INVESTIGATION OF PROCESS PARAMETERS AND DEVELOPMENT OF A MATHEMATICAL MODEL FOR THE PURPOSES OF CONTROL DESIGN AND IMPLEMENTATION FOR A WASTEWATER TREATMENT PROCESS

SYDNEY C. DU PLESSIS

CAPE PENINSULA
UNIVERSITY OF TECHNOLOGY
Library and Information Services
Dewey · 628.3 Dup

CAPE PENINSULA
UNIVERSITY OF TECHNOLOGY

9001598

CAPE PENINSULA UNIVERSITY OF TECHNOLOGY
LIBRARY AND INFORMATION SERVICES
BELLVILLE CAMPUS

TEL: (021) 959-6210 FAX:(021)959-6109

Renewals may be made telephonically.
This book must be returned on/before the last date shown.
Please note that fines are levied on overdue books

24 AUG 2010

11 AUG 2010

L THE 628.3 DUP
green

CAPE PENINSULA
UNIVERSITY OF TECHNOLOGY
9001598

BEL THE 628.3 DUP
green



Cape Peninsula
University of Technology

INVESTIGATION OF PROCESS PARAMETERS AND DEVELOPMENT OF A MATHEMATICAL MODEL FOR THE PURPOSES OF CONTROL DESIGN AND IMPLEMENTATION FOR A WASTEWATER TREATMENT PROCESS

by

SYDNEY CHARLES du PLESSIS

Dissertation submitted in fulfilment of the requirements for the degree

Doctor of Technology: Electrical Engineering

in the Faculty of Engineering

at the Cape Peninsula University of Technology

Supervisor: Prof. Raynitchka Tzoneva

Bellville
May 2009

DECLARATION

I, Sydney Charles du Plessis, declare that the contents of this thesis represent my own unaided work, and that the thesis has not previously been submitted for academic examination towards any qualification. Furthermore, it represents my own opinions and not necessarily those of the Cape Peninsula University of Technology.

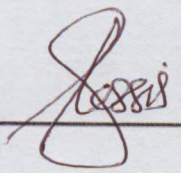

Signed _____

18/9/09

Date _____

ABSTRACT

The problem for effective and optimal control of wastewater treatment plants is very important recently because of the increased requirements to the quality of the effluent. The activated sludge process is a type of wastewater process characterized with complex dynamics and because of this proper control design and implementation strategies are necessary and important for its operation. Since the early seventies, when a major leap forward was made by the widespread introduction of dissolved oxygen control, little progress has been made.

The most critical phase in the solution of any control problem is the modelling stage. The primary building block of any modern control exercise is to construct and identify a model for the system to be controlled. The existing full Activated Sludge Model 1 (ASM1) and especially University of Cape Town (UCT) models of the biological processes in the activated sludge process, called in the thesis biological models, are highly complex because they are characterised with a lot of variables that are difficult to be measured on-line, complex dependencies and nonlinear interconnections between the biological variables, many kinetic parameters that are difficult to be determined, different time scales for the process dynamics.

The project considers reduction of the impact of the complexity of the process model over the methods for control design and proposes a solution to the above difficulties by development of a reduced model with small number of variables, but still with the same characteristics as the original full model for the purposes of real time control design.

Then the research problem can be stated in the following way: To develop mathematical methods, algorithms and programmes for transformation of the complex biological and mass balance models of the activated sludge process into simpler reduced models of the process convenient to be used for optimal parameter estimation, control design and control implementation in real- time. The thesis chapters describe the solution of this problem:

- Chapter 1 considers the problems for the complexity of the mathematical models of the activated sludge process and states the thesis aim and objectives, hypothesis, assumptions, methodology.
- Chapter 2 provides a study of the activated sludge technology and its characteristics as an object of control. The complex relationships between the process variables are described. The place of the problem for modelling and parameter estimation in the plant multi-layer control hierarchy is stated.
- Chapter 3 defines a system within a state space, important criteria for process model development and various model types are given. The wastewater treatment biological models such as UCT biological model and Activated Sludge model No. 1 are described. The similarities and differences between these two models are discussed. The default values for kinetic, stoichiometric and switching functions in the UCT model and ASM1 model are given. The processes and processes' rates of the UCT model Peterson matrix and the ASM1 Peterson matrix are explained in a detailed manner. Three wastewater treatment plant structures viz., Benchmark, Mitchell's Plain and Athlone are introduced and described. Their mass balance equations are derived for every tank and component.
- Chapter 4 elucidates the need for reduced model development of both the ASM1 and UCT models. The assumptions for model reduction are also studied. The dissolved oxygen concentration is considered as a control input for the reduced models. The ASM1 and UCT reduced biological models are developed. The mass balance equations for the three wastewater treatment plants are derived on the basis of the reduced UCT and ASM1 biological models. The matrices and vectors for each of the plants are separately built and the reduced model characteristics are compared and contrasted.
- Chapter 5 gives answer to the question which parameters to be estimated on the basis of sensitivity study of the model parameters. It examines the changes of the model variables according to the changes in the model parameters. State space models of sensitivity for the three considered plants are developed and used for calculation of the sensitivity functions in Matlab environment. Parameters with large values of the sensitivity functions are found.
- Chapter 6 states the problem for parameter estimation and proposes a method for its solution based on time domain decomposition.The aim is to determine

values of model parameters that provide the best fit to measured data, based on least squares criterion. Matlab software is developed and applied to solve the problem for the considered plants for the ASM1 and UCT biological models.

- Chapter 7 gives a theoretical analysis of the problem for state and parameter estimation. Different approaches are compared in order to find the techniques suitable for the activated sludge process characteristics. Kalman filter is selected as the most convenient one.
- Chapter 8 gives short comparative analysis of the existing simulators of the activated sludge process. SIMBA simulator is selected and its structure is described. Simulation of the mass balance full and reduced models of the considered plants is provided and described. Discussion of the results is done.
- Chapter 9 investigates the Sensitivity function simulation and Parameter Estimation for the Benchmark process and the Athlone process model based on the reduced ASM1 and UCT biological model.
- Chapter 10 gives the conclusion and future research directions.

ACKNOWLEDGEMENTS

I wish to thank:

- Prof. R. Tzoneva for the advice and support which she provided towards my project and thesis.
- Mr Carl Kriger for the support he provided during my research work
- Mr Mohamed Kalimullah provided the IT expertise backup for my work.
- the late Prof. Hilton Fransman for motivating me to write my proposal and his Research Committee for accepting it.

The financial assistance of the National Research Foundation and Cape Peninsula University of Technology towards this research is acknowledged. Opinions expressed in this dissertation and the conclusions arrived at, are those of the author, and are not necessarily to be attributed to the National Research Foundation.

DEDICATION

I dedicated this dissertation to our God and my late parents, Sydney Charles du Plessis (Senior) and Martha Magdalena du Plessis who inculcated in me the spirit, ethos and promise what education can do for humankind providing an opportunity and freedom for my personal growth and a vista to my future knowledge for the environment and for people with disabilities.

TABLE OF CONTENTS

	Declaration	ii
	Abstract	iii
	Acknowledgements	vi
	Dedication	vii
	Glossary	xxxiii

CHAPTER ONE: STATEMENT OF THE PROBLEM. PROJECT OBJECTIVES, HYPOTHESIS AND ASSUMPTIONS

1.1	Introduction	1
1.2	Awareness of the problem	1
1.3	Statement of the Problem	3
1.3.1	Design based subproblems	4
1.3.1.1	Subproblem 1	4
1.3.1.2	Subproblem 2	4
1.3.1.3	Subproblem 3	4
1.3.1.4	Subproblem 4	4
1.3.1.5	Subproblem 5	4
1.3.2	Real time implementation subproblems	4
1.3.2.1	Subproblem 6	4
1.3.2.2	Subproblem 7	5
1.3.2.3	Subproblem 8	5
1.3.2.4	Subproblem 9	5
1.4	Research objectives	5
1.5	The Hypothesis	6
1.6	Delimitation of the research	6
1.7	Assumptions	7
1.8	Phases in the model building	7
1.8.1	Development of models	7
1.8.2	Parameter and variable estimation	8
1.8.3	Model Verification and Validation	9
1.9	Research methods	9
1.10	Thesis chapters	10
1.11	The significance of the research	11
1.12	Conclusion	11

CHAPTER TWO: THE WASTEWATER TREATMENT PLANT PROCESS

2.1	Introduction	13
2.2	The waste water treatment plant	13
2.3	Activated sludge processes of industrial wastewaters	14
2.3.1	Plug-flow activated sludge	14
2.3.2	Complete Mixed Activated Sludge (CMAS)	15
2.3.3	Pure Oxygen systems	15
2.4	Treatment of Industrial wastewater in municipal activated	16

	sludge Plants	
2.4.1	Effect on effluent quality	17
2.4.2	Effect on sludge quality	17
2.4.3	Effect on temperature	17
2.4.4	Sludge handling	18
2.4.5	Bioinhibition and aquatic toxicity	18
2.4.6	Nutrient(N and P) requirements	18
2.5	The activated sludge process as an object of control	18
2.6	Multilayer control strategy of the wastewater treatment process	21
2.6.1	Hierarchical control structure functions	21
2.6.2	The process modelling and estimation - task of the adaptation layer	22
2.7	Conclusion	24

CHAPTER THREE: MATHEMATICAL MODELS OF THE ACTIVATED SLUDGE PROCESS

3.1	Introduction	25
3.2	Definition of a system	25
3.2.1	Definition of a mathematical model	27
3.2.2	Important criteria in the process of model development	28
3.2.2.1	Model Purpose	28
3.2.2.2	System Boundaries	28
3.2.2.3	Time Constraints	28
3.2.2.4	Accuracy	29
3.2.3	Model Types	29
3.2.3.1	Reductionist versus Holistic Models	29
3.2.3.2	Internal versus External Models	29
3.2.3.3	Dynamic versus Static Models	30
3.2.3.4	Deterministic versus Stochastic Models	30
3.2.3.5	Continuous-Time versus Discrete-Time Models	30
3.2.3.6	Distributed versus Lumped-Parameter Models	31
3.3	Biological models	31
3.3.1	UCT biological model	31
3.3.1.1	Carbon Biological Removal	32
3.3.1.2	Nitrification	34
3.3.1.3	Alterations to the model	34
3.3.1.3.1	The Influence of Energy Requirement for Adsorption	34
3.3.1.3.2	The Influence of the Function of Adsorption	35
3.3.1.3.3	The Influence of Function of Enmeshment	35
3.3.1.3.4	The Influence of Synthesis of Active Mass	36
3.3.1.3.5	The Influence of Soluble substrate	36
3.3.1.3.6	The Influence of Particulate substrate	36
3.3.1.3.7	The Influence of Endogenous Respiration	38
3.3.2	Description of the UCT mathematical model equations	39
3.4	Discussion	47
3.4.1	Activated Sludge Model No.1 (ASM1)	48

3.4.2	Model Process Operation Rates	48
3.4.3	The basic principles of the model building	49
3.4.3.1	The influence of non-biodegradable organic matter	50
3.4.3.2	The influence of biodegradable organic matter	50
3.4.3.3	The influence of heterotrophic biomass	51
3.4.3.4	The influence of nitrogenous matter	51
3.5	Fundamental Processes in the Peterson Matrix	53
3.6	Default values	54
3.6.1	Main differences between UCT and ASM1 biological models	56
3.7	Model assumptions, restrictions and simplifications	58
3.8	Mass balance models	58
3.8.1	Mass balance equations for the Benchmark structure	59
3.8.2	Plant layout	59
3.8.3	Plant specifications	60
3.9	Discrete form of equations	61
3.9.1	Mass balance equations for the Mitchell's Plain wastewater treatment plant	62
3.9.1.1	Plant layout	62
3.9.1.2	Plant Specifications	63
3.9.2	Mass balance equations for the Athlone wastewater treatment Plant	65
3.9.2.1	Plant layout	65
3.9.2.2	Plant Specifications	65
3.10	Conclusion	67

CHAPTER FOUR: DEVELOPMENT OF REDUCED BIOLOGICAL AND MASS BALANCE MODELS OF ACTIVATED SLUDGE PROCESS

4.1	Introduction	69
4.2	The need for reduced model development	69
4.3	Assumptions for the development of the reduced biological models	73
4.3.1	Dissolved oxygen concentration	75
4.3.2	Description of the organic matter for the reduced model	75
4.3.3	Nitrogen consumption	76
4.3.4	Microorganism components	76
4.4	Reduced ASM1 biological model	77
4.4.1	Biological processes included in the reduced model	77
4.5	Reduced UCT biological model	78
4.6	Mass balance process models	82
4.6.1	Development of the mass balance process model for the benchmark structure with reduced ASM1 and UCT biological models	82
4.6.1.1	Mass balance equations for benchmark model	82
4.6.1.2	Process models in a vector-matrix form	86
4.6.2	Development of the mass balance process model for the Mitchell's Plain structure with reduced UCT and ASM1 biological models	90

4.6.2.1	Mass balance equations for the Mitchell's Plain plant	90
4.6.2.2	Process model in a vector-matrix form	91
4.6.3	Development of the mass balance process model for the Athlone structure with the reduced ASM1 and UCT biological models	93
4.6.3.1	Mass balance equations for the Athlone plant	93
4.6.3.2	Process model in a vector-matrix form	95
4.7	Reduced models characteristics	96
4.8	Conclusion	97

CHAPTER FIVE: SENSITIVITY STUDY FOR THE DETERMINATION OF THE KEY PARAMETERS OF THE WASTEWATER TREATMENT SYSTEM

5.1	Introduction	98
5.2	Sensitivity functions	98
5.3	Development of the sensitivity functions and model for the Benchmark Structure with ASM1 and UCT biological models	99
5.3.1	Benchmark structure with ASM1 biological model	99
5.3.1.1	Sensitivity equations derivation	99
5.3.1.2	Sensitivity state space model	104
5.3.2	Benchmark structure with UCT model	108
5.3.2.1	Sensitivity equations derivation	109
5.3.2.2	Sensitivity state space model	117
5.4	Derivation of the sensitivity functions and reduced model for the Athlone process	122
5.4.1	Reduced process model based on the ASM1 biological model	122
5.4.1.1	Sensitivity equations derivation	122
5.4.1.2	State space sensitivity model	123
5.4.2	Sensitivity model based on the UCT biological model	126
5.4.2.1	Sensitivity equations derivation	126
5.4.2.2	State space sensitivity model	128
5.5	Matlab simulation of the sensitivity models	131
5.6	Conclusion	131

CHAPTER SIX: PARAMETER ESTIMATION

6.1	Introduction	132
6.2	Assessment of the structurally identifiable parameters	132
6.2.1	Study of the identifiability of the reduced model on the basis of the Taylor series expansion	133
6.2.1.1	Theory and practical application	133
6.2.1.2	Study of the identifiability of the reduced model for the Benchmark process	134
6.2.2	Reduced version of the vector of the parameters. Identifiability of the growth parameters for the ASM1 model	138
6.2.3	Application to the case of the UCT reduced model.	138

	Identifiability according to the yield and growth parameters	
6.2.4	Reduced version of the vector of the parameters. Identifiability of the growth parameters	140
6.3	The problem for parameter estimation	141
6.3.1	Definitions	141
6.3.2	Preliminary steps in Parameter estimation	141
6.3.2.1	Selecting data subsets for estimation and validation	141
6.3.2.2	Selection of parameters to be estimated	142
6.3.2.3	Differentiating Linear and Nonlinear parameters	142
6.4	Techniques for parameter estimation	142
6.4.1	On-line and off-line estimation methods	143
6.4.2	Objectives in parameter estimation	143
6.4.3	Minimization approach	144
6.5	Basic components of the parameter estimation	144
6.5.1	Deterministic Models	144
6.5.1.1	Structural Model	144
6.5.1.2	Reduced Model	145
6.5.2	Data-Experiments and Data Matrix	146
6.5.3	Residuals	147
6.6	Analysis of the conventional linear techniques for calculation of the parameter estimates	148
6.6.1	Maximum Likelihood (ML) Estimation	148
6.6.2	Bayesian Estimation	151
6.6.2.1	Mode of the Posterior Distribution	152
6.6.3	Least Squares-Unweighted Least Squares	153
6.6.4	Derivation of the Principle of Least-Squares	154
6.6.5	Weighted Least Squares	155
6.6.6	Constrained Least Squares	156
6.6.7	Nonlinear Process Identification	157
6.6.7.1	Methods of the least square correction	157
6.6.7.2	Methods of theoretically sound nonlinear functions	158
6.6.7.2.1	Model Parametrization and Problem Statement of Hammerstein Model	159
6.7	Estimation of the growth parameters of the wastewater treatment process	161
6.7.1	Estimation of the kinetic parameters through biological tests	161
6.7.2	Parameter estimation with the aid of sensitivity functions	161
6.7.3	Modelling using automatic estimation methods	162
6.8	Approach for linear batch parameter estimation of growth kinetics of the microorganisms in wastewater treatment	163
6.8.1	Estimation of the growth parameters of the Benchmark process	164
6.8.1.1	Application of the ASM1 biological model	164
6.8.1.1.1	Transformation of the state space model (6.115) to the form of (6.113)	164
6.8.1.1.2	Formulation and solution of the problem for linear batch least squares estimation	166
6.8.1.1.3	Algorithm and a MATLAB program	168
6.8.1.2	Application for the UCT biological model	168

6.8.1.2.1	Transformation of the state space model (6.115) to the form of the model (6.113)	168
6.8.2	Estimation of the growth parameters of the Athlone process	169
6.8.2.1	Application of the ASM1 biological model	169
6.8.2.2	Application of the UCT biological model	170
6.8.3	Properties of the least square estimator for the parameters $\hat{\theta}$	170
6.8.3.1	Mean value of the least squares estimator	170
6.8.3.2	Covariance matrix of the least squares estimator	170
6.9	Recursive Least square estimation	171
6.9.1	Application of the method to the Benchmark process	174
6.9.1.1	Using of the ASM1 model	174
6.9.1.2	Using of the UCT model	175
6.9.2	Application of the method to the Athlone process	175
6.10	Recursive least square estimation with exponential forgetting	175
6.11	Conclusion	177

CHAPTER SEVEN: STATE AND PARAMETER ESTIMATION

7.1	Introduction	179
7.2	Theoretical concepts in system observability	180
7.2.1	Notion of observability	180
7.2.2	State estimation for continuous systems	181
7.2.3	State estimation for discrete time systems	182
7.2.4	State estimation for noisy systems	183
7.2.5	Observers for linear systems	184
7.2.5.1	Luenberger observer	184
7.2.5.2	Kalman filter	185
7.2.6	Nonlinear system estimation. Extended Kalman filter	186
7.3	Estimation of the biotechnological processes	187
7.3.1	General observer	188
7.3.1.1	Exponential observability	189
7.3.1.2	Asymptotic observers	190
7.3.1.3	Extended Luenberger and Kalman Observers	190
7.3.2	Different applications	191
7.3.2.1	Asymptotic observers for state estimation when the growth reaction rates are unknown	191
7.3.2.1.1	Statement of the estimation problem	191
7.3.2.1.2	An observer-based estimator	192
7.3.2.1.3	A linear regression estimator	193
7.3.2.1.4	Extended Kalman Filtering for on-line estimation of reaction rates	194
7.3.2.2	State and Parameter Estimation with unknown Yield Coefficients	196
7.3.2.2.1	Conditions for estimating ρ independently of the unknown yield coefficients	196
7.3.2.2.2	Joint Estimation of Yield Coefficients and Specific Reaction Rates	197
7.3.2.2.2.1	Full State measurement	197
7.3.2.2.2.2	Partial state measurement	199

7.3.2.2.3	Adaptive Observers	200
7.3.3	Estimation of yield coefficients	201
7.3.3.1	The estimation problem	201
7.3.3.2	A linear regression form	201
7.3.3.3	Estimators of the parameter vector θ	202
7.3.4	Other Parameter Estimation Issues in Bioreactors	203
7.3.4.1	Estimation of specific liquid gas transfer rates	203
7.3.4.2	Estimation of oxygen related parameters	204
7.4	Overview and comparison of the methods for parameter and state estimation of the activated sludge process	205
7.4.1	Interval observers	206
7.4.2	Joint state and parameter estimation	207
7.4.2.1	Case of measurement of DO	207
7.4.2.2	Case of measurement of nitrate-nitrogen concentration (process product)	208
7.4.2.3	Case of measurements of the substrate concentration	208
7.4.2.4	State and parameter estimation for phosphorus removal	209
7.4.3	Estimation of the parameters associated with the oxygen consumption and transfer	209
7.4.3.1	Oxygen Transfer Function Models	209
7.4.3.2	Respiration rate model	210
7.4.4	Estimation of the influent characteristics as on unknown input	212
7.5	Discrete Kalman filter design for state estimation of the reduced models of the Benchmark and Athlone wastewater treatment plant	213
7.5.1	Development of a linearised tangent model of the reduced nonlinear models for the Benchmark and Athlone processes with ASM1 and UCT reduced biological models	214
7.5.1.1	Linearised model for the Benchmark and Athlone processes based on the ASM reduced biological model	215
7.5.1.2	Linearised model for the Benchmark and Athlone processes based on the reduced UCT biological model	218
7.5.1.3	State observability	221
7.5.2	Design of a discrete Kalman filter for the estimation of the immeasurable state variables on the basis of the process linearised model	224
7.5.3	Steady state Kalman filter	228
7.5.4	Design of a discrete extended Kalman filter for estimation of concentrations of the immeasurable process variables	228
7.5.5	Application of the discrete Kalman filters to the wastewater state variables estimation	230
7.6	Conclusion	230

CHAPTER EIGHT: THE SIMULATION OF THE WASTEWATER PROCESSES

8.1	Introduction	232

8.2	The importance of simulation	232
8.3	Simulators / Comparative analysis	233
8.4	Application Specific Simulators	235
8.4.1	Short description of the simulators capabilities	235
8.4.2	Comparison of the simulators characteristics	238
8.5	MATLAB/ Simulink	239
8.6	SIMBA	239
8.7	Development of the ASM1 and UCT biological models in SIMBA environment	241
8.7.1	Variables, parameters, input flow fractions	241
8.7.2	Peterson matrix and stoichiometric balances for the ASM1 full and reduced models	244
8.7.2.1	ASM1 full model	244
8.7.2.2	Reduced ASM1 Model	244
8.7.3	Peterson matrix and balances for the UCT model full and reduced models	244
8.7.3.1	UCT full model	244
8.7.3.2	Reduced UCT model	244
8.8	Simulation of the Mitchell's Plain plant on the basis of the UCT full biological model	249
8.8.1	SIMBA diagrams	249
8.8.2	Results from the simulation	250
8.8.2.1	Dynamic behaviour of the influent (point h1) in Mitchell Plain plant wastewater simulated over a of 100 days for total sludge age of 16 days at 22 C	251
8.8.2.2	Dynamic behaviour of the process variables after the anaerobic tank (point h2) in Mitchell Plain plant activated sludge simulated over a period of 100 days for total sludge age of 16 days at 22 C	253
8.8.2.3	Dynamic behaviour of the process variables after the anoxic tank (point h3) in Mitchell Plain plant activated sludge simulated over a period of 100 days for total sludge age of 16 days at 22 C	256
8.8.2.4	Dynamic behaviour of the process variables after the aerobic tank (point h4) in Mitchell Plain plant activated sludge simulated over a period of 100 days for total sludge age of 16 days at 22 C	259
8.8.3	Discussion of the obtained results	261
8.9	Simulation of the Athlone plant on the basis of ASM1 full and reduced and UCT full and reduced models	263
8.9.1	SIMBA diagrams	263
8.9.2	Results from the simulation of the Athlone plant with the full and reduced ASM1 biological model	264
8.9.2.1	Dynamic behaviour of the influent (point h1) in wastewater for Athlone UCT plant simulated over a period of 100 days for total sludge age of 20 days at 22 C	264
8.9.2.2	Dynamic behaviour of the process variables (point h2) in wastewater for Athlone UCT plant simulated over a period of 100 days for total sludge age of 20 days at 22 C	269
8.9.2.3	Dynamic behaviour of the process variables after the anoxic	275

	tank(point h3) in wastewater for Athlone UCT plant simulated over a period of 100 days for total sludge age of 20 days at 22 C	
8.9.2.4	Dynamic behaviour of the process variables after the aerobic tank (point h4) in wastewater for Athlone UCT plant simulated over a period of 100 days for total sludge age of 20 days at 22 C	281
8.9.2.5	Discussion of the results	287
8.9.3	Results from the simulation of the Athlone plant with the full and reduced UCT biological model	289
8.9.3.1	Dynamic behaviour of the influent (point h1) in wastewater for Athlone plant simulated over a period of 100 days for total sludge age of 20 days at 22 C	289
8.9.3.2	Dynamic behaviour of the process variables after the anaerobic tank (point h2) in wastewater for Athlone plant simulated over a period of 100 days for total sludge age of 20 days at 22 C	294
8.9.3.3	Dynamic behaviour of the process variables after the anoxic tank (point h3) in wastewater for Athlone plant simulated over a period of 100 days for total sludge age of 20 days at 22 C	299
8.9.3.4	Dynamic behaviour of the process variables after the aerobic tank (point h4) in wastewater for Athlone plant simulated over a period of 100 days for total sludge age of 20 days at 22 C	304
8.9.4	Discussion of the results	309
8.10	Conclusion	314

CHAPTER NINE: RESULTS FROM THE APPLICATION OF METHODS FOR SENSITIVITY ANALYSIS AND PARAMETER ESTIMATION TO THE BENCHMARK AND ATHLONE PLANTS

9.1	Introduction	316
9.2	Sensitivity analysis of the Activated Sludge process	316
9.2.1	Software for the sensitivity analysis	316
9.2.2	Sensitivity function simulation for the Benchmark process model based on the reduced ASM1 and UCT biological model	317
9.2.2.1	Results for the ASM1 reduced biological model	318
9.2.2.2	Results for the UCT reduced biological model	334
9.2.2.3	Discussion of the results	356
9.2.2.3.1	Benchmark process with ASM1 reduced biological model	356
9.2.2.3.2	Benchmark process with UCT reduced biological model	356
9.2.3	Sensitivity function simulation for the Athlone process model Based on the reduced ASM1 and UCT biological models	358
9.2.3.1	Results for the ASM1 reduced biological model	358
9.2.3.2	Results for the UCT reduced biological model	368
9.2.3.3	Discussion of the results	381
9.2.3.3.1	Athlone process with ASM1 reduced biological model	381
9.2.3.3.2	Athlone process with the UCT reduced biological model	381
9.3	Parameter estimation of the reduced models of the Activated Sludge Process	383
9.3.1	Software for the parameter estimation	383

9.3.2	Reduced ASM1 model parameter estimation used for the Benchmark process and Athlone process mass balance models	386
9.3.2.1	Results for the Benchmark mass balance process model	386
9.3.2.2	Results for the Athlone mass balance process model	392
9.3.2.3	Discussion of the results	397
9.3.3	Reduced UCT model parameter estimation used for the Benchmark process	397
9.3.3.1	Results for the Benchmark mass balance process model	397
9.3.3.2	Results for the Benchmark process	405
9.4	Conclusion	405

CHAPTER TEN: CONCLUSION, DELIVERABLES AND FUTURE DIRECTIONS OF RESEARCH

10.1	Introduction	406
10.2	Aims and Objectives	406
10.2	Achievements of the thesis	407
10.3	Discussion and importance of the achievements	412
10.4	Recommendations	413
10.4.1	Applications	413
10.4.2	Future directions	413
10.5	Publications	414

BIBLIOGRAPHY 415

LIST OF FIGURES

Figure 2.1: Schematic of the wastewater treatment plant 14
Figure 2.2: Complex dependencies in the microorganism cells. The biomass growth process components 19
Figure 2.3: Dependence between chemical and biological variables 20
Figure 2.4: Activated sludge process 20
Figure 2.5: Three layer hierarchical control structure 22
Figure 2.6: Estimation algorithm 24
Figure 3.1: "Black box" model of the system 26
Figure 3.2: Phases in utilization of slowly biodegradable COD in UCT model 56
Figure 3.3 : Biodegradable COD utilization concept in UCT model 57
Figure 3.4: Biodegradable COD utilization in the ASM1 model 57
Figure 3.5: Wastewater treatment plant layout of the Benchmark model 60
Figure 3.6: Mitchell's Plain wastewater treatment plant configuration 62
Figure 3.7: Athlone plant configuration 65
Figure 6.1: Hammerstein model 159
Figure 7.1: Basic structure of the observer and plant 181
Figure 7.2: Predictor/ corrector observer 183
Figure 8.1: A schematic SIMBA diagram of the overall Mitchell's Plain wastewater treatment plant 249
Figure 8.2: A schematic SIMBA diagram of the internal structure of the Mitchell's Plain wastewater treatment plant 250
Figure 8.3: Front panel of the SIMBA simulation package 250
Figure 8.4: The dynamic behaviour of biological (active) heterotrophic biomass fraction at h1 251
Figure 8.5: The dynamic behaviour of biological (active) autotrophic biomass fraction at h1 251
Figure 8.6: The dynamic behaviour of endogenous mass fraction at h1 251
Figure 8.7: The dynamic behaviour of inert mass fraction at h1 251
Figure 8.8: The dynamic behaviour of adsorbed slowly biodegradable substrate fraction at h1 251
Figure 8.9: The dynamic behaviour of enmeshed slowly biodegradable substrate fraction at h1 251
Figure 8.10: The dynamic behaviour of biodegradable particulate organic nitrogen fraction at h1 252
Figure 8.11: The influence of readily biodegradable (soluble) substrate fraction at h1 252
Figure 8.12: The dynamic behaviour of ammonia nitrogen at h1 252
Figure 8.13: The dynamic behaviour of bio-degradable soluble organic nitrogen at h1 252
Figure 8.14: The dynamic behaviour of nitrate nitrogen at h1 252
Figure 8.15: The dynamic behaviour of alkalinity at h1 252
Figure 8.16: The dynamic behaviour of unbiodegradable soluble substrate at h1 253
Figure 8.17: The dynamic behaviour of oxygen at h1 253
Figure 8.18: The dynamic behaviour of flow rate at h1 253
Figure 8.19: The dynamic behaviour of biological (active) heterotrophic biomass fraction at h2 253
Figure 8.20: The dynamic behaviour of biological (active) autotrophic mass fraction at h2 253
Figure 8.21: The dynamic behaviour of endogenous mass fraction at h2 254
Figure 8.22: The dynamic behaviour of inert mass fraction at h2 254
Figure 8.23: The dynamic behaviour of adsorbed slowly biodegradable substrate fraction at h2 254

Figure 8.24: The dynamic behaviour of enmeshed slowly biodegradable substrate fraction at h2 254
Figure 8.25: The dynamic behaviour of biodegradable particulate organic nitrogen fraction at h2 254
Figure 8.26: The dynamic behaviour of readily biodegradable (soluble) substrate fraction at h2 254
Figure 8.27: The dynamic behaviour of ammonia nitrogen fraction at h2 255
Figure 8.28: The dynamic behaviour of biodegradable particulate organic nitrogen fraction at h2 255
Figure 8.29: The dynamic behaviour of nitrate nitrogen fraction at h2 255
Figure 8.30: The dynamic behaviour of alkalinity at h2 255
Figure 8.31: The dynamic behaviour of unbiodegradable soluble substrate fraction at h2 255
Figure 8.32: The dynamic behaviour of oxygen at h2 255
Figure 8.33: The dynamic behaviour of flow rate at h2 255
Figure 8.34: The dynamic behaviour of biological (active) heterotrophic biomass fraction at h3 256
Figure 8.35: The dynamic behaviour of biological (active) autotrophic mass fraction at h3 256
Figure 8.36: The dynamic behaviour of endogenous mass fraction at h3 256
Figure 8.37: The dynamic behaviour of inert mass fraction at h3 256
Figure 8.38: The dynamic behaviour of adsorbed slowly biodegradable substrate fraction at h3 256
Figure 8.39: The dynamic behaviour of enmeshed slowly biodegradable substrate fraction at h3 256
Figure 8.40: The dynamic behaviour of biodegradable particulate organic nitrogen fraction at h3 257
Figure 8.41: The dynamic behaviour of readily biodegradable (soluble) substrate fraction at h3 257
Figure 8.42: The dynamic behaviour of ammonia nitrogen fraction at h3 257
Figure 8.43: The dynamic behaviour of biodegradable particulate organic nitrogen fraction at h3 257
Figure 8.44: The dynamic behaviour of nitrate nitrogen fraction at h3 257
Figure 8.45: The dynamic behaviour of alkalinity at h3 257
Figure 8.46: The dynamic behaviour of unbiodegradable soluble substrate fraction at h3 258
Figure 8.47: The dynamic behaviour of oxygen at h3 258
Figure 8.48: The dynamic behaviour of flow rate at h3 258
Figure 8.49: The dynamic behaviour of biological (active) heterotrophic biomass fraction at h4 259
Figure 8.50: The influence of biological (active) autotrophic biomass fraction at h4 259
Figure 8.51: The dynamic behaviour of endogenous mass fraction at h4 259
Figure 8.52: The dynamic behaviour of inert mass fraction at h4 259
Figure 8.53: The dynamic behaviour of adsorbed slowly biodegradable substrate fraction at h4 259
Figure 8.54: The dynamic behaviour of enmeshed slowly biodegradable substrate fraction at h4 259
Figure 8.55: The dynamic behaviour of biodegradable particulate organic nitrogen fraction at h4 260
Figure 8.56: The dynamic behaviour of readily biodegradable (soluble) substrate fraction at h4 260
Figure 8.57: The dynamic behaviour of ammonia nitrogen fraction at h4 260
Figure 8.58: The dynamic behaviour of biodegradable particulate organic nitrogen fraction at h4 260

Figure 8.59: The dynamic behaviour of nitrate nitrogen fraction at h4 260
Figure 8.60: The dynamic behaviour of alkalinity at h4 260
Figure 8.61: The influence of unbiodegradable soluble substrate fraction at h4 261
Figure 8.62: The influence of oxygen at h4 261
Figure 8.63: The dynamic behaviour of flow rate at h4 261
Figure 8.64: A schematic SIMBA diagram of the overall Athlone wastewater treatment plant 263
Figure 8.65: A schematic SIMBA diagram of the internal structure of the Athlone wastewater treatment plant 263
Figure 8.66a: The dynamic behaviour of unbiodegradable soluble substrate at h1 for ASM1 full model 264
Figure 8.66b: The dynamic behaviour of unbiodegradable soluble substrate at h1 for ASM1 reduced model 264
Figure 8.67a: The dynamic behaviour of readily biodegradable (soluble) substrate fraction at h1 for ASM1 full model 264
Figure 8.67b: The dynamic behaviour of readily biodegradable (soluble) substrate fraction at h1 for ASM1 reduced model 264
Figure 8.68a: The dynamic behaviour of inert mass fraction at h1 for ASM1 full model 264
Figure 8.68b: The dynamic behaviour of inert mass fraction at h1 for ASM1 reduced model 264
Figure 8.69a: The dynamic behaviour of enmeshed slowly biodegradable substrate fraction at h1 for ASM1 full model 265
Figure 8.69b: The dynamic behaviour of enmeshed slowly biodegradable substrate fraction at h1 for ASM1 reduced model 265
Figure 8.70a: The dynamic behaviour of biological (active) heterotrophic mass fraction at h1 for ASM1 full model 265
Figure 8.70b: The dynamic behaviour of biological (active) heterotrophic mass fraction at h1 for ASM1 reduced model 265
Figure 8.71a: The dynamic behaviour of biological (active) autotrophic mass fraction at h1 for ASM1 full model 265
Figure 8.71b: The dynamic behaviour of biological (active) autotrophic mass fraction at h1 for ASM1 reduced model 265
Figure 8.72a: The dynamic behaviour of endogenous mass fraction at h1 for ASM1 full model 266
Figure 8.72b: The dynamic behaviour of endogenous mass fraction at h1 for ASM1 reduced model 266
Figure 8.73a: The dynamic behaviour of oxygen at h1 for ASM1 full model 266
Figure 8.73b: The dynamic behaviour of oxygen at h1 for ASM1 reduced model 266
Figure 8.74a: The dynamic behaviour of nitrate nitrogen at h1 for ASM1 full model 266
Figure 8.74b: The dynamic behaviour of nitrate nitrogen at h1 for ASM1 reduced model 266
Figure 8.75a: The dynamic behaviour of ammonia nitrogen at h1 for ASM1 full model 267
Figure 8.75b: The dynamic behaviour of ammonia nitrogen at h1 for ASM1 reduced model 267
Figure 8.76a: The dynamic behaviour of biodegradable soluble organic nitrogen at h1 for ASM1 full model 267
Figure 8.76b: The dynamic behaviour of biodegradable soluble organic nitrogen at h1 for ASM1 reduced model 267
Figure 8.77a: The dynamic behaviour of biodegradable particulate organic nitrogen fraction at h1 for ASM1 full model 267
Figure 8.77b: The dynamic behaviour of biodegradable particulate organic nitrogen fraction at h1 for ASM1 reduced model 267
Figure 8.78a: The dynamic behaviour of alkalinity at h1 for ASM1 full model 268
Figure 8.78b: The dynamic behaviour of alkalinity at h1 for ASM1 reduced model 268
Figure 8.79a: The dynamic behaviour of flow rate at h1 for ASM1 full model 268

Figure 8.79b: The dynamic behaviour of flow rate at h1 for ASM1 reduced model 268
Figure 8.80a: The dynamic behaviour of chemical oxygen demand at h1 for ASM1 full model 268
Figure 8.80b: The dynamic behaviour of chemical oxygen demand at h1 for ASM1 reduced model 268
Figure 8.81a: The dynamic behaviour of nitrogen at h1 for ASM1 full model 269
Figure **8.81b:** The dynamic behaviour of nitrogen at h1 for ASM1 reduced model 269
Figure 8.82a: The dynamic behaviour of total Kjeldahl nitrogen at h1 for ASM1 full model 269
Figure 8.82b: The dynamic behaviour of total Kjeldahl nitrogen at h1 for ASM1 reduced model 269
Figure 8.83a: The dynamic behaviour of unbiodegradable soluble substrate at h2 for ASM1 full model 270
Figure 8.83b: The dynamic behaviour of unbiodegradable soluble substrate at h2 for ASM1 reduced model 270
Figure 8.84a: The dynamic behaviour of readily biodegradable (soluble) substrate fraction at h2 for ASM1 full model 270
Figure 8.84b: The dynamic behaviour of readily biodegradable (soluble) substrate fraction at h2 for ASM1 reduced model 270
Figure 8.85a: The dynamic behaviour of inert mass fraction at h2 for ASM1 full model 271
Figure 8.85b: The dynamic behaviour of inert mass fraction at h2 for ASM1 reduced model 271
Figure 8.86a: The dynamic behaviour of enmeshed slowly biodegradable substrate fraction at h2 for ASM1 full model 271
Figure 8.86b: The dynamic behaviour of enmeshed slowly biodegradable substrate fraction at h2 for ASM1 reduced model 271
Figure 8.87a: The dynamic behaviour of biological (active) heterotrophic mass fraction at h2 for ASM1 full model 271
Figure 8.87b: The dynamic behaviour of biological (active) heterotrophic mass fraction at h2 for ASM1 reduced model 271
Figure 8.88a: The dynamic behaviour of biological (active) autotrophic mass fraction at h2 for ASM1 full model 272
Figure 8.88b: The dynamic behaviour of biological (active) autotrophic mass fraction at h2 for ASM1 reduced model 272
Figure 8.89a: The dynamic behaviour of endogenous mass fraction at h2 for ASM1 full model 272
Figure 8.89b: The dynamic behaviour of endogenous mass fraction at h2 for ASM1 reduced model 272
Figure 8.90a: The dynamic behaviour of oxygen at h2 for ASM1 full model 272
Figure 8.90b: The dynamic behaviour of oxygen at h2 for ASM1 reduced model 272
Figure 8.91a: The dynamic behaviour of nitrate nitrogen at h2 for ASM1 full model 273
Figure 8.91b: The dynamic behaviour of nitrate nitrogen at h2 for ASM1 reduced model 273
Figure 8.92a: The dynamic behaviour of ammonia nitrogen at h2 for ASM1 full model 273
Figure 8.92b: The dynamic behaviour of ammonia nitrogen at h2 for ASM1 reduced model 273
Figure 8.93a: The dynamic behaviour of biodegradable soluble organic nitrogen at h2 for ASM1 full model 273
Figure 8.93b: The dynamic behaviour of biodegradable soluble organic nitrogen at h2 for ASM1 reduced model 273
Figure 8.94a: The dynamic behaviour of biodegradable particulate organic nitrogen fraction at h2 for ASM1 full model 274
Figure 8.94b: The dynamic behaviour of biodegradable particulate organic nitrogen fraction at h2 for ASM1 reduced model 274
Figure 8.95a: The dynamic behaviour of alkalinity at h2 for ASM1 full model 274

Figure 8.95b: The dynamic behaviour of alkalinity at h2 for ASM1 reduced model 274
Figure 8.96a: The dynamic behaviour of flow rate at h2 for ASM1 full model 274
Figure 8.96b: The dynamic behaviour of flow rate at h2 for ASM1 reduced model 274
Figure 8.97a: The dynamic behaviour of chemical oxygen demand at h2 for ASM1 full model 275
Figure 8.97b: The dynamic behaviour of chemical oxygen demand at h2 for ASM1 reduced model 275
Figure 8.98a: The dynamic behaviour of nitrogen at h2 for ASM1 full model 275
Figure 8.98b: The dynamic behaviour of nitrogen at h2 for ASM1 reduced model 275
Figure 8.99a: The dynamic behaviour of total Kjeldahl nitrogen at h2 for ASM1 full model 275
Figure 8.99b: The dynamic behaviour of total Kjeldahl nitrogen at h2 for ASM1 reduced model 275
Figure 8.100a: The dynamic behaviour of unbiodegradable soluble substrate at h3 for ASM1 full model 276
Figure 8.100b: The dynamic behaviour of unbiodegradable soluble substrate at h3 for ASM1 reduced model 276
Figure 8.101a: The dynamic behaviour of readily biodegradable (soluble) substrate fraction at h3 for ASM1 full model 276
Figure 8.101b: The dynamic behaviour of readily biodegradable (soluble) substrate fraction at h3 for ASM1 reduced model 276
Figure 8.102a: The dynamic behaviour of inert mass fraction at h3 for ASM1 full model 277
Figure 8.102b: The dynamic behaviour of inert mass fraction at h3 for ASM1 reduced model 277
Figure 8.103a: The dynamic behaviour of enmeshed slowly biodegradable substrate fraction at h3 for ASM1 full model 277
Figure 8.103b: The dynamic behaviour of enmeshed slowly biodegradable substrate fraction at h3 for ASM1 reduced model 277
Figure 8.104a: The dynamic behaviour of biological (active) heterotrophic mass fraction at h3 for ASM1 full model 277
Figure 8.104b: The dynamic behaviour of biological (active) heterotrophic mass fraction at h3 for ASM1 reduced model 277
Figure 8.105a: The dynamic behaviour of biological (active) autotrophic biomass fraction at h3 for ASM1 full model 278
Figure 8.105b: The dynamic behaviour of biological (active) autotrophic biomass fraction at h3 for ASM1 reduced model 278
Figure 8.106a: The dynamic behaviour of endogenous mass fraction at h3 for ASM1 full model 278
Figure 8.106b: The dynamic behaviour of endogenous mass fraction at h3 for ASM1 reduced model 278
Figure 8.107a: The dynamic behaviour of oxygen at h3 for ASM1 full model 278
Figure 8.107b: The dynamic behaviour of oxygen at h3 for ASM1 reduced model 278
Figure 8.108a: The dynamic behaviour of nitrate nitrogen at h3 for ASM1 full model 279
Figure 8.108b: The dynamic behaviour of nitrate nitrogen at h3 for ASM1 reduced model 279
Figure 8.109a: The dynamic behaviour of ammonia nitrogen at h3 for ASM1 full model 279
Figure 8.109b: The dynamic behaviour of ammonia nitrogen at h3 for ASM1 reduced model 279
Figure 8.110a: The dynamic behaviour of biodegradable soluble organic nitrogen at h3 for ASM1 full model 279
Figure 8.110b: The dynamic behaviour of biodegradable soluble organic nitrogen at h3 for ASM1 reduced model 279

Figure 8.111a: The dynamic behaviour of biodegradable particulate organic nitrogen fraction at h3 for ASM1 full model 280
Figure 8.111b: The dynamic behaviour of biodegradable particulate organic nitrogen fraction at h3 for ASM1 reduced model 280
Figure 8.112a: The dynamic behaviour of alkalinity at h3 for ASM1 full model 280
Figure 8.112b: The dynamic behaviour of alkalinity at h3 for ASM1 reduced model 280
Figure 8.113a: The dynamic behaviour of flow rate at h3 for ASM1 full model 280
Figure 8.113b: The dynamic behaviour of flow rate at h3 for ASM1 reduced model 280
Figure 8.114a: The dynamic behaviour of chemical oxygen demand at h3 for ASM1 full model 281
Figure 8.114b: The dynamic behaviour of chemical oxygen demand at h3 for ASM1 reduced model 281
Figure 8.115a: The dynamic behaviour of nitrogen at h3 for ASM1 full model 281
Figure 8.115b: The dynamic behaviour of nitrogen at h3 for ASM1 reduced model 281
Figure 8.116a: The dynamic behaviour of total Kjeldahl nitrogen at h3 for ASM1 full model 281
Figure 8.116b: The dynamic behaviour of total Kjeldahl nitrogen at h3 for ASM1 reduced model 281
Figure 8.117a: The dynamic behaviour of unbiodegradable soluble substrate at h4 for ASM1 full model 282
Figure 8.117b: The dynamic behaviour of unbiodegradable soluble substrate at h4 for ASM1 reduced model 282
Figure 8.118a: The dynamic behaviour of readily biodegradable (soluble) substrate fraction at h4 for ASM1 full model 282
Figure 8.118b: The dynamic behaviour of readily biodegradable (soluble) substrate fraction at h4 for ASM1 reduced model 282
Figure 8.119a: The dynamic behaviour of inert mass fraction at h4 for ASM1 full model 283
Figure 8.119b: The dynamic behaviour of inert mass fraction at h4 for ASM1 reduced model 283
Figure 8.120a: The dynamic behaviour of enmeshed slowly biodegradable substrate fraction at h4 for ASM1 full model 283
Figure 8.120b: The dynamic behaviour of enmeshed slowly biodegradable substrate fraction at h4 for ASM1 reduced model 283
Figure 8.121a: The dynamic behaviour of biological (active) heterotrophic mass fraction at h4 for ASM1 full model 283
Figure 8.121b: The dynamic behaviour of biological (active) heterotrophic mass fraction at h4 for ASM1 reduced model 283
Figure 8.122a: The dynamic behaviour of biological (active) autotrophic mass fraction at h4 for ASM1 full model 284
Figure 8.122b: The dynamic behaviour of biological (active) autotrophic mass fraction at h4 for ASM1 reduced model 284
Figure 8.123a: The dynamic behaviour of endogenous mass fraction at h4 for ASM1 full model 284
Figure 8.123b: The dynamic behaviour of endogenous mass fraction at h4 for ASM1 reduced model 284
Figure 8.124a: The dynamic behaviour of oxygen at h4 for ASM1 full model 284
Figure 8.124b: The dynamic behaviour of oxygen at h4 for ASM1 reduced model 284
Figure 8.125a: The dynamic behaviour of nitrate nitrogen at h4 for ASM1 full model 285
Figure 8.125b: The dynamic behaviour of nitrate nitrogen at h4 for ASM1 reduced model 285
Figure 8.126a: The dynamic behaviour of ammonia nitrogen at h4 for ASM1 full model 285
Figure 8.126b: The dynamic behaviour of ammonia nitrogen at h4 for ASM1 reduced model 285

Figure 8.127a: The dynamic behaviour of biodegradable soluble organic nitrogen at h4 for ASM1 full model 285
Figure 8.127b: The dynamic behaviour of biodegradable soluble organic nitrogen at h4 for ASM1 reduced model 285
Figure 8.128a: The dynamic behaviour of biodegradable particulate organic nitrogen fraction at h4 for ASM1 full model 286
Figure 8.128b: The dynamic behaviour of biodegradable particulate organic nitrogen fraction at h4 for ASM1 reduced model 286
Figure 8.129a: The dynamic behaviour of alkalinity at h4 for ASM1 full model 286
Figure 8.129b: The dynamic behaviour of alkalinity at h4 for ASM1 reduced model 286
Figure 8.130a: The dynamic behaviour of flow rate at h4 for ASM1 full model 286
Figure 8.130b: The dynamic behaviour of flow rate at h4 for ASM1 reduced model 286
Figure 8.131a: The dynamic behaviour of chemical oxygen demand at h4 for ASM1 full model 287
Figure 8.131b: The dynamic behaviour of chemical oxygen demand at h4 for ASM1 reduced model 287
Figure 8.132a: The dynamic behaviour of nitrogen at h4 for ASM1 full model 287
Figure 8.132b: The dynamic behaviour of nitrogen at h4 for ASM1 reduced model 287
Figure 8.133a: The dynamic behaviour of total Kjeldahl nitrogen at h4 for ASM1 full model 287
Figure 8.133b: The dynamic behaviour of total Kjeldahl nitrogen at h4 for ASM1 reduced model 287
Figure 8.134a: The dynamic behaviour of biological (active) heterotrophic mass fraction at h1 for Athlone plant UCT full model 290
Figure 8.134b: The dynamic behaviour of biological (active) heterotrophic mass fraction at h1 for Athlone plant UCT reduced model 290
Figure 8.135a: The dynamic behaviour of biological (active) autotrophic biomass fraction at h1 for Athlone plant UCT full model 290
Figure 8.135b: The dynamic behaviour of biological (active) autotrophic biomass fraction at h1 for Athlone plant UCT reduced model 290
Figure 8.136a: The dynamic behaviour of endogenous mass fraction at h1 for Athlone plant UCT full model 290
Figure 8.136b: The dynamic behaviour of endogenous mass fraction at h1 for Athlone plant UCT reduced model 290
Figure 8.137a: The dynamic behaviour of inert mass fraction at h1 for Athlone plant UCT full model 291
Figure 8.137b: The dynamic behaviour of inert mass fraction at h1 for Athlone plant UCT reduced model 291
Figure 8.138a: The dynamic behaviour of adsorbed slowly biodegradable substrate fraction at h1 for Athlone plant UCT full model 291
Figure 8.138b: The dynamic behaviour of adsorbed slowly biodegradable substrate fraction at h1 for Athlone plant UCT reduced model 291
Figure 8.139a: The dynamic behaviour of enmeshed slowly biodegradable substrate fraction at h1 for Athlone plant UCT full model 291
Figure 8.139b: The dynamic behaviour of enmeshed slowly biodegradable substrate fraction at h1 for Athlone plant UCT reduced model 291
Figure 8.140a: The dynamic behaviour of biodegradable particulate organic nitrogen fraction at h1 for Athlone plant UCT full model 292
Figure 8.140b: The dynamic behaviour of biodegradable particulate organic nitrogen fraction at h1 for Athlone plant UCT reduced model 292
Figure 8.141a: The dynamic behaviour of readily biodegradable (soluble) substrate fraction at h1 for Athlone plant UCT full model 292
Figure 8.141b: The dynamic behaviour of readily biodegradable (soluble) substrate fraction at h1 for Athlone plant UCT reduced model 292
Figure 8.142a: The dynamic behaviour of ammonia nitrogen at h1 for Athlone plant 292

UCT full model
Figure 8.142b: The dynamic behaviour of ammonia nitrogen fraction at h1 for Athlone plant UCT reduced model 292
Figure 8.143a: The dynamic behaviour of biodegradable soluble organic nitrogen fraction at h1 for Athlone plant UCT full model 293
Figure 8.143b: The dynamic behaviour of biodegradable soluble organic nitrogen fraction at h1 for Athlone plant UCT reduced model 293
Figure 8.144a: The dynamic behaviour of nitrate nitrogen fraction at h1 for Athlone plant UCT full model 293
Figure 8.144b: The dynamic behaviour of nitrate nitrogen fraction at h1 for Athlone plant UCT reduced model 293
Figure 8.145a: The dynamic behaviour of alkalinity at h1 for Athlone plant UCT full model 293
Figure 8.145b: The dynamic behaviour of alkalinity at h1 for Athlone plant UCT reduced model 293
Figure 8.146a: The dynamic behaviour of unbiodegradable soluble substrate at h1 for Athlone plant UCT full model 294
Figure 8.146b: The dynamic behaviour of unbiodegradable soluble substrate fraction at h1 for Athlone plant UCT reduced model 294
Figure 8.147a: The dynamic behaviour of oxygen at h1 for Athlone plant UCT full model 294
Figure 8.147b: The dynamic behaviour of oxygen at h1 for Athlone plant UCT reduced model 294
Figure 8.148a: The dynamic behaviour of flow rate at h1 for Athlone plant UCT full model 294
Figure 8.148b: The dynamic behaviour of flow rate at h1 for Athlone plant UCT reduced model 294
Figure 8.149a: The dynamic behaviour of biological (active) heterotrophic mass fraction at h2 for Athlone plant UCT full model 295
Figure 8.149b: The dynamic behaviour of biological (active) heterotrophic mass fraction at h2 for Athlone plant UCT reduced model 295
Figure 8.150a: The dynamic behaviour of biological (active) autotrophic biomass fraction at h2 for Athlone plant UCT full model 295
Figure 8.150b: The dynamic behaviour of biological (active) autotrophic biomass fraction at h2 for Athlone plant UCT reduced model 295
Figure 8.151a: The dynamic behaviour of endogenous mass fraction at h2 for Athlone plant UCT full model 296
Figure 8.151b: The dynamic behaviour of endogenous mass fraction at h2 for Athlone plant UCT reduced model 296
Figure 8.152a: The dynamic behaviour of inert mass fraction at h2 for Athlone plant UCT full model 296
Figure 8.152b: The dynamic behaviour of inert mass fraction at h2 for Athlone plant UCT reduced model 296
Figure 8.153a: The dynamic behaviour of adsorbed slowly biodegradable substrate fraction at h2 for Athlone plant UCT full model 296
Figure 8.153b: The dynamic behaviour of adsorbed slowly biodegradable substrate fraction at h2 for Athlone plant UCT reduced model 296
Figure 8.154a: The dynamic behaviour of enmeshed slowly biodegradable substrate fraction at h2 for Athlone plant UCT full model 297
Figure 8.154b: The dynamic behaviour of enmeshed slowly biodegradable substrate fraction at h2 for Athlone plant UCT reduced model 297
Figure 8.155a: The dynamic behaviour of biodegradable particulate organic nitrogen fraction at h2 for Athlone plant UCT full model 297
Figure 8.155b: The dynamic behaviour of biodegradable particulate organic nitrogen fraction at h2 for Athlone plant UCT reduced model 297
Figure 8.156a: The dynamic behaviour of readily biodegradable (soluble) substrate 297

fraction at h2 for Athlone plant UCT full model
Figure 8.156b: The dynamic behaviour of readily biodegradable (soluble) substrate fraction at h2 for Athlone plant UCT reduced model 297
Figure 8.157a: The dynamic behaviour of ammonia nitrogen fraction at h2 for Athlone plant UCT full model 298
Figure 8.157b: The dynamic behaviour of ammonia nitrogen fraction at h2 for Athlone plant UCT reduced model 298
Figure 8.158a: The dynamic behaviour of biodegradable soluble organic nitrogen fraction at h2 for Athlone plant UCT full model 298
Figure 8.158b: The dynamic behaviour of biodegradable soluble organic nitrogen fraction at h2 for Athlone plant UCT reduced model 298
Figure 8.159a: The dynamic behaviour of nitrate nitrogen fraction at h2 for Athlone plant UCT full model 298
Figure 8.159b: The dynamic behaviour of nitrate nitrogen fraction at h2 for Athlone plant UCT reduced model 298
Figure 8.160a: The dynamic behaviour of alkalinity at h2 for Athlone plant UCT full model 299
Figure 8.160b: The dynamic behaviour of alkalinity at h2 for Athlone plant UCT reduced model 299
Figure 8.161a: The dynamic behaviour of unbiodegradable soluble substrate at h2 for Athlone plant UCT full model 299
Figure 8.161b: The dynamic behaviour of unbiodegradable soluble substrate fraction at h2 for Athlone plant UCT reduced model 299
Figure 8.162a: The dynamic behaviour of oxygen at h2 for Athlone plant UCT full model 299
Figure 8.162b: The dynamic behaviour of oxygen at h2 for Athlone plant UCT reduced model 299
Figure 8.163a: The dynamic behaviour of flow rate at h2 for Athlone plant UCT full model 300
Figure 8.163b: The dynamic behaviour of flow rate at h2 for Athlone plant UCT reduced model 300
Figure 8.164a: The dynamic behaviour of biological (active) heterotrophic mass fraction at h3 for Athlone plant UCT full model 300
Figure 8.164b: The dynamic behaviour of biological (active) heterotrophic mass fraction at h3 for Athlone plant UCT reduced model 300
Figure 8.165a: The dynamic behaviour of biological (active) autotrophic biomass fraction at h3 for Athlone plant UCT full model 301
Figure 8.165b: The dynamic behaviour of biological (active) autotrophic biomass fraction at h3 for Athlone plant UCT reduced model 301
Figure 8.166a: The dynamic behaviour of endogenous mass fraction at h3 for Athlone plant UCT full model 301
Figure 8.166b: The dynamic behaviour of endogenous mass fraction at h3 for Athlone plant UCT reduced model 301
Figure 8.167a: The dynamic behaviour of inert mass fraction at h3 for Athlone plant UCT full model 301
Figure 8.167b: The dynamic behaviour of inert mass fraction at h3 for Athlone plant UCT reduced model 301
Figure 8.168a: The dynamic behaviour of adsorbed slowly biodegradable substrate fraction at h3 for Athlone plant UCT full model 302
Figure 8.168b: The dynamic behaviour of adsorbed slowly biodegradable substrate fraction at h3 for Athlone plant UCT reduced model 302
Figure 8.169a: The dynamic behaviour of enmeshed slowly biodegradable substrate fraction at h3 for Athlone plant UCT full model 302
Figure 8.169b: The dynamic behaviour of enmeshed slowly biodegradable substrate fraction at h3 for Athlone plant UCT reduced model 302
Figure 8.170a: The dynamic behaviour of biodegradable particulate organic nitrogen 302

fraction at h3 for Athlone plant UCT full model
Figure 8.170b: The dynamic behaviour of biodegradable particulate organic nitrogen fraction at h3 for Athlone plant UCT reduced model 302
Figure 8.171a: The dynamic behaviour of readily biodegradable (soluble) substrate fraction at h3 for Athlone plant UCT full model 303
Figure 8.171b: The dynamic behaviour of readily biodegradable (soluble) substrate fraction at h3 for Athlone plant UCT reduced model 303
Figure 8.172a: The dynamic behaviour of ammonia nitrogen at h3 for Athlone plant UCT full model 303
Figure 8.172b: The dynamic behaviour of ammonia nitrogen fraction at h3 for Athlone plant UCT reduced model 303
Figure 8.173a: The dynamic behaviour of biodegradable soluble organic nitrogen at h3 for Athlone plant UCT full model 303
Figure 8.173b: The dynamic behaviour of biodegradable soluble organic nitrogen fraction at h3 for Athlone plant UCT reduced model 303
Figure 8.174a: The dynamic behaviour of nitrate nitrogen fraction at h3 for Athlone plant UCT full model 304
Figure 8.174b: The dynamic behaviour of nitrate nitrogen fraction at h3 for Athlone plant UCT reduced model 304
Figure 8.175a: The dynamic behaviour of alkalinity at h3 for Athlone plant UCT full model 304
Figure 8.175b: The dynamic behaviour of alkalinity at h3 for Athlone plant UCT reduced model 304
Figure 8.176a: The dynamic behaviour of unbiodegradable soluble substrate at h3 for Athlone plant UCT full model 304
Figure 8.176b: The dynamic behaviour of unbiodegradable soluble substrate fraction at h3 for Athlone plant UCT reduced model 304
Figure 8.177a: The dynamic behaviour of oxygen at h3 for Athlone plant UCT full model 305
Figure 8.177b: The dynamic behaviour of oxygen at h3 for Athlone plant UCT reduced model 305
Figure 8.178a: The dynamic behaviour of biological (active) heterotrophic mass fraction at h4 for Athlone plant UCT full model 305
Figure 8.178b: The dynamic behaviour of biological (active) heterotrophic mass fraction at h4 for Athlone plant UCT reduced model 305
Figure 8.179a: The dynamic behaviour of biological (active) autotrophic biomass fraction at h4 for Athlone plant UCT full model 306
Figure 8.179b: The dynamic behaviour of biological (active) autotrophic biomass fraction at h4 for Athlone plant UCT reduced model 306
Figure 8.180a: The dynamic behaviour of endogenous mass fraction at h4 for Athlone plant UCT full model 306
Figure 8.180b: The dynamic behaviour of endogenous mass fraction at h4 for Athlone plant UCT reduced model 306
Figure 8.181a: The dynamic behaviour of inert mass fraction at h4 for Athlone plant UCT full model 306
Figure 8.181b: The dynamic behaviour of inert mass fraction at h4 for Athlone plant UCT reduced model 306
Figure 8.182a: The dynamic behaviour of adsorbed slowly biodegradable substrate fraction at h4 for Athlone plant UCT full model 307
Figure 8.182b: The dynamic behaviour of adsorbed slowly biodegradable substrate fraction at h4 for Athlone plant UCT reduced model 307
Figure 8.183a: The dynamic behaviour of enmeshed slowly biodegradable substrate fraction at h4 for Athlone plant UCT full model 307
Figure 8.183b: The dynamic behaviour of enmeshed slowly biodegradable substrate fraction at h4 for Athlone plant UCT reduced model 307
Figure 8.184a: The dynamic behaviour of biodegradable particulate organic nitrogen 307

fraction at h4 for Athlone plant UCT full model
Figure 8.184b: The dynamic behaviour of biodegradable particulate organic nitrogen fraction at h4 for Athlone plant UCT reduced model 307
Figure 8.185a: The dynamic behaviour of readily biodegradable (soluble) substrate fraction at h4 for Athlone plant UCT full model 308
Figure 8.185b: The dynamic behaviour of readily biodegradable (soluble) substrate fraction at h4 for Athlone plant UCT reduced model 308
Figure 8.186a: The dynamic behaviour of ammonia nitrogen fraction at h4 for Athlone plant UCT full model 308
Figure 8.186b: The dynamic behaviour of ammonia nitrogen fraction at h4 for Athlone plant UCT reduced model 308
Figure 8.187a: The dynamic behaviour of biodegradable soluble organic nitrogen at h4 for Athlone plant UCT full model 308
Figure 8.187b: The dynamic behaviour of biodegradable soluble organic nitrogen fraction at h4 for Athlone plant UCT reduced model 308
Figure 8.188a: The dynamic behaviour of nitrate nitrogen fraction at h4 for Athlone plant UCT full model 309
Figure 8.188b: The dynamic behaviour of nitrate nitrogen fraction at h4 for Athlone plant UCT reduced model 309
Figure 8.189a: The dynamic behaviour of alkalinity at h4 for Athlone plant UCT full model 309
Figure 8.189b: The dynamic behaviour of alkalinity at h4 for Athlone plant UCT reduced model 309
Figure 8.190a: The dynamic behaviour of unbiodegradable soluble substrate fraction at h4 for Athlone plant UCT full model 309
Figure 8.190b: The dynamic behaviour of unbiodegradable soluble substrate fraction at h4 for Athlone plant UCT reduced model 309
Figure 8.191a: The dynamic behaviour of oxygen at h4 for Athlone plant UCT full model 310
Figure 8.191b: The dynamic behaviour of oxygen at h4 for Athlone plant UCT reduced model 310
Figure 8.192a: The dynamic behaviour of flow rate at h4 for Athlone plant UCT full model 310
Figure 8.192b: The dynamic behaviour of flow rate at h4 for Athlone plant UCT reduced model 310
Figure 9.1a: Flow chart of the main program for sensitivity functions calculation 317
Figure 9.1b: Flow chart of the subprogram for sensitivity functions calculation 317
Figure 9.2: Process variable S_{NH1} and its sensitivity functions towards the model parameters 319
Figure 9.3: Process variable S_{NH2} and its sensitivity functions towards the model parameters 320
Figure 9.4: Process variable S_{NH3} and its sensitivity functions towards the model parameters 321
Figure 9.5: Process variable S_{NH4} and its sensitivity functions towards the model parameters 322
Figure 9.6: Process variable S_{NH5} and its sensitivity functions towards the model parameters 323
Figure 9.7: Process variable S_{NO1} and its sensitivity functions towards the model parameters 324
Figure 9.8: Process variable S_{NO2} and its sensitivity functions towards the model parameters 325
Figure 9.9: Process variable S_{NO3} and its sensitivity functions towards the model parameters 326
Figure 9.10: Process variable S_{NO4} and its sensitivity functions towards the model parameters 327
Figure 9.11: Process variable S_{NO5} and its sensitivity functions towards the model 328

parameters
Figure 9.12: Process variable S_{S1} and its sensitivity functions towards the model parameters 329
Figure 9.13: Process variable S_{S2} and its sensitivity functions towards the model parameters 330
Figure 9.14: Process variable S_{S3} and its sensitivity functions towards the model parameters 331
Figure 9.15: Process variable S_{S4} and its sensitivity functions towards the model parameters 332
Figure 9.16: Process variable S_{S5} and its sensitivity functions towards the model parameters 333
Figure 9.17: Process variable S_{NH1} and its sensitivity functions towards the model parameters 335
Figure 9.18: Process variable S_{NH2} and its sensitivity functions towards the model parameters 336
Figure 9.19: Process variable S_{NH3} and its sensitivity functions towards the model parameters 337
Figure 9.20: Process variable S_{NH4} and its sensitivity functions towards the model parameters 338
Figure 9.21: Process variable S_{NH5} and its sensitivity functions towards the model parameters 339
Figure 9.22: Process variable S_{NO1} and its sensitivity functions towards the model parameters 340
Figure 9.23: Process variable S_{NO2} and its sensitivity functions towards the model parameters 341
Figure 9.24: Process variable S_{NO3} and its sensitivity functions towards the model parameters 342
Figure 9.25: Process variable S_{NO4} and its sensitivity functions towards the model parameters 343
Figure 9.26: Process variable S_{NO5} and its sensitivity functions towards the model parameters 344
Figure 9.27: Process variable S_{S1} and its sensitivity functions towards the model parameters 345
Figure 9.28: Process variable S_{S2} and its sensitivity functions towards the model parameters 346
Figure 9.29: Process variable S_{S3} and its sensitivity functions towards the model parameters 347
Figure 9.30: Process variable S_{S4} and its sensitivity functions towards the model parameters 348
Figure 9.31: Process variable S_{S5} and its sensitivity functions towards the model parameters 349
Figure 9.32: Process variable S_{Sads1} and its sensitivity functions towards the model parameters 350
Figure 9.33: Process variable S_{Sads2} and its sensitivity functions towards the model parameters 351
Figure 9.34: Process variable S_{Sads3} and its sensitivity functions towards the model parameters 352
Figure 9.35: Process variable S_{Sads4} and its sensitivity functions towards the model parameters 353
Figure 9.36: Process variable S_{Sads5} and its sensitivity functions towards the model parameters 354
Figure 9.37: Process variable S_{SNH1} and its sensitivity functions towards the model parameters 358
Figure 9.38: Process variable S_{SNH2} and its sensitivity functions towards the model parameters 359
Figure 9.39: Process variable S_{SNH3} and its sensitivity functions towards the model 360

parameters
Figure 9.40: Process variable S_{SNO1} and its sensitivity functions towards the model parameters 361
Figure 9.41: Process variable S_{SNO2} and its sensitivity functions towards the model parameters 362
Figure 9.42: Process variable S_{SNO3} and its sensitivity functions towards the model parameters 363
Figure 9.43: Process variable S_{SS1} and its sensitivity functions towards the model parameters 364
Figure 9.44: Process variable S_{SS2} and its sensitivity functions towards the model parameters 365
Figure 9.45: Process variable S_{SS3} and its sensitivity functions towards the model parameters 366
Figure 9.46: Process variable S_{SNH1} and its sensitivity functions towards the model parameters 368
Figure 9.47: Process variable S_{SNH2} and its sensitivity functions towards the model parameters 369
Figure 9.48: Process variable S_{SNH3} and its sensitivity functions towards the model parameters 370
Figure 9.49: Process variable S_{SNO1} and its sensitivity functions towards the model parameters 371
Figure 9.50: Process variable S_{SNO2} and its sensitivity functions towards the model parameters 372
Figure 9.51: Process variable S_{SNO3} and its sensitivity functions towards the model parameters 373
Figure 9.52: Process variable S_{SS1} and its sensitivity functions towards the model parameters 374
Figure 9.53: Process variable S_{SS2} and its sensitivity functions towards the model parameters 375
Figure 9.54: Process variable S_{SS3} and its sensitivity functions towards the model parameters 376
Figure 9.55: Process variable S_{Sads1} and its sensitivity functions towards the model parameters 377
Figure 9.56: Process variable S_{Sads2} and its sensitivity functions towards the model parameters 378
Figure 9.57: Process variable S_{Sads3} and its sensitivity functions towards the model parameters 379
Figure 9.58a: Flow chart of the main program for sensitivity functions 384
Figure 9.58b: Flow chart of the subprogram for sensitivity functions 384
Figure 9.59: Trajectories of the reduced ASM1 biological model parameters for the Benchmark process 387
Figure 9.60: Trajectories of the ASM1 full (solid line), reduced estimated (dashed line) and the error between them as applied for the Benchmark process for the process variable SNH 388
Figure 9.61: Trajectories of the ASM1 full (solid line), reduced estimated (dashed line) and the error between them as applied for the Benchmark process for the process variable SNO 389
Figure 9.62: Trajectories of the ASM1 full (solid line), reduced estimated (dashed line) and the error between them as applied for the Benchmark process for the process variable SS 390
Figure 9.63: Trajectories of the reduced ASM1 biological model parameters for the Athlone process 392
Figure 9.64: Trajectories of the ASM1 full (solid line), reduced estimated (dashed line) and the error between them as applied for the Athlone process for the process variable SNH 393
Figure 9.65: Trajectories of the ASM1 full (solid line), reduced estimated (dashed 394

line) and the error between them as applied for the Athlone process for the process variable SNO
Figure 9.66: Trajectories of the ASM1 full (solid line), reduced estimated (dashed line) and the error between them as applied for the Athlone process for the process variable SS 395
Figure 9.67: Trajectories of the reduced UCT biological model parameters for the Benchmark process 399
Figure 9.68: Trajectories of the UCT full (solid line), reduced estimated (dashed line) and the error between them as applied for the Benchmark process for the process variable SNH 400
Figure 9.69: Trajectories of the UCT full (solid line), reduced estimated (dashed line) and the error between them as applied for the Benchmark process for the process variable SNO 401
Figure 9.70: Trajectories of the UCT full (solid line), reduced estimated (dashed line) and the error between them as applied for the Benchmark process for the process variable SS 402
Figure 9.71: Trajectories of the UCT full (solid line), reduced estimated (dashed line) and the error between them as applied for the Benchmark process for the process variable XSA 403

LIST OF TABLES

Table 3.1: Biological fractions, descriptions and units of the UCT model 39
Table 3.2: Peterson Matrix representation of the UCT model 41
Table 3.3: Switching functions and formulae of the UCT biological model 42
Table 3.4: Default values for kinetic, stoichiometric and switching function constants in the UCT model 43
Table 3.5: ASM1 Peterson Matrix Model 52
Table 3.6: Typical parameter values at neutral pH 55
Table 3.7: Benchmark plant specifications 60
Table 3.8: Plant specifications of Mitchell's Plain 63
Table 3.9: Athlone plant specifications 65
Table 4.1: The reduced ASM1 biological model in matrix format 77
Table 4.2: ASM1 process parameters with their common values 78
Table 4.3: The reduced UCT biological model in matrix format 79
Table 4.4: The nominal parameters of the UCT biological model 80
Table 4.5: Reduced UCT process parameters with their common values 81
Table 4.6 : Dimensions of the matrices and vectors of the derived reduced models 97
Table 8.1: A Comparative Analysis of the existing Simulators 238
Table 8.2: The fractions of Activated Sludge Model UCT process biological model 241
Table 8.3: User defined fraction properties 242
Table 8.4: User defined fraction properties values 242
Table 8.5: External inputs (EI) and instrumental variables (IV) 242
Table 8.6: The values and units of the Parameters of the UCT biological model 243
Table 8.7: Peterson matrix for the full ASM1 model 245
Table 8.8: Peterson matrix of the reduced ASM1 model 245
Table 8.9: The Peterson matrix of the full UCT model 246
Table 8.10: COD-Balance (COD content of unit) for the full UCT model 246
Table 8.11: N-Balance (N content of unit) for the full UCT model 247
Table 8.12: Peterson matrix for the reduced UCT model 247
Table 8.13: Stoichiometry of the UCT reduced model 248

Table 8.14: COD-Balance (COD content of unit) of UCT reduced model 248
Table 8.15: N-Balance (N content of unit) of the UCT reduced model 249
Table 9.1: The maximum or minimum values of sensitivity functions simulation for the Benchmark process model based on the reduced ASM1 biological model 355
Table 9.2: The maximum or minimum values of sensitivity function simulation for the Benchmark process model based on the reduced UCT biological model 356
Table 9.3: The maximum or minimum values of sensitivity function simulation for the Athlone process model based on the reduced ASM1 biological model 380
Table 9.4: The maximum or minimum values of sensitivity function simulation for the Athlone process model based on the reduced UCT biological model 381
Table 9.5: The obtained weighted errors of reduced ASM1 model parameter estimation used for the Benchmark process mass balance models 396
Table 9.6: The obtained weighted errors of reduced ASM1 model parameter estimation used for the Athlone process mass balance models 396
Table 9.7: The obtained weighted errors of reduced UCT model parameter estimation used for the Benchmark process mass balance models 404

Appendices	
APPENDIX A: CALCULATION OF THE INFLUENT OF THE UCT MODEL	436
APPENDIX B: SET THE BIOLOGICAL PARAMETERS FOR UCT MODEL	439
APPENDIX C : BENCHMARK AND ATHLONE PROCESSES WITH ASM1 AND UCT REDUCED BIOLOGICAL MODELS FOR SENSITIVITY STUDIES	441
APPENDIX D: SOFTWARE FOR SIMULATION OF SENSITIVITY FUNCTIONS OF THE PROCESS VARIABLES OF THE BENCHMARK AND ATHLONE MASS BALANCES MODEL BASED ON THE REDUCED ASM1 AND UCT BIOLOGICAL MODELS TOWARDS ITS PARAMETERS	474
APPENDIX E: REDUCED ASM1 AND UCT MODEL PARAMETER ESTIMATION USED FOR THE BENCHMARK AND ATHLONE PROCESS MASS BALANCE MODELS	532
APPENDIX F: SOFTWARE FOR PARAMETER ESTIMATION OF THE BENCHMARK MASS BALANCES MODEL FOR THE CASE OF ASM1 AND UCT REDUCED MODELS	538

GLOSSARY

Terms/Acronyms/Abbreviations	Definition/Explanation
activated sludge process	**Treatment efficiency** is normally used to describe The overall efficiency of the treatment process, that is both an activated sludge pond and a settling tank. **Sludge concentration** (biomass concentration), χ, in wastewater in the aeration tank or in the flow of recycle sludge is often given in the unit suspended solids, χ_{SS}, volatile solids, χ_{VSS}, or as COD, χ_{COD}. **Sludge mass,** M_{χ}, in an activated sludge plant comprises any sludge in the part of the treatment plant handling activated sludge, including the sludge which is not currently being aerated in the activated sludge pond. **Sludge loading** states the amount of organic matter applied to the sludge per day.
adaptive	Model that interacts with the real system and changes the values of its inputs or state variables depending on past output values.
aggregated	Model that contains state variables that represent functional classes of different constituents (e.g. organisms) or that simplifies that spatial configuration of a system by lumping it together (cf. segregated).
black-box	Model that describes the observed behaviour of the corresponding subsystem without being based on the mechanisms of this subsystem (cf. white-box).
complex	A relative attribute that values whether the model contains more state variables, parameters, forcing functions, etc. or an attribute that qualifies that (irrespective of the number of the variables) there exists chaotic solutions of the model equations (cf. simple).
continuous time	The model resolves the time axis continuously; the time evolution is usually described by differential equations (cf. discrete time).
deterministic	The time evolution of the model solution is uniquely determined by the initial state (for state-space

	models) and the time evolution of inputs (cf. stochastic).
discrete time	The model divides the time axis into periods of finite length and the output or the state of the model in the next period is given as an algebraic equation depending on the old inputs or states (cf. continuous time).
distributed parameter	Model with more than one independent variable, i.e. model behaviour is governed by partial differential equation in time and space.
dynamic	The model describes the time evolution of a system; a solution of the model may anyway be in steady-state (cf. static, steady-state).
empirical	The model equations are not based on generally accepted laws but are just of a descriptive nature (cf. mechanistic).
input/output model	Model that describes system behaviour as being a function of only present input and past inputs and outputs.
linear	Model equations are linear in input variables (for input-output models) or in state variables (for state-space models).
lumped	Equal to aggregated.
nonlinear	Model equations are nonlinear in input variables (for input-output models) or in input and state variables (for state-space models).
parameter	Model constituent, whose value needs to be determined for each specific application of the model.
parameter estimation	Process of finding parameter values that lead to an optimal agreement of model results with measured data by using statistical methods. Time series of data can be used as a whole (batch estimation) or data points from within a moving data window can be used. In the latter the parameters become time-dependent and algorithm can be implemented to modify the previous estimate by considering the omitted and new data points (recursive estimation).

reduced order	Model of reduced complexity obtained by direct deduction (e.g. by aggregation/lumping).
reductionist	Hierarchical description of a system by resolving it in subsystems that again are resolved in sub-subsystems until a description level is reached at which a satisfying description is possible without empirical assumptions (in the ideal case down to a description that is based on natural laws).
static	The model describes the steady-state of the solution of a system (cf. dynamic).
stochastic	The time evolution of the model contains random elements (cf. deterministic).
validation	Test of a model with a data set not used for identification; note that such tests only increase the belief in the correctness of the model, it is not possible to prove that the model is correct (cf. verification).
verification	The same as validation (cf. validation).
$p(\boldsymbol{\theta})$	Probability density
$p(\mathbf{y}_{meas} \mid \boldsymbol{\theta})$	Conditional probability density
$L(\mathbf{y}_{meas} \mid \boldsymbol{\theta})$	Likelihood function
$y_i(\boldsymbol{\theta})$	Calculated value of the model
$\sigma_{meas,i}$	Standard deviation of $y_{meas,i}$.
$y(t)$	Observed variable
$\{\theta_1, \theta_2, ..., \theta_n\}$	A set of constant parameters
$x_1(t), x_2(t), ..., x_n(t)$	Known functions
N	Samples of measurements
Φ	Square matrix
$\hat{\theta}$	Estimate of θ
$\varepsilon(t)$	Residual (error)
V_{LS}	Loss function
u(t)	Input
f(u)	Static nonlinear function
G(q)	Linear time-invariant transfer function
v(t)	Stationary stochastic process
θ	Parameter vector
$x \in R^n$	State variable vector
$y \in R^l$	Output variable vector
$u \in R^m$	Control variable vector

$z \in R^p$	System variable vector
$\theta \in R^r$	System parameter vector
n	Dimension of state space
m	Dimension of the control space
l	Dimension of the output space
r	Dimension of the system parameter space
e	Error between the measured and true values of variables
p	Dimension of the system space
q	Dimension of the reduced model
$\sum_i$	Covariance matrix of the response variables **y** at the $\mathbf{i}^{th}$ experiment and hence of $\mathbf{e}_i$
CMAS	Completely Mixed Activated Sludge
$z(t)$	State variables
COD	Chemical oxygen demand
DO	Dissolved oxygen
TKN	Total Kjeldahl Nitrogen
ASM1	Activated sludge model No. 1
UCT	University of Cape Town
$\mathbf{y} = y_1, y_2, ..., y_l$	Dependent variables
$\mathbf{u} = u_1, u_2, ..., u_m$	Independent variables
$f = f_1, f_2, ..., f_l$	*l*-Dimensional vector of functions
$m = s - l$	Independent variables
m	A big number of samples
μ	Sample mean value
σ	Sample standard deviation
$\mathbf{e}_i$	Residuals
$L(\theta)$	Likelihood function
pdf	$p_0(\theta)$ the prior
λ	A vector of the Lagrange multipliers
H	Jacobian matrix
φ	Observation functions
$v(k)$	A sequence of independent random variables
$\omega(k) \in R^{15\times15}$	The symmetrical positive definite matrix
z_0	The vector of the initial state
$v(t)$	The vector of the noise
ϕ	Known nonlinear function
$\hat{z}(t)$	Current state estimate
Y	Yield matrix
D	Dilution rate
Q	Rate of the released by the process gas
F	Inflow rate
$\Omega(\hat{\xi})$	Gain matrix
F_{out}	Effluent flow rate

β_i	Specific liquid-gas transfer rates
OUR	Oxygen uptake rate
K_{La}	Oxygen transfer function
$R(t)$	Respiration rate

Nomenclature

SIMBA model	ASM1 model	UCT model	Kinetic Parameters
myH	$\hat{\mu}_H$	$\hat{\mu}_H$	Maximum specific growth rate of the heterotrophs when utilizing soluble readily biodegradable COD
KSH	$\mathbf{K}_{SH}$	$\mathbf{K}_{SH}$	Half-saturation coefficient for heterotroph growth when utilizing soluble readily biodegradable COD
KMP	k_h	$\mathbf{K}_{MP}$	Maximum specific growth rate of the heterotrophs when utilizing adsorbed particulate slowly biodegradable COD
KSP		$\mathbf{K}_{SP}$	Half-saturation coefficient for heterotroph growth when utilizing adsorbed particulate slowly biodegradable COD
bH	$\mathbf{b}_H$	$\mathbf{b}_H$	Heterotrophic organism specific death rate
KA		$\mathbf{K}_A$	Slowly biodegradable COD adsorption rate
KR	$\mathbf{K}_R$	$\mathbf{K}_R$	Conversion rate of soluble organic nitrogen to free and saline ammonia
nyG	η_G	η_G	Correction factor for anoxic heterotrophic growth
myA	$\hat{\mu}_A$	$\hat{\mu}_A$	Maximum specific growth rate of the autotrophs (nitrifiers)
KSA	$\mathbf{K}_{SA}$	$\mathbf{K}_{SA}$	Half-saturation coefficient for autotroph growth on ammonia
bA	$\mathbf{b}_A$	$\mathbf{b}_A$	Autotrophic organism specific death rate
KH	K_H		Maximum specific hydrolysis rate
KX	K_X		Half-saturation coefficient for hydrolysis
muS	η_S		Correction factor for anoxic hydrolysis
			Stoichiometric Parameters
YH	$\mathbf{Y}_{ZH}$	$\mathbf{Y}_{ZH}$	Heterotroph yield in COD units
YA	$\mathbf{Y}_{ZA}$	$\mathbf{Y}_{ZA}$	Autotroph yield in COD units

		$\mathbf{f}_{MA}$	Maximum ratio of adsorbed substrate to heterotroph mass
Fp	$\mathbf{f}_{E}$	$\mathbf{f}_{E}$	Inert fraction of the active organism mass
iXB	$\mathbf{f}_{ZB,N}$	$\mathbf{f}_{ZB,N}$	Fraction of biological (active) mass which is nitrogen
iXP	$\mathbf{f}_{ZE,N}$	$\mathbf{f}_{ZE,N}$	Fraction of endogenous/inert mass which is nitrogen
			Switching functions parameters
KOH	$\mathbf{K}_{OH}$	$\mathbf{K}_{OH}$	Switching constant for oxygen-limited heterotroph growth (switch from aerobic to anoxic growth)
KOA	$\mathbf{K}_{OA}$	$\mathbf{K}_{OA}$	Switching constant for oxygen-limited autrophic growth
KHA	$\mathbf{K}_{HA}$	$\mathbf{K}_{HA}$	Switching constant for ammonia-limited aerobic heterotroph growth
KNO	$\mathbf{K}_{NO}$	$\mathbf{K}_{NO}$	Switch constant for nitrate-limited anoxic heterotroph growth

CHAPTER ONE

STATEMENT OF THE PROBLEM. PROJECT OBJECTIVES, HYPOTHESIS AND ASSUMPTIONS

1.1 Introduction

The development of a dynamic model, describing an activated sludge process performing carbonaceous removal, nitrification, denitrification and phosphate removal is described considering the aims and objectives. The main purpose is to combine knowledge of the process dynamics with mathematical methods for parameter estimation and identification. The simplified model may serve as a tool for predicting the dynamic behaviour of the activated sludge process, since the parameters can be tracked on-line during varying operating conditions. The proposed model would be aimed for operation and control purposes as an integral part of a hierarchical control structure. This chapter describes also the hypothesis, assumptions made, main steps in building of a mathematical model and the contents of the separate chapters of the thesis.

1.2 Awareness of the problem

The problem for effective and optimal control of wastewater treatment plants is very important recently because of the increased requirements to the quality of the effluent. The activated sludge process is a type of wastewater process characterized with complex dynamics and because of this proper control design and implementation strategies are necessary and important for it operation.

It should be noted that few plants are equipped with more than a few rudimentary sensing elements and control loops, mostly concerning flow metering and control, and for monitoring the basic plant performance over longer periods of time. Since the early seventies, when a major leap forward was made by the widespread introduction of dissolved oxygen control, little progress has been made. Several reasons for this lack of instrumentation, control and automation have been proposed (Beck, 1986; Olsson, 1993):

- *Understanding*: Insight in the treatment processes is still insufficient and there is a lack of suitable mathematical models.
- *Inadequate instrumentation*: Non-existent or insufficiently reliable technology.
- *Plant constraints*: Inapt and insufficient flexibility to manipulate the process.
- *Economic motivation*: There exists a lack of fundamental knowledge concerning benefits versus costs of automated treatment processes. In addition, wastewater treatment processes are not productive and automation can only contribute to a decrease of operating costs but does not directly lead to increased profit.

- *Education and training*: Operators are not always adequately trained to operate advanced sensor and control equipment and most environmental engineers would need more basic understanding of process dynamics and control in order to appreciate the potential of instrumentation, control and automation.
- *Communication*: The interaction between operators, designers, equipment suppliers, researchers and government regulatory agencies is often unsatisfactory and leads to poorly designed plants.

Control of wastewater treatment plants relies on four building blocks:

- insight in the plant operations and dynamics summarized in an appropriate mathematical process model;
- sensors that provide on-line data from some of the output variables of the process and disturbances acting upon it;
- adequate control strategies which try to minimize deviations from the control objectives;
- actuators which implement the controller outputs on the plant.

Not only the organic carbon pollution of wastewater must be eliminated but also nutrients (i.e., nitrogen and phosphorus). With biological nutrient removal being the most economic way of treatment (in most cases), rather complex process configurations have resulted. The numerous interactions that occur among the different unit processes and the fact that the biological potential is taken to its limit, lead to nutrient removal plants being quite vulnerable to external disturbances or erroneous manipulations (Takacs et al., 1990). Hence, the increased complexity is a major driving force for the introduction of advanced instrumentation, modelling and control that can provide the necessary information and operation of the process condition.

The most critical phase in the solution of any control problem is the modeling stage. This is because nearly all control techniques require knowledge of the dynamics of the system to be controlled before an attempt can be made to make a controller for it. This means that the primary building block of any modern control exercise is to construct and identify a model for the system to be controlled.

One has a complex kinetic model and has to use the model for real time control. There are couple of difficulties with the complex models:

- many variables are difficult to determine
- many kinetic parameters are difficult to be determined.

A way to solve the difficulties would be to simplify the complex model by development of a reduced model with small number of variables, but still with the same characteristics as the original full model. Kinetic parameters can be determined by development and application of methods for parameter estimation.

Many model construction and identification studies are conducted using general linear statistical models and corresponding identification algorithms. It is easy to assume more or less complete ignorance of a system and then let a general algorithm find an empirical model for it. This approach works fairly well on linear processes but a vast number (Holmberg, 1983), (Ingilsen, 2002a), (Jeppsson, 1996) and (Olsson, 1992) of important systems (such as wastewater treatment processes) cannot be described adequately by linear equations.

Another approach for modelling is to develop models of the wastewater processes using the first principles of conservation of mass and energy. The obtained mass-balance models describe the process technological structure and biological reactions. They are nonlinear and with big dimension. Examples of such models are the COST Benchmark model (Copp, 2002) and the University of Cape Town (UCT) (Dold et al, 1980) model. The most used biological models are the IAWQ1 (Henze et al, 1987) – the model of the International Association for Water Quality and UCT model – the model developed at the Department of Civil Engineering, (UCT).

It is currently not possible to model and identify general non-linear systems (Jeppsson, 1996) because of their great variety and because of their structural complexity. There are numerous non-linear systems which must be controlled in the present industrial world. Thus, it is important to develop methods to model non-linear systems and to estimate the model parameters. Once the models are available, it is also important to investigate how they can be used to establish the concept of understanding and effective control of the relevant system.

1.3 Statement of the Problem

The research work on the project is concentrated on the development of reduced biological ASM1 and UCT and mass balance models for the purposes of process control design and implementation. The selection of these models was done on the basis of a comparative literature study and interviews with the models' developers. The full ASM1 and especially UCT models are highly complex and problematic with their limitations and drawbacks in respect to their use for control purposes. These limitations and drawbacks are

- big dimension of the model variables
- complex dependencies and interconnections between the biological variables
- different time scales for the process dynamics
- the control actions for the process are not included in explicit way in model equations.

The research work on the project is provided to overcome these difficulties. Then the research problem can be stated in the following way:

Problem: To develop mathematical methods, algorithms and programmes for transformation of the complex biological and mass balance models of the activated sludge process into simpler reduced models of the process convenient to be used for optimal parameter estimation, control design and control implementation in real-time.

The research problem is divided in the following subproblems:

1.3.1 Design based subproblems

1.3.1.1 Subproblem 1: Activated sludge process study.

To acquire knowledge for the connections between the process technology, physiochemical and enzyme reactions, mass balances and their description by the original UCT model.

1.3.1.2 Subproblem 2: Reduction of the number of the biological variables in the model equations.

To reduce the complexity of the model. The comparison between the original and reduced models to be done by simulation.

1.3.1.3 Subproblem 3: Development of senditivity models of the reduced process models for sensitivity functions simulation and analysis

To study the the influence of the model parameters over the dynamic behaviour of the process for the purposes of parameter estimation.

1.3.1.4 Subproblem 4: Development of a method and algorithm for parameter etimation of the obtained reduced models.

Decomposition method for minimum least square parameter estimation to be developed. Validation of the model to be done by simulation with different input signals.

1.3.1.5. Subproblem 5: Development of a method for estimation of some of the nonmeasureable process variables using the real time data of some of the measurable variables.

A method to be developed for estimation of the reduced models biological variables on the basis of measurement of the Dissolved Oxygen (DO) concentration

1.3.2 Real implementation subproblems

1.3.2.1 Subproblem 6: Development of reduced mass balance models of 3 processes – Benchmark, Athlone and Mitchell's Plain on the bais of both ASM1 and UCT biological models.

The models to be developed based on data from the real plants

1.3.2.2 Subproblem 7: SIMBA software for simulation of the full and reduced mass balance models

The software to be developed for the considered three real plants

1.3.2.3 Subproblem 8: Development of Matlab software for analysis of the process sensitivity functions

The software to be applied to the considered three real plants

1.3.2.4. Subproblem 9: Development of Matlab software for parameter estimation of the real processes

The software to be applied to the considered above three plants

1.4 Research objectives

The project considers reduction of the impact of the complexity of the process model over the methods for control design by development of reduced models and methods for parameter estimation of these models.

The aim of the project is to develop theoretical methods, algorithms and software for simplification and parameter estimation of the mathematical mass balance and biological models of the activated sludge process under the condition for fully representation of the process dynamics.

The aim of the project can be achieved through the following objectives:

1. Study of the complex relationships between the process variables in connection with the kinetic differential equations describing the process.

2. Reducing the complexity of the model through grouping or cutting some of the mathematical representation in the model with criterion keeping the dynamical behaviour of the reduced model not changed in comparison with the original one.

3. Development of sensitivity functions of the reduced models' variables towards the models' parameters. Analysis of the dynamics of the models of sensitivity.

4. Development method for parameter estimation of the transformed models on the basis of the least-squares approach. Validation of the model.

5. Analysis of the existing methods for parameter and state estimation of biological processes

6. Development of algorithms and programmes for simulation, parameter estimation, real time variables estimation using SIMBA and MATLAB/Simulink software.

1.5 The Hypothesis

1. Is it possible to develop a simplified reduced model of the activated sludge process, which still represents the important process characteristics.

2. The difference on the time scale of process dynamics allows the process model to be decomposed in time domain and every part of it to be considered separately making assumptions for the value of the variables of the other parts of the model.

3. The real time data from the measured variables can be used to estimate the values of the nonmeasured variables.

4. The reduced model allows reduction of the complexity and number of calculations for control design and implementation and can be used in real time. The resulting control will not differ from the control obtained using the original full model.

1.6 Delimitation of the research

The research project is concentrated on the modelling of the activated sludge process, the main part of the wastewater treatment process. Other parts of the process will not be considered.

Only the ASM1 and UCT biological models are considered and transformed. Other existing activated sludge models are not considered.

Only Benchmark and UCT mass balance models are considered. Other mass balance models are not considered.

The real time data is obtained from the Benchmark COST model literature (Copp, 2002), Athlone and Mitchell's Plain plants.

Software for the implementation of the developed methods is programmed using SIMBA and MATLAB/Simulink environment.

The problems for parameter and state estimation are solved using the optimal control theory and methods of variational calculus, applying time domain decomposition of the necessary conditions for optimality of the problems for estimation.

1.7 Assumptions

The following assumptions are made:

1. The process under study is in operation according to the prescribed technology.
2. The used original biological models ASM1 and UCT can fully describe the process kinetics in all technological parts.
3. The complex dependencies between the enzymes and biomass in the wastewater treatment process can be represented through the values of the parameters in the kinetic model.
4. The least-squares method for parameter estimation can be extended to solve a complex problem for estimation with nonlinear parameter dependencies.
5. The method of least-squares can be extended to solve the problem for estimation of the nonmeasurable process variables using real time data from the measurable variables.
6. The activated sludge process can be represented through fully observable and fully controllable model.

1.8 Phases in the model building

After the definition of the modelling objectives and selection of a model type, several key steps can be found in all current model building methodologies. These steps are outlined below as follows:

1.8.1 Development of models

System Characterization

The first step is to characterize the process. This is achieved by developing a set of axioms or description of the process. These axioms can be formed by intuitively describing the process or in some idealizing or approximating the process behaviour. They could be result of some prior knowledge of the process or based on postulated mechanisms within the process. The end result of this step is a set of relationships. The expert modellers will adequately describe the process to the accuracy which is required. The description invariably is incomplete so that a number of different possible models and processes could satisfy them. The axioms may also contain information which is incorrectly characterized from the process. Identification of all important characteristics may, however, be impossible due to the

complexity of the process and the limited expertise and knowledge of the modeller. Therefore, the task of the modeller is to strive for a good characterization, i.e., identify many of the most important characteristics whilst limiting incorrect and non-essential identifications.

Model Construction

In this step of model building process, the axioms developed during the system characterization are refined into mathematical relationships. This requires a quantitative assessment of the physical phenomena judged to be important during the characterization step and involves determining a mathematical structure for the model and assigning parameters to the model.

The distinction between conservative and constitutive relationships should be emphasized. Conservation relationships are fundamental physical laws whereas constitutive relationships are postulated mechanisms usually based on empirical evidence. In using constitutive relations, the modeller is incorporating more questionable but necessary information into the model.

In a completely different direction, arbitrary structure for the model can be chosen. Model parameters are then varied to achieve agreement between the process and the model. This type of model orginates from the field of system identification and is only suitable for model realization from observed process data. However, it should be noted that methods for parameter estimation are becoming increasingly important also for modellers working with deterministic models of complex systems.

1.8.2 Parameter and variable estimation

Parameter estimation consists of determining the 'optimal' values of the parameters of a given model with the aid of the measured data. Although this procedure uses a given model structure, it is not completely independent of model structure evaluation, because the model may degenerate to a simpler structure for particular values of some parameters. Since the initial state of a simulation, the boundary conditions and the external variables can also be formulated with the aid of parameters, all these parameters, together with the model parameters, can be combined to yield a single array of parameters to be estimated simultaneously using the same estimation technique.

There are four important conventional techniques which can be used for parameter estimation, for example, Beck (1987) and Ljung (1987):

- Bayesian estimation;

- Maximum likelihood estimation;
- Weighted least squares estimation;
- Least squares estimation.

These four methods are listed in decreasing order of the amount of information that has to be provided by user of the method, or, equivalently, in increasing order of the number of a *priori* assumptions (Jeppsson, 1996) already included in the method. For the most complicated case of Bayesian estimation, the probability distribution of the parameters and the conditional probability distribution of the measurements for given parameter values have to be parameterized, whereas the simplest case of least squares estimation can be performed without extrinsic information. Weighted least squares and least squares estimation are special cases of the maximum likelihood method in which the measurements are assumed to be uncorrelated and normally distributed. Practical experience has shown that the methods above do not always suffice, since distribution of real data is never known exactly. This leads to the development of methods for robust estimation, see for example, Birkes and Dodge (1993).

1.8.3 Model Verification and Validation

Model verification and validation may be regarded as a part of the model construction methodology or a concluding step. However, it is clear that model construction and model validation are closely related and require an iterative procedure.

The constructed model must be tested by simulations. In the first simulation the model behaviour is analysed/verified. This amounts to checking that the simulated responses are consistent with the axioms proposed during the process characterization and the mathematical structure used in the model. It also means debugging the model code and ensuring that the simulated responses appear feasible.

The validation step involves checking that the model responses generated during the model analysis agree with that obtained from the true process. This is the ultimate check on the success of the model building.

1.9 Research methods

The field of modelling of industrial processes is a multidisciplinary field, which requires integrated approach for providing research activities. That is why different

research methods are used during the different phases of the research work on the project. They include;

- descriptive method – to describe the process to be modelled using the first principles of mass and energy balances. The information is gathered by observation, technology study, measurements, questionnaires and interviews with the operational personnel, conversations with specialist from the field.
- design method – to transform the model describing the process according to the first principles to model convenient for the real time control design and implementation. Transformation is based on mathematical dependencies, deep study on the process variables interrelations. The work is based on the comparison dynamic behaviour of the original and transformed model by simulation.
- design method – to connect in explicit way the process inputs and outputs in the process model. The work is based on some assumptions for the type of dependencies between the process parameters and variables and on comparison of the behaviour of the original and transformed models by simulation.
- experimental method – to obtain data which to be compared with the results from of the transformed models. The experiments are based on the information of the previous steps and planning for the phases of the experiments.
- design method – development of mathematical method to solve the problem for parameter estimation of the transformed model. The method uses the knowledge of the optimal estimation theory from the variational calculus. The software is developed and the simulation with different outputs is done for verification of the model using the software.
- descriptive method – to describe the developed methods, programs and system for real time simulation with all characteristics and functions. The information is gathered from all of the above steps.

1.10 Thesis chapters

The chapter one outlines the statement of the problem, project objectives, hypothesis and assumptions of the thesis. This is followed by sketching the goals of each of the chapters in a clear concise and explanatory reason. The chapter two describes the wastewater treatment plant process and shows the various scenarios when the municipal wastewater and industrial wastewater are combined. In chapter three the mathematical models of the activated sludge process are investigated whilst in chapter four the reduced biological and mass balance models of the activated sludge process for the Benchmark model, Athlone plant and Mitchel's plant based on ASM1 and UCT biological models are developed. In chapter five the sensitivity study involves the determination of the key parameters of the wastewater treatment system. The chapter six describes and develops the parameter estimation and applies it to the Benchmark and Athlone mass balance models, based on ASM1 and UCT biological models. In chapter seven methods for estimation of both state and parameters are analysed for the cases of biological processes. Chapter eight describes the results from simulation of the models using SIMBA software. Chapter nine describes the results from sensitivity study and parameter estimation. Chapter ten discusses the results, gives conclusion and the future directions of work.

1.11 The significance of the research

South African science has very good results in design technology and modelling of activated sludge process. In South Africa there are many wastewater treatment works where the activated sludge process is not monitored properly and control is manual. The keys to building a competitive industrial base are knowledge, innovation and productivity. These keys in the project are: the project will innovate the existing and will develop and apply new knowledge about the process, the developed models application will lead to saving of energy and improve the quality of the effluent water; Transfer of knowledge and technology is another of the main aims. Development of the project will: Promote links with one important sector of the industry and identify the needs of this sector; establish and grow the research skills within the research community in tertiary institutions. Different potential benefits can be obtained as a result of introduction of the modern control strategies in wastewater treatment plants. Some of them are:

- **Performance.** Maintenance of the plat efficiency nearer the maximum by improved operation could result in significant decreases in the pollution load placed on the water resources.
- **Productivity.** This is another advantage of good operation. It can be reached through an increase in the amount of waste that can be treated per unit of process capacity.
- **Reliability**. It is well recognised that bypassing of raw wastewater and gross process failures occur all too frequently. This frequency can be greatly reduced by improved operational procedures, whether they are manual or automatic.
- **Process stability**. Through adequate control actions the growth of biomass will be stable.
- **Operational personnel** reduction.
- **Operational cost** reduction. The power and chemicals addition can be regulated according with the needs for such addition.

Development of the research project will have positive impact on both – wastewater treatment plant and staff and students from Department of Electrical Engineering with

- The application of new technologies for modelling, monitoring and optimal control for waste water treatment process
- Work in collaboration with people from the industry,
- Develop research work and control system for a real process.

1.12 Conclusion

Aim and objectives for development of a dynamic model, describing an activated sludge process performing carbonaceous removal, nitrification, denitrification and phosphate removal is described. The main purpose is to combine knowledge of the process dynamics with mathematical methods for parameter estimation and identification. The simplified model may serve as tool for predicting the dynamic

behaviour of the activated sludge process, since the parameters can be tracked on-line during varying operating conditions. The proposed model would be aimed for operation and control purposes as an integral part of a hierarchical control structure. The chapter describes also the hypothesis, made assumptions, main steps in building of a mathematical model and the contents of the separate chapters of the thesis. The description of the activated sludge process is done in the following chapter 2.

CHAPTER TWO

THE WASTEWATER TREATMENT PLANT PROCESS: MULTILAYER CONTROL STRATEGY

2.1 Introduction

The wastewater treatment plant process is described and carefully explained in this chapter. The activated sludge is considered as an object of control further to the fermentation process modelling and estimation are considered in this chapter. The activated sludge processes of industrial wastewaters and treatment of industrial wastewater in municipal activated sludge plants are dealt with and carefully explained in detail. The multilayer control strategy of the wastewater treatment process was implemented and exercised in the hierarchial operation.

2.2 The wastewater treatment process

The wastewater treatment process based on using of biological process of activated sludge is considered. The function of the wastewater treatment plant is to speed up the natural process by which the water purifies itself. The main objective of the plant is to produce an effluent meeting the required standards at the lowest possible cost, working in two directions (Dold et al., 1991):

- Reduction of organic bound energy to a level such that the heterotrophic growth and associated deoxygenating effects in the receiving body of water are acceptably low,
- Reduction of the autotrophic substances, phosphates, ammonia and nitrates, to levels such that photosynthetic autotrophic growth and their capacity to fix solar energy as organic energy in the receiving body of water are acceptably low.

The schematic diagram of the wastewater treatment plant is given on Figure 2.1. The sewerage flows through the screens where the heavy debris are removed and continues through small tank where the grit are removed. Then the influent flows towards the primary settling tanks where some small particles of the waste is going to the bottom and continues onto the activated sludge reactor where where it passes through different tanks according to the selected technology (anaerobi, anoxic, aerobic). After the treatment the water goes to the final clarifier from where it exits as final effluent. The sludge from the primary settling tanks continues to the gravity thickener which then goes to the flotation process and onto the sump or alternatively the primary thickened sludge flows to the sump. The final clarifier has the product recycled back to just before the activated sludge reactor. The waste activated sludge which leaves after the activated sludge reactor goes to the flotation unit and then onto the sump.

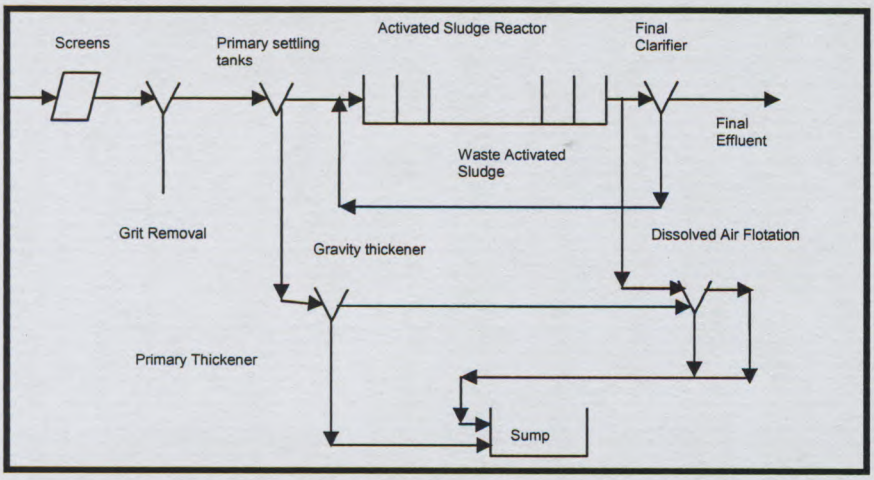

Figure 2.1: Schematic diagram of the wastewater treatment plant

2.3 Activated sludge processes of industrial wastewaters

The objective of the activated sludge processes in treating industrial wastewaters is to remove soluble and insoluble organics and to convert this material into a flocculent microbial suspension that settles well in conventional gravity clarifiers. A number of modifications of the activated sludge process have been developed to accommodate specific waste characteristics and/or operational needs (Eckenfelder & Grau, 1992). As a general rule, the nature of the wastewater will dictate the preferred process modification, primarily for the purpose of maintaining mixed liquor quality.

2.3.1 Plug-flow activated sludge

This activated sludge process modification uses long, narrow aeration basins to provide a mixing regime that approaches plug-flow conditions. A plug-flow regime promotes the growth of a flocculent and well-settling sludge by introducing influent wastewater and return sludge at the head-end of the basin. This provides a high substrate gradient that promotes growth of floc-forming rather than filamentous biomass. If the wastewater contains toxic or bioinhibitory organics, however they must be removed or equalized prior to entering the head-end of the aeration basin since there is negligible dilution available in the aeration basin itself. The oxygen utilization rate is high at the beginning of the basin and decreases with aeration time. Under normal operating conditions the mixed liquor oxygen utilization rate approaches the endogenous level towards the end of the aeration basin.

Modification of the way in which wastewater and return sludge are brought in contact in a plug-flow system can have a number of benefits. Provision of a separate zone at the inlet, with a volume of about 15 percent of the total aeration

volume and a low-energy subsurface mechanical mixing, can achieve controlled anoxic conditions. These conditions generally promote good floc formation and control of filamentous growth. In cases where nitrification occurs, recycle of nitrified mixed liquor (and NO_2) from the end of the aeration basin to the anoxic zone at the head-end can achieve significant denitrification and remove some of the influent COD.

2.3.2 Complete Mixed Activated Sludge (CMAS)

In a complete mixed activated sludge process, the wastewater and the return sludge are introduced into the aeration basin at multiple points to facilitate their rapid blending with the basin contents. The objective is to maximize equalization of the influent load within the aeration basin. This process is particularly applicable to wastewaters that contain toxic/bioinhibitory substances or that have highly variable loading patterns. Furthermore, wastewaters with variable pH are neutralized by the basin contents and biological activity. Another advantage of a complete mixed process is that the oxygen uptake rate is equalized throughout the basin, thus permitting uniform spacing of the aeration equipment.

Complete mixed activated sludge should not be employed when treating readily degradable wastewaters unless a biological selector is installed in front of the aeration basin in order to maintain good sludge settling characteristics.

2.3.3 Pure Oxygen systems

The pure oxygen system is a series of well-mixed reactors employing concurrent gas-liquid contact in a covered aeration tank. Feed wastewater, recycle sludge, and oxygen gas are introduced into the first stage. The oxygen gas is fed at low pressure (~ 1.5ml H_2O). Two gas-liquid contacting systems can be employed: submerged turbine aeration and surface aeration. The pumping action of the impeller on the shaft as the sparger promotes adequate liquid mixing and yields relatively long residence times for dispersed oxygen bubbles. Gas is recirculated within a stage at a rate that is usually higher than the rate of the gas flow between stages. A slight pressure drop occurs from stage to stage to prevent gas back-mixing. Since the relative mixing and oxygen transfer requirements vary from stage to stage, each stage is equipped with an independent mixer-compressor combination designed to provide the required level of mixing and oxygenation.

The gas-liquid contact mechanism provided by surface aerators eliminates the need for gas recirculating compressors and associated piping. The mixing intensity

required to maintain the sludge in suspension is provided by a low-speed, low-shear impeller. Oxygen gas is automatically fed to either system on a demand basis (based on headspace gas pressure) with the entire unit operating, in effect, as a respirometer. As organic loading rate increases, the oxygen gas pressure decreases, resulting in an automatic increase in feed-oxygen flow.

Due the high mixed liquor solids maintained in the oxygen system, the major portion of soluble BOD (biochemical oxygen demand) removal, and thus the highest oxygen demand, occurs in the first stage, which requires the highest mixer and compressor horsepower. The subsequent stages are then utilized to stabilize sludge that has progressively decreasing oxygen demand. Effluent mixed liquor from the system settled and the clarifier underflow is returned to the first stage for blending the feed. The exhaust gas from final stage is vented to the atmosphere. The oxygen normally operates with a vent-gas composition of 30 to 50 percent oxygen. Due to net transfer of gas to the liquid, the vent-gas flow rate will be only 10 to 20 percent of the gas feed rate. Based upon economic considerations, about 90 percent oxygen utilization is desired.

The maintenance of a fully aerobic floc will maximize the endogenous rate coefficient and thereby minimize the excess sludge under moderate to high F/M (Food/Mass) loading conditions. The sludge settling rate will also be at a maximum under fully aerobic conditions. These conditions are promoted under the high DO operating levels that are available with the pure oxygen-activated sludge process especially for high-strength wastewaters.

2.4 Treatment of Industrial wastewater in municipal activated sludge plants

Municipal wastewater is unique in that a major portion of the organics is present in suspended or colloidal form. Typically, the COD in municipal sewage will be 33 percent suspended 33 percent colloidal and 33 percent soluble. The COD of industrial wastewaters, however, is frequently 100 percent soluble. In an activated sludge plant treating municipal wastewater, the suspended organics are rapidly enmeshed in the flocs, the colloids are adsorbed on the flocs, and a portion of the soluble organics is adsorbed. These reactions occur in the first few minutes of the wastewater-biomass contact in the aeration basin. By contrast, for readily degradable industrial wastewaters, such as food processing, a portion of COD is rapidly sorbed and the remainder removed as a function of time and biological solids concentration. Very little sorption occurs in refractory wastewaters. The kinetics of the activated sludge process of the municipal plants will therefore vary

depending on the percentage and type of the industrial wastewater in the combined wastewater flow to the plant.

The percentage of biological solids in the aeration basin will also vary with the amount and nature of the industrial wastewater contribution. For example, domestic wastewater without primary clarification will yield a sludge that is approximately 47 percent biomass. Primary clarification will increase the biomass percentage to about 53 percent. Increasing the sludge age will also increase the biomass percentage as influent volatile suspended solids under degradation and synthesis. Similiarly, the addition of soluble industrial wastewater will increase the biomass percentage in the activated sludge.

As a result of these considerations, there are a number of factors that must be considered in the process design for activated sludge treatment of combined municipal and industrial wastewaters.

2.4.1 Effect on effluent quality

Soluble industrial wastewaters will affect the overall substrate removal rate coefficient. Refractory wastewaters such as those from chemical factories will reduce the overall rate while readily degradable wastewaters such as those from food processing will increase the rate. It has been shown that for process design purposes, the mean value of the rate coefficient can be computed as a substrated mass-weighted average of the individual components constituting the wastewater.

2.4.2 Effect on sludge quality

Readily degradable wastewaters will stimulate filamentous bulking while refractory wastewaters will frequently suppress filamentous bulking. Municipal wastewater itself is subject to filamentous bulking under certain conditions. Addition of the readily degradable wastewater will enhance this potential, implying the use of plug-flow configuration may be warranted. Depending on the wastewater mixture, bioinhibitory wastewaters may be effectively treated when mixed with municipal wastewaters in a complete mix configuration.

2.4.3 Effect on temperature

Addition of an industrial wastewater that has a high soluble substrate load will increase the temperature coefficient, of the combined process. This will decrease process efficency at reduced mixed liquor operating temperatures.

2.4.4 Sludge handling

An increase in soluble organics will increase the percentage of biological sludge in the waste sludge mixture. This generally will decrease thickening and dewaterability, decrease cake solids, and increase chemical conditioning requirements. An evaluation should be made of changes in sludge handling requirements and production rates that may result from the addition of the industrial wastewater.

2.4.5 Bioinhibition and aquatic toxicity

Many industrial wastewaters exhibit inhibition of the activated sludge process, particularly with respect to nitrification. Similarly they may be a new source of potential aquatic toxicity if the toxicants "pass through" the municipal works. It is therefore essential that the industrial wastewater be fully evaluated for compatibility with existing activated sludge process to ensure future permit compliance.

2.4.6 Nutrient (N and P) requirements

Since many industrial wastewaters are nutrient deficient, the COD:N:P ratio of the combined wastewater should be determined. If the industrial load contribution is not large, the background excess nutrient concentration of the municipal wastewater may provide the required nutrient balance.

2.5 The activated sludge process as an object of control

The activated sludge process is a biological process based on the intrinsic capability of the microorganism to perform complex chemical transformations upon organic compounds by means of the metabolic activity and the action of enzymes. The activation sludge processes have been subjects of intensive research in the last 20 years (Nejjari et al., 1999; Henze et al., 1994; Henze et al., 1995; Henze et al., 1998; Gujer et al.,1999; Gernaey et al., 2004; Fuerhacker et al., 2000; Ekama & Wentzel, 1999; Eckenfelder & Grau, 1992).

The ability to control activated sludge processes at their optimal states accurately and automatically is of considerable interest to the municipalities since it can enable them to reduce their production costs and increase and maintain the quality of the effluent. It should be noted, however, that the control system design of these bio-reactors is not straightly-forward as is described in the papers due to the specific process characteristics as object of control: significant model uncertainty, time varying and nonlinear nature of the process, lack of reliable on-line sensors, slow response.

It is also important that the micro-organisms themselves have complex regulatory mechanisms within the cells and that the external control system can only manipulate the extra-cellular environment which may indirectly affects the intracellular metabolic reactions –Figure 2.2

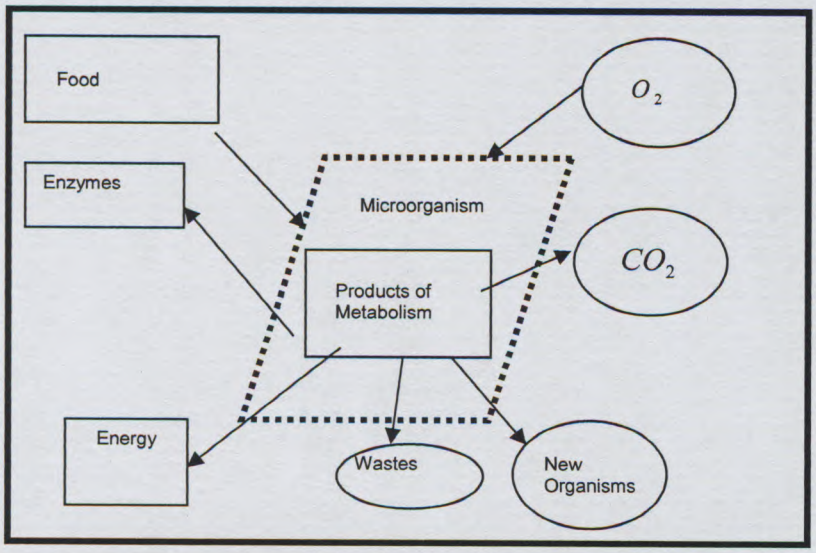

Figure 2.2: Complex dependencies in the microorganism cells. The biomass growth process components

That is why the best results of the control will be received if the control system succeeds to optimise the environmental conditions for the cells – temperature, Dissolved Oxygen (DO) concentration, pH, and flow rate. The activity of a particular enzyme is controlled by the concentration of several medium components. The important thing in considering the control problem is not simply to apply sophisticated control theory but to consider it with deep understanding of the dynamics of the physiological state changes. It is therefore quite important to investigate how the physiological state changes in relation to genetic change and environmental change. In order to achieve the full biological potential of the cells, the environmental conditions must be maintained optimal. The first step towards this goal is the identification of the key variables, which can be used as control variables. For the considered thesis the dissolved oxygen concentration is selected as a key control variable. This selection is considered in the model development. Other variables are considered as constant ones. Then the activated sludge processes can be considered as represented by two key groups of variables – chemical and biological – Figure 2.3. The first group consists of such variables as temperature, dissolved oxygen, dissolved carbon dioxide, pH, flow rate, etc. These variables can be measured very easily in real time. The second group consists of concentrations of the substrate, biomass and product. The real time values of these variables are usually difficult to be measured by sensors. The chemical variables

control the enzyme activity and in this way they control the biological variables. This means if the optimal conditions for the chemical variables are reached according to some optimisation criterion, then the optimal conditions for the biological variables will be also reached. This idea is not new but at the moment in industry the values of the chemical variables are kept constant, equals to some their nominal values. The influence of different disturbances during the process as input flow composition, flow, waste concentration is not considered from control system point of view. In reality the micro-organisms need different, not constant values for the chemical variables during the different phases of the process. These values can be determined using some of the methods of optimal control towards both chemical and biological variables.

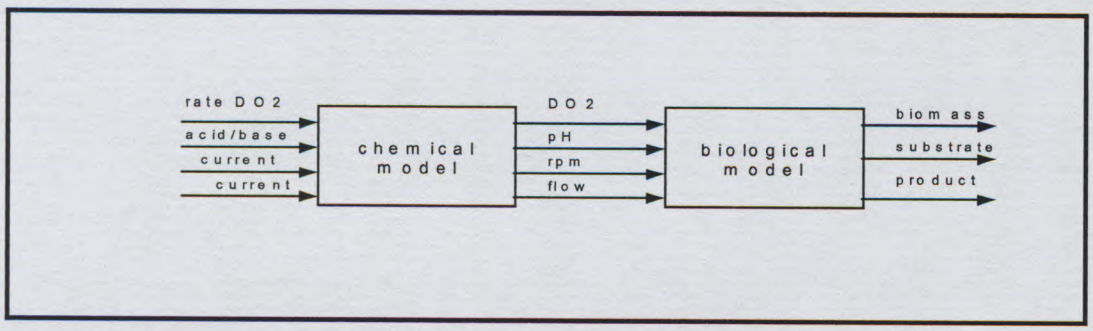

Figure 2.3: Dependence between chemical and biological variables

Furthermore, the activated sludge process – Figure 2.4 has not been studied fully yet as an object of control. It is not clear which kind of models are convenient; which are dependencies between inputs and outputs; what process variables are the most significant and in what way they affect the quality of the process or of its products; what the optimal combination of settings for these significant variables is, according to the goals posed on the process quality and the product quantity. There is lack of methods for measuring of important variables, for modelling and parameter estimation and for optimisation and control calculation.

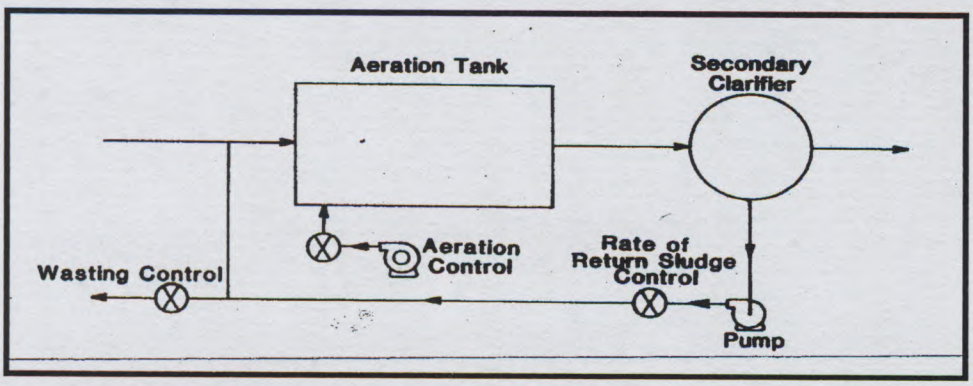

Figure 2.4: Activated sludge process

The project development is in accordance with the mention above important characteristics and drawbacks and will aim to develop models that would be capable to be used in a SCADA system for implementation of a strategy for real time optimisation and control of the waste treatment process, based on

- the characteristics of the process as an object of control,
- the existing instrumentation and control structures in industry for the considered processes,
- the possibilities to apply new instrumentation techniques for measurement, monitoring, modelling and control.

2.6 Multilayer control strategy of the wastewater treatment process

2.6.1 Hierarchical control structure functions

The research work on the thesis is a part of a bigger departmental project for development of an optimal adaptive strategy for control of the activated sludge process. The main research question is if a real time adaptive control strategy implemented in the software environment of the used at the present process SCADA systems can lead the wastewater treatment process to fulfillment of the requirements for quality of the effluent flow. The implementation of the adaptive control strategy is based on:

- complex dependencies between the process variables
- using measurement only of the chemical variables, which means using only widespread in the plants sensors
- existing operational structure of the plant

Activated sludge process is a dynamic process, which involves both rapidly and slowly changing parameters. The main dynamic processes in wastewater reactors can be separated into three timescales: fast DO dynamics, slower substrate (amongst others Nitrogen) dynamics and slow biomass (sludge) dynamics. The respective characteristic time constants of these three timescales are minutes, hours and weeks. Substrate plays the keyrole as it is directly related to effluent quality. That is why its control s the most important for the proper water treatment. The dissolved oxygen and the biomass control are used to create a proper environment for optimal substrate removal. The optimality is considered as an optimized balance between effluent quality and operational costs. On the basis of the said above it is natural that a substrate optimal control determines the setpoints for both DO and sludge controllers according to the influence of the main process disturbances. In accordance with the above an approach of an adaptive control is used in the project by which the process is optimised in a certain sense and the optimal control is obtained by a computer. This approach is based on three types of problems:

- adaptive estimation of state and process parameters,
- steady state or dynamic process optimisation and
- direct control.

The set of problems realising the adaptive control strategy can be solved in the framework of the multi-layer control hierarchical structures, Figure 2.5. In such a way the solution of all problems is subordinated to one joint goal. The problems solved on each layer are:

- adaptation - estimation the model and state parameters according to the values of the process disturbances;
- optimisation - steady state or dynamic optimisation of the process state and control according to the predictions and estimation from the adaptation layer;
- direct control - determination and implementation of closed loop linear and non-linear control according to the predictions and estimations from the adaptation layer and according to the set point/reference trajectories obtained from the optimisation layer.

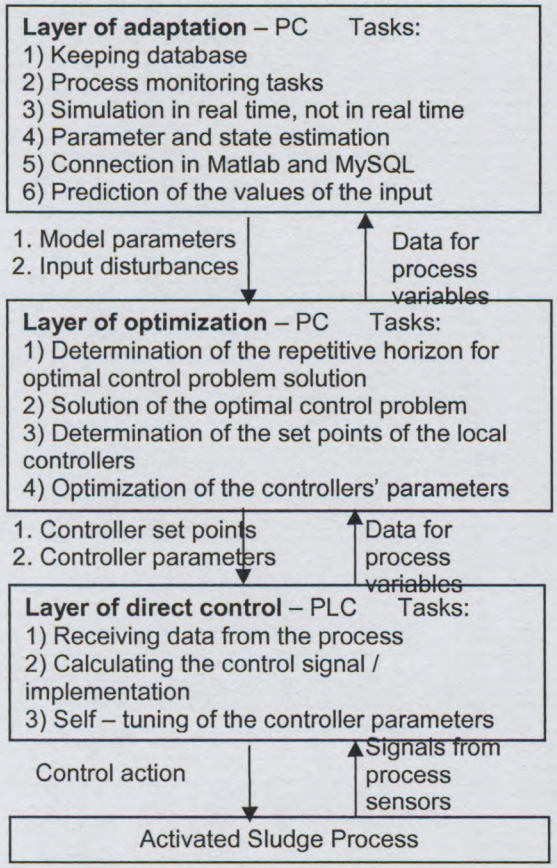

Figure 2.5: Three layer hierarchical control structure

2.6.2. The process modelling and estimation - task of the adaptation layer.

To postulate rational process control procedures, it is necessary to work with a mathematical model that relates process performance (organics and solids

removal) to process variables (influent strength and biodegradability, aeration, active microbial mass). Dynamic modelling and simulation is used to evaluate the effects of various inputs and process characteristics with respect to process stability. Two types of models are considered:

- models describing the behaviour of the chemical variables only. They are used for the optimal tuning of the controllers of the chemical variables. These models are not developed in the thesis.
- models describing the behavior of the biological variables.They can be described on the basis of nonlinear differential and difference equations and state space models with or without time delays. These equations describe dynamics of the biological variables - concentrations of substrate, biomass or product (metabolite) by applying material and energy balances using the fundamental transport, stoichiometric, termodinamic and kinetic relationships.

Both amongst scientists and practitioners a reasonable consensus exists that the Activated Sludge Model no. 1 (ASM no. 1) by Henze et al. (1987) and UCT model are the most popular mathematical description of the biochemical processes in ASP reactors for carbon and Nitrogen removal. The most popular model for the settling process probably is the double exponential model (Takacs, 1991). These models are used in the project as bases for development of the simpler models for the purposes of control design.

The model parameters can be determined using different methods for parameter estimation. Over the last decades there has been a large and ongoing interest in (nonlinear) system identification (e.g. Young, 1984; Ljung, 1987) and its application to activated sludge processes (e.g. Busby & Andrews, 1975; Vanrolleghem, 1994; Jeppsson, 1996; Tenno & Uronen, 1996). The objective of identification is to reduce the uncertainty about process dynamics, such that designs of processes and controllers can be improved. Good control can improve the utilization of the reactor volume and reduce the required over-dimensioning of plant designs.

The model parameters can be determined using different methods for parameter estimation. The methods for off-line and real-time estimation can be used. The information for the off-line parameter estimation can be received on the basis of experiments with the real or lab/pilot scale fermentor. The information for a real value of both types of variables during the process running can be obtained through a data acquisition system. The estimation algorithm is based on the least square method, according to the Fig.2.6. Dynamic modelling and simulation can be used to evaluate the effects of various inputs and process characteristics with respect to process stability.

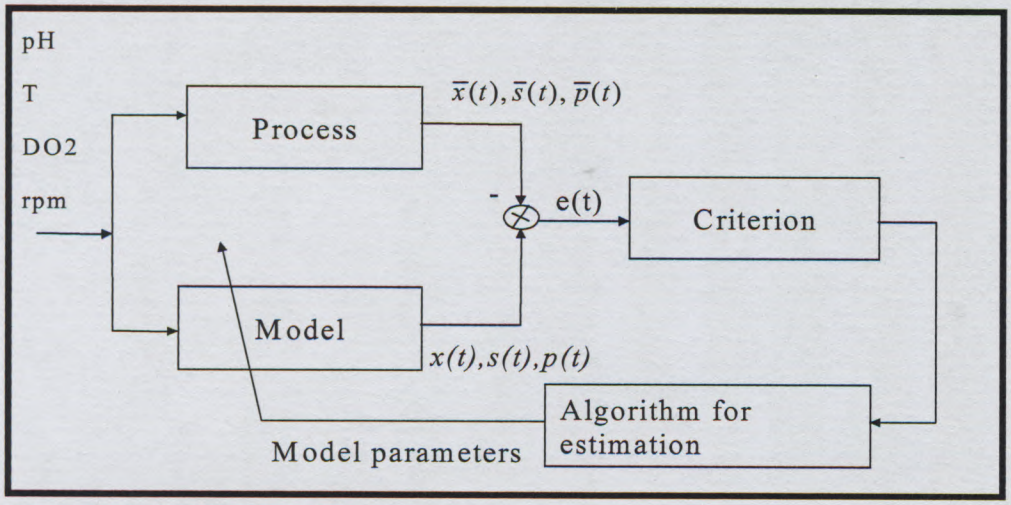

Figure 2.6: Estimation algorithm

2.7 Conclusion

Wastewater treatment technological structure is considered. The main part of the process called activated sludge process is described and its characteristics are outlined. The influence of the industrial wastewater over the municipality wastewater is summarised. The problems for modelling and estimation of the activated sludge mathematical models as a part of the process three layer control structure are introduced. These problems are considered in the following chapters.

The chapter 3 describes the problems for modelling of the biological processes in the activated sludge process.

CHAPTER THREE
MATHEMATICAL MODELS OF THE ACTIVATED SLUDGE PROCESS

3.1 Introduction

A definition of a system is given within a certain mathematical nomenclature and important criteria for process model development are defined and various model types are named. The wastewater treatment biological models such as UCT biological model and Activated Sludge model No. 1 are described. The similarities and differences between these two models are discussed. The default values for kinetic, stoichiometric and switching functions in the UCT model and ASM1 model are given. The processes and processes' rates of the UCT model Peterson matrix and the ASM1 Peterson matrix are explained in a detailed manner. Three wastewater treatment structures are introduced and described. Their mass balance equations are derived for every tank and component.

3.2 Definition of a system

A system is a process built to manufacture some products or materials and in the process there are different types of variables that interact and produce other variables. The process is affected by external variables which can be manipulated inputs or can be disturbances. The disturbances can be measured or unmeasured.

People who are "system thinkers" usually expect that systems are

(1) based on a set of cause-effect relationships that can be
(2) decomposed into subsystems and
(3) applied over a restricted application domain.

It can be defined that a system is a collection of objects arranged in an ordered form to serve some purpose.

Causes in systems nomenclature are usually referred to as inputs, and effects as outputs. The system approach assumes that all observed outputs are functions only of the system inputs. In practice a ubiquitous background noise is often present as well. This combined with the fact that we rarely, if ever, know everything about any system, means that the observed output is more often a function of the inputs and so-called white noise. From an engineering viewpoint, this means that proposed designs

need to rely on models that are less than ideal (Andrews &Mclone, 1971), (Aris, 1999), (Aris, 1994), (Bogaerts, 1999), (Bogaerts & Hanus, 2000), (Close & Frederick, 1994), (Director & Rohrer, 1988), (Gernshenfeld, 1999) and (Law & Kelton, 1991). Whether the system model is adequate depends on its functions. Regardless of this, any model is rarely perfect in the sense of exactness.

There are two basic means by which systems are designed: top-down and bottom-up. In top-down design, one begins with highly abstract modules and progressively decomposes these down to an atomic level. Just the opposite occurs in the bottom-up design. Here the designer begins with invisible atoms and builds ever more abstract structures until the entire system is defined.

Usually the system is considered as a "black box", as illustrated in Figure 3.1. It is apparent from this diagram that a system is an entity completely isolated from its environment except for an entry point called the input and an exit point called output.

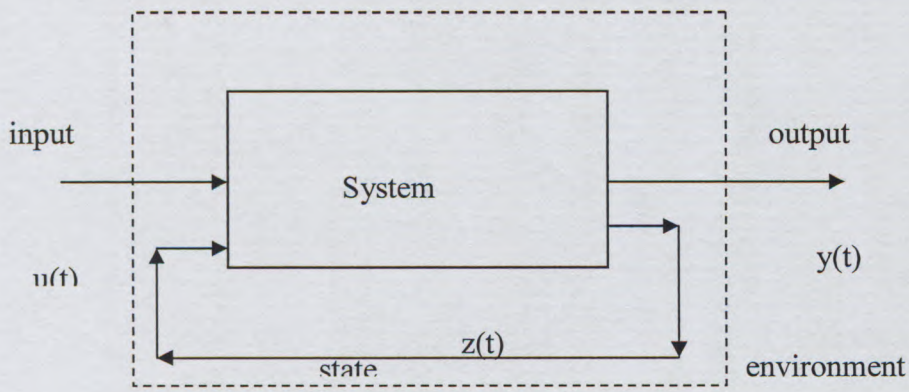

Figure 3.1: "Black box" model of the system

More specifically, the following system properties are considered in the thesis:

- All environmental influences in a system can be reduced to a vector of *m* real variables that vary with time, $u(t)=[u_1(t),...,u_m(t)]$. In general, $u(t)$ is called the input and the components $u_i(t)$ are input signals.
- All system effects can be summarized by a vector of *l* real variables that vary with time, $y(t)=[y_1(t),...,y_l(t)]$. In general, $y(t)$ is called the output and the components $y_i(t)$ are output signals.
- All internal system variables can be summarized by a vector on *n* real variables that vary with time. $z(t)=[z_1(t),...,z_n(t)]$ In general, *z(t)* is called the state and

the components $z_i(t)$ are the state variables.

Using these notations the system can be mathematically written by two algebraic equations involving the input, state and output:

$$z(t) = f_1(u(t)),$$

$$y(t) = f_2(u(t), z(t)), \tag{3.1}$$

for suitable functions f_1 and f_2. Since the state *z(t)* is given explicitly, an equivalent algebraic input-output relationship can be found. That is, for suitable function g ,

$$y(t) = f_2(u(t), f_1(u(t))) \equiv g(u(t)) \tag{3.2}$$

If the output signals are algebraic functions of only the current input, the system is said to be of zero-th order, since there can be no system dynamics. If the output signal depends dynamically on the input, there must also be system memory. For instance, suppose that the system samples a given signal every *t* = 0,1 , 2, ..., seconds and that the output *y(t)* depends on input *u(t-1)*. It follows that there must be two memory elements present in order to recall *u(t-1)* and *u(t-2)* as needed. Each such implied memory element increases the number of system state variables by one. Thus, the state and output equations comparable to Equations (3.1) and (3.2) are dynamic in that f_1 and f_2 now depend on time delays, advances, derivatives and integrals.

3.2.1 Definition of a mathematical model

A model is a representation of the essential aspects of the system. It presents knowledge for the system in a usable form. The mathematical model describes the relationship amongst the system variables in terms of differential, difference or algebraic equations.

Models are characterized by their system behaviour and type of the input accepted by the system. Once both the input and system behaviour is known, the output can be found. This is known as the analysis problem (Ljung, 1999), (Profozich, 1997), (Roberts et al., 1983), (Sage, 1995), (Sage & Armstrong, 2000), (Sandquist, 1985) and (Thompson, 2000).

Mathematical models of continuous systems are often defined in term of differential equations. Differential equations are particularly elegant, since they are able to describe the system dynamic behaviour.

3.2.2 Important criteria in the process of model development

Any given process may have different required models. The chose of a required model will depend on its objectives. Some of the more relevant objectives concern model purpose, system boundaries, time constraints and accuracy.

3.2.2.1 Model Purpose

A clear statement of the model intention is needed as a first step in setting the model objectives. This entails listing all the relevant process variables and the accuracy to which they must be modeled. Within the field of wastewater treatment a number of general purposes for mathematical models can be defined. These are listed below.

- Design – models allow the exploration of the impact of changing system parameters and development of plants designed to meet the desired process objectives at minimal cost.
- Research – models serve as a tool to develop and test hypotheses and thereby gaining new knowledge about the process.
- Process control – models allow for the development of new control strategies by investigating the system response to a wide range of inputs without endangering the actual plant.
- Forecasting – models are used to predict future plant performance when exposed to foreseen input changes and provide a framework for testing appropriate counteractions.
- Performance analysis – models allow for analysis of the total plant performance over time when compared with laws and regulations and what the impact of new output requirements on plant design and operational costs will be.
- Education – models provide students with a tool to actively explore new ideas and improve the learning process as well as allowing plant operators training facilities and thereby increasing their ability to handle unforeseen situations.

The models developed in thesis are intended for all mentioned above purposes.

3.2.2.2 System Boundaries

The system boundaries define the scope of the model. A correct choice of the system boundaries is necessary so that all the important dynamics in the process are modeled.

If uncertainty exists about the correct choice of boundary, a criterion for boundary selection is to check whether the streams crossing the proposed boundary are easy to characterize. If the streams are well characterized, then the correct boundary has been chosen.

3.2.2.3 Time Constraints

Time constraints are important model restrictions to be chosen before construction of the dynamic models. Sometimes the process under investigation will contain a wide range of dynamic activity with widely varying speeds of response. Characteristic time constants in the process may range over several orders of magnitude. Invariably the modeler is interested in a simulation over a defined period of time.

The modeler should identify a 'time-scale-of-interest' and not model any latent dynamic effects outside this time-scale. This identification should be in the form of maximum and minimum characteristic time constant. Selection of an appropriate time-scale will also have the added advantage of possibly avoiding ultra-stable or stiff problems in the model numerical solution. These numerical problems occur in systems with widely varying time constants or speed of response (Willoughby, 1974). The wastewater treatment process belongs to this class.

3.2.2.4 Accuracy

The appropriateness of the model depends on the ability to predict the system performance within a prescribed accuracy. The accuracy sought will affect the degree of simplification which can be achieved in building the model. It is important that the desired accuracy of the model be specified before the model is constructed and that this accuracy reflected the purpose of the model. A measure of accuracy must be created to confirm this, or the accuracy must be confirmed during model validation.

3.2.3 Model Types

Many different classifications have been produced for the different model types which are available (e.g. Murthy et al., 1990; Jorgensen, 1992). The model types depend on the model philosophies.

3.2.3.1 Reductionist versus Holistic Models

Reductionist models are based on the attempt to include as many details as possible into the model and to describe the behaviour of a system as the net effect of all processes. In contrast to this approach, holistic models are based on a few important global parameters and on general principles.

3.2.3.2 Internal versus External Models

Internal (or mechanistic) models describe system response as a consequence of input

using the mechanistic structure of the system, whereas external (or input/output, black-box, empirical) models are based on empirical relationships between the input and output. Typical external models are time-series models (e.g., ARMAX models) and neural networks. A mechanistic model is a model based on fundamental engineering and scientific knowledge about the physical, chemical and biological mechanisms that affect a system. A model based on elementary principles tends to produce more reliable results when used for extrapolation. In complex systems it can be very difficult to obtain the necessary fundamental relationships of the process and, consequently a model must be based on empirical relationships. In practice, models are often a mixture of mechanistic and empirical models, using different concepts at different levels of resolution.

Depending on the mathematical form of their describing equations the models can be separated in several ways. Some of the most common ones are presented below:

3.2.3.3 Dynamic versus Static Models

This category arises between models that do or do not vary with time. Static model are often classified as steady-state models which model the equilibrium behaviour of the system. Conversely dynamic models account for the time varying responses of a system.

3.2.3.4 Deterministic versus Stochastic Models

Another classification arises between models that contain uncertainty or randomness in their final results and those that do not. Stochastic models are models in which the final outcome is not known with certainty but can be expressed as a distribution of all possible outcomes. In deterministic models all future outcomes are known with precision by the present state and the future values of the external variables (inputs) of the model.

3.2.3.5 Continuous-Time versus Discrete-Time Models

Continuous-time models are based on formulation of the rates of change of state variables. The values of the state variables as functions of time are then obtained as the solution of a system of differential equations. In contrast to this approach, discrete-time models are based on a division of time-scale into discrete intervals and specifying the state variables in a given time interval as algebraic functions of the values in the

immediately preceding time interval.

3.2.3.6 Distributed versus Lumped-Parameter Models

Many courses of events which are of interest to modeling are distributed not only in time but also in space. Mathematically, variables distributed in space can be described by partial differential equations and the resulting models are called distributed models. Application of such equations will, however, result in a complex simulation problem. A common way of overcoming this difficulty is to use the lumped-parameter approximation of these distributed equations. To use this approach, isotropic regions in the process are identified. These are regions in which composition, specific energy and momentum are approximately invariant with spatial dimension. The time-varying properties of this 'lump' are then calculated from the transfer of mass, energy and momentum over the boundary.

Other possible ways of classifying mathematical models are, for example, linear versus non-linear and continuous versus discrete-event models.

3.3 Biological models of the activated sludge process

Over the past two decades significant advances have been made in the areas of engineering design, implementation and operation of the activated sludge system (Cronje et al., 2002). The progressively biological removal of carbon (C), nitrogen (N) and phosphorus (P) by the activated sludge systems have been successfully designed and implemented at full-scale. A suite of steady state design models (WRC, 1984; Wentzel et al., 1990 and Maurer & Gujer, 1994) and kinetic simulation models (Dold et al., 1980; Dold et al., 1991; Henze et al., 1987; Henze et al., 1995; van Haandel et al., 1981 & Wentzel et al., 1992) had been developed. The University of Cape Town (UCT) (Dold et al., 1980) and Activated Sludge Model 1 (Henze et al., 1987) biological models are considered in the thesis.

3.3.1 UCT biological model

The UCT model is developed by Marais and Ekama at UCT. It gives mathematical representation of the biochemical processes of carbon and nitrogen removal at the beginning of the model development and of phosphorus removal at the later developments, going through different stages of model improvement. The full UCT model (Dold et al., 1991) consists of 14 different process including 14 state variables

and 21 parameters.

3.3.1.1 Carbon removal biological model

The UCT model is a mechanistic type of model. In the development of the UCT model Marais and Ekama (1976) included into the Lawrence and McCarty model (1970) some of the concepts proposed earlier by McKinney (1962), i.e. the generation of endogenous residue due to endogenous respiration and the accumulation of inert volatile solids due to the presence of this material in the influent. Furthermore, on the basis of a constant equivalence between organic mass (VSS) and substrate (COD), they functionally integrated the oxygen consumption with the growth and endogenous respiration of the microorganisms. The BOD was rejected as a suitable parameter for defining the organic material. They accepted the theory of electron donating capacity in its equivalent form, the COD. It should be noticed the greatest advantage of the Marais and Ekama (1976) model is that it

- differentiates between the active and inert sludge fractions,
- shows the biological reactions in terms of active mass, and
- permits the oxygen utilization rate to be determined directly from the biological reactions

Ekama and Marais (1979) applied the model to cyclically loaded completely mixed activated sludge processes where the influent is domestic wastewater. It was found impossible to correlate the predicted and observed oxygen consumption for low sludge ages. A rapid change in the oxygen consumption rate was observed at the moment of feed termination. The oxygen consumption continued for 1,5 to 2 hours at a rate of about 90 per cent of that measured just before the feed terminated, this was followed by a period of approximately 5 hours during which the oxygen consumption rate slowly decreased until, fairly abruptly, the rate steadied at a value which could be associated with endogenous respiration.

The difference between the observed and predicted response was ascribed by Ekama and Marais to the nature of the influent substrate. It was found that in domestic waste flows 60 to 70 per cent of the COD was in a fine particulate form (Morris and Stumm, 1960; Ford and Eckenfelder, 1967 and Wilson and Marais, 1976). The use of particulate substrate necessarily requires to be preceded by adsorption and storage on the organism, followed by extracellular enzymatic reactions prior to transfer through the cell wall. It is found that an adsorption mechanism is incorporated to store the particulate biodegradable material on the organism. They adopted the modified adsorption

mechanism which had been proposed by Blackwell (1971), the adapted mathematical equation is:

$$\frac{dS_b}{dt} = -K_a S_b X_a \left(f_{ma} - {X_s}/{X_a} \right) \qquad (3.3)$$

where K_a is the substrate transfer rate (mg COD/mg VASS/d), X_a is the active volatile solids concentration (mg VASS/l), S_b is the biodegradable substrate concentration in the liquid phase (mg COD/l), X_s is the stored substrate concentration (mg VSS/l), f_{ma} is the maximum fraction of substrate that can be stored on the active organism mass (mg VSS/mg VASS).

The explanation for the sudden drop in oxygen consumption rate at feed termination was due to an energy requirement for carbonaceous substrate adsorption as hypothesized by Ekama and Marais (1979). It was further a forecast that all the biodegradable COD in the domestic wastewater can be taken to be of a particulate nature although approximately 30 per cent of the COD is not removed by filtration. It is likely that the filtrate COD consists of large complex organic molecules which also require extracellular enzymatic breakdown. Now they accepted that all biodegradable COD must pass through the adsorption and storage stage. The conclusion of the hypothesis was that biological adsorption is an energy demanding reaction and they found the step change in oxygen consumption rate to determine the energy required for adsorption and storage of COD and calculated it to be 7,8 per cent of the COD mass removed from bulk concentration.

The use of the stored substrate for synthesis was modeled by a Monod type relationship linking the stored substrate concentration to the specific growth rate of the active organisms i.e.

$$\frac{1}{X_a}\frac{dX_a}{dt} = Y_h \left[\frac{K_m X_s P}{K_s + X_s P} \right] \qquad (3.4)$$

where Y_h is the growth yield coefficient in terms of stored substrate as mg COD/l (mg VSS/mg COD), K_m is the maximum specific substrate utilization rate (mg COD/mg VSS/d), K_s is the half saturation coefficient (mg COD/l), P is the COD:VSS ratio (mg COD/mg VSS)

A number of previous investigators had proposed this relationship (Blackwell, 1971; Jacquart et al., 1973 and Busby & Andrews, 1973) and the modeling for the synthesis of stored COD reaction was found to be adequate by Ekama and Marais.

3.3.1.2 Nitrification

The model proposed by (Downing et al., 1964) was the forerunner to the model of Ekama and Marais (1979) for biological nitrification. For this model the Monod relationship is used to relate the ammonia substrate concentration to the specific growth rate of the nitrifying bacteria. The influence of the presence of organic nitrogen on the nitrification kinetics is however not considered by the Downing model (1964).The inclusion of the effect of organic nitrogen into the model required two additions:

- A conversion of the organic nitrogen derived from the influent and from mass loss to ammonia, a relatively slow reaction which was found necessary to be included. It explains the experimental observation that in certain instances the nitrification rate is no longer governed by the ammonia concentration, but rather by the rate of conversion of organic nitrogen to ammonia.
- The incorporation of storage of organic nitrogen is necessitated by the storage of COD.

With this alteration, the model was found to give good performance with TKN, ammonia and nitrate concentrations observed during diurnal cyclic square wave loading tests.

3.3.1.3 Alterations to the model

The Alterations to the model of the Ekama and Marais (1979) is reviewed under the following considerations:

3.3.1.3.1 The Influence of Energy Requirement for Adsorption

The adsorbed state is thermodynamically associated with a lower energy level than the unadsorbed one. It should be noted that should this be true also for biologically mediated adsorption of organic material onto the organisms, the assumption that the adsorption is energy necessitating would appear to be suspect. From the appearance being reinforced consequently the experiments on completely mixed activated sludge behaviour using soluble, easily biodegradable substrate were performed. The oxygen utilization rate exhibited a sudden decrease at the feed termination under square wave cyclic loading conditions and usually the response of the plant was in accordance with the forecastings of the modified Lawrence and McCarty model. The hypothesis that sewage wastewater is composed of two fractions was obtained from pure

substrate experiments. The fractions are:

- a readily ingestible soluble fraction which is utilized at a very fast rate,
- a slowly biodegradable particulate fraction which requires storage and enzymatic breakdown prior to transfer through the cell wall.

The step change in the oxygen consumption rate at feed termination using sewage wastewater in terms of this hypothesis may be featured to the cessation of the oxygen utilization for the metabolism of the rapidly biodegradable substrate (COD) fraction in the influent. After the step change the behaviour remains a consequence of the storage of COD originated from the particulate, slowly biodegradable portion of the influent; it is found the mechanism of adsorption and storage of particulate COD remains unaltered, apart from that this operates on only the particulate fraction of the influent and does not require energy for adsorption.

For the bisubstrate hypothesis it was found that simulating the step change at feed termination, is estimated at 24 per cent of the biodegradable COD in the influent necessarily must be readily ingestible. The hypothesis was formulated in the following way: For the synthesis reaction the oxygen requirement forms 34 per cent of the COD metabolized; the balance, i.e. 66 per cent, becomes new cell mass (Marais and Ekama, 1976). The fraction of the biodegradable influent COD which is rapidly ingestible therefore, is 1/0,34 times the size of the step change in the oxygen utilization rate, i.e. 0,08/0,34 = 0,24. It is noted that 30 to 40 per cent of the COD in domestic wastewater is soluble compared to the fraction found which is not unreasonable.

3.3.1.3.2 The Influence of the Function of Adsorption

The adsorption is a mass transfer process and its mathematical equation as expressed in Eq. (3.3) is in compliance with mass transfer principles. For this reason there appeared to be no need to reconsider its detail, i.e. Eq. (3.3) was retained.

3.3.1.3.3 The Influence of Function of Enmeshment

The complete insensitivity of the effluent COD to severe cyclic load variations from the behaviour of the experimental Completely Mixed Activated Sludge (CMAS) process could not be explained by the adsorption hypothesis alone. An additional hypothesis was required that all the particulate material not adsorbed was enmeshed in the sludge mass, densified in the settling tank and recycled to the reactor. This assumption has

great support from the observation that inert particulate material does not appear in the overflow from the settling tank.

3.3.1.3.4 The Influence of Synthesis of Active Mass

The adoption of the bi-substrate postulate immediately adds the dilemma of the reaction of the organism mass to the dual substrates. The precise mechanism cannot be given because more detailed simulation studies are required. Now the two substrates are acted on independently by the same active mass and that the sludge synthesized is the sum of these two metabolic reactions.

3.3.1.3.5 The Influence of Soluble substrate

Lawrence and McCarty (1970) had an identical relationship for the synthesis of active mass from readily ingestible substrate fraction i.e. a Monod formulation linking the specific growth rate of the active mass to the soluble substrate concentration in the liquid phase:

$$\frac{1}{X_a}\frac{dX_a}{dt} = Y_h\left[\frac{K_{ms}S_{bs}}{K_{ss}+S_{bs}}\right] \tag{3.5}$$

where S_{bs} is the soluble biodegradable substrate concentration (mg COD/l), K_{ms} is the maximum specific substrate utilization rate for soluble substrate (mg COD/mg VSS/d), K_{ss} is the half-saturation coefficient for soluble substrate (mg COD/l). This correlation have been appraised by Gaudy et al. (1971) as inappropriate for modeling transient behaviour of the activated sludge treating readily ingestible soluble substrates. They found that the correlation did not accurately forecast the change in organism growth behaviour for a period after a step change in the feed rate. Gaudy et al (1971) found the process behaviour had noticeable differences in the experimental conditions. They found after the transitory behaviour between the two steady state conditions for the duration of an experiment that a change in the food to micro-organism ratio was approximately 170 times. In comparison, the activated sludge process is usually concerned with relatively small disturbances about a steady state condition for which the maximum point food to micro-organism ratio is usually 5 times the average value.

3.3.1.3.6 The Influence of Particulate substrate

The use of particulate substrate requires

- adsorption and storage

- extracellular enzymatic breakdown of the complex organic molecules to simpler ones in order to pass through the cell wall for synthesis by the organism.

The total reaction rate is prolonged and an order of magnitude slightly delayed than that for a soluble substrate for example like glucose. The bound rate is unlikely to be in the metabolism of the material that has been secreted through the cell wall. It is believed the bound rate is determined by the extracellular breakdown rate of stored particulate substrate to smaller molecules. Should this reason be correct, then Eq. (3.4) is no longer valid to express the growth rate of the active mass for using particulate substrate because it does not recognize the true rate bound mechanism, i.e. extracellular enzymatic breakdown rate. The reason equation (3.4) can be justified is because its use has given satisfactory predictions of the dynamic behaviour of the CMAS process treating domestic sewage. It has been found that this explanation no longer holds. If looking at simulations of the BOD-time curve in the BOD test on municipal effluents, now the primary active mass concentration is minute approximately very much less than 1mg/l. Practically no growth (and no oxygen demand) and no removal of the particulate biodegradable organic fraction in the BOD sample was forecasted for the use of the particulate BOD. If Eq. (3.4) was applied in the forecast of the behaviour of the aerated lagoon activated sludge process, at sludge ages (retention times) less than two days and low temperatures (12 C), an operational paradigm was forecasted that indicated an insufficient sludge growth rate and partial failure by washout.

A comprehensively analysis of the atypical behaviour described before indicated that it arises from equation (3.4). The adsorption and synthesis operations (equations (3.3) and (3.4)) respectively, behave in conjunction. The stored substrate concentration (X_s) is restricted by the active mass concentration (X_a) as shown by equation (3.3) and the amount of the maximum fraction of substrate that can be stored on the active organism mass (f_{ma}). The value of f_{ma} appears to be close to unity, this can be shown from simulation research and proof in the scientific papers (Porges, Jasewicz and Hoover, 1956).Subsequently if X_a is low, X_s is essentially also low and from equation (2) the synthesis rate also will be low. It has been found to be quite the opposite to the assumption in the event the growth rate should be near to the peak amount because there is a large amount of X_s relative to X_a. This inadequacy stems from the fact that the stored substrate is defined in concentration units relative to the bulk liquid phase but

rather should be defined relative to the active organism concentration. This inadequacy was recognized by Stenstrom (1975) and he proposed the following change:

$$\frac{1}{X_a}\frac{dX_a}{dt} = Y_h\left[\frac{K_m(X_s/X_v)}{K_{fs} + (X_s/X_v)}\right] = Y_h\left[\frac{K_m f_s}{K_{fs} + f_s}\right] \qquad (3.6)$$

where f_s is the X_s/X_v (mg VSS/mg VSS), K_{fs} is the half saturation coefficient for synthesis (mg VSS/mg VSS), X_v is the total volatile solids concentration (mg VSS/l).

3.3.1.3.7 The Influence of Endogenous Respiration

The occurrence generally known as endogenous respiration shows itself by reduction of active volatile mass per unit active mass per unit time if there is no biodegradable substrate present. The mass of the sludge that disappears is used by the organisms and therefore is directly equated to the oxygen consumption for the endogenous respiration. An unbiodegradable fraction remains and therefore accumulates in the process as endogenous residue.

The endogenous respiration has due to the energy requirement for organism maintenance since a fraction of the organism mass disappears to supply energy for maintenance of the mass remaining. For the requirement to make the energy available an electron acceptor must be present. It should be noted that in the activated sludge process, either oxygen or nitrate can serve as the electron acceptor. The single sludge nitrification-denitrification process showed a main difficulty in situations where both the oxygen and nitrate concentrations in a reactor are zero, that is when nitrate has been completely denitrified in an anoxic reactor. If no oxygen or nitrate is present, maintenance energy cannot be released. Now what happens to the organism under these circumstances? A qualitative change in the organism behavioral pattern can be accommodated by the introduction of dissolved oxygen and nitrate deficient conditions. Therefore this presented complexities in the model which could not be verified when fundamental endogenous respiration mechanism was not clearly understood. Subsequently, the goal became to find an easy alternative model which could logically answer the discrepancies regarding endogenous respiration in both aerobic and anoxic conditions, which in situations where aerobically generated organisms are placed in an anaerobic state for a short time. This instituted the evolution of the death –regeneration model.

In the death-regeneration model an endeavor is made to split reactions which possibly take place during the death phase of the organisms. It is proposed that the percentage of live mass that disappears in fact dies, lyses biodegradable substrate back in to the liquid and leaves the balance as unbiodegradable endogenous residue. The biodegradable COD in the liquid is added to the lased biodegradable and passes through the same phases of adsorption, storage and storage abstraction for synthesis. This proposal, states that endogenous respiration (cell maintenance) it is believed does not exist and that oxygen is consumed only for synthesis of new cell material from the lysed energy. It is found that the death-regeneration approach provides a convenient, simple and reliable framework in which to propose the biological kinetics of the anoxic-aerobic activated sludge process.

3.3.2 Description of the UCT mathematical model equations

The variables used to mathematically describe the activated sludge process in the UCT model are 14. Their notations and names according to UCT and ASM1 model (SIMBA software package (SIMBA 4, User guide 2001) are given in Table 3.1

Table 3.1: Biological fractions, descriptions and units of the UCT model

Variable notation UCT/SIMBA	Description	Unit
Z_{BH} /XBH	Heterotrophic biomass	$g\ COD/m^3$
Z_{BA} /XBA	Autotrophic biomass	$g\ COD/m^3$
Z_E /XP	Endogenous biomass	$g\ COD/m^3$
Z_I /XI	Inert biomass	$g\ COD/m^3$
S_{ads} /XSA	Adsorbed slowly biodegradable substrate	$g\ COD/m^3$
S_{enm} /XSE	Enmeshed slowly biodegradable substrate	$g\ COD/m^3$
N_{obp} /XND	Biodegradable particulate organic nitrogen	$g\ COD/m^3$
S_{bs} /SS	Soluble substrate	$g\ COD/m^3$
N_a /SNH	Ammonia nitrogen	$g\ N/m^3$
N_{obs} /SND	Biodegradable soluble organic nitrogen	$g\ N/m^3$
N_{o3} /SNO	Nitrate nitrogen	$g\ N/m^3$
Alk/SALK	Alkalinity	Mol/m^3
S_{us} /SI	Unbiodegradable soluble substrate	$g\ COD/m^3$
O/SO	Oxygen	$g\ COD/m^3$

The UCT model characterizes the biochemical processes, their kinetics and the compounds on which they act and describes their behaviour at a single point in the system. The process model is presented in a matrix form known as the Paterson matrix in Table 3.2. This matrix provides a quantitative description of interrelationships between the processes and associated compounds. The switching functions are described in a Table 3.3. The default values of the process parameters are given in a Table3.4.

Table 3.2: Peterson Matrix representation of the UCT model

COMPOUND → PROCESS ↓ $f_{ZB,N}$ $-f_E f_{ZE,N}$	1 Z_{BH}	2 Z_{BA}	3 Z_E	4 Z_I	5 S_{ads}	6 S_{enm}	7 N_{obp}	8 S_{bs}	9 N_a	10 N_{obs}	11 N_{o3}	12 Alk	13 S_{us}	14 O	PROCESS RATES, P_j
1 Aerobic growth of Z_{BH} on S_{bs} with N_a	1							$-1/Y_{ZH}$	$-f_{ZB,N}$			$-f_{ZB,N}/14$		$-\frac{1-Y_{ZH}}{Y_{ZH}}$	$\hat{\mu}_H \left[\frac{S_{bs}}{K_{SH}+S_{bs}}\right] \begin{bmatrix} HAir \\ on \end{bmatrix} \left[\frac{N_a}{Limit}\right] Z_{BH}$
2 Aerobic growth of Z_{BH} on S_{bs} with N_{o3}	1							$-1/Y_{ZH}$			$-f_{ZB,N}$	$f_{ZB,N}/14$		$-\frac{1-Y_{ZH}}{Y_{ZH}}$	$\hat{\mu}_H \left[\frac{S_{bs}}{K_{SH}+S_{bs}}\right] \begin{bmatrix} HAir \\ on \end{bmatrix} \left[\frac{1-N_a}{Limit}\right] \left[\frac{N_{o3}}{Limit}\right] Z_{BH}$
3 Anoxic growth of Z_{BH} on S_{bs} with N_a	1							$-1/Y_{ZH}$	$-f_{ZB,N}$		$-\frac{1-Y_{ZH}}{2.86Y_{ZH}}$	A*			$\hat{\mu}_H \left[\frac{S_{bs}}{K_{SH}+S_{bs}}\right] \begin{bmatrix} H\ Air \\ Off \end{bmatrix} \left[\frac{N_a}{Limit}\right] \left[\frac{N_{o3}}{Limit}\right] Z_{BH}$
4 Anoxic growth of Z_{BH} on S_{bs} with N_{o3}	1							$-1/Y_{ZH}$			B*	C*			$\hat{\mu}_H \left[\frac{S_{bs}}{K_{SH}+S_{bs}}\right] \begin{bmatrix} H\ Air \\ Off \end{bmatrix} \left[\frac{1-N_a}{Limit}\right] \left[\frac{N_{o3}}{Limit}\right] Z_{BH}$
5 Aerobic growth of Z_{BH} on S_{ads} with N_a	1				$-1/Y_{ZH}$				$-f_{ZB,N}$			$-f_{ZB,N}/14$		$-\frac{1-Y_{ZH}}{Y_{ZH}}$	$\left[\frac{(S_{ads}/Z_{BH})}{K_{SP}+(S_{ads}/Z_{BH})}\right] \begin{bmatrix} HAir \\ on \end{bmatrix} \left[\frac{N_a}{Limit}\right] Z_{BH} K_{MP}$
6 Aerobic growth of Z_{BH} on S_{ads} with N_{o3}	1				$-1/Y_{ZH}$						$-f_{ZB,N}$	$f_{ZB,N}/14$		$-\frac{1-Y_{ZH}}{Y_{ZH}}$	$\left[\frac{(S_{ads}/Z_{BH})}{K_{SP}+(S_{ads}/Z_{BH})}\right] \begin{bmatrix} HAir \\ on \end{bmatrix} \left[\frac{1-N_a}{Limit}\right] \left[\frac{N_{o3}}{Limit}\right] Z_{BH} K_{MP}$

7 Anoxic growth of Z_{BH} on S_{ads} With N_a	1				$-1/Y_{ZH}$				$-f_{ZB,N}$		$-\frac{1-Y_{ZH}}{2.86Y_{ZH}}$	A*			$\left[\frac{(S_{ads}/Z_{BH})}{K_{SP}+(S_{ads}/Z_{BH})}\right]$ $\begin{bmatrix} H\ Air \\ Off \end{bmatrix}\left[\begin{matrix} N_a \\ Limit \end{matrix}\right]\left[\begin{matrix} N_{O3} \\ Limit \end{matrix}\right] Z_{BH} K_{MP} \eta_G$
8 Anoxic growth of Z_{BH} on S_{ads} With N_{o3}	1				$-1/Y_{ZH}$		$f_{ZB,N}-f_E f_{ZE,N}$				B*	C*			$\left[\frac{(S_{ads}/Z_{BH})}{K_{SP}+(S_{ads}/Z_{BH})}\right]$ $\begin{bmatrix} H\ Air \\ Off \end{bmatrix}\left[\begin{matrix} 1-N_a \\ Limit \end{matrix}\right]\left[\begin{matrix} N_{O3} \\ Limit \end{matrix}\right] Z_{BH} K_{MP} \eta_G$
9 Death of Z_{BH}			f_E			$1-f_E$									$b_H Z_{BH}$
10 Adsorption of S_{enm}						-1									$K_A S_{enm} Z_{BH}(f_{MA}-S_{ads}/Z_{BH})$
11 Hydrolysis of N_{obp}							-1			1					$(p_5+p_6+p_7+p_8)$ (N_{obp}/S_{ads})
12 Ammonification of N_{obs}									1	-1		1/14			$K_R N_{obs} Z_{BH}$
13 Aerobic growth of Z_{BA}		1							$-1/Y_{ZA}$ $-f_{ZB,N}$		$1/Y_{ZA}$	$-f_{ZB,N}/14$ $-1/(7Y_{ZA})$		$-\frac{4.57-Y_{ZA}}{Y_{ZA}}$	$\hat{\mu}_A\left[\frac{N_a}{K_{SA}+N_a}\right]\begin{bmatrix} A\ Air \\ on \end{bmatrix} Z_{BA}$
14 Death of Z_{BA}		-1	f_E			$1-f_E$	$f_{ZB,N}-f_E f_{ZE,N}$								$b_A Z_{BA}$
KEY	A* = $\frac{1-Y_{ZH_Z}}{14*2.86Y_{ZH}}-f_{ZB,N}/14$, B* = $\frac{1-Y_{ZH}}{2.86Y_{ZH}}-f_{ZB,N}$, C* = $\frac{1-Y_{ZH_Z}}{14*2.86Y_{ZH}}+f_{ZB,N}/14$														

Table 3.3: Switching functions and formulae of the UCT biological model

Switching function	$\begin{bmatrix} H\ Air \\ On \end{bmatrix}$	$\begin{bmatrix} H\ Air \\ Off \end{bmatrix}$	$\begin{bmatrix} H\ Air \\ On \end{bmatrix}$	$\begin{bmatrix} N_a \\ Limit \end{bmatrix}$	$\begin{bmatrix} 1-N_a \\ Limit \end{bmatrix}$	$\begin{bmatrix} N_{O3} \\ Limit \end{bmatrix}$
Formula	$\frac{O}{K_{OH}+O}$	$\frac{K_{OH}}{K_{OH}+O}$	$\frac{O}{K_{OA}+O}$	$\frac{N_a}{K_{HA}+N_a}$	$\frac{K_{HA}}{K_{HA}+N_a}$	$\frac{N_{O3}}{K_{NO}+N_{O3}}$

Table 3.4: Default values for kinetic, stoichiometric and switching function constants in the UCT model

SIMBA SYMBOL	VALUE	UNITS	UCTold
Kinetic parameters $(20\ ^{\circ}C)$			
myH	2,5	d^{-1}	$\hat{\mu}_H$
KSH	5,0	$g\ COD\ m^{-3}$	K_{SH}
KMP	1,35	$g\ COD\ \ (g\ cell\ COD.d)^{-1}$	K_{MP}
KSP	0,027	$g\ COD\ \ (g\ cell\ COD)^{-1}$	K_{SP}
BH	0,62	d^{-1}	b_H
KA	0,17	$g\ COD\ \ (g\ cell\ COD.d)^{-1}$	K_A
KR	0,032	$m^3\ (g\ cell\ COD.d)^{-1}$	K_R
myA	0,5	d^{-1}	$\hat{\mu}_A$
KSA	1,0	$g\ NH_3 - N\ m^{-3}$	K_{SA}
bA	0,04	d^{-1}	b_A
nyG	0,33	-	η_G
Stoichiometric parameters			
YH	0,666	$g\ cell\ COD\ (g\ COD\ utilized)^{-1}$	Y_{ZH}
YA	0,15	$g\ cell\ COD\ (g\ N\ utilized)^{-1}$	Y_{ZA}
fMA	1,00	$g\ COD\ (g\ cell\ COD)^{-1}$	f_{MA}
fP	0,08	-	f_E
iXB	0,068	$g\ N\ (g\ COD)^{-1}$ *in active mass*	$f_{ZB,N}$
iXP	0,068	$g\ N\ (g\ COD)^{-1}$ *in endogenous mass*	$f_{ZE,N}$
Switching Function Parameters			
KOH	0,002	$g\ O_2\ m^{-3}$	K_{OH}
KOA	0,002	$g\ O_2\ m^{-3}$	K_{OA}

KNA	0,01	$g\ NH_3 - N\ m^{-3}$	K_{NA}
KNO	0,1	$g\ NO_3 - N\ m^{-3}$	K_{NO}
Arrhenius temperature dependency constants			
$K_{i,T} = K_{i,20}\theta^{(T-20)}$			
		where $K_{i,T} = K_i\ at\ T\ °C$ $\theta = Arrhenius\ cons\tan t$	
myH	1,200	-	$\hat{\mu}_H$
KSH	1,000	-	K_{SH}
KMP	1.080	-	K_{MP}
KSP	0,910	-	K_{SP}
BH	1,029	-	b_H
KA	1,029	-	K_A
fMA	1,000	-	f_{MA}
KR	1,029	-	K_R
myA	1,123	-	$\hat{\mu}_A$
KSA	1,123	-	K_{SA}
bA	1,029	-	b_A

A short description of the processes and their stoichiometric interactions with the compounds is given below (Dold et al., 1991).

Processes 1 and 2: Aerobic growth of heterotrophs on readily biodegradable COD. These two processes are accountable for elimination of the readily biodegradable substrate under aerobic conditions. A fraction of the readily biodegradable COD is utilized for the production (growth) of heterotrophic biological (active) organism mass (synthesis) and the balance is oxidized for energy giving rise to an associated synthesis oxygen demand. The growth is replicated using Monod kinetics. In the process 1, concomitant with the growth, ammonia is used as a nitrogen source for synthesis, and there is an associated alkalinity change. Should ammonia become limiting, nitrate can serve as an alternative nitrogen source for synthesis, Process 2. This is achieved by incorporating switching functions dependent on the

ammonia concentration, which switch Process 1 off and Process 2 on when ammonia reduces to near zero but nitrate is available as a nitrogen source. Should both ammonia and nitrate reduce to zero, growth Processes 1 and 2 are switched off. Additional switching functions in both Processes 1 and 2 ensure that these processes only operate if oxygen is present as electron acceptor- as the oxygen concentration reduces to zero there is a switch from aerobic to anoxic growth (Processes 3 and 4) with nitrate as electron acceptor.

Processes 3 and 4: Anoxic growth of heterotrophs on readily biodegradable COD
In the absence of oxygen, the heterotrophic organism population is capable of utilizing nitrate, if available, as acceptor with readily biodegradable COD as substrate. In these two processes, a fraction of the readily biodegradable COD is used for production (growth) of heterotrophic biological (active) organism mass and balance is oxidized giving rise to reduction of nitrate to nitrogen gas. The anoxic growth is replicated on the basis of the same Monod kinetics used for aerobic growth (Processes 1 and 2). As in aerobic growth (with readily biodegradable COD), ammonia (Process 3) or nitrate (Process 4) can serve as nitrogen source for cell synthesis, this is accommodated through switching functions. Further switching functions in both Processes 3 and 4 ensure that the anoxic growth rates decrease to zero at low nitrate concentrations.

Processes 5 and 6: Aerobic growth of heterotrophs on adsorbed slowly biodegradable COD.
In these two processes the slowly biodegradable COD, which has been adsorbed on the organism (Process 10), is utilized under aerobic conditions. This use consists of two steps, hydrolysis of the adsorbed slowly biodegradable COD and direct utilization of the hydrolysis products for the production (growth) of active organism mass (synthesis) and its associated oxygen demand. Since the rate limiting step is hydrolysis, only this step is modeled, using Levenspiel's surface reaction kinetics (Dold et al, 1980). As in aerobic growth on readily biodegradable COD, ammonia (Process 5) or nitrate (Process 6) can serve as a nitrogen source for cell synthesis; this is achieved by incorporating switching functions dependent on the ammonia concentration. Also, switching functions ensure that both processes operate only if oxygen is present as electron acceptor; at low oxygen concentrations there is a switch to anoxic growth(Processes 7 and 8) with nitrate as electron acceptor.

Processes 7 and 8: Anoxic growth of heterotrophs on adsorbed slowly biodegradable COD.

These processes are modeled in the same way as for aerobic growth Processes 5 and 6 except that in absence of oxygen, nitrate serves as an alternative electron acceptor and that the Levenspiel surface reaction for hydrolysis/utilization kinetic rate expression is multiplied by the factor of .33 (nyG). Again, either ammonia (Process 7) or nitrate (Process 8) can serve as nitrogen source for cell synthesis. Switching functions in both Processes 7 and 8 ensure that the anoxic growth rates decrease to zero at low nitrate concentrations.

Process 9: Death of heterotrophs.

The process is modeled according to the death- regeneration hypothesis. That is, the heterotrophic organism mass dies at a certain rate per unit organism mass; a portion of the material from the death is unbiodegradable particulate and adds to the unbiodegradable endogenous residue while the remainder adds to the pool of slowly biodegradable COD. Nitrogen associated with the biodegradable portion adds to the pool of particulate organic nitrogen. The process of organism death is assumed to continue under aerobic, anoxic and anaerobic conditions.

Process 10: Adsorption of slowly biodegradable COD.

Slowly biodegradable COD is assumed to be enmeshed in the sludge mass immediately on contact with mixed liquor. The absorption process transfer the enmeshed slowly biodegradable to the adsorbed slowly biodegradable COD.

Process 11: Hydrolysis of particulate organic nitrogen.

Biodegradable particulate organic nitrogen is broken down to soluble organic nitrogen at a rate linked directly to the rate of hydrolysis/utilization of adsorbed slowly biodegradable COD under both aerobic (Processes 5 and 6) and anoxic (Processes 7 and 8) conditions. The product of breakdown adds to the pool of soluble organic nitrogen.

Process 12: Ammonification of soluble nitrogen.

Biodegradable soluble organic nitrogen is converted to free and saline ammonia, a process mediated by heterotrophic biological active mass. Hydrogen ions consumed in the conversion process results in an alkalinity change.

Process 13: Aerobic growth of autotrophs.

In this process ammonia is oxidized to nitrate via a single step resulting in production (growth) of autotrophic biological active mass and giving rise to an associated nitrification oxygen demand. The process requires the presence of oxygen; a switching function ensures that the process operates only if oxygen is present. This operation has a marked effect on the estimated total oxygen demand; the effect on total Mixed Liquor Volatile Suspended Solids (MLVSS) is small as the yield of autotrophic nitrifiers is low. As with the growth of heterotrophs, ammonia nitrogen is included in the new cells and the alkalinity is affected.

Process 14: Death of autotrophs.

This operation is similar to that of the heterotrophs (Process 9).

3.4 Discussion

Marais and Ekama (1976) hypothesized the Lawrence and McCarty model (1970) which was proposed by McKinney (1962) for the generation of endogenous residue due to endogenous respiration and accumulation of inert volatile solids due to presence of this material in the influent. Marais and Ekama (1976) contributed three salient points namely, differentiating between active and inert sludge fractions; showing the biological reactions in terms of active mass; permitting oxygen utilization rate (o.u.r.) to be determined directly from biological reactions.

The Peterson matrix has equations modeled on the Monod kinetics and switching functions for example if one looks at the fraction of the aerobic growth of heterotrophs on readily biodegradable COD can see from the first row which are the process compounds affected by this growth process. Every compound dynamics is influenced by different processes. Mathematically this dependence can be described by the differential equation summing the products between the stoichiometric coefficients from the corresponding column with the associated process rate, for example for the dynamics of the heterotrophs:

$$\frac{dZ_{BH(a)}}{dt} = \hat{\mu}_H \left[\frac{S_{bs}}{K_{SH}+S_{bs}}\right]\left[\begin{matrix}HAir\\on\end{matrix}\right]\left[\frac{N_a}{Limit}\right]Z_{BH} + \hat{\mu}_H \left[\frac{S_{bs}}{K_{SH}+S_{bs}}\right]\left[\begin{matrix}HAir\\on\end{matrix}\right]\left[\frac{1-N_a}{Limit}\right]\left[\frac{N_{o3}}{Limit}\right]Z_{BH} +$$
$$+\hat{\mu}_H \left[\frac{S_{bs}}{K_{SH}+S_{bs}}\right]\left[\begin{matrix}HAir\\Off\end{matrix}\right]\left[\frac{N_a}{Limit}\right]\left[\frac{N_{o3}}{Limit}\right]Z_{BH} + \hat{\mu}_H \left[\frac{S_{bs}}{K_{SH}+S_{bs}}\right]\left[\begin{matrix}HAir\\Off\end{matrix}\right]\left[\frac{1-N_a}{Limit}\right]\left[\frac{N_{o3}}{Limit}\right]Z_{BH} + \quad (3.7)$$
$$+\left[\frac{(S_{ads}/Z_{BH})}{K_{SP}+(S_{ads}/Z_{BH})}\right]\left[\begin{matrix}HAir\\on\end{matrix}\right]\left[\frac{N_a}{Limit}\right]Z_{BH}K_{MP} + \left[\frac{(S_{ads}/Z_{BH})}{K_{SP}+(S_{ads}/Z_{BH})}\right]\left[\begin{matrix}HAir\\on\end{matrix}\right]\left[\frac{1-N_a}{Limit}\right]\left[\frac{N_{o3}}{Limit}\right]Z_{BH}K_{MP} +$$
$$+\left[\frac{(S_{ads}/Z_{BH})}{K_{SP}+(S_{ads}/Z_{BH})}\right]\left[\begin{matrix}HAir\\Off\end{matrix}\right]\left[\frac{N_a}{Limit}\right]\left[\frac{N_{o3}}{Limit}\right]Z_{BH}K_{MP}\eta_G + \left[\frac{(S_{ads}/Z_{BH})}{K_{SP}+(S_{ads}/Z_{BH})}\right]\left[\begin{matrix}HAir\\Off\end{matrix}\right]\left[\frac{1-N_a}{Limit}\right]\left[\frac{N_{o3}}{Limit}\right]Z_{BH}K_{MP}\eta_G$$

The Ekama's and Marais's model (1979) uses the Monod relationship to relate the ammonia substrate concentration to the specific growth rate of the nitrifying bacteria. Since the inclusion of the effect of organic nitrogen is considered in this model but was not considered for the forerunner model (Downing et al, 1964) namely the nitrification rate is no longer dominated by the ammonia concentration but rather by the conversion rate of organic nitrogen to ammonia; the incorporation of storage nitrogen is required by the storage of COD.

The influence of synthesis of active mass which has adopted the bisubstrate postulate, immediately adds the dilemma of the reaction of the organism mass of dual substrates. It has been suggested that the two substrates are acted on independently by the same active mass and that the sludge synthesized is the total of these two metabolic reactions.

3.4.1 Activated Sludge Model No.1 (ASM1)

The International Association on Water Pollution Research (IAWPR) in 1983 established a Task Group on Mathematical Modeling for Design and Operation of Activated Sludge Processes which developed the Activated Sludge Model No.1 (ASM1) in 1987. When the ASM1 was published, biological phosphorus removal had already being used in a limited capacity on full-scale treatment plants. The ASM1 is simpler than UCT model having the capability of realistically describing the behaviour of single sludge systems carrying out carbon oxidation, nitrification and denitrification.

3.4.2 Model Process Operation Rates

The task group developed the ASM1 model on the basis of the following considerations:

- The establishment of a mathematical model involves balancing contradiction requirements. This involves balancing on the one hand, a model

which must include the large occurrences within a system in a degree which is consistent with the known information about the system. Whilst on the other side, the model equations must be soluble within certain reason and effort. The model solution difficulty increases with the increasing series of processes. It is found the more closely the process rate expressions resemble reality, the more difficulty they would be.

- Those processes which are essential to a real solution would be included by the modeler who will select rate expression for them that allow the utilizing of simplified solution methods without detracting from the applicability of the conclusion. This may require the choice of greatly simplified rate expressions in many cases. Because the rate expressions do not copy real-life events which occur in a system, they could be used to simulate the outcome of those events.
- On the above base processes and rate expressions were selected to be included in the model. The task group found the major events to focus on and choose the simplest rate expressions consistent with them. The modifications of the UCT model were proposed in terms of enmeshment-adsorption (storage) and in the volatilization (hydrolysis) concepts. The task group rejected the concept that the biodegradable particulate COD was adsorbed and stored on the organism mass. They proposed that the enmeshed biodegradable material was hydrolyzed to readily biodegradable COD and released to bulk liquid by the action of extracellular enzymes secreted by the organisms. For the denitrification the group separated the processes of hydrolysis and growth.
- Furthermore the task group developed the notion of switching functions to turn process rate equations on and off as environmental conditions deem fit such as the classical case of the electron acceptor present. Where the bacteria which are responsible for nitrification would be capable of growth only under aerobic conditions and their growth rate will drop to zero as the dissolved oxygen concentration approaches zero, no matter the concentration of their energy yielding substrate. This can be replicated by including dissolved oxygen 'switch' in the process rate equations. The task group adopted the following oxygen switching function: $\frac{S_O}{K_O + S_O}$ where S_O is the concentration of dissolved oxygen. The choice of a small value for K_O indicates that the value of the switching function is near unity under moderate dissolved oxygen (DO) concentrations but decreases to zero as the DO concentration approaches zero. Because the function is mathematically continuous this leads to the elimination of problems of numerical instability which would happen during simulations which include the rate equations that are switched on and off discontinuously. The alternative may occur where the dissolved oxygen is absent which may be turned on by the following switching function: $\frac{K_O}{K_O + S_O}$

3.4.3 The basic principles of the model building

A lot of assumptions and principles of the UCT model were accepted for development of the ASM1 model. The primary focus of the task group was the predictions of activated sludge concentration and not the concentrations of soluble constituents in the vessels and the electron acceptor requirements for the development of the model. A matter of confusion has been lead by development of activated sludge theory due to the inhibition of a regular measure of the concentration of organic material in

wastewater. Three values have been measured and used: biochemical oxygen demand (BOD), total organic carbon (TOC), and chemical oxygen demand (COD). COD is the best measure because it alone provides a connection between electron equivalents in the organic substrate, biomass and oxygen utilized (Gaudy and Gaudy, 1971). For COD, mass balances can be made and subsequently the concentrations of all organic materials, including biomass are in COD units in the ASM1 model. COD provides the link between electron equivalent in the organic substrate, the biomass and the oxygen utilized. The organic matter may be tabulated into a number of sections, (McKinney & Ooten, 1969) and (Dold et al.,1980). The first important subclass is based on biodegradability.

3.4.3.1 The influence of non-biodegradable organic matter

The non-biodegradable organic matter passes through an activated sludge system in a biologically inert fashion. The fractions can be divided into two depending on their physical state, viz., soluble and particulate. The inert soluble organic matter S_I remains unchanged in concentration when it enters and leaves the system. The inert suspended organic matter X_I becomes enmeshed in the activated sludge and is finally removed from the system through sludge wastage. Since the waste sludge flow rate is smaller than the system inflow rate, a mass balance requires the concentration of X_I in the system to be higher than the inflow concentrations.

3.4.3.2 The influence of biodegradable organic matter

The biodegradable organic matter could be divided into two fractions, viz., readily biodegradable and slowly biodegradable. For modeling purposes, the readily biodegradable matter S_S is treated as soluble where the slowly biodegradable matter, X_S is treated as if it is particulate but this is certainly not the case because it could be soluble. S_S consists of small molecules which are consumed by heterotrophic bacteria and utilized for growth of biomass. A part of the energy (COD) in conjunction with the molecules combined into the biomass and the balance is required for the energy for synthesis. The electrons associated with that portion are transferred to oxygen or nitrate which are known as exogenous electron acceptors. In comparison, X_S consist of complex molecules which are digested and adsorbed extracellularly and conversion into readily biodegradable substrate by means of hydrolysis which

involves no energy utilization. Thus no utilization of electron acceptor associated with it.

The X_S has a specific rate of hydrolysis which is usually considerably lower than the utilization specific rate of S_S, so that it becomes the rate-limiting factor in the growth of biomass when X_S alone is present as substrate. The hydrolysis rate is furthermore lower under anoxic conditions (for the terminal electron acceptor there is only nitrate available) than under aerobic situations and is apparently stopped under anaerobic conditions (neither nitrate nor oxygen are present) as stated by van Haandel et al. (1981). The branching of substrate into two forms provides a built–in lag in uptake of electron acceptors that allows for space-time dependent differences in oxygen and nitrate utilization to be modeled.

3.4.3.3 The influence of heterotrophic biomass

The S_S has heterotrophic biomass generated by growth on it under following situation of either aerobic or anoxic conditions whereas under anaerobic conditions it is assumed to be stopped. A whole of decay mechanisms come in play for when the biomass is lost which involves endogenous metabolism, death, predation and lysis. The decay is assumed to result in the conversion of biomass into X_S and particulate end products, X_P which are inert and not prone to further biological attack as found by Dold et al (1980). The latter is similar formalization to the endogenous mass of McKinney and Ooten (1969) which act to reduce the viability of the suspended matter in the bioreactor. The loss of the biomass by decay is assumed to occur at a rate which is independent of the concentration (nature) of the electron acceptor present. But the conversion of end product X_S to form that can be used for regrowth of new cells influenced by the electron acceptor.

3.4.3.4 The influence of nitrogenous matter

In WWTP nitrogenous matter, like carbonaceous matter can be divided into two different categories: non-biodegradable and biodegradable with further subdivisions. The non-biodegradable fraction has a particulate part connected with the non-biodegradable particulate COD whilst the soluble part is relatively small and not included into the model. The biodegradable nitrogenous material may be divided into

three branches, namely free saline ammonia, S_{NH}; soluble organic nitrogen, S_{ND}; and particulate organic nitrogen, X_{ND}. The particulate organic nitrogen reacts by means of hydrolysis to soluble organic nitrogen in conjunction with hydrolysis of slowly biodegradable organic material whilst soluble organic nitrogen is acted on by heterotrophic bacteria and converted to ammonia nitrogen. The nitrogen supply for the synthesis for heterotrophic bacteria is served by ammonia nitrogen and as the energy supply for the growth of autotrophic nitrifying bacteria which is converted to nitrate nitrogen in a unitary step requiring oxygen. The terminal electron acceptor for heterotrophic bacteria is served and formed by the nitrate under anoxic conditions with the evolution of nitrogen gas. Either autotrophic or heterotrophic biomass of cell decay leads to evolution of particulate organic nitrogen which can re-enter the cycle.

The ASM1 model is represented by its Peterson matrix given in Table 3.5

Table 3.5: ASM1 Peterson Matrix Model

Component → i		1	2	3	4	5	6	7	8	9	10	11	12	13	Process Rate, ρ_j [ML^{-3}T^{-1}]
j	Process ↓	S_I	S_S	X_I	X_S	$X_{B,H}$	$X_{B,A}$	X_P	S_O	S_{NO}	S_{NH}	S_{ND}	X_{ND}	S_{ALK}	
1	Aerobic growth of heterotrophs		$-\frac{1}{Y_H}$			1			$-\frac{1-Y_H}{Y_H}$		$-i_{XB}$			$-\frac{i_{XB}}{14}$	$\hat{\mu}_H\left(\frac{S_S}{K_S+S_S}\right)\left(\frac{S_O}{K_{O,H}+S_O}\right)X_{B,H}$
2	Anoxic growth of heterotrophs		$-\frac{1}{Y_H}$			1				$-\frac{1-Y_H}{2.86Y_H}$	$-i_{XB}$			$\frac{1-Y_H}{14\cdot 2.86Y_H}-\frac{i_{XB}}{14}$	$\hat{\mu}_H\left(\frac{S_S}{K_S+S_S}\right)\left(\frac{K_{O,H}}{K_{O,H}+S_O}\right)\left(\frac{S_{NO}}{K_{NO}+S_{NO}}\right)\eta_g X_{B,H}$
3	Aerobic growth of autotrophs						1		$-\frac{4.57}{Y_A}+1$	$\frac{1}{Y_A}$	$-i_{XB}-\frac{1}{Y_A}$			$-\frac{i_{XB}}{14}-\frac{1}{7Y_A}$	$\hat{\mu}_A\left(\frac{S_{NH}}{K_{NH}+S_{NH}}\right)\left(\frac{S_O}{K_{O,A}+S_O}\right)X_{B,A}$
4	'Decay' of heterotrophs				$1-f_P$	-1		f_P					$i_{XB}-f_P i_{XP}$		$b_H X_{B,H}$
5	'Decay' of autotrophs				$1-f_P$		-1	f_P					$i_{XB}-f_P i_{XP}$		$b_A X_{B,A}$
6	Ammonification of soluble organic nitrogen										1	-1		$\frac{1}{14}$	$k_a S_{ND} X_{B,H}$
7	'Hydrolysis' of entrapped organics		1		-1										$k_h\frac{X_S/X_{B,H}}{K_X+(X_S/X_{B,H})}\left[\left(\frac{S_O}{K_{O,H}+S_O}\right)+\eta_h\left(\frac{K_{O,H}}{K_{O,H}+S_O}\right)\left(\frac{S_{NO}}{K_{NO}+S_{NO}}\right)\right]X_{B,H}$
8	'Hydrolysis' of entrapped organic nitrogen											1	-1		$\rho_7(X_{ND}/X_S)$

3.5 Fundamental Processes in the Peterson Matrix

There are four fundamental processes. They are growth of biomass, decay of biomass, ammonification of organic nitrogen and hydrolysis of particulate organics which are entrapped in the bioflocs. These processes are

Processes 1: Aerobic growth of heterotrophic biomass.

A fraction of the readily biodegradable substrate is used for growth of heterotrophic biomass and the balance is oxidized for energy giving rise to an associated oxygen demand. The growth is modeled using Monod kinetics. Ammonia is used as the nitrogen source for synthesis and incorporated into the cell mass. Both the concentration of S_S and S_O may be rate limiting for the growth process. This process is generally the main contributor to the production of the new biomass and removal of COD. It is also associated with an alkalinity change.

Process 2: Anoxic growth of heterotrophs

In the absence of oxygen the heterotrophic organisms are capable of using nitrate as the terminal electron acceptor with S_S as substrate. The process will lead to a production of heterotrophic biomass and nitrogen gas (denitrification). The nitrogen gas is a result of the reduction of nitrate with associated alkalinity change. The same Monod kinetics as used for the aerobic growth is applied except that the kinetic rate expression is multiplied by a factor η_g (<1). This reduced rate could either be caused by a lower maximum growth rate under anoxic conditions or because only a fraction of the heterotrophic biomass is able to function with nitrate as electron acceptor. Ammonia serves as the nitrogen source for cell synthesis, which in turn changes the alkalinity.

Process 3: Aerobic growth of autotrophs

Ammonia is oxidized to nitrate via a single-step process (nitrification) resulting in production of autotrophic biomass and giving rise to an associated oxygen demand. Ammonia is also used as the nitrogen source for synthesis and incorporated into the cell mass. The process has a marked effect on the alkalinity (both from the conversion of ammonia into biomass and by the oxidation of ammonia to nitrate) and the total oxygen demand. The effect on the amount of formed biomass is small as the yield of the autotrophic nitrifiers is low. Once again the growth is modeled using Monod

kinetics.

Process 4: Decay of heterotrophs

The process is modeled according to the death-regeneration hypothesis (Dold et al., 1980). The organisms die at a certain rate and a portion of the material is considered to be non-biodegradable and adds to the X_P fraction. The remainder adds to the pool of slowly biodegradable substrate. The organic nitrogen associated with the X_S becomes available as particulate organic nitrogen. No loss of COD is involved and no electron acceptor is utilized. The process is assumed to continue with the same rate under aerobic, anoxic and anaerobic conditions.

Process 5: Decay of autotrophs

The process is modeled in the same way as used to describe decays of heterotrophs.

Process 6: Ammonification of soluble organic nitrogen

Biodegradable soluble organic nitrogen is converted to free and saline ammonia in a first-order process mediated by the active heterotrophs. Hydrogen ions consumed in the conversion process results in an alkalinity change.

Process 7: Hydrolysis of entrapped organics

Slowly biodegradable substrate enmeshed in the sludge mass is broken down extracellularly, producing readily biodegradable substrate available to the organisms for growth. The process is modeled on the basis of surface reaction kinetics and occurs under aerobic and anoxic conditions. The rate of hydrolysis is reduced under anoxic conditions compared with aerobic conditions by a factor η_h (<1). The rate is also first-order with respect to the heterotrophic biomass present but saturates as the amount of entrapped substrate becomes large in proportion to the biomass.

Process 8: Hydrolysis of entrapped organic nitrogen

Biodegradable particulate organic nitrogen is broken down to soluble organic nitrogen at a rate defined by the hydrolysis reaction for entrapped organics described above.

3.6 Default values

The parameter values used by IAWPRC group are listed in the table for 10 °C and 20 °C. The values are given in Table 3.6.

Table3.6: Typical parameter values at neutral pH

Symbol	Unit	Value at 20 °C	Value at 10 °C
Stoichiometric Parameters Y_A	g cell COD formed $(g\ N\ oxidised)^{-1}$	0.24	0.24
Y_H	g cell COD formed $(g\ COD\ oxidised)^{-1}$	0.67	0.67
f_P	dimensionless	0.08	0.08
i_{XB}	$g\ N(g\ COD)^{-1}$ in biomass	0.086	0.086
i_{XE}	$g\ N(g\ COD)^{-1}$ in endogenous mass	0.06	0.06
Kinetic Parameters			
$\hat{\mu}_H$	day^{-1}	6.0	3.0
K_S	$g\ COD\ m^{-3}$	20.0	20.0
K_{OH}	$g\ O_2\ m^{-3}$	0.20	0.20
K_{NO}	$g\ NO_3 - N\ m^{-3}$	0.50	0.50
b_H	day^{-1}	0.62	0.20
η_g	dimensionless	0.8	0.8
η_h	-	0.4	0.4
k_h	$g\ slowly\ biodegradable\ COD\ (g\ cell\ COD day)^{-1}$	3.0	1.0
K_X	$g\ slowly\ biodegradable\ COD\ (g\ cell\ COD)^{-1}$	0.03	0.01
$\hat{\mu}_A$	day^{-1}	0.80	0.3
K_{NH}	$g\ NH_3 - N\ m^{-3}$	1.0	1.0
K_{OA}	$g\ O_2\ m^{-3}$	0.4	0.4
k_a	$m^3 COD(g day)^{-1}$	0.08	0.04

3.6.1 Main differences between UCT and ASM1 biological models

The main difference between the models is in the way the slowly biodegradable particulate carbonaceous matter is utilized during the processes of nitrification and denitrification.

- In UCT model the product of hydrolysis of SBCOD are utilized directly by the organisms
- In ASM1 model the products of hydrolysis are released as readily biodegradable COD which is utilized

In UCT model utilization of the slowly biodegradable COD is independent of the readily biodegradable COD. It involves four distinct phases (Ekama & Wentzel, 1999):

- Enmeshment – this is a physical phenomenon due to the flows in the process. It is assumed to be instantaneous. The inflow slowly biodegradable substrate S_{bpi} is transformed to enmeshed substrate S_{enm}. The rate of transformation is not modelled.
- Adsorption of S_{enm} onto the organism's active sites for breakdown. The transformation is S_{enm} to S_{ads} and is determined by the rate of adsorption K_A. This is a rapid process.
- Extracellular breakdown (hydrolysis) to simpler units which pass directly through the cell wall for use. This is a process with slow rate.
- Metabolism/synthesis of the smaller molecules by the organisms.
- The rate of the phases 3) and 4) is limited by the rate of hydrolysis. This rate is related to a concentration per unit of the active mass (S_{ads}/Z_{BH}) and is expressed as:

$$\rho = K_{MP}\frac{S_{ads}/Z_{BH}}{K_{SP}+S_{ads}/Z_{BH}}Z_{BH} \qquad (3.8)$$

The schematic diagram of the above four processes is given in (Ekama & Wentzel, 1999).

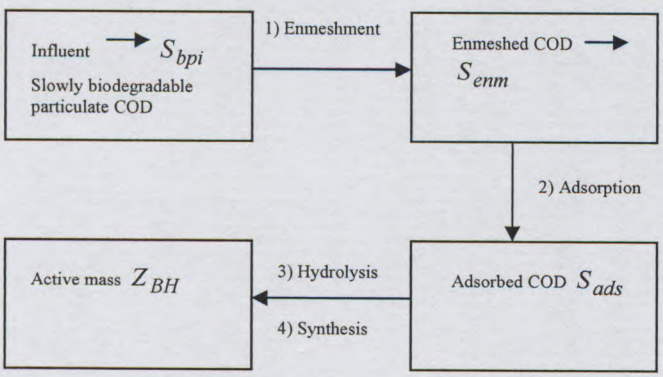

Figure 3.2: Phases in utilization of slowly biodegradable COD in UCT model

The differences in the total utilization of the biodegradable COD , considering both readily biodegradable and slowly biodegradable COD are shown on the following schematic diagrams, (Ekama & Wentzel, 1999).

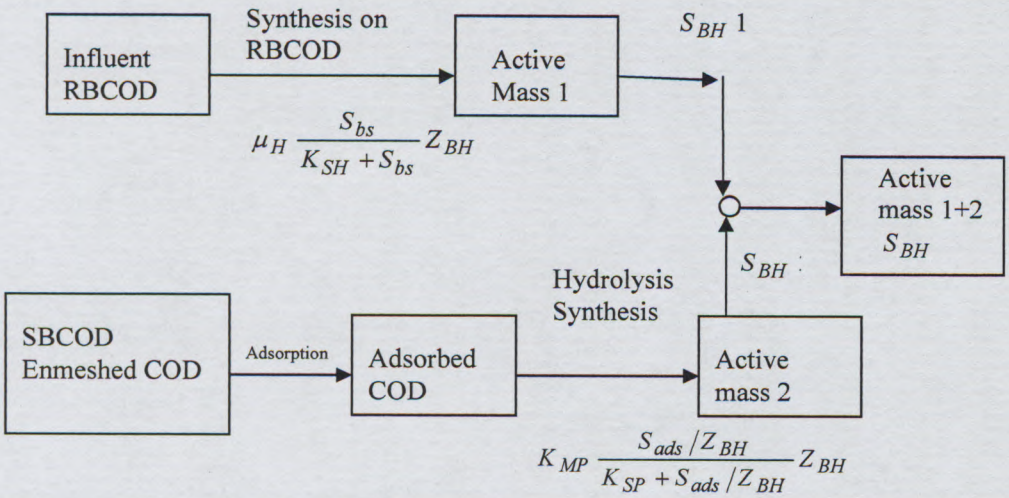

Figure 3.3 : Biodegradable COD utilization concept in UCT model

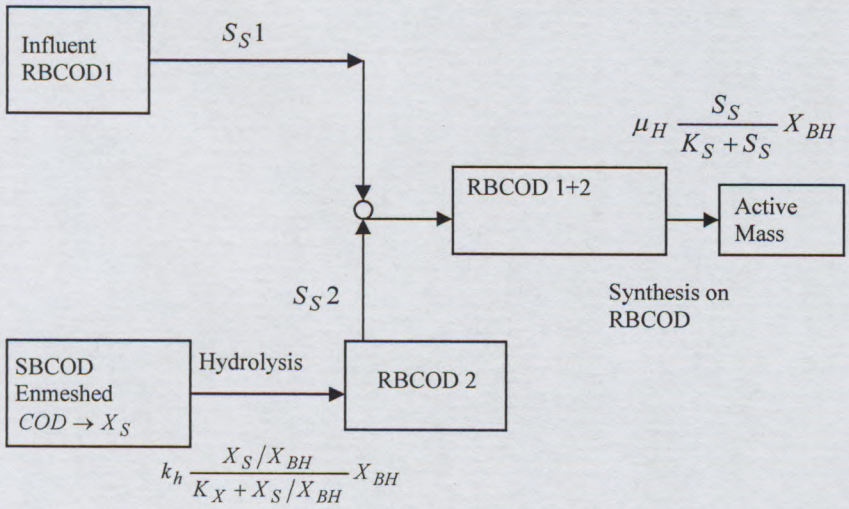

Figure 3.4: Biodegradable COD utilization in the ASM1 model

These differences result in the fact that the adsorption process is not included in ASM1 model equations and the number of variables in ASM1 model is 13 not 14 as in

the UCT model.

3.7 Model assumptions, restrictions and simplifications

The model assumptions, restrictions and simplifications are made during the model development and model use. They are very similar for both UCT and ASM1 model. For the ASM1 model Henze et al. (1987) give a list of these assumptions and restrictions, as follows:

- The system operates at constant temperature. The Arrhenius equation has to be used to adjust the model parameters for different than 20° C temperatures.
- The pH e approximately neutral and constant. The alkalinity variable in the model can be used to developed pH control.
- The nature of the organic matter in the given fractions is not changeable. On the basis of this the coefficients in the rate expressions are assumed to have constant values. This means that the model cannot describe properly changes in the wastewater character.
- The limitation of the nitrogen, phosphorus and other inorganic nutrients on the removal of the organic substrate and on the cell growth is not considered. This means enough amounts of these nutrients have to be present for balanced growth.
- The correction factors for denitrification are fixed and constant for given wastewater.
- The coefficients for nitrification are assumed to be constant and to include also the inhibitory influence of other waste components.
- The heterotrophic biomass is homogeneous and does not change with its species with time. This assumption can have effect on the sludge settleability.
- The entrapment of particulate organic material in the biomass is assumed to be instantaneous.
- Hydrolysis of organic matter and organic nitrogen are coupled and occur simultaneously with equal rates.
- The type of electron acceptor present in the different tanks does not affect the loss of active biomass by decay.

3.8 Mass balance models

According to Billings and Dold (1988, Part1&2), (Mazouni et al., 2004), (Rauh et al., 2004a), (Bernard, 2002) and (Copp, 2002), in the biological wastewater treatment system growth is harnessed in a plethora of applications. In sewage treatment the objective is to minimize the residual soluble material and it is useful to quantify the system behaviour on the basis of a model of the process (Manesis et al., 1998). Since biological growth is a key feature in this application, it is likely that consideration is given to setting up and solving a mathematical model (Keirn-Jesperson & Henze, 1993), (Marsili-Libelli et al., 2000), (Murnleitner et al., 1997) and (Smolder et al., 1995). The computer simulation program for predicting the response of a biological system can be implemented on the basis of a mathematical model.

The mass balance equations are developed under the assumptions made for the biological models and additionally made for the physical processes

- All reactors are completely mixed
- Municipal wastewater is used only
- The waste flow is taken from the last reactor
- The settling tank is efficient 100%. All particulates are recycled. The effluent contains only soluble material. No biological reactions occur in the settling tank, which is treated as a separation point with no hold-up
- The settler has different mass balances for the particulate and soluble compounds

The mathematical model derivation of a given wastewater treatment process is based on the use of mass balance laws for every of its tanks. The basic expression for the mass balance within any defined system boundary is:

$$\begin{bmatrix} Rate\ of \\ accumulation \end{bmatrix} = \begin{bmatrix} Rate\ of \\ input \end{bmatrix} - \begin{bmatrix} Rate\ of \\ output \end{bmatrix} + \begin{bmatrix} Rate\ of\ production \\ in\ the\ reaction \end{bmatrix} \tag{3.9}$$

The input and output terms are transport terms modelled using the physical characteristics of the system. The steady state conditions prevail where the flow rates and concentrations (inputs) of the biological reaction system remain constant. The rates for production by reaction of the soluble organic matter S_I and particulate organic matter X_i are zero $r_{SI}=0, r_{Xi}=0.$

3.8.1 Mass balance equations for the COST Benchmark process structure

3.8.2 Plant layout

The COST Benchmark process structure is developed by the COST 682 working group for comparison and verifying of different simulators and control strategies (Copp, 2002). The Benchmark format has 2 anoxic tanks, 3 aerobic tanks and a secondary settler with two recycle flows (from aerobic tank 5 to the input and from the settler to the input) as depicted in Figure.3.6, where: Q_o is the input flow rate, Q_a is the internal recycle flow rate, $Q_k, k=\overline{1,5}$ is the output flow rate of the k-th tank, Q_r is the recycle flow rate, Q_e is the effluent flow rate, and Q_w is the waste flow rate, Z is the vector of the waste concentrations in the wastewater

$Z=[S_I, S_S, X_I, X_S, X_{BH}, X_{BA}, X_P, S_O, S_{NO}, S_{NH}, S_{ND}, X_{ND}, S_{ALK}]'$, V_k is the volume of the *kth* tank, k is the tank number.

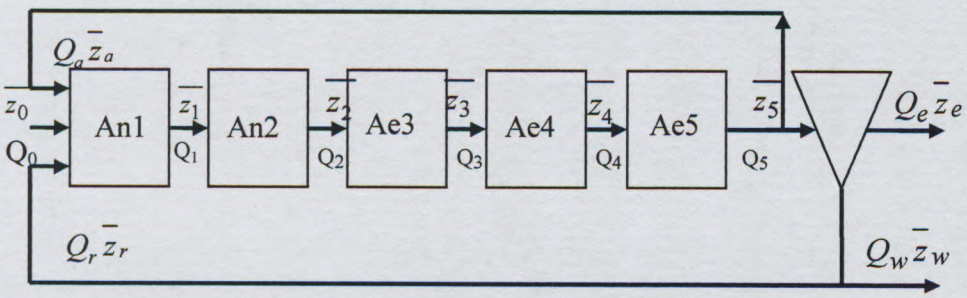

Figure 3.5: Wastewater treatment plant layout of the Benchmark model

3.8.3 Plant specifications

The process is characterized with the values of the flow rates and the tanks' volumes, as is given in the Table 3.7

Table 3.7: Benchmark plant specifications

Anoxic volume	V anoxic	1000 m^3
Aerobic volume	V aerobic	1333 m^3
Settler volume	V settler	6000 m^3
Degree of sludge recirculation	Q_r	18 446 m^3/day
Internal recirculation flow rate	Q_a	55 338 m^3/day
Waste flow rate	Q_w	385 m^3/day (sludge age = 10 days)
Influent flow	Q_{in}	18 446 m^3/day

The mass balance equations deduced from the plant lay-out for each individual tank are as follows.

- tank 1 anoxic

$$\frac{dz_1}{dt} = \frac{1}{V_1}\left(Q_a z_a + Q_r z_r + Q_0 z_0 + r_1 V_1 - Q_1 z_1\right), Q_1 = Q_a + Q_r + Q_0 \tag{3.10}$$

- tank 2 anoxic, and tank 3, 4 & 5 aerobic

$$\frac{dz_k}{dt} = \frac{1}{V_k}\left(Q_{k-1} z_{k-1} + r_k V_k - Q_k z_k\right), Q_k = Q_{k-1},\ k = \overline{3,5} \tag{3.11}$$

- tanks 3 – 5 aerobic, special case of oxygen concentration balance ($S_{O,k}$)

$$\frac{dS_{O,k}}{dt} = \frac{1}{V_k}\left(Q_{k-1} S_{O,k-1} + (K_{La})_k V_k \left(S_{O,SAT} - S_{O,k}\right) - Q_k S_{O,k}\right) \tag{3.12}$$

where the concentration at saturation of oxygen is $S_{O,SAT}$, r_k, $k = \overline{3,5}$ is

the rate of the biological processes in the corresponding tank

- balance for settler

The input to the settler for the concentration vector and flow can be expressed as

$z_F = z_5, z_w = z_r,\ \ Q_F = Q_5 - Q_a = Q_0 + Q_a + Q_r - Q_a = Q_0 + Q_r$

$Q_F = Q_0 + Q_r = Q_e + Q_w + Q_r \ \rightarrow\ Q_e = Q_0 + Q_r - Q_w - Q_r = Q_0 - Q_w$ '

where for micro organisms and particulate materials, the effluent concentration is $z_e = 0$, then the balance for the settler is $(Q_0 + Q_r)z_5 = Q_r z_r + Q_w z_r + Q_e z_e$,

$(Q_0 + Q_r)z_5 = (Q_r + Q_w)z_r + Q_e z_e$, or $z_r = \dfrac{(Q_0 + Q_r)z_5 - Q_e z_e}{Q_r + Q_\omega}$. (3.13)

As for the particulate compounds $z_e = 0$, then

$$z_r = \frac{(Q_0 + Q_r)z_5}{Q_r + Q_w} = \lambda z_5,\ where\ \lambda = \frac{Q_0 + Q_r}{Q_r + Q_w} \tag{3.14}$$

For the soluble compounds $z_e \neq 0, z_e = z_5$, $Q_e = Q_0 - Q_w$, then

$$z_r = \frac{(Q_0 + Q_r)z_5 - Q_e z_e}{Q_r + Q_w} = \frac{(Q_r + Q_w)z_5}{Q_r + Q_w} = z_5 \tag{3.15}$$

3.9 Discrete form of the equations

The discrete form of the equations is developed for the simplification of the computer simulation. Introducing sampling with interval Δt , the derivatives for all equations are presented as first a difference

$$\frac{dz}{dt} = \frac{z(k+1) - z(k)}{\Delta t} = f(z) \tag{3.16}$$

and $z(k+1) = z(k) + \Delta t f(z)$ is the discrete equation describing the concentration of the moment *(k+1)* on the basis of the concentration at the k-th moment. The common equations for tanks are as follows:

$$z_1(k+1) = z_1(k) + \frac{\Delta t}{V_1}[Q_0 z_0 + (Q_a + \lambda Q_r)z_5(k) - (Q_0 + Q_a + Q_r)z_1(k)] + r_{z1}.\Delta t \tag{3.17}$$

$$z_1(k+1) = z_1(k) + \frac{\Delta t}{V_1}[Q_0 z_0 + (Q_a + Q_r)z_5(k) - (Q_0 + Q_a + Q_r)z_1(k)] + r_{z1}.\Delta t \tag{3.18}$$

$$z_2(k+1) = z_2(k) + \frac{\Delta t}{V_2}[(Q_0 + Q_a + Q_r)(z_1(k) - z_2(k))] + r_{z2}.\Delta t \tag{3.19}$$

$$z_3(k+1) = z_3(k) + \frac{\Delta t}{V_3}[(Q_0 + Q_a + Q_r)(z_2(k) - z_3(k))] + r_{z3}.\Delta t \tag{3.20}$$

$$z_4(k+1) = z_4(k) + \frac{\Delta t}{V_4}[(Q_0 + Q_a + Q_r)(z_3(k) - z_4(k))] + r_{z4}.\Delta t \quad (3.21)$$

$$z_5(k+1) = z_5(k) + \frac{\Delta t}{V_5}[(Q_0 + Q_a + Q_r)(z_4(k) - z_5(k))] + r_{z5}.\Delta t \quad (3.22)$$

The equations for the oxygen for tanks 3 to 5 are:

$$S_{O3}(k+1) = S_{O3}(k) + \frac{\Delta t}{V_3}[Q_3(S_{O2}(k) - S_{O3}(k))] + \Delta t r_{SO3} + \Delta t K_{la3}(S_{OSAT} - S_{O3}(k)) \quad (3.23)$$

$$S_{O4}(k+1) = S_{O4}(k) + \frac{\Delta t}{V_4}[Q_4(S_{O3}(k) - S_{O4}(k))] + \Delta t r_{SO4} + \Delta t K_{la4}(S_{OSAT} - S_{O4}(k)) \quad (3.24)$$

$$S_{O5}(k+1) = S_{O5}(k) + \frac{\Delta t}{V_5}[Q_5(S_{O4}(k) - S_{O5}(k))] + \Delta t r_{SO5} + \Delta t K_{La5}(S_{OSAT} - S_{O5}(k)) \quad (3.25)$$

3.9.1 Mass balance equations for the Mitchell's Plain wastewater treatment plant

Mitchell's Plain plant is situated in the south part of Cape Town. The structure of the Mitchell's Plain plant is shown on Figure 3.6. This process consists of one anaerobic, one anoxic and one aerobic reactor. The secondary settler is placed after the aerobic tank. The process has two recycles-returns from the settler and internal one from the end of the aerobic tank to the input of the anoxic tank.

3.9.1.1 Plant layout

The incoming raw sewage which is the influent enters the anaerobic reactor, which has no oxygen and no presence of nitrates and nitrites, then proceeds further. The partially treated sludge enters the anoxic reactor which resides in the presence of nitrates and nitrites. Then enters the aerobic tank where it is treated with dissolved oxygen resulting in activated sludge. The activated sludge is dewatered and surplus sludge recycled to the anoxic tank. There is a recycle between the aerobic tank and the anoxic tank.

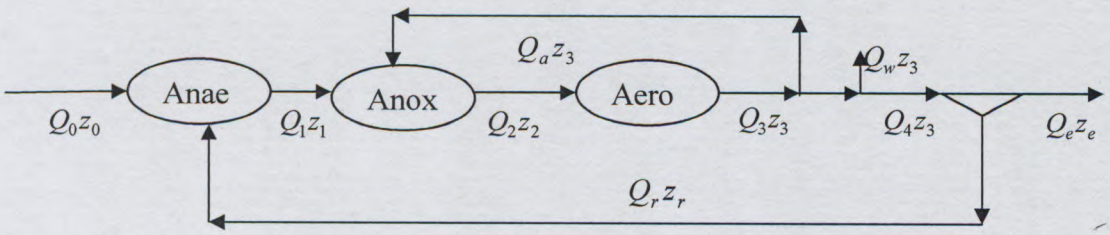

Figure 3.6: Mitchell's Plain wastewater treatment plant configuration

3.9.1.2 Plant Specifications

The values for the plant's volumes of the tanks and flow rates are given in Table 3.8.

Table 3.8: Plant specifications of Mitchell's Plain

Anoxic volume	V anoxic	1598,3 m^3
Aerobic volume	V aerobic	3727,1 m^3
Anaerobic volume	V anaerobic	914,3 m^3
Degree of sludge	Q_r	30200 m^3/day
Internal recycle	Q_a	93 000 m^3/day
Waste flow rate	Q_w	397 m^3/day
Influent	Q_0	31 500 m^3/day

A derivation of the mass balance equations for the Mitchell's Plain wastewater treatment plant is based on the flow rates, volumes of the tanks and the concentrations of the process variables.

- tank 1, anaerobic

$$\frac{dz_1}{dt} = \frac{1}{V_1}[Q_0 z_0 + Q_r z_r + r_1 V_1 - Q_1 z_1] \qquad Q_1 = Q_0 + Q_r \tag{3.26}$$

- tank 2, anoxic

$$\frac{dz_2}{dt} = \frac{1}{V_2}[Q_1 z_1 + Q_a z_3 + r_2 V_2 - Q_2 z_2] \qquad Q_2 = Q_1 + Q_a = Q_0 + Q_r + Q_a \tag{3.27}$$

- tank 3, aerobic

$$\frac{dz_3}{dt} = \frac{1}{V_3}[Q_2 z_2 + r_3 V_3 - Q_3 z_3] \qquad Q_3 = Q_2 = Q_0 + Q_r + Q_a \tag{3.28}$$

- tank 3, dissolved oxygen balance

$$\frac{dS_{O,3}}{dt} = \frac{1}{V_3}[Q_2 S_{O,2} + r_{O,3} V_3 + (K_L a)_3 V_3 (S_{OSAT} - S_{O,3}) - Q_3 S_{O,3}] \tag{3.29}$$

- settler balance, Q_4 is input for the settler.

$$Q_4 = Q_3 - Q_a - Q_w$$

$$Q_e = Q_4 - Q_r = Q_3 - Q_a - Q_w - Q_r = Q_0 + Q_r + Q_a - Q_a - Q_w - Q_r = Q_0 - Q_w \tag{3.30}$$

The concentration for the particulate compounds is $z_e = 0, z_w = z_3$. Then the balance for the settler is

$$Q_e.0 = (Q_3 - Q_a - Q_w)z_3 - Q_r z_r \rightarrow z_r = \frac{(Q_r + Q_0 - Q_w)z_3}{Q_r} = \lambda z_3, \ \lambda = \frac{Q_r + Q_0 - Q_w}{Q_r} \tag{3.31}$$

The concentration for the soluble compounds is $z_e \neq 0, z_e = z_3$. Then the balance for the settler is

$$Q_e z_3 = (Q_3 - Q_a - Q_w) z_3 - Q_r z_r \tag{3.32}$$

$$Q_r z_r = (Q_3 - Q_a - Q_w - Q_e) z_3 = (Q_0 + Q_r + Q_a - Q_a - Q_w - Q_0 + Q_w) z_3 = Q_r z_3 \quad \text{or} \quad z_r = z_3 \tag{3.33}$$

For the soluble compounds the concentrations of the return recycle are equal to the concentration of the output flow of the third tank:

$$S_{Ir} = S_{I3}, S_{Sr} = S_{S3}, X_{Sr} = X_{S3}, S_{Or} = S_{O3}, S_{NOr} = S_{NO3}, S_{NHr} = S_{NH3}$$

$$S_{NDr} = S_{ND3}, S_{ALKr} = S_{ALK3}, S_{Nobr} = S_{Nob3} \tag{3.34}$$

For the particulate compounds the concentrations of the return recycle are equal to the concentration of the output flow of the third tank multiplied by the ratio $\lambda = \dfrac{Q_r + Q_0 - Q_w}{Q_r}$, as follows:

$$X_{BH,r} = \lambda X_{BH,3}, X_{BA,r} = \lambda X_{BA,3}, X_{P,r} = \lambda X_{P,3}, X_{S,r} = \lambda X_{S,3}, X_{ND,r} = X_{ND,3} \tag{3.35}$$

The mass balance equations can now be simplified.

- tank 1, anaerobic

For soluble compounds

$$\frac{dz_1}{dt} = \frac{1}{V_1}[Q_0 z_0 + Q_r z_3 - Q_1 z_1] + r_1 = \frac{1}{V_1}[Q_0 z_0 + Q_r z_3 - Q_0 z_1 - Q_r z_1] + r_1 =$$

$$= \frac{1}{V_1}[Q_0 (z_0 - z_1) + Q_r (z_3 - z_1)] + r_1 \tag{3.36}$$

For particulate compounds

$$\frac{dz_1}{dt} = \frac{1}{V_1}[Q_0 z_0 + \lambda Q_r z_3 - Q_1 z_1] + r_1 = \frac{1}{V_1}[Q_0 z_0 + \lambda Q_r z_3 - Q_0 z_1 - Q_r z_1] + r_1 =$$

$$= \frac{1}{V_1}[Q_0 (z_0 - z_1) + Q_r (\lambda z_3 - z_1)] + r_1 \tag{3.37}$$

- tank 2, anoxic

For the soluble and particulate compounds

$$\frac{dz_2}{dt} = \frac{1}{V_2}[Q_1 z_1 + Q_a z_3 - Q_2 z_2] + r_2 = \frac{1}{V_2}[(Q_0 + Q_r) z_1 + Q_a z_3 - (Q_0 + Q_r + Q_a) z_2] + r_2$$

$$=\frac{1}{V_2}[(Q_0+Q_r)(z_1-z_2)+Q_a(z_3-z_2)]+r_2 \tag{3.38}$$

- tank 3, aerobic

For the soluble and particulate compounds

$$\frac{dz_3}{dt} = \frac{1}{V_3}[Q_2z_2-Q_3z_3]+r_3 = \frac{1}{V_3}[(Q_0+Q_r+Q_a)z_2-(Q_0+Q_r+Q_a)z_3]+r_3 =$$

$$=\frac{1}{V_3}[(Q_0+Q_r+Q_a)(z_2-z_3)]+r_3 \tag{3.39}$$

For the dissolved oxygen concentration – soluble and particulate compounds

$$\frac{dS_{O,3}}{dt} = \frac{1}{V_3}[Q_2S_{O,2}-Q_3S_{O,3}]+r_{O,3}+(K_{La})_3(S_{O,sat}-S_{O,3}) =$$

$$=\frac{1}{V_3}[(Q_0+Q_r+Q_a)(S_{O,2}-S_{O,3})]+r_{O,3}+(K_{La})_3(S_{OSAT}-S_{O,3}) \tag{3.40}$$

3.9.2 Mass balance equations for the Athlone wastewater treatment plant

3.9.2.1 Plant layout

Athlone treatment plant consists of anaerobic, anoxic and aerobic tanks, Figure 3.8, connected according to the UCT process technology (Dold et al, 1991; Dold et al, 1980). The process has one return activated sludge recycle and two internal recycles- from the end of the aerobic to the input of the anoxic tank and from the end of the anoxic to the input of anaerobic tank. The Athlone plant is situated in the northern part of Cape Town.

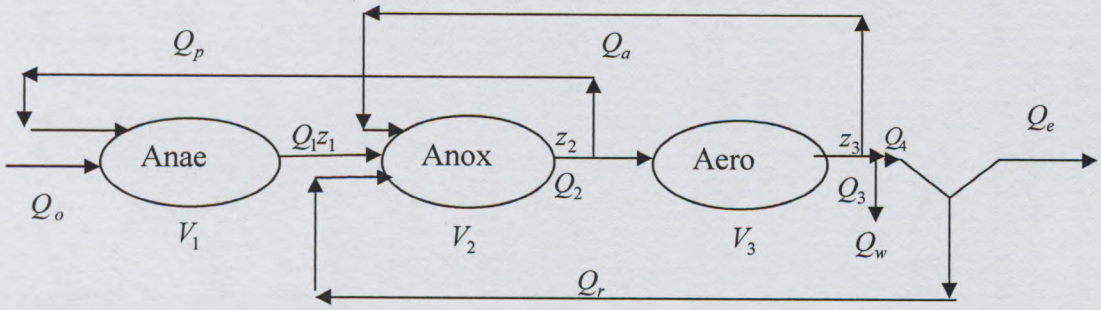

Figure 3.7: Athlone plant configuration

3.9.2.2 Plant Specifications

The values of the flow rates and volumes for the process are given in Table 3.9.

Table 3.9: Athlone plant specifications

Anaerobic volume	V anaerobic	1148 m^3
Anoxic volume	V anoxic	1148 m^3
Aerobic volume	V aerobic	5273 m^3
Internal recirculation flow rate 2	Q_a	39916.8 m^3/day
Return recycle flow rate	Q_r	40003.2 m^3/day
Internal recirculation flow rate 1	Q_p	39916.8 m^3/day
Waste flow rate	Q_w	3840 m^3/day
Influent flow	Q_0	40003 m^3/day

Mass balance equations are derived for every tank, as follows:

The flow rates for every tank are

$$Q_1 = Q_p + Q_0, \quad Q_2 = Q_1 + Q_r + Q_a = Q_p + Q_o + Q_r + Q_a \tag{3.41}$$

$$Q_3 = Q_2 = Q_p + Q_0 + Q_r + Q_a \tag{3.42}$$

$$Q_r = Q_3 - Q_w - Q_e \tag{3.43}$$

tank 1, anaerobic

$$\frac{dz_1}{dt} = \frac{1}{V_1}\left[Q_0 z_0 + Q_p z_2 - Q_1 z_1 + V_1 r_1\right] \tag{3.44}$$

tank 2, anoxic

$$\frac{dz_2}{dt} = \frac{1}{V_2}\left[Q_1 z_1 + Q_a z_3 + Q_r z_r - Q_2 z_2 + V_2 r_2\right] \tag{3.45}$$

tank 3, aerobic

$$\frac{dz_3}{dt} = \frac{1}{V_3}\left[Q_2 z_2 - Q_3 z_3 + V_3 r_3\right] \tag{3.46}$$

tank 3, dissolved oxygen balance

$$\frac{dS_{O,3}}{dt} = \frac{1}{V_3}\left[Q_2 S_{O,2} - Q_3 S_{O,3}\right] + r_{O,3} + (K_{La})_3 (S_{OSAT} - S_{O,3}) \tag{3.47}$$

settler, Q_4 is the input to the settler

$$Q_4 = Q_3 - Q_a - Q_w \tag{3.48}$$

$$Q_e = Q_4 - Q_r = Q_3 - Q_a - Q_w - Q_r = Q_p + Q_0 + Q_r + Q_a - Q_a - Q_w - Q_r =$$

$$= Q_p + Q_0 - Q_w \tag{3.49}$$

Concentration in the settler for the particulate compounds is $z_e = 0, z_w = z_3$. Then the balance for settler for particulate is

$$Q_e.0 = Q_4 z_3 - Q_r z_r = (Q_3 - Q_a - Q_w) z_3 - Q_r z_r, \quad z_r = \frac{(Q_p + Q_0 + Q_r - Q_w) z_3}{Q_r} = \lambda z_3 \tag{3.50}$$

Concentration in the settler for the soluble compounds is $z_e \neq 0$, $z_e = z_3$. Then the balance for settler for soluble is

$$Q_e z_3 = (Q_4 z_3 - Q_r z_r) = (Q_3 - Q_a - Q_w) z_3 - Q_r z_r = (Q_p + Q_0 + Q_r + Q_a - Q_a - Q_w) z_3 - Q_r z_r$$

After some transformations it is obtained

$$Q_r z_3 = Q_r z_r \text{ and } z_r = z_3 \tag{3.51}$$

The soluble compounds are

$$S_{I\,r} = S_{I\,3}, S_{S\,r} = S_{S\,3}, X_{X\,r} = X_{S\,3}, S_{O\,r} = S_{O\,3}, S_{NO\,r} = S_{NO\,3}, S_{NH\,r} = S_{NH\,3}$$
$$S_{ND\,r} = S_{ND\,3}, S_{ALK\,r} = S_{ALK\,3} \tag{3.52}$$

The particulate compounds for $\lambda = \dfrac{Q_p + Q_0 + Q_r - Q_w}{Q_r}$ are

$$X_{BH,r} = \lambda X_{BH,3}, X_{BA,r} = \lambda X_{BA,3}, X_{P,r} = \lambda X_{P,3}, X_{S,r} = \lambda X_{s,3}, X_{ND,r} = \lambda X_{ND,3} \tag{3.53}$$

The mass balance equations for the tanks can be written according to the types of the compounds. The equations for the tanks 1 and 3 are the same as Equations (3.44) and (3.46). The equation for the tank 2 is:

For the particulate compounds

$$\frac{dz_2}{dt} = \frac{1}{V_2}[Q_1 z_1 + Q_a z_3 + Q_r \lambda z_3 - Q_2 z_2] + r_2 = \frac{1}{V_2}[Q_1 z_1 - Q_2 z_2 + (Q_a + \lambda Q_r) z_3] + r_2 \tag{3.54}$$

For the soluble compounds

$$\frac{dz_2}{dt} = \frac{1}{V_2}[Q_1 z_1 + Q_a z_3 + Q_r z_3 - Q_2 z_2] + r_2 = \frac{1}{V_2}[Q_1 z_1 - Q_2 z_2 + (Q_a + Q_r) z_3] + r_2 \tag{3.55}$$

The discrete form of the obtained mass balance equations can be obtained in the same way as for the Benchmark and Mitchell's Plain plant models.

3.10 Conclusion

The system and a model of the system have been defined within a certain mathematical nomenclature. Some important criteria for process model development have been defined and various model types have been named.

The biological models such as UCT model and Activated Sludge model No. 1 have been described as complex mechanistic models. The default values for kinetic, stoichiometric and switching functions of these two models are given. The similarities and differences in the model building principles for both models are discussed.

Three plant structures - Benchmark, Mitchell's Plain and Athlone are introduced and described. Their mathematical models on the basis of mass balances for every tank and every process component are derived. These models will be used further in Chapter 4 for development of the corresponding reduced models, that can be used for real time estimation and optimal control.

CHAPTER FOUR

DEVELOPMENT OF REDUCED BIOLOGICAL AND MASS BALANCE MODELS OF THE ACTIVATED SLUDGE PROCESS

4.1 Introduction

This chapter elucidates the need for reduced model development of both the ASM1 and UCT models where the assumptions for model reduction are also studied. The dissolved oxygen concentration is considered as a control input for the reduced models. The ASM1 reduced model and UCT reduced biological model are studied where the parameters are established for the parameter estimation determined in Chapter 6.

The mass balance equations for the three wastewater treatment plants viz., Benchmark, Mitchell's Plain and Athlone are developed in this Chapter on the basis of the reduced UCT and ASM1 biological models. The matrices and vectors for each of the plants are separately developed and the reduced model characteristics are compared and contrasted.

4.2 The need for reduced model development

Many authors have noted the difficulty of developing nonlinear models necessary for the real time control as nonlinear model predictive control. One reason for the difficulties is that the proper model strongly depends on initially selection of a reasonable structure of this model (Pearson, 2003).

The practical difficulty of nonlinear dynamic model development arises from several sources, from which the main two are: the model utility can be measured in several, general conflicting ways and the class of nonlinear models does not exhibit the unity that the class of linear models does.

Pearson gives a list of four important measures of model utility.

- approximation accuracy
- physical interpretation
- suitability for control
- ease of development

Fundamental models are generally far superior to empirical and semi-empirical ones with respect to the first two criteria but they can not give good response to the last two criteria.

In contrast, the most popular models for process control application are low-order linear models despite their inability to approximate a wide range of important qualitative behaviour. This is due to the fact that these models are very good according to the last two criteria despite their limitations towards the first ones. The nonlinear models with moderate complexity are some compromise between the two groups, especially if they are based on the "grey box" conceptions. The second key difficulty with nonlinear dynamic model development is the enormous structure heterogeneity that models have.

The main objectives of the WWTP operations are (Jeppson, 1996)

- maintaining liquid and sludge inventories
- maintaining required effluent quality
- disturbance rejection
- efficient operation and reduction of cost through proper monitoring and control

Major difficulties when attempting to control the ASP following the above objectives are:

- When one variable in the process is manipulated it affects a large number of measurable variables in a complex way. Over a longer period of time the total system behaviour may change considerably. The ideal situation would naturally be that a change of one control variable would produce a well defined response in one process variable; instead the situation is practically the opposite. This is the indication that it may be necessary to use control strategies based on multi-variable control to solve the problems in some cases.
- From a modeling point of view a similar problem exists. Changing process behaviour will naturally have an impact on the microbial population in the system as the microorganisms adapt to a new environmental conditions (due to changing in characteristics, operational modifications, physical, chemical reactions, etc.). The model parameters can consequently not be regarded as constants but must be dynamically updated as the plant conditions change. More adequate and adaptive models are necessary in order to predict both the long and short term behaviour of the AS system and to determine and implement better control strategies.

The most popular mathematical description of the biological processes in the reactors for nitrogen and carbon removal is the Activated Sludge Model No.1(ASM1).The model contains 13 different components, 20 parameters and eight models representing biological processes in the wastewater treatment plants. The first ever-developed model, UCT biological model consists of 14 components, 14 processes and 21 parameters. The Peterson matrix representations of the two models are shown in Chapter 3. The full models are used for design, prediction, simulation, control purposes.

Biological model of the activated sludge process that incorporate kinetics of the ASM1 or UCT models are large and complex. If these models are coupled with the model of the associated equipment such as secondary settling tank, return sludge tank, this will result in an increased complexity of the entire model of the process. For real time parameter and state estimation, monitoring and control, a reduction of the order of the high dimensional model is required.

Due to the complexity of the full models, the reduced versions of the models are used for the purpose of computational solutions. The full models are hard to calibrate in real time and use directly for control purposes. They are also time consuming and computer intensive. A reduced model is a more feasible model for controller design as well as has to be a good approximation of the full model.

The different process time scales allow many control actions to be decoupled. As a result, slow phenomena can be controlled while considering the fast dynamics instantaneous. For the control of fast varying variables, the slow modes are considered constant. This approach is also useful for model development, in the sense that models can be simplified based on their range of applicability in time domain. From a complete set of models, describing the different dynamics of the process, a fairly simple model suited for the specific purpose can be selected.

Different methods and techniques have been applied for reducing the high dimensional models of the activated sludge process. The first one was based on some qualitative assumptions based on the IAWQ model No.1 (Jeppson & Olson, 1993). Another assumption is reported in (Jannssen, Hopkins, Petersen & Vanrolleghem, 2000).The developed by Jeppson and Olson model is applied by (Ayesa, Oyarbide, Larrea & Garcia-Heras, 1995) in the evaluation of observability of two wastewater plants. Another used technique is the singular perturbation (Kokotovic, O'Malley & Sannuti, 1976). It is applied by (Steffens, Lant & Newell, 1997) to carbon removal and nitrifying ASP.

There are other techniques proposed for different types of processes and still have not been used for wastewater plants. One of the first is of retaining the dominant system eigenvalues and eigenvectors (Davison, 1966). Similar technique in frequency domain was proposed by (Langholz & Feinmesser, 1978). The reduced order model based on system poles was not optimized.

An optimal reduced order model was proposed in (Wilson, 1974) and (Lepschy, Mian & Viaro, 1987). Optimization of the reduced model in the frequency domain was developed by (Luus, 1980). The above optimization techniques suffer from bad convergence of the optimization process.

Good improvement in reduced model automation is achieved in (Moore, 1981) using the balanced truncating method and in (Glover, 1984) using the optimal Hankel norm approximation. These techniques are simpler and require fewer computations (Safanov & Chiang, 1989), (Latham & Anderson, 1985), (Al-Saggaf & Franklin, 1988), (Wisnewski & Doyle, 1996).

A number of new computational algorithms were lately proposed to improve the practical applications of the methods. Halevi, Ziochevsky & Gilat (1997) proposed an algorithm for updating optimum reduced order model either on-line or off-line based on the series expansion. Beck, Doyle & Glover (1996) used linear fraction transformation technique together with the balanced truncation technique of Moore to reduce the model of MIMO systems with uncertainties. In (Lee, Wang & Newell, 2002) a linear reduced order state space model is developed for the ASP described by partial differential equations based on the kinetics of ASM2.

On the basis of the analysis of the literature describing the reduced order model development it can be concluded that the requirements to be followed when the reduced model is developed from control engineering point of view (Lee, Wang & Newell, 2002) can be stated in the following way:

- Simplification of the best available process model in such a way that the design of a control system utilizing the reduced order model is able to meet certain specifications
- Fictitious and unobservable or uncontrollable states generated by the model reduction algorithm can be systematically "stripped" away
- If modern control methods such as linear quadratic Gaussian LQG or HB (H-norm methods like H-infinity) control laws are to be employed for controlling the process, usage of the reduced-order model can significantly reduce the control law complexity without pronounced change in control system performance.

The reduced models in the thesis are developed for the purpose of state and parameter estimation in real time and for a process optimization in real time. First reduced biological models are developed for the ASM1 and UCT biological models. Using the mass-balance models developed for the Benchmark, Athlone and Mitchell's Plain plants, the respective reduced mass balance models are proposed.

4.3 Assumptions for the development of the reduced biological models

The reduced order model is developed based on a number of simplifying assumptions. Comparison of the behaviour of the reduced and the full model has performed, considering different types of process operations in Chapter 6.

The basis for development of reliable mathematical model is a thorough understanding of the involved processes. The aim of the work is to develop reduced order models which can adequately describe both carbonaceous and nitrogenous activities for the purpose of on-line control. A fundamental requirement is that the models contain a minimum number of state variables and parameters to allow for model identification based on available on-line measurements and for on-line calculation of the process optimal control.

The reduction is not based on the general mathematical methods for reduction of nonlinear models mentioned in the previous considerations above. It is based on the traditional reasoning and means of analysis of the ASP characteristics. The reduced biological models are developed for

- IAWQ No.1-(ASM1) model
- UCT model

The aim is to follow the same principles of development of every one of these models and to preserve the differences between them according the process of adsorption and hydrolysis.

The reduced models will be used for control of the carbon and nitrogen removal using control of the dissolved oxygen concentration in the aeration tanks. The carbon and nitrogen removal dynamics are considered in comparison with the dynamics of all process variables. The activated sludge process dynamics can be decomposed in 3 time scales with time constants values equal to

- weeks or months – the process variables with these characteristics are the heterotrophic and autotrophic microorganisms and slowly biodegradable biomass.
- hours - the process variables with these characteristics are carbonaceous and nitrogenous substrates and the inflow flow rate and concentrations.
- minutes – the process variables with these characteristics are the physico-chemical variables such as dissolved oxygen, pH, conductivity, redox potential.

The main disturbances over the activated sludge process are the load disturbances determined by the inflow flow rate and waste concentrations. The control of the ASP will be effective if it can overcome the effect of the inflow disturbances. This means that the model of the process has to have dynamics in the same time scale as these of the disturbances. That is why for the purpose of optimal control of the process the calculation of the optimal control can be done using a reduced model of the process in which only dynamics of the carbonaceous and nitrogenous substrate and inflow disturbances are included. It is possible to neglect the equations from the full biological model describing the concentrations of X_S, X_{BA}, X_{BH}, for the ASM1 model and S_{enm}, Z_{BH}, Z_{BA} for the UCT model because they have a couple of time slower dynamics and can be considered to be in a steady state. It is also possible to neglect the equation for dissolved oxygen concentration because it is used to design a controller for the control of this concentration. Its dynamics are couple times faster than the dynamics of the substrate concentrations and it can be assumed that the value of the DO is equal of this of the required set-point. The dissolved oxygen concentration as a control variable is included in the switching functions of the process rates.

Then the reduced biological model is proposed to consist from three equations for the three variables – concentrations of ammonia S_{NH}, nitrate S_{NO} and biodegradable substrate S_S.

Models for on-line control must be related to quantities and variables which are possible to be measured on-line. This is especially important as the model parameters are not constant but vary with time and operational conditions. The following set of quality variables are assumed to be measured on-line for the purpose of the model parameter estimation:

- biodegradable organic substrate concentration - S_S
- ammonia nitrogen concentration - S_{NH}
- nitrate nitrogen concentration - S_{NO}
- volumetric flow rates – Q
- Dissolved oxygen concentration - S_O

The reduced model equations include different biochemical processes, according to the corresponding Peterson matrix. Not all processes are incorporated in the model. Some

reasoning for the simplification is based on physical and biological viewpoints mainly on a discussion how the following components are treated in the model:

- dissolved oxygen
- organic matter
- nitrogen
- microorganisms

4.3.1 Dissolved oxygen concentration

For the reduced models states, measurements of the DO concentration are not considered although the DO sensor is usually regarded as the most reliable on-line instrument for the ASP. This is because the DO concentration is excluded as a state variable. There are 2 possibilities which are accepted for DO concentration variable in the proposed reduced model:

- DO is a control variable for the biological model and its value is optimized through solution of an optimal control problem with given criterion
- it is assumed that DO is separately controlled on a routine basis according to its optimal trajectory obtained from the optimal control problem solution.

The effect of DO changes can be combined with other inhibitory circumstances and reflected as variations in the estimated growth rate factors. In ASM1 and UCT models switching functions to single out the effect of different concentrations are used and this will be kept in the reduced model.

4.3.2 Description of the organic matter for the reduced model

The four fractions of the organic matter S_I (soluble inert organic matter), S_S (readily biodegradable organic matter), X_I and X_P (particulate inert organic matter) and X_S (slowly biodegradable organic matter) are replaced by a simple variable S_S, which is considered to be made up of all biodegradable organic matter and is assumed to be directly measurable

This approach can be motivated following (Jeppson, 1996)

- The two inert fractions are not important from a biological point of view. The S_I fraction simply follows the wastewater flow and passes from the WWTP without having any effect. The particulate inert fraction is used for prediction the total amount of sludge in the system to determine wastage and recirculation rates. Variations of the amount of sludge in the system are a slow process and, consequently, it is not necessary to include this in a model for control with a prediction over hours.
- On the other hand the two biodegradable fractions are of utmost importance for describing the biological reactions. S_S is considered to be directly available for the

microorganisms, while X_S first has to be enzymatically broken down into S_S (the hydrolysis mechanism) before the organisms can use it for metabolism. The dynamics of X_S are very slow (days), the hydrolysis process is also, not very well understood. The IAWQ description of it is quite complex, but it is still a simplification of the true reaction. Due to the slow dynamics, uncertainty and complex description of the mechanism it is not included in the reduced order model.

- Another reason for lumping the biodegradable organic matter together is the difficulty of measuring the S_S and X_S fractions separately. On-line respirometer can be used to determine the so-called short-term COD content of wastewater. In practice, COD measurement on filtered samples of wastewater is often considered to be equal to the amount of S_S.

4.3.3 Nitrogen consumption

The considered nitrogen fractions in the ASM1 and UCT models are four:

- nitrate and nitrite nitrogen S_{NO}
- ammonia nitrogen S_{NH}
- soluble biodegradable organic nitrogen S_{ND}
- particulate biodegradable organic nitrogen X_{ND}

The only two nitrogen fractions included in the reduced models are the nitrate nitrogen S_{NO} and the ammonia nitrogen S_{NH}, which are both assumed to be measured on-line. The reasons for this selection are:

- To reduce the complexity of the model structure and the number of parameters
- The two organic fractions S_{ND} and X_{ND} primarily describe the internal formation of S_{NH} by hydrolysis and ammonification. (Jeppson, 1996) proposes that as in the reduced model ammonia nitrogen is assumed to be measured, therefore, its formation mechanism is not considered to be crucial for control purposes. Moreover, as the hydrolysis mechanism was excluded to describe the transformation of the organic matter it should consequently not be used to describe the transformation of nitrogen (as it is basically the same process). (Lucasse et al., 1999) proposes that the equation for the soluble biodegradable organic nitrogen S_{ND} to be not included if the input concentration of $S_{NH,in}$ is multiplied by a factor of f. This is based on the knowledge that a certain percentage (around 20%) of the influent nitrogen is entrapped in organic components and it is also ammonified. Then f can be selected as f = 1.2. The later is accepted in the thesis.

4.3.4 Microorganism components

The two types of microorganisms are maintained in the reduced models, i.e. active heterotrophic biomass (X_{BH}), and active autotrophic biomass (X_{BA}) are with slow dynamics and are accepted constant.

4.4 Reduced ASM1 biological model

4.4.1 Biological processes included in the reduced model

Aerobic growth of heterotrophs X_{BH} for the degrading of organic matter, Anoxic growth of heterotrophs for de-nitrification process, Aerobic growth of Autotrophs X_{BA} for nitrification process and lastly the hydrolysis of entrapped organics nitrogen are the processes that characterize the dynamic behaviour of the three components used in describing the removal of carbon and nitrogen :

- Soluble ammonium nitrogen S_{NH}
- Soluble nitrate nitrogen S_{NO}
- Soluble readily biodegradable substrate S_S

The Peterson matrix for the reduced ASM1 model is given in Table 4.1.

Table 4.1: The reduced ASM1 biological model in a matrix format

Compound → i process ↓ j	S_{Sn}	S_{NOn}	S_{NHn}	P_{nj} (n = tank, j = state)
1. Aerobic growth of heterotrophs	$-\frac{1}{Y_H}$	0	$-i_{XB}$	$\hat{\mu}_H\left(\frac{S_{S_n}}{K_S+S_{S_n}}\right)\left(\frac{S_{O_n}}{K_{OH}+S_{O_n}}\right)X_{BH_n}$
2. Anoxic growth of heterotrophs	$-\frac{1}{Y_H}$	$-\frac{1-Y_H}{2.86Y_H}$	$-i_{XB}$	$\hat{\mu}_H\left(\frac{S_{S_n}}{K_S+S_{S_n}}\right)\left(\frac{K_{OH}}{K_{OH}+S_{O_n}}\right)\left(\frac{S_{NO_n}}{K_{NO}+S_{NO_n}}\right)\eta_g X_{BH_n}$
3. Aerobic growth of autotrophs	0	$\frac{1}{Y_A}$	$-i_{XB}-\frac{1}{Y_A}$	$\hat{\mu}_A\left(\frac{S_{NH_n}}{K_{NH}+S_{NH_n}}\right)\left(\frac{S_{O_n}}{K_{OA}+S_{O_n}}\right)X_{BA_n}$
4. Hydrolysis	1	0	0	$k_h X_{BH_n}\left(\frac{X_{S_n}/X_{BH_n}}{K_X+X_{S_n}/X_{BH_n}}\right)$ $\left[\left(\frac{S_{O_n}}{K_{OH}+S_{O_n}}\right)+\eta_h\left(\frac{K_{OH}}{K_{OH}+S_{O_n}}\right)\left(\frac{S_{NO_n}}{K_{NO}+S_{NO_n}}\right)\right]$

The biological behavior of each component is described by the following set of nonlinear differential equations taken from the Peterson matrix table above.

$$r_{S_{NH}}=\left[-i_{XB}\hat{\mu}_H\left(\frac{S_S}{K_S+S_S}\right)\left(\frac{S_O}{K_{OH}+S_O}\right)X_{BH}\right]-i_{XB}\left[\hat{\mu}_H\left(\frac{S_S}{K_S+S_S}\right)\left(\frac{S_{NO}}{K_{NO}+S_{NO}}\right)\left(\frac{K_{OH}}{K_{OH}+S_O}\right)X_{BH}\eta_g\right]+ \\ +\left[\left(-i_{XB}-\frac{1}{Y_A}\right)\hat{\mu}_A\left(\frac{S_O}{K_{OA}+S_O}\right)\left(\frac{S_{NH}}{K_{NH}+S_{NH}}\right)X_{BA}\right] \quad (4.1)$$

$$r_{S_{NO}}=\left[-\frac{1-Y_H}{2.86Y_H}X_{BH}\hat{\mu}_H\left(\frac{S_S}{K_S+S_S}\right)\left(\frac{K_{OH}}{K_{OH}+S_O}\right)\left(\frac{S_{NO}}{K_{NO}+S_{NO}}\right)\eta_g\right]+\left[\frac{1}{Y_A}\hat{\mu}_A\left(\frac{S_O}{K_{OA}+S_O}\right)\left(\frac{S_{NH}}{K_{NH}+S_{NH}}\right)X_{BA}\right] \quad (4.2)$$

$$r_{S_S} = \left[-\frac{1}{Y_H}\hat{\mu}_H \left(\frac{S_S}{K_S + S_S} \right) \left(\frac{S_O}{K_{OH} + S_O} \right) X_{BH} \right] - \left[\frac{1}{Y_H}\hat{\mu}_H \left(\frac{S_S}{K_S + S_S} \right) \left(\frac{S_{NO}}{K_{NO} + S_{NO}} \right) \left(\frac{K_{OH}}{K_{OH} + S_O} \right) X_{BH}\eta_g \right] + \\ + k_h \left(\frac{X_s / X_{BH}}{K_x + (X_s / X_{BH})} \right) \left[\left(\frac{S_O}{K_{OH} + S_O} \right) + \eta_h \left(\frac{S_{NO}}{K_{NO} + S_{NO}} \right) \left(\frac{K_{OH}}{K_{OH} + S_O} \right) \right] X_{BH} \quad (4.3)$$

The 14 process parameters used in the reduced ASM1 model and their typical values are given in Table 4.2. As not all processes are included in the reduced model the typical values of the parameters cannot be used anymore. The new values have to be determined in such a way that the behaviour of the reduced model is very close to this of the full model. This will be done through parameter estimation method developed in Chapter 6.

Table 4.2: ASM1 process parameters with their common values

Symbol	Value	Explanation
Y_A	0.24	Autotrophic biomass yield
Y_H	0.67	Heterotrophic biomass yield
i_{XB}	0.086	Nitrogen mass per mass of COD in biomass
μ_A	0.8	Maximum specific growth rate autotrophic biomass
μ_H	6	Maximum specific growth rate heterotrophic biomass
K_S	20	Half saturation coefficient for heterotrophic biomass
K_{OH}	0.2	Oxygen half saturation coefficient for heterotrophic biomass
K_{NO}	0.5	Nitrate for denitrifying heterotrophs
K_{NH}	1.0	Ammonium half saturation coefficient for autotrophic biomass
K_{OA}	0.4	Oxygen half saturation coefficient for autotrophic biomass
$?_g$	0.8	Correction factor for μ_H under anoxic conditions
$?_h$	0.4	Correction factor for hydrolysis under anoxic conditions
k_h	3	Maximum hydrolysis rate
K_X	0.03	Half saturation coefficient for hydrolysis of slowly biodegradable substrate

4.5 Reduced UCT biological model

The differences in the two full models, discussed in chapter 3.2.2.3 determine differences in the reduced model structures- the reduced UCT model includes on the place of the hydrolysis process four processes for the aerobic (2) and anoxic (2) growth of heterotrophs on the S_{ads} and one adsorption of S_{enm} process. This means that an additional variable (compound) S_{ads} is included. All considerations made for the ammonia and organic nitrogen for the ASM1 biological model are the same for the UCT

biological model. The parameter f = 1.2 is introduced to substitute S_{ND} compound. As a result the model has ten processes describing the removal of nitrogen and carbon from wastewater. The ASM1 notation is accepted also for the UCT model in order to follow the mathematical equations development in the unified way. The correspondence between the notations for the variables in the ASM1 and UCT models is:

- Soluble ammonium nitrogen S_{NH} - *Na* in the notation of the UCT model
- Soluble nitrate nitrogen S_{NO} - N_{O3} in the notation of the UCT model
- Soluble biodegradable substrate S_S - *Sbs* in the notation of the UCT model
- Particulate biodegradable substrate adsorbed - S_{ads} in the notation of the UCT model.
- Particulate slowly biodegradable substrate X_S - S_{enm} in the notation of the UCT model.
- Active heterotroph biomass $X_{BH} - Z_{BH}$ in the notation of the UCT model.
- Active autotroph biomass $X_{BA} - Z_{BA}$ in the notation of the UCT model.

The representation of the UCT reduced model is given in Table 4.3 where the compounds are represented using the ASM1 model notations. The reduced UCT model has 16 parameters, Table 4.4. Their original notations are used in the Peterson matrix in to distinguish the reduced models. These parameters are determined by parameter estimating method described in Chapter 6.

Table 4.3: The reduced UCT biological model in a matrix format

Compound → i process ↓ j	S_{ads}	S_S	S_{NH}	S_{NO}	Process rates, ρ_j
1) Aerobic growth of X_{BH} on S_S with S_{NH}	0	$-\frac{1}{Y_{ZH}}$	$-f_{ZB,H}$	0	$\hat{\mu}_H\left(\frac{S_S}{K_S+S_S}\right)\left(\frac{S_O}{K_{OH}+S_O}\right)\left(\frac{S_{NH}}{K_{HA}+S_{NH}}\right)X_{BH}$
2) Aerobic growth of X_{BH} on S_S with S_{NO}	0	$-\frac{1}{Y_{ZH}}$	0	$-f_{ZB,H}$	$\hat{\mu}_H\left(\frac{S_s}{K_s+S_s}\right)\left(\frac{S_O}{K_{OH}+S_O}\right)\left(\frac{K_{HA}}{K_{HA}+S_{NH}}\right)\left(\frac{S_{NO}}{K_{NO}+S_{NO}}\right)X_{BH}$
3) Anoxic growth of X_{BH} on S_S with S_{NH}	0	$-\frac{1}{Y_{ZH}}$	$-f_{ZB,H}$	$-\frac{1-Y_{ZH}}{2.86Y_{ZH}}$	$\hat{\mu}_H\left(\frac{S_S}{K_s+S_s}\right)\left(\frac{K_{OH}}{K_{OH}+S_O}\right)\left(\frac{S_{NH}}{K_{HA}+S_{NH}}\right)\left(\frac{S_{NO}}{K_{NO}+S_{NO}}\right)X_{BH}$
4) Anoxic growth of X_{BH} on S_S with S_{NO}	0	$-\frac{1}{Y_{ZH}}$	0	$\frac{1-Y_{ZH}}{2.86Y_{ZH}}-f_{ZB,H}$	$\hat{\mu}_H\left(\frac{S_S}{K_{SH}+S_S}\right)\left(\frac{K_{OH}}{K_{OH}+S_O}\right)\left(\frac{K_{HA}}{K_{HA}+S_{NH}}\right)\left(\frac{S_{NO}}{K_{NO}+S_{NO}}\right)X_{BH}$
5) Aerobic growth of X_{BH} on S_{ads} with S_{NH}	$-\frac{1}{Y_{ZH}}$	0	$-f_{ZB,H}$	0	$K_{MP}\left(\frac{S_{ads}/X_{BH}}{K_{SP}+S_{ads}/X_{BH}}\right)\left(\frac{S_O}{K_{OH}+S_O}\right)\left(\frac{S_{NH}}{K_{HA}+S_{NH}}\right)X_{BH}$

6) Aerobic growth of X_{BH} on S_{ads} with S_{NO}	$-\frac{1}{Y_{ZH}}$	0	0	$-f_{ZB,H}$	$K_{MP}\left(\frac{S_{ads}/X_{BH}}{K_{SP}+S_{ads}/X_{BH}}\right)\left(\frac{S_O}{K_{OH}+S_O}\right)\left(\frac{K_{HA}}{K_{HA}+S_{NH}}\right)\left(\frac{S_{NO}}{K_{NO}+S_{NO}}\right)X_{BH}$
7) Anoxic growth of X_{BH} on S_{ads} with S_{NH}	$-\frac{1}{Y_{ZH}}$	0	$-f_{ZB,H}$	$-\frac{1-Y_{ZH}}{2.86Y_{ZH}}$	$K_{MP}\left(\frac{S_{ads}/X_{BH}}{K_{SP}+S_{ads}/X_{BH}}\right)\left(\frac{K_{OH}}{K_{OH}+S_O}\right)\left(\frac{S_{NH}}{K_{HA}+S_{NH}}\right)\left(\frac{S_{NO}}{K_{NO}+S_{NO}}\right)\eta_g X_{BH}$
8) Anoxic growth of X_{BH} on S_{ads} with S_{NO}	$-\frac{1}{Y_{ZH}}$	0	0	$\frac{1-Y_{ZH}}{2.86Y_{ZH}}-f_{ZB,H}$	$K_{MP}\left(\frac{S_{ads}/X_{BH}}{K_{SP}+S_{ads}/X_{BH}}\right)\left(\frac{K_{OH}}{K_{OH}+S_O}\right)\left(\frac{K_{HA}}{K_{HA}+S_{NH}}\right)\left(\frac{S_{NO}}{K_{NO}+S_{NO}}\right)\eta_g X_{BH}$
9) Adsorption of X_S	1	0	0	0	$K_A X_S X_{BH}\left(f_{MA}-S_{ads}/X_{BH}\right)$
10) Aerobic growth of X_{BA}	0	0	$-\frac{1}{Y_{ZA}}-f_{ZB,A}$	$\frac{1}{Y_{ZA}}$	$\hat{\mu}_A\left(\frac{S_O}{K_{OA}+S_O}\right)\left(\frac{S_{NH}}{K_{SA}+S_{NH}}\right)X_{BA}$

Table 4.4: The nominal parameters of the UCT biological model

Symbol	Value	Units
Kinetic parameters $(20^\circ C)$		
μ_H	1.5 ÷3.5	d^{-1}
K_{SH}	5.0	$g\ COD\ m^{-3}$
K_{MP}	1.35	$g\ COD\ (g\ cell\ COD.d)^{-1}$
K_{SP}	0.027	$g\ COD\ (g\ cell\ COD)^{-1}$
K_A	0.17	$g\ COD\ (g\ cell\ COD.d)^{-1}$
μ_A	0.2 ÷0.75	d^{-1}
K_S	1.0	$g\ NH_3-N\ m^{-3}$
η_g	0.33	-
Stoichiometric parameters		
Y_{ZH}	0.666	$g\ cells\ COD(g\ COD\ utilized)^{-1}$
Y_{ZA}	0.15	$g\ cel\ COD(g\ N\ utilized)^{-1}$
f_{MA}	1.00	$g\ COD\ (g\ cell\ COD)^{-1}$
$f_{ZB,H}$	0.068	$g\ N(g\ COD)^{-1}$ in active mass
Switching functions parameters		
K_{OH}	0.002	$g\ O_2\ m^{-3}$
K_{OA}	0.002	$g\ O_2\ m^{-3}$
K_{HA}	0.01	$g\ NH_3-N\ m^{-3}$
K_{NO}	0.1	$g\ NO_3-N\ m^{-3}$

Table 4.5: Reduced UCT process parameters with their common values

ASM1 / UCT notations	Value	Explanation
Y_A / Y_{ZA}	0.15	Autotrophic biomass yield
Y_H / Y_{ZH}	0.666	Heterotrophic biomass yield
i_{XB} / f_{zbN}	0.068	Nitrogen mass per mass of COD in biomass
μ_A/ my_A	0.5	Maximum specific growth rate for autotrophic biomass
μ_H / my_H	2.5	Maximum specific growth rate for heterotrophic biomass
K_S / K_{SH}	5	Half saturation coefficient for heterotrophic biomass
K_{OH} / K_{OH}	0.002	Oxygen half saturation coefficient for heterotrophic biomass
K_{NO} / K_{NO}	0.1	Nitrate half saturation coefficient for denitrifying heterotrophic biomass
K_{SA} / K_{NH}	1	Ammonium half saturation coefficient for autotrophic biomass
K_{OA} / K_{OA}	0.002	Oxygen half saturation coefficient for autotrophic biomass
$?_g$ / ny_G	0.33	Correction factor for μ_H under anoxic conditions
k_h / K_{MP}	1.35	Maximum specific growth rate of the heterotrophs when utilizing adsorbed particulate slowly biodegradable COD

The equations describing the reduced UCT biological model can be written according to the Table 4.3 as follows:

$$r_{ads} = -\frac{1}{Y_{ZH}} K_{MP}\left(\frac{S_{ads}/X_{BH}}{K_{SP}+(S_{ads}/X_{BH})}\right) X_{BH}\left\{\begin{array}{l}\left(\frac{S_{NH}}{K_{HA}+S_{NH}}\right)\left[\left(\frac{S_O}{K_{OH}+S_O}\right)+\left(\frac{K_{OH}}{K_{OH}+S_O}\right)\left(\frac{S_{NO}}{K_{NO}+S_{NO}}\right)\eta_g\right]+\\ +\left(\frac{K_{HA}}{K_{HA}+S_{NH}}\right)\left(\frac{S_{NO}}{K_{NO}+S_{NO}}\right)\left[\left(\frac{S_O}{K_{OH}+S_O}\right)+\left(\frac{K_{OH}}{K_{OH}+S_O}\right)\eta_g\right]\end{array}\right\}+ \quad (4.4)$$

$$+K_A X_S X_{BH}\left(f_{MA}-S_{ads}/X_{BH}\right)$$

$$r_{SS} = -\frac{1}{Y_{ZH}}\mu_H X_{BH}\left(\frac{S_S}{K_{SH}+S_S}\right)\left\{\begin{array}{l}\left(\frac{S_{NH}}{K_{HA}+S_{NH}}\right)\left[\left(\frac{S_O}{K_{OH}+S_O}\right)+\left(\frac{K_{OH}}{K_{OH}+S_O}\right)\left(\frac{S_{NO}}{K_{NO}+S_{NO}}\right)\right]+\\ +\left(\frac{K_{HA}}{K_{HA}+S_{NH}}\right)\left(\frac{S_{NO}}{K_{NO}+S_{NO}}\right)\left[\left(\frac{S_O}{K_{OH}+S_O}\right)+\left(\frac{K_{OH}}{K_{OH}+S_O}\right)\right]\end{array}\right\} \quad (4.5)$$

$$r_{SNH} = -f_{ZB,H}\mu_H\left(\frac{S_S}{K_{SH}+S_S}\right)X_{BH}\left(\frac{S_{NH}}{K_{HA}+S_{NH}}\right)\left[\left(\frac{S_O}{K_{OH}+S_O}\right)+\left(\frac{K_{OH}}{K_{OH}+S_O}\right)\left(\frac{S_{NO}}{K_{NO}+S_{NO}}\right)\right]-$$

$$-f_{ZB,H}K_{MP}\left[\frac{S_{ads}/X_{BH}}{K_{SP}+(S_{ads}/X_{BH})}\right]X_{BH}\left(\frac{S_{NH}}{K_{HA}+S_{NH}}\right)\left[\left(\frac{S_O}{K_{OH}+S_O}\right)+\left(\frac{K_{OH}}{K_{OH}+S_O}\right)\left(\frac{S_{NO}}{K_{NO}+S_{NO}}\right)\eta_g\right]- \quad (4.6)$$

$$-\left[\frac{1}{Y_{ZA}}+f_{ZB,H}\right]\mu_A\left(\frac{S_{NH}}{K_{SA}+S_{NH}}\right)\left(\frac{S_O}{K_{OH}+S_O}\right)X_{BA}$$

$$r_{SNO} = -f_{ZB,H}X_{BH}\left(\frac{S_O}{K_{OH}+S_O}\right)\left(\frac{S_{NO}}{K_{NO}+S_{NO}}\right)\left[\left(\frac{K_{HA}}{K_{HA}+S_{NH}}\right)\left[\mu_H\left(\frac{S_S}{K_{SH}+S_S}\right)+K_{MP}\left[\frac{S_{ads}/X_{BH}}{K_{SP}+(S_{ads}/X_{BH})}\right]\right]\right]-$$

$$-\frac{1-Y_{ZH}}{2.86Y_{ZH}}X_{BH}\left(\frac{K_{OH}}{K_{OH}+S_O}\right)\left(\frac{S_{NH}}{K_{HA}+S_{NH}}\right)\left(\frac{S_{NO}}{K_{NO}+S_{NO}}\right)\left[\mu_H\left(\frac{S_S}{K_{SH}+S_S}\right)+K_{MP}\eta_g\left(\frac{S_{ads}/X_{BH}}{K_{SP}+S_{ads}/X_{BH}}\right)\right]-$$

$$-\left[-\frac{1-Y_{ZH}}{2.86Y_{ZH}}+f_{ZB,H}\right]X_{BH}\left[\left(\frac{K_{OH}}{K_{OH}+S_O}\right)\left(\frac{K_{HA}}{K_{HA}+S_{NH}}\right)\left(\frac{S_{NO}}{K_{NO}+S_{NO}}\right)\left[\mu_H\left(\frac{S_S}{K_{SH}+S_S}\right)+K_{MP}\eta_g\left(\frac{S_{ads}/X_{BH}}{K_{SP}+S_{ads}/X_{BH}}\right)\right]\right]+$$

$$+\frac{\mu_A}{Y_{ZA}}\left(\frac{S_{NH}}{K_{SA}+S_{NH}}\right)\left(\frac{S_O}{K_{OH}+S_O}\right)X_{BA} \quad (4.7)$$

4.6 Mass balance process models

Mass balance equations for 3 wastewater treatment plants were developed in Chapter 3.4 on the basis of the full UCT and ASM1 biological models. The above mass balance models are developed here on the basis of the reduced UCT and ASM1 biological models. A state space representation for everyone of them is obtained in a discrete time domain. The state space models are used for investigation of the sensitivity of the model variables towards the model parameters and for parameters estimations in Chapters 5 and 6 respectively. The structure and specifications of the benchmark process are described in Chapter 3. The mass balance equations are described by the equations (3.9) – (13.11).

4.6.1 Development of the mass balance process models for the Benchmark structure with the reduced ASM1 and UCT biological models

4.6.1.1 Mass balance equations for the benchmark model

Following the mass balance equations (3.9) – (3.14) the obtained reduced simplified mass balance models for the Benchmark structure for each tank are presented below. These equations are written here for the UCT model, as this model has its first 3 process compounds the same as the ASM1 model plus one compound more (S_{ads}).

For Tank 1:

$$\frac{dS_{NH_1}(t)}{dt} = \frac{1}{V_1}\left[Q_a S_{NH5}(t) + Q_r S_{NH3}(t) + fQ_0 S_{NH\phi_1}(t) - QS_{NH_1}(t)\right] + r_{S_{NH_1}}(t)$$

$$\frac{dS_{NO_1}(t)}{dt} = \frac{1}{V_1}\left[Q_a S_{NO_5}(t) + Q_r S_{NO_5}(t) + Q_0 S_{NO\phi_1}(t) - QS_{NO_1}(t)\right] + r_{S_{NO_1}}(t)$$

$$\frac{dS_{S_1}(t)}{dt} = \frac{1}{V_1}\left[Q_a S_{S5}(t) + Q_r S_{S_5}(t) + Q_0 S_{S\phi_1}(t) - QS_{S_1}(t)\right] + r_{S_{S_1}}(t)$$

$$\frac{dS_{ads_1}(t)}{dt} = \frac{1}{V_1}\left[Q_a S_{ads_5}(t) + Q_r S_{ads_5}(t) + Q_o S_{ads\phi_1}(t) - QS_{ads_1}(t) + r_{Sads1}(t)\right] \quad (4.8)$$

For Tank 2:

$$\frac{dS_{NH_2}(t)}{dt} = \frac{1}{V_2}\left[Q\left(S_{NH_1}(t) - S_{NH_2}(t)\right)\right] + r_{S_{NH_2}}(t)$$

$$\frac{dS_{NO_2}(t)}{dt} = \frac{1}{V_2}\left[Q\left(S_{NO_1}(t) - S_{NO_2}(t)\right)\right] + r_{S_{NO_2}}(t)$$

$$\frac{dS_{S_2}(t)}{dt} = \frac{1}{V_2}\left[Q\left(S_{S_1}(t) - S_{S_2}(t)\right)\right] + r_{S_{S_2}}(t)$$

$$\frac{dS_{ads_2}(t)}{dt} = \frac{1}{V_2}\left[Q\left(S_{ads_1}(t) - S_{ads_2}(t)\right)\right] + r_{Sads_2}(t) \qquad (4.9)$$

For Tank 3:

$$\frac{dS_{NH_3}(t)}{dt} = \frac{1}{V_3}\left[Q\left(S_{NH_2}(t) - S_{NH_3}(t)\right)\right] + r_{S_{NH_3}}(t)$$

$$\frac{dS_{NO_3}(t)}{dt} = \frac{1}{V_3}\left[Q\left(S_{NO_2}(t) - S_{NO_3}(t)\right)\right] + r_{S_{NO_3}}(t)$$

$$\frac{dS_{S_3}(t)}{dt} = \frac{1}{V_3}\left[Q\left(S_{S_2}(t) - S_{S_3}(t)\right)\right] + r_{S_{S_3}}(t)$$

$$\frac{dS_{ads_3}(t)}{dt} = \frac{1}{V_3}\left[Q\left(S_{ads_2}(t) - S_{ads_3}(t)\right)\right] + r_{Sads_3}(t) \qquad (4.10)$$

For Tank 4:

$$\frac{dS_{NH_4}(t)}{dt} = \frac{1}{V_4}\left[Q\left(S_{NH_3}(t) - S_{NH_4}(t)\right)\right] + r_{S_{NH_4}}(t)$$

$$\frac{dS_{NO_4}(t)}{dt} = \frac{1}{V_4}\left[Q\left(S_{NO_3}(t) - S_{NO_4}(t)\right)\right] + r_{S_{NO_4}}(t)$$

$$\frac{dS_{S_4}(t)}{dt} = \frac{1}{V_4}\left[Q\left(S_{S_3}(t) - S_{S_4}(t)\right)\right] + r_{S_{S_4}}(t)$$

$$\frac{dS_{ads_4}(t)}{dt} = \frac{1}{V_4}\left[Q\left(S_{ads_3}(t) - S_{ads_4}(t)\right)\right] + r_{Sads_4}(t) \qquad (4.11)$$

For Tank 5:

$$\frac{dS_{NH_5}(t)}{dt} = \frac{1}{V_5}\left[Q\left(S_{NH_4}(t) - S_{NH_5}(t)\right)\right] + r_{S_{NH_5}}(t)$$

$$\frac{dS_{NO_5}(t)}{dt} = \frac{1}{V_5}\left[Q\left(S_{NO_4}(t) - S_{NO_5}(t)\right)\right] + r_{S_{NO_5}}(t)$$

$$\frac{dS_{S_5}(t)}{dt} = \frac{1}{V_5}\left[Q\left(S_{S_4}(t) - S_{S_5}(t)\right)\right] + r_{S_{S_5}}(t)$$

$$\frac{dS_{ads_5}(t)}{dt} = \frac{1}{V_5}\left[Q\left(S_{ads_4}(t) - S_{ads_5}(t)\right)\right] + r_{Sads_5}(t) \tag{4.12}$$

where for the *ith* tank Q_i are the flow rates, V_i are the volumes of the tanks and r_i represent the process rates given by the expression $r_i = \sum_{j=1} C_{ij}\rho_j$ where C_{ij} are the coefficients from the ASM1 and UCT reduced model Peterson matrices. The ASM1 model process rates and the UCT model process rates in the equations are given in Table 4.1 and Table 4.3 respectively.

The input concentration of S_{NH} is multiplied by a factor *f* in order to represent around 20% of influent nitrogen that is entrapped in organic components. This simplification allows for the omission of soluble biodegradable organic nitrogen S_{ND}, from the model variables.

The system equations are written in a discrete form by representing the derivatives $\frac{dz}{dt}$ with the first difference equation $\frac{z(k+1)-z(k)}{\Delta t}$ where *?t* is the sampling interval.

The discrete mass balance models for the Benchmark structure are:

For Tank 1:

$$S_{NH_1}(k+1) = S_{NH_1}(k) + \frac{\Delta t}{V_1}\left[Q_a S_{NH_5}(k) + Q_r S_{NH_5}(k) + Q_0 f S_{NH\phi_1}(k) - Q S_{NH_1}(k)\right] + \Delta tr_{S_{NH_1}}(k)$$

$$S_{NO_1}(k+1) = S_{NO_1}(k) + \frac{\Delta t}{V_1}\left[Q_a S_{NO_5}(k) + Q_r S_{NO_5}(k) + Q_0 S_{NO0_1}(k) - Q S_{NO_1}(k)\right] + \Delta tr_{S_{NO_1}}(k)$$

$$S_{S_1}(k+1) = S_{S_1}(k) + \frac{\Delta t}{V_1}\left[Q_a S_{S_5}(k) + Q_r S_{S_5}(k) + Q_0 S_{S0_1}(k) - Q S_{S_1}(k)\right] + \Delta tr_{S_{S_1}}(k)$$

$$S_{ads_1}(k+1) = S_{ads_1}(k) + \frac{\Delta t}{V_1}\left[Q_a S_{ads_5}(k) + Q_r S_{ads_5}(k) + Q_O S_{ads\phi_1}(k) - Q S_{ads_1}(k)\right] + \Delta tr_{Sads_1}(k) \tag{4.13}$$

For Tank 2:

$$S_{NH_2}(k+1) = S_{NH_2}(k) + \frac{\Delta t}{V_2}\left[Q\left(S_{NH_1}(k) - S_{NH_2}(k)\right)\right] + \Delta tr_{S_{NH_2}}(k)$$

$$S_{NO_2}(k+1) = S_{NO_2}(k) + \frac{\Delta t}{V_2}\left[Q\left(S_{NO_1}(k) - S_{NO_2}(k)\right)\right] + \Delta tr_{S_{NO_2}}(k)$$

$$S_{S_2}(k+1) = S_{S_2}(k) + \frac{\Delta t}{V_2}\left[Q\left(S_{S_1}(k) - S_{S_2}(k)\right)\right] + \Delta tr_{S_{S_2}}(k)$$

$$S_{ads_2}(k+1) = S_{ads_2}(k) + \frac{\Delta t}{V_2}\left[Q\left(S_{ads_1}(k) - S_{ads_2}(k)\right)\right] + \Delta tr_{Sads_2}(k) \quad (4.14)$$

For Tank 3:

$$S_{NH_3}(k+1) = S_{NH_3}(k) + \frac{\Delta t}{V_3}\left[Q\left(S_{NH_2}(k) - S_{NH_3}(k)\right)\right] + \Delta tr_{S_{NH_3}}(k)$$

$$S_{NO_3}(k+1) = S_{NO_3}(k) + \frac{\Delta t}{V_3}\left[Q\left(S_{NO_2}(k) - S_{NO_3}(k)\right)\right] + \Delta tr_{S_{NO_3}}(k)$$

$$S_{S_3}(k+1) = S_{S_3}(k) + \frac{\Delta t}{V_3}\left[Q\left(S_{S_2}(k) - S_{S_3}(k)\right)\right] + \Delta tr_{S_{S_3}}(k)$$

$$S_{ads3}(k+1) = S_{ads3}(k) + \frac{\Delta t}{V_3}\left[Q\left(S_{ads2}(k) - S_{ads3}(k)\right)\right] + \Delta tr_{Sads3}(k) \quad (4.15)$$

For Tank 4:

$$S_{NH_4}(k+1) = S_{NH_4}(k) + \frac{\Delta t}{V_4}\left[Q\left(S_{NH_3}(k) - S_{NH_4}(k)\right)\right] + \Delta tr_{S_{NH_4}}(k)$$

$$S_{NO_4}(k+1) = S_{NO_4}(k) + \frac{\Delta t}{V_4}\left[Q\left(S_{NO_3}(k) - S_{NO_4}(k)\right)\right] + \Delta tr_{S_{NO_4}}(k)$$

$$S_{S_4}(k+1) = S_{S_4}(k) + \frac{\Delta t}{V_4}\left[Q\left(S_{S_3}(k) - S_{S_4}(k)\right)\right] + \Delta tr_{S_{S_4}}(k)$$

$$S_{ads4}(k+1) = S_{ads4}(k) + \frac{\Delta t}{V_4}\left[Q\left(S_{ads1}(k) - S_{ads4}(k)\right)\right] + \Delta tr_{Sads4} \quad (4.16)$$

For Tank 5:

$$S_{NH_5}(k+1) = S_{NH_5}(k) + \frac{\Delta t}{V_5}\left[Q\left(S_{NH_4}(k) - S_{NH_5}(k)\right)\right] + \Delta tr_{S_{NH_5}}(k)$$

$$S_{NO_5}(k+1) = S_{NO_5}(k) + \frac{\Delta t}{V_5}\left[Q\left(S_{NO_4}(k) - S_{NO_5}(k)\right)\right] + \Delta tr_{S_{NO_5}}(k)$$

$$S_{S_5}(k+1) = S_{S_5}(k) + \frac{\Delta t}{V_5}\left[Q\left(S_{S_4}(k) - S_{S_5}(k)\right)\right] + \Delta tr_{S_{S_5}}(k)$$

$$S_{ads5}(k+1) = S_{ads5}(k) + \frac{\Delta t}{V_5}\left[Q\left(S_{ads4}(k) - S_{ads5}(k)\right)\right] + \Delta tr_{Sads5}(k) \quad (4.17)$$

4.6.1.2 Process models in a vector-matrix form

The vectors of the every tank Peterson matrix compound concentrations and dissolved oxygen concentration form the system state and control vectors. The concentrations of $z = [S_{NH}\ S_{NO}\ S_S]^T$ and $z = [S_{NH}\ S_{NO}\ S_S\ S_{ads}]^T$ are selected to form the vector of state space for the ASM1 and UCT reduced models respectively. Control inputs are the concentrations of dissolved oxygen in the wastewater in every of the tanks. The vectors are:

1) for the ASM1 reduced mass balance model

- for the state space:

$$z=[z_1\ \ z_2\ \ z_3\ \ z_4\ \ z_5]^T = \\ =[S_{NH_1}\ \ S_{NO_1}\ \ S_{S_1}\ \ S_{NH_2}\ \ S_{NO_2}\ \ S_{S_2}\ \ S_{NH_3}\ \ S_{NO_3}\ \ S_{S_3}\ \ S_{NH_4}\ \ S_{NO_4}\ \ S_{S_4}\ \ S_{NH_5}\ \ S_{NO_5}\ \ S_{S_5}]^T, z \varepsilon R^{15} \quad (4.18)$$

- for the control:

$$\bar{u} = [u_1\ \ u_2\ \ u_3\ \ u_4\ \ u_5]^T = [S_{O_1}\ \ S_{O_2}\ \ S_{O_3}\ \ S_{O_4}\ \ S_{O_5}]^T,\ u\ \varepsilon\ R^5 \quad (4.19)$$

- for the input concentration :

$$z_{i\phi} = [S_{NH_\phi}\ \ S_{NO_\phi}\ \ S_{S_\phi}\ \ 0\ 0\ 0\ 0\ 0\ 0\ 0\ 0\ 0\ 0\ 0]^T, z_{i\phi}\ \varepsilon R^{15} \quad (4.20)$$

- for the biological rates :

$$\bar{r}(z,\bar{u},k) = [r(z_1,u_1,k)\ \ r(z_2,u_2,k)\ \ r(z_3,u_3,k)\ \ r(z_4,u_4,k)\ \ r(z_5,u_5,k)]^T, \\ k = \overline{0,K-1}\ \ r\ \varepsilon\ R^{15} \quad (4.21)$$

2) For the UCT reduced mass balance model

- For the state space

$$z = [z_1\ \ z_2\ z_3\ z_4\ z_5]^T = [S_{NH1}\ S_{NO1}\ S_{S1}\ S_{ads1}...S_{NH5}\ S_{NO5}\ S_{S5}\ S_{ads5}]^T, z \in R^{20} \quad (4.22)$$

- The control vector is the same $\bar{u} \in R^5$ (4.23)
- For the input concentration $z_{i\phi} = [S_{NH\phi}\ S_{NO\phi}\ S_{S\phi}\ S_{ads\phi}]^T, z_{i\phi} \in R^4$ (4.24)
- the vector of rates is the same but its components are

$$r(z_n,u_n,k) = [\Delta tr_{SNH,n}\ \Delta tr_{SNO,n}\ \Delta tr_{SS,n}\ \Delta tr_{ads,n}]^T \text{ and } \bar{r}(z,\bar{u},k) \in R^{20} \quad (4.25)$$

From the above notations and mass balance equations the whole system can be written in a vector/matrix form in the following way:

$$z(k+1) = Az(k) + \bar{r}(z,\bar{u},k) + Bz_{i\phi}(k) \qquad z(0) = z_0$$

where $z_{i\phi}$ is the vector of the inflow concentration, $\bar{r}(z,\bar{u},k)$ is the vector of the biological rates, $\bar{u}$ is the vector of the control, and

- For the ASM1 model

$$n = \overline{1,5},\ S_{On} = u_n, \qquad S_{NH_n} = z_{n1}, \qquad S_{NO_n} = z_{n2}, \qquad S_{S_n} = z_{n3}$$

- For UCT model

$S_{NHn} = z_{n1}$ $S_{NOn} = z_{n2}$ $S_{Sn} = z_{n3}$ $S_{adsn} = z_{n4}$

The vector $\bar{r}(z,\bar{u},k)$ in the above equation can be represented according to the Peterson matrix as a product $C^T\rho$ where ρ are the process rates and the matrix C consists of weighting coefficients from the Peterson matrices for all tanks. The vectors ρ_n where $n=\overline{1,5}$ contain process rates from the ASM1 and UCT reduced model Tables 4.1 and 4.3 respectively. The vector for the growth rates is $\rho=[\rho_1 \quad \rho_2 \quad \rho_3 \quad \rho_4 \quad \rho_5]^T$. The vector ρ for the whole system from the reduced ASM1 model is $\rho \varepsilon R^{20}$ and $\rho \varepsilon R^{50}$ for the reduced UCT model. The matrix C_n where $n=\overline{1,5}$ contains coefficients from the ASM1 and UCT reduced model matrix Tables 4.1 and 4.2 respectively. The matrices C for the whole system are:

$$C_{\substack{ASM1\\UCT}} = \Delta t.\begin{bmatrix} C_1 & 0 & 0 & 0 & 0 \\ 0 & C_2 & 0 & 0 & 0 \\ 0 & 0 & C_3 & 0 & 0 \\ 0 & 0 & 0 & C_4 & 0 \\ 0 & 0 & 0 & 0 & C_5 \end{bmatrix}, C_{ASM1} \varepsilon R^{20\times 15}, C_{UCT} \varepsilon R^{45\times 15} \tag{4.26}$$

$$C_{n,ASM1} = \begin{bmatrix} -i_{xB} & 0 & -1 \\ -i_{xB} & -\frac{1-Y_H}{2.86Y_H} & -\frac{1}{Y_H} \\ -i_{xB}-\frac{1}{Y_A} & \frac{1}{Y_A} & 0 \\ 0 & 0 & 1 \end{bmatrix} \in R^{4\times 3}, C_{n,UCT} = \begin{bmatrix} -f_{ZB,H} & 0 & -\frac{1}{Y_{ZH}} & 0 \\ 0 & -f_{ZB,H} & -\frac{1}{Y_{ZH}} & 0 \\ -f_{ZB,H} & -\frac{1-Y_{ZH}}{2.86Y_{ZH}} & -\frac{1}{Y_{ZH}} & 0 \\ 0 & \frac{1-Y_{ZH}}{2.86Y_{ZH}}-f_{ZB,H} & -\frac{1}{Y_{ZH}} & 0 \\ -f_{ZB,H} & 0 & 0 & -\frac{1}{Y_{ZH}} \\ 0 & 0 & 0 & -\frac{1}{Y_{ZH}} \\ -f_{ZB,H} & -\frac{1-Y_{ZH}}{2.86Y_{ZH}} & 0 & -\frac{1}{Y_{ZH}} \\ 0 & \frac{1-Y_{ZH}}{2.86Y_{ZH}}-f_{ZB,H} & 0 & -\frac{1}{Y_{ZH}} \\ 0 & 0 & 0 & 1 \\ -\frac{1}{Y_{ZA}}-f_{ZB,H} & \frac{1}{Y_{ZA}} & 0 & 0 \end{bmatrix} \in R^{9\times 3}$$

The matrices B are:

$$B_{ASM1} = \begin{bmatrix} f\frac{\Delta t}{V_1}Q_o & 0 & 0 \\ 0 & \frac{\Delta t}{V_1}Q_o & 0 \\ 0 & 0 & \frac{\Delta t}{V_1}Q_o \\ 0 & 0 & 0 \\ 0 & 0 & 0 \\ 0 & 0 & 0 \\ 0 & 0 & 0 \\ 0 & 0 & 0 \\ 0 & 0 & 0 \\ 0 & 0 & 0 \\ 0 & 0 & 0 \\ 0 & 0 & 0 \\ 0 & 0 & 0 \\ 0 & 0 & 0 \\ 0 & 0 & 0 \end{bmatrix} \quad B \varepsilon R^{15\times 3} \qquad B_{UCT} = \begin{bmatrix} f\frac{\Delta t}{V_1}Q_o & 0 & 0 & 0 \\ 0 & \frac{\Delta t}{V_1}Q_o & 0 & 0 \\ 0 & 0 & \frac{\Delta t}{V_1}Q_o & 0 \\ 0 & 0 & 0 & \frac{\Delta t}{V_1}Q_o \\ 0 & 0 & 0 & 0 \\ 0 & 0 & 0 & 0 \\ 0 & 0 & 0 & 0 \\ 0 & 0 & 0 & 0 \\ 0 & 0 & 0 & 0 \\ 0 & 0 & 0 & 0 \\ 0 & 0 & 0 & 0 \\ 0 & 0 & 0 & 0 \\ 0 & 0 & 0 & 0 \\ 0 & 0 & 0 & 0 \\ 0 & 0 & 0 & 0 \end{bmatrix} \in R^{20\times 4} \qquad (4.27)$$

The matrices A are:

- For ASM1 reduced model

$$A_{ASM1} = \begin{bmatrix} 1-\frac{\Delta t}{V_1}Q & 0 & 0 & 0 & 0 & 0 & 0 & 0 & 0 & 0 & 0 & 0 & \frac{\Delta t}{V_1}(Q_a+Q) & 0 & 0 \\ 0 & 1-\frac{\Delta t}{V_1}Q & 0 & 0 & 0 & 0 & 0 & 0 & 0 & 0 & 0 & 0 & 0 & \frac{\Delta t}{V_1}(Q_a+Q) & 0 \\ 0 & 0 & 1-\frac{\Delta t}{V_1}Q & 0 & 0 & 0 & 0 & 0 & 0 & 0 & 0 & 0 & 0 & 0 & \frac{\Delta t}{V_1}(Q_a+Q) \\ \frac{\Delta t}{V_2}Q & 0 & 0 & 1-\frac{\Delta t}{V_2}Q & 0 & 0 & 0 & 0 & 0 & 0 & 0 & 0 & 0 & 0 & 0 \\ 0 & \frac{\Delta t}{V_2}Q & 0 & 0 & 1-\frac{\Delta t}{V_2}Q & 0 & 0 & 0 & 0 & 0 & 0 & 0 & 0 & 0 & 0 \\ 0 & 0 & \frac{\Delta t}{V_2}Q & 0 & 0 & 1-\frac{\Delta t}{V_2}Q & 0 & 0 & 0 & 0 & 0 & 0 & 0 & 0 & 0 \\ 0 & 0 & 0 & \frac{\Delta t}{V_3}Q & 0 & 0 & 1-\frac{\Delta t}{V_3}Q & 0 & 0 & 0 & 0 & 0 & 0 & 0 & 0 \\ 0 & 0 & 0 & 0 & \frac{\Delta t}{V_3}Q & 0 & 0 & 1-\frac{\Delta t}{V_3}Q & 0 & 0 & 0 & 0 & 0 & 0 & 0 \\ 0 & 0 & 0 & 0 & 0 & \frac{\Delta t}{V_3}Q & 0 & 0 & 1-\frac{\Delta t}{V_3}Q & 0 & 0 & 0 & 0 & 0 & 0 \\ 0 & 0 & 0 & 0 & 0 & 0 & \frac{\Delta t}{V_4}Q & 0 & 0 & 1-\frac{\Delta t}{V_4}Q & 0 & 0 & 0 & 0 & 0 \\ 0 & 0 & 0 & 0 & 0 & 0 & 0 & \frac{\Delta t}{V_4}Q & 0 & 0 & 1-\frac{\Delta t}{V_4}Q & 0 & 0 & 0 & 0 \\ 0 & 0 & 0 & 0 & 0 & 0 & 0 & 0 & \frac{\Delta t}{V_4}Q & 0 & 0 & 1-\frac{\Delta t}{V_4}Q & 0 & 0 & 0 \\ 0 & 0 & 0 & 0 & 0 & 0 & 0 & 0 & 0 & \frac{\Delta t}{V_5}Q & 0 & 0 & 1-\frac{\Delta t}{V_5}Q & 0 & 0 \\ 0 & 0 & 0 & 0 & 0 & 0 & 0 & 0 & 0 & 0 & \frac{\Delta t}{V_5}Q & 0 & 0 & 1-\frac{\Delta t}{V_5}Q & 0 \\ 0 & 0 & 0 & 0 & 0 & 0 & 0 & 0 & 0 & 0 & 0 & \frac{\Delta t}{V_5}Q & 0 & 0 & 1-\frac{\Delta t}{V_5}Q \end{bmatrix} \in \in R^{51:} \qquad (4.28)$$

- For the UCT reduced model

$$A_{UCT} = \begin{bmatrix}
1-\frac{\Delta t}{V_1}Q & 0 & 0 & 0 & 0 & 0 & 0 & 0 & 0 & 0 \\
0 & 1-\frac{\Delta t}{V_1}Q & 0 & 0 & 0 & 0 & 0 & 0 & 0 & 0 \\
0 & 0 & 1-\frac{\Delta t}{V_1}Q & 0 & 0 & 0 & 0 & 0 & 0 & 0 \\
0 & 0 & 0 & 1-\frac{\Delta t}{V_1}Q & 0 & 0 & 0 & 0 & 0 & 0 \\
\frac{\Delta t}{V_2}Q & 0 & 0 & 0 & 1-\frac{\Delta t}{V_2}Q & 0 & 0 & 0 & 0 & 0 \\
0 & \frac{\Delta t}{V_2}Q & 0 & 0 & 0 & 1-\frac{\Delta t}{V_2}Q & 0 & 0 & 0 & 0 \\
0 & 0 & \frac{\Delta t}{V_2}Q & 0 & 0 & 0 & 1-\frac{\Delta t}{V_2}Q & 0 & 0 & 0 \\
0 & 0 & 0 & \frac{\Delta t}{V_2}Q & 0 & 0 & 0 & 1-\frac{\Delta t}{V_2}Q & 0 & 0 \\
0 & 0 & 0 & 0 & \frac{\Delta t}{V_3}Q & 0 & 0 & 0 & 1-\frac{\Delta t}{V_3}Q & 0 \\
0 & 0 & 0 & 0 & 0 & \frac{\Delta t}{V_3}Q & 0 & 0 & 0 & 1-\frac{\Delta t}{V_3}Q \\
0 & 0 & 0 & 0 & 0 & 0 & \frac{\Delta t}{V_3}Q & 0 & 0 & 0 \\
0 & 0 & 0 & 0 & 0 & 0 & 0 & \frac{\Delta t}{V_3}Q & 0 & 0 \\
0 & 0 & 0 & 0 & 0 & 0 & 0 & 0 & \frac{\Delta t}{V_4}Q & 0 \\
0 & 0 & 0 & 0 & 0 & 0 & 0 & 0 & 0 & \frac{\Delta t}{V_4}Q \\
0 & 0 & 0 & 0 & 0 & 0 & 0 & 0 & 0 & 0 \\
0 & 0 & 0 & 0 & 0 & 0 & 0 & 0 & 0 & 0 \\
0 & 0 & 0 & 0 & 0 & 0 & 0 & 0 & 0 & 0 \\
0 & 0 & 0 & 0 & 0 & 0 & 0 & 0 & 0 & 0 \\
0 & 0 & 0 & 0 & 0 & 0 & 0 & 0 & 0 & 0 \\
0 & 0 & 0 & 0 & 0 & 0 & 0 & 0 & 0 & 0
\end{bmatrix}$$

$$\begin{bmatrix}
0 & 0 & 0 & 0 & 0 & 0 & \frac{\Delta t}{V_1}(Q_a+Q_r) & 0 & 0 & 0 \\
0 & 0 & 0 & 0 & 0 & 0 & 0 & \frac{\Delta t}{V_1}(Q_a+Q_r) & 0 & 0 \\
0 & 0 & 0 & 0 & 0 & 0 & 0 & 0 & \frac{\Delta t}{V_1}(Q_a+Q_r) & 0 \\
0 & 0 & 0 & 0 & 0 & 0 & 0 & 0 & 0 & \frac{\Delta t}{V_1}(Q_a+Q_r) \\
0 & 0 & 0 & 0 & 0 & 0 & 0 & 0 & 0 & 0 \\
0 & 0 & 0 & 0 & 0 & 0 & 0 & 0 & 0 & 0 \\
0 & 0 & 0 & 0 & 0 & 0 & 0 & 0 & 0 & 0 \\
0 & 0 & 0 & 0 & 0 & 0 & 0 & 0 & 0 & 0 \\
0 & 0 & 0 & 0 & 0 & 0 & 0 & 0 & 0 & 0 \\
0 & 0 & 0 & 0 & 0 & 0 & 0 & 0 & 0 & 0 \\
1-\frac{\Delta t}{V_3}Q & 0 & 0 & 0 & 0 & 0 & 0 & 0 & 0 & 0 \\
0 & 1-\frac{\Delta t}{V_3}Q & 0 & 0 & 0 & 0 & 0 & 0 & 0 & 0 \\
0 & 0 & 1-\frac{\Delta t}{V_4}Q & 0 & 0 & 0 & 0 & 0 & 0 & 0 \\
0 & 0 & 0 & 1-\frac{\Delta t}{V_4}Q & 0 & 0 & 0 & 0 & 0 & 0 \\
\frac{\Delta t}{V_4}Q & 0 & 0 & 0 & 1-\frac{\Delta t}{V_4}Q & 0 & 0 & 0 & 0 & 0 \\
0 & \frac{\Delta t}{V_4}Q & 0 & 0 & 0 & 1-\frac{\Delta t}{V_4}Q & 0 & 0 & 0 & 0 \\
0 & 0 & \frac{\Delta t}{V_5}Q & 0 & 0 & 0 & 1-\frac{\Delta t}{V_5}Q & 0 & 0 & 0 \\
0 & 0 & 0 & \frac{\Delta t}{V_5}Q & 0 & 0 & 0 & 1-\frac{\Delta t}{V_5}Q & 0 & 0 \\
0 & 0 & 0 & 0 & \frac{\Delta t}{V_5}Q & 0 & 0 & 0 & 1-\frac{\Delta t}{V_5}Q & 0 \\
0 & 0 & 0 & 0 & 0 & \frac{\Delta t}{V_5}Q & 0 & 0 & 0 & 1-\frac{\Delta t}{V_5}Q
\end{bmatrix} \in R^{20\times 20} \qquad 4.29)$$

4.6.2 Development of the mass balance process models for the Mitchell's Plain structure with the reduced ASM1 and UCT biological models

4.6.2.1 Mass balance equations for the Mitchell's Plain plant

The input concentration, S_{NH} is multiplied by a factor *f* in order to represent the 20 % entrapped in the organic components influent nitrogen. System equations expressed for every of the reduced model process variables are

Tank 1

$$\frac{dS_{NH,1}(t)}{dt} = \frac{1}{V_1}\left[Q_0 f S_{NH,\phi}(t) + Q_r S_{NH,3}(t) - Q_1 S_{NH,1}(t)\right] + r_{SNH,1}(t)$$

$$\frac{dS_{NO,1}(t)}{dt} = \frac{1}{V_1}\left[Q_0 f S_{NO,\phi}(t) + Q_r S_{NO,3}(t) - Q_1 S_{NO,1}(t)\right] + r_{NO,1}(t) \qquad (4.30)$$

$$\frac{dS_{S,1}(t)}{dt} = \frac{1}{V_1}\left[Q_0 S_{S,\phi}(t) + Q_r S_{S,3}(t) - Q_1 S_{S,1}(t)\right] + r_{SS,1}(t)$$

$$\frac{dS_{ads,1}}{dt} = \frac{1}{V_1}\left[Q_0 S_{ads\phi}(t) + Q_r S_{ads,3}(t) - Q_1 S_{ads,1}(t)\right] + r_{Sads,1}(t)$$

Tank 2

$$\frac{dS_{NH,2}(t)}{dt} = \frac{1}{V_2}\left[Q_1 S_{NH,1}(t) + Q_a S_{NH,3}(t) - Q_2 S_{NH,2}(t)\right] + r_{SNH,2}(t)$$

$$\frac{dS_{NO,2}(t)}{dt} = \frac{1}{V_2}\left[Q_1 S_{NO,2}(t) + Q_a S_{NO,3}(t) - Q_2 S_{NO,2}(t)\right] + r_{SNO,2}(t) \qquad (4.31)$$

$$\frac{dS_{S,2}(t)}{dt} = \frac{1}{V_2}\left[Q_1 S_{S,2}(t) + Q_a S_{S,3}(t) - Q_2 S_{S,2}(t)\right] + r_{SS,2}(t)$$

$$\frac{dS_{ads,2}}{dt} = \frac{1}{V_2}\left[Q_1 S_{ads,2}(t) + Q_a S_{ads,3}(t) - Q_2 S_{ads,2}(t)\right] + r_{Sads,2}(t)$$

Tank 3

$$\frac{dS_{NH,3}(t)}{dt} = \frac{1}{V_3}\left[Q_2 S_{NH,2}(t) - Q_3 S_{NH,3}(t)\right] + r_{SNH,3}(t)$$

$$\frac{dS_{NO,3}(t)}{dt} = \frac{1}{V_3}\left[Q_2 S_{NO,2}(t) - Q_3 S_{NO,3}(t)\right] + r_{SNO,3}(t) \qquad (4.32)$$

$$\frac{dS_{S,3}(t)}{dt} = \frac{1}{V_3}\left[Q_2 S_{S,2}(t) - Q_3 S_{S,3}(t)\right] + r_{SS,3}(t)$$

$$\frac{dS_{ads,3}}{dt} = \frac{1}{V_3}\left[Q_2 S_{ads,2}(t) - Q_3 S_{ads,3}(t)\right] + r_{Sads,3}(t)$$

The discrete form of the equations is:

Tank 1

$$S_{NH,1}(k+1)=S_{NH,1}(k)+\frac{\Delta t}{V_1}\left[Q_0 fS_{NH,\phi}(k)+Q_r S_{NH,3}(k)-Q_1 S_{NH,1}(k)\right]+\Delta tr_{SNH,1}(k)$$

$$S_{NO,1}(k+1)=S_{NO,1}(k)+\frac{\Delta t}{V_1}\left[Q_0 S_{NO,\phi}(k)+Q_r S_{NO,3}(k)-Q_1 S_{NO,1}(k)\right]+\Delta tr_{SNO,1}(k) \quad (4.33)$$

$$S_{S,1}(k+1)=S_{S,1}(k)+\frac{\Delta t}{V_1}\left[Q_0 S_{S,\phi}(k)+Q_r S_{S,3}(k)-Q_1 S_{S,1}(k)\right]+\Delta tr_{SS,1}(k)$$

$$S_{ads,1}(k+1)=S_{ads,1}(k)+\frac{\Delta t}{V_1}\left[Q_0 S_{ads\phi}(k)+Q_r S_{ads,3}(k)-Q_1 S_{ads,1}(k)\right]+\Delta tr_{Sads,1}(k)$$

Tank 2

$$S_{NH,2}(k+1)=S_{NH,2}(k)+\frac{\Delta t}{V_2}\left[Q_1 S_{NH,1}(k)+Q_a S_{NH,3}(k)-Q_2 S_{NH,2}(k)\right]+\Delta tr_{SNH,2}(k)$$

$$S_{NO,2}(k+1)=S_{NO,2}(k)+\frac{\Delta t}{V_2}\left[Q_1 S_{NO,1}(k)+Q_a S_{NO,3}(k)-Q_2 S_{NO,2}(k)\right]+\Delta tr_{SNO,2}(k) \quad (4.34)$$

$$S_{S,2}(k+1)=S_{S,2}(k)+\frac{\Delta t}{V_2}\left[Q_1 S_{S,1}(k)+Q_a S_{S,3}(k)-Q_2 S_{S,2}(k)\right]+\Delta tr_{SS,2}(k)$$

$$S_{ads,2}(k+1)=S_{ads,2}(k)+\frac{\Delta t}{V_2}\left[Q_1 S_{ads,1}(k)+Q_a S_{ads,3}(k)-Q_2 S_{ads,2}(k)\right]+\Delta tr_{Sads,2}(k)$$

Tank 3

$$S_{NH,3}(k+1)=S_{NH,3}(k)+\frac{\Delta t}{V_3}\left[Q_2 S_{NH,2}(k)-Q_3 S_{NH,3}(k)\right]+\Delta tr_{SNH,3}(k)$$

$$S_{NO,3}(k+1)=S_{NO,3}(k)+\frac{\Delta t}{V_3}\left[Q_2 S_{NO,2}(k)-Q_3 S_{NO,3}(k)\right]+\Delta tr_{SNO,3}(k) \quad (4.35)$$

$$S_{S,3}(k+1)=S_{S,3}(k)+\frac{\Delta t}{V_3}\left[Q_2 S_{S,2}(k)-Q_3 S_{S,3}(k)\right]+\Delta tr_{SS,3}(k)$$

$$S_{ads,3}(k+1)=S_{ads,3}(k)+\frac{\Delta t}{V_3}\left[Q_2 S_{ads,2}(k)-Q_3 S_{ads,3}(k)\right]+\Delta tr_{Sads,3}(k)$$

4.6.2.2 Process model in a vector-matrix form

The state space vector is formed in the same way as for the Benchmark plant. The equation of the whole system is

$$z(k+1)=Az(k)+r(z,u,k)+Bz_{i\phi}(k),\ z(0)=z_0 \quad (4.36)$$

$$z(k+1)=Az(k)+C^T\overline{\rho}(z,\overline{u},k)+Bz_{i\phi}(k),\ z(0)=z_0 \quad (4.37)$$

where the state, control and compound rates are formed in the same way as for the Benchmark model. For the ASM1 reduced model $z_{ASM1} = [z_1\ z_2\ z_3]^T \in R^9$. For the UCT reduced model $z_{UCT} \in R^{12}$. Then the state space matrices are $A_{ASM1} \in R^{9\times 9}$ and $A_{UCT} \in R^{12\times 12}$. These matrices are as follows:

$$A_{ASM1} = \begin{bmatrix}
1-\frac{\Delta t Q_1}{V_1} & 0 & 0 & 0 & 0 & 0 & \frac{\Delta t Q_r}{V_1} & 0 & 0 \\
0 & 1-\frac{\Delta t Q_1}{V_1} & 0 & 0 & 0 & 0 & 0 & \frac{\Delta t Q_r}{V_1} & 0 \\
0 & 0 & 1-\frac{\Delta t Q_1}{V_1} & 0 & 0 & 0 & 0 & 0 & \frac{\Delta t Q_r}{V_1} \\
\frac{\Delta t Q_1}{V_2} & 0 & 0 & 1-\frac{\Delta t Q_2}{V_2} & 0 & 0 & \frac{\Delta t}{V_2} Q_a & 0 & 0 \\
0 & \frac{\Delta t Q_1}{V_2} & 0 & 0 & 1-\frac{\Delta t Q_2}{V_2} & 0 & 0 & \frac{\Delta t}{V_2} Q_a & 0 \\
0 & 0 & \frac{\Delta t Q_1}{V_2} & 0 & 0 & 1-\frac{\Delta t Q_2}{V_2} & 0 & 0 & \frac{\Delta t}{V_2} Q_a \\
0 & 0 & 0 & \frac{\Delta t Q_2}{V_3} & 0 & 0 & 1-\frac{\Delta t Q_3}{V_3} & 0 & 0 \\
0 & 0 & 0 & 0 & \frac{\Delta t Q_2}{V_3} & 0 & 0 & 1-\frac{\Delta t Q_3}{V_3} & 0 \\
0 & 0 & 0 & 0 & 0 & \frac{\Delta t Q_2}{V_3} & 0 & 0 & 1-\frac{\Delta t Q_3}{V_3}
\end{bmatrix}, A \in R^{9\times 9} \tag{4.38}$$

$$A_{UCT} = \begin{bmatrix}
1-\frac{\Delta t}{V_1} Q_1 & 0 & 0 & 0 & 0 & 0 & 0 & 0 & \frac{\Delta t Q_r}{V_1} & 0 & 0 & 0 \\
0 & 1-\frac{\Delta t}{V_1} Q_1 & 0 & 0 & 0 & 0 & 0 & 0 & 0 & \frac{\Delta t Q_r}{V_1} & 0 & 0 \\
0 & 0 & 1-\frac{\Delta t}{V_1} Q_1 & 0 & 0 & 0 & 0 & 0 & 0 & 0 & \frac{\Delta t Q_r}{V_1} & 0 \\
0 & 0 & 0 & 1-\frac{\Delta t}{V_1} Q_1 & 0 & 0 & 0 & 0 & 0 & 0 & 0 & \frac{\Delta t Q_r}{V_1} \\
\frac{\Delta t}{V_2} Q_1 & 0 & 0 & 0 & 1-\frac{\Delta t}{V_2} Q_2 & 0 & 0 & 0 & \frac{\Delta t}{V_2} Q_a & 0 & 0 & 0 \\
0 & \frac{\Delta t}{V_2} Q_1 & 0 & 0 & 0 & 1-\frac{\Delta t}{V_2} Q_2 & 0 & 0 & 0 & \frac{\Delta t}{V_2} Q_a & 0 & 0 \\
0 & 0 & \frac{\Delta t}{V_2} Q_1 & 0 & 0 & 0 & 1-\frac{\Delta t}{V_2} Q_2 & 0 & 0 & 0 & \frac{\Delta t}{V_2} Q_a & 0 \\
0 & 0 & 0 & \frac{\Delta t}{V_2} Q_1 & 0 & 0 & 0 & 1-\frac{\Delta t}{V_2} Q_2 & 0 & 0 & 0 & \frac{\Delta t}{V_2} Q_a \\
0 & 0 & 0 & 0 & \frac{\Delta t}{V_3} Q_2 & 0 & 0 & 0 & 1-\frac{\Delta t}{V_3} Q_3 & 0 & 0 & 0 \\
0 & 0 & 0 & 0 & 0 & \frac{\Delta t}{V_3} Q_2 & 0 & 0 & 0 & 1-\frac{\Delta t}{V_3} Q_3 & 0 & 0 \\
0 & 0 & 0 & 0 & 0 & 0 & \frac{\Delta t}{V_3} Q_2 & 0 & 0 & 0 & 1-\frac{\Delta t}{V_3} Q_3 & 0 \\
0 & 0 & 0 & 0 & 0 & 0 & 0 & \frac{\Delta t}{V_3} Q_2 & 0 & 0 & 0 & 1-\frac{\Delta t}{V_3} Q_3
\end{bmatrix} \in R^{12\times 12} \tag{4.39}$$

The matrices B are as follows

$$B_{UCT} = \begin{bmatrix} f\frac{\Delta t}{V_1}Q_0 & 0 & 0 & 0 \\ 0 & \frac{\Delta t}{V_1}Q_0 & 0 & 0 \\ 0 & 0 & \frac{\Delta t}{V_1}Q_0 & 0 \\ 0 & 0 & 0 & \frac{\Delta t}{V_1}Q_0 \\ 0 & 0 & 0 & 0 \\ 0 & 0 & 0 & 0 \\ 0 & 0 & 0 & 0 \\ 0 & 0 & 0 & 0 \\ 0 & 0 & 0 & 0 \\ 0 & 0 & 0 & 0 \\ 0 & 0 & 0 & 0 \\ 0 & 0 & 0 & 0 \end{bmatrix} \in R^{12\times 4} \qquad B_{ASM1} = \begin{bmatrix} f\frac{\Delta t}{V_1}Q_0 & 0 & 0 \\ 0 & \frac{\Delta t}{V_1}Q_0 & 0 \\ 0 & 0 & \frac{\Delta t}{V_1}Q_2 \\ 0 & 0 & 0 \\ 0 & 0 & 0 \\ 0 & 0 & 0 \\ 0 & 0 & 0 \\ 0 & 0 & 0 \\ 0 & 0 & 0 \end{bmatrix} \in R^{9\times 3} \tag{4.40}$$

The matrices $C_{n,UCT}$ and $C_{n,ASM1}$ are the same as above. The dimensions of the vectors $\rho = [\rho_1, \rho_2, \rho_3]^T$ is $\rho_{ASM1} \in R^{12}$ and $\rho_{UCT} \in R^{30}$ where $\rho_{n,ASM1} \in R^4$ and $\rho_{n,UCT} \in R^{10}$, respectively.

4.6.3 Development of the mass balance process models for the Athlone structure with reduced UCT and ASM1 biological models

4.6.3.1 Mass balance equations for the Athlone plant

System equations expressed for every of the reduced model process variables are:

Tank 1:

$$\frac{dS_{NH_1}(t)}{dt} = \frac{1}{V_1}\left[Q_p S_{NH_2}(t) + fQ_0 S_{NH\phi_1}(t) - Q_1 S_{NH_1}(t)\right] + r_{S_{NH_1}}(t)$$

$$\frac{dS_{NO_1}(t)}{dt} = \frac{1}{V_1}\left[Q_p S_{NO_2}(t) + Q_0 S_{NO\phi_1}(t) - Q_1 S_{NO_1}(t)\right] + r_{S_{NO_1}}(t)$$

$$\frac{dS_{S_1}(t)}{dt} = \frac{1}{V_1}\left[Q_p S_{S_2}(t) + Q_0 S_{S\phi_1}(t) - Q_1 S_{S_1}(t)\right] + r_{S_{S_1}}(t) \tag{4.41}$$

$$\frac{dS_{ads,1}(t)}{dt} = \frac{1}{V_1}\left[Q_p S_{ads,2}(t) + Q_0 S_{ads\phi}(t) - Q_1 S_{ads,1}(t)\right] + r_{Sads,1}(t)$$

Tank 2:

$$\frac{dS_{NH_2}(t)}{dt} = \frac{1}{V_2}\left[Q_1 S_{NH_1}(t) + Q_a S_{NH_3}(t) + Q_r S_{NH_3}(t) - Q_2 S_{NH_2}(t)\right] + r_{S_{NH_2}}(t)$$

$$\frac{dS_{NO_2}(t)}{dt} = \frac{1}{V_2}\left[Q_1 S_{NO_1}(t) + Q_a S_{NO_3}(t) + Q_r S_{NO_3}(t) - Q_2 S_{NO_2}\right] + r_{S_{NO_2}}(t)$$

$$\frac{dS_{S_2}(t)}{dt} = \frac{1}{V_2}\left[Q_1 S_{S_1}(t) + Q_a S_{S_3}(t) + Q_r S_{S_3}(t) - Q_2 S_{S_2}(t)\right] + r_{S_{S_2}}(t) \tag{4.42}$$

$$\frac{dS_{ads,2}(t)}{dt} = \frac{1}{V_2}\left[Q_1 S_{ads,1}(t) + Q_a S_{ads,3}(t) Q_r S_{ads,3} - Q_2 S_{ads,2}(t)\right] + r_{Sads,2}(t)$$

Tank 3:

$$\frac{dS_{NH_3}(t)}{dt} = \frac{1}{V_3}\left[Q_2 S_{NH_2}(t) - Q_3 S_{NH_3}(t)\right] + r_{S_{NH_3}}(t)$$

$$\frac{dS_{NO_3}(t)}{dt} = \frac{1}{V_3}\left[Q_2 S_{NO_2}(t) - Q_3 S_{NO_3}(t)\right] + r_{S_{NO_3}}(t)$$

$$\frac{dS_{S_3}(t)}{dt} = \frac{1}{V_3}\left[Q_2 S_{S_2}(t) - Q_3 S_{S_3}(t)\right] + r_{S_{S_3}}(t) \qquad (4.43)$$

$$\frac{dS_{ads,3}(t)}{dt} = \frac{1}{V_1}\left[Q_2 S_{ads,2}(t) - Q_3 S_{ads,3}(t)\right] + r_{Sads,3}(t)$$

The discrete mass balance models for the Athlone structure are:

Tank 1:

$$S_{NH_1}(k+1) = S_{NH_1}(k) + \frac{\Delta t}{V_1}\left[\ \left[Q_p S_{NH_2}(k) + fQ_0 S_{NH\phi_1}(k) - Q_1 S_{NH_1}(k)\right]\ \right] + \Delta tr_{S_{NH_1}}(k)$$

$$\mathrm{S_{NO_1}(k+1) = S_{NO_1}(k) + \frac{\Delta t}{V_1}\left[Q_p S_{NO_2}(k) + Q_0 S_{NO\phi_1}(k) - Q_1 S_{NO_1}(k)\right] + \Delta tr_{S_{NO_1}}(k)}$$

$$\mathrm{S_{S_1}(k+1) = S_{S_1}(k) + \frac{\Delta t}{V_1}\left[Q_p S_{S_2}(k) + Q_0 S_{S\phi_1}(k) - Q_1 S_{S_1}(k)\right] + \Delta tr_{S_{S_1}}(k)} \qquad (4.44)$$

$$S_{ads,1}(k+1) = S_{ads,1}(k) + \frac{\Delta t}{V_1}\left[Q_p S_{ads,2}(k) + Q_0 S_{ads\phi}(k) - Q_1 S_{ads,1}(k)\right] + \Delta tr_{ads,1}(k)$$

Tank 2:

$$S_{NH_2}(k+1) = S_{NH_2}(k) + \frac{\Delta t}{V_2}\left[Q_1 S_{NH_1}(k) + (Q_a + Q_r) S_{NH_3}(k) - Q_{21} S_{NH_2}(k)\right] + \Delta tr_{S_{NH_2}}(k)$$

$$S_{NO_2}(k+1) = S_{NO_2}(k) + \frac{\Delta t}{V_2}\left[Q_1 S_{NO_1}(k) + (Q_a + Q_r) S_{NO_3}(k) - Q_2 S_{NO_2}(k)\right] + \Delta tr_{S_{NO_2}}(k)$$

$$S_{S_2}(k+1) = S_{S_2}(k) + \frac{\Delta t}{V_2}\left[Q_1 S_{S_1}(k) + (Q_a + Q_r) S_{S_3}(k) - Q_2 S_{S_2}(k)\right] + \Delta tr_{S_{S_2}}(k) \qquad (4.45)$$

$$S_{ads,2}(k+1) = S_{ads,2}(k) + \frac{\Delta t}{V_2}\left[Q_1 S_{ads,1}(k) + (Q_a + Q_r) S_{ads,3}(k) - Q_2 S_{ads,2}(k)\right] + \Delta tr_{ads,2}(k)$$

Tank 3:

$$\mathrm{S_{NH_3}(k+1) = S_{NH_3}(k) + \frac{\Delta t}{V_3}\left[Q_2 S_{NH_2}(k) - Q_3 S_{NH_3}(k)\right] + \Delta tr_{S_{NH_3}}(k)}$$

$$\mathrm{S_{NO_3}(k+1) = S_{NO_3}(k) + \frac{\Delta t}{V_3}\left[Q_2 S_{NO_2}(k) - Q_3 S_{NO_3}(k)\right] + \Delta tr_{S_{NO_3}}(k)}$$

$$S_{S_3}(k+1) = S_{S_3}(k) + \frac{\Delta t}{V_3}\left[Q_2 S_{S_2}(k) - Q_3 S_{S_3}(k)\right] + \Delta tr_{S_{S_3}}(k) \quad (4.46)$$

$$S_{ads,3}(k+1) = S_{ads,3}(k) + \frac{\Delta t}{V_3}\left[Q_2 S_{ads,2}(k) - Q_3 S_{ads,3}(k)\right] + \Delta tr_{ads,3}(k)$$

4.6.3.2 Process model in a vector-matrix form

The model vectors for the Athlone plant have the same components as for the Mitchell's Plain plant as both have the same number of tanks and are based on the same biological models. The structure of the matrices A_{ASM1} and A_{UCT} are different because the two plants have different recycles. The matrices C_n where $n = \overline{1,3}$ contain coefficients from the ASM1 and UCT reduced models are given in the Tables 4.1 and 4.3 respectively. The matrices C for the whole system are:

$$C = \Delta t. \begin{bmatrix} C_1 & 0 & 0 \\ 0 & C_2 & 0 \\ 0 & 0 & C_3 \end{bmatrix}, C_{ASM1} \varepsilon R^{12\times 9}, C_{UCT} \varepsilon R^{30\times 12}$$

(4.47)

The matrices B are the same for the Mitchell's Plain plant. The matrices A are:

$$A_{ASM} = \begin{bmatrix} 1-\frac{\Delta t}{V_1}Q_1 & 0 & 0 & \frac{\Delta t}{V_1}(Q_p) & 0 & 0 & 0 & 0 & 0 \\ 0 & 1-\frac{\Delta t}{V_1}Q_1 & 0 & 0 & \frac{\Delta t}{V_1}(Q_p) & 0 & 0 & 0 & 0 \\ 0 & 0 & 1-\frac{\Delta t}{V_1}Q_1 & 0 & 0 & \frac{\Delta t}{V_1}(Q_p) & 0 & 0 & 0 \\ \frac{\Delta t}{V_2}Q_1 & 0 & 0 & 1-\frac{\Delta t}{V_2}Q_2 & 0 & 0 & \frac{\Delta t}{V_2}(Q_a+Q_1) & 0 & 0 \\ 0 & \frac{\Delta t}{V_2}Q_1 & 0 & 0 & 1-\frac{\Delta t}{V_2}Q_2 & 0 & 0 & \frac{\Delta t}{V_2}(Q_a+Q_1) & 0 \\ 0 & 0 & \frac{\Delta t}{V_2}Q_1 & 0 & 0 & 1-\frac{\Delta t}{V_2}Q_2 & 0 & 0 & \frac{\Delta t}{V_2}(Q_a+Q_1) \\ 0 & 0 & 0 & \frac{\Delta t}{V_3}Q_2 & 0 & 0 & 1-\frac{\Delta t}{V_3}Q_3 & 0 & 0 \\ 0 & 0 & 0 & 01 & \frac{\Delta t}{V_3}Q_2 & 0 & 0 & 1-\frac{\Delta t}{V_3}Q_3 & 0 \\ 0 & 0 & 0 & 0 & 0 & \frac{\Delta t}{V_3}Q_2 & 0 & 0 & 1-\frac{\Delta t}{V_3}Q_3 \end{bmatrix} \varepsilon R^{9\times 9}$$

(4.48)

$$A_{UCT} = \begin{bmatrix}
1-\frac{\Delta t}{V_1}Q_1 & 0 & 0 & 0 & \frac{\Delta t}{V_1}Q_5 & 0 & 0 & 0 & 0 & 0 & 0 & 0 \\
0 & 1-\frac{\Delta t}{V_1}Q_1 & 0 & 0 & 0 & \frac{\Delta t}{V_1}Q_p & 0 & 0 & 0 & 0 & 0 & 0 \\
0 & 0 & 1-\frac{\Delta t}{V_1}Q_1 & 0 & 0 & 0 & \frac{\Delta t}{V_1}Q_p & 0 & 0 & 0 & 0 & 0 \\
0 & 0 & 0 & 1-\frac{\Delta t}{V_1}Q_1 & 0 & 0 & 0 & \frac{\Delta t}{V_1}Q_p & 0 & 0 & 0 & 0 \\
\frac{\Delta t}{V_2}Q_1 & 0 & 0 & 0 & 1-\frac{\Delta t}{V_2}Q_2 & 0 & 0 & 0 & \frac{\Delta t}{V_2}(Q_a+Q_r) & 0 & 0 & 0 \\
0 & \frac{\Delta t}{V_2}Q_1 & 0 & 0 & 0 & 1-\frac{\Delta t}{V_2}Q_2 & 0 & 0 & 0 & \frac{\Delta t}{V_2}(Q_a+Q_r) & 0 & 0 \\
0 & 0 & \frac{\Delta t}{V_2}Q_1 & 0 & 0 & 0 & 1-\frac{\Delta t}{V_2}Q_2 & 0 & 0 & 0 & \frac{\Delta t}{V_2}(Q_a+Q_r) & 0 \\
0 & 0 & 0 & \frac{\Delta t}{V_2}Q_1 & 0 & 0 & 0 & 1-\frac{\Delta t}{V_2}Q_2 & 0 & 0 & 0 & \frac{\Delta t}{V_2}(Q_a+Q_r) \\
0 & 0 & 0 & 0 & \frac{\Delta t}{V_2}Q_1 & 0 & 0 & 0 & 1-\frac{\Delta t}{V_3}Q_3 & 0 & 0 & 0 \\
0 & 0 & 0 & 0 & 0 & \frac{\Delta t}{V_2}Q_1 & 0 & 0 & 0 & 1-\frac{\Delta t}{V_3}Q_3 & 0 & 0 \\
0 & 0 & 0 & 0 & 0 & 0 & \frac{\Delta t}{V_2}Q_1 & 0 & 0 & 0 & 1-\frac{\Delta t}{V_3}Q_3 & 0 \\
0 & 0 & 0 & 0 & 0 & 0 & 0 & \frac{\Delta t}{V_2}Q_1 & 0 & 0 & 0 & 1-\frac{\Delta t}{V_3}Q_3
\end{bmatrix} \in R^{12\times 12} \tag{4.49}$$

4.7 Reduced models characteristics

The derivations of the reduced models for different process configurations and for different biological models lead to the same structure of the model, given by equations (4.36) with matrices and vectors of different dimension and structure according to the plant structures. It can be seen that the models have three main parts:

- State space linear form *Az(k)* which describes input/output mass balances in the structure of the process. The structure and dimensions of the matrix *A* depend on the structure and number of tanks in the process and on the number of the compounds in the biological models.
- Input disturbance part $Bz_{i\varphi}$. The structure of the matrix B is the same for all processes but the dimensions depend on the number of tanks and on the number of compounds in the biological models. In the considered structures the input flow is coming always to the first tank, which is the anaerobic tank.
- The biological rate part $C^T\rho$. The structure of the matrix *C* is a block diagonal one. The structure of the blocks C_n is the same and the values of the elements in the blocks are the same for ASM1 or UCT reduced biological models because they represent the Peterson matrix coefficients. The dimensions of the $C_{n,UCT}$ and $C_{n,ASM1}$ are different because 4 biological processes and 3 compounds are considered in the ASM1 reduced model and 10 biological processes and 4 compounds are considered in the UCT reduced model. The biological rate is a nonlinear part of the models. It represents the nonlinear connections between the state and control variables. The change of behaviour of the process is based on the influence of the oxygen over the biological rates and in this way on the concentrations of t he process variables.

Dimensions of the vectors and matrices of the obtained mass balance reduced models for the three considered processes are shown in the Table 4.6.

Table 4.6: Dimensions of the matrices and vectors of the derived reduced models

Plant	Models	Matrices' and vectors' dimensions				
		A	B	C	ρ	z
Benchmark	ASM1	15×15	15×5	20×15	20	15
	UCT	20×20	20×5	50×20	50	20
Mitchell's Plain	ASM1	9×9	9×3	12×9	12	9
	UCT	12×12	12×3	30×12	30	12
Athlone	ASM1	9×9	9×3	12×9	12	9
	UCT	12×12	12×3	30×12	30	12

4.8 Conclusion

This chapter elucidates the need for reduced model development for both the ASM1 and UCT biological models. The assumptions for the model reduction procedure are also studied. The dissolved oxygen concentration is considered as a control input for the reduced models. The ASM1 and UCT reduced biological model structures are studied and the corresponding mass balance equations are derived.

The mass balance for three wastewater treatment plants viz., Benchmark, Mitchell's Plain and Athlone are developed in this chapter on the basis of the full UCT and ASM1 biological models which results in the UCT reduced and ASM1 reduced models. The matrices and vectors for each of the plants are separately described.

The models developed in the chapter 4 are used for sensitivity analysis and simulation purposes in chapter 5 and for parameter estimation purposes in chapter 6.

CHAPTER FIVE

SENSITIVITY STUDY FOR THE DETERMINATION OF THE KEY PARAMETERS OF THE WASTEWATER TREATMENT SYSTEM

5.1 Introduction

The sensitivity study of the model inputs and parameters gives answer to the question which parameters to estimate. Many of the biological nutrient removal models are not identifiable since there are many more parameters than there are feasible measurements. That is why if some insensitive parameters could be found the problem for parameter estimation could be simplified (Holmberg & Ranta, 1982). The sensitivity study of the model dynamic set of equations is to examine the changes of the model variables towards the changes in the system parameters. In order to establish sensitivity of the model variables towards the parameters in steady state also the steady state model is considered. Parameters with large values of the sensitivity functions have to be estimated (Sato & Ohmori, 2002).

Sensitivity functions, equations and state space models are derived in the chapter for the cases of Benchmark and Athlone plants. Two biological models – ASM1 and UCT are considered for every plant. Matlab software for the sensitivity functions calculation and sensitivity models simulation is developed. The results are described and discussed.

5.2 Sensitivity functions

The sensitivity function $z^{\theta}(t)$ of the nonlinear system

$$\dot{z}(\theta,t) = f\left(z(\theta,t), \theta, u\right) \quad z(0) = z_0 \tag{5.1}$$

where θ is the vector of the parameters is defined as

$$z^{\theta}(t) = \frac{\partial z(\theta,t)}{\partial \theta(t)} \tag{5.2}$$

or in terms of the components of the vector of parameters

$$\left(z^{\theta}\right)_{ij} = \frac{\partial z_i}{\partial \theta_j} \tag{5.3}$$

In other words, the sensitivity function $\left(z^{\theta}\right)_{ij}$ is a mathematical description which indicates influence of slight change in parameter θ_j on the state variable.

Differentiating (5.1) according to parameter vector θ gives

$$\dot{z}^{\theta}(t) = \frac{\partial f}{\partial z} z^{\theta}(t) + \frac{\partial f(t)}{\partial \theta} \quad z^{\theta}(0) = z_0^{\theta} \tag{5.4}$$

The solution of the equation (5.4) gives the sensitivity function behavior.

5.3 Development of the sensitivity functions and model for the Benchmark Structure with ASM1 and UCT biological models

5.3.1. Benchmark structure with ASM1 biological model

The mass-balance model for the Benchmark structure described by Equations (4.13) – (4.17) with ASM1 reduced model described by Equations (4.1) – (4.3) is considered. The parameters characterized these models are given in Table 4.2. They are $y_A, y_H, i_{XB}, \mu_A, \mu_H, K_S, K_{OH}, K_{NH}, K_{OA}, \eta_g, \eta_h, k_h, K_X$. Additionally the parameter *f* is included. This parameter is not a part of the biological model. The sensitivity of the process variables towards these parameters is evaluated by using the theory of sensitivity (Schermann & Garag-Gabin, 2005; Montgomery, 1997; Breyfogle & Breyfogle, 2003).

5.3.1.1 Sensitivity equations derivation

The derivations of the sensitivity functions and models are analogous for every process tanks. That is why they are calculated for the n-th tank, as follows:

- for the parameter *f*

$$\left(\frac{dS_{NH,n}}{dt}\right)\Big/df = \frac{1}{V_n}\left[Q\left(\frac{dS_{NH,n-1}}{df} - \frac{dS_{NH,n}}{df}\right)\right] + \frac{\partial r_{SNH,n}}{\partial S_{NH,n}} \bullet \frac{dS_{NH,n}}{df} + \frac{\partial r_{SNH,n}}{\partial S_{NO,n}} \bullet \frac{dS_{NO,n}}{df} + \frac{\partial r_{SNH,n}}{\partial S_{S,n}} \bullet \frac{dS_{S,n}}{df} + \frac{dr_{SNH,n}}{df} \tag{5.5}$$

$$\left(\frac{dS_{NO,n}}{dt}\right)\Big/df = \frac{1}{V_n}\left[Q\left(\frac{dS_{NO,n-1}}{df} - \frac{dS_{NO,n}}{df}\right)\right] + \frac{\partial r_{SNO,n}}{\partial S_{NO,n}} \bullet \frac{dS_{NO,n}}{df} + \frac{\partial r_{SNO,n}}{\partial S_{NH,n}} \bullet \frac{dS_{NH,n}}{df} + \frac{\partial r_{SNO,n}}{\partial S_{S,n}} \bullet \frac{dS_{S,n}}{df} + \frac{dr_{SNO,n}}{df} \tag{5.6}$$

$$\left(\frac{dS_{S,n}}{dt}\right)\Big/df = \frac{1}{V_n}\left[Q\left(\frac{dS_{S,n-1}}{df} - \frac{dS_{S,n}}{df}\right)\right] + \frac{\partial r_{SS,n}}{\partial S_{S,n}} \bullet \frac{dS_{S,n}}{df} + \frac{\partial r_{SS,n}}{\partial S_{NH,n}} \bullet \frac{dS_{NH,n}}{df} + \frac{\partial r_{SS,n}}{\partial S_{NO,n}} \bullet \frac{dS_{NO,n}}{df} + \frac{dr_{SS,n}}{df} \tag{5.7}$$

where $\frac{dr_{SNH,n}}{df} = \frac{dr_{SNO,n}}{df} = \frac{dr_{SS,n}}{df} = 0$, and $\frac{dS_{NH,n}}{df} = S^f_{NH,n}, \frac{dS_{NO,n}}{df} = S^f_{NO,n}, \frac{dS_{S,n}}{df} = S^f_{S,n}$

are the sensitivity functions of the process variables towards the parameter *f*. The process rate derivatives are:

$$\frac{\partial r_{SNH,n}}{\partial S_{NH,n}} = -\left(i_{XB} + \frac{1}{Y_A}\right)\hat{\mu}_A X_{BA} \frac{S_{O,n}}{(K_{OA} + S_{O,n})}\left(\frac{K_{NH}}{(K_{NH} + S_{NH,n})^2}\right) = r^{SNH,n}_{SNH,n} \tag{5.8}$$

$$\frac{\partial r_{SNH,n}}{\partial S_{NO,n}} = -i_{XB}\hat{\mu}_H \left(\frac{S_S}{K_S + S_{S,n}}\right)\left(\frac{K_{OH}}{K_{OH} + S_{O,n}}\right) X_{BH}\eta_g \left(\frac{K_{NO}}{(K_{NO} + S_{NO,n})^2}\right) = r^{SNO,n}_{SNH,n} \tag{5.9}$$

$$\frac{\partial r_{SNH,n}}{\partial S_{S,n}} = -i_{XB}\hat{\mu}_H X_{BH}\left(\frac{S_{O,n}}{K_{OH}+S_{O,n}}\right)\left(\frac{K_S}{(K_S+S_{S,n})^2}\right) = r_{SNH,n}^{SS,n} \tag{5.10}$$

$$\frac{\partial r_{SNO,n}}{\partial S_{NH,n}} = \frac{1}{Y_A}\hat{\mu}_A X_{BA}\left(\frac{S_{O,n}}{K_{OA}+S_{O,n}}\right)\left(\frac{K_{NH}}{(K_{NH}+S_{NH,n})^2}\right) = r_{SNO,n}^{NH,n} \tag{5.11}$$

$$\frac{\partial r_{SNO,n}}{\partial S_{NO,n}} = -\frac{1-Y_H}{2.86Y_H}X_{BH}\hat{\mu}_H\eta_g\left(\frac{S_{S,n}}{K_S+S_{S,n}}\right)\left(\frac{K_{OH}}{K_{OH}+S_{O,n}}\right)\left(\frac{K_{NO}}{(K_{NO}+S_{NO,n})^2}\right) = r_{SNO,n}^{NO,n} \tag{5.12}$$

$$\frac{\partial r_{SNO,n}}{\partial S_{S,n}} = -\frac{1-Y_H}{2.86Y_H}X_{BH}\hat{\mu}_H\eta_g\left(\frac{K_{OH}}{K_{OH}+S_{O,n}}\right)\left(\frac{S_{NO,n}}{K_{NO}+S_{NO,n}}\right)\left(\frac{K_S}{(K_S+S_{S,n})^2}\right) = r_{SNO,n}^{SS,n} \tag{5.13}$$

$$\frac{\partial r_{SS,n}}{\partial S_{NH,n}} = 0 \tag{5.14}$$

$$\frac{\partial r_{SS,n}}{\partial S_{NO,n}} = \left[-\frac{1}{Y_H}\hat{\mu}_H\left(\frac{S_{S,n}}{K_S+S_{S,n}}\right)+k_h\eta_h\frac{X_{S,n}/X_{BH,n}}{K_X+(X_{S,n}/X_{BH,n})}\right]X_{BH}\left(\frac{K_{OH}}{K_{OH}+S_{O,n}}\right)\left(\frac{K_{NO}}{(K_{NO}+S_{NO,n})^2}\right) = r_{SS,n}^{SNO,n} \tag{5.15}$$

$$\frac{\partial r_{SS,n}}{\partial S_{S,n}} = -\frac{1}{Y_H}\hat{\mu}_H X_{BH,n}\left[\left(\frac{S_{O,n}}{K_{OH}+S_{O,n}}\right)+\left(\frac{S_{NO,n}}{K_{NO}+S_{NO,n}}\right)\left(\frac{K_{OH}}{K_{OH}+S_{O,n}}\right)\right]\left(\frac{K_S}{(K_S+S_{S,n})}\right) = r_{SS,n}^{SS,n} \tag{5.16}$$

On the basis of the above derivations, the equations describing the sensitivity model according to the parameter *f* are

1) for tanks 2 ÷ 5

$$\dot{S}_{NH,n}^f = \frac{1}{V_n}\left[Q\left(S_{NH,n-1}^f - S_{NH,n}^f\right)\right]+r_{SNH,n}^{SNH,n}S_{NH,n}^f + r_{SNH,n}^{SNO,n}\bullet S_{NO,n}^f + r_{SNH,n}^{SS,n}S_{S,n}^f \tag{5.17}$$

$$\dot{S}_{NO,n}^f = \frac{1}{V_n}\left[Q\left(S_{NO,n-1}^f - S_{NO,n}^f\right)\right]+r_{SNO,n}^{SNH,n}\bullet S_{NH,n}^f + r_{SNO,n}^{SNO,n}\bullet S_{NO,n}^f + r_{SNO,n}^{SS,n}\bullet S_{S,n}^f \tag{5.18}$$

$$\dot{S}_{S,n}^f = \frac{1}{V_n}\left[Q\left(S_{S,n-1}^f - S_{S,n}^f\right)\right]+r_{SS,n}^{SNH,n}\bullet S_{NH,n}^f + r_{SS,n}^{SNO,n}\bullet S_{NO,n}^f + r_{SS,n}^{SS,n}\bullet S_{S,n}^f \tag{5.19}$$

2) for the first tank

$$\dot{S}_{NH,1}^f = \frac{1}{V_1}\left[Q_a S_{NH,5}^f + Q_r S_{NH,5}^f + Q_o S_{NH,1}^f - QS_{NH,1}^f\right]+r_{SNH,1}^{SNH,1}\bullet S_{NH,1}^f + r_{SNH,1}^{SNO,1}\bullet S_{NO,1}^f + r_{SNH,1}^{SS,1}\bullet S_{S,1}^f \tag{5.20}$$

$$\dot{S}_{NO,1}^f = \frac{1}{V_1}\left[Q_a S_{NO,5}^f + Q_r S_{NO,5}^f - QS_{NO,1}^f\right]+r_{SNO,1}^{SNH,1}\bullet S_{NH,1}^f + r_{SNO,1}^{SNO,1}\bullet S_{NO,1}^f + r_{SNO,1}^{SS,1}\bullet S_{S,1}^f \tag{5.21}$$

$$\dot{S}_{S,1}^f = \frac{1}{V_1}\left[Q_a S_{S,5}^f + Q_r S_{S,5}^f - QS_{S,1}^f\right]+r_{SS,1}^{SNH,1}\bullet S_{NH,1}^f + r_{SS,1}^{SNO,1}\bullet S_{NO,1}^f + r_{SS,1}^{SS,1}\bullet S_{S,1}^f \tag{5.22}$$

- for the parameters $\theta = Y_H, Y_A, i_{XB}, \mu_A, \mu_H, K_S, K_{OH}, K_{NO}, K_{NH}, K_{OA}, \eta_g, \eta_h, k_h, K_X$

1) for the first tank

$$\dot{S}_{NH,1}^\theta = \frac{1}{V_1}\left[(Q_a+Q_r)S_{NH,5}^\theta - QS_{NH,1}^\theta\right]+r_{SNH,1}^{SNH,1}\bullet S_{NH,1}^\theta + r_{SNH,1}^{SNO,1}\bullet S_{NO,1}^\theta + r_{SNH,1}^{SS,1}\bullet S_{S,1}^\theta + r_{SNH,1}^\theta \tag{5.23}$$

$$\dot{S}^{\theta}_{NO,1} = \frac{1}{V_1}\left[(Q_a + Q_r)S^{\theta}_{NO,5} - QS^{\theta}_{NO,1}\right] + r^{SNH,1}_{SNO,1} \bullet S^{\theta}_{NH,1} + r^{SNO,1}_{SNO,1} \bullet S^{\theta}_{NO,1} + r^{SS,1}_{SNO,1} \bullet S^{\theta}_{S,1} + r^{\theta}_{SNO,1} \tag{5.24}$$

$$\dot{S}^{\theta}_{S,1} = \frac{1}{V_1}\left[(Q_a + Q_r)S^{\theta}_{S,5} - QS^{\theta}_{S,1}\right] + r^{SNH,1}_{SS,1} \bullet S^{\theta}_{NH,1} + r^{SNO,1}_{SS,1} \bullet S^{\theta}_{NO,1} + r^{SS,1}_{SS,1} \bullet S^{\theta}_{S,1} + r^{\theta}_{SS,1} \tag{5.25}$$

2) for the tanks $n = \overline{2,5}$

$$\dot{S}^{\theta}_{NH,n} = \frac{1}{V_1}\left[Q\left(S^{\theta}_{NH,n-1} - S^{\theta}_{NH,n}\right)\right] + r^{SNH,n}_{SNH,n} \bullet S^{\theta}_{SNH,n} + r^{SNO,n}_{SNH,n} \bullet S^{\theta}_{NO,n} + r^{SS,n}_{SNH,n} \bullet S^{\theta}_{S,n} + r^{\theta}_{SNH,n} \tag{5.26}$$

$$\dot{S}^{\theta}_{NO,n} = \frac{1}{V_1}\left[Q\left(S^{\theta}_{NO,n-1} - S^{\theta}_{NO,n}\right)\right] + r^{SNH,n}_{SNO,n} \bullet S^{\theta}_{SNH,n} + r^{SNO,n}_{SNO,n} \bullet S^{\theta}_{NO,n} + r^{SS,n}_{SNO,n} \bullet S^{\theta}_{S,n} + r^{\theta}_{SNO,n} \tag{5.27}$$

$$\dot{S}^{\theta}_{S,n} = \frac{1}{V_1}\left[Q\left(S^{\theta}_{S,n-1} - S^{\theta}_{S,n}\right)\right] + r^{SS,n}_{SS,n} \bullet S^{\theta}_{SNH,n} + r^{SNO,n}_{SS,n} \bullet S^{\theta}_{NO,n} + r^{SS,n}_{SS,n} \bullet S^{\theta}_{S,n} + r^{\theta}_{SS,n} \tag{5.28}$$

where $S^{\theta}_{NH,n}, S^{\theta}_{NO,n}, S^{\theta}_{S,n}$ are the corresponding to the parameters θ sensitivity functions, the partial derivatives of the process rates are determined above and the derivatives of the rates according to the parameters are as follows:

- for Y_H

$$r^{Y_H}_{SNH,n} = 0 \tag{5.29}$$

$$r^{Y_H}_{SNO,n} = -\hat{\mu}_H \eta_g X_{BH,n}\left(\frac{S_{S,n}}{K_S + S_{S,n}}\right)\left(\frac{K_{OH}}{K_{OH} + S_{O,n}}\right)\left(\frac{S_{NO,n}}{K_{NO,n} + S_{NO,n}}\right)\left(\frac{1}{2.86Y_H^2}\right) \tag{5.30}$$

$$r^{Y_H}_{SS,n} = \frac{1}{Y_H^2}\hat{\mu}_H X_{BH,n}\left(\frac{S_{S,n}}{K_S + S_{S,n}}\right)\left[\left(\frac{S_{O,n}}{K_{OH} + S_{O,n}}\right) + \left(\frac{S_{NO,n}}{K_{NO,n} + S_{NO,n}}\right)\left(\frac{K_{OH}}{K_{OH} + S_{O,n}}\right)\right] \tag{5.31}$$

- for Y_A

$$r^{Y_A}_{SNH,n} = \frac{1}{Y_A^2}\hat{\mu}_A\left(\frac{S_{O,n}}{K_{OA} + S_{O,n}}\right)\left(\frac{S_{NH,n}}{K_{NH} + S_{NH,n}}\right)X_{BA,n} \tag{5.32}$$

$$r^{Y_A}_{SNO,n} = -\frac{1}{Y_A^2}\hat{\mu}_A\left(\frac{S_{O,n}}{K_{OA} + S_{O,n}}\right)\left(\frac{S_{NH,n}}{K_{NH} + S_{NH,n}}\right)X_{BA,n} = -r^{Y_A}_{SNH,n} \tag{5.33}$$

$$r^{Y_A}_{SS,n} = 0 \tag{5.34}$$

- for i_{XB}

$$r^{i_{XB}}_{SNH,n} = -\hat{\mu}_H X_{BH,n}\left(\frac{S_{S,n}}{K_S + S_{S,n}}\right)\left[\left(\frac{S_{O,n}}{K_{OH} + S_{O,n}}\right) + \left(\frac{S_{NO,n}}{K_{NO} + S_{NO,n}}\right)\left(\frac{K_{OH}}{K_{OH} + S_{O,n}}\right)\eta_g\right] - \tag{5.35}$$
$$-\hat{\mu}_A\left(\frac{S_{O,n}}{K_{OA} + S_{O,n}}\right)\left(\frac{S_{NH,n}}{K_{NH} + S_{NH,n}}\right)X_{BA,n}$$

$$r_{SNO,n}^{i_{XB}} = 0 \tag{5.36}$$

$$r_{SS,n}^{i_{XB}} = 0 \tag{5.37}$$

- for $\hat{\mu}_A$

$$r_{SNH,n}^{\hat{\mu}_A} = -\left(i_{XB} + \frac{1}{Y_A}\right)\left(\frac{S_{O,n}}{K_{OA}+S_{O,n}}\right)\left(\frac{S_{NH,n}}{K_{NH}+S_{NH,n}}\right)X_{BA,n} \tag{5.38}$$

$$r_{SNO,n}^{\hat{\mu}_A} = \frac{1}{Y_A}\left(\frac{S_{O,n}}{K_{OA}+S_{O,n}}\right)\left(\frac{S_{NH,n}}{K_{NH}+S_{NH,n}}\right)X_{BA,n} \tag{5.39}$$

$$r_{SS,n}^{\hat{\mu}_A} = 0 \tag{5.40}$$

- for $\hat{\mu}_H$

$$r_{SNH,n}^{\hat{\mu}_H} = -i_{XB}X_{BH,n}\left(\frac{S_{S,n}}{K_S+S_{S,n}}\right)\left[\left(\frac{S_{O,n}}{K_{OH}+S_{O,n}}\right)+\eta_g\left(\frac{S_{NO,n}}{K_{NO}+S_{NO,n}}\right)\left(\frac{K_{OH}}{K_{OH}+S_{O,n}}\right)\right] \tag{5.41}$$

$$r_{SNO,n}^{\hat{\mu}_H} = -\frac{1-Y_H}{2.86Y_H}X_{BH,n}\left(\frac{S_{S,n}}{K_S+S_{S,n}}\right)\left(\frac{K_{OH}}{K_{OH}+S_{O,n}}\right)\left(\frac{S_{NO,n}}{K_{NO}+S_{NO,n}}\right)\eta_g \tag{5.42}$$

$$r_{SS,n}^{\hat{\mu}_H} = -\frac{1}{Y_H}X_{BH,n}\left(\frac{S_{S,n}}{K_S+S_{S,n}}\right)\left[\left(\frac{S_{O,n}}{K_{OH}+S_{O,n}}\right)+\left(\frac{S_{NO,n}}{K_{NO}+S_{NO,n}}\right)\left(\frac{K_{OH}}{K_{OH}+S_{O,n}}\right)\right] \tag{5.43}$$

- for K_S

$$r_{SNH,n}^{K_S} = i_{XB}\hat{\mu}_H X_{BH,n}\left(\frac{S_{S,n}}{(K_S+S_{S,n})^2}\right)\left[\left(\frac{S_{O,n}}{K_{OH}+S_{O,n}}\right)+\eta_g\left(\frac{S_{NO,n}}{K_{NO}+S_{NO,n}}\right)\left(\frac{K_{OH}}{K_{OH}+S_{O,n}}\right)\right] \tag{5.44}$$

$$r_{SNO,n}^{K_S} = \frac{1-Y_H}{2.86Y_H}X_{BH,n}\hat{\mu}_H\left(\frac{S_{S,n}}{K_S+S_{S,n}}\right)\left(\frac{K_{OH}}{K_{OH}+S_{O,n}}\right)\left(\frac{S_{NO,n}}{K_{NO}+S_{NO,n}}\right)\eta_g \tag{5.45}$$

$$r_{SS,n}^{K_S} = \frac{1}{Y_H}\hat{\mu}_H X_{BH,n}\left(\frac{S_{S,n}}{(K_S+S_{S,n})^2}\right)\left[\left(\frac{S_{O,n}}{K_{OH}+S_{O,n}}\right)+\left(\frac{S_{NO,n}}{K_{NO}+S_{NO,n}}\right)\left(\frac{K_{OH}}{K_{OH}+S_{O,n}}\right)\right] \tag{5.46}$$

- for K_{OH}

$$r_{SNH,n}^{K_{OH}} = i_{XB}\hat{\mu}_H X_{BH,n}\left(\frac{S_{S,n}}{K_S+S_{S,n}}\right)\left(\frac{S_{O,n}}{(K_{OH}+S_{O,n})^2}\right)\left[1-\eta_g\left(\frac{S_{NO,n}}{K_{NO}+S_{NO,n}}\right)\right] \tag{5.47}$$

$$r_{SNO,n}^{K_{OH}} = -\frac{1-Y_H}{2.86Y_H}X_{BH,n}\hat{\mu}_H\left(\frac{S_{S,n}}{K_S+S_{S,n}}\right)\left(\frac{S_{O,n}}{(K_{OH}+S_{O,n})^2}\right)\left(\frac{S_{NO,n}}{K_{NO}+S_{NO,n}}\right)\eta_g \tag{5.48}$$

$$r_{SS,n}^{K_{OH}} = \frac{1}{Y_H}\hat{\mu}_H X_{BH,n}\left(\frac{S_{S,n}}{K_S + S_{S,n}}\right)\left(\frac{S_{O,n}}{(K_{OH} + S_{O,n})^2}\right)\left[1 - \left(\frac{S_{NO,n}}{K_{NO} + S_{NO,n}}\right)\right] + k_h X_{BH,n} \cdot \left[\frac{X_{S,n}/X_{BH,n}}{K_X + (X_{S,n}/X_{BH,n})}\right]\left(\frac{S_{O,n}}{(K_{OH} + S_{O,n})^2}\right)\left[-1 + \eta_h\left(\frac{S_{NO,n}}{K_{NO} + S_{NO,n}}\right)\right] \quad (5.49)$$

- for K_{NO}

$$r_{SNH,n}^{K_{NO}} = i_{XB}\hat{\mu}_H X_{BH,n}\eta_g\left(\frac{S_{S,n}}{K_S + S_{S,n}}\right)\left(\frac{S_{NO,n}}{(K_{NO} + S_{NO,n})^2}\right)\left(\frac{K_{OH}}{K_{OH} + S_{O,n}}\right) \quad (5.50)$$

$$r_{SNO,n}^{K_{NO}} = \frac{1 - Y_H}{2.86 Y_H}\hat{\mu}_H X_{BH,n}\eta_g\left(\frac{S_{S,n}}{K_S + S_{S,n}}\right)\left(\frac{S_{NO,n}}{(K_{NO} + S_{NO,n})^2}\right)\left(\frac{K_{OH}}{K_{OH} + S_{O,n}}\right) \quad (5.51)$$

$$r_{SS,n}^{K_{NO}} = \frac{1}{Y_H}\hat{\mu}_H X_{BH,n}\left(\frac{S_{S,n}}{K_S + S_{S,n}}\right)\left(\frac{S_{NO,n}}{(K_{NO} + S_{NO,n})^2}\right)\left(\frac{K_{OH}}{K_{OH} + S_{O,n}}\right) - k_h X_{BH,n}\eta_h \cdot \left[\frac{X_{S,n}/X_{BH,n}}{(K_X + X_{S,n}/X_{BH,n})}\right]\left(\frac{S_{NO,n}}{(K_{NO} + S_{NO,n})^2}\right)\left(\frac{K_{OH}}{K_{OH} + S_{O,n}}\right) \quad (5.52)$$

- for K_{NH}

$$r_{SNH,n}^{K_{NH}} = \left(i_{XB} + \frac{1}{Y_A}\right)\hat{\mu}_A\left(\frac{S_{O,n}}{K_{OA} + S_{O,n}}\right)\left(\frac{S_{NH,n}}{(K_{NH} + S_{NH,n})^2}\right)X_{BA,n} \quad (5.53)$$

$$r_{SNO,n}^{K_{NH}} = -\frac{1}{Y_A}\hat{\mu}_A\left(\frac{S_{O,n}}{K_{OA} + S_{O,n}}\right)\left(\frac{S_{NH,n}}{(K_{NH} + S_{NH,n})^2}\right)X_{BA,n} \quad (5.54)$$

$$r_{SS,n}^{K_{NH}} = 0 \quad (5.55)$$

- for K_{OA}

$$r_{SNH,n}^{K_{OA}} = \left(i_{XB} + \frac{1}{Y_A}\right)\hat{\mu}_A\left(\frac{S_{O,n}}{(K_{OA} + S_{O,n})^2}\right)\left(\frac{S_{NH,n}}{K_{NH} + S_{NH,n}}\right)X_{BA} \quad (5.56)$$

$$r_{SNO,n}^{K_{OA}} = -\frac{1}{Y_A}\hat{\mu}_A\left(\frac{S_{O,n}}{(K_{OA} + S_{O,n})^2}\right)\left(\frac{S_{NH,n}}{K_{NH} + S_{NH,n}}\right)X_{BA} \quad (5.57)$$

$$r_{SS,n}^{K_{OA}} = 0 \quad (5.58)$$

- for η_g

$$r_{SNH,n}^{\eta_g} = -i_{XB}\hat{\mu}_H\left(\frac{S_{S,n}}{K_S + S_{S,n}}\right)\left(\frac{S_{NO,n}}{K_{NO} + S_{NO,n}}\right)\left(\frac{K_{OH}}{K_{OH} + S_{O,n}}\right)X_{BH,n} \quad (5.59)$$

$$r_{SNO,n}^{\eta_g} = -\frac{1-Y_H}{2.86Y_H}\hat{\mu}_H\left(\frac{S_{S,n}}{K_S+S_{S,n}}\right)\left(\frac{S_{NO,n}}{K_{NO}+S_{NO,n}}\right)\left(\frac{K_{OH}}{K_{OH}+S_{O,n}}\right)X_{BH,n} \tag{5.60}$$

$$r_{SS,n}^{\eta_g} = 0 \tag{5.61}$$

- for η_h

$$r_{SNH,n}^{\eta_h} = 0 \tag{5.62}$$

$$r_{SNO,n}^{\eta_h} = 0 \tag{5.63}$$

$$r_{SS,n}^{\eta_h} = k_h\left[\frac{X_{S,n}/X_{BH,n}}{\left(K_X+\left(X_{S,n}/X_{BH,n}\right)\right)}\right]\left(\frac{S_{O,n}}{K_{OH}+S_{O,n}}\right)\left(\frac{S_{NO,n}}{K_{NO}+S_{NO,n}}\right)\left(\frac{K_{OH}}{K_{OH}+S_{O,n}}\right)X_{BH,n} \tag{5.64}$$

- for k_h

$$r_{SNH,n}^{k_h} = 0 \tag{5.65}$$

$$r_{SNO,n}^{k_h} = 0 \tag{5.66}$$

$$r_{SS,n}^{k_h} = \left[\frac{X_{S,n}/X_{BH,n}}{\left(K_X+\left(X_{S,n}/X_{BH,n}\right)\right)}\right]\left[\left(\frac{S_{O,n}}{K_{OH}+S_{O,n}}\right)+\eta_h\left(\frac{S_{NO,n}}{K_{NO}+S_{NO,n}}\right)\left(\frac{K_{OH}}{K_{OH}+S_{O,n}}\right)\right]X_{BH,n} \tag{5.67}$$

- for K_X

$$r_{SNH,n}^{K_X} = 0 \tag{5.68}$$

$$r_{SNO,n}^{K_X} = 0 \tag{5.69}$$

$$r_{SS,n}^{K_X} = k_h\left[\left(\frac{S_{O,n}}{K_{OH}+S_{O,n}}\right)+\eta_h\left(\frac{S_{NO,n}}{K_{NO}+S_{NO,n}}\right)\left(\frac{K_{OH}}{K_{OH}+S_{O,n}}\right)\right]X_{BH,n}\left[-\left(\frac{X_{S,n}/X_{BH,n}}{\left(K_X+\left(X_{S,n}/X_{BH,n}\right)\right)^2}\right)\right] \tag{5.70}$$

5.3.1.2 Sensitivity state space model

The sensitivity state space model is formed for the whole plant. The vector of the sensitivity state space consists of all sensitivity functions according to the model parameters, as follows for the *n*-th tank.

$$S_n^{\theta} = \begin{bmatrix} S_{NH,n}^{f} & S_{NO,n}^{f} & S_{S,n}^{f} & S_{NH,n}^{Y_H} & S_{NO,n}^{Y_H} & S_{S,n}^{Y_H} & S_{NH,n}^{Y_A} & S_{NO,n}^{Y_A} & S_{S,n}^{Y_A} & S_{NH,n}^{i_{XB}} & S_{NO,n}^{i_{XB}} & S_{S,n}^{i_{XB}} \cdots \\ S_{NH,n}^{\mu_A} & S_{NO,n}^{\mu_A} & S_{S,n}^{\mu_A} & S_{NH,n}^{\mu_H} & S_{NO,n}^{\mu_H} & S_{S,n}^{\mu_H} & S_{NH,n}^{K_S} & S_{NO,n}^{K_S} & S_{S,n}^{K_S} & S_{NH,n}^{K_{OH}} & S_{NO,n}^{K_{OH}} & S_{S,n}^{K_{OH}} \cdots \\ S_{NH,n}^{K_{NO}} & S_{NO,n}^{K_{NO}} & S_{S,n}^{K_{NO}} & S_{NH,n}^{K_{NH}} & S_{NO,n}^{K_{NH}} & S_{S,n}^{K_{NH}} & S_{NH,n}^{K_{OA}} & S_{NO,n}^{K_{OA}} & S_{S,n}^{K_{OA}} & S_{NH,n}^{\eta_g} & S_{NO,n}^{\eta_g} & S_{S,n}^{\eta_g} \cdots \\ S_{NH,n}^{\eta_h} & S_{NO,n}^{\eta_h} & S_{S,n}^{\eta_h} & S_{NH,n}^{k_h} & S_{NO,n}^{k_h} & S_{S,n}^{k_h} & S_{NH,n}^{K_X} & S_{NO,n}^{K_X} & S_{S,n}^{K_X} & & & \end{bmatrix}^T \in R^{45} \tag{5.71}$$

The state process variables vector for the *n*-th tank is

$$X_n = \left[S_{NH,n}\ S_{NO,n}\ S_{S,n}\right]^T \in R^3 \tag{5.72}$$

The combined vector for the process variables and sensitivity functions for the *n*-th tank is

$$X_n^S = \left\lfloor X_n\ \ S_n^\theta \right\rfloor \in R^{48} \tag{5.73}$$

This vector is used to for the state space process and sensitivity model derivation.

The matrix of the process rates derivatives towards the process variables is

$$\frac{\partial r_n}{\partial X_n} = \left[r_{SNH,n}^{SNH,n}\ r_{SNH,n}^{SNO,n}\ r_{SNH,n}^{SS,n};\ r_{SNO,n}^{SNH,n}\ r_{SNO,n}^{SNO,n}\ r_{SNO,n}^{SS,n};\ r_{SS,n}^{SNH,n}\ r_{SS,n}^{SNO,n}\ r_{SS,n}^{SS,n}\right] \in R^{3x3} \tag{5.74}$$

The vector of the derivatives of the process rates to the model parameters is

$$\frac{\partial r_n}{\partial \theta} = \begin{bmatrix} r_{SNH,n}^{f}\ r_{SNO,n}^{f}\ r_{SS,n}^{f}\ r_{SNH,n}^{Y_H}\ r_{SNO,n}^{Y_H}\ r_{SS,n}^{Y_H}\ r_{SNH,n}^{Y_A}\ r_{SNO,n}^{Y_A}\ r_{SS,n}^{Y_A}\ r_{SNH,n}^{i_{XB}}\ r_{SNO,n}^{i_{XB}}\ r_{SS,n}^{i_{XB}} \\ r_{SNH,n}^{\mu_A}\ r_{SNO,n}^{\mu_A}\ r_{SS,n}^{\mu_A}\ r_{SNH,n}^{\mu_H}\ r_{SNO,n}^{\mu_H}\ r_{SS,n}^{\mu_H}\ r_{SNH,n}^{K_S}\ r_{SNO,n}^{K_S}\ r_{SS,n}^{K_S}\ r_{SNH,n}^{K_{OH}}\ r_{SNO,n}^{K_{OH}}\ r_{SS,n}^{K_{OH}} \\ r_{SNH,n}^{K_{NO}}\ r_{SNO,n}^{K_{NO}}\ r_{SS,n}^{K_{NO}}\ r_{SNH,n}^{K_{NH}}\ r_{SNO,n}^{K_{NH}}\ r_{SS,n}^{K_{NH}}\ r_{SNH,n}^{K_{OA}}\ r_{SNO,n}^{K_{OA}}\ r_{SS,n}^{K_{OA}}\ r_{SNH,n}^{\eta_g}\ r_{SNO,n}^{\eta_g}\ r_{SS,n}^{\eta_g} \\ r_{SNH,n}^{\eta_h}\ r_{SNO,n}^{\eta_h}\ r_{SS,n}^{\eta_h}\ r_{SNH,n}^{k_h}\ r_{SNO,n}^{k_h}\ r_{SS,n}^{k_h}\ r_{SNH,n}^{K_X}\ r_{SNO,n}^{K_X}\ r_{SS,n}^{K_X} \end{bmatrix}^T \in R^{45} \tag{5.75}$$

The description in the state space is given for every tank separately because of the big dimension of the vector of the state space.

- The state space equation for the first tank in the discrete form is incorporating process variables and the sensitivity functions, as follows:

$$X_1^S(k+1) = A_1^S(x_1, u_1, k\ )X_1^S(k) + C_1^{ST}\rho\ (x_1, u_1, k) + B_1^S X_{i\phi}(k) + D_1^S(x_1, u_1, k) + A_{15}^S(x_1, u_1, k)X_5^S(k) \tag{5.76}$$

where

$$A_1^S(x_1, u_1, k) = diag\left\{A_1, \left(A_1^\theta, \theta = f, Y_H, Y_A, i_B, \mu_A, \mu_H, K_S, K_{OH}, K_{NO}, K_{NH}, K_{OA}, \eta_g, \eta_h, k_h, K_X\right)\right\} \in R^{48\times 48} \tag{5.77}$$

$$A_1 = \begin{bmatrix} 1-\frac{\Delta t}{V_1}Q_1 & 0 & 0 \\ 0 & 1-\frac{\Delta t}{V_1}Q_1 & 0 \\ 0 & 0 & 1-\frac{\Delta t}{V_1}Q_1 \end{bmatrix} \quad A_1 \in R^{3\times 3} \tag{5.78}$$

$$A_1^\theta = \begin{bmatrix} 1+\Delta t\left(-\frac{Q_1}{V_1}+r_{SNH,1}^{SNH,1}\right) & \Delta t r_{SNH,1}^{SNO,1} & \Delta t r_{SNH,1}^{SS,1} \\ \Delta t r_{SNO,1}^{SNH,1} & 1+\Delta t\left(-\frac{Q_1}{V_1}+r_{SNO,1}^{SNO,1}\right) & \Delta t r_{SNO,1}^{SS,1} \\ \Delta t r_{SS,1}^{SNH,1} & \Delta t r_{SS,1}^{SNO,1} & 1+\Delta t\left(-\frac{Q_1}{V_1}+r_{SS,1}^{SS,1}\right) \end{bmatrix} \quad A_1^\theta \in R^{3\times 3} \tag{5.79}$$

The matrices A_1^θ are identical for all parameters.

The matrix C_1^S is $C_1^S = [C_1 : 0_{4\times 45}] \in R^{4\times 48}$ (5.80)

where $C_1 = \Delta t * \begin{bmatrix} -i_{XB} & 0 & -\frac{1}{Y_H} \\ -i_{XB} & -\frac{1-Y_H}{2.86Y_H} & -\frac{1}{Y_H} \\ -i_{XB} - \frac{1}{Y_A} & -\frac{1}{Y_A} & 0 \\ 0 & 0 & 1 \end{bmatrix}$

The matrix B_1^S is

$$B_1^S = \begin{bmatrix} B_1^{3\times 3} \\ B_{1,45\times 3}^{\theta} \end{bmatrix} \in R^{48\times 3}, B_1^{\theta} = \begin{bmatrix} \frac{\Delta t}{V_1} Q_0 \, 0 \, 0 \\ \cdots\cdots\cdots \\ 0_{47\times 3} \end{bmatrix}, \; B_1 = \begin{bmatrix} f\frac{\Delta t}{V_1} Q_0 & 0 & 0 \\ 0 & \frac{\Delta t}{V_1} Q_0 & 0 \\ 0 & 0 & \frac{\Delta t}{V_1} Q_0 \end{bmatrix} \quad (5.81)$$

The inflow waste concentration vector is $X_{i\phi} = [S_{NH\phi}, S_{NO\phi}, S_{S\phi}]^T$ (5.82)

The vector D_1^S is representing the derivatives of the process rates towards the model parameters.

$$D_1^S = \begin{bmatrix} 0_{1\times 3} : \left[r_{SNH,1}^{\theta} \; r_{SNO,1}^{\theta} \; r_{SS,1}^{\theta} \right] \theta = f, Y_H, Y_A, i_{XB}, \mu_A, \mu_H, K_S, K_{OH}, K_{NO}, \\ K_{NH}, K_{OA}, \eta_g, \eta_h, k_h, K_X \end{bmatrix}^T \in R^{48} \quad (5.83)$$

The matrix A_{15}^S describes the connections between the end of the fifth tank and the beginning of the first one. The connections are done by the vector $X_5^S = [X_5 \; S_5^{\theta}] \in R^{48}$

$$A_{15}^{\theta} = diag\left\{ A_{15}, A_{15}^{\theta}, \theta = f, Y_H, Y_A, i_{XB}, \mu_A, \mu_H, K_S, K_{OH}, K_{NO}, \\ K_{NH}, K_{OA}, \eta_g, \eta_h, k_h, K_X \right\} \in R^{48\times 48} \quad (5.84)$$

where

$$A_{15} = \begin{bmatrix} \frac{\Delta t}{V_1}(Q_a + Q_r) & 0 & 0 \\ 0 & \frac{\Delta t}{V_1}(Q_a + Q_r) & 0 \\ 0 & 0 & \frac{\Delta t}{V_1}(Q_a + Q_r) \end{bmatrix} \in R^{3\times 3}$$

$$A_{15}^{\theta} = \begin{bmatrix} \frac{\Delta t}{V_1}(Q_a + Q_r) & 0 & 0 \\ 0 & \frac{\Delta t}{V_1}(Q_a + Q_r) & 0 \\ 0 & 0 & \frac{\Delta t}{V_1}(Q_a + Q_r) \end{bmatrix} \in R^{3\times 3} \quad (5.85)$$

All matrices A_{15} are identical and $A_{15}^S = diag\left\{ \frac{\Delta t}{V_1}(Q_a + Q_r) \right\}_{48\times 48}$

- Derivation of the model equations for the other tanks $2 \div 5$

The state space model incorporating, the process variables and sensitivity functions is derived for the *n*-th tank, as follows:

$$X_n^S(k+1) = A_n^S(x_n, u_n, k)X_n^S(k) + C_n^{ST}\rho(x_n, u_n, k) + D_n^S(x_n, u_n, k) + A_{n,n-1}^S X_{n-1}^S \tag{5.86}$$

where $A_n^S = diag\left\{ \begin{matrix} A_n, A_n^\theta, \theta = f, Y_H, Y_A, i_{XB}, \mu_A, \mu_H, K_S, K_{OH}, K_{NO}, \\ K_{NH}, K_{OA}, \eta_g, \eta_h, k_h, K_X \end{matrix} \right\} \in R^{48\times 48}$

$$A_n^\theta = \begin{bmatrix} 1-\frac{\Delta t}{V_n}Q + \Delta tr_{SNH,n}^{SNH,n} & \Delta tr_{SNH,n}^{SNO,n} & \Delta tr_{SNH,n}^{SS,n} \\ \Delta tr_{SNO,n}^{SNH,n} & 1-\frac{\Delta t}{V_n}Q + \Delta tr_{SNO,n}^{SNO,n} & \Delta tr_{SNO,n}^{SS,n} \\ \Delta tr_{SS,n}^{SS,n} & \Delta tr_{SS,n}^{SNO,n} & 1-\frac{\Delta t}{V_n}Q + \Delta tr_{SS,n}^{SS,n} \end{bmatrix} \in R^{3\times 3} \tag{5.87}$$

$$A_n = \begin{bmatrix} 1-\frac{\Delta t}{V_n}Q_n & 0 & 0 \\ 0 & 1-\frac{\Delta t}{V_n}Q_n & 0 \\ 0 & 0 & 1-\frac{\Delta t}{V_n}Q_n \end{bmatrix} \in R^{3\times 3} \tag{5.88}$$

The matrices $A_{n,n-1}^S$ are

$$A_{n,n-1}^S = diag\left\{ \begin{matrix} A_{n,n-1}, A_{n,n-1}^\theta, \theta = f, Y_H, Y_A, i_{XB}, \mu_A, \mu_H, K_S, K_{OH}, K_{NO}, \\ K_{NH}, K_{OA}, \eta_g, \eta_h, k_h, K_X \end{matrix} \right\} \in R^{48\times 48} \tag{5.89}$$

where $A_{n,n-1} = \begin{bmatrix} \frac{\Delta t}{V_n}Q_{n-1} & 0 & 0 \\ 0 & \frac{\Delta t}{V_n}Q_{n-1} & 0 \\ 0 & 0 & \frac{\Delta t}{V_n}Q_{n-1} \end{bmatrix} \in R^{3\times 3}$, $A_{n,n-1}^\theta = \begin{bmatrix} \frac{\Delta t}{V_n}Q_{n-1} & 0 & 0 \\ 0 & \frac{\Delta t}{V_n}Q_{n-1} & 0 \\ 0 & 0 & \frac{\Delta t}{V_n}Q_{n-1} \end{bmatrix}$

The matrices $A_{n,n-1}$ and $A_{n,n-1}^\theta$ are identical.

The vector D_n^S is

$$D_n^S = \left[0_{1\times 3} : \left[r_{SNH,n}^\theta \; r_{SNO,n}^\theta \; r_{SS,n}^\theta \right] \left\{ \begin{matrix} \theta = f, Y_H, Y_A, i_{XB}, \mu_A, \mu_H, K_S, K_{OH}, K_{NO}, \\ K_{NH}, K_{OA}, \eta_g, \eta_h, k_h, K_X \end{matrix} \right\} \right]^T \in R^{48} \tag{5.90}$$

The matrices C_n^S are equal to C_1^S, with the same coefficients.

- State space model of the whole system

The model of process variables and sensitivity functions for the whole model is described by the following state space equation:

$$X^S(k+1) = A^S X^S(k) + C^{ST}\rho(x, u, k) + B^S X_{i\phi} + D^S(x, u, k) \tag{5.91}$$

The matrix A^S is

$$A^S = \begin{bmatrix} A_1^S & 0 & 0 & 0 & A_{15}^S \\ A_{21}^S & A_2^S & 0 & 0 & 0 \\ 0 & A_{32}^S & A_3^S & 0 & 0 \\ 0 & 0 & A_{43}^S & A_4^S & 0 \\ 0 & 0 & 0 & A_{54}^S & A_5^S \end{bmatrix} \in R^{240\times 240} \tag{5.92}$$

The matrix C^S is

$$C^S = \begin{bmatrix} C_1^S & 0 & 0 & 0 & 0 \\ 0 & C_2^S & 0 & 0 & 0 \\ 0 & 0 & C_3^S & 0 & 0 \\ 0 & 0 & 0 & C_4^S & 0 \\ 0 & 0 & 0 & 0 & C_5^S \end{bmatrix} \in R^{20\times 240} \tag{5.93}$$

The vector of the process rates is

$$\rho(x,u,k) = \begin{bmatrix} \rho_{11}\ \rho_{12}\ \rho_{13}\ \rho_{14}\ \rho_{15}\ \rho_{21}\ \rho_{22}\ \rho_{23}\ \rho_{24}\ \rho_{25}\ \rho_{31}\ \rho_{32}\ \rho_{33}\ \rho_{34}\ \rho_{35} \\ \rho_{41}\ \rho_{42}\ \rho_{43}\ \rho_{44}\ \rho_{45}\ \rho_{51}\ \rho_{52}\ \rho_{53}\ \rho_{54}\ \rho_{55} \end{bmatrix}^T \in R^{20} \tag{5.94}$$

The matrix B^S is

$$B^S = \begin{bmatrix} B_1^S \\ \cdots \\ 0_{192\times 3} \end{bmatrix} \in R^{240\times 3} \tag{5.95}$$

The vector D^S is

$$D^S = \begin{bmatrix} D_1^S\ D_2^S\ D_3^S\ D_4^S\ D_5^S \end{bmatrix}^T \in R^{240} \tag{5.96}$$

The model (5.91) – (5.96) is used to calculate the sensitivity functions of the benchmark structure with the ASM1 reduced model. A Matlab program is developed for these calculations, Appendix C. The results are given in Chapter 9.

5.3.2 Benchmark structure with UCT model

The mass-balance for the Benchmark structure is described by equations (4.13) – (4.17). The UCT reduced model is described by equations (4.4) – (4.6). The parameters of the UCT model are given in Table 4.4.

The mass-balance equations have the same structure as above. Only the expressions for the process rates are different.

5.3.2.1 Sensitivity equations derivation

The order of calculation is done in the same way as above.

- for the parameter *f*

  1) for the first tank

  The sensitivity functions are given by equations

$$\dot{S}^f_{NH,1} = \frac{1}{V_1}\left[Q_a S^f_{NH,5} + Q_r S^f_{NH,5} + Q_0 S_{NH\phi 1} - Q S^f_{NH,1}\right] + r^{SNH,1}_{SNH,1} S^f_{NH,1} + r^{SNO,1}_{SNH,1} S^f_{NO,1} + r^{SS,1}_{SNH,1} S^f_{S,1} + r^{S_{ads,1}}_{SNH,1} S^f_{ads,1} + r^f_{SNH,1} \quad (5.97)$$

$$\dot{S}^f_{NO,1} = \frac{1}{V_1}\left[Q_a S^f_{NO,5} + Q_r S^f_{NO,5} - Q S^f_{NO,1}\right] + r^{SNH,1}_{SNO,1} S^f_{NH,1} + r^{SNO,1}_{SNO,1} S^f_{NO,1} + r^{SS,1}_{SNO,1} S^f_{S,1} + r^{S_{ads,1}}_{SNO,1} S^f_{ads,1} + r^f_{SNO,1} \quad (5.98)$$

$$\dot{S}^f_{S,1} = \frac{1}{V_1}\left[Q_a S^f_{S,5} + Q_r S^f_{S,5} - Q S^f_{S,1}\right] + r^{SNH,1}_{SS,1} S^f_{NH,1} + r^{SNO,1}_{SS,1} S^f_{NO,1} + r^{SS,1}_{SS,1} S^f_{S,1} + r^{S_{ads,1}}_{SS,1} S^f_{ads,1} + r^f_{SS,1} \quad (5.99)$$

$$\dot{S}^f_{ads,1} = \frac{1}{V_1}\left[Q_a S^f_{ads,5} + Q_r S^f_{ads,5} - Q S^f_{ads,1}\right] + r^{SNH,1}_{ads,1} S^f_{NH,1} + r^{SNO,1}_{ads,1} S^f_{NO,1} + r^{SS,1}_{ads,1} S^f_{S,1} + r^{S_{ads,1}}_{ads,1} S^f_{ads,1} + r^f_{ads,1} \quad (5.100)$$

  2) for the other n = 2÷5 tanks

  The sensitivity functions are given equations

$$\dot{S}^f_{NH,n} = \frac{1}{V_n}\left[Q\left(S^f_{NH,n-1} - S^f_{NH,n}\right)\right] + r^{SNH,n}_{SNH,n} S^f_{NH,n} + r^{SNO,n}_{SNH,n} S^f_{NO,n} + r^{SS,n}_{SNH,n} S^f_{S,n} + r^{Sads,n}_{SNH,n} S^f_{ads,n} + r^f_{SNH,n} \quad (5.101)$$

$$\dot{S}^f_{NO,n} = \frac{1}{V_n}\left[Q\left(S^f_{NO,n-1} - S^f_{NO,n}\right)\right] + r^{SNH,n}_{SNO,n} S^f_{NH,n} + r^{SNO,n}_{SNO,n} S^f_{NO,n} + r^{SS,n}_{SNO,n} S^f_{S,n} + r^{Sads,n}_{SNO,n} S^f_{ads,n} + r^f_{SNO,n} \quad (5.102)$$

$$\dot{S}^f_{S,n} = \frac{1}{V_n}\left[Q\left(S^f_{S,n-1} - S^f_{S,n}\right)\right] + r^{SNH,n}_{SS,n} S^f_{NH,n} + r^{SNO,n}_{SS,n} S^f_{NO,n} + r^{SS,n}_{SS,n} S^f_{S,n} + r^{Sads,n}_{SS,n} S^f_{ads,n} + r^f_{SS,n} \quad (5.103)$$

$$\dot{S}^f_{ads,n} = \frac{1}{V_n}\left[Q\left(S^f_{ads,n-1} - S^f_{ads,n}\right)\right] + r^{SNH,n}_{Sads,n} S^f_{NH,n} + r^{SNO,n}_{Sads,n} S^f_{NO,n} + r^{SS,n}_{Sads,n} S^f_{S,n} + r^{Sads,n}_{Sads,n} S^f_{ads,n} + r^f_{Sads,n} \quad (5.104)$$

- for the parameter $\theta = Y_{ZH}, Y_{ZA}, f_{ZBH}, \mu_A, \mu_H, K_S, K_{OH}, K_{NO}, K_{NA}, K_{OA}, \eta_g, K_{MP}, K_{SP}, K_{SA}$

  The equations are as follows:

  1) for the first tank

$$\dot{S}^\theta_{NH,1} = \frac{1}{V_1}\left[(Q_a + Q_r) S^\theta_{Nh,5} - Q S^\theta_{NH,1}\right] + r^{SNH,1}_{SNH,1} S^\theta_{NH,1} + r^{SNO,1}_{SNH,1} S^\theta_{NO,1} + r^{SS,1}_{SNH,1} S^\theta_{S,1} + r^{Sads,1}_{SNH,1} S^\theta_{ads,1} + r^\theta_{SNH,1} \quad (5.105)$$

$$\dot{S}^\theta_{NO,1} = \frac{1}{V_1}\left[(Q_a + Q_r) S^\theta_{NO,5} - Q S^\theta_{NO,1}\right] + r^{SNH,1}_{SNO,1} S^\theta_{NH,1} + r^{SNO,1}_{SNO,1} S^\theta_{NO,1} + r^{SS,1}_{SNO,1} S^\theta_{S,1} + r^{Sads,1}_{SNO,1} S^\theta_{ads,1} + r^\theta_{SNO,1} \quad (5.106)$$

$$\dot{S}^\theta_{S,1} = \frac{1}{V_1}\left[(Q_a + Q_r) S^\theta_{S,5} - Q S^\theta_{S,1}\right] + r^{SNH,1}_{SS,1} S^\theta_{NH,1} + r^{SNO,1}_{SS,1} S^\theta_{NO,1} + r^{SS,1}_{SS,1} S^\theta_{S,1} + r^{Sads,1}_{SS,1} S^\theta_{ads,1} + r^\theta_{SS,1} \quad (5.107)$$

$$\dot{S}^\theta_{ads,1} = \frac{1}{V_1}\left[(Q_a + Q_r) S^\theta_{ads,5} - Q S^\theta_{ads,1}\right] + r^{SNH,1}_{ads,1} S^\theta_{NH,1} + r^{SNO,1}_{ads,1} S^\theta_{NO,1} + r^{SS,1}_{ads,1} S^\theta_{S,1} + r^{Sads,1}_{ads,1} S^\theta_{ads,1} + r^\theta_{ads,1} \quad (5.108)$$

2) for the tanks n = 2÷5

$$\dot{S}^{\theta}_{NH,n} = \frac{1}{V_n}\left[Q\left(S^{\theta}_{NH,n-1} - S^{\theta}_{NH,n}\right)\right] + r^{SNH,n}_{SNH,n} S^{\theta}_{NH,n} + r^{SNO,n}_{SNH,n} S^{\theta}_{NO,n} + r^{SS,n}_{SNH,n} S^{\theta}_{S,n} + r^{Sads,n}_{SNH,n} S^{\theta}_{ads,n} + r^{\theta}_{SNH,n} \quad (5.109)$$

$$\dot{S}^{\theta}_{NO,n} = \frac{1}{V_n}\left[Q\left(S^{\theta}_{NO,n-1} - S^{\theta}_{NO,n}\right)\right] + r^{SNH,n}_{SNO,n} S^{\theta}_{NH,n} + r^{SNO,n}_{SNO,n} S^{\theta}_{NO,n} + r^{SS,n}_{SNO,n} S^{\theta}_{S,n} + r^{Sads,n}_{SNO,n} S^{\theta}_{ads,n} + r^{\theta}_{SNO,n} \quad (5.110)$$

$$\dot{S}^{\theta}_{S,n} = \frac{1}{V_n}\left[Q\left(S^{\theta}_{S,n-1} - S^{\theta}_{S,n}\right)\right] + r^{SNH,n}_{SS,n} S^{\theta}_{NH,n} + r^{SNO,n}_{SS,n} S^{\theta}_{NO,n} + r^{SS,n}_{SS,n} S^{\theta}_{S,n} + r^{Sads,n}_{SS,n} S^{\theta}_{ads,n} + r^{\theta}_{SS,n} \quad (5.111)$$

$$\dot{S}^{\theta}_{ads,n} = \frac{1}{V_n}\left[Q\left(S^{\theta}_{ads,n-1} - S^{\theta}_{ads,n}\right)\right] + r^{SNH,n}_{Sads,n} S^{\theta}_{NH,n} + r^{SNO,n}_{Sads,n} S^{\theta}_{NO,n} + r^{SS,n}_{Sads,n} S^{\theta}_{S,n} + r^{Sads,n}_{Sads,n} S^{\theta}_{ads,n} + r^{\theta}_{Sads,n} \quad (5.112)$$

The partial derivatives of the process rates are determined as follows:

- for the parameter *f*

$$dr^{f}_{SNH,n} = dr^{f}_{SNO,n} = dr^{f}_{SS,n} = dr^{f}_{Sads,n} = 0,\ n = 1 \div 5$$

- for the process variables

$$r^{SNH,n}_{SNH,n} = -f_{ZBH} X_{BH}\left(\frac{K_{NA}}{\left(K_{NA} + S_{NH,n}\right)^2}\right)\left(\frac{S_{O,n}}{K_{OH} + S_{O,n}}\right)\left[\mu_H\left(\frac{S_{S,n}}{K_S + S_{S,n}}\right) + K_{MP}\left(\frac{S_{ads,n}/X_{BH,n}}{K_{SP} + S_{ads,n}/X_{BH,n}}\right)\right] +$$
$$+\left(\frac{K_{OH}}{K_{OH} + S_{O,n}}\right)\left(\frac{S_{NO,n}}{K_{NO} + S_{NO,n}}\right)\mu_H\left(\frac{S_{S,n}}{K_S + S_{S,n}}\right)K_{MP}\eta_g\left(\frac{S_{ads,n}/X_{BH,n}}{K_{SP} + S_{ads,n}/X_{BH}}\right) - \quad (5.113)$$
$$-\left(\frac{1}{Y_{ZA}} + f_{ZBH}\right)\mu_A\left(\frac{S_{O,n}}{K_{OA} + S_{O,n}}\right)\left(\frac{K_{SA}}{\left(K_{SA} + S_{NH,n}\right)^2}\right)X_{BA}$$

$$r^{SNO,n}_{SNH,n} = -f_{ZBH} X_{BH}\left(\frac{K_{NO}}{\left(K_{NO} + S_{NO,n}\right)^2}\right)\left(\frac{K_{OH}}{K_{OH} + S_{O,n}}\right)\left(\frac{S_{NH,n}}{K_{NA} + S_{NH,n}}\right). \quad (5.114)$$
$$\cdot\left[\mu_H\left(\frac{S_{S,n}}{K_S + S_{S,n}}\right) + \eta_g K_{MP}\left(\frac{S_{ads,n}/X_{BH}}{K_{SP} + S_{ads,n}/X_{BH}}\right)\right]$$

$$r^{SS,n}_{SNH,n} = -f_{ZBH}\mu_H\left(\frac{K_S}{\left(K_S + S_{S,n}\right)^2}\right)X_{BH}\left(\frac{S_{NH,n}}{K_{NA} + S_{NH,n}}\right)\left[\left(\frac{S_{O,n}}{K_{OH} + S_{O,n}}\right) + \left(\frac{K_{OH}}{K_{OH} + S_{O,n}}\right)\left(\frac{S_{NO,n}}{K_{NO} + S_{NO,n}}\right)\right] \quad (5.115)$$

$$r^{Sads,n}_{SNH,n} = -f_{ZBH} K_{MP}\left(\frac{K_{SP}/X_{BH,n}}{\left(K_{SP} + S_{ads,n}/X_{BH,n}\right)^2}\right)X_{BH}\left(\frac{S_{NH,n}}{K_{NA} + S_{NH,n}}\right). \quad (5.116)$$
$$\cdot\left[\left(\frac{S_{O,n}}{K_{OH} + S_{O,n}}\right) + \eta_g\left(\frac{K_{OH}}{K_{OH} + S_{O,n}}\right)\left(\frac{S_{NO,n}}{K_{NO} + S_{NO,n}}\right)\right]$$

$$r^{SNH,n}_{SNO,n} = f_{ZBH}\left(\frac{S_{O,n}}{K_{OH} + S_{O,n}}\right)\left(\frac{K_{NA}}{\left(K_{NA} + S_{NH,n}\right)^2}\right)\left(\frac{S_{NO,n}}{K_{NO} + S_{NO,n}}\right)X_{BH,n}\left[\mu_H\left(\frac{S_{S,n}}{K_S + S_{S,n}}\right) + K_{MP}\left(\frac{S_{ads,n}/X_{BH,n}}{K_{SP} + S_{ads,n}/X_{BH,n}}\right)\right] +$$
$$+ f_{ZBH}\left(\frac{K_{OH}}{K_{OH} + S_{O,n}}\right)\left(\frac{K_{NA}}{\left(K_{NA} + S_{NH,n}\right)^2}\right)\left(\frac{S_{NO,n}}{K_{NO} + S_{NO,n}}\right)X_{BH,n}\left[\mu_H\left(\frac{S_{S,n}}{K_S + S_{S,n}}\right) + K_{MP}\eta_g\left(\frac{S_{ads,n}/X_{BH,n}}{K_{SP} + S_{ads,n}/X_{BH,n}}\right)\right] + \quad (5.117)$$
$$+\frac{1}{Y_{ZA}}\mu_A\cdot\left(\frac{K_{SA}}{\left(K_{SA} + S_{NH,n}\right)^2}\right)\left(\frac{S_{NO,n}}{K_{OA} + S_{NO,n}}\right)X_{BA}$$

$$r_{SNO,n}^{SNO,n} = -f_{ZBH}\left(\frac{S_{O,n}}{K_{OH}+S_{O,n}}\right)\left(\frac{K_{NA}}{K_{NA}+S_{NH,n}}\right)\left(\frac{K_{NO}}{(K_{NO}+S_{NO,n})^2}\right)X_{BH,n}\left[\mu_H\left(\frac{S_{S,n}}{K_S+S_{S,n}}\right)+K_{MP}\left(\frac{S_{ads,n}/X_{BH,n}}{K_{SP}+S_{ads,n}/X_{BH,n}}\right)\right]-$$
$$-\left(\frac{K_{OH}}{K_{OH}+S_{O,n}}\right)\left(\frac{K_{NO}}{(K_{NO}+S_{NO,n})^2}\right)X_{BH,n}\left[\mu_H\left(\frac{S_{S,n}}{K_S+S_{S,n}}\right)+K_{MP}\eta_g\left(\frac{S_{ads,n}/X_{BH,n}}{K_{SP}+S_{ads,n}/X_{BH,n}}\right)\right].$$
$$.\left[\left(\frac{1-Y_{ZH}}{2.86Y_{ZH}}\right)\left(\frac{S_{NH,n}}{K_{NA}+S_{NH,n}}\right)+\left(\frac{1-Y_{ZH}}{2.86Y_{ZH}}+f_{ZBH}\right)\left(\frac{K_{NA}}{K_{NA}+S_{NH,n}}\right)\right] \quad (5.118)$$

$$r_{SNO,n}^{SS,n} = -\mu_H\left(\frac{K_S}{(K_S+S_{S,n})^2}\right)\left(\frac{S_{NO,n}}{K_{NO}+S_{NO,n}}\right)X_{BH,n}[f_{ZBH}\left(\frac{S_{O,n}}{K_{OH}+S_{O,n}}\right)\left(\frac{K_{NA}}{K_{NA}+S_{NH,n}}\right)+ \quad (5.119)$$
$$+\left(\frac{1-Y_{ZH}}{2.86Y_{ZH}}\right)\left(\frac{K_{OH}}{K_{OH}+S_{O,n}}\right)\left(\frac{S_{NH,n}}{K_{NA}+S_{NH,n}}\right)+\left(\frac{1-Y_{ZH}}{2.86Y_{ZH}}+f_{ZBH}\right)\left(\frac{K_{OH}}{K_{OH}+S_{O,n}}\right)\left(\frac{K_{NA}}{K_{NA}+S_{NH,n}}\right)$$

$$r_{SNO,n}^{Sads,n} = -K_{MP}\left(\frac{K_{SP}/X_{BH}}{(K_{SP}+K_{SP}/X_{BH})^2}\right)\left(\frac{S_{NO,n}}{K_{NO}+S_{NO,n}}\right)X_{BH,n}.$$
$$.[f_{ZBH}\left(\frac{S_{O,n}}{K_{OH}+S_{O,n}}\right)\left(\frac{K_{NA}}{K_{NA}+S_{NH,n}}\right)+\left(\frac{1-Y_{ZH}}{2.86Y_{ZH}}\right)\left(\frac{K_{OH}}{K_{OH}+S_{O,n}}\right)\left(\frac{S_{NH,n}}{K_{NA}+S_{NH,n}}\right)\eta_g+ \quad (5.120)$$
$$+\left(\frac{1-Y_{ZH}}{2.86Y_{ZH}}+f_{ZBH}\right)\left(\frac{K_{OH}}{K_{OH}+S_{O,n}}\right)\left(\frac{K_{NA}}{K_{NA}+S_{NH,n}}\right)\eta_g]$$

$$r_{SS,n}^{SNH,n} = -\frac{1}{Y_{ZH}}\mu_H\left(\frac{S_{S,n}}{K_S+S_{S,n}}\right)\left(\frac{S_{O,n}}{K_{OH}+S_{O,n}}\right)\left(\frac{K_{NA}}{(K_{NA}+S_{NH,n})^2}\right)X_{BH,n}\left[1-\left(\frac{S_{NO,n}}{K_{NO}+S_{NO,n}}\right)\right] \quad (5.121)$$

$$r_{SS,n}^{SNO,n} = -\frac{1}{Y_{ZH}}\mu_H\left(\frac{S_{S,n}}{K_S+S_{S,n}}\right)\left(\frac{K_{NO}}{(K_{NO}+S_{NO,n})^2}\right)X_{BH,n}. \quad (5.122)$$
$$.\left[\left(\frac{S_{O,n}}{K_{OH}+S_{O,n}}\right)\left(\frac{K_{NA}}{K_{NA}+S_{NH,n}}\right)+\left(\frac{K_{OH}}{K_{OH}+S_{O,n}}\right)\left(\frac{S_{NH,n}}{K_{NA}+S_{NH,n}}\right)+\left(\frac{K_{OH}}{K_{OH}+S_{O,n}}\right)\left(\frac{K_{NA}}{K_{NA}+S_{NH,n}}\right)\right]$$

$$r_{SS,n}^{SS,n} = -\frac{1}{Y_{ZH}}\left(\frac{K_S}{(K_S+S_S)^2}\right)\left[\left(\frac{S_{O,n}}{K_{OH}+S_{O,n}}\right)\left[\left(\frac{S_{NH,n}}{K_{NA}+S_{NH,n}}\right)+\left(\frac{K_{NA}}{K_{NA}+S_{NH,n}}\right)\left(\frac{S_{NO}}{K_{NO}+S_{NO}}\right)\right]+\right. \quad (5.123)$$
$$\left.+\left(\frac{K_{OH}}{K_{OH}+S_O}\right)\left(\frac{S_{NO}}{K_{NO}+S_{NO}}\right)\left[\left(\frac{S_{NH,n}}{K_{NA}+S_{NH,n}}\right)+\left(\frac{K_{NA}}{K_{NA}+S_{NH,n}}\right)\right]\right]$$

$$r_{SS,n}^{Sads,n} = 0 \quad (5.124)$$

$$r_{Sads,n}^{SNH,n} = -\frac{1}{Y_{ZH}}K_{MP}\left(\frac{S_{ads,n}/X_{BH,n}}{K_{SP}+S_{ads,n}/X_{BH,n}}\right)\left(\frac{S_{O,n}}{K_{OH}+S_{O,n}}\right)\left(\frac{K_{NA}}{(K_{NA}+S_{NH,n})^2}\right)X_{BH,n}\left[1-\left(\frac{S_{NO,n}}{K_{NO}+S_{NO,n}}\right)\right] \quad (5.125)$$

$$r_{Sads,n}^{SNO,n} = -\frac{1}{Y_{ZH}}K_{MP}\left(\frac{S_{ads,n}/X_{BH,n}}{K_{SP}+S_{ads,n}/X_{BH,n}}\right)\left(\frac{K_{NO}}{(K_{NO}+S_{NO,n})^2}\right)X_{BH,n}. \quad (5.126)$$
$$.\left[\left(\frac{S_{O,n}}{K_{OH}+S_{O,n}}\right)\left(\frac{K_{NA}}{K_{NA}+S_{NH,n}}\right)+\left(\frac{K_{OH}}{K_{OH}+S_{O,n}}\right)\left(\frac{S_{NH,n}}{K_{NA}+S_{NH,n}}\right)+\left(\frac{K_{OH}}{K_{OH}+S_{O,n}}\right)\left(\frac{K_{NA}}{K_{NA}+S_{NH,n}}\right)\right]$$

$$r_{Sads,n}^{SS,n} = 0 \quad (5.127)$$

$$r_{Sads,n}^{Sads,n} = -\frac{1}{Y_{ZH}} K_{MP} \left(\frac{K_{SP}/X_{BH,n}}{\left(K_{SP} + S_{ads,n}/X_{BH,n}\right)^2} \right) \left(\frac{S_{O,n}}{K_{OH} + S_{O,n}} \right) X_{BH,n} \cdot$$

$$\cdot \left[\left(\frac{S_{NH,n}}{K_{NA} + S_{NH,n}} \right) + \left(\frac{K_{NA}}{K_{NA} + S_{NH,n}} \right) \left(\frac{S_{NO,n}}{K_{NO} + S_{NO,n}} \right) \right] -$$

$$- \frac{1}{Y_{ZH}} K_{MP} \left(\frac{K_{SP}/X_{BH,n}}{\left(K_{SP} + S_{ads,n}/X_{BH,n}\right)^2} \right) \left(\frac{K_{OH}}{K_{OH} + S_{O,n}} \right) \left(\frac{S_{NO,n}}{K_{NO} + S_{NO,n}} \right) \eta_g X_{BH,n} \left[\left(\frac{S_{NH,n}}{K_{NA} + S_{NH,n}} \right) + \left(\frac{K_{NA}}{K_{NA} + S_{NH,n}} \right) \right]$$

(5.128)

The partial derivatives of the process rates according to the model coefficients $\theta = Y_{ZH}, Y_{ZA}, f_{ZBH}, \mu_A, \mu_H, K_S, K_{OH}, K_{NO}, K_{NA}, K_{OA}, \eta_g, K_{MP}, K_{SP}, K_{SA}$ are as follows:

- for the process rate $r_{SNH,n}$

$$r_{SNH,n}^{Y_{ZH}} = 0, \qquad r_{SNH,n}^{Y_{ZA}} = \frac{1}{Y_{ZA}} \mu_A \left(\frac{S_{NH,n}}{K_{SA} + S_{NH,n}} \right) \left(\frac{S_{O,n}}{K_{OA} + S_{O,n}} \right) X_{BA,n} \tag{5.129}$$

$$r_{SNH,n}^{f_{ZBH}} = -\left(\frac{S_{O,n}}{K_{OH} + S_{O,n}} \right) \left(\frac{S_{NH,n}}{K_{NA} + S_{NH,n}} \right) X_{BH,n} \left[\mu_H \left(\frac{S_{S,n}}{K_S + S_{S,n}} \right) + K_{MP} \left(\frac{S_{ads,n}/X_{BH,n}}{K_{SP} + S_{ads,n}/X_{BH,n}} \right) \right] -$$

$$- \left(\frac{K_{OH}}{K_{OH} + S_{O,n}} \right) \left(\frac{S_{NH,n}}{K_{NA} + S_{NH,n}} \right) \left(\frac{S_{NO,n}}{K_{NO} + S_{NO,n}} \right) X_{BH,n} \left[\mu_H \left(\frac{S_{S,n}}{K_S + S_{S,n}} \right) + K_{MP} \eta_g \left(\frac{S_{ads,n}/X_{BH,n}}{K_{SP} + S_{ads,n}/X_{BH,n}} \right) \right] -$$

$$- \mu_A \left(\frac{S_{NH,n}}{K_{SA} + S_{NH,n}} \right) \left(\frac{S_{O,n}}{K_{OA} + S_{O,n}} \right) X_{BA,n}$$

(5.130)

$$r_{SNH,n}^{\mu_H} = -f_{ZBH} \left(\frac{S_{S,n}}{K_S + S_{S,n}} \right) X_{BH,n} \left[\left(\frac{S_{NH,n}}{K_{NA} + S_{NH,n}} \right) \left(\frac{S_{O,n}}{K_{OH} + S_{O,n}} \right) + \left(\frac{K_{OH}}{K_{OH} + S_{O,n}} \right) \left(\frac{S_{NO,n}}{K_{NO} + S_{NO,n}} \right) \right] \tag{5.131}$$

$$r_{SNH,n}^{\mu_A} = -\left(\frac{1}{Y_{ZA}} - f_{ZBH} \right) \left(\frac{S_{NH,n}}{K_{SA} + S_{NH,n}} \right) \left(\frac{S_{O,n}}{K_{OA} + S_{O,n}} \right) X_{BA,n} \tag{5.132}$$

$$r_{SNH,n}^{K_S} = f_{ZBH} \mu_H \left(\frac{S_{S,n}}{\left(K_S + S_{S,n}\right)^2} \right) \left(\frac{S_{NH,n}}{K_{NA} + S_{NH,n}} \right) X_{BH,n} \left[\left(\frac{S_{O,n}}{K_{OH} + S_{O,n}} \right) + \left(\frac{K_{OH}}{K_{OH} + S_{O,n}} \right) \left(\frac{S_{NO,n}}{K_{NO} + S_{NO,n}} \right) \right] \tag{5.133}$$

$$r_{SNH,n}^{K_{OH}} = f_{ZBH} \left(\frac{S_{O,n}}{\left(K_{OH} + S_{O,n}\right)^2} \right) \left(\frac{S_{NH,n}}{K_{NA} + S_{NH,n}} \right) X_{BH,n} \left\{ \mu_H \left(\frac{S_{S,n}}{K_S + S_{S,n}} \right) + K_{MP} \left(\frac{S_{ads,n}/X_{BH,n}}{K_{SP} + S_{ads,n}/X_{BH,n}} \right) \right\} -$$

$$- f_{ZBH} \left(\frac{S_{O,n}}{\left(K_{OH} + S_{O,n}\right)^2} \right) \left(\frac{S_{NH,n}}{K_{NA} + S_{NH,n}} \right) \left(\frac{S_{NO,n}}{K_{NO} + S_{NO,n}} \right) X_{BH,n} \left\{ \mu_H \left(\frac{S_{S,n}}{K_S + S_{S,n}} \right) + K_{MP} \eta_g \left(\frac{S_{ads,n}/X_{BH,n}}{K_{SP} + S_{ads,n}/X_{BH,n}} \right) \right\}$$

(5.134)

$$r_{SNH,n}^{K_{NO}} = f_{ZBH} \left(\frac{K_{OH}}{K_{OH} + S_{O,n}} \right) \left(\frac{S_{NH,n}}{K_{NA} + S_{NH,n}} \right) \left(\frac{S_{NO,n}}{\left(K_{NO} + S_{NO,n}\right)^2} \right) X_{BH,n} \left[\mu_H \left(\frac{S_{S,n}}{K_S + S_{S,n}} \right) + K_{MP} \eta_g \left(\frac{S_{ads,n}/X_{BH,n}}{K_{SP} + S_{ads,n}/X_{BH,n}} \right) \right] \tag{5.135}$$

$$r_{SNH,n}^{K_{NA}} = f_{ZBH}\left(\frac{S_{O,n}}{K_{OH}+S_{O,n}}\right)\left(\frac{S_{NH,n}}{\left(K_{NA}+S_{NH,n}\right)^2}\right)X_{BH,n}\left[\mu_H\left(\frac{S_{S,n}}{K_S+S_{S,n}}\right)+K_{MP}\left(\frac{S_{ads,n}/X_{BH,n}}{K_{SP}+S_{ads,n}/X_{BH,n}}\right)\right]+$$

$$+f_{ZBH}\left(\frac{K_{OH}}{K_{OH}+S_{O,n}}\right)\left(\frac{S_{NH,n}}{\left(K_{NA}+S_{NH,n}\right)^2}\right)\left(\frac{S_{NO,n}}{K_{NO}+S_{NO,n}}\right)X_{BH,n}\left[\mu_H\left(\frac{S_{S,n}}{K_S+S_{S,n}}\right)+K_{MP}\eta_g\left(\frac{S_{ads,n}/X_{BH,n}}{K_{SP}+S_{ads,n}/X_{BH,n}}\right)\right] \quad (5.136)$$

$$r_{SNH,n}^{K_{OA}} = \left(\frac{1}{Y_{ZA}}+f_{ZBH}\right)\mu_A\left(\frac{S_{NH,n}}{K_{SA}+S_{NH,n}}\right)\left(\frac{S_{O,n}}{\left(K_{OA}+S_{O,n}\right)^2}\right)X_{BA,n} \quad (5.137)$$

$$r_{SNH,n}^{\eta_g} = -K_{MP}\left(\frac{S_{ads,n}/X_{BH,n}}{K_{SP}+S_{ads,n}/X_{BH,n}}\right)\left(\frac{K_{OH}}{K_{OH}+S_{O,n}}\right)\left(\frac{S_{NH,n}}{K_{NA}+S_{NH,n}}\right)\left(\frac{S_{NO,n}}{K_{NO}+S_{NO,n}}\right)X_{BH,n}f_{ZBH} \quad (5.138)$$

$$r_{SNH,n}^{K_{MP}} = \left(\frac{S_{ads,n}/X_{BH,n}}{K_{SP}+S_{ads,n}/X_{BH,n}}\right)\left(\frac{S_{NH,n}}{K_{NA}+S_{NH,n}}\right)X_{BH,n}f_{ZBH}\left[\left(\frac{S_{O,n}}{K_{OH}+S_{O,n}}\right)+\left(\frac{K_{OH}}{K_{OH}+S_{O,n}}\right)\left(\frac{S_{NO,n}}{K_{NO}+S_{NO,n}}\right)\eta_g\right] \quad (5.139)$$

$$r_{SNH,n}^{K_{SP}} = f_{ZBH}K_{MP}\left(\frac{S_{ads,n}/X_{BH,n}}{K_{SP}+S_{ads,n}/X_{BH,n}}\right)\left(\frac{S_{NH,n}}{K_{NA}+S_{NH,n}}\right)\left[\left(\frac{S_{O,n}}{K_{OH}+S_{O,n}}\right)+\left(\frac{K_{OH}}{K_{OH}+S_{O,n}}\right)\left(\frac{S_{NO,n}}{K_{NO}+S_{NO,n}}\right)\right]X_{BH,n} \quad (5.140)$$

$$r_{SNH,n}^{K_{SA}} = \left(\frac{1}{Y_{ZA}}+f_{ZBH}\right)\mu_A\left(\frac{S_{NH,n}}{\left(K_{SA}+S_{NH,n}\right)^2}\right)\left(\frac{S_{O,n}}{K_{OA}+S_{O,n}}\right)X_{BA,n} \quad (5.141)$$

$$r_{SNO,n}^{Y_{ZH}} = \frac{1}{2.86Y_{ZH}^2}\left(\frac{K_{OH}}{K_{OH}+S_{O,n}}\right)\left(\frac{S_{NO,n}}{K_{NO}+S_{NO,n}}\right)X_{BH,n}\left[\mu_H\left(\frac{S_{S,n}}{K_S+S_{S,n}}\right)+K_{MP}\eta_g\left(\frac{S_{ads,n}/X_{BH,n}}{K_{SP}+S_{ads,n}/X_{BH,n}}\right)\right]\cdot$$

$$\cdot\left[\left(\frac{S_{NH,n}}{K_{NA}+S_{NH,n}}\right)+\left(\frac{K_{NA}}{K_{NA}+S_{NH,n}}\right)\right] \quad (5.142)$$

$$r_{SNO,n}^{Y_{ZA}} = \frac{1}{2.86Y_{ZH}^2}\mu_A\left(\frac{S_{NH,n}}{K_{SA}+S_{NH,n}}\right)\left(\frac{S_{O,n}}{\left(K_{OA}+S_{O,n}\right)^2}\right)X_{BA,n} \quad (5.143)$$

$$r_{SNO,n}^{f_{ZBH}} = -\left(\frac{S_{O,n}}{K_{OH}+S_{O,n}}\right)\left(\frac{K_{NA}}{K_{NA}+S_{NH,n}}\right)\left(\frac{S_{NO,n}}{K_{NO}+S_{NO,n}}\right)X_{BH,n}\left[\mu_H\left(\frac{S_{S,n}}{K_S+S_{S,n}}\right)+K_{MP}\left(\frac{S_{ads,n}/X_{BH,n}}{K_{SP}+S_{ads,n}/X_{BH,n}}\right)\right] \quad (5.144)$$

$$r_{SNO,n}^{\mu_H} = -2f_{ZBH}\left(\frac{S_{S,n}}{K_S+S_{S,n}}\right)\left(\frac{K_{NA}}{K_{NA}+S_{NH,n}}\right)\left(\frac{S_{NO,n}}{K_{NO}+S_{NO,n}}\right)X_{BH,n}\cdot$$

$$\cdot\left[\left(\frac{S_{O,n}}{K_{OH}+S_{O,n}}\right)+\left(\frac{K_{OH}}{K_{OH}+S_{O,n}}\right)\right]-\left(\frac{1-Y_{ZH}}{2.86Y_{ZH}}\right)\left(\frac{S_{S,n}}{K_S+S_{S,n}}\right)\left(\frac{K_{OH}}{K_{OH}+S_{O,n}}\right)\cdot \quad (5.145)$$

$$\cdot\left(\frac{S_{NO,n}}{K_{NO}+S_{NO,n}}\right)X_{BH,n}\left[\left(\frac{S_{NH,n}}{K_{NA}+S_{NH,n}}\right)+\left(\frac{K_{NA}}{K_{NA}+S_{NH,n}}\right)\right]$$

$$r_{SNO,n}^{\mu_A} = \frac{1}{Y_{ZA}}\left(\frac{S_{NH,n}}{\left(K_{SA}+S_{NH,n}\right)^2}\right)\left(\frac{S_{O,n}}{K_{OA}+S_{O,n}}\right)X_{BA,n} \tag{5.146}$$

$$r_{SNO,n}^{K_S} = f_{ZBH}\mu_H\left(\frac{S_{S,n}}{\left(K_S+S_{S,n}\right)^2}\right)\left(\frac{K_{NA}}{K_{NA}+S_{NH,n}}\right)\left(\frac{S_{NO,n}}{K_{NO}+S_{NO,n}}\right)X_{BH,n}\left[\left(\frac{S_{O,n}}{K_{OH}+S_{O,n}}\right)+\left(\frac{K_{OH}}{K_{OH}+S_{O,n}}\right)\right]+$$
$$+\left(\frac{1-Y_{ZH}}{2.86Y_{ZH}}\right)\mu_H\left(\frac{S_{S,n}}{\left(K_S+S_{S,n}\right)^2}\right)\left(\frac{K_{OH}}{K_{OH}+S_{O,n}}\right)\left(\frac{S_{NO,n}}{K_{NO}+S_{NO,n}}\right)X_{BH,n}\left[\left(\frac{S_{NH,n}}{K_{NA}+S_{NH,n}}\right)+\left(\frac{K_{NA}}{K_{NA}+S_{NH,n}}\right)\right] \tag{5.147}$$

$$r_{SNO,n}^{K_{OH}} = -\frac{1-Y_{ZH}}{2.86Y_{ZH}}\left(\frac{K_{OH}}{\left(K_{OH}+S_{O,n}\right)^2}\right)\left(\frac{S_{NO,n}}{K_{NO}+S_{NO,n}}\right)X_{BH,n}\left[\mu_H\left(\frac{S_{S,n}}{K_S+S_{S,n}}\right)+K_{MP}\eta_g\left(\frac{S_{ads,n}/X_{BH,n}}{K_{SP}+S_{ads,n}/X_{BH,n}}\right)\right]+$$
$$+f_{ZBH}\left(\frac{S_{O,n}}{\left(K_{OH}+S_{O,n}\right)^2}\right)\left(\frac{K_{NA}}{K_{NA}+S_{NH,n}}\right)\left(\frac{S_{NO,n}}{K_{NO}+S_{NO,n}}\right)X_{BH,n}K_{MP}\left(\frac{S_{ads,n}/X_{BH,n}}{K_{SP}+S_{ads,n}/X_{BH,n}}\right)\left[1-\eta_g\right] \tag{5.148}$$

$$r_{SNO,n}^{K_{NO}} = f_{ZBH}\left(\frac{S_{O,n}}{K_S+S_{O,n}}\right)\left(\frac{K_{NA}}{K_{NA}+S_{NH,n}}\right)\left(\frac{S_{NO,n}}{\left(K_{NO}+S_{NO,n}\right)^2}\right)X_{BH,n}\left[\mu_H\left(\frac{S_{S,n}}{K_S+S_{S,n}}\right)+K_{MP}\left(\frac{S_{ads,n}/X_{BH,n}}{K_{SP}+S_{ads,n}/X_{BH,n}}\right)\right]+$$
$$+\left(\frac{1-Y_{ZH}}{2.86Y_{ZH}}\right)\left(\frac{K_{OH}}{K_{OH}+S_{O,n}}\right)\left(\frac{S_{NH,n}}{K_{NA}+S_{NH,n}}\right)\left(\frac{S_{NO,n}}{\left(K_{NO}+S_{NO,n}\right)^2}\right)X_{BH,n}\left[\mu_H\left(\frac{S_{S,n}}{K_S+S_{S,n}}\right)+K_{MP}\eta_g\left(\frac{S_{ads,n}/X_{BH,n}}{K_{SP}+S_{ads,n}/X_{BH,n}}\right)\right]+$$
$$+\left(\frac{1-Y_{ZH}}{2.86Y_{ZH}}+f_{ZBH}\right)\left(\frac{K_{OH}}{K_{OH}+S_{O,n}}\right)\left(\frac{K_{NA}}{K_{NA}+S_{NH,n}}\right)\left(\frac{S_{NO,n}}{\left(K_{OH}+S_{NO,n}\right)^2}\right)X_{BH,n}\left[\mu_H\left(\frac{S_{S,n}}{K_S+S_{S,n}}\right)+K_{MP}\eta_g\left(\frac{S_{ads,n}/X_{BH,n}}{K_{SP}+S_{ads,n}/X_{BH,n}}\right)\right] \tag{5.149}$$

$$r_{SNO,n}^{K_{NA}} = -f_{ZBH}\left(\frac{S_{O,n}}{K_S+S_{O,n}}\right)\left(\frac{S_{NH,n}}{\left(K_{NA}+S_{NH,n}\right)^2}\right)\left(\frac{S_{NO,n}}{K_{NO}+S_{NO,n}}\right)X_{BH,n}\left[\mu_H\left(\frac{S_{S,n}}{K_S+S_{S,n}}\right)+K_{MP}\left(\frac{S_{ads,n}/X_{BH,n}}{K_{SP}+S_{ads,n}/X_{BH,n}}\right)\right]-$$
$$-f_{ZBH}\left(\frac{K_{OH}}{K_{OH}+S_{O,n}}\right)\left(\frac{S_{NH,n}}{\left(K_{NA}+S_{NH,n}\right)^2}\right)\left(\frac{S_{NO,n}}{K_{NO}+S_{NO,n}}\right)X_{BH,n}\left[\mu_H\left(\frac{S_{S,n}}{K_S+S_{S,n}}\right)+K_{MP}\eta_g\left(\frac{S_{ads,n}/X_{BH,n}}{K_{SP}+S_{ads,n}/X_{BH,n}}\right)\right] \tag{5.150}$$

$$r_{SNO,n}^{K_{OA}} = -\frac{1}{Y_{ZA}}\mu_A\left(\frac{S_{NH,n}}{\left(K_{SA}+S_{NH,n}\right)^2}\right)\left(\frac{S_{O,n}}{K_{OA}+S_{O,n}}\right)X_{BA,n} \tag{5.151}$$

$$r_{SNO,n}^{\eta_g} = -\frac{1-Y_{ZH}}{2.86Y_{ZH}}K_{MP}\left(\frac{S_{ads,n}/X_{BH,n}}{K_{SP}+S_{ads,n}/X_{BH,n}}\right)\left(\frac{K_{OH}}{K_{OH}+S_{O,n}}\right)\left(\frac{S_{NO,n}}{K_{NO}+S_{NO,n}}\right)X_{BH,n}\left[\left(\frac{S_{NH,n}}{K_{NA}+S_{NH,n}}\right)+\left(\frac{K_{NA}}{K_{NA}+S_{NH,n}}\right)\right]-$$
$$-f_{ZBH}K_{MP}\left(\frac{S_{ads,n}/X_{BH,n}}{K_{SP}+S_{ads,n}/X_{BH,n}}\right)\left(\frac{K_{OH}}{K_{OH}+S_{O,n}}\right)\left(\frac{K_{NA}}{K_{NA}+S_{NH,n}}\right)\left(\frac{S_{NO,n}}{K_{NO}+S_{NO,n}}\right)X_{BH,n} \tag{5.152}$$

$$r_{SNO,n}^{K_{MP}} = -f_{ZBH}\left(\frac{S_{ads,n}/X_{BH,n}}{K_{SP}+S_{ads,n}/X_{BH,n}}\right)\left(\frac{K_{NA}}{K_{NA}+S_{NH,n}}\right)\left(\frac{S_{NO,n}}{K_{NO}+S_{NO,n}}\right)X_{BH,n}\left[\left(\frac{S_{O,n}}{K_{OH}+S_{O,n}}\right)+\eta_g\left(\frac{K_{OH}}{K_{OH}+S_{O,n}}\right)\right]-$$
$$-\frac{1-Y_{ZH}}{2.86Y_{ZH}}\left(\frac{S_{ads,n}/X_{BH,n}}{K_{SP}+S_{ads,n}/X_{BH,n}}\right)\left(\frac{K_{OH}}{K_{OH}+S_{O,n}}\right)\left(\frac{S_{NO,n}}{K_{NO}+S_{NO,n}}\right)\eta_g X_{BH,n}\left[\left(\frac{S_{NH,n}}{K_{NA}+S_{NH,n}}\right)+\left(\frac{K_{NA}}{K_{NA}+S_{NH,n}}\right)\right] \tag{5.153}$$

$$r_{SNO,n}^{K_{SP}} = f_{ZBH} K_{MP} \left(\frac{S_{ads,n}/X_{BH,n}}{K_{SP} + S_{ads,n}/X_{BH,n}} \right) \left(\frac{K_{NA}}{K_{NA} + S_{NH,n}} \right) \left(\frac{S_{NO,n}}{K_{NO} + S_{NO,n}} \right) X_{BH,n} \left[\left(\frac{S_{O,n}}{K_{OH} + S_{O,n}} \right) + \eta_g \left(\frac{K_{OH}}{K_{OH} + S_{O,n}} \right) \right] +$$

$$+ \frac{1 - Y_{ZH}}{2.86 Y_{ZH}} \left(\frac{S_{ads,n}/X_{BH,n}}{K_{SP} + S_{ads,n}/X_{BH,n}} \right) \left(\frac{K_{OH}}{K_{OH} + S_{O,n}} \right) \left(\frac{S_{NO,n}}{K_{NO} + S_{NO,n}} \right) \eta_g X_{BH,n} \left[\left(\frac{S_{NH,n}}{K_{NA} + S_{NH,n}} \right) + \left(\frac{K_{NA}}{K_{NA} + S_{NH,n}} \right) \right] \quad (5.154)$$

$$r_{SNO,n}^{K_{SA}} = -\frac{1}{Y_{ZA}} \mu_A \left(\frac{S_{NH,n}}{(K_{SA} + S_{NH,n})^2} \right) \left(\frac{S_{O,n}}{K_{OA} + S_{O,n}} \right) X_{BA,n} \quad (5.155)$$

$$r_{SNO,n}^{f_{MA}} = 0 \quad (5.156)$$

$$r_{SNO,n}^{K_A} = 0 \quad (5.157)$$

- for the process rate $r_{SS,n}$

$$r_{SS,n}^{Y_{ZH}} = \frac{1}{Y_{ZH}^2} \mu_H \left(\frac{S_{S,n}}{K_S + S_{S,n}} \right) X_{BH,n} [\left(\frac{S_{O,n}}{K_{OH} + S_{O,n}} \right) \left[\left(\frac{S_{NH,n}}{K_{NA} + S_{NH,n}} \right) + \left(\frac{K_{NA}}{K_{NA} + S_{NH,n}} \right) \left(\frac{S_{NO,n}}{K_{NO} + S_{NO,n}} \right) \right] + \quad (5.158)$$

$$+ \left(\frac{K_{OH}}{K_{OH} + S_{O,n}} \right) \left(\frac{S_{NO,n}}{K_{NO} + S_{NO,n}} \right) \left[\left(\frac{S_{NH,n}}{K_{NA} + S_{NH,n}} \right) + \left(\frac{K_{NA}}{K_{NA} + S_{NH,n}} \right) \right]]$$

$$r_{SS,n}^{Y_{ZA}} = 0 \quad (5.159)$$

$$r_{SS,n}^{f_{ZBH}} = 0 \quad (5.160)$$

$$r_{SS,n}^{\mu_H} = -\frac{1}{Y_{ZA}} \left(\frac{S_{S,n}}{K_S + S_{S,n}} \right) X_{BH,n} [\left(\frac{S_{O,n}}{K_{OH} + S_{O,n}} \right) \left[\left(\frac{S_{NH,n}}{K_{NA} + S_{NH,n}} \right) + \left(\frac{K_{NA}}{K_{NA} + S_{NH,n}} \right) \left(\frac{S_{NO,n}}{K_{NO} + S_{NO,n}} \right) \right] + \quad (5.161)$$

$$. + \left(\frac{K_{OH}}{K_{OH} + S_{O,n}} \right) \left(\frac{S_{NO,n}}{K_{NO} + S_{NO,n}} \right) \left[\left(\frac{S_{NH,n}}{K_{NA} + S_{NH,n}} \right) + \left(\frac{K_{NA}}{K_{NA} + S_{NH,n}} \right) \right]]$$

$$r_{SS,n}^{\mu_A} = 0 \quad (5.162)$$

$$r_{SS,n}^{K_S} = \frac{1}{Y_{ZH}} \mu_H \left(\frac{S_{S,n}}{(K_S + S_{S,n})^2} \right) X_{BH,n} [\left(\frac{S_{O,n}}{K_{OH} + S_{O,n}} \right) \left[\left(\frac{S_{NH,n}}{K_{NA} + S_{NH,n}} \right) + \left(\frac{K_{NA}}{K_{NA} + S_{NH,n}} \right) \left(\frac{S_{NO,n}}{K_{NO} + S_{NO,n}} \right) \right] + \quad (5.163)$$

$$+ \left(\frac{K_{OH}}{K_{OH} + S_{O,n}} \right) \left(\frac{S_{NO,n}}{K_{NO} + S_{NO,n}} \right) \left[\left(\frac{S_{NH,n}}{K_{NA} + S_{NH,n}} \right) + \left(\frac{K_{NA}}{K_{NA} + S_{NH,n}} \right) \right]]$$

$$r_{SS,n}^{K_{OH}} = \frac{1}{Y_{ZH}} \mu_H \left(\frac{S_{S,n}}{K_S + S_{S,n}} \right) \left(\frac{S_{O,n}}{(K_{OH} + S_{O,n})^2} \right) X_{BH,n} \left[\left(\frac{S_{NH,n}}{K_{NA} + S_{NH,n}} \right) \left(1 - \left(\frac{S_{NO,n}}{K_{NO} + S_{NO,n}} \right) \right) \right] \quad (5.164)$$

$$r_{SS,n}^{K_{NO}} = \frac{1}{Y_{ZH}} \mu_H \left(\frac{S_{S,n}}{K_S + S_{S,n}} \right) \left(\frac{S_{NO,n}}{(K_{NO} + S_{NO,n})^2} \right) X_{BH,n} [\left(\frac{S_{O,n}}{K_{OH} + S_{O,n}} \right) \left(\frac{K_{NA}}{K_{NA} + S_{NH,n}} \right) + \quad (5.165)$$

$$+ \left(\frac{K_{OH}}{K_{OH} + S_{O,n}} \right) \left[\left(\frac{S_{NH,n}}{K_{NA} + S_{NH,n}} \right) + \left(\frac{K_{NA}}{K_{NA} + S_{NH,n}} \right) \right]]$$

$$r_{SS,n}^{K_{NA}} = \frac{1}{Y_{ZH}} \mu_H \left(\frac{S_{S,n}}{K_S + S_{S,n}} \right) \left(\frac{S_{NH,n}}{(K_{NA} + S_{NH,n})^2} \right) X_{BH,n} \left(\frac{S_{O,n}}{K_{OH} + S_{O,n}} \right) \left[1 - \left(\frac{S_{NO,n}}{K_{NO} + S_{NO,n}} \right) \right] \quad (5.166)$$

$$r_{SS,n}^{K_{OA}} = 0 \quad (5.167)$$

$$r_{SS,n}^{\eta_g} = 0 \quad (5.168)$$

$$r_{SS,n}^{K_{MP}} = 0 \quad (5.169)$$

$$r_{SS,n}^{K_{SP}} = 0 \quad (5.170)$$

$$r_{SS,n}^{K_{SA}} = 0 \quad (5.171)$$

$$r_{SS,n}^{f_{MA}} = 0 \quad (5.172)$$

$$r_{SS,n}^{K_A} = 0 \quad (5.173)$$

-derivatives of the process rate $r_{ads,n}$ towards the model parameters

$$r_{Sads}^{Y_{ZH}} = \frac{1}{Y_{ZH}^2} K_{MP} \left(\frac{S_{ads,n}/X_{BH,n}}{K_{SP} + S_{ads,n}/X_{BH,n}} \right) X_{BH,n} [\left(\frac{S_{O,n}}{K_{OH} + S_{O,n}} \right) \left[\left(\frac{S_{NH,n}}{K_{NA} + S_{NH,n}} \right) + \left(\frac{K_{NA}}{K_{NA} + S_{NH,n}} \right) \left(\frac{S_{NO,n}}{K_{NO} + S_{NO,n}} \right) \right] +$$
$$+ \eta_g \left(\frac{K_{OH}}{K_{OH} + S_{O,n}} \right) \left(\frac{S_{NO,n}}{K_{NO} + S_{NO,n}} \right) \left[\left(\frac{S_{NH,n}}{K_{NA} + S_{NH,n}} \right) + \left(\frac{K_{NA}}{K_{NA} + S_{NH,n}} \right) \right]] \quad (5.174)$$

$$r_{Sads,n}^{Y_{ZA}} = 0 \quad (5.175)$$

$$r_{Sads,n}^{f_{ZBH}} = 0 \quad (5.176)$$

$$r_{Sads,n}^{\mu_H} = 0 \quad (5.177)$$

$$r_{Sads,n}^{\mu_A} = 0 \quad (5.178)$$

$$r_{Sads,n}^{K_S} = 0 \quad (5.179)$$

$$r_{Sads}^{K_{OH}} = \frac{1}{Y_{ZH}} K_{MP} \left(\frac{S_{ads,n}/X_{BH,n}}{K_{SP} + S_{ads,n}/X_{BH,n}} \right) \left(\frac{S_{O,n}}{(K_{OH} + S_{O,n})^2} \right) X_{BH,n} \left(\frac{S_{NH,n}}{K_{NA} + S_{NH,n}} \right) \left[1 - \left(\frac{S_{NO,n}}{K_{NO} + S_{NO,n}} \right) \right] \quad (5.180)$$

$$r_{Sads}^{K_{NO}} = \frac{1}{Y_{ZH}} K_{MP} \left(\frac{S_{ads,n}/X_{BH,n}}{K_{SP} + S_{ads,n}/X_{BH,n}} \right) \left(\frac{S_{NO,n}}{(K_{NO} + S_{NO,n})^2} \right) X_{BH,n} \left(\frac{S_{O,n}}{K_{OH} + S_{O,n}} \right) \left(\frac{K_{NA}}{K_{NA} + S_{NH,n}} \right) + \quad (5.181)$$
$$+ \eta_g \left(\frac{K_{OH}}{K_{OH} + S_{O,n}} \right) \left[\left(\frac{S_{NH,n}}{K_{NA} + S_{NH,n}} \right) + \left(\frac{K_{NA}}{K_{NA} + S_{NH,n}} \right) \right]]$$

$$r_{Sads}^{K_{NA}} = \frac{1}{Y_{ZH}} K_{MP} \left(\frac{S_{ads,n}/X_{BH,n}}{K_{SP} + S_{ads,n}/X_{BH,n}} \right) \left(\frac{S_{NH,n}}{(K_{NA} + S_{NH,n})^2} \right) X_{BH,n} \left(\frac{S_{O,n}}{K_{OH} + S_{O,n}} \right) \left[1 - \left(\frac{S_{NO,n}}{K_{NO} + S_{NO,n}} \right) \right] \quad (5.182)$$

$$r_{Sads,n}^{K_{OA}} = 0 \quad (5.183)$$

$$r_{Sads}^{\eta_g} = -\frac{1}{Y_{ZH}} K_{MP} \left(\frac{S_{ads,n}/X_{BH,n}}{K_{SP} + S_{ads,n}/X_{BH,n}} \right) \left(\frac{K_{OH}}{K_{OH} + S_{O,n}} \right) \left(\frac{S_{NO,n}}{K_{NO} + S_{NO,n}} \right) \eta_g X_{BH,n} \left[\left(\frac{S_{NH,n}}{K_{NA} + S_{NH,n}} \right) + \left(\frac{K_{NA}}{K_{NA} + S_{NH,n}} \right) \right] \tag{5.184}$$

$$r_{Sads}^{K_{MP}} = -\frac{1}{Y_{ZH}} \left(\frac{S_{ads,n}/X_{BH,n}}{K_{SP} + S_{ads,n}/X_{BH,n}} \right) X_{BH,n} [\left(\frac{S_{O,n}}{K_{OH} + S_{O,n}} \right) \left[\left(\frac{S_{NH,n}}{K_{NA} + S_{NH,n}} \right) + \left(\frac{K_{NA}}{K_{NA} + S_{NH,n}} \right) \left(\frac{S_{NO,n}}{K_{NO} + S_{NO,n}} \right) \right] +$$
$$+ \eta_g \left(\frac{K_{OH}}{K_{OH} + S_{O,n}} \right) \left(\frac{S_{NO,n}}{K_{NO} + S_{NO,n}} \right) \left[\left(\frac{S_{NH,n}}{K_{NA} + S_{NH,n}} \right) + \left(\frac{K_{NA}}{K_{NA} + S_{NH,n}} \right) \right]] \tag{5.185}$$

$$r_{Sads}^{K_{SP}} = -\frac{1}{Y_{ZH}} \left(\frac{S_{ads,n}/X_{BH,n}}{\left(K_{SP} + S_{ads,n}/X_{BH,n}\right)^2} \right) X_{BH,n} [\left(\frac{S_{O,n}}{K_{OH} + S_{O,n}} \right) \left[\left(\frac{S_{NH,n}}{K_{NA} + S_{NH,n}} \right) + \left(\frac{K_{NA}}{K_{NA} + S_{NH,n}} \right) \left(\frac{S_{NO,n}}{K_{NO} + S_{NO,n}} \right) \right] +$$
$$+ \eta_g \left(\frac{K_{OH}}{K_{OH} + S_{O,n}} \right) \left(\frac{S_{NO,n}}{K_{NO} + S_{NO,n}} \right) \left[\left(\frac{S_{NH,n}}{K_{NA} + S_{NH,n}} \right) + \left(\frac{K_{NA}}{K_{NA} + S_{NH,n}} \right) \right]] \tag{5.186}$$

$$r_{Sadsn}^{K_{SA}} = 0 \tag{5.187}$$

$$r_{Sads,n}^{K_{OA}} = K_A X_{S,n} X_{BH,n} \tag{5.188}$$

$$r_{Sads,n}^{K_A} = X_{S,n} X_{BH,n} \left(f_{MA} - S_{ads,n}/X_{BH,n} \right) \tag{5.189}$$

5.3.2.2 Sensitivity state space model

The sensitivity state space model is formed. It is based on the model of the plant extended with the model of the sensitivity functions.

The vector of the sensitivity functions consists of all sensitivity functions according to the model parameters, as follows for the *n*-th tank :

$$S_n^\theta = \begin{bmatrix} S_{NH,n}^f & S_{NO,n}^f & S_{S,n}^f & S_{ads,n}^f & S_{NH,n}^{Y_{ZH}} & S_{NO,n}^{Y_{ZH}} & S_{S,n}^{Y_{ZH}} & S_{ads,n}^{Y_{ZH}} & S_{NH,n}^{Y_{ZA}} & S_{NO,n}^{Y_{ZA}} & S_{S,n}^{Y_{ZA}} & S_{ads,n}^{Y_{ZA}} \cdots \\ S_{NH,n}^{f_{ZBH}} & S_{NO,n}^{f_{ZBH}} & S_{S,n}^{f_{ZBH}} & S_{ads,n}^{f_{ZBH}} & S_{NH,n}^{\mu_A} & S_{NO,n}^{\mu_A} & S_{S,n}^{\mu_A} & S_{ads,n}^{\mu_A} & S_{NH,n}^{\mu_H} & S_{NO,n}^{\mu_H} & S_{S,n}^{\mu_H} & S_{ads,n}^{\mu_H} \cdots \\ S_{NH,n}^{K_S} & S_{NO,n}^{K_S} & S_{S,n}^{K_S} & S_{ads,n}^{K_S} & S_{NH,n}^{K_{OH}} & S_{NO,n}^{K_{OH}} & S_{S,n}^{K_{OH}} & S_{ads,n}^{K_{OH}} & S_{NH,n}^{K_{NO}} & S_{NO,n}^{K_{NO}} & S_{S,n}^{K_{NO}} & S_{ads,n}^{K_{NO}} \cdots \\ S_{NH,n}^{K_{NA}} & S_{NO,n}^{K_{NA}} & S_{S,n}^{K_{NA}} & S_{ads,n}^{K_{NA}} & S_{NH,n}^{K_{OA}} & S_{NO,n}^{K_{OA}} & S_{S,n}^{K_{OA}} & S_{ads,n}^{K_{OA}} & S_{NH,n}^{\eta_g} & S_{NO,n}^{\eta_g} & S_{S,n}^{\eta_g} & S_{ads,n}^{\eta_g} \cdots \\ S_{NH,n}^{K_{MP}} & S_{NO,n}^{K_{MP}} & S_{S,n}^{K_{MP}} & S_{ads,n}^{K_{MP}} & S_{NH,n}^{K_{SP}} & S_{NO,n}^{K_{SP}} & S_{S,n}^{K_{SP}} & S_{ads,n}^{K_{SP}} & S_{NH,n}^{K_{SA}} & S_{NO,n}^{K_{SA}} & S_{S,n}^{K_{SA}} & S_{ads,n}^{K_{SA}} \cdots \\ S_{NH,n}^{f_{MA}} & S_{NO,n}^{f_{MA}} & S_{S,n}^{f_{MA}} & S_{ads,n}^{f_{MA}} & S_{NH,n}^{K_A} & S_{NO,n}^{K_A} & S_{S,n}^{K_A} & S_{ads,n}^{K_A} \end{bmatrix}^T \in R^{68} \tag{5.190}$$

The process state space vector for the *n*-th system is

$$X_n = \left[S_{NH,n} \; S_{NO,n} \; S_{S,n} \; S_{ads,n} \right] \in R^4 \tag{5.191}$$

The combined vector for the process variables and sensitivity functions is

$$X_n^S = \left[X_n \quad S_n^\theta \right]^T \in R^{72} \tag{5.192}$$

This vector is used to describe the model of the process variables and sensitivity functions. The matrix of the process rates derivatives towards the process variables is

$$\frac{\partial r_n}{\partial X_n} = \begin{bmatrix} r_{SNH,n}^{SNH,n} & r_{SNH,n}^{SNO,n} & r_{SNH,n}^{SS,n} & r_{SNH,n}^{Sads,n} \\ r_{SNO,n}^{SNH,n} & r_{SNO,n}^{SNO,n} & r_{SNO,n}^{SS,n} & r_{SNO,n}^{Sads,n} \\ r_{SS,n}^{SNH,n} & r_{SS,n}^{SNO,n} & r_{SS,n}^{SS,n} & r_{SS,n}^{Sads,n} \\ r_{Sads,n}^{SNH,n} & r_{Sads,n}^{SNO,n} & r_{Sads,n}^{SS,n} & r_{Sads,n}^{Sads,n} \end{bmatrix} \in R^{4x4} \tag{5.193}$$

The vector of the process rates derivatives towards the parameters can be represented in the following way

$$\frac{\partial r_n}{\partial \theta} = \begin{bmatrix} r_{NH,n}^{f} & r_{NO,n}^{f} & r_{S,n}^{f} & r_{ads,n}^{f} & r_{NH,n}^{Y_{ZH}} & r_{NO,n}^{Y_{ZH}} & r_{S,n}^{Y_{ZH}} & r_{ads,n}^{Y_{ZH}} & r_{NH,n}^{Y_{ZA}} & r_{NO,n}^{Y_{ZA}} & r_{S,n}^{Y_{ZA}} & r_{ads,n}^{Y_{ZA}} \cdots \\ r_{NH,n}^{f_{ZBH}} & r_{NO,n}^{f_{ZBH}} & r_{S,n}^{f_{ZBH}} & r_{ads,n}^{f_{ZBH}} & r_{NH,n}^{\mu_A} & r_{NO,n}^{\mu_A} & r_{S,n}^{\mu_A} & r_{ads,n}^{\mu_A} & r_{NH,n}^{\mu_H} & r_{NO,n}^{\mu_H} & r_{S,n}^{\mu_H} & r_{ads,n}^{\mu_H} \cdots \\ r_{NH,n}^{K_S} & r_{NO,n}^{K_S} & r_{S,n}^{K_S} & r_{ads,n}^{K_S} & r_{NH,n}^{K_{OH}} & r_{NO,n}^{K_{OH}} & r_{S,n}^{K_{OH}} & r_{ads,n}^{K_{OH}} & r_{NH,n}^{K_{NO}} & r_{NO,n}^{K_{NO}} & r_{S,n}^{K_{NO}} & r_{ads,n}^{K_{NO}} \cdots \\ r_{NH,n}^{K_{NA}} & r_{NO,n}^{K_{NA}} & r_{S,n}^{K_{NA}} & r_{ads,n}^{K_{NA}} & r_{NH,n}^{K_{OA}} & r_{NO,n}^{K_{OA}} & r_{S,n}^{K_{OA}} & r_{ads,n}^{K_{OA}} & r_{NH,n}^{\eta_g} & r_{NO,n}^{\eta_g} & r_{S,n}^{\eta_g} & r_{ads,n}^{\eta_g} \cdots \\ r_{NH,n}^{K_{MP}} & r_{NO,n}^{K_{MP}} & r_{S,n}^{K_{MP}} & r_{ads,n}^{K_{MP}} & r_{NH,n}^{K_{SP}} & r_{NO,n}^{K_{SP}} & r_{S,n}^{K_{SP}} & r_{ads,n}^{K_{SP}} & r_{NH,n}^{K_{SA}} & r_{NO,n}^{K_{SA}} & r_{S,n}^{K_{SA}} & r_{ads,n}^{K_{SA}} \cdots \\ r_{NH,n}^{f_{MA}} & r_{NO,n}^{f_{MA}} & r_{S,n}^{f_{MA}} & r_{ads,n}^{f_{MA}} & r_{NH,n}^{K_A} & r_{NO,n}^{K_A} & r_{S,n}^{K_A} & r_{ads,n}^{K_A} \end{bmatrix}^T \in R^{68} \tag{5.194}$$

The common process and sensitivity state space model is described for every tank separately because of the big dimension of the vector of state space and the number of tanks.

- The state space model for the first tank in discrete form is

$$X_1^S(k+1) = A_1^S(x_1, u_1, k)X_1^S(k) + C_1^{S\,T}\rho(x_1, u_1, k) + B_1^S X_{1\phi}(k) + D_1^S(x_1, u_1, k) + A_{15}^S(x_1, u_1, k)X_5^S(k) \tag{5.195}$$

where

$$A_1^S = diag\left\{A_1, A_1^\theta\left(\begin{matrix}\theta = f, Y_{ZH}, Y_{ZA}, f_{ZBH}, \mu_A, \mu_H, K_S, K_{OH}, K_{NO}, K_{NA}, \\ K_{OA}, \eta_g, K_{MP}, K_{SP}, K_{SA}, f_{MA}, K_A\end{matrix}\right)\right\},\ A_1^S \in R^{72\times 72} \tag{5.196}$$

$$A_1 = \begin{bmatrix} 1-\frac{\Delta t}{V_1}Q_1 & 0 & 0 & 0 \\ 0 & 1-\frac{\Delta t}{V_1}Q_1 & 0 & 0 \\ 0 & 0 & 1-\frac{\Delta t}{V_1}Q_1 & 0 \\ 0 & 0 & 0 & 1-\frac{\Delta t}{V_1}Q_1 \end{bmatrix} \in R^{4\times 4} \tag{5.197}$$

The matrices A_1^θ are identical for all model parameters

$$A_1^S = \begin{bmatrix} 1+\Delta t\left(-\frac{Q_1}{V_1}+r_{SNH,1}^{SNH,1}\right) & \Delta t r_{SNH,1}^{SNO,1} & \Delta t r_{SNH,1}^{SS,1} & \Delta t r_{SNH,1}^{Sads,1} \\ \Delta t r_{SNO,1}^{SNH,1} & 1+\Delta t\left(-\frac{Q_1}{V_1}+r_{SNO,1}^{SNO,1}\right) & \Delta t r_{SNO,1}^{SS,1} & \Delta t r_{SNO,1}^{Sads,1} \\ \Delta t r_{SS,1}^{SNH,1} & \Delta t r_{SS,1}^{SNO,1} & 1+\Delta t\left(-\frac{Q_1}{V_1}+r_{SS,1}^{SS,1}\right) & \Delta t r_{SS,1}^{Sads,1} \\ \Delta t r_{Sads,1}^{SNH,1} & \Delta t r_{Sads,1}^{SNO,1} & \Delta t r_{Sads,1}^{SS,1} & 1+\Delta t\left(-\frac{Q_1}{V_1}+r_{Sads,1}^{Sads,1}\right) \end{bmatrix} \in R^{4\times 4} \quad (5.198)$$

The matrix $C_1^S = [C_1 : 0_{10\times 68}] \in R^{10\times 72}$, where

$$C_1 = \Delta t * \begin{bmatrix} -f_{ZBH} & 0 & -1/Y_{ZH} & 0 \\ 0 & -f_{ZBH} & -1/Y_{ZH} & 0 \\ -f_{ZBH} & -\frac{1-Y_{ZH}}{2.86Y_{ZH}} & -1/Y_{ZH} & 0 \\ 0 & -\frac{1-Y_{ZH}}{2.86Y_{ZH}}-f_{ZBH} & -1/Y_{ZH} & 0 \\ -f_{ZBH} & 0 & 0 & -1/Y_{ZH} \\ 0 & -f_{ZBH} & 0 & -1/Y_{ZH} \\ -f_{ZBH} & -\frac{1-Y_{ZH}}{2.86Y_{ZH}} & 0 & -1/Y_{ZH} \\ 0 & -\frac{1-Y_{ZH}}{2.86Y_{ZH}}-f_{ZBH} & 0 & -1/Y_{ZH} \\ 0 & 0 & 0 & 1 \\ -\frac{1}{Y_{ZH}}-f_{ZBH} & 1/Y_{ZA} & 0 & 0 \end{bmatrix} \in R^{10\times 4} \quad (5.199)$$

The matrix

$$B_1^S = \begin{bmatrix} B_1 \\ B_1^\theta \end{bmatrix} \in R^{72\times 4} \quad B_1 \in R^{4\times 4} \quad B_1^\theta \in R^{68\times 4},\ X_{i\phi} = \left[S_{NH\phi}\ S_{NO\phi}\ S_{S\phi}\ S_{ads\phi}\right]^T\ X_{i\phi} \in R^4, S_{NO\phi} = 0,\ S_{ads\phi} = X_{S\phi}$$

$$B_1^S = \begin{bmatrix} \frac{\Delta t Q_0}{V_1} & 0 & 0 & 0 \\ 0 & 0 & 0 & 0 \\ 0 & 0 & 0 & 0 \\ 0 & 0 & 0 & 0 \\ \cdots\cdots\cdots\cdots & & & \\ 0_{68\times 4} & & & \end{bmatrix} \qquad B_1 = diag(f\ \frac{\Delta t Q_0}{V_1}\ \frac{\Delta t Q_0}{V_1}\ \frac{\Delta t Q_0}{V_1}\ \frac{\Delta t Q_0}{V_1}) \quad (5.200)$$

The vector D_1^S represents the derivatives of the process rates towards the model parameters

$$D_1^S = \left[0_{1\times 4} : \left[r_{SNH,1}^{\theta} \; r_{SNO,1}^{\theta} \; r_{SS,1}^{\theta} \; r_{ads,1}^{\theta} \right], \theta = f, Y_{ZH}, Y_{ZA}, f_{ZBH}, \mu_A, \mu_H, K_S, K_{OH}, K_{NO}, K_{NA}, K_{OA}, \eta_g, K_{MP}, K_{SP}, K_{SA}, f_{MA}, K_A \right]^T \in R^{72} \tag{5.201}$$

The matrix A_{15}^S describes the connections between the end of the fifth tank, recycle and the beginning of the first one. The vector X_5^S is formed in the same way as the vector $X_1^S : X_5^S = \left[X_5 \; S_5^{\theta} \right]^T \in R^{72}$

$$A_{15}^S = diag\left\{ A_{15}, A_{15}^{\theta} \left(\begin{matrix} \theta = f, Y_{ZH}, Y_{ZA}, f_{ZBH}, \mu_A, \mu_H, K_S, K_{OH}, \\ K_{NO}, K_{NA}, K_{OA}, \eta_g, K_{MP}, K_{SP}, K_{SA}, f_{MA}, K_A \end{matrix} \right) \right\}^T \in R^{72\times 72} \tag{5.202}$$

where

$$A_{15} = diag\left(\frac{\Delta t(Q_a + Q_r)}{V_1}, \frac{\Delta t(Q_a + Q_r)}{V_1}, \frac{\Delta t(Q_a + Q_r)}{V_1}, \frac{\Delta t(Q_a + Q_r)}{V_1} \right) \in R^{4\times 4} \quad A_{15}^{\theta} = diag\left\{ \frac{\Delta t(Q_a + Q_r)}{V_1} \right\}_{68\times 68}$$

because all sensitivity functions and process variables have the same internal recycle flows. This means that

$$A_1^S = diag\left\{ \frac{\Delta t(Q_a + Q_r)}{V_1} \right\}_{72\times 72}$$

- Derivation of the equations for the other tanks, n = 2÷5

The return flow dynamics for all other tanks are identical, that is why the models will be with the same structure, as follows

$$X_n^S(k+1) = A_n^S(x_n, u_n, k) X_n^S(k) + C_n^{S\,T} \rho(x_n, u_n, k) + D_n^S(x_n, u_n, k) + A_{n,n-1}^S(x_n, u_n, k) X_{n-1}^S(k) \tag{5.203}$$

where $A_n^S = diag\left\{ A_n, A_n^{\theta} \left(\begin{matrix} \theta = f, Y_{ZH}, Y_{ZA}, f_{ZBH}, \mu_A, \mu_H, K_S, K_{OH}, \\ K_{NO}, K_{NA}, K_{OA}, \eta_g, K_{MP}, K_{SP}, K_{SA}, f_{MA}, K_A \end{matrix} \right) \right\}^T \in R^{72\times 72}$ (5.204)

$$A_n = diag\left\{ 1 - \frac{\Delta t}{V_n} Q_n \right\}_{4\times 4}$$

$$A_n^{\theta} = \begin{bmatrix} 1 + \Delta t\left(-\frac{Q_n}{V_n} + r_{SNH,n}^{SNH,n} \right) & \Delta t r_{SNH,n}^{SNO,n} & \Delta t r_{SNH,n}^{SS,n} & \Delta t r_{SNH,n}^{Sads,n} \\ \Delta t r_{SNO,n}^{SNH,n} & 1 + \Delta t\left(-\frac{Q_n}{V_n} + r_{SNO,n}^{SNO,n} \right) & \Delta t r_{SNO,n}^{SS,n} & \Delta t r_{SNO,n}^{Sads,n} \\ \Delta t r_{SS,n}^{SNH,n} & \Delta t r_{SS,n}^{SNO,n} & 1 + \Delta t\left(-\frac{Q_n}{V_n} + r_{SS,n}^{SS,n} \right) & \Delta t r_{SS,n}^{Sads,n} \\ \Delta t r_{Sads,n}^{SNH,n} & \Delta t r_{Sads,n}^{SNO,n} & \Delta t r_{Sads,n}^{SS,n} & 1 + \Delta t\left(-\frac{Q_n}{V_n} + r_{Sads,n}^{Sads,n} \right) \end{bmatrix} \in R^{4\times 4} \tag{5.205}$$

The matrix A_n^{θ} has the same structure for all parameter θ and for all tanks $n = \overline{2,5}$.

The matrices $A^S_{n,n-1}$ are $A^S_{n,n-1} = diag\left\{ \begin{matrix} A_{n,n-1}, A^\theta_{n,n-1}, \theta = f, Y_{ZH}, Y_{ZA}, f_{ZBH}, \mu_A, \mu_H, K_S, K_{OH}, \\ K_{NO}, K_{NA}, K_{OA}, \eta_g, K_{MP}, K_{SP}, K_{SA}, f_{MA}, K_A \end{matrix} \right\}$

where $A_{n,n-1} = diag\left\{\frac{\Delta t Q_{n-1}}{V_n}\right\}_{4\times4}$ $A^\theta_{n,n-1} = diag\left\{\frac{\Delta t Q_{n-1}}{V_n}\right\}_{4\times4}$ for one parameter.

Then $A^S_{n,n-1} = diag\left\{\frac{\Delta t Q_{n-1}}{V_n}\right\}_{72\times72}$ for all parameters θ. (5.206)

The vector D^S_n is

$$D^S_n = \left[0_{1\times4} : \left[r^\theta_{SNH,n}\ r^\theta_{SNO,n}\ r^\theta_{SS,n}\ r^\theta_{ads,n} \right] \theta = f, Y_{ZH}, Y_{ZA}, f_{ZBH}, \mu_A, \mu_H, K_S, K_{OH}, K_{NO}, K_{NA}, K_{OA}, \eta_g, K_{MP}, K_{SP}, K_{SA}, f_{MA}, K_A \right]^T \in R^{72} \quad (5.207)$$

The matrices C^S_n are equal to C^S_1 with the same coefficients.

- State space process and sensitivity model of the whole process

  Combining all equations for the tanks, the full model is

$$X^S(k+1) = A^S X^S(k) + C^{S\,T} \rho\left(x^S, u, k\right) + B^S X_{i\phi}(k) + D^S\left(x^S, u, k\right), \quad X^S(0) = X^S_0 \quad (5.208)$$

where

$$A^S = \begin{bmatrix} A^S_1 & 0 & 0 & 0 & A_{15} \\ A^S_{21} & A^S_2 & 0 & 0 & 0 \\ 0 & A^S_{32} & A^S_3 & 0 & 0 \\ 0 & 0 & A^S_{43} & A^S_4 & 0 \\ 0 & 0 & 0 & A^S_{54} & A^S_5 \end{bmatrix} \in R^{360\times360} \quad (5.209)$$

The matrix C^S is $C^S = diag\left\{C^S_1, C^S_2, C^S_3, C^S_4, C^S_5\right\} \in R^{50\times360}$ (5.210)

The vector ρ is $\rho = \begin{bmatrix} \rho_{11}\ \rho_{12}\ \rho_{13}\ \rho_{14}\ \rho_{15}\ \rho_{16}\ \rho_{17}\ \rho_{18}\ \rho_{19}\ \rho_{110}\ \rho_{21}\ \rho_{22} \\ \rho_{23}\ \rho_{24}\ \rho_{25}\ \rho_{26}\ \rho_{27}\ \rho_{28}\ \rho_{29}\ \rho_{210}\ \rho_{31}\ \rho_{32}\ \rho_{33}\ \rho_{34} \\ \rho_{35}\ \rho_{36}\ \rho_{37}\ \rho_{38}\ \rho_{39}\ \rho_{310}\ \rho_{41}\ \rho_{42}\ \rho_{43}\ \rho_{44}\ \rho_{45}\ \rho_{46} \\ \rho_{47}\ \rho_{48}\ \rho_{49}\ \rho_{410}\ \rho_{51}\ \rho_{52}\ \rho_{53}\ \rho_{54}\ \rho_{55}\ \rho_{56}\ \rho_{57}\ \rho_{58} \\ \rho_{59}\ \rho_{510} \end{bmatrix} \in R^{50}$ (5.211)

The matrix B^S is $B^S = \begin{bmatrix} B^S_1 \\ \ldots\ldots \\ 0_{288\times4} \end{bmatrix} \in R^{360\times4}$ (5.212)

The vector D^S is $D^S = \left[D^S_1\ D^S_2\ D^S_3\ D^S_4\ D^S_5\right]^T \in R^{360}$ (5.213)

The full model is used for calculation of the sensitivity functions, Chapter 9.

5.4 Derivation of the sensitivity functions and reduced model for the Athlone process

5.4.1 Reduced process model based on the ASM1 biological model

The process mass balance equations for the Athlone process are given by the equations (4.34) – (4.36). The reduced model parameters are the same as for the Benchmark process model.

5.4.1.1 Sensitivity equations derivation

The sensitivity functions are derived as follows:

- For the parameter f

1) For the first tank

$$\dot{S}^f_{NH,1} = \frac{1}{V_1}\left[Q_p S^f_{NH,2} + Q_0 S_{NH\phi} - Q_1 S^f_{NH,1}\right] + r^{SNH,1}_{SNH,1} S^f_{NH,1} + r^{SNO,1}_{SNH,1} S^f_{NO,1} + r^{SS,1}_{SNH,1} S^f_{S,1} + r^f_{SNH,1} \quad (5.214)$$

$$\dot{S}^f_{NO,1} = \frac{1}{V_1}\left[Q_p S^f_{NO,2} - Q_1 S^f_{NO,1}\right] + r^{SNH,1}_{SNO,1} S^f_{NH,1} + r^{SNO,1}_{SNO,1} S^f_{NO,1} + r^{SS,1}_{SNO,1} S^f_{S,1} + r^f_{SNO,1} \quad (5.215)$$

$$\dot{S}^f_{S,1} = \frac{1}{V_1}\left[Q_p S^f_{S,2} - Q_1 S^f_{S,1}\right] + r^{SNH,1}_{SS,1} S^f_{NH,1} + r^{SNO,1}_{SS,1} S^f_{NO,1} + r^{SS,1}_{SS,1} S^f_{S,1} + r^f_{SS,1} \quad (5.216)$$

2) For the second tank

$$\dot{S}^f_{NH,2} = \frac{1}{V_2}\left[Q_1 S^f_{NH,1} + Q_a S^{f}{}_{NH,3} + Q_r S^f_{NH,3} - Q_2 S^f_{NH,2}\right] + r^{SNH,2}_{SNH,2} S^f_{NH,2} + r^{SNO,2}_{SNH,2} S^f_{NO,2} + r^{SS,2}_{SNH,2} S^f_{S,2} + r^f_{SNH,2} \quad (5.217)$$

$$\dot{S}^f_{NO,2} = \frac{1}{V_2}\left[Q_1 S^f_{NO,1} + Q_a S^{f}{}_{NO,3} + Q_r S^f_{NO,3} - Q_2 S^f_{NO,2}\right] + r^{SNH,2}_{SNO,2} S^f_{NH,2} + r^{SNO,2}_{SNO,2} S^f_{NO,2} + r^{SS,2}_{SNO,2} S^f_{S,2} + r^f_{SNO,2} \quad (5.218)$$

$$\dot{S}^f_{S,2} = \frac{1}{V_2}\left[Q_1 S^f_{S,1} + Q_a S^{f}{}_{S,3} + Q_r S^f_{S,3} - Q_2 S^f_{S,2}\right] + r^{SNH,2}_{SS,2} S^f_{NH,2} + r^{SNO,2}_{SS,2} S^f_{NO,2} + r^{SS,2}_{SS,2} S^f_{S,2} + r^f_{SS,2} \quad (5.219)$$

3) For the third tank

$$\dot{S}^f_{NH,3} = \frac{1}{V_3}\left[Q_2 S^f_{NH,2} - Q_3 S^f_{NH,3}\right] + r^{SNH,3}_{SNH,3} S^f_{NH,3} + r^{SNO,3}_{SNH,3} S^f_{NO,3} + r^{SS,3}_{SNH,3} S^f_{S,3} + r^f_{SNH,3} \quad (5.220)$$

$$\dot{S}^f_{NO,3} = \frac{1}{V_3}\left[Q_2 S^f_{NO,2} - Q_3 S^f_{NO,3}\right] + r^{SNH,3}_{SNO,3} S^f_{NH,3} + r^{SNO,3}_{SNO,3} S^f_{NO,3} + r^{SS,3}_{SNO,3} S^f_{S,3} + r^f_{SNO,3} \quad (5.221)$$

$$\dot{S}^f_{S,3} = \frac{1}{V_3}\left[Q_2 S^f_{S,2} - Q_3 S^f_{S,3}\right] + r^{SNH,3}_{SS,3} S^f_{NH,3} + r^{SNO,3}_{SS,3} S^f_{NO,3} + r^{SS,3}_{SS,3} S^f_{S,3} + r^f_{SS,3} \quad (5.222)$$

- For the parameters $\theta = Y_H, Y_A, i_{XB}, \mu_A, \mu_H, K_S, K_{OH}, K_{NO}, K_{NA}, K_{OA}, \eta_g, \eta_h, k_h, K_X$

1) For the first tank:

$$\dot{S}^\theta_{NH,1} = \frac{1}{V_1}\left[Q_p S^\theta_{Nh,2} - Q_1 S^\theta_{NH,1}\right] + r^{SNH,1}_{SNH,1} S^\theta_{NH,1} + r^{SNO,1}_{SNH,1} S^\theta_{NO,1} + r^{SS,1}_{SNH,1} S^\theta_{S,1} + r^\theta_{SNH,1} \quad (5.223)$$

$$\dot{S}^{\theta}_{NO,1} = \frac{1}{V_1}\left[Q_p S^{\theta}_{NO,2} - Q_1 S^{\theta}_{NO,1}\right] + r^{SNH,1}_{SNO,1} S^{\theta}_{NH,1} + r^{SNO,1}_{SNO,1} S^{\theta}_{NO,1} + r^{SS,1}_{SNO,1} S^{\theta}_{S,1} + r^{\theta}_{SNO,1} \tag{5.224}$$

$$\dot{S}^{\theta}_{S,1} = \frac{1}{V_1}\left[Q_p S^{\theta}_{S,2} - Q_1 S^{\theta}_{S,1}\right] + r^{SNH,1}_{SS,1} S^{\theta}_{NH,1} + r^{SNO,1}_{SS,1} S^{\theta}_{NO,1} + r^{SS,1}_{SS,1} S^{\theta}_{S,1} + r^{\theta}_{SS,1} \tag{5.225}$$

2) For the second and third tank

The sensitivity equations for the parameters θ are equivalent to the structure to these for the parameter *f*, but all derivatives are taken according to the parameters θ.

The derivatives of the process rates towards the process variables are the same as for the Benchmark model because they are based on the ASM1 biological model. The same is applied for the derivatives of the process rates towards the parameters.

5.4.1.2 State space sensitivity model

The state space sensitivity vector S^{θ}_n is given by the equation (5.189). The state process variable and sensitivity vector is $X^S_n = \left[X_n; S^{\theta}_n\right] \in R^{48}$. The matrix of the process rate derivatives towards the process variables and the vector of the process rate derivatives towards the parameters θ are the same as these for the Benchmark structure.

- The state space equation for the first tank in a discrete form is

$$X^S_1(k+1) = A^S_1\left(x^S_1, u_1, k\right)X^S_1(k) + C^{ST}_1 \rho\left(x^S_1, u_1, k\right) + B^S_1 X_{i\phi} + D^S_1\left(x^S_1, u_1, k\right) + A^S_{1,2} X^S_2 \tag{5.226}$$

where A^S_1 is determined in the same way as for the benchmark model $A^S_1 \in R^{48\times 48}$,

$$A_1 = \begin{bmatrix} 1-\frac{\Delta t}{V_1}Q_1 & 0 & 0 \\ 0 & 1-\frac{\Delta t}{V_1}Q_1 & 0 \\ 0 & 0 & 1-\frac{\Delta t}{V_1}Q_1 \end{bmatrix} \in R^{3\times 3} \tag{5.227}$$

$$A^{\theta}_1 = \begin{bmatrix} 1+\Delta t\left(-\frac{Q_1}{V_1} + r^{SNH,1}_{SNH,1}\right) & \Delta t r^{SNO,1}_{SNH,1} & \Delta t r^{SS,1}_{SNH,1} \\ \Delta t r^{SNH,1}_{SNO,1} & 1+\Delta t\left(-\frac{Q_1}{V_1} + r^{SNO,1}_{SNO,1}\right) & \Delta t r^{SS,1}_{SNO,1} \\ \Delta t r^{SNH,1}_{SS,1} & \Delta t r^{SNO,1}_{SS,1} & 1+\Delta t\left(-\frac{Q_1}{V_1} + r^{SS,1}_{SS,1}\right) \end{bmatrix} \in R^{3\times 3} \tag{5.228}$$

The matrices A_1^θ are identical for all parameters. The matrices $C_1^S \in R^{4\times 48}$, $B_1^S \in R^{48\times 3}$ and the vector $D_1^S \in R^{48}$ are the same as for the Benchmark model.

The matrix A_{12}^S describes the connections between end of the second tank and the beginning of the first one. This matrix can be expressed in the following way.

$$A_{12}^S = diag\left\{ \begin{matrix} A_{12}, A_{12}^\theta, \theta = f, Y_H, Y_A, i_{XB}, \mu_A, \mu_H, K_S, K_{OH}, K_{NO}, \\ K_{NH}, K_{OA}, \eta_g, \eta_h, k_h, K_X \end{matrix} \right\} \in R^{48\times 48} \tag{5.229}$$

where $A_{12} = \begin{bmatrix} \frac{\Delta t Q_p}{V_1} & 0 & 0 \\ 0 & \frac{\Delta t Q_p}{V_1} & 0 \\ 0 & 0 & \frac{\Delta t Q_p}{V_1} \end{bmatrix} \in R^{3\times 3}$, $A_{12}^\theta = \begin{bmatrix} \frac{\Delta t Q_p}{V_1} & 0 & 0 \\ 0 & \frac{\Delta t Q_p}{V_1} & 0 \\ 0 & 0 & \frac{\Delta t Q_p}{V_1} \end{bmatrix} \in R^{3\times 3}$

Then $A_{12}^S = diag\left\{ \frac{\Delta t Q_p}{V_1} \right\} \in R^{48\times 48}$ (5.230)

- The state space equation for the second tank is

$$X_2^S(k+1) = A_2^S\left(x_2^S, u_2, k\right) + C_2^{ST}\rho_2\left(x_2^S, u_2, k\right) + D_2^S\left(x_2^S, u_2, k\right) + A_{21}^S X_1^S(k) + A_{23}^S X_3^S(k) \tag{5.231}$$

The matrices are

$$A_2 = \begin{bmatrix} 1-\frac{\Delta t Q_2}{V_2} & 0 & 0 \\ 0 & 1-\frac{\Delta t Q_2}{V_2} & 0 \\ 0 & 0 & 1-\frac{\Delta t Q_2}{V_2} \end{bmatrix} \in R^{3\times 3} \tag{5.232}$$

$$A_2^\theta = \begin{bmatrix} 1+\Delta t\left(-\frac{Q_2}{V_2}+r_{SNH,2}^{SNH,2}\right) & \Delta t r_{SNH,2}^{SNO,2} & \Delta t r_{SNH,2}^{SS,2} \\ \Delta t r_{SNO,2}^{SNH,2} & 1+\Delta t\left(-\frac{Q_2}{V_2}+r_{SNO,2}^{SNO,2}\right) & \Delta t r_{SNO,2}^{SS,2} \\ \Delta t r_{SS,2}^{SNH,2} & \Delta t r_{SS,2}^{SNO,2} & 1+\Delta t\left(-\frac{Q_2}{V_2}+r_{SS,2}^{SS,2}\right) \end{bmatrix} \in R^{3\times 3} \tag{5.233}$$

$$A_2^S = diag\left\{A_2, A_2^\theta, \theta = f \ldots K_X\right\} \in R^{48\times 48} \tag{5.234}$$

$$A_{21} = A_{21}^\theta = \begin{bmatrix} \frac{\Delta t Q_1}{V_2} & 0 & 0 \\ 0 & \frac{\Delta t Q_1}{V_2} & 0 \\ 0 & 0 & \frac{\Delta t Q_1}{V_2} \end{bmatrix} \in R^{3\times 3} \tag{5.235}$$

$$A_{23} = A_{23}^{\theta} = \begin{bmatrix} \frac{\Delta t(Q_a + Q_r)}{V_2} & 0 & 0 \\ 0 & \frac{\Delta t(Q_a + Q_r)}{V_2} & 0 \\ 0 & 0 & \frac{\Delta t(Q_a + Q_r)}{V_2} \end{bmatrix} \in R^{3\times 3} \quad (5.236)$$

$$A_{21}^{S} = diag\{A_{21}, A_{21}^{\theta}, \theta = f \ldots K_X\} \in R^{48\times 48} \quad (5.237)$$

$$A_{23}^{S} = diag\{A_{23}, A_{23}^{\theta}, \theta = f \ldots K_X\} \in R^{48\times 48} \quad (5.238)$$

The matrix C_2^S and the vector D_2^S have the same structure as the corresponding ones for the second tank of the Benchmark process.

- The state space equation for the third tank is

$$X_3^S(k+1) = A_3^S(x_3^S, u_3, k)X_3^S(k) + C_3^{ST}\rho_3(x_3^S, u_3, k) + D_3^S(x_3^S, u_3, k) + A_{32}^S X_2^S(k) \quad (5.239)$$

where

$$A_3 = \begin{bmatrix} 1 - \frac{\Delta t Q_3}{V_3} & 0 & 0 \\ 0 & 1 - \frac{\Delta t Q_3}{V_3} & 0 \\ 0 & 0 & 1 - \frac{\Delta t Q_3}{V_3} \end{bmatrix} \in R^{3\times 3} \quad (5.240)$$

$$A_3^{\theta} = \begin{bmatrix} 1 + \Delta t\left(-\frac{Q_3}{V_3} + r_{SNH,3}^{SNH,3}\right) & \Delta t r_{SNH,3}^{SNO,3} & \Delta t r_{SNH,3}^{SS,3} \\ \Delta t r_{SNO,3}^{SNH,3} & 1 + \Delta t\left(-\frac{Q_3}{V_3} + r_{SNO,3}^{SNO,3}\right) & \Delta t r_{SNO,3}^{SS,3} \\ \Delta t r_{SS,3}^{SNH,3} & \Delta t r_{SS,3}^{SNO,3} & 1 + \Delta t\left(-\frac{Q_3}{V_3} + r_{SS,3}^{SS,3}\right) \end{bmatrix} \in R^{3\times 3} \quad (5.241)$$

$$A_3^S = diag\{A_3, A_3^{\theta}, \theta = f, \ldots, K_X\} \in R^{48\times 48} \quad (5.242)$$

$$A_{32} = A_{32}^{\theta} = \begin{bmatrix} \Delta t\frac{Q_2}{V_3} & 0 & 0 \\ 0 & \Delta t\frac{Q_2}{V_3} & 0 \\ 0 & 0 & \Delta t\frac{Q_2}{V_3} \end{bmatrix} \in R^{3\times 3} \quad (5.243)$$

$$A_{32}^S = diag\{A_{32}, A_{32}^{\theta}, \theta = f, \ldots, K_X\} \in R^{48\times 48} \quad (5.244)$$

The matrix C_3^S and the vector D_3^S have the same structure as the corresponding ones for the third tank of the Benchmark process.

- sensitivity model for the whole plant

The state space equation for the whole Athlone plant is

$$X^S(k+1) = A^S(x^S, u, k)X^S(k) + C^{S\,T}\rho(x^S, u, k) + B^S X_{i\phi} + D^S(x^S, u, k) \tag{5.245}$$

where the matrices are

$$A^S = \begin{bmatrix} A_1 & A_{12} & 0 \\ A_{21} & A_2 & A_{23} \\ 0 & A_{32} & A_3 \end{bmatrix} \in R^{144x144} \tag{5.246}$$

$$C^S = diag\{C_1^S, C_2^S, C_3^S\} \in R^{12x144} \tag{5.247}$$

$$B^S = \begin{bmatrix} B_1^S \\ B_1^\theta \\ 0_{96\times 3} \end{bmatrix} \in R^{144\times 3} \tag{5.248}$$

$$D^S = \begin{bmatrix} D_1^S \\ D_2^S \\ D_3^S \end{bmatrix} \in R^{144} \tag{5.249}$$

and the corresponding vectors are $X^S \in R^{144}, u \in R^3, \rho \in R^{12}, X_{i\phi} \in R^3$. This model is used for simulation of the sensitivity functions behaviour in Matlab.

5.4.2 Sensitivity model based on the UCT biological model

The process mass balance equations are given by the Equations (4.34) – (4.36). The reduced model parameters are the same as for the Benchmark process model with the UCT biological model. The vectors of the process state space variables, the vector of the sensitivity functions, the matrix of the process rate derivatives towards the process variables, the vector of the process rate derivatives towards the model parameters have the same structure as the one for the Benchmark process with the UCT biological model and $\theta = Y_{ZH}, Y_{ZA}, f_{ZBH}, \mu_A, \mu_H, K_S, K_{OH}, K_{NO}, K_{NA}, K_{OA}, \eta_g, K_{MP}, K_{SP}, K_{SA}, f_{MA}, K_A$.

5.4.2.1 Sensitivity equations derivation

The sensitivity equations are derived in a similar manner to the Benchmark structure way.

- for the parameter *f*

1) For the first tank

$$\dot{S}^f_{NH,1}=\frac{1}{V_1}\left[Q_p S^f_{NH,2}+Q_0 S^f_{NH,\phi}-Q_1 S^f_{NH,1}\right]+r^{SNH,1}_{SNH,1}S^f_{NH,1}+r^{SNO,1}_{SNH,1}S^f_{NO,1}+r^{SS,1}_{SNH,1}S^f_{S,1}+r^{Sads,1}_{SNH,1}S^f_{ads,1}+r^f_{SNH,1} \quad (5.250)$$

$$\dot{S}^f_{NO,1}=\frac{1}{V_1}\left[Q_p S^f_{NO,2}-Q_1 S^f_{NO,1}\right]+r^{SNH,1}_{SNO,1}S^f_{NH,1}+r^{SNO,1}_{SNO,1}S^f_{NO,1}+r^{SS,1}_{SNO,1}S^f_{S,1}+r^{S_{ads},1}_{SNO,1}\dot{S}^f_{ads,1}+r^f_{SNO,1} \quad (5.251)$$

$$\dot{S}^f_{S,1}=\frac{1}{V_1}\left[Q_p S^f_{S,2}-Q_1 S^f_{S,1}\right]+r^{SNH,1}_{SS,1}S^f_{NH,1}+r^{SNO,1}_{SS,1}S^f_{NO,1}+r^{SS,1}_{SS,1}S^f_{S,1}+r^{S_{ads},1}_{SS,1}\dot{S}^f_{ads,1}+r^f_{SS,1} \quad (5.252)$$

$$\dot{S}^f_{ads,1}=\frac{1}{V_1}\left[Q_p S^f_{ads,2}-Q_1 S^f_{ads,1}\right]+r^{SNH,1}_{ads,1}S^f_{NH,1}+r^{SNO,1}_{ads,1}S^f_{NO,1}+r^{SS,1}_{ads,1}S^f_{S,1}+r^{S_{ads},1}_{ads,1}\dot{S}^f_{ads,1}+r^f_{ads,1} \quad (5.253)$$

2) For the second tank

$$\dot{S}^f_{NH,2}=\frac{1}{V_2}\left[Q_1 S^f_{NH,1}+Q_a S^f_{NH,3}+Q_r S^f_{NH,3}-Q_2 S^f_{NH,2}\right]+r^{SNH,2}_{SNH,2}S^f_{NH,2}+r^{SNO,2}_{SNH,2}S^f_{NO,2}+r^{SS,2}_{SNH,2}S^f_{S,2}+r^{Sads,2}_{SNH,2}S^f_{ads,2}+r^f_{SNH,2} \quad (5.254)$$

$$\dot{S}^f_{NO,2}=\frac{1}{V_2}\left[Q_1 S^f_{NO,1}+Q_a S^f_{NO,3}+Q_r S^f_{NO,3}-Q_2 S^f_{NO,2}\right]+r^{SNH,2}_{SNO,2}S^f_{NH,2}+r^{SNO,2}_{SNO,2}S^f_{NO,2}+r^{SS,2}_{SNO,2}S^f_{S,2}+r^{Sads,2}_{SNO,2}\dot{S}^f_{ads,2}+r^f_{SNO,2} \quad (5.255)$$

$$\dot{S}^f_{S,2}=\frac{1}{V_2}\left[Q_1 S^f_{S,1}+Q_a S^f_{S,3}+Q_r S^f_{S,3}-Q_2 S^f_{S,2}\right]+r^{SNH,2}_{SS,2}S^f_{NH,2}+r^{SNO,2}_{SS,2}S^f_{NO,2}+r^{SS,2}_{SS,2}S^f_{S,2}+r^{Sads,2}_{SS,2}\dot{S}^f_{ads,2}+r^f_{SS,2} \quad (5.256)$$

$$\dot{S}^f_{ads,2}=\frac{1}{V_2}\left[Q_1 S^f_{ads,1}+Q_a S^f_{ads,3}+Q_r S^f_{ads,3}-Q_2 S^f_{ads,2}\right]+r^{SNH,2}_{ads,2}S^f_{NH,2}+r^{SNO,2}_{ads,2}S^f_{NO,2}+r^{SS,2}_{ads,2}S^f_{S,2}+r^{Sads,2}_{ads,2}\dot{S}^f_{ads,2}+r^f_{ads,2} \quad (5.257)$$

3) For the third tank

$$\dot{S}^f_{NH,3}=\frac{1}{V_3}\left[Q_2 S^f_{NH,2}-Q_3 S^f_{NH,3}\right]+r^{SNH,3}_{SNH,3}S^f_{NH,3}+r^{SNO,3}_{SNH,3}S^f_{NO,3}+r^{SS,3}_{SNH,3}S^f_{S,3}+r^{Sads,3}_{SNH,3}S^f_{ads,3}+r^f_{SNH,3} \quad (5.258)$$

$$\dot{S}^f_{NO,3}=\frac{1}{V_3}\left[Q_2 S^f_{NO,2}-Q_3 S^f_{NO,3}\right]+r^{SNH,3}_{SNO,3}S^f_{NH,3}+r^{SNO,3}_{SNO,3}S^f_{NO,3}+r^{SS,3}_{SNO,3}S^f_{S,3}+r^{Sads,3}_{SNO,3}\dot{S}^f_{ads,3}+r^f_{SNO,3} \quad (5.259)$$

$$\dot{S}^f_{S,3}=\frac{1}{V_3}\left[Q_2 S^f_{S,2}-Q_3 S^f_{S,3}\right]+r^{SNH,3}_{SS,3}S^f_{NH,3}+r^{SNO,3}_{SS,3}S^f_{NO,3}+r^{SS,3}_{SS,3}S^f_{S,3}+r^{Sads,3}_{SS,3}\dot{S}^f_{ads,3}+r^f_{SS,3} \quad (5.260)$$

$$\dot{S}^f_{ads,3}=\frac{1}{V_3}\left[Q_2 S^f_{ads,2}-Q_3 S^f_{ads,3}\right]+r^{SNH,3}_{ads,3}S^f_{NH,3}+r^{SNO,3}_{ads,3}S^f_{NO,1}+r^{SS,3}_{ads,3}S^f_{S,3}+r^{Sads,3}_{ads,3}\dot{S}^f_{ads,3}+r^f_{ads,3} \quad (5.261)$$

- for the parameters $\theta=Y_{ZH},Y_{ZA},f_{ZBH},\mu_A,\mu_H,K_S,K_{OH},K_{NO},K_{NA},K_{OA},\eta_g,K_{MP},K_{SP},K_{SA},f_{MA},K_A$

1) For the first tank

$$\dot{S}^\theta_{NH,1}=\frac{1}{V_1}\left[Q_p S^\theta_{NH,2}-Q_1 S^\theta_{NH,1}\right]+r^{SNH,1}_{SNH,1}S^\theta_{NH,1}+r^{SNO,1}_{SNH,1}S^\theta_{NO,1}+r^{SS,1}_{SNH,1}S^\theta_{S,1}+r^{Sads,1}_{SNH,1}S^\theta_{ads,1}+r^\theta_{SNH,1} \quad (5.262)$$

$$\dot{S}^\theta_{NO,1}=\frac{1}{V_1}\left[Q_p S^\theta_{NO,2}-Q_1 S^\theta_{NO,1}\right]+r^{SNH,1}_{SNO,1}S^\theta_{NH,1}+r^{SNO,1}_{SNO,1}S^\theta_{NO,1}+r^{SS,1}_{SNO,1}S^\theta_{S,1}+r^{Sads,1}_{SNO,1}S^\theta_{ads,1}+r^\theta_{SNO,1} \quad (5.263)$$

$$\dot{S}^{\theta}_{S,1} = \frac{1}{V_1}\left[Q_p S^{\theta}_{S,2} - Q_1 S^{\theta}_{S,1}\right] + r^{SNH,1}_{SS,1} S^{\theta}_{NH,1} + r^{SNO,1}_{SS,1} S^{\theta}_{NO,1} + r^{SS,1}_{SS,1} S^{\theta}_{S,1} + r^{Sads,1}_{SS,1} S^{\theta}_{ads,1} + r^{\theta}_{SS,1} \quad (5.264)$$

$$\dot{S}^{\theta}_{ads,1} = \frac{1}{V_1}\left[Q_p S^{\theta}_{ads,2} - Q S^{\theta}_{ads,1}\right] + r^{SNH,1}_{ads,1} S^{\theta}_{NH,1} + r^{SNO,1}_{ads,1} S^{\theta}_{NO,1} + r^{SS,1}_{ads,1} S^{\theta}_{S,1} + r^{Sads,1}_{ads,1} S^{\theta}_{ads,1} + r^{\theta}_{ads,1} \quad (5.265)$$

2) For the second and third tank

The sensitivity equations have the same structure like these for the tanks two and three according to the parameter *f*, but here the derivatives are taken according to the parameters θ.

5.4.2.2 State space sensitivity model

The state space sensitivity vector $S^{\theta}_n \in R^{68}$ is given by Equation (5.190). The state process variables and sensitivity vector is $X^S_n = \left[X_n; S^{\theta}_n\right] \in R^{72}, n = 1,2,3$. The matrix of the process rates derivatives according to the process variables $\frac{\partial r_n}{\partial x_n} \in R^{4\times 4}$ is given by the Equation (5.193). The vector of the process rates derivatives towards the model parameters. $\frac{\partial r_n}{\partial \theta} \in R^{68}$ is given by the Equation (5.194). The process and sensitivity state space model is described for every tank separately because of the big dimension of the vector of the state space.

- The state space model for the first tank in discrete form is

$$X^S_1(k+1) = A^S_1\left(x^S_1, u_1, k\right) X^S_1(k) + C^{S\,T}_1 \rho_1\left(x^S_1, u_1, k\right) + B^S_1 X_{i\phi} + D^S_1\left(x^S_1, u_1, k\right) + A^S_{1,2} X^S_2 \quad (5.266)$$

where A^S_1 is determined in the same way as for the Benchmark structure with the UCT biological model, $A^S_1 = diag\left\{A_1, A^{\theta}_1, \theta = \ldots\right\}$, $A^S_1 \in R^{72\times 72}$

$$A_1 = \begin{bmatrix} 1-\frac{\Delta t}{V_1}Q_1 & 0 & 0 & 0 \\ 0 & 1-\frac{\Delta t}{V_1}Q_1 & 0 & 0 \\ 0 & 0 & 1-\frac{\Delta t}{V_1}Q_1 & 0 \\ 0 & 0 & 0 & 1-\frac{\Delta t}{V_1}Q_1 \end{bmatrix} \in R^{4\times 4} \quad (5.267)$$

$$A_1^{\theta}=\begin{bmatrix} 1+\Delta t\left(-\frac{Q}{V_1}+r_{SNH,1}^{SNH,1}\right) & \Delta tr_{SNH,1}^{SNO,1} & \Delta tr_{SNH,1}^{SS,1} & \Delta tr_{SNH,1}^{Sads,1} \\ \Delta tr_{SNO,1}^{SNH,1} & 1+\Delta t\left(-\frac{Q}{V_1}+r_{SNO,1}^{SNO,1}\right) & \Delta tr_{SNO,1}^{SS,1} & \Delta tr_{SNO,1}^{Sads,1} \\ \Delta tr_{SS,1}^{SNH,1} & \Delta tr_{SS,1}^{SNO,1} & 1+\Delta t\left(-\frac{Q}{V_1}+r_{SS,1}^{SS,1}\right) & \Delta tr_{SS,1}^{Sads,1} \\ \Delta tr_{Sads,1}^{SNH,1} & \Delta tr_{Sads,1}^{SNO,1} & \Delta tr_{Sads,1}^{SS,1} & 1+\Delta t\left(-\frac{Q}{V_1}+r_{Sads,1}^{Sads,1}\right) \end{bmatrix}\in R^{4\times 4} \tag{5.268}$$

$\theta = f, Y_{ZB}, Y_{ZA}, \ldots$

The matrices A_1^{θ} are identical for all parameters θ.

The matrix $C_1^S = [C_1 : \theta_{10\times 68}] \in R^{10\times 72}$ is the same as for the Benchmark structure with the UCT model. It is the same for the matrix $B_1^S = \begin{bmatrix} B_1 \\ B_1^{\theta} \end{bmatrix} \in R^{72\times 4}, B_1 \in R^{4\times 4}, B_1^{\theta} \in R^{68\times 4}$ and for the vector $D_1^S \in R^{72}$. The vector $\rho_1 \in R^{10}$.

The matrix $A_{12}^S = diag\{A_{12}, A_{12}^{\theta}, \theta = f, Y_{ZH}, Y_{ZA}, \ldots, K_X\} \in R^{72\times 72}$ describes the connections between the end of the second tank and the beginning of the first tank, where

$$A_{12}=\begin{bmatrix} \frac{\Delta tQ_p}{V_1} & 0 & 0 & 0 \\ 0 & \frac{\Delta tQ_p}{V_1} & 0 & 0 \\ 0 & 0 & \frac{\Delta tQ_p}{V_1} & 0 \\ 0 & 0 & 0 & \frac{\Delta tQ_p}{V_1} \end{bmatrix} = A_{12}^{\theta} \in R^{4\times 4} \quad A_{12}^S = diag\left\{\frac{\Delta tQ_p}{V_1}\right\} \in R^{72\times 72} \tag{5.269}$$

- The state space equation for the second tank is

$$X_2^S(k+1) = A_2^S\left(x_2^S, u_2, k\right) + C_2^{ST}\rho_2\left(x_2^S, u_2, k\right) + D_2^S\left(x_2^S, u_2, k\right) + A_{2,1}^S X_1^S(k) + A_{2,3}^S X_3^S(k) \tag{5.270}$$

where the matrices are

$$A_2 = diag\left\{1-\frac{\Delta tQ_2}{V_2}\right\} \in R^{4\times 4}$$

$$A_2^{\theta}=\begin{bmatrix} 1+\Delta t\left(-\frac{Q_2}{V_2}+r_{SNH,2}^{SNH,2}\right) & \Delta tr_{SNH,2}^{SNO,2} & \Delta tr_{SNH,2}^{SS,2} & \Delta tr_{SNH,2}^{Sads,2} \\ \Delta tr_{SNO,2}^{SNH,2} & 1+\Delta t\left(-\frac{Q_2}{V_2}+r_{SNO,2}^{SNO,2}\right) & \Delta tr_{SNO,2}^{SS,2} & \Delta tr_{SNO,2}^{Sads,2} \\ \Delta tr_{SS,2}^{SNH,2} & \Delta tr_{SS,2}^{SNO,2} & 1+\Delta t\left(-\frac{Q_2}{V_2}+r_{SS,2}^{SS,2}\right) & \Delta tr_{SS,2}^{Sads,2} \\ \Delta tr_{Sads,2}^{SNH,2} & \Delta tr_{Sads,2}^{SNO,2} & \Delta tr_{Sads,2}^{SS,2} & 1+\Delta t\left(-\frac{Q_2}{V_2}+r_{Sads,2}^{Sads,2}\right) \end{bmatrix}\in R^{4\times 4} \tag{5.271}$$

$$A_{21} = diag\left\{\Delta t \frac{Q_1}{V_2}\right\} = A_{21}^{\theta} \in R^{4\times4},\ A_{21}^{S} \in R^{72} \tag{5.272}$$

$$A_{23} = A_{23}^{\theta} = diag\left\{\Delta t \frac{Q_a + Q_r}{V_2}\right\} \in R^{4\times4},\ A_{23}^{S} \in R^{72\times72} \tag{5.273}$$

The matrix C_2^S and the vector D_2^S have the same structure as the corresponding ones for the Benchmark structure with the UCT model.

- The state space equation for the third tank is

$$X_3^S(k+1) = A_3^S\left(x_3^S, u_3, k\right)X_3^S(k) + C_3^{ST}\rho_3\left(x_3^S, u_3, k\right) + D_3^S\left(x_3^S, u_3, k\right) + A_{32}^S X_2^S(k) \tag{5.274}$$

where

$$A_3 = diag\left\{1 - \frac{\Delta t Q_3}{V_3}\right\} \in R^{4\times4}$$

$$A_3^{\theta} = \begin{bmatrix} 1+\Delta t\left(-\frac{Q_3}{V_3} + r_{SNH,3}^{SNH,3}\right) & \Delta t r_{SNH,3}^{SNO,3} & \Delta t r_{SNH,3}^{SS,3} & \Delta t r_{SNH,3}^{Sads,3} \\ \Delta t r_{SNO,3}^{SNH,3} & 1+\Delta t\left(-\frac{Q_3}{V_3} + r_{SNO,3}^{SNO,3}\right) & \Delta t r_{SNO,3}^{SS,3} & \Delta t r_{SNO,3}^{Sads,3} \\ \Delta t r_{SS,3}^{SNH,3} & \Delta t r_{SS,3}^{SNO,3} & 1+\Delta t\left(-\frac{Q_3}{V_3} + r_{SS,3}^{SS,3}\right) & \Delta t r_{SS,3}^{Sads,3} \\ \Delta t r_{Sads,3}^{SNH,3} & \Delta t r_{Sads32}^{SNO,3} & \Delta t r_{Sads,3}^{SS,3} & 1+\Delta t\left(-\frac{Q_3}{V_3} + r_{Sads,3}^{Sads,3}\right) \end{bmatrix} \in R^{4\times4} \tag{5.275}$$

$$A_{32} = A_{32}^{\theta} = diag\left\{\Delta t \frac{Q_2}{V_3}\right\} \in R^{4\times4},\ A_{32}^{S} \in R^{72\times72} \tag{5.276}$$

The matrix C_3^S and the vector D_3^S have the same structure as the corresponding ones for the third tank of the Benchmark plant with the UCT biological model.

- State space process and sensitivity model of the Athlone plant

The state space equation for the whole Athlone plant is

$$X^S(k+1) = A^S\left(x^S, u, k\right)X^S(k) + C^{ST}\rho\left(x^S, u, k\right) + B^S X_{i\phi} + D^S\left(x^S, u, k\right) \tag{5.277}$$

where the matrices are

$$A^S = \begin{bmatrix} A_1 & A_{12} & 0 \\ A_{21} & A_2 & A_{23} \\ 0 & A_{32} & A_3 \end{bmatrix} \in R^{216\times216} \tag{5.278}$$

$$C^S = diag\left\{C_1^S, C_2^S, C_3^S\right\} \in R^{30\times216} \tag{5.279}$$

$$B^S = \begin{bmatrix} B_1^S \\ B_1^\theta \\ 0_{144\times4} \end{bmatrix} \in R^{216\times4} \tag{5.280}$$

$$D^S = \begin{bmatrix} D_1^S \\ D_2^S \\ D_3^S \end{bmatrix} \in R^{216} \tag{5.281}$$

and the corresponding vectors are $X^S \in R^{216}, u \in R^3, \rho \in R^{30}, X_{i\phi} \in R^4$. This model is used for simulation of the sensitivity functions behaviour in Matlab, Chapter 9.

5.5. Matlab simulation of the sensitivity models

Matlab software for simulation of the state space models of sensitivity is developed for the considered plants, Appendix C. The results are described in Chapter 9.

5.6 Conclusion

Sensitivity functions, equations and state space models are derived in the chapter for the cases of Benchmark and Athlone plants. Two biological models – ASM1 and UCT are considered for every plant. Matlab software for the sensitivity functions calculation and sensitivity models simulation is developed. The results are described and discussed.

The sensitivity study of the model inputs and parameters give answer to the question which parameters to estimate. The biological nutrient removal models may be not identifiable since there are many more parameters than there are feasible measurements. That is why if some insensitive parameters could be found the problem for parameter estimation could be simplified (Holmberg & Ranta, 1982). The sensitivity of the model dynamic set of equations is to examine the changes of the model variables towards the changes in the system parameters. Parameters with large values over the sensitivity functions have to be estimated (Sato & Ohmori, 2002)

CHAPTER SIX
PARAMETER ESTIMATION

6.1 Introduction

Parameter estimation is a common feature in many areas of process modeling, both in on-line applications such as real time optimization and in off-line applications such as the modeling of reaction kinetics and biotechnological processes (Lennox et al, 2001), (Montague, 1997), (Nomikos and MacGregor, 1994), (Luyben, 1993), (Gudi et al, 1995), (Dacosta et al, 1997), (Wang et al, 1999), (Fisher et al, 1988), (Stecha et al, 2005), (Dochain, 2003) and (Wang and Gawthrop, 2001). The aim is to determine values of model parameters that provide the best fit to measured data, generally based on some type of least squares or maximum likelihood criterion (Bjorck, 1996), (Huffel and van de Walle, 1991), (Soderstrom, 1974), (Clarke, 1967), (Geladi and Kowalski, 1986), (Hulhoven and Bogaerts). In the most general case, this requires the solution of a nonlinear and frequently nonconvex optimization problem (James et al, 2002), (Francisco et al, 2003), (Sakizlis et al, 2004), (Lakshminarayanan et al, 1996), (Valdes et al, 2003), (Wang et al, 2005), (Gawthrop and Wang, 2004), (Adby and Dempster, 1974) and (Boyd and Vandenberghe, 2002).

6.2 Assessment of the structurally identifiable parameters

A study of the structural identifiability of model parameters prior to practical parameter estimation or model calibration is very important in order to obtain reliable parameter estimates (Petersen et al., 2003). The problem for identifiability of the parameters is based on the possibility for measurement of some of the state variables and for unique calculation of the model parameters using model structure (structural identifiability) or type and quality of the available data (practical identifiability). The two types of identifiability are very different – in the study of the first one perfect noise-free data are assumed whereas in the practical one the data may be noise corrupted. As a result the parameters could be structural identifiable and practically unidentifiable.

The structural identifiability for linear system is well understood. An overview of the existing methods is given in (Godfrey & Di Stefano, 1985). Assessment of the structural identifiability for nonlinear models is more complex and only a few methods are available (Margaria et al., 2001). The approach for nonlinear models is to derive necessary and/or sufficient conditions that may allow taking conclusion for the

structural identifiability. The methods available for models with Monod kinetics are (Dochain & Vanrolleghem, 2001)

- Transformation of the nonlinear model into linear one (Godfrey & Di Stefano, 1985), (Walter, 1982), (Dochain et al., 1995), (Ljung & Glad, 1994)
- Series expansion – Taylor series and generating series (Dochain et al., 1995), (Holmberg, 1982), (Walter, 1982), (Pohjanpalo, 1978)
- Similarity transformation or local state isomorphism (Ljung & Glad, 1994), (Chappell et al., 1990), (Julien et al., 1998)
- Study of the observability properties of the nonlinear systems (Casti, 1985)

On the basis of the overview of the existing literature the following conclusion can be made (Dochain & Vanrolleghem, 2001), (Peterson et al., 2003):

- In general for both linear and nonlinear models, it could be very difficult to predict which approach is easiest to be implemented. The series expansion methods are relatively simple to be applied. In the Taylor series approach the series is generated with respect to time domain. In the generating series approach the series is generated with respect to the input domain.
- Most of the structural identifiability tests give only local structural identifiability results for nonlinear models. The results are applicable strictly only for the values for which are obtained. In order to become global, the results have to be calculated for the whole physical state space via the computation of the different terms required for the test in this space for all admissible state space values.
- The methods may give sufficient or necessary identifiability results. The Taylor series expansion gives a sufficient structural identifiability because no upper bound on the number of parameters to be considered in the test.
- The computation burden of the test for more parameters is enormous, that is why the use of symbolic software can be very helpful.

The Taylor expansion method is used in the thesis to investigate the identifiability of the reduced model.

6.2.1 Study of the identifiability of the reduced model on the basis of the Taylor series expansion

6.2.1.1 Theory and practical application

The Taylor series expansion method was developed by Pohjanpalo (1978). The basis of this method is that the output of the model (measured variable) and its derivatives with respect to time, developed around initial time, $t = 0$, can be assumed to be known

The algorithm for practical applications is:

- The model is written in a state space form

$$\dot{z}(t) = f(z,u,\theta,t),\ z(0) = z_0(\theta) \tag{6.1}$$

$$y(t,\theta) = h(z,\theta,t) \tag{6.2}$$

- The method is based on a Taylor series expansion of the observations $y(t)$ around time $t = 0$

$$y(t) = y(0) + t\frac{dy}{dt}(0) + \frac{t^2}{2!}\frac{d^2y}{dt^2}(0) + \ldots \tag{6.3}$$

and is based on looking at the successive derivatives to check if they contain information about the parameters to be identified.

- The output *y(0)* and the successive derivatives can be expressed from the model equations (6.1), (6.2) as functions of the unknown parameters θ.

$$\begin{aligned} y(0) &= H0(\theta) \\ \dot{y}(0) &= H1(\theta) \\ &\ldots\ldots\ldots\ldots \\ y^q(0) &= Hq(\theta) \end{aligned} \tag{6.4}$$

- The system of equations (6.4) is solved according to θ. The parameters θ are expressed as functions of the output, the derivatives and the input u

$$\begin{aligned} \theta_1 &= \beta_1\left(y(0), \dot{y}(0), \ldots, y^q(0), u(0)\right) \\ \theta_2 &= \beta_2\left(y(0), \dot{y}(0), \ldots, y^q(0), u(0)\right) \\ &\ldots\ldots\ldots\ldots\ldots\ldots\ldots\ldots\ldots\ldots \\ \theta_p &= \beta_p\left(y(0), \dot{y}(0), \ldots, y^q(0), u(0)\right) \end{aligned} \tag{6.5}$$

If the solution (6.5) exists, this means the parameters $\theta_i, i = \overline{1, p}$ are structurally identifiable. If the solution (6.5) can be written only for combination of the parameters θ_i, then only these combinations are identifiable.

Generally speaking the number of the successive derivatives *(q)* is not equal to the number of the unknown parameters *(p)*. The number of derivatives is at minimum equal to the number of parameters, but it may be larger in order to obtain new expressions that are independent of the preceding ones. In this way new information can be introduced for the analysis.

The parameters or parameters combinations to be identified are determined by the user. Thus the procedure is an iterative one where different parameters and combinations are analyzed.

6.2.1.2 Study of the identifiability of the reduced model for the Benchmark process

The common model developed in Chapter 3, equations (3.10)-(3.12) are considered. The reduced biological ASM1 model has 14 parameters and the biological UCT model has 16 parameters. The following approach is applied:

a) selection of the parameter is provided
b) the Taylor series expansion of the model is developed

c) the equations are solved according to the selected parameters or combination of parameters

The following measurement are supposed to be available

- the dissolved oxygen concentration at tanks 3, 4, 5
- the concentrations of the state variables are measured in the inflow, the outflows of every tank
- the values of the tank volumes and flow rates are measureable
- the initial values of the state variables are known $z(0) = z_0$

In considered case the output equation is

$$y(t) = z(t) \tag{6.6}$$

The calculation of the consecutive derivatives of the output is as follows:

$$\begin{aligned}
&\dot{y}(\theta)\big|_0 = \dot{z}(\theta)\big|_0 = A_c z(\theta)\big|_0 + C_c^T \rho(z,u,\theta)\big|_0 + B_c z_{i\phi}\big|_0 \\
&\ddot{y}(\theta)\big|_0 = \ddot{z}(\theta)\big|_0 = A_c \dot{z}(\theta)\big|_0 + C_c^T \dot{\rho}(z,u,\theta)\big|_0 \\
&\qquad = A_c^2 z(\theta)\big|_0 + A_c C_c^T \rho(z,u,\theta)\big|_0 + A_c B_c z_{i\phi}\big|_0 + C_c^T \dot{\rho}(z,u,\theta)\big|_0 \\
&\dddot{y}(\theta)\big|_0 = \dddot{z}(\theta)\big|_0 = A_c^2 \dot{z}(\theta)\big|_0 + A_c C_c^T \dot{\rho}(z,u,\theta)\big|_0 + C_c^T \ddot{\rho}(z,u,\theta)\big|_0 \\
&\qquad = A_c^3 z(\theta)\big|_0 + A_c^2 C_c^T \rho(z,u,\theta)\big|_0 + A_c^2 B_c z_{i\phi}\big|_0 + A_c C_c^T \dot{\rho}(z,u,\theta)\big|_0 + C_c^T \ddot{\rho}(z,u,\theta)\big|_0 \\
&y^4(\theta)\big|_0 = A_c^4 z(\theta)\big|_0 + A_c^3 C_c^T \rho(z,u,\theta)\big|_0 + A_c^3 B_c z_{i\phi}\big|_0 + A_c^2 C_c^T \dot{\rho}(z,u,\theta)\big|_0 + A_c C_c^T \ddot{\rho}(z,u,\theta)\big|_0 + C_c^T \dddot{\rho}(z,u,\theta)\big|_0 \\
&\cdots\cdots\cdots

because the parameters appear only in the expressions for the process rates and in the matrix C_c. At the moment $t = 0$ the left hand side of the equation (6.8) is a constant and the right hand side can be written as a linear combination according to the parameters θ as follows for the *n- th* tank

$$H1_{SNH,n} = -\theta_1\left(\frac{S_{S,n}}{K_S + S_{S,n}}\right)\left(\frac{S_{O,n}}{K_{OH} + S_{O,n}}\right)X_{BH,n} - \theta_2\left(\frac{S_{S,n}}{K_S + S_{S,n}}\right)\left(\frac{S_{NO,n}}{K_{NO} + S_{NO,n}}\right)\left(\frac{K_{OH}}{K_{OH} + S_{O,n}}\right)X_{BH,n} -$$
$$-\theta_3\left(\frac{S_{O,n}}{K_{OA} + S_{O,n}}\right)\left(\frac{S_{NH,n}}{K_{NH} + S_{NH,n}}\right)X_{BA,n} - \theta_4\left(\frac{S_{O,n}}{K_{OA} + S_{O,n}}\right)\left(\frac{S_{NH,n}}{K_{NH} + S_{NH,n}}\right)X_{BA,n}$$
$$H1_{SNO,n} = \theta_5\left(\frac{S_{S,n}}{K_S + S_{S,n}}\right)\left(\frac{K_{OH}}{K_{OH} + S_{O,n}}\right)\left(\frac{S_{NO,n}}{K_{NO} + S_{NO,n}}\right)X_{BH,n} + \theta_4\left(\frac{S_{O,n}}{K_{OA} + S_{O,n}}\right)\left(\frac{S_{NH,n}}{K_{NH} + S_{NH,n}}\right)X_{BA,n}$$
$$H1_{SS,n} = -\theta_6\left(\frac{S_{S,n}}{K_S + S_{S,n}}\right)\left(\frac{S_{O,n}}{K_{OH} + S_{O,n}}\right)X_{BH,n} - \theta_7\left(\frac{S_{S,n}}{K_S + S_{S,n}}\right)\left(\frac{S_{NO,n}}{K_{NO} + S_{NO,n}}\right)\left(\frac{K_{OH}}{K_{OH} + S_{O,n}}\right)X_{BH,n} +$$
$$+\theta_8\left(\frac{X_{S,n}/X_{BH,n}}{K_X + (X_{S,n}/X_{BH,n})}\right)\left(\frac{S_{O,n}}{K_{OH} + S_{O,n}}\right)X_{BH,n} + \theta_9\left(\frac{X_{S,n}/X_{BH,n}}{K_X + (X_{S,n}/X_{BH,n})}\right)\left(\frac{S_{NO,n}}{K_{NO} + S_{NO,n}}\right)\left(\frac{K_{OH}}{K_{OH} + S_{O,n}}\right)X_{BH,n} \tag{6.9}$$

where

$$\theta_1 = i_{xB}\mu_H, \theta_2 = i_{xB}\mu_H\eta_g, \theta_3 = i_{xB}\mu_A, \theta_4 = \mu_A/Y_A, \theta_5 = \frac{1-Y_H}{2.86Y_H}\mu_H\eta_g, \theta_6 = \mu_H/Y_H, \tag{6.10}$$
$$\theta_7 = \mu_H\eta_g/Y_H, \theta_8 = k_h, \theta_9 = k_h\eta_h$$

It is accepted that the parameters θ are constant and the same for all tanks (Cost Benchmark model). Then the vector of the parameters is $\theta = [\theta_1\ \theta_2\ \theta_3\ \theta_4\ \theta_5\ \theta_6\ \theta_7\ \theta_8\ \theta_9]^T$

For $t = 0$ the expressions after the parameters θ are constant and if it is noted

$$\left(\frac{S_{S,n}}{K_S + S_{S,n}}\right)\left(\frac{S_{O,n}}{K_{OH} + S_{O,n}}\right)X_{BH,n}\Big|_0 = p_{n1}$$
$$\left(\frac{S_{S,n}}{K_S + S_{S,n}}\right)\left(\frac{S_{NO,n}}{K_{NO} + S_{NO,n}}\right)\left(\frac{K_{OH}}{K_{OH} + S_{O,n}}\right)X_{BH,n}\Big|_0 = p_{n2}$$
that $$\left(\frac{S_{O,n}}{K_{OA} + S_{O,n}}\right)\left(\frac{S_{NH,n}}{K_{NO} + S_{NH,n}}\right)X_{BA,n}\Big|_0 = p_{n3} \tag{6.11}$$
$$\left(\frac{X_{S,n}/X_{BH,n}}{K_X + (X_{S,n}/X_{BH,n})}\right)\left(\frac{S_{O,n}}{K_{OH} + S_{O,n}}\right)X_{BH,n}\Big|_0 = p_{n4}$$
$$\left(\frac{X_{S,n}/X_{BH,n}}{K_X + (X_{S,n}/X_{BH,n})}\right)\left(\frac{S_{NO,n}}{K_{NO} + S_{NO,n}}\right)\left(\frac{K_{OH}}{K_{OH} + S_{O,n}}\right)X_{BH,n}\Big|_0 = p_{n5}$$

The equations for the expression of the first derivative $H1_n$ can be written as

$$H1_{SNH,n} = -p_{n1}\theta_1 - p_{n2}\theta_2 - p_{n3}\theta_3 - p_{n3}\theta_4$$
$$H1_{SNO,n} = -p_{n2}\theta_5 + p_{n3}\theta_4 \qquad (6.12)$$
$$H1_{SS,n} = -p_{n1}\theta_6 - p_{n2}\theta_7 + p_{n4}\theta_8 + p_{n5}\theta_9$$

$$H1_n = \begin{bmatrix} -p_{n1} & -p_{n2} & p_{n3} & p_{n3} & 0 & 0 & 0 & 0 & 0 \\ 0 & 0 & 0 & p_{n3} & -p_{n2} & 0 & 0 & 0 & 0 \\ 0 & 0 & 0 & 0 & 0 & -p_{n1} & -p_{n2} & p_{n4} & p_{n5} \end{bmatrix}.\theta \qquad (6.13)$$

$$H1_n = p_n\theta,\ p_n \in R^{3\times 9}, \theta \in R^9$$

For the whole process (5 tanks) the above dependence is

$$H1 = p\theta, p \in R^{15\times 9}, \theta \in R^9, H1 \in R^{15} \qquad (6.14)$$

The vector of parameters θ can be obtained in a unique way from the obtained dependence, which is linear according to the parameters. As a result it could be concluded that the parameters' values can be estimated from the known date for the process variables (substrates and dissolved oxygen concentrations).

The next step is to determine the growth and yield coefficients of the model on the basis of the equation (6.10) and the estimated values of θ. It is obtained

$$\eta_g = \frac{\theta_2}{\theta_1},\ Y_H = \frac{\theta_6\theta_2 - 2.86\theta_1\theta_5}{\theta_6\theta_2},\ \mu_H = \frac{\theta_6\theta_2 - 2.86\theta_1\theta_5}{\theta_2},\ i_{xB} = \frac{\theta_1\theta_2}{\theta_6\theta_2 - 2.86\theta_1\theta_5},$$
$$\mu_A = \frac{\theta_3(\theta_6\theta_2 - 2.86\theta_1\theta_5)}{\theta_1\theta_2},\ Y_A = \frac{\theta_3(\theta_6\theta_2 - 2.86\theta_1\theta_5)}{\theta_1\theta_2\theta_4},\ k_h = \theta_8, \eta_h = \frac{\theta_9}{\theta_8} \qquad (6.15)$$

The value of the estimate of θ_7 can be used for checking the calculation of the parameters.

The results (6.14), (6.15) show that the calculation of the growth and yield parameters is possible and that the reduced model is identifiable according to the parameters $\mu_H, \mu_A, k_h, \eta_g, \eta_h, Y_H, Y_A, i_{xB}$. The model is linear according to a combination of these parameters. This result is obtained on the basis of using only the first derivative of the model output according to the time. The values of this derivative can be obtained on the basis of the measured data for the considered process variables by discrete calculation of the first derivative.

The identifiability of the above parameters is obtained on the basis of calculation of the model for the whole process. This means that the number of the needed data is increased, but at the same time the number of the estimated parameters is increased and the number of the high order derivatives of the Taylor series necessary to be derived and calculated is reduced.

6.2.2 Reduced version of the vector of the parameters. Identifiability of the growth parameters for the ASM1 model

If not all parameters is necessary to be determined a reduced version of the vector of the parameters can be considered. If the yield parameters are known, then the parameters of the growth $\mu_H, \mu_A \text{ and } k_h$ could be estimated. In this case the expression for the rate of change of the corresponding concentrations in the *n-th* tank is presented as

$r_n = C_c^T \rho_n(z,u,\theta)$, *where* $\theta = [\mu_H, \mu_A, k_h]^T$.

Again the first derivative *H1* is considered, according to equation (6.8) but representation for the separate variables is different. The parameters θ are part only of the vector $\rho = [\rho_1 \ \rho_2 \ \rho_3 \ \rho_4]^T$. Then these process rates are expressed as

$$\begin{aligned}
\rho_{n1} &= \theta_1 \left(\frac{S_{S,n}}{K_S + S_{S,n}}\right)\left(\frac{S_{O,n}}{K_{OH} + S_{O,n}}\right) X_{BH,n} = p_{n1}\theta_1 \\
\rho_{n2} &= \theta_1 \left(\frac{S_{S,n}}{K_S + S_{S,n}}\right)\left(\frac{S_{NO,n}}{K_{NO} + S_{NO,n}}\right)\left(\frac{K_{OH}}{K_{OH} + S_{O,n}}\right)\eta_g X_{BH,n} = p_{n2}\theta_1 \\
\rho_{n3} &= \theta_2 \left(\frac{S_{O,n}}{K_{OA} + S_{O,n}}\right)\left(\frac{S_{NH,n}}{K_{NH} + S_{NH,n}}\right) X_{BA,n} = p_{n3}\theta_2 \\
\rho_{n4} &= \theta_3 \left(\frac{X_{S,n}/X_{BH,n}}{K_X + (X_{S,n}/X_{BH,n})}\right)\left[\left(\frac{S_{O,n}}{K_{OA} + S_{O,n}}\right) + \eta_h \left(\frac{K_{OH}}{K_{OH} + S_{O,n}}\right)\left(\frac{S_{NO,n}}{K_{NO} + S_{NO,n}}\right)\right] X_{BH,n} = (p_{n4} + \eta_h p_{n5})\theta_3
\end{aligned} \tag{6.16}$$

Then the vector ρ_n is

$$\begin{bmatrix} \rho_{n1} \\ \rho_{n2} \\ \rho_{n3} \\ \rho_{n4} \end{bmatrix} = \begin{bmatrix} p_{n1} & 0 & 0 \\ p_{n2}\eta_g & 0 & 0 \\ 0 & p_{n3} & 0 \\ 0 & 0 & p_{n4} + \eta_h p_{n5} \end{bmatrix} \begin{bmatrix} \theta_1 \\ \theta_2 \\ \theta_3 \end{bmatrix} = p_n \theta \tag{6.17}$$

and the derivatives are

$$\begin{aligned}
H1_n &= C_{c,n}^T p_n \theta, \ p_n \in R^{4x3} \\
H1 &= C_c^T p\theta, \ p = [p_1 \ p_2 \ p_3 \ p_4 \ p_5]^T \in R^{20\times 3}, \ H1 \in R^{15}
\end{aligned} \tag{6.18}$$

Again the unique solution can be found for the vector of parameters and the model is identified according to them.

6.2.3 Application to the case of the UCT reduced model. Identifiability according to the yield and growth parameters

The same considerations are done. This model has more processes that ASM1 model.

The vector of the introduced parameters is

$$\theta = [\theta_1\ \theta_2\ \theta_3\ \theta_4\ \theta_5\ \theta_6\ \theta_7\ \theta_8\ \theta_9\ \theta_{10}\ \theta_{11}\ \theta_{12}]^T \tag{6.19}$$

$$\theta_1 = f_{ZB,H}\mu_H \quad \theta_2 = f_{ZB,H}K_{MP}\ \theta_3 = f_{ZBH}K_{MP}\eta_g\ \theta_4 = \mu_A/Y_{ZA},\ \theta_5 = f_{ZB,H}\mu_A \quad \theta_6 = \frac{1-Y_{ZH}}{2.86Y_{ZH}}\mu_H$$
$$\theta_7 = \frac{1-Y_{ZH}}{2.86Y_{ZH}}\mu_H\eta_g,\ \theta_8 = \mu_H/Y_{ZH},\ \theta_9 = K_{MP}/Y_{ZH},\ \theta_{10} = K_{MP}\eta_g/Y_{ZH},\ \theta_{11} = K_A f_{MA},\ \theta_{12} = K_A \tag{6.20}$$

Then the corresponding derivatives are

$$\begin{aligned}
H1_{SNH,n} &= -\theta_1 p_{n1} - \theta_1 p_{n3} - \theta_2 p_{n5} - \theta_3 p_{n7} - \theta_4 p_{n11} - \theta_5 p_{n11} \\
H1_{SNO,n} &= -\theta_1 p_{n2} - \theta_6 p_{n3} + \theta_6 p_{n4} - \theta_1 p_{n4} - \theta_2 p_{n6} - \theta_7 p_{n7} + \theta_1 p_{n8} - \theta_8 p_{n8} + \theta_4 p_{n11} \\
H1_{SS,n} &= -\theta_8 p_{n1} - \theta_8 p_{n2} - \theta_8 p_{n3} - \theta_8 p_{n4} \\
H1_{Sads} &= -\theta_9 p_{n5} - \theta_9 p_{n6} - \theta_{10} p_{n7} - \theta_{10} p_{n8} + \theta_{11} p_{n9} - \theta_{12} p_{n10}
\end{aligned} \tag{6.21}$$

The expression for the derivatives for the *n-th* tank is

$$H1_n = \begin{bmatrix}
-(p_{n1}+p_{n3}) & -p_{n5} & -p_{n7} & -p_{n11} & -p_{n11} & 0 & 0 & 0 & 0 & 0 & 0 & 0 \\
-(p_{n2}+p_{n7}) & -p_{n6} & -p_{n8} & p_{n11} & 0 & -p_{n3}+p_{n4} & -p_{n7}+p_{n8} & 0 & 0 & 0 & 0 & 0 \\
0 & 0 & 0 & 0 & 0 & 0 & 0 & -\sum_{i=1}^{4} p_{ni} & 0 & 0 & 0 & 0 \\
0 & 0 & 0 & 0 & 0 & 0 & 0 & 0 & -\sum_{i=5}^{6} p_{ni} & -\sum_{i=7}^{8} p_{ni} & -p_{n9} & -p_{n10}
\end{bmatrix}\theta$$
$$= p_n\theta,\ H1_n \in R^4,\ p_n \in R^{4\times 12},\ \theta \in R^{12} \tag{6.22}$$

The above representation for the whole system is

$$H1 = p\theta,\ H1 \in R^{20},\ p \in R^{20\times 12} \tag{6.23}$$

The obtained expression for the first derivative shows that the vector of the parameter can be calculated according to equation (6.23). When the values of the parameters θ are calculated the values of the yield and growth parameters can be obtained using the equations (6.20) and the estimated values of the parameters θ are as follows:

$$K_A = \theta_{12},\ f_{MA} = \theta_{11}/\theta_{12},\ \eta_g = \theta_3/\theta_2,\ \mu_H = \theta_8 - 2.86\theta_6,\ f_{ZB,H} = \frac{\theta_1}{\theta_8 - 2.86\theta_6}$$
$$K_{MP} = \frac{\theta_2(\theta_8 - 2.86\theta_6)}{\theta_1},\ \mu_A = \frac{\theta_5(\theta_8 - 2.86\theta_6)}{\theta_1},\ Y_{ZA} = \frac{\theta_5(\theta_8 - 2.86\theta_6)}{\theta_1\theta_4} \tag{6.24}$$

The value of the parameter θ_7 again can be used to check the calculations. The conclusion for the UCT model is that it is identifiable according to the selected vector of parameters θ.

6.2.4 Reduced version of the vector of the parameters. Identifiability of the growth parameters

For this case the parameters are selected as $\theta = [\mu_H, K_{MP}, K_A, \mu_A] \in R$. It is supposed that the yield coefficients and the parameters η_g, f_{MA} are known. Then the process rates are represented as in the equations (6.16) where $\mu_H = \theta_1, K_{MP} = \theta_2, K_A = \theta_3, \mu_A = \theta_4$.

Then the vector ρ_n is

$$\rho_n = \begin{bmatrix} p_{n1} & 0 & 0 & 0 \\ p_{n2} & 0 & 0 & 0 \\ p_{n3} & 0 & 0 & 0 \\ p_{n4} & 0 & 0 & 0 \\ 0 & p_{n5} & 0 & 0 \\ 0 & p_{n6} & 0 & 0 \\ 0 & \eta_g p_{n7} & 0 & 0 \\ 0 & \eta_g p_{n8} & 0 & 0 \\ 0 & 0 & p_{n9} f_{MA} - p_{n10} & 0 \\ 0 & 0 & 0 & p_{n11} \end{bmatrix} \begin{bmatrix} \theta_1 \\ \theta_2 \\ \theta_3 \\ \theta_4 \end{bmatrix} = p_n \theta \qquad (6.25)$$

$\rho_n \in R^{10}, p_n \in R^{10\times 4}, \theta \in R^4$

Then the expressions for the derivatives are

$$H1_n = C_{c_n}^T p_n \theta,\ p_n \in R^{10\times 4}$$
$$H1 = C_c^T p \theta, H1 \in R^{20},\ p \in R^{50\times 4} \qquad (6.26)$$

and the θ is found by equation (6.26)

On the basis of the above derivations for the study of the identifiability of the reduced models can be concluded;

- The identifiability of the model can be calculated for the selected parameters only on the basis of the first derivative of the output of the models
- The identifiability of the mass-balance model is determined only by the identifiability of the reduced biological models
- The Taylor series method is applied to the model of the whole process which allows reducing the number of the output derivatives necessary to be derived and calculated.

Matlab software is developed for calculation of the parameters θ on the basis of the data for the output variables of the process, Appendix D. The analytical results for identifiability of the Benchmark plant with ASM1 and UCT biological models are applied further to develop procedures for calculation of parameters θ on the basis of the method of least squares, Appendix D, Chapter 9.

6.3 The problem for parameter estimation

Modelling and parameter estimation have become prerequisites for the development of the optimization and control methods (Holmberg & Ranta, 1982). Further more estimation of the non-measurable state variables is necessary for practical implementation of control and supervising systems.

6.3.1 Definitions

The problem for parameter estimation is one of the problems for system identification. The task of system identification consists of making optimal use of available information in order to find the most adequate process model. The problem for system identification consists of model structure evaluation, parameter estimation, model validation.

Parameter estimation is defined as (Dochain & vanRolleghem, 2001) "the determination of the optimum values of the parameters that arise in a mathematical description with the aid of experimental data, assuming that the structure of the process model, in other words the relationship between the variables and the parameters are explicitly known"

The structure of a typical estimation problem has the following form (Crassidis and Jenkins, 2004):.

- A dynamic system is given. Its mathematical model is hypothesized according to the experience of the scientist and according to the physical laws governing the system, number and nature of the available measurements and the needed accuracy. Usually the parameters of the constructed model are poorly known.
- The poorly known parameters have to be estimated in such a way that the mathematical model gives an optimal estimate of the real system behaviour.
- The problem for estimation is solved as an optimization problem.

Any method which solves a problem of the above structure could be considered as an estimation process. Depending on the type of the mathematical model of the physical process and on the statistical properties of the measurements errors the solution of the estimation process varies from near-trivial to impossible.

6.3.2 Preliminary steps in Parameter estimation process

6.3.2.1 Selecting data subsets for estimation and validation

The quality of the model is assessed by a validation step. For the validation model predictions are compared to a data set that is not being used for identification. The

independence of the data used for estimation and the data used for validation is fundamental for reliable validation. The separation of the data must be done in such a way that the first data set is sufficiently informative and covers a sufficiently large spectrum of experimental conditions (Using for instance optimal experiment design methodology). The remaining data must still contain sufficient data to allow for a validation that is as credible as possible.

6.3.2.2 Selection of parameters to be estimated

The selection of the parameters to be estimated is important because these parameters have to be identifiable and also they have to be capable to influence the process behaviour in a maximum way. Different methods for selection of the parameters can be used as: structural and practical identifiability analysis, sensitivity analysis and numerical properties of the estimation algorithm. The method of sensitivity functions is used in the project. The sensitivity function represents a change in the variables of the process for a change of a parameter. The large the values of the sensitivity functions, the more accurately a single parameter can be identified. In the case of several parameters, the sensitivity functions of the parameters as functions of the independent variable of the measurement (time) have to be linearly independent. Otherwise the parameters are not individually identifiable because a change in one parameter can be compensated for by changes in the other parameters.

6.3.2.3 Differentiating Linear and Nonlinear parameters

The technique used to evaluate whether a function is nonlinear in a parameter is to take the partial derivative of the function with respect to the parameter and check whether the result is still a function of that parameter. If the answer is affirmative the model is nonlinear in that parameter.

6.4 Techniques for parameter estimation

There are 4 conventional techniques for the calculation of parameter estimates:

- Bayesian estimation
- Maximum likelihood estimation
- Weighted least squares estimation
- Least squares estimation

These methods are listed in decreasing order of the amount of information that has to be provided by the user of the method. Weighted and least squares estimation are special cases of the maximum likelihood method in which the measurements are assumed to be uncorrelated and normally distributed. Bayesian estimation treats both

measurements and model parameters as random variables. Maximum likelihood estimation treats the parameters not as random variables but as constant parameters of the distributions of the measurements.

6.4.1 On-line and off-line estimation methods

When performing off-line estimation a complete set of data is available in time series form. The procedure consists of performing a simulation with constant parameter values over the whole time interval containing measurements, and locating the minimum. The estimation becomes an optimization problem. Different algorithms are available to solve this problem as Newton's method, conjugate gradient method, Levenberg-Marquardt method and many others.

The on-line methods (Kalman filter, recursive instrumental variable method) gives estimates recursively as the measurements are obtained. It is the only alternative if the identification is used for adaptive controller or if the process is time varying.

6.4.2 Objectives in parameter estimation

In order to objectify the estimation of parameters, functions are defined that represent the wish to fit a model to the date. The model parameters are then adjusted to achieve a minimum in these functions, yielding best-fit parameters. The functions are termed loss, merit, cost or objective functions. The choice of such is indeed one of the first problems to be solved when model parameters are to be estimated. The best known objective function for parameter estimation is the sum of squared errors function

$$J(\theta)=\sum_{i=1}^{N}\left[y_i-\hat{y}_i(\theta)\right]^2 \tag{6.27}$$

where y_i are the observations (in total N observations are available) and $\hat{y}_i(\theta)$ are the model predictions (output) for the given parameter set θ. The above function is called ordinary least square function. Weights can be assigned to every variable and then cost function has the form

$$J(\theta)=\sum_{i=1}^{N} w_i\left[y_i-\hat{y}_i(\theta)\right]^2 \tag{6.28}$$

where w_i are the weights.

6.4.3 Minimization approach

Finding the best parameter estimates involves minimizing the deviation of the model predictions from the data points using one of the objectives functions. Depending on whether the parameters are linear in the model or nonlinear, the solutions methods of this minimization problem are quite different. For linear parameters a one step calculation gives the best estimates whereas for nonlinear parameters the numerical methods that search the parameter space in a systematic way are used.

6.5 Basic components of the parameter estimation

6.5.1 Deterministic Models

The theory of mathematical relationships among certain quantities is often described by scientists whilst the properties of structures or the operation of processes involves the derivation of equations by the engineer (Soderstrom and Stoica, 1989), (Betancour et al, 2004), (Khalil, 2002), (Fosssard and Normand-Cyrot, 1995), (Mehra, 1979), (Chavent, 1979), (Carson et al, 1979), (Kumar and Moore, 1979) and (van den Bos, 1979). The relations which supposedly describe a certain physical situation are called a mathematical model; the model consists of one or more equations. The equations have quantities which are classified into variables and parameters. It is not clearly cut to distinction between these two and it depends on the context in which the variables appear. Normally a model is developed to describe the relationships that exist among quantities which can be measured independently in an experiment. They are called the variables of the model. For the formulation of these relationships, however, one frequently introduces inherent properties of nature or of materials and equipment used in a given experiment. They are called the parameters.

6.5.1.1 Structural Model

The models which are considered take the general function

$$\mathbf{g}(\mathbf{x},\boldsymbol{\theta}) = \mathbf{0} \tag{6.29}$$

where: $\mathbf{g} = \{g_1, g_2, ..., g_s\}^T$ (6.30)

is an *s*-dimensional vector of functions.

$$\mathbf{x} = \{x_1, x_2, ..., x_p\}^T \tag{6.31}$$

is a *p*-dimensional vectors of variables.

$$\boldsymbol{\theta} = \{\theta_1, \theta_2, ..., \theta_r\}^T \tag{6.32}$$

is an *r*-dimensional vector of parameters whose values are not precisely known.

A model whose form corresponds to the above Equation (6.29) is called a deterministic model, since all the quantities appearing in it are assumed at least in principle to be well determined. Unless the values of its parameters are known, the model can be of little practical value. There are two sets of criteria by which the values of the parameters may be established:

1. Calculate the value of a parameter by applying the established laws of nature to already known quantities.
2. The values of the model variables are measured in actual physical situations and then the parameter values which cause the model equations to be satisfied and fit to the data are calculated

6.5.1.2 Reduced Model

The above structural equations are suitable for checking the validity of the model. Should values be found for parameters such that the equations are at least approximately satisfied then the model is not rejected. The prediction is the most important practical use to which the model (6.29) could be put to. For this purpose, the variables $\boldsymbol{x}$ are classified into two groups:

1. The *l* variables $\mathbf{y} = y_1, y_2, ..., y_l$ whose values have to be predicted. These are called the dependent variables.
2. The *m* variables $\mathbf{u} = u_1, u_2, ..., u_m$ on the basis of which the prediction has to be done. They are called the independent variables (control variables).

The problem of prediction then is that of determining in advance the values that the dependent variables will take for given values of the independent variables. Rearranging the structural equations with $\boldsymbol{u}$ and $\boldsymbol{y}$ replacing $\boldsymbol{x}$

$$\mathbf{g}(\mathbf{u}, \mathbf{y}, \theta) = \mathbf{0} \tag{6.33}$$

Intuitively, the prediction is possible if all of the following conditions are met:

1. The model is reasonably correct.
2. The values of the parameters are known to a good approximation.
3. The structural equations can be solved for the dependent variables, yielding the reduced equations

$$\mathbf{y} = \mathbf{f}(\mathbf{u}, \theta) \tag{6.34}$$

where $f = f_1, f_2, ..., f_l$ is an *l*-dimensional vector of functions.

Since the number of structural equations is *l*, it is possible usually to solve for values of up to *l* dependent variables, leaving $m = s - l$ independent variables. The model (6.34) is used for simulation and control design of different processes.

A linear reduced model is one in which the functions f are linear in the θ. A linear structural model may result in a nonlinear reduced model. For example, the linear structural model $\log y + \theta x = 0$ reduces to the nonlinear model $y = e^{-\theta x}$.

6.5.2 Data-Experiments and Data Matrix

Parameter Estimation is modeled on data, and data consist of observed or measured values of the model variables. The data may be obtained by observing situations occurring in nature, or one may set up experiments which conditions are controlled so as to favor the process of observation. It is not important where and how the data were obtained but rather intrinsic measurements process affects the errors in the observations.

In most cases the data acquisition process forms a certain pattern. Implementing an experiment consists of recording the observed values of a set of variables under a given set of experimental conditions. Sometimes this means that the dependent variables are observed for given values of the independent variables. Sometimes, however, the experimental conditions themselves are not among the variables of the model.

As a matter of course for an investigation, several experiments are performed, each under a different set of experimental conditions. A variable subscripted by a character $\mu, \eta \text{ or } \phi$ denotes the value of that variable as measured in the corresponding experiment

$$\mathbf{x}_{\mu} = [x_{\mu 1}, x_{\mu 2}, ..., x_{\mu p}]^T \qquad (6.35)$$

are the values of the model variables observed in the μ th experiment. A function subscripted with one of these characters denotes that function computed for the values observed in the corresponding experiment

The large characters are used to designate the data matrix, the matrix whose μ th row consists of the data vector for the μ th experiment. Thus, $\boldsymbol{X}$ and $\boldsymbol{G}$ are the matrices

whose μ th rows are $\mathbf{x}_\mu^T$ and $\mathbf{g}_\mu^T$ respectively, e.g., where the number of experiments is N

$$\mathbf{X} \equiv \begin{bmatrix} z_{11} & z_{12} & \cdots & z_{1p} \\ \vdots & & & \\ z_{N1} & z_{N2} & \cdots & z_{Np} \end{bmatrix} \qquad \mathbf{G} \equiv \begin{bmatrix} g_{11} & g_{12} & \cdots & g_{1s} \\ \vdots & & & \\ g_{N1} & g_{N2} & \cdots & g_{Ns} \end{bmatrix} \tag{6.36}$$

6.5.3 Residuals

Two basic equations are important in the estimation process

$y_\mu = y + v$ (measured value = true value + measurement error) (6.37)

$y_\mu = \hat{y} + e$ (measured value = estimated value + residual error) (6.38)

The error $\varepsilon_{\mu a}$ could be defined as the difference between the measured and the true values of a variable. In case of a reduced model $\mathbf{y} = \mathbf{f(u,\theta)}$, if the true value $\hat{\boldsymbol{\theta}}$ of $\boldsymbol{\theta}$ is known, the error

$$\varepsilon_{\mu a} = y_{\mu a} - f_a(\mathbf{u}_\mu, \hat{\boldsymbol{\theta}}) \tag{6.39}$$

could be computed where $\mu = \overline{1,N}$ is the number of the experiments and $a = \overline{1,r}$ is the number of the variable.

These differences could be computed for any other value of $\boldsymbol{\theta}$. This defines functions

$$e_{\mu a}(\boldsymbol{\theta}) \equiv y_{\mu a} - f_a(\mathbf{u}_\mu, \boldsymbol{\theta}) \tag{6.40}$$

which are referred as the residuals. The errors are equal to the residuals evaluated with true value $\boldsymbol{\theta} = \hat{\boldsymbol{\theta}}$.

The residuals in an inexact structural model $\mathbf{g(x,\theta)} = \gamma$ are obtained simply by evaluation of the model equations

$$e_{\mu a}(\boldsymbol{\theta}) = g_a(\mathbf{x}_\mu, \boldsymbol{\theta}) \tag{6.41}$$

When the structural model is exact, the residuals are the differences between the observed and estimated values of the variables

$$e_{\mu a}(\theta) = y_{\mu a} - f_a\left(\mathbf{u}_\mu, \hat{\boldsymbol{\theta}}\right) \tag{6.42}$$

In order to have an accurate model fit, the residual errors must have an absolute mean of ≤ 0.0075 and a standard deviation of ≤ 0.125 with a big number of samples *(N)*, the sample mean value $(m)$and the sample standard deviation (σ) for the residual error can be computed using the formulas:

$$m = \frac{1}{N}\sum_{\mu=1}^{N}\left[y_{\mu_a}(t_\mu) - \hat{y}(t_\mu)\right] \tag{6.43}$$

$$\sigma^2 = \frac{1}{N-1}\sum_{\mu=1}^{N}\left\{\left[y(t_\mu) - \hat{y}(t_\mu) - m\right]\right\}^2 \tag{6.44}$$

6.6 Analysis of the conventional linear techniques for calculation of the parameter estimates

6.6.1 Maximum Likelihood (ML) Estimation

If the mathematical model of the process under consideration is adequate, it is very reasonable to assume that the measured responses from the $\mathbf{i}^{th}$ experiment are normally distributed (Young, 1979), (Chow, 1964), (Cragg, 1967) and (Carney and Goldwyn, 1967). In particular the joint probability density function conditional on the value of the parameters $(\boldsymbol{\theta}\ and\ \sum_i)$ is of the form,

$$p\left(\hat{y}_i \middle| \boldsymbol{\theta}\sum_i\right) \sim \det\left(\sum_i\right)^{-1/2} \exp\left\{-\frac{\mathbf{e}_i^T \sum_i^{-1} \mathbf{e}_i}{2}\right\} \tag{6.45}$$

where $\sum_i$ is the covariance matrix of the response variables $\boldsymbol{y}$ at the $\mathbf{i}^{th}$ experiment and hence, of the residuals $\mathbf{e}_i$ too.

If it is assumed that measurements from different experiments are independent, the joint probability density function for the all measured responses is simply the product,

$$p\left(\hat{\mathbf{y}}_1, \hat{\mathbf{y}}_2, ..., \hat{\mathbf{y}}_N \middle| \boldsymbol{\theta}, \sum_1, \sum_2, ..., \sum_N\right) \sim \det\left(\sum_1\right)^{-1/2} \det\left(\sum_2\right)^{-1/2} ...$$

$$\det\left(\sum_N\right)^{-1/2} \exp\left\{-\frac{\mathbf{e}_1^T \sum_1^{-1} \mathbf{e}_1}{2}\right\} \exp\left\{-\frac{\mathbf{e}_2^T \sum_2^{-1} \mathbf{e}_2}{2}\right\} ... \exp\left\{-\frac{\mathbf{e}_N^T \sum_1^{-1} \mathbf{e}_N}{2}\right\} \tag{6.46}$$

Grouping together the similar terms where N is the number of experiments, it can be written:

$$p\left(\hat{\mathbf{y}}_1, \hat{\mathbf{y}}_2, ..., \hat{\mathbf{y}}_N \middle| \boldsymbol{\theta}, \sum_1, \sum_2, ..., \sum_N\right) \sim \left(\prod_{i=1}^{N} \det\left(\sum_i\right)\right)^{-\frac{1}{2}} \exp\left\{-\frac{1}{2}\sum_{i=1}^{N} \mathbf{e}_i^T \sum_i^{-1} \mathbf{e}_i\right\} \tag{6.47}$$

The Loglikelihood function is the log of the joint probability density and is regarded as a function of the parameters conditional on the observed responses. Hence,

$$L\left(\boldsymbol{\theta}, \sum_1, \sum_2, ..., \sum_N \middle| \hat{\mathbf{y}}_1, \hat{\mathbf{y}}_2, ..., \hat{\mathbf{y}}_N\right) = A - \frac{1}{2}\sum_{i=1}^{N} \log\left(\det\left(\sum_i\right)\right) - \frac{1}{2}\sum_{i=1}^{N} \mathbf{e}_i^T \sum_i^{-1} \mathbf{e}_i \tag{6.48}$$

where A is a constant quantity. The maximum likelihood estimates of the unknown parameters are obtained by maximizing the Loglikelihood function.

If it is assumed that the covariance matrices $(\sum_i)$ of the measured responses (and hence of the error terms) during each experiment are known precisely. Obviously, in such a case the *ML* parameter estimates are obtained by minimizing the following objective function

$$S_{ML}(\boldsymbol{\theta}) = \sum_{i=1}^{N} \mathbf{e}_i^T \sum_i^{-1} \mathbf{e}_i = \sum_{i=1}^{N} e_i^T Q_i e_i \tag{6.49}$$

Therefore, on statistical grounds, if the error terms (e_i) are normally distributed with zero mean and with a known covariance matrix, then $\mathbf{Q}_i$ should be the inverse of this covariance matrix, i.e.,

$$\mathbf{Q}_i = [COV(e_i)]^{-1} = \sum_i^{-1} \quad ; \; i = 1,2, \ldots, N \tag{6.50}$$

where Q_i is the weighting matrix for the *i-th* experiment.

If the mathematical model of Maximum Likelihood Estimation process under consideration is adequate then the measured responses are normally distributed. The Loglikelihood function is the joint probability density and is regarded as a function of the parameters conditional on the observed responses. The covariance matrices of the measured responses and the error terms are known exactly. The *ML* estimates are obtained by minimizing the objective function. The *MLE* may be divided into three cases which all reduce to special case of Least Squares (LS).

Case I: Let the stringent assumption that the error terms in each response variable and for each experiment $(e_{ij}, i = 1,\ldots,N; j = 1,\ldots,l)$ are all identical and independently distributed (i.i.d.) normally with zero mean and variance, σ_e^2. Namely,

$$\sum_i = \sigma_e^2 \mathbf{I} \quad ; i = 1,2, \ldots, N \tag{6.51}$$

where $\boldsymbol{I}$ is the $l \times l$ identity matrix. Substitution of $\sum_i$ into Equation (6.23) yields

$$S_{ML}(\boldsymbol{\theta}) = \frac{1}{\sigma_e^2} \sum_{i=1}^{N} \mathbf{e}_i^T \mathbf{e}_i \tag{6.52}$$

Obviously minimization of $S_{ML}(\boldsymbol{\theta})$ in the above equation does not require the prior knowledge of the common factor σ_e^2. Therefore, under these conditions the *ML* estimation is equivalent to simple Least Squares (*LS*) estimation $(\mathbf{Q}_i = \mathbf{I})$.

Case II: If the more realistic assumption that the variance of a particular response variable is constant from experiment to experiment is considered and however, different response variables have different variances, i.e.,

$$\sum_i = \begin{bmatrix} \sigma_{e1}^2 & 0 & \cdots & 0 \\ 0 & \sigma_{e2}^2 & \cdots & 0 \\ \vdots & \vdots & \ddots & \vdots \\ 0 & 0 & \cdots & \sigma_{el}^2 \end{bmatrix}; \; i = 1,2, \ldots, N \tag{6.53}$$

and although the elements of the diagonal matrix $\sum_i$ given by Equation (6.53), may be not known, it is assumed that their relative value are known. Namely, it is assumed that the following ratios $(v_i, i = 1,2,\ldots,l)$ are known,

$$v_1 = \sigma_{e1}^2 / \sigma^2 \tag{6.54}$$

$$v_2 = \sigma_{e2}^2 / \sigma^2 \tag{6.55}$$

$$v_l = \sigma_{el}^2 / \sigma^2 \tag{6.56}$$

where σ^2 is an unknown scaling factor. Therefore $\sum_i$ can be written as

$$\sum_i = \sigma^2 diag(v_1, v_2, \ldots, v_l), \qquad i = 1, 2, \ldots, N \tag{6.57}$$

Upon substitution of $\sum_i$ into Equation (6.48) it becomes apparent that the ML parameter estimates are the same as the weighted *LS* estimates when the following weighting matrices are used,

$$\mathbf{Q}_i = \mathbf{Q} = diag\left(v_1^{-1}, v_2^{-1}, \ldots, v_l^{-1}\right) \tag{6.58}$$

If the variances in Equation (6.53) are totally unknown, the *ML* parameter estimates can only be obtained by the determinant criterion.

Case III: Generalized LS estimation will yield ML estimates whenever the errors are distributed with variances that change from experiment to experiment. Therefore, in this case the choice for $\mathbf{Q}_i$ should be $[COV(e_i)]^{-1}$ for $i = 1, \ldots, N$. An interesting situation

that arises often in engineering practice is when the errors are represented with a constant, yet unknown, scaling constant factor for each variable, i.e.,

$$\sigma_{eij}^2 = \sigma^2 y_{ij}^2 \quad ; i = 1, 2, ..., N \text{ and } j = 1, 2, ..., m \tag{6.59}$$

where σ^2 is an unknown scaling factor. Again, upon substitution of $\sum_i$ into Equation (6.63) it is readily seen that the *ML* parameter estimates are the same as the generalized *LS* estimates when the following weighting matrices are used,

$$\mathbf{Q}_i = diag\left(y_{i1}^{-2}, y_{i2}^{-2}, ..., y_{il}^{-2}\right); i = 1, 2, ..., N \tag{6.60}$$

The above choice has the computational disadvantage that the weights are function of the unknown parameters as shown by Englezos and Kalogerakis (2001). If the magnitude of the errors is not excessive, the measurements in the weighting matrix could be used with equally good results, namely

$$\mathbf{Q}_i = diag\left(\hat{y}_{i1}^{-2}, \hat{y}_{i2}^{-2}, ..., \hat{y}_{il}^{-2}\right); i = 1, 2, ..., N \tag{6.61}$$

6.6.2 Bayesian Estimation

The Bayesian Estimation uses the prior information which means the estimates are physically meaningful and the model equations may be degenerated relative to some of the parameters. The *MLE* may reduce to the Bayesian Estimation under the circumstance of looking for the mode of posterior distribution

In the estimation methods explained thus far no use were made of the prior information. It could be seen, the posterior **pdf** $p^*(\theta)$ is given by Bayes's theorem as

$$p^*(\theta) = cL(\theta)p_0(\theta) \tag{6.62}$$

where $L(\theta)$ is the likelihood function, and $p_0(\theta)$ the prior **pdf**, which summarizes the prior information. The estimates which make use of the prior information are usually based on the posterior distribution, and are therefore known as *Bayesian* estimates (Young, 1979).

If $p^*(\theta)$ is to be a **pdf**, then $\int p^*(\theta)d\theta = 1$, and hence c must be $1/I$, where

$$I \equiv \int L(\theta)p_0(\theta)d\theta \tag{6.63}$$

The function $p^*(\theta)$ is referred to as a proper or improper posterior distribution if the integral *I* does or does not exist, respectively. In the latter case, it is let *c=1*. The following are sufficient but by no means necessary conditions for the existence of *I*:

1. $L(\theta)$ is bounded and $p_0(\theta)$ is normal.

2. $L(\theta)$ and $p_0(\theta)$ are bounded, and $p_0(\theta)$ vanishes everywhere except in a bounded region of θ space.

To select an estimate for the parameters θ, some typical values of the posterior distribution, such as the mean, median or mode are picked. These values are referred to as location parameters of the distribution since they locate the region in θ space where most realizations of the random variable occur. Some of these location parameters exist even if the posterior distribution is improper, while others may not exist even for proper distributions. At this point it is well to summarize some of the benefits that accrue from the Bayesian estimation:

- One is sure to obtain estimates which are physically meaningful. It is guaranteed that estimates for parameters known to be positive are indeed positive.
- The model equations may be degenerated relative to some of the parameters.

6.6.2.1 Mode of the Posterior Distribution

The natural extension of the maximum likelihood method to Bayesian estimation problems consists of looking for the mode of the posterior distribution. That is, it is accepted for estimate the value of θ for which $p^*(\theta)$ is maximum. This method, to which referred as *MPD* (maximum of posterior distribution), offers the following advantages:

- The estimate coincides with the maximum likelihood estimate in case of a uniform prior distribution, since then $p^*(\theta)$ is proportional to $L(\theta)$. The estimates coincide even if $p_0(\theta)$ is uniform only within a bounded region and zero elsewhere, provided only the maximum of $L(\theta)$ occurs within this region. The practitioner who accepts the *MLE* when no prior information is given would naturally wish his estimates to be affected only when a slight amount of prior information becomes available. *MPD* satisfies this requirement.
- It is known from a theorem by von Mises (1919), that if $p_0(\theta)$ is continuous and does not vanish at the maximum of $L(\theta)$, then the *MPD* converges to the *MLE* as the number of experiments is increased indefinitely. The *MPD* shares the consistency and asymptotic efficiency of the *MLE*.
- The MPD can be obtained whether or not $p^*(\theta)$ is a proper distribution.
- It is usually much easier to compute the *MPD* than other Bayesian estimates.

In computing *MPD* estimates, two cases are distinguished:

- The prior distribution does not vanish anywhere. In this case, the maximization is of:

$$\Phi(\theta) = \log L(\theta) + \log p_0(\theta) \tag{6.64}$$

The same techniques as above are used for *MLE* can be applied here. Care must be taken, however, to retain any constants multiplying the concentrated likelihood.

$$\Phi(\boldsymbol{\theta}) = (N/2)\log\det\mathbf{M}(\boldsymbol{\theta}) - \log p_0(\boldsymbol{\theta}) \tag{6.65}$$

which is to be minimized. Note that in the presence of $\log p_0(\boldsymbol{\theta})$, the factor $N/2$ may not be dropped. In case of single equation least square with unknown σ, the term $(N/2)\log\det\mathbf{M}$ takes the form $(N/2)\log\sum_{\mu=1}^{N}\mathbf{e}_\mu^2(\boldsymbol{\theta})$.

- The prior distribution vanishes outside the region defined by a set of constraints

$$h(\theta) \geq 0 \tag{6.66}$$

6.6.3 Least Squares-Unweighted Least Squares

The technique of least squares is the oldest and most widely used estimation method (Bard, 1974),(Chavent, 1979), (Kumar and Moore, 1979) and (van den Bos, 1979). It can be applied in an ad hoc manner directly to the deterministic model, without any cognizance being taken of the probability distribution of the observations. Estimates obtained in such a way may be very satisfactory indeed, although one can think of situations in which nothing better can be done. This is certainly not true and where the observations have certain probability distributions, these estimates even possess optimal statistical properties.

In cases of pure curve fitting, where the coefficients have no physical significance, the least squares method is usually adequate.

The following notation is used: A small character denotes the vector formed by adjoining to each other the rows of the matrix dented by the same character. Thus

$$\mathbf{E}^{\mathrm{T}} \equiv [E_{11}, E_{12}, ..., E_{1l}, E_{21}, ..., E_{Nl}] \tag{6.67}$$

The least squares procedure in its simplest form consists of finding the values of $\boldsymbol{\theta}$ which minimize the function

$$\mathfrak{I}(\boldsymbol{\theta}) \equiv \mathbf{E}^{\mathrm{T}}(\boldsymbol{\theta})\mathbf{E}(\boldsymbol{\theta}) = Tr[\mathbf{E}^{\mathrm{T}}(\boldsymbol{\theta})\mathbf{E}(\boldsymbol{\theta})] \tag{6.68}$$

which is , in the component form

$$\mathfrak{I}(\boldsymbol{\theta}) = \sum_{a=1}^{l}\sum_{\mu=1}^{N} e_{\mu a}^2(\boldsymbol{\theta}) \tag{6.69}$$

i.e., the sum of the squares of the residuals is minimized. When $l = 1$, single equation least squares are obtained.

The necessary condition for optimality of the function (6.69) is:

$$\partial\mathfrak{I}/\partial\boldsymbol{\theta} = 2\sum_{a=1}^{l}\sum_{\mu=1}^{N} e_{\mu a}\,\partial e_{\mu a}/\partial\boldsymbol{\theta} = \mathbf{0} \tag{6.70}$$

In the most common case of a single reduced equation, $e_\mu = y_\mu - f(\mathbf{u}_\mu, \boldsymbol{\theta})$, then:

$$\Im(\boldsymbol{\theta}) = \sum_{\mu=1}^{N} \left[y_\mu - f(\mathbf{u}_\mu, \boldsymbol{\theta}) \right]^2 \tag{6.71}$$

$$\partial \Im / \partial \theta_\alpha = -2 \sum_{\mu=1}^{N} e_\mu \, \partial f(\mathbf{u}_\mu, \boldsymbol{\theta}) / \partial \theta_\alpha \qquad (\alpha = 1, 2, ..., r) \tag{6.72}$$

Weighted least squares can improve the estimates if some knowledge of the relative accuracy of the measurements is known and can also be used to impose constraints in the estimation process.

6.6.4 Derivation of the Principle of Least-Squares

The least-squares technique is a mathematical procedure by which the unknown parameters of a mathematical model are chosen such that the sum of the squares of some chosen error (Ikonem and Najim, 2002), (Zhu, 2001) is minimized. Suppose a mathematical model is given in the form

$$y(t) = u_1(t)\theta_1 + u_2(t)\theta_2 + ... + u_r(t)\theta_r \tag{6.73}$$

where $y(t)$ is the observed variable, $\{\theta_1, \theta_2, ..., \theta_r\}$ is a set of constant parameters, $u_1(t), u_2(t), ..., u_r(t)$ are known functions that may depend on other known variables.

Assume that N samples of measurements of $y(t)$ and $u_1(t), u_2(t), ..., u_r(t)$ are made at time *1, 2, ..., N*. Filling the data samples into equation (6.73) results in a set of linear equations.

$$y(t) = u_1(t)\theta_1 + u_2(t)\theta_2 + ... + u_r(t)\theta_r \qquad t = 1, 2, ..., N \tag{6.74}$$

This can be arranged in a simple matrix form

$$\mathbf{y} = \Phi\theta \tag{6.75}$$

where

$$\mathbf{y} = \begin{bmatrix} y(1) \\ y(2) \\ \vdots \\ y(N) \end{bmatrix}, \quad \Phi = \begin{bmatrix} u_1(1) & u_2(1) & \cdots & u_r(1) \\ u_1(2) & u_2(2) & & u_r(2) \\ \vdots & \vdots & \ddots & \vdots \\ u_1(N) & u_2(N) & \cdots & u_r(N) \end{bmatrix}, \quad \theta = \begin{bmatrix} \theta_1 \\ \theta_2 \\ \vdots \\ \theta_r \end{bmatrix} \quad v = \begin{bmatrix} v(1) \\ v(2) \\ \vdots \\ v(N) \end{bmatrix} \tag{6.76}$$

A necessary condition that this set of equations has a solution is $N \geq r$. For $N = r$, an unique solution exists:

$$\hat{\theta} = \Phi^{-1}\mathbf{y} \tag{6.77}$$

provided Φ^{-1}, the inverse of the square matrix Φ, exists. $\hat{\theta}$ denotes the estimate of θ. This is well known. However, when N > r, it is generally not possible to find a $\hat{\theta}$ vector which can fit the data samples exactly, because the data may be contaminated by disturbances and measurement noise. A too low model order or wrong model structure are other possible causes of misfit. A way to determine the parameters is to estimate them on the basis of least-squares-error.

To achieve this introduce a residual (error), $e(t)$, and let

$$e(t) = y(t) - \hat{y}(t) = y(t) - \Phi(t)\theta \tag{6.78}$$

Now $\hat{\theta}$ is choosen such that the criterion (loss function)

$$V_{LS} = \frac{1}{N}\sum_{t=1}^{N} e(t)^2 = \frac{1}{N}\sum_{t=1}^{N} | y(t) - \Phi(t)\theta |\, e^2 = \frac{1}{N} e^T e \tag{6.79}$$

is minimized. Here

$$e = [e(1) \quad e(2) \quad \cdots \quad e(N)]^t \tag{6.80}$$

To carry out the minimization, the equation (6.78) is expressed as

$$V_{LS}(\theta) = \frac{1}{N}(\mathbf{y} - \Phi\theta)^T(\mathbf{y} - \Phi\theta) = \frac{1}{N}[\mathbf{y}^T\mathbf{y} - \theta^T\Phi^T\mathbf{y} - \mathbf{y}^T\Phi\theta + \theta^T\Phi^T\Phi\theta] \tag{6.81}$$

Taking the first derivative of $V_{LS}(\theta)$ with respect to θ and equating the result to zero, it is obtained

$$\frac{\partial V_{LS}(\theta)}{\partial\theta}|_{\theta=\hat{\theta}} = \frac{1}{N}[-2\Phi^T\mathbf{y} + 2\Phi^T\Phi\hat{\theta}] = 0 \tag{6.82}$$

Hence the solution is given by the equation

$$\Phi^T\Phi\theta = \Phi^T\mathbf{y} \tag{6.83}$$

or

$$\hat{\theta} = [\Phi^T\Phi]^{-1}\Phi^T\mathbf{y} \tag{6.84}$$

6.6.5 Weighted Least Squares

An objective function consisting of a simple sum of squares is often unsatisfactory for the following reasons:

- The various quantities $y_{\mu a}(or\ g_{\mu a})$ may represent entities having different physical dimensions, or measured on different scales.
- Some observations may be known to be less reliable than others, and it would make sure that the obtained parameter estimates will be less influenced by those than by the

more accurate ones. It should be remembered that one cannot always escape the statistical structure of the data.

The solution to both of these problems is one and the same; assign a non-negative weight factor in the criterion function.

$$\Im = (1/2)e^T we \tag{6.85}$$

where $w \in R^{e \times l}$ is the symmetric weighting matrix.

Then the optimal value of the parameter vector is

$$\hat{\theta} = \left(\Phi^T w \Phi\right)^{-1} \Phi^T wy \tag{6.86}$$

6.6.6 Constrained Least Squares

Minimization of the weighted least square criterion (6.79),(6.85) is used when some of the measurements agreed more closely with the model than others. For perfect measurements the corresponding diagonal element of the weight matrix should be infinity (∞), which could be presented by sufficiently large number. The case of perfect measurement could be represented by introducing an equity constraint in the estimation process (Junkins, 1969). The considered measurements are

$$\begin{bmatrix} \tilde{y}_1 \\ \cdots \\ \tilde{y}_2 \end{bmatrix} = \begin{bmatrix} \varphi_1 \\ \cdots \\ \varphi_2 \end{bmatrix} \hat{\theta} + \begin{bmatrix} e_1 \\ \cdots \\ 0 \end{bmatrix} \tag{6.87}$$

where $\tilde{y}_1 \in R^{l_1}, \varphi_1 \in R^{l_1 \times r}, e_1 \in R^{l_1}, \tilde{y}_2 \in R^{l_2}, \varphi_2 \in R^{l_2 \times r}$ *and* $l_1 \geq r, m_2 \leq r$. The absence of the residual error e_2 reflects the fact that $\varphi_2 \theta$ is required to equals $\tilde{y}_2$ exactly. Then the problem for parameter estimation can be formulated as a constrained optimization problem.

$$\Im = 1/2 e_1 w_1 e_1 = 1/2 \left(\tilde{y}_1 - \varphi_1 \hat{\theta}\right) w_1 \left(\tilde{y}_1 - H_1 \hat{\theta}\right) \tag{6.88}$$

Subject to the equity constraint

$$\tilde{y}_2 - \varphi_2 \hat{\theta} = 0 \tag{6.89}$$

The problem could be solved using the Lagrange multiplier method

$$L = \Im + \lambda^T \left(\tilde{y}_2 - \varphi_2 \hat{\theta}\right), \quad \lambda = \left[\lambda_1 \ \lambda_2 \ \ldots \ \lambda_{l_2}\right]^T \in R^{l_2}$$

λ is a vector of the Lagrange multipliers. The necessary conditions for optimality are

$$\frac{\partial L}{\partial \theta} = -\varphi_1^T w_1 \tilde{y}_1 + \left(\varphi_1^T w_1 \varphi_1\right) \hat{\theta} - \varphi_2^T \lambda = 0 \tag{6.90}$$

$$\frac{\partial L}{\partial \lambda} = \tilde{y}_2 - \varphi_2 \hat{\theta} = 0 \quad \rightarrow \quad \tilde{y}_2 = \varphi_2 \hat{\theta} \tag{6.91}$$

Solution of the problem (6.90), (6.91) is

$$\hat{\theta} = \bar{\theta} + K\left(\tilde{y}_2 - \varphi_2 \bar{\theta}\right) \tag{6.92}$$

where $K = \left(\varphi_1^T w_1 \varphi_1\right)^{-1} \varphi_2^T \left[\varphi_2 \left(H_1^T w_1 H_1\right)^{-1} H_2^T\right]^{-1}$ (6.93)

$$\bar{\theta} = \left(\varphi_1^T w_1 \varphi_1\right)^{-1} \varphi_1 w_1 \tilde{y}_1 \tag{6.94}$$

$\bar{\theta}$ in equation (6.94) is the least square estimate of θ in absence of the constraint equation. The second term in equation (6.92) is an additive correction in which an optimal gain matrix K multiplies the constraint residual $\left(\tilde{y}_2 - \varphi_2 \bar{x}\right)$ before the correction.

6.6.7 Nonlinear Process Identification

Nonlinear system identification is more challenging and it has received less attention compared to linear system identification. From a control point of view, being able to identify nonlinear models will extend the working range of model based controllers.

There are several approaches to nonlinear system identification:

- methods of the differential correction
- methods of theoretically sound nonlinear functions

6.6.7.1 Methods of the least square correction

The method is a generalization of Newton's root solving method for finding θ values satisfying $y - f(\theta) = 0$. The convergence of the method is guaranteed only under strict requirements on the functions (*f*) and their first two partial derivatives as well as on the closeness of the starting estimates.

The problem is formulated in the following way: find the estimate $\hat{\theta}$ that minimizes

$$\Im = (1/2) e^T w e = (1/2)\left[\hat{y} - f\left(\hat{\theta}\right)\right]^T w\left[\tilde{y} - f\left(\hat{\theta}\right)\right] \tag{6.95}$$

And satisfies the model

$$\tilde{y} = f\left(\hat{\theta}\right) + e \tag{6.96}$$

In most practical problems $\Im$ cannot be directly minimized by applying the ordinary calculus because $\hat{\theta}$ cannot be expressed analytically. Because of this a successive approximation procedure is used based on approximate starting value

$$\theta_e = [\theta_{1e} \ \theta_{2e} \ \dots \ \theta_{re}]^T \tag{6.97}$$

Then the parameter estimates are

$$\hat{\theta} = \theta_e + \Delta\theta \tag{6.98}$$

where $\Delta\theta$ is a correction vector. If the components of $\Delta\theta$ are sufficiently small the function $f(\hat{\theta})$ could be linearized about θ_e using a first order Taylor series expansion

$$f(\hat{\theta}) = f(\theta_e) + H\frac{\partial f}{\partial\theta}\bigg|_{\theta_e} \tag{6.99}$$

where H is the Jacobian matrix. The measurement residual after the correction can be linearly approximated as

$$\Delta y = \hat{y} - f(\hat{\theta}) \approx \tilde{y} - f(\theta_e) - H\Delta\theta = \Delta y_e - H\Delta\theta \tag{6.100}$$

where the residual before the correction is

$$\Delta y_e = \tilde{y} - f(\theta_e) \tag{6.101}$$

The determination of the optimal $\Delta\theta$ is based on the minimization of the criterion

$$\Im = (1/2)\Delta y^T w \Delta y \approx \Im_p = 1/2(\Delta y_e - H\Delta\theta)^T w(\Delta y_e - H\Delta\theta) \tag{6.102}$$

Minimization of (6.102) is equivalent to the minimization of (6.95) and the solution is

$$\Delta\theta = (H^T wH)^{-1} H^T w \Delta y_e \tag{6.103}$$

The calculation process is iterative. It will stop if a condition for accuracy is satisfied, as

$$\partial\Im = \frac{|\Im_i - \Im_{i-1}|}{\Im_i} < \frac{\varepsilon}{\|\omega\|}$$

where ε is a prescribed small value. Convergence difficulties can be caused by:

- the initial estimate is too far from the minimizing $\hat{\theta}$
- numerical difficulties in solving for the corrections $\Delta\theta$

6.6.7.2 Methods of theoretically sound nonlinear functions

One way is to use theoretically sound nonlinear functions (Zhu, 2001) and to develop identification schemes for these models. Identification using Volterra series, neural networks and nonlinear ARMAX models belong to this methodology. The advantage of this approach is the ability to obtain a global model of the underlying system. The main difficulty of the approach is the high cost in identification tests and computation. Another approach is to combine linear dynamic models with static or memoryless nonlinear functions. This type of models is called block-oriented nonlinear models. There are several advantages when using block-oriented models:

- low cost in identification tests;
- low cost in identification and control computations and
- it is easy to comprehend and to incorporate a *priori* process knowledge.

The shortcoming of block-oriented models is the lack of global description of the system. The third approach is to construct global models by combining several local models which is called operating regime based identification or multiple model approach. The local models can be linear models or simple nonlinear models. The motivation of the operating regime based identification is to obtain the advantages of both first and second approaches.

Three types of block-oriented nonlinear models are mostly used: Hammerstein model, Wiener model and combined Hammerstein-Wiener model.

6.6.7.2.1 Model Parametrization and Problem Statement of Hammerstein Model

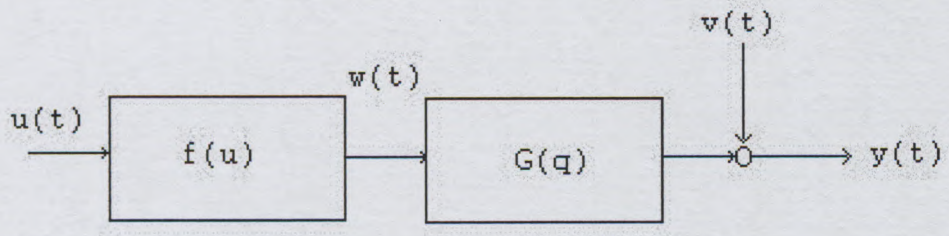

Figure 6.1: Hammerstein model

A nonlinear Hammerstein model in discrete-time is given in Figure 6.1. The input *u(t)* is first scaled by the static nonlinear function *f(u)* and then passes the linear time-invariant transfer function *G(q)*. It is assumed that

1) the nonlinear function *f(u)* is continuous;
2) the linear block *G(q)* is stable and
3) the process output is disturbed by a stationary stochastic process*{v(t)}*.

$$f[u(t)] = \beta_1 u(t) + \beta_2 u^2(t) + \ldots + \beta_m u^m(t) \tag{6.104}$$

$$G(q) = \frac{b_0 + b_1 q^{-1} + \ldots + b_n q^{-l}}{1 + a_1 q^{-1} + \ldots + a_n q^{-l}} = \frac{B(q)}{A(q)} \tag{6.105}$$

$$v(t) = H(q)e(t) = \frac{1 + c_1 q^{-1} + \ldots + c_n q^{-l}}{1 + d_1 q^{-1} + \ldots + d_n q^{-l}} e(t) = \frac{C(q)}{D(q)} e(t) \tag{6.106}$$

Denote the parameter vector as

$$\theta = [\beta_1, \beta_2, ..., \beta_m, a_1, ..., a_l, b_0, b_1, ..., b_l, c_1, ..., c_n, d_1, ..., d_l]^T \quad (6.107)$$

Assuming that $\beta_1 \neq 0$, then without loss of generality it can be set $\beta_1 = 1$.

With these notations the process model can be written in more compact form as

$$y(t) = \frac{B(q)}{A(q)} \sum_{k=1}^{m} \beta_k u^k(t) + \frac{C(q)}{D(q)} e(t) \quad (6.108)$$

It is known that polynomials have several drawbacks. They do not extrapolate well; high degree polynomials have oscillatory behaviour and parameter estimation is often numerically ill-conditioned. The problems with polynomials do not occur with linear splines, but linear splines are not smooth meaning that their derivatives are not continuous at their break points or knots. To overcome this last problem, the cubic splines could be used to model the nonlinear block.

Let K denotes a set of knots $\{u_1, u_2, ..., u_m\}$ which are real numbers and satisfies

$$u_1 = u_{\min} < u_2 < u_3 < ... < u_m = u_{\max} \quad (6.109)$$

A cubic spline function defined for all real numbers u is given as

$$w(u) = \sum_{k=2}^{m-1} \beta_k \mid u - u_k \mid^3 + \beta_m + \beta_{m+1} u + \beta_{m+2} u^2 + \beta_{m+3} u^3 \quad (6.110)$$

where $[\beta_2, \beta_3, ..., \beta_{m+3}]$ are fixed real numbers, namely, the parameters to be estimated. Here m is called the number of knots which can be seen as the "degree" or "order" of the cubic splines. Now, identification problem for the model (6.108) can be stated as follows:

1) **Test design.** Design an identification test using excitation signals so that the parameters of model are identifiable. If possible, the test should be designed so that the identified model is most suitable for model application. Denote the collected input-output data as $\{u(1), y(1), u(2), y(2), ..., u(N), y(N)\}$, where N is the number of samples.

2) **Parameter estimation.** Determine the parameters of model (6.108) using the test data by minimizing the loss function

$$V_{PE} = \sum_{t=1}^{N} e^2(t) \quad (6.111)$$

where

$$e(t) = H^{-1}(q)\{y(t) - G(q) f[u(t)]\} = \frac{D(q)}{C(q)} [y(t) - \frac{B(q)}{A(q)} \sum_{k=1}^{m} \beta_k u^k(t)] \quad (6.112)$$

3) **Order Selection.** Determine the orders l and m so that the obtained model is the most accurate for control.

4) **Model validation.** Verify if the identified model is suitable for its application, namely, control. If not, provide a remedy that should include redesigning the identification test.

The identification of the Wiener Model and the NLN Hammerstein-Wiener Model follows a similar mathematical modelling and analysis with variations as proposed by the Hammerstein model.

6.7. Estimation of the growth parameters of the wastewater treatment process

The estimation of the growth parameters is mainly done by fitting of the model of the process to the measured values of biomass and substrate.

6.7.1. Estimation of the kinetic parameters through biological tests

Another way of determination of the kinetic parameters $Y, K_d, \mu_{\max}, K_S$, a nitrification and denitrification rate is by biological test methods (Pala &Bolukbas, 2005). The experiment data is used to best fit the substrate and biomass concentration whose behaviour later is used to calculate the kinetic parameters.

Laboratory procedures for parameter estimation of the ASM No. 1 are presented in (Ekama et al., 1984, 1986). However this approach requires several time and resource consuming laboratory experiments which are rarely performed by design engineers and process operators. Furthermore, the calculated parameters continuously will be changed because of changing process load and environmental conditions which makes the extensive laboratory experiments unpractical.

6.7.2. Parameter estimation with the aid of sensitivity functions

Manual fitting with the aid of the sensitivity functions is described in (Holmberg & Ranta, 1982). This method according to the authors is the most suitable because of the small amount of available data, big deviations between measurements and the aim to retain the physical meaning of the parameters. The values of the parameters are adjusted by studying the sensitivity function in the intervals where the model fit should be improved and by altering the parameter to which the system is most sensitive. It was established that the parameters μ_m and K_S are strongly interdependent and they cannot be separated. The sensitivity according to Y parameters is the greatest at steady-state.

The application of the sensitivity analysis in order to determine the key parameters of the Activated Sludge Model No. 1 is done in (Salo & Ohmori, 2002). An identification algorithm is developed further based on the results obtained from the sensitivity analysis for the linear representation of the oxygen transfer coefficient. The considered model has two inputs, 6 state space and output variables with 18 growth and oxygen transfer parameters that need to be identified. Sensitivity model of the process is developed and the sensitivity functions of the state variables towards the parameters are calculated. It is established that the parameter $\mu_H, \mu_A, Y_H, Y_A, b_H, K_a, i_{xB}$ *and* $S_{O,Sat}$ have high sensitivity for at least one water component. These are parameters that are identified. It is supposed that the components of the state vector are measurable. A procedure for identification of the parameters μ_H, b_H is developed. The ASM 1 mass balance equation for the heterotroph biomass is rewritten as a function of the unknown parameters as a regression model. The parameters are estimated using recursive least square algorithm.

6.7.3. Modelling using automatic estimation methods

Pohjanpalo (1978) developed a test for a global system identifiability based on power series expansion. A test provided by Holmberg and Ranta (1982) showed that if the transient behaviour of the biomass and substrate are completely known all the parameters (including μ_m and K_S can be uniquely determined. This implies that the model is theoretically globally identifiable. The practical identifiability which is more important because of the incomplete measurements, cannot be studied with this test.

Estimation of the growth parameters by minimizing the sum of squares error index using gradient method was done in (Holmberg & Ranta, 1982). The algorithm converges to the real value of Y while the estimates of K_S and μ_m are very sensitive to the initial values. Unique solution for these parameters could not be obtained by this method. If noise data from measurement is introduced, the results show that the estimations is very sensitive to measurement noise.

The practical nonidentifiability does not mean that models using Michaelis-Menten kinetics could not be used. They are used very often nevertheless that the parameter set is not unique. This means that different sets of value fit the data with the same error. Because of these properties the Michaelis-Menten model should be regarded as

a black-box than as a physical model. Another property of this model is that for measurements of the substrate $S \langle\langle K_S$ the model reduces to a linear form $\mu = \mu_m / K_S \bullet S$. In this case the estimation of K_S and μ_m is not unique. This situation is typical for the activated sludge process. As a result the obtained parameters should not be considered as biological characteristics of the processes nor should they be used for comparing the influences of changes in environmental conditions.

6.8. Approach for linear batch parameter estimation of growth kinetics of the microorganisms in wastewater treatment

A major problem in identification is how to parameterize the characteristics and properties of a process using a model with suitable structure. Linear models provide a good starting point in the selection of the structure for parameter estimation. The wastewater process model is a nonlinear one, but according to some of its parameters it can be considered as a linear one.

Linear regression models are considered

$$y(k) = \varphi(k)\theta + v(k) \tag{6.113}$$

where the model is linear according to the parameters θ. The model functions $\varphi(k)$ can be linear or nonlinear functions of input and output signals. If the statistical characteristics of the disturbance term $v(k)$ are not known, it could be accepted that

$$\hat{y}(k) = \varphi(k)\theta \tag{6.114}$$

is a natural prediction of what $y(k)$ will be. The expression (6.114) becomes a prediction in an exact statistical (means square) sense if $\{v(k)\}$is a sequence of independent random variables, independent also of the observation functions φ, with zero mean and finite variance.

The method of the linear batch parameter estimation is considered for the reduced benchmark and Athlone processes incorporating ASM1 and UCT biological models. The common mass balance equation describing these processes is

$$z(k+1) = Az(k) + C^T \rho(z,u,k) + Bz_{i\phi}(k) \tag{6.115}$$

where the dimension of the vectors and matrices is different, determined according to the process and to the used biological model. The kinetic parameters are components of the mathematical expressions for the process rates $r(z,u,k) = C^T \rho(z,u,k)$. The model (6.115) has parameters describing the mass balance expressions and the

biological model kinetics. The parameters describing the mass balance of the tanks are accepted to be constant. Such are the tank volumes, flow rates. The parameters used in the biological models are three types

- parameters in the matrix C describing the yield of the heterotrophs and autotrophs are accepted to be constant and known. These are :
  - for the ASM1 model: i_{xB}, Y_H, Y_A
  - for the UCT model : $f_{ZB,H}, Y_{ZH}, Y_{ZA}$
- the parameters of the switching functions are accepted to be constant and known:
  - for ASM1 these are $K_S, K_{NH}, K_{OA}, K_{OH}, K_{NO}, K_X, \eta_g, \eta_h$
  - for UCT model these are $K_S, K_{OA}, K_{HA}, K_{OH}, K_{NO}, K_{SP}$
- parameter of the growth rates are considered as time variable and unknown. These are
  - for the ASM1 model these are μ_A, μ_H, k_h
  - for the UCT model these are $\mu_A, \mu_H, K_{MP}, K_A$

The growth rate parameters are determined in this chapter through least square estimation techniques.

6.8.1 Estimation of the growth parameters of the Benchmark process

6.8.1.1 Application of the ASM1 biological model

6.8.1.1.1 Transformation of the state space model (6.115) to the form of (6.113)

The model (6.115) has to be transformed in a form of model (6.113) – linear according to the parameters μ_A, μ_H, k_h. Following the process rate expressions from the Table 4.1 every of the growth rates is represented as a product between the unknown parameter and the rest of the process rates in the following way:

$$\rho_{n,1} = p_{n,1}(z_n, u_n, k)\theta_1 \tag{6.116}$$

$$\rho_{n,2} = p_{n,2}(z_n, u_n, k)\theta_1 \tag{6.117}$$

$$\rho_{n,3} = p_{n,3}(z_n, u_n, k)\theta_2 \tag{6.118}$$

$$\rho_{n,4} = p_{n,4}(z_n, u_n, k)\theta_3 \tag{6.119}$$

Where n is the number of the tank, $n = \overline{1.5}$, $\theta_1(k) = \mu_H(k), \theta_2(k) = \mu_A(k), \theta_3(k) = k_h(k)$ and the expressions for the $\rho_{n,i}(z_n, u_n, k), i = \overline{1.4}$ are as follows

$$p_{n,1}(z_n, u_n, k) = \left(\frac{S_{S,n}}{K_S + S_{S,n}}\right)\left(\frac{S_{O,n}}{K_{OH} + S_{O,n}}\right)X_{BH,n} \tag{6.120}$$

$$p_{n,2}(z_n, u_n, k) = \left(\frac{S_{S,n}}{K_S + S_{S,n}}\right)\left(\frac{K_{OH}}{K_{OH} + S_{O,n}}\right)\left(\frac{S_{NO,n}}{K_{NO} + S_{NO,n}}\right)\eta_g X_{BH,n} \tag{6.121}$$

$$p_{n,3}(z_n,u_n,k)=\left(\frac{S_{NH,n}}{K_{NH}+S_{NH,n}}\right)\left(\frac{S_{O,n}}{K_{OA}+S_{O,n}}\right)X_{BA,n} \tag{6.122}$$

$$p_{n,4}(z_n,u_n,k)=\left(\frac{X_{S,n}/X_{BH,n}}{K_X+X_{S,n}/X_{BH,n}}\right)X_{BH,n}\left[\left(\frac{S_{O,n}}{K_{OH}+S_{O,n}}\right)+\eta_h\left(\frac{K_{OH}}{K_{OH}+S_{O,n}}\right)\left(\frac{S_{NO,n}}{K_{NO}+S_{NO,n}}\right)\right] \tag{6.123}$$

Then the expression for the biological rates is

$$r_n(z_n,u_n,k)=C_n^T p_n(k)\theta(k),\ n=\overline{1,5},\ k=\overline{0,N} \tag{6.124}$$

$$r(z,u,k)=C^T p(k)\theta(k) \tag{6.125}$$

where the vector of the parameters is $\theta=[\theta_1\ \theta_2\ \theta_3]^T$ and the matrix $p(k)$is

$$p(k)=\begin{bmatrix}p_1(k)\\p_2(k)\\p_3(k)\\p_4(k)\\p_5(k)\end{bmatrix}\in R^{20\times 3} \tag{6.126a}$$

and $$p_n(k)=\begin{bmatrix}p_{n,1}(k) & 0 & 0\\ p_{n,2}(k) & 0 & 0\\ 0 & p_{n,3}(k) & 0\\ 0 & 0 & p_{n,4}(k)\end{bmatrix}\in R^{4\times 3},\ n=\overline{1,5} \tag{6.126b}$$

Then the model equation (6.115) can be written in the following way

$$\begin{aligned}&z(k+1)-Az(k)-Bz_{i\phi}(k)=y(k)=C^T p(k)\theta(k)=\varphi(k)\theta(k)\\ &y(k)=z(k+1)-Az(k)-Bz_{i\phi}(k),\quad y\in R^{15}\\ &\varphi(k)=C^T p(k),\qquad\qquad \varphi\in R^{15\times 3}\end{aligned} \tag{6.127}$$

The model (6.127) is used to estimate the values of the parameters θ.

This model could be written in a matrix form paying attention to the measurements of the input and output variables for a given period of time. If the number of measurements are N, then it can be written for every moment

$$\begin{aligned}&y(1)=\varphi(1)\theta(1)\\ &y(2)=\varphi(2)\theta(2)\\ &\cdots\cdots\cdots\cdots\\ &y(N)=\varphi(N)\theta(N)\end{aligned} \tag{6.128}$$

The system of equations (6.128) can be written by one vector/matrix equation, if a new output vector is introduced

$$y=\begin{bmatrix} y(1) \\ y(2) \\ \cdots \\ y(N) \end{bmatrix} \in R^{15*N}, \quad \theta=\begin{bmatrix} \theta(1) \\ \theta(2) \\ \cdots \\ \theta(N) \end{bmatrix} \in R^{3*N} \tag{6.129}$$

$$y=\Phi\theta, \quad \Phi \in R^{(15*N)\times 3*N}$$

In model (6.129) the vector y is formed by measurements of the state and input disturbances and the matrix Φ is formed as a nonlinear matrix function of the state and control variables.

6.8.1.1.2Formulation and solution of the problem for linear batch least squares estimation

The goal of the parameter estimation is to obtain an estimate of the model parameters such that the sum of the squared residuals is minimized

$$\Im(\theta,k)=\sum_{k=1}^{N}\left\|y(k)-\hat{y}(\theta)\right\|^{2}_{w(k)} \rightarrow \min \tag{6.130}$$

$$\hat{y}(\theta,k)=\varphi(k)\hat{\theta}(k) \tag{6.131}$$

where $\varphi(k)\in R^{15\times 15}$ is the symmetrical positive definite matrix.

The quadratic cost function expresses the weighted squared errors between the N observed outputs $y(k)$ and their predictions $\varphi(k)\hat{\theta}$ provided by the model. The scalar coefficients in the matrices w give the weighting of different observation functions. The quadratic function of the criterion allows single optimum solution as it has the shape of a parabola. The linear model (6.127) and the quadratic criterion allow an analytical solution to be obtained.

The solution of the problem (6.130), (6.131) is standard one. Equation (6.131) is substituted in Equation (6.130).

$$\Im(\theta,k)=\sum_{k=1}^{N}\left\|y(k)-\varphi(k)\hat{\theta}(k)\right\|^{2}_{w(k)} \rightarrow \min \tag{6.132}$$

The necessary condition for optimality of (6.132) according to the parameter vector is

$$\begin{aligned}\frac{\partial\Im}{\partial\hat{\theta}}&=\sum_{k=1}^{N}w(k)\left[y(k)-\varphi(k)\hat{\theta}(k)\right]\left[-\varphi(k)\right]+\left[\left[y(k)-\varphi(k)\hat{\theta}(k)\right]w(k)\right]^{T}\left[-\varphi(k)\right]= \\ &=\sum_{k=1}^{N}\varphi^{T}(k)\left[y(k)-\varphi(k)\hat{\theta}(k)\right]^{T}w(k)+\varphi^{T}(k)\left[y(k)-\varphi(k)\hat{\theta}(k)\right]w(k)= \\ &=-2\sum_{k=1}^{N}\varphi^{T}(k)w(k)\left[y(k)-\varphi(k)\hat{\theta}(k)\right]=0\end{aligned} \tag{6.133}$$

Equation (6.133) can be written in the following way:

$$-\varphi^T(k)w(k)y(k)+\varphi^T(k)\omega(k)\varphi(k)\hat{\theta}(k)=0, k=\overline{1,N} \tag{6.134}$$

The sufficient condition for minimization of (6.132) is the positive definiteness of the second derivative of the criterion function towards the vector of the parameters

$$\frac{\partial^2\Im(\theta)}{\partial\theta^2}=\sum_{k=1}^{N}\varphi^T(k)\omega(k)\varphi(k) \tag{6.135}$$

The requirement is the matrix $\frac{\partial^2\Im(\theta)}{\partial\theta^2}$ to be positive definite for all values of $\varphi(k)$ not equal to zero. As the matrices $w(k)$ are selected to be positive definite, the second derivative will be positive definite if the $\varphi(k)=C^T p(k)$ are not zero.

The optimal estimate of the vector of the parameters $\hat{\theta}$ is obtained from the equation (6.134), under the assumption that the second derivative is positive definite, then its inverse exists and

$$\hat{\theta}(k)=\left[\varphi^T(k)w(k)\varphi(k)\right]^{-1}\varphi^T(k)w(k)y(k),\ k=\overline{1,N} \tag{6.136}$$

Often it is more convenient to calculate the least squares estimate from the compact matrix form (6.129). In this case the cost function is

$$\Im(\theta)=(y-\Phi\theta)^T w(y-\Phi\theta)$$

$$w=\begin{bmatrix}\omega(1) & 0 & \cdots & 0\\ 0 & \omega(2) & \cdots & \cdots\\ \cdots & \cdots & \cdots & \cdots\\ 0 & 0 & \cdots & \omega(N)\end{bmatrix}\in R^{(15*N)\times(15*N)} \tag{6.137}$$

The optimal estimate then is given by the solution

$$\hat{\theta}=\left[\Phi^T w\Phi\right]^{-1}\Phi^T y \tag{6.138}$$

where $\frac{\partial^2\Im}{\partial\theta^2}=\Phi^T w\Phi$ must be positive definite

The optimal estimates (6.136) and (6.138) can be obtained using the model vectors and matrices as follows

$$\hat{\theta}(k)=\left[\left[C^T p(k)\right]^T w(k)C^T p(k)\right]^{-1}\left[C^T p(k)\right]^T w(k)\left[z(k+1)-Az(k)-Bz_{i\phi}(k)\right],\ k=\overline{1,N} \tag{6.139}$$

$$\hat{\theta}=\left[\begin{bmatrix} C^T p(1) \\ C^T p(2) \\ \cdots\cdots \\ C^T p(N) \end{bmatrix}^T w \begin{bmatrix} C^T p(1) \\ C^T p(2) \\ \cdots\cdots \\ C^T p(N) \end{bmatrix}\right]^{-1} \begin{bmatrix} C^T p(1) \\ C^T p(2) \\ \cdots\cdots \\ C^T p(N) \end{bmatrix}^T w \begin{bmatrix} z(2)-Az(1)-Bz_{i\phi}(1) \\ z(3)-Az(2)-Bz_{i\phi}(2) \\ \cdots\cdots\cdots\cdots \\ z(N+1)-Az(N)-Bz_{i\phi}(N) \end{bmatrix} \tag{6.140}$$

6.8.1.1.3 Algorithm and a MATLAB program

The steps of the algorithm are:

- Input all known coefficients of the model and state and control measurements $z(k),\ k=\overline{1,N+1},\ u(k),\ k=\overline{1,N}$
- Calculate the vector $y(k)=z(k+1)-Az(k)-Bz_{i\phi}(k),\ k=\overline{1,N}$
- Form the vector y
- Calculate the matrices p and Φ
- Calculate $\hat{\theta}$ from equation (6.140)
  A program is written in MATLAB for batch calculation of the parameter estimates following the applied algorithm, Appendix D.

6.8.1.2 Application for the UCT biological model

6.8.1.2.1 Transformation of the state space model (6.115) to the form of the model (6.113)

The parameters that have to be estimated are $\mu_H, \mu_A, K_{MP}, K_A$

The process rate expressions from the Table 4.3 are represented as a product of the parameters and the part of the process rate in the following way (for the *n*-th tank)

$$\begin{aligned}
&\rho_{n,1}(k)=p_{n,1}(z_n,u_n,k)\theta_1(k),\ \rho_{n,2}(k)=p_{n,2}(z_n,u_n,k)\theta_1(k),\ \rho_{n,3}(k)=p_{n,3}(z_n,u_n,k)\theta_1(k),\\
&\rho_{n,4}(k)=p_{n,4}(z_n,u_n,k)\theta_1(k),\ \rho_{n,5}(k)=p_{n,5}(z_n,u_n,k)\theta_2(k),\ \rho_{n,6}(k)=p_{n,6}(z_n,u_n,k)\theta_2(k)\\
&\rho_{n,7}(k)=p_{n,7}(z_n,u_n,k)\theta_2(k),\ \rho_{n,8}(k)=p_{n,8}(z_n,u_n,k)\theta_2(k),\ \rho_{n,9}(k)=p_{n,9}(z_n,u_n,k)\theta_3(k),\\
&\rho_{n,10}(k)=p_{n,10}(z_n,u_n,k)\theta_4(k)
\end{aligned} \tag{6.141}$$

where n is the number of the tank, $n=\overline{1,5}$, $\theta_1=\mu_H$, $\theta_2=K_{MP}$, $\theta_3=\mu_A$ *and* $\theta_4=\mu_A$ and the expressions for the $p_{n,i}(z_{n,i},u_{n,i},k),\ i=\overline{1,10}$ are as follows

$$\begin{aligned}
p_{n,1} &= \left(\frac{S_{S,n}}{K_S+S_{S,n}}\right)\left(\frac{S_{O,n}}{K_{OH}+S_{O,n}}\right)\left(\frac{S_{NH,n}}{K_{HA}+S_{NH,n}}\right)X_{BH,n}\\
p_{n,2} &= \left(\frac{S_{S,n}}{K_S+S_{S,n}}\right)\left(\frac{S_{O,n}}{K_{OH}+S_{O,n}}\right)\left(\frac{K_{HA}}{K_{HA}+S_{NH,n}}\right)\left(\frac{S_{NO,n}}{K_{NO}+S_{NO,n}}\right)X_{BH,n}\\
p_{n,3} &= \left(\frac{S_{S,n}}{K_S+S_{S,n}}\right)\left(\frac{K_{OH}}{K_{OH}+S_{O,n}}\right)\left(\frac{S_{NH,n}}{K_{HA}+S_{NH,n}}\right)\left(\frac{S_{NO,n}}{K_{NO}+S_{NO,n}}\right)X_{BH,n}\\
p_{n,4} &= \left(\frac{S_{S,n}}{K_S+S_{S,n}}\right)\left(\frac{K_{OH}}{K_{OH}+S_{O,n}}\right)\left(\frac{K_{HA}}{K_{HA}+S_{NH,n}}\right)\left(\frac{S_{NO,n}}{K_{NO}+S_{NO,n}}\right)X_{BH,n}\\
p_{n,5} &= \left(\frac{S_{ads,n}/X_{BH,n}}{K_{SP}+S_{ads,n}/X_{BH,n}}\right)\left(\frac{S_{O,n}}{K_{OH}+S_{O,n}}\right)\left(\frac{S_{NH,n}}{K_{HA}+S_{NH,n}}\right)X_{BH,n}
\end{aligned} \tag{6.142a}$$

$$
\begin{aligned}
p_{n,6} &= \left(\frac{S_{ads,n}/X_{BH,n}}{K_{SP}+S_{ads,n}/X_{BH,n}}\right)\left(\frac{S_{O,n}}{K_{OH}+S_{O,n}}\right)\left(\frac{K_{HA}}{K_{HA}+S_{NH,n}}\right)\left(\frac{S_{NO,n}}{K_{NO}+S_{NO,n}}\right)X_{BH,n}\\
p_{n,7} &= \left(\frac{S_{ads,n}/X_{BH,n}}{K_{SP}+S_{ads,n}/X_{BH,n}}\right)\left(\frac{K_{OH}}{K_{OH}+S_{O,n}}\right)\left(\frac{S_{NH,n}}{K_{HA}+S_{NH,n}}\right)\left(\frac{S_{NO,n}}{K_{NO}+S_{NO,n}}\right)\eta_g X_{BH,n}\\
p_{n,8} &= \left(\frac{S_{ads,n}/X_{BH,n}}{K_{SP}+S_{ads,n}/X_{BH,n}}\right)\left(\frac{K_{OH}}{K_{OH}+S_{O,n}}\right)\left(\frac{K_{HA}}{K_{HA}+S_{NH,n}}\right)\left(\frac{S_{NO,n}}{K_{NO}+S_{NO,n}}\right)\eta_g X_{BH,n}\\
p_{n,9} &= X_{S,n}X_{BH,n}\left(f_{MA}-S_{ads,n}/X_{BH,n}\right)\\
p_{n,10} &= \left(\frac{S_{O,n}}{K_{OA}+S_{O,n}}\right)\left(\frac{S_{NH,n}}{K_{HA}+S_{NH,n}}\right)X_{BA,n}
\end{aligned}
\qquad (6.142b)
$$

The expression for the biological rates is

$$
\begin{aligned}
&r_n(z_n,u_n,k)=C^T p_n(k)\theta(k),\ n=\overline{1,5},\ k=\overline{0,N}\\
&r(z,u,k)=C^T p\theta
\end{aligned}
\qquad (6.143)
$$

where the vector of the parameters is $\theta=[\theta_1\ \theta_2\ \theta_3\ \theta_4]^T$

$$
p(k)=\begin{bmatrix} p_1(k)\\ p_2(k)\\ p_3(k)\\ p_4(k)\\ p_5(k)\end{bmatrix}\in R^{50\times 4}\quad p_n(k)=\begin{bmatrix} p_{n,1} & 0 & 0 & 0\\ p_{n,2} & 0 & 0 & 0\\ p_{n,3} & 0 & 0 & 0\\ p_{n,4} & 0 & 0 & 0\\ 0 & p_{n,5} & 0 & 0\\ 0 & p_{n,6} & 0 & 0\\ 0 & p_{n,7} & 0 & 0\\ 0 & p_{n,8} & 0 & 0\\ 0 & 0 & p_{n,9} & 0\\ 0 & 0 & 0 & p_{n,10}\end{bmatrix}\in R^{10\times 4} \qquad (6.144)
$$

The model for estimation of the parameters is presented in the same way as equation (6.127) where $y\in R^{15}$ *and* $\varphi\in R^{20\times 4}, C_n\in R^{10\times 4}$ *and* $C\in R^{50\times 20}, \varphi=C^T p\in R^{20\times 4}$

The derivation of the optimal estimate vector θ is the same as in the case of the ASM1 model and has the form of equations (6.136) and (6.138), or equations (6.139) and (6.140). The algorithm and the MATLAB program are with the same structure, but with different dimensions and matrix p, Appendix D.

6.8.2 Estimation of the growth parameters of the Athlone process

6.8.2.1 Application of the ASM1 biological model

The equation of the model is the same but the number of tanks is different $n=\overline{1,3}$.

Then the dimension of the vector and matrices is as follows: $z \in R^9, C_n \in R^{4\times3}, C \in R^{12\times9}, \rho \in R^{12}, \theta \in R^3, p_n \in R^{4\times3}, p \in R^{12\times3}$.

6.8.2.2 Application of the UCT biological model

The dimensions and vector and matrices are $z \in R^{10}, C_n \in R^{10\times4}, C \in R^{30\times12}, \rho \in R^{30}$

$\theta \in R^4, p_n \in R^{10\times4}, p \in R^{30\times4}$.

The algorithm and the MATLAB programs have the same structure as for the Benchmark process, but the dimensions and the structure of the model vectors and matrices are different, Appendix D.

6.8.3 Properties of the least square estimator for the parameters $\hat{\theta}$

6.8.3.1 Mean value of the least squares estimator

The vector of the estimated parameter $\hat{\theta}$ is a random one as the measurements are disturbed. If the mathematical expectation of the parameter estimation is equal to the true parameter θ, the estimator is unbiased. This is the case when the noise $v = \left[v^T(1), v^T(2), ..., v^T(N)\right]^T \in R^{nl*N}$, where nl is the dimension of the state space has zero mean, and the noise and data matrix φ are statistically independent.

The estimation error is $\tilde{\theta} = \theta - \hat{\theta}$ (6.145)

The mathematical expectation of the estimation error $\tilde{\theta}$ is

$$E(\tilde{\theta}) = E\left\{\theta - \left[\Phi^T w \Phi\right]^{-1} \Phi^T w y\right\} = E\left\{\theta - \left[\Phi^T w \Phi\right]^{-1} \Phi^T w \left[\Phi\theta + v\right]\right\} = E\left\{\left[\Phi^T w \Phi\right]^{-1} \Phi^T w\right\} E\{v\} \quad (6.146)$$

where $\left[\Phi^T w \Phi\right]^{-1} \Phi^T w \Phi = I, v, \Phi$ are statistically independent. From here if $E\{v\} = 0$ (zero mean), the least squares estimator is unbiased and

$$E\{\tilde{\theta}\} = 0, \; and \; E\{\hat{\theta}\} = \theta \quad (6.147)$$

6.8.3.2 Covariance matrix of the least squares estimator

The covariance matrix of the estimation error represents the dispersion of $\tilde{\theta}$ about its mean value, as follows

$$\mathrm{cov}(\tilde{\theta}) = E\left\{\left[\tilde{\theta} - E\{\tilde{\theta}\}\right]\left[\tilde{\theta} - E\{\tilde{\theta}\}\right]^T\right\} = E\{\hat{\theta}\theta^T\} \quad (6.148)$$

as the estimation error has zero mean value $E\{\tilde{\theta}\} = 0$.

Then the covariance matrix of the estimation error is

$$\begin{aligned}\sigma_1 &= E\left\{\tilde{\theta}\tilde{\theta}^T\right\} = E\left\{\left[\theta-\hat{\theta}\right]\left[\theta-\hat{\theta}\right]^T\right\} = \\ &= E\left\{\left[\theta-\left[\Phi^T w\Phi\right]^{-1}\Phi^T w\right]\left[\Phi\theta+v\right]\left[\theta\left[\Phi^T w\Phi\right]^{-1}\Phi^T w\right]\left[\Phi\theta+v\right]^T\right\} \\ &= E\left\{\left[\Phi^T w\Phi\right]^{-1}\Phi^T wvv^T w\Phi\left[\Phi^T w\Phi\right]^{-1}\right\} = E\left\{\left[\Phi^T w\Phi\right]^{-1}\Phi^T w\Phi\left[\Phi^T w\Phi\right]^{-1}\right\}E\left\{vv^T\right\} = \\ &= E\left\{\left[\Phi^T w\Phi\right]^{-1}\right\}\sigma^2\end{aligned} \tag{6.149}$$

where v has zero mean and variance σ^2 with equally distributed components. v and Φ are statistically independent. As the estimation is based on a given data, the matrix Φ is known and then

$$E\left\{\left[\Phi^T w\Phi\right]^{-1}\right\} = \left[\Phi^T w\Phi\right]^{-1} \tag{6.150}$$

Then the correlation matrix is

$$\sigma_1 = \left[\Phi^T w\Phi\right]^{-1}\sigma^2 \tag{6.151}$$

Matrix σ_1 is a measure how well the unknown vector of the parameter can be estimated. The square root of the diagonal elements of σ_1, $\sqrt{\sigma_{1_{i,i}}}$ represents the standard errors of each element $\hat{\theta}_i$ of the estimate $\hat{\theta}$. The variance can be estimated, according to the formula

$$\sigma^2 = \frac{\left[y-\Phi\hat{\theta}\right]^T\left[y-\Phi\hat{\theta}\right]}{N-n^2} \tag{6.152}$$

Where n^2 is the number of parameters to be estimated and $N-n^2$ is called a degree of freedom of the estimation.

6.9 Recursive Least square estimation

The method of the recursive estimation is used for the situation where the measurements of input and output from the process are obtained one- by-one. The aim is to update the parameters estimate whenever new information is available. Normally this is done by adding the new measurement to the previous set of measurements and recomputing the estimates. The approach is not to recompute estimates with the all available data, but to update the previous parameter estimates with the new data.

The form of the recursive method then is:

New estimate = old estimate + correction (6.153)

Let it is supposed that the estimate of the parameters is obtained for the first k-1 instants. Then according to Equation (6.136)

$$\hat{\theta}(k-1) = \left[\sum_{i=1}^{k-1}\varphi^T(i)w(i)\varphi(i)\right]^{-1}\sum_{i=1}^{k-1}\varphi^T(i)w(i)y(i) \tag{6.154}$$

Then at the moment $i = k$ new information is obtained for the input and output of the process and the new function $\varphi(k)$ is calculated. The least square estimate is

$$\hat{\theta}(k)=\left[\sum_{i=1}^{k-1}\left[\varphi^T(i)w(i)\varphi(i)\right]+\varphi^T(k)w(k)\varphi(k)\right]^{-1}\left[\sum_{i=1}^{k-1}\left[\varphi^T(i)w(i)y(i)\right]+\varphi^T(k)w(k)y(k)\right] \tag{6.155}$$

The aim is to use the information for the new and previous estimate from equations (6.155) and (6.154) and to obtain the new estimate using the information for the previous one according to the equation (6.127). The derivation follows:

A new matrix is defined

$$R(k)=\sum_{i=1}^{k}\varphi^T(i)w(i)\varphi(i) \tag{6.156}$$

which using (6.155) allows a recursive formula for $R(k)$ to be written

$$R(k)=R(k-1)+\varphi^T(k)w(k)\varphi(k) \tag{6.157}$$

Using (6.156) the new estimate $\hat{\theta}(k)$ is

$$\hat{\theta}(k)=R^{-1}(k)\left[\sum_{i=1}^{k-1}\left[\varphi^T(i)w(i)y(i)\right]+\varphi^T(k)w(k)y(k)\right] \tag{6.158}$$

and the previous estimate is

$$\hat{\theta}(k-1)=R^{-1}(k-1)\sum_{i=1}^{k-1}\varphi^T(i)w(i)y(i) \tag{6.159}$$

In order to include $\hat{\theta}(k-1)$ into the expression for $\hat{\theta}(k)$ the sum for $i=\overline{1,k-1}$ from (6.159) can be expressed and substituted in (6.158)

$$\sum_{i=1}^{k-1}\varphi^T(i)w(i)y(i)=R(k-1)\hat{\theta}(k-1) \tag{6.160}$$

$$\hat{\theta}(k)=R^{-1}(k)\left[R(k-1)\hat{\theta}(k-1)+\varphi^T(k)w(k)y(k)\right] \tag{6.161}$$

R(k-1) can be expressed by R(k) according (6.157) and substituted in (6.161)

$$R(k-1)=R(k)-\varphi^T(k)w(k)\varphi(k) \tag{6.162}$$

$$\hat{\theta}(k)=R^{-1}(k)\left\{\left[R(k)-\varphi^T(k)w(k)\varphi(k)\right]\hat{\theta}(k-1)+\varphi^T(k)w(k)y(k)\right\} \tag{6.163}$$

After some mathematical transformation it is obtained :

$$\hat{\theta}(k)=\hat{\theta}(k-1)-R^{-1}(k)\varphi^T(k)w(k)\varphi(k)\hat{\theta}(k-1)+R^{-1}(k)\varphi^T(k)w(k)y(k) \tag{6.164}$$

$$\hat{\theta}(k)=\hat{\theta}(k-1)+R^{-1}(k)\varphi^T(k)w(k)\left[y(k)-\varphi(k)\hat{\theta}(k-1)\right] \tag{6.165}$$

The equation (6.165) together with equation (6.157) is a recursive formula for the least square estimate. The matrix *R(k)* in equation (6.165) is necessary to be inverted at

every step. There is possibility to calculate the estimate without matrix inversion. It is supposed that

$$p1(k) = R^{-1}(k) \tag{6.166}$$

Then the formula (6.157) is

$$p^{-1}1(k) = p^{-1}1(k-1) + \varphi^T(k) w(k) \varphi(k) \tag{6.167}$$

The matrix $\rho(k)$ is also symmetrical and positive definite.

$$p1(k) = \left[p^{-1}1(k-1) + \varphi^T(k) w(k) \varphi(k)\right]^{-1} \tag{6.168}$$

The equation (6.168) can be simplified using the Matrix inversion lemma stating that if A,B,C,D are matrices with appropriate dimension such that A+BCD exists, then (Najim & Ikonen, 1999).

$$\left[A + BCD\right]^{-1} = A^1 A^{-1} B\left[DA^{-1}B + C^{-1}\right]^{-1} DA^{-1} \tag{6.169}$$

It can be substituted in (6.168) that

$$A \leftarrow \rho^{-1}1(k-1),\ B \leftarrow \varphi^T(k),\ C \leftarrow \omega(k),\ D \leftarrow \varphi(k) \tag{6.170}$$

Then

$$\begin{aligned} p1(k) &= \left[p^{-1}1(k-1)\right]^{-1} - \left[p^{-1}1(k-1)\right]^{-1} \varphi^T(k)\left[\varphi(k)\left[p^{-1}1(k-1)\right]\varphi^T(k) + w^{-1}(k)\right]^{-1} \varphi(k)\left[p^{-1}1(k-1)\right]^{-1} \\ &= p1(k-1) - p1(k-1)\varphi^T(k)\left[\varphi(k)p1(k-1)\varphi^T(k) + w^{-1}(k)\right]^{-1} \varphi(k)p1(k-1) \end{aligned} \tag{6.171}$$

The expression $L(k) = R^{-1}(k)\Phi^T(k)w(k) = p1(k)\Phi^T(k)w(k)$ can be written using equation (6.171) in the following way

$$\begin{aligned} L(k) &= \left[p1(k-1) - p1(k-1)\varphi^T(k)\left[\varphi(k)p1(k-1)\varphi^T(k) + \omega^{-1}(k)\right]^{-1}.\varphi(k)p1(k-1)\right]\varphi^T(k)\omega(k) \\ &= p1(k-1)\varphi^T(k)\left[I - \left[\varphi(k)p1(k-1)\varphi^T(k) + \omega^{-1}(k)\right]^{-1}.\varphi(k)p1(k-1)\varphi^T(k)\right]w(k) \end{aligned} \tag{6.172}$$

Taking $\left[\varphi(k)p1(k-1)\varphi^T(k) + w^{-1}(k)\right]^{-1}$ outside of the first brackets gives

$$\begin{aligned} L(k) &= p1(k-1)\varphi^T(k)\left[\varphi(k)p1(k-1)\varphi^T(k) + w^{-1}(k)\right]^{-1} \\ &\left[\varphi(k)p1(k-1)\varphi^T(k) + w^{-1}(k) - \varphi(k)p1(k-1)\varphi^T(k)\right]w(k) \\ &= p1(k-1)\varphi^T(k)\left[\varphi(k)p1(k-1)\varphi^T(k) + w^{-1}\right]^{-1} \end{aligned} \tag{6.173}$$

Then the expression (6.165) becomes

$$\hat{\theta}(k) = \hat{\theta}(k-1) + L(k)\left[y(k) - \varphi(k)\hat{\theta}(k-1)\right] \tag{6.174}$$

where $L(k)$ is calculated from equation (6.173) and $p1(k)$ is calculated from (6.171) and (6.173)

$$p1(k) = [I - L(k)\varphi(k)]p1(k-1) \tag{6.175}$$

The equation (6.174) is the covariance requisition form. This form is more computational effective.

Algorithm for calculation:

1. Select initial values for $p1(k_0)$ and $\hat{\theta}(k_0)$ by using batch least square algorithm on the first $k_0 \rangle \dim\theta$ samples of data

$$p1(k_0) = \left[\sum_{i=1}^{k_0} \varphi^T(i) w(i) \varphi(i)\right]^{-1} \tag{6.176}$$

$$\hat{\theta}(k_0) = p1(k_0) \sum_{i=1}^{k_0} \varphi^T(i) w(i) y(i) \tag{6.177}$$

2. Calculate the value of *L(k)* from equation (6.173)
3. Calculate the estimate of the parameters from Eq. (6.174)
4. Update the value of the matrix p from equation (6.175)

Another choice is to set the initial vector of parameters to zero, $\hat{\theta}(k_0) = 0$ and let the initial error covariance matrix to be a multiple of identity matrix $p1(k_0) = CI$, where C is some large positive constant. A large value of $p1$ implies that the confidence in $\hat{\theta}(k_0)$ is poor and ensures a high degree of correction.

If the model of the process is linear according to the parameters and if there is no correlation between the measurement error of different stages of measurement so that the assumed diagonal structure of $w(k)$ is strictly valid, then the sequential solution for $\hat{\theta}(k)$ will be the same as the batch solution.

6.9.1. Application of the method to the Benchmark process

6.9.1.1 Using of the ASM1 model

The process described by equation (6.127) is considered. The dimension of the vector of the parameter θ is 3. The above Algorithm is followed:

1. The initial conditions for $\rho 1(k_0)$ *and* $\hat{\theta}(k_0)$ are determined according to Equations (6.112) and (6.114) where $N = 5 \rangle \dim\theta$

$$p1(5)=\left[\begin{bmatrix} C^T p(1) \\ C^T p(2) \\ \vdots \\ C^T p(5) \end{bmatrix}^T w \begin{bmatrix} C^T p(1) \\ C^T p(2) \\ \vdots \\ C^T p(5) \end{bmatrix}\right]^{-1} \equiv p1(k-1),\ w \in R^{15\times 15}, \tag{6.178}$$

$$\hat{\theta}(5)=p1(5)\begin{bmatrix} C^T p(1) \\ \vdots \\ C^T p(5) \end{bmatrix}\begin{bmatrix} z(2)-Az(1)-Bz_{i\phi}(1) \\ \cdots\cdots\cdots\cdots \\ z(6)-Az(5)-Bz_{i\phi}(5) \end{bmatrix} \equiv \hat{\theta}(k-1) \tag{6.179}$$

2. Calculation of $L(k)$ from equation (6.147)

- Calculation of the inverse matrix for the moment $k \rangle 5$

$$\varphi(k)=C^T p(k) \in R^{3\times 3},\ w(k) \in R^{3\times 3}$$
$$L(k)=\left[C^T p(k) p1(k-1) p^T(k) C + w^{-1}(k)\right]^{-1} \in R^{3\times 3} \tag{6.180}$$

- Calculation of $L(k)$

$$L(k)=p1(k-1)p^T(k)CL1(k) \in R^{3\times 3} \tag{6.181}$$

Calculation of $\hat{\theta}(k)$

$$\hat{\theta}(k)=\hat{\theta}(k-1)+L(k)\left[z(k+1)-Az(k)-Bz_{i\phi}(k)-C^T\rho(k)\hat{\theta}(k-1)\right] \tag{6.182}$$

3. Calculation of the updated form of $p1(k)$

$$p1(k)=\left[I-L(k)C^T p(k)\right]p1(k-1) \tag{6.183}$$

4. Recursive calculation following points 2, 3, 4.

6.9.1.2 Using of the UCT model

In this case the number of estimated parameters is 4. The above steps are followed, but the dimension of the matrices for the *n-th* tank is different

$$\varphi(k) \in R^{4\times 4}, L(k) \in R^{4\times 4}, p1(k) \in R^{4\times 4}$$

6.9.2. Application of the method to the Athlone process

The equations of the process have the same form as above. The difference is in the dimension of the vectors and matrices because of the different numbers of tanks and different biological models.

6.10. Recursive least square estimation with exponential forgetting

The least square criterion (6.130) gives an average estimate of the parameters, based on the values of the data samples used in the identification. If the process is time varying, it is necessary to have an estimate that is representative of the current properties of the system. This can be achieved by weighting the newer samples more than the old ones, i.e. by forgetting old information

The criterion with forgetting factor can be written in the following way

$$\Im(\theta)=\sum_{i=1}^{k}\left\|y(i)-\varphi(i)\theta\right\|^{2}_{\lambda^{k-1}w(k)} \tag{6.184}$$

where $\lambda \rangle 0$ is a forgetting factor. The derivation of the recursive estimate formula is following the same steps as in the previous case, where on the places of the weighting matrix w, the new one $\lambda\omega(k)$ is substituted. Then equation (6.156) becomes

$$\begin{aligned} R(k)&=\sum_{i=1}^{k}\varphi^{T}(i)\lambda^{k-i}w(i)\varphi(i)=\sum_{i=1}^{k-1}\left[\varphi^{T}(i)\lambda^{k-i}w_{i}(k)\varphi(i)\right]+\varphi^{T}(k)\lambda^{k-k}w(k)\varphi(k)= \\ &=\lambda R(k-1)+\varphi^{T}(k)w(k)\varphi(k) \end{aligned} \tag{6.185}$$

Then the estimate at the moment k is

$$\hat{\theta}(k)=R^{-1}(k)\left[\sum_{i=1}^{k-1}\left[\varphi^{T}(i)\lambda^{k-i}w(i)y(i)\right]+\varphi^{T}(k)w(k)y(k)\right] \tag{6.186}$$

The previous estimate is

$$\hat{\theta}(k-1)=\frac{R^{-1}(k-1)}{\lambda}\sum_{i=1}^{k-1}\varphi^{T}(i)\lambda^{k-i}w(i)y(i) \tag{6.187}$$

From here

$$\sum_{i=1}^{k-1}\varphi^{T}(i)\lambda^{k-i}w(i)y(i)=\lambda R(k-1)\hat{\theta}(k-1) \tag{6.188}$$

$$\hat{\theta}(k)=R^{-1}(k)\left[\lambda R(k-1)\hat{\theta}(k-1)+\varphi^{T}(k)w(k)y(k)\right] \tag{6.189}$$

R(k-1) can be expressed by *R(k)* from equation (6.185)

$$R(k-1)=\frac{1}{\lambda}R(k)-\frac{1}{\lambda}\varphi^{T}(k)w(k)\varphi(k) \tag{6.190}$$

Then

$$\hat{\theta}(k)=R^{-1}(k)\left[\left[\frac{1}{\lambda}R(k)-\frac{1}{\lambda}\varphi^{T}(k)w(k)\varphi(k)\right]\hat{\theta}(k-1)+\frac{1}{\lambda}\varphi^{T}(k)w(k)y(k)\right] \tag{6.191}$$

And after some mathematical transformations it is obtained

$$\hat{\theta}(k)=\hat{\theta}(k-1)+R^{-1}(k)\varphi^{T}(k)w(k)\left[y(k)-\varphi(k)\hat{\theta}(k-1)\right] \tag{6.192}$$

This is the same expression as equation (6.165)

The same transformations are done to overcome the inversion of the matrix R(k)

$$p1(k)=R^{-1}(k)$$

$$p1(k)=\left[\lambda p^{-1}1(k-1)+\varphi^T(k)w(k)\varphi(k)\right]^{-1}= \tag{6.193}$$

$$=\frac{1}{\lambda}\left[p1(k-1)-p1(k-1)\varphi^T(k)\left[\varphi(k)\frac{p1(k-1)}{\lambda}\varphi^T(k)+\omega^{-1}(k)\right]^{-1}\varphi(k)\frac{p1(k-1)}{\lambda}\right]$$

$$L(k)=p1(k)\varphi^T(k)\omega(k)=$$

$$=\frac{1}{\lambda}\left[p1(k-1)-\rho1(k-1)\varphi^T(k)\left[\varphi(k)\frac{p1(k-1)}{\lambda}\varphi^T(k)+\omega^{-1}(k)\right]^{-1}\varphi(k)\frac{\rho1(k-1)}{\lambda}\right]\varphi^T(k)w(k)=$$

$$=\frac{1}{\lambda}p1(k-1)\varphi^T(k)\left[I-\left[\varphi(k)\frac{p1(k-1)}{\lambda}\varphi^T(k)+w^{-1}(k)\right]^{-1}\varphi(k)\frac{p1(k-1)}{\lambda}\varphi^T(k)\right]w(k)=$$

$$=\frac{1}{\lambda}p1(k-1)\varphi^T(k)\left[\varphi(k)\frac{p1(k-1)}{\lambda}\varphi^T(k)+w^{-1}(k)\right]^{-1}$$

(6.194)

From here

$$p1(k)=\frac{1}{\lambda}\left[I-L(k)\varphi(k)\right]p1(k-1) \tag{6.195}$$

$$\hat{\theta}(k)=\hat{\theta}(k-1)+L(k)\left[y(k)-\varphi(k)\hat{\theta}(k-1)\right] \tag{6.196}$$

The algorithm for calculation is following the steps of the algorithm for recursive estimation, but the calculation of the matrix $L(k)$ is according equation (6.195) and of $p1(k)$ according to equation (6.194). The effect of the forgetting factor is that $p1(k)$ and L(k) are kept larger. With $0 \langle \lambda \langle 1$, $p(k)$ will not tend to zero and the algorithm always will react quickly to the changes in θ. A common choice of λ is $0.95 \div 0.99$.

6.11 Conclusion

Parameter estimation is a common feature in many areas of process modeling, both in on-line applications such as real time optimization and in off-line applications such as the modeling of reaction kinetics and biotechnological processes (Lennox et al, 2001), (Montague, 1997), (Nomikos and MacGregor, 1994), (Luyben, 1993), (Gudi et al, 1995), (Dacosta et al, 1997), (Wang et al, 1999), (Fisher et al, 1988), (Stecha et al, 2005), (Dochain, 2003) and (Wang and Gawthrop, 2001).

This chapter starts with the problem for identifiability of the models of nonlinear processes and the existing methods for checking it. Then the identifiability of the considered two plants for wastewater treatment models is proved on the basis of the Taylor series method. Equations for calculation of the selected parameters are derived.

Overview of the existing methods for parameter estimation is given and on it basis a method for parameter estimation of the growth parameters for ASM1 and UCT biological models as a part of the corresponding Benchmark and Athlone plant mass balance models is developed. Algorithms and Matlab programmes for calculation are developed, Appendix D. The results are given in Chapter 9.

CHAPTER SEVEN
STATE AND PARAMETER ESTIMATION

7.1 Introduction

The lack of on-line measurement technology for product quality variables is a common problem in the process industry. As temperatures, pressures, flow rates, levels and composition are routinely measured on-line, key quality variables are only available at intervals, often hours apart shown (Biagiola and Figueroa, 2004), (Ferreira et al, 2005), (Nejjari et al, 1996), (Pons et al, 2005), (Ahmad and Reynolds, 1999), (Hart,1998), (Marsili-Libelli, 1992), (Marsili-Libelli and Tabani, 2002) (Papastratos, 1999), (Bastin and Gevers, 1988), (Bastin and Dochain, 1990), (Ossenbruggen et al., 1991), (Larrea et al., 1992), (Lesouef et al., 1992), (Gehan et al, 1999), (Johnson and Tiedeman, 1985), (Siegrist and Tschui, 1992), (Tenno and Uronen, 1995) and (Marsili-Libelli and Giovannini, 1996). For on-line model predictive control some kind of process monitoring schemes are necessary to provide accurate continuous real time and future predictions for those key quality variables which are no measurable and essential (Bernard and Gouze, 2002), (Gaslan et al, 2003), (Aschemann et al, 2005), (Rauh et al, 2004) and (Slotine and Li, 1991).

A major difficulty in the application of advanced monitoring and control strategies for the wastewater treatment is the difficulty in on-line measuring of the chemical and biological variables, such as biomass concentration, specific bacterial activity or intermediate product concentrations. The idea for using observers, also called software sensors that combine a number of readily available on-line measurements (gaseous flow rates, pH, dissolved gases, etc.,) with a process model for estimating the values of unmeasured state variables appeared and was developed during the last years. Different methods were proposed to design such observers based on different principles. In practice the choice between them depends on the specificities of the considered problem, reliability of the process model, as well as the amount and accuracy of data. If a reliable process model is available and if this model has been thoroughly identified and validated, either a Kalman filter or a high gain observer can be developed. When the process model is not accurate enough, an asymptotic observer relying on mass-balance principles, but not on the uncertain kinetics, shall be used instead. If bounds are known for the uncertain inputs or parameters, an interval

observer can be used for predicting intervals in which the unmeasured variables are guaranteed to belong.

Another important point in the design of the observer, additional to the model quality is the objective to be achieved according to its use - for control, for diagnostics, observation and so on.

The chapter analyses the existing methods for design of observers and/or estimators for biotechnological and wastewater treatment processes and describes development of two methods for design of discrete Kalman filters for estimation of the immeasurable state variables of the reduced nonlinear mass balance models based on ASM1 and UCT biological models for the Benchmark and Athlone plants.

7.2 Theoretical concepts in system observability

The state variables can be reconstructed from the measurements by an observer (when no disturbances are modeled) or a filter (when the disturbances are modeled as stochastic processes). It is first fundamental to study the observability property of the system before designing an observer for its states. The observability determines whether the measured signals contain sufficiently information to estimate the unmeasured state variables. It also guarantees that an estimator can be found so that the estimated state converges to the real state arbitrarily fast. Then the system is called to be observable if it satisfies this property from a theoretical point of view. The next step is to design the observer (Luenberger, 1979).

The theory of observability of the dynamic system is mainly developed for linear systems. The methods, proposed for nonlinear system are not general ones; they are tailored to the specifics of the considered problem.

7.2.1 Notion of observability

A general nonlinear model is considered

$$\dot{z}(t) = f(z(t), u(t)), \qquad z(0) = z_0 \tag{7.1}$$

$$y(t) = h(z(t)) \tag{7.2}$$

where $u \in R^m$, $z \in R^n$ and $y \in R^l$ are the system input, state and output vectors respectively, z_0 is the vector of the initial state. The functions f and h provide dynamics of the process and the links between the states and measurements.

The objective is to estimate $z(t)$ from the measurement $y(t)$. Observability is a structural property of the system that states whether this is possible or not (Gautier and Kupka, 2001), (Luenberger, 1979).

Definition: The system is said to be observable, if $z(t)$ can be uniquely determined from

$$y(t), \frac{dy(t)}{dt}, \frac{d^2y(t)}{dt^2}, \ldots, \frac{d^{n_y}y(t)}{dt^{n_y}} \text{ and } u(t), \frac{du(t)}{dt}, \ldots, \frac{d^{n_u}u(t)}{dt^{n_u}}$$

for some $n_y \geq 0$ and $n_u \geq 0$. (7.3)

The unobservability results from some state or subsystem being disconnected physically from the output and therefore not influencing the measurements. The observer then can be designed to estimate state $z(t)$ based on a model of the process and a set of input/output measurements. The observer is an auxiliary dynamic system coupled to the original system via the measured inputs and outputs, Figure 7.1:

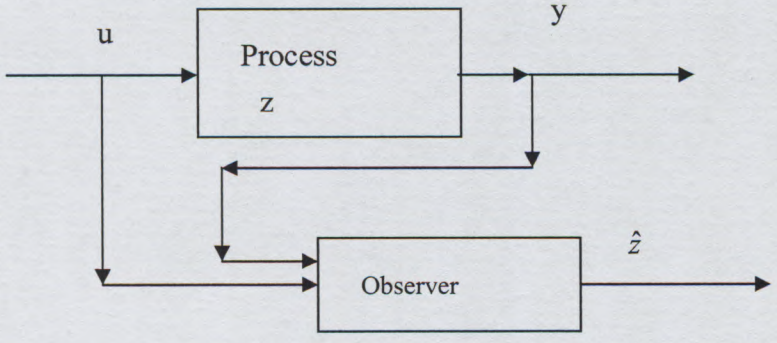

Figure 7.1: Basic structure of the observer and plant

7.2.2 State estimation for continuous systems

Definition: An observer is an auxiliary system coupled to the original system as :

$$\dot{q}(t) = \hat{f}(q(t), u(t), y(t)), \qquad q(0) = q_0 \tag{7.4}$$

$$\hat{z}(t) = \hat{h}(q(t), u(t), y(t)) \tag{7.5}$$

where $q \in R^p$ is the observer state vector, $\hat{f}$ is the function of the observer dynamics and $\hat{h}$ relates the state q to the estimate $\hat{z}$ of the real system. The required property of the observer is that the observation error asymptotically converges to zero.

$$\lim_{t\to\infty}\|\hat{z}(t)-z(t)\|=0 \tag{7.6}$$

A desirable property of the observer is the possibility to tune the convergence rate in order for the estimates to converge more rapidly than the dynamics of the estimated process. Another desirable property is that the estimate $\hat{z}$ should remain equal to $z(t)$ under proper initialization, this means when it is initialized with the true value of $z(0)$. Based on the above requirements the structure of the observers is accepted to be of the following type

$$\dot{\hat{z}}(t)=f(z(t),u(t))+K[q(t),h(\hat{z}(t))-y(t)] \tag{7.7}$$

$$\dot{q}(t)=\hat{f}(q(t),u(t),y(t)) \quad with \quad K(q(t),0)=0 \tag{7.8}$$

This observer consists of the model of the original system corrected by a term that depends on the discrepancy between the measured and the predicted outputs. The correction value is tuned by the function K, called the observer gain.

7.2.3 State estimation for discrete time systems

For the case of discrete nonlinear systems the state space model of the system is

$$z(k+1)=f[z(k),u(k)] \tag{7.9}$$

and the measurement equation is

$$y(k+1)=h[z(k+1)] \tag{7.10}$$

where k is the discrete time

For this case the mathematical form of the state observer consists of three parts:

- prediction of the next state according to the current estimate $z(k)$ and equation (7.9)

$$\hat{z}(k+1|k)=f[\hat{z}(k|k),u(k)] \tag{7.11}$$

where $\hat{z}(k|k)$ denotes the estimate at the moment k according to the measurements up to time k, $\hat{z}(k+1|k)$ is the estimate at the moment $k+1$, given the same data from the measurement, $u(k)$ are the process inputs at the moment k.

- correction of the estimation done by a filter and according to the latest measurement at a time $k+1$

$$\hat{z}(k+1|k+1)=\hat{z}(k+1|k)+K(k+1)[y(k+1)-h(\hat{z}(k+1|k))] \tag{7.12}$$

where $y(k+1)$ are the actual process measurements. The function

$$\hat{y}(k+1|k) = h(\hat{z}(k+1|k)) \tag{7.13}$$

corresponds to the estimated output at the moment $k + 1$ according to the given measurements up to time k. The filter parameter K is also function of time, but normally is accepted to be a constant in order to be capable to implement the filter. According to equation (7.13) if the actual measurement $y(k+1)$ is the same as the predicted one $\hat{y}(k+1|k)$ the correction will be zero. The structure of the predictor/ corrector estimator is given in Figure 7.2 (Olson & Newell, 2001).

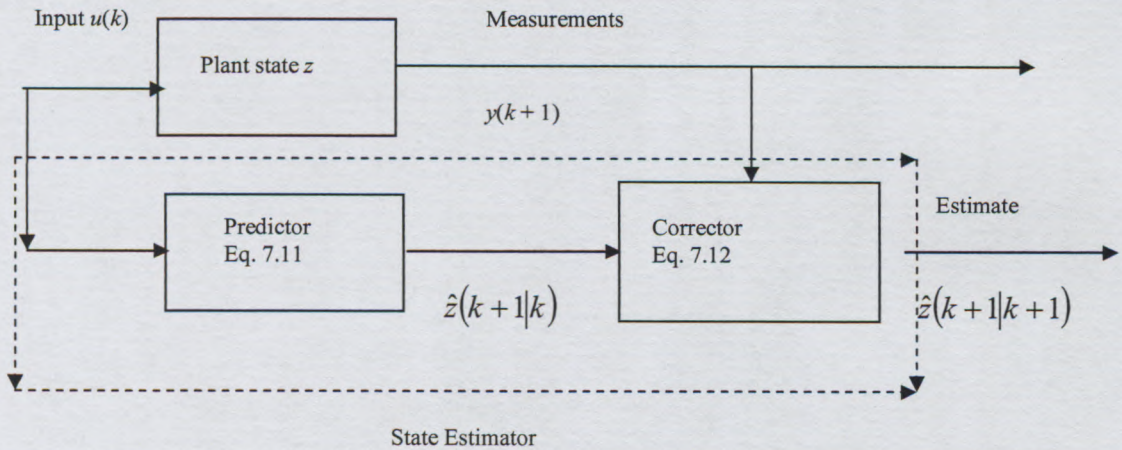

Figure 7.2: Predictor/ corrector observer

7.2.4 State estimation for noisy systems

The stochastic processes are used to mathematically model the process disturbances and the errors (random) in the sensors measurements. This means that some random variable with given probability distribution is added to the process variables at each moment of time and in the same way to a sensor signal. In points 7.1-7.3 it is assumed that the data information sent to the estimator is perfect one. But this is ideal, not the real situation. In reality the electrical noise to a sensor signal can be described as an additional random variable $v(t)$

$$y(t) = h[z(t)] + v(t) \tag{7.14}$$

where $v(t)$ is the vector of the noise $v \in R^l$, modelled as a sequence of stochastic variables. If they are independent, the amplitude of the noise at a moment t does not depend on the amplitudes at previous times. Then the random noise is normally

distributed (Gaussian) and its mean value and standard deviations completely characterize it.

In the same way the nonmodelled disturbances to the process can be modeled as a random numbers $\omega(t)$ added to the state

$$\dot{z}(t) = f[z(t), u(t)] + \omega(t) \tag{7.15}$$

where $\omega(t)$ is considered in the same way as the noise $v(t)$. If the noise description is given, the estimator can take the model uncertainty into consideration. Any correction K in the presence of both types of noises has to be optimally selected according to the noise characteristics. The Kalman filter (Kalman, 1986) is develop to achieve optimal estimation. It has the structure of equations (7.4), (7.5) but the required property of the estimator is the observation error, calculated as

$$\varepsilon(t) = h[z(t)] + v(t) - h[\hat{z}(t)] \tag{7.16}$$

has asymptotically to converge to the sensor noise. In practice statistical test has to be done of the residual $\varepsilon(t)$ to find out if the filter is convergent. The corrector factor K obtained from the Kalman filter is time varying and represents the optimal compromise between process and sensor disturbances and the estimation error.

7.2.5 Observers for linear systems

The linear time invariant system is described by a linear state space model

$$\dot{z}(t) = Az(t) + Bu(t) \tag{7.17}$$

$$y(t) = Cz(t) \tag{7.18}$$

Where $A \in R^{n \times n}$, $B \in R^{n \times m}$, $C \in R^{l \times n}$ are the system matrices. The observability criterion is given by the rank condition

$$rank\left[C^T \; A^T C^T \; \ldots \left(A^{n-1}\right)^T C^T\right] = n \tag{7.19}$$

7.2.5.1 Luenberger observer (Luenberger, 1966)

The structure of the observer is

$$\dot{\hat{z}}(t) = A\hat{z}(t) + Bu(t) + K[C\hat{z}(t) - y(t)] \tag{7.20}$$

where $\hat{z} \in R^n$ is the state of the observer, $K \in R^{n \times l}$ is the gain matrix that is used to tune the convergence rate of the observer and can be chosen in order for the observation error to converge to zero arbitrary fast. Pole placement methods are normally used to make the observation error system stable, where the dynamics of the error is given by the equation

$$\dot{e}(t) = (A - KC)e(t) \tag{7.21}$$

If the system is observable then K always can be found such that the error goes to zero. The gain K could not be selected to be very big because it can increase the sensitivity of the observer to external perturbations (noise). If there is only one sensor (y is a scalar output) the correcting gain K is a vector, otherwise K is a matrix. A good solution is to design the observer paying attention to both stability and accuracy. The Kalman filter proposes a way of achieving such a compromise.

A special kind of Luenberger observer can be designed for a nonlinear system where nonlinearities depend on the output y only:

$$\dot{z}(t) = Az(t) + \phi(y(t), t) + Bu(t) \tag{7.22}$$

$$y(t) = Cz(t) \tag{7.23}$$

where ϕ is known nonlinear function. Then the Luenberger-like observer has linear dynamics with respect to the observation error and can be written as

$$\dot{\hat{z}}(t) = A\hat{z}(t) + \phi(y(t), t) + Bu(t) + K[C\hat{z}(t) - y(t)] \tag{7.24}$$

The gain K can be chosen arbitrarily.

7.2.5.2 **Kalman filter** (1960, 1986)

The Kalman filter can be considered as a Luenberger observer with a time varying gain. The gain is chosen in such a way that the variance of the observation error is minimized (or equivalently, the integral between t_0 and t of the squared error is minimized). Because of this minimization, the Kalman filter is called an optimal estimator.

The stochastic model of the observable linear system is considered:

$$\dot{z}(t) = Az(t) + Bu(t) + Gw(t) \qquad z(t_0) = z_0 \tag{7.25}$$

where $w(t) \sim (0, Q(t))$ is a white noise with zero mean and covariance $Q(t)$. It is supposed that the initial state z_0 is unknown, but there is a priori knowledge $z \sim (\bar{z}_0, P_0)$ and that the measurements are given at discrete times t_k according to

$$y(k) = Cz(t_k) + v(k) \tag{7.26}$$

where $v(k) \sim (0, R_k)$ is uncorrelated with $w(t)$ and z_0, white noise. Besides initialization a continuous/ discrete Kalman filter consists of two steps: a prediction (propagation) step (between two successive measurements) followed by a correction step (at measurement times). The sequence is:

- Initialization $\left(t = t_0^+\right)$

$$P(t_0) = P_0,\ \hat{z}(t_0) = \bar{z}_0,\ P_0 = E\left\{\varepsilon(t_0).\varepsilon^T(t_0)\right\} \tag{7.27}$$

- Prediction step: $\left(t_{k-1}^+ \le t \le t_k^-,\ k \ge 1\right)$

$$\dot{P}(t) = AP(t) + P(t)A^T + GQ(t)G^T \tag{7.28}$$

$$\dot{\hat{z}}(t) = A\hat{z}(t) + Bu(t) \tag{7.29}$$

- Correction step: $\left(t = t_k^+,\ k \ge 1\right)$

$$K(k) = P(t_k^-)G^T\left[GP(t_k^-)G^T + R_k\right]^{-1} \tag{7.30}$$

$$P(t_k^+) = (I - K_k(t))P(t_k^-) \tag{7.31}$$

$$z(t_k^+) = z(t_k^-) + K_k\left(y_k - Cz(t_k^-)\right) \tag{7.32}$$

In these equations the model matrices depend on time. The Kalman filter can be extended by adding a term $-QP(t),\ Q \rangle 0$ in the prediction equation for P. This exponential forgetting factor allows to consider the case where $Q = 0$. The calculation of the positive definite matrices P, Q and P_0 can be very tricky in practice, especially when the noise properties are not known precisely.

7.2.6 Nonlinear system estimation. Extended Kalman filter

The extended Kalman filter is developed for nonlinear systems of the kind

$$\dot{z}(t) = f\left[z(t), u(t), t\right] + G(t)\omega(t),\ z(0) = z_0 \tag{7.33}$$

with measurements at discrete time t_k given by

$$y(t) = h\left[z(t), t\right] + v(t) \tag{7.34}$$

where f and h are continuously differentiable functions. The problem with the nonlinear models is that the Gaussian input does not necessarily produce a Gaussian output because distortions caused by the nonlinear elements. The accepted principle in connection with estimation of state is that when the system is subjected to small inputs the outputs will be Gaussian. The extended Kalman filter for nonlinear systems is based on this principle. The fundamental concept of this filter is the notion that the true state is very close to the estimated state and as a result the error dynamics can be represented accurately enough by a linearized first order Taylor series expansion.

The idea is to linearise the nonlinear system around its current state estimate $\hat{z}(t)$. Then the problem becomes equivalent to building Kalman filter for a nonstationary linear system with matrices A and C taken as

$$A(t_k)=\frac{\partial f}{\partial z}\Big|_{\hat{z}(t_k)},\quad C(t_k)=\frac{\partial h}{\partial z}\Big|_{\hat{z}(t_k)} \tag{7.35}$$

The extended Kalman filter is used for many applications. This filter suffers from low convergence (Bastin and Dochain, 1990). A multirate extended Kalman filter can be developed for measurements with different sampling rates.

7.3 Estimation of the biotechnological processes

The structure of the models of the biotechnological processes such as the fermentation and the ASP consists of two parts (Bernard, Hadj-Sadoc & Gouze, 2000)

- a linear part based on mass-balance considerations
- a number of nonlinear terms that describe the biological reaction rates (kinetics)

The kinetic terms are often poorly known in practice and it is very difficult or impossible to construct a reliable observer by accounting for such uncertain terms. One of the directions of design of the observer uses the above structure of the ASP models in order to construct observers that are independent on the uncertain reaction rates. This is obtained via a linear change of variables. The main condition to design this so-called asymptotic observer is that enough number of variables is measured. The asymptotic observers fall into the broad class of observers with unknown inputs, whose principle relies on cancellation of the unknown part via a change of variables (Darouach, Zasadninski & Xu 1994), (Hou & Muller, 1991), (Kudva,Viswanadham & Ramaurishna, 1980).

Construction of such observer requires the following assumptions that:

- there are more measured quantities than the model reactions
- matrix introducing the measured state variables has a full rank

The linear unknown input observer method is a two step strategy which then allows implementing any state observer to the transformed system (Hou & Muller, 1991). Additional parameter uncertainties in the linearized process model orient the observation strategy to the use of the robust state observers. For linear system such efficient uncertain estimation approaches are given in (Takahashi & Peres, 1999), (Yin & Park, 2001), (Gomez-Quintero & Queinnec, 2002).

The development of the methods for parameter and state estimation for these processes often is very difficult and complex because of the specific process

characteristics. Some of the first methods are developed for the fermentation processes and later they are extended for the cases of ASP.

7.3.1. General observer

Lets consider the biotechnological process described by the general state space model, that is (Bastin & Dochain, 1990):

$$\dot{z}(t) = Y\varphi(z) - Dz(t) - Q + F \tag{7.36}$$

where the notations used are as follows: $z \in R^n$ is the state vector, Y is the yield matrix, D is the dilution rate, Q is the rate of the released by the process gas, F is the inflow rate. It is suppose that full knowledge of this model i.e. the structure of the reaction kinetics $\varphi(z)$ is completely known and also the numerical values of all the coefficients involved in the model, for example yield coefficients and kinetic coefficients are given.

It is assumed that the dilution rate D, the feed rates F and the gaseous outflow rates Q are known on-line, and that a subset of the state variables is measured on-line. The vector of these measurements is denoted z_1 and is related to the state of the system as follows: $z_1 = Lz$, where the $q \times n$ matrix L is an elementary matrix which selects the measured components of z. On the other hand, the vector of the unmeasured states is denoted z_2, so that (z_1, z_2) constitutes a partition of z.

A "state observer" is an algorithm designed to reconstruct the non measured state variables from the measured ones. A general class of state observers for nonlinear systems of the form (7.36) is as follows:

$$\dot{\hat{z}} = Y\varphi(\hat{z}) - D\hat{z} - Q + F + K(\hat{z})(z_1 - \hat{z}_1) \tag{7.37}$$

where $\hat{z}$ denotes the on-line estimate of $z, K(\hat{z})$ is a $q \times n$ "gain" matrix depending on $\hat{z}$ and $\hat{z}_1 = L\hat{z}$. The observer equation (7.37) can be seen as a copy of the model (7.36) with an additional driving term which is proportional to the observation error of the measured part of the state $(z_1 - \hat{z}_1)$ and which disappears in the case of perfect estimation (Gauthier et al, 1992).

In practice, the on-line (observation) of the missing states is obtained simply by integrating equation (7.37) on the supervising computer (Rocha and Ferreira, 2004),

(Williamson, 1977). The estimated state vector $\hat{z}$ includes all the state variables, even those which are measured (Bogaerts and Hanus, 2001).

The state observer design problem reduces to that of a reasonable choice of the gain matrix $K(\hat{z})$. To solve this problem, the observation error is introduced:

$$e = z - \hat{z} \tag{7.38}$$

whose dynamics are easily shown to be governed by the following differential equation obtained by subtracting (7.37) from (7.36) :

$$\dot{e} = Y[\varphi(\hat{z}+e) - \varphi(\hat{z})] - De - K(\hat{z})Le \tag{7.39}$$

A zero observation error $e = 0$ is clearly an equilibrium point of the error model (7.38). Hence, it makes sense to consider the linearized tangent approximation of (7.38) around $e = 0$. It is written as follows

$$\dot{e} = [A(\hat{z}) - K(\hat{z})L]e \tag{7.40a}$$

where $A(\hat{z}) \triangleq Y\left[\frac{\partial \varphi(z)}{\partial z}\right]_{z=\hat{z}} - DI_n$ (7.40b)

Thus, the design problem can be stated as the problem of choosing $K(\hat{z})$ in such a way that the linear time-varying model (7.40) has desirable properties.

7.3.1.1 Exponential observability

The variant form (7.40a) of the observation error dynamics indicates that an arbitrarily fast (exponential) convergence rate of the observation $\hat{z}(t)$ to its true value $z(t)$ can be assigned if the eigenvalues of the matrix $[A(\hat{z}) - K(\hat{z})L]$ by an appropriate choice of the matrix $K(\hat{z})$ can be freely fixed. When such a possibility exists, the system (7.36) is said to be exponentially observable and the observation scheme (7.37) is called an exponential observer.

A simple test to check whether a given system is exponentially observable or not is expressed by the following necessary condition: for the process (7.36) to be exponentially observable the following rank condition holds:

$$rank(O) \triangleq rank \begin{bmatrix} L \\ LA(z) \\ LA(z)^2 \\ \vdots \\ LA(z)^{n-1} \end{bmatrix} = n \qquad A(z) \triangleq Y\left[\frac{\partial \varphi(z)}{\partial z}\right] - DI_n \tag{7.41}$$

along the process trajectories. The matrix O is called the "observability matrix". It is important to note that condition (7.41) is only a necessary (but not a sufficient) exponential observability condition. Its main interest is to provide an easy way to detect those processes which are generically not exponentially observable.

7.3.1.2 Asymptotic observers

When the system (7.36) is not exponentially observable (i.e. when the eigenvalues of $A(\hat{z})-K(\hat{z})L$ cannot be freely assigned) but when the error system (7.40a) has nevertheless an asymptotically stable equilibrium point at $e = 0$, the process can still be observed but with its dynamics partially determined by the experimental conditions through $A(\hat{z})$. Observers of this kind are called asymptotic observers (since one cannot freely assign their dynamics).

7.3.1.3 Extended Luenberger and Kalman Observers

Assume that the system (7.36) is exponentially observable and the observation scheme (7.37) is considered. As have been previously mentioned, the observer design problem is the problem of selecting the gain matrix $K(\hat{z})$. Two standard solutions are respectively the extended Luenberger observer and the extended Kalman observer which are shown below (Brown and Hwang, 1992), (Kwakernaak and Sivan, 1972):

- The extended Luenberger observer

  The design rule for Luenberger observers is to choose the matrix $K(\hat{z})$ such that $e = 0$ is an asymptotically stable equilibrium point of the linear tangent error model (7.40) (Luenberger, 1984), (Luenberger, 1969). This is achieved by choosing $K(\hat{z})$ such that:

  a) the matrix $A(\hat{z})-K(\hat{z})L$ and its time derivative are bounded:

  $$\|A(\hat{z})-K(\hat{z})L\| \le C_1 \qquad \forall \hat{z} \tag{7.42}$$

  $$\left\| \frac{d}{dt}[A(\hat{z})-K(\hat{z})L] \right\| \le C_2 \qquad \forall \hat{z} \tag{7.43}$$

  b) the eigenvalues of $A(\hat{z})-K(\hat{z})L$ have strictly negative real parts

  $$\mathrm{Re}\{\lambda_i[A(\hat{z})-K(\hat{z})L]\} \le C_3 < 0 \qquad \forall \hat{z} \qquad i=\overline{1,n} \tag{7.44}$$

  Under these conditions, it can be shown that $e = 0$ is a stable equilibrium point provided C_2 is sufficiently small.

- The extended Kalman observer

In a Kalman observer, the design is based on a "quadratic optimization" approach. The problem is to find the gain matrix $K(\hat{z})$ which minimizes the mean square observation error :

$$E = \int_0^1 \| z - \hat{z} \|^2 d\tau = \int_0^1 \| e(\tau) \|^2 d\tau \quad (7.45)$$

under the constraint of the linear tangent error model (7.40). The solution is as follows:

$$K(\hat{z}) = P(\hat{z}) L^T \quad (7.46)$$

where the $n \times n$ square symmetric matrix $P(\hat{z})$ is generated by the Riccati equation :

$$\dot{P} = -PL^T LP + PA^T(\hat{z}) + A(\hat{z})P \quad (7.47)$$

It should be noted that this yields a time-varying gain K even in such case where A would be independent of $\hat{z}$.

7.3.2. Different applications

7.3.2.1 Asymptotic observers for state estimation when the growth reaction rates are unknown

Previously the design of state observers was considered under two very restrictive conditions :

- the model (7.36) is exponentially observable
- the structure of the model is fully known.

However there are many simple processes of practical interest which are known to be not exponentially observable. Moreover, the requirement of a full knowledge of the process kinetics is too severe in most engineering applications (Bastin, 1988), (Hulhoven and Bogaerts, 2004). There is therefore a clear incentive to look for a class of observers which allows one to asymptotically reconstruct the missing states even when the process is not exponentially observable and the kinetics are unknown. In this section the problem of estimating the reaction rates from on-line knowledge of the state variables (either from measurements or by means of asymptotic observers) is considered.

7.3.2.1.1 Statement of the estimation problem

The biotechnological process described by the general state space model (7.36) is considered. It is assumed that :

- The yield coefficients (matrix Y) are known.
- The dilution rate D, the feed rates F and gaseous outflow rates Q are measured on-line.
- The vector of state variables z is measured and known.

It is assumed that the vector $\varphi(z)$ of reaction rates is partially unknown and written as:

$$\varphi(z)=H(z)\rho(z) \tag{7.48}$$

where $H(z)$ is an $M \times r$ matrix of known functions of the state and $\rho(z)$ a vector of unknown functions of z with $\dim \rho(z)=r$. With this definition, the process dynamics (7.36) are rewritten as:

$$\dot{z}=YH(z)\rho(z)-Dz-Q+F \tag{7.49}$$

The problem of estimating $\rho(z)$ from the on-line knowledge of *D, F, Q* and z has to be solved.

Two different solutions to this problem are presented (Pomerieau and Perrier, 1988), (Pomerieau, 1988), (Pomerieau and Perrier, 1989) and (Pomerieau, 1990). The first one is called an observer-based estimator because it is based on the use of a type of the state observers described in Section 7.2.6. The second one is based on a reformulation of the process model in a linear regression form.

7.3.2.1.2 An observer-based estimator

The primary idea is to use a state observer, not to estimate the state (since it is known) but to provide real-time information (Moisan and Bernard, 2005) for the updating of the estimate of $\rho(z)$. The estimation algorithm is as follows:

- The observer-based estimator equation

$$\dot{\hat{z}}=YH(z)\hat{\rho}(t)-Dz-Q+F-K(z-\hat{z}) \tag{7.50}$$

$$\dot{\hat{\rho}}=[YH(z)]^T \Gamma(z-\hat{z}) \tag{7.51}$$

where $\hat{\rho}$ denotes the real-time estimate of $\rho(z)$. Equation (7.50) is clearly similar to the general state observer (7.37) but with three decisive alterations:

a) the square matrix K may be dependent on z but must be stable for all $z(t)$.
b) the actual value of the state z is used in the right hand side of the equation (terms $H(z)$ and Dz).
c) The actual value of $\rho(z)$, which is unknown, is replaced by an estimate $\hat{\rho}$ which is reformulated by the second equation (7.51).

Γ is the gain matrix of the reformulating law (7.51), it must be chosen such that the matrix $K^T\Gamma+\Gamma K$ is negative definite. This reformulating law (7.51) is in turn driven by the deviation $(z-\hat{z})$ which is supposed to reflect the mismatch between $\hat{\rho}(t)$ and $\rho(z)$.

- Tuning the estimator

The matrices K and Γ are design parameters at the user's disposal to control the stability and the tracking properties of the algorithm (Oliviera et al, 2002), (Perrier et al, 2000), (Oliviera et al, 1996). A common choice is to take:

$$K=diag\{-\omega_i\},\ i=1,...,n, \quad \Gamma=diag\{\gamma_j\},\ j=1,...,r, \quad \omega_i,\gamma_j \in \Re^* \tag{7.52}$$

With this choice, the condition on $K^T\Gamma+\Gamma K$ is automatically verified. In such case the tuning of the estimator reduces to the calibration by trial and error of the $n + r$ scalar constants ω_i and γ_j.

- Analysis of the estimator
  Define the observation error e and the tracking error $\bar{p}$ as follows:

$$e=z-\hat{z} \qquad \bar{p}=p(z)-\hat{p} \tag{7.53}$$

  Their dynamics are easily shown to be governed by the following linear time-varying system (obtained by subtracting (7.50) from (7.36)) :

$$\begin{bmatrix}\dot{e}\\ \dot{\bar{p}}\end{bmatrix}=A(z)\begin{bmatrix}e\\ \bar{p}\end{bmatrix}+v \tag{7.54}$$

  with

$$A(z)=\begin{bmatrix}K & YH(z)\\ -H^T(z)Y^T\Gamma & 0\end{bmatrix} \qquad v=\begin{bmatrix}0 & \frac{d\rho}{dt}\end{bmatrix}^T \tag{7.55}$$

  Suppose that K is constant with all eigenvalues having strictly real parts and that $\rho(z)$ is differentiable function of z. Then it is the standard result of adaptive system theory that the error system (7.53), (7.54) is stable if the matrix $YH(z)$ is persistently exciting.

- Numerical Implementation
  A numerical implementation of the estimator requires a discrete-time definition. A forward Euler discretization of the continuous-time algorithm (7.50), (7.51) gives :

$$\hat{z}_{t+1}=\hat{z}_t+T\left[YH(z_t)\hat{\rho}_t-Dz_t-Q_t+F_t-K(z_t-\hat{z}_t)\right] \tag{7.56}$$

$$\hat{\rho}_{t+1}=\hat{\rho}_t+T\left[YH(\hat{z}_t)\right]^T\Gamma(z_t-\hat{z}_t) \tag{7.57}$$

  where T denotes the sampling period. As for the numerical implementation of asymptotic observers, the change from the continuous-time observer-based estimator to the discrete-time version sets specific stability questions in which the sampling period T, design parameters K and Γ and the regressor $YH(z_t)$ play a vital role.

The observer-based estimator (7.50), (7.51) and its discrete-time counterpart (7.56), (7.57) are based on the full dynamical model of the process. It is often sufficient to select a subset of the state equations, provided they involve all the parameters $\rho(z)$ which need to be estimated (Farza et al, 1997), (Gauthier and Kupka, 1994).

7.3.2.1.3 A linear regression estimator

An alternative of $\rho(z)$ based on a model reformulation is presented in terms of linear regression.

- Model reformulation
  The solution of the differential equation (7.49) which describes the process dynamics can be shown to be written as follows:

$$z=\psi^T\rho+\psi_0+\varepsilon \tag{7.58}$$

  ψ, ψ_0 and ε are outputs of the following linear filters :

$$\frac{d\psi^T}{dt}=\Omega\psi^T+YH(z) \tag{7.59}$$

$$\frac{d\psi_0}{dt}=\Omega\psi_0-(\Omega+DI_n)z-Q+F \tag{7.60}$$

$$\frac{d\varepsilon}{dt}=\Omega\varepsilon-\psi^T\frac{d\rho}{dt} \tag{7.61}$$

with Ω an arbitrary stable symmetric matrix.

- Introduce the notation :

$$y\underline{\Delta}z-\psi_0 \tag{7.62}$$

It is then obvious that the process dynamics (7.49) are described by the following linear regression model:

$$y=\psi^T\rho+\varepsilon \tag{7.63}$$

where y is the output, ψ is the regressor, ρ is the unknown parameter to be estimated and ε is interpreted as an unknown additive disturbance.

It should be noted that the output y and regressor ψ can be calculated in real-time from the available data *(z , D, Q, F)* with the aid of filtering equations (7.59) – (7.61). The important point is that the linear regression model (7.63) allows to use a standard least squares algorithm for the estimation of $\rho(z)$.

7.3.2.1.4 Extended Kalman Filtering for on-line estimation of reaction rates

In Section 7.2.6 it has been shown how extended Kalman observers can be designed for on-line state estimation when the model structure (and hence the kinetics structure) is fully known. The same technique can be used to solve the dual problem of estimating the reaction rates from full state measurement (Bellgardt et al, 1984), (Caminal et al, 1987), (Dekkers, 1983), (Katoh et al, 1981), (Kotob et al, 1987), (Leigh and Ng, 1984), (Moilanen, 1981), (Nihtila et al, 1984), (Shimizu et al, 1989), (Staniskis and Simutis, 1986), (Takamatsu, 1981) and (Yoo et al, 1985). The basic idea is to consider the unknown parameter ρ as an additional unknown state of the process. The state space model (7.49) is therefore augmented as follows:

$$\begin{bmatrix}\dot{z}\\ \dot{\rho}\end{bmatrix}=\begin{bmatrix}YH(z)\rho-Dz+F-Q\\ w(t)\end{bmatrix} \tag{7.64}$$

where *w(t)* is a completely unknown time-varying function. A state observer, analogous to (7.37), is written for that system:

$$\frac{d}{dt}\begin{bmatrix}\hat{z}\\ \hat{\rho}\end{bmatrix}=\begin{bmatrix}KH(\hat{z})\hat{\rho}-D\hat{z}+F-Q\\ 0\end{bmatrix}+\begin{bmatrix}K_1(\hat{z},\hat{\rho})\\ K_2(\hat{z},\hat{\rho})\end{bmatrix}(z-\hat{z}) \tag{7.65}$$

w(t) is replaced by zero in the observer equation since it is an a priori unknown quantity.

The extended Kalman filtering (EKF) technique is then used to compute the gain matrices K_1 and K_2 on-line. The linearized tangent approximation of (7.65) is written:

$$\frac{d}{dt}\begin{bmatrix} z-\hat{z} \\ \rho-\hat{\rho} \end{bmatrix} = \begin{bmatrix} A(\hat{z},\hat{\rho})-K_1(\hat{z},\hat{\rho}) & YH(\hat{z}) \\ -K_2(\hat{z},\hat{\rho}) & 0 \end{bmatrix}\begin{bmatrix} z-\hat{z} \\ \rho-\hat{\rho} \end{bmatrix} \tag{7.66}$$

with $$A(\hat{z},\hat{\rho}) = K\left[\frac{\partial H(z)\hat{\rho}}{\partial z}\right]_{z=\hat{z}} - DI_n \tag{7.67}$$

The gain matrices K_1 and K_2 are computed in order to minimize the following quadratic criterion :

$$J(t) = \int_0^t \left\{ \left(\frac{d\hat{\rho}^T}{dt}(\tau)\right)\Sigma^{-1}\left(\frac{d\hat{\rho}}{dt}(\tau)\right) + \| z(\tau)-\hat{z}(\tau)\|^2 \right\} dt \tag{7.68}$$

under the constraint of the linearized tangent model (7.66). The criterion is a weighted sum of two terms (weighting matrix Σ^{-1}) : the first term penalizes fast variations of the parameter estimate $\hat{\rho}$ while the second term penalizes too large deviations between the actual state value z and its estimate $\hat{z}$.

The solution of this optimization problem is as follows. The time-varying symmetric matrix *P(t)* :

$$P(t) \triangleq \begin{bmatrix} P_{11}(t) & P_{12}(t) \\ P_{12}(t) & P_{22}(t) \end{bmatrix} \tag{7.69}$$

is updated via the following Riccati equation :

$$\frac{dP}{dt} = -PE_0P + PA_0^T(\hat{z},\hat{\rho}) + A_0(\hat{z},\hat{\rho})P + \Sigma_0 \tag{7.70}$$

where $$E_0 \triangleq \begin{bmatrix} I_n & 0 \\ 0 & 0 \end{bmatrix} \qquad \Sigma_0 \triangleq \begin{bmatrix} 0 & 0 \\ 0 & \Sigma \end{bmatrix} \tag{7.71}$$

and $A_0(\hat{z},\hat{\rho})$ is the coefficient matrix of the system (7.66). The gains K_1 and K_2 are given by :

$$K_1(\hat{z},\hat{\rho}) = P_{11}(t) \tag{7.72}$$

$$K_2(\hat{z},\hat{\rho}) = P_{12}(t) \tag{7.73}$$

The EKF estimator thus consists of equations (7.65), (7.70) (7.72) and (7.73). It appears to have a similar structure to that of the observer-based estimator (7.50). However the computation complexity is increased by the need to solve the Riccati

equation (7.70) on-line. An additional drawback of the EKF approach is that its stability and convergence properties are extremely difficult to analyze and are still an open problem in the case of parameter estimation in nonlinear systems. It is well known, however, that an EKF estimator may give biased estimates or may even diverge if it is not carefully initialized (Ljung, 1999). Therefore, although the EKF estimator may often yields interesting results, there is no a priori guarantee as to its stability.

7.3.2.2 State and parameter estimation with unknown yield coefficients

A biotechnological process described by the general space model (7.49) is considered: i.e. where the reaction rate vector $\varphi(z)$ is expressed as the product of a $M \times r$ matrix $H(z)$ of known functions of z and a vector $\rho(z)$ of unknown function of z $(\dim \rho(z)=\tau)$. In addition, it is supposed that (some of) the yield coefficients (matrix Y) are unknown.

7.3.2.2.1 Conditions for estimating ρ independently of the unknown yield coefficients

The dynamics of the vector ζ are stated as:

$$\zeta = A_0 z_a + z_b \tag{7.74}$$

defined in the structural property which is equal to :

$$\dot{\zeta} = -D\zeta + A_0(F_a - Q_a) + (F_b - Q_b) \tag{7.75}$$

Assume that the $(n-p)$ vector ζ can be expressed as a linear combination of vectors z_1 and z_2 of measured and non measured variables (Bastin and Dochain, 1986) and (Bernard and Gouze, 2004) i.e.

$$\zeta = A_1 z_1 + A_2 z_2 \tag{7.76}$$

The dynamics of the measured variables z_1 are equal to:

$$\frac{dz_1}{dt} = Y_1 H(z_1, z_2)\rho(z_1, z_2) - Dz_1 + F_1 - Q_1 \tag{7.78}$$

The kinetics term $Y_1 H(z_1, z_2)\rho(z_1, z_2)$ is in general a function of some of the unknown components of z_2. Assume that these components can be expressed from (7.76) as function of z_1 and ζ only (in the particular situation when all the components of z_2 explicitly appear in $Y_1 H(z_1, z_2)\rho(z_1, z_2)$, this means that then A_2 must be left invertible.

Then the kinetics term $Y_1 H(z_1, z_2)\rho$ can be rewritten in terms of the measured states z_1 and of the auxiliary states ζ :

$$Y_1 H(z_1, z_2)\rho = \Phi(z_1, \zeta)\rho \tag{7.78}$$

where $\Phi(z_1, \zeta)$ is $q \times M$ matrix which is a function of z_1 and ζ .

7.3.2.2.2 Joint Estimation of Yield Coefficients and Specific Reaction Rates

A general method was described in (7.3.2.1) where the yield coefficients (i.e. the matrix Y) are known. Earlier on, the case where some of the yield coefficients are unknown but can be eliminated from the estimation procedure by appropriate model transformations was discussed. In this section, the situation where all the yield coefficients are unknown is considered. The possibility of simultaneous on-line estimation of both specific reaction rates $\alpha(z)$ and yield coefficients (matrix Y), from full state measurement and partial state measurement (Bastin et al, 1988) is considered.

7.3.2.2.2.1 Full State measurement

Let's consider biotechnological processes described by the state space model (7.79):

$$\frac{dz}{dt} = YG(z)\alpha - Dz + F - Q \tag{7.79}$$

It is assumed that:

1) The full state z is measured on-line
2) The dilution rate D, the feed rates F and the gaseous outflow rates are known on-line.
3) The yield coefficients (matrix Y) and the specific reaction rates α are unknown.

The problem is to design an estimator of Y and α .

If N_j is the number of components involved in the reaction with index j, it is then easy to see that the total number m of unknown yield coefficients in K (denoted $k_1, k_2, ..., k_m$) is given by :

$$m = \sum_{i=1}^{M} (N_j - 1) \tag{7.80}$$

Moreover, there are obviously M parameters α_j (j = 1, ..., M) in the model (7.79). Hence the total number of unknown parameters is :

$$m + M = \sum_{i=1}^{M} N_j \tag{7.81}$$

Now, due to its particular structure, the vector $YG(z)\alpha$ may be rewritten in a linear regression form as follows:

$$YG(z)\alpha \underline{\underline{\Delta}} \Phi(z)\theta \tag{7.82}$$

In this expression, $\Phi(z)$ is a $N \times (m+M)$ matrix of known multilinear combinations of state variables. $\theta^T = [\theta_1, \theta_2, ..., \theta_{m+M}]$ is a vector of bilinear combinations of the unknown parameters $d_i\,(i=1,...,m)$ and $\alpha_j\,(j=1,...,M)$. It is formally written as follows:

$$\theta = f(\alpha, d) \tag{7.83}$$

An important point is that the function f in (7.83) is invertible, that is α and d can be computed uniquely from θ

$$\begin{bmatrix} \alpha \\ d \end{bmatrix} = f^{-1}(\theta) \tag{7.84}$$

With the definition (7.82), the process model (7.79) is rewritten as follows:

$$\frac{dz}{dt} = \Phi(z)\theta - Dz + F - Q \tag{7.85}$$

Since the unknown parameter θ enters linearly in (7.85), a natural solution is to estimate it with algorithms similar to the previous point and then recover α and d with the inverse function (7.84). The algorithms are written as follows:

- Observer-based Estimator

$$\frac{d\hat{z}}{dt} = \Phi(z)\hat{\theta} - Dz + F - Q - K(z - \hat{z}) \tag{7.86}$$

$$\frac{d\hat{\theta}}{dt} = \Phi^T(z)\Gamma(z - \hat{z}) \tag{7.87}$$

$$\begin{bmatrix} \hat{\alpha} \\ \hat{d} \end{bmatrix} = f^{-1}(\hat{\theta}) \tag{7.88}$$

- Linear Regression Estimator

$$\frac{d\psi^T}{dt} = \Omega\psi^T + \Phi(z) \tag{7.89}$$

$$\frac{d\psi_0}{dt} = K\psi_0 + (K - DI_n)z - Q + F \tag{7.90}$$

$$\frac{d\hat{\theta}}{dt} = \Gamma\psi(\xi - \psi_0 - \psi^T\hat{\theta}) \tag{7.91}$$

$$\frac{d\Gamma}{dt} = -\Gamma\psi\psi^T\Gamma + \lambda\Gamma \tag{7.92}$$

$$\begin{bmatrix} \hat{\alpha} \\ \hat{d} \end{bmatrix} = f^{-1}(\hat{\theta}) \tag{7.93}$$

7.3.2.2.2.2 Partial state measurement

The problem of joint estimation of yield coefficients and specific reaction rates, but when only a part of the state is measured on-line is considered.

It is assumed that:

1) the subset of measured state variables is denoted z_1; the set of remaining non measured states is denoted z_2, so that (z_1, z_2) is a state partition which in turn induces the similar partitions $(Y_1, Y_2), (F_1, F_2), (Q_1, Q_2)$
2) there exist a nice state partition (z_a, z_b), with an associated auxiliary state ζ:

$$\zeta = A_0 z_a + z_b = A_1 z_1 + A_2 z_2 \tag{7.94}$$

which obeys the following dynamics:

$$\dot{\zeta} = -D\zeta + F_b - Q_b \tag{7.95}$$

3) the matrix A_2 is left invertible

Under these assumptions, the state space model (7.36) is equivalent to:

$$\frac{dz_1}{dt} = Y_1 G\left(z_1, A_2^+(\zeta - A_1 z_1)\right)\alpha - Dz_1 + F_1 - Q_1 \tag{7.96}$$

$$\dot{\zeta} = -D\zeta + F_b - Q_b \tag{7.97}$$

Now, as in the previous section, it is easily seen that the term $Y_1 G\left(z_1, A_2^+(\zeta - A_1 z_1)\right)\alpha$ may be rewritten as:

$$Y_1 G\left(z_1, A_2^+(\zeta - A_1 z_1)\right)\alpha \triangleq \Phi(z_1, Z)\theta \tag{7.98}$$

The structures of Φ and θ are however slightly different from the previous ones. $\Phi(z_1, \zeta)$ is now a matrix of known polynomial combinations of measured states z_1 and the auxiliary state ζ. θ is a vector of polynomial combinations of some of the unknown parameters d_i and α_j, denoted as before in (7.84). It may arise, however, that this function f is not completely invertible. Then, in contrast with the previous case, only a few d_i and α_j can be recovered from θ. With the "reparametrization" (7.98), the model (7.96), (7.97) is rewritten:

$$\frac{dz_1}{dt} = \Phi(z_1, Z)\theta - Dz_1 + F_1 - Q_1 \tag{7.99}$$

$$\frac{d\zeta}{dt} = -D\zeta + F_b - Q_b \tag{7.100}$$

The solution to the estimation problem appears readily: it suffices to combine a parameter estimator for θ with an asymptotic observer for ζ. For instance, an observer-based estimator is written as follows:

- Observer-based Estimator

$$\dot{\zeta} = -D\zeta + F_b - Q_b \tag{7.101}$$

$$\dot{\hat{z}} = \Phi\left(z_1, \hat{\zeta}\right)\hat{\theta} - Dz_1 + F_1 - Q_1 - K_1\left(z_1 - \hat{z}_1\right) \tag{7.102}$$

$$\frac{d\hat{\theta}}{dt} = \Phi^T\left(z_1, \hat{\zeta}\right)\Gamma\left(z_1 - \hat{z}_1\right) \tag{7.103}$$

7.3.2.2.3 Adaptive Observers

The problem of joint estimation of the yield coefficients d_i and specific reaction rates α_j from partial state measurement z_1 (Hulhoven and Bogaerts, 2005), (van Impe and Bastin, 1995), (Marcos et al, 2004), (Titica et al, 2003), (Nejjari et al, 1999), (Bastin and Gevers, 1988), (Gouze et al, 2000), (Mailleret et al, 2004), and (Rapaport and Gouze, 2003) was considered. The possibility of estimating jointly the yield coefficients, the specific reaction rates and missing states is considered now. The algorithms designed for the purpose are called adaptive observers which are made adaptive by introducing on-line parameter estimation (Kreisselmeier, 1977),(McInnis et al, 1979) (Mareels et al, 1987) and (Narenda and Annaswany, 1989).

- Extended Luenberger adaptive observer

A first solution is to combine a Luenberger observer with the observer-based parameter estimator (7.101) – (7.103) (Luenberger, 1984), (Luenberger, 1969). The adaptive observer is as follows:

$$\frac{d\hat{z}}{dt} = \Phi\left(\hat{z}\right)\hat{\theta} - D\hat{z} + F - Q + K\left(z - \hat{z}\right) \tag{7.145}$$

$$\frac{d\hat{\theta}}{dt} = \Phi^T\left(\hat{z}\right)\Gamma\left(z_1 - \hat{z}_1\right) \tag{7.105}$$

- Extended Kalman filtering

Extended Kalman filtering can be used for state estimation (Krauss et al, 1994) or for parameter estimation. Obviously, it can also be used for both together. In that case, the adaptive observer is written as follows:

$$\frac{d\hat{z}}{dt} = \Phi\left(z\right)\hat{\theta} - D\hat{z} + F - Q + K_1\left(\hat{z}, \hat{\theta}\right)\left(z_1 - \hat{z}_1\right) \tag{7.106}$$

$$\frac{d\hat{\theta}}{dt} = K_2\left(\hat{z}, \hat{\theta}\right)\left(z_1 - \hat{z}_1\right) \tag{7.107}$$

where K_1 and K_2 are updated by an appropriate Riccati equation.

- An asymptotic adaptive observer

A third solution is the following one. It is supposed that all the yield coefficients involved in A_1 and A_2 (equation (7.94)) can be calculated from θ. Then, an adaptive observer is readily obtained by augmenting the observer-based parameter estimator as follows:

$$\dot{\zeta} = -D\hat{\zeta} + F_b - Q_b \tag{7.108}$$

$$\dot{\hat{z}} = \Phi\left(z_1, \hat{\zeta}\right)\hat{\theta} - Dz_1 + F_1 - Q_1 - K_1\left(z_1 - \hat{z}_1\right) \tag{7.109}$$

$$\frac{d\hat{\theta}}{dt} = \Phi^T\left(z_1, \hat{\zeta}\right)\Gamma\left(z_1 - \hat{z}_1\right) \tag{7.110}$$

$$\hat{z}_2 = \hat{A}_2^+\left(\hat{\zeta} - \hat{A}_1 z_1\right) \tag{7.111}$$

where $\hat{A}_2^+$ and $\hat{A}_1$ respectively denote the matrices A_2^+ and A_1 whose nonzero entries are substituted by the corresponding estimates.

7.3.3 Estimation of yield coefficients

7.3.3.1 The estimation problem

The problem of estimating the yield coefficients independently of the reaction rates is considered for biotechnological processes described by the general dynamical model (7.36) under the following conditions:

1) the yield coefficients (matrix Y) are unknown;
2) the reaction rates $\varphi(z)$ are unknown;
3) the full state z is measured;
4) the substrate feed rates F, the gaseous outflow rates Q and the volume V are measured

On this basis, the possibility of estimating the yield coefficients independently of the reaction rates is considered. For the first step, a linear regression form equivalent to the model (7.36) but independent of the reaction rates $\varphi(z)$ is considered.

7.3.3.2 A linear regression form

Let's consider a partition of the model (7.36):

$$\frac{dz_a}{dt} = Y_a\varphi(z) - Dz_a + F_a - Q_a \tag{7.112}$$

$$\frac{dz_b}{dt} = Y_b\varphi(z) - Dz_b + F_b - Q_b \tag{7.113}$$

with $\dim(z_a) = p = rank(Y)$ and $\dim(z_b) = n - p$

The auxiliary time-varying quantities:

$$\eta_a(t) \triangleq V(t)z_a(t) - V(0)z_a(0) + \int_0^t \left[F_{out}z_a + V\left(Q_a - F_a\right)\right]d\tau \tag{7.114}$$

$$\eta_b(t) \triangleq V(t)z_b(t) - V(0)z_b(0) + \int_0^t \left[F_{out}z_b + V\left(Q_b - F_b\right)\right]d\tau \tag{7.115}$$

where V denotes the volume and F_{out} the effluent flow rate. Note in the integral of expressions (7.114) and (7.115) that the first term $\left(F_{out}z_a,\ F_{out}z_b\right)$ respectively is equal to zero in first and second reactors and that the second term $\left(V\left(Q_a - F_a\right) and V\left(Q_b - F_b\right)\right)$ respectively represents the cumulated mass of introduced

feed and produced gas. Then, straightforward calculations and integration lead to the following relationship between $\eta_a(t)$ and $\eta_b(t)$:

$$\eta_b(t) = -A_0 \eta_a(t) \tag{7.116}$$

where A_0 is the solution of the matrix equation:

$$A_0 Y_a + Y_b = 0 \tag{7.117}$$

Most often, K_a is a square $M \times M$ nonsingular matrix, such that $A_0 = -Y_b Y_a^{-1}$ and (7.116) is rewritten as:

$$\eta_b(t) = (Y_b Y_a^{-1}) \eta_a(t) \tag{7.118}$$

Let us now denote by $\theta = [\theta_1, ..., \theta_l]$ $(\dim(\theta) = l)$ the vector of the entries of the matrix A_0 which are not identically zero. Expression (7.118) is rewritten in the following linear regression form:

$$\eta_b(t) = R^T(\eta_a(t))\theta \tag{7.119}$$

where $R^T(\eta_a(t))$ is a $(n-p) \times l$ matrix, function of $\eta_a(t)$. This form is independent of the kinetics.

7.3.3.3 Estimators of the parameter vector θ

Suppose that measurements of z, F and Q have been collected during a time interval $[0, t_i]$. Obviously, expression (7.120) naturally suggests using a linear regression technique to estimate θ independently of the reaction rates $\varphi(z)$. The standard least squares algorithm is written as follows in this case:

$$\hat{\theta} = \left\{ \int_0^{t_i} [R(\eta_a) R^T(\eta_a)] d\tau \right\}^{-1} \int_0^{t_i} [R(\eta_a) \eta_b] d\tau \tag{7.120}$$

The matrix inversion can be avoided by using a recursive form of this algorithm:

$$\frac{d\hat{\theta}}{dt} = \Gamma R(\eta_a) [\eta_b - R^T(\eta_a)\hat{\theta}] \tag{7.121}$$

$$\frac{d\Gamma}{dt} = -\Gamma R(\eta_a) R^T(\eta_a) \Gamma \tag{7.122}$$

The algorithm (7.120) is a tool for estimating the parameter θ. But the goal is actually to estimate the yield coefficients, which is the vector $d = d_1, d_2, ..., d_m$. θ is a nonlinear rational function of d which is writtten formally as follows:

$$\theta = f(d) \tag{7.123}$$

Therefore the question arises whether d can be calculated from the knowledge of θ or not. This is called the structural identifiability issue (Chen et al, 1990) and (Chen, 1990). It is evidently of interest to be able to detect beforehand those models which are not identifiable whatever the experimental conditions. A trivial condition is obviously that the number of unknown yield coefficients cannot be larger than the number of parameters θ_i.

7.3.4 Other Parameter Estimation Issues in Bioreactors

The general dynamical model (7.36) is a combination of two terms - $K\varphi(z)$ describes the process kinetics while $-Dz+F-Q$ represents the mass transport (or dilution) dynamics.

In the previous parts of this chapter, the focus was either on real time estimation of the state z or on estimation of the parameters related to the kinetics $Y\varphi(z)$ (Goldbic et al, 2000), (Barbu et al, 2005), (Barbu et al, 2004), (Brdys and Zhang, 2001a), (Nejjari et al, 1999), (Sotomayer and Garcia, 2002), (Vega and Gutierrez, 1999), (Al-Ghazzawi, 2001), (Ali and Zafiriou, 1993), (Marsili-Libelli and Guinti, 2002), (Marsili-Libelli, 1990), (Goodwin et al, 1980), (Holmberg and Ranta, 1982) and (Holmberg, 1983b). But unknown parameters can also be hidden in the transport dynamics, for which the methods followed so far are easily extended (Betanair et al, 2004b), (Moreno, 1999), (Smits et al, 2002), (van Impe, 1998). These two issues are discussed below:

7.3.4.1 Estimation of specific liquid gas transfer rates

It is legitimate to consider that the gaseous outflow rates Q_i are proportional to the concentrations z_i in the liquid phase:

$$Q_i = \beta_i z_i \tag{7.124}$$

as long as z_i is lower than the saturation level. The parameters β_i are termed specific liquid-gas transfer rates. Define the vector β containing those parameters β_i. Then, it is clear the model (7.36) can be rewritten as follows:

$$\frac{dz}{dt} = \Phi(z)\theta - Dz + F - \psi(z)\beta \tag{7.125}$$

where $\psi(z)$ is a $n \times \dim(\beta)$ matrix which depends linearly on z. If it is defined:

$$\Phi^*(z)=[\Phi(z),\psi(z)] \qquad \theta^*=\begin{bmatrix}\theta\\ \beta\end{bmatrix} \tag{7.126}$$

the model (7.125) is also written as:

$$\frac{dz}{dt}=\Phi^*(z)\theta^*-Dz+F \tag{7.127}$$

It is evident that the augmented parameter θ^* can be estimated by any of the algorithms which have been built for θ, just replacing Φ by Φ^* and θ by θ^*. It is however needed that the augmented regressor Φ^* is persistently exciting.

7.3.4.2 Estimation of oxygen related parameters

Numerous studies has given rise to concerns about parameters related to the dissolved oxygen concentration which is often the most easily measurable state (Aubrun et al, 2001), (Bogaerts and Wouwer, 2004), (Assis and Filho, 2000), (Spagni et al, 2001), (Assis and Filho, 2000), (Brdys and Konarczak, 2001b), (Ingildsen, 2002a), (Ingildsen et al, 2002b), (Francisco et al, 2005), (Wimberger and Verde, 2005), (Lindberg and Carlson, 1996), (Tromans, 1999), (Vogelaar et al, 1996), (O'Brien et al, 2005), (Brdys and Diaz-Marquez, 2002), (Maciejowski, 2002), (Zhang et al, 2005), (Holmberg and Olsson, 1986) and (Ko et al, 1982). Let's consider the aerobic process described by the following scheme: $S+S_0\rightarrow X$ with S the substrate, X the biomass and S_0 the dissolved oxygen. The biomass and dissolved oxygen dynamics are written as follows:

$$\frac{dX}{dt}=\mu X-DX \tag{7.128}$$

$$\frac{dS_0}{dt}=-k_2\mu X-DS_0+K_La(S_{0S}-S_0) \tag{7.129}$$

where K_La and S_{0S} denote the mass transfer coefficient and the saturation concentration respectively. These equations may be reformulated as follows:

$$\frac{d}{dt}\begin{bmatrix}X\\ S_0\end{bmatrix}=\begin{bmatrix}X & 0 & 0 & 0\\ 0 & -X & 1 & -S_0\end{bmatrix}\begin{bmatrix}\mu\\ k_2\mu\\ K_LaS_{0S}\\ K_La\end{bmatrix}-D\begin{bmatrix}X\\ S_0\end{bmatrix} \qquad \underline{\underline{\Delta}}\,\Phi^*(z)\theta^*-Dz \tag{7.130}$$

$$\text{with } \Phi^*(z)=\begin{bmatrix}X & 0 & 0 & 0\\ 0 & -X & 1 & -S_0\end{bmatrix} \text{ and } \theta^*=\begin{bmatrix}\theta_1'\\ \theta_2'\\ \theta_3'\\ \theta_4'\end{bmatrix}=\begin{bmatrix}\mu\\ k_2\mu\\ K_LaS_{0S}\\ K_La\end{bmatrix} \tag{7.131}$$

The model is thus clearly in the format for parameter estimation. We see, in addition, that the reparametrization θ^* is invertible, that is estimates of μ, k_2, $K_L a$ and S_{0S} can be recovered as follows:

$$\hat{\mu}=\hat{\theta}_1' \quad \hat{k}_2=\frac{\hat{\theta}_2'}{\hat{\theta}_1'} \quad \hat{K}_L a=\hat{\theta}_4' \quad \hat{S}_{0S}=\frac{\hat{\theta}_3'}{\hat{\theta}_4'} \tag{7.132}$$

In addition, an on-line estimate of the "oxygen uptake rate", OUR is given by:

$$\hat{OUR}=\hat{\theta}_2' X \tag{7.133}$$

Various relationships for the estimation of oxygen related parameters in aerobic processes have been proposed (Marsili-Libeili, 1983) and (Marsili-Libeili, 1985). For instance, one can assume that the mass transfer coefficient $K_L a$ is proportional to the aeration flow rate:

$$K_L a=k_0 F_g \tag{7.134a}$$

and hence, rewrite (7.134a) as follows:

$$\frac{dS_0}{dt}=\begin{bmatrix}-1 & F_g & -S_0 F_g\end{bmatrix}\begin{bmatrix}OUR \\ k_0 S_{0S} \\ k_0\end{bmatrix}-DS_0 \tag{7.134b}$$

that is directly proceed to the estimation of the oxygen uptake rate OUR, together with the parameters k_0 and S_{0S}.

7.4 Overview and comparison of the methods for parameter and state estimation of the activated sludge process

The most difficult problems in the implementation of the advanced control strategies in fermentation and wastewater treatment processes are the possibilities of obtaining reliable on-line values of the state of the process. Measurement of the different components of the biomass and substrate requires time consuming and expensive analyses. Real time analyzers such as respirometers, optical density meters, ATP-analyzers, organic carbon analyzers are developed, but they are expensive, not enough reliable and not in common use. That is why the need for mathematical state estimation is great. The limitation on the estimation problem formulation and solution is that in the real plant very little types of variables could be measured on-line, such as the dissolved oxygen concentration, oxygen transfer, temperature, pH, flow rates of air, mixed liquor flow rates. Most important variables to be estimated are the OUR, influent load S_S, effluent load S_e, organism growth μ, biomass concentration $x(t)$.

The approaches relevant to estimation in the field of wastewater treatment are considered here. In recent years there has been the development of the so called software sensors. A software sensor is an algorithm for the on-line estimation of state variables and parameters which are not measurable in real time, based on related measurements which are more easily acceptable. Very often biomass identification is estimated through measurement of related variables and an on-line estimation algorithm observer based on the process model.

The principles underlying the design of the observers can be quite different because the choice of the observer inherently depends on the problem under consideration. In practice this choice is strongly related to the reliability of the process model as well as the amount and accuracy of the data

- if a reliable process model is available and if this model has been thoroughly estimated and validated, a Kalman filter or high gain observer can be designed
- if the process model is not accurate enough, an asymptotic observer using mass-balance models with uncertain kinetics can be developed
- if bounds of uncertain inputs or parameters are known an interval observer can be developed to predict the intervals in which the immeasurable variables are guaranteed to belong.

7.4.1. Interval observers

There are many cases in the wastewater treatment where the mathematical models are not good approximation of the process or where the measurement errors are big. In these situations an exact observer cannot be developed because there is not guarantee that the observation error will converge to zero asymptotically. Then in order to solve the problem the observation principle can be weakened. Not the exact states are estimated, but rigorous bounds enclosing the estimated state are derived by accounting for the uncertainty of the process model (Rapaport & Gouze, 1999), (Gouze et al., 2000).

Interval observers require knowledge of the uncertainty time varying bounds $v^-(t) \le v(t) \le v^+(t)$. These bounds are used to calculate the time-varying bounds of the state variables under estimation. For the case of the general model

$$\dot{x}(t) = f[x(t), u(t), \omega(t)] \qquad x(t_0) = x_0 \tag{7.135}$$

$$y(t) = h[x(t), v(t)] \tag{7.136}$$

where $\omega \in R^r$ and $v \in R^s$ are the uncertain quantities, lower and upper bounds are known

$$\omega^-(t) \le \omega(t) \le \omega^+(t), \quad t > t_0 \tag{7.137}$$

$$v^-(t) \le v(t) \le v^+(t), \quad t > t_0 \tag{7.138}$$

The development of the interval observer is based on the fixed model structure set of measured data and on the lower and upper bounds of the uncertainties. This observer has the form

$$\dot{z}^- = f\left(z^-, z^+, u, y, \omega^-, \omega^+, v^-, v^+\right), \; z^-(t_0) = g^-\left(x_0^-, x_0^+\right) \tag{7.139}$$

$$\dot{z}^+ = f\left(z^-, z^+, u, y, \omega^-, \omega^+, v^-, v^+\right), \; z^+(t_0) = g^+\left(x_0^-, x_0^+\right) \tag{7.140}$$

$$x^- = h^-\left(z^-, z^+, u, y, \omega^-, \omega^+, v^-, v^+\right) \tag{7.141}$$

$$x^+ = h^+\left(z^-, z^+, u, y, \omega^-, \omega^+, v^-, v^+\right) \tag{7.142}$$

and provides lower and upper bounds of the state variables. The interval observer exists if for any initial condition $x^-(t_0) \le x(t_0) \le x^+(t_0)$ there exist bounds $z^-(t_0), z^+(t_0)$ such that the solution of the system of the model and observer always results in

$$x^-(t) \le x(t) \le x^+(t), t > t_0 \tag{7.143}$$

The bounds x^-, x^+ can be very large and practically not applicable. However for linear system it is proved that the x^- and x^+ converge to a limit interval of finite magnitude (Gouze et al., 2000).

7.4.2 Joint state and parameter estimation

Because of the nonlinear feature of the biological process dynamics and the large uncertainty of some process parameters, mainly the process kinetics, the implementation of extended version of classical observers is difficult. In this case joint state and parameter estimation procedures are very successful as observer based estimator, least squares observers or joint observer estimator variants.

7.4.2.1 Case of measurement of DO.

An asymptotic estimator for on-line tracking of unavailable states and unknown parameters of the bioprocess is developed in (Nejjari et al, 1999). The asymptotic estimator uses process physics in a direct manner to develop a nonlinear observer applicable to the activated sludge process. The asymptotic estimator is developed for a single variable, simplified model of the ASP under the following assumptions:

- the dilution rate $D(t) = Q_{in}/V$ and the aeration flow rate u(t) are the two control variables
- the yield coefficient is known
- a noisy measure of the dissolved oxygen S_O is available
- the biomass, substrate and recycled biomass concentrations are unavailable on-line
- the control variables are bounded

The asymptotic estimator consists of an adaptive observer which combines a priori knowledge of the physical bioprocess with the experimental data. It computes estimated values of the unavailable biomass, substrate and recycled biomass variables and the specific growth rate $\mu(t)$ using the dissolved oxygen concentration $S_O(t)$ as a unique measured variable. A bootstrap method for joint state and parameter estimation for bilinear systems with one input and one output is presented in (Dai et al., 1989). It is applicable to the dissolved oxygen dynamics, which are also described by a bilinear model.

7.4.2.2 Case of measurement of nitrate-nitrogen concentration (process product).

A two stage algorithm for on-line estimation of nitrification process is presented in (Marsili-Libelli & Giovannini, 1997). An asymptotic observer for the autotrophic biomass is derived first based on output nitrate-nitrogen measurements under the assumptions that

- the process runs in a completely mixed aerator
- no denitrification exists either in the aeration basin or in the secondary settler

Discrete version of the estimator is derived and its stability is investigated. The second stage of the algorithm represents estimation of the nitrification kinetics using conventional recursive least squares. The estimators derived in the two phases are coupled together. The effectiveness of the combined algorithm is tested by computer simulations.

7.4.2.3 Case of measurements of the substrate concentration

An asymptotic interval observer for estimation of the concentration of biomass on the basis of measurement of substrate concentration and the specific growth rate is developed in (Fuchard et al., 2002). The interval observer is based on the principle of comparative systems. This approach assumes a bounded uncertainty and provides tools to determine the bounds in which the state must lie. It is a very robust approach,

but it can be too conservative. The development is done only for single substrate-single organism mass balance model of aerobic tank.

Measurement of the substrate concentration and an extended Kalman filter in order to estimate the biomass concentration are developed in (Albiol et al., 1993).

7.4.2.4 State and parameter estimation for phosphorus removal

Biological phosphorus removal involved in the activated sludge process requires more efficient on-line monitoring and process control. However the corresponding models are more complex and the on-line measurements are not available. State and parameter estimation technique are developed in (Zhao & Kummel, 1995) for the phosphorus removal dynamics using specially developed reduced model based on process insights and ASM No. 2. Application of the extended Kalman filter is developed for the state estimation. Least squares algorithm is applied for parameter estimation. Simultaneous state and parameter estimation algorithm is developed on the basis of the previous two by describing the process using an augmented model in which the uncertain parameters are considered as additional states. Then the Kalman filter algorithm is applied to the augmented model. The filter calculates the substrate concentration in the aeration tank and two important model parameters using only the available phosphate measurements.

7.4.3 Estimation of the parameters associated with the oxygen consumption and transfer

7.4.3.1 Oxygen Transfer Function Models

There are different models of K_{La} described in the literature. The simplest one is when there is no aeration control, it is assumed that the aerators are on during the whole time. This type is known as the constant K_{La} function. The second type is a linear function (Heersman & Keesman, 1995), (Holmberg & Olsson, 1985), (Holmberg, 1990), (Lukasse et al, 1996). Different nonlinear models are proposed: second order model (Holmberg, 1990), a squared root model is proposed by Lukasse et al., 1996. An exponential model is proposed by Lindberg, 1997 and a Monod type of model is given in (Lira et al.,2004)

$$K_{La}(u) = K_1 \tag{7.144}$$

$$K_{La}(u) = K_1 u \tag{7.145}$$

$$K_{La}(u) = K_1 u + K_3 u^2 \tag{7.146}$$

$$K_{La}(u) = K_3\sqrt{u} \tag{7.147}$$

$$K_{La}(u) = K_1\left(1 - e^{-K_2 u}\right) \tag{7.148}$$

$$K_{La}(u) = K_1 u/(u + K_2) \tag{7.149}$$

The function $K_{La}(u)$ varies slowly with time constant of hours or day.

7.4.3.2 Respiration rate model

The oxygen transfer coefficient and oxygen uptake rate (respiration rate) are both important control variables which cannot be measured directly. Knowledge of the oxygen uptake rate can be used as an indicator of sludge activity for on-line control of sludge return. The importance of these variables gives additional incentive for providing research in their identification (Ko et al., 1982). One of the first papers identifying both of them together on the basis of recursive Bayesian approach is (Holmberg & Olsson, 1985) for linear representation of the oxygen transfer rate.

The respiration rate is closely related to the amount of biomass and biodegradation of substrates. The respiration rate is a disturbance input to the dissolved oxygen model because of the respiration rate is affected by microbial activity, influent characteristics, flow rate etc. it is not possible to represent it by a mathematical formulation. It is established that:

- the respiration in many domestic wastewater treatment processes has sinusoidal behaviour due to the large diurnal fluctuations in the flow rate and the concentration of the input waste materials
- the respiration rate in industrial wastewater has a step-like behaviour
- Some models of the respiration rate are proposed in (Lindberg, 1997). These models are random walk model, filtered random walk model, integrated random walk model (Olsson & Newell, 1999)

In general, the oxygen transfer rate varies much more slowly (in a matter of days) in comparison with the respiration rate $R(t)$ which is directly related to the biological activity and varies in a matter of minutes (Yoo & Lee, 2004).

In closed reactor fermentation processes the oxygen transfer rate $K_{La}[S_{OS} - S_O(t)]$ can be computed from the analyses of O_2 and CO_2 in the exhaust gases and from the air flow rate into the reactor. In the activated sludge process the oxygen transfer rate cannot be determined directly and then the parameters representing the oxygen transfer coefficient as a function of the air flow rate must be estimated. In (Holmberg &

Ranta, 1982) the oxygen transfer coefficient is represented as linear function of the air flow rate

$$K_{La} = K_1 + K_2 u(t) \tag{7.150}$$

After substitution into the equation for the oxygen mass balance it could be obtained

$$\dot{S}_O = \frac{1}{V}\left[Q_{in} S_{O,in} - Q_{out} S_O(t)\right] + \left(K_1 + K_2 u(t)\right)\left[S_{O,Sat} - S_O(t)\right] - R(t) \tag{7.151}$$

The first term in the above equation can be omitted as it is negligible in comparison with the others terms. An recursive least-square algorithm on the basis of measurements of S_O and u is developed in (Holmberg & Ranta, 1982). The algorithm give estimates of the parameters K_1, K_2 and $OUR\ R(t)$. The algorithm gives goods results when applied to situations with marked dynamic changes and bad results in the continuous closed loop conditions. The performance is improved if the data for estimation are taken during the transition behaviour caused by the step changes of the air flow rate.

Additionally to the above estimation an estimation of parameters representing the *OUR* as a function of the concentration of the microorganisms and the growth rate μ could be done. (Holmberg & Ranta, 1982) considered the following representation

$$R(t) = a\mu(t)x(t) + bx(t) = \theta \frac{\mu_m S(t)x(t)}{K_S + S(t)} + bx(t) \tag{7.152}$$

where θ and b represent the growth rate and the maintenance consumption of oxygen, x is the biomass and μ is the growth rate.

The Kalman filter is used for parameter estimation of the oxygen transfer rate and the respiration rate in (Yoo et al., 2004) as a part of a nonlinear control strategy from the measurement of DO and air flow rate for the case where

$$K_{La}(u(t)) = K_1\left(1 - e^{-\frac{K_2 u(t)}{a}}\right) \tag{7.153}$$

where a is the scaling factor and K_1 and K_2 are parameters.

Prediction of the oxygen transfer coefficient and oxygen uptake rate for the purpose of the adaptive control is proposed in (Ko et al., 1982) using simplification of the equation describing the dissolved oxygen dynamics. A least-squares estimate of these parameters is obtained in a recursive form.

Two step procedure is described in (Lira et al., 2004) for real time application:

- non-recursive step – in the first minutes of the reaction the mean respiration rate R and the K_{La} are estimated as a function of the control input. The measured values of the dissolved oxygen are used and the system behaviour is represented as a linear regressor

$$S_0(K) = \varphi^T(K)\theta \tag{7.154}$$

$$\text{The estimate is } \hat{\theta} = \left[\sum_{K=1}^{N} \varphi(K)\varphi^T(K)\right]^{-1}\left[\sum_{K=1}^{N} \varphi(K)S_O(K)\right] \tag{7.155}$$

- recursive step – the K_{La} function estimated from the first step is used as true and the respiration rate is estimated recursively with initial value R from the first step. The forgetting factor algorithm is applied and this is the only one algorithm that is able to track the respiration rate.

  The two step procedure is developed for two types of K_{La} representations – constant) and linear.

On-line estimation of the oxygen uptake rate for the purpose of control of the dissolved oxygen concentration is described in (Gerksic et al., 2004) for the ASM1 process with control input K_{La} for an equation

$$\dot{S}_O(t) = K_{La}\left(S_{O,Sat} - S_O(t)\right) - R(t) \tag{7.156}$$

From here $R(t)$ is estimated on-line from the S_O and K_{La} signals assuming that $S_{O,Sat}$ is a known parameter. The value of the derivative $\dot{S}_O(t)$ is estimated using numerical differentiation which requires additionally to suppress the effect of measurement noise amplified by the differentiation.

7.4.4 Estimation of the influent characteristics as an unknown input

Estimation of the unmeasured influent concentrations is very important for development of a proper control strategy. However, abundant material treating inflow constituents estimation is far from being available. Some of the existing developments are: unknown input Kalman filter to estimate the variation of the influent organic concentration in an anaerobic fluidized bed reactor (Aubrun et al., 2001), extended Kalman filter to estimate the nitrogen concentration and the influent ammonia by using a reduced nonlinear model. The problem is to estimate the unknown input and state of the system. This method is based on a two steps strategy presented by Hou and Muller (1982):

- First, the linear system is transformed by matrix operations into two decoupled systems: one unknown input-free system, and one directly related to the unknown input
- Second, the unknown input-free system state vector estimation is done by applying a robust observer technique. Then the unknown input is calculated by using the remaining system.

This two step procedure is applied in (Gomez-Quintero & Queinnec, 2002) to uncertain linear system for estimation of the influent ammonia concentration and the process state variables. Robust unknown input estimation is proposed in (Takahashi & Peres, 1999). A recursive parameter estimation technique is developed in (Lukasse et al., 1999) for reduced process model to identify the influent NH_4^{in}, maximum nitrification rate and maximum denitrification rate on the basis of measurement from standard $NH_4(NO_3), Q_{in}$, DO sensors. The Kalman filter is used because the filter gain varies as a function of the Jacobian, which is directly related to the parameter observability.

Asymptotic observer of the biotechnological processes with unknown kinetics is considered in (Bernard et al., 2000). The accepted approach is to consider the kinetic expression as an unknown input (Hou & Muller, 1991), (Darouach et al., 1994), (Gillijns & De Moor, 2007). These observers are based on mass-balance considerations, in order to eliminate the unknown kinetics. But since they are in open-loop they are not very robust to errors on the estimation of the influent masses. They also require measurement of some output gaseous flow rates. In (Bernard et al., 2000) these gaseous flow rates together with some easy to perform measurements are used to build a closed-loop nonlinear observer that achieves better than described in (Bastin & Dochain, 1990) asymptotic observers, according to the properties of robustness and convergence rate.

7.5 Discrete Kalman filter design for state estimation of the reduced models of the Benchmark and Athlone wastewater treatment plant

Many of biological variables of the activated sludge process can not be measured on-lone because of lack of cheap sensors. Then if the control id necessary to be implemented the real-time values of the process variables are necessary to be known. This requires their estimation using the data which can e obtained from the possible to be measured variables.

It is supposed that there is stable and reliable reduced model of the Benchmark and Athlone activated sludge processes on the basis of the reduced ASM1 and UCT

biological models. Then a Kalman filter can be designed. As the reduced models are nonlinear two approaches are considered. First one is based on linearization of the nonlinear models on the basis of Taylor's series and design of a Kalman filter for the linearised model. The second approach is based on design an extended Kalman filter where the Taylor series derivatives are calculated at every sampling period for the estimated state

Different applications of the extended Kalman filter are described in (Steyer, Bouvier, Conte, Gras &Sousbie, 2002), (Zhao & Kummel, 1995), (Chachnat, Roche & Lafiti, 2003). A multirate extended Kalman filter is developed for a reduced nonlinear model in (Chachnat, Roche & Lafiti, 2003). This five state model describes dynamics of COD, NO, NH, organic nitrogen ND and DO and is observable under both aerobic and anoxic conditions. Numerical simulations have been performed using a set of data produced from the full ASM1 model corrupted with white noise. The DO, NO and NH measurements are assumed to be available every 10 sec, 10 min and 10 min respectively. The results show satisfactory performance for COD estimation. But the obtained COD estimates are very sensitive to model-parameter mismatch. This motivates the development of a mass-balance based observer that is independent on the uncertain kinetic terms.

Since previous results addressing the on-line state estimation can be founded in the literature, most of them for nonlinear models (Tatiraju, Soroush & Mutharasau, 1999), (Bogaerts & Hanus, 2001). Some of the papers estimate the inflow characteristics, for example Aubrun, Theilliol, Harmaud & Steyer, (2001) has presented an unknown input Kalman filter to estimate the variation of the influent organic concentration in an anaerobic fluidized bed reactor. In (Gomez-Quintero & Queinnec, 2002) an extended Kalman filter is used to estimate the nitrogen concentration and the influent ammonia by using a reduced nonlinear model.

7.5.1 Development of a linearised tangent model of the reduced nonlinear models for the Benchmark and Athlone processes with ASM1 and UCT reduced biological models

The mass balance model derived in Chapters 3 and 4 can be written in the common notations as

$$\frac{dz(t)}{dt} = f_c(z,u,t) \tag{7.157}$$

$$z(k+1) = f(z,u,k) \tag{7.158}$$

The equilibrium point(s) are the values of $\bar{z}$ for which

$$0 = f_c(\bar{z},\bar{u}) \tag{7.159}$$

$$\bar{z}(k) = f(\bar{z},\bar{u},k) \tag{7.160}$$

for constant values of the control $\bar{u}$. Then the derivation of the linearised tangent model around the steady state $\bar{z}$ is based on the Taylor series expansion of the function f_c *or* f around the steady state for small deviations of the state and control from their equilibrium values

$$\tilde{z} = z - \bar{z},\ \tilde{u} = u - \bar{u} \tag{7.161}$$

The Taylor series expansion is

$$f(z,u) = f(\bar{z},\bar{u}) + \frac{\partial f(\bar{z},\bar{u})}{\partial z}\tilde{z} + \frac{\partial f(\bar{z},\bar{u})}{\partial u}\tilde{u} + \frac{1}{2!}\frac{\partial^2 f(\bar{z},\bar{u})}{\partial z^2}\tilde{z}^2 + \frac{1}{2!}\frac{\partial^2 f(\bar{z},\bar{u})}{\partial u^2}\tilde{u}^2 + \ldots \tag{7.162}$$

The linearised tangent model is derived using only the first order derivatives as

$$\tilde{z}(k+1) = F\tilde{z}(k) + G\tilde{u}(k) \tag{7.163}$$

$$F = \frac{\partial f(\bar{z},\bar{u})}{\partial z} \qquad G = \frac{\partial f(\bar{z},\bar{u})}{\partial u} \tag{7.164}$$

The above procedure is followed to derive the linearised tangent models for the Benchmark and Athlone processes.

7.5.1.1 Linearised model for the Benchmark and Athlone processes based on the ASM1 reduced biological model

For the Benchamrk process with the ASM1 reduced biological model nonlinear function $f(z,u,k)$ is

$$f(z,u,k) = Az(k) + C^T\rho(z,u,k) + Bz_{in\phi}(k) \tag{7.165}$$

Then
$$\frac{\partial f(z,u,k)}{\partial z(k)} = A + C^T\frac{\partial \rho(z,u,k)}{\partial z(k)}$$
$$\frac{\partial f(z,u,k)}{\partial u(k)} = C^T\frac{\partial \rho(z,u,k)}{\partial u(k)} \tag{7.166}$$

where for the *n-th* tank, according to the Table 4.1

$$\frac{\partial \rho(z,u,k)}{\partial z(k)} = \begin{bmatrix} \frac{\partial \rho_{n1}}{\partial S_{NH,n}} & \frac{\partial \rho_{n1}}{\partial S_{NO,n}} & \frac{\partial \rho_{n1}}{\partial S_{S,n}} \\ \frac{\partial \rho_{n2}}{\partial S_{NH,n}} & \frac{\partial \rho_{n2}}{\partial S_{NO,n}} & \frac{\partial \rho_{n2}}{\partial S_{S,n}} \\ \frac{\partial \rho_{n3}}{\partial S_{NH,n}} & \frac{\partial \rho_{n3}}{\partial S_{NO,n}} & \frac{\partial \rho_{n3}}{\partial S_{S,n}} \\ \frac{\partial \rho_{n4}}{\partial S_{NH,n}} & \frac{\partial \rho_{n4}}{\partial S_{NO,n}} & \frac{\partial \rho_{n4}}{\partial S_{S,n}} \end{bmatrix} \tag{7.167}$$

$$\frac{\partial \rho(z,u,k)}{\partial u(k)} = \begin{bmatrix} \frac{\partial \rho_{n1}}{\partial S_{O,n}} & \frac{\partial \rho_{n2}}{\partial S_{O,n}} & \frac{\partial \rho_{n3}}{\partial S_{O,n}} & \frac{\partial \rho_{n4}}{\partial S_{O,n}} \end{bmatrix}^T \tag{7.168}$$

The separate derivatives according to the state vector are as follows:

$$\begin{aligned}
&\frac{\partial \rho_{n1}}{\partial S_{NH,n}} = 0, \ \frac{\partial \rho_{n1}}{\partial S_{NO,n}} = 0, \frac{\partial \rho_{n1}}{\partial S_{S,n}} = \left(\frac{K_S}{(K_S + S_{S,n})^2}\right)\hat{\mu}_H\left(\frac{S_{O,n}}{K_{OH} + S_{O,n}}\right)X_{BH,n} = f_n 13(k) \\
&\frac{\partial \rho_{n2}}{\partial S_{NH,n}} = 0, \ \frac{\partial \rho_{n2}}{\partial S_{NO,n}} = \hat{\mu}_H\left(\frac{S_{S,n}}{K_S + S_{S,n}}\right)\left(\frac{S_{O,n}}{K_{OH} + S_{O,n}}\right)\left(\frac{K_{NO}}{(K_{NO} + S_{NO,n})^2}\right)\eta_g X_{BH,n} = f_n 22(k) \\
&\frac{\partial \rho_{n2}}{\partial S_{S,n}} = \hat{\mu}_H\left(\frac{K_S}{(K_S + S_{S,n})^2}\right)\left(\frac{K_{OH}}{K_{OH} + S_{O,n}}\right)\left(\frac{S_{NO,n}}{K_{NO} + S_{NO,n}}\right)\eta_g X_{BH,n} = f_n 23(k) \\
&\frac{\partial \rho_{n3}}{\partial S_{NH,n}} = \hat{\mu}_A\left(\frac{K_{NH}}{(K_{NH} + S_{NH,n})^2}\right)\left(\frac{S_{O,n}}{K_{OA} + S_{O,n}}\right)X_{BA,n} = f_n 31(k), \frac{\partial \rho_{n3}}{\partial S_{NO,n}} = 0, \frac{\partial \rho_{n3}}{\partial S_{S,n}} = 0 \\
&\frac{\partial \rho_{n4}}{\partial S_{NH,n}} = 0, \frac{\partial \rho_{n4}}{\partial S_{NO,n}} = k_h X_{BH,n}\left(\frac{X_{S,n}/X_{BH,n}}{K_X + X_{S,n}/X_{BH,n}}\right)\eta_h\left(\frac{K_{OH}}{K_{OH} + S_{O,n}}\right)\left(\frac{K_{NO}}{(K_{NO} + S_{NO,n})^2}\right) = f_n 42(k) \\
&\frac{\partial \rho_{n4}}{\partial S_{S,n}} = 0
\end{aligned} \tag{7.169}$$

Using the derivatives (7.169) the matrix $\frac{\partial \rho(z,u,k)}{\partial z}$ as calculated for the equilibrium point $\bar{z}, \bar{u}$ for which the derivatives are constant is

$$\frac{\partial \rho_n(\bar{z},\bar{u})}{\partial \bar{z}} = \begin{bmatrix} 0 & 0 & f_n 13 \\ 0 & f_n 22 & f_n 23 \\ f_n 31 & 0 & 0 \\ 0 & f_n 42 & 0 \end{bmatrix} \tag{7.170}$$

Then for the whole process $F = \frac{\partial f(\bar{z},\bar{u})}{\partial \bar{z}} = A + C^T \frac{\partial \rho(\bar{z},\bar{u})}{\partial z} = A + C1$ (7.171)

where $C1 = diag\{C1_1, C1_2, C1_3, C1_4, C1_5\}$ for the Benchmark process,
$C1 = diag\{C1_1, C1_2, C1_3\}$ for the Athlone process, and

$$C1_n = \begin{bmatrix} -\left(i_{xB} + \frac{1}{Y_A}\right) f_n 31 & -i_{xB} f_n 22 & -i_{xB}\left(f_n 13 + f_n 23\right) \\ \frac{f_n 31}{Y_A} & -\frac{1-Y_H}{2.86Y_H} f_n 22 & -\frac{1-Y_H}{2.86Y_H} f_n 22 \\ 0 & -\frac{f_n 22}{Y_H} + f_n 42 & -\frac{f_n 13 + f_n 23}{Y_H} \end{bmatrix} \tag{7.172}$$

It can be concluded from equation (7.171) that the off diagonal elements of matrix F are the same as for the matrix A and the block diagonal elements are

$$F_n = \begin{bmatrix} 1 - \frac{\Delta t}{V_n} Q - \left(i_{xB} + \frac{1}{Y_A} f 31n\right) & -i_{xB} f 22n & -i_{xB}\left(f 13n + f 23n\right) \\ \frac{f 31n}{Y_A} & 1 - \frac{\Delta t}{V_n} Q - \frac{1-Y_H}{2.86Y_H} f 22n & -\frac{1-Y_H}{2.86Y_H} f 23n \\ 0 & -\frac{f 22n}{Y_H} + f 42n & 1 - \frac{\Delta t}{Y_H} Q - \frac{f 13n + f 23n}{Y_H} \end{bmatrix} \tag{7.173}$$

The structures of the matrix for both Benchmark and Athlone processes linearised models have the same character.

The derivatives according to the control vector are

$$\begin{aligned} \frac{\partial \rho_{n1}}{\partial S_{O,n}} &= \mu_H \left(\frac{S_{S,n}}{K_S + S_{S,n}}\right)\left(\frac{K_{OH}}{\left(K_{OH} + S_{O,n}\right)^2}\right) X_{BH,n} = g_{n1} \\ \frac{\partial \rho_{n2}}{\partial S_{O,n}} &= -\mu_H \left(\frac{S_{S,n}}{K_S + S_{S,n}}\right)\left(\frac{K_{OH}}{\left(K_{OH} + S_{O,n}\right)^2}\right)\left(\frac{S_{NO,n}}{K_{NO} + S_{NO,n}}\right)\eta_g X_{BH,n} = g_{n2} \\ \frac{\partial \rho_{n3}}{\partial S_{O,n}} &= \mu_A \left(\frac{K_{NH}}{K_{NH} + S_{NH,n}}\right)\left(\frac{K_{OA}}{\left(K_{OA} + S_{O,n}\right)^2}\right) X_{BA,n} = g_{n3} \\ \frac{\partial \rho_{n4}}{\partial S_{O,n}} &= k_h X_{BH,n} \left(\frac{X_{S,n}/X_{BH,n}}{K_X + X_{S,n}/X_{BH,n}}\right)\left[\left(\frac{K_{OH}}{\left(K_{OH} + S_{O,n}\right)^2}\right) - \eta_h \left(\frac{K_{OH}}{\left(K_{OH} + S_{O,n}\right)^2}\right)\left(\frac{S_{NO,n}}{K_{NO} + S_{NO,n}}\right)\right] = g_{n4} \end{aligned} \tag{7.174}$$

Then the matrix

$$G_n = C_n^T \begin{bmatrix} g_{n1} & g_{n2} & g_{n3} & g_{n4} \end{bmatrix} = \Delta t_i \begin{bmatrix} -i_{xB}\left(g_{n1} + g_{n2} + g_{n3}\right) - \frac{g_{n3}}{Y_A} \\ -\frac{1-Y_H}{2.86Y_H} g_{n2} + \frac{g_{n3}}{Y_A} \\ -\frac{g_{n1} + g_{n2}}{Y_H} + g_{n4} \end{bmatrix} \tag{7.175}$$

For the whole process $G = \begin{bmatrix} G_1 & G_2 & G_3 & G_4 & G_5 \end{bmatrix}^T$ for the Benchmark plant and $G = \begin{bmatrix} G_1 & G_2 & G_3 \end{bmatrix}^T$ for the Athlone plant.

7.5.1.2 Linearised model for the Benchmark and Athlone processes based on the reduced UCT biological model

The derivation of the matrices of the linearised model is done in the same way, but the dimensions of the state variable vector and of the vector of the process rate is different.

$$\text{The matrix } \frac{\partial \rho(z,u,k)}{\partial z} = \begin{bmatrix} \frac{\partial \rho_{n1}}{\partial S_{NH,n}} & \frac{\partial \rho_{n1}}{\partial S_{NO,n}} & \frac{\partial \rho_{n1}}{\partial S_{S,n}} & \frac{\partial \rho_{n1}}{\partial S_{ads,n}} \\ \cdots\cdots & \cdots\cdots & \cdots\cdots & \cdots\cdots \\ \frac{\partial \rho_{n10}}{\partial S_{NH,n}} & \frac{\partial \rho_{n10}}{\partial S_{NO,n}} & \frac{\partial \rho_{n10}}{\partial S_{S,n}} & \frac{\partial \rho_{n10}}{\partial S_{ads,n}} \end{bmatrix} \tag{7.176}$$

The vector

$$\frac{\partial \rho(z,u,k)}{\partial u} = \begin{bmatrix} \frac{\partial \rho_{n1}}{\partial S_{O,n}} & \frac{\partial \rho_{n2}}{\partial S_{O,n}} & \cdots & \frac{\partial \rho_{n10}}{\partial S_{O,n}} \end{bmatrix}^T \tag{7.177}$$

The separate derivatives according to the state vector for the n-th tank are

$$\begin{aligned}
&\frac{\partial \rho_{n1}}{\partial S_{NH,n}} = \mu_H \left(\frac{S_{S,n}}{K_S + S_{S,n}} \right) \left(\frac{S_{O,n}}{K_{OH} + S_{O,n}} \right) \left(\frac{K_{HA}}{(K_{HA} + S_{NH,n})^2} \right) X_{BH,n} = f_n 11(k) \\
&\frac{\partial \rho_{n1}}{\partial S_{NO,n}} = 0 \\
&\frac{\partial \rho_{n1}}{\partial S_{S,n}} = \mu_H \left(\frac{K_S}{(K_S + S_S)^2} \right) \left(\frac{S_{O,n}}{K_{OH} + S_{O,n}} \right) \left(\frac{S_{NH,n}}{K_{HA} + S_{NH,n}} \right) X_{BH,n} = f_n 13(k) \\
&\frac{\partial \rho_{n1}}{\partial S_{ads,n}} = 0 \\
&\frac{\partial \rho_{n2}}{\partial S_{NH,n}} = -\mu_H \left(\frac{S_{S,n}}{K_S + S_{S,n}} \right) \left(\frac{S_{O,n}}{K_{OH} + S_{O,n}} \right) \left(\frac{K_{HA}}{(K_{HA} + S_{NH,n})^2} \right) \left(\frac{S_{NO,n}}{K_{NO} + S_{NO,n}} \right) X_{BH,n} = f_n 21(k) \\
&\frac{\partial \rho_{n2}}{\partial S_{NO,n}} = \mu_H \left(\frac{S_{S,n}}{K_S + S_{S,n}} \right) \left(\frac{S_{O,n}}{K_{OH} + S_{O,n}} \right) \left(\frac{K_{HA}}{K_{HA} + S_{NH,n}} \right) \left(\frac{K_{NO}}{(K_{NO} + S_{NO,n})^2} \right) X_{BH,n} = f_n 22(k) \\
&\frac{\partial \rho_{n2}}{\partial S_{S,n}} = \mu_H \left(\frac{K_S}{(K_S + S_S)^2} \right) \left(\frac{S_{O,n}}{K_{OH} + S_{O,n}} \right) \left(\frac{K_{HA}}{K_{HA} + S_{NH,n}} \right) \left(\frac{S_{NO,n}}{K_{NO} + S_{NO,n}} \right) X_{BH,n} = f_n 23(k) \\
&\frac{\partial \rho_{n2}}{\partial S_{ads,n}} = 0 \\
&\frac{\partial \rho_{n3}}{\partial S_{NH,n}} = \mu_H \left(\frac{S_{S,n}}{K_S + S_{S,n}} \right) \left(\frac{K_{OH}}{K_{OH} + S_{O,n}} \right) \left(\frac{K_{HA}}{(K_{HA} + S_{NH,n})^2} \right) \left(\frac{S_{NO,n}}{K_{NO} + S_{NO,n}} \right) X_{BH,n} = f_n 31(k) \\
&\frac{\partial \rho_{n3}}{\partial S_{NO,n}} = \mu_H \left(\frac{S_{S,n}}{K_S + S_{S,n}} \right) \left(\frac{K_{OH}}{K_{OH} + S_{O,n}} \right) \left(\frac{S_{NH,n}}{K_{HA} + S_{NH,n}} \right) \left(\frac{K_{NO}}{(K_{NO} + S_{NO,n})^2} \right) X_{BH,n} = f_n 32(k)
\end{aligned} \tag{7.178}$$

$$\frac{\partial \rho_{n3}}{\partial S_{S,n}} = \mu_H \left(\frac{K_S}{(K_S + S_S)^2} \right) \left(\frac{K_{OH}}{K_{OH} + S_{O,n}} \right) \left(\frac{S_{NH,n}}{K_{HA} + S_{NH,n}} \right) \left(\frac{S_{NO,n}}{K_{NO} + S_{NO,n}} \right) X_{BH,n} = f_n 33(k)$$

$$\frac{\partial \rho_{n3}}{\partial S_{ads,n}} = 0$$

$$\frac{\partial \rho_{n4}}{\partial S_{NH,n}} = -\mu_H \left(\frac{S_{S,n}}{K_S + S_{S,n}} \right) \left(\frac{K_{OH}}{K_{OH} + S_{O,n}} \right) \left(\frac{K_{HA}}{(K_{HA} + S_{NH,n})^2} \right) \left(\frac{S_{NO,n}}{K_{NO} + S_{NO,n}} \right) X_{BH,n} = f_n 41(k)$$

$$\frac{\partial \rho_{n4}}{\partial S_{NO,n}} = \mu_H \left(\frac{S_{S,n}}{K_S + S_{S,n}} \right) \left(\frac{K_{OH}}{K_{OH} + S_{O,n}} \right) \left(\frac{K_{HA}}{K_{HA} + S_{NH,n}} \right) \left(\frac{K_{NO}}{K_{NO} + S_{NO,n}} \right) X_{BH,n} = f_n 42(k)$$

$$\frac{\partial \rho_{n4}}{\partial S_{S,n}} = \mu_H \left(\frac{K_S}{K_S + S_S} \right) \left(\frac{K_{OH}}{K_{OH} + S_{O,n}} \right) \left(\frac{K_{HA}}{K_{HA} + S_{NH,n}} \right) \left(\frac{S_{NO,n}}{K_{NO} + S_{NO,n}} \right) X_{BH,n} = f_n 43(k)$$

$$\frac{\partial \rho_{n4}}{\partial S_{ads,n}} = 0$$

$$\frac{\partial \rho_{n5}}{\partial S_{NH,n}} = K_{MP} \left(\frac{S_{ads,n}/X_{BH,n}}{K_{SP} + S_{ads,n}/X_{BH,n}} \right) \left(\frac{S_{O,n}}{K_{OH} + S_{O,n}} \right) \left(\frac{K_{HA}}{(K_{HA} + S_{NH,n})^2} \right) X_{BH,n} = f_n 51(k)$$

$$\frac{\partial \rho_{n5}}{\partial S_{NO,n}} = K_{MP} \left(\frac{S_{ads,n}/X_{BH,n}}{K_{SP} + S_{ads,n}/X_{BH,n}} \right) \left(\frac{S_{O,n}}{K_{OH} + S_{O,n}} \right) \left(\frac{K_{NO}}{(K_{NO} + S_{NO,n})^2} \right) \left(\frac{K_{HA}}{K_{HA} + S_{NH,n}} \right) X_{BH,n} = f_n 52(k)$$

$$\frac{\partial \rho_{n5}}{\partial S_{S,n}} = 0$$

$$\frac{\partial \rho_{n5}}{\partial S_{ads,n}} = K_{MP} \left(\frac{S_{ads,n}/X_{BH,n}}{(K_{SP} + S_{ads,n}/X_{BH,n})^2} \right) \left(\frac{S_{O,n}}{K_{OH} + S_{O,n}} \right) \left(\frac{S_{NH,n}}{K_{HA} + S_{NH,n}} \right) X_{BH,n} = f_n 54(k)$$

$$\frac{\partial \rho_{n6}}{\partial S_{NH,n}} = -K_{MP} \left(\frac{S_{ads,n}/X_{BH,n}}{K_{SP} + S_{ads,n}/X_{BH,n}} \right) \left(\frac{S_{O,n}}{K_{OH} + S_{O,n}} \right) \left(\frac{K_{NO}}{K_{NO} + S_{NO,n}} \right) \left(\frac{K_{HA}}{(K_{HA} + S_{NH,n})^2} \right) X_{BH,n} = f_n 61(k)$$

$$\frac{\partial \rho_{n6}}{\partial S_{NO,n}} = K_{MP} \left(\frac{S_{ads,n}/X_{BH,n}}{K_{SP} + S_{ads,n}/X_{BH,n}} \right) \left(\frac{S_{O,n}}{K_{OH} + S_{O,n}} \right) \left(\frac{K_{HA}}{K_{HA} + S_{NH,n}} \right) \left(\frac{K_{NO}}{(K_{NO} + S_{NO,n})^2} \right) X_{BH,n} = f_n 62(k)$$

$$\frac{\partial \rho_{n6}}{\partial S_{S,n}} = 0$$

$$\frac{\partial \rho_{n6}}{\partial S_{ads,n}} = K_{MP} \left(\frac{S_{ads,n}/X_{BH,n}}{(K_{SP} + S_{ads,n}/X_{BH,n})^2} \right) \left(\frac{S_{O,n}}{K_{OH} + S_{O,n}} \right) \left(\frac{K_{HA}}{K_{HA} + S_{NH,n}} \right) \left(\frac{S_{NO,n}}{K_{NO} + S_{NO,n}} \right) X_{BH,n} = f_n 64(k)$$

$$\frac{\partial \rho_{n7}}{\partial S_{NH,n}} = K_{MP} \left(\frac{S_{ads,n}/X_{BH,n}}{K_{SP} + S_{ads,n}/X_{BH,n}} \right) \left(\frac{K_{OH}}{K_{OH} + S_{O,n}} \right) \left(\frac{K_{HA}}{(K_{HA} + S_{NH,n})^2} \right) \left(\frac{S_{NO,n}}{K_{NO} + S_{NO,n}} \right) \eta_g X_{BH,n} = f_n 71(k)$$

$$\frac{\partial \rho_{n7}}{\partial S_{NO,n}} = K_{MP} \left(\frac{S_{ads,n}/X_{BH,n}}{K_{SP} + S_{ads,n}/X_{BH,n}} \right) \left(\frac{K_{OH}}{K_{OH} + S_{O,n}} \right) \left(\frac{S_{NH,n}}{K_{HA} + S_{NH,n}} \right) \left(\frac{K_{NO}}{(K_{NO} + S_{NO,n})^2} \right) \eta_g X_{BH,n} = f_n 72(k)$$

$$\frac{\partial \rho_{n7}}{\partial S_{S,n}} = 0$$

$$\frac{\partial \rho_{n7}}{\partial S_{ads,n}} = K_{MP}\left(\frac{S_{ads,n}/X_{BH,n}}{\left(K_{SP}+S_{ads,n}/X_{BH,n}\right)^2}\right)\left(\frac{K_{OH}}{K_{OH}+S_{O,n}}\right)\left(\frac{S_{NH,n}}{K_{HA}+S_{NH,n}}\right)\left(\frac{S_{NO,n}}{K_{NO}+S_{NO,n}}\right)\eta_g X_{BH,n} = f_n 74(k)$$

$$\frac{\partial \rho_{n8}}{\partial S_{NH,n}} = -K_{MP}\left(\frac{S_{ads,n}/X_{BH,n}}{K_{SP}+S_{ads,n}/X_{BH,n}}\right)\left(\frac{K_{OH}}{K_{OH}+S_{O,n}}\right)\left(\frac{K_{HA}}{\left(K_{HA}+S_{NH,n}\right)^2}\right)\left(\frac{S_{NO,n}}{K_{NO}+S_{NO,n}}\right)\eta_g X_{BH,n} = f_n 81(k)$$

$$\frac{\partial \rho_{n8}}{\partial S_{NO,n}} = K_{MP}\left(\frac{S_{ads,n}/X_{BH,n}}{K_{SP}+S_{ads,n}/X_{BH,n}}\right)\left(\frac{K_{OH}}{K_{OH}+S_{O,n}}\right)\left(\frac{K_{HA}}{K_{HA}+S_{NH,n}}\right)\left(\frac{K_{NO}}{\left(K_{NO}+S_{NO,n}\right)^2}\right)\eta_g X_{BH,n} = f_n 82(k)$$

$$\frac{\partial \rho_{n8}}{\partial S_{S,n}} = 0$$

$$\frac{\partial \rho_{n8}}{\partial S_{ads,n}} = K_{MP}\left(\frac{S_{ads,n}/X_{BH,n}}{\left(K_{SP}+S_{ads,n}/X_{BH,n}\right)^2}\right)\left(\frac{K_{OH}}{K_{OH}+S_{O,n}}\right)\left(\frac{K_{HA}}{K_{HA}+S_{NH,n}}\right)\left(\frac{S_{NO,n}}{K_{NO}+S_{NO,n}}\right)\eta_g X_{BH,n} = f_n 84(k)$$

$$\frac{\partial \rho_{n9}}{\partial S_{NH,n}} = 0,\ \frac{\partial \rho_{n9}}{\partial S_{NO,n}} = 0,\ \frac{\partial \rho_{n9}}{\partial S_{S,n}} = 0$$

$$\frac{\partial \rho_{n9}}{\partial S_{ads,n}} = -K_A X_{S,n} X_{BH,n}/X_{BH,n} f_n 94(k)$$

$$\frac{\partial \rho_{n10}}{\partial S_{NH,n}} = \mu_A\left(\frac{S_{O,n}}{K_{OA}+S_{O,n}}\right)\left(\frac{K_{HA}}{\left(K_{HA}+S_{NH,n}\right)^2}\right)X_{BA,n} = f_n 101(k)$$

$$\frac{\partial \rho_{n10}}{\partial S_{NO,n}} = 0,\ \frac{\partial \rho_{10}}{\partial S_{NO,n}} = 0,\ \frac{\partial \rho_{n10}}{\partial S_{ads,n}} = 0$$

The matrix of the derivatives is

$$\frac{\partial \rho_n(\bar{z},\bar{u})}{\partial z_n} = \begin{bmatrix} f_n 11 & 0 & f_n 13 & 0 \\ f_n 21 & f_n 22 & f_n 23 & 0 \\ f_n 31 & f_n 32 & f_n 33 & 0 \\ f_n 41 & f_n 42 & f_n 43 & 0 \\ f_n 51 & f_n 52 & 0 & f_n 54 \\ f_n 61 & f_n 62 & 0 & f_n 64 \\ f_n 71 & f_n 72 & 0 & f_n 74 \\ f_n 81 & f_n 82 & 0 & f_n 84 \\ 0 & 0 & 0 & f_n 94 \\ f_n 101 & 0 & 0 & 0 \end{bmatrix} \tag{7.179}$$

The matrix $C1_n = C_n^T \frac{\partial \rho_n(\bar{z},\bar{u})}{\partial z_n}$ and $C1 = diag\{C1, C2, C3, C4, C5\}$ for the Benchmark and $C1 = diag\{C1, C2, C3\}$ for the Athlone process.

The derivatives according to the control vector are:

$$\frac{\partial \rho_{n1}}{\partial S_{O,n}} = \mu_H \left(\frac{S_{S,n}}{K_S + S_{S,n}} \right) \left(\frac{K_{OH}}{(K_{OH} + S_{O,n})^2} \right) \left(\frac{S_{NH,n}}{K_{HA} + S_{NH,n}} \right) X_{BH,n} = g_{n1}$$

$$\frac{\partial \rho_{n2}}{\partial S_{O,n}} = -\mu_H \left(\frac{S_{S,n}}{K_S + S_{S,n}} \right) \left(\frac{K_{OH}}{(K_{OH} + S_{O,n})^2} \right) \left(\frac{K_{HA}}{K_{HA} + S_{NH,n}} \right) \left(\frac{S_{NO,n}}{K_{NO} + S_{NO,n}} \right) X_{BH,n} = g_{n2}$$

$$\frac{\partial \rho_{n3}}{\partial S_{O,n}} = -\mu_H \left(\frac{S_{S,n}}{K_S + S_{S,n}} \right) \left(\frac{K_{OH}}{(K_{OH} + S_{O,n})^2} \right) \left(\frac{S_{NH,n}}{K_{HA} + S_{NH,n}} \right) \left(\frac{S_{NO,n}}{K_{NO} + S_{NO,n}} \right) X_{BH,n} = g_{n3} \quad (7.180)$$

$$\frac{\partial \rho_{n4}}{\partial S_{O,n}} = -\mu_H \left(\frac{S_{S,n}}{K_S + S_{S,n}} \right) \left(\frac{K_{OH}}{(K_{OH} + S_{O,n})^2} \right) \left(\frac{K_{HA}}{K_{HA} + S_{NH,n}} \right) \left(\frac{S_{NO,n}}{K_{NO} + S_{NO,n}} \right) X_{BH,n} = g_{n4}$$

$$\frac{\partial \rho_{n5}}{\partial S_{O,n}} = K_{MP} \left(\frac{S_{ads,n}/X_{BH,n}}{K_{SP} + S_{ads,n}/X_{BH,n}} \right) \left(\frac{K_{OH}}{(K_{OH} + S_{O,n})^2} \right) \left(\frac{S_{NH,n}}{K_{HA} + S_{NH,n}} \right) X_{BH,n} = g_{n5}$$

$$\frac{\partial \rho_{n6}}{\partial S_{O,n}} = K_{MP} \left(\frac{S_{ads,n}/X_{BH,n}}{K_{SP} + S_{ads,n}/X_{BH,n}} \right) \left(\frac{K_{OH}}{(K_{OH} + S_{O,n})^2} \right) \left(\frac{S_{NO,n}}{K_{NO} + S_{NO,n}} \right) X_{BH,n} = g_{n6}$$

$$\frac{\partial \rho_{n7}}{\partial S_{O,n}} = -K_{MP} \left(\frac{S_{ads,n}/X_{BH,n}}{K_{SP} + S_{ads,n}/X_{BH,n}} \right) \left(\frac{K_{OH}}{(K_{OH} + S_{O,n})^2} \right) \left(\frac{S_{NH,n}}{K_{HA} + S_{NH,n}} \right) \left(\frac{S_{NO,n}}{K_{NO} + S_{NO,n}} \right) X_{BH,n} = g_{n7}$$

$$\frac{\partial \rho_{n8}}{\partial S_{O,n}} = -K_{MP} \left(\frac{S_{ads,n}/X_{BH,n}}{K_{SP} + S_{ads,n}/X_{BH,n}} \right) \left(\frac{K_{OH}}{(K_{OH} + S_{O,n})^2} \right) \left(\frac{K_{HA}}{K_{HA} + S_{NH,n}} \right) \left(\frac{S_{NO,n}}{K_{NO} + S_{NO,n}} \right) \eta_g X_{BH,n} = g_{n8}$$

$$\frac{\partial \rho_{n9}}{\partial S_{O,n}} = 0, \quad \frac{\partial \rho_{n10}}{\partial S_{O,n}} = \mu_A \left(\frac{K_{OA}}{(K_{OA} + S_{O,n})^2} \right) \left(\frac{S_{NH,n}}{K_{HA} + S_{NH,n}} \right) X_{BA,n} = g_{n10}$$

The matrix $G_n = C_n^T \begin{bmatrix} g_{n1} & g_{n2} & g_{n3} & g_{n4} & g_{n5} & g_{n6} & g_{n7} & g_{n8} & g_{n9} & g_{n10} \end{bmatrix}^T$ (7.181)

$$G_n = \Delta t \begin{bmatrix} -f_{ZB,H}(g_{n1} + g_{n3} + g_{n5} + g_{n7}) - \left(\frac{1}{Y_{ZA}} + f_{ZB,H} \right) g_{n10} \\ -f_{ZB,H}(g_{n2} + g_{n4} + g_{n6} + g_{n8}) - \left(\frac{1 - Y_{ZH}}{2.86 Y_{ZH}} \right)(g_{n3} - g_{n4} + g_{n7} - g_{n8}) + \frac{1}{Y_{ZA}} g_{n10} \\ -\frac{1}{Y_{ZH}}(g_{n1} + g_{n2} + g_{n3} + g_{n4}) \\ -\frac{1}{Y_{ZH}}(g_{n5} + g_{n6} + g_{n7} + g_{n8}) \end{bmatrix} \quad (7.182)$$

And the control matrix for the whole process is $G = \begin{bmatrix} G_1 & G_2 & G_3 & G_4 & G_5 \end{bmatrix}^T$ for the Benchmark and $G = \begin{bmatrix} G_1 & G_2 & G_3 \end{bmatrix}^T$ for the Athlone plan.

The linearised models are used as a part of the algorithm for a Kalman filter for estimation of the immeasurable state variables.

7.5.1.3 State observability

The notion of observability can be defined as the possibility to connect the state variables of a dynamical system to the measured variables via the dynamical model of

the system. The system is observable if every its state variable affects some of the measured process variables. The observability of the system allows reconstructing the time behaviour of the state variables from measured variables in an arbitrary finite time from any initial condition. If the system is observable it is possible to design an observer that is theoretically capable of correct reconstruction of the time behaviour of the unmeasured variables.

The linearised system is observable if the matrix of observability.

$$0 = \begin{bmatrix} C \\ CA \\ CA^2 \\ \vdots \\ CA^{n-1} \end{bmatrix} \tag{7.183}$$

has a rank n, where the dimension of the state vector is n. In the considered case of wastewater treatment $A=F$, where F is determined by Equation (7.171), $C=C2$, where $C2$ is determined on the basis of measurable variables. The observability test is very difficult for the nonlinear systems and especially for the wastewater processes because of the large uncertainties in the kinetics of the biochemical reactions and the used analytical expressions describing them.

Normally linear approximation of the nonlinear model is used to provide the identifiability test. Then the observability results for the nonlinear system are only sufficient ones – if the linearised tangent model is observable around the equilibrium state and control variables, then the nonlinear system is observable around this point. In (Dochain & Chen, 1992) is proved that a necessary condition for the observability of the linearised tangent system is $p+R \geq n$, where p is the number of the measured components, R is the rank of the yield matrix C and n is the number of the process state variables. The observability test is independent of the mathematical structure of the reaction rates $\rho(z)$. The fulfillment of the condition $p+R \geq n$ does not guarantee the system observability, but it can be very useful to detect in a very simple way the observability of the process.

The application of the condition is considered for the above linearised models. It can be seen from Equation (7.171) that the yield matrices C determine the structure of the

linearised model state space matrix F. That is why they play very big role in the model observability.

For the ASM1 biological model the matrix C_n^T is

$$C_n^T = \begin{bmatrix} -i_{xB} & -i_{xB} & -i_{xB} - \frac{1}{Y_A} & 0 \\ 0 & -\frac{1-Y_H}{2.86Y_H} & \frac{1}{Y_A} & 0 \\ -\frac{1}{Y_H} & -\frac{1}{Y_H} & 0 & 1 \end{bmatrix} \tag{7.184}$$

The rank C_n^T is 3, $n=3$, this means the measurement of one of the state variables will be necessary to build a state observer. For the UCT biological model the rank $C_n^T = 4, n = 4$ and again one state variable will be necessary to be measured. Which of the variables to be measured depends on their dynamic rate equations. The equations must incorporate connections with the unmeasured variables. It can be seen from the Table 4.1 that the variable $S_{SH,n}$ has the connection through the process rate for the anoxic growth of heterotrophs to the other two variables $S_{S,n}$ and $S_{NO,n}$ for the reduced ASM1 model. This means if $S_{NH,n}$ is measurable the other two variables can be determined using observers – first $S_{NO,n}$ using $S_{NO,n}$ and $S_{NH,n}$ and then $S_{S,n}$ using the process of anoxic growth of heterotrophs. If $S_{S,n}$ is only measured then $S_{NH,n}$ can be obtained using the process rate for aerobic growth of heterotrophs and then $S_{NO,n}$ using the process rate of the aerobic growth of heterotrophs. If $S_{NO,n}$ is measured then $S_{S,n}$ can be obtained through the process rate of hydrolysis and $S_{NH,n}$ through the process rate of anoxic growth of heterotrophs. Similar considerations can be done for the UCT reduced model using Table 4.3.

7.5.2 Design of a discrete Kalman filter for the estimation of the immeasurable state variables on the basis of the process linearised model

The linearised models of the Benchmark and Athlone processes are considered

$$\tilde{z}(k+1) = F(k)\tilde{z}(k) + G(k)\tilde{u}(k) + H(k)\omega(k) \tag{7.185}$$

$$\tilde{y}(k) = C2(k)\tilde{z}(k) + v(k) \tag{7.186}$$

where $\tilde{z}(k) = z(k) - \bar{z}$, $\tilde{u}(k) = u(k) - \bar{u}$, $\bar{z}$, $\bar{u}$ are the state and control equilibrium points, $\omega(k)$, $v(k)$ are zero-mean Gaussian white noise processes with errors not correlated forward or backward in time so that

$$E\{v(k)v(j)^T\} = \begin{Bmatrix} 0 & k \neq j \\ R(k) & k = j \end{Bmatrix}, \quad E\{\omega(k)\ \omega(j)\} = \begin{Bmatrix} 0 & k \neq j \\ Q(k) & k = j \end{Bmatrix} \tag{7.187}$$

The requirement for the noise characteristics preserves the block diagonal structure of the covariance matrices. Further the noises $\omega(k)$, $v(k)$ are not correlated and $E\{v(k)\omega(k)^T\} = 0$ for all k. The $\omega(k)$ is a forcing process noise and $v(k)$ is the measurement noise.

If it is supposed that the current estimate $\hat{\tilde{z}}(k)$ is known. It is necessary to update it to obtain $\hat{\tilde{z}}(k+1)$ based on all $k+1$ measurement subsets determined by the matrix *C2(k)* in the following form

$$\hat{\tilde{z}}^-(k+1) = F(k)\hat{\tilde{z}}^+(k) + G(k)\tilde{u}(k) \tag{7.188}$$

$$\hat{\tilde{z}}^+(k) = \hat{z}^-(k) + K(k)\left[\tilde{y}(k) - C2(k)\hat{z}^-(k)\right] \tag{7.189}$$

An optimal choice of the matrix $K(k)$ has to be derived in such a way that the minimum of the variances of all state estimates from their through values are minimized according to the criterion

$$J = \frac{1}{2}E\left\{\left[\hat{\tilde{z}}(k) - \tilde{z}(k)\right]^2\right\} \tag{7.190}$$

The following error covariance matrices can be defined

$$P^-(k) \equiv E\{\delta\tilde{z}^-(k)\delta\tilde{z}^-(k)^T\} \quad P^-(k+1) \equiv E\{\delta\tilde{z}^-(k+1)\delta\tilde{z}^-(k+1)^T\} \tag{7.191}$$

$$P^+(k) \equiv E\{\delta\tilde{z}^+(k)\delta\tilde{z}^+(k)^T\} \quad P^+(k+1) \equiv E\{\delta\tilde{z}^+(k+1)\delta\tilde{z}^+(k+1)^T\} \tag{7.192}$$

where

$$\delta\tilde{z}^-(k) = \hat{\tilde{z}}^-(k) - \tilde{z}^-(k) \quad \delta\tilde{z}^-(k+1) = \hat{\tilde{z}}^-(k+1) - \tilde{z}^-(k+1) \tag{7.193}$$

$$\delta\tilde{z}^+(k) = \hat{\tilde{z}}^+(k) - \tilde{z}^+(k) \quad \delta\tilde{z}^+(k+1) = \hat{\tilde{z}}^+(k+1) - \tilde{z}^+(k+1) \tag{7.194}$$

are the state errors in the prediction and uptake respectively.

From here it follows that it is necessary to derive optimal expressions for $P^-(k+1)$ and $P^+(k+1)$. Since the first equation (7.191) is not a direct function of *K(k)* the expression for $P^-(k+1)$ can be derivated by :

- substitution of equations (7.185) and (7.188) into equation (7.193)

$$\begin{aligned}&\delta\tilde{z}^-(k+1)=\hat{\tilde{z}}^-(k+1)-\tilde{z}(k+1)=\left[F(k)\hat{\tilde{z}}^+(k)+G(k)\tilde{u}(k)\right]-\\&-\left[F(k)\tilde{z}(k)+G(k)\tilde{u}(k)+H(k)\omega(k)\right]=F(k)\left[\hat{\tilde{z}}^+(k)-\tilde{z}(k)\right]-H(k)\omega(k)=\\&=F(k)\delta\tilde{z}^+(k)-H(k)\omega(k)\end{aligned} \qquad (7.195)$$

- substitution of equation (7.195) into equation (7.191)

$$\begin{aligned}&p^-(k+1)=E\left\{\delta\tilde{z}^-(k+1)\delta\tilde{z}^-(k+1)^T\right\}=E\left\{F(k)\tilde{z}^+(k)\tilde{z}^+(k)^T F(k)^T\right\}-\\&-E\left\{F(k)\tilde{z}^+(k)\omega(k)^T H(k)^T\right\}-E\left\{H(k)\omega(k)\tilde{z}^+(k)^T F(k)^T\right\}+\\&+E\left\{H(k)\omega(k)\omega(k)^T H(k)^T\right\}\end{aligned} \qquad (7.196)$$

It can be seen that $\omega(k)+\delta z^+(k)$ are not correlated as $\tilde{z}^+(k+1)$, *not* $\delta\tilde{z}^+$ directly depends on $\omega(k)$ *and* $E\left\{\delta\tilde{z}^+(k)\omega(k)^T\right\}=0$. $E\left\{\omega(k)\delta\tilde{z}^+(k)\right\}=0$ and the expression for $P^-(k+1)$ becomes

$$P^-(k+1)=F(k)P^+(k)F(k)^T+H(k)Q(k)H(k)^T \qquad (7.197)$$

where $P^+(k)$ *and* $Q(k)$ are determined from the noise characteristics given by equation (7.187). Equation (7.197) connects the process dynamics given by the model matrix *F(k)* with the noise characteristics given by the covariance matrices $P(k)$, $Q(k)$. It can be solved using the initial condition

$$p^-(0)=E\left\{\delta\tilde{z}^-(0)\delta\tilde{z}(0)^T\right\} \qquad (7.198)$$

The next step is to develop an optimal expression for $P(k)$ by:

- substitution of equation (7.186) into equation (7.189) it is obtained

$$\begin{aligned}&\hat{\tilde{z}}^+(k)=\hat{\tilde{z}}^-(k)+K(k)\left[C2(k)\hat{z}(k)+v(k)-C2(k)\hat{\tilde{z}}^-(k)\right]=\\&=\left[I-K(k)C2(k)\right]\hat{\tilde{z}}^-(k)+K(k)C2(k)\tilde{z}(k)+K(k)v(k)\end{aligned} \qquad (7.199)$$

- substitution of equation (7.199) into equation (7.194) gives

$$\begin{aligned}\delta\tilde{z}^+(k)&=\hat{\tilde{z}}^+(k)-\tilde{z}(k)=\left[I-K(k)C2(k)\right]\hat{\tilde{z}}^-(k)+K(k)C2(k)\tilde{z}(k)+K(k)v(k)-\tilde{z}(k)=\\&=\left[I-K(k)C2(k)\right]\delta\tilde{z}^-(k)+K(k)v(k)\end{aligned} \qquad (7.200)$$

- calculation of $p^+(k)$ according to equation (7.192)

$$P^+(k)=E\{\delta z^+(k)\delta\tilde{z}^+(k)^T\}=E\{[I-K(k)C2(k)]\delta\tilde{z}^-(k)\delta\tilde{z}^-(k)[I-K(k)C2(k)]^T\}+$$
$$+E\{[I-K(k)C2(k)]\delta\tilde{z}^-(k)v(k)^TK(k)^T\}+ \quad (7.201)$$
$$+E\{K(k)v(k)\delta\tilde{z}^-(k)^T[I-K(k)C2(k)]^T\}+E\{K(k)v(k)v(k)^TK(k)^T\}$$

It can be seen that $v(k)$, $\delta\tilde{z}^-(k)$ are not correlated as $\delta\tilde{z}^+(k)$, not $\delta\tilde{z}^-(k)$ directly depends on *v(k)*. Then $E\{\delta z^-(k)v(k)\}=E\{v(k)\delta\tilde{z}^-(k)^T\}=0$. Equation (7.201) becomes

$$P^+(k)=\{[I-K(k)C2(k)]\delta\tilde{z}^-(k)\delta\tilde{z}^-(k)^T[I-K(k)C2(k)]^T\}+E\{K(k)v(k)v(k)^TK(k)^T\} \quad (7.202)$$

Using the characteristics of the measurement noise, equation (7.202) and the definition of the correlation matrix given by equation (191), (7.192), it can be written

$$P^+(k)=[I-K(k)C2(k)]P^-(k)[I-K(k)C2(k)]^T+K(k)R(k)K(k)^T \quad (7.203)$$

The next step is to determine the gain $K(k)$ such that the estimation error vector is minimized according to the criterion

$$\min|_{K(k)}\Im[K(k)]=Tr(P^+(k))=Tr\{[I-K(k)C2(k)]P^-(k)[I-K(k)C2(k)]^T+K(k)R(k)K(k)^T\} \quad (7.204)$$

The optimal value of $K(k)$ has to be determined on the basis of the necessary condition for optimality

$$\frac{\partial\Im(k)}{\partial K(k)}=0 \quad (7.205)$$

The equation (7.205) can be derived following the trace dependencies

$$\frac{\partial Tr}{\partial A}(ABA^T)=A(B+B^T) \quad (7.206)$$

Then

$$\frac{\partial\Im}{\partial K(k)}=-2[I-K(k)C2(k)]P^-(k)C2(k)^T+2K(k)R(k)=0 \quad (7.207)$$

In equation (7.207) is used that $[I-K(k)C2(k)]$ and $R(k)$ are symmetrical matrices. From (7.207)

$$K(k)=P^-(k)C2(k)^T[C2(k)P^-(k)C2(k)^T+R(k)]^{-1} \quad (7.208)$$

The optimal value of $K(k)$ can be used to calculate the optimal value of $P^+(k)$, by substitution of equation (7.208) into equation (7.203)

$$P^+(k) = P^-(k) - K(k)C2(k)P^-(k) - P^-(k)C2(k)^T K(k) + K(k)\left[C2(k)P^-(k)C2(k)^T + R(k)\right]K(k)^T =$$
$$= P^-(k) - K(k)C2(k)P^-(k) = \left[I - K(k)C2(k)\right]P^-(k)$$

(7.209)

From equation (7.209) follows that the update stage of the Kalman filter decreases the covariance of the estimation error, while the propagation stage in equation (7.197) increases the covariance

Algorithm: The Kalman filter algorithm is given by the following steps:

1. Determine the model equations (7.183), (7.184) and determine the noise characteristics, equation (7.185),
2. Initialization step
   - determine the initial state estimate $\hat{\tilde{z}}(t_0) = \hat{\tilde{z}}_0$
   - determine the initial covariance matrix $p_0 = E\left\{\delta\tilde{z}(t_0)\delta\tilde{z}(t_0)^T\right\}$
3. Calculate the Kalman filter gain from equation (7.208) with

   $$\hat{\tilde{z}}_0^- = \hat{\tilde{z}}_0 \text{ and } p_0^- = p_0 \qquad (7.210)$$
4. Update the state estimate according to equation (7.187) and update the covariance matrix for the estimation error according to the equation (7.209)
5. Propagate the calculated at the step 4 state estimate to the next step using the equation (7.186) and propagate the calculated at the step 4 covariance matrix to the next step using the equation (7.197)

If the measurement is not given at the initial point then the state estimates are propagated first to the next available measurement point $\hat{\tilde{z}}_0^+ = \hat{\tilde{z}}_0$ and $p_0^+ = p_0$.
This algorithm determines the predictor-corrector form of the Kalman filter.

The propagation and measurement update equations can be combined to form the a priori recursive form of the Kalman filter. To achieve this equation (7.189) is substituted in equation (7.188) and equation (7.207) into equation (7.197). The obtained estimation algorithm is

$$\hat{\tilde{z}}(k+1) = F(k)\hat{\tilde{z}}(k) + G(k)\hat{u}(k) + F(k)K(k)\left[\tilde{y}(k) - C2(k)\hat{\tilde{z}}(k)\right] \qquad (7.211)$$

$$K(k) = P(k)C2(k)^T\left[C2(k)P(k)C2(k)^T + R(k)\right]^{-1} \qquad (7.212)$$

$$P(k+1) = F(k)P(k)F(k)^T - F(k)K(k)C2(k)P(k)F(k)^T + H(k)Q(k)H(k)^T \qquad (7.213)$$

Equation (7.213) forms the discrete Riccati equation of the Kalman filter.

7.5.3 Steady state Kalman filter

For time invariant systems the error covariance matrix P reaches a steady state values very quickly. In this case a steady state (constant) value of the gain K can be pre-computed using the steady state covariance matrix and the number of computations is reduced significantly. The steady- state versions of the equations (7.211) – (7.213) is

$$\hat{\tilde{z}}(k+1) = F\tilde{z}(k) + G\tilde{u}(k) + FK\left[\tilde{y}(k) - C2\hat{\tilde{z}}(k)\right] \tag{7.214}$$

$$K = PC2^T\left[C2PC2^T + R\right]^{-1} \tag{7.215}$$

$$P = FPF^T - FPC2^T\left[C2PC2^T + R\right]^{-1}C2PF^T + HQH^T \tag{7.216}$$

7.5.4 Design of a discrete extended Kalman filter for estimation of concentrations of the immeasurable process variables

The discrete Kalman filter is derived assuming that both the model and the measurements are available in discrete-time form. Suppose that:

- the initial condition of state z_0 is known
- the discrete time model and measurements are corrupted by noise.

The truth model for the process is

$$z(k+1) = f(z,u,k) = Az(k) + C^T\rho(z,u,k) + Bz_{i\phi}(k) + H(k)\omega(k) \tag{7.217}$$

$$\tilde{y}(k) = \varphi[z(k)] + v(k) \tag{7.218}$$

where $v(k), \omega(k)$ are assumed to be zero mean Gaussian white-noise processes which means that the errors are not correlated forward or backward in time so that

$$E\left\{v(k)\,v(j)^T\right\} = \begin{cases} 0 & k \neq j \\ R(k), & k = j \end{cases} \tag{7.219}$$

and

$$E\left\{\omega(k)\,\omega(j)^T\right\} = \begin{cases} 0 & k \neq j \\ Q(k) & k = j \end{cases} \tag{7.220}$$

This requirement preserves the block diagonal structure of the covariance and weight matrices. It is assumed also that $v(k)$ and $\omega(k)$ are uncorrelated so that $E\left\{v(k)\,\omega(k)^T\right\} = 0$ for all k. The process $\omega(k)$ is forcing noise on the system of difference equations.

The problem is to update the current estimate of the state $\hat{z}(k)$ to obtain $\hat{z}(k+1)$ based upon all $k+1$ measurement subsets. To achieve this, the approach of the extended Kalman filter is used (Gelb, 1974), (Jazwinski, 1970). The idea for development of this filter is based on the notion that the true state is sufficiently close to the estimated state. Then the error dynamics can be represented sufficiently accurately by a linearised first order Taylor series expansion

$$f(z(k),u(k),k) \cong f(\bar{z}(k),u(k),k) + \frac{\partial f}{\partial z}\Big|_{\bar{z}}[z(k)-\bar{z}(k)] \tag{7.221}$$

$$\varphi[z(k),k] \cong \varphi[\bar{z}(k),k] + \frac{\partial \varphi}{\partial z}\Big|_{\bar{z}}[z(k)-\bar{z}(k)] \tag{7.222}$$

where $\bar{z}(k)$ is close to $z(k)$.

The idea in the extended Kalman filter is to use the current estimate (conditional mean) for the nominal state estimate, which means $\bar{z}(k)=\hat{z}(k)$. Taking the expectations of the equations (7.221), (7.222) to both sides with $\bar{z}(k)=\hat{z}(k)$ it is obtained

$$E\{f[z,u,k]\} = f[\hat{z},u,k] \tag{7.223}$$

$$E\{\varphi[z(k),k]\} = \varphi[\hat{z},k] \tag{7.224}$$

Equations (7.223), (7.224) are used in the extended Kalman filter structure for the state and output estimate using the measurements of the output $\tilde{y}$ and the values of the control u, in the corresponding data points

$$\hat{z}^-(k+1) = f[\hat{z}(k),u(k),k] \tag{7.225}$$

$$\hat{z}^+(k) = \hat{z}^-(k) + K(k)[y(k) - \varphi[\hat{z}^-(k),k]] \tag{7.226}$$

After substitution of equations (7.221), (7.222) into equations (7.225), (7.226) and after applying equations (7.215), (7.216) it is obtained for $\bar{z}(k)=\hat{z}(k)$ that

$$\hat{z}^-(k+1) = f[\hat{z}(k),u(k),k] - \frac{\partial f}{\partial z}\Big|_{\hat{z}(k)}[z(k)-\hat{z}(k)] = z(k+1) - H(k)\omega(k) - \frac{\partial f}{\partial z}\Big|_{\hat{z}(k)} \tag{7.227}$$

$$\delta z^-(k+1) = \hat{z}^-(k+1) - z^+(k+1) = F[\hat{z}(k),k]\delta z(k) - H(k)\omega(k) \tag{7.228}$$

$$\begin{aligned}\hat{z}^+(k) &= \hat{z}^-(k) + K(k)[\tilde{y}(k) - \varphi[\bar{z}^-(k),k]] + \frac{\partial \varphi}{\partial z}\Big|_{\hat{z}(k)}[z(k)-\hat{z}(k)] = \\ &= \hat{z}^-(k) + K(k)v(k) - K(k)C2[\hat{z}^-(k),k]z(k) + K(k)C2[\hat{z}(k),k]\end{aligned} \tag{7.229}$$

$$\delta z^+(k) = \hat{z}^+(k) - z(k) = [I - K(k)C2[\hat{z}^-(k),k]]\delta z(k) + K(k)v(k) \tag{7.230}$$

where

$$F[\hat{z}(k),k]=\frac{\partial f}{\partial z}\Big|_{\hat{z}(k)} \qquad C2[\hat{z}(k),k]=\frac{\partial \varphi}{\partial z}\Big|_{\hat{z}(k)} \tag{7.231}$$

The equations (7.226), (7.228) have the same structure as the equations (7.195), (7.199), which describe the behaviour of the prediction and measurement errors. This means that the same equations for the corresponding covariance matrices can be used, equations (7.197), (7.209). The same algorithm, described in the previous point for the linear discrete time model can be used with $F(k)$ replaced by $F[\hat{z}(k),k]$ and $C2(k)$ *by* $C2[\hat{z}(k),k]$. These matrices have to be recalculated for every step of the algorithm. They can not be constant in general and a steady-state gain of the filter cannot be calculated. The iterations are continued until the estimate is no longer improved.

7.5.5 Application of the discrete Kalman filters to the wastewater state variables estimation

The application of the extended Kalman filter to the Benchmark and Athlone processes is given by equation (7.217), (7.218) where the dimension and coefficients of the matrices C, ρ depends on the type of the biological model. The matrices $F(k), C2(k)$ are given by equation (7.231) were the derivatives according to the state are given for the ASM1 model by equation (7.171), (7.172) and for the UCT model equations (7.171), (7.179) and the derivatives according to the control are given by the equations (7.175) for the ASM1 model and by the equations (7.182) for the UCT model.

The application of the developed Kalman filters to the Benchmark and Athlone processes with reduced ASM1 and UCT bilogical model can be based on measurement of the concentration $S_{NH,n}$.

7.6 Conclusion

A major difficulty in the application of advanced monitoring and control strategies for the wastewater treatment is the difficulty in on-line measurement of the chemical and biological variables, such as biomass concentration, specific bacterial activity or intermediate product concentrations. The idea for using observers, also called software sensors that combine a number of readily available on-line measurements (gaseous flow rates, pH, dissolved gases, etc.,) with a process model for estimating the values of unmeasured state variables appeared and was developed during the last years. This

chapter groups and analyses the existing literature for estimation of biotechnological and wastewater treatment processes according to the existing models and the type of measured and estimated variables. It considers also the existing types of observers. Different methods were proposed to design such observers based on different principles. In practice the choice between them depends on the specificities of the considered problem, reliability of the process model, as well as the amount and accuracy of data. If a reliable process model is available and if this model has been thoroughly identified and validated, either a Kalman filter or a high gain observer can be developed. When the process model is not accurate enough, an asymptotic observer relying on mass-balances principles, but not on the uncertain kinetics, shall be used instead. If bounds are known for the uncertain inputs or parameters, an interval observer can be used for predicting intervals in which the unmeasured variables are guaranteed to belong.

The last part of the chapter proposes derivation of two types of discrete Kalman filters for the considered Benchmark and Athlone plant reduced mass balance models based on ASM1 and UCT biological models. The first derivation is for the linearised nonlinear models, obtained using Taylor series for the equilibrium points of the process. The second derivation is for an extended discrete Kalman filter, where the nonlinear models are used directly in the filtering process. The measured variables in both cases are the dissolved oxygen concentration (control input) and the concentration ammonia for every tank of the process.

The next chapters of the thesis represent simulation results for the methods developed till now.

CHAPTER EIGHT

THE SIMULATION OF THE WASTEWATER PROCESSES

8.1 Introduction

The problem for simulation of the activated sludge process (Katebi & Graells, 2005), (Mazouni, Ignatova & Harmand, 2005), (Kletting, 2005), (Lije, Chai & Cong, 2005), (Alex, Ogurek & Jumar, 2005), (Gernaey, Rosen, Batstone & Alex, 2004), (Hucka, 2003), (Rauch, Aalderink, Drebs, Snelling & Vanrolleghem, 1998) is solved in the software environment of SIMBA package. The chapter starts with a comparative analysis of the existing simulators and description of SIMBA. The Mitchell's Plain and Athlone plant configurations are considered and the corresponding mass balance equations are used. The building of Mitchell's Plain and Athlone processes in Simba is undertaken developing the requisite software. The results for the dynamic behaviour of the variables of the Mitchell's Plain (UCT), Athlone (ASM1) and Athlone (UCT) wastewater treatment plant are generated from the software implementation.

8.2 The importance of simulation

The role of simulation in the processes of design, planning, operating control, optimization of the activated sludge process is growing. The planning phase of wastewater treatment plants is done in simulation which helps to economise investment costs. The static assessment of the plant according binding instructions can be improved by adding studies of the dynamic behaviour of the plants (Katebi et al, 1999) and (Larsson and Skogestad, 2000). Numerous combinations of plants and tanks for design and modelling can also be compared for the various loads.

The operating costs of a wastewater treatment plant can be reduced by an intelligent automation. The development of advanced strategies of control is achieved by simulation which is a very beneficial tool since one gain high process stability as well as low operation costs.

Adaptable strategies for operating the plant are necessary for full advantage of its treatment behaviour. The success of design and modelling improves the understanding of the processes of wastewater treatment and aids the development of the best operation strategy in contrasting conditions.

The aim of utilizing mathematical modelling and simulation for the wastewater treatment process plant is to predict the behaviour of the activated sludge process so that the plant can be optimized efficiently. At the present moment this analysis is done manually rather than using computer software. It should be noted that the fundamental level of diagnosis is performed when monitoring the machinery and the plant equipment is done by the operator (Olsson and Newell, 2001). For essential pieces of information such as behaviour or basic physical parameters for example flowrates, pressures or levels the alarm of the equipment is activated which will warn the operator. But the alarm signals can be very late to take preventative measures as the activated sludge microorganisms react very slowly. Hence an early warning signal becomes vital in the biological wastewater treatment process. The real time simulation can solve this problem.

The problem for simulation of the dynamic behaviour of the activated sludge process is considered and solved in this chapter, on the basis of different process configurations and biological models. First, a short comparative analysis of the existing simulators in the field of wastewater treatment is done.

A Matlab/Simulink Simulator is developed for the COST Benchmark configuration with ASM1 model. It is described in part 5.3.
SIMBA simulator is used in part 5 to simulate the behaviour of the activated sludge process in the Athlone and Mitchell's Plain plant on the basis of ASM1 and UCT full and reduced models.
The results from the simulation are displayed at the end of the corresponding parts.

8.3 Simulators / Comparative analysis

Simulators have been used extensively in many disciplines over the years and are powerful tools for design, planning, process analysis, operator guidance, education and training. Simulators can also be considered as packages of knowledge of the dynamics of the process.

A simulation is the mimicking or imitating the behaviour of a particular system whereby a computer is used as an experimental platform (Olsson and Newell, 2001). The dynamic models can be packaged in special software platforms known as simulators. So using the

simulator one can study the effects of different parameter values, model complexities and initial conditions. It should be advised that simulators must be used with care because they are never better than the models and the data they are using.

Simulators have increasingly gained acceptance in the last ten years for wastewater treatment. The general hardware and software development as well as mathematical modelling applications have together made a contribution towards this. The complexities of nutrient removal systems utilise simulators which are considered important tools to better understand these processes. The integration of several sub-processes within a plant makes it necessary to analyse all the interactions. On a larger scale, the interactions with the sewerage network and the influent are important to be understood which require the possibilities of the total wastewater system to be fully utilized since they are dynamic and the time frame is crucial.

There are two kinds of simulators, block diagram simulators and general-purpose simulation languages. They allow for the simulation of continuous-time (differential equation) and discrete-time (difference equation) models and their variants.

- Block Diagram Simulators

  The representation for the control system structure is a block diagram which offers a block-diagram editor as graphical front end to their simulation engines. Such simulators are:
  1) Simulink from the MathWorks Inc.
  2) SystemBuild from Integrated Systems Inc.
  3) Easy-5 from Boeing

- General-Purpose Simulation Languages

  The general-purpose simulation language software is usually based on the equation oriented systems which have been enhanced by graphical front end. Such simulators are:
  1) Simnon from SSPA Systems
  2) ACSL from Mitchell & Gauthier Assoc.

- Combined Block and Language Simulators

  The more sophisticated user can program blocks for the libraries in high-level simulation language. They resemble general-purpose simulation languages which offer flexibility and ease of use of the graphical block diagram interface. Such type simulators are:
  1) Aspen Dynamics from AspenTech
  2) Nimbus from The University of Queensland

- Object-Oriented Modelling Languages

A limitation of the block-diagram simulators has to do with computational causality. One always defined what the input is and what the output is but unfortunately, causality is not sometimes defined since simultaneous events are acausal. Such simulators are:
1) Dynasim AB

- From Simulation to Real-Time Implementation

The automatic code from simulator to a real-time environment is highly sought-after. Such simulators are:
1) Simnon from SSPA Systems
2) Real-Time Workshop from the MathWorks Inc.
3) RealSim from Integrated Systems Inc.

8.4 Application Specific Simulators

A number of widespread simulators and simulation languages have been used in the wastewater treatment design and operation studies. The most used ones are:

1) BioWin from Envirosim Associates Ltd. of Oakville, Ontario, in partnership with Reid Crowther & Partners Ltd., Vancouver, B.C. Canada
2) EFOR from *Krüger* Systems, Denmark
3) Fortran
4) GPS-X from Hydromantis
5) Matlab Simulink
6) SIMBA (Otterpohl Wasserkonzepte)
7) STOAT from WRc, Software Services, Swindon, Wiltshire, UK
8) WEST from Hemmis n.v., Belgium
9) JASS, Uppsala University
10) SIMNON from SSPA Systems
11) AQUASIM
12) SSSP from Clemson University, S.C., USA
13) DSP from The University of Queensland, Australia

8.4.1 Short description of the simulators' capabilities

A short description and comparative study of some the above simulators is given below:

BioWin is a dedicated process simulator that makes use of linked process units to simulate biological wastewater treatment systems. It has been developed as a Microsoft Windows™ application and runs on an IBM PC-type computer.

EFOR™ is a software tool dedicated to the modeling of wastewater treatment systems, which makes it easy to construct a wide variety of wastewater treatment plants. Even treatment plants with a complex and dynamic operation are easily to be described and simulated with **EFOR™**.

FORTRAN has been recognized for years as a powerful programming language for scientific applications. FORTRAN permits a rigorous translation of the mathematical description into a set of code lines, which can be used to simulate the plant operation without any further plant assumptions. On the other hand, user-friendliness is restricted, especially with respect to data management.

GPS-X is a modular, multipurpose modeling environment for the simulation of wastewater treatment systems.

MATLAB (MATrix LABoratory) is a general, high-performance language for technical computing. It integrates computation, visualization and programming in a common environment. MATLAB is an interactive system and includes a large library of predefined mathematical functions. It also provides the user with the possibility to extend this library with new functions. The code for such functions are based on mathematical notation and can often be formulated in a fraction of the time it would take to write similar programs in a scalar language, such as C or Fortran. MATLAB features a family of application-specific toolboxes that extend the MATLAB environment in order to solve particular classes of problems. Furthermore, it is possible to use MATLAB for on-line applications, to build application specific graphical user interfaces and to create standalone (and platform independent) applications by automatic translation of MATLAB programs into C code. The wide field of applications that the toolboxes support is definitely one of the major advantages of MATLAB.

SIMBA® is a simulation environment based on Matlab™ & Simulink™ for the simulation of wastewater treatment systems and includes a specific user interface for wastewater treatment system simulation. SIMBA extends Matlab/Simulink using block libraries for biological and chemical treatment processes (i.e. activated sludge and biofilm processes, chemical precipitation and sedimentation using different models, sewer systems...).

STOAT is a modular multipurpose modelling environment for the simulation of wastewater treatment systems. STOAT includes an implementation of ASM1, called *IAWQ #1*, and the Takács settler model, called *Generic*.

WEST is a multi-platform modelling and experimentation system for the simulation of any system that can be represented by algebraic and differential equations. In WEST, ease of modelling a wide range of systems with maximum reuse of model knowledge is combined with high calculation performance. So far, WEST mainly has been used in the context of wastewater treatment research.

JASS stands for Java Activated Sludge process Simulator and is a Java program that simulates activated sludge processes.Version 3.0 was developed as a Master thesis work at the Department of Systems and Control, Uppsala University. Version 3.1 was developed shortly afterwards, implementing some minor updates and new features.

Simnon (SSPA Systems, 1991) is designed for solving ordinary differential and difference equations and for simulating dynamic systems. Numerical integration routines used to simulate differential equations and difference equations are solved by iterations. No symbolic analysis of the systems is possible. The systems may be described as an interconnection of subsystems (promoting a hierarchical system description) which may be either in continuous or discrete time. The user interacts with the program by typing commands (a graphical interface is available as an add-on product). Parameters, initial conditions and system descriptions can be modified interactively and the results are graphically or numerically displayed on the screen. A built-in macro facility allows the user to create own set of commands. The allowed complexity of the developed models is limited, although this is seldom a problem (the maximum number of state variables is 300). The program also has real-time capabilities, i.e., data can be transferred on-line from and to a real process connected to the I/O-devices of the computer.

AQUASIM (Reichert and Ruchti, 1994) is an interactive system for simulating and analysing the dynamics of aquatic systems. It is a graphical, mouse-driven program that includes a number of predefined compartment models (at present: mixed reactors, biofilm reactors and river section). The introduction of compartment models limits the generality of the program but allows the selection of efficient numerical algorithms according to the type of partial differential equation used to describe the transport mechanisms. The internal dynamic processes within a compartment are formulated by the user without any restrictions. Different compartments can be combined by using different types of links. The program also contains built-in tools for identifiability analysis (by sensitivity analysis), parameter estimation and

uncertainty analysis. Results are presented graphically (though not on-line and only as traditional two-dimensional plots) or saved as ASCII files. The program does not have any real-time capabilities but is only intended for off-line use.

8.4.2 Comparison of the simulators characteristics

There is a wide range of simulators available today, both for general purpose simulation of dynamic systems and with specific application to waste water treatment systems. They come in all shades and prices, specialized for different application areas, for different computing platforms and embracing different modelling paradigms. It is an impossible task to analyse all of them. The usual criteria for selection are models available, model library, modularity of the models, model validation flexibility to build larger plant models, graphical representations, numerics available, real time simulation, measurement data, output presentation, optimizers, and cost. Table 8.1 gives analysis of the simulator according to some of these criteria.

Table 8.1: A Comparative Analysis of the existing Simulators

Criteria	Model Avail.	Model Library	Modu-larity	Valid Model	Flexi-bility	Graph. Repres	Num. Avail.	R-T Simul.	Meas. Data	Output Presen	Opti-misers
Simulink	X	X	X	X	X	X	X	X	X	X	X
Systembuild	X	X	X	X	X	X	X	X	X	X	X
Easy-5	X	X	X	X	X	X	X	X	X		X
Simnon	X	X	X		X	X	X	X	X	X	
ACSL	X	X		X	X	X	X	X	X	X	
Aspen Dynamics	X	X	X		X	X	X	X	X	X	X
Nimbus	X	X	X		X	X	X	X	X	X	X
Dynasim AB	X	X				X	X	X	X	X	X
RealSim	X	X	X	X	X	X	X	X	X	X	X
GPS-X	X	X		X	X	X	X	X	X	X	X
SIMBA	X	X	X	X	X	X	X	X	X	X	X
AQUASIM	X	X	X	X		X	X		X		
BioWin	X	X	X			X	X		X		
EFOR	X	X	X	X	X	X	X	X	X	X	
STOAT	X	X	X	X	X	X	X	X	X	X	
WEST	X	X	X	X	X	X	X		X		
SSSP	X	X	X			X	X		X		
DSP	X	X	X		X	X	X		X	X	X

Matlab/Simulink and SIMBA software are used in this study. Matlab/Simulink is used for sensitivity analysis and for parameter estimation. The SIMBA simulator was used for both steady state and dynamic simulation. Description of these two software environments is done below:

8.5 MATLAB/ Simulink

Simulink (MathWorks, 1995) is an interactive system for simulating dynamic systems. It is a graphical, mouse-driven program that allows the user to model a system by drawing a block diagram in a graphical editor and manipulating it dynamically. It handles linear, non-linear, continuous time, discrete-time, multi-variable and multi-rate systems. A large number of predefined building blocks are included in the program and it is easy for the user to extend this library with blocks of their own. Hierarchical models are recommended since blocks may include other blocks and allows for graphical 'information zooming'. Results are numerically and graphically available in numerous ways. The major advantage of Simulink is the fact that it is an integrated part (toolbox) of the complete Matlab™ (*mat*rix *lab*oratory) computing environment (MathWorks, 1992). Matlab is an interactive system whose basic data element is a matrix that does not require dimensioning. It includes a large library of predefined functions and a simple way for the user to define own functions expressed as they are written mathematically – without any traditional programming. However, it is possible to include models written in C (using a special format) into the program, as well as creating stand-alone applications. Moreover, data can be transferred on-line in and out of the program from a real process connected to the I/O-devices of the computer, allowing for real-time analysis and online control. A large number of application-specific toolboxes that extend the Matlab environment in order to solve particular classes of problems are available. These toolboxes include signal processing, control system design, system identification, optimization, neural networks, fuzzy logic, statistics, partial differential equations, symbolic math, etc. Altogether this means that the Simulink user not only has the possibility to perform simulations but an enormous capability to manipulate and further validate the results. All this power is available at the user's fingertips in one integrated environment.

8.6 SIMBA

SIMBA, the German acronym for ***Sim****ulierung von* ***B****iologische* ***A****bwasser* (Simulation of Wastewater Treatment) is a dedicated software package for modelling and simulating wastewater treatment processes which was developed by IFAK, Magdeburg, Germany (SIMBA 4, Userguide 2001).

SIMBA is considered a custom made version of MATLAB/Simulink for wastewater treatment applications and utilizes Simulink as a general platform which allows the simulator client to

concentrate all the development work on modelling and has an attractive and intuitive user interface. As one can see SIMBA uses all of the features of Simulink and also can use MATLAB for all the latter-processing. It also includes facilities for software sensors and supervision of sensors, SIMBA 4, Userguide (2001). Many computer simulation users can readily extend the model library and can document their model developments in Simulink format. It is found that academic consumers make a valuable contribution to the modelling efforts and SIMBA enjoys increasing popularity in industrial applications. Now SIMBA can import historical data and can also be connected for Real-Time simulation to a SCADA system for data acquisition.

The modelling allows the analysis of wastewater treatment and the complex biochemical processes without any intervention in the real plant (Katebi, 1999) and (Schutze et al, 2002). The dynamic simulation which is based on a model of the time behaviour of concentrations can be implemented in any configuration of plants. With simulations, it is possible to strategise for the technology, structure and operation mode of the plant for example municipal sewage plants where the activated sludge processes are used.

The IWA work group Henze et al (1987) established the model ASM 1 which is the model mostly used in simulated activated sludge plants and generally accepted for control and process studies of biological wastewater treatment plants. Hence this model was adopted for SIMBA. The model ASM 3 described by Gujer et al (1999) was also made by the IWA as an available alternative. Now it can be seen that both proposals describe the COD and N elimination. ASM 1 has been updated to an alternative Model ASM 2d which has been developed by Henze et al., (1998). It contains extra processes of chemical and biological phosphorus elimination.

.

The modelling and simulation for the whole wastewater treatment section of a treatment plant, models for primary and secondary clarification, for storage of wastewater and models for other parts of a plant were attached to SIMBA. The primary clarifier model derived by Otterpohl et al (1994) establishes the COD and N elimination depending on the composition of the wastewater and the hydraulic retention time whilst various models are available for secondary clarifiers. One of them is the model which was originated by Takacs et al (1987), another is a two component layer model developed by Otterpohl and Freund (1992). In addition, tools for simulation of the anaerobic sludge digestion, the processes in sewer

systems, the wastewater treatment in biofilms and a simple river quality model are integrated.

The simulation system of SIMBA is completed for biological wastewater treatment plants which makes the main components these plants available as blocks of a library. SIMBA 4.0 is based on an open library in a new uniform model format since the creation of updated or the modification of existing model approaches is much simplified. Hence the special libraries of ASM 1, ASM 2d, ASM 3, SIMBA sewer, sludge and biofilm as well as applications for the implementation of the special control algorithms are available.

8.7 Development of the ASM1 and UCT biological models in SIMBA environment

8.7.1 Variables, parameters, input flow fractions

The model fractions of the activated sludge are sometimes separated into two components before the primary clarifier and after the clarifier. The fraction of each compound before the clarifier differs because of the hierarchical influence within the biomass. The ASM1 biological model is a part of the SIMBA software. The UCT biological model was developed in the thesis. The ASM1 model in SIMBA environment was used to be extrapolated for the UCT model fractions. The fractions of the UCT model are shown in Table 8.2 using the notations of the ASM1 model. This table is necessary to be determined in SIMBA in order to start the simulations. In the table Sol.(1) is a notation for soluble components, Part.(2) is for the particulate components and TS(3) is for the total solids. The particulate and solids are settled in the primary clarifier. The user defined fraction properties for each of the compounds describe the fraction of COD and N within them, whereby this would be used in future calculations for the SIMBA simulation.The fraction properties are shown in Table 8.3. The Numerical values for stoichiometry balance according to Table 8.3 are given in Table 8.4. The next step of the the simulation is to determine the instrumental variables and the parameters, a3÷a11, A, B, C from the Peterson matrix in Chapter 3.

In Table 8.5, the mass transfer coefficient for oxygen K_{La} (akla20) at 20 C is the external input. The instrumental variables are shorthand names for the expanded equations of each respective rate coefficient.The values of the parameters of the models are given in Table 8.6.

Table 8.2: The fractions of the UCT Activated Sludge process biological model

Name	Unit	Sol.(1),Part.(2), no TS(3)	Settl. in PC (0-1)	TSS content	Default value
XBH	gCOD/m^3	2	1	0	500
XBA	gCOD/m^3	2	1	0	100
XP	gCOD/m^3	2	1	0	0.01
XI	gCOD/m^3	2	1	0	0.01
XSA	gCOD/m^3	2	1	0	10
XSE	gCOD/m^3	2	1	0	10
XND	gCOD/m^3	3	1	0	1
SS	gCOD/m^3	1	0	0	10
SNH	g N/m^3	1	0	0	10
SND	g N/m^3	1	0	0	1
SNO	g N/m^3	1	0	0	10
SALK	Mol/m^3	1	0	0	7
SI	gCOD/m^3	1	0	0	0.01
SO	gCOD/m^3	1	0	0	0.01

Table 8.3: User defined fraction properties

Property	XBH	XBA	XP	XI	XSA	XSE	XND	SS	SNH	SND	SNO	SALK	SI	SO	Description
COD	1	1	1	1	1	1	0	1	0	0	-64/14	0	0	-1	COD content of unit
N	iXB	iXB	iXP	0	0	0	1	0	1	1	1	0	0	0	N content of unit

Table 8.4: User defined fraction properties values

Property	XBH	XBA	XP	XI	XSE	XSA	XND	SS	SNH	SND	SNO	SALK	SI	SO	Description
COD	1	1	1	1	1	1	0	1	0	0	-4.5714	0	0	-1	COD content of unit
N	0.068	0.068	0.068	0	0	0	1	0	1	1	1	0	0	0	N content of unit

Table 8.5: External inputs (EI) and instrumental variables (IV)

Name	Formula	Description	Unit
a3to11	0-(1-YH)/(40/14*YH)	IV	-
A	(1-YH)/(14*40/14*YH)-iXB/14	IV	-
B	(1-YH)/(40/14*YH)-iXB	IV	-
C	(1-YH)/(14*40/14*YH)+iXB/14	IV	-
a7to11	0-(1-YH)/(40/14*YH)	IV	-
a13to12	0-(iXB/14)-1/(7*YA)	IV	-
akla20	-	EI	-

Table 8.6: The values and units of the Parameters of the UCT biological model

Name	Formula	Description	Unit
YH	0.666	-	g COD/g COD
iXB	0.068	-	g N/g COD
iXP	0.068	-	g N/g COD
YA	0.15	-	g COD/g N
fP	0.08	-	-
myH	2.5*1.2^(T-20)	-	-
myA	0.5*1.123^(T-20)	-	-
KSH	5*1^(T-20)	-	g COD/m^3
KNO	0.1	-	g N/m^3
KOH	0.002	-	g O/m^3
KNA	0.01	-	g N/m^3
KMP	1.35*1.080^(T-20)	-	-
KSP	0.027*0.91^(T-20)	-	-
nyG	0.33	-	-
bH	0.62*1.029^(T-20)	-	1/d
bA	0.04*1.029^(T-20)	-	1/d
KA	0.17*1.029^(T-20)	-	g COD/g COD
fMA	1.0*1^(T-20)	-	-
KR	0.032*1.029^(T-20)	-	m^3/g COD
KSA	1.0*1.123^(T-20)	-	g N/m^3
KOA	0.002	-	g O/m^3
fTS	1.024^(T-20)	Temperature term for kla	-
SOsat	13.89-T*0.3825+T*T*0.007311-T*T*T*0.00006588	DO Saturation Concentr for 20 grd C	g/m^3

In Table 8.6, the operating temperature is at 20 C which means that the exponent for T-20 is equal to zero and then the expressions for the power of zero equal to unity and the value of the parameters are equal to the default value.

The influent has a steady state input and flow rate values from 0 to 24 hours, for COD, TKN and alkalinity. The characterization of the carbonaceous material and nitrogenous material in the influent is in terms of the COD and Total Kjeldahl Nitrogen (TKN) and it is necessary to specify the magnitudes of the various fractions of the influent COD and TKN. The research undertaken by the UCT group has indicated a division of the carbonaceous material and nitrogenous material in fractions. They are used to generated the various biological fractions in SIMBA where the influent is in the steady state. A Matlab function file is developed -

uct_influent which calculates the different COD and TKN fractions. The same file is used also for the ASM1 model. The file *uct_influent* is presented in the Appendix A.

The next step in simulation in SIMBA is to build the Peterson matrices and to calculate the stoichiometric balances. This is done for the ASM1 and UCT full and reduced models.

8.7.2 Peterson matrix and stoichiometric balances for the ASM1 full and reduced models

8.7.2.1 ASM1 full model

The Peterson matrix for the full ASM1 model consists of 9 processes and 13 variables. The SIMBA representation of this matrix is given in Table 8.7.

8.7.2.2 Reduced ASM1 Model

The reduced model developed in Chapter 4 is considered. The Peterson matrix of the reduced ASM1 model is given in Table 8.8.

8.7.3 Peterson matrix and balances for the UCT full and reduced models

8.7.3.1 UCT full model

The SIMBA UCT full model Peterson matrix is given in Table 8.9. The COD and TKN balances are given respectively in Table 8.10 and Table 8.11. The rates r3, r4 and r7, r8 are not equal to zero due to the evolution of nitrogen gas in the anoxic reactor as can be clearly seen in Table 8.11. The used default values for the UCT model are given in Table 3.4 . The default values of the parameter of the UCT original model has been assigned to the SIMBA equivalent which was developed for the UCT model.

8.7.3.2 Reduced UCT model

The SIMBA Peterson matrix for the reduced UCT model is given in Table 8.12. The stoichiometry and balances for the reduced model are given respectively in Table 8.13, Table 8.14 and Table 8.15.

Table 8.7: Peterson matrix for the full ASM1 model

FOX Editor ASM1m (ASM)

File Properties... Model spec. Properties... Options

	1 SI	2 SS	3 XI	4 XS	5 XBH	6 XBA	7 XP	8 SO	9 SNO	10 SNH	11 SND	12 XND	13 SALK
1	0	-1/YH	0	0	1	0	0	(YH - 1)/YH	0	-1*iXB	0	0	-1*iXB/
2	0	-1/YH	0	0	1	0	0	(YH - 1)/YH	-1*iXB	0	0	0	iXB/1
3	0	-1/YH	0	0	1	0	0	0	(YH - 1)/(2.86*YH)	-1*iXB	0	0	(1 - YH)/(14*2.86
4	0	-1/YH	0	0	1	0	0	0	(YH - 1)/(2.86*YH) - iXB	0	0	0	(1 - YH)/(14*2.86
5	0	0	0	0	0	1	0	-1*(4.57 - YA)/YA	1/YA	-1*iXB - 1/YA	0	0	-1*iXB/14 -
6	0	0	0	1 - fP	-1	0	fP	0	0	0	0	iXB - fP*iXP	0
7	0	0	0	1 - fP	0	-1	fP	0	0	0	0	iXB - fP*iXP	0
8	0	0	0	0	0	0	0	0	0	1	-1	0	1/14
9	0	1	0	-1	0	0	0	0	0	0	0	0	0
10	0	0	0	0	0	0	0	0	0	0	1	-1	0
11	0	0	0	0	0	0	0	1	0	0	0	0	0

FOX Editor ASM1m (ASM)

File Properties... Model spec. Properties... Options

	Process	
1	p1a	muH*LimSS*SO/(KOH + SO)*LimSALKH*SNH/(SNH + KNHNO)*XBH
2	p1b	muH*LimSS*SO/(KOH + SO)*LimSALKH*KNHNO/(SNH + KNHNO)*SNO/(SNO + KNHNO)*XBH
3	p2a	muH*LimSS*KOH/(KOH + SO)*SNO/(KNO + SNO)*SNH/(SNH + KNHNO)*nuG*LimSALKH*XBH
4	p2b	muH*LimSS*KOH/(KOH + SO)*SNO/(KNO + SNO)*nuG*LimSALKH*KNHNO/(SNH + KNHNO)*XBH
5	p3	muA*SNH/(KNH + SNH)*SO/(KOA + SO)*LimSALKA*XBA
6	p4	bH*XBH
7	p5	bA*XBA
8	p6	kA*SND*XBH
9	p7	kH*XS/XBH/(KX + XS/XBH)*(SO/(KOH + SO) + nuH*KOH/(KOH + SO)*SNO/(KNO + SNO) + nuHA*KOan/(KOan + SO + SNO))*XBH
10	p8	p7*XND/XS
11	p9	fTs*akla20*(SOsat - SO)

Table 8.8: Peterson matrix of the reduced ASM1 model

FOX Editor ASM1m (ASM)

File Properties... Model spec. Properties... Options

	1 SI	2 SS	3 XI	4 XS	5 XBH	6 XBA	7 XP	8 SO	9 SNO	10 SNH	11 SND	12 XND	13 SALK
1	0	-1/YH	0	0	0	0	0	0	(YH - 1)/(2.86*YH) - iXB	0	0	0	0
2	0	0	0	0	0	0	0	-1*(4.57 - YA)/YA	1/YA	-1*iXB - 1/YA	0	0	0
3	0	0	0	0	0	0	0	0	0	0	0	0	0
4	0	0	0	0	0	0	0	0	0	0	0	0	0
5	0	0	0	0	0	0	0	0	0	1	0	0	0
6	0	1	0	0	0	0	0	0	0	0	0	0	0
7	0	0	0	0	0	0	0	0	0	0	0	0	0
8	0	0	0	0	0	0	0	1	0	0	0	0	0
9	0	0	0	0	0	0	0	0	0	0	0	0	0

FOX Editor ASM1m (ASM)

File Properties... Model spec. Properties... Options

	Process	
1	p2b	muH*LimSS*KOH/(KOH + SO)*SNO/(KNO + SNO)*nuG*LimSALKH*KNHNO/(SNH + KNHNO)*XBH
2	p3	muA*SNH/(KNH + SNH)*SO/(KOA + SO)*LimSALKA*XBA
3	p4	bH*XBH
4	p5	bA*XBA
5	p6	kA*SND*XBH
6	p7	kH*XS/XBH/(KX + XS/XBH)*(SO/(KOH + SO) + nuH*KOH/(KOH + SO)*SNO/(KNO + SNO) + nuHA*KOan/(KOan + SO + SNO))*XBH
7	p8	p7*XND/XS
8	p9	fTs*akla20*(SOsat - SO)
9	r9	1.0

Table 8.9: The Peterson matrix of the full UCT model

Process	XBH	XBA	XP	XI	XSA	XSE	XND	SS	SNH	SND	SNO	SALK	SI	SO	Rate
r1	1	0	0	0	0	0	0	-1/YH	0-iXB	0	0	0-iXB/14	0	0-(1-YH)/YH	myH*SS/(KSH+SS)*SO/(KOH+SO)* *SNH/(KNA+SNH)*XBH
r2	1	0	0	0	0	0	0	-1/YH	0	0	0-iXB	iXB/14	0	0-((1-YH)/YH-iXB*64/14)	myH*SS/(KSH+SS)*SO/(KOH+SO)* *KNA/(KNA+SNH)*SNO/(KNO+SNO)*XBH
r3	1	0	0	0	0	0	0	-1/YH	0-iXB	0	a3to11	A	0	0	myH*SS/(KSH+SS)*KOH/(KOH+SO)* *SNH/(KNA+SNH)*SNO/(KNO+SNO)*XBH
r4	1	0	0	0	0	0	0	-1/YH	0	0	B	C	0	0	myH*SS/(KSH+SS)*KOH/(KOH+SO)* *KNA/(KNA+SNH)*SNO/(KNO+SNO)*XBH
r5	1	0	0	0	-1/YH	0	0	0	0-iXB	0	0	0-iXB/14	0	0-(1-YH)/YH	KMP*((XSA/XBH)/(KSP+(XSA/XBH)))* *SO/(KOH+SO)*SNH/(KNA+SNH)*XBH
r6	1	0	0	0	-1/YH	0	0	0	0	0	0-iXB	iXB/14	0	0-((1-YH)/YH-iXB*64/14)	KMP*((XSA/XBH)/(KSP+(XSA/XBH)))* *SO/(KOH+SO)*KNA/(KNA+SNH)* *SNO/(KNO+SNO)*XBH
r7	1	0	0	0	-1/YH	0	0	0	0-iXB	0	a7to11	A	0	0	KMP*((XSA/XBH)/(KSP+(XSA/XBH)))* *KOH/(KOH+SO)*SNH/(KNA+SNH)* *SNO/(KNO+SNO)*XBH*nyG
r8	1	0	0	0	-1/YH	0	0	0	0	0	B	C	0	0	MP*((XSA/XBH)/(KSP+(XSA/XBH)))* *KOH/(KOH+SO)*KNA/(KNA+SNH)* *SNO/(KNO+SNO)*XBH*nyG
r9	-1	0	fP	0	0	1-fP	0+iXB-fP*iXP	0	0	0	0	0	0	0	bH*XBH
r10	0	0	0	0	1	-1	0	0	0	0	0	0	0	0	KA*XSE*XBH*(fMA-XSA/XBH)
r11	0	0	0	0	0	0	-1	0	0	1	0	0	0	0	(r5+r6+r7+r8)*(XND/XSA)
r12	0	0	0	0	0	0	0	0	1	-1	0	1/14	0	0	KR*SND*XBH
r13	0	1	0	0	0	0	0	0	0-1/YA-iXB	0	0+1/YA	a13to12	0	0-(64/14-YA)/YA	myA*(SNH/(KSA+SNH))* *(SO/(KOA+SO))*XBA
r14	0	-1	fP	0	0	1-fP	0+iXB-fP*iXP	0	0	0	0	0	0	0	bA*XBA
r15	0	0	0	0	0	0	0	0	0	0	0	0	0	1	fTS*akla20*(SOsat-SO)

Table 8.10: COD-Balance (COD content of unit) for the full UCT model

Process	XBH	XBA	XP	XI	XSE	XSA	XND	SS	SNH	SND	SNO	SALK	SI	SO	Sum
r1	1	0	0	0	0	0	0	-1.5015	0	0	0	0	0	0.5015	0
r2	1	0	0	0	0	0	0	-1.5015	0	0	0.31086	0	0	0.19064	0
r3	1	0	0	0	0	0	0	-1.5015	0	0	0.8024	0	0	0	0.3009
r4	1	0	0	0	0	0	0	-1.5015	0	0	-0.49155	0	0	0	-0.99305
r5	1	0	0	0	-1.5015	0	0	0	0	0	0	0	0	0.5015	0
r6	1	0	0	0	-1.5015	0	0	0	0	0	0.31086	0	0	0.19064	0
r7	1	0	0	0	-1.5015	0	0	0	0	0	0.8024	0	0	0	0.3009
r8	1	0	0	0	-1.5015	0	0	0	0	0	-0.49155	0	0	0	-0.99305
r9	-1	0	0.08	0	0	0.92	0	0	0	0	0	0	0	0	0
r10	0	0	0	0	1	-1	0	0	0	0	0	0	0	0	0
r11	0	0	0	0	0	0	0	0	0	0	0	0	0	0	0
r12	0	0	0	0	0	0	0	0	0	0	0	0	0	0	0
r13	0	1	0	0	0	0	0	0	0	0	-30.4762	0	0	29.4762	0
r14	0	-1	0.08	0	0	0.92	0	0	0	0	0	0	0	0	0
r15	0	0	0	0	0	0	0	0	0	0	0	0	0	-1	-1

Table 8.11: N-Balance (N content of unit) for the full UCT model

Process	XBH	XBA	XP	XI	XSE	XSA	XND	SS	SNH	SND	SNO	SALK	SI	SO	Sum
r1	0.068	0	0	0	0	0	0	0	-0.068	0	0	0	0	0	0
r2	0.068	0	0	0	0	0	0	0	0	0	-0.068	0	0	0	0
r3	0.068	0	0	0	0	0	0	0	-0.068	0	-0.17553	0	0	0	-0.17553
r4	0.068	0	0	0	0	0	0	0	0	0	0.10753	0	0	0	0.17553
r5	0.068	0	0	0	0	0	0	0	-0.068	0	0	0	0	0	0
r6	0.068	0	0	0	0	0	0	0	0	0	-0.068	0	0	0	0
r7	0.068	0	0	0	0	0	0	0	-0.068	0	-0.17553	0	0	0	-0.17553
r8	0.068	0	0	0	0	0	0	0	0	0	0.10753	0	0	0	0.17553
r9	-0.068	0	0.00544	0	0	0	0.06256	0	0	0	0	0	0	0	0
r10	0	0	0	0	0	0	0	0	0	0	0	0	0	0	0
r11	0	0	0	0	0	0	-1	0	0	1	0	0	0	0	0
r12	0	0	0	0	0	0	0	0	1	-1	0	0	0	0	0
r13	0	0.068	0	0	0	0	0	0	-6.7347	0	6.6667	0	0	0	0
r14	0	-0.068	0.00544	0	0	0	0.06256	0	0	0	0	0	0	0	0
r15	0	0	0	0	0	0	0	0	0	0	0	0	0	0	0

Table 8.12: Peterson matrix for the reduced UCT model

FOX Editor UCT model (ASM)

File Properties... Model spec. Properties... Options

	1 XBH	2 XBA	3 XP	4 XI	5 XSA	6 XSE	7 XND	8 SS	9 SNH	10 SND	11 SNO	12 SALK	13 SI	14 SO
1	0	0	0	0	0	0	0	-1/YH	0-iXB	0	0	0	0	0-(1-YH)/YH
2	0	0	0	0	0	0	0	-1/YH	0	0	0-iXB	0	0	0-((1-YH)/YH-iXB*64/14)
3	0	0	0	0	0	0	0	-1/YH	0-iXB	0	a3toll	0	0	0
4	0	0	0	0	0	0	0	-1/YH	0	0	B	0	0	0
5	0	0	0	0	0	0	0	0	0-iXB	0	0	0	0	0-(1-YH)/YH
6	0	0	0	0	0	0	0	0	0	0	0-iXB	0	0	0-((1-YH)/YH-iXB*64/14)
7	0	0	0	0	0	0	0	0	0-iXB	0	a7toll	0	0	0
8	0	0	0	0	0	0	0	0	0	0	B	0	0	0
9	0	0	0	0	0	0	0	0	0	0	0	0	0	0
10	0	0	0	0	0	0	0	0	0	0	0	0	0	0
11	0	0	0	0	0	0	0	0	0	0	0	0	0	0
12	0	0	0	0	0	0	0	0	1	0	0	0	0	0
13	0	0	0	0	0	0	0	0	0-1/YA-iXB	0	0+1/YA	0	0	0
14	0	0	0	0	0	0	0	0	0	0	0	0	0	0
15	0	0	0	0	0	0	0	0	0	0	0	0	0	0

FOX Editor UCT model (ASM)

File Properties... Model spec. Properties... Options

	Process	
1	r1	myH*SS/(KSH+SS)*SO/(KOH+SO)*SNH/(KNA+SNH)*XBH
2	r2	myH*SS/(KSH+SS)*SO/(KOH+SO)*KNA/(KNA+SNH)*SNO/(KNO+SNO)*XBH
3	r3	myH*SS/(KSH+SS)*KOH/(KOH+SO)*SNH/(KNA+SNH)*SNO/(KNO+SNO)*XBH
4	r4	myH*SS/(KSH+SS)*KOH/(KOH+SO)*KNA/(KNA+SNH)*SNO/(KNO+SNO)*XBH
5	r5	KMP*((XSA/XBH)/(KSP+(XSA/XBH)))*SO/(KOH+SO)*SNH/(KNA+SNH)*XBH
6	r6	KMP*((XSA/XBH)/(KSP+(XSA/XBH)))*SO/(KOH+SO)*KNA/(KNA+SNH)*SNO/(KNO+SNO)*XBH
7	r7	KMP*((XSA/XBH)/(KSP+(XSA/XBH)))*KOH/(KOH+SO)*SNH/(KNA+SNH)*SNO/(KNO+SNO)*XBH*nyG
8	r8	KMP*((XSA/XBH)/(KSP+(XSA/XBH)))*KOH/(KOH+SO)*KNA/(KNA+SNH)*SNO/(KNO+SNO)*XBH*nyG
9	r9	bH*XBH
10	r10	KA*XSE*XBH*(fMA-XSA/XBH)
11	r11	(r5+r6+r7+r8)*(XND/XSA)
12	r12	KR*SND*XBH
13	r13	myA*(SNH/(KSA+SNH))*(SO/(KOA+SO))*XBA
14	r14	bA*XBA
15	r15	fTS*akla20*(SOsat-SO)

Table 8.13: Stoichiometry of the UCT reduced model

Process	XBH	XBA	XP	XI	XSA	XSE	XND	SS	SNH	SND	SNO	SALK	SI	SO	Rate
r1	0	0	0	0	0	0	0	-1.5015	-0.068	0	0	0	0	-0.5015	56765.984
r2	0	0	0	0	0	0	0	-1.5015	0	0	-0.068	0	0	-0.19064	56.2039
r3	0	0	0	0	0	0	0	-1.5015	-0.068	0	-0.17553	0	0	0	11240.7889
r4	0	0	0	0	0	0	0	-1.5015	0	0	0.10753	0	0	0	11.2408
r5	0	0	0	0	0	0	0	0	-0.068	0	0	0	0	-0.5015	708334.219
r6	0	0	0	0	0	0	0	0	0	0	-0.068	0	0	-0.19064	701.321
r7	0	0	0	0	0	0	0	0	-0.068	0	-0.17553	0	0	0	46287.1866
r8	0	0	0	0	0	0	0	0	0	0	0.10753	0	0	0	46.2872
r9	0	0	0	0	0	0	0	0	0	0	0	0	0	0	310
r10	0	0	0	0	0	0	0	0	0	0	0	0	0	0	0
r11	0	0	0	0	0	0	0	0	0	0	0	0	0	0	0
r12	0	0	0	0	0	0	0	0	1	0	0	0	0	0	407
r13	0	0	0	0	0	0	0	0	-6.7347	0	6.6667	0	0	0	6.5985
r14	0	0	0	0	0	0	0	0	0	0	0	0	0	0	4
r15	0	0	0	0	0	0	0	0	0	0	0	0	0	0	8.6274

Table 8.14: COD-Balance (COD content of unit) of UCT reduced model

Process	XBH	XBA	XP	XI	XSA	XSE	XND	SS	SNH	SND	SNO	SALK	SI	SO	Sum
r1	0	0	0	0	0	0	0	-1.5015	0	0	0	0	0	0.5015	-1
r2	0	0	0	0	0	0	0	-1.5015	0	0	0.31086	0	0	0.19064	-1
r3	0	0	0	0	0	0	0	-1.5015	0	0	0.8024	0	0	0	-0.6991
r4	0	0	0	0	0	0	0	-1.5015	0	0	-0.49155	0	0	0	-1.993
r5	0	0	0	0	0	0	0	0	0	0	0	0	0	0.5015	0.5015
r6	0	0	0	0	0	0	0	0	0	0	0.31086	0	0	0.19064	0.5015
r7	0	0	0	0	0	0	0	0	0	0	0.8024	0	0	0	0.8024
r8	0	0	0	0	0	0	0	0	0	0	-0.49155	0	0	0	-0.49155
r9	0	0	0	0	0	0	0	0	0	0	0	0	0	0	0
r10	0	0	0	0	0	0	0	0	0	0	0	0	0	0	0
r11	0	0	0	0	0	0	0	0	0	0	0	0	0	0	0
r12	0	0	0	0	0	0	0	0	0	0	0	0	0	0	0
r13	0	0	0	0	0	0	0	0	0	0	-30.4762	0	0	0	-30.4762
r14	0	0	0	0	0	0	0	0	0	0	0	0	0	0	0
r15	0	0	0	0	0	0	0	0	0	0	0	0	0	0	0

Table 8.15: N-Balance (N content of unit) of the UCT reduced model

Process	XBH	XBA	XP	XI	XSA	XSE	XND	SS	SNH	SND	SNO	SALK	SI	SO	Sum
r1	0	0	0	0	0	0	0	0	-0.068	0	0	0	0	0	-0.068
r2	0	0	0	0	0	0	0	0	0	0	-0.068	0	0	0	-0.068
r3	0	0	0	0	0	0	0	0	-0.068	0	-0.17553	0	0	0	-0.24353
r4	0	0	0	0	0	0	0	0	0	0	0.10753	0	0	0	0.10753
r5	0	0	0	0	0	0	0	0	-0.068	0	0	0	0	0	-0.068
r6	0	0	0	0	0	0	0	0	0	0	-0.068	0	0	0	-0.068
r7	0	0	0	0	0	0	0	0	-0.068	0	-0.17553	0	0	0	-0.24353
r8	0	0	0	0	0	0	0	0	0	0	0.10753	0	0	0	0.10753
r9	0	0	0	0	0	0	0	0	0	0	0	0	0	0	0
r10	0	0	0	0	0	0	0	0	0	0	0	0	0	0	0
r11	0	0	0	0	0	0	0	0	0	0	0	0	0	0	0
r12	0	0	0	0	0	0	0	0	1	0	0	0	0	0	1
r13	0	0	0	0	0	0	0	0	-6.7347	0	6.6667	0	0	0	-0.068
r14	0	0	0	0	0	0	0	0	0	0	0	0	0	0	0
r15	0	0	0	0	0	0	0	0	0	0	0	0	0	0	0

8.8 Simulation of the Mitchell's Plain plant on the basis of the UCT full biological model

8.8.1. SIMBA diagrams

The Mitchell's Plain structure and mass balances described in Chapter 3 are used to build the SIMBA diagram of the plant. The overall diagram is given in Figure 8.1. The exact connections between the tanks are shown in Figure 8.2

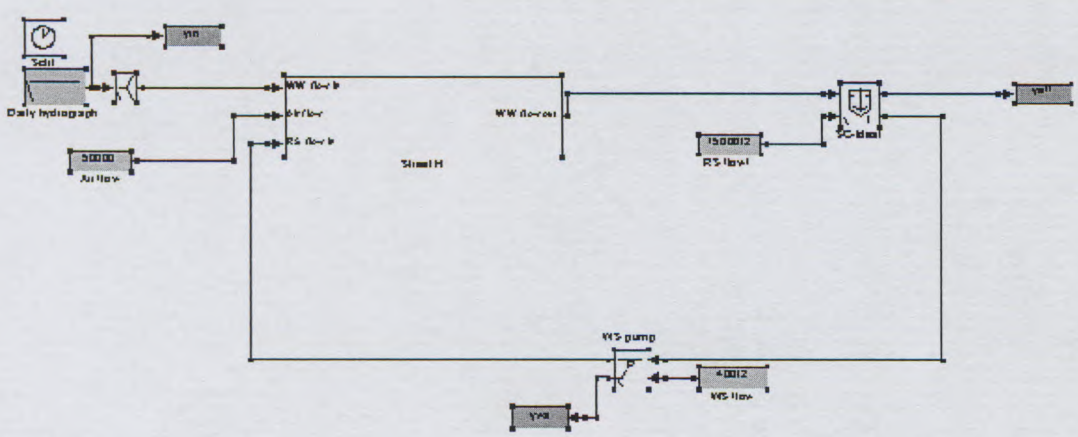

Figure 8.1: A schematic SIMBA diagram of the overall Mitchell's Plain wastewater treatment plant

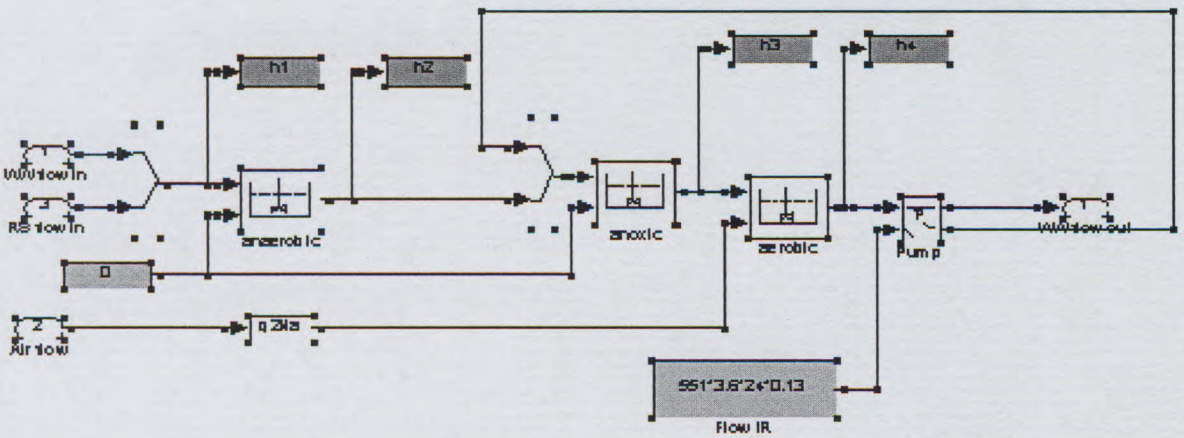

Figure 8.2: A schematic SIMBA diagram of the internal structure of the Mitchell's Plain wastewater treatment plant

Point h1-h4 show the places for measurement the values of the variables of the process as follows – h1 is for the influent, h2 is after the anaerobic tank, h3 is after the anoxic tank and h4 is after the aerobic tank.

8.8.2 Results from the simulation

The simulation is done for a period of 100 days. The results from the simulations are read from the communication window of SIMBA, given in Figure 5.3.

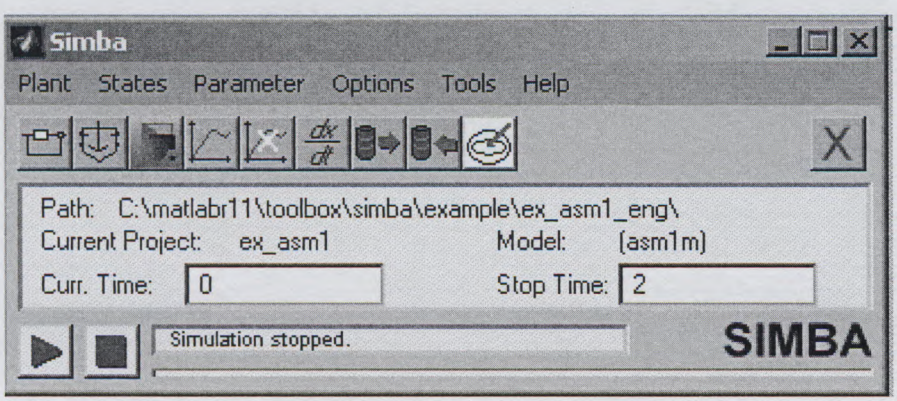

Figure 8.3: Front panel of the SIMBA simulation package

The results are shown for every of the process tanks and variables as follows:

8.8.2.1 Dynamic behaviour of the influent (point h1) in Mitchell Plain wastewater plant simulated over a period of 100 days for total sludge age of 16 days at 22 C

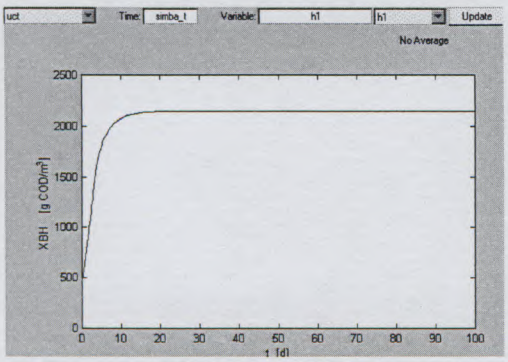

Figure 8.4: The dynamic behaviour of biological (active) heterotrophic biomass fraction at h1

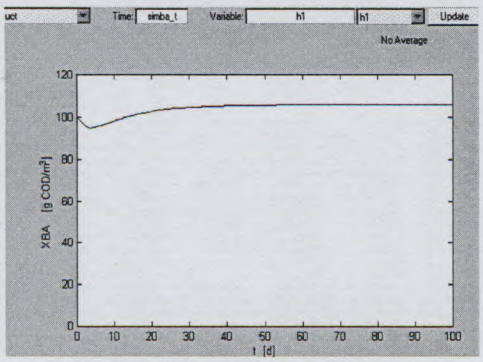

Figure 8.5: The dynamic behaviour of biological (active) autotrophic biomass fraction at h1

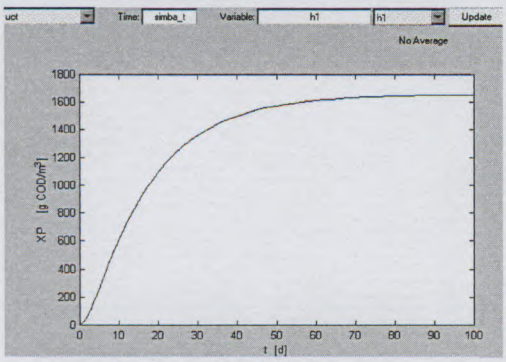

Figure 8.6: The dynamic behaviour of endogenous mass fraction at h1

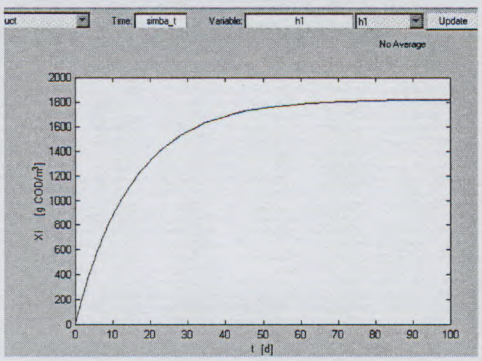

Figure 8.7: The dynamic behaviour of inert mass fraction at h1

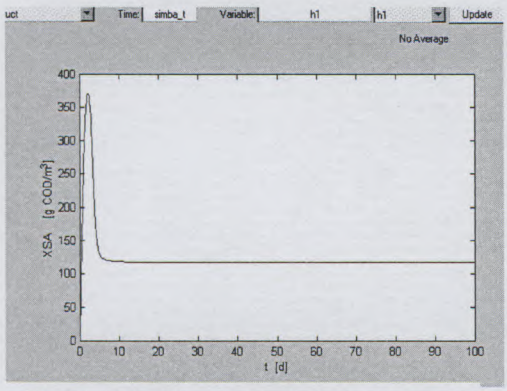

Figure 8.8: The dynamic behaviour of adsorbed slowly biodegradable substrate fraction at h1

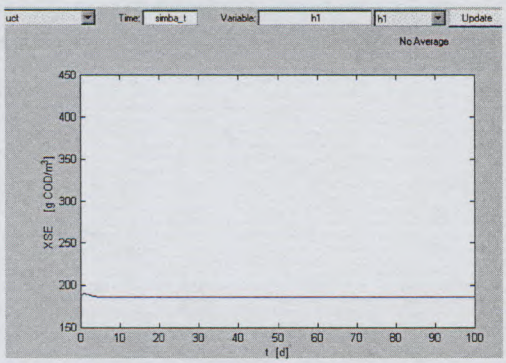

Figure 8.9: The dynamic behaviour of enmeshed slowly biodegradable substrate fraction at h1

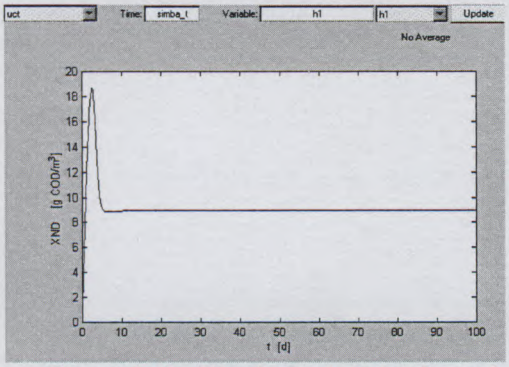

Figure 8.10: The dynamic behaviour of biodegradable particulate organic nitrogen fraction at h1

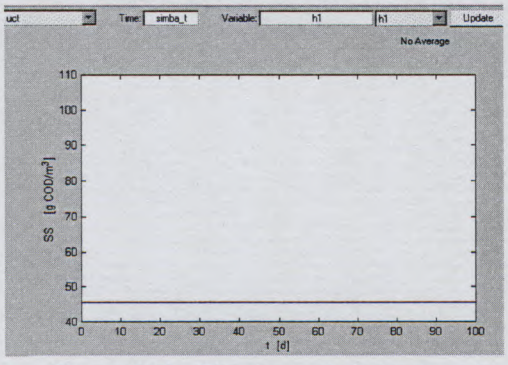

Figure 8.11: The dynamic behavior of readily biodegradable (soluble) substrate fraction at h1

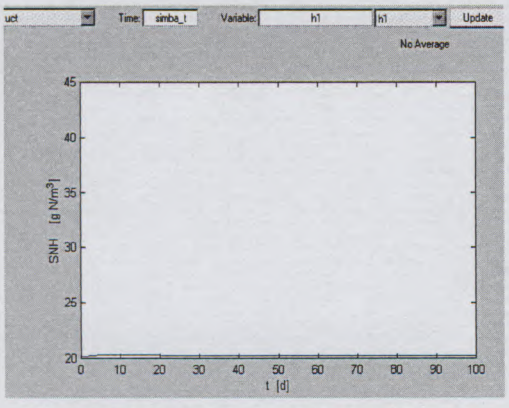

Figure 8.12: The dynamic behaviour of ammonia nitrogen at h1

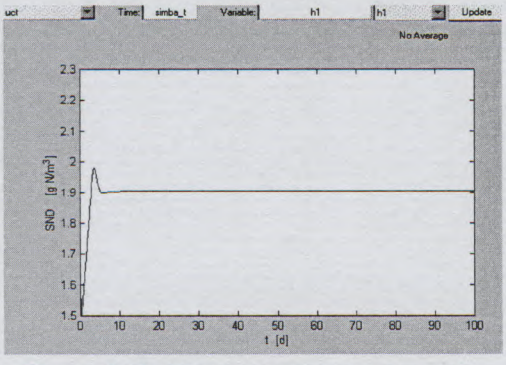

Figure 8.13: The dynamic behaviour of biodegradable soluble organic nitrogen at h1

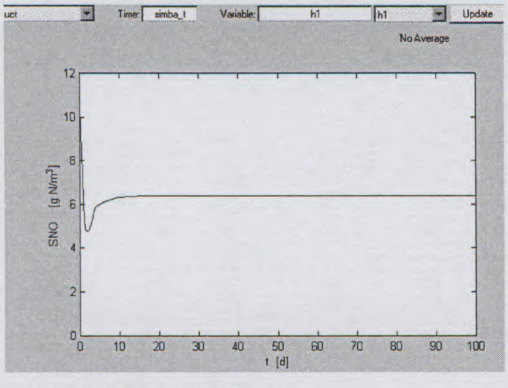

Figure 8.14: The dynamic behaviour of nitrate nitrogen at h1

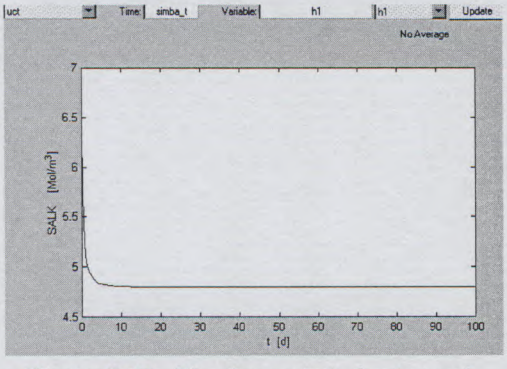

Figure 8.15: The dynamic behaviour of alkalinity at h1

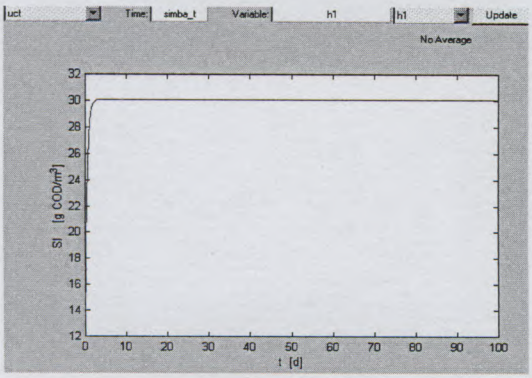

Figure 8.17: The dynamic behaviour of unbiodegradable soluble substrate fraction at h1

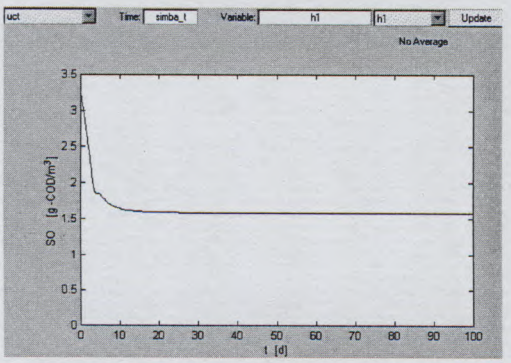

Figure 8.17: The dynamic behaviour of oxygen at h1

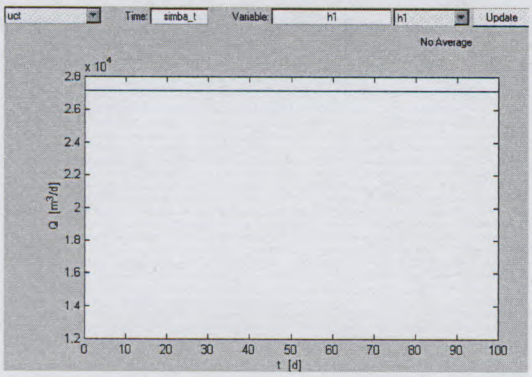

Figure 8.18: The dynamic behaviour of flow rate at h1

8.8.2.2 Dynamic behaviour of the process variables after the anaerobic tank (point h2) in Mitchell Plain activated sludge plant simulated over a period of 100 days for total sludge age of 16 days at 22 C

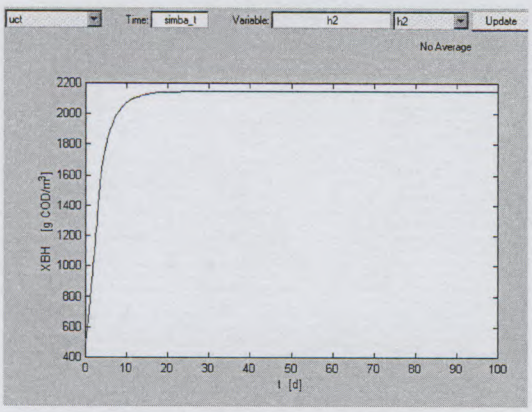

Figure 8.19: The dynamic behaviour of biological (active) heterotrophic biomass fraction at h2

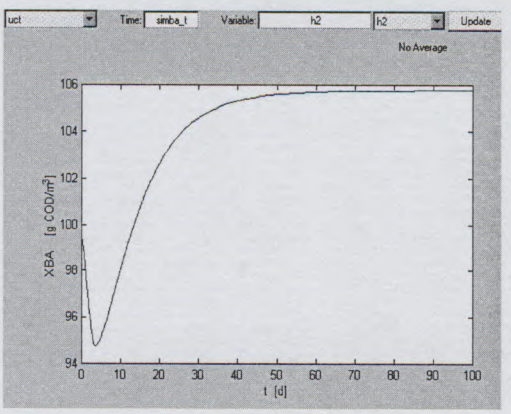

Figure 8.20: The dynamic behaviour of biological (active) autotrophic mass fraction at h2

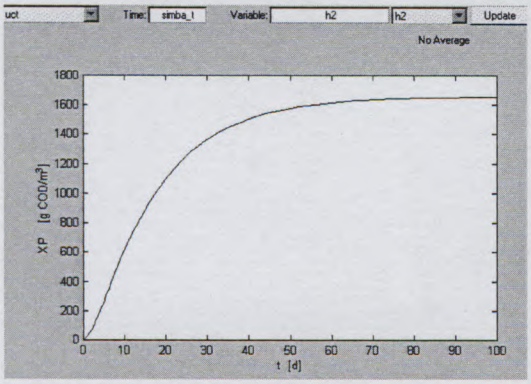

Figure 8.21: The dynamic behaviour of endogenous mass fraction at h2

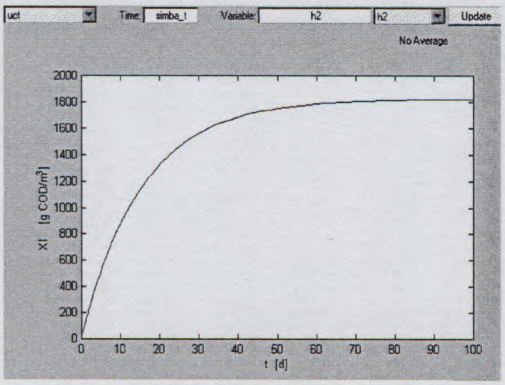

Figure 8.22: The dynamic behaviour of inert mass fraction at h2

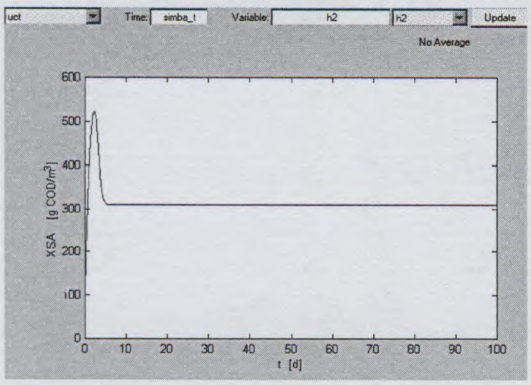

Figure 8.23: The dynamic behaviour of adsorbed slowly biodegradable substrate fraction at h2

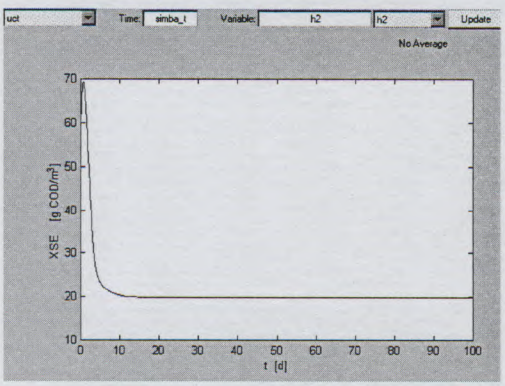

Figure 8.24: The dynamic behaviour of enmeshed slowly biodegradable substrate fraction at h2

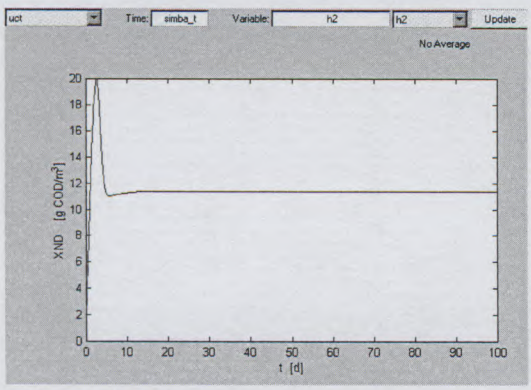

Figure 8.25: The dynamic behaviour of biodegradable particulate organic nitrogen fraction at h2

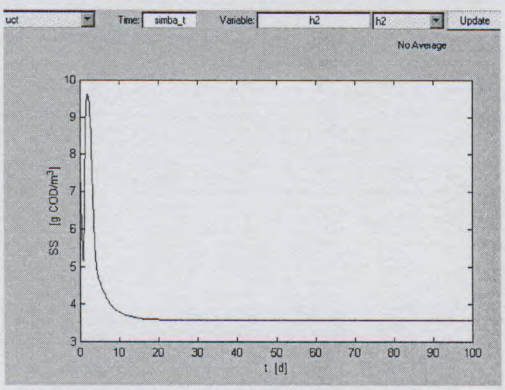

Figure 8.26: The dynamic behaviour of readily biodegradable (soluble) substrate fraction at h2

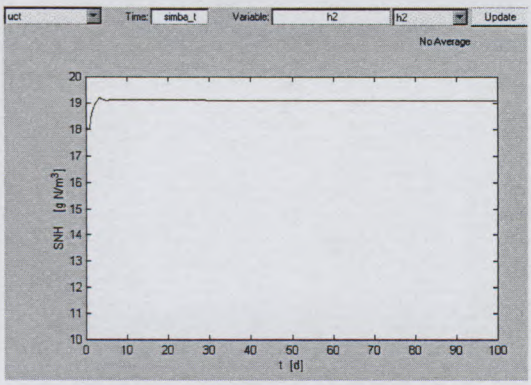

Figure 8.27: The dynamic behaviour of ammonia nitrogen fraction at h2

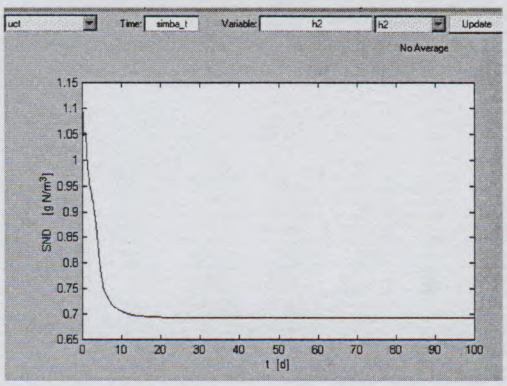

Figure 8.28: The dynamic behaviour of biodegradable particulate organic nitrogen fraction at h2

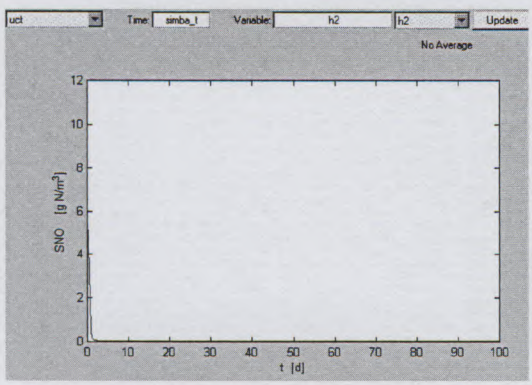

Figure 8.29: The dynamic behaviour of nitrate nitrogen fraction at h2

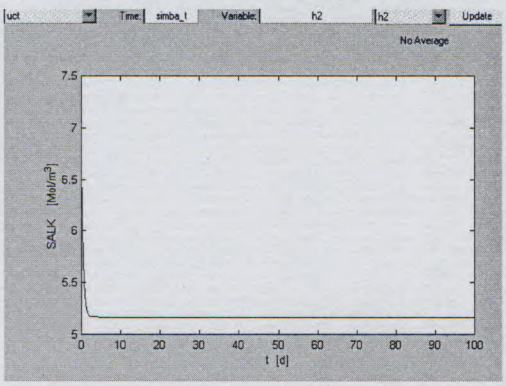

Figure 8.30: The dynamic behaviour of alkalinity at h2

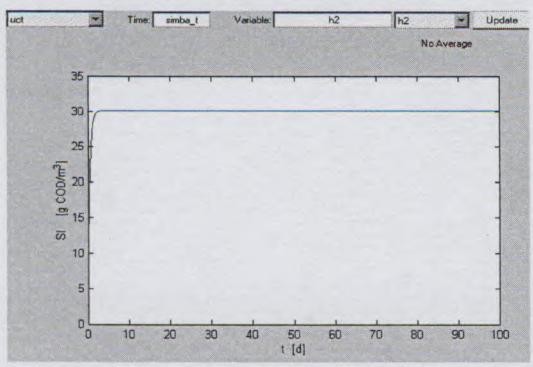

Figure 8.31: The dynamic behaviour of unbiodegradable soluble substrate fraction at h2

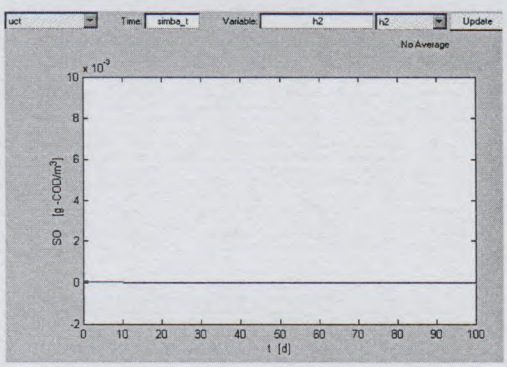

Figure 8.32: The dynamic behaviour of oxygen at h2

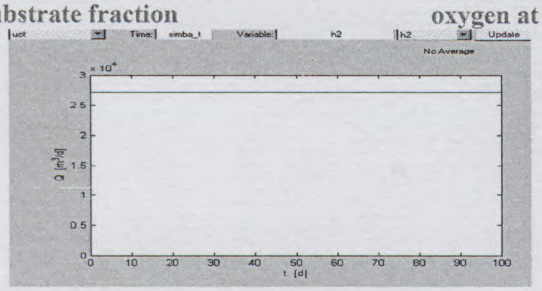

Figure 8.33: The dynamic behaviour of flow rate at h2

8.8.2.3 Dynamic behaviour of the process variables after the anoxic tank (point h3) in Mitchell Plain activated sludge plant simulated over a period of 100 days for total sludge age of 16 days at 22 C

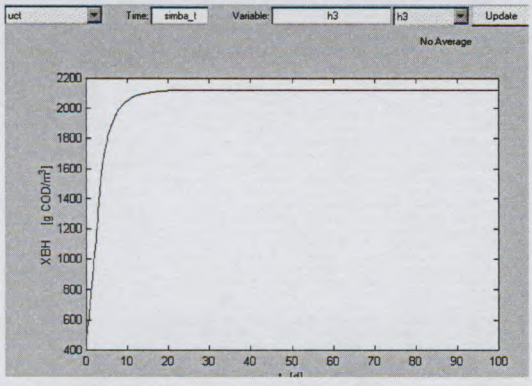

Figure 8.34: The dynamic behaviour of biological (active) heterotrophic biomass fraction at h2

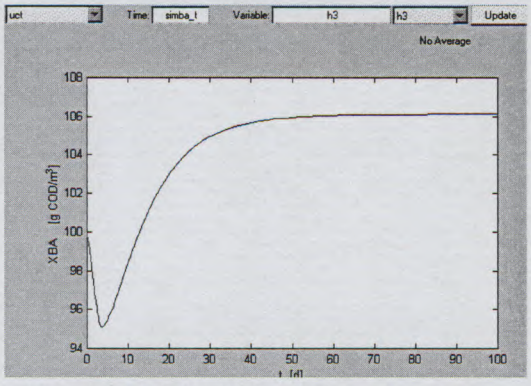

Figure 8.35: The dynamic behaviour of biological (active) autotrophic mass fraction at h3

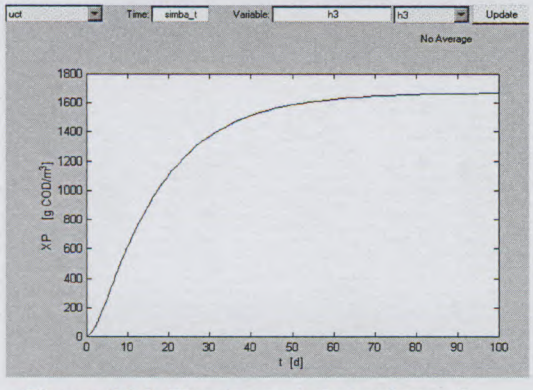

Figure 8.36: The dynamic behaviour of endogenous mass fraction at h3

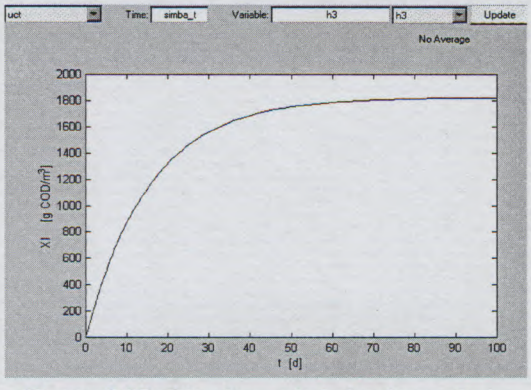

Figure 8.37: The dynamic behaviour of inert mass fraction at h3

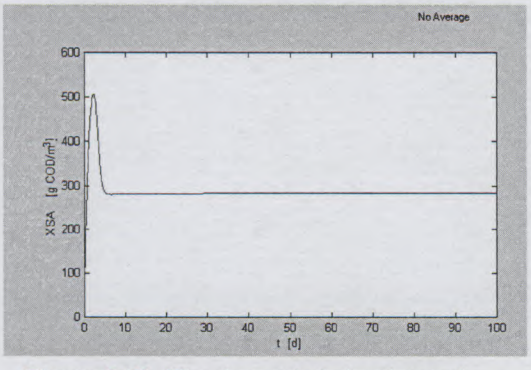

Figure 8.38: The dynamic behaviour of adsorbed slowly biodegradable substrate fraction at h3

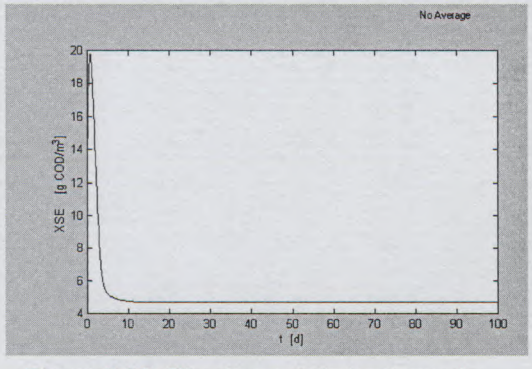

Figure 8.39: The dynamic behaviour of enmeshed slowly biodegradable substrate fraction at h3

Figure 8.34: The dynamic behaviour

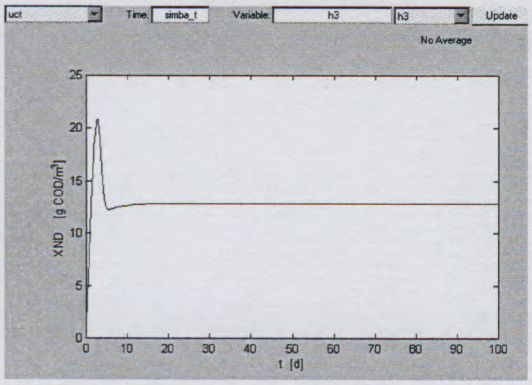

Figure 8.40: The dynamic behaviour of biodegradable particulate organic nitrogen fraction at h3

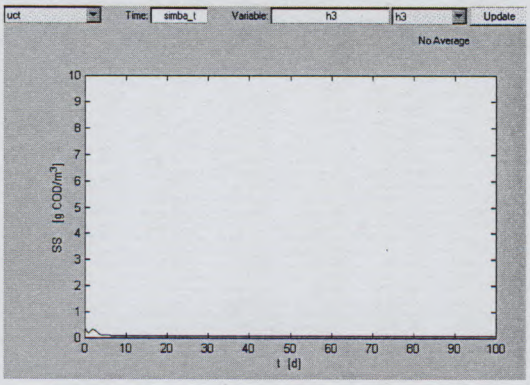

Figure 8.41: The dynamic behaviour of readily biodegradable (soluble) substrate fraction at h3

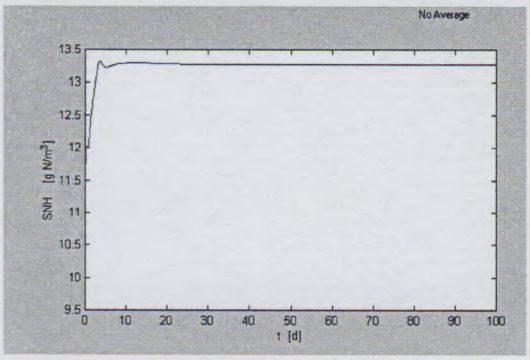

Figure 8.42: The dynamic behaviour of ammonia nitrogen fraction at h3

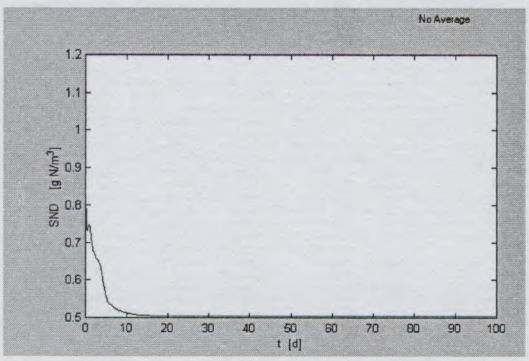

Figure 8.43: The dynamic behaviour of biodegradable particulate organic nitrogen fraction at h3

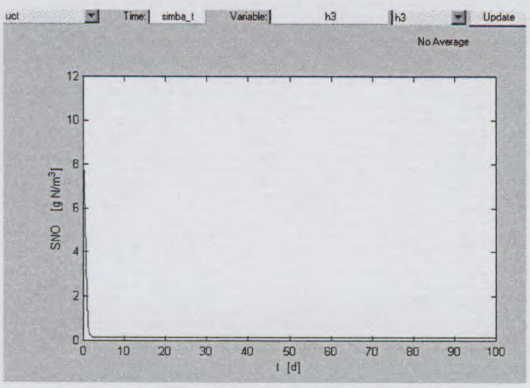

Figure 8.44: The dynamic behaviour of nitrate nitrogen fraction at h3

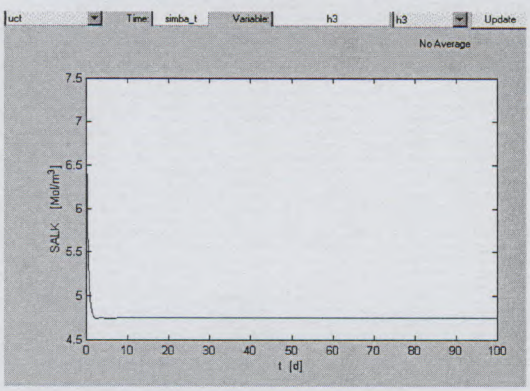

Figure 8.45: The dynamic behaviour of alkalinity at h3

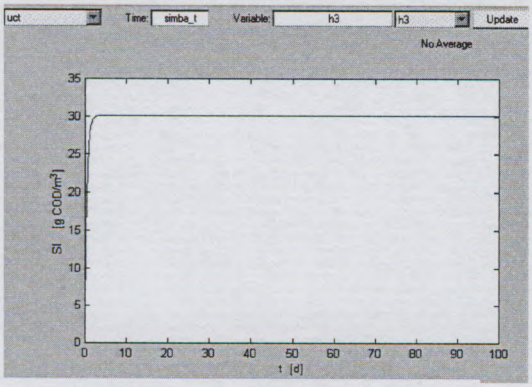

Figure 8.46: The dynamic behaviour of unbiodegradable soluble substrate fraction at h3

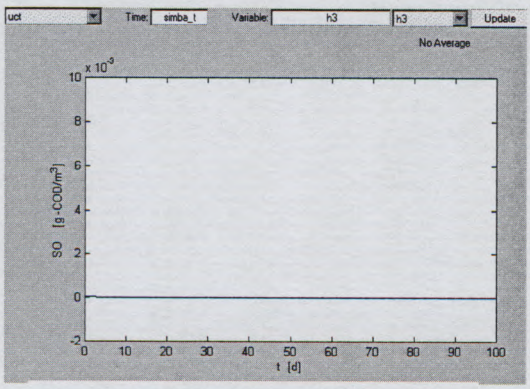

Figure 8.47: The dynamic behaviour of oxygen at h3

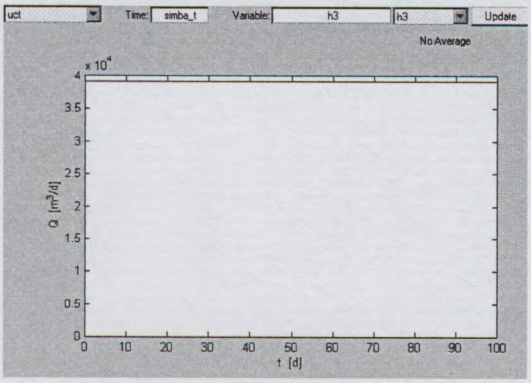

Figure 8.48: The dynamic behaviour of flow rate at h3

8.8.2.4 Dynamic behaviour of the process variables after the aerobic tank (point h4) in Mitchell Plain activated sludge plant simulated over a period of 100 days for total sludge age of 16 days at 22 C

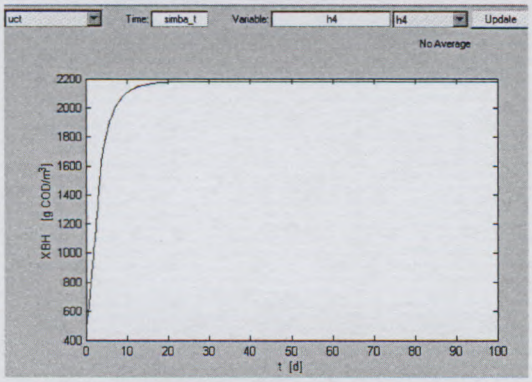

Figure 8.49: The dynamic behaviour of biological (active) heterotrophic biomass fraction at h4

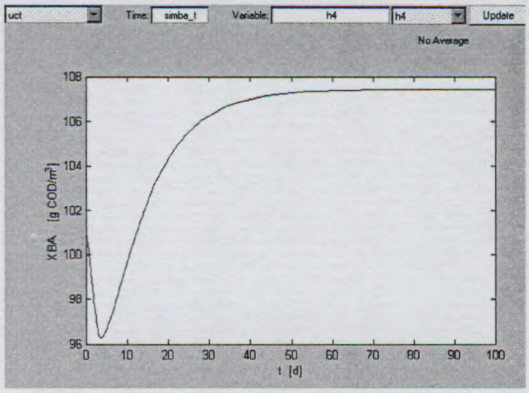

Figure 8.50: The dynamic behavior of biological (active) autotrophic biomass fraction at h4

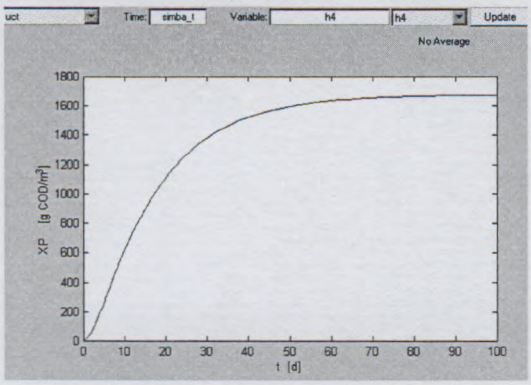

Figure 8.51: The dynamic behaviour of endogenous mass fraction at h4

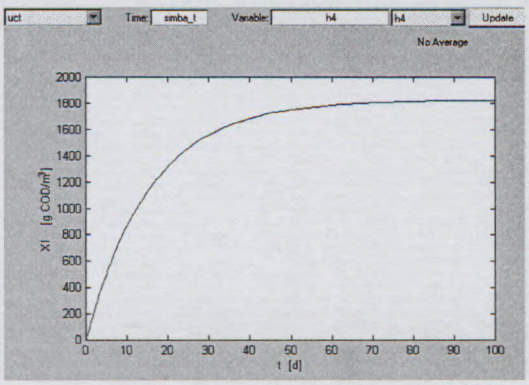

Figure 8.52: The dynamic behaviour of inert mass fraction at h4

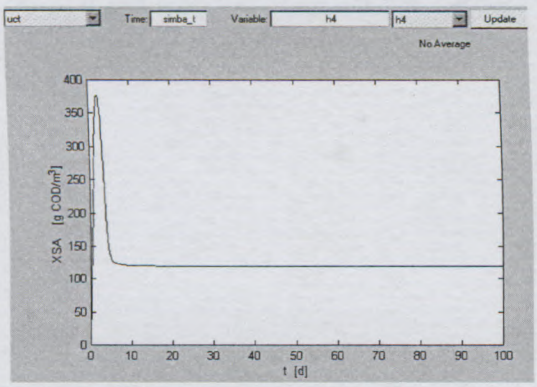

Figure 8.53: The dynamic behaviour of adsorbed slowly biodegradable substrate fraction at h4

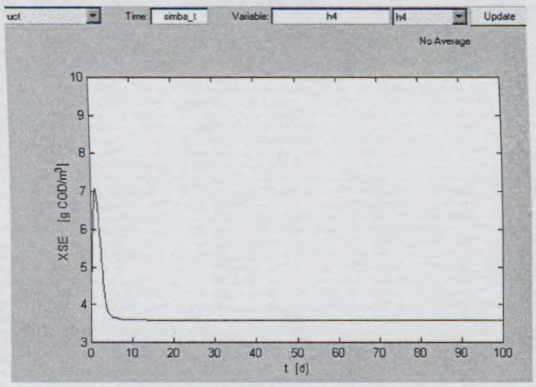

Figure 8.54: The dynamic behaviour of enmeshed slowly biodegradable substrate fraction at h4

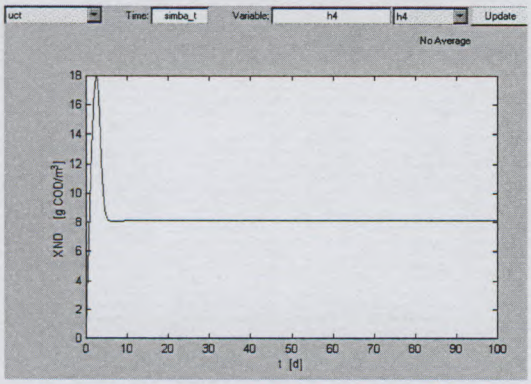

Figure 8.55: The dynamic behaviour of biodegradable particulate organic nitrogen fraction at h4

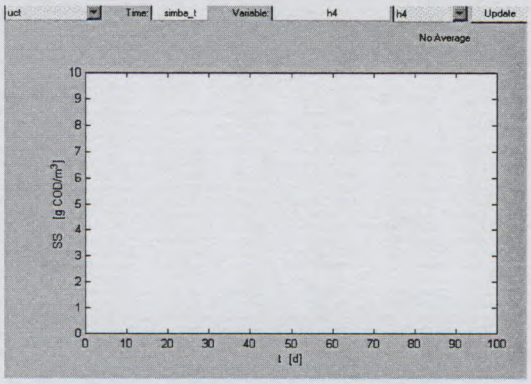

Figure 8.56: The dynamic behaviour of readily biodegradable (soluble) substrate fraction at h4

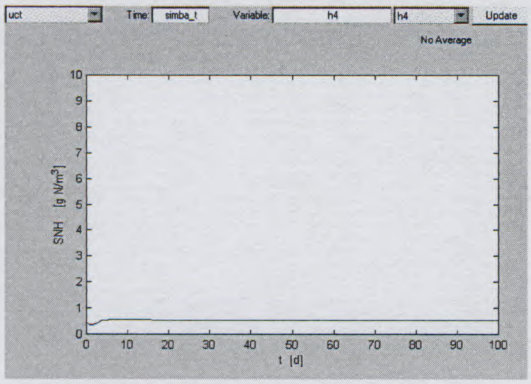

Figure 8.57: The dynamic behaviour of ammonia nitrogen fraction at h4

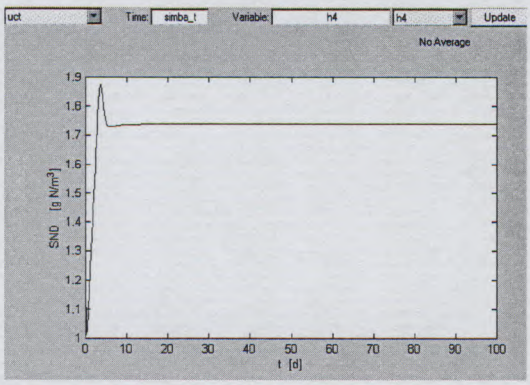

Figure 8.58: The dynamic behaviour of biodegradable particulate organic nitrogen fraction at h4

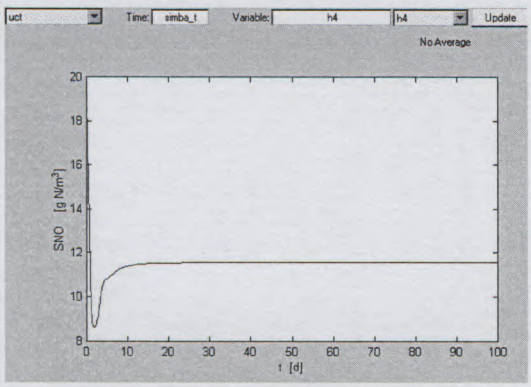

Figure 8.59: The dynamic behaviour of nitrate nitrogen fraction at h4

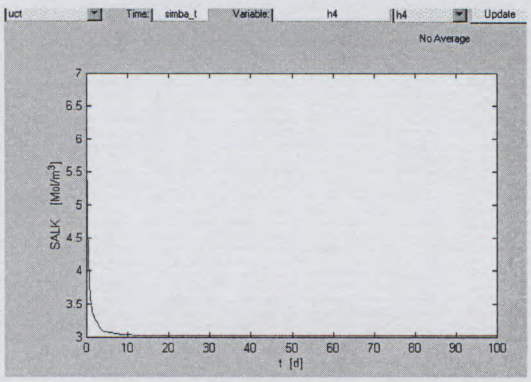

Figure 8.60 The dynamic behaviour of alkalinity at h4

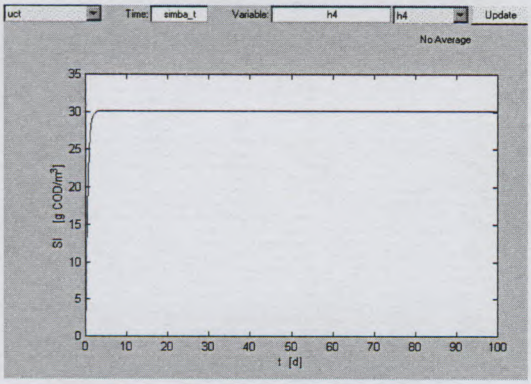

Figure 8.61: The dynamic behavior of unbiodegradable soluble substrate fraction at h4

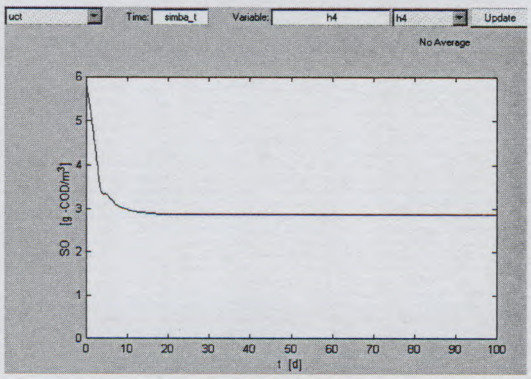

Figure 8.62: The dynamic behavior of oxygen at h4

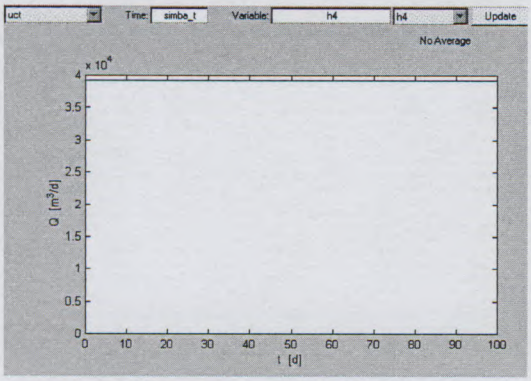

Figure 8.63: The dynamic behaviour of flow rate at h4

8.8.3 Discussion of the obtained results

- The growth of heterotrophs within the various reaction zones.

  The heterotrophs start to grow from 400 $g\,COD/m^3$ to below 2200 $g\,COD/m^3$ and the growth rate remains uniformly constant after 10 days in the anaerobic reactor (see Figure 8.19) The growth rate of the heterotrophs remain unchanged in the anoxic and aerobic reactors (see Figures 8.34 and 8.49) for the same period. The heterotrophs growth rate have increased to 2200 $g\,COD/m^3$ constant in the aerobic reactor (see Figure 8.49).

- The growth of autotrophs within the various reaction zones.

  The autotrophs start to decay from 100 $g\,COD/m^3$ to reach a minimum of 95 $g\,COD/m^3$ after 4 days and then attain a constant growth rate of 105 $g\,COD/m^3$ after 50 days in the anaerobic reactor (see Figure 8.20). After the anaerobic tank the autotrophs decays from below a 100 $g\,COD/m^3$ to a minimum of 95 $g\,COD/m^3$ after 4 days then

grows to below a maximum of 106 $g\,COD/m^3$ in 50 days which remains fairly constant in the anoxic reactor (see Figure 8.35). In the aerobic reactor the autotrophs start to decay below 100 $g\,COD/m^3$ with a constant growth rate in 50 days, and then remains constant (see Figure 8.50).

- The dynamic behaviour of the readily biodegradable (soluble) substrate within the various reaction zones.

  The soluble substrate starts to grow from 5 $g\,COD/m^3$ to a maximum of 9,5 before it decays to below 4 $g\,COD/m^3$, a constant baseline minimum value in 10 days in the anaerobic reactor. (see Figure 8.26). The soluble substrate is insignificant and approximately zero in the anoxic and aerobic zones (see Figures 8.41 and 8.56).

- The dynamic behaviour of ammonia nitrogen within the various reaction zones.

  In the anaerobic reactor the ammonia nitrogen grows from 18 $g\,N/m^3$ to just over 19 $g\,N/m^3$ then decays to a constant 19 $g\,N/m^3$ value (see Figure 8.27). The ammonia nitrogen initially grows from 11,75 $g\,N/m^3$ to 13,4 $g\,N/m^3$ in 5 days then remain constant in the anoxic reactor. (see Figure 8.42). The ammonia nitrogen is minimal in the aerobic reactor at 0,5 $g\,N/m^3$ (see Figure 8.57).

- The dynamic behaviour of nitrates nitrogen within the various reaction zones

  In the anaerobic tank the nitrates at zero days spike up to 5,2 $g\,N/m^3$ whilst in the anoxic tank after zero days it spike up to 8 $g\,N/m^3$. In the aerobic tank at zero days the concentration is 18 $g\,N/m^3$ and drops to a minimum of 7 $g\,N/m^3$ after 2 days then steeply ascends after 10 days to 10,5 $g\,N/m^3$. Then remains constant after 11 days at 11 $g\,N/m^3$

- The dynamic behaviour of oxygen within the various reaction zones.

  After the oxygen leaves the anaerobic reactor, it remains at a constant value of zero (seen Figure 8.32). In the anoxic reactor the oxygen level is also zero (see Figure 8.47). After the aerobic reactor the oxygen initially declines from 6 $g\,COD/m^3$ to 2,9 $g\,COD/m^3$ in 10 days and remain constant at that value (see Figure 8.62).

8.9 Simulation of the Athlone plant on the basis of ASM1 full and reduced and UCT full and reduced models

8.9.1 SIMBA diagrams

The Athlone plant structures and mass balances described in Chapter 4 are used to build the SIMBA diagram of the plant. The reduced ASM1 models is simulated with the estimated parameters and the reduced UCT model is simulated with the nominal parameters of the full model in order to see the differences between the two models.The overall diagram is given in Figure 8.64. The exact connections between the tanks are given in Figure 8.65.

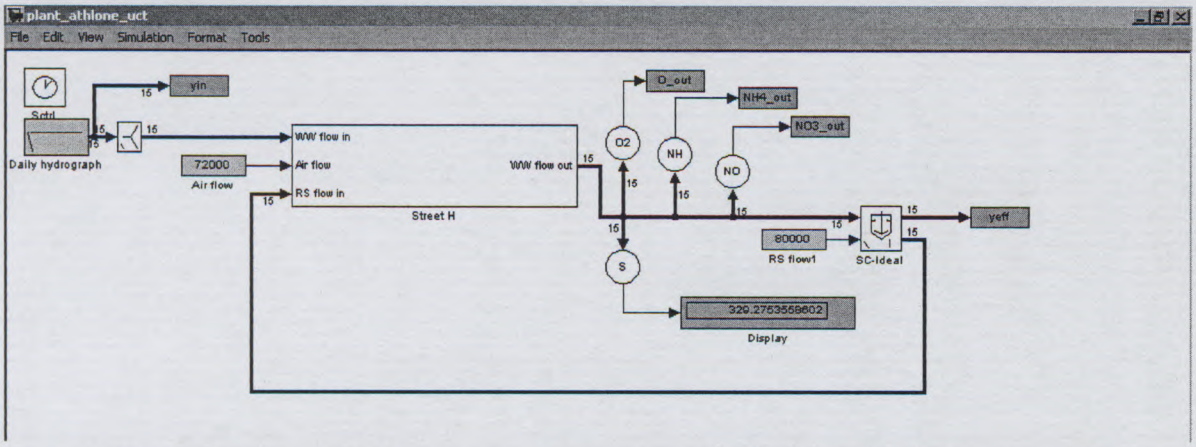

Figure 8.64: A schematic SIMBA diagram of the overall Athlone wastewater treatment plant

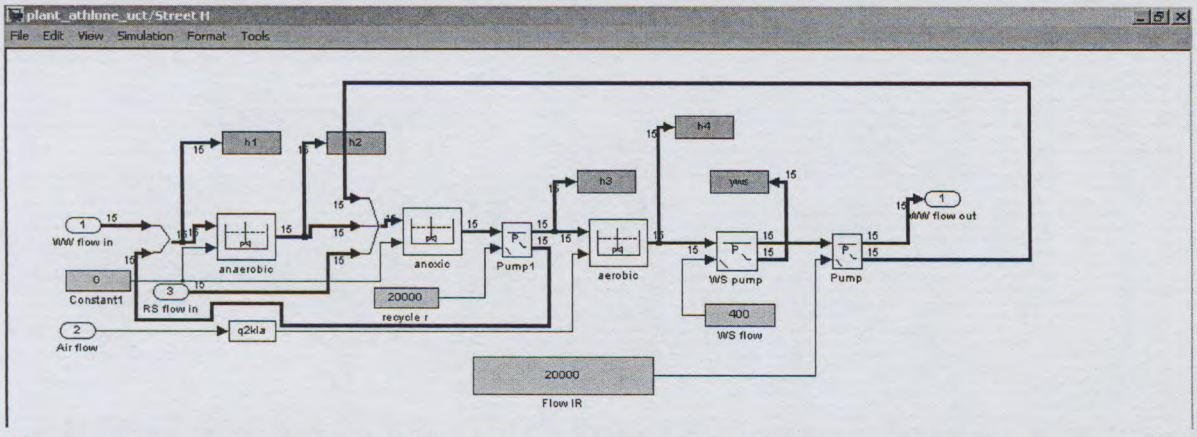

Figure 8.65: A schematic SIMBA diagram of the internal structure of the Athlone wastewater treatment plant

8.9.2 Results from the simulation of the Athlone plant with the full and reduced ASM1 biological models

The results are given according to the point of measurement and for full and reduced ASM1 model in order to see the differences in the process dynamic behaviour.

8.9.2.1 Dynamic behaviour of the anaerobic tank input (point h1) for Athlone wastewater plant simulated over a period of 100 days for total sludge age of 20 days at 22 C

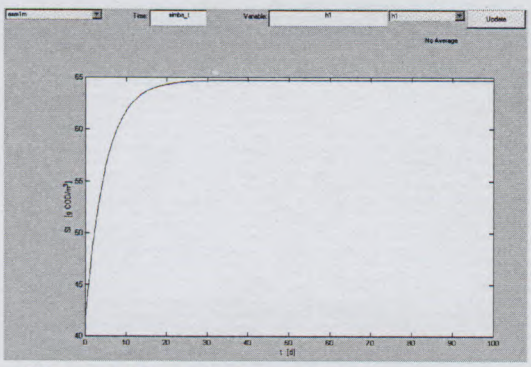

Figure 8.66a: The dynamic behaviour of unbiodegradable soluble substrate at h1 for ASM1 full model

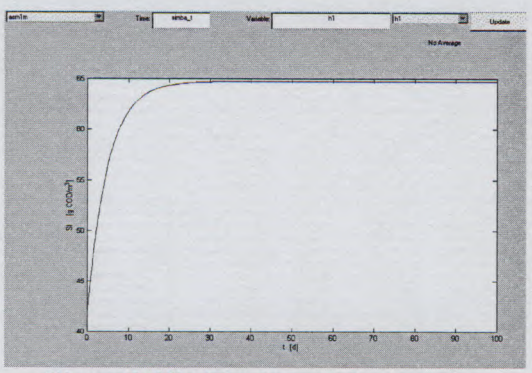

Figure 8.66b: The dynamic behaviour of unbiodegradable soluble substrate at h1 for ASM1 reduced model

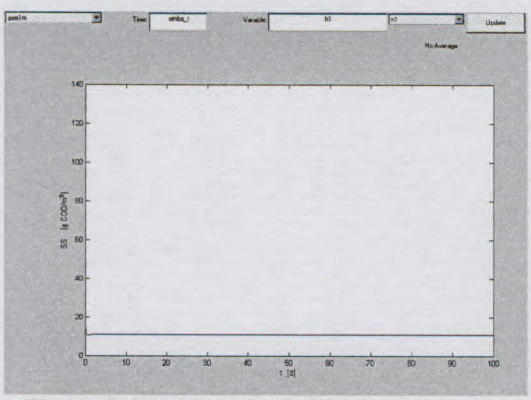

Figure 8.67a: The dynamic behaviour of readily biodegradable (soluble) substrate fraction at h1 for ASM1 full model

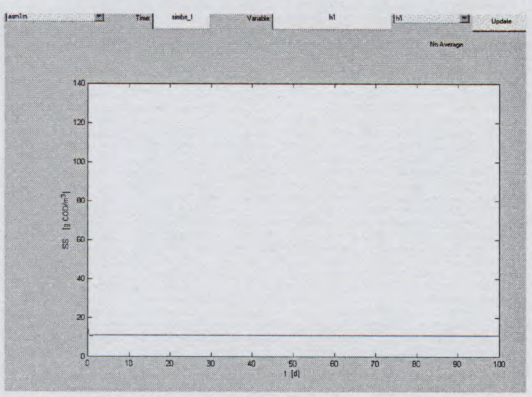

Figure 8.67b: The dynamic behaviour of readily biodegradable (soluble) substrate fraction at h1 for ASM1 reduced model

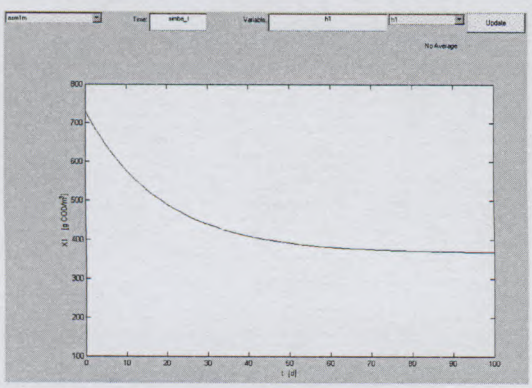

Figure 8.68a: The dynamic behaviour of inert mass fraction at h1 for ASM1 full model

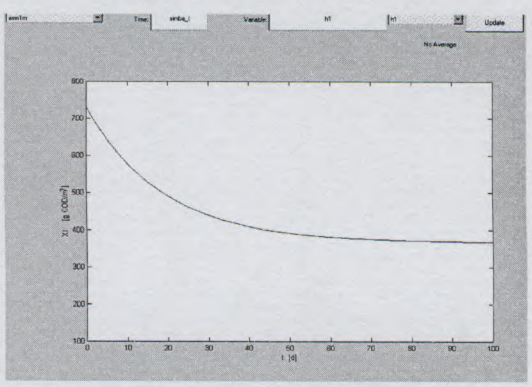

Figure 8.68b: The dynamic behaviour of inert mass fraction at h1 for ASM1 reduced model

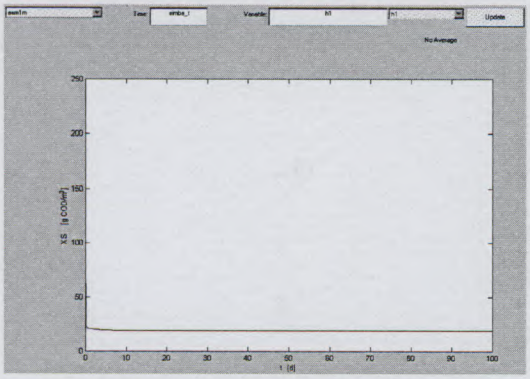

Figure 8.69a: The dynamic behaviour of enmeshed slowly biodegradable substrate fraction at h1 for ASM1 full model

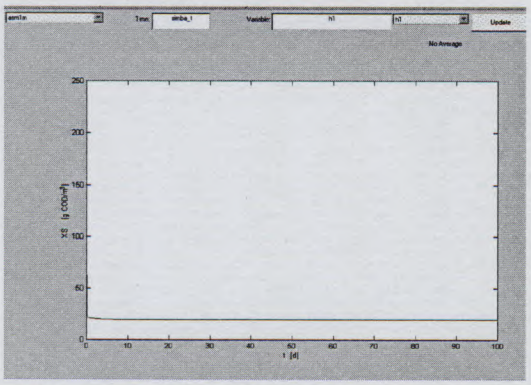

Figure 8.69b: The dynamic behaviour of enmeshed slowly biodegradable substrate fraction at h1 for ASM1 reduced model

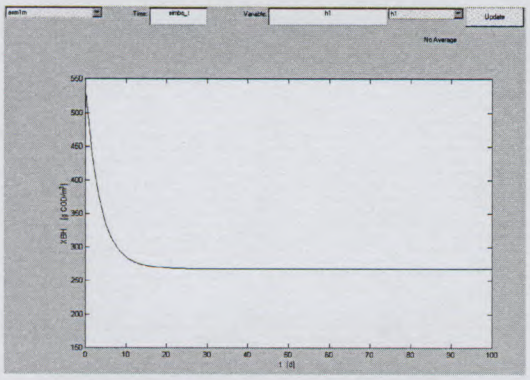

Figure 8.70a: The dynamic behaviour of biological (active) heterotrophic mass fraction at h1 for ASM1 full model

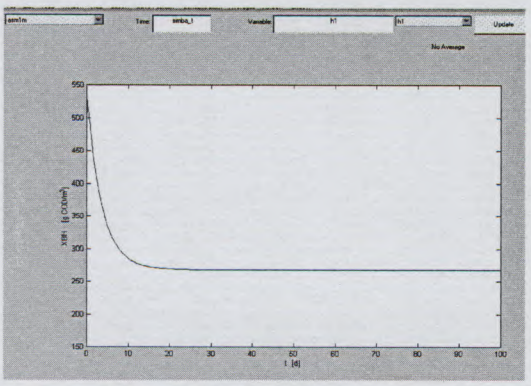

Figure 8.70b: The dynamic behaviour of biological (active) heterotrophic mass fraction at h1 for ASM1 reduced model

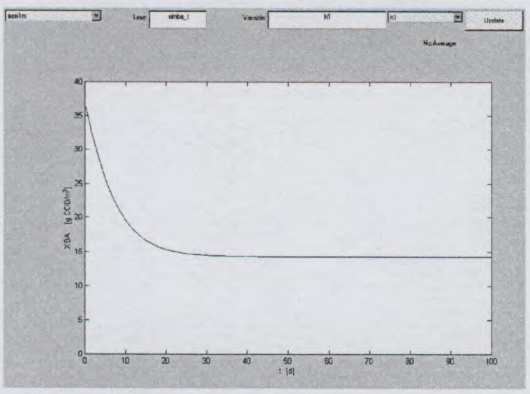

Figure 8.71a: The dynamic behaviour of biological (active) autotrophic mass fraction at h1 for ASM1 full model

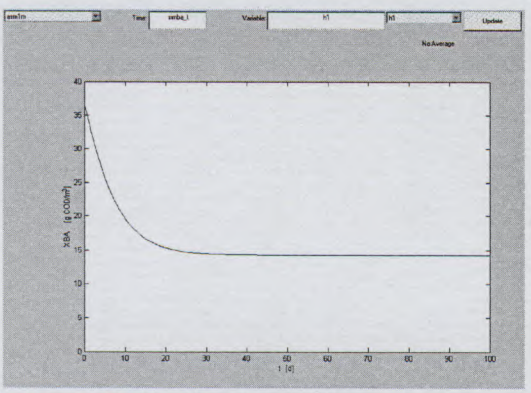

Figure 8.71b: The dynamic behaviour of biological (active) autotrophic mass fraction at h1 for ASM1 reduced model

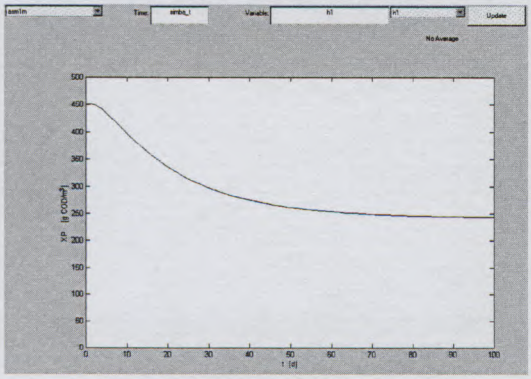

Figure 8.72a: The dynamic behaviour of endogenous mass fraction at h1 for ASM1 full model

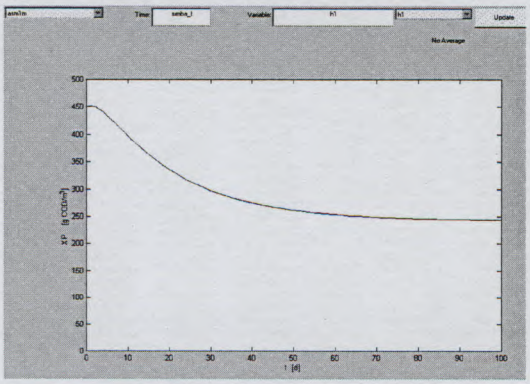

Figure 8.72a: The dynamic behaviour of endogenous mass fraction at h1 for ASM1 reduced model

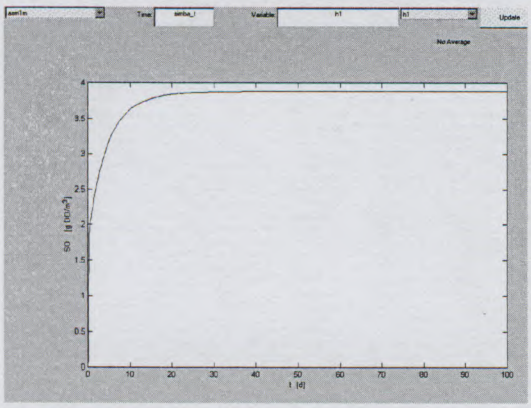

Figure 8.73a: The dynamic behaviour of oxygen at h1 for ASM1 full model

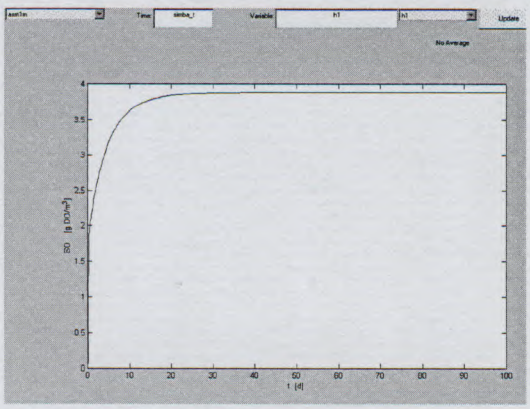

Figure 8.73b: The dynamic behaviour of oxygen at h1 for ASM1 reduced model

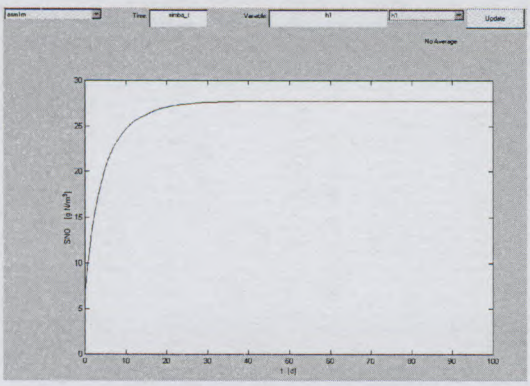

Figure 8.74a: The dynamic behaviour of nitrate nitrogen at h1 for ASM1 full model

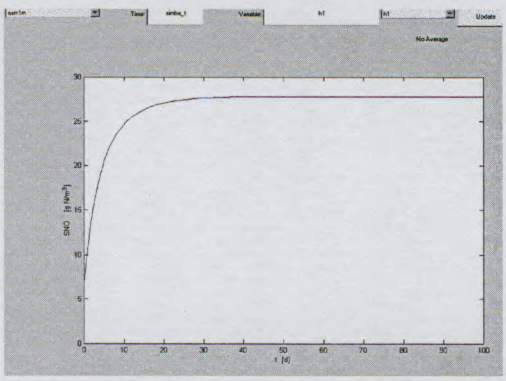

Figure 8.74b: The dynamic behaviour of nitrate nitrogen at h1 for ASM1 reduced model

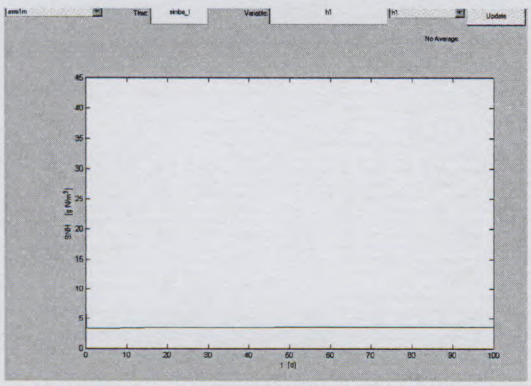

Figure 8.75a: The dynamic behaviour of ammonia nitrogen at h1 for ASM1 full model

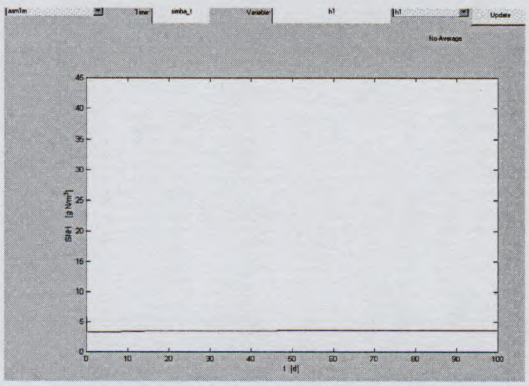

Figure 8.75b: The dynamic behaviour of ammonia nitrogen at h1 for ASM1 reduced model

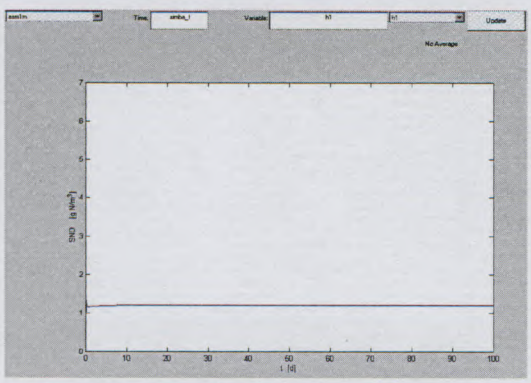

Figure 8.76a: The dynamic behaviour of biodegradable particulate organic nitrogen fraction at h1 for ASM1 full model

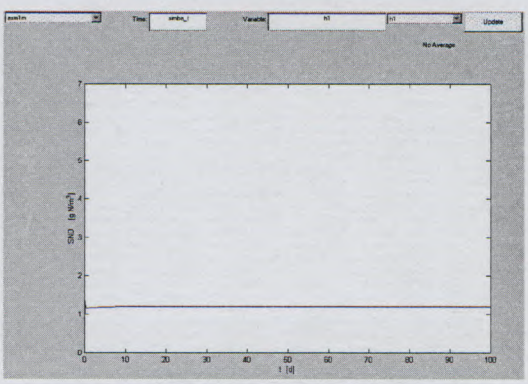

Figure 8.76b: The dynamic behaviour of biodegradable particulate organic nitrogen fraction at h1 for ASM1 reduced model

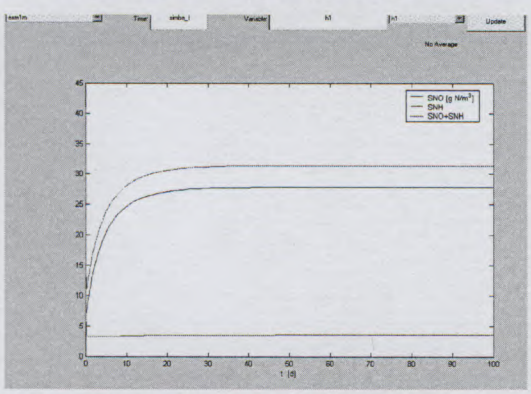

Figure 8.77a: The dynamic behaviour of biodegradable soluble organic nitrogen at h1 for ASM1 full model

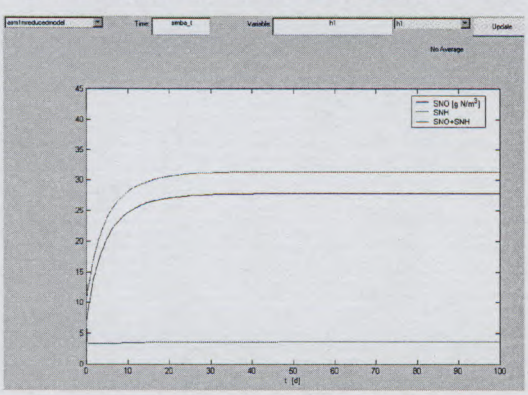

Figure 8.77b: The dynamic behaviour of biodegradable soluble organic nitrogen at h1 for ASM1 reduced model

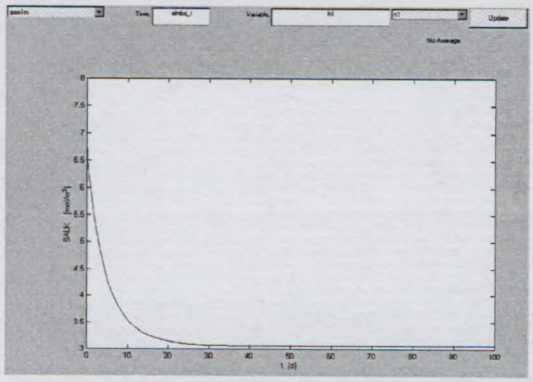

Figure 8.78a: The dynamic behaviour of alkalinity at h1 for ASM1 full model

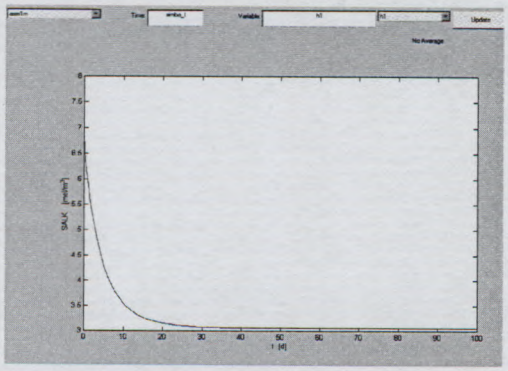

Figure 8.78b: The dynamic behaviour of alkalinity at h1 for ASM1 reduced model

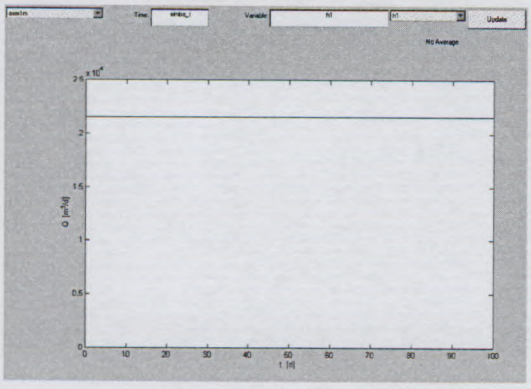

Figure 8.79a: The dynamic behaviour of flow rate at h1 for ASM1 full model

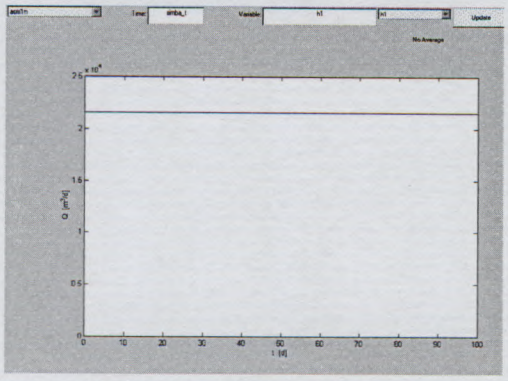

Figure 8.79b: The dynamic behaviour of flow rate at h1 for ASM1 reduced model

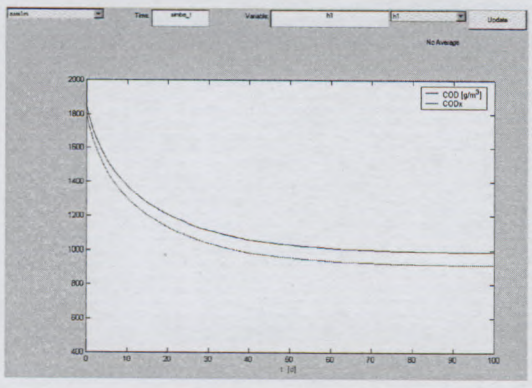

Figure 8.80a: The dynamic behaviour of chemical oxygen demand at h1 for ASM1 full model

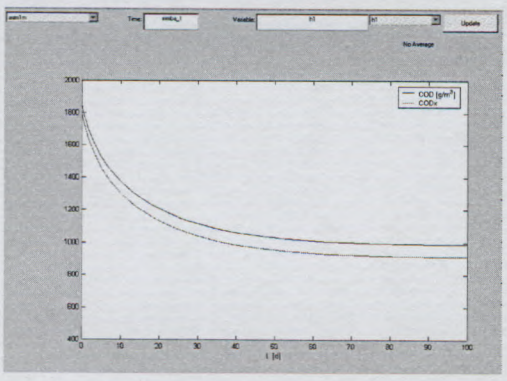

Figure 8.80b: The dynamic behaviour of chemical oxygen demand at h1 for ASM1 reduced model

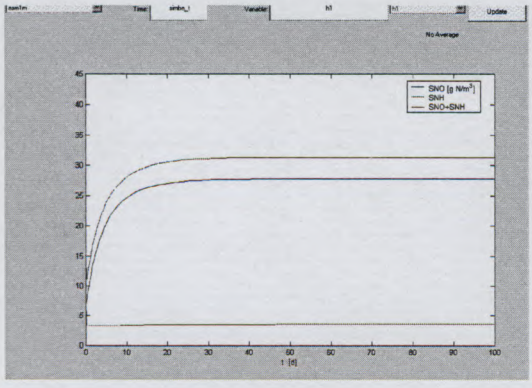

Figure 8.81a: The dynamic behaviour of nitrogen at h1 for ASM1 full model

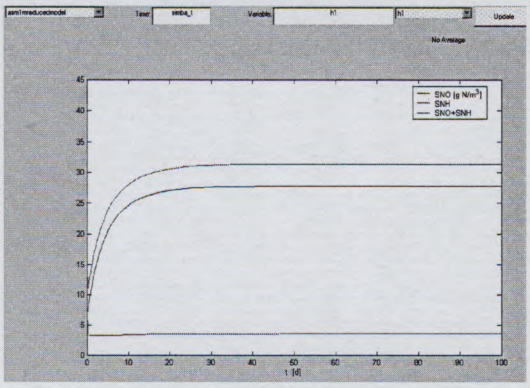

Figure 8.81b: The dynamic behaviour of nitrogen at h1 for ASM1 reduced model

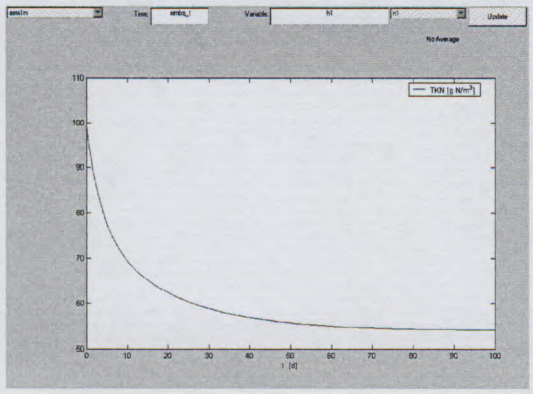

Figure 8.82a: The dynamic behaviour of total Kjedahl nitrogen at for ASM1 full model

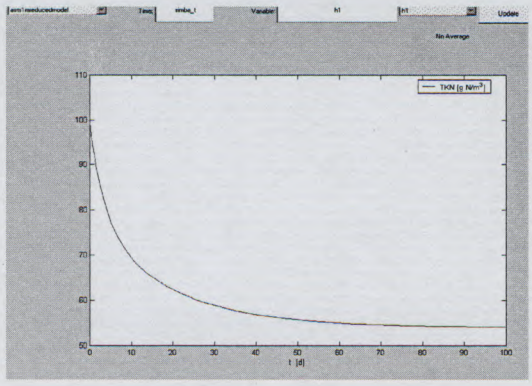

Figure 8.82b: The dynamic behaviour of total Kjedahl nitrogen at for ASM1 reduced model

8.9.2.2 Dynamic behaviour of the process variables after the anaerobic tank (point h2) in Athlone wastewater plant simulated over a period of 100 days for total sludge age of 20 days at 22 C°

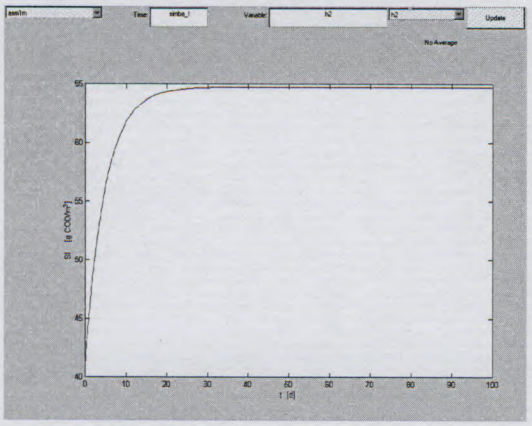

Figure 8.83a: The dynamic behaviour of unbiodegradable soluble substrate at h2 for ASM1 full model

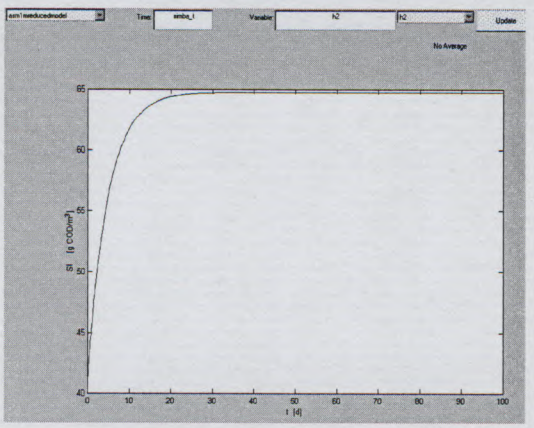

Figure 8.83b: The dynamic behaviour of unbiodegradable soluble substrate at h2 for ASM1 reduced model

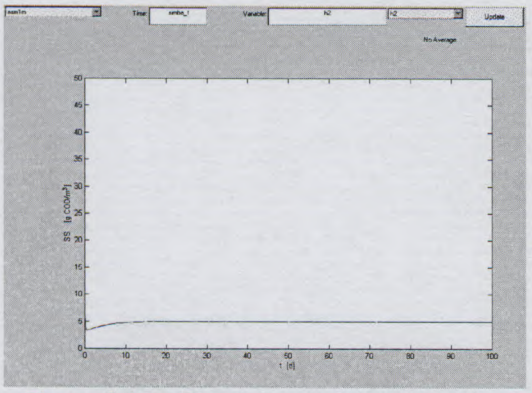

Figure 8.84a: The dynamic behaviour of readily biodegradable (soluble) substrate fraction at h2 for ASM1 full model

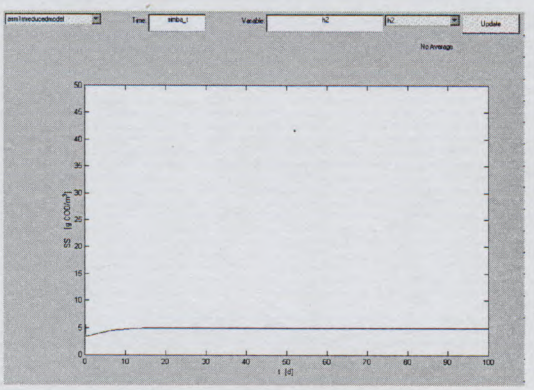

Figure 8.84b: The dynamic behaviour of readily biodegradable (soluble) substrate fraction at h2 for ASM1 reduced model

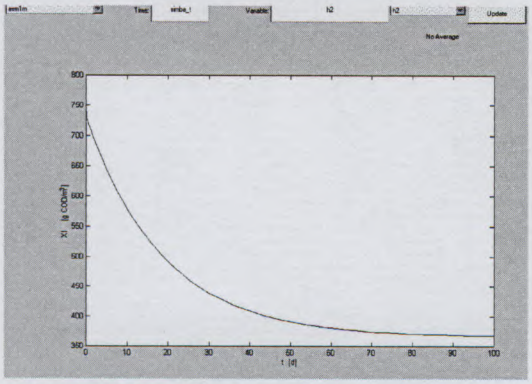

Figure 8.85a: The dynamic behaviour of inert mass fraction at h2 for ASM1 full model

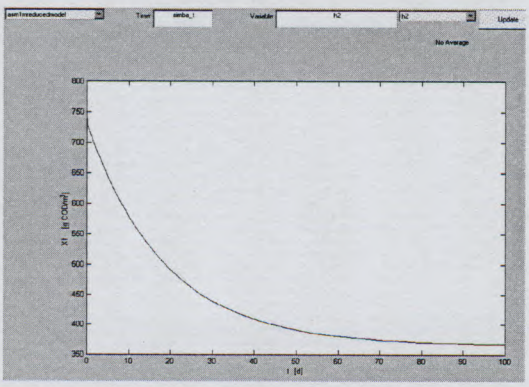

Figure 8.85b: The dynamic behaviour of inert mass fraction at h2 for ASM1 reduced model

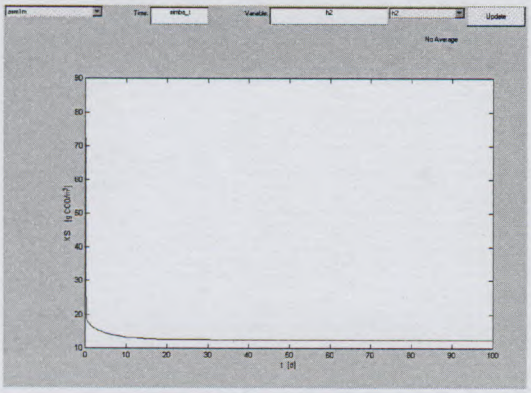

Figure 8.86a: The dynamic behaviour of enmeshed slowly biodegradable substrate fraction at h2 for ASM1 full model

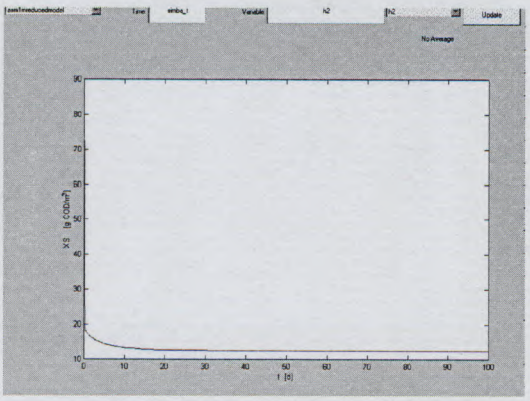

Figure 8.86b: The dynamic behaviour of enmeshed slowly biodegradable substrate fraction at h2 for ASM1 reduced model

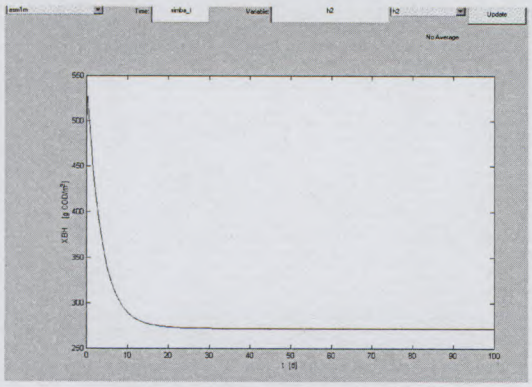

Figure 8.87a: The dynamic behaviour of biological (active) heterotrophic mass fraction at for ASM1 full model

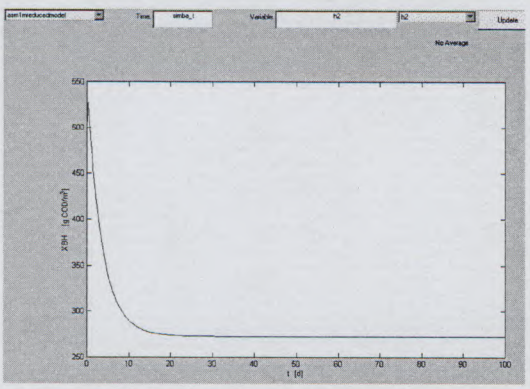

Figure 8.87b: The dynamic behaviour of biological (active) heterotrophic mass fraction at h2 for ASM1 reduced model

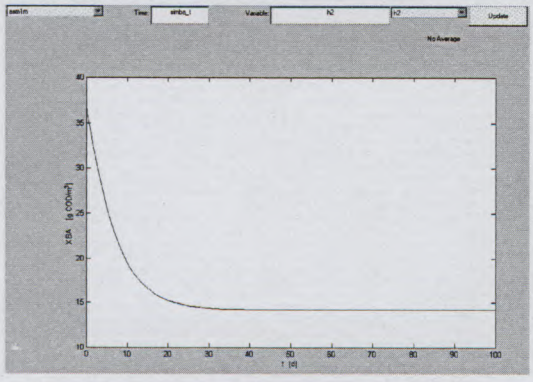

Figure 8.88a: The dynamic behaviour of biological (active) autotrophic mass fraction at for ASM1 full model

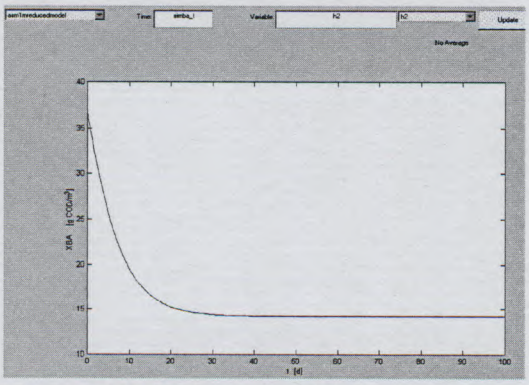

Figure 8.88b: The dynamic behaviour of biological (active) autotrophic mass fraction at h2 for ASM1 reduced model

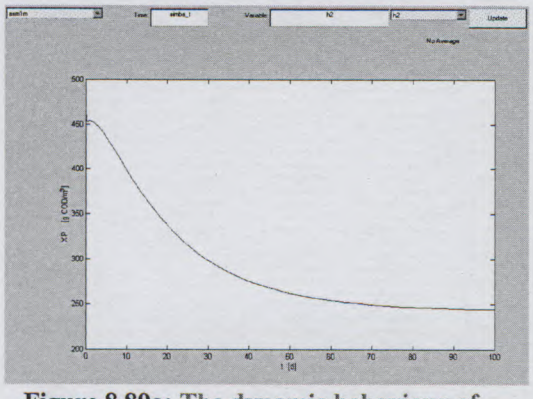

Figure 8.89a: The dynamic behaviour of endogenous mass fraction at h2 for ASM1 full model

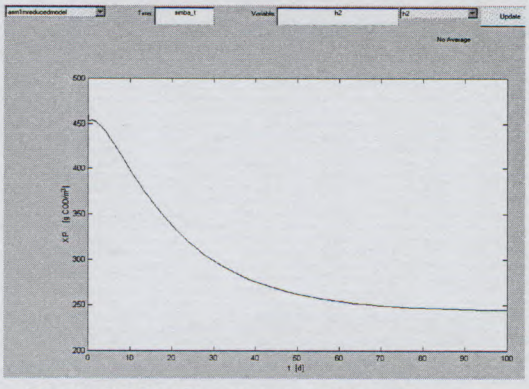

Figure 8.89b: The dynamic behaviour of endogenous mass fraction at h2 for ASM1 reduced model

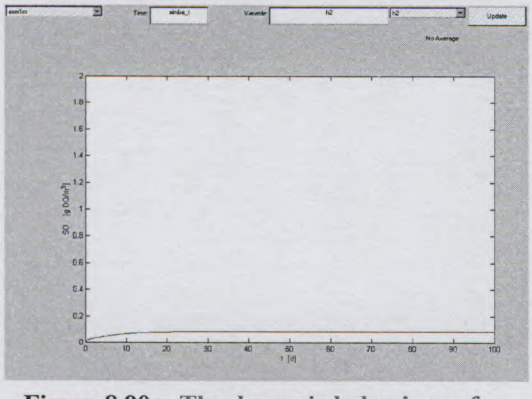

Figure 8.90a: The dynamic behaviour of oxygen at h2 for ASM1 full model

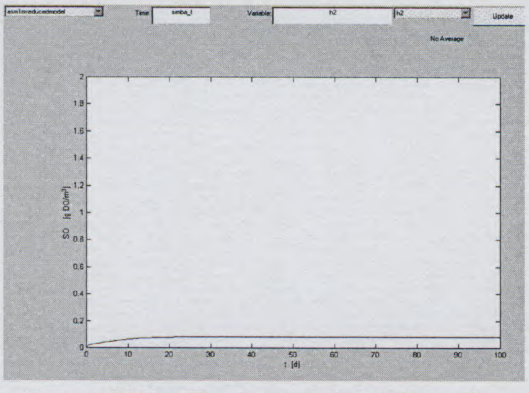

Figure 8.90b: The dynamic behaviour of oxygen at h2 for ASM1 reduced model

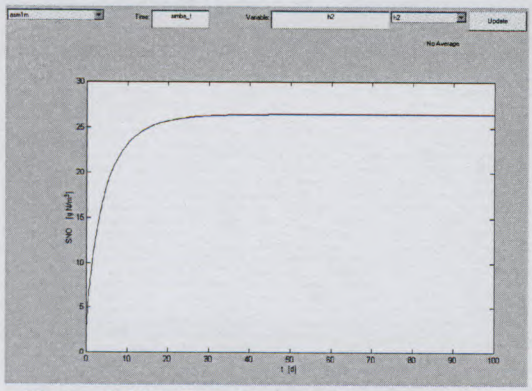

Figure 8.91a: The dynamic behaviour of nitrate nitrogen at h2 for ASM1 full model

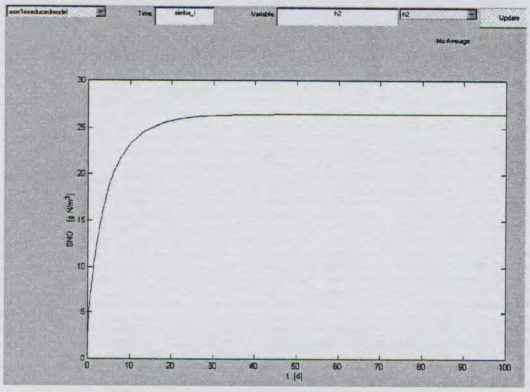

Figure 8.91b: The dynamic behaviour of nitrate nitrogen at h2 for ASM1 reduced model

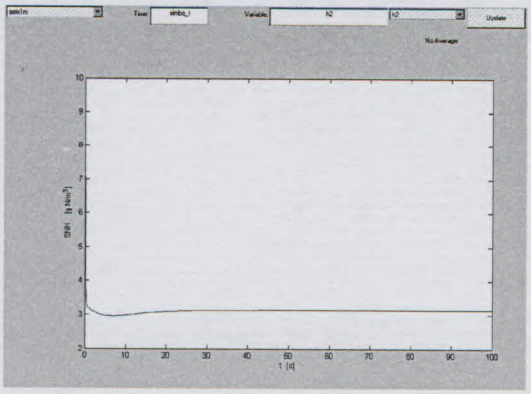

Figure 8.92a: The dynamic behaviour of ammonia nitrogen at h2 for ASM1 full model

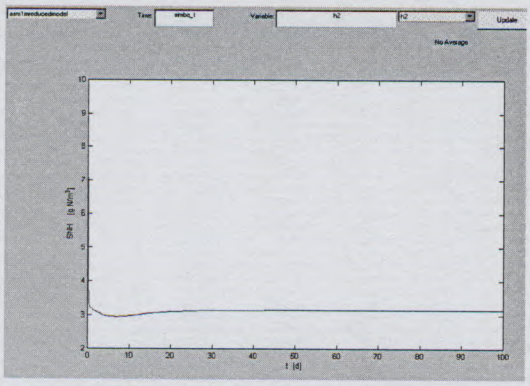

Figure 8.92b: The dynamic behaviour of ammonia nitrogen at h2 for ASM1 reduced model

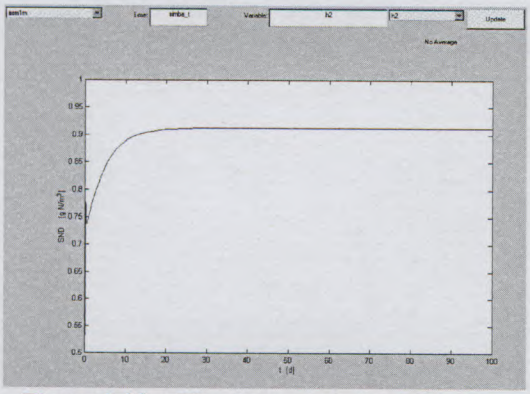

Figure 8.93a: The dynamic behaviour of biodegradable soluble organic nitrogen at h2 for ASM1 full model

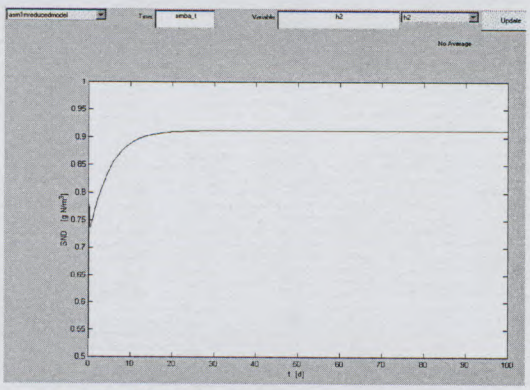

Figure 8.93b: The dynamic behaviour of biodegradable soluble organic nitrogen at h2 for ASM1 reduced model

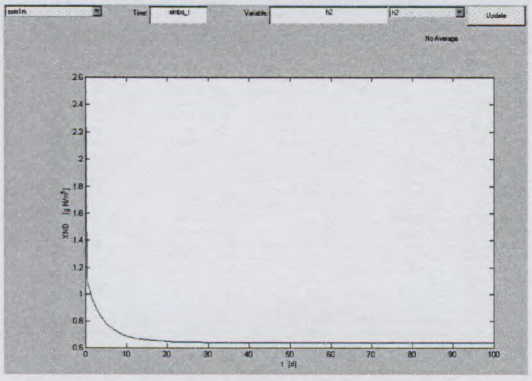

Figure 8.94a: The dynamic behaviour of biodegradable particulate organic nitrogen fraction at h2 for ASM1 full model

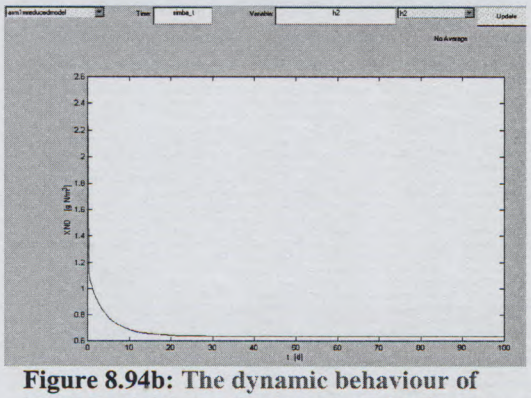

Figure 8.94b: The dynamic behaviour of biodegradable particulate organic nitrogen fraction at h2 for ASM1 reduced model

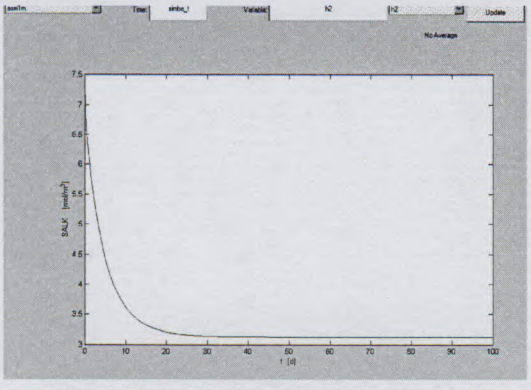

Figure 8.95a: The dynamic behaviour of alkalinity at h2 for ASM1 full model

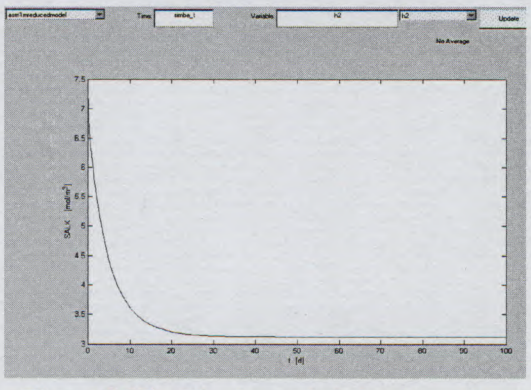

Figure 8.95b: The dynamic behaviour of alkalinity at h2 for ASM1 reduced model

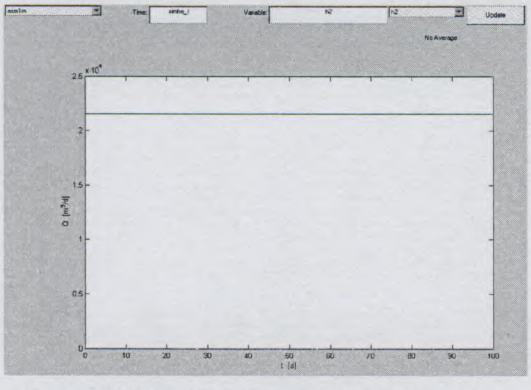

Figure 8.96a: The dynamic behaviour of flow rate at h2 for ASM1 full model

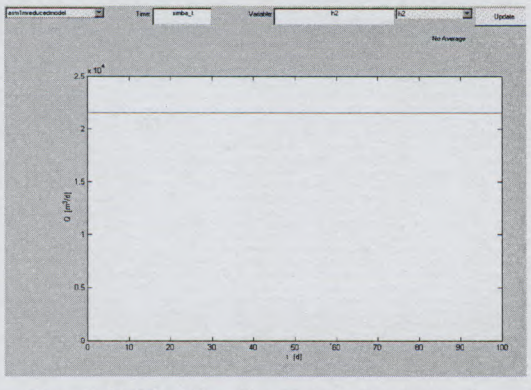

Figure 9.96b: The dynamic behaviour of flow rate at h2 for ASM1 reduced model

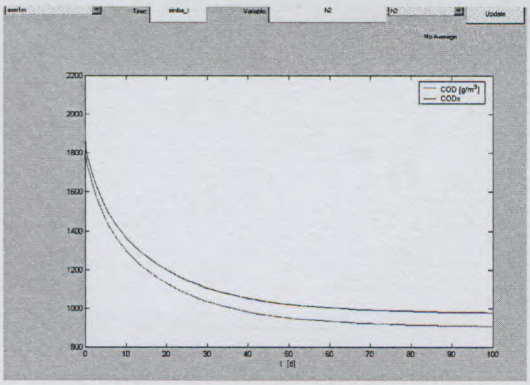

Figure 8.97a: The dynamic behaviour of chemical oxygen demand at h2 for ASM1 full model

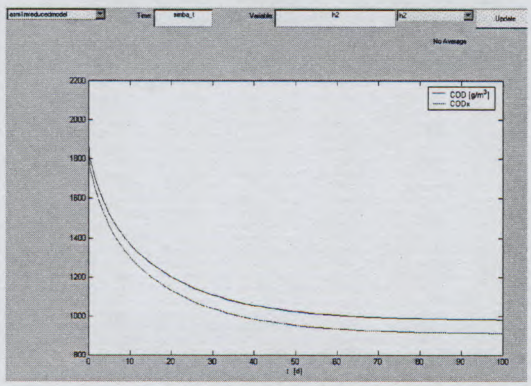

Figure 8.97b: The dynamic behaviour of chemical oxygen demand at h2 for ASM1 reduced model

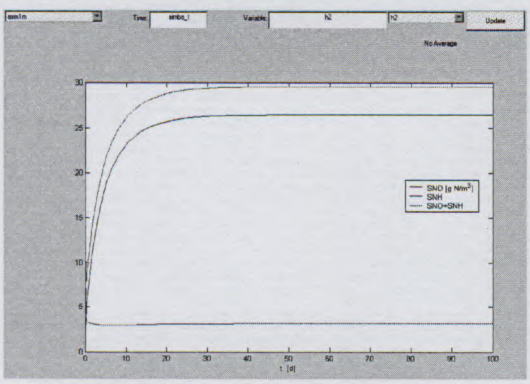

Figure 8.98a: The dynamic behaviour of nitrogen at h2 for ASM1 full model

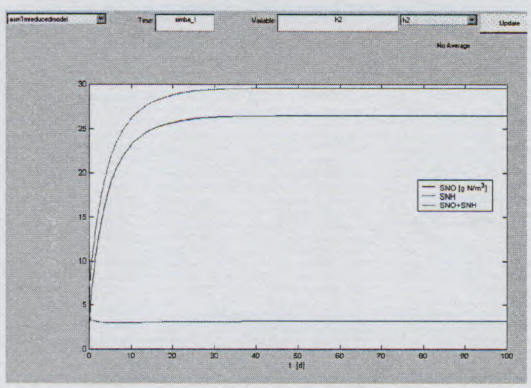

Figure 8.98b: The dynamic behaviour of nitrogen at h2 for ASM1 reduced model

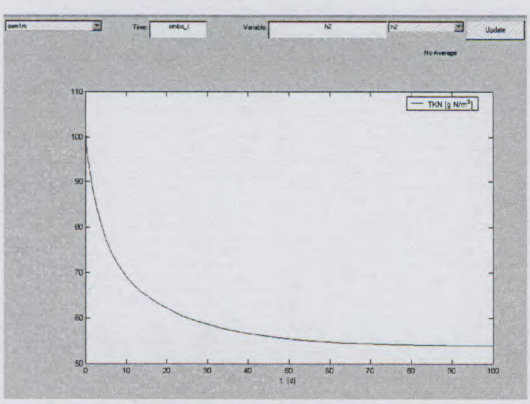

Figure 8.99a: The dynamic behaviour of total Kjedahl nitrogen at h2 for ASM1 full model

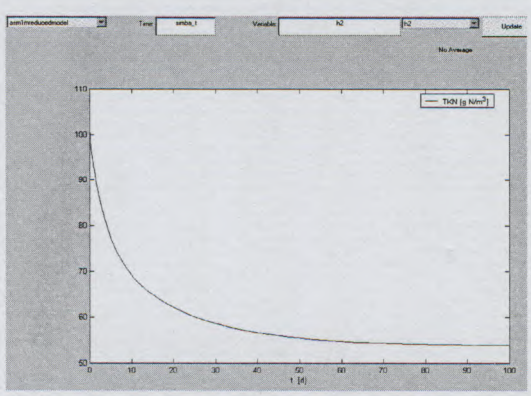

Figure 8.99b: The dynamic behaviour of total Kjedahl nitrogen at h2 for ASM1 reduced model

8.9.2.3 Dynamic behaviour of the process variables after the anoxic tank (point h3) in Athlone wastewater plant simulated over a period of 100 days for total sludge age of 20 days at 22 C°

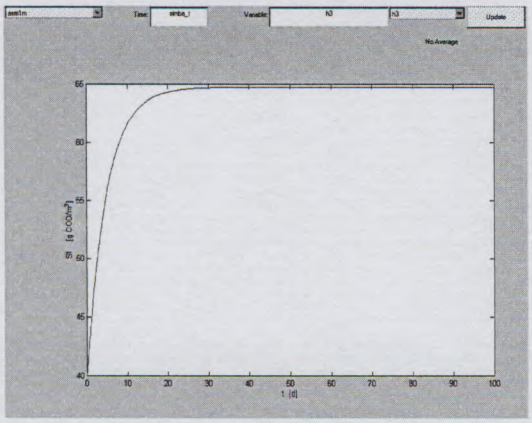

Figure 8.100a: The dynamic behaviour of unbiodegradable soluble substrate at h3 for ASM1 full model

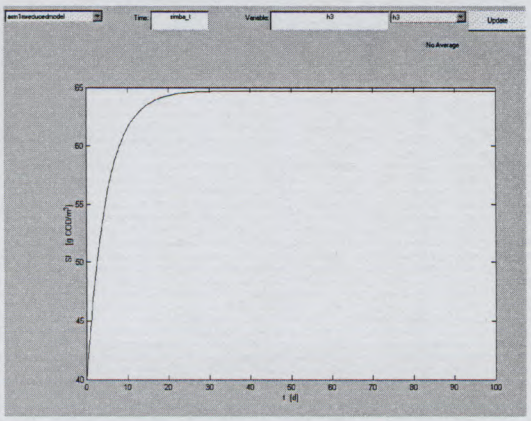

Figure 8.100b: The dynamic behaviour of unbiodegradable soluble substrate at h3 for ASM1 reduced model

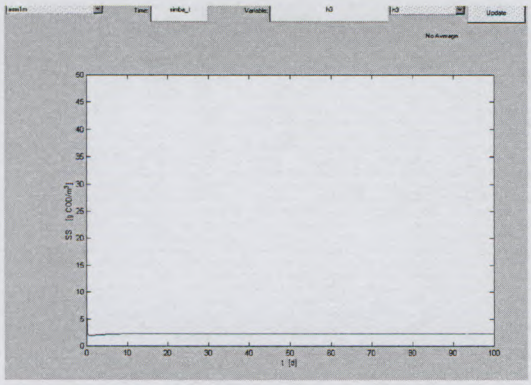

Figure 8.101a: The dynamic behaviour of readily biodegradable (soluble) substrate fraction at h3 for ASM1 full model

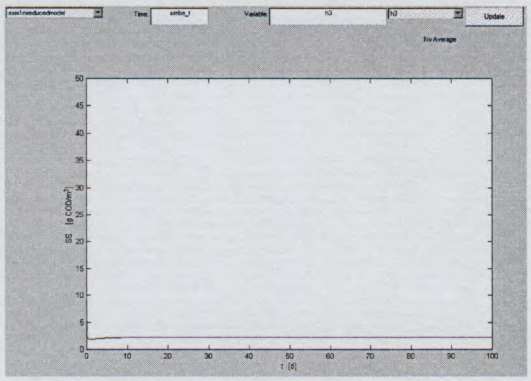

Figure 8.101b: The dynamic behaviour of readily biodegradable (soluble) substrate fraction at h3 for ASM1 reduced model

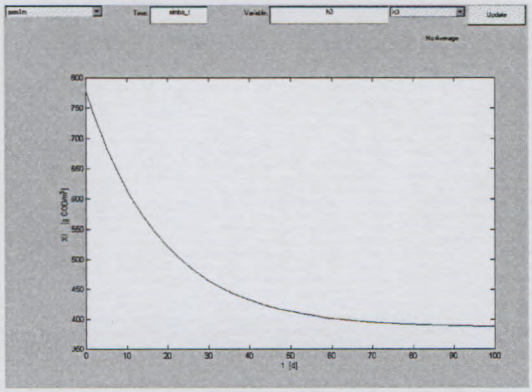

Figure 8.102a: The dynamic behaviour of inert mass fraction at h3 for ASM1 full model

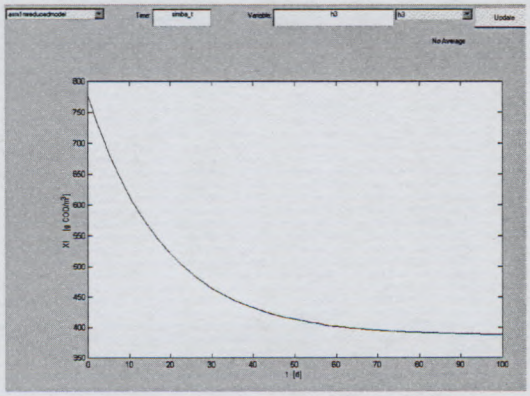

Figure 8.102b: The dynamic behaviour of inert mass fraction at h3 for ASM1 reduced model

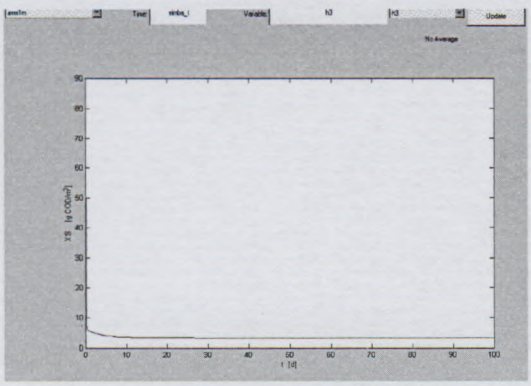

Figure 8.103a: The dynamic behaviour of enmeshed slowly biodegradable substrate fraction at h3 for ASM1 full model

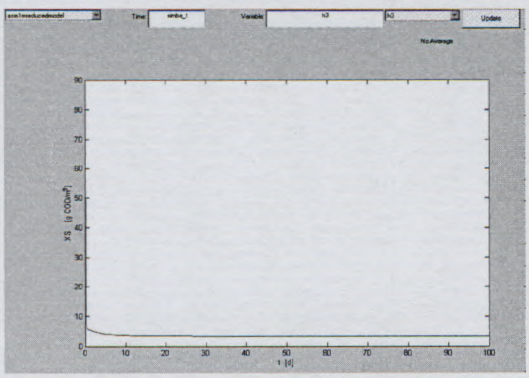

Figure 8.103b: The dynamic behaviour of enmeshed slowly biodegradable substrate fraction at h3 for ASM1 reduced model

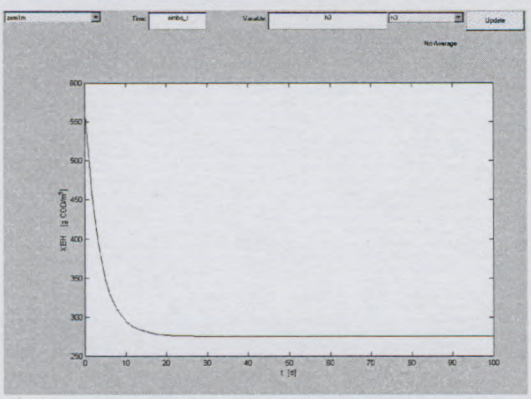

Figure 8.104a: The dynamic behaviour of biological (active) heterotrophic mass fraction at h3 for ASM1 full model

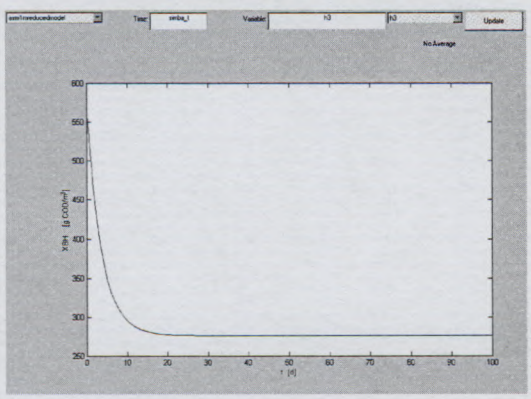

Figure 8.104b: The dynamic behaviour of biological (active) heterotrophic mass fraction at h3 for ASM1 reduced model

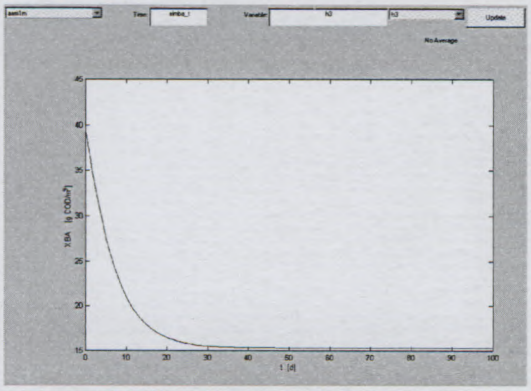

Figure 8.105a: The dynamic behaviour of biological (active) autotrophic biomass fraction at h3 for ASM1 full model

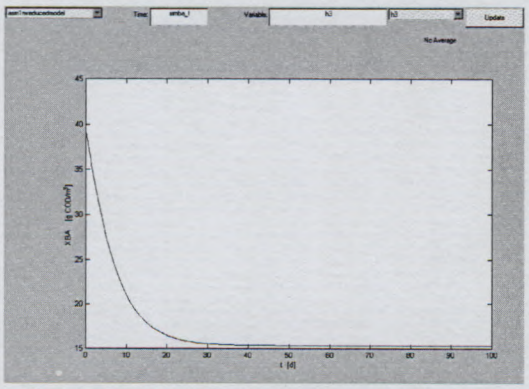

Figure 8.105b: The dynamic behaviour of biological (active) autotrophic biomass fraction at h3 for ASM1 reduced model

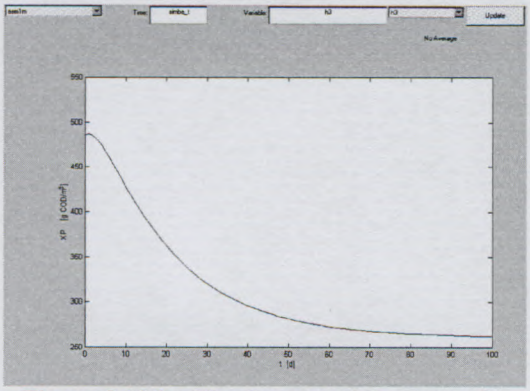

Figure 8.106a: The dynamic behaviour of endogenous mass fraction at h3 for ASM1 full model

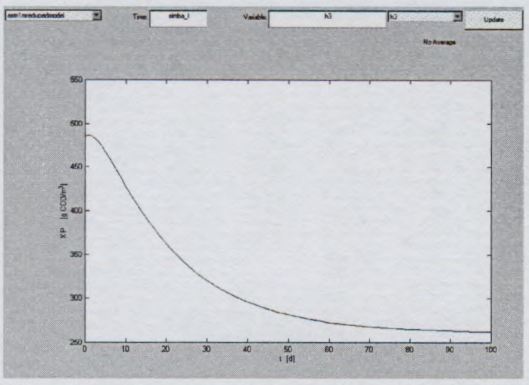

Figure 8.106b: The dynamic behaviour of endogenous mass fraction at h3 for ASM1 reduced model

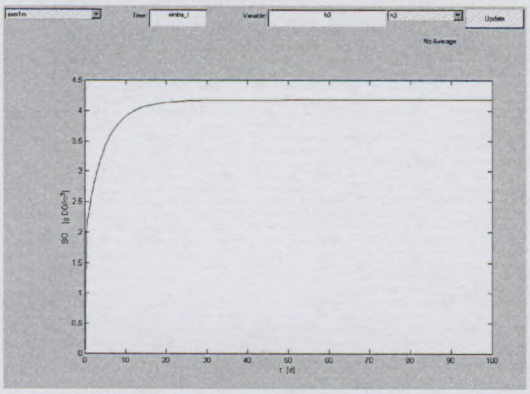

Figure 8.107a: The dynamic behaviour of oxygen at h3 for ASM1 full model

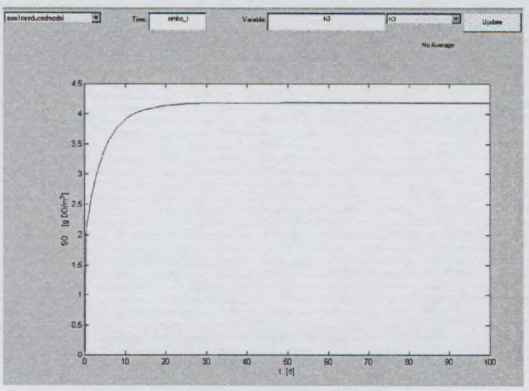

Figure 8.107b: The dynamic behaviour of oxygen at h3 for ASM1 reduced model

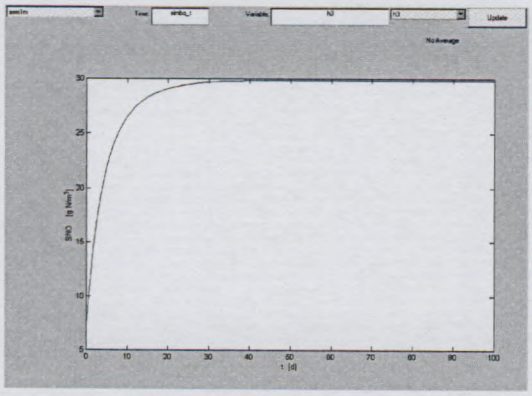

Figure 8.108a: The dynamic behaviour of nitrate nitrogen at h3 for ASM1 full model

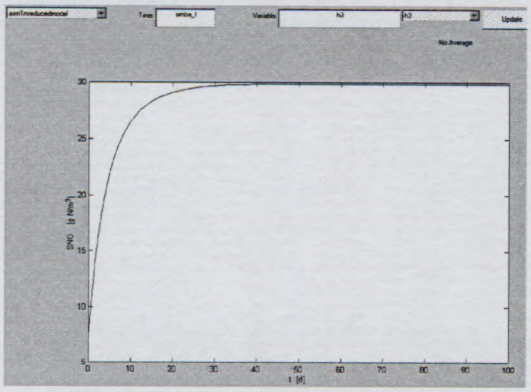

Figure 8.108b: The dynamic behaviour of nitrate nitrogen at h3 for ASM1 reduced model

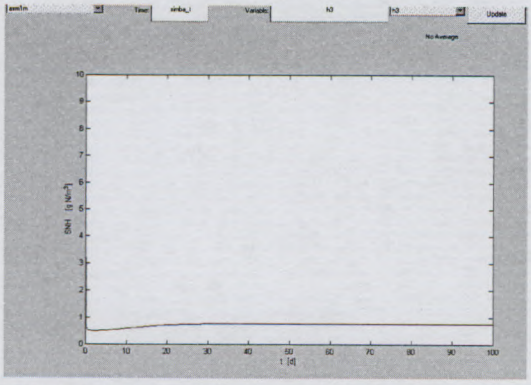

Figure 8.109a: The dynamic behaviour of ammonia nitrogen at h3 for ASM1 full model

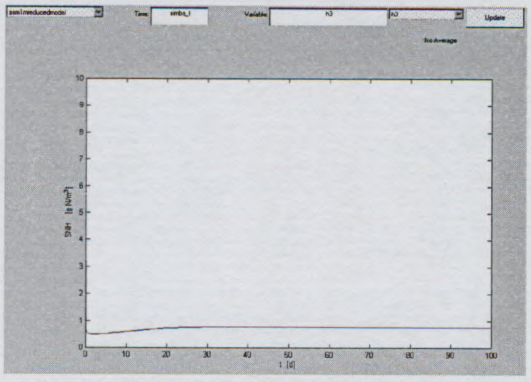

Figure 8.109b: The dynamic behaviour of ammonia nitrogen at h3 for ASM1 reduced model

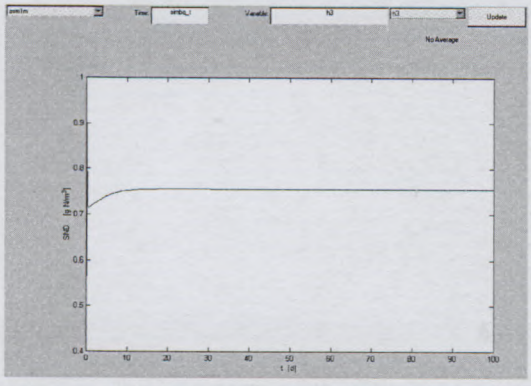

Figure 8.110a: The dynamic behaviour of biodegradable soluble organic nitrogen at h3 for ASM1 full model

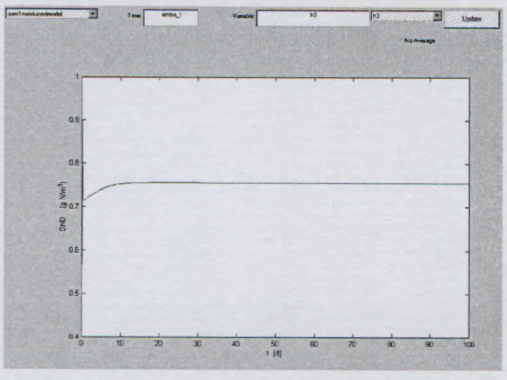

Figure 8.110b: The dynamic behaviour of biodegradable soluble organic nitrogen at h3 for ASM1 reduced model

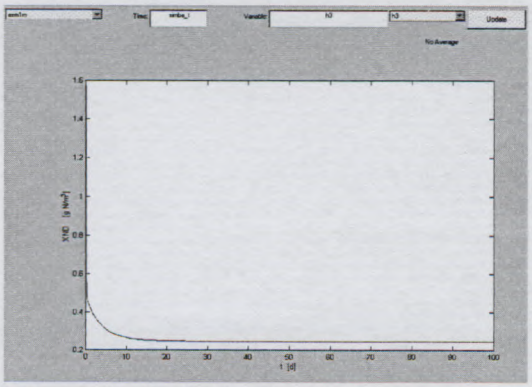

Figure 8.111a: The dynamic behaviour of biodegradable particulate organic nitrogen fraction at h3 for ASM1 full model

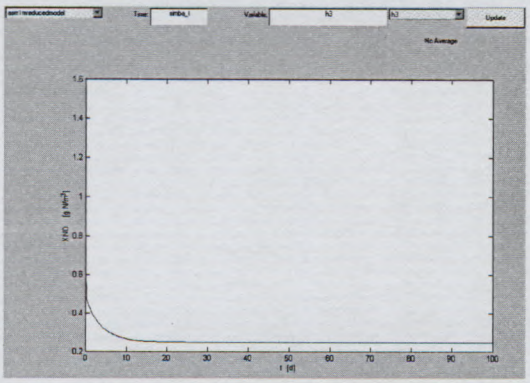

Figure 8.111b: The dynamic behaviour of biodegradable particulate organic nitrogen fraction at h3 for ASM1 reduced model

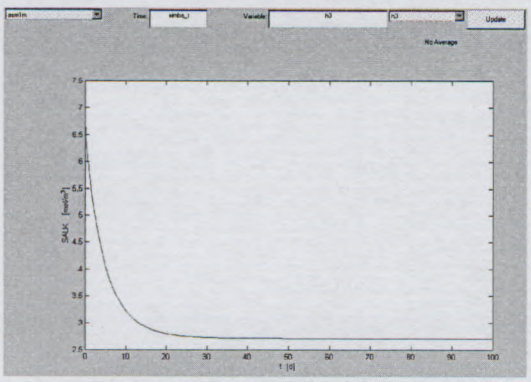

Figure 8.112a: The dynamic behaviour of alkalinity at h3 for ASM1 full model

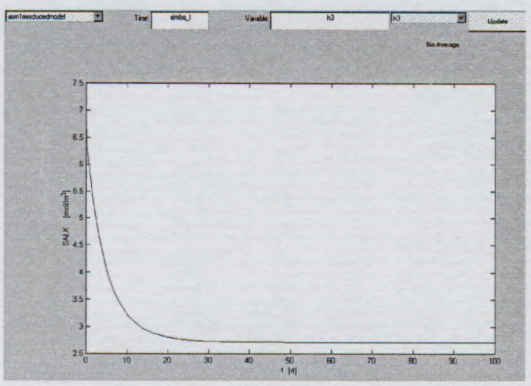

Figure 8.112b: The dynamic behaviour of alkalinity at h3 for ASM1 reduced model

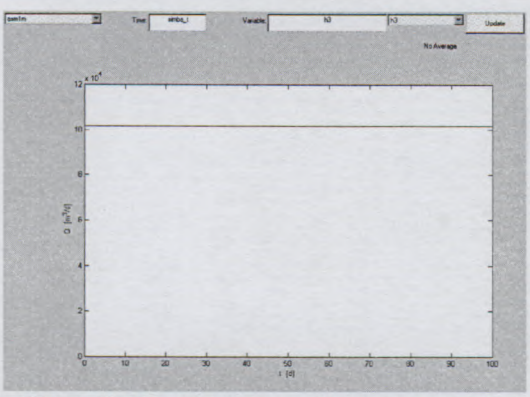

Figure 8.113a: The dynamic behaviour of flow rate at h3 for ASM1 full model

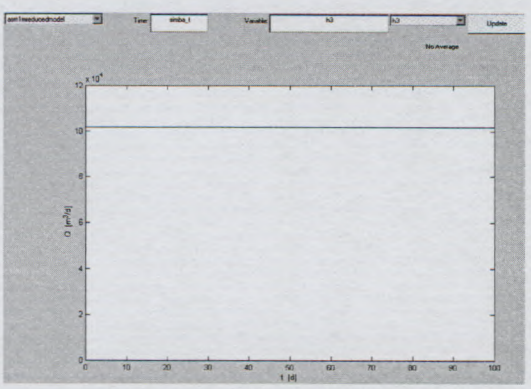

Figure 8.113b: The dynamic behaviour of flow rate at h3 for ASM1 reduced model

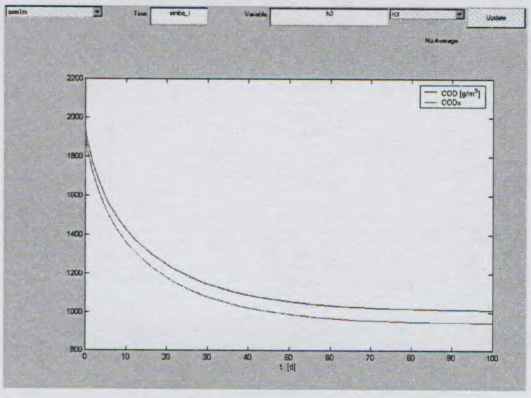

Figure 8.114a: The dynamic behaviour of chemical oxygen demand at h3 for ASM1 full model

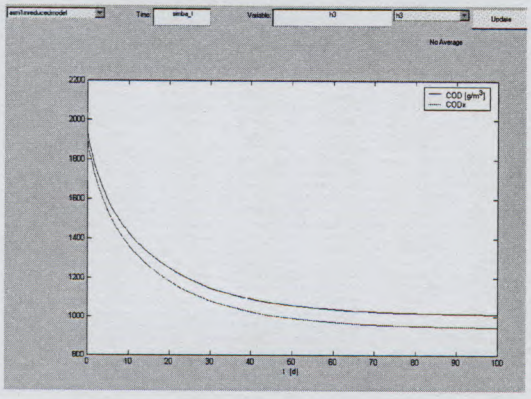

Figure 8.114b: The dynamic behaviour of chemical oxygen demand at h3 for ASM1 reduced model

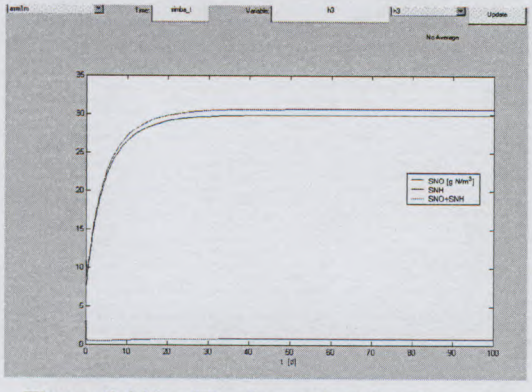

Figure 8.115a: The dynamic behaviour of nitrogen at h3 for ASM1 full model

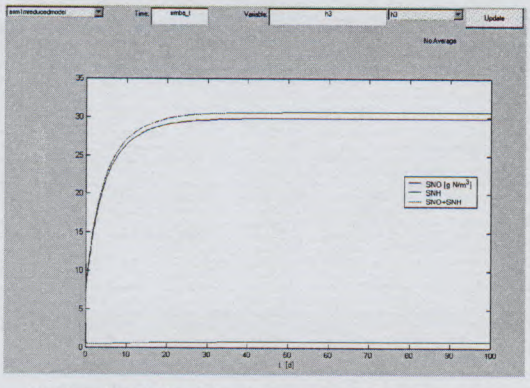

Figure 8.115b: The dynamic behaviour of nitrogen at h3 for ASM1 reduced model

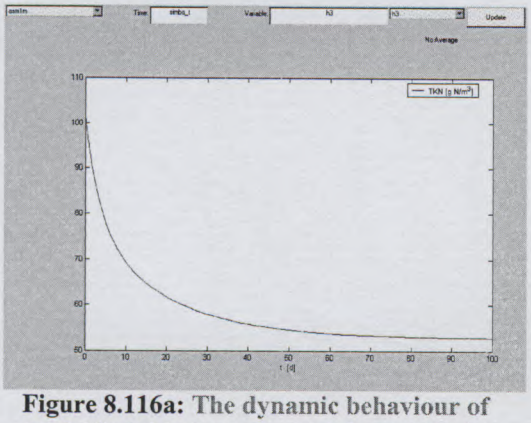

Figure 8.116a: The dynamic behaviour of total Kjedahl nitrogen at h3 for ASM1 full model

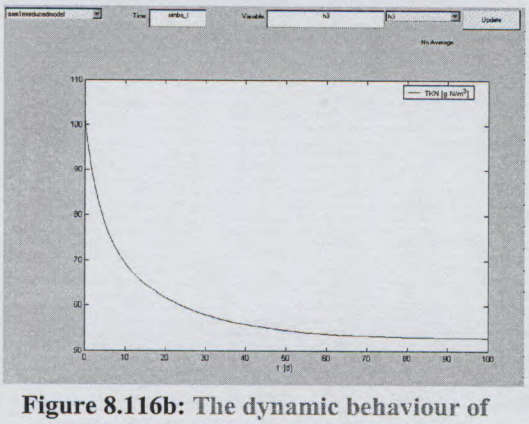

Figure 8.116b: The dynamic behaviour of total Kjedahl nitrogen at h3 for ASM1 reduced model

8.9.2.4 Dynamic behaviour of the process variables after the aerobic tank (point h4) in Athlone wastewater plant simulated over a period of 100 days for total sludge age of 20 days at 22 C

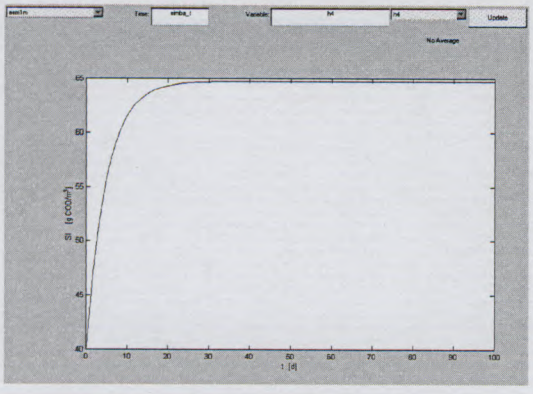

Figure 8.117a: The dynamic behaviour of unbiodegradable soluble substrate at h4 for ASM1 full model

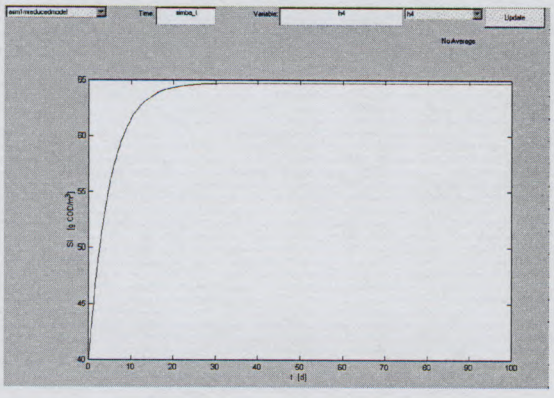

Figure 8.117b: The dynamic behaviour of unbiodegradable soluble substrate at h4 for ASM1 reduced model

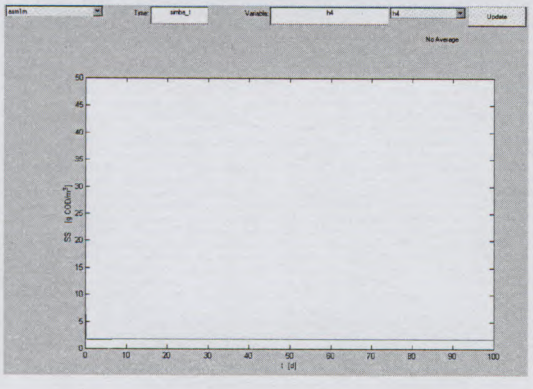

Figure 8.118a: The dynamic behaviour of readily biodegradable (soluble) substrate fraction at h4 for ASM1 full model

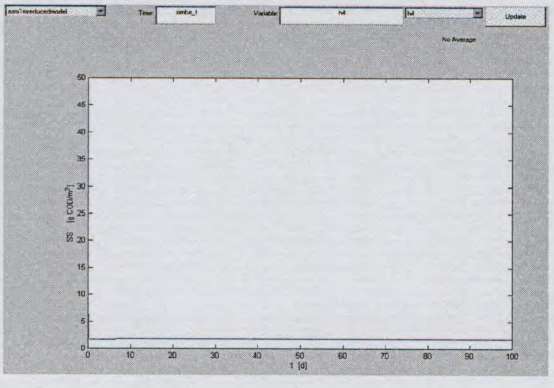

Figure 8.118b: The dynamic behaviour of readily biodegradable (soluble) substrate fraction at h4 for ASM1 reduced model

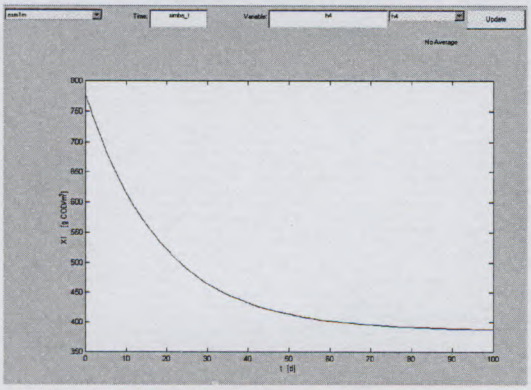

Figure 8.119a: The dynamic behaviour of inert mass fraction at h4 for ASM1 full model

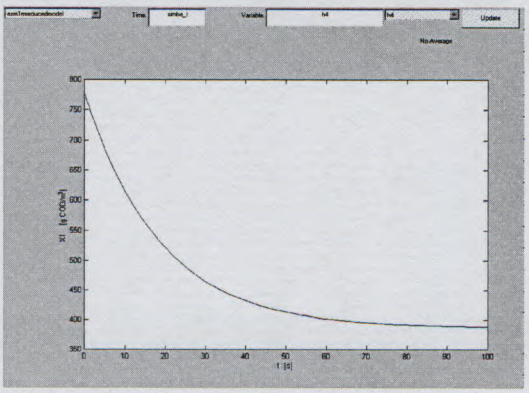

Figure 8.119b: The dynamic behaviour of inert mass fraction at h4 for ASM1 reduced model

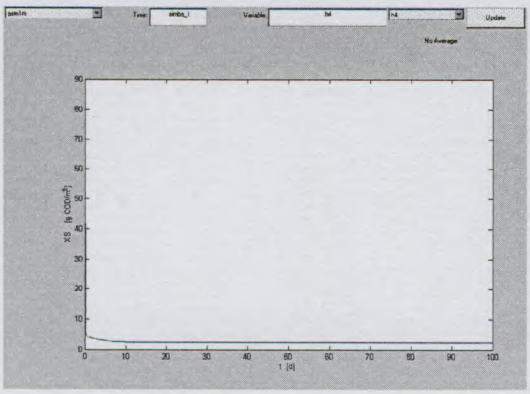

Figure 8.120a: The dynamic behaviour of enmeshed slowly biodegradable substrate fraction at h4 for ASM1 full model

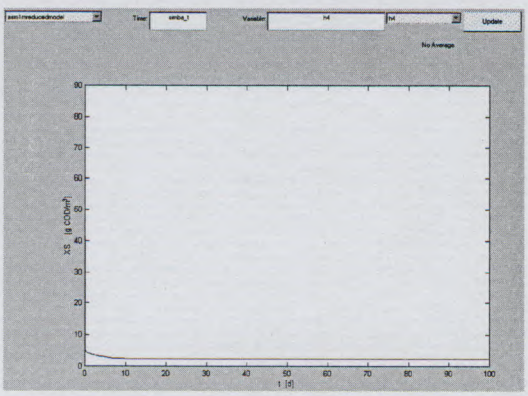

Figure 8.120b: The dynamic behaviour of enmeshed slowly biodegradable substrate fraction at h4 for ASM1 reduced model

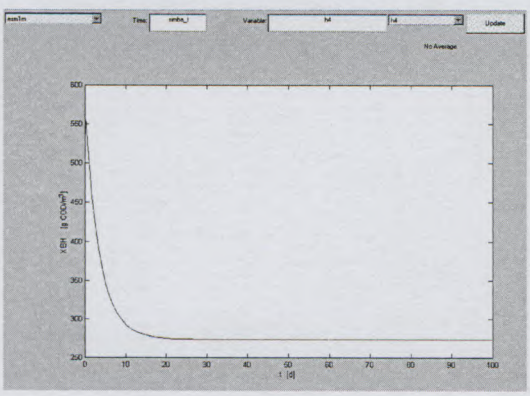

Figure 8.121a The dynamic behaviour of biological (active) heterotrophic mass fraction at h4 for ASM1 full model

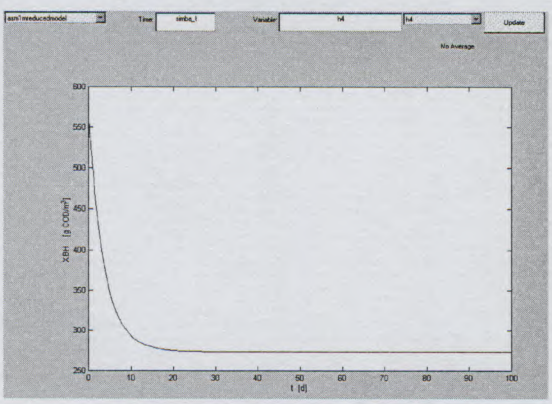

Figure 8.121b: The dynamic behaviour of biological (active) heterotrophic mass fraction at h4 for ASM1 reduced model

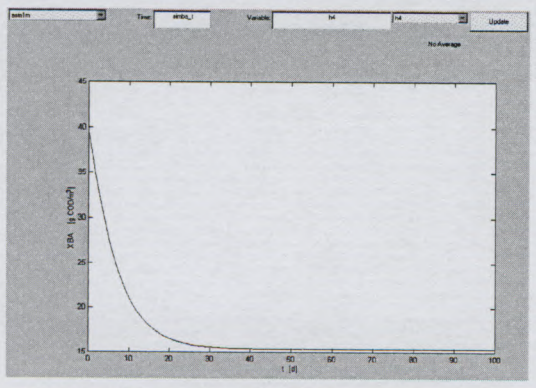

Figure 8.122a: The dynamic behaviour of biological (active) autotrophic mass fraction at h4 for ASM1 full model

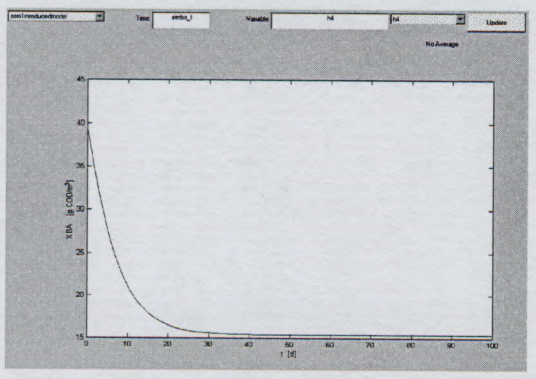

Figure 8.122b: The dynamic behaviour of biological (active) autotrophic mass fraction at h4 for ASM1 reduced model

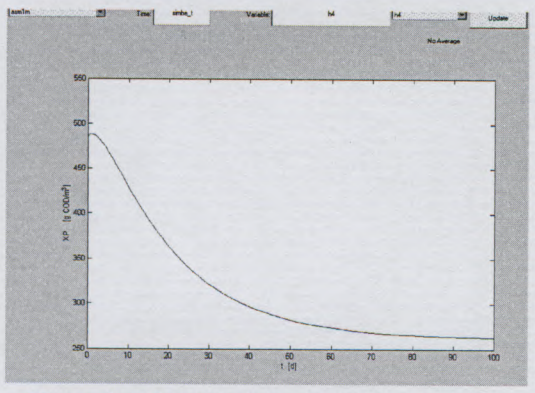

Figure 8.123a: The dynamic behaviour of endogenous mass fraction at h4 for ASM1 full model

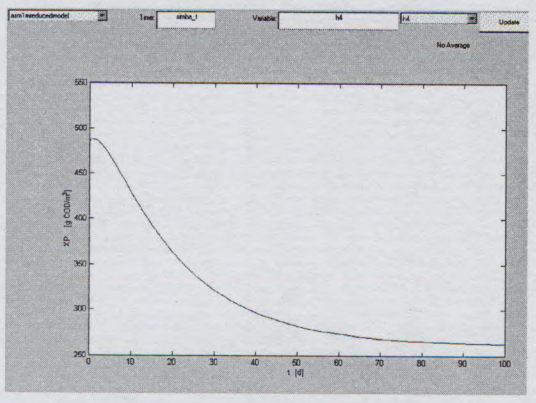

Figure 8.123b: The dynamic behaviour of endogenous mass fraction at h4 for ASM1 reduced model

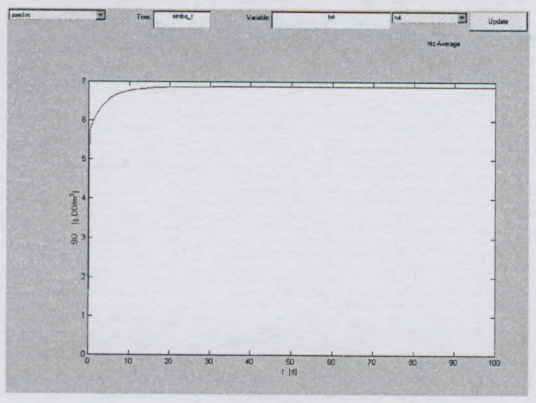

Figure 8.124a: The dynamic behaviour of oxygen at h4 for ASM1 full model

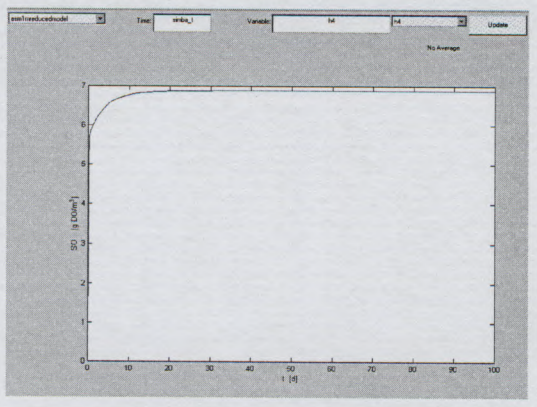

Figure 8.124b: The dynamic behaviour of oxygen at h4 for ASM1 reduced model

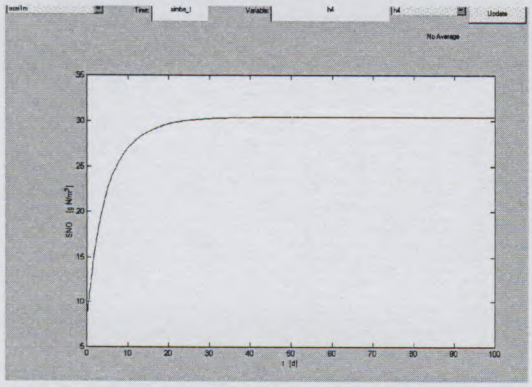

Figure 8.125a: The dynamic behaviour of nitrate nitrogen at h4 for ASM1 full model

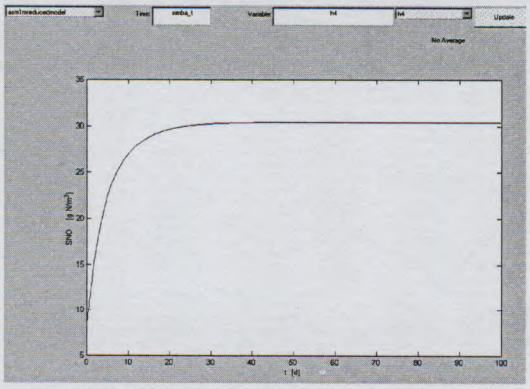

Figure 8.125b: The dynamic behaviour of nitrate nitrogen at h4 for ASM1 reduced model

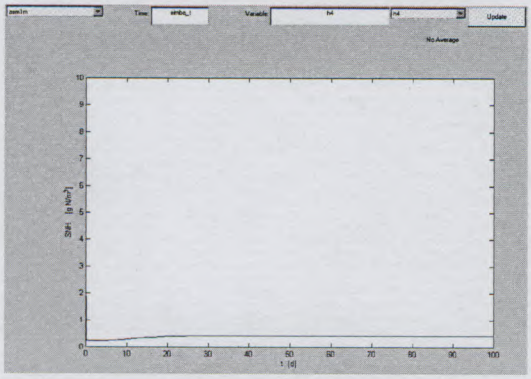

Figure 8.126a: The dynamic behaviour of ammonia nitrogen at h4 for ASM1 full model

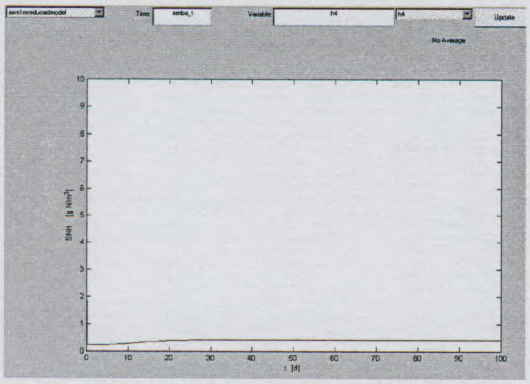

Figure 8.126b: The dynamic behaviour of ammonia nitrogen at h4 for ASM1 reduced model

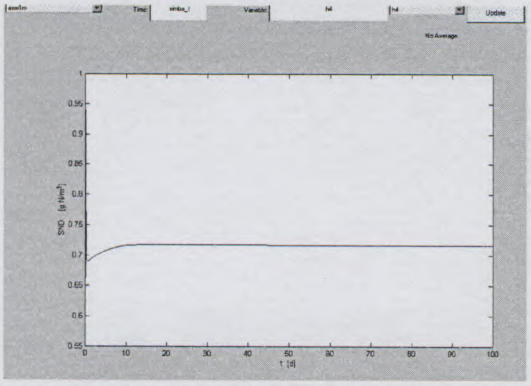

Figure 8.127a: The dynamic behaviour of biodegradable soluble organic nitrogen at h4 for ASM1 full model

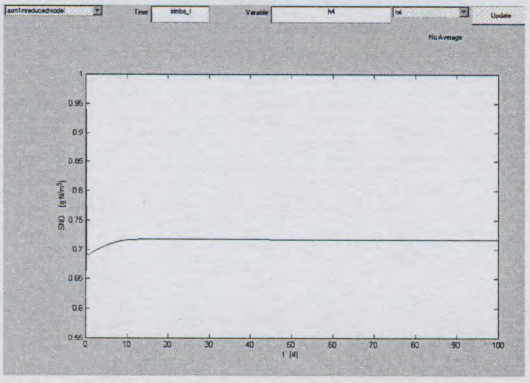

Figure 8.127b: The dynamic behaviour of biodegradable soluble organic nitrogen at h4 for ASM1 reduced model

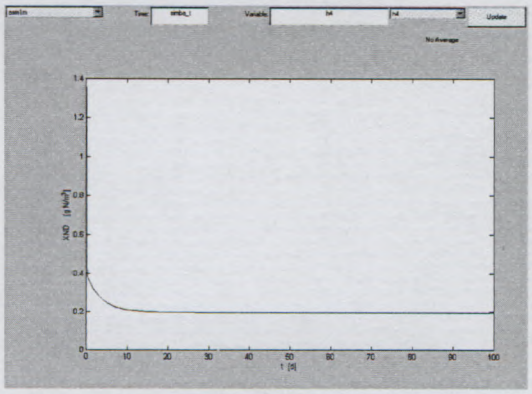

Figure 8.128a: The dynamic behaviour of biodegradable particulate organic nitrogen fraction at h4 for ASM1 full model

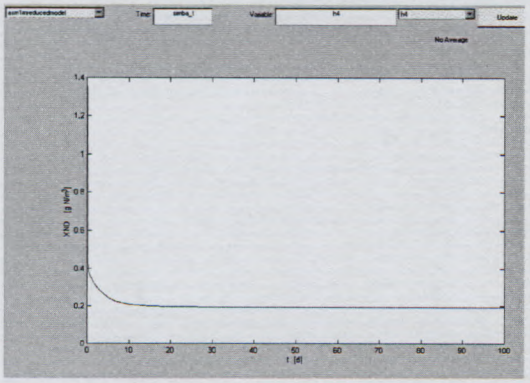

Figure 8.128b: The dynamic behaviour of biodegradable particulate organic nitrogen fraction at h4 for ASM1 reduced model

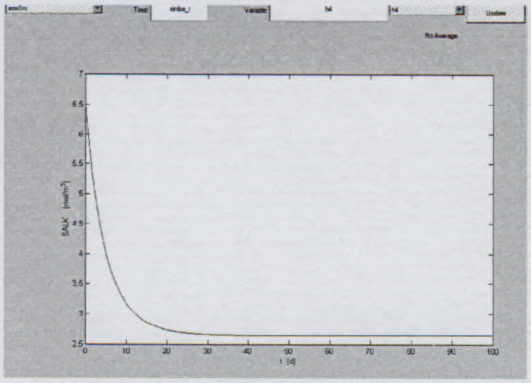

Figure 8.129a: The dynamic behaviour of alkalinity at h4 for ASM1 full model

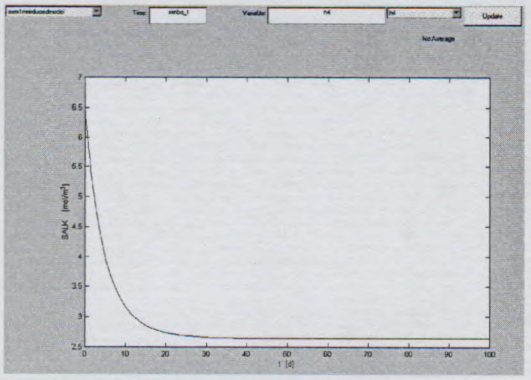

Figure 8.129b: The dynamic behaviour of alkalinity at h4 for ASM1 reduced model

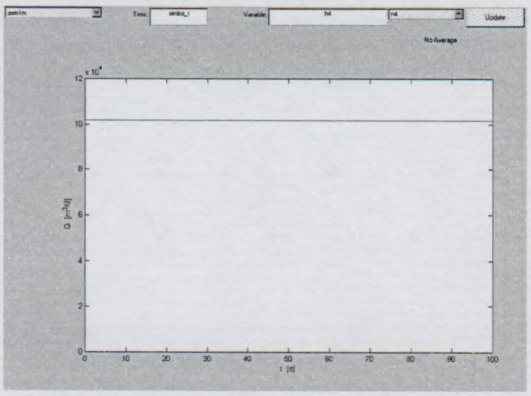

Figure 8.130a: The dynamic behaviour of flow rate at h4 for ASM1 full model

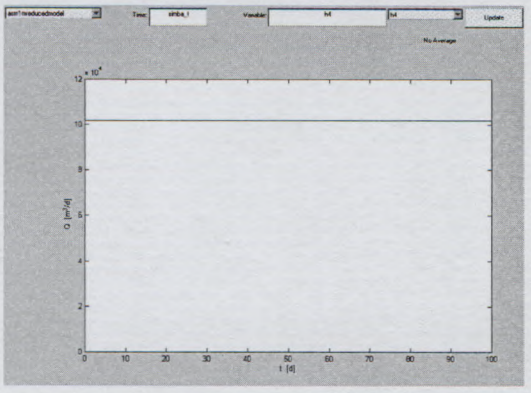

Figure 8.130b The dynamic behaviour of flow rate at h4 for ASM1 reduced model

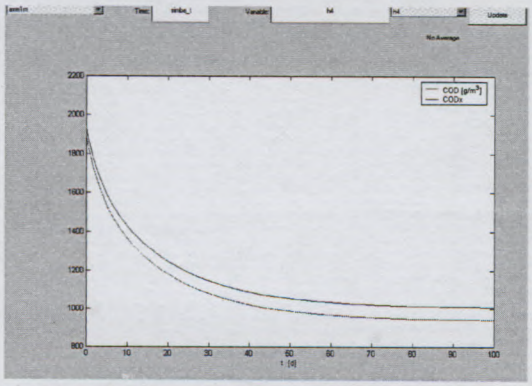

Figure 8.131a: The dynamic behaviour of chemical oxygen demand at h4 for ASM1 full model

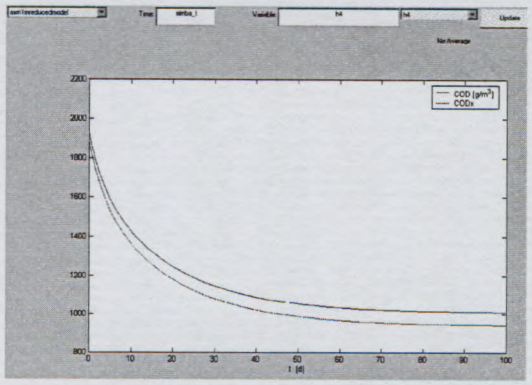

Figure 8.131b: The dynamic behaviour of chemical oxygen demand at h4 for ASM1 reduced model

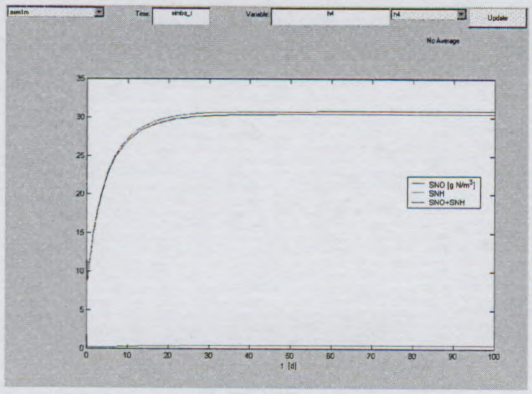

Figure 8.132a: The dynamic behaviour of nitrogen at h4 for ASM1 full model

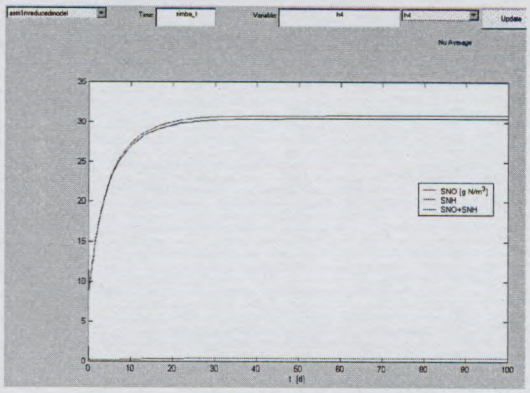

Figure 8.132b: The dynamic behaviour of nitrogen at h4 for ASM1 reduced model

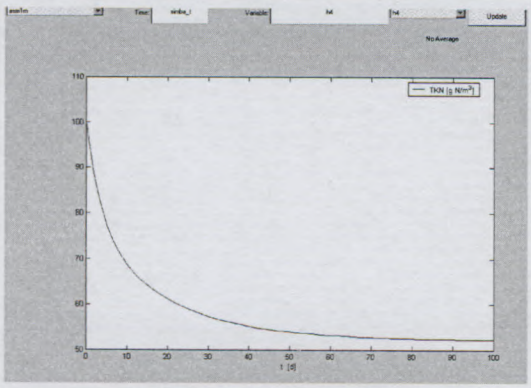

Figure 8.133a: The dynamic behaviour of total Kjedahl nitrogen at h4 for ASM1 full model

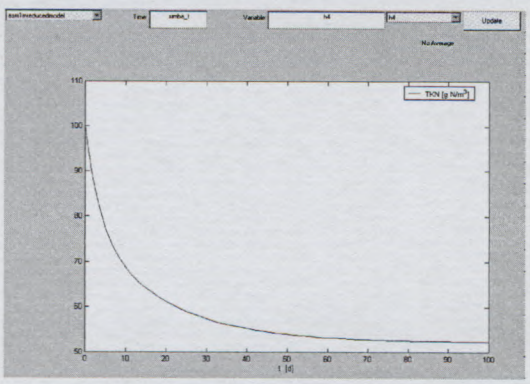

Figure 8.133b: The dynamic behaviour of total Kjedahl nitrogen at h4 for ASM1 reduced model

8.9.2.5 Discussion of the results

The graphs of the variables at the points h1, h2, h3 and h4 are all exactly the same for the ASM1 fullmodel and the ASM1 reduced model.

- The growth of heterotrophs within the various reaction zones.
  After the anaerobic tank the hetertrophs are at 750 $g\,COD/m^3$ at zero day and decay down to 250 $g\,COD/m^3$ after 10 days then further decay to 240 $g\,COD/m^3$ after 15 days and remain constant (See Figures 8.85a & 8.85b). In the anoxic tank the heterotrophs follow a similar pattern from 750 $g\,COD/m^3$ at zero day decay to 250 $g\,COD/m^3$ after 10 days and then a further to 240 $g\,COD/m^3$ at 15 days with a constant concentration after that (See Figures 8.102a & 8.102b). In the aerobic tank the heterotrophs are at 750 $g\,COD/m^3$ at zero day decaying to 260 $g\,COD/m^3$ after 10 days, then from 15 days have a stable concentration of 240 $g\,COD/m^3$ (See Figures 8.119a & 8.119b).

- The growth of autotrophs within the various reaction zones.
  In the anaerobic tank the autotrophs are 37 $g\,COD/m^3$ at zero days, then decaying to 18 $g\,COD/m^3$ after 10 days, then stabilizing after 20 days at 14 $g\,COD/m^3$ which remains constant after that value (See Figures 8.86a & 8.86b). In the anoxic tank the autrotrophs are at 40 $g\,COD/m^3$ at zero days, then decaying to 18after 10 days whilst remaining constant after 40 days at 15 $g\,COD/m^3$ (See Figures 8.103a & 8.103b). In the aerobic tank the autotrophs are at 39 $g\,COD/m^3$ at zero days decaying to 19 $g\,COD/m^3$ after 10 days then remaining constant at 15 $g\,COD/m^3$ after 40 days (See Figures 8.120a & 8.120b).

- The dynamic behaviour of the readily biodegradable (soluble) substrate within the various reaction zones.
  In the anaerobic tank the soluble substrate is at 4 $g\,COD/m^3$ for zero days increasing to 5 $g\,COD/m^3$ after 10 days, then remaining constant (stable) at this concentration (See Figures 8.82a & 8.82b). In the anoxic tank the soluble substrate is at 5 $g\,COD/m^3$ for zero days dropping down to 2,5 $g\,COD/m^3$ at zero days, and after 10 days at 3 $g\,COD/m^3$ which remains constant (See Figures 8.99a & 8.99b). In the aerobic tank the soluble substrate is at 6 $g\,COD/m^3$ for zero days dropping down to 2 $g\,COD/m^3$ for zero days then slightly increasing to 2,5 $g\,COD/m^3$ after 10 days and remaining constant at that concentration (See Figures 8.116a & 8.116b).

- The dynamic behaviour of ammonia nitrogen within the various reaction zones.
  In the anaerobic tank the ammonia is at 7 $g\,N/m^3$ for zero days dropping to 3,2 $g\,N/m^3$ for zero days. After 5 days the concentration is at a minimum of 3 $g\,N/m^3$ then slightly increases to 3,2 $g\,N/m^3$ after 20 days which remains constant at that value (See Figures 8.90a & 8.90b). In the anoxic tank the ammonia is at 3,2 $g\,N/m^3$ for zero days and drops to

1,6 $g\,N/m^3$ for zero days (minimum) which slightly increases to 1,8 $g\,N/m^3$ after 20 days and remains constant at this concentration (See Figures 8.107a & 107b). In the aerobic tank the ammonia is at $2\,g\,N/m^3$ for zero days dropping to 0,2 $g\,N/m^3$ for zero days (minimum) which then slightly increases to 0,4 $g\,N/m^3$ for 20 days which remain constant after that concentration (See Figures 8.124a & 8.124b).

- The dynamic behaviour of nitrates nitrogen within the various reaction zones
  In the anaerobic tank the nitrates are 4,5 $g\,N/m^3$ for zero days which increases to 25 $g\,N/m^3$ after 10 days. Then after 20 days the concentration is 27 $g\,N/m^3$ after which it remains constant (See Figures 8.89a & 8.89b). In the anoxic tank the nitrates are at 7,5 $g\,N/m^3$ for zero days which increases to 28 $g\,N/m^3$ after 10 days. Then thereafter 40 days at 30 $g\,N/m^3$ which remains constant (See Figures 8.106a & 8.106b). In the aerobic tank the nitrates are at 8 $g\,N/m^3$ for zero days and increases to 27,5 $g\,N/m^3$ for 10 days. Then after 30 days the concentration is 31 $g\,N/m^3$ (See Figures 8.123a & 8.123b).

- The dynamic behaviour of oxygen within the various reaction zones.
  In the anaerobic tank the oxygen is at zero concentration for zero days and slightly increased to 0,08 $g\,COD/m^3$ after 10 days. The concentration of oxygen stabilizes at 20 days to 0,1 $g\,COD/m^3$ and remains constant (See Figures 8.88a & 8.88b). In the anoxic tank the oxygen starts at zero concentration to 2 $g\,COD/m^3$ for zero days. Then increases to 4 $g\,COD/m^3$ for 10 days and after 20 days has a constant value of 4,4 $g\,COD/m^3$ (See Figures 8.105a & 8.105b). In the aerobic tank the oxygen is at 1,8 $g\,COD/m^3$ increasing to 5,8 $g\,COD/m^3$ for zero days. Then increases to 6,8 $g\,COD/m^3$ for 10 days and after 20 days has a constant value of 6,9 $g\,COD/m^3$ (See Figures 8.122a & 8.122b).

8.9.3 Results from the simulation of the Athlone plant models using the full and reduced UCT biological models

8.9.3.1 Dynamic behaviour of the anaerobic tank input (point h1) in wastewater for Athlone plant simulated over a period of 100 days for total sludge age of 20 days at 22 C

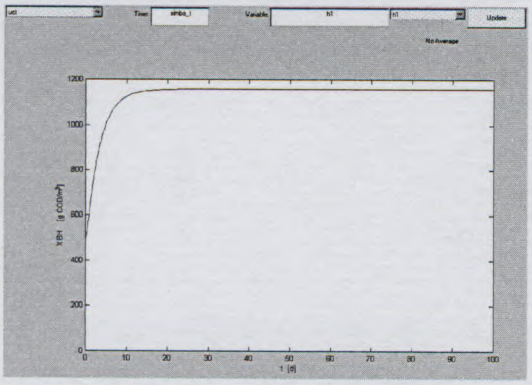

Figure 8.134a: The dynamic behaviour of biological (active) heterotrophic mass fraction at h1, full UCT model

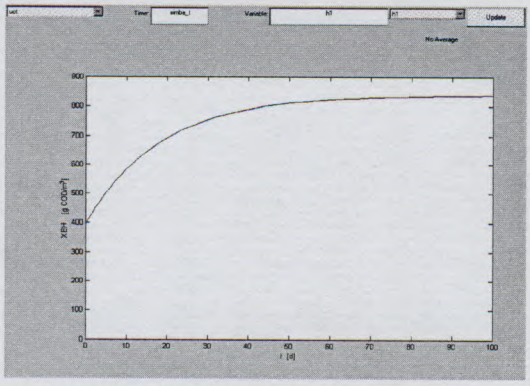

Figure 8.134b: The dynamic behaviour of biological (active) heterotrophic mass fraction, UCT reduced model at h1

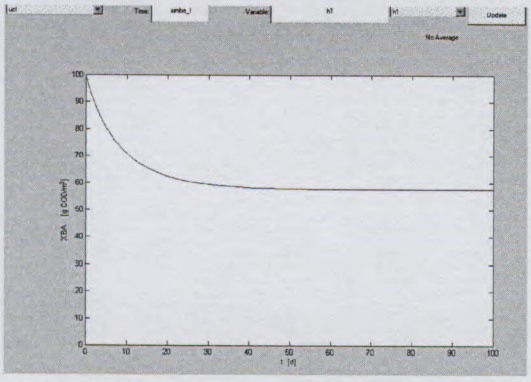

Figure 8.135a: The dynamic behaviour of biological (active) autotrophic biomass fraction at h1 full UCT model

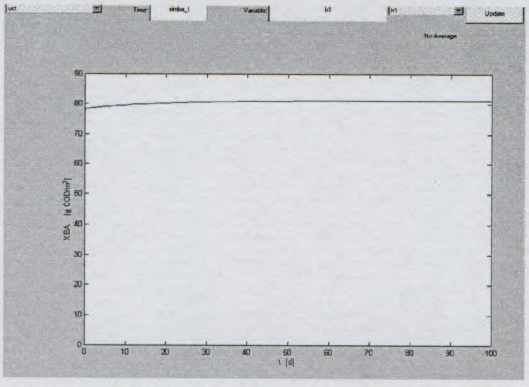

Figure 8.135b: The dynamic behaviour of biological (active) autotrophic biomass fraction UCT reduced model at h1

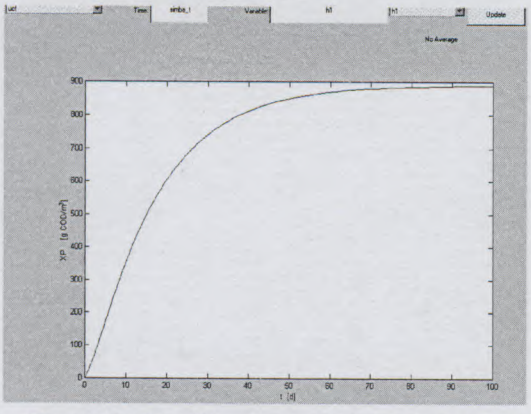

Figure 8.136a: The dynamic behaviour of endogenous mass fraction at h1 full UCT model

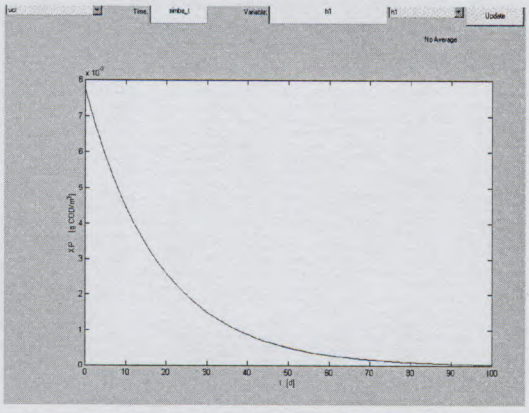

Figure 8.136b: The dynamic behaviour of endogenous mass fraction UCT reduced model at h1

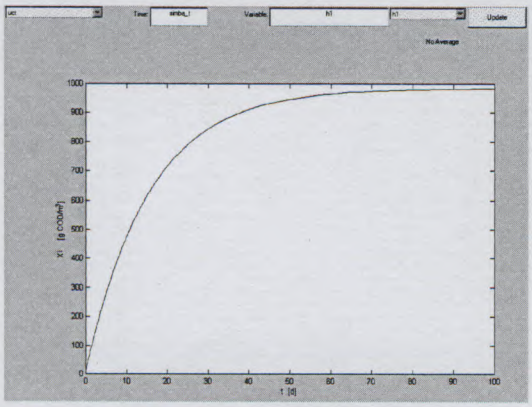

Figure 8.137a: The dynamic behaviour of inert mass fraction at h1, full UCT model

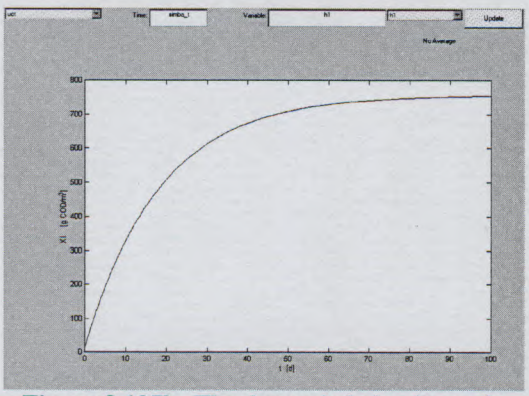

Figure 8.137b: The dynamic behaviour of inert mass fraction at h1, UCT reduced model

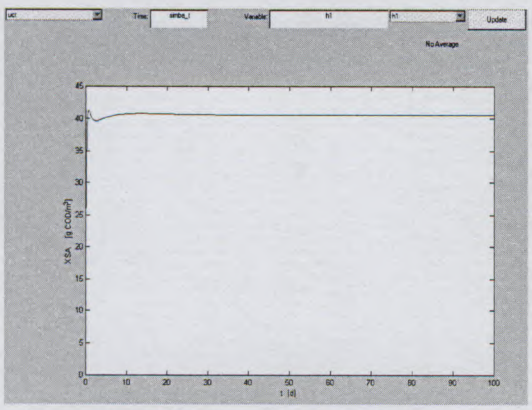

Figure 8.138a: The dynamic behaviour of adsorbed slowly biodegradable substrate fraction at h1 full UCT model

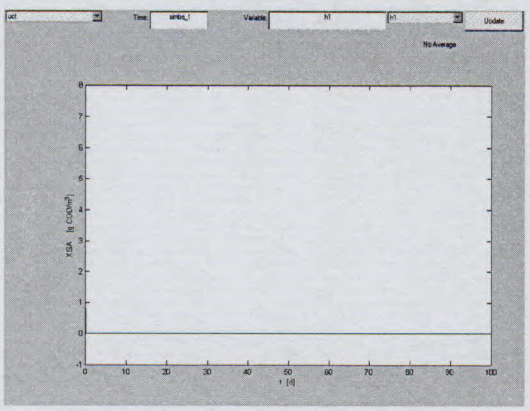

Figure 8.138b: The dynamic behaviour of adsorbed slowly biodegradable substrate fraction at h1 UCT reduced model

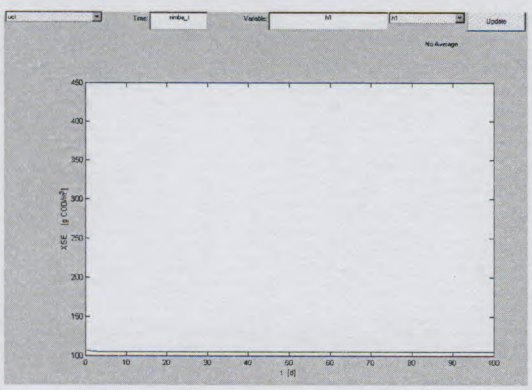

Figure 8.139a: The dynamic behaviour of enmeshed slowly biodegradable substrate fraction at h1 full UCT model

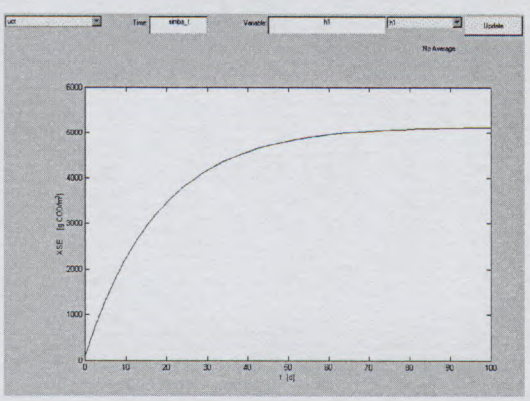

Figure 8.139b: The dynamic behaviour of enmeshed slowly biodegradable substrate fraction at h1 UCT reduced model

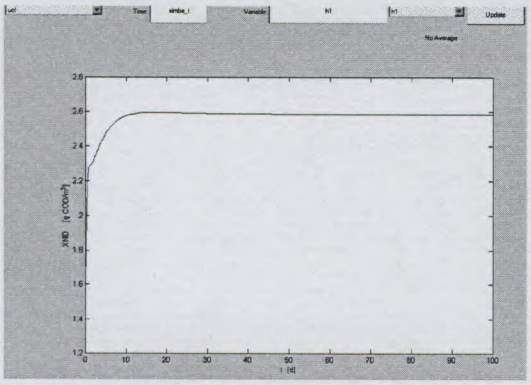

Figure 8.140a: The dynamic behaviour of biodegradable particulate organic nitrogen fraction at h1 full UCT model

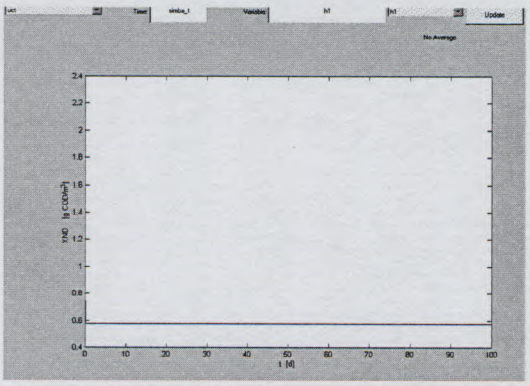

Figure 8.140b: The dynamic behaviour of biodegradable particulate organic nitrogen fraction at h1 UCT reducedmodel

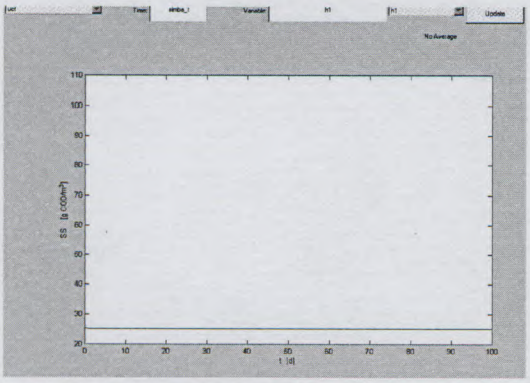

Figure 8.141a: The dynamic behaviour of readily biodegradable (soluble) substrate fraction at h1 full UCT model

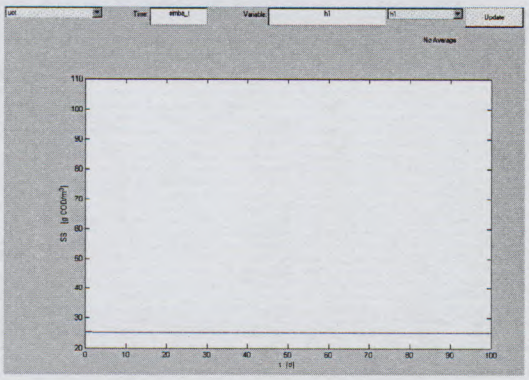

Figure 8.141b: The dynamic behaviour of readily biodegradable (soluble) substrate fraction at h1 UCT reduced model

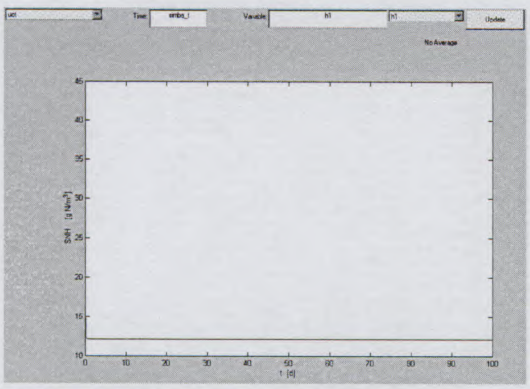

Figure 8.142a: The dynamic behaviour of ammonia nitrogen at h1 full UCT model

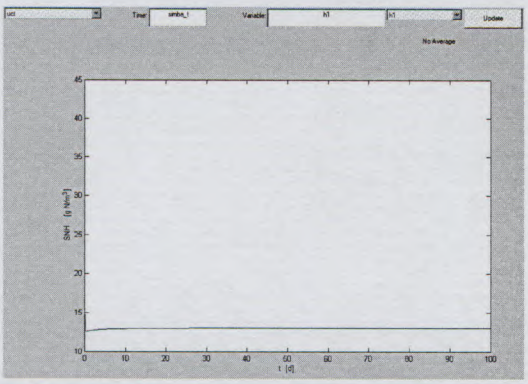

Figure 8.142b The dynamic behaviour of ammonia nitrogen fraction at h1 UCT reduced model

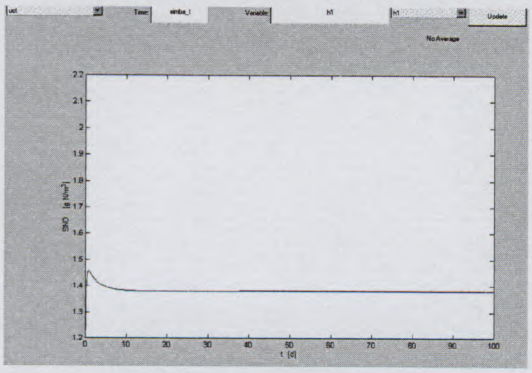

Figure 8.143a: The dynamic behaviour of biodegradable soluble organic nitrogen at h1 full UCT model

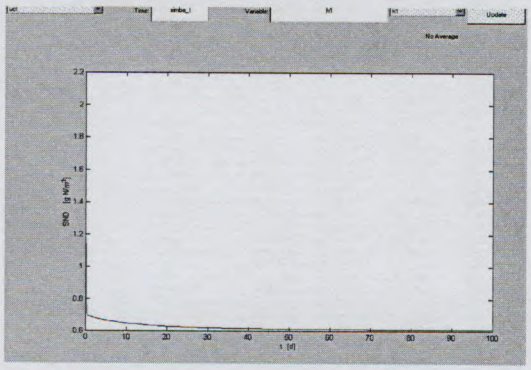

Figure 8.143b: The dynamic behaviour of biodegradable soluble organic nitrogen fraction at h1 UCT reduced model

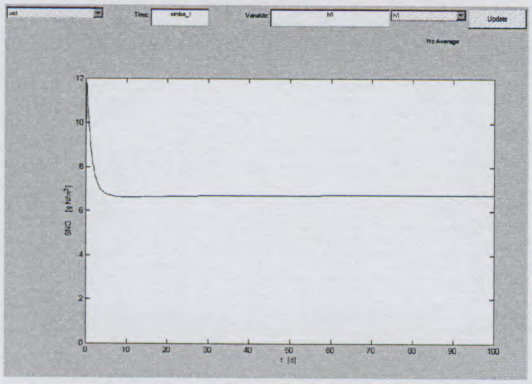

Figure 8.144a: The dynamic behaviour of nitrate nitrogen at h1 UCT full model

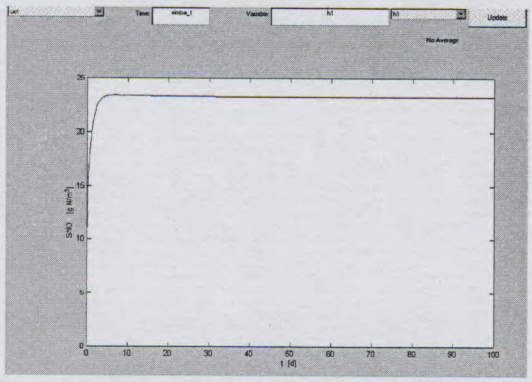

Figure 8.144b: The dynamic behaviour of nitrate nitrogen fraction at h1 UCT reduced model

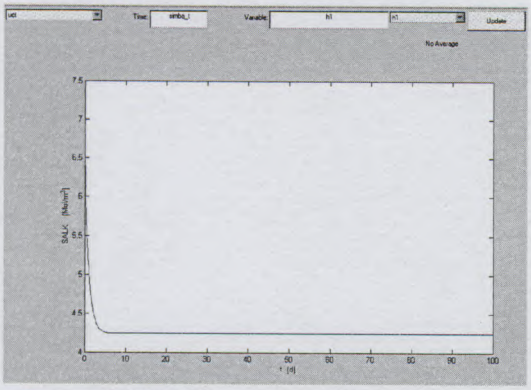

Figure 8.145a: The dynamic behaviour of alkalinity at h1 UCT full model

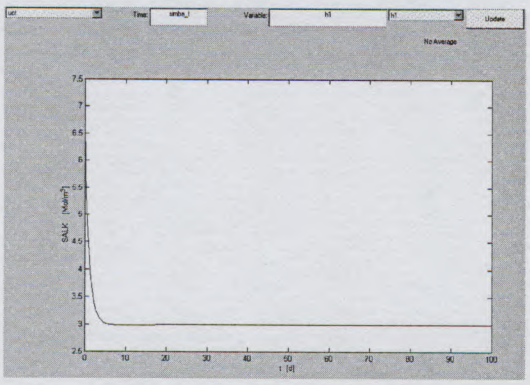

Figure 8.145b: The dynamic behaviour of alkalinity at h1 UCT reduced model

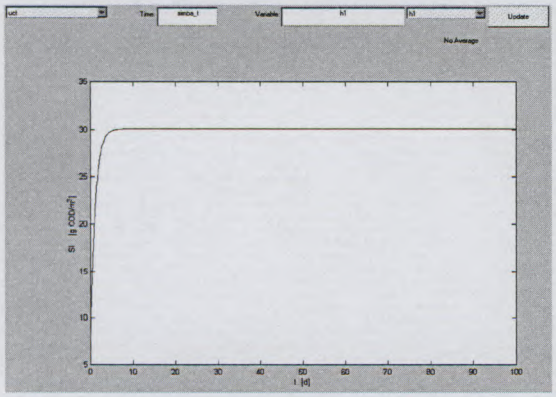

Figure 8.146a: The dynamic behaviour of unbiodegradable soluble substrate at h1 UCT full model

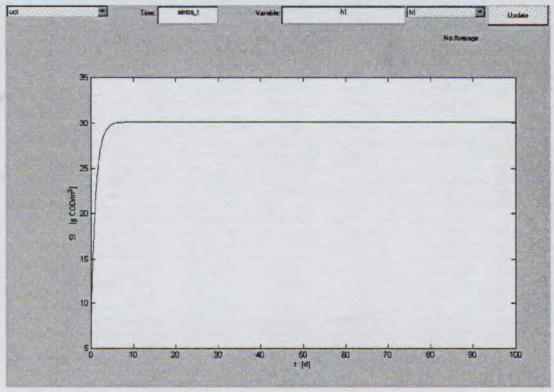

Figure 8.146b: The dynamic behaviour of unbiodegradable soluble substrate fraction at h1 UCT reduced model

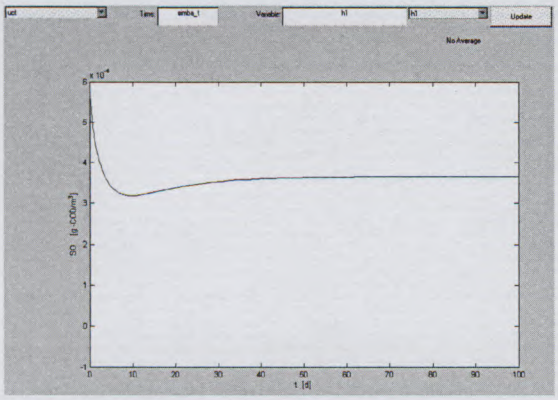

Figure 8.147a: The dynamic behaviour of oxygen at h1 in wastewater UCT full model

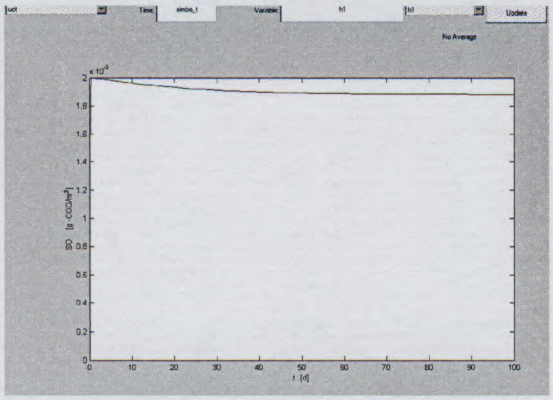

Figure 8.147b: The dynamic behaviour of oxygen at h1 UCT reduced model

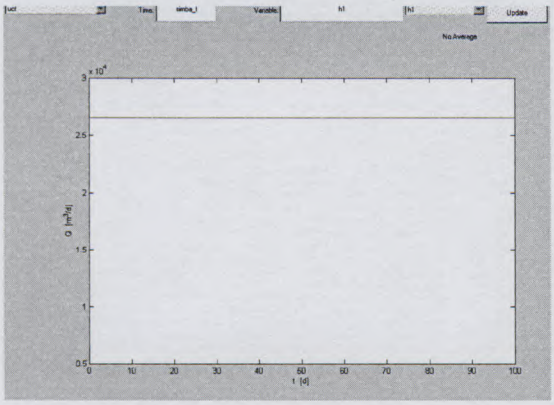

Figure 8.148a: The dynamic behaviour of flow rate at h1 UCT full model

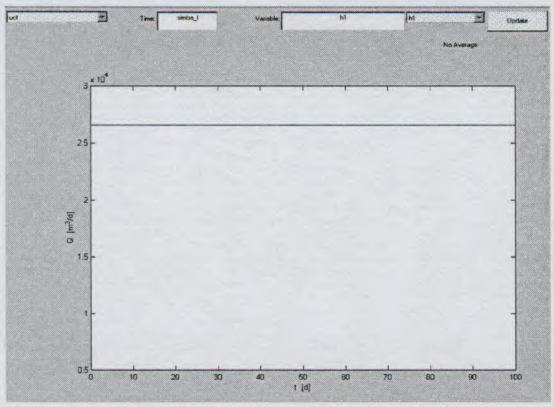

Figure 8.148b: The dynamic behaviour of flow rate at h1 UCT reduced model

8.9.3.2 Dynamic behaviour of the process variables after the anaerobic tank (point h2) in Athlone wastewater plant simulated over a period of 100 days for total sludge age of 20 days at 22 C

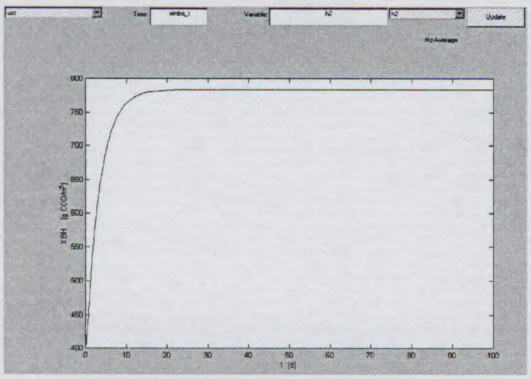

Figure 8.149a: The dynamic behaviour of biological (active) heterotrophic mass fraction at h2 UCT full model

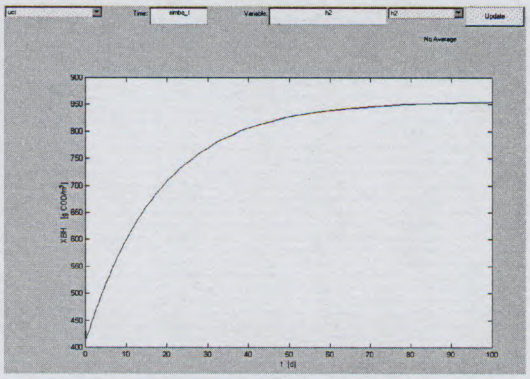

Figure 8.149b: The dynamic behaviour of biological (active) heterotrophic mass fraction at h2 UCT reduced model

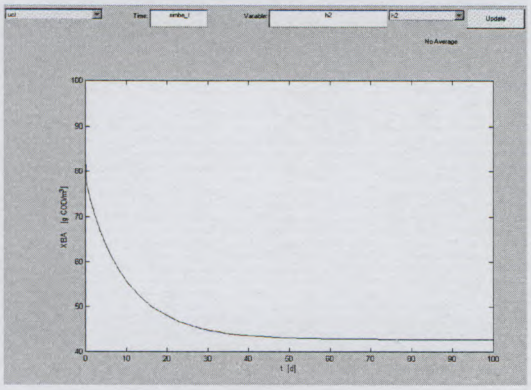

Figure 8.150a: The dynamic behaviour of biological (active) autotrophic biomass fraction at UCT full model at h2

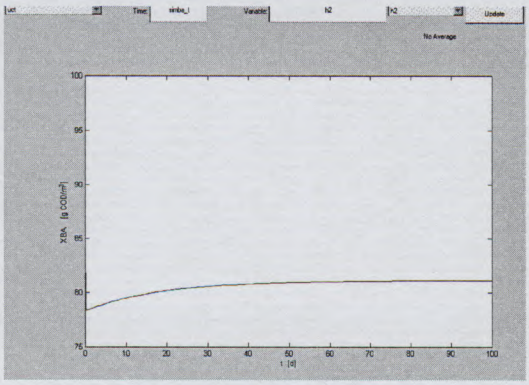

Figure 8.150b: The dynamic behaviour of biological (active) autotrophic biomass fraction at h2 UCT reduced model

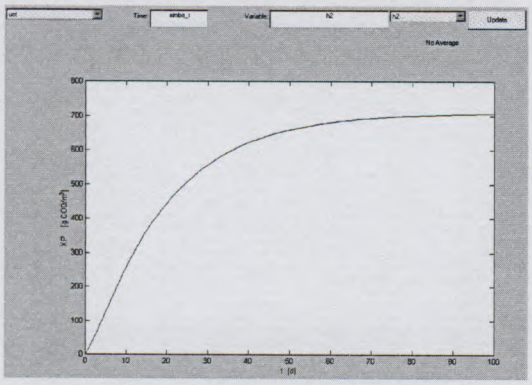

Figure 8.151a: The dynamic behaviour of endogenous mass fraction at h2 UCT full model

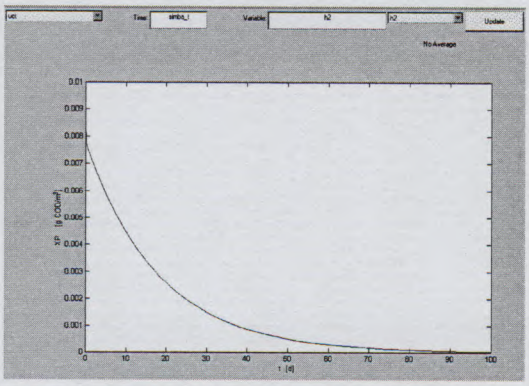

Figure 8.151b: The dynamic behaviour of endogenous mass fraction at h2 UCT reduced model

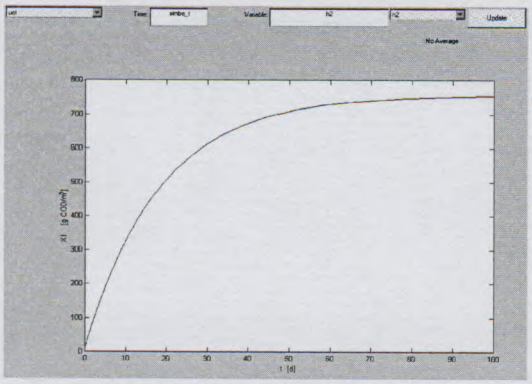

Figure 8.152a: The dynamic behaviour of inert mass fraction at h2 UCT full model

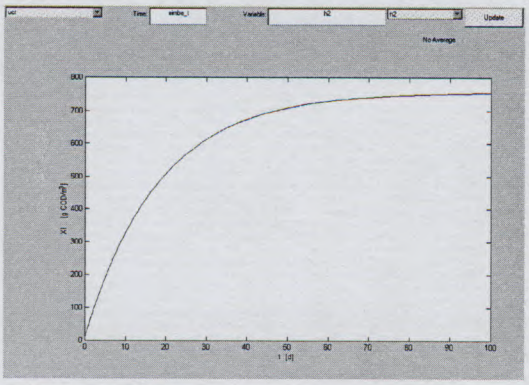

Figure 8.152b: The dynamic behaviour of inert mass fraction at h2 UCT reduced model

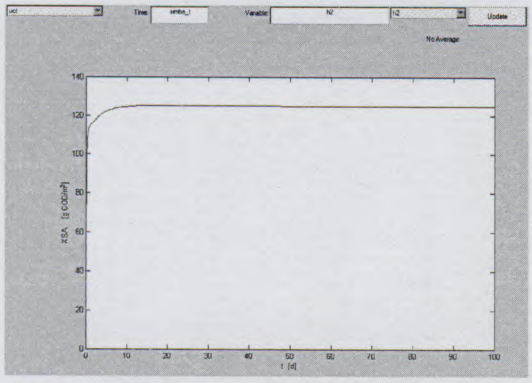

Figure 8.153a: The dynamic behaviour of adsorbed slowly biodegradable substrate fraction at h2 UCT full model

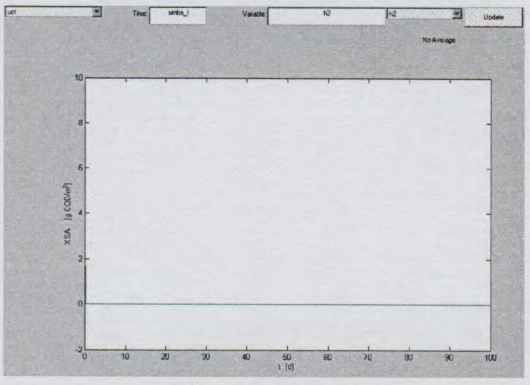

Figure 8.153b: The dynamic behaviour of adsorbed slowly biodegradable substrate at h2 UCT reduced model

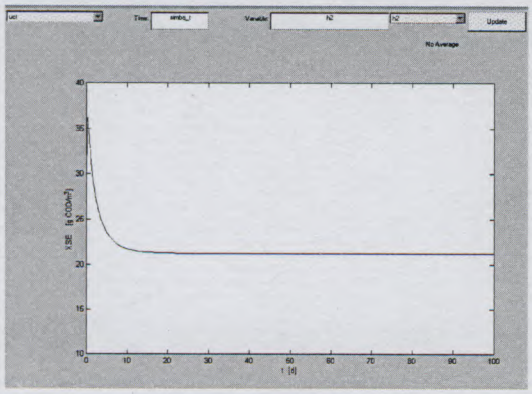

Figure 8.154a: The dynamic behaviour of enmeshed slowly biodegradable substrate fraction at h2 UCT full model

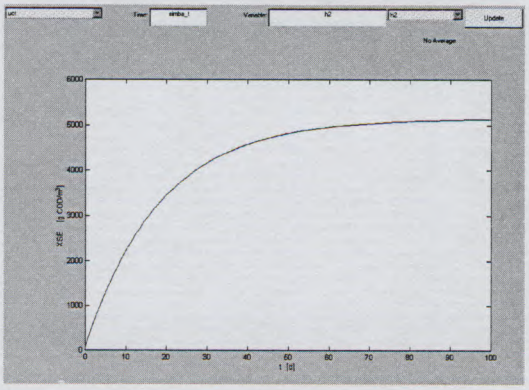

Figure 8.154b: The dynamic behaviour of enmeshed slowly biodegradable substrate fraction at h2 UCT reduced model

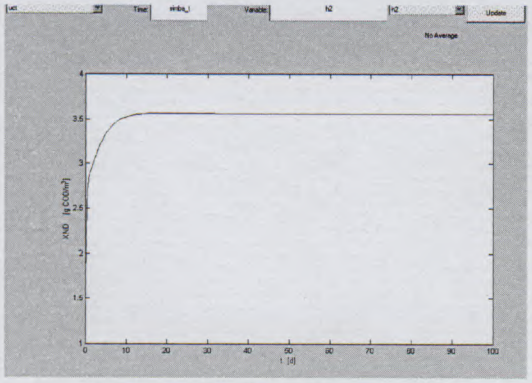

Figure 8.155a: The dynamic behaviour of biodegradable particulate organic nitrogen fraction at h2 UCT full model

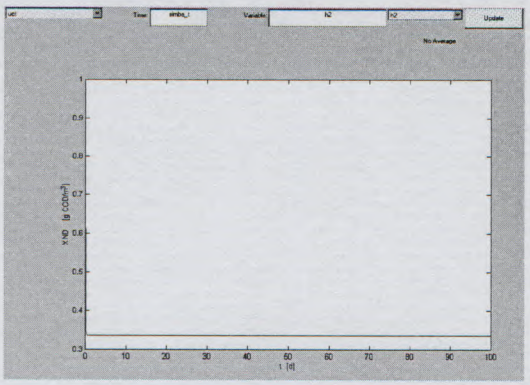

Figure 8.155b: The dynamic behaviour of biodegradable particulate organic nitrogen fraction at h2 UCT reduced model

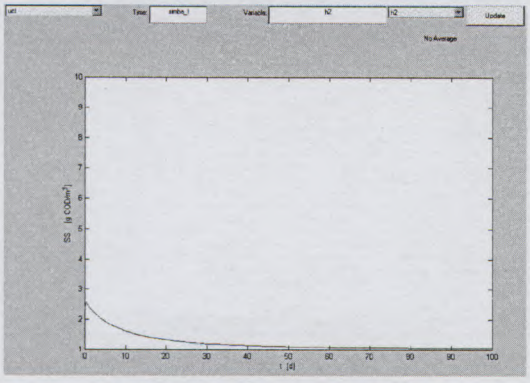

Figure 8.156a: The dynamic behaviour of readily biodegradable (soluble) substrate fraction at h2 UCT full model

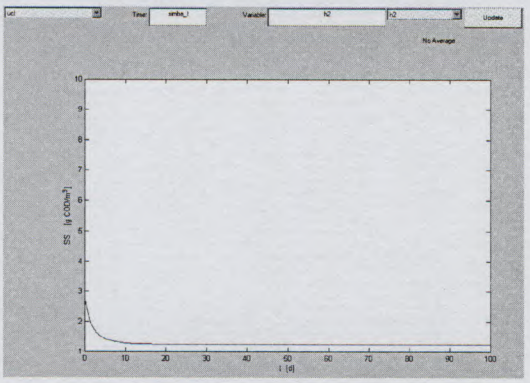

Figure 8.156b: The dynamic behaviour of readily biodegradable (soluble) substrate fraction at h2 UCT reduced model

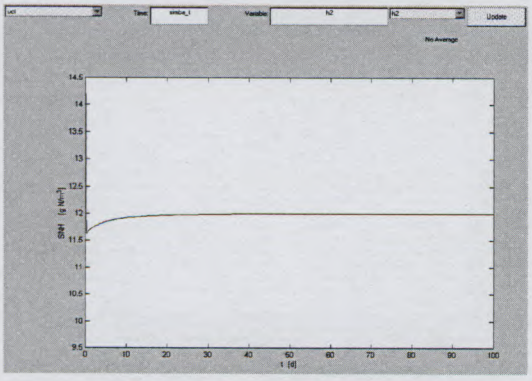

Figure 8.157a: The dynamic behaviour of ammonia nitrogen at h2 UCT full model

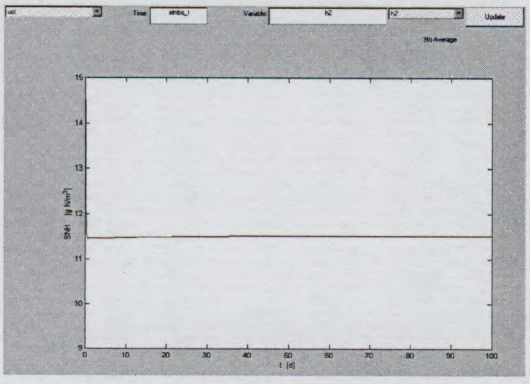

Figure 8.157b: The dynamic behaviour of ammonia nitrogen fraction at h2 UCT reduced model

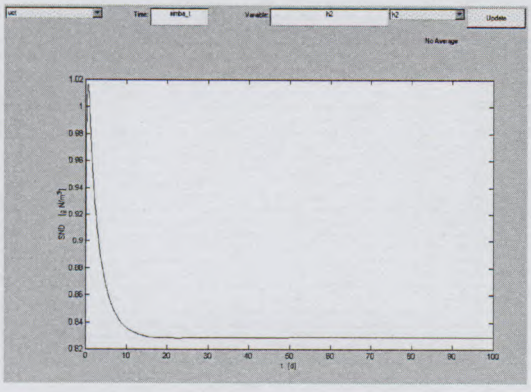

Figure 8.158a: The dynamic behaviour of biodegradable soluble organic nitrogen at h2 UCT full model

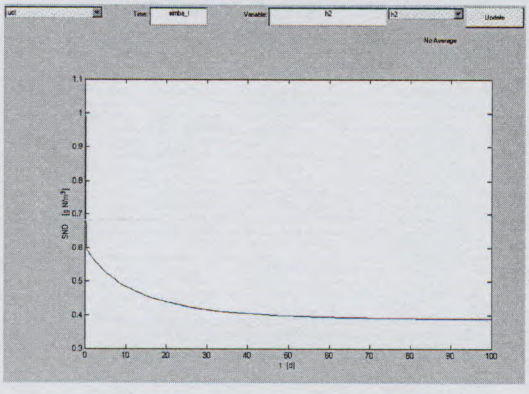

Figure 8.158b: The dynamic behaviour of biodegradable soluble organic nitrogen fraction at h2 UCT reduced model

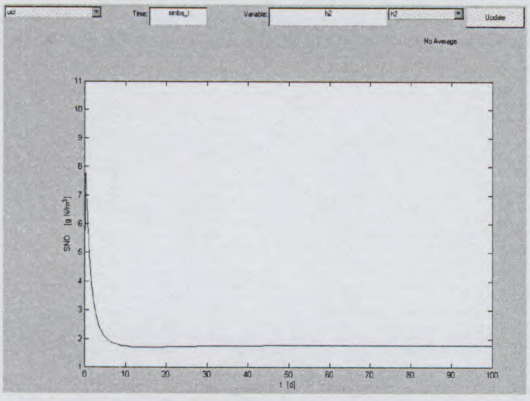

Figure 8.159a: The dynamic behaviour of nitrate nitrogen at h2 UCT full model

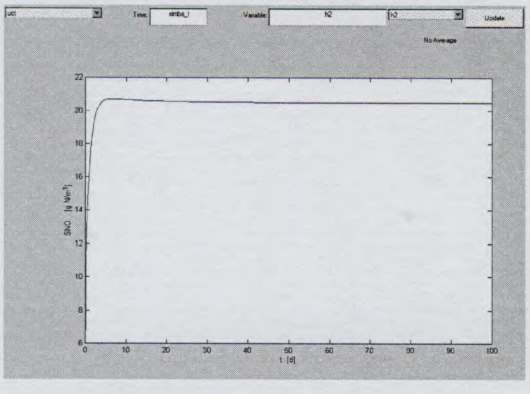

Figure 8.159b: The dynamic behaviour of nitrate nitrogen fraction at h2 UCT reduced model

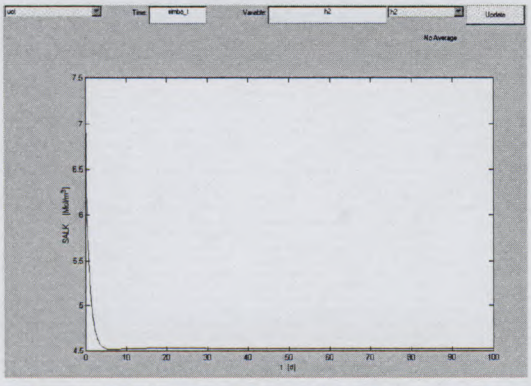

Figure 8.160a: The dynamic behaviour of alkalinity at h2 UCT full model

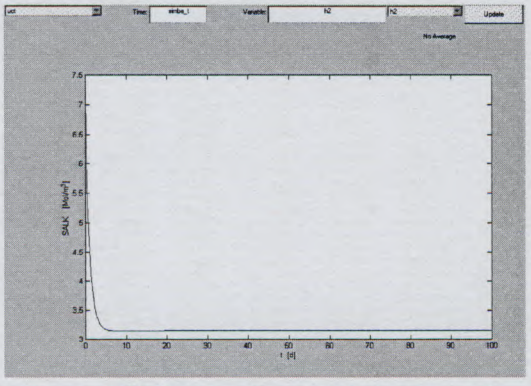

Figure 8.160b: The dynamic behaviour of alkalinity at h2 UCT reduced model

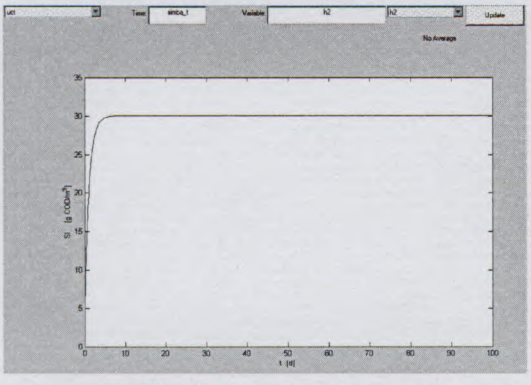

Figure 8.161a: The dynamic behaviour of unbiodegradable soluble substrate at h2 UCT full model

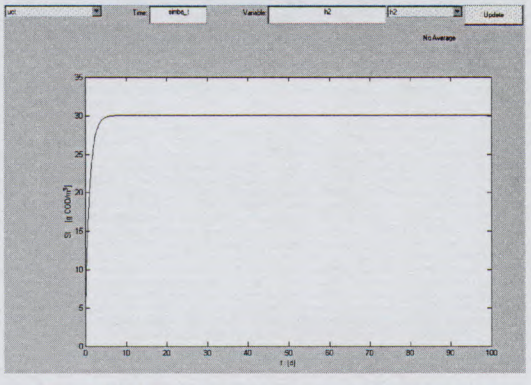

Figure 8.161b: The dynamic behaviour of unbiodegradable soluble substrate fraction at h2 UCT reduced model

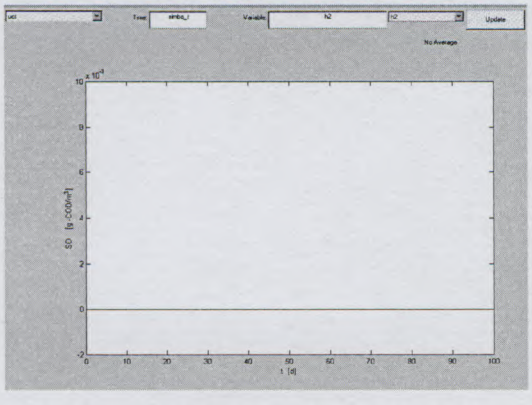

Figure 8.162a: The dynamic behaviour of oxygen at h2 UCT full model

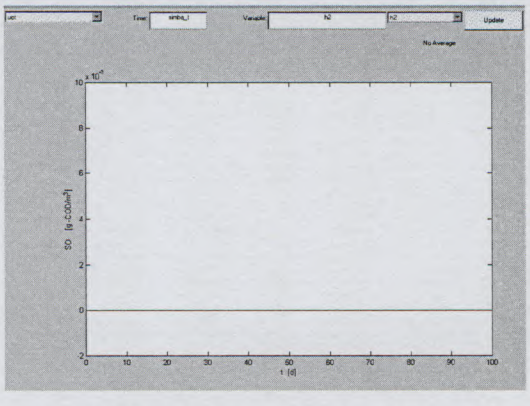

Figure 8.162b: The dynamic behaviour of oxygen at h2 UCT reduced model

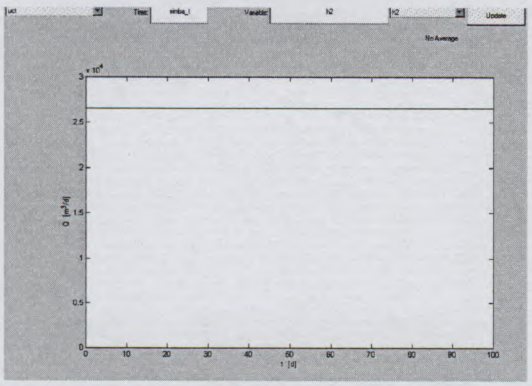

Figure 8.163a: The dynamic behaviour of flow rate at h2 UCT full model

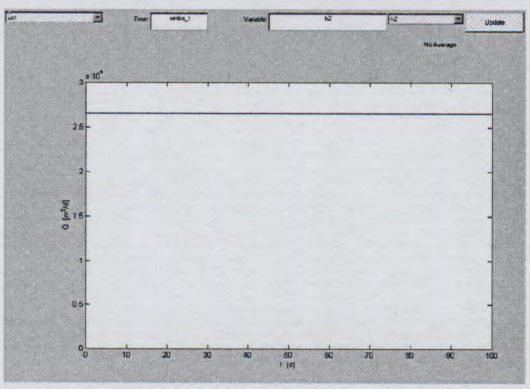

Figure 8.163b: The dynamic behaviour of flow rate at h2 UCT reduced model

8.9.3.3 Dynamic behaviour of the process variables after the anoxic tank (point h3) for Athlone wastewater plant simulated over a period of 100 days for total sludge age of 20 days at 22 Co

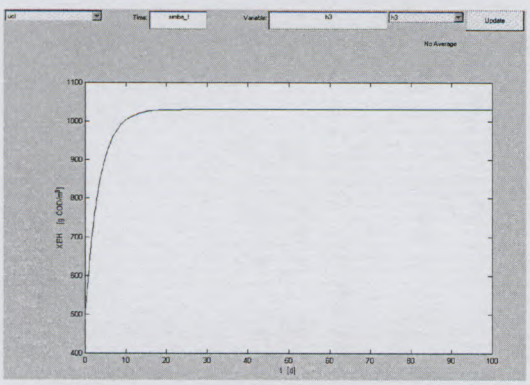

Figure 8.164a: The dynamic behaviour of biological (active) heterotrophic mass fraction at h3 UCT full model

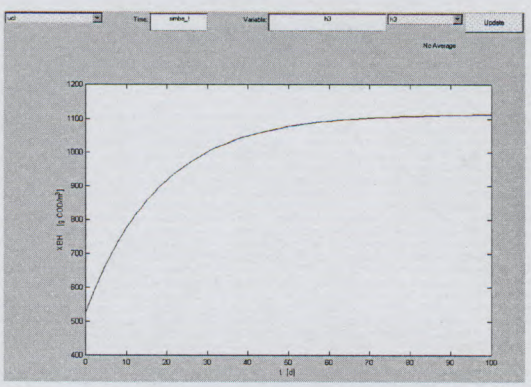

Figure 8.164b: The dynamic behaviour of biological (active) heterotrophic mass fraction at h3 UCT reduced model

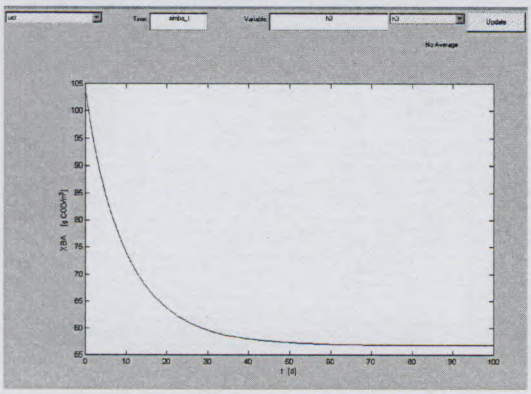

Figure 8.165a: The dynamic behaviour of biological (active) autotrophic biomass fraction at h3 full UCT model

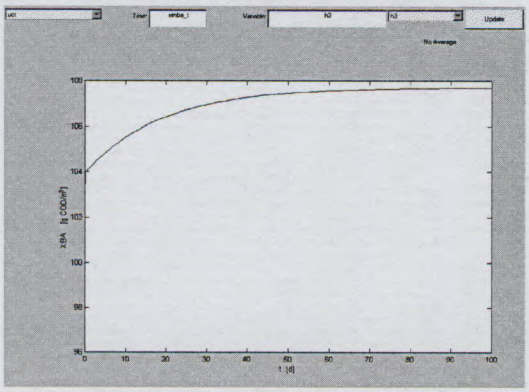

Figure 8.165b: The dynamic behaviour of biological (active) autotrophic biomass fraction at h3 UCT reduced model

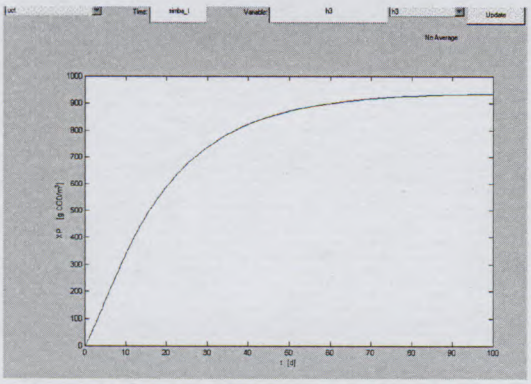

Figure 8.166a: The dynamic behaviour of endogenous mass fraction at h3 UCT full model

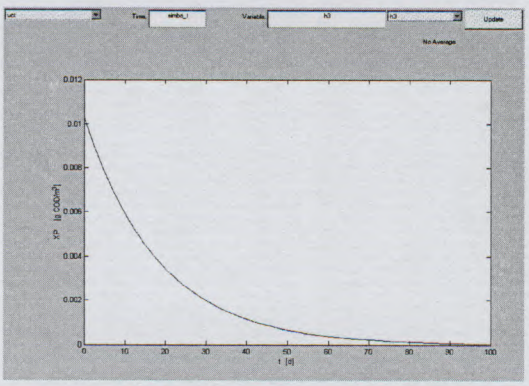

Figure 8.166b: The dynamic behaviour of endogenous mass fraction at h3 UCT reduced model

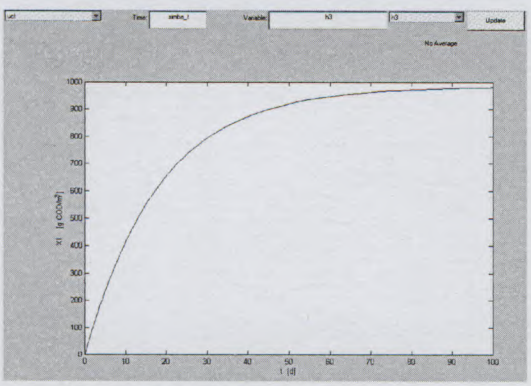

Figure 8.167a: The dynamic behaviour of inert mass fraction at h3 UCT full model

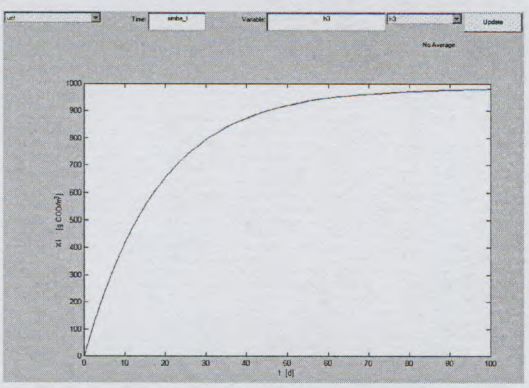

Figure 8.167b: The dynamic behaviour of inert mass fraction UCT reduced model at h3

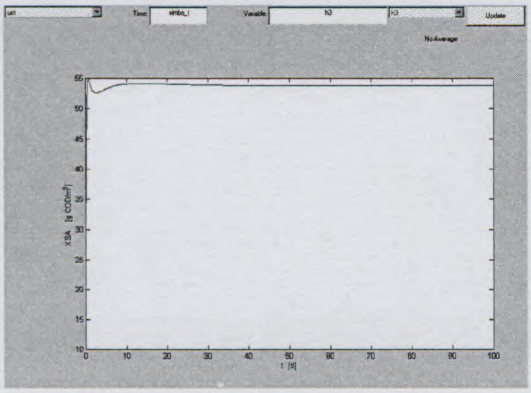

Figure 8.168a: The dynamic behaviour of adsorbed slowly biodegradable substrate fraction at h3 UCT full model

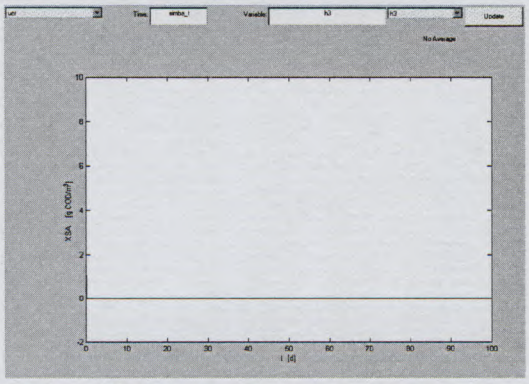

Figure 8.168b: The dynamic behaviour of adsorbed slowly biodegradable substrate fraction at h3 UCT reduced model

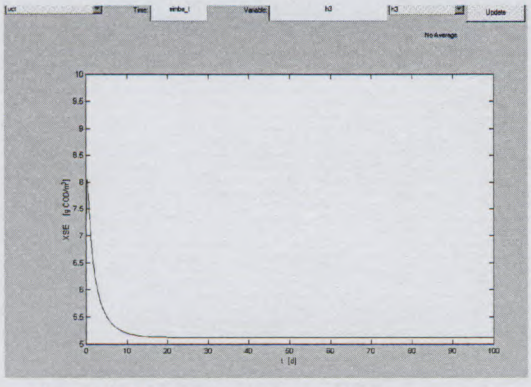

Figure 8.169a: The dynamic behaviour of enmeshed slowly biodegradable substrate fraction at h3 UCT full model

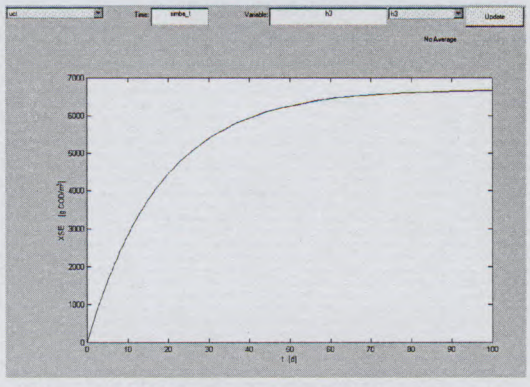

Figure 8.169b: The dynamic behaviour of enmeshed slowly biodegradable substrate fraction at h3 UCT reduced model

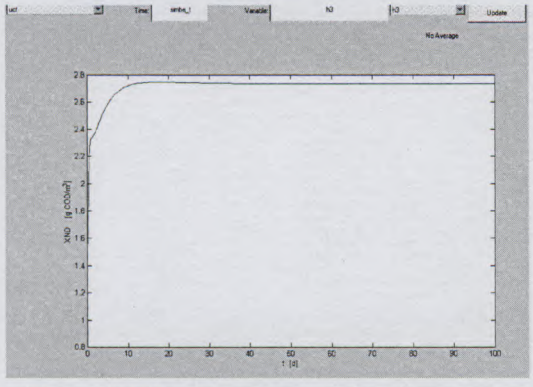

Figure 8.170a: The dynamic behaviour of biodegradable particulate organic nitrogen fraction at h3 UCT full model

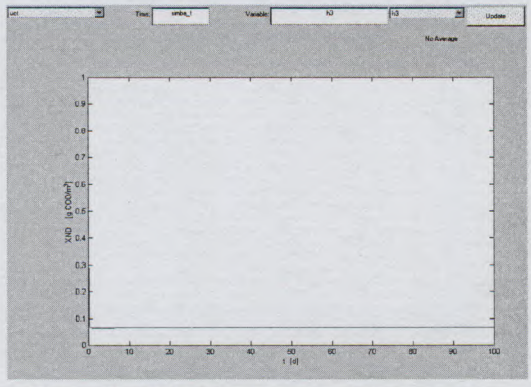

Figure 8.170b: The dynamic behaviour of biodegradable particulate organic nitrogen fraction at h3 UCT reduced model

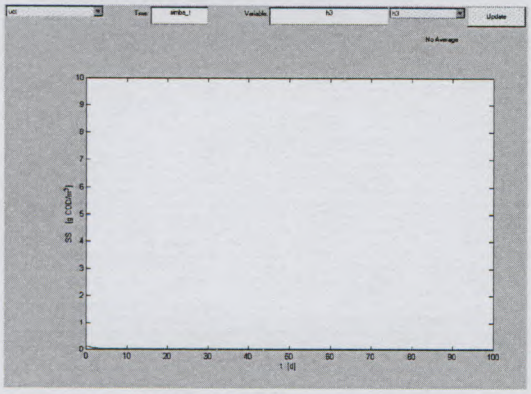

Figure 8.171a: The dynamic behaviour of readily biodegradable (soluble) substrate fraction at h3 UCT full model

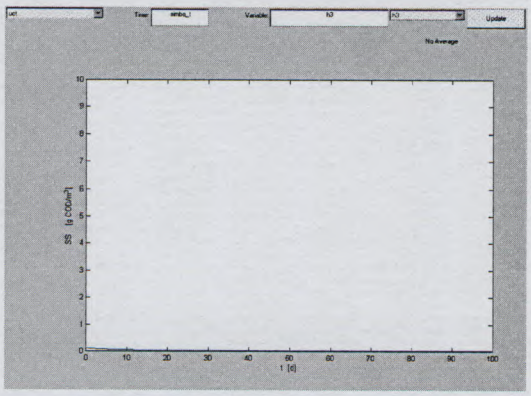

Figure 8.171b: The dynamic behaviour of readily biodegradable (soluble) substrate fraction at h3 UCT reduced model

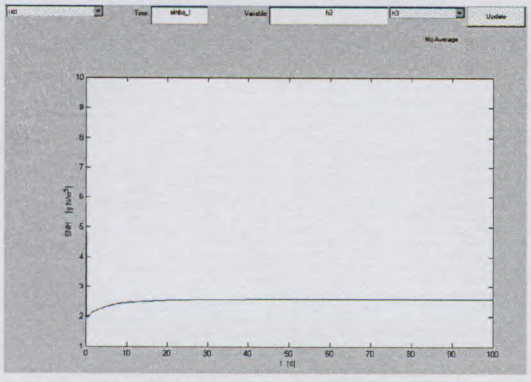

Figure 8.172a: The dynamic behaviour of ammonia nitrogen at h3 in UCT full model

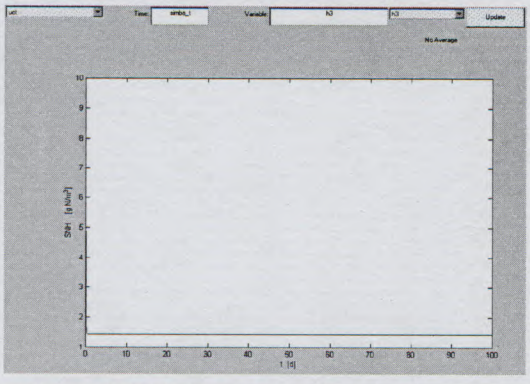

Figure 8.172b: The dynamic behaviour of ammonia nitrogen fraction at h3 UCT reduced model

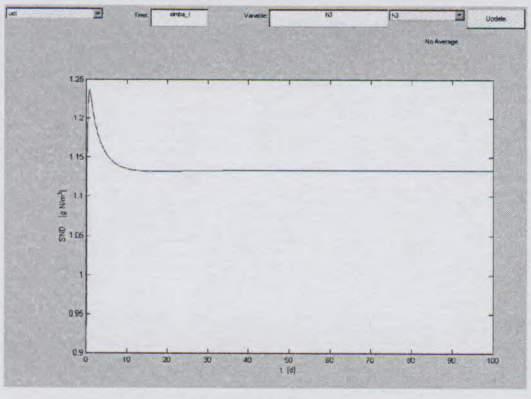

Figure 8.173a: The dynamic behaviour of biodegradable soluble organic nitrogen at h3 UCT full model

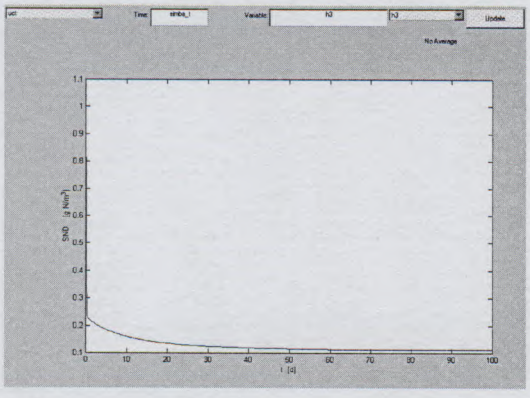

Figure 8.173b: The dynamic behaviour of biodegradable soluble organic nitrogen fraction UCT reduced model at h3

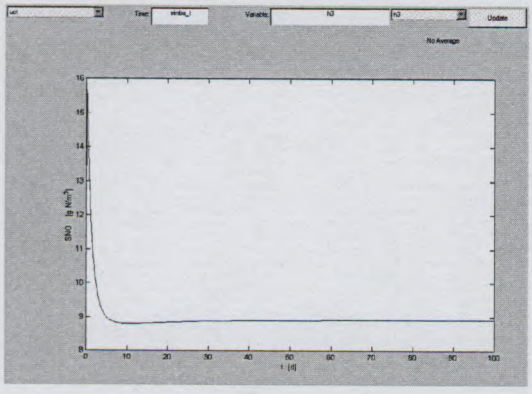

Figure 8.174a: The dynamic behaviour of nitrate nitrogen at h3 UCT full model

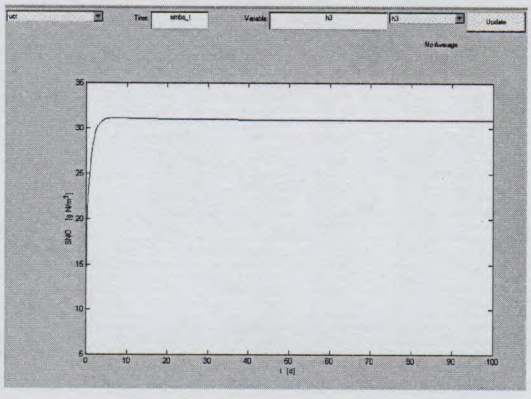

Figure 8.174b: The dynamic behaviour of nitrate nitrogen fraction at h3 UCT reduced model

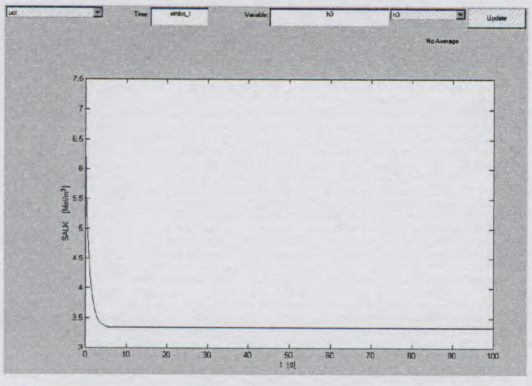

Figure 8.175a: The dynamic behaviour of alkalinity at h3 UCT full model

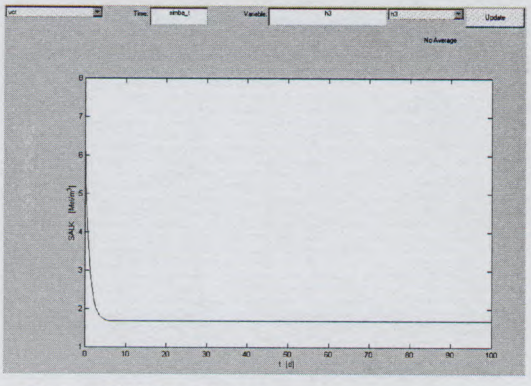

Figure 8.175b: The dynamic behaviour of alkalinity at h3 UCT reduced model

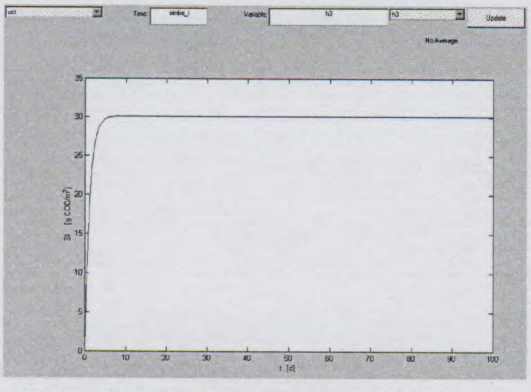

Figure 8.176a: The dynamic behaviour of unbiodegradable soluble substrate at h3 UCT full model

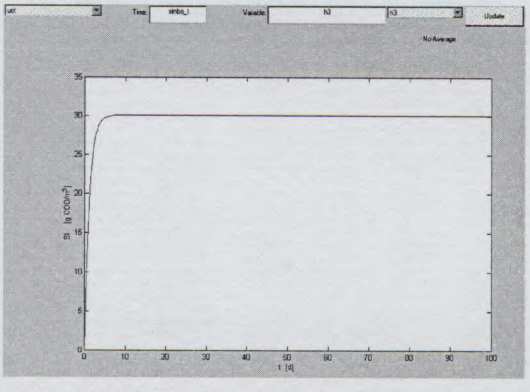

Figure 8.176b: The dynamic behaviour of unbiodegradable soluble substrate fraction at h3 UCT reduced model

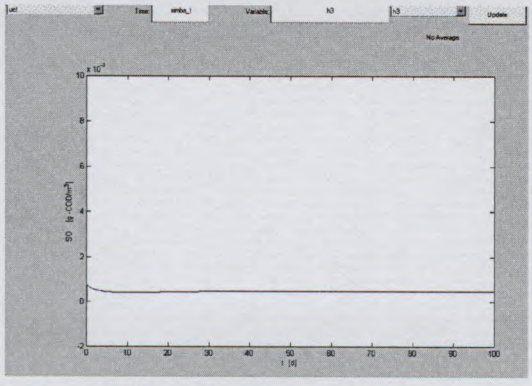

Figure 8.177a: The dynamic behaviour of oxygen at h3 UCT full model

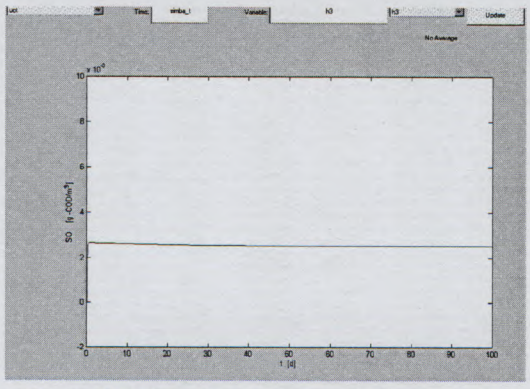

Figure 8.177b: The dynamic behaviour of oxygen at h3 UCT reduced model

8.9.3.4 Dynamic behaviour of the process variables after the aerobic tank (point h4) in Athlone wastewater plant simulated over a period of 100 days for total sludge age of 20 days at 22 C°

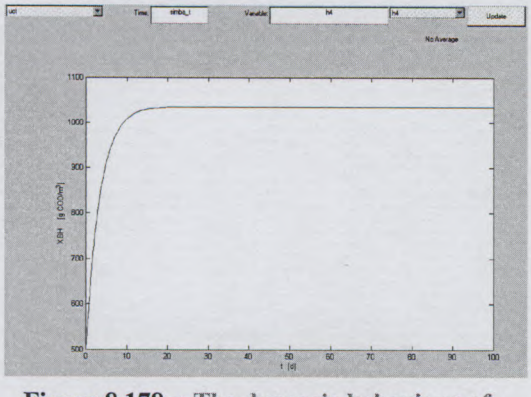

Figure 8.178a: The dynamic behaviour of biological (active) heterotrophic mass fraction at h4 UCT full model

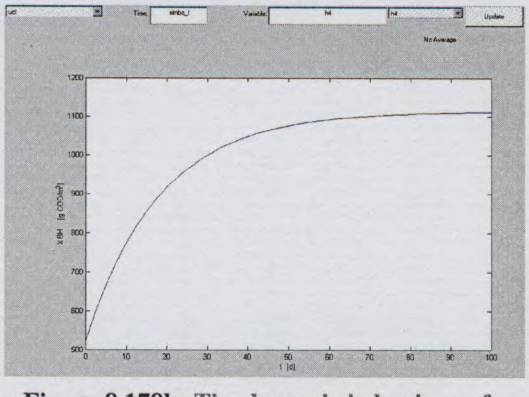

Figure 8.178b: The dynamic behaviour of biological (active) heterotrophic mass fraction at h4 UCT reduced model

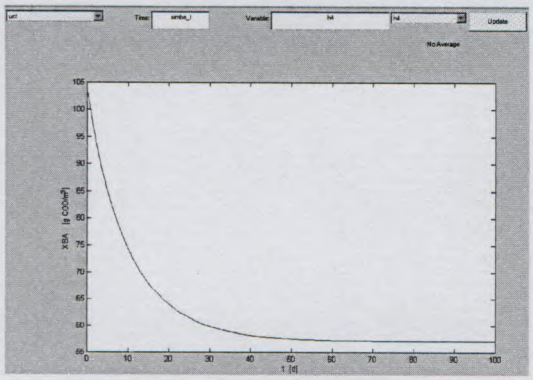

Figure 8.179a: The dynamic behaviour of biological (active) autotrophic biomass fraction at h4 UCT full model

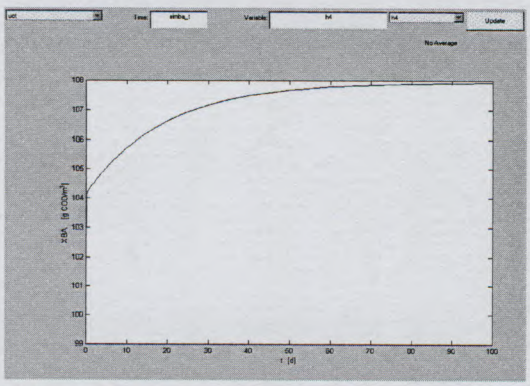

Figure 8.179b: The dynamic behaviour of biological (active) autotrophic biomass fraction at h4 UCT reduced model

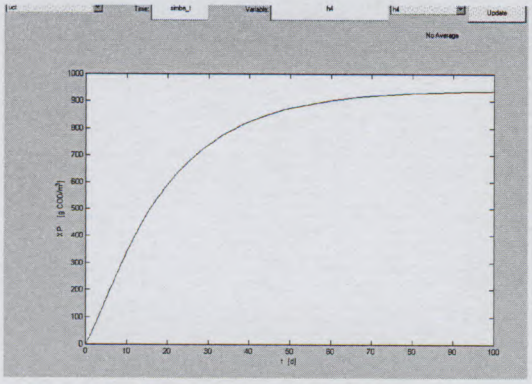

Figure 8.180a: The dynamic behaviour of endogenous mass fraction at h4 UCT full model

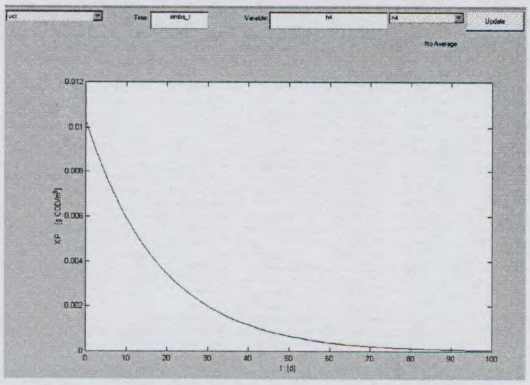

Figure 8.180b: The dynamic behaviour of endogenous mass fraction at h4 UCT reduced model

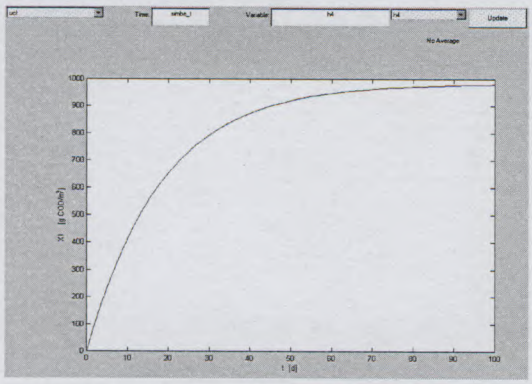

Figure 8.181a: The dynamic behaviour of inert mass fraction at h4 UCT full model

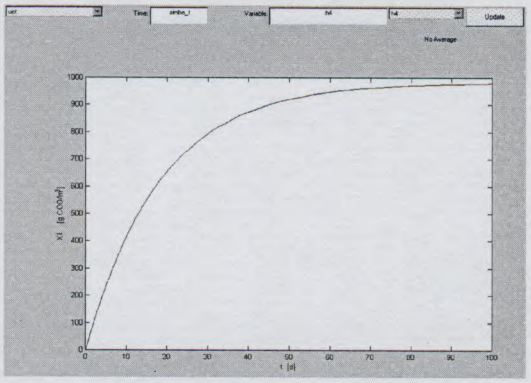

Figure 8.181b: The dynamic behaviour of inert mass fraction at h4 UCT reduced model

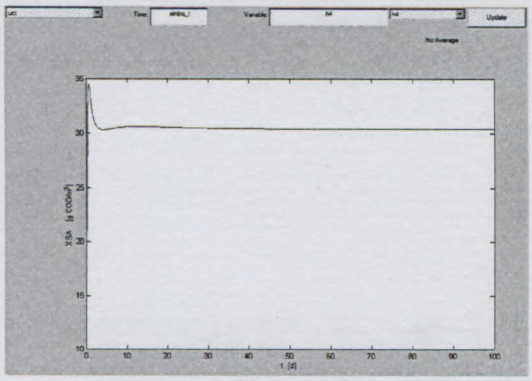

Figure 8.182a: The dynamic behaviour of adsorbed slowly biodegradable substrate fraction at h4 UCT full model

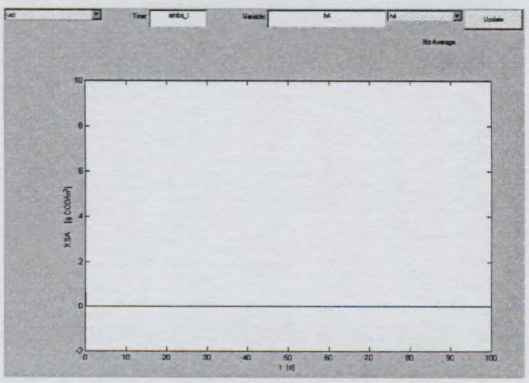

Figure 8.182b: The dynamic behaviour of adsorbed slowly biodegradable substrate fraction at h4 UCT reduced model

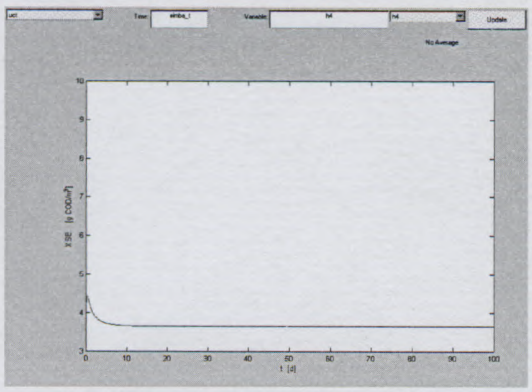

Figure 8.183a: The dynamic behaviour of enmeshed slowly biodegradable substrate fraction at h4 UCT full model

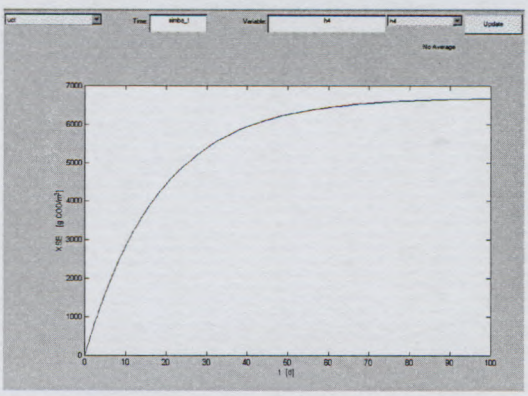

Figure 8.183b: The dynamic behaviour of enmeshed slowly biodegradable substrate fraction at h4 UCT reduced model

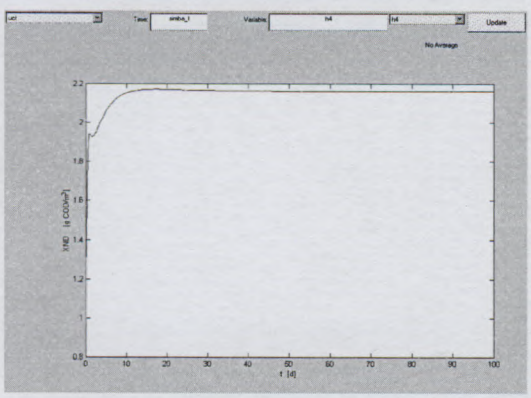

Figure 8.184a: The dynamic behaviour of biodegradable particulate organic nitrogen fraction at h4 UCT full model

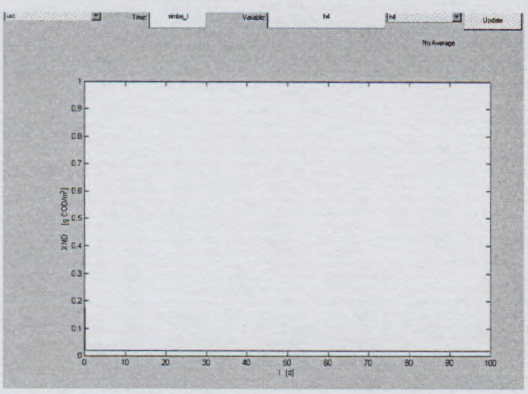

Figure 8.184b: The dynamic behaviour of biodegradable particulate organic nitrogen fraction at h4UCT reduced model

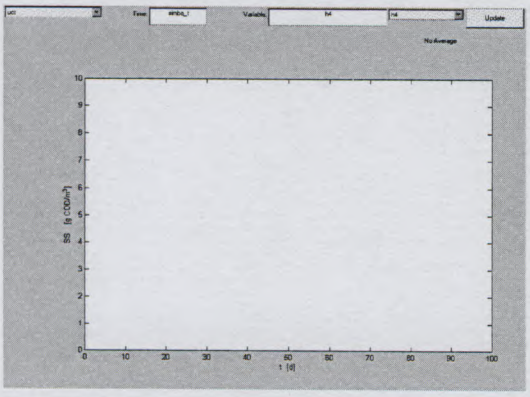

Figure 8.185a: The dynamic behaviour of readily biodegradable (soluble) substrate fraction at h4 UCT full model

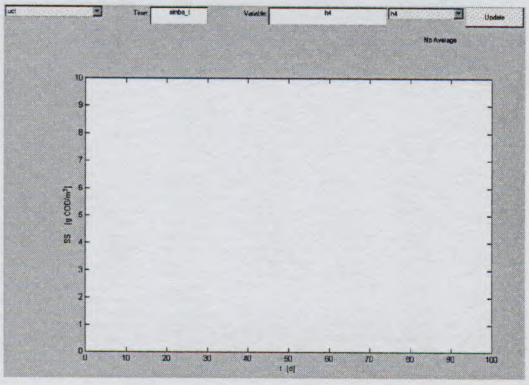

Figure 8.185b: The dynamic behaviour of readily biodegradable (soluble) substrate fraction at h4 UCT reduced model

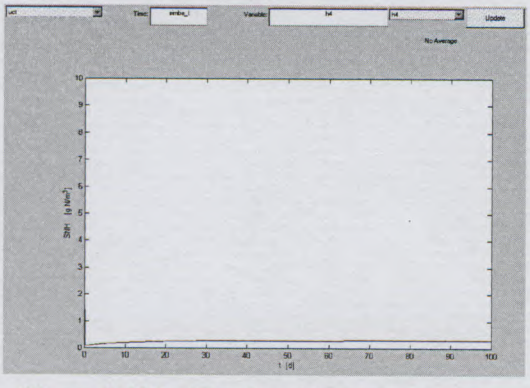

Figure 8.186a: The dynamic behaviour of ammonia nitrogen at h4 UCT full model

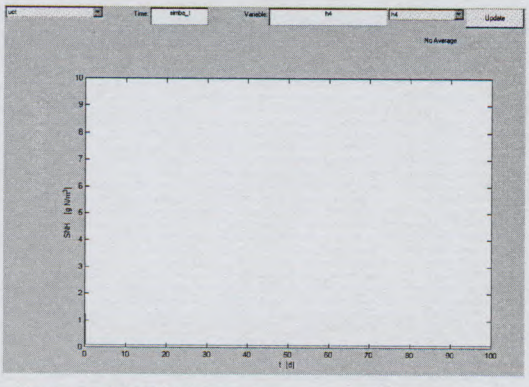

Figure 8.186b: The dynamic behaviour of ammonia nitrogen fraction at h4 UCT reduced model

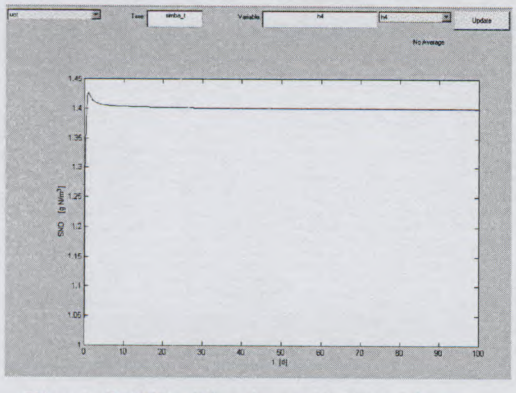

Figure 8.187a: The dynamic behaviour of biodegradable soluble organic nitrogen fraction at h4 UCT full model

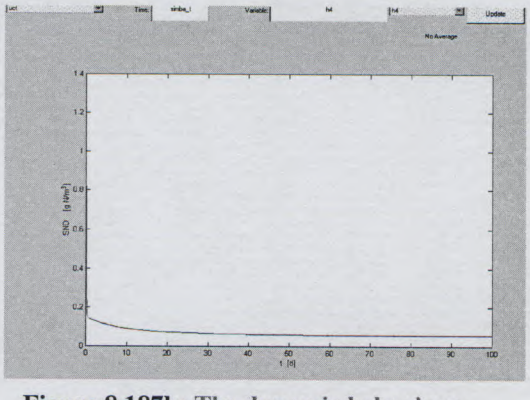

Figure 8.187b: The dynamic behaviour of biodegradable soluble organic nitrogen fraction at h4 UCT reduced model

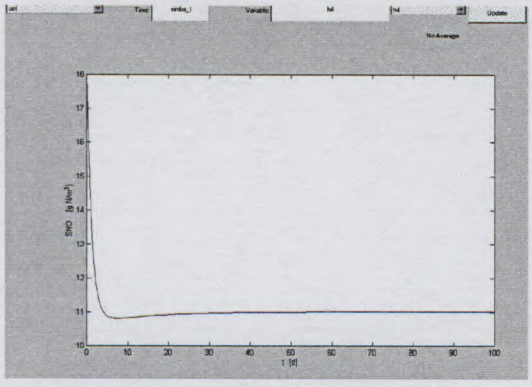

Figure 8.188a: The dynamic behaviour of nitrate nitrogen at h4 UCT full model

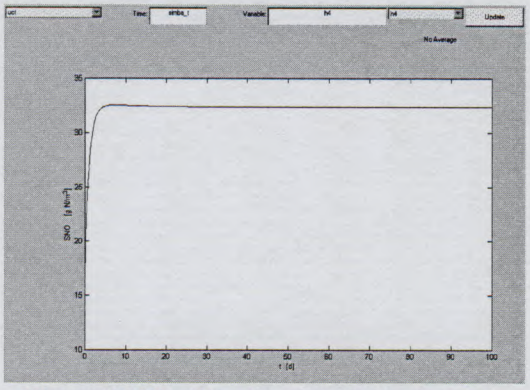

Figure 8.188b: The dynamic behaviour of nitrate nitrogen fraction at h4 UCT reduced model

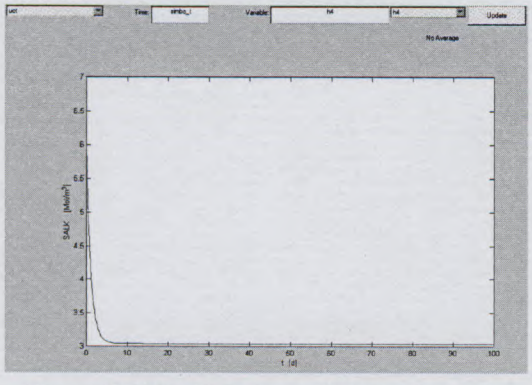

Figure 8.189a: The dynamic behaviour of alkalinity at h4 UCT full model

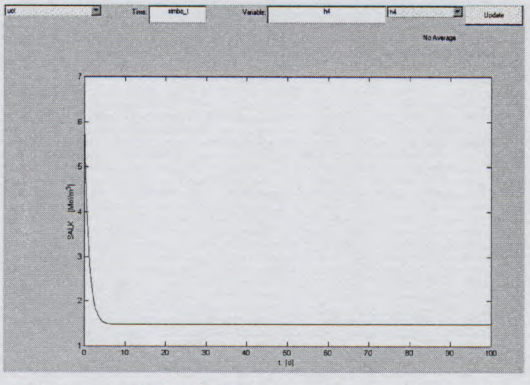

Figure 8.189b: The dynamic behaviour of alkalinity at h4 UCT reduced model

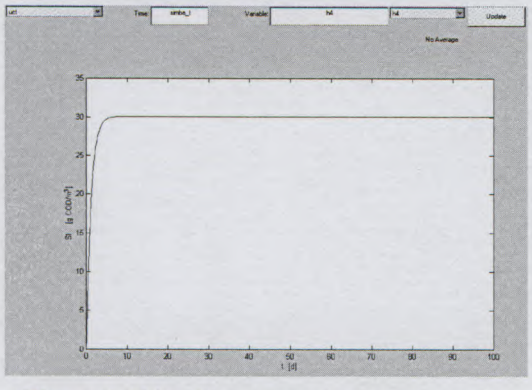

Figure 8.190a: The dynamic behaviour of unbiodegradable soluble substrate at h4 UCT full model

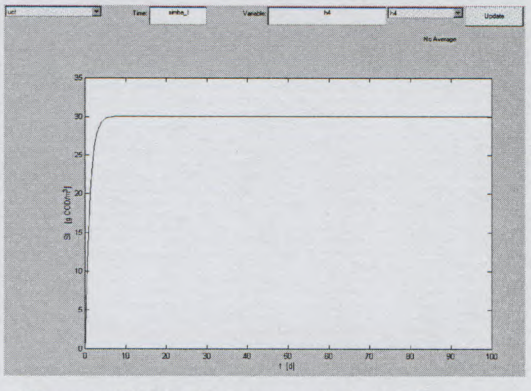

Figure 8.190b: The dynamic behaviour of unbiodegradable soluble substrate fraction at h4 UCT reduced model

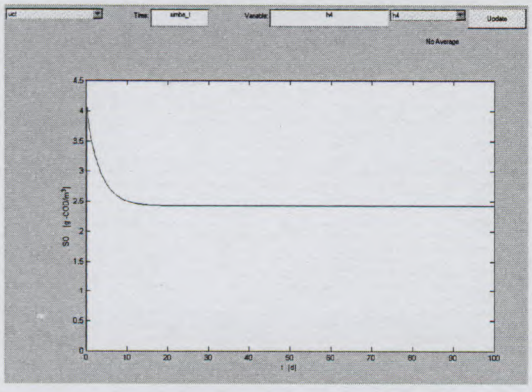

Figure 8.191a: The dynamic behaviour of oxygen at h4 UCT full model

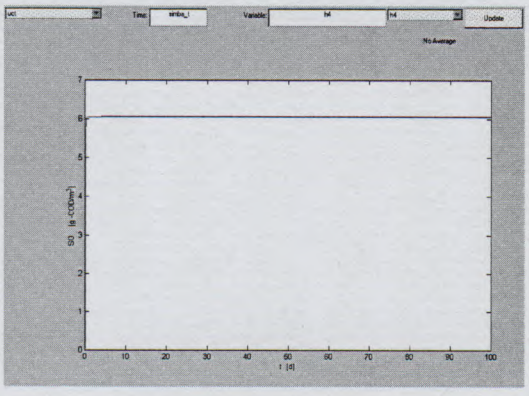

Figure 8.191b: The dynamic behaviour of oxygen at h4 UCT reduced model

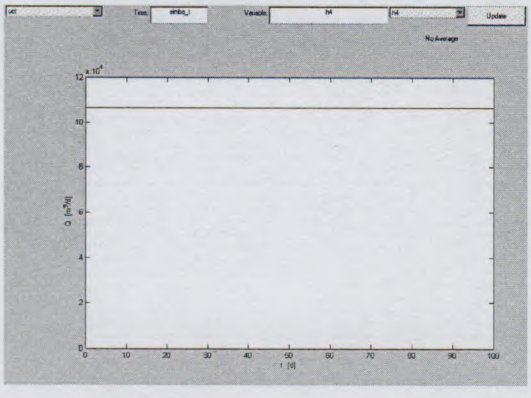

Figure 8.192a: The dynamic behaviour of flow rate at h4 UCT full model

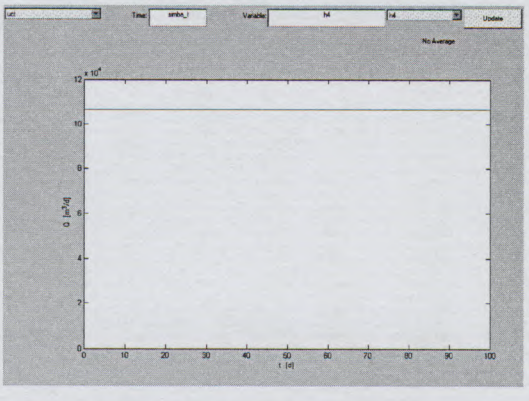

Figure 8.192b: The dynamic behaviour of flow rate at h4 UCT reduced model

8.9.4 Discussion of the results

The influent zone for the heterotrophic biomass for the Athlone plant full UCT model grows from 700 $g\,COD/m^3$ to 1200 $g\,COD/m^3$ after 10 days and remains constant after 10 days (see Figure 8.132a) whilst for the Athlone plant reduced model the heterotrophic biomass grows from 500 $g\,COD/m^3$ to 840 $g\,COD/m^3$ after 50 days and remain constant at that value. (see Figure 8.132b). The influent zone for autotrophic biomass for the Athlone plant full UCT model decays from 100 $g\,COD/m^3$ to 60 $g\,COD/m^3$ after 15 days and remains at this constant baseline (see Figure 8.133a) whilst the Athlone plant reduced UCT model

remains constant at 80 $g\,COD/m^3$ (see Figure 8.135b). In the influent zone the enmeshed slowly biodegradable substrate in the Athlone plant full UCT model remains at a constant 100 $g\,COD/m^3$ for a period of a 100days (see Figure 8.137a) whilst the Athlone plant reduced UCT model grows from 0 $g\,COD/m^3$ to 5100 $g\,COD/m^3$ after 60 days and remain constant (see Figure 8.137b). In the influent zone the biodegradable particulate organic nitrogen in the Athlone plant full UCT model grows from 2,2 $g\,COD/m^3$ to 2,6 $g\,COD/m^3$ after 10days and remains constant at that value (see Figure 8.138a) whilst the Athlone reduced UCT model remains constant at 0,6 $g\,N/m^3$ (see Figure 8.138b). In the influent zone the biodegradable soluble organic nitrogen in the Athlone plant full UCT model grows from 1,4 $g\,N/m^3$ and reaches a maximum at 1,45 $g\,N/m^3$ then decays to 1,38 after 5 days and remains constant (see Figure 8.141a) whilst the Athlone plant reduced UCT model remains fairly constant at zero (see Figure 8.141b). In the influent zone the nitrate nitrogen in the Athlone plant full UCT model decays from 12 $g\,N/m^3$ to 6,8 $g\,N/m^3$ after 4 days and remains constant at that value (see Figure 8.142a) whilst the Athlone plant reduced UCT model grows from 12 $g\,N/m^3$ to 25 $g\,N/m^3$ after 4 days and remains constant at that value (see figure 8.142b). In the influent zone the oxygen in the Athlone plant full UCT model decays from $8\times10^{-4}\,g\,COD/m^3$ to above 3×10^{-4} $g\,COD/m^3$ and level out to $3{,}7\times10^{-4}\,g\,COD/m^3$ after 40 days and remain at a constant value (see Figure 8.145a) whilst in the Athlone plant reduced UCT model decays from $2\times10^{-4}\,g\,COD/m^3$ to $1{,}8\times10^{-4}\,g\,COD/m^3$ leveling off after 40 days at that value (see Figure 8.145b).

After the anaerobic reactor the heterotrophic biomass for the Athlone plant full UCT model grows from 400 $g\,COD/m^3$ to 780 $g\,COD/m^3$ in 10 days and remain constant at that value (see Figure 8.147a) whilst the Athlone plant reduced UCT model undergoes a gradual increase in growth rate from 400 $g\,COD/m^3$ to 780 $g\,COD/m^3$ after 50 days then remains at constant value (see Figure 8.147b). After the anaerobic reactor the autotrophic biomass for the Athlone full UCT model decays from 80 $g\,COD/m^3$ to 45 $g\,COD/m^3$ after 15 days and remain constant at that value (see Figure 8.148a) whilst the Athlone plant reduced UCT

model gradually increases to 78 $g\,COD/m^3$ after 20 days and remains constant at that value (see Figure 8.148b). After the anaerobic reactor the endogenous biomass for the Athlone plant full UCT model grows from 0 $g\,COD/m^3$ to 700 $g\,COD/m^3$ after 60 days and remain constant at that value (see Figure 8.149a) whilst the Athlone plant reduced UCT model decays from 0,008 $g\,COD/m^3$ to zero (see Figure 8.149b). After the anaerobic reactor the adsorbed slowly biodegradable substrate for the Athlone plant full UCT model grows from 65 $g\,COD/m^3$ to 125 $g\,COD/m^3$ after 10 days and remain constant at that value (see Figure 8.151a) whilst the Athlone plant reduced UCT model does not deviate from the value of zero. (see Figure 8.151b).After the anaerobic reactor the enmeshed slowly biodegradable substrate for the Athlone plant full UCT model decays from 32 $g\,COD/m^3$ to 22 $g\,COD/m^3$ after 10 days and remain constant at that value (see Figure 8.152a) whilst the Athlone plant reduced UCT model grows from zero to 5100 $g\,COD/m^3$ after 60 days and remain constant at that value (see Figure 8.152b). After the anaerobic reactor biodegradable particulate organic nitrogen for the Athlone plant full UCT model grows from 1,9 $g\,COD/m^3$ to 3,6 $g\,COD/m^3$ after 10 days and remain constant at that value (see Figure 8.153a) whilst the Athlone plant reduced UCT model remains constant at 0,3 $g\,N/m^3$ (see Figure 8.153b). After the anaerobic reactor the biodegradable soluble organic nitrogen for the Athlone plant full UCT model decays from 1,02 $g\,N/m^3$ to 0,03 $g\,N/m^3$ after 10 days and remain constant at that value (see Figure 8.156a) whilst the Athlone plant reduced UCT model decays gradually from 0,8 $g\,N/m^3$ to 0,4 $g\,N/m^3$ after 30 days and remain constant at that value (see Figure 8.156b). After the anaerobic reactor the nitrate nitrogen for the Athlone plant full UCT model decays from 7,8 $g\,N/m^3$ to 1,8 $g\,N/m^3$ after 5 days and remain constant at that value (see Figure 8.157a) whilst the Athlone plant reduced UCT model grows from 14 $g\,N/m^3$ to 22 $g\,N/m^3$ after 5 days and remain constant at that value (see Figure 8.157b).

After the anoxic reactor the heterotrophic biomass for the Athlone plant full UCT model grows rapidly from 500 $g\,COD/m^3$ to 1000 $g\,COD/m^3$ after 10 days and remain constant at that value (see Figure 8.162a) whilst the Athlone plant reduced UCT model gradually grows from 540 $g\,COD/m^3$ to 1200 $g\,COD/m^3$ after 60 days and remain constant at that

value (see Figure 8.162b). After the anoxic reactor the autotrophic biomass for the Athlone plant full UCT model decays from 105 $gCOD/m^3$ to 55 $gCOD/m^3$ after 50 days and remain constant at that value (see Figure 8.163a) whilst the Athlone plant reduced UCT model grows from 150 $gCOD/m^3$ to 148 $gCOD/m^3$ after 70 days and remain constant at that value (see Figure 8.163b). After the anoxic reactor the endogenous biomass for the Athlone plant full UCT model grow gradually from zero to 940 $gCOD/m^3$ after 70 days and remain constant at that value (see Figure 8.164a) whilst the Athlone plant reduced UCT model decays from 0,04 $gCOD/m^3$ to zero (see Figure 8.164b). After the anoxic reactor the adsorbed slowly biodegradable substrate for the Athlone plant full UCT model remains at a constant value of 53 $gCOD/m^3$ (see Figure 8.166a) whilst the Athlone plant reduced UCT model remains at a value of zero (see Figure 8.166b). After the anoxic reactor the enmeshed slowly biodegradable substrate for the Athlone plant full UCT model decays from 8 $gCOD/m^3$ to 5,2 $gCOD/m^3$ after 10 days and remain constant at that value (see Figure 8.167a) whilst the Athlone plant reduced UCT model grows from zero to 6800 $gCOD/m^3$ after 60 days and remain constant at that value (see Figure 8.167b). After the anoxic reactor the biodegradable particulate organic nitrogen for the Athlone plant full UCT model grows from 2,2 $gCOD/m^3$ to 2,9 $gCOD/m^3$ after 10days and remain constant at that value (see Figure 8.170a) whilst the Athlone plant reduced UCT model remains constant at 0,05 gN/m^3 value (see Figure 8.168b). After the anoxic reactor the ammonia nitrogen for the Athlone plant full UCT model gradually grows from 2,0 gN/m^3 to 2,5 gN/m^3 after 10 days and remain constant at that value (see Figure 8.170a) whilst the Athlone plant reduced UCT model remains constant at 1,5 gN/m^3 value (see Figure 8.170b). After the anoxic reactor the biodegradable soluble organic nitrogen for the Athlone plant full UCT model decays from 1,25 gN/m^3 to 1,13 gN/m^3 after 10 days and remain constant at that value (see Figure 8.171a) whilst the Athlone plant reduced UCT model gradually decays from 0,25 gN/m^3 to 0,1 gN/m^3 after 30 days and remain constant at that value (see Figure 8.171b). After the anoxic reactor the nitrate nitrogen for the Athlone plant full UCT model decays from 15,8 gN/m^3 to 9,0 gN/m^3 after 5 days and remain constant at that value (see Figure 8.172a) whilst the Athlone plant reduced UCT model

grows from 15 gN/m^3 to 27 gN/m^3 after 5 days and remain constant at that value (see Figure 8.172b).

After the aerobic reactor the heterotrophic biomass for the Athlone plant full UCT model rapidly grows from 500 $gCOD/m^3$ to 1300 $gCOD/m^3$ after 10 days and remain constant at that value (see Figure 8.176a) whilst the Athlone plant reduced UCT model gradually grows from 500 $gCOD/m^3$ to 1050 $gCOD/m^3$ after 70 days and remain constant at that value (see Figure 8.176b). After the aerobic reactor the autotrophic biomass for the Athlone plant full UCT model decays from 105 $gCOD/m^3$ to 50 $gCOD/m^3$ after 40 days and remain constant at that value (see Figure 8.177a) whilst the Athlone plant reduced UCT model gradually grows from 110 $gCOD/m^3$ to 180 $gCOD/m^3$ after 80 days and remain constant at that value (see Figure 8.177b). After the aerobic reactor the endogenous biomass for the Athlone plant full UCT model gradually grows from zero to 920 $gCOD/m^3$ after 80 days and remain constant at that value (see Figure 8.178a) whilst the Athlone plant reduced UCT model decays from 0,01 $gCOD/m^3$ to zero in 90 days (see Figure 8.178b). After the aerobic reactor the adsorbed slowly biodegradable substrate for the Athlone plant full UCT model gradually decays from 35 $gCOD/m^3$ to 30 $gCOD/m^3$ after 2 days and remain constant at that value (see Figure 8.1820) whilst the Athlone plant reduced UCT model remins constant at zero value (see Figure 8.180b). After the aerobic reactor the enmeshed slowly biodegradable substrate for the Athlone plant full UCT model slowly decays from 4,4 $gCOD/m^3$ to 3,8 $gCOD/m^3$ after 2 days and remain constant at that value (see Figure 8.181a) whilst the Athlone plant reduced UCT model gradually grows from zero to 6700 $gCOD/m^3$ after 70 days and remain constant at that value (see Figure 8.181b). After the aerobic reactor the biodegradable particulate organic nitrogen for the Athlone plant full UCT model grows from 1,9 $gCOD/m^3$ to 2,19 $gCOD/m^3$ after 10 days and remain constant at that value (see Figure 8.182a) whilst the Athlone plant reduced UCT model remains constant near zero (see Figure 8.182b). After the aerobic reactor the biodegradable soluble organic nitrogen for the Athlone plant full UCT model gradually decays from 1,43 gN/m^3 to 1,40 gN/m^3 after 4 days and remain constant at that value (see Figure 8.185a) whilst the Athlone plant reduced UCT model gradually decays from

0,18 gN/m^3 to 0,08 gN/m^3 after 10 days and remain constant at that value (see Figure 8.185b). After the aerobic reactor the nitrate nitrogen for the Athlone plant full UCT model decays from 18 gN/m^3 to 11 gN/m^3 after 6 days and remain constant at that value (see Figure 8.186a) whilst the Athlone plant reduced UCT model grows from 18 gN/m^3 to 33 gN/m^3 after 5 days and remain constant at that value (see Figure 8.186b). After the aerobic reactor the oxygen for the Athlone plant full UCT model decays from 4,0 $gCOD/m^3$ to 2,5 $gCOD/m^3$ after 8 days and remain constant at that value (see Figure 8.189a) whilst the Athlone plant reduced UCT model remains constant at 6,0 $gCOD/m^3$ value (see Figure 8.189b).

The results show that the use of the nominal parameters for the UCT reduced model can not give the same dynamic behavior of the process variables. Estimation of some of the parameters is necessary to be done

8.10 Conclusion

The problem for simulation of the activated sludge process (Katebi & Graells, 2005), (Mazouni, Ignatova & Harmand, 2005), (Kletting, 2005), (Lije, Chai & Cong, 2005), (Alex, Ogurek & Jumar, 2005), (Gernaey, Rosen, Batstone & Alex, 2004), (Hucka, 2003), (Rauch, Aalderink, Drebs, Snelling & Vanrolleghem, 1998) is solved using the simulator SIMBA. The chapter starts with a comparative analysis of existing simulators and description of SIMBA software.The derived at Chapter 3 and Chapter 4 mass balance equations of the Mitchels Plain and Athlone plants based on UCT and ASM1 biological models are used to develop the software for the simulation in SIMBA environment. The results of the Mitchell's Plain (UCT), Athlone (ASM1) and Athlone (UCT) wastewater treatment plant variables behavior are generated from the software implementation. The results are discussed. The dynamic behaviour of the variables for the Athlone process described by ASM1 biological models are the same for the full and reduced model. The results for the reduced and full UCT models are not so close. The obtained results show that the use of reduced models requires parameter estimation technique to find new values for the growth parameters. The software and results for the sensitivity analysis and parameter estimation are shown in the next chapter.

CHAPTER NINE

RESULTS FROM THE APPLICATION OF THE METHODS FOR SENSITIVITY ANALYSIS AND PARAMETER ESTIMATION TO THE BENCHMARK AND ATHLONE PLANTS

9.1. Introduction

The solution of the problems for sensitivity analysis and parameter estimation of the Activated sludge process is described in Chapters 5 and 6 respectively. The methods developed are implemented in the frameworks of the software environment of Matlab and the results are presented in this chapter.

9.2. Sensitivity analysis of the Activated Sludge process

The sensitivity analysis of the wastewater treatment model process variables towards the kinetic parameters is investigated in order to determine which parameters have to be recalculated (estimated) during the real-time operation and control of the process. The calculations are done for the reduced ASM1 and UCT models applied to the Benchmark and Athlone plants structures.

9.2.1. Software for the sensitivity analysis

Four software programmes are developed in Matlab:

- Calculation of the sensitivity functions of the Benchmark process based on ASM1 reduced biological model: *BASM1S.m, rateASM1.m*
- Calculation of the sensitivity functions of the Benchmark process based on UCT biological model: *BUCTS1.m, rateBUCTS.m*
- Calculation of the sensitivity functions of the Athlone process based on ASM1 reduced biological model: *AASM1.m, rateAASM1.m*
- Calculation of the sensitivity functions of the Athlone process based on UCT biological model:*AUCTS.m, rateAUCTS.m*

The developed software is given in the Appendix C and every application consists of two parts:

- main programme for input of the nominal process parameters, initial conditions, average values of the biomass concentrations, calculation of the process model matrices and organization of the calculation algorithm
- sub-programme for calculation of the biological rates, sensitivity functions and formation of the sensitivity model state space and rates matrices and vectors.

The algorithm of the calculation is given on Figure 9.1.a)for the main programme and in Figure 9.1.b) for the sub-programmes. The number of variables and parameters for

different plants and biological models is different. The corresponding values are shown under the separate process and model descriptions.

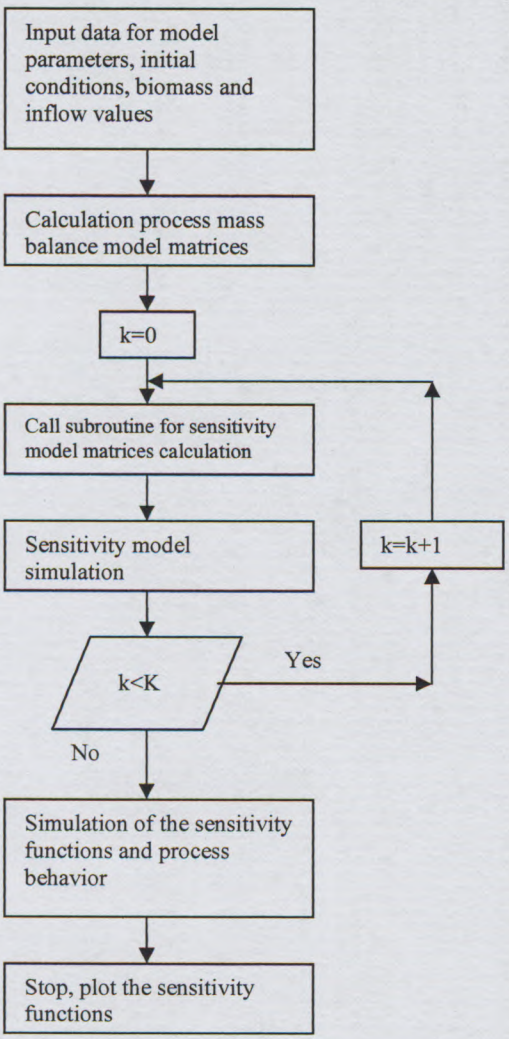

Figure 9.1a: Flow chart of the main program for sensitivity functions calculation

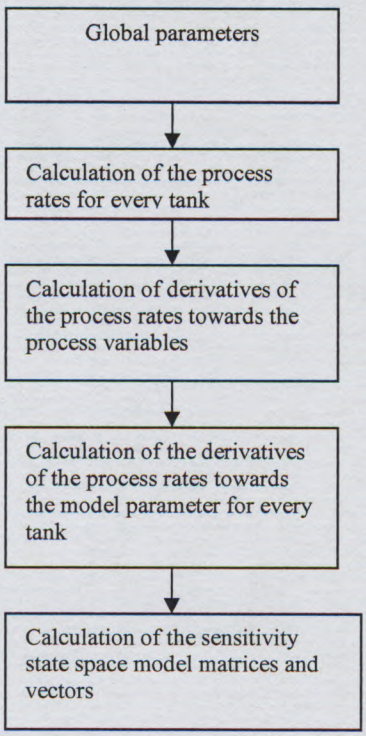

Figure 9.1b: Flow chart of the subprogram for sensitivity functions calculation

9.2.2. Sensitivity function simulation for the Benchmark process model based on the reduced ASM1 and UCT biological models

The reduced ASM1 biological model is described in the Chapter 4, point 4.4 and the reduced UCT biological model is described in point 4.5. The mass balance models for Benchmark process based on both ASM1 and UCT reduced models are described in point 4.6.1. The corresponding sensitivity models are derived in Chapter 5, point 5.3. The values of the processes tank's volumes are given in the Chapter 3. Table 3.7. The

nominal kinetic parameters are given in Table 4.2 for the reduced ASM1 and in Table 4.4 for the reduced UCT biological models.

9.2.2.1 Results for the ASM1 reduced biological model

Simulations of the sensitivity functions are done for the initial conditions of the process variables given by the vector x_0 and zero for the sensitivity functions. The sampling period DT = 0.01042 is selected as it is the sampling period of the data used by the developers of the Benchmark process. The data of this process is used for simulation. The value of the sampling period is selected on the basis of the ASP dynamics and is convenient for all existing plant for wastewater treatment. The inflow concentration is hundred times less than the average one for dry weather, given by the vector X_i

X_0=[7.918;5.37;2.808;8.344;3.662;1.459;5.548;6.541;1.15;2.967;9.299;0.995;1.733;10.415;0.889]
Xi=[0.3156 0 0.6950]

The simulation is done for steady state conditions of the biomass and the slowly biodegradable substrate given by the vectors

XBH = 0.05*[2551.76*ones(1,K);2553.38*ones(1,K);2557.13*ones(1,K);2559.18*ones(1,K);2559.34*ones(1,K)];
XBA = 0.05*[148.389*ones(1,K);148.309*ones(1,K);148.941*ones(1,K);149.527*ones(1,K);149.797*ones(1,K)];
XS = 0.05*[82.135*ones(1,K);76.386*ones(1,K);64.855*ones(1,K);55.694*ones(1,K);49.306*ones(1,K)];

The vector of the dissolved oxygen concentration is: U=[0.2;0.2;2.0;2.29;1.91]

The process reduced state space mass balance model matrices as taken from the Matlab program are:

A_{ASM1}=

0.0390	0	0	0	0	0	0	0	0	0	0	0	0.7688	0	0
0	0.0390	0	0	0	0	0	0	0	0	0	0	0	0.7688	0
0	0	0.0390	0	0	0	0	0	0	0	0	0	0	0	0.7688
0.9610	0	0	0.0390	0	0	0	0	0	0	0	0	0	0	0
0	0.9610	0	0	0.0390	0	0	0	0	0	0	0	0	0	0
0	0	0.9610	0	0	0.0390	0	0	0	0	0	0	0	0	0
0	0	0	0.7210	0	0	0.2790	0	0	0	0	0	0	0	0
0	0	0	0	0.7210	0	0	0.2790	0	0	0	0	0	0	0
0	0	0	0	0	0.7210	0	0	0.2790	0	0	0	0	0	0
0	0	0	0	0	0	0.7210	0	0	0.2790	0	0	0	0	0
0	0	0	0	0	0	0	0.7210	0	0	0.2790	0	0	0	0
0	0	0	0	0	0	0	0	0.7210	0	0	0.2790	0	0	0
0	0	0	0	0	0	0	0	0	0.7210	0	0	0.2790	0	0
0	0	0	0	0	0	0	0	0	0	0.7210	0	0	0.2790	0
0	0	0	0	0	0	0	0	0	0	0	0.7210	0	0	0.2790

0.2306	0	0
0	0.1922	0

C_{nASM1}=

-0.0008	0	-0.0156
-0.0008	-0.0018	-0.0156
-0.0443	0.0434	0
0	0	0.0104

, n= 1:5

B_{ASM1}= 0 0 0.1922
zeros(12,3)

The results from the simulations are given from Figures 9.2 till Figure 9.16.

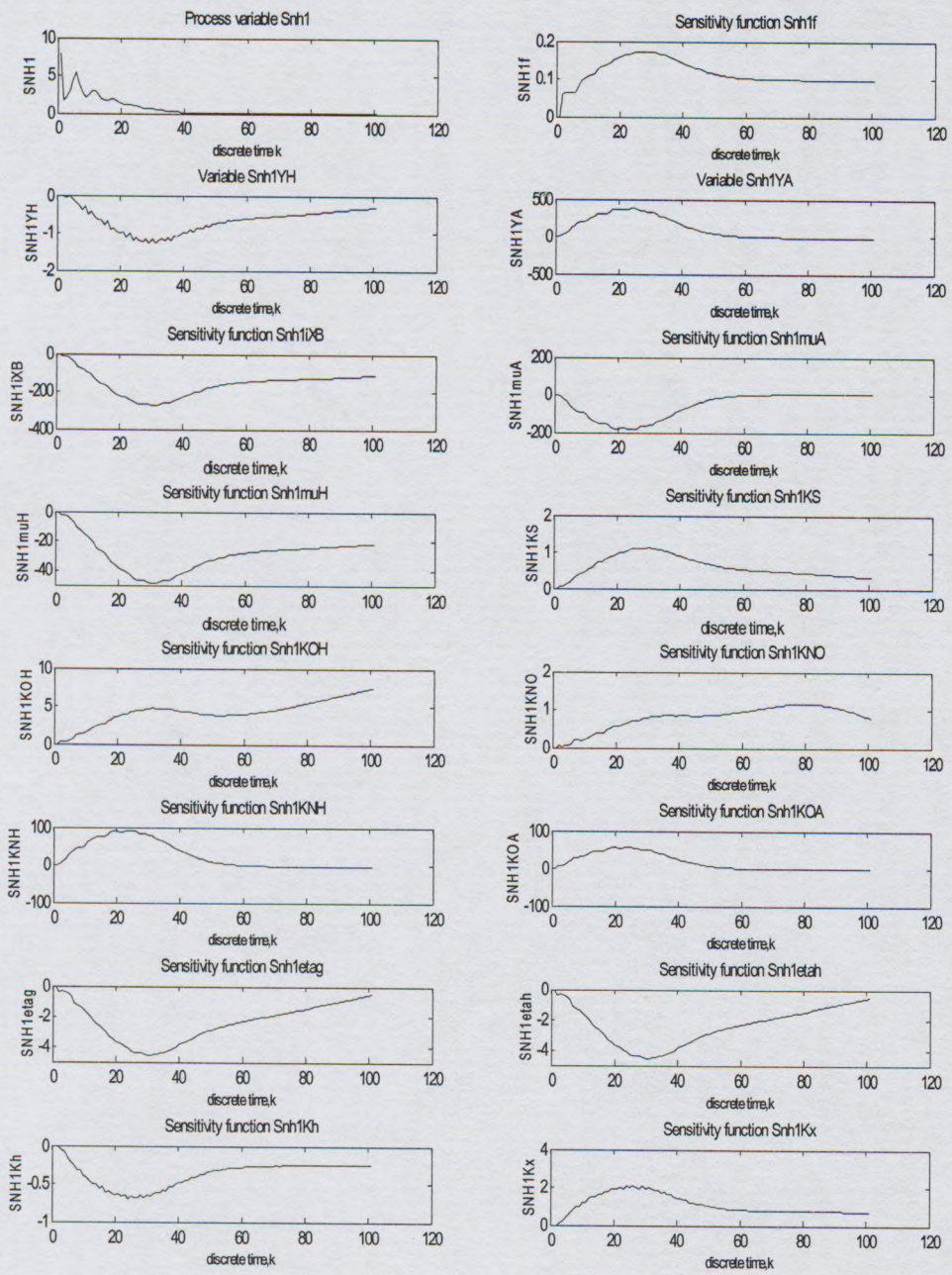

Figure 9.2: Process variable S_{NH1} and its sensitivity functions towards the model parameters

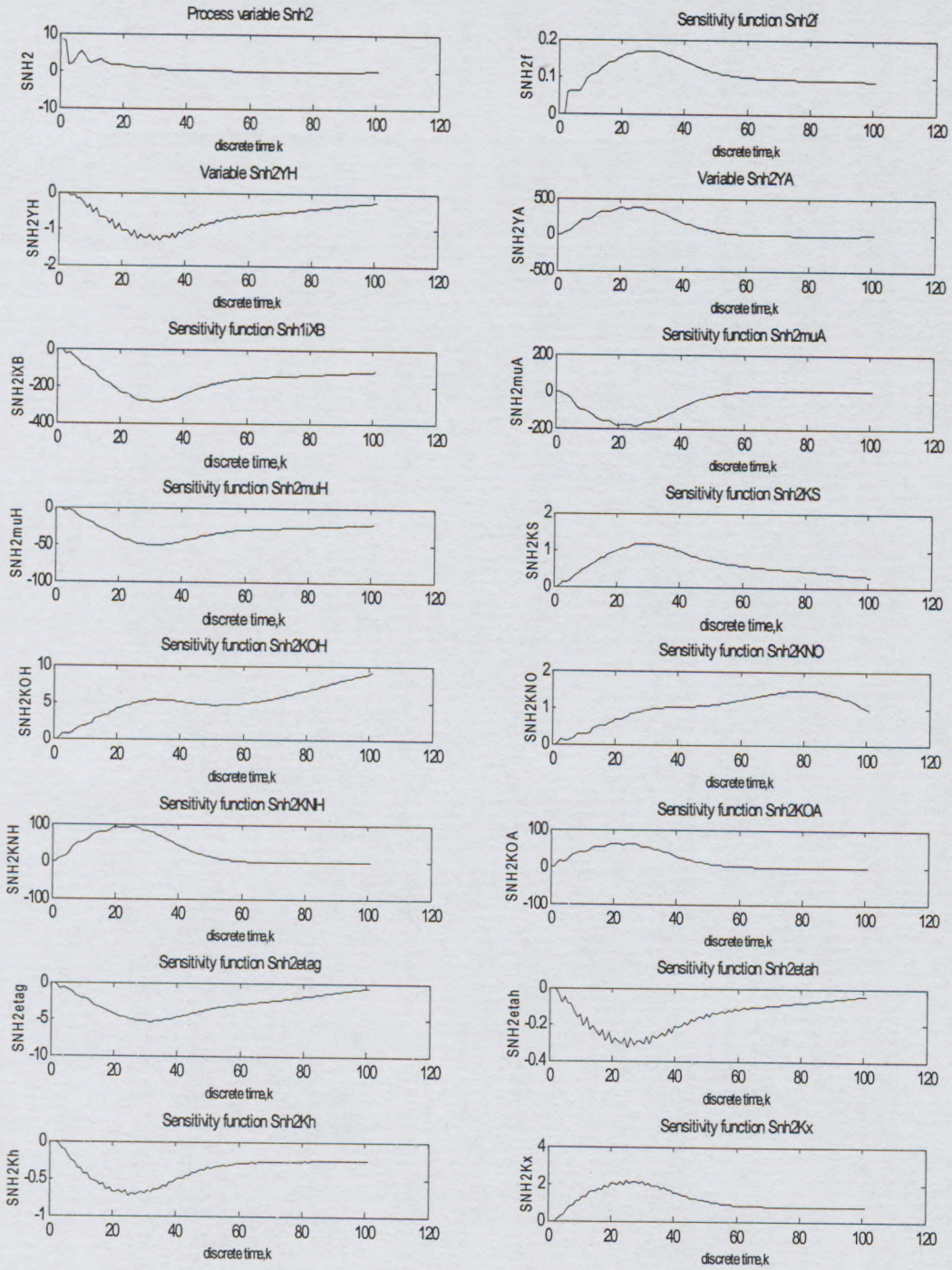

Figure 9.3: Process variable S_{NH2} and its sensitivity functions towards the model parameters

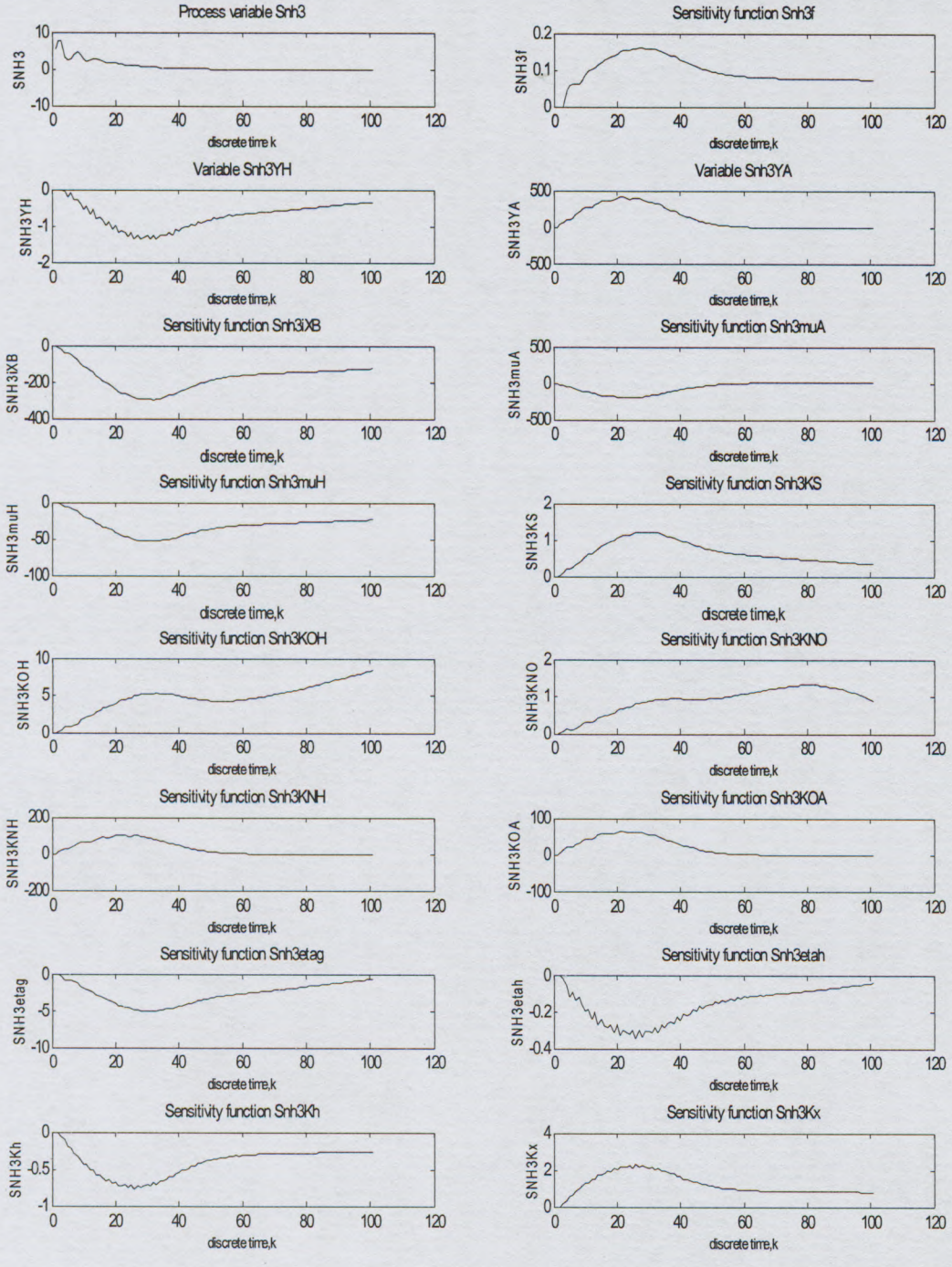

Figure 9.4: Process variable S_{NH3} and its sensitivity functions towards the model parameters

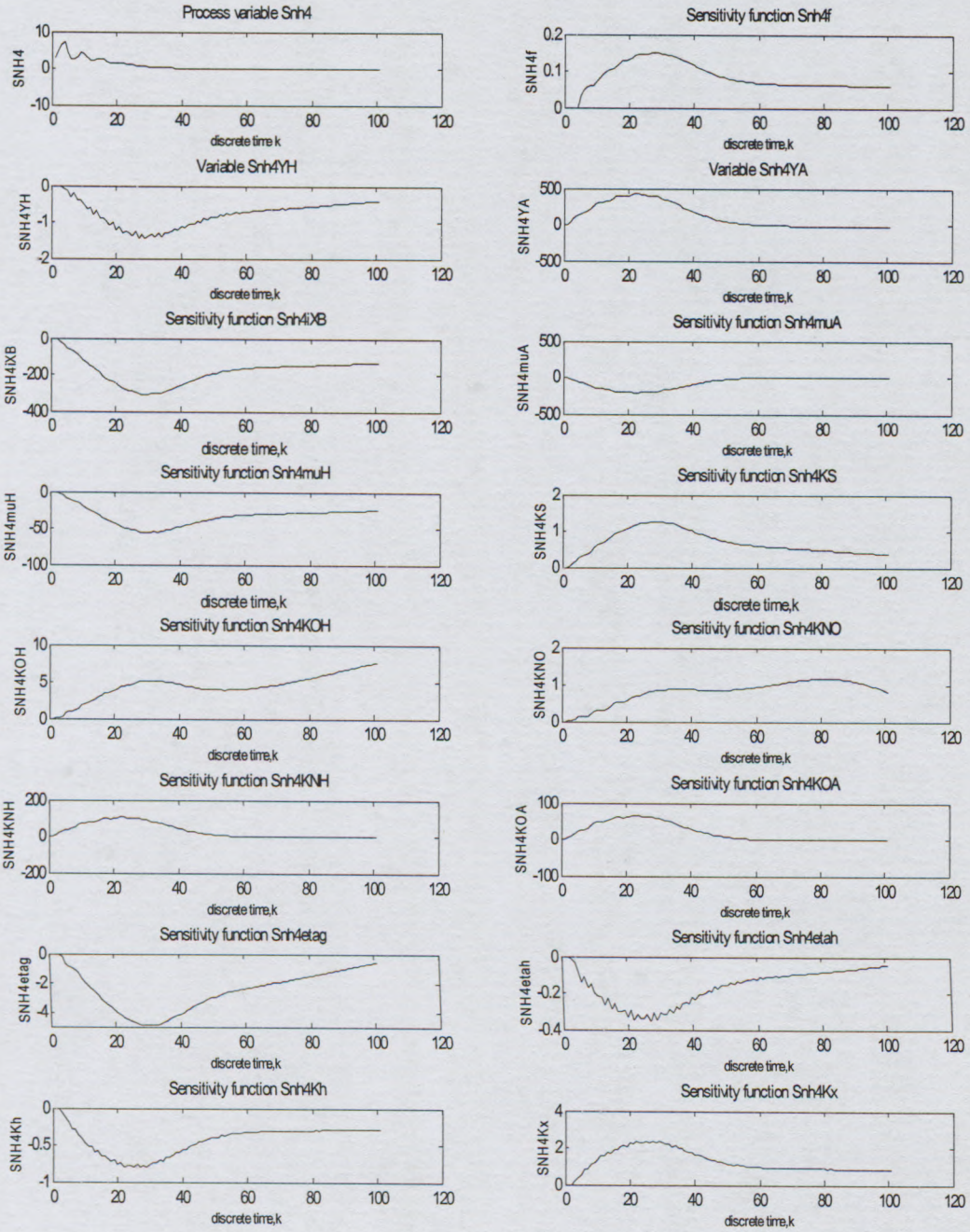

Figure 9.5: Process variable S_{NH4} and its sensitivity functions towards the model parameters

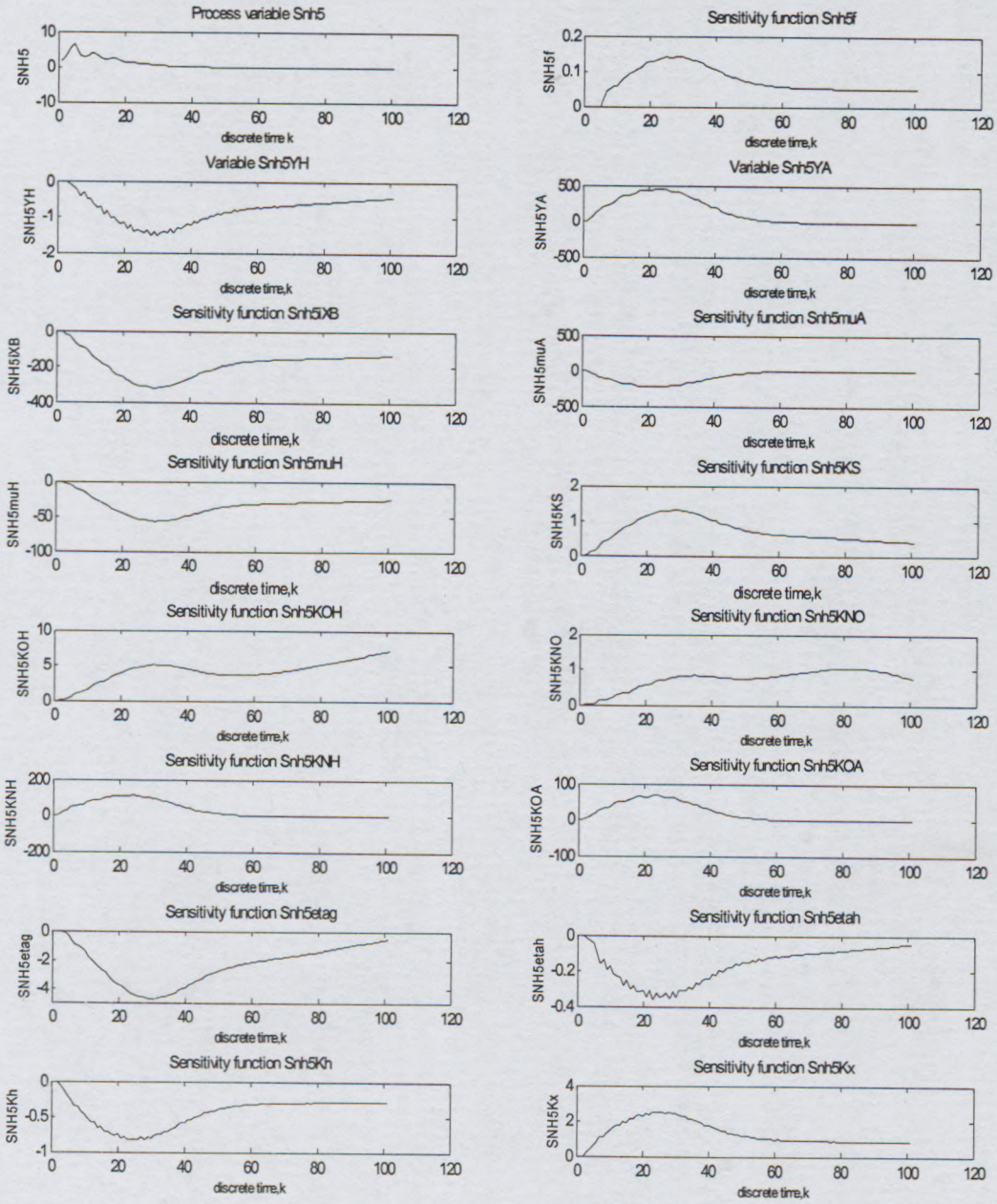

Figure 9.6: Process variable S_{NH5} and its sensitivity functions towards the model parameters

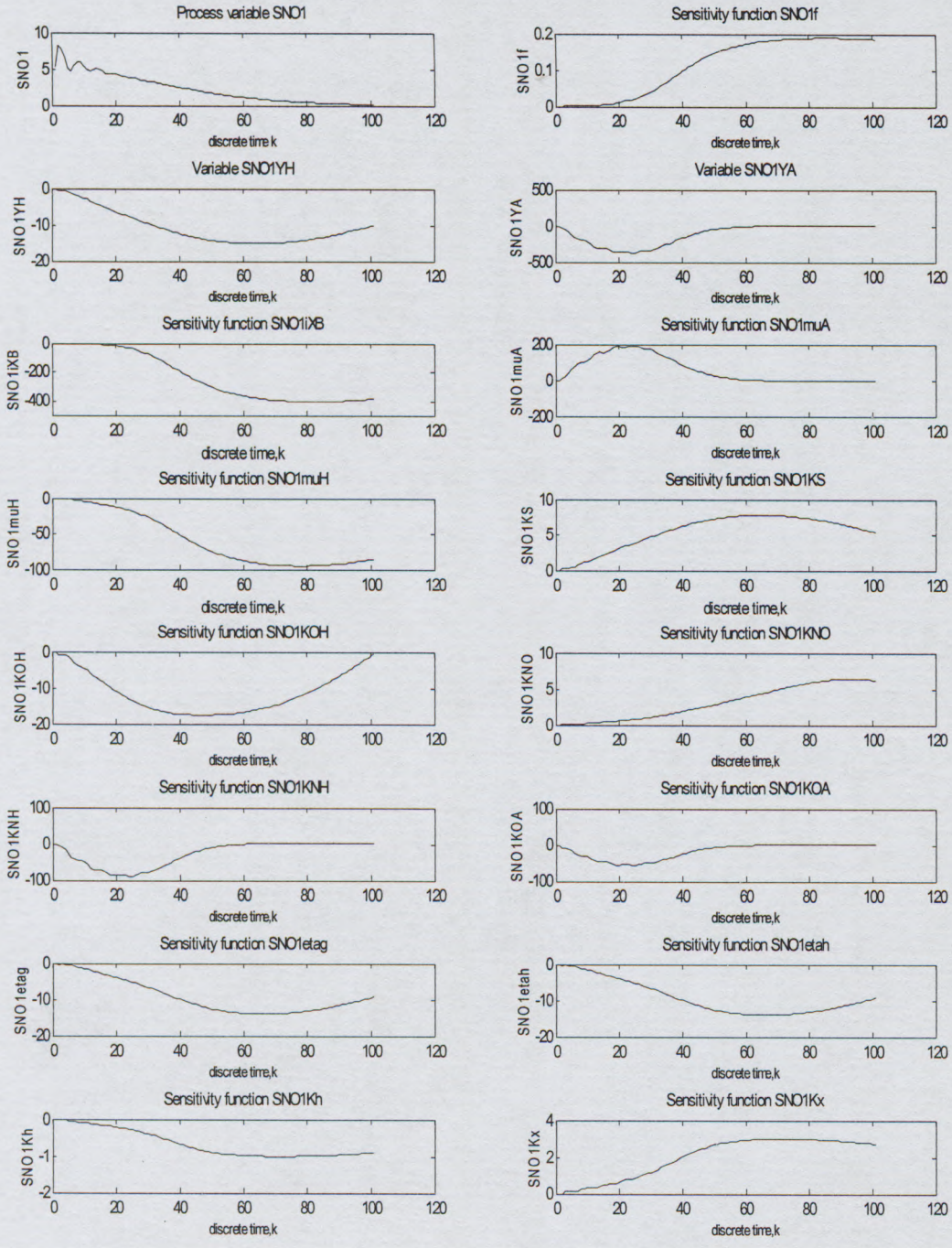

Figure 9.7: Process variable S_{NO1} and its sensitivity functions towards the model parameters

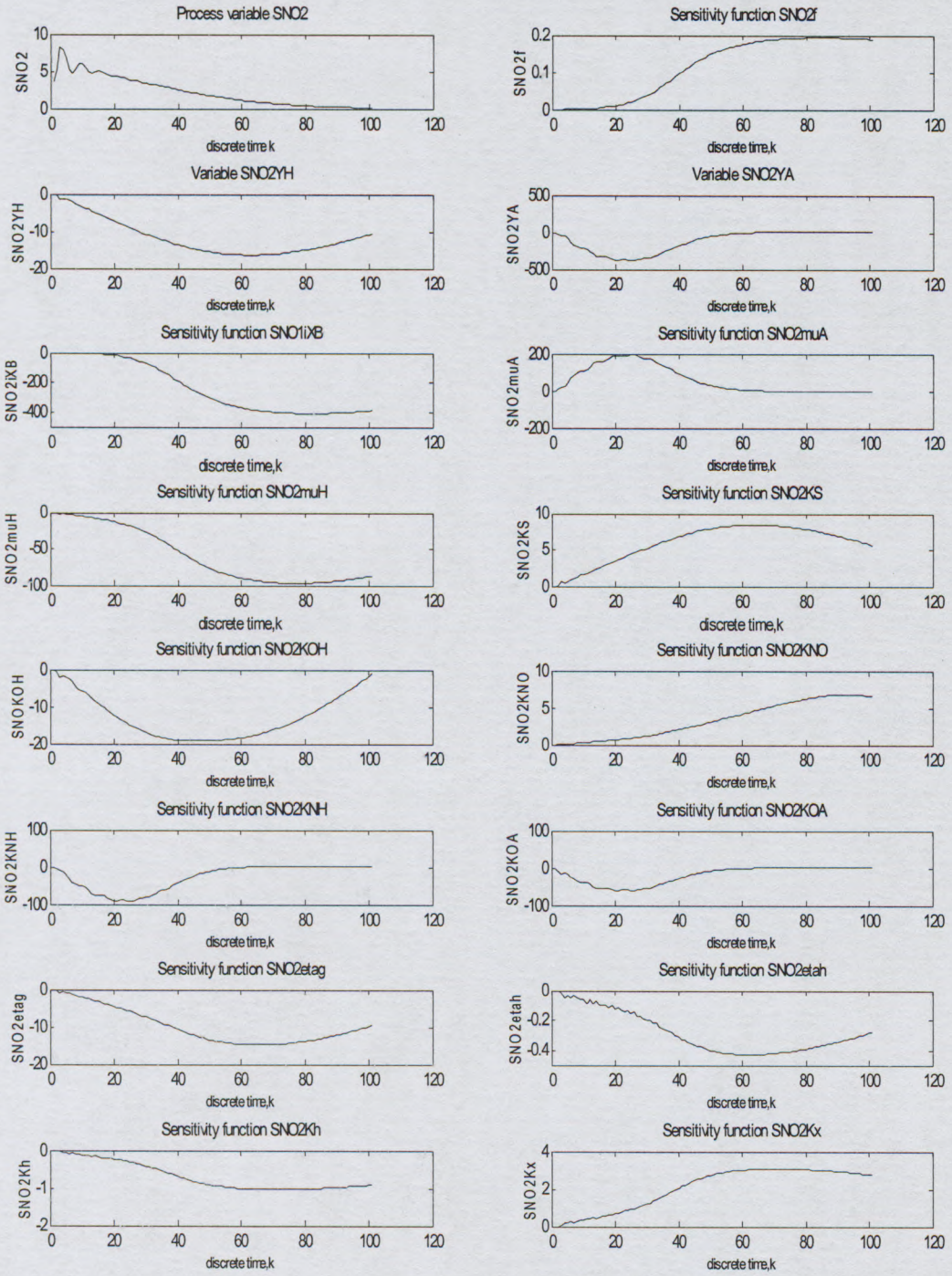

Figure 9.8: Process variable S_{NO2} and its sensitivity functions towards the model parameters

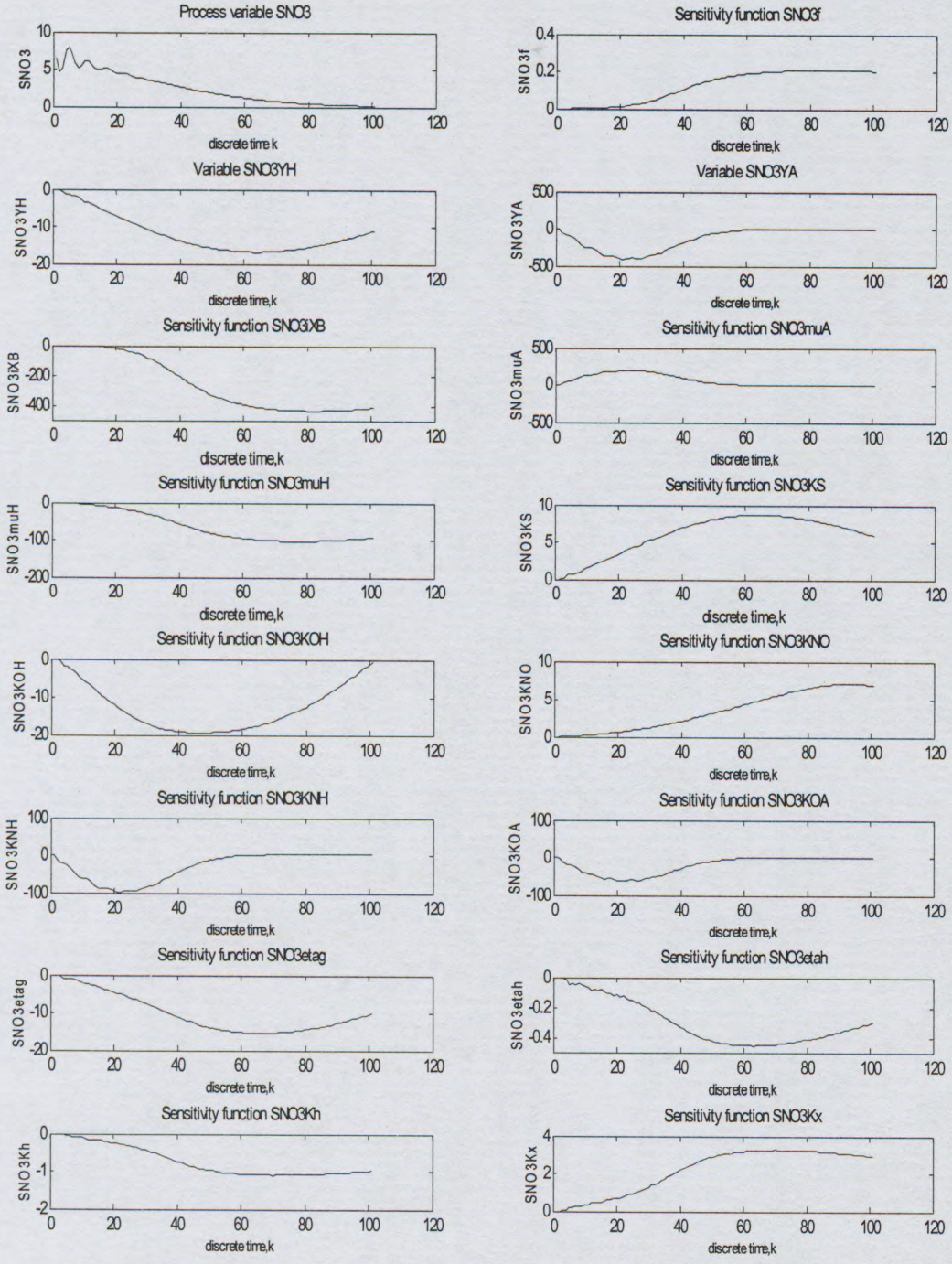

Figure 9.9: Process variable S_{NO3} and its sensitivity functions towards the model parameters

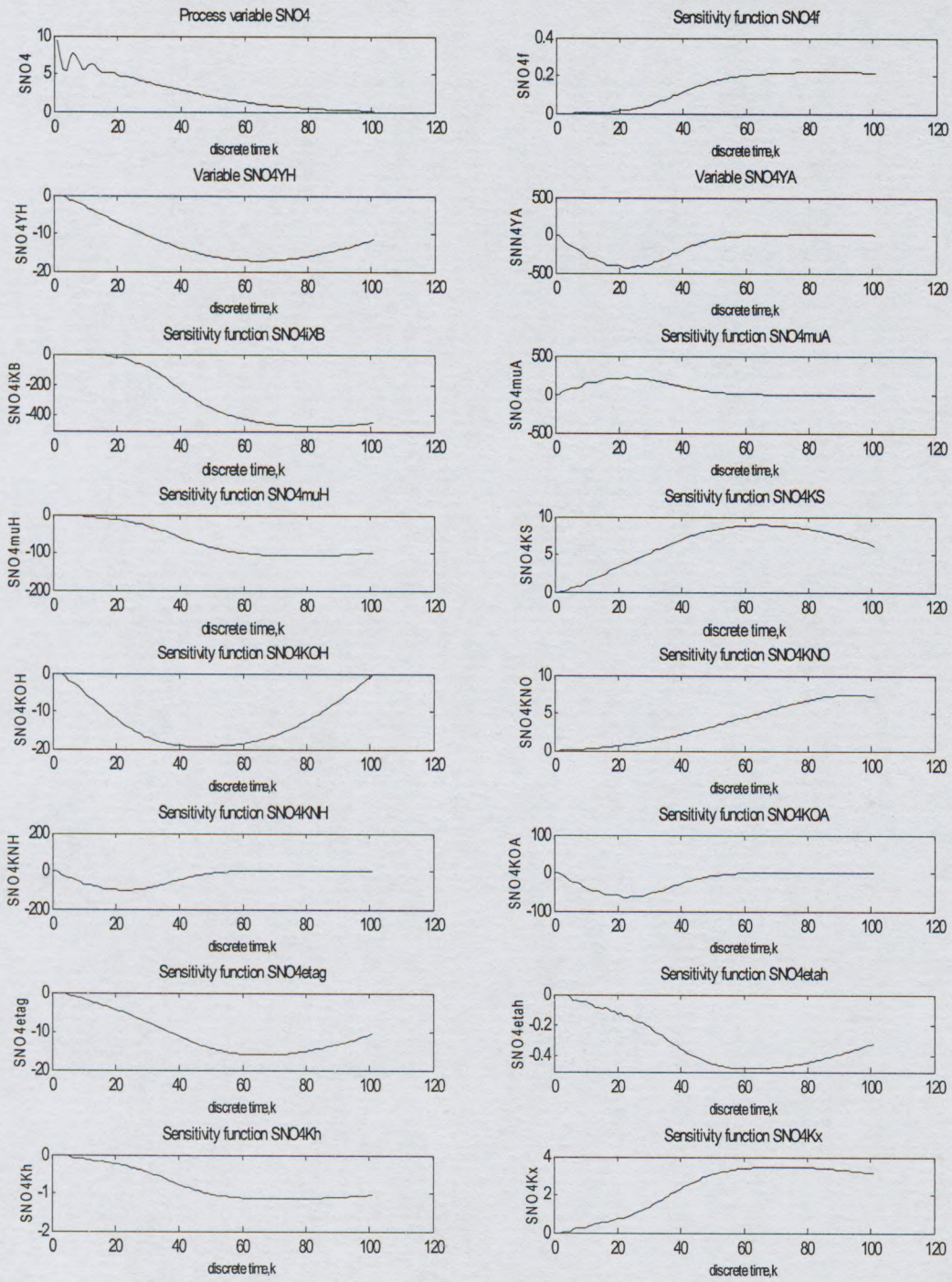

Figure 9.10: Process variable S_{NO4} and its sensitivity functions towards the model parameters

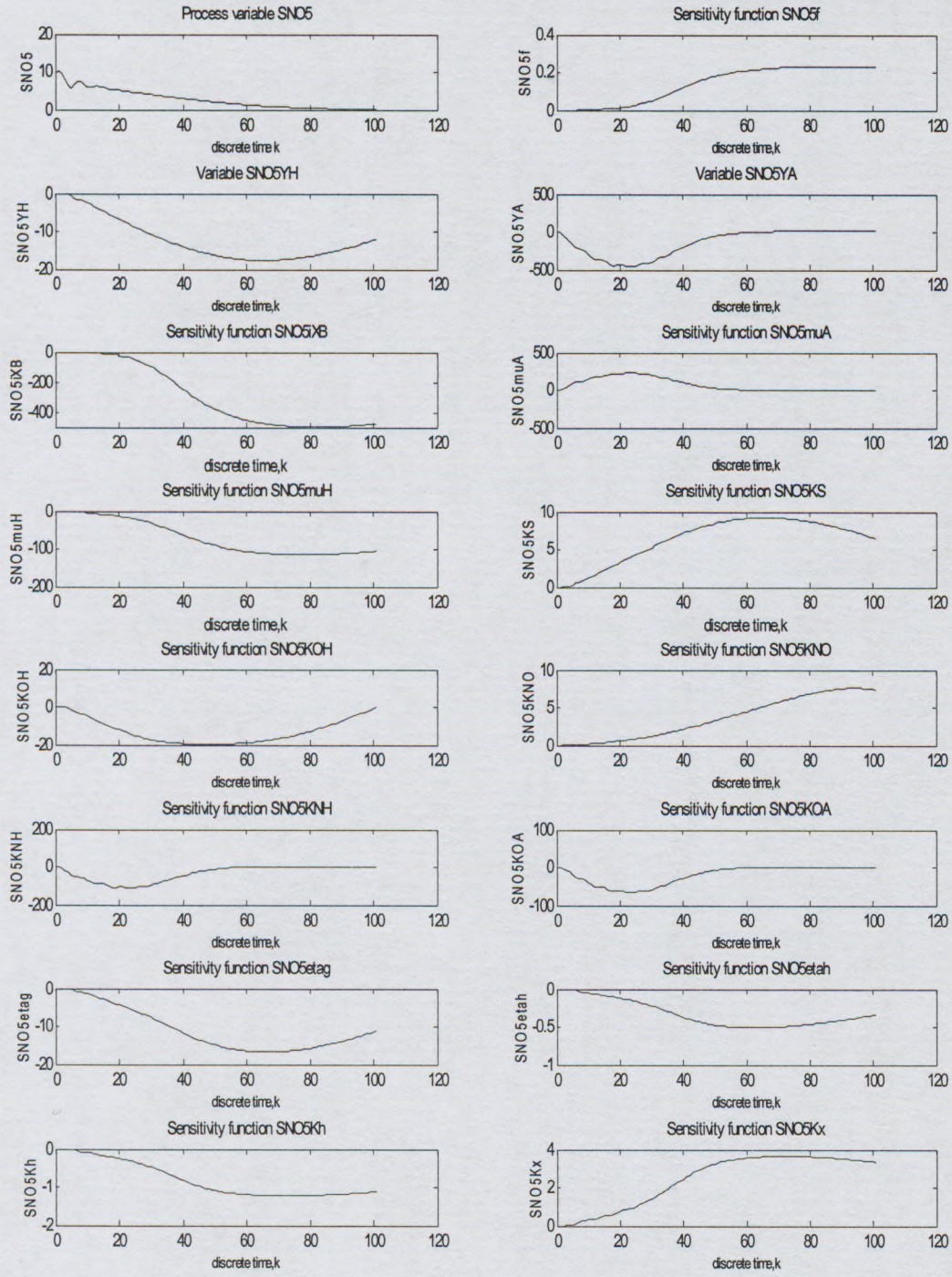

Figure 9.11: Process variable S_{NO5} and its sensitivity functions towards the model parameters

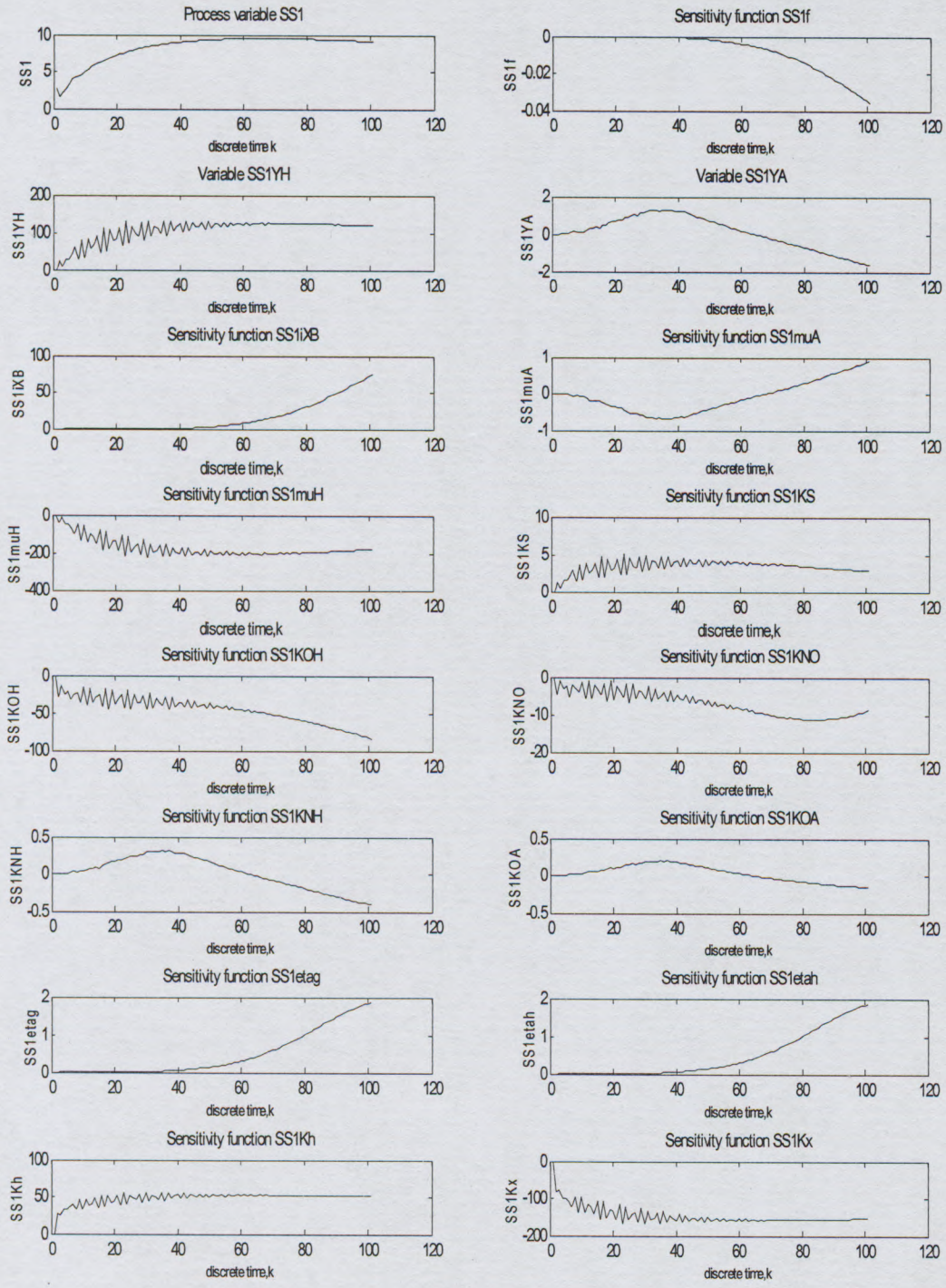

Figure 9.12: Process variable S_{S1} and its sensitivity functions towards the model parameters

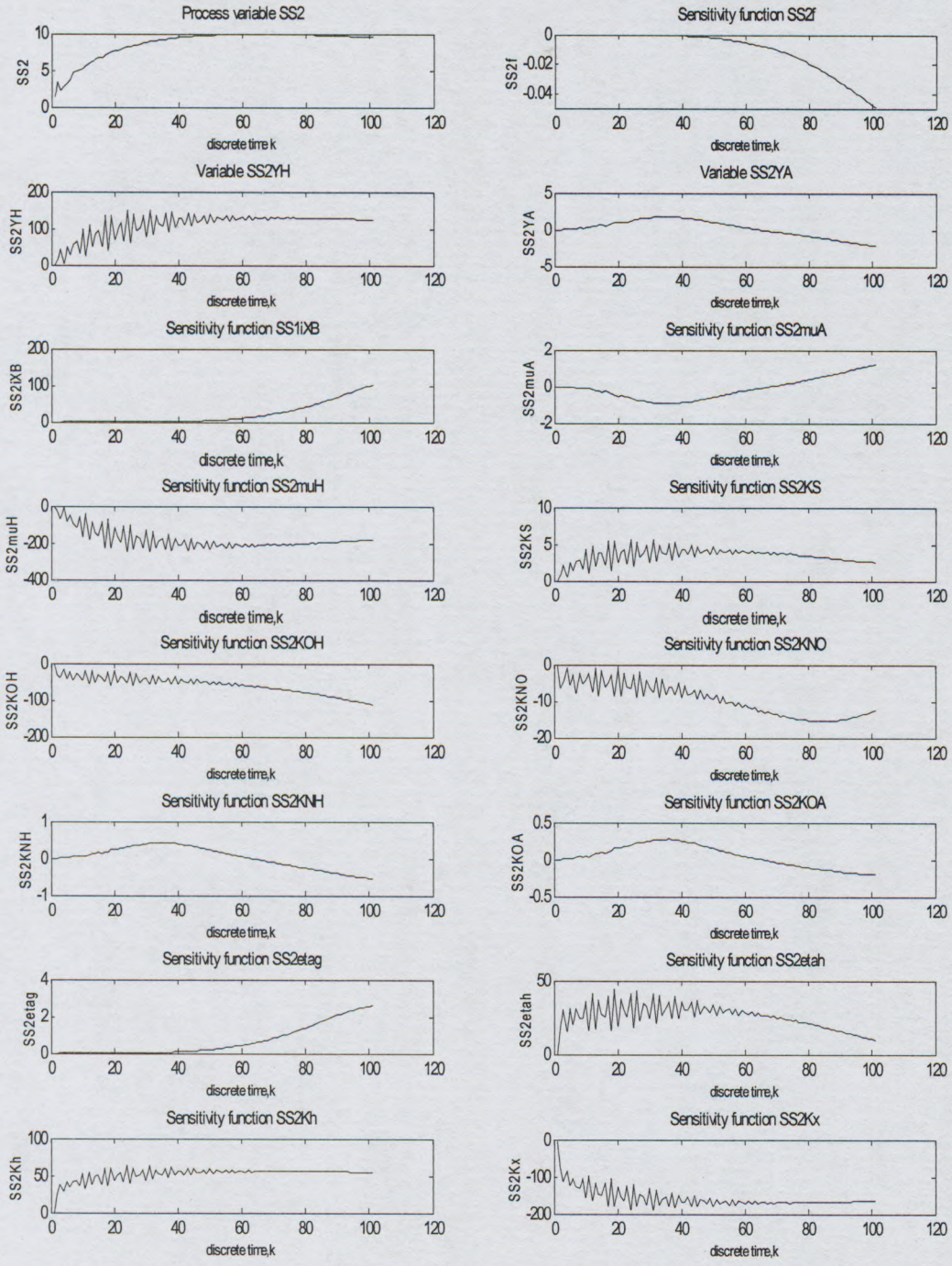

Figure 9.13: Process variable S_{S2} and its sensitivity functions towards the model parameters

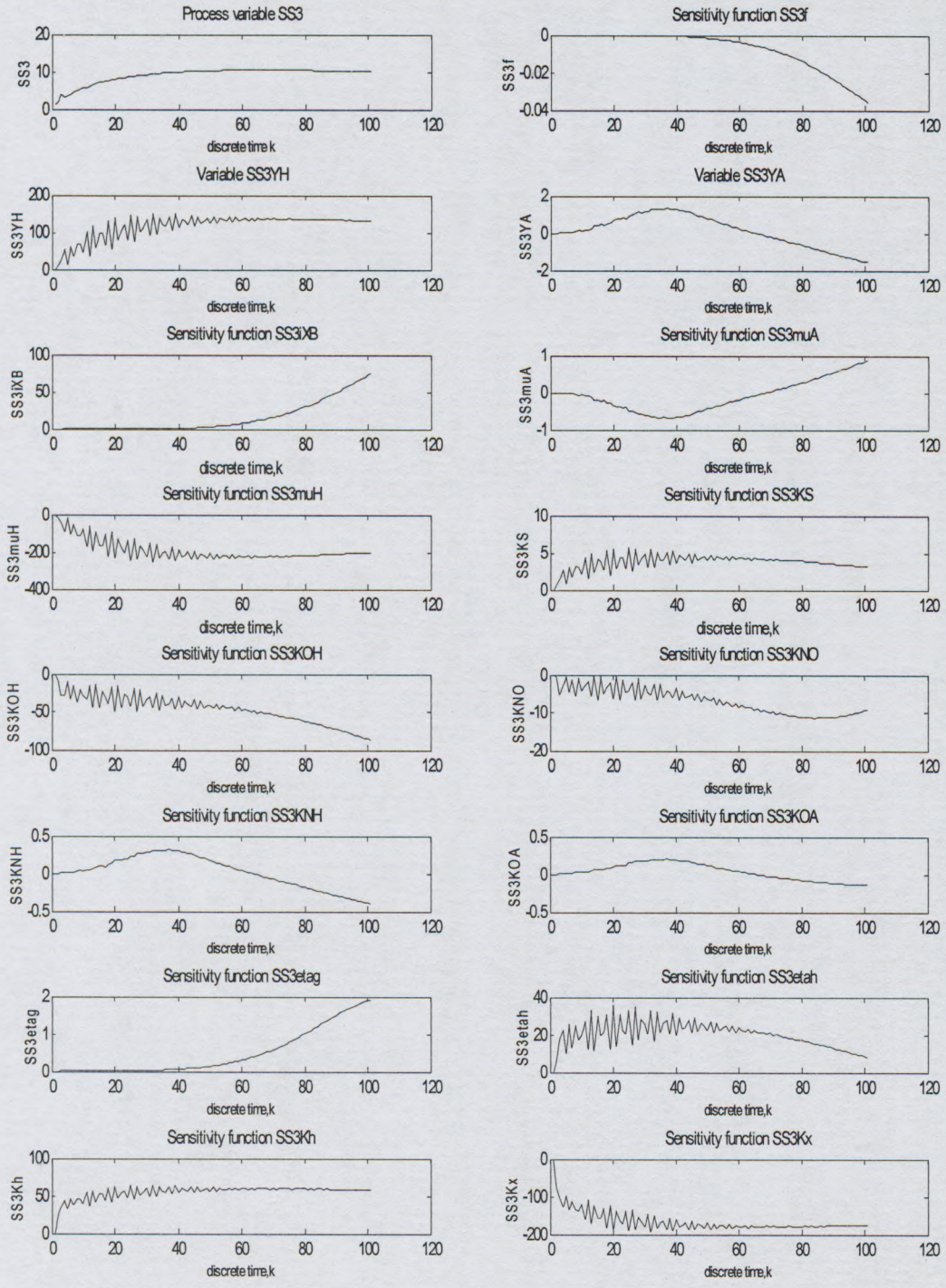

Figure 9.14: Process variable S_{S3} and its sensitivity functions towards the model parameters

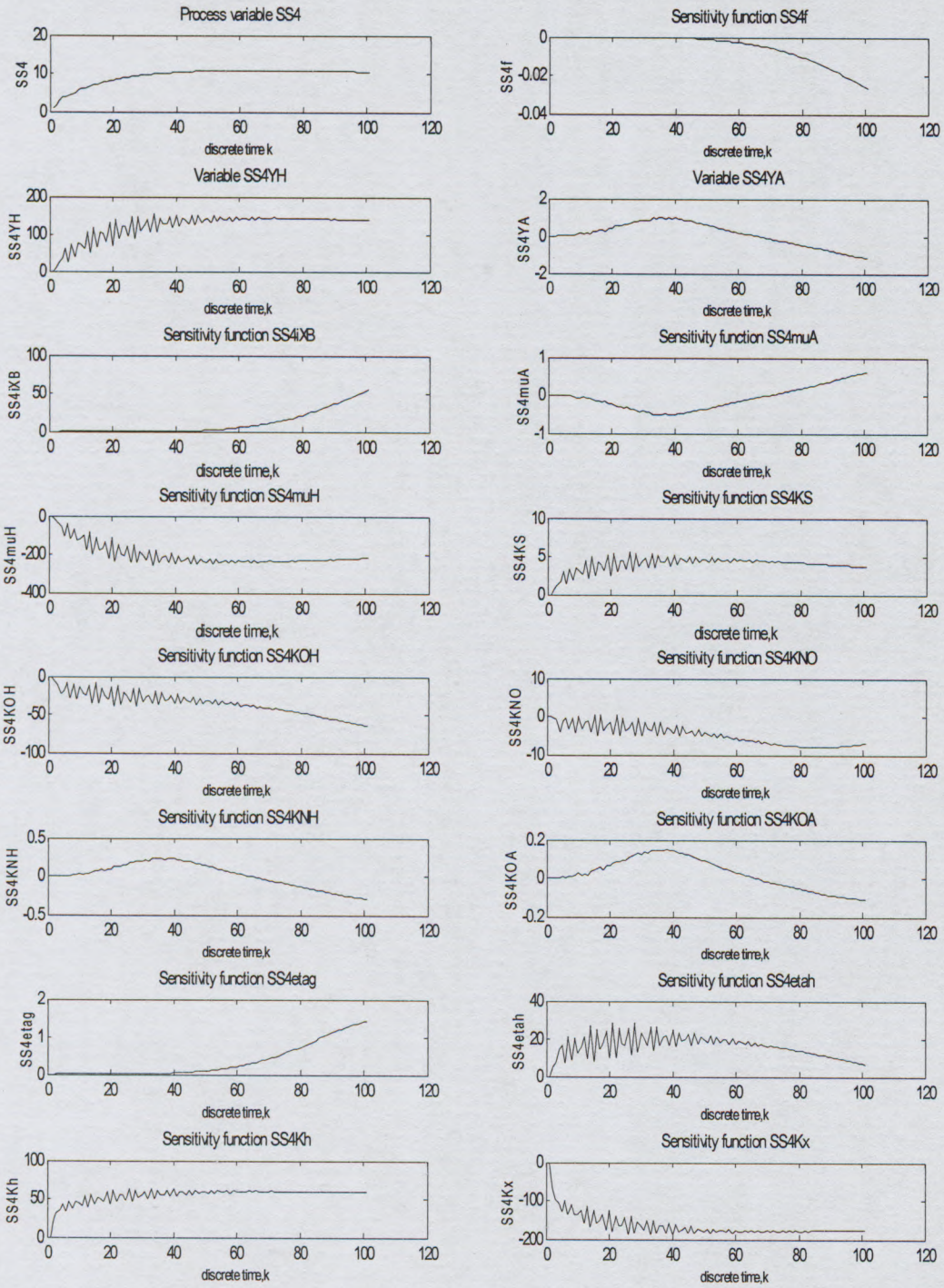

Figure 9.15: Process variable S_{S4} and its sensitivity functions towards the model parameters

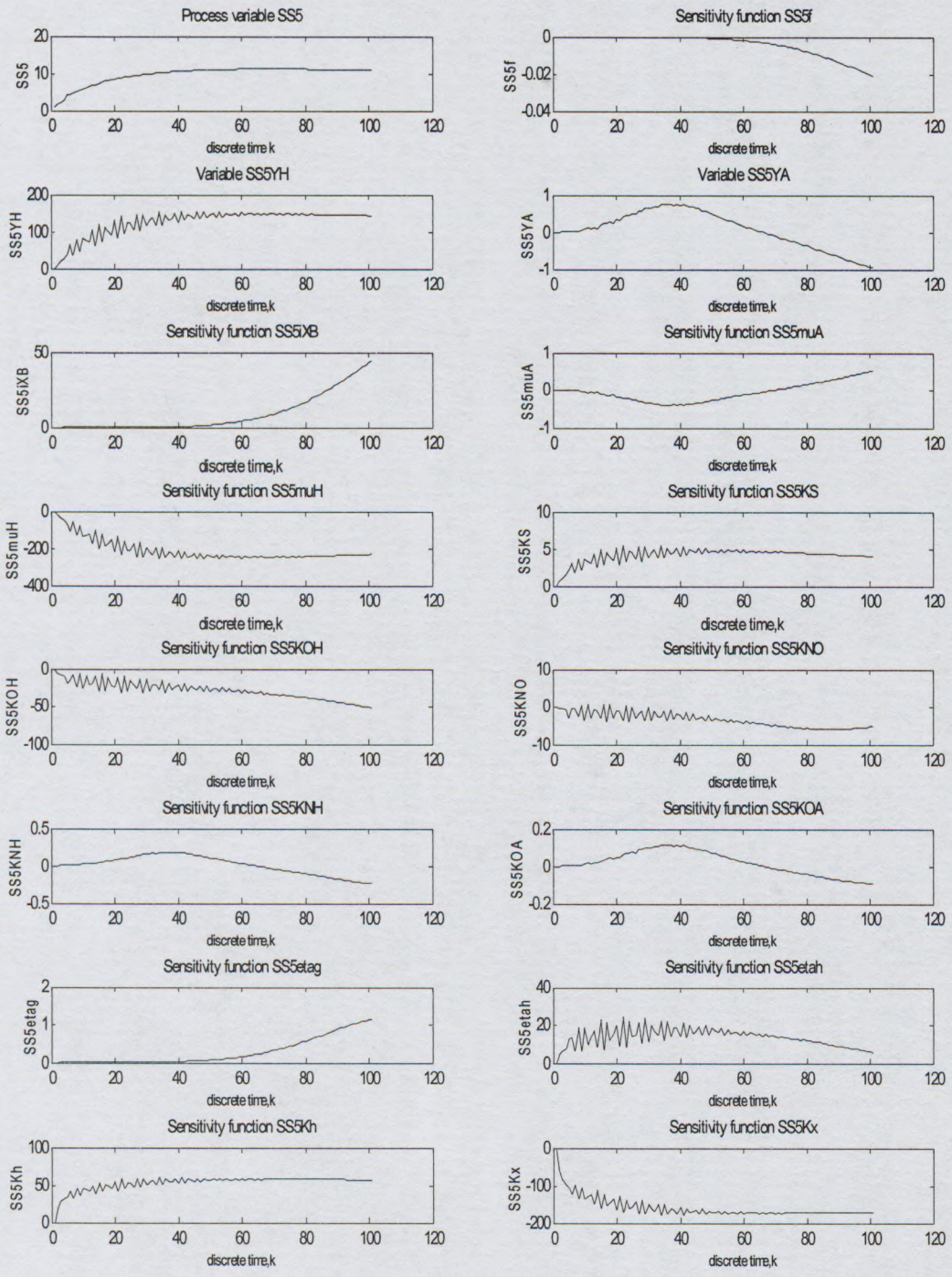

Figure 9.16: Process variable S_{S5} and its sensitivity functions towards the model parameters

9.2.2.2 Results for the UCT reduced biological model

The simulations are done for the inflow average concentration for dry weather given by the vector X_i. The initial conditions for the process variables are given by the vector x_0 and they are zero for the vector of the sensitivity functions. The values for the biomass and the slowly biodegradable substarte are given by the vectors XBH, XBA and XS.

```
Xi=[31.56; 0.0;69.5;202.3];
X0=[7.918;5.37;2.808;5.3;8.344;3.662;1.459;5.15;5.548;6.541;1.15;5.1;
     2.967;9.299;0.995;4.8;1.733;0.415;0.889;4.2]
XBH = 0.02*[2551.76*ones(1,K);2553.38*ones(1,K);2557.13*ones(1,K);
            2559.18*ones(1,K);2559.34*ones(1,K)];
XBA = 0.02*[148.389*ones(1,K);148.309*ones(1,K);148.941*ones(1,K);
            149.527*ones(1,K);149.797*ones(1,K)];
XS = 0.02*[82.135*ones(1,K);76.386*ones(1,K);64.855*ones(1,K);
           55.694*ones(1,K);49.306*ones(1,K)];
```

The vector of the dissolved oxygen concentration is: U=[0.2;0.2;2.0;2.29;1.91]

The process state space reduced model matrices are:

Au=

0.0390	0	0	0	0	0	0	0	0	0	0	0	0	0	0	0	0.7688	0	0	0
0	0.0390	0	0	0	0	0	0	0	0	0	0	0	0	0	0	0	0.7688	0	0
0	0	0.0390	0	0	0	0	0	0	0	0	0	0	0	0	0	0	0	0.7688	0
0	0	0	0.0390	0	0	0	0	0	0	0	0	0	0	0	0	0	0	0	0.7688
0.9610	0	0	0	0.0390	0	0	0	0	0	0	0	0	0	0	0	0	0	0	0
0	0.9610	0	0	0	0.0390	0	0	0	0	0	0	0	0	0	0	0	0	0	0
0	0	0.9610	0	0	0	0.0390	0	0	0	0	0	0	0	0	0	0	0	0	0
0	0	0	0.9610	0	0	0	0.0390	0	0	0	0	0	0	0	0	0	0	0	0
0	0	0	0	0.7210	0	0	0	0.2790	0	0	0	0	0	0	0	0	0	0	0
0	0	0	0	0	0.7210	0	0	0	0.2790	0	0	0	0	0	0	0	0	0	0
0	0	0	0	0	0	0.7210	0	0	0	0.2790	0	0	0	0	0	0	0	0	0
0	0	0	0	0	0	0	0.7210	0	0	0	0.2790	0	0	0	0	0	0	0	0
0	0	0	0	0	0	0	0	0.7210	0	0	0	0.2790	0	0	0	0	0	0	0
0	0	0	0	0	0	0	0	0	0.7210	0	0	0	0.2790	0	0	0	0	0	0
0	0	0	0	0	0	0	0	0	0	0.7210	0	0	0	0.2790	0	0	0	0	0
0	0	0	0	0	0	0	0	0	0	0	0.7210	0	0	0	0.2790	0	0	0	0
0	0	0	0	0	0	0	0	0	0	0	0	0.7210	0	0	0	0.2790	0	0	0
0	0	0	0	0	0	0	0	0	0	0	0	0	0.7210	0	0	0	0.2790	0	0
0	0	0	0	0	0	0	0	0	0	0	0	0	0	0.7210	0	0	0	0.2790	0
0	0	0	0	0	0	0	0	0	0	0	0	0	0	0	0.7210	0	0	0	0.2790

Bu=

0.2306	0	0	0
0	0.1922	0	0
0	0	0.1922	0
0	0	0	0.1922

Cn=

-0.0680	0	-1.4925	0
0	-0.0680	-1.4925	0
-0.0680	-0.1722	-1.4925	0
0	0.1042	-1.4925	0
-0.0680	0	0	-1.4925
0	-0.0680	0	-1.4925
-0.0680	-0.1722	0	-1.4925
0	0.1042	0	-1.4925
0	0	0	1.0000
-6.7347	6.6667	0	0

n=1,5

The results from the simulation are given from Figure 9.17 till Figure 9.36.

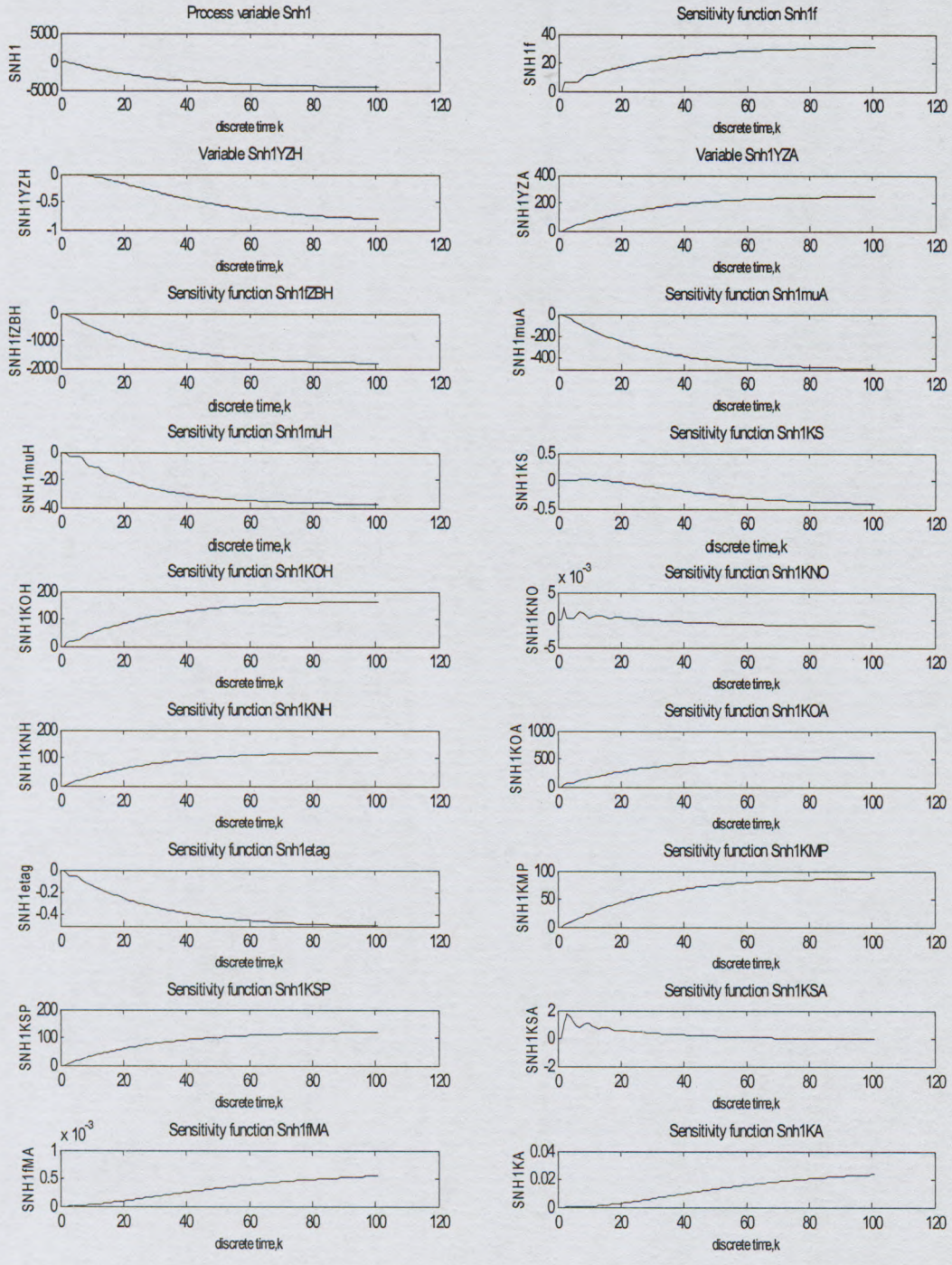

Figure 9.17: Process variable S_{NH1} and its sensitivity functions towards the model parameters

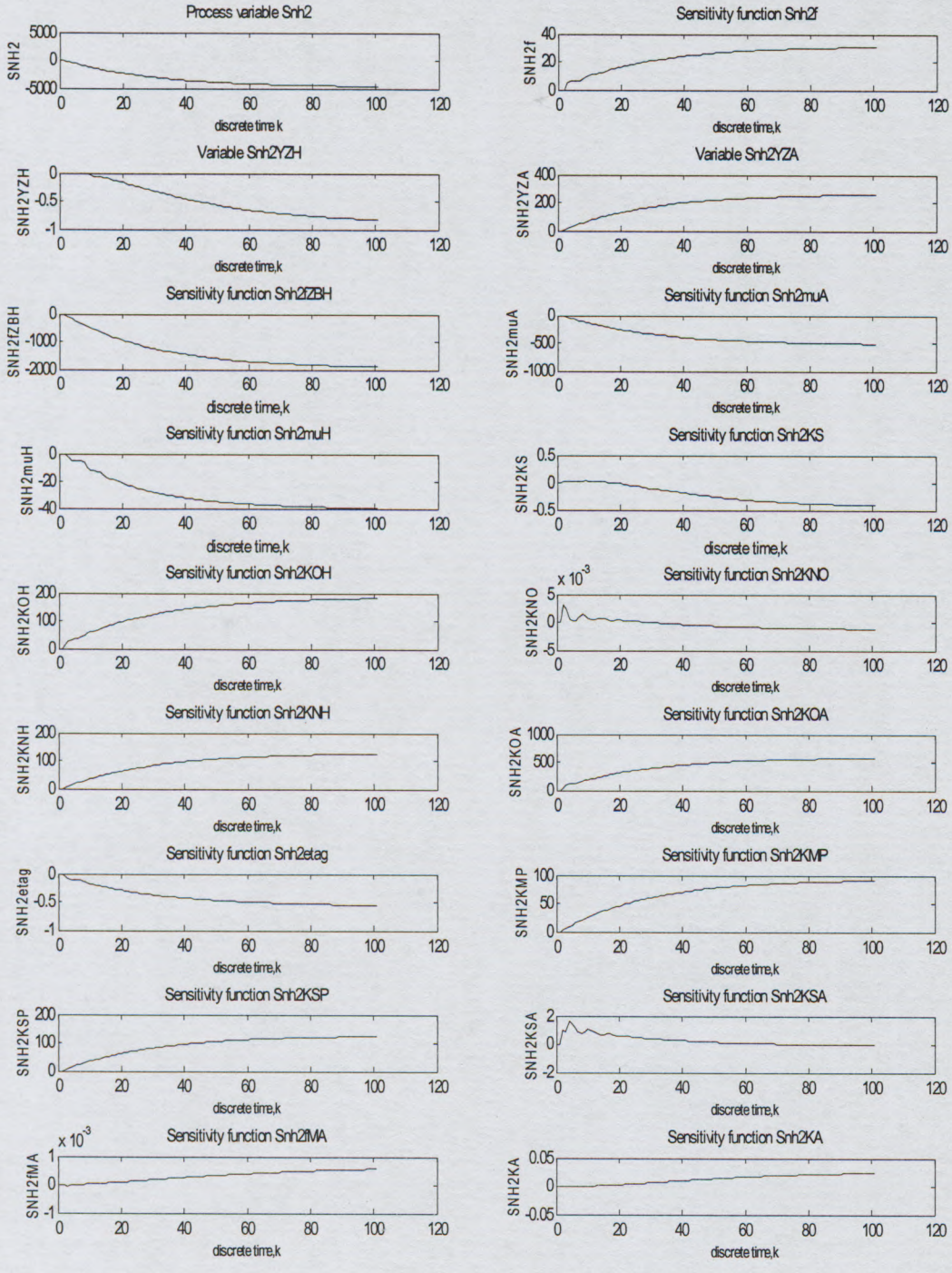

Figure 9.18: Process variable S_{NH2} and its sensitivity functions towards the model parameters

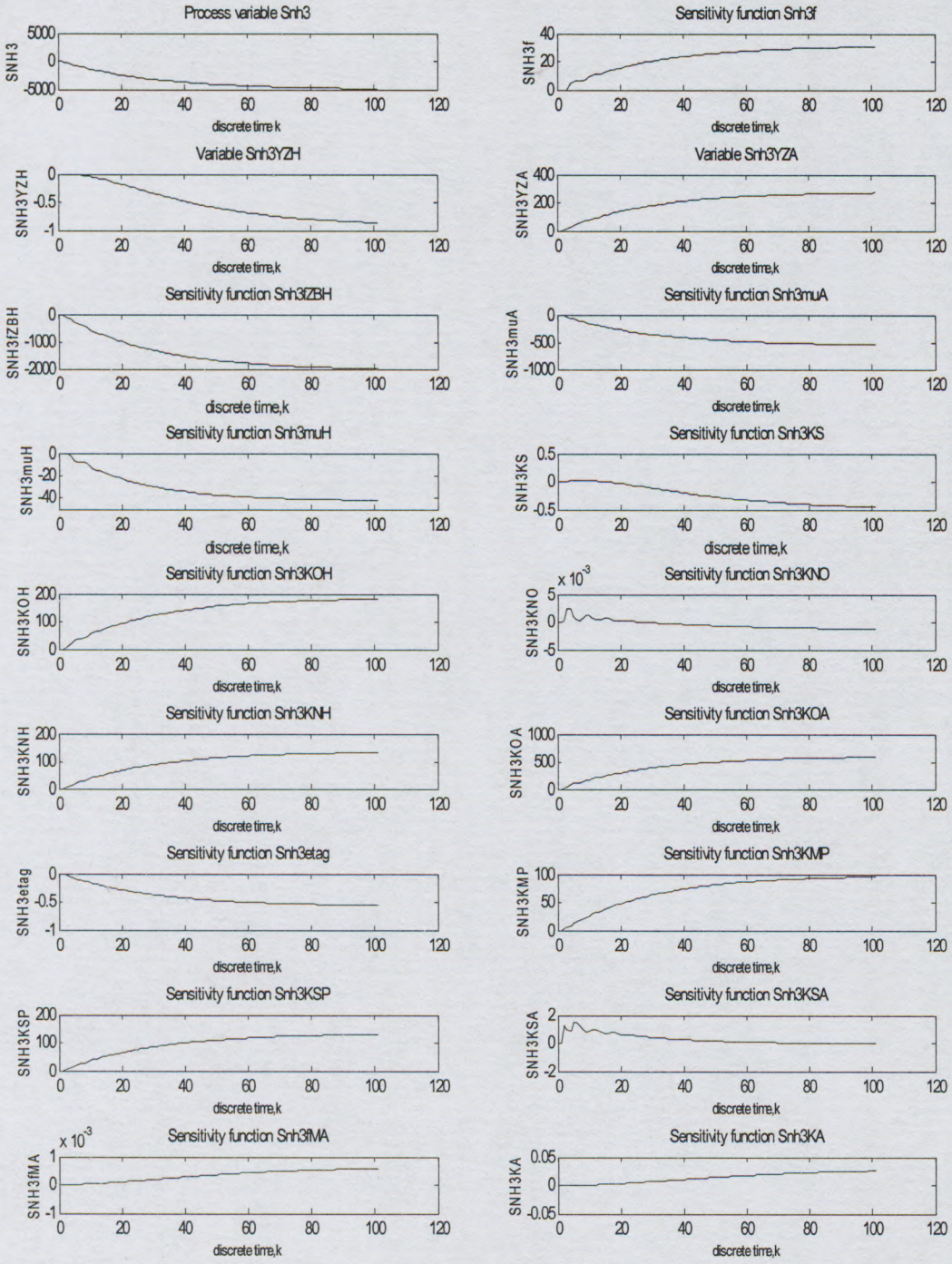

Figure 9.19: Process variable S_{NH3} and its sensitivity functions towards the model parameters

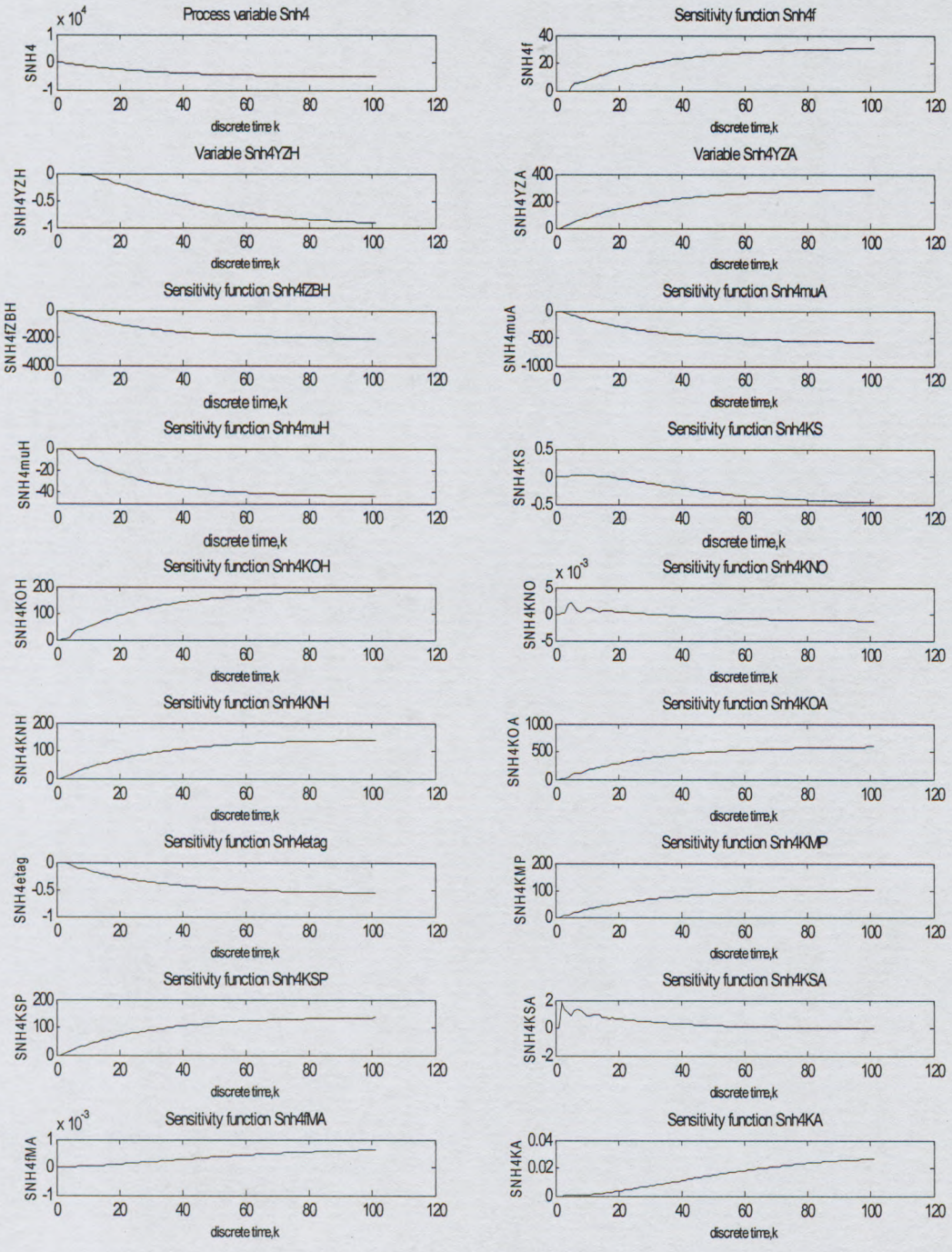

Figure 9.20: Process variable S_{NH4} and its sensitivity functions towards the model parameters

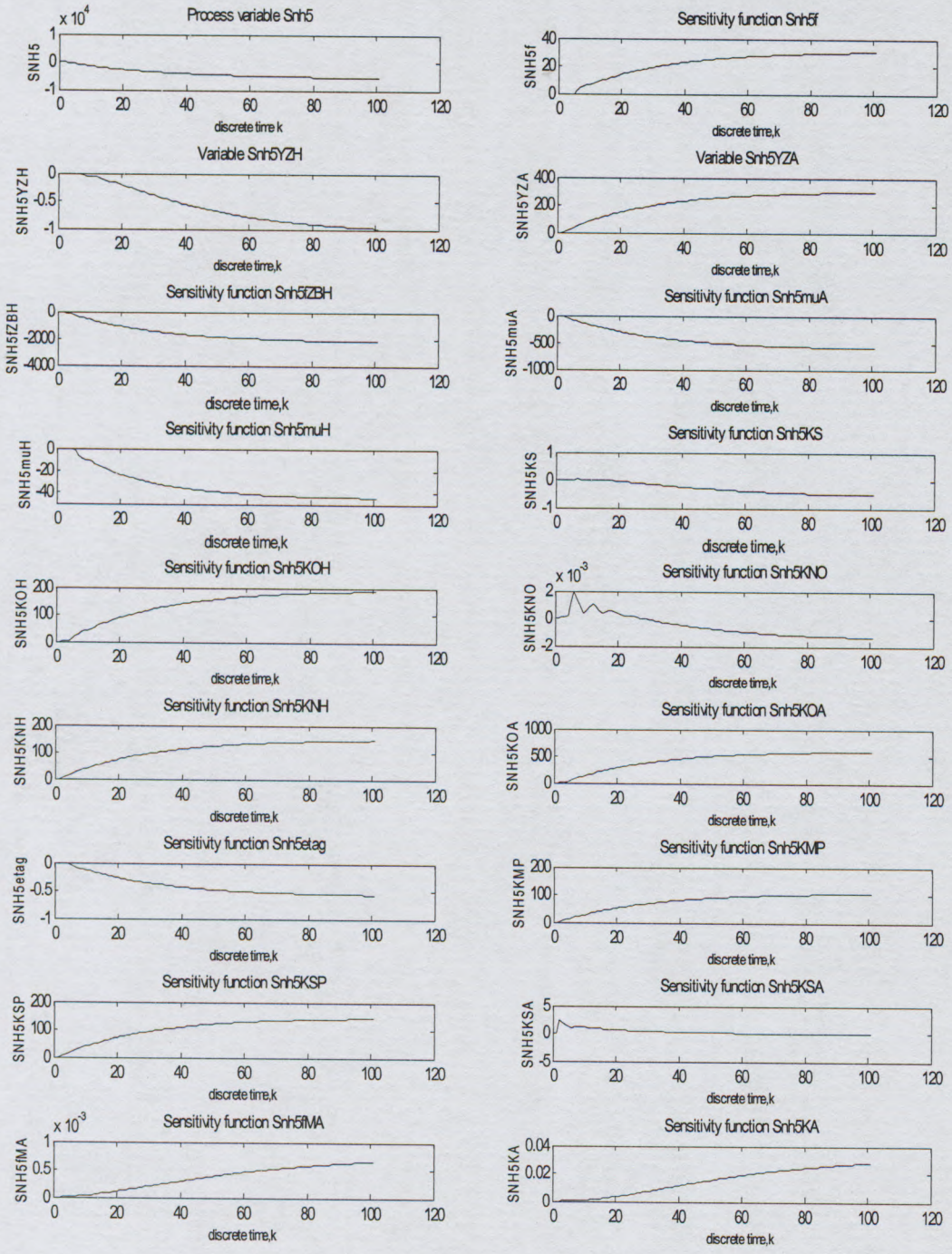

Figure 9.21: Process variable S_{NH5} and its sensitivity functions towards the model parameters

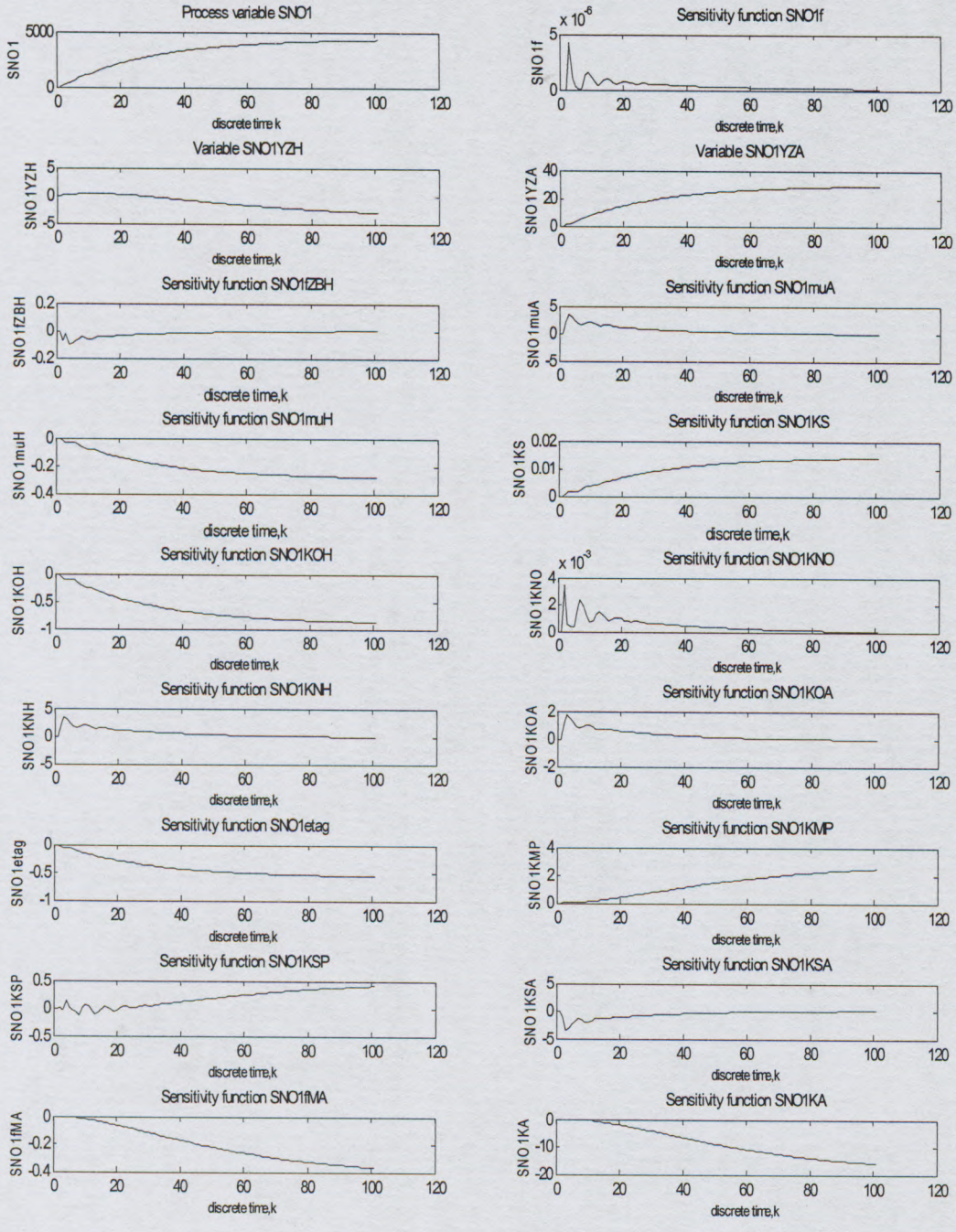

Figure 9.22: Process variable S_{NO1} and its sensitivity functions towards the model parameters

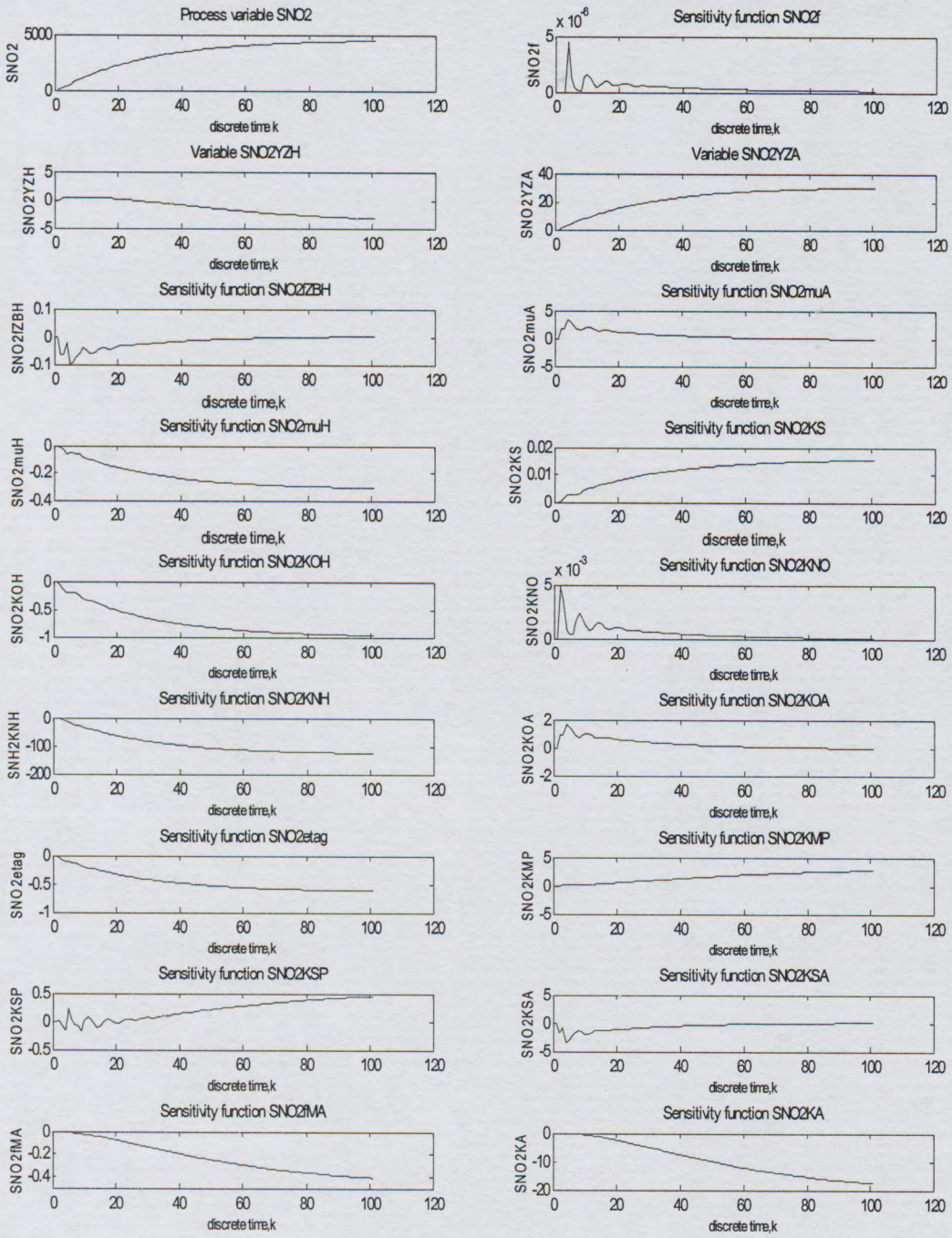

Figure 9.23: Process variable S_{NO2} and its sensitivity functions towards the model parameters

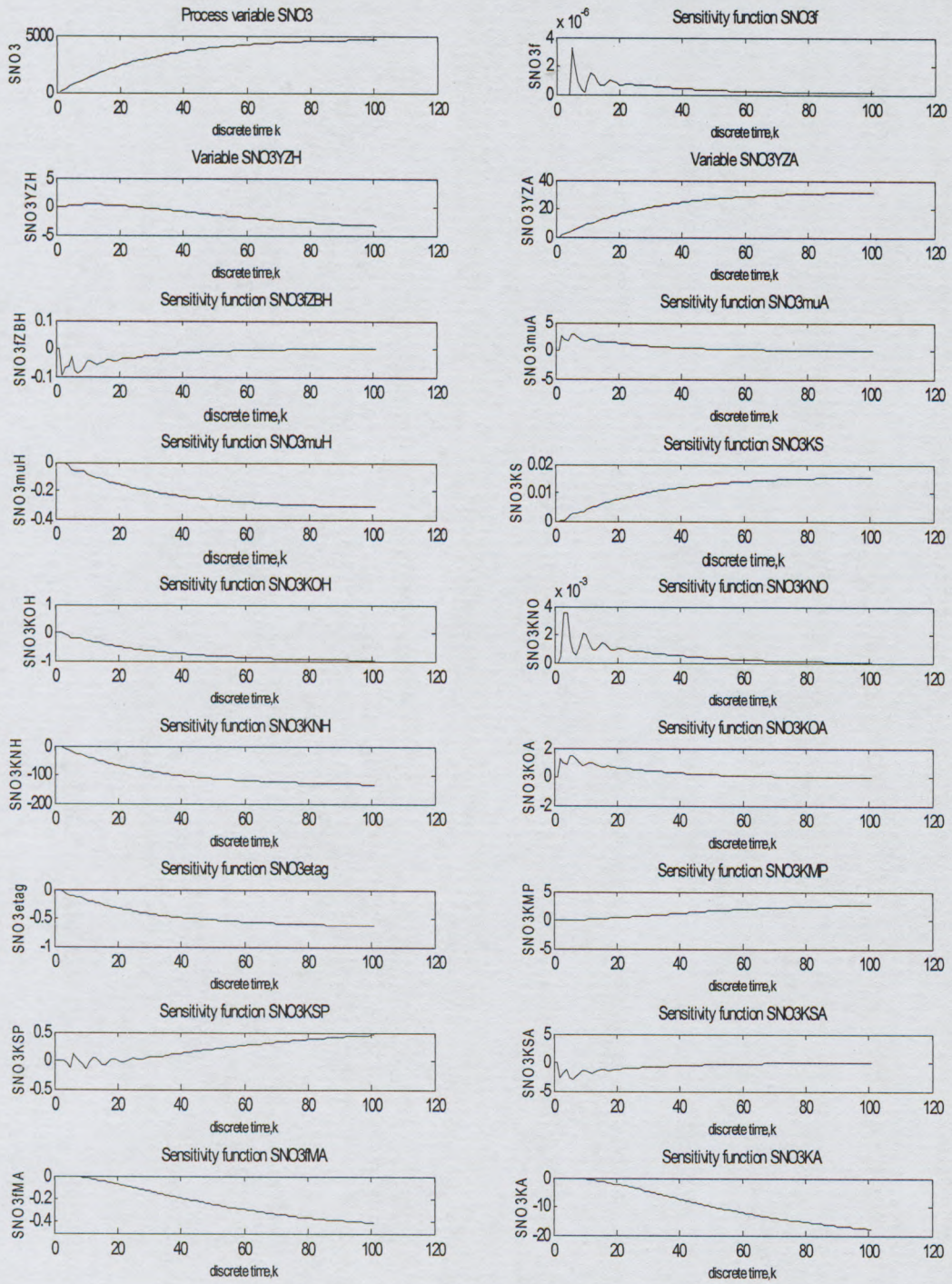

Figure 9.24: Process variable S_{NO3} and its sensitivity functions towards the model parameters

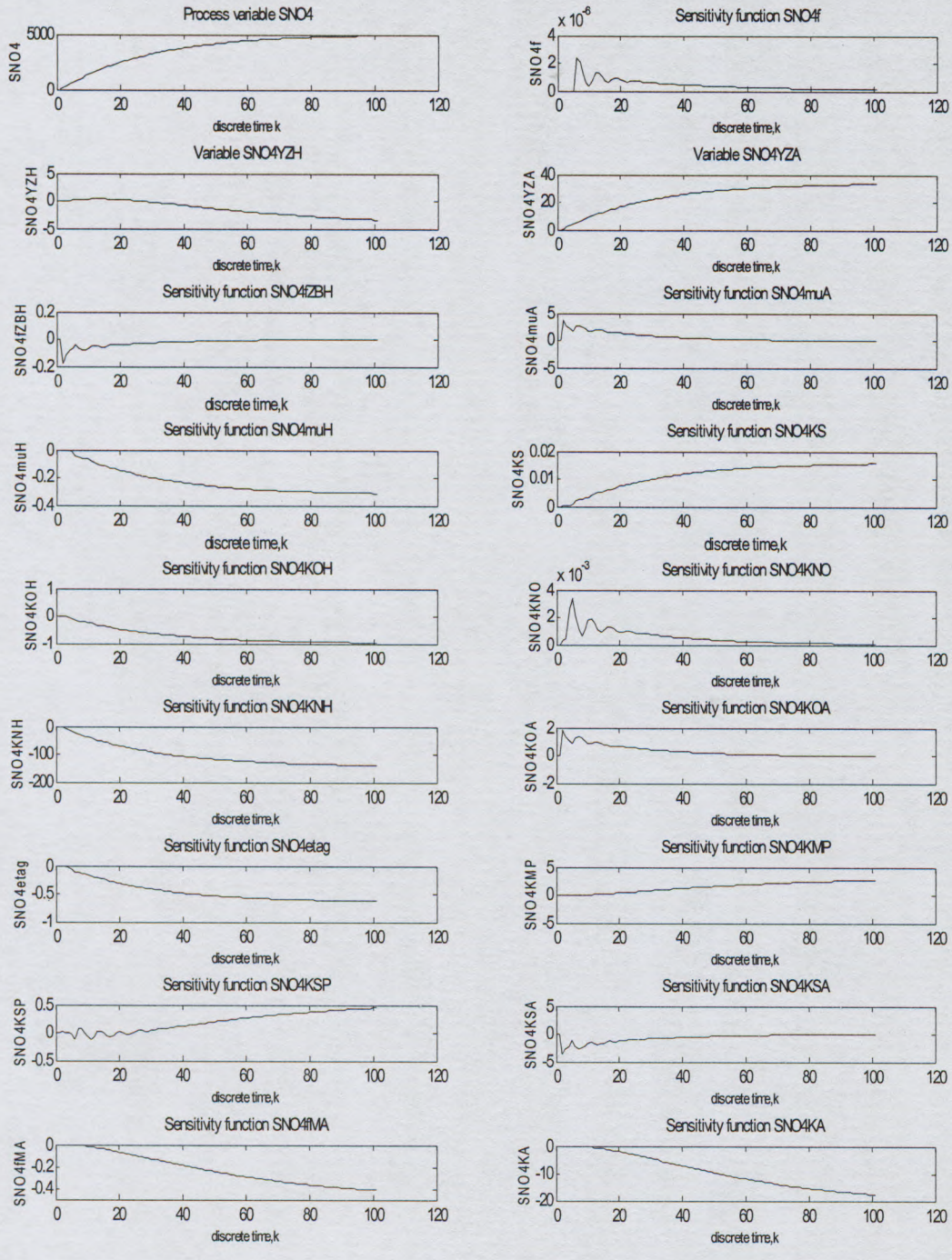

Figure 9.25: Process variable S_{NO4} and its sensitivity functions towards the model parameters

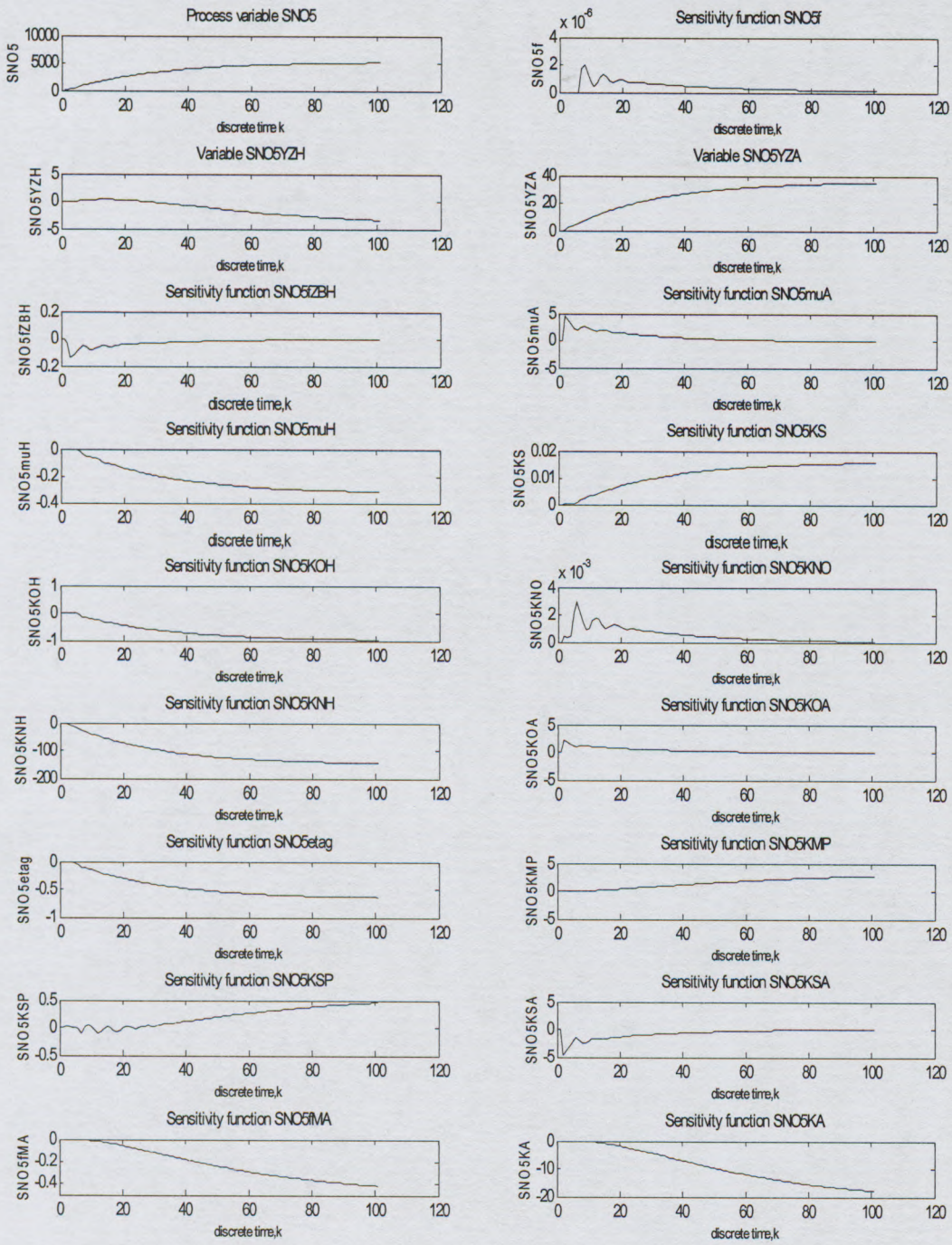

Figure 9.26: Process variable S_{NO5} and its sensitivity functions towards the model parameters

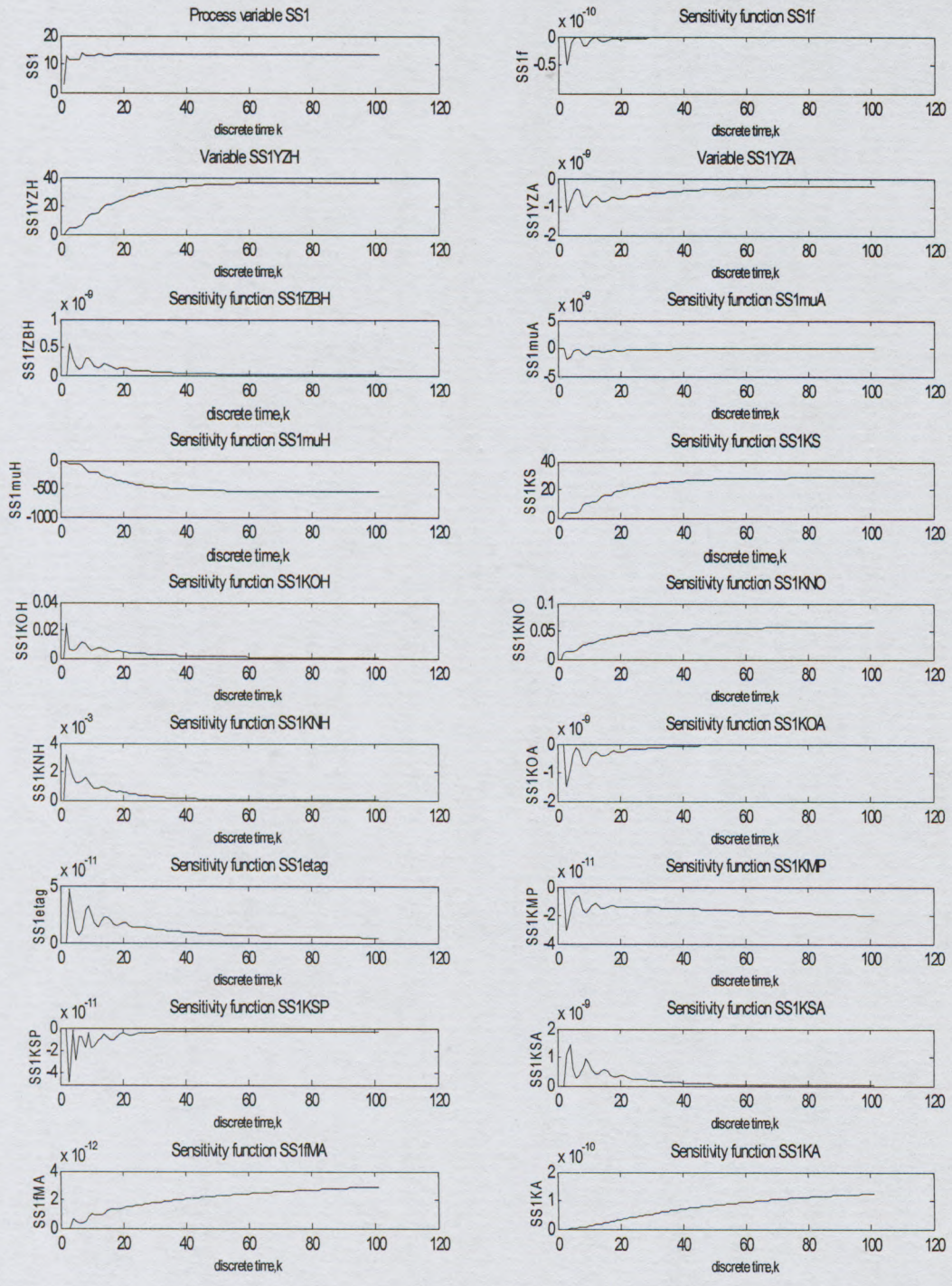

Figure 9.27: Process variable S_{S1} and its sensitivity functions towards the model parameters

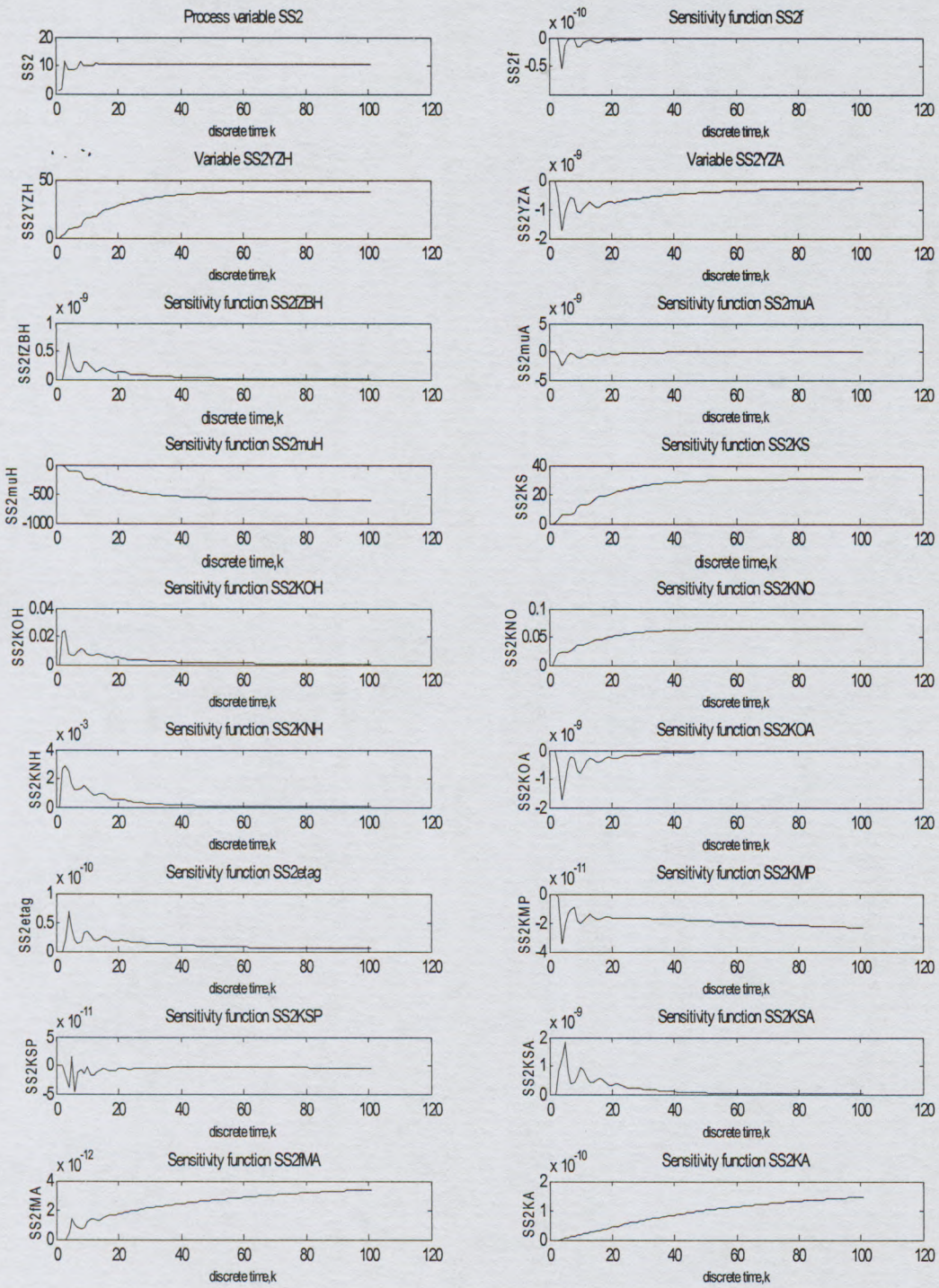

Figure 9.28: Process variable S_{S2} and its sensitivity functions towards the model parameters

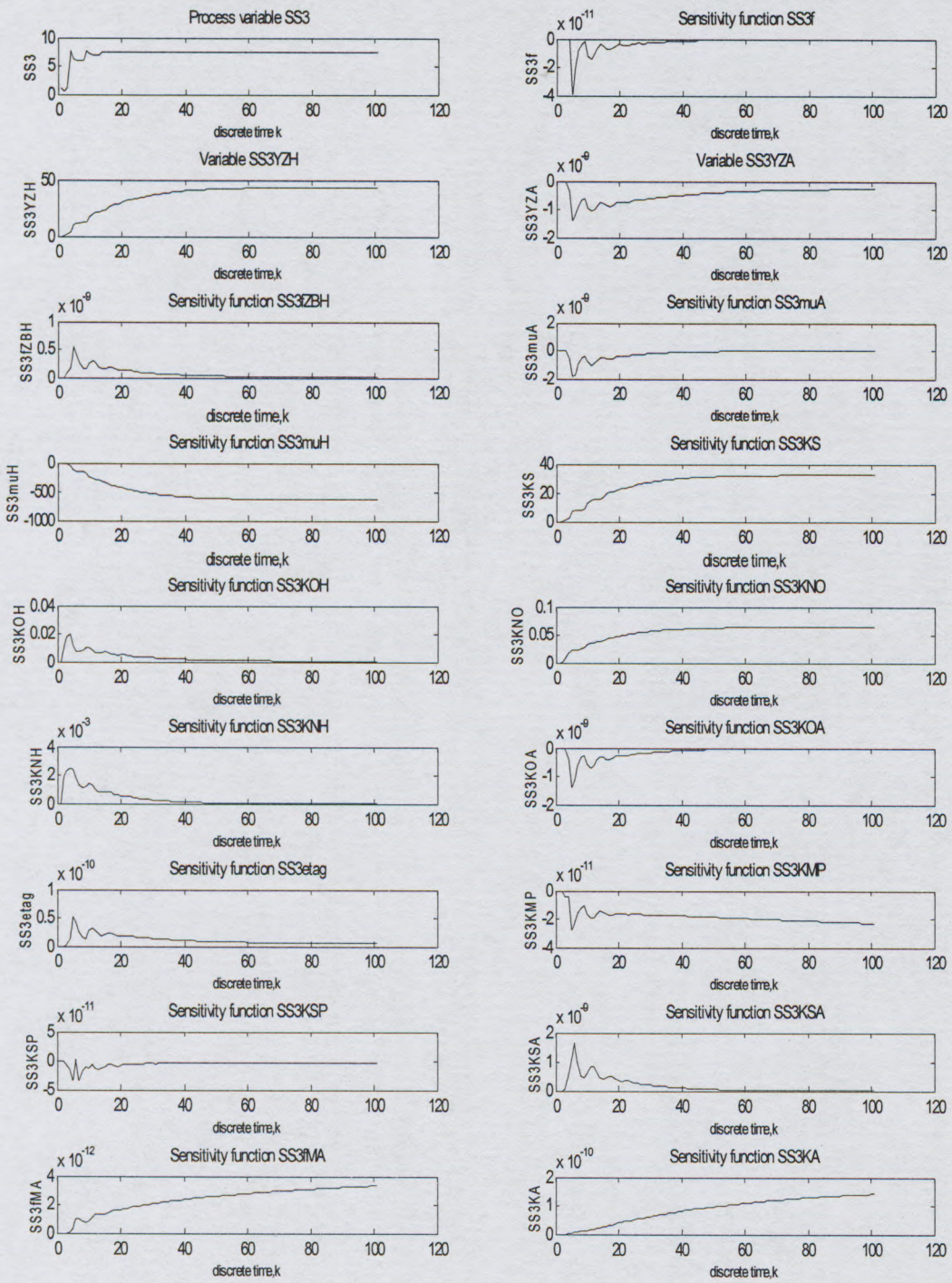

Figure 9.29: Process variable S_{S3} and its sensitivity functions towards the model parameters

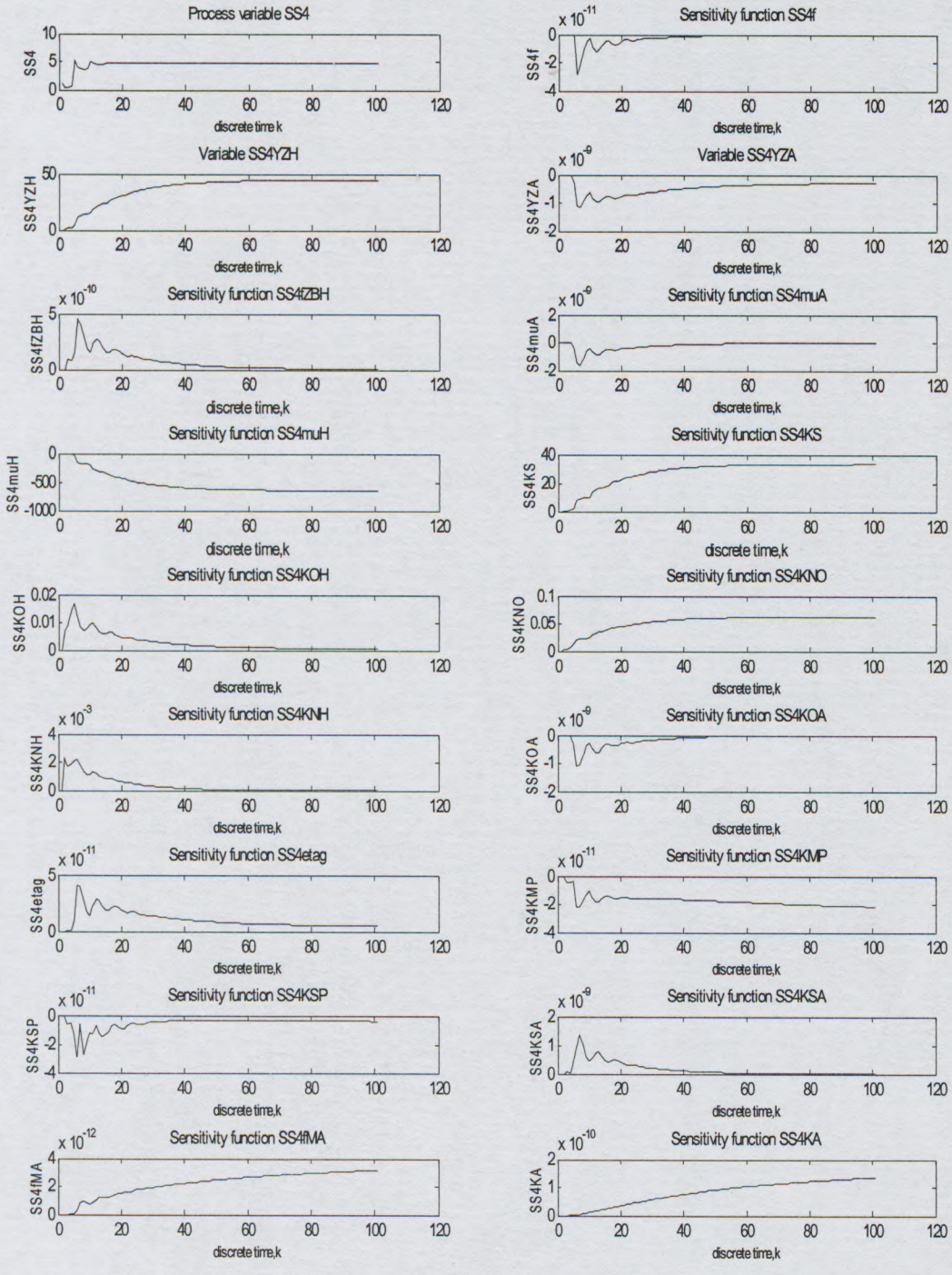

Figure 9.30: Process variable S_{S4} and its sensitivity functions towards the model parameters

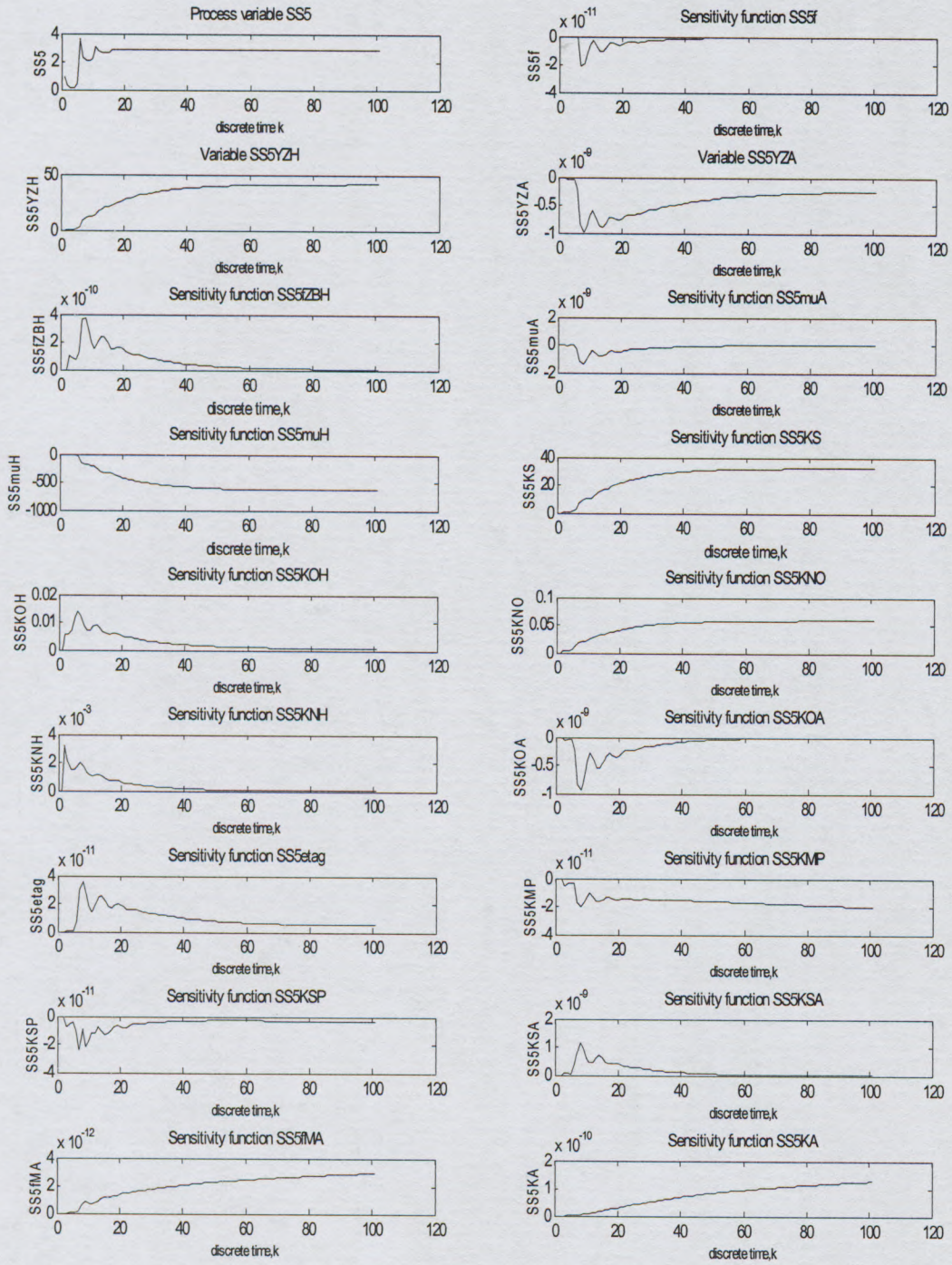

Figure 9.31: Process variable S_{S5} and its sensitivity functions towards the model parameters

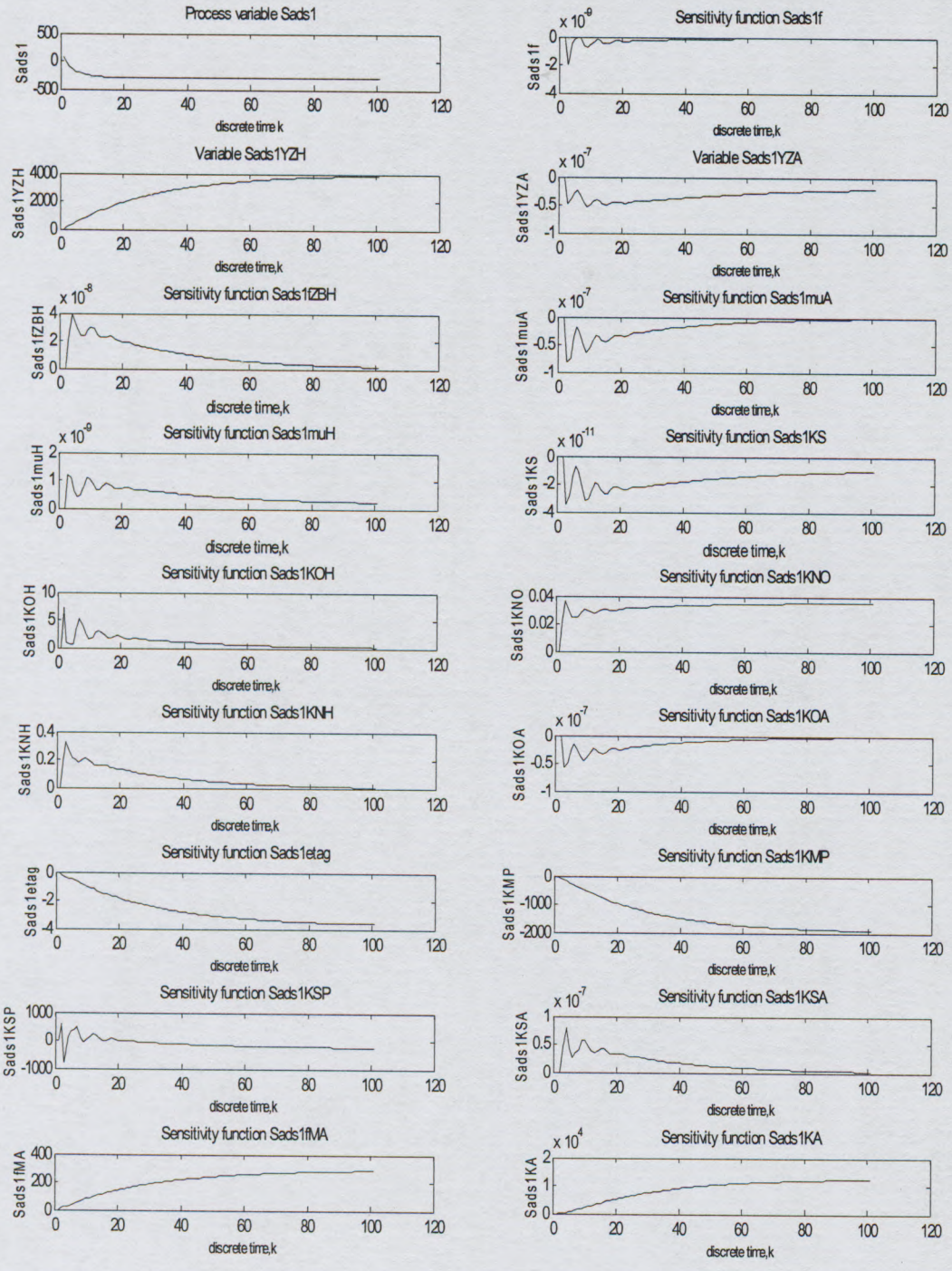

Figure 9.32: Process variable S_{Sads1} and its sensitivity functions towards the model parameters

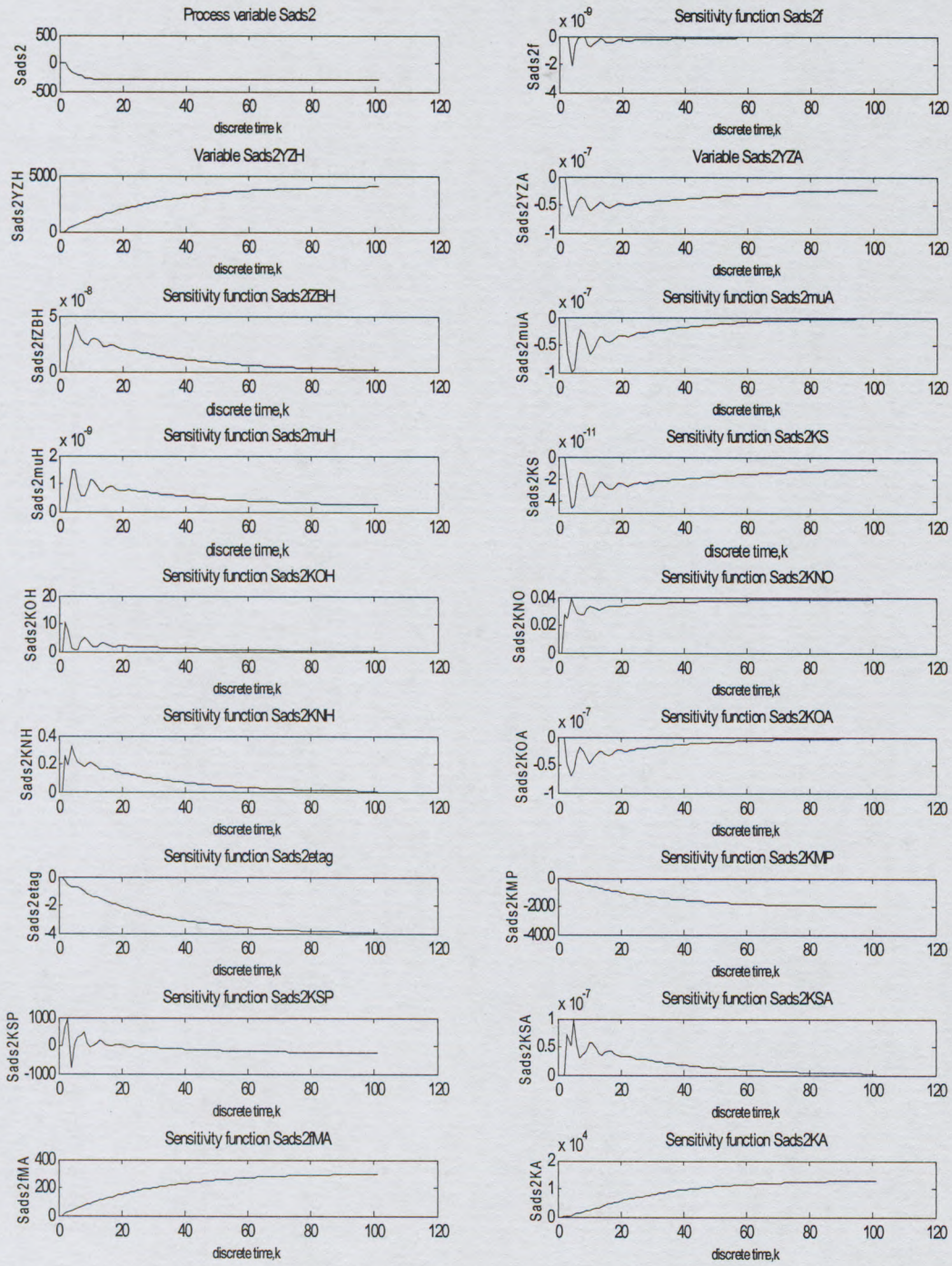

Figure 9.33: Process variable S_{Sads2} and its sensitivity functions towards the model parameters

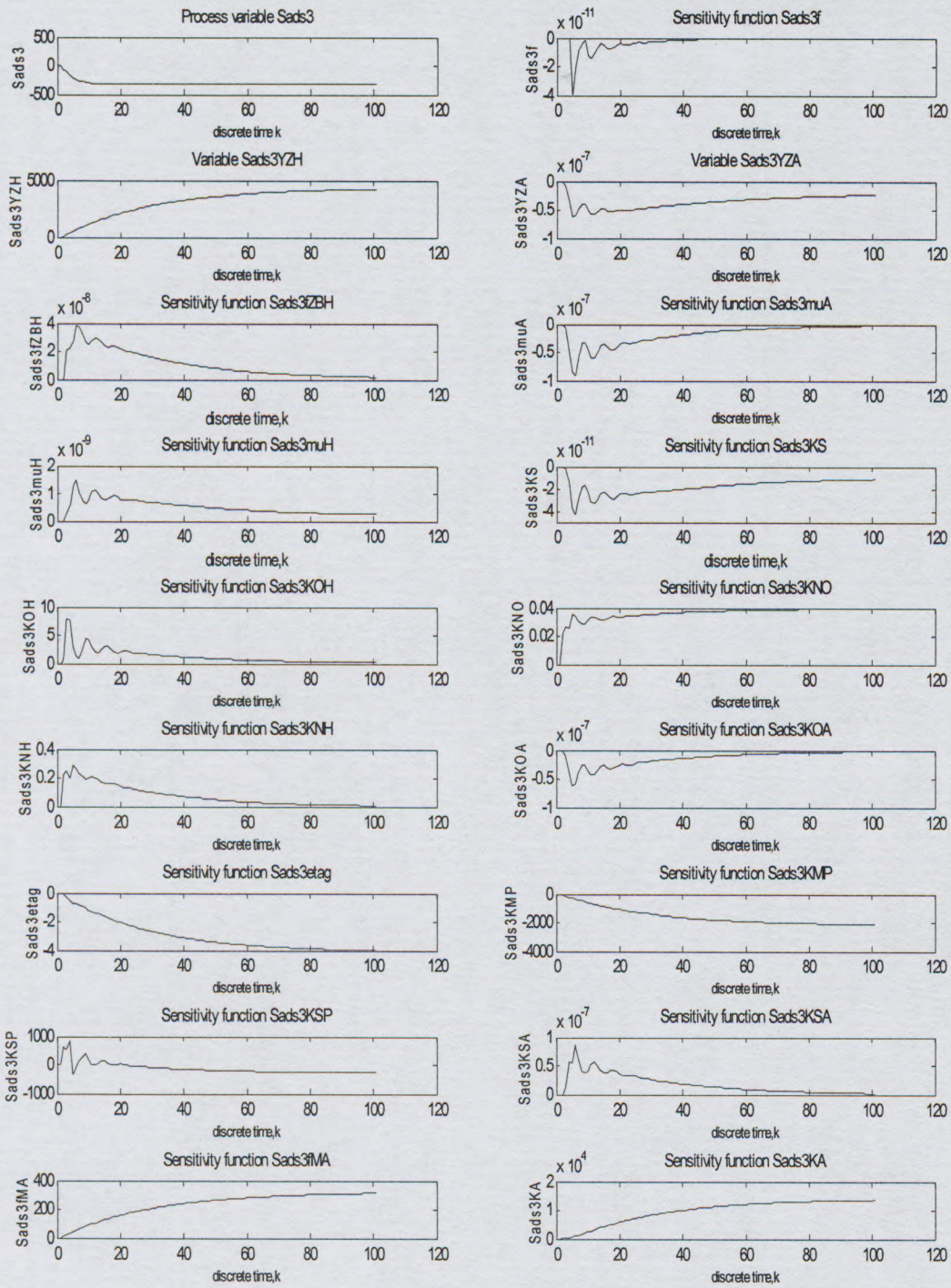

Figure 9.34: Process variable S_{Sads3} and its sensitivity functions towards the model parameters

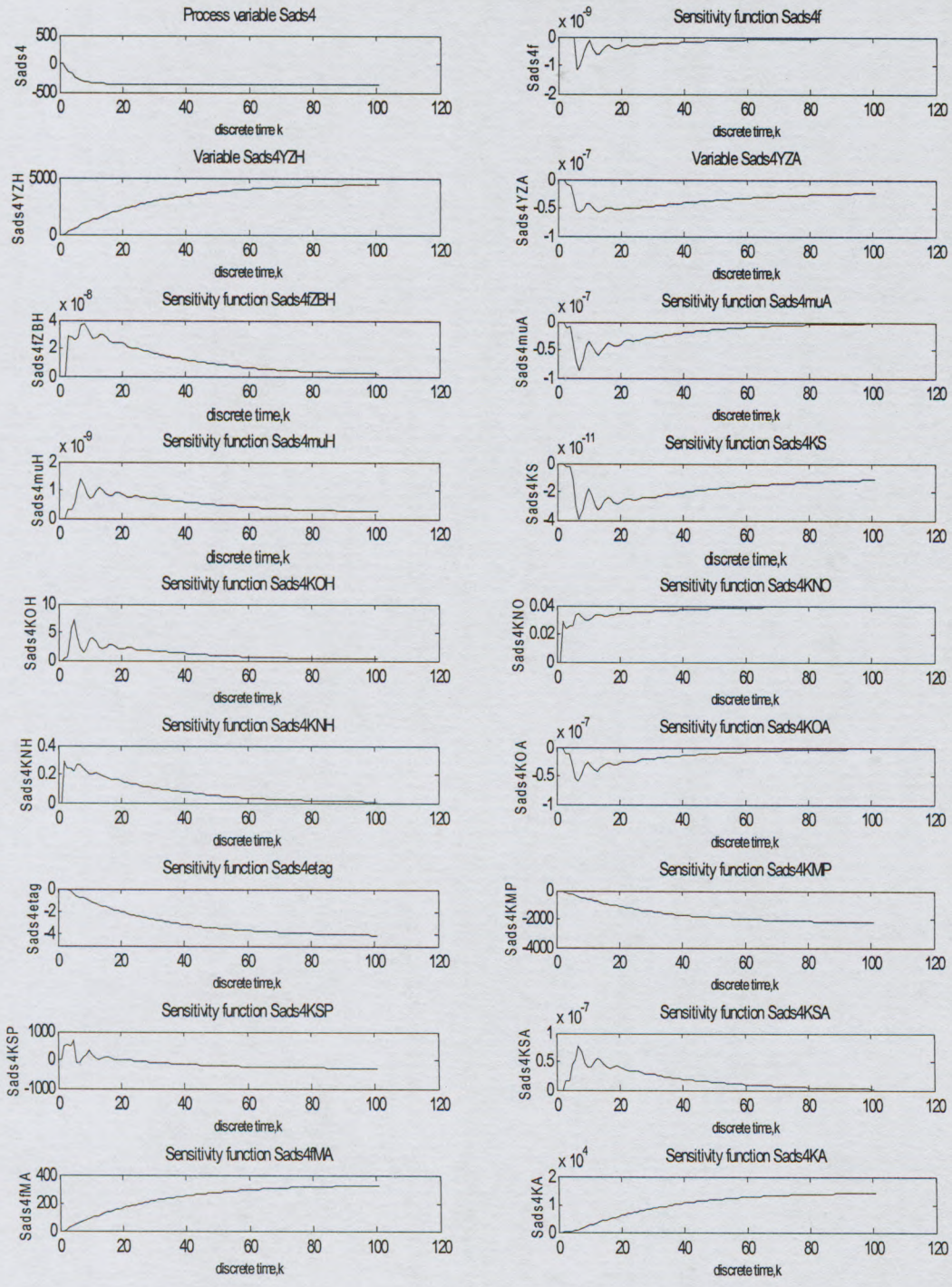

Figure 9.35: Process variable S_{Sads4} and its sensitivity functions towards the model parameters

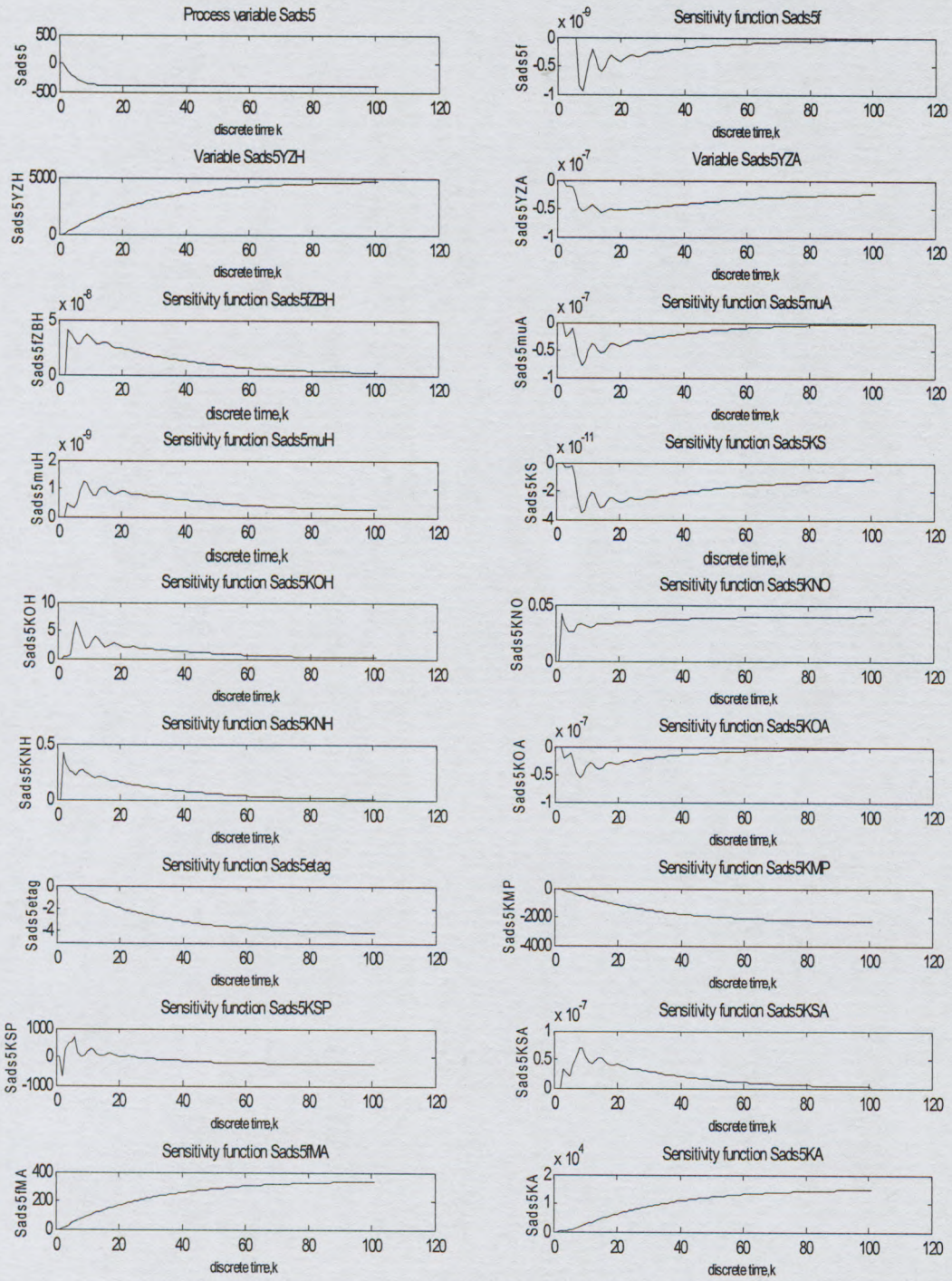

Figure 9.36: Process variable S_{Sads5} and its sensitivity functions towards the model parameters

9.2.2.3. Discussion of the results

9.2.2.3.1 Benchmark process with ASM1 reduced biological model

In order to compare behaviour of different sensitivity functions the minimum and maximum values of the sensitivity functions according to the model parameters are given in Table 9.1.

Table 9.1: The maximum or minimum values of sensitivity functions simulation for the Benchmark process model based on the reduced ASM1 biological model

Para / Frac	Maximum or minimum values of the sensitivity functions														
	f	YH	YA	iXB	muA	muH	KS	KOH	KNO	KNH	KOA	etag	etah	Kh	Kx
Snh 1-2	0.18	-1	490	-300	-200	-45	1	8	1.2	100	80	-5	-5	0.6	2
SNO 1-2	0.2	-15	-490	-400	200	-95	8	-18	8	-98	-50	-15	-15	-1	3
SS 1-2	-0.4	100	-1.8	75	-0.75	-200	4	-90	-10.5	± 0.4	0.25	3	25	60	-150
Snh 3-5	0.18	-1	490	-300	-200	-45	1	8	1.2	100	80	-5	-3	0.6	2
SNO 3-5	0.2	-15	-490	-400	200	-95	8	-18	6	-98	-50	-15	-0.4	-1	3
SS 3-5	-0.4	150	-1.8	75	-0.75	-200	4	-90	-10.5	0.4	0.25	2	25	60	-150

The sensitivity functions of Snh for the parameters YA, KNH and KOA grow progressively for tanks 1 and 2 (see Table 9.1). The sensitivity functions of Snh for the parameters iXB, muA and muH decay progressively for tanks 1 and 2 (see Table 9.1). The sensitivity functions of SNO for the parameter muA grow progressively for tanks 1 and 2 (see Table 9.1). The sensitivity functions of SNO for the parameters YH, YA,iXB,muH, KNH, KOA, etag and etah decay progressively for tanks 1 and 2 (see Table 9.1). The sensitivity functions of SS for the parameters YH, iXB, etah and Kh grow progressively for tanks 1 and 2 (see Table 9.1). The sensitivity functions of SS for the parameters muH, KOH and Kx decay progressively for tanks 1 and 2 (see Table 9.1). The sensitivity functions of Snh for the parameters YA, KNH and KOA grow significantly for tanks 3 to 5 (see Table 9.1). The sensitivity functions of Snh for the parameters iXB, muA and muH decay significantly for tanks 3 to 5 (see Table 9.1). The sensitivity functions of SNO for the parameter muA grow significantly for tanks 3 to 5 (see Table 9.1). The sensitivity functions of SNO for the parameters YH, YA, iXB, muH, KOH, KNH, KOA and etag decay significantly for tanks 3 to 5 (see Table 9.1). The sensitivity functions of SS for the parameters YH, iXB, etah and Kh grow significantly for tanks 3 to 5 (see Table 9.1). The sensitivity functions of SS for the parameters muH, KOH and Kx decay significantly for tanks 3 to 5 (see Table 9.1).

It can be concluded from Table 9.1 that the process variables are more sensitive towards the parameters YA, iXB, muA, muH, KNH, KOH, KOA and Kh. The sensitivity of the variables SNH and SNO is higher than this of the variables SS for the parameters YA, YH, muA, KNH and KOA. The sensitivity of the variable SS is higher for the parameters KOH, Kh and Kx.

9.2.2.3.2 Benchmark process with UCT reduced biological model

The minimum and maximum values of the sensitivity functions of the variables towards the UCT model parameters are summarized in Table 9.2.

Table 9.2: The maximum or minimum values of sensitivity function simulation for the Benchmark process model based on the reduced UCT biological model

para / Frac	Maximum or minimum values of the sensitivity functions																
	f	YZH	YZA	fZBH	muA	muH	KS	KOH	KNO	KNH	KOA	etag	KMP	KSP	KSA	fMA	KA
Snh1-2	35	-0.8	275	-1900	-500	-39	-0.4	190	-0.1 E-3	110	500	-0.5	95	105	2	0.5 E-3	0.02
SNO 1-2	4E-3	-4	30	-0.1	4	-0.3	0.015	-0.8	3E-3	-120	2	-0.5	3	0.49	-4	-0.4	17
SS1-2	-0.5 E-10	38	-1E-9	0.5 E-9	-1E-9	-500	35	0.25	0.06	3.5 E-3	-1.5E-7	0.6 E-10	-1E-11	-5E-11	1.5 E-7	3E-12	1.5E-10
Sads 1-2	-2E-9	4000	-0.2 E-7	4E-8	-0.8 E-7	1.2 E-9	-0.8 E-11	10	0.037	0.38	-0.25 E-7	-3.8	-2000	-200	1E-7	350	1.2E4
Snh3-5	35	-0.8	275	-1900	-500	-39	-0.4	190	-0.1 E-3	110	500	-0.5	100	105	2	0.5 E-3	0.02
SNO 3-5	3.5 E-3	-4	30	-0.1	4	-0.3	0.015	-0.8	3E-3	-120	2	-0.5	3	0.49	-4	-0.4	17
SS3-5	-3E-11	38	-1E-9	0.5 E-9	-1E-9	-500	35	0.25	0.06	3.5 E-3	-1.5E-7	0.6 E-10	-1E-11	-5E-11	1.5 E-7	3E-12	1.5E-10
Sads 3-5	-2E-9	4500	-0.2 E-7	4E-8	-0.8 E-7	1.2 E-9	-0.8 E-11	10	0.037	0.38	-0.25 E-7	-3.8	-2000	-200	1E-7	350	1.2E4

The sensitivity functions of Snh for the parameters f, YZA, KOH, KNH, KOA, KMP and KSP grow significantly for tanks 1 and 2 (see Table 9.2). The sensitivity functions of Snh for the parameters fZBH, muA and muH decay significantly for tanks 1 and 2 (see Table 9.2). The sensitivity functions of SNO for the parameter YZA grow significantly for tanks 1 and 2 (see Table 9.2). The sensitivity functions of SNO for the parameter KNH decay significantly for tanks 1 and 2 (see Table 9.2). The sensitivity functions of SS for the parameters YZH and KS grow significantly for tanks 1 and 2 (see table 9.2). The sensitivity functions of Sads for the parameters YZH and fMA grow significantly for tanks 1 and 2 (see Table 9.2). The sensitivity functions of Sads for the parameters KMP and KSP decay significantly for tanks 1 and 2 (see Table 9.2). The sensitivity functions of Snh for the parameters f, YZA, KOH, KNH, KOA, KMP and KSP grow significantly for tanks 3 to 5 (see Table 9.2). The sensitivity functions of Snh for the parameters fZBH, muA and muH decay significantly for tanks 3 to 5 (see Table 9.2). The sensitivity functions of SNO for the parameters YZA and KA grow significantly for tanks 3 to 5 (see Table 9.2). The sensitivity functions of SNO for the parameter KNH decay significantly for tanks 3 to 5 (see Table 9.2). The sensitivity functions of SS for the parameter YZH and KS grow significantly for tanks 3 to 5 (see Table 9.2). The sensitivity functions of SS for the parameter muH decay significantly for tanks 3 to 5 (see Table 9.2). The sensitivity functions of Sads for the parameters YZH, fMA and KA grow significantly for tanks 3 to 5 (see Table 9.2).

The following can be concluded on the basis of analysis of the data from Table 9.2. The process variable SNH is most sensitive towards parameters f, YZA, fZBH, muA, muH, KOH, KNH, KOA, KMP and KSP. The variable SNO is more sensitive towards parameters YZA, KA, and KNH. The variable SS is more sensitive towards the parameters YZH and KS. The variable Sads is more sensitive towards the parameters YZH, KA, KMP and KSP.

9.2.3. Sensitivity function simulation for the Athlone process model based on the reduced ASM1 and UCT biological models

The reduced ASM1 biological model is described in the Chapter 4, point 4.4 and the reduced UCT biological model is described in point 4.5. The nominal kinetic parameters are given in Table 4.2 for the reduced ASM1 and in Table 4.4 for the reduced UCT biological models. The values of the processes tank's volumes for the Athlone process are given in the Chapter 3, Table 3.9.The mass balance models for Athlone process based on both ASM1 and UCT reduced models are described in point 4.6.3. The corresponding sensitivity models are derived in Chapter 5, point 5.4.

9.2.3.1 Results for the ASM1 reduced biological model

Simulations of the sensitivity functions are done for the initial conditions of the process variables given by the vector x_0 and zero for the sensitivity functions. The sampling period is DT = 0.01042. The inflow concentration is hundred times less than the average one for dry weather, given by the vector Xi

X_0=[7.918;5.37;2.808;8.344;3.662;1.459;5.548;6.541;1.15]
Xi=[0.3156 0 0.6950]

The simulation is done for steady state conditions of the biomass and the slowly biodegradable substrate given by the vectors

```
XBH = 0.01*[2551.76*ones(1,K);2553.38*ones(1,K);2557.13*ones(1,K)];
XBA = 0.01*[148.389*ones(1,K);148.309*ones(1,K);148.941*ones(1,K)];
XS =  0.01*[82.135*ones(1,K);76.386*ones(1,K);64.855*ones(1,K)];
```

The dissolved oxygen concentration is U=[0.2;0.2;4].

The process reduced state space mass balance model matrices are:

A=

0.2746	0	0	0.3623	0	0	0	0	0
0	0.2746	0	0	0.3623	0	0	0	0
0	0	0.2746	0	0	0.3623	0	0	0
0.7254	0	0	-0.4508	0	0	0.7254	0	0
0	0.7254	0	0	-0.4508	0	0	0.7254	0
0	0	0.7254	0	0	-0.4508	0	0	0.7254
0	0	0	0.3159	0	0	0.6841	0	0
0	0	0	0	0.3159	0	0	0.6841	0
0	0	0	0	0	0.3159	0	0	0.6841

B=

0.4537	0	0
0	0.3631	0
0	0	0.3631
zeros(6,3)		

C_n=

-0.0008	0	-0.0156	
-0.0008	-0.0018	-0.0156	, n= 1:3
-0.0443	0.0434	0	
0	0	0.0104	

The results from the simulations are given from Figure 9.37 till Figure 9.45.

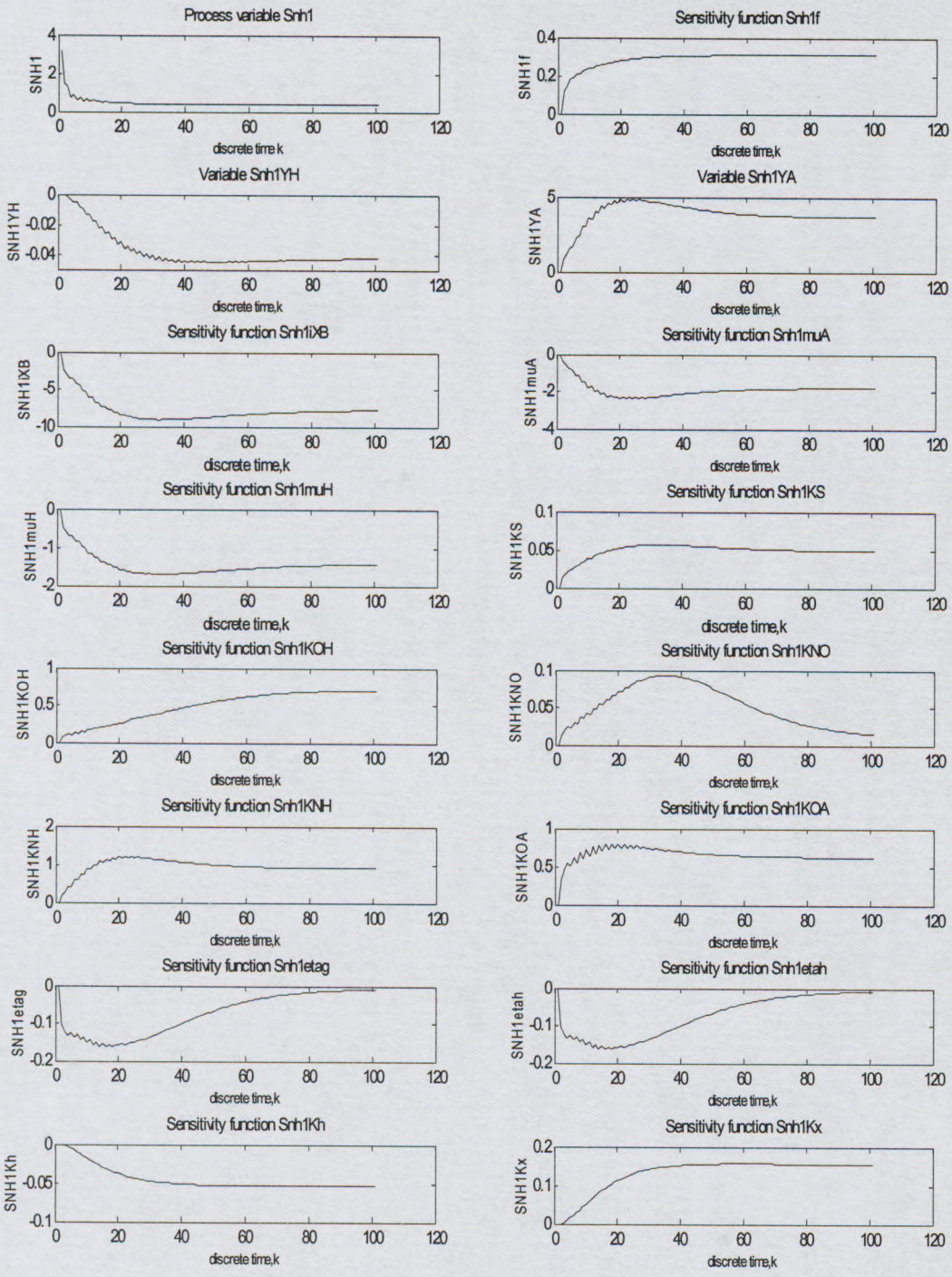

Figure 9.37: Process variable S_{SNH1} and its sensitivity functions towards the model parameters

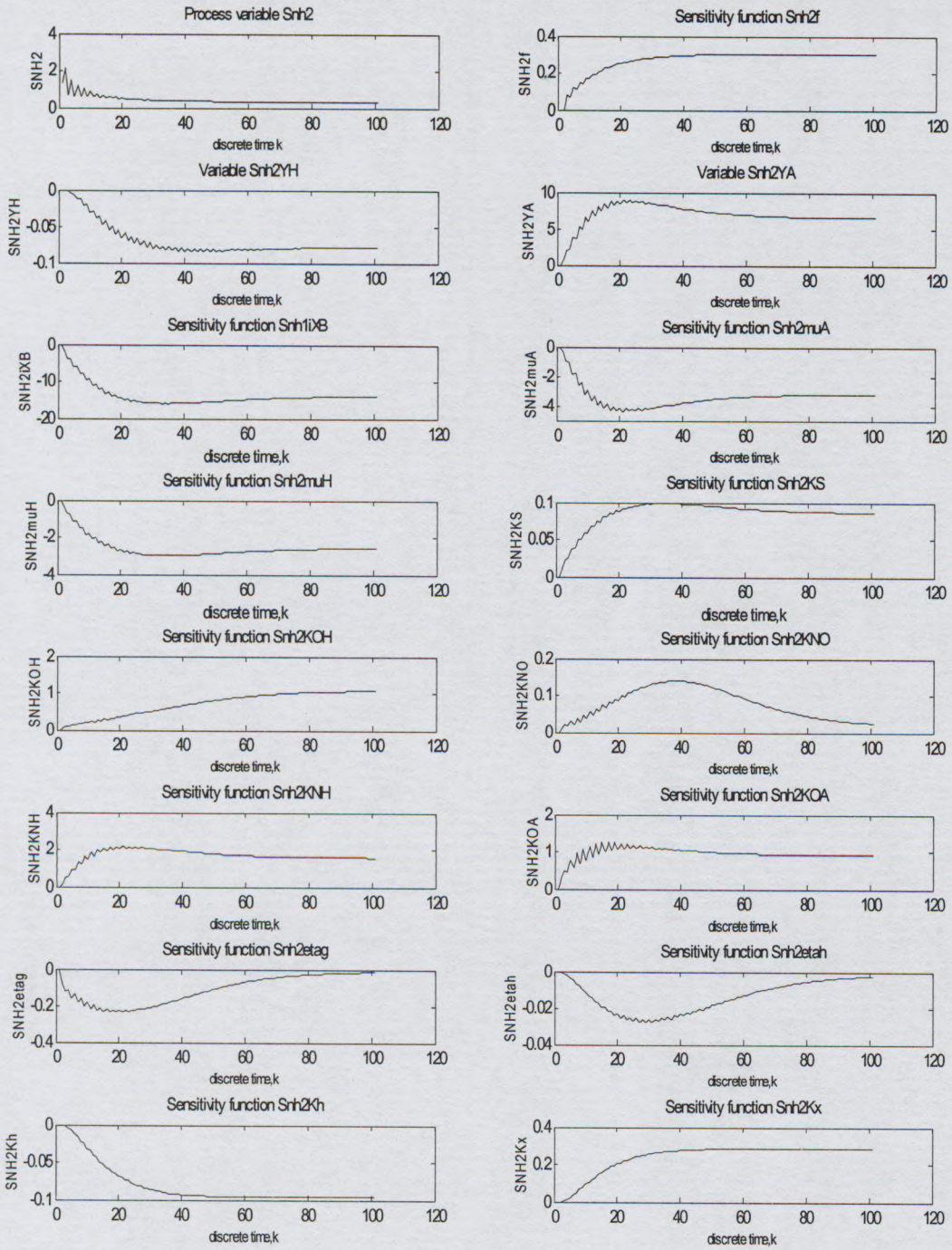

Figure 9.38: Process variable S_{SNH2} and its sensitivity functions towards the model parameters

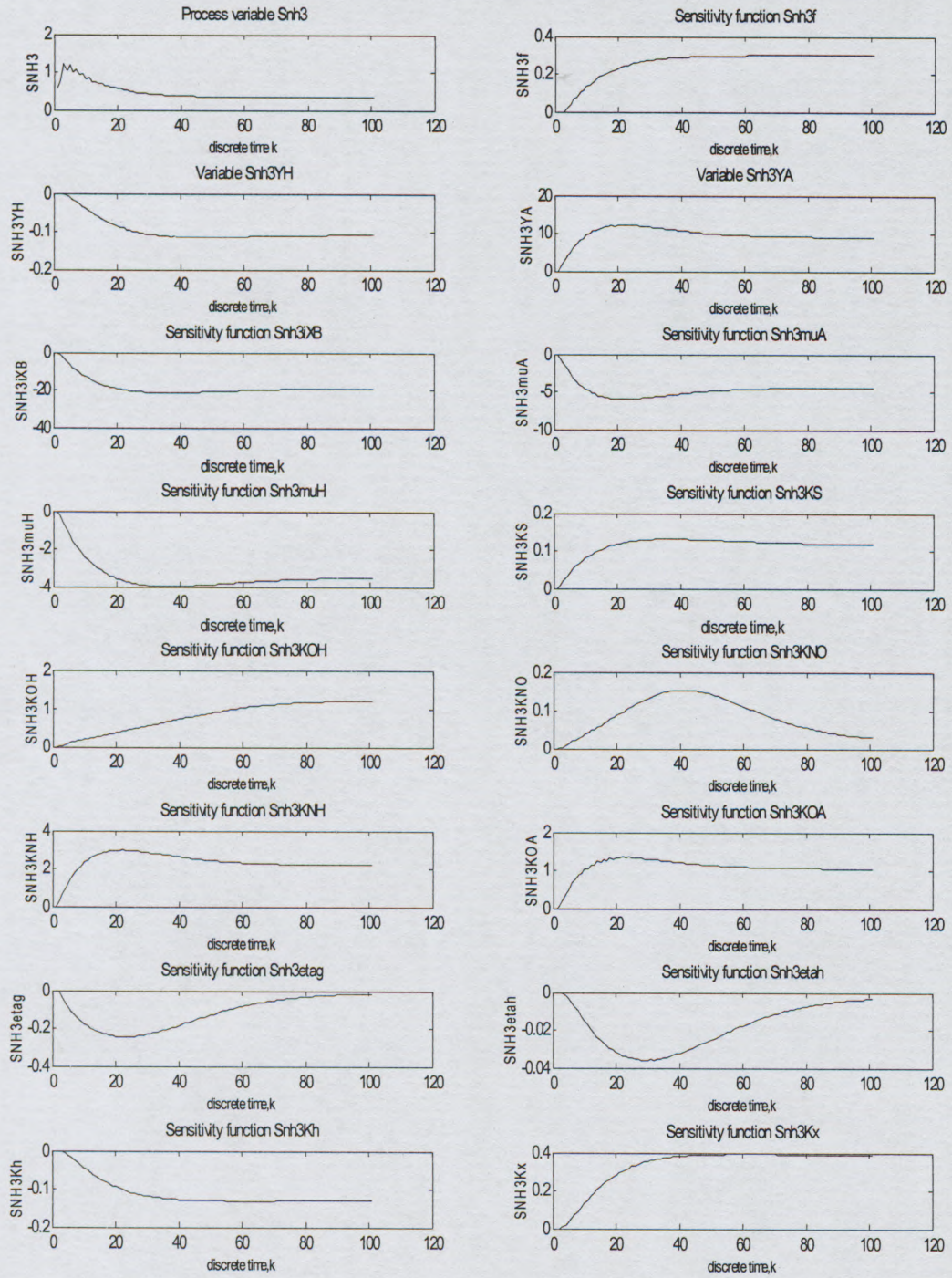

Figure 9.39: Process variable S_{SNH3} and its sensitivity functions towards the model parameters

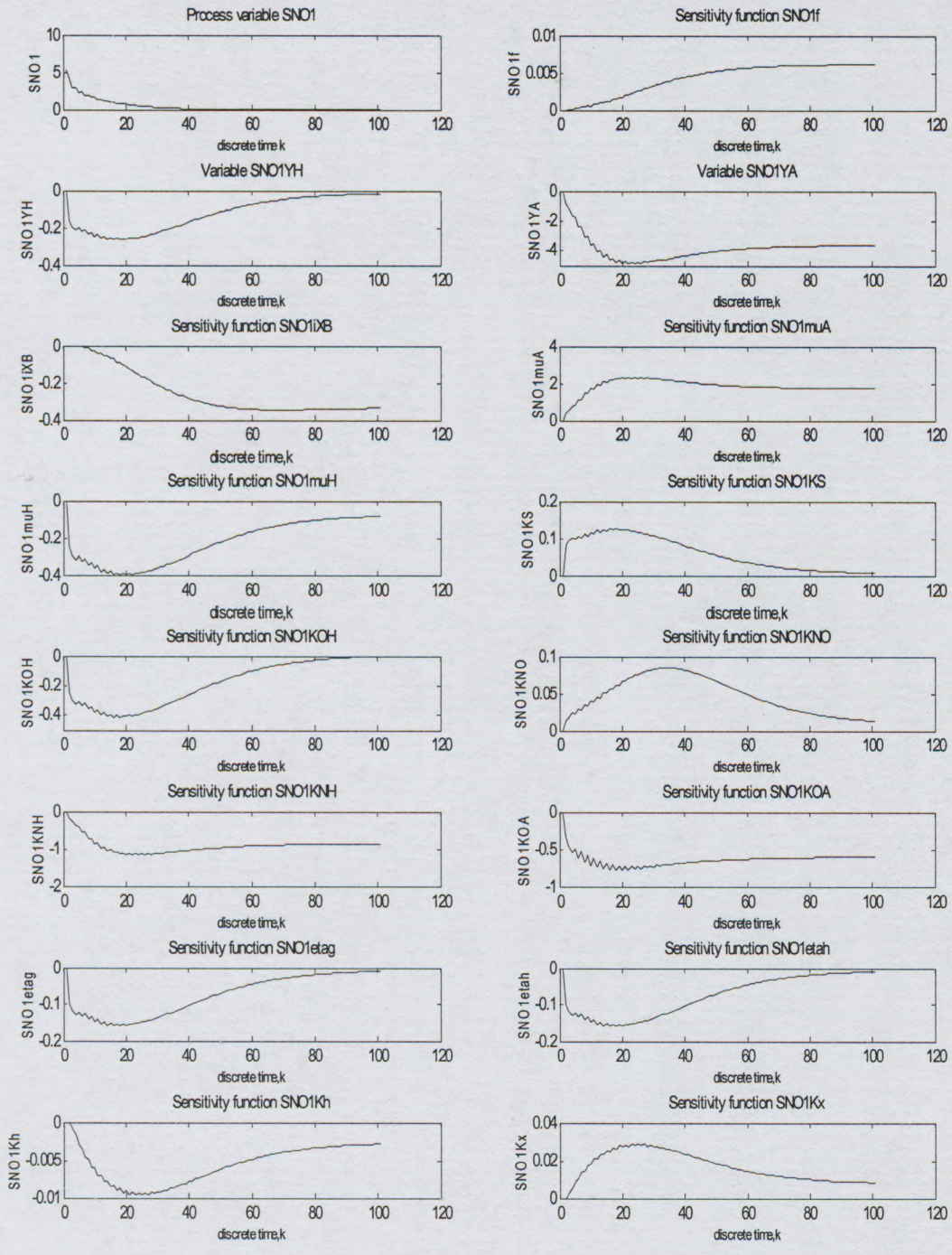

Figure 9.40: Process variable S_{SNO1} and its sensitivity functions towards the model parameters

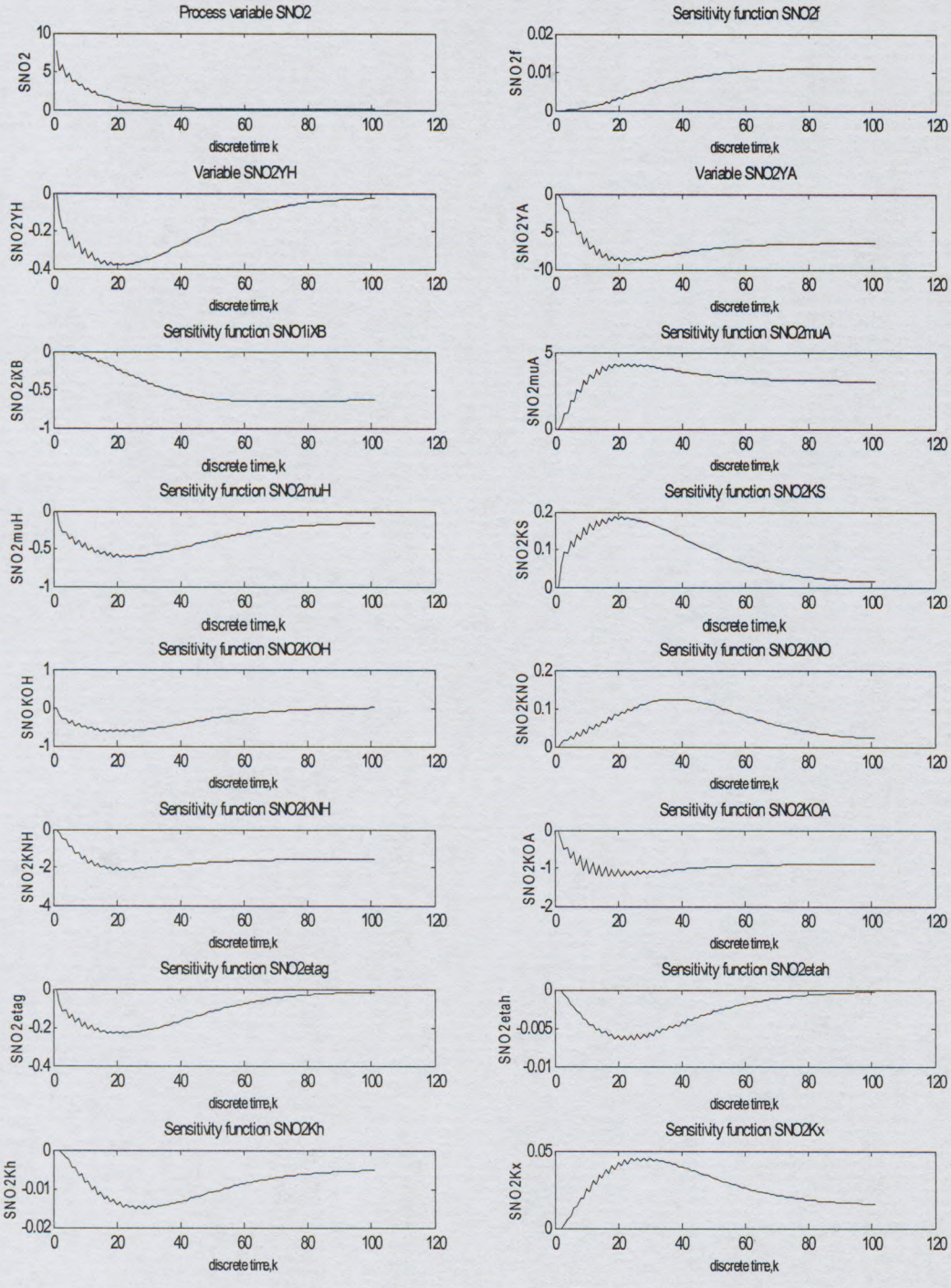

Figure 9.41: Process variable S_{SNO2} and its sensitivity functions towards the model parameters

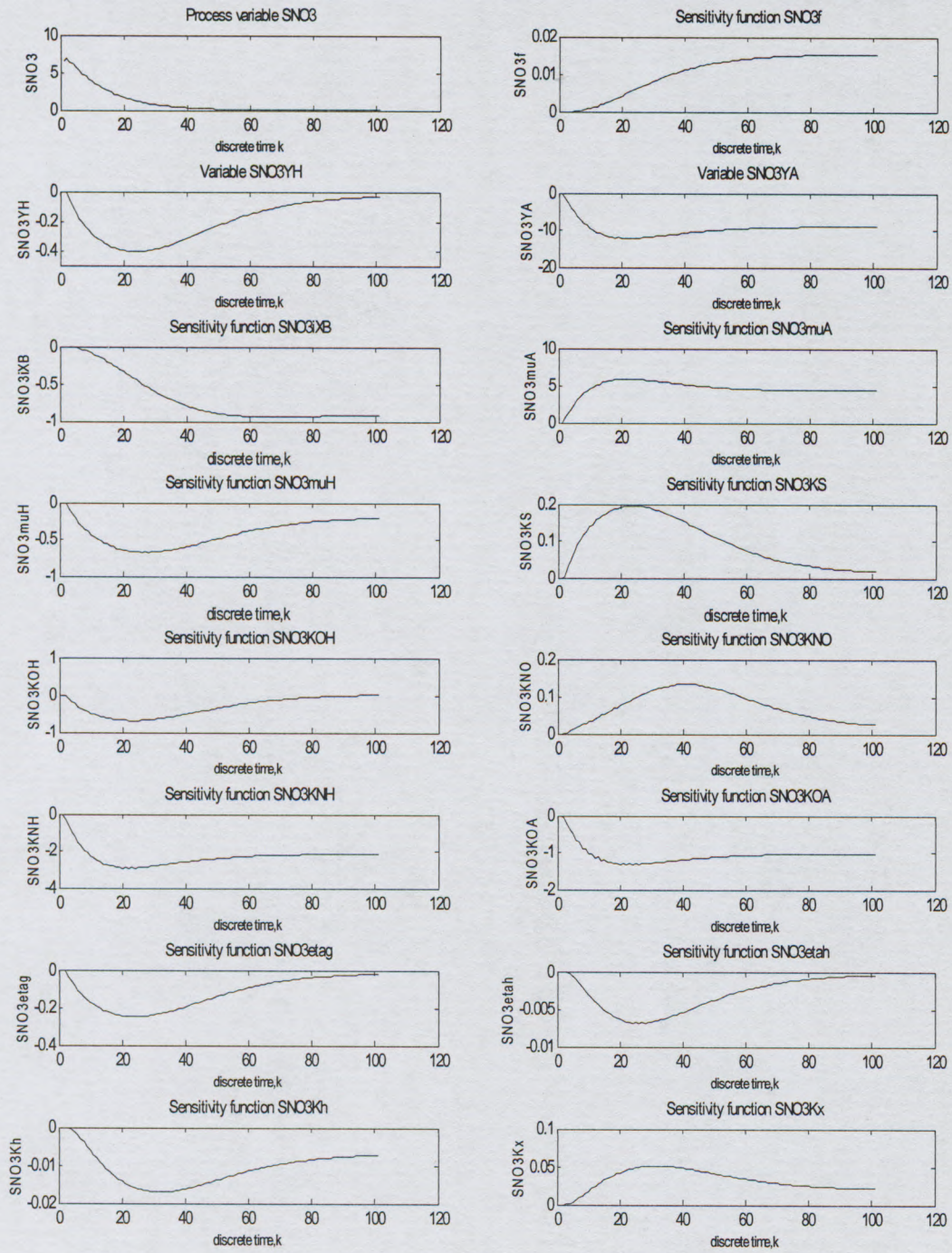

Figure 9.42: Process variable S_{SNO3} and its sensitivity functions towards the model parameters

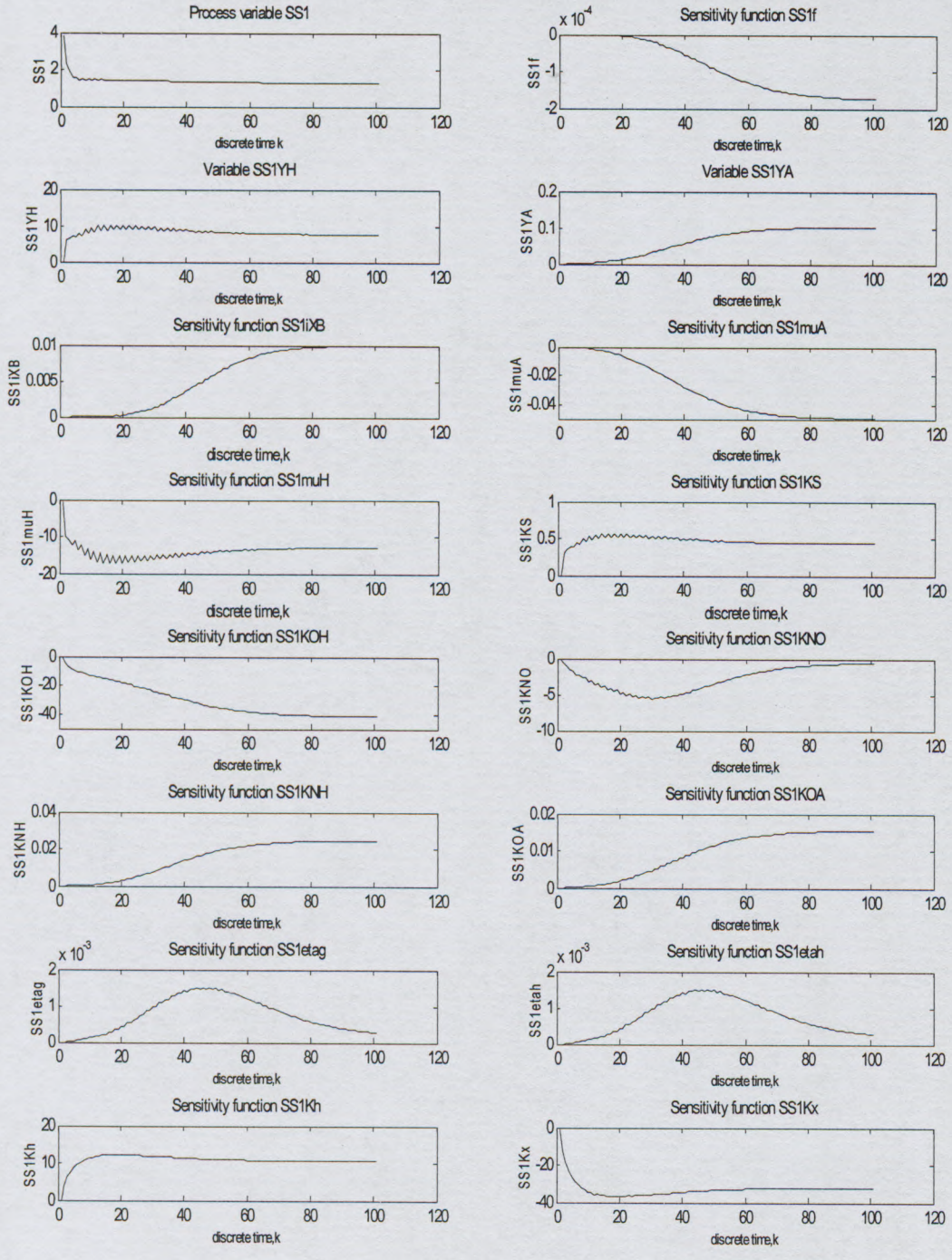

Figure 9.43: Process variable S_{SS1} and its sensitivity functions towards the model parameters

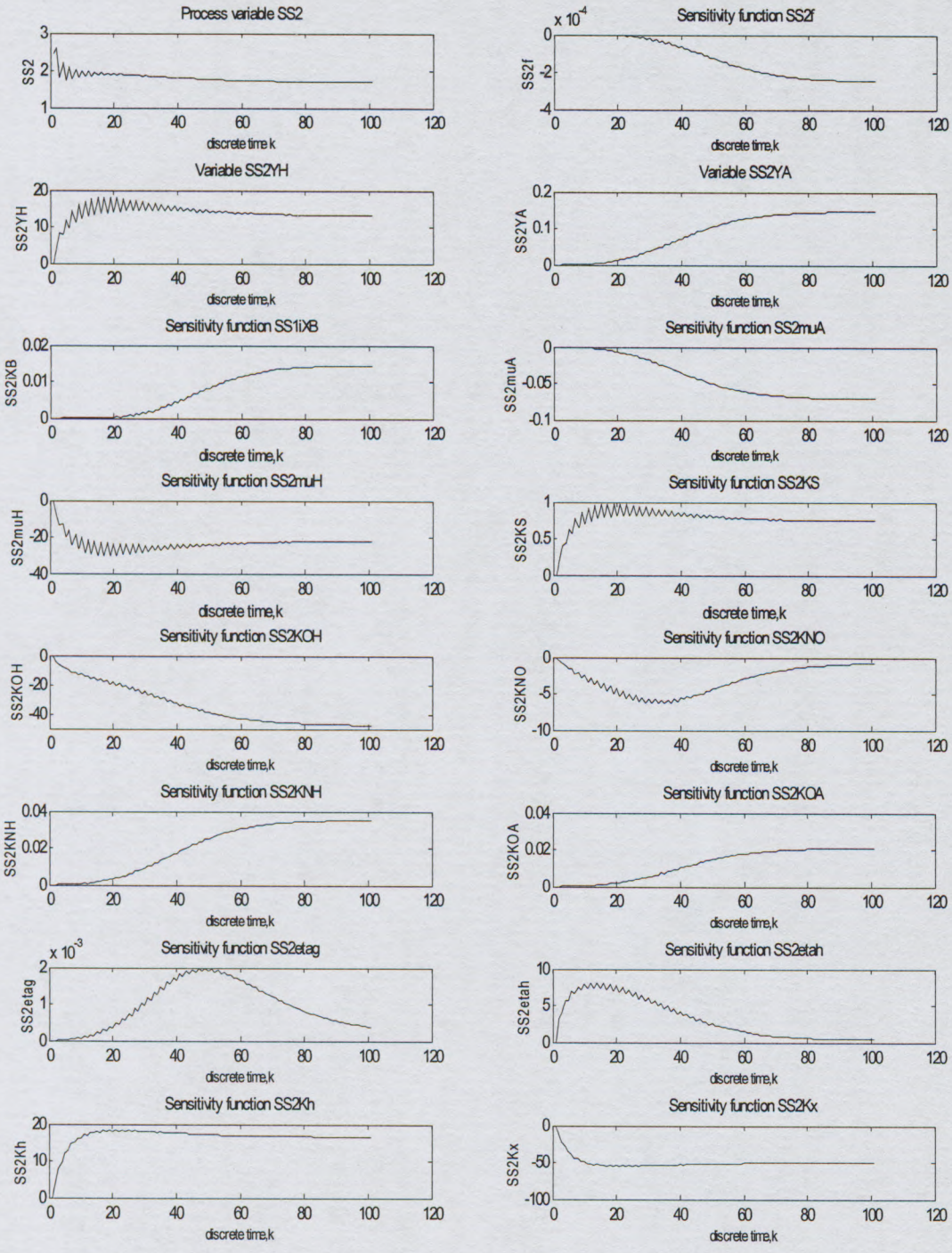

Figure 9.44: Process variable S_{SS2} and its sensitivity functions towards the model parameters

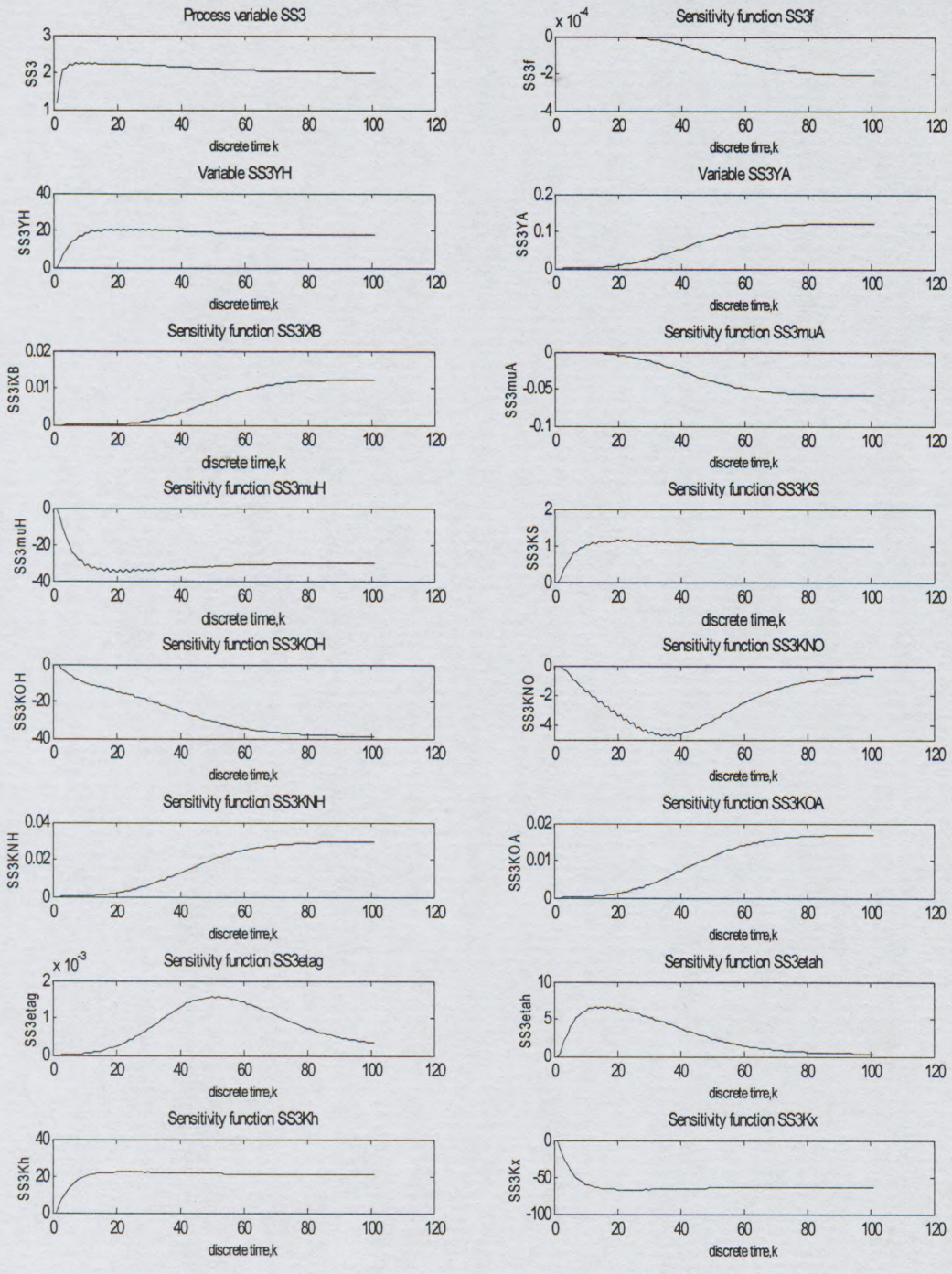

Figure 9.45: Process variable S_{SS3} and its sensitivity functions towards the model parameters

9.2.3.2 Results for the UCT reduced biological model

Simulations of the sensitivity functions are done for the initial conditions of the process variables given by the vector x_0 and zero for the sensitivity functions. The sampling period is DT = 0.01042. The inflow concentration is hundred times less than the average one for dry weather, given by the vector X_{iUCT}

X_0=[7.918;5.37;2.808;5.3;8.344;3.662;1.459;5.15;5.548;6.541;1.15;5.1]
X_i=[3.156 0 6.950 20.2]
The simulation is done for steady state conditions of the biomass and the slowly biodegradable substrate given by the vectors

```
XBH = 0.05*[2551.76*ones(1,K);2553.38*ones(1,K);2557.13*ones(1,K)];
XBA = 0.05*[148.389*ones(1,K);148.309*ones(1,K);148.941*ones(1,K)];
XS =  0.05*[82.135*ones(1,K);76.386*ones(1,K);64.855*ones(1,K)];
```

The vector of the dissolved oxygen concentration is U=[0.2;0.2;4].

The process reduced state space mass balance model matrices are:

```
Au=
 0.2746       0       0       0  0.3623       0       0       0       0       0       0       0
      0  0.2746       0       0       0  0.3623       0       0       0       0       0       0
      0       0  0.2746       0       0       0  0.3623       0       0       0       0       0
      0       0       0  0.2746       0       0       0  0.3623       0       0       0       0
 0.7254       0       0       0 -0.4508       0       0       0  0.7254       0       0       0
      0  0.7254       0       0       0 -0.4508       0       0       0  0.7254       0       0
      0       0  0.7254       0       0       0 -0.4508       0       0       0  0.7254       0
      0       0       0  0.7254       0       0       0 -0.4508       0       0       0  0.7254
      0       0       0       0  0.3159       0       0       0  0.6841       0       0       0
      0       0       0       0       0  0.3159       0       0       0  0.6841       0       0
      0       0       0       0       0       0  0.3159       0       0       0  0.6841       0
      0       0       0       0       0       0       0  0.3159       0       0       0  0.6841
```

```
Bu=
 0.4357       0       0       0
      0  0.3631       0       0
      0       0  0.3631       0
      0       0       0  0.3631
 zeros(8,4)
```

```
Cn=
-0.0680       0  -1.4925       0
      0 -0.0680  -1.4925       0
-0.0680 -0.1722  -1.4925       0
      0  0.1042  -1.4925       0
-0.0680       0        0  -1.4925
      0 -0.0680        0  -1.4925
-0.0680 -0.1722        0  -1.4925
      0  0.1042        0  -1.4925
      0       0        0   1.0000
-6.7347  6.6667        0        0
```

The results from simulation are shown from Figure 9.46 till Figure 9.57

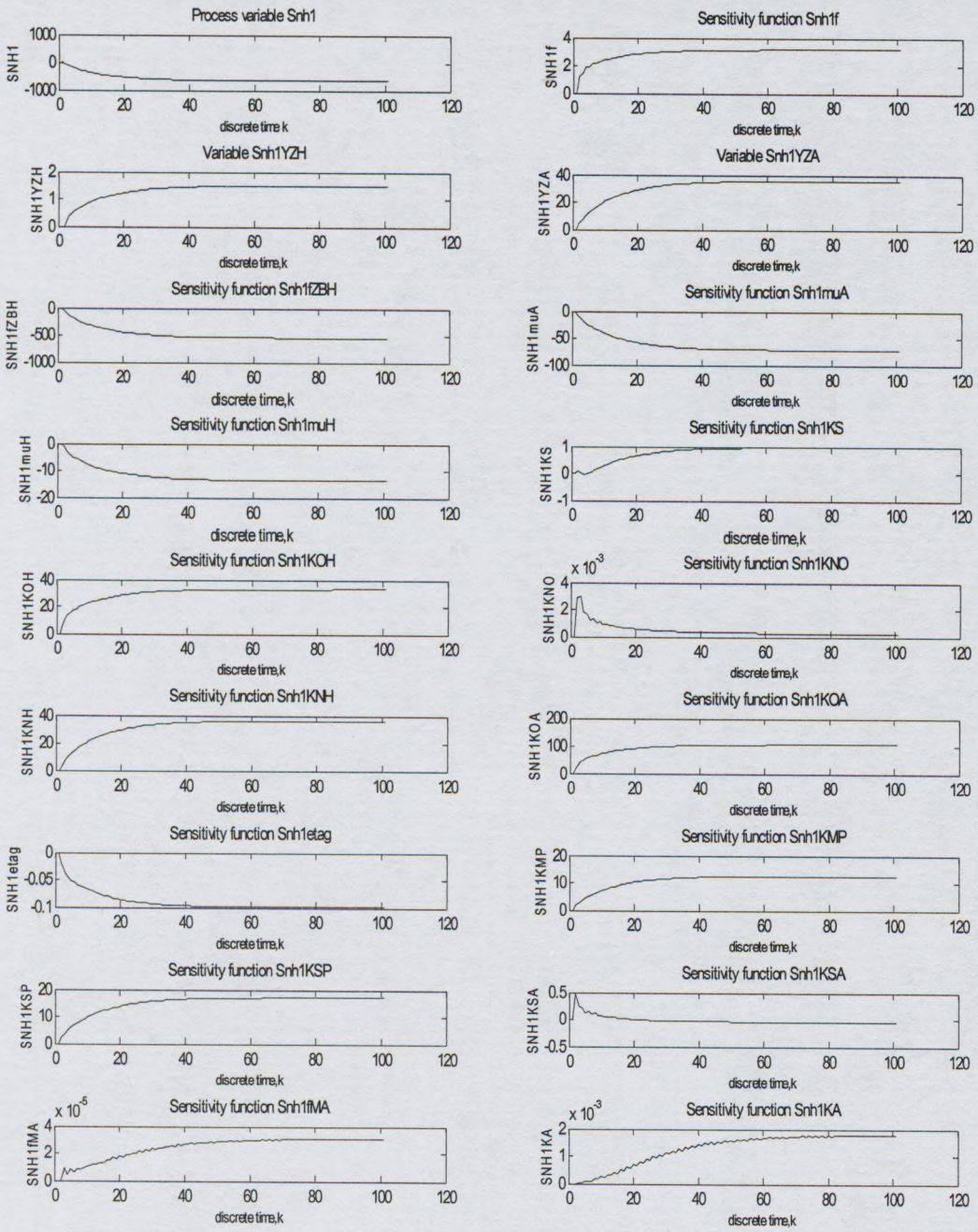

Figure 9.46: Process variable S_{SNH1} and its sensitivity functions towards the model parameters

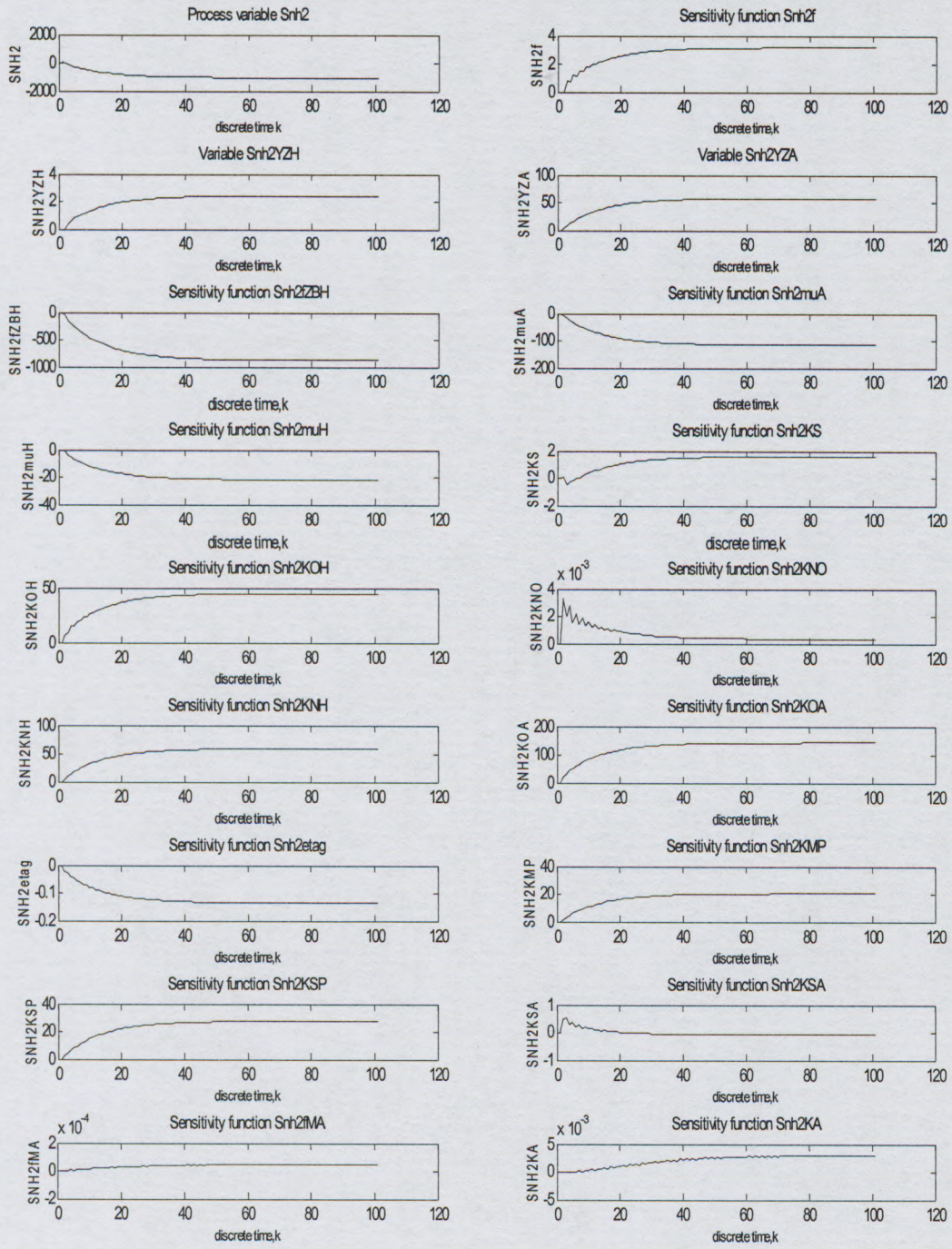

Figure 9.47: Process variable S_{SNH2} and its sensitivity functions towards the model parameters

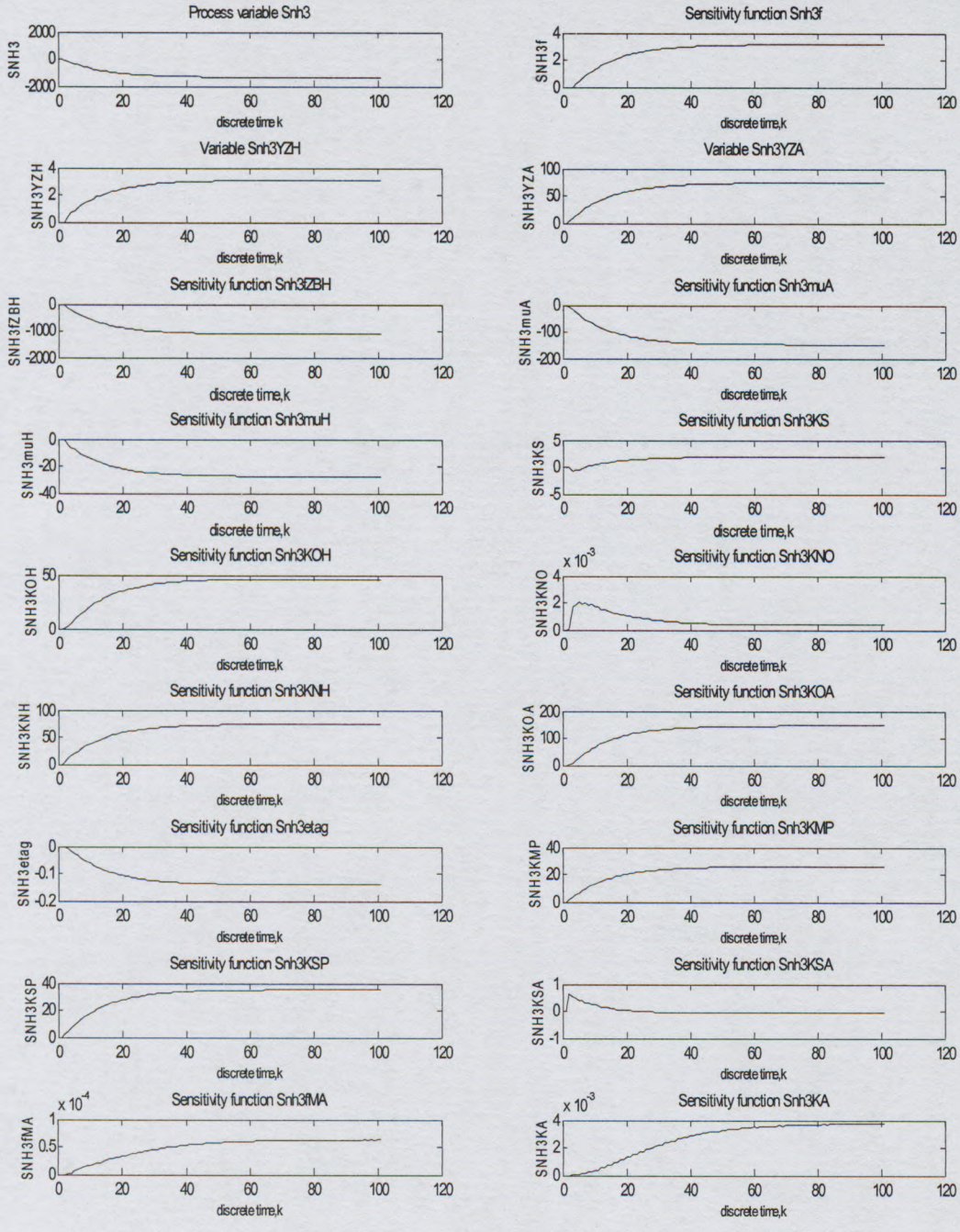

Figure 9.48: Process variable S_{SNH3} and its sensitivity functions towards the model parameters

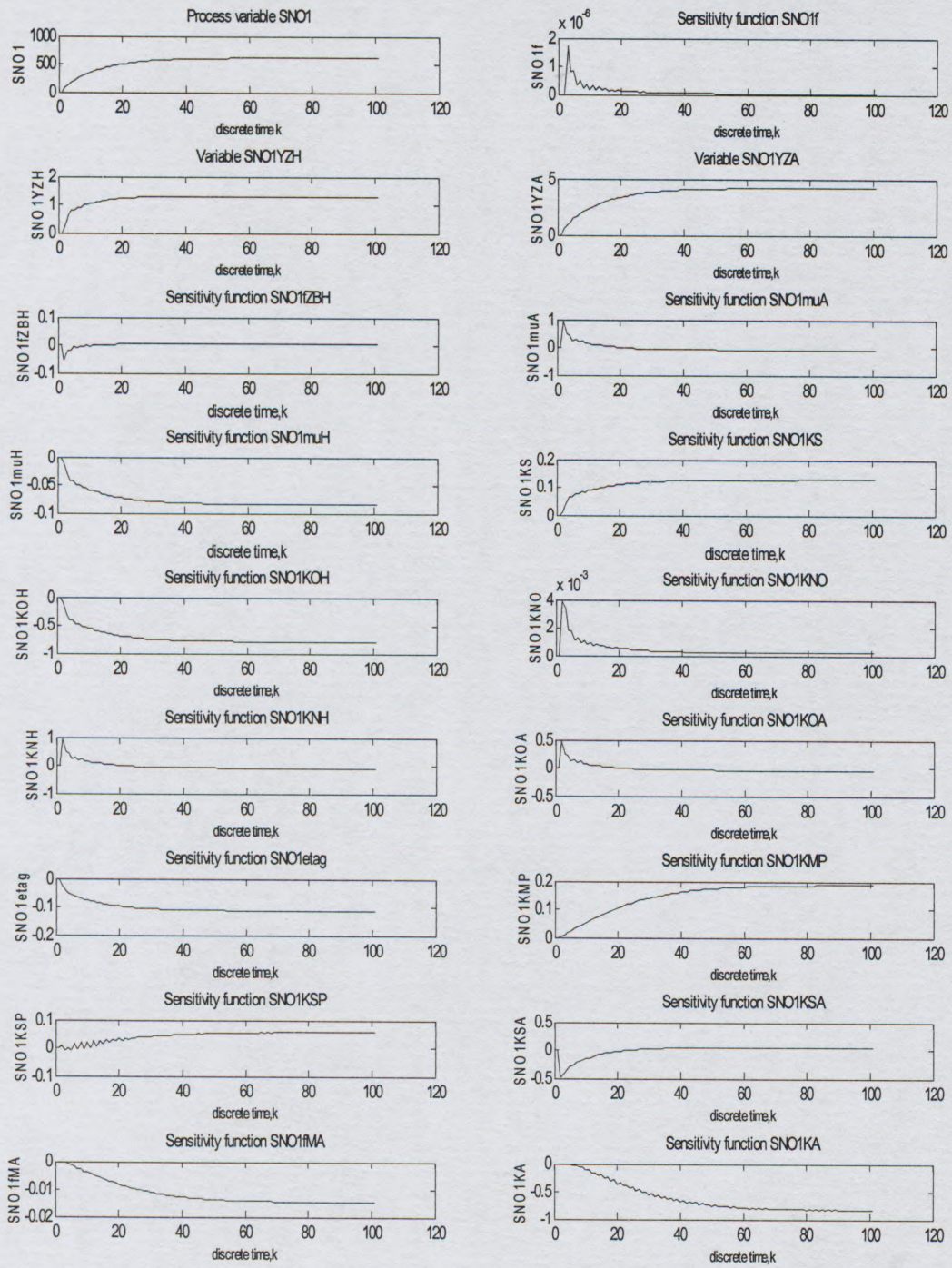

Figure 9.49: Process variable S_{SNO1} and its sensitivity functions towards the model parameters

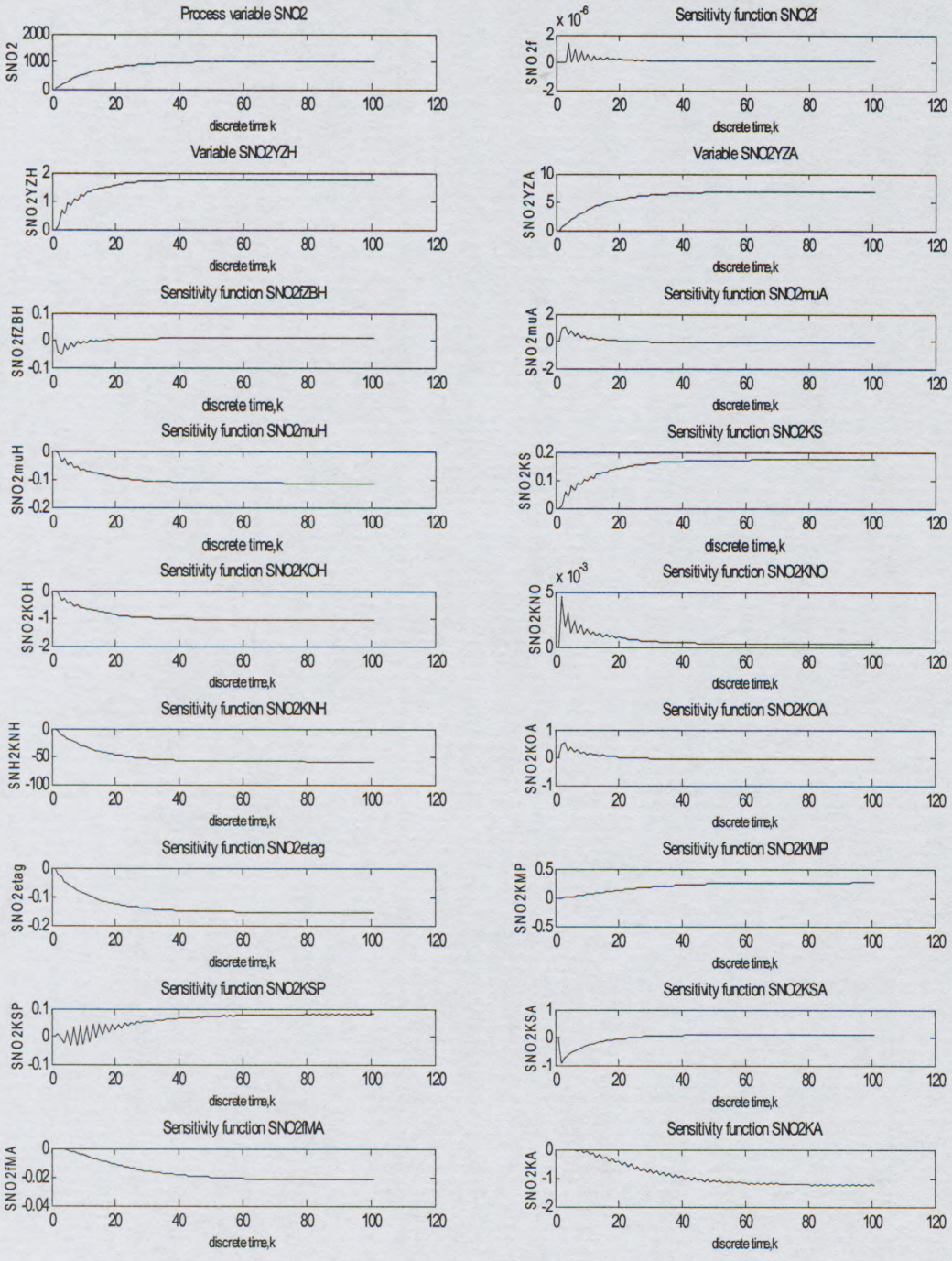

Figure 9.50: Process variable S_{SNO2} and its sensitivity functions towards the model parameters

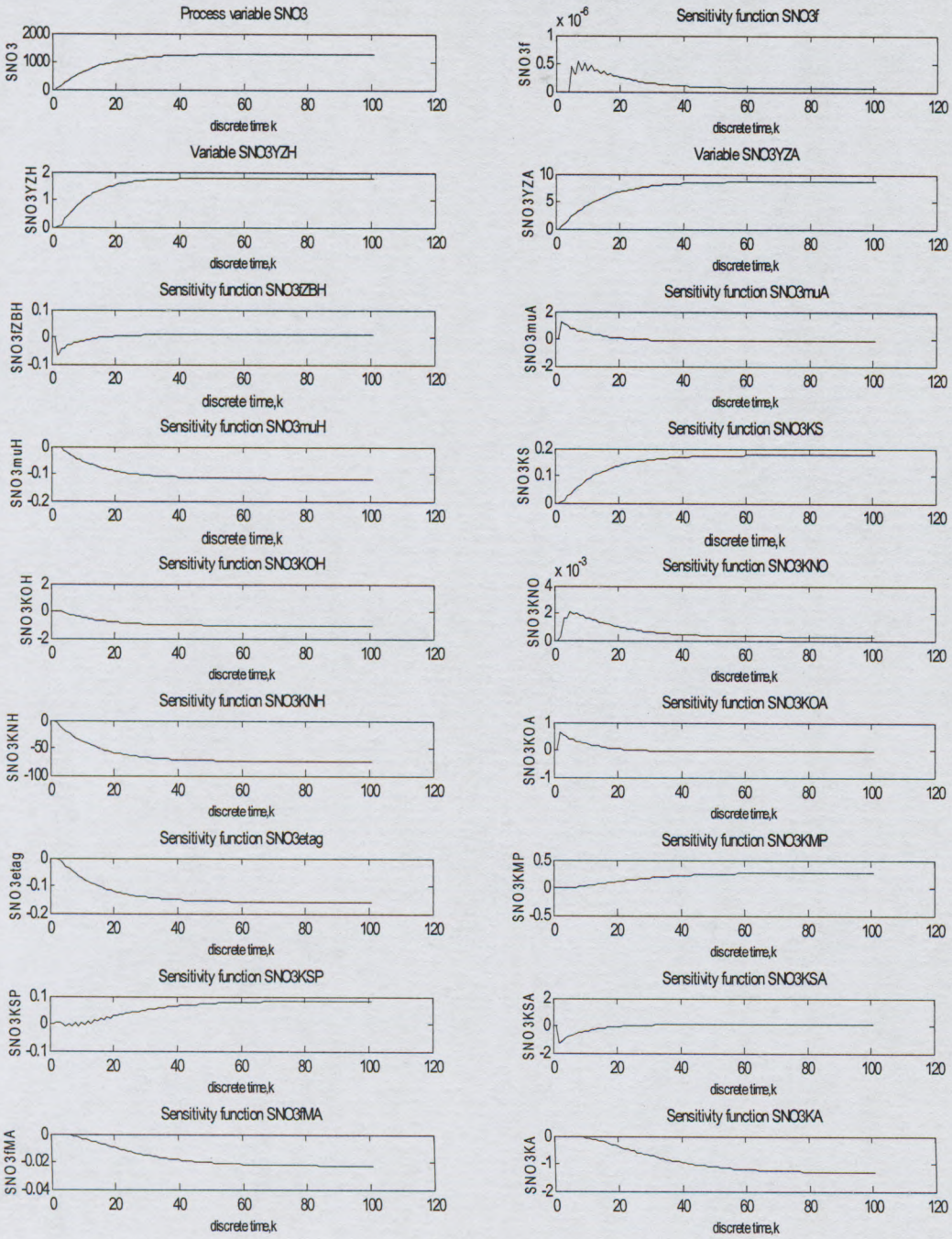

Figure 9.51: Process variable S_{SNO3} and its sensitivity functions towards the model parameters

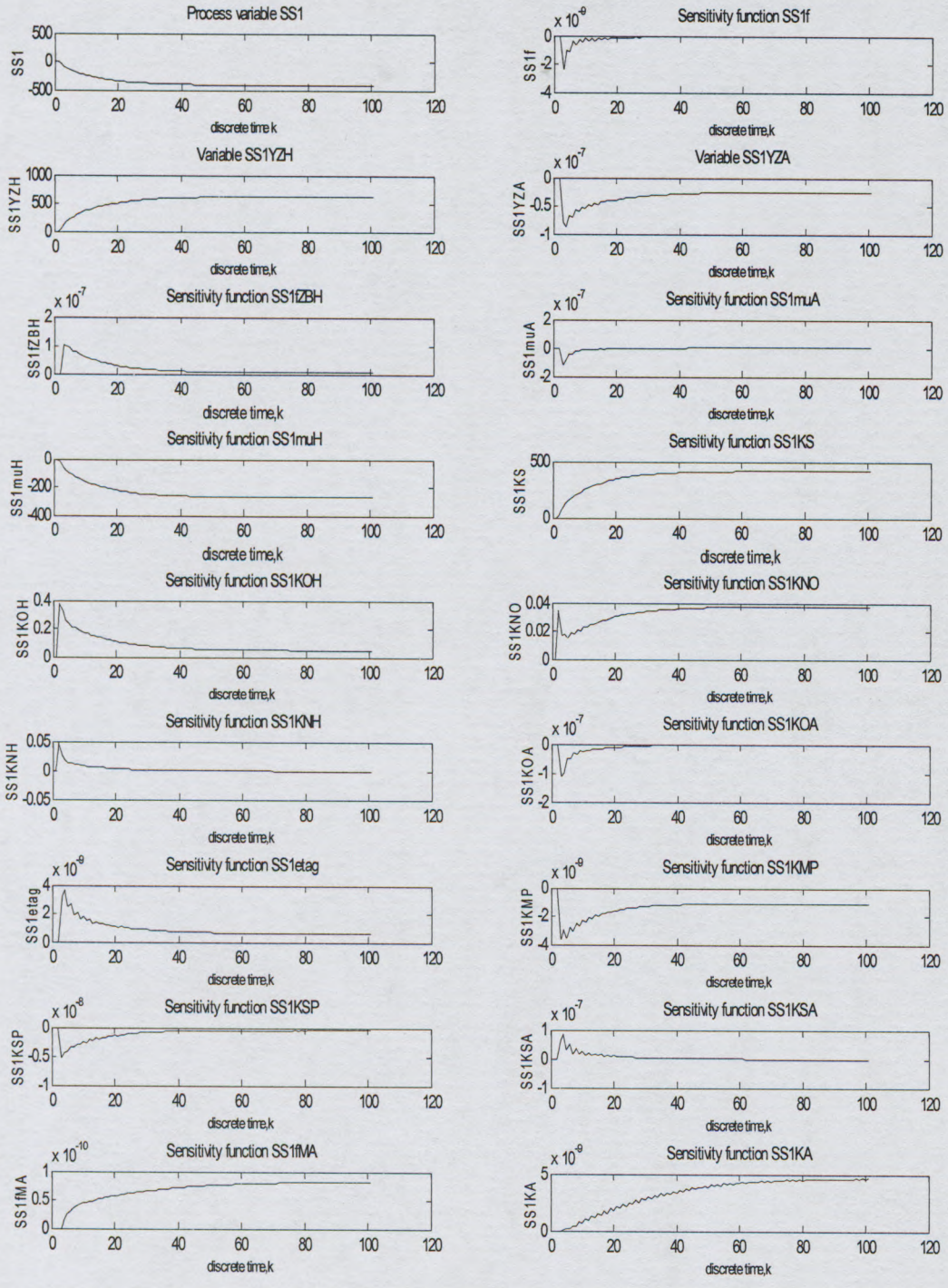

Figure 9.52: Process variable S_{SS1} and its sensitivity functions towards the model parameters

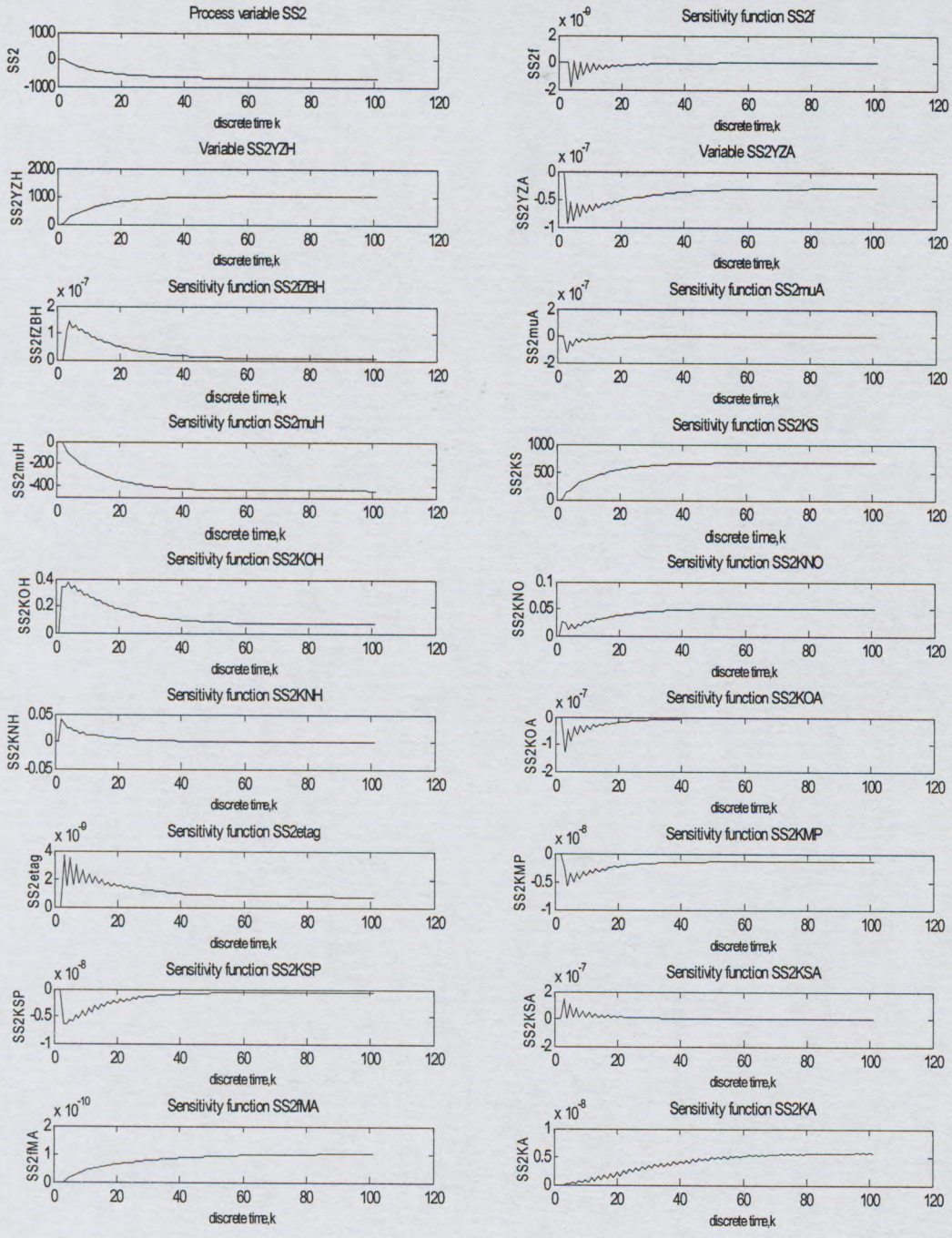

Figure 9.53: Process variable S_{SS2} and its sensitivity functions towards the model parameters

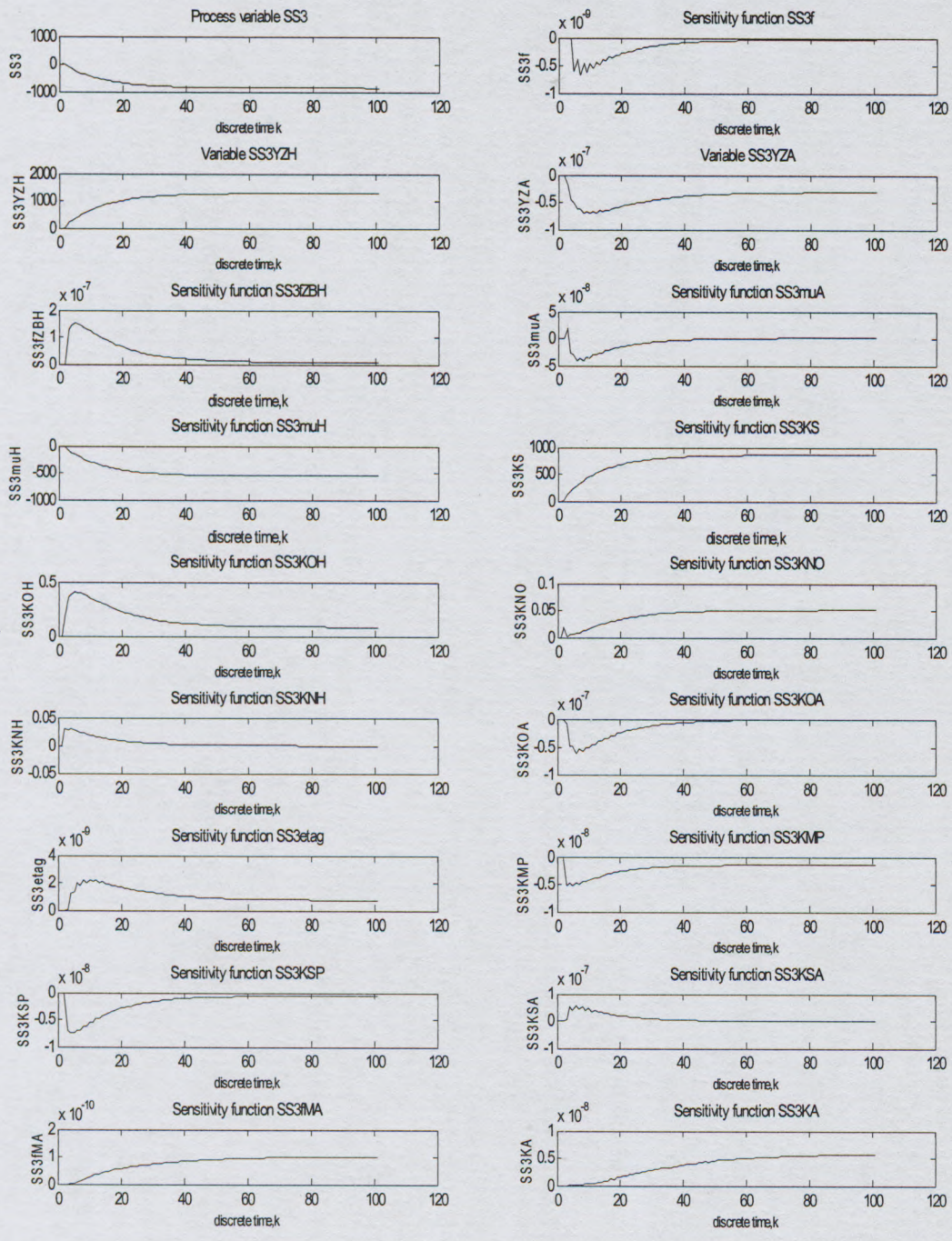

Figure 9.54: Process variable S_{SS3} and its sensitivity functions towards the model parameters

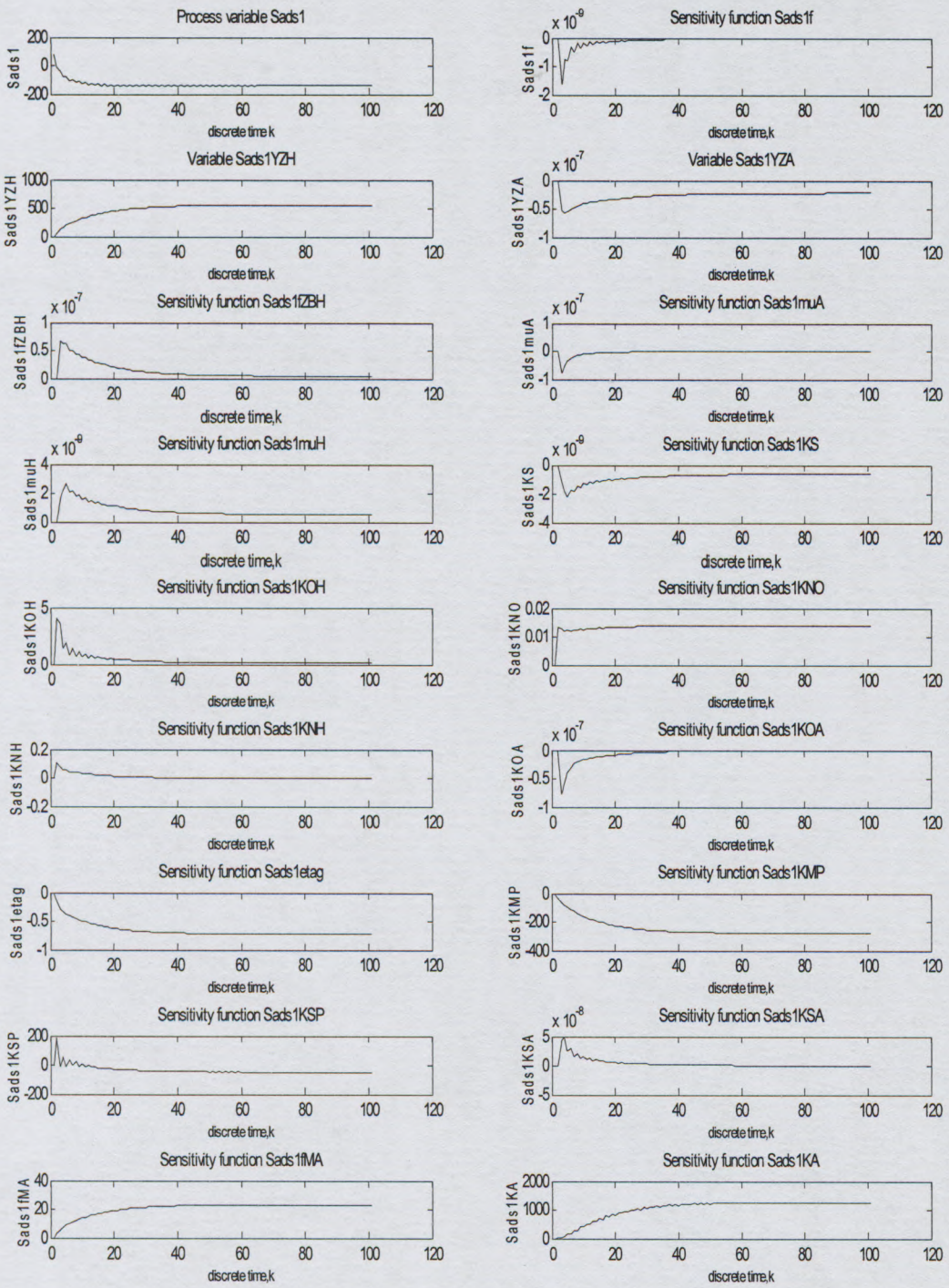

Figure 9.55: Process variable S_{Sads1} and its sensitivity functions towards the model parameters

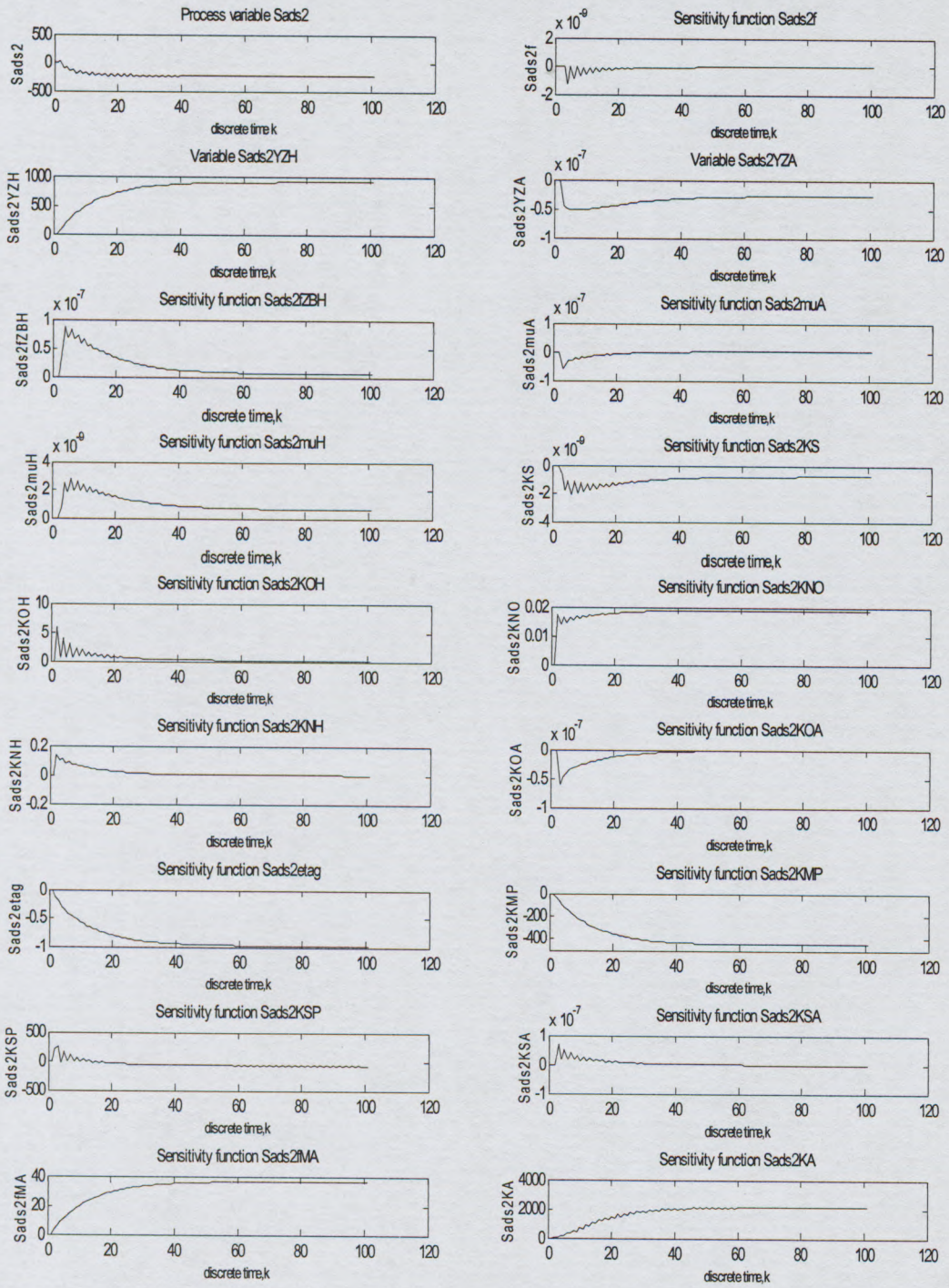

Figure 9.56: Process variable S_{Sads2} and its sensitivity functions towards the model parameters

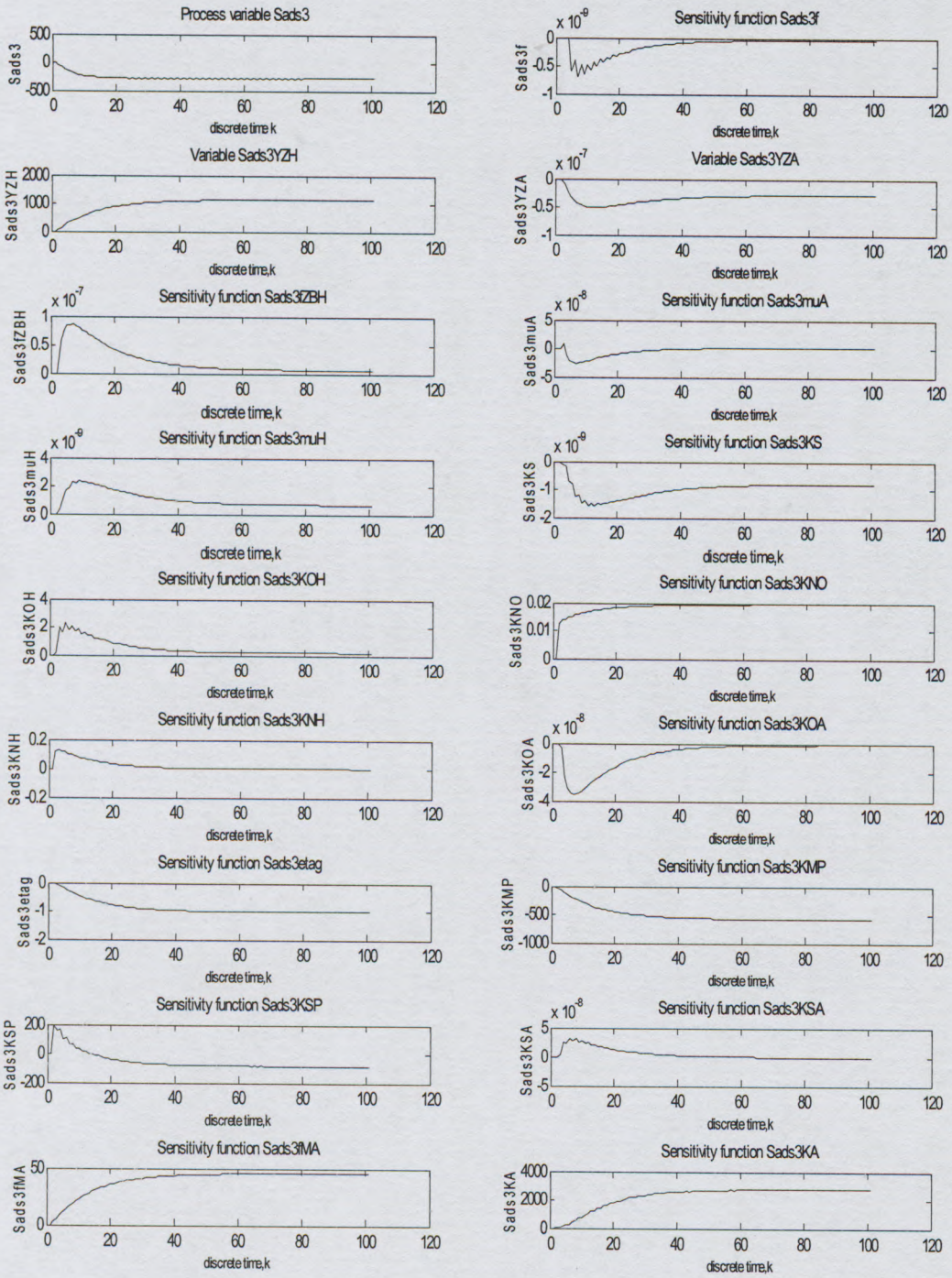

Figure 9.57: Process variable S_{Sads3} and its sensitivity functions towards the model parameters

9.2.3.3 Discussion of the results

9.2.3.3. 1Athlone process with ASM1 reduced biological model

In order to compare the results the minimum and maximum values of the sensitivity functions of the process variables towards the model parameters are summarized in Table 9.3.

Table 9.3: The maximum or minimum values of sensitivity function simulation for the Athlone process model based on the reduced ASM1 biological model

para / Frac	Maximum or minimum values of the sensitivity functions														
	f	YH	YA	iXB	muA	muH	KS	KOH	KNO	KNH	KOA	etag	etah	Kh	Kx
Snh1	0.35	-0.04	5	-9	-2	-18	0.06	0.7	0.09	1.2	0.8	-0.16	-0.16	-0.05	0.18
SNO1	0.007	-0.26	-5	-0.4	2	-0.4	0.12	-0.4	0.08	-1	-0.8	-0.15	0.15	-0.01	0.03
SS1	-1.8E-4	10	0.1	0.01	-0.05	-18	0.5	-40	-5	0.025	0.018	1.8E-3	1.8E-3	11	-38
Snh2	0.35	-0.08	9.5	-18	-4	-3	0.1	0.8	0.09	2	1.2	-0.2	-0.03	-0.09	0.18
SNO2	0.012	-0.4	-8	-0.7	4	-0.5	0.2	-0.4	0.12	-2	-1	-0.2	-0.007	-0.015	0.048
SS2	-2E-4	18	0.18	0.018	-0.075	-30	1	-40	-5	0.035	0.02	2E-3	8	18	-50
Snh3	0.35	-0.1	9.5	-20	-6	-4	0.1	1	0.15	3	1.2	-0.2	-0.038	-0.013	0.4
SNO3	0.018	-0.4	-8	-1	5	-0.5	0.2	-0.4	0.12	-2	-1	-0.2	-0.007	-0.015	0.048
SS3	-2E-4	20	0.16	0.016	-0.075	-30	1	-40	-5	0.03	0.018	1.8E-3	6	18	50

The sensitivity functions of Snh for the parameter muH decay significantly for tank 1 (see Table 9.3). The sensitivity functions of SS for the parameters muH, KOH and Kx decay significantly for tanks 1 (see Table 9.3). The sensitivity functions of SNO for the parameter iXB decay significantly for tank 2 (see Table 9.3). The sensitivity functions of SS for the parameters YH and Kh grow significantly for tank 2 (see Table 9.3). The sensitivity functions of SS for the parameters muH, KOH and Kx decay significantly for tank 2 (see Table 9.3). The sensitivity function of Snh for the parameter iXB decays significantly for tank 3 (see Table 9.3). The sensitivity functions of SS for the parameters YH, Kh and Kx grow significantly for tank 3 (see Table 9.3). The sensitivity functions of SS for the parameters muH and KOH decays significantly for tank 3 (see Table 9.3).

It can be concluded that the variable SNH1's is more senitive towards the parameters muH, SNH2 for SNH2 for iXB and SNH3 for iXB. The variable SNO1 is not strongly sensitive towards the parameters, SNO2 towards the parameter YA, and SNO3 is strongly dependent towards YA. The variable SS1 is more sensitive towards the parameters muH, KOh and Kx, the variable SS2 is more sensitive towards the parameters Yh, muH, KOH and Kx, and the variable SS3 is more sensitive towards the parameters Yh, muH, KOH, Kh and Kx.

9.2.3.3.2 Athlone process with the UCT reduced biological model

The minimum and maximum values of the process variables sensitivity functions towards the model parameters are summarized in Table 9.4.

Table 9.4: The maximum or minimum values of sensitivity function simulation for the Athlone process model based on the reduced UCT biological model

para / Frac	Maximum or minimum values of the sensitivity functions																
	f	YZH	YZA	fZBH	muA	muH	KS	KOH	KNO	KNH	KOA	etag	KMP	KSP	KSA	fMA	KA
Snh 1	3.8	1.8	39	-500	-75	-15	1	38	3E-3	38	100	-0.1	15	18	0.5	3.2E-5	2E-3
SNO 1	1.8 E-9	1.7	4.8	-0.04	1	0.08	0.18	-0.8	4E-3	1	0.5	-0.12	0.19	0.08	-0.5	-0.017	-0.08
SS1	-2.2 E-9	600	-0.7 E-7	1E-7	-1E-8	-300	480	0.4	0.038	0.05	-1E-7	4E-9	-3.8 E-9	-0.5 E-7	0.9 E-7	0.8E-7	5E-7
Sads 1	-1.5 E-9	500	-0.5 E-7	0.6 E-7	-0.8 E-7	2.4 E-7	-2E-7	4.8	0.016	0.1	-0.75 E-7	-0.75	-300	200	5E-9	20	1200
Snh 2	3.8	2.6	50	-800	-110	-20	1.8	48	3E-3	60	170	-0.15	20	30	0.75	0.75 E-9	4E-3
SNO 2	1.8 E-9	1.9	8	-0.04	1	0.12	0.18	-1	4.9E-3	-60	0.5	-0.17	0.4	0.09	-1	-0.02	-1.2
SS2	-2.2 E-9	1000	-0.7 E-7	1.4 E-7	-1E-8	-420	750	0.4	0.05	0.05	-1E-7	4E-7	-3.8 E-9	-0.5 E-9	0.9 E-7	0.8E-10	5E-9
Sads 2	-1.5 E-9	980	-0.5 E-7	0.8 E-7	-0.8 E-7	2.4 E-9	-2E-9	5	0.02	0.1	-0.6E-7	-1	-420	250	0.7 E-7	39	2000
Snh 3	3.8	3.8	80	-1000	-180	-30	1.8	48	2E-3	80	170	-0.15	20	39	0.75	0.75 E-9	4E-3
SNO 3	0.5 E-9	1.9	8	-0.04	1	-0.12	0.18	-1	2E-3	-80	0.5	-0.17	0.4	0.09	-1	-0.02	-1.2
SS3	-0.5 E-9	1000	-0.7 E-7	1.4 E-7	-1E-8	-500	900	0.4	0.05	0.05	-0.5E-7	2.2 E-9	-3.8 E-9	-0.5 E-9	0.5 E-9	0.8E-10	5E-7
Sads 3	-1.5 E-9	980	-0.5 E-7	0.8 E-7	0.8 E-7	2.4 E-9	-2E-9	2	0.02	0.1	-3.8E-9	-1	-500	250	0.7 E-7	49	3000

The sensitivity functions of Snh for the parameters YZA, KOH, KNH, KOA, KMP and KSP grow significantly for tank 1 (see Table 9.4). The sensitivity functions of Snh for the parameters fZBH, muA and muH decay significantly for tank 1 (see Table 9.4). The sensitivity functions of SS for the parameters YZH and KS grow significantly for tank 1 (see Table 9.4). The sensitivity function of SS for the parameter muH decays significantly for tank 1 (see Table 9.4). The sensitivity functions of Sads for the parameter YZH, KSP, fMA and KA grow significantly for tank 1 (see Table 9.4). The sensitivity function of Sads for the parameter KMP decays significantly for tank 1 (see Table 9.4). The sensitivity functions of Snh for the parameters YZA, KNH, KOA, KMP and KSP grow significantly for tank 2 (see Table 9.4). The sensitivity functions of Snh for the parameters fZBH and muA decay significantly for tank 2 (see Table 9.4). The sensitivity function of SNO for the parameter KNH decays significantly for tank 2 (see Table 9.4). The sensitivity functions of SS for the parameters YZH and KS grows significantly for tank 2 (see Table 9.4). The sensitivity function of SS for the parameter muH decays significantly for tank 2 (see Table 9.4). The sensitivity functions of Sads for the parameters YZH, KSP, fMA and KA grow significantly for tank 2 (see Table 9.4). The sensitivity function of Sads for the parameter KMP decays significantly for tank 2 (see Table 9.4). The sensitivity functions of Snh for the parameters YZA, KOH, KNH, KOA, KMP and KSP grows significantly for tank 3 (see Table 9.4). The sensitivity functions of Snh for the parameters fZBH, muA and muH decays significantly for tank 3 (see Table 9.4). The sensitivity function of parameter KNH decays significantly for tank 3 (see Table 9.4). The sensitivity functions of SS for the parameters YZH and KS grow

significantly for tank 3 (see Table 9.4). The sensitivity function of SS for the parameter muH decays significantly for tank 3 (see Table 9.4). The sensitivity functions of Sads for the parameters YZH, KSP, fMA and KA grows significantly for tank 3 (see Table 9.4). The sensitivity function of Sads for the parameter KMP decays significantly for tank 3 (see Table 9.4).

In conclusion the variable Snh1 is more sensitive for the parameters YZA, fZBH, muA, muH, KOH, KNH, KOA and KSA, Snh2 towards the parameters KNH and Snh3towards the parameters YZA, fZBH, muA, muH, KOH, KNH, KOA, KMP and KSP. The variable SNO1 is not sensitive towards the parameters, SNO2 towards the parameter KNH, and SNO3 towards KNH. The variable SS1 is more sensitive towards the parameters Yzh, muH and KS, SS2 towards YZH, muH and KS, SS3 YZH, muH and KS. The variable Sads1 is more sensitive towards the parameters YZH, KMP, KSP, KA and fMA, Sads2 toward parameters YZH, KMP, KSP, fMA and KA; Sads3 towards YZH, KMP, KSP, fMA and KA.

9.3. Parameter estimation of the reduced models of the Activated Sludge Process

The parameter estimation methods developed in Chapter 6 are used to develop software for estimation of the reduced model parameter. The calculations are done for the reduced ASM1 and UCT models applied to the Benchmark and Athlone plants structures.

9.3.1. Software for the parameter estimation

Four software programmes are developed in Matlab:

- Calculation of the parameters of the ASM1 reduced biological model applied to the Benchmark process: *BASM1parest.m, rateASM1F.m, prateASM1R.m and rateASM1RE.m.*
- Calculation of the parameters of the ASM1 reduced biological model applied to the Athlone process: A*ASM1parest.m, rateAASM1F.m, prateAASM1R.m and rateAASM1RE.m.*
- Calculation of the parameters of the UCT reduced biological model applied to the Benchmark process: *BUCTparest.m, rateBUCTF.m, prateBUCTR.m and rateBUCTRE.m.*
- Calculation of the parameters of the UCT reduced biological model applied to the Athlone process: AUCT*parest.m, rateAUCTF.m, prateAUCTR.m and rateAUCTRE.m.*

The developed software is given in the Appendix D and every application consists of two parts:

- main programme for input of the nominal process parameters, initial conditions, average values of the biomass concentrations, calculation of the process model matrices and organization of the calculation algorithm
- sub-programmes for calculation of the biological rates for the full, reduced and estimated model,

The estimation of the parameters follows the algorithm:

1. The model of the corresponding process with the full ASM1 or UCT biological models are simulated with control inputs determined by the values of the Benchmark process Kla oxygen transfer functions values.

2. The reduced model parameter estimation is done for the same values of the control variables and for the obtained from point 1 trajectories of the reduced model process variables.

3. The obtained trajectories of the model parameters are used for reduced model simulation and for the error between the full and reduced model calculation.

The algorithm of the calculation is given on Figure 9.58.a) for the main programme and in Figure 9.58.b) for the sub-programmes. The number of variables and parameters for different plants and biological models is different. The corresponding values are shown under the separate process and model descriptions.

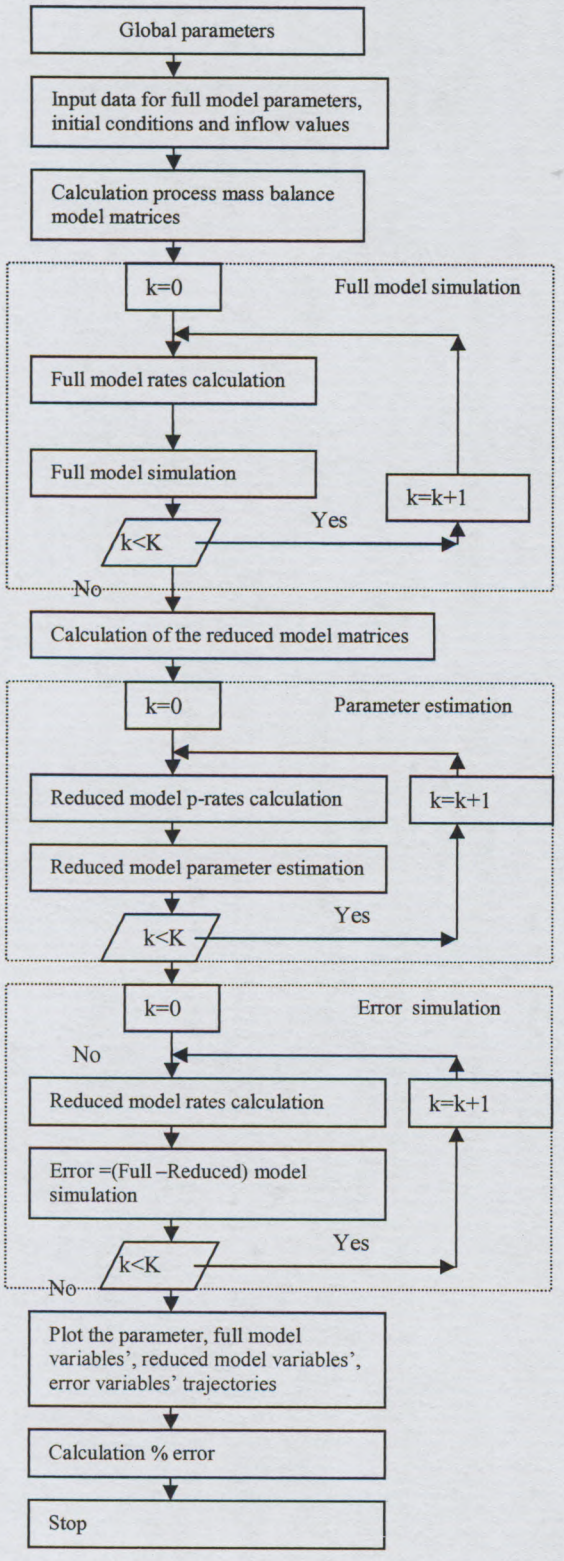

Figure 9.58a: Flow chart of the main program for sensitivity functions

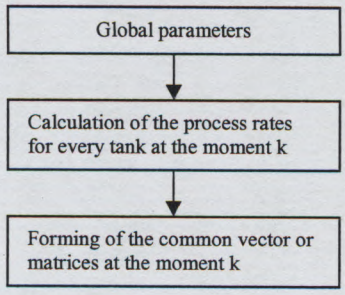

Figure 9.58b: Flow chart of the subprogram for sensitivity functions

9.3.2. Reduced ASM1 model parameter estimation used for the Benchmark process and Athlone process mass balance models

The reduced ASM1 biological model is described in the Chapter 4, point 4.4. The mass balance models for Benchmark process based on both ASM1 and UCT reduced models are described in point 4.6.1. The values of the processes tank's volumes are given in the Chapter 3, Table 3.7. The nominal kinetic parameters are given in Table 4.2 for the reduced ASM1 biological model.

9.3.2.1 Results for the Benchmark mass balance process model

The calculations of the full model variables trajectories is done for the average values of the inflow given by the vector

Zi=[SIi*ones(1,K);SSi*ones(1,K);XIi*ones(1,K);XSi*ones(1,K);XBHi*ones(1,K);XBAi*ones(1,K);XPi*ones(1,K);
S0i*ones(1,K);SNOi*ones(1,K);SNHi*ones(1,K);SNDi*ones(1,K);XNDi*ones(1,K);SALKi*ones(1,K)];
where
SSi=69.5;XBHi=28.17;XSi=202.32;XIi=51.2;SNHi=31.56;SIi=30.0;SNDi=6.95;XNDi=10.59;S0i=0.0;XBAi=0.0;
XPi=0.0;SNOi=0.0;SALKi=7.0;

The control vector is given by the matrix K_{la}, where
S0sat = 8, Kla1=4.8; Kla2=4.8; Kla3 = 240; Kla4=240; Kla5 = 84;
Kl=[Kla1 Kla2 Kla3 Kla4 Kla5];
Kla=diag(Kl);

The initial conditions are given as the steady state values of the Benchmark full model after two week simulation with the average values of in inflow concentration for the dry weather by the vectors
Z0=[Z10;Z20;Z30;Z40;Z50]*0.1
Z10 = [Si_1 ;Ss_1 ;Xi_1 ;Xs_1 ;Xbh_1 ;Xba_1 ;Xp_1 ;So_1 ;Sno_1 ;Snh_1 ;Snd_1 ;Xnd_1 ;Salk_1];
Si_1 = 3.0000000e+01; Ss_1 = 2.8082131e+00; Xi_1 = 1.1491252e+03; Xs_1 = 8.2134908e+01;
Xbh_1 = 2.5517658e+03; Xba_1 = 1.4838943e+02; Xp_1 = 4.4885186e+02; So_1 = 4.2984433e-03;
Sno_1 = 5.3699400e+00; Snh_1 = 7.9178845e+00; Snd_1 = 1.2166405e+00; Xnd_1 = 5.2848894e+00;
Salk_1 = 4.9277103e+00;

Z20 = [Si_2 ;Ss_2 ;Xi_2 ;Xs_2 ;Xbh_2 ;Xba_2 ;Xp_2 ;So_2 ;Sno_2 ;Snh_2 ;Snd_2 ;Xnd_2 ;Salk_2];
Si_2 = 3.0000000e+01; Ss_2 = 1.4587940e+00; Xi_2 = 1.1491252e+03; Xs_2 = 7.6386187e+01;
Xbh_2 = 2.5533851e+03; Xba_2 = 1.4830914e+02; Xp_2 = 4.4952273e+02; So_2 = 6.3131911e-05;
Sno_2 = 3.6619672e+00; Snh_2 = 8.3444148e+00; Snd_2 = 8.8206477e-01; Xnd_2 = 5.0290873e+00;
Salk_2 = 5.0801748e+00;

Z30 = [Si_3 ;Ss_3 ;Xi_3 ;Xs_3 ;Xbh_3 ;Xba_3 ;Xp_3 ;So_3 ;Sno_3 ;Snh_3 ;Snd_3 ;Xnd_3 ;Salk_3];
Si_3 = 3.0000000e+01; Ss_3 = 1.1495418e+00; Xi_3 = 1.1491252e+03; Xs_3 = 6.4854922e+01;
Xbh_3 = 2.5571314e+03; Xba_3 = 1.4894126e+02; Xp_3 = 4.5041834e+02; So_3 = 1.7183778e+00;
Sno_3 = 6.5408820e+00; Snh_3 = 5.5479452e+00; Snd_3 = 8.2888682e-01; Xnd_3 = 4.3924277e+00;
Salk_3 = 4.6747902e+00;

Z40 = [Si_4 ;Ss_4 ;Xi_4 ;Xs_4 ;Xbh_4 ;Xba_4 ;Xp_4 ;So_4 ;Sno_4 ;Snh_4 ;Snd_4 ;Xnd_4 ;Salk_4];
Si_4 = 3.0000000e+01; Ss_4 = 9.9532389e-01; Xi_4 = 1.1491252e+03; Xs_4 = 5.5693982e+01;
Xbh_4 = 2.5591826e+03; Xba_4 = 1.4952712e+02; Xp_4 = 4.5131469e+02; So_4 = 2.4288838e+00;
Sno_4 = 9.2989988e+00; Snh_4 = 2.9673854e+00; Snd_4 = 7.6678656e-01; Xnd_4 = 3.8790101e+00;
Salk_4 = 4.2934562e+00;

Z50 = [Si_5 ;Ss_5 ;Xi_5 ;Xs_5 ;Xbh_5 ;Xba_5 ;Xp_5 ;So_5 ;Sno_5 ;Snh_5 ;Snd_5 ;Xnd_5 ;Salk_5];
Si_5 = 3.0000000e+01; Ss_5 = 8.8949280e-01; Xi_5 = 1.1491252e+03; Xs_5 = 4.9305586e+01;
Xbh_5 = 2.5593436e+03; Xba_5 = 1.4979714e+02; Xp_5 = 4.5221112e+02; So_5 = 4.9094351e-01;
Sno_5 = 1.0415220e+01; Snh_5 = 1.7333316e+00; Snd_5 = 6.8828001e-01; Xnd_5 = 3.5271755e+00;
Salk_5 = 4.1255794e+00;

The obtained trajectories of the full model state variables are given by the solid lines in Figures 9.60-9.62. They are used as target variables for the estimation of the parameters of the reduced model. The parameter estimation is done for the initial conditions of the process variables given for the reduced model by the vector x_0. The inflow concentration for the reduced model is the average one for dry weather, given by the vector X_i

X_0=[7.918;5.37;2.808;8.344;3.662;1.459;5.548;6.541;1.15;2.967;9.299;0.995;1.733;10.415;0.889]
Xi=[31.56 0 69.50]

The simulation for the reduced model is done for steady state conditions of the biomass and the slowly biodegradable substrate given by the vectors

XBH = 0.05*[2551.76*ones(1,K);2553.38*ones(1,K);2557.13*ones(1,K);2559.18*ones(1,K);2559.34*ones(1,K)];
XBA = 0.05*[148.389*ones(1,K);148.309*ones(1,K);148.941*ones(1,K);149.527*ones(1,K);149.797*ones(1,K)];
XS = 0.05*[82.135*ones(1,K);76.386*ones(1,K);64.855*ones(1,K);55.694*ones(1,K);49.306*ones(1,K)];

The vector of the dissolved oxygen concentration for the reduced model is the same as for the full model. The sampling period is DT = 0.01042. The process reduced state space mass balance model matrices as taken from the Matlab program are the same as the given in point 9.2.2.1.

The results from the simulations are given from Figures 9.59 till Figure 9.62 where the trajectories of the full model process variables are given by the solid lines and the values of the reduced model state variables are given by the dashed lines.

The errors of the estimation are calculated as a weighted value of the sum of the squares of the errors of the process variables at the discrete points for the corresponding sum of the respective variables of the full model, as

$$e_S = \frac{ERR_S * ERR_S^T}{S * S^T}$$

where the S is one of the variables.

The obtained weighted errors are:

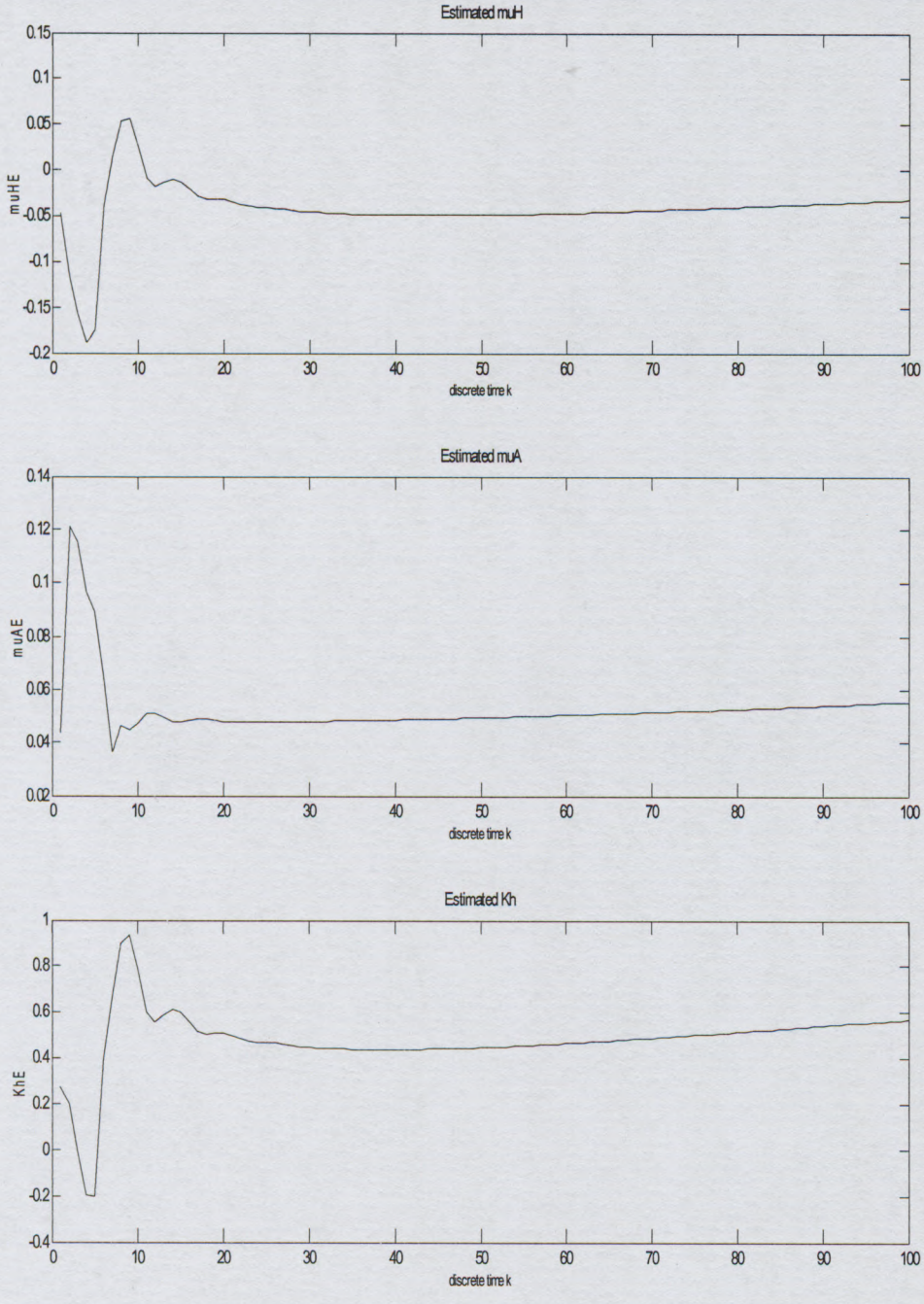

Figure 9.59: Trajectories of the reduced ASM1 biological model parameters for the Benchmark process

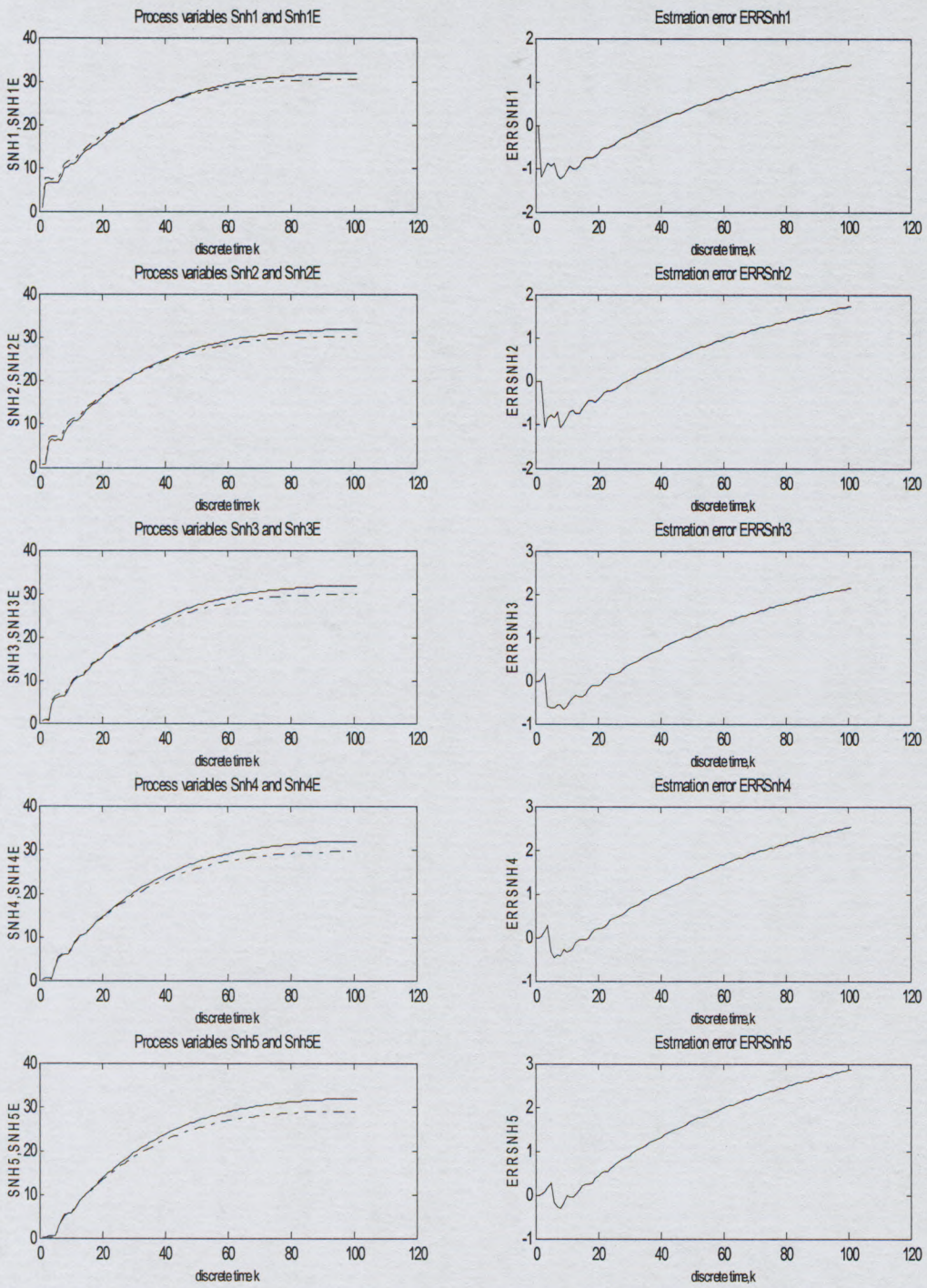

Figure 9.60: Trajectories of the ASM1 full (solid line), reduced estimated (dashed line) and the error between them as applied for the Benchmark process for the process variable SNH

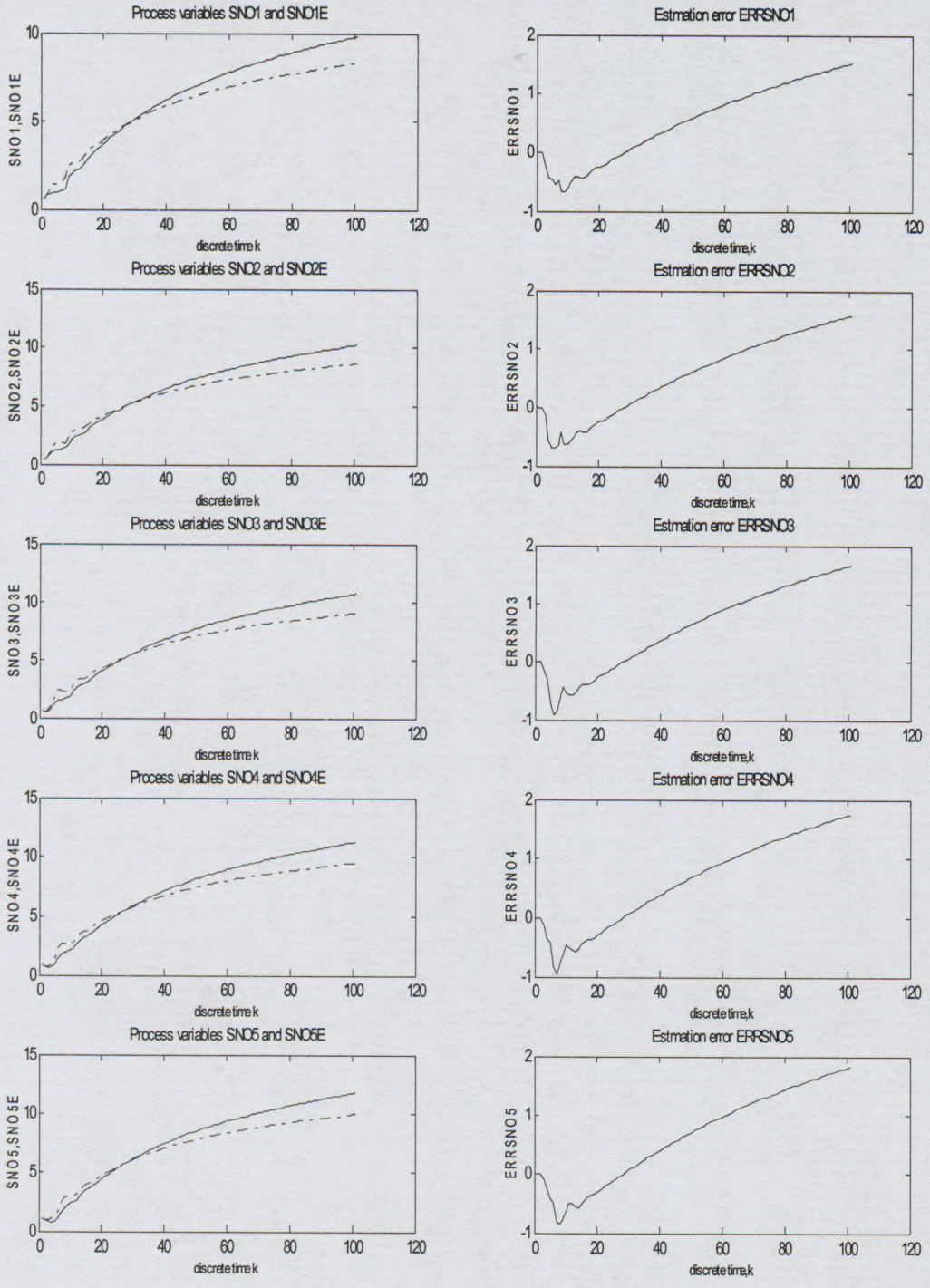

Figure 9.61: Trajectories of the ASM1 full (solid line), reduced estimated (dashed line) and the error between them as applied for the Benchmark process for the process variable SNO

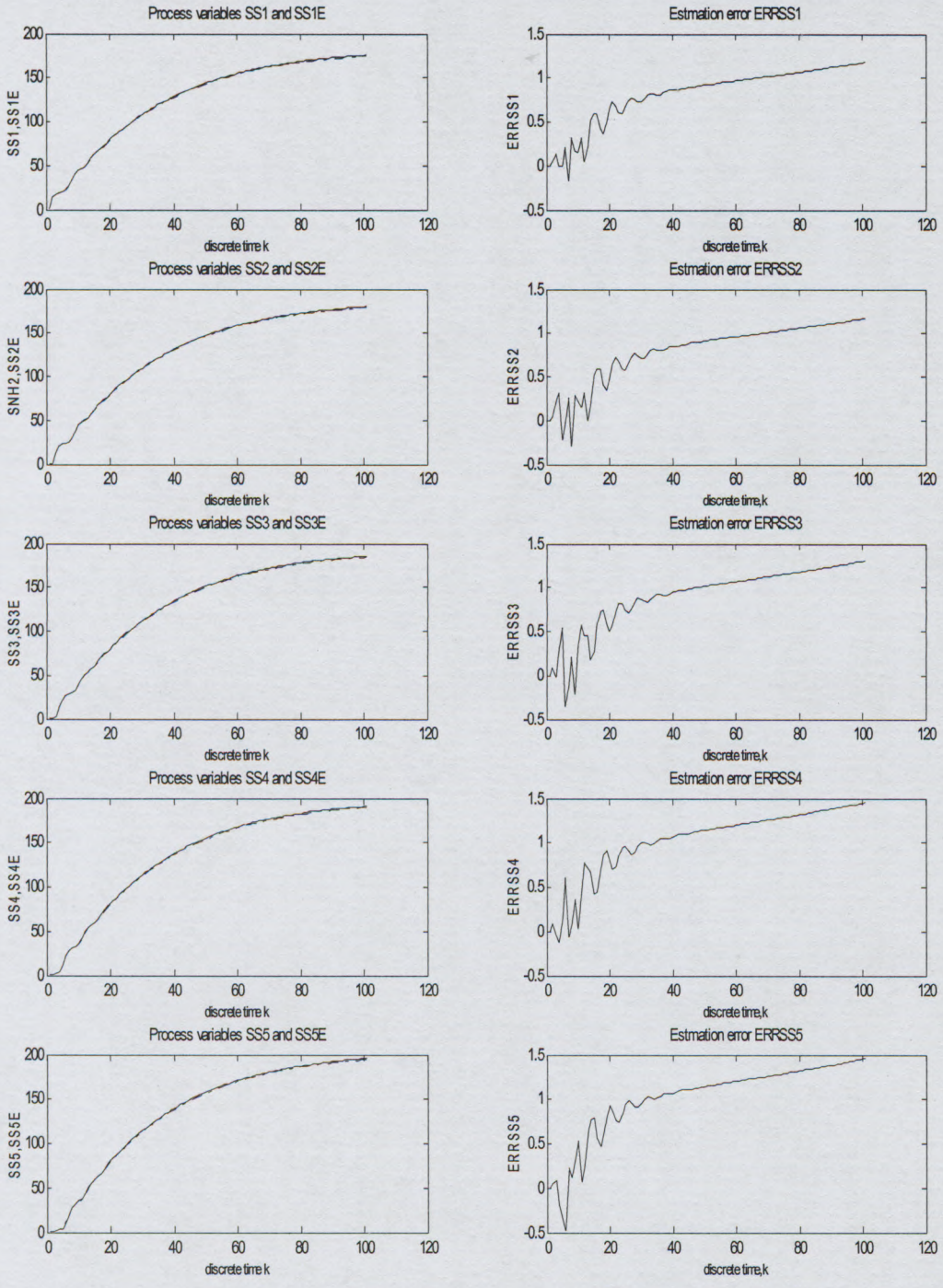

Figure 9.62: Trajectories of the ASM1 full (solid line), reduced estimated (dashed line) and the error between them as applied for the Benchmark process for the process variable SS

9.3.2.2 Results for the Athlone mass balance process model

The calculations of the full model variables trajectories is done for the average values of the inflow given by the vector

Zi=[SIi*ones(1,K);SSi*ones(1,K);XIi*ones(1,K);XSi*ones(1,K);XBHi*ones(1,K);XBAi*ones(1,K);XPi*ones(1,K);
S0i*ones(1,K);SNOi*ones(1,K);SNHi*ones(1,K);SNDi*ones(1,K);XNDi*ones(1,K);SALKi*ones(1,K)];
where
SSi=69.5;XBHi=28.17;XSi=202.32;XIi=51.2;SNHi=31.56;SIi=30.0;SNDi=6.95;XNDi=10.59;S0i=0.0;XBAi=0.0;
XPi=0.0;SNOi=0.0;SALKi=7.0;

The control vector is given by the matrix K_{la}, where
S0sat = 8, Kla1=4.8; Kla2=4.8; Kla3 = 240;
Kl=[Kla1 Kla2 Kla3];
Kla=diag(Kl);

The initial conditions are given as the steady state values of the Benchmark full model after two week simulation with the average values of in inflow concentration for the dry weather by the vectors
Z0=[Z10;Z20;Z30;Z40;Z50]*0.1
Z10 = [Si_1 ;Ss_1 ;Xi_1 ;Xs_1 ;Xbh_1 ;Xba_1 ;Xp_1 ;So_1 ;Sno_1 ;Snh_1 ;Snd_1 ;Xnd_1 ;Salk_1];
Si_1 = 3.0000000e+01; Ss_1 = 2.8082131e+00; Xi_1 = 1.1491252e+03; Xs_1 = 8.2134908e+01;
Xbh_1 = 2.5517658e+03; Xba_1 = 1.4838943e+02; Xp_1 = 4.4885186e+02; So_1 = 4.2984433e-03;
Sno_1 = 5.3699400e+00; Snh_1 = 7.9178845e+00; Snd_1 = 1.2166405e+00; Xnd_1 = 5.2848894e+00;
Salk_1 = 4.9277103e+00;

Z20 = [Si_2 ;Ss_2 ;Xi_2 ;Xs_2 ;Xbh_2 ;Xba_2 ;Xp_2 ;So_2 ;Sno_2 ;Snh_2 ;Snd_2 ;Xnd_2 ;Salk_2];
Si_2 = 3.0000000e+01; Ss_2 = 1.4587940e+00; Xi_2 = 1.1491252e+03; Xs_2 = 7.6386187e+01;
Xbh_2 = 2.5533851e+03; Xba_2 = 1.4830914e+02; Xp_2 = 4.4952273e+02; So_2 = 6.3131911e-05;
Sno_2 = 3.6619672e+00; Snh_2 = 8.3444148e+00; Snd_2 = 8.8206477e-01; Xnd_2 = 5.0290873e+00;
Salk_2 = 5.0801748e+00;

Z30 = [Si_3 ;Ss_3 ;Xi_3 ;Xs_3 ;Xbh_3 ;Xba_3 ;Xp_3 ;So_3 ;Sno_3 ;Snh_3 ;Snd_3 ;Xnd_3 ;Salk_3];
Si_3 = 3.0000000e+01; Ss_3 = 1.1495418e+00; Xi_3 = 1.1491252e+03; Xs_3 = 6.4854922e+01;
Xbh_3 = 2.5571314e+03; Xba_3 = 1.4894126e+02; Xp_3 = 4.5041834e+02; So_3 = 1.7183778e+00;
Sno_3 = 6.5408820e+00; Snh_3 = 5.5479452e+00; Snd_3 = 8.2888682e-01; Xnd_3 = 4.3924277e+00;
Salk_3 = 4.6747902e+00;

The obtained trajectories of the full model state variables are given by the solid lines in Figures 9.63-9.66. They are used as target variables for the estimation of the parameters of the reduced model. The parameter estimation is done for the initial conditions of the process variables given for the reduced model by the vector x_0. The inflow concentration for the reduced model is the average one for dry weather, given by the vector X_i

X_0=[7.918;5.37;2.808;8.344;3.662;1.459;5.548;6.541;1.15]
Xi=[31.56 0 69.50]

The simulation for the reduced model is done for steady state conditions of the biomass and the slowly biodegradable substrate given by the vectors

XBH = 0.01*[2551.76*ones(1,K);2553.38*ones(1,K);2557.13*ones(1,K))];
XBA = 0.01*[148.389*ones(1,K);148.309*ones(1,K);148.941*ones(1,K)];
XS = 0.01*[82.135*ones(1,K);76.386*ones(1,K);64.855*ones(1,K)];

The vector of the dissolved oxygen concentration for the reduced model is the same as for the full model. The sampling period is DT = 0.01042. The process reduced state space mass balance model matrices as taken from the Matlab program are the same as the given in point 9.2.2.2.

The results from the simulations are given from Figures 9.63 till Figure 9.66 where the trajectories of the full model process variables are given by the solid lines and the values of the reduced model state variables are given by the dashed lines.

The errors of the estimation are calculated as in the previous point.

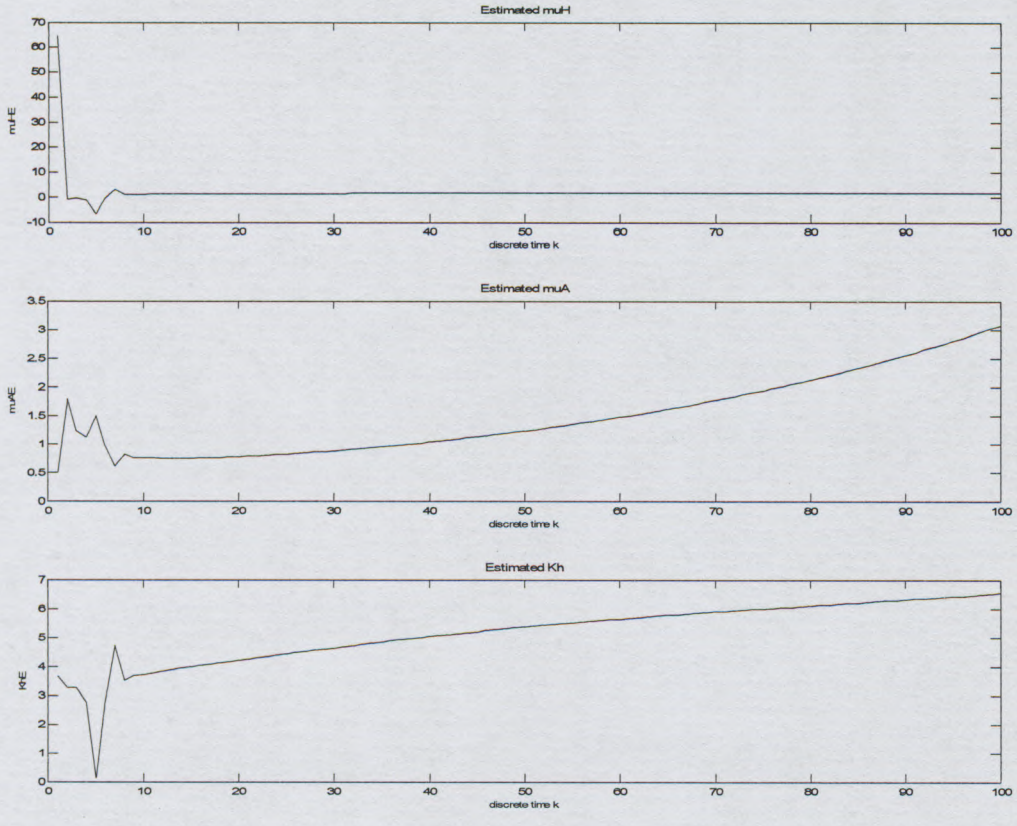

Figure 9.63: Trajectories of the reduced ASM1 biological model parameters for the Athlone process

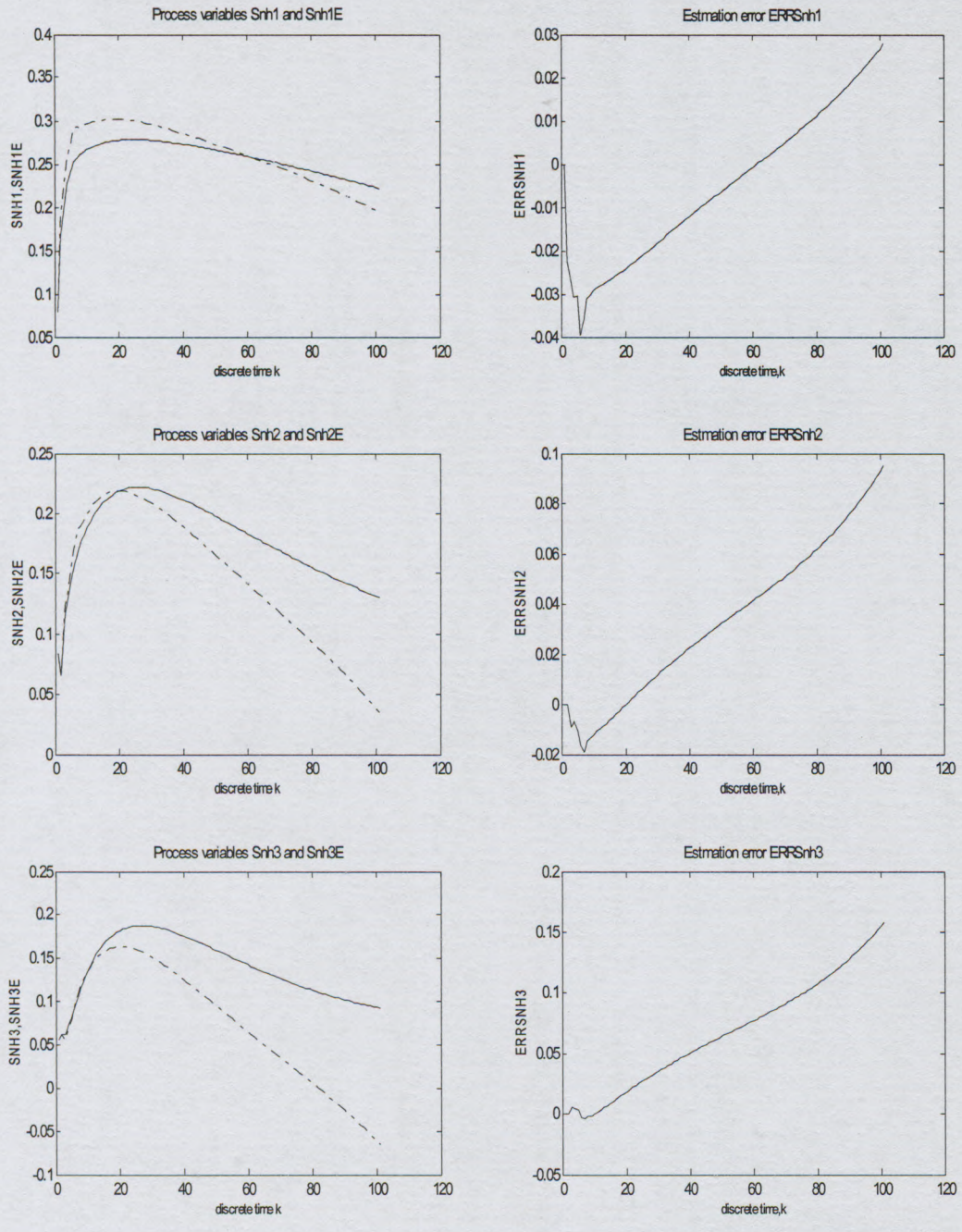

Figure 9.64: Trajectories of the ASM1 full (solid line), reduced estimated (dashed line) and the error between them as applied for the Athlone process for the process variable SNH

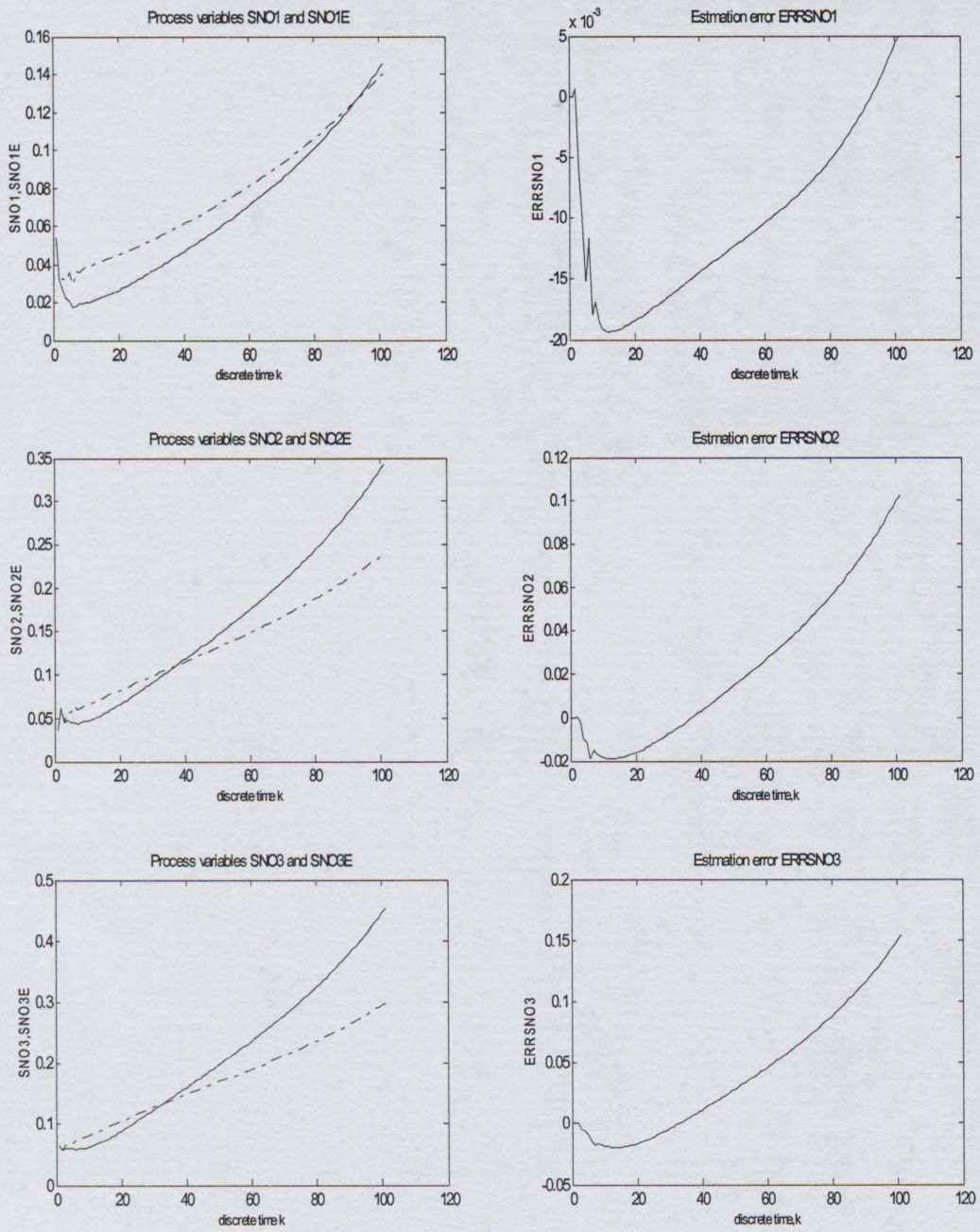

Figure 9.65: Trajectories of the ASM1 full (solid line), reduced estimated (dashed line) and the error between them as applied for the Athlone process for the process variable SNO

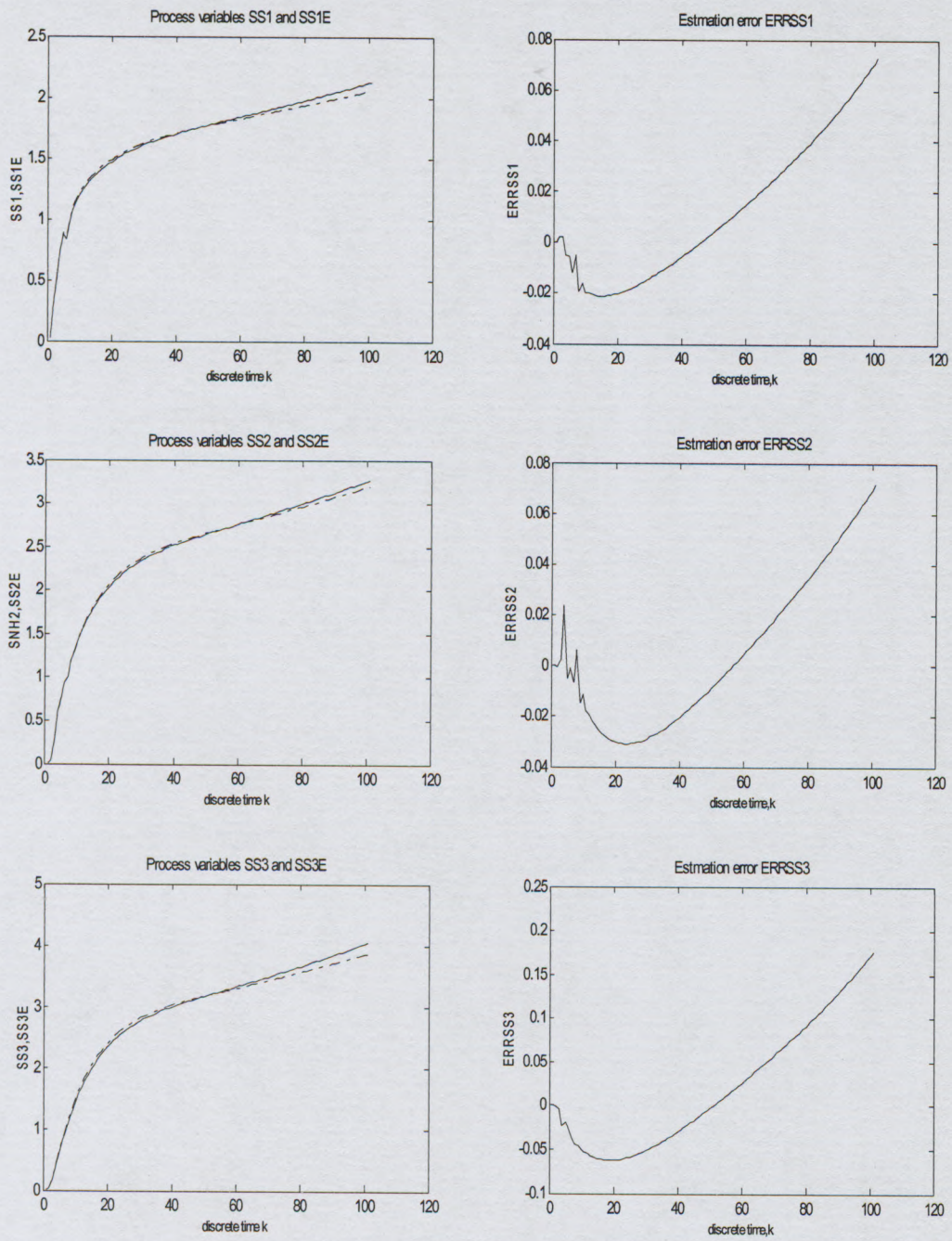

Figure 9.66: Trajectories of the ASM1 full (solid line), reduced estimated (dashed line) and the error between them as applied for the Athlone process for the process variable SS

9.3.2.3 Discussion of the results

The values of the calculated errors are summarized in Table 9.5.

Table 9.5: The obtained weighted errors of reduced ASM1 model parameter estimation used for the Benchmark process mass balance models

Error predict. / tank	eSnh	eSNO	eSS
tank 1	0.0011	0.0148	4.2244E-005
tank 2	0.0016	0.0149	3.9315E-005
tank 3	0.0025	0.0149	4.6888E-005
tank 4	0.0038	0.0148	5.6684E-005
tank 5	0.0053	0.0147	5.4716E-005

The trajectories of the ASM1 full model and ASM1reduced model exhibit common behaviour which are very close to each other. The smallest error for the ASM1 reduced model can be seen to be 3.9315E-005 for SS in tank 2 but relatively speaking the errors are not that significantly different to influence a major change. However the SS has a crucial bearing on the error prediction of the ASM1 reduced model due to the smaller critical error. Hence the ASM1 reduced model can be used for process optimization and controller design due to reduced number of calculations for parameter estimation of Snh, SNO and SS compared to the ASM1 full model which depends on the complete Peterson matrix.

The values of the calculated errors of the estimation are given in Table 9.6

Table 9.6: The obtained weighted errors of reduced ASM1 model parameter estimation used for the Athlone process mass balance models

Error pred / tank	eSnh	eSNO	eSS
tank 1	0.0049	0.0266	3.0995E-004
tank 2	0.0622	0.0540	1.4452E-004
tank 3	0.3133	0.0718	5.9436E-004

The trajectories of the ASM1 full and ASM1 reduced model for the Athlone process show slight difference with the same profile. The smallest error for the ASM1 reduced model can be seen to be 1.4452E-004 in tank 2 similar to the Benchmark, with relatively speaking errors are not significantly different to have major influence. Hence the ASM1 reduced model can be used for process optimization and controller design due to reduced number of calculations for parameter estimation of Snh, SNO and SS compared to the ASM1 full model which depends on the complete Peterson matrix.

9.3.3. Reduced UCT model parameter estimation used for the Benchmark process

The reduced UCT biological model is described in the Chapter 4, point 4.6. The mass balance models for Benchmark process based on both ASM1 and UCT reduced models are described in point 4.6.1. The values of the processes tank's volumes are given in the Chapter 3, Table 3.7. The nominal kinetic parameters are given in Table 4.4 for the reduced UCT biological model.

9.3.3.1 Results for the Benchmark mass balance process model

The calculations of the full model variables trajectories are done for the average values of the inflow given by the vector

Zi=[XBHi*ones(1,K);XBAi*ones(1,K);XPi*ones(1,K);XIi*ones(1,K);XSAi*ones(1,K);XSEi*ones(1,K);XNDi*ones(1,K);SSi*ones(1,K);SNHi*ones(1,K);SNDi*ones(1,K);SNOi*ones(1,K);SALKi*ones(1,K);SIi*ones(1,K);S0i*ones(1,K)]*0.1;
SSi=69.5;XBHi=28.17;XSEi=202.32;XIi=51.2;SNHi=31.56;SIi=30.0;SNDi=6.95;XNDi=10.59;S0i=0.0;XBAi=0.0;XPi=0.0;SNOi=0.0;SALKi=7.0;XSAi=0.0;

The control vector for the full model is given by the matrix K_{la}, where
S0sat = 8, Kla1=4.8; Kla2=4.8; Kla3 = 240; Kla4=240; Kla5 = 84;
Kl=[Kla1 Kla2 Kla3 Kla4 Kla5];
Kla=diag(Kl);

The initial conditions are given as the steady state values of the Benchmark full model after two week simulation with the average values of inflow concentration for the dry weather by the vectors
Z0=[Z10;Z20;Z30;Z40;Z50]*0.01
Z10 = [Xbh_1 ;Xba_1 ;Xp_1 ;Xi_1 ;Xsa_1 ;Xse_1;Xnd_1 ;Ss_1 ;Snh_1 ;Snd_1 ;Sno_1 ;Salk_1;Si_1 ;So_1];
Si_1 = 3.0000000e+01; Ss_1 = 2.8082131e+00; Xi_1 = 1.1491252e+03; Xsa_1 = 8.2134908e+01;
Xbh_1 = 2.5517658e+03; Xba_1 = 1.4838943e+02; Xp_1 = 4.4885186e+02; So_1 = 4.2984433e-03;
Sno_1 = 5.3699400e+00; Snh_1 = 7.9178845e+00; Snd_1 = 1.2166405e+00; Xnd_1 = 5.2848894e+00;
Salk_1 = 4.9277103e+00;Xse_1=500.0

Z20 = [Xbh_2 ;Xba_2 ;Xp_2 ;Xi_2 ;Xsa_2 ;Xse_2;Xnd_2 ;Ss_2 ;Snh_2 ;Snd_2 ;Sno_2 ;Salk_2;Si_2 ;So_2];
Si_2 = 3.0000000e+01; Ss_2 = 1.4587940e+00; Xi_2 = 1.1491252e+03; Xsa_2 = 7.6386187e+01;
Xbh_2 = 2.5533851e+03; Xba_2 = 1.4830914e+02; Xp_2 = 4.4952273e+02; So_2 = 6.3131911e-05;
Sno_2 = 3.6619672e+00; Snh_2 = 8.3444148e+00; Snd_2 = 8.8206477e-01; Xnd_2 = 5.0290873e+00;
Salk_2 = 5.0801748e+00;Xse_2=480.0

Z30 = [Xbh_3 ;Xba_3 ;Xp_3 ;Xi_3 ;Xsa_3 ;Xse_3;Xnd_3 ;Ss_3 ;Snh_3 ;Snd_3 ;Sno_3 ;Salk_3;Si_3 ;So_3];
Si_3 = 3.0000000e+01; Ss_3 = 1.1495418e+00; Xi_3 = 1.1491252e+03; Xsa_3 = 6.4854922e+01;
Xbh_3 = 2.5571314e+03; Xba_3 = 1.4894126e+02; Xp_3 = 4.5041834e+02; So_3 = 1.7183778e+00;
Sno_3 = 6.5408820e+00; Snh_3 = 5.5479452e+00; Snd_3 = 8.2888682e-01; Xnd_3 = 4.3924277e+00;
Salk_3 = 4.6747902e+00; Xse_3=420.0

Z40 = [Xbh_4 ;Xba_4 ;Xp_4 ;Xi_4 ;Xsa_4 ;Xse_4;Xnd_4 ;Ss_4 ;Snh_4 ;Snd_4 ;Sno_4 ;Salk_4;Si_4 ;So_4];
Si_4 = 3.0000000e+01; Ss_4 = 9.9532389e-01; Xi_4 = 1.1491252e+03; Xsa_4 = 5.5693982e+01;
Xbh_4 = 2.5591826e+03; Xba_4 = 1.4952712e+02; Xp_4 = 4.5131469e+02; So_4 = 2.4288838e+00;
Sno_4 = 9.2989988e+00; Snh_4 = 2.9673854e+00; Snd_4 = 7.6678656e-01; Xnd_4 = 3.8790101e+00;
Salk_4 = 4.2934562e+00; Xse_4=350.0

Z50 = [Xbh_5 ;Xba_5 ;Xp_5 ;Xi_5 ;Xsa_5 ;Xse_5;Xnd_5 ;Ss_5 ;Snh_5 ;Snd_5 ;Sno_5 ;Salk_5;Si_5 ;So_5];
Si_5 = 3.0000000e+01; Ss_5 = 8.8949280e-01; Xi_5 = 1.1491252e+03; Xsa_5 = 4.9305586e+01;
Xbh_5 = 2.5593436e+03; Xba_5 = 1.4979714e+02; Xp_5 = 4.5221112e+02; So_5 = 4.9094351e-01;
Sno_5 = 1.0415220e+01; Snh_5 = 1.7333316e+00; Snd_5 = 6.8828001e-01; Xnd_5 = 3.5271755e+00;
Salk_5 = 4.1255794e+00; Xse_5=250.0

The obtained trajectories of the full model state variables are given by the solid lines in Figures 9.60-9.62. They are used as target variables for the estimation of the parameters of the reduced model. The parameter estimation is done for the initial conditions of the process variables given for the reduced model by the vector x_0. The inflow concentration for the reduced model is the average one for dry weather, given by the vector X_i

X_0=[7.918;5.37;2.808;500.0;8.344;3.662;1.459;480.0;5.548;6.541;1.15;420.0;2.967;9.299;0.995;350.0;1.733;10.415;0.889;250.0]*0.01
Xi=[31.56 0 69.50]*0.1

The simulation for the reduced model is done for steady state conditions of the biomass and the slowly biodegradable substrate given by the vectors

```
XBH = 0.1*[2551.76*ones(1,K);2553.38*ones(1,K);2557.13*ones(1,K);2559.18*ones(1,K);2559.34*ones(1,K)];
XBA = 0.1*[148.389*ones(1,K);148.309*ones(1,K);148.941*ones(1,K);149.527*ones(1,K);149.797*ones(1,K)];
XSE =  0.1*[82.135*ones(1,K);76.386*ones(1,K);64.855*ones(1,K);55.694*ones(1,K);49.306*ones(1,K)];
```

The vector of the dissolved oxygen concentration for the reduced model is the same as for the full model. The sampling period is DT = 0.01042. The process reduced state space mass balance model matrices as taken from the Matlab program are the same as the given in point 9.2.2.1.

The results from the simulations are given from Figures 9.63 till Figure 9.67 where the trajectories of the full model process variables are given by the solid lines and the values of the reduced model state variables are given by the dashed lines.

The errors of the estimation are calculated as a weighted value of the sum of the squares of the errors of the process variables at the discrete points for the corresponding sum of the respective variables of the full model, as

$$e_S = \frac{ERR_S * ERR_S^T}{S * S^T}$$

where the S is one of the variables.

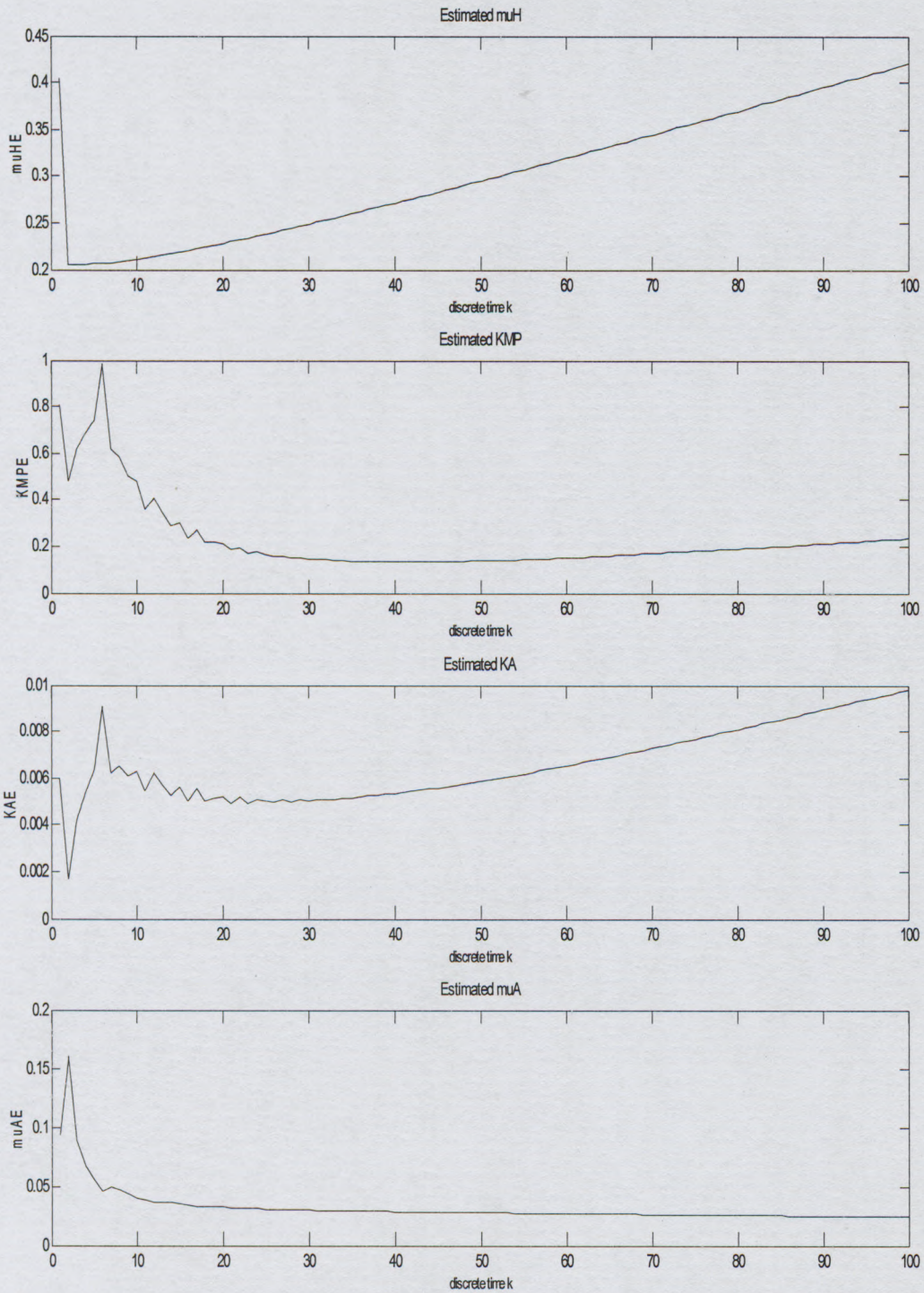

Figure 9.67: Trajectories of the reduced UCT biological model parameters for the Benchmark process

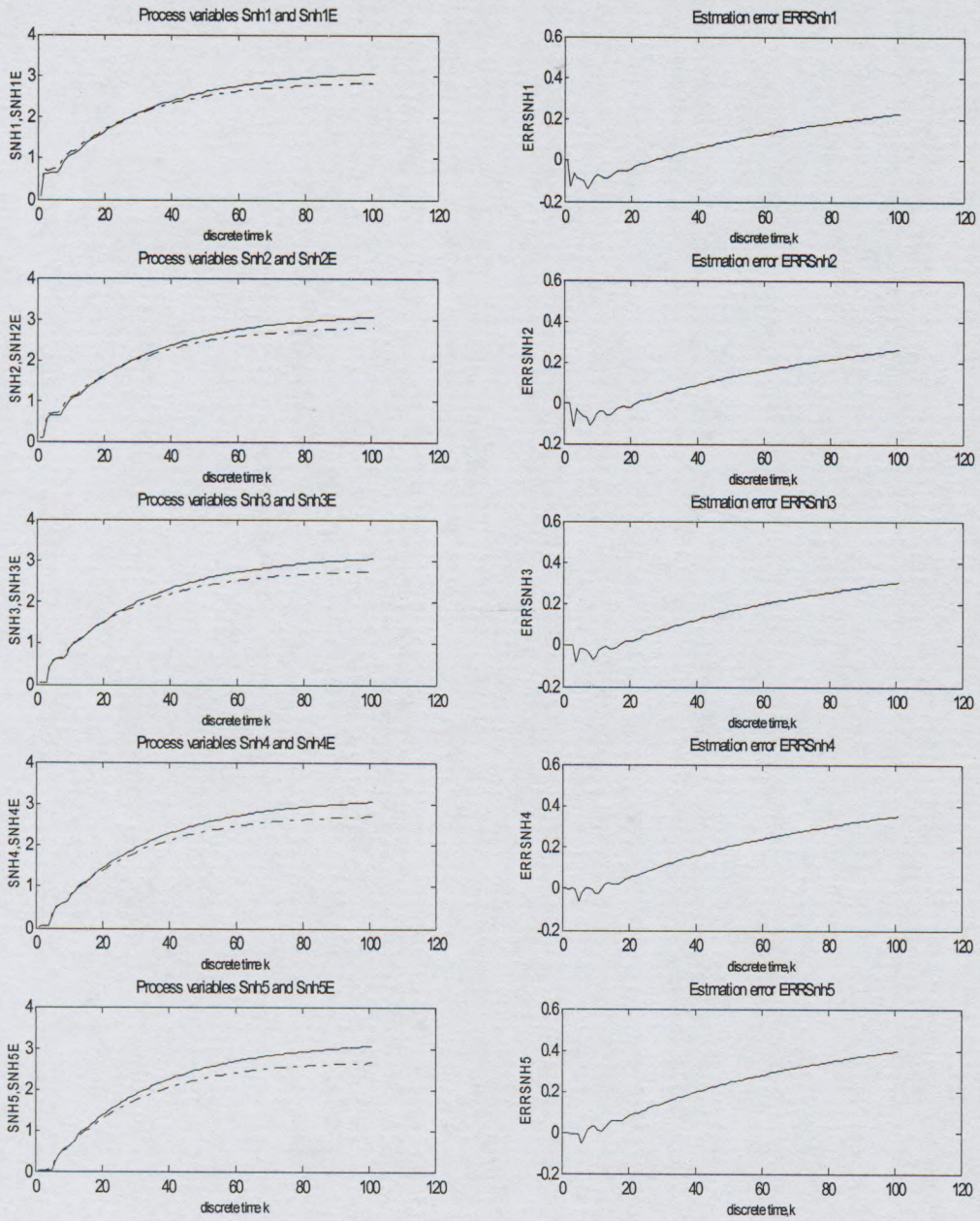

Figure 9.68: Trajectories of the UCT full (solid line), reduced estimated (dashed line) and the error between them as applied for the Benchmark process for the process variable SNH

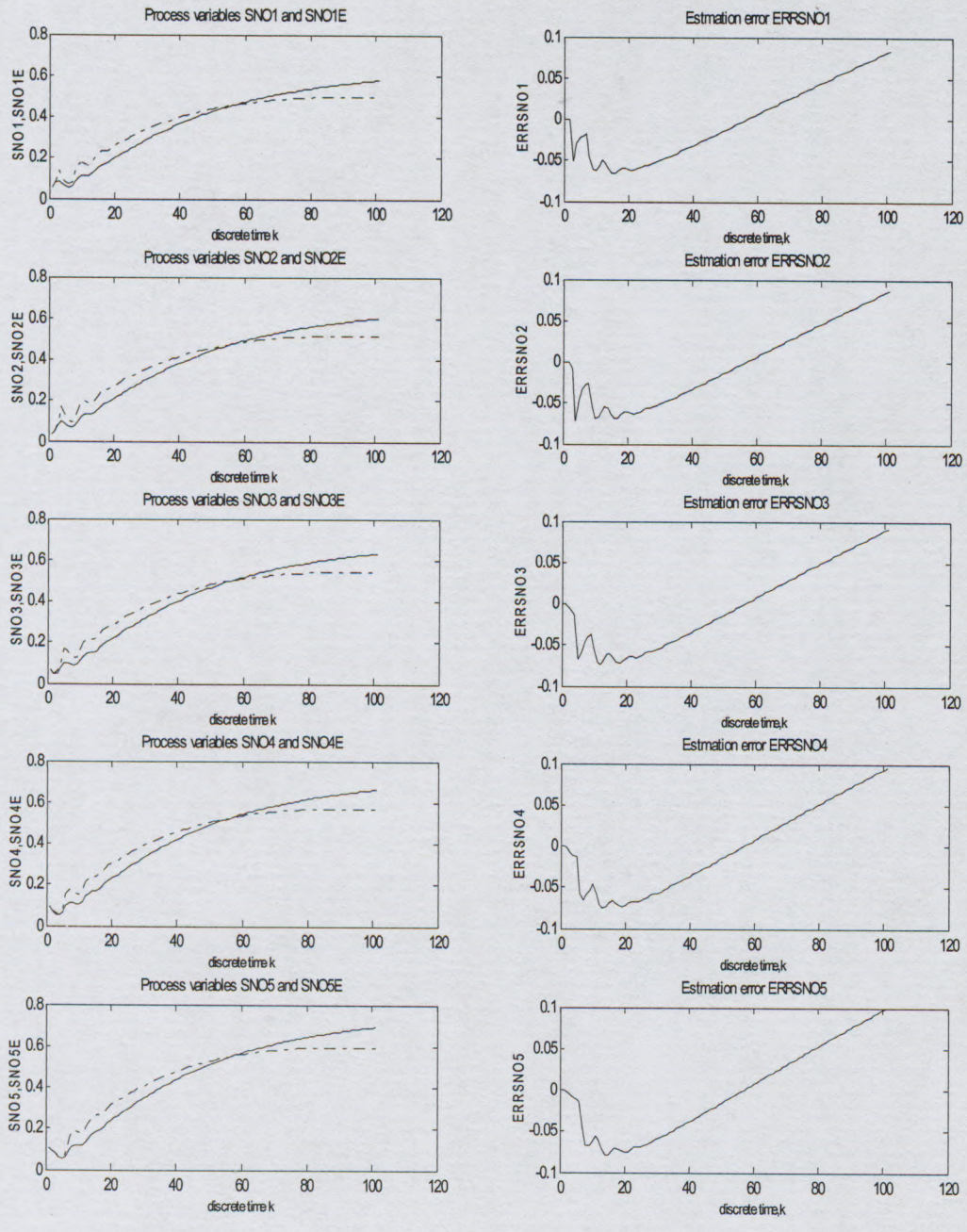

Figure 9.69: Trajectories of the UCT full (solid line), reduced estimated (dashed line) and the error between them as applied for the Benchmark process for the process variable SNO

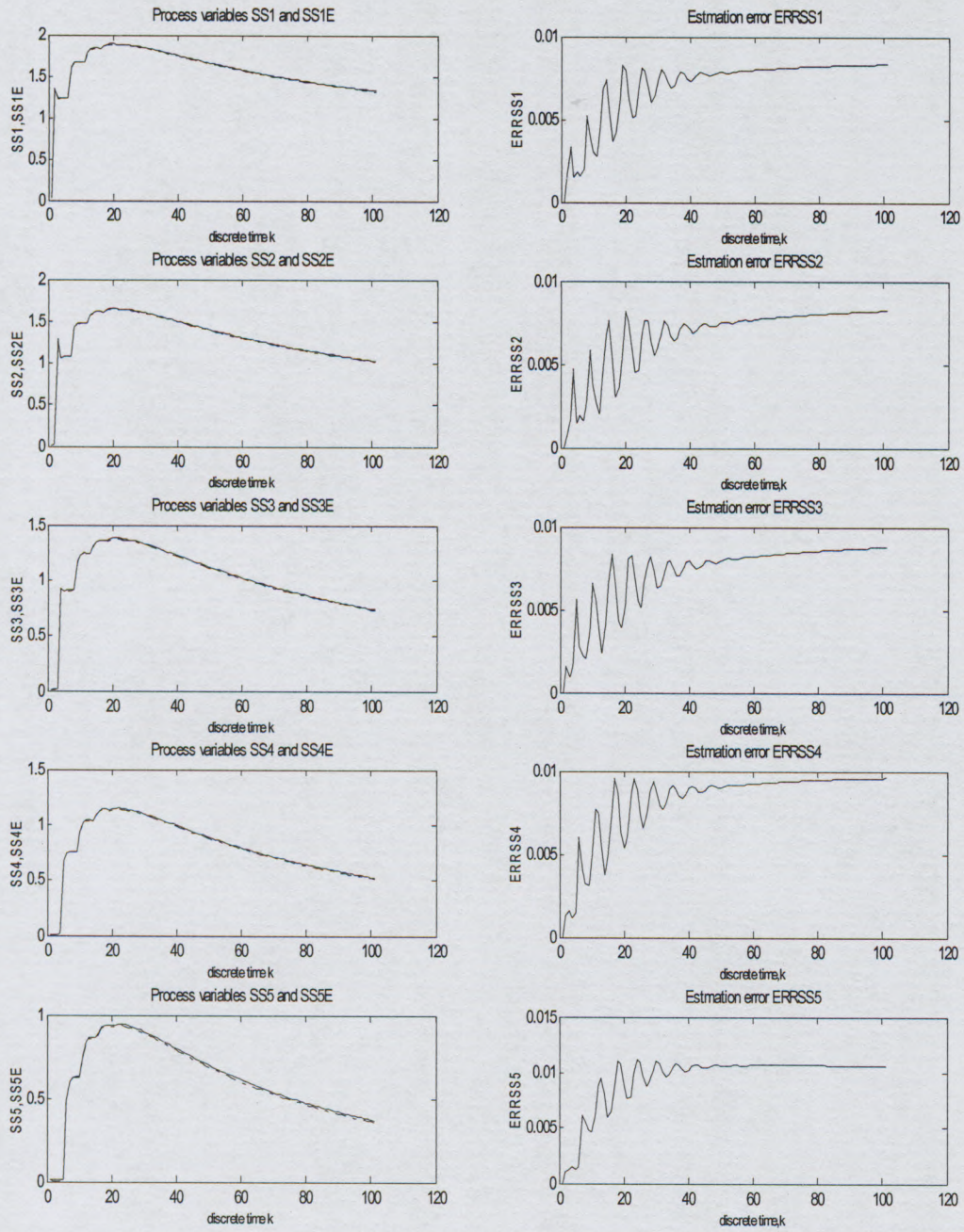

Figure 9.70: Trajectories of the UCT full (solid line), reduced estimated (dashed line) and the error between them as applied for the Benchmark process for the process variable SS

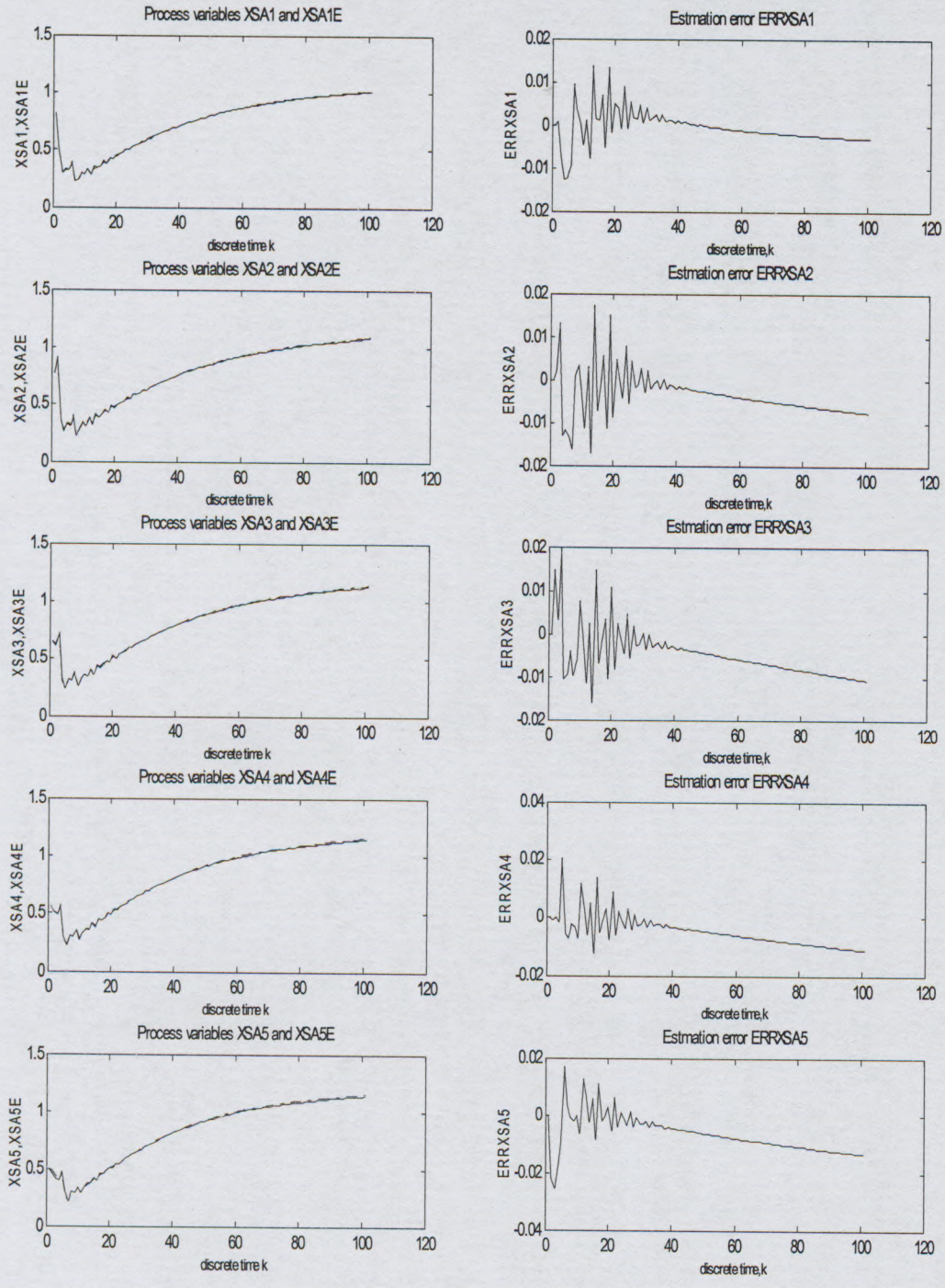

Figure 9.71: Trajectories of the UCT full (solid line), reduced estimated (dashed line) and the error between them as applied for the Benchmark process for the process variable XSA

9.3.3.2 Results for the Benchmark process

The calculated errors are given in Table 9.7

Table 9.7: The obtained weighted errors of reduced UCT model parameter estimation used for the Benchmark process mass balance models

Error pred / tank	eSnh	eSNO	eSS	eXSA
tank 1	0.0029	0.0120	2.0912E-005	2.6040E-005
tank 2	0.0040	0.0122	2.7614E-005	6.0335E-005
tank 3	0.0060	0.0121	4.9503E-005	7.4898E-005
tank 4	0.0086	0.0120	1.0142E-004	0.0118
tank 5	0.0118	0.0118	2.1773E-004	1.1166E-004

The trajectories of the UCT full model and UCT reduced model exhibit common behaviour which are very close to each other. The smallest error for the UCT reduced model can be seen to be 2.0912E-005 for SS in tank 1 but relatively speaking the errors are not that significantly different to influence major change. However the SS and XSA has a crucial bearing on the error prediction of the UCT reduced model due to the smaller critical error. Hence the UCT reduced model can be used for process optimization and controller design due to the reduced number of calculations for parameter estimation of SNH, SNO, SS and XSA compared to the UCT full model which depends on the complete Peterson matrix.

9.3 Conclusion

The methods of solution for sensitivity analysis and parameter estimation of the Activated sludge process are implemented in the frameworks of the software environment of Matlab and the results are presented in this chapter.

The maximum or minimum values of sensitivity function simulation for the Benchmark and Athlone process model based on the reduced ASM1 and UCT biological model are positively large or negatively large for the respective parameters concerned.

From the results in parameter estimation, it appears that SS has the least error but the errors are not that significantly different to influence major change. Hence the ASM1 and UCT reduced models can be used for process optimization and controller design due to the reduced number of calculations for parameter estimation of (SNH, SNO and SS) and (SNH, SNO, SS and XSA) compared to the ASM1 and UCT full models.

CHAPTER TEN

CONCLUSION, DELIVERABLES AND FUTURE DIRECTIONS OF RESEARCH

10.1 Introduction

The problem for effective and optimal control of wastewater treatment plants is very important recently because of the increased requirements to the quality of the effluent. The activated sludge process is a type of wastewater process characterized with complex dynamics and because of this proper control design and implementation strategies are necessary and important for its operation.

The most critical phase in the solution of any control problem is the modelling stage. The primary building block of any modern control exercise is to construct and identify a model for the system to be controlled. The existing full ASM1 and especially UCT biological models of the activated sludge process are highly complex because they are characterised with :-

- a lot of variables that are difficult to be measured on-line,
- complex dependencies and nonlinear interconnections between the biological variables,
- many kinetic parameters that are difficult to be determined,
- different time scales for the process dynamics,
- the control actions for the process are not included in explicit way in model equations.

All these difficulties require simpler and with reduced size models to be developed for the purpose of real-time control design and implementation.

10.2 Aims and Objectives

The project considers reduction of the impact of the complexity of the process model over the methods for control design by development of reduced models and methods for parameter and state estimation of these models.

The aim of the project is to analyze the existing and to develop theoretical methods, algorithms and software for simplification, parameter and state estimation of the mathematical mass balance and biological models of the

activated sludge process under the condition for fully representation of the process dynamics.

The aim of the project is achieved through the following objectives/ deliverables:

1. Study of the complex relationships between the process variables in connection with the kinetic differential equations describing the process.

2. Reducing the complexity of the model through grouping or cutting some of the mathematical representation in the model with criterion keeping the dynamical behaviour of the reduced model not changed in comparison with the original one.

3. Development of sensitivity functions of the reduced models' variables towards the models' parameters. Analysis of the dynamics of the models of sensitivity.

4. Development method for parameter estimation of the transformed models on the basis of the least-squares approach. Validation of the model.

5. Comparative analysis of the methods for state estimation. Development of tangent linear models of the nonlinear wastewater reduced models and application of Kalman filter for state estimation

6. Development of algorithms and programmes for simulation, sensitivity functions calculation and simulation and for parameter estimation using SIMBA and MATLAB/Simulink software.

10.2 Achievements of the thesis

10.2.1 A REDUCED ASM1 BIOLOGICAL AND MASS BALANCE MODELS OF THE COST BENCHMARK AND ATHLONE PLANTS ARE DEVELOPED ON THE BASIS OF CRITICAL ANALYSIS OF THE PROCESS VARIABLES

10.2.2 A REDUCED UCT BIOLOGICAL AND MASS BALANCE MODELS OF THE COST BENCHMARK AND ATHLONE PLANTS ARE DEVELOPED ON THE BASIS OF CRITICAL ANALYSIS OF THE PROCESS VARIABLES

10.2.3 METHOD FOR CALCULATION OF THE SENSITIVITY FUNCTIONS TOWARDS ALL MODEL PARAMETERS OF THE REDUCED ASM1 BIOLOGICAL MODEL FOR THE COST BENCHMARK AND ATHLONE PLANTS IS DEVELOPED

10.2.4 METHOD FOR CALCULATION OF THE SENSITIVITY FUNCTIONS TOWARDS ALL MODEL PARAMETERS OF THE REDUCED UCT BIOLOGICAL MODEL FOR THE COST BENCHMARK AND ATHLONE PLANTS IS DEVELOPED

10.2.5 METHOD FOR CALCULATION PARAMETER ESTIMATES OF THE REDUCED ASM1 BIOLOGICAL MODEL FOR THE COST BENCHMARK AND ATHLONE PLANTS IS DEVELOPED ON THE BASIS OF THE LEAST SQUARES TECHNIQUES

10.2.6 METHOD FOR CALCULATION PARAMETER ESTIMATES OF THE REDUCED UCT BIOLOGICAL MODEL FOR THE COST BENCHMARK AND ATHLONE PLANTS IS DEVELOPED ON THE BASIS OF THE LEAST SQUARES TECHNIQUES

10.2.7 THEORETICAL ANALYSIS OF THE EXISTING METHODS FOR PARAMETER AND STATE ESTIMATION OF BIOTECHNOLOGICAL PROCESSES IS DONE. A LINEARIZED TANGENT MODEL OF THE BENCHMARK MASS BALANCE MODELS BASED ON ASM1 AND UCT BIOLOGICAL MODELS ARE DEVELOPED. THE LINEAR KALMAN FILTER ALORITHM IS DEVELOPED FOR THESE MODELS.

10.2.8 SIMBA SOFTWARE FOR SIMULATION OF THE MITCHELL'S PLAIN PLANT BASED ON THE UCT BIOLOGICAL MODEL IS DEVELOPED

10.2.9 SIMBA SOFTWARE FOR SIMULATION OF THE ATHLONE PLANT BASEDD ON THE ASM1 AND UCT BIOLOGICAL MODELS IS DEVELOPED

10.2.10 SOFTWARE FOR SIMULATION OF SENSITIVITY FUNCTIONS OF THE PROCESS VARIABLES TOWARDS THE MODEL PARAMETERS FOR THE BENCHMARK MASS BALANCE MODEL BASED ON THE REDUCED ASM1 BIOLOGICAL MODEL IS DEVELOPED

The main program, BASM1S.m calculates the sensitivity model and simulates the sensitivity functions for the process variables of the Benchmark process based on ASM1 reduced biological model towards the model parameters. The program calls the function subroutine rateASM1.m. The calculation uses reduced biological model with 3 variables SNH, SNO and SS

The subprogram function rateASM1.m calculates the process rates, derivatives of the process rates towards the model parameters and variables and forms the sensitivity model matrices necessary for simulation of the process variables and the sensitivity functions for the Benchmark process based on the reduced ASM1 biological model.

10.2.11 SOFTWARE FOR SIMULATION OF SENSITIVITY FUNCTIONS OF THE PROCESS VARIABLES TOWARDS THE MODEL PARAMETERS FOR THE BENCHMARK MASS BALANCE MODEL BASED ON THE REDUCED UCT BIOLOGICAL MODEL IS DEVELOPED

The main program, BUCTS1.m calculates the sensitivity model and simulates the sensitivity functions for the process variables of the Benchmark process based on UCT reduced biological model towards the model parameters. The program call the function subroutine rate BUCTS.m. The calculation uses reduced biological model with 3 variables SNH, SNO, SS and Sads

The subprogram function rateASM1.m calculates the process rates, derivatives of the process rates towards the model parameters and variables and forms the sensitivity model matrices necessary for simulation of the process variables and the sensitivity functions for the Benchmark process based on the reduced UCT biological model.

10.2.12 SOFTWARE FOR SIMULATION OF SENSITIVITY FUNCTIONS OF THE

PROCESS VARIABLES TOWARDS THE MODEL PARAMETERS FOR THE ATHLONE MASS BALANCE MODEL BASED ON THE REDUCED ASM1 BIOLOGICAL MODEL IS DEVELOPED

The main program, AASM1S.m calculates the sensitivity model and simulates the sensitivity functions for the process variables of the Athlone process based on ASM1 reduced biological model towards the model parameters. The program call the function subroutine rateAASM1.m. The calculation uses reduced biological model with 3 variables SNH, SNO and SS

The subprogram function rateAASM1.m calculates the process rates, derivatives of the process rates towards the model parameters and variables and forms the sensitivity model matrices necessary for simulation of the process variables and the sensitivity functions for the Athlone process based on the reduced ASM1 biological model.

10.2.13 SOFTWARE FOR SIMULATION OF SENSITIVITY FUNCTIONS OF THE PROCESS VARIABLES TOWARDS THE MODEL PARAMETERS FOR THE ATHLONE MASS BALANCE MODEL BASED ON THE REDUCED UCT BIOLOGICAL MODEL IS DEVELOPED

The main program function rateAUCTS.m calculates the process rates, derivatives of the process rates towards the model parameters and variables and forms the sensitivity model matrices necessary for simulation of the process variables and the sensitivity functions for the Athlone process based on the reduced UCT biological model.

The subprogram function rate AUCTS.m calculates the process rates, derivatives of the process rates towards the model parameters and variables and forms the sensitivity model matrices necessary for simulation of the process variables and the sensitivity functions for the Athlone process based on the reduced UCT biological model.

10.2.14 SOFTWARE FOR GROWTH PARAMETER ESTIMATION OF THE BENCHMARK MASS BALANCE MODEL FOR THE CASE OF ASM1 REDUCED MODEL

The main program, BASM1parest.m estimates the reduced ASM1 model parameters for the Benchmark process, the estimations of the kinetic parameters muH, muA and Kh and calculates the errors between the process variables behaviour for the full and reduced ASM1 models. The program call the

function subroutines rateASM1F.m, prateASM1R.m and rateASM1RE.m. The calculation uses reduced biological model with 3 variables SNH, SNO and SS

The subprogram function rate ASM1F.m calculates the process rates of the full ASM1 biological model at every moment of the time.

The subprogram function prateASM1.m calculates the functions of the process rates which multiply the process estimated parameters for the Benchmark process based on the reduced ASM1 biological model at every moment of time.

The subprogram function rateASM1.m calculates at every moment the process rates of the reduced ASM1 model using the estimated values of the model parameters.

10.2.15 SOFTWARE FOR GROWTH PARAMETER ESTIMATION OF THE ATHLONE MASS BALANCE MODEL FOR THE CASE OF ASM1 REDUCED MODEL IS DEVELOPED

The main program, BASM1parest.m estimates the reduced ASM1 model parameters for the Athlone process and calculates the errors between the process variables behaviour for the full and reduced models. The program call the function subroutines rateASM1F.m, prateASM1R.m and rateASM1RE.m. The calculation uses the reduced biological model with 3 variables SNH, SNO and SS. The program uses global definition of the model parameters

The subprogram function rateASM1F.m calculates the process rates of the full ASM1 biological model for the Athlone process.

The subprogram function prateASM1R.m calculates at every moment the functions of the process rates which multiply the process estimated parameters for the Athlone process based on the reduced ASM1 biological model.

The subprogram function rateASM1RE.m calculates at every moment the process rates of the reduced ASM1 model using the estimated parameters.

10.2.16 SOFTWARE FOR GROWTH PARAMETER ESTIMATION OF THE BENCHMARK MASS BALANCE MODEL FOR THE CASE OF UCT REDUCED MODEL IS DEVELOPED

The main program, BUCTparest.m calculates the trajectories of the full mass-balance model, the estimations of the kinetic parameters muH, muA, KMP and KA, and the trajectories of the process variables of the reduced mass-balance model for the Benchmark process with the UCT reduced biological model. The program calls the function subroutines rateBUCTF.m, rateBUCTE.m and prateBUCTR.m. The calculation uses the reduced biological model with 4 variables SNH, SNO,SS and Sads

The subprogram function rateBUCTF.m calculates at every moment the process rates of the full UCT biological model for the Benchmark process.

The subprogram function prateBUCTR.m calculates at every moment the function P, which multiplies the estimated parameters for the reduced UCT biological model and Benchmark process.

The subprogram function rateBUCTE.m calculates at every moment the process rates using the estimated values of the parameters for the reduced UCT biological model and the Benchmark process.

10.3 Discussion and importance of the achievements

10.3.1 The developed ASM1 and UCT reduced models are based on the existing process variables considered in their respective time scales of dynamic behaviour. The reduced models do not introduce new or combined variables, which makes the use of models simpler than some similar ones proposed in the literature.

10.3.2 The development of the reduced UCT model is based on the UCT full model principles for the enzyme reactions of the activated sludge and in this way the reduced model keeps the UCT approach. The obtained reduced model is a first attempt for reduction of the very complex UCT full model for purposes of optimal control calculation.

10.3.3 The sensitivity functions of the developed reduced mass-balance models are calculated towards all parameters which gives vast amount of data for proper selection of the parameters with the biggest influence over the variables behaviour. This means that only the parameters with the bigger influence can be considered for estimation, which makes the process of estimation simpler and faster.

10.3.4 The mass-balance equations for the dissolved oxygen are not a part of the reduced models as the time scale of the dissolved oxygen dynamics are a couple of times faster than those of the substrate , ammonia and nitrogen compounds. This fact makes the models very convenient for purposes of state and parameter estimation and process optimization.

10.3.5 The method for estimation of the reduced model parameters requires steady state data for the biomass concentrations and slowly biodegradable substrate, real-time data for the dissolved oxygen concentration, readily biodegradable substrate, ammonia and nitrate nitrogen. The steady state values can be taken from laboratory measurements every week. There are still difficulties for real time measurements of the required above variables in the municipality waste-water plants

10.4 Recommendations

10.4.1 Applications

The developed methods, algorithms and software serve for:

- *Understanding*: Insight in the treatment processes is still insufficient and there is a lack of suitable mathematical models.
- *Inadequate instrumentation*: Non-existent or insufficiently reliable technology.
- *Plant constraints*: Inapt and insufficient flexibility to manipulate the process.
- *Economic motivation*: There exists a lack of fundamental knowledge concerning benefits versus costs of automated treatment processes. In addition, wastewater treatment processes are not productive and automation can only contribute to a decrease of operating costs but does not directly lead to increased profit.
- *Education and training*: Operators are not always adequately trained to operate advanced sensor and control equipment and most environmental engineers would need more basic understanding of process dynamics and control in order to appreciate the potential of instrumentation, control and automation.
- *Communication*: The interaction between operators, designers, equipment suppliers, researchers and government regulatory agencies is often unsatisfactory and leads to poorly designed plants
- *Real time control.* Parameter estimation is a common feature in many areas of process modeling, both in on-line applications such as real time optimization and in off-line applications such as the modeling of reaction kinetics and biotechnological processes

10.4.2 Future directions

10.4.2.1 The structure of SIMBA package allows to integrate the sensitivity studies and parameter estimation work within SIMBA such as providing a Graphic User Interface (GUI) for the operators or researchers in a user-friendly environment. This technological advance should to readily attainable for the control and computer engineers to be able to make the paradigm shift to another level for

easy access to Wastewater engineers. The state and parameter estimation research could primarily focus on the development of more user-friendly applications such as hands-on usage.

10.4.2.2 The development of the method for nonlinear parameter estimation require s more in-depth investigation on the plethora of the techniques at it's disposal and fine tuning and identifying the methods which are favourably suitable for study.

10.4.2.3 The future research should involve the real time study of biological excess phosphorus removal, ASM2 and ASM2d systems developing software for this type of activated sludge.

10.4 Publications

10.4.1 Sensitivity study of the activated sludge reduced models for the purposes of parameter estimation and process optimization 1. Benchmark process with the ASM1 and UCT reduced biological models – WaterSA journal (under revision).

10.4.2 Sensitivity study of the activated sludge reduced models for the purposes of parameter estimation and process optimization 2. Athlone process with the ASM1 and UCT reduced biological models – WaterSA journal (under revision).

BIBLIOGRAPHY

Adby, P.R. & Dempster, M.A.H. 1974. Introduction to Optimization Methods, London, Chapman and Hall.

Ahmad, S.R. & Reynolds, D.M. 1999: "Monitoring of water quality using fluorescence technique: prospect of on-line process control". Water Research, 33(9): 2069-2074.

Albiol, J., Robuste, J., Casas, C. & Poch, M. 1993. Biomass estimation in plant cell cultures using an extended Kalman filter, Biotechnology Progress, 9, 174-178.

Alcaraz-Gonzalez, V., Salazar-Pena, R., Gonzalez-Alvarez, V., Gouze, J-L. & Steyer, J-P. 2005. A tunable multivariable nonlinear robust observer for biological systems. C.R.Biologies, 328: 317-325.

Alex, J., Ogurek, M. & Jumar, U. 2005. Formalised Model Representation for wastewater systems. . Preprints from Proceedings of the 16th IFAC World Congress, 4 July – 8 July, Prague, Czech Republic.

Al-Ghazzawi, A., Ali, E., Nouh, A. & Zafiriou, E. 2001. On line tuning strategy for model predictive controllers. Journal of Process Control, 11: 265-284.

Ali, E. & Zafiriou, E. 1993. On the tuning of Nonlinear Model Predictive Control Algorithms. Proceedings of the American Control Conference: 786-790.

Al-Saggaf, U.M. & Franklin, G.F. 1988. Model reduction via balanced realisations: an extension and frequency weighting techniques. IEEE Transactions Automatic Control AC-33(7): 687-692.

Anderson,B.D.O. & Liu, Y. 1989. Controller reduction: concepts and approaches. IEEE transactions Automatic Control, 34(8): 802-811.

Anderson, B.D.O. & Moore, J.B. 1989. Linear Quadratic Methods, Prentice Hall.

Andrews, J.G.& Mclone, R.R. 1971: Mathematical Modeling, New York, Butterworth.

Aris, R. 1999. Mathematical Modeling, Vol. VI, New York, Academic Press.

Aris, R. 1994. Mathematical Modeling Techniques, Dover.

Aschemann, H., Rauh, A., Kletting, M., Hofer, E.P., Gennat, M. & Tibken, B. 2005. Interval Analysis and Nonlinear Control of Wastewater Plants with Parameter Uncertainty. Preprints from Proceedings of the 16th IFAC World Congress, 4 July – 8 July, Prague, Czech Republic.

Assis, A.J. & Filho, R.M. 2000. Soft sensors development for on-line bioreactor state estimation. Computers and Chemical Engineering, 24: 1099-1103.

Astrom, K.J. & Wittenmark, B. 1990. Computer-Controlled Sytems, Theory and Design, (2nd ed.), Englewood Cliffs, New Jersey, USA. Prentice Hall, Inc.

Aubrun, C., Theilliol, D., Harmand, J. & Steyer, J.P. 2001. Software sensor design for COD estimation in an anaerobic fluidised bed reactor. Water Science Technology, 43(7): 115-122.

Ayesa, E., Oyarbide, G., Larrea, L. & Garcia-Heras, J.L. 1995. Observability of reduced order models-application to a model for control of Alpha process. Water Science Technology, 31(2): 161-170.

Barbu, M., Caraman, S. & Ceanga, E. 2005.QFT (Quantitative Feedback Theory) Robust Control of Wastewater Treatment Process. Preprints from Proceedings of the 16th IFAC World Congress, 4 July – 8 July, Prague, Czech Republic.

Barbu, M., Barbu, G. & Ceanga, E. 2004. The Multi-model Control of Wastewater Treatment Process with Activated Sludge, 12th Mediterranean Conference on Control and Automation – Med'04, Kusadasi, Turkey, Proc. CD-ROM, 6-9 June.

Bard, Y. 1974. Nonlinear Parameter Estimation, New York, Academic Press.

Barker, P.S. & Dold, P.L. 1997. General model for biological nutrient removal activated sludge systems: model presentation, Water Environmental Research, 69(5): 969-984.

Bastin, G. & Dochain, D. 1990. On-line Estimation and Adaptive Control of Bioreactor, New York, Elsevier.

Bastin, G. & Gevers, M. 1988: Stable adaptive estimator for nonlinear time varying systems. IEEE Trans. AC 33: 650-658.

Bastin, G. 1988: State estimation and adaptive control of multilinear compartmental systems : theoretical framework and application to biotechnological processes, in New trends in nonlinear systems theory, Lecture Notes on Control and Information Science, : 122, Springer Verlag.

Bastin, G., Mareels, I.M.Y., Dochain, D. & Gevers, M. 1988: Sufficient experimental conditions for the convergence of an adaptive observer for nonlinear systems. Proceedings of 8th IFAC Symposium on identification and System Parameter Estimation, Beijing, China: 1762-1766.

Bastin, G. & Dochain, D. 1986. On-line estimation of microbial specific growth rates. Automatica, 22(6): 705-711.

Beck, C., Doyle, J. & Glover, K. 1996. Model reduction of multi-dimensional and uncertain systems. IEEE Transactions Automatic Control, 41(10): 1466-1477.

Beck, M.B. 1986 . Identification, Estimation and Control of Biological Wastewater Treatment Processes. Proceedings of Institute Electrical Engineering, 133: 254-264.

Beck, M.B. 1987. Water Quality Modelling. A Review of the Analysis of Uncertainty. Water Resources Research, 23(8): 1393-1442.

Bellgardt, K.H., Meyer, H.D., Kuhlmann, W., Schurgeri, K. & Thoma, M. 1984. On-line estimation of biomass and fermentation parameters by a Kalman filter during during a cultivation of Saccharomyces cerevisiae. 3rd European Congress Biotechnology, Verlag Chemie, Weinheim, 2: 607-616.

Bennett, W.R. 1976. Scientific and Engineering Problem-Solving with the Computer, New Jersey, Englewood Cliffs, Prentice-Hall.

Ben Youssef, C. & Dahhou, B. 1996. Multivariable adaptive control of an aerated lagoon for a wastewater treatment process. J. Proc. Cont., 6(5): 265-275.

Bernard, O. & Gouze, J.L. 2004. Closed loop observers bundle for uncertain biotechnological models. J. Proc. Control, 14: 765-774.

Bernard, O. 2002. Mass balance modeling of bioprocesses, Mathematical Control Theory, ICTP lecture notes.

Bernard, O., Hadj-Sadok, Z. & Gouze, J. 2000. Observers for the biotechnological processes with unknown kinetics. Application to wastewater treatment. Proceedings of the 39th IEEE Conference on Decision and Control, Sydney, 4526-4531.

Betanair, M.J., Moreno, J. & Buitron, G. 2004b. Practical Optimal Control for Fed-Batch Bioreactors.

Preprints of NOCCOS 2004, Stuttgart, Germany, 1-3 Sept.: 1517-1522.

Betancour, M., Dochain, D., Fibrianto, H. 2004. Eoli workpackage 2: Model selection and parameter identification. Technical Report Deliverable D2.3: Validated Model. European Community Research.

Biagiola, S.I. & Figueroa, J.L. 2004. Application of state estimation based NMPC to an unstable nonlinear process. Chemical Engineering Science, 59: 4601-4612.

Bich Pham, H.T., Larsson, G. & Enfor, S.-O. 1998. Growth and energy metabolism in aerobic fed-batch cultures of Saccharomyces cerevisiae : Simulation and model verification. Biotechnology Bioengineering, 60(4): 474-482.

Billing, A.E. & Dold, P.L. 1988. Modelling techniques for biological reaction systems. 1. Mathematical description and model representation. Water SA, 14(4): 185-192.

Billing, A.E. & Dold, P.L. 1988. Modelling techniques for biological reaction systems. 2. Modelling of the steady state case . Water SA,14(4): 193-206.

Birkes, D., Dodge, Y. 1993. Alternative Methods of Regression, New York, New York, USA. John Wiley and Sons, Ltd.

Bjorck, A. 1996. Numerical Methods for Least Squares Problems. SIAM, Philadelphia.

Blackwell, L.G. 1971. A theoretical and experimental evaluation of the transient response of the activated sludge process. Ph D thesis. Clemson Univ. Clemson. S Carolina.

Bogaerts, Ph. & Wouwer, A.V. 2004. Parameter identification for state estimation – application to bioprocess software sensors. Chemical Engineering Science, 59: 2465-2476.

Bogaerts, Ph. & Hanus, R. 2001. On-line estimation of bioprocesses with full horizon observers. Mathematics Computer Simulation, 56: 425-441.

Bogaerts, Ph. & Hanus, R. 2000. Macroscopic modeling of bioprocesses with a view to engineering applications. In : Focus on Biotechnology, Thonard, Ph., Hofman, M., (ed.), vol. 5, Engineering and Manufacturing for biotechnology, Kluwer Academic Publishers.

Bogaerts, Ph. 1999. Contribution a la modelisation mathematique pour la simulation et l'observation d etat des bioprocedes, Ph. D. thesis, Universite libre de Bruxelles.

Boyd, S. & Vandenberghe, L. 2002. Introduction to Convex Optimization with Engineering Applications. Lecture Notes, Stanford University, (Available at : isl.stanford.edu/pub/boyd/)

Brdys, M.A. & Diaz-Marquez, J. 2002. Application of Fuzzy Model predictive control to the dissolved oxygen concentration tracking in an activated sludge process. 15th IFAC Triennial World Congress, Barcelona, Spain.

Brdys, M.A., Zhang, Y. 2001a. Robust Hierachial Optimising Control of Municipal Wastewater Treatment Plants. Preprints of the 9th IFAC/IFORS/IMACS/IFIP Symposium Large Sclae Systems:Theory & Applications, Bucharest, Romania, 18-20 July: 540-547.

Brdys, M.A., Konarczak, K. 2001b. Dissolved Oxygen Control for Activated Sludge Processes. Preprints of the 9th IFAC/IFORS/IMACS/IFIP Symposium Large Scale Systems:Theory & Applications, Bucharest, Romania, 18-20 July: 548-553.

Breyfogle, F.W.& Breyfogle F.W. III. 2003. Implementing Six Sigma: Smart Solution using Statistical Methods, Technology & Engineering, 275.

Bronson, R. 1973. Theory and Problems of Modern Introductory Differential Equations [Schaum's Outline Series], New York, McGraw-Hill.

Brouzes, P. 1968. Automated Activated sludge Plants with respiratory metabolizm control, Proceeding of the 4th International Conference on Water Pollution Control Research, Prague.

Brown, R.G. & Hwang, P.Y.C. 1992. Introduction to random signals and applied Kalman Filtering, 2nd ed, New York., John Wiley & Sons.

Burden, R.L., Douglas Faires, J. & Reynold, S. 1981. Numerical Analysis, 2nd ed, Pacific Grove, Carlifornia., Prindle, Webber & Schmidt.

Busby, J.L. & Andrews, J.F. 1973. Dynamic modeling and control strategies for the activated sludge process. Research Report, Dept of Environmental Systems Engineering, Clemson University, Clemson, S Carolina.

Caminal, G., Lafuente, J., Lopez-Santin, J., Poch, M. & Sola, C. 1987. Application of Extended Kalman Filter to identification of Enzymatic Deactivation. Biotechnology Bioengineering, 29: 366-369.

Carlson, B. 1993. On-line estimation of the respiration rate in an Activated Sludge Process, Water Science Technology, 28, 427-432.

Carney, T.M. & Goldwyn, R.M. 1967. Numerical experiments with various optimal estimators. Journal of Optimization Theory Applications, 1: 113-130.

Carson, E.R., Cobelli, C. & Finkelstein, L. 1979. The Identification of Metabolic Systems – A Review. In Iserman, R., Identification and System Parameter Estimation, Oxford, Pergamon Press, 1: 151-171.

Chavent, G. 1979. Identification of Distributed Parameter Systems: About the Output Least Square Method, its Implementation, and Identifiability. In Iserman, R., Identification and System Parameter Estimation, Oxford, Pergamon Press, 1: 85-97.

Chen, L., Bastin, G. & Dochain, D. 1990. Parameter identifiability of a class of nonlinear compartmental models for bioprocesses. Proc. IFAC World Congress, Tallinn, USSR.

Chen, L. 1990 Identification and Control of Biological Systems. Doctoral Dissertation, University Catholic Louvain, Belgique.

Chidambara, M.P. 1969. Further comments by M.R. Chidambara. IEEE Transactions Automatic Control, AC-12:799-800.

Childers, D.G. 1997. Probability and Random Processes, New York, McGraw-Hill-Irwin.

Chow, G.C. 1964. A comparison of alternative estimators for simultaneous equations. Econometrica, 32: 532-553.

Christofides, P.D. & Daoutidis, P. 1998. Robust control of hyperbolic PDE systems. Chemical Engineering Science, 53(1): 85-105.

Christofides, P.D. & Daoutidis, P. 1996. Feedback control of hyperbolic PDE systems. American Institute of Chemical Engineers Journal, 42(11): 3063-3086.

Cinlar, E. 1975. Introduction to Stochastic Processes, Englewood Cliffs, Prentice-Hall.

Clark, D.W. 1967.Generalised least squares estimation of parameters of a dynamic model. 1st IFAC Symposuim on Identification and Automatic Control and Systems, Prague.

Close, C.M. & Frederick, D.K. 1994. Modeling and Analysis of Dynamic Systems, 2nd ed, New York., Wiley.

Conte,C.M., Dean, S.K. & de Boor, C. 1980. Elementary Numerical Analysis, 3rd ed, NewYork., McGraw-Hill.

Cooper, G.R. & McGillem, C.D. 1998. Probabilistic Methods of Signal and System Analysis, 3rd ed., Oxford, Oxford University Press.

Copp, J. 2002. COST Action 624 - - The Cost Simulation Benchmark: Description and Simulation Manual, European Commission.

Cragg, J.G. 1967. On the relative small sample properties of several structural-equation estimators. Econometrica, 35: 89-110.

Crassidis, J. & Jenkins, J. 2004. Optimal estimation of dynamic systems, New Jersey, Chapan & Hall/CRC.

Cronje, G.L., Beeharry, A.O., Wentzel, M.C. & Ekama, G.A. 2002. Active biomass in activated sludge mixed liquor. Water Res., 36: 439-444.

Dacosta, P., Kordich, C., Williams, D. & Gomm, J.B. 1997. Estimation of inaccessible fermentation states with variable inoculum sizes. Artificial Intelligence Engineering, 11(4): 383-392.

Dai, H., Sinha, N. & Puthenpura, S. 1989. Robust combined estimation of states and parameters of bilinear systems, Automatica, 25(4), 613-616.

Darouach, M., Zasadzinski, M. & Xu, S. 1994. Full order observers for linear systems with unknown inputs, IEEE Transaction Automation Control, 39(3), 1068-1072.

Davison, E.J. 1966. A method for simplifying linear dynamic systems. IEEE Transactions Automatic Control, AC-11: 93-101.

Dekkers, R.M., 1983. State estimation of fed-batch Baker's yeast fermentation. In A. Halme (Ed.), Modelling and Control of Biotechnical Processes, Pergamon, Oxford: 201-212.

Director, S.W. & Rohrer, R.A. 1988. Introduction to System Theory, New York, McGraw-Hill.

Dochain, D. 2003. State and parameter estimation in the chemical and biochemical processes: a tutorial. Journal of Process Control, 13: 801-818.

Dochain, D. & Vanrolleghem, P.A., 2001. Dynamical Modelling and Estimation in Wastewater Treatment Processes, London, UK. IWA Publishing.

Dochain, D., Vanrolleghem, P.A. & Van Daele, M. 1995. Structural identifiability of biokinetic models of activated sludge respiration. Water Research, 29: 2571-2579.

Dold, P.L., Wentzel, M.C., Billing, A.E., Ekama, G.A. & Marais G.v.R. 1991.Activated sludge simulation programs. Water Research Commission, P.O. Box 824, Pretoria 0001, South Africa.

Dold, P.L., Ekama, G.A. & Marais, G.v.R. 1980. A general model for the activated sludge process. Progress Water Technology, 12: 47-77.

Downing, A.L., Painter, H.A. & Knowles, G. 1964. Nitrification in the activated sludge process. Journal of Proceedings Institute Sewerage Purification, 64: 130-158.

Drazin, P.G. 1992. Nonlinear Systems, Cambridge, Cambridge University Press.

Eckenfelder, W.W. & Grau, P. 1992. Activated sludge process design and control: Theory and practice, Lancaster, Pennsylvania, Technomic Publishing Company.

Ekama, G.A. & Wentzel, M.C. 1999. Denitrification kinetics in biological N and P removal activated sludge systems treating municipal wastewaters, Water Science Technology, 39(6):69-77.

Ekama, G., Dold, P. & Marais, G. 1986. Procedures for determining influent COD fractions and maximum specific growth rate of heterotrophs in activated sludge systems, Water Science Technology, 18, 91-114.

Ekama, G., Marais, G., Pitman, A., Keay, G., Buchan, L., Gerber, A. & Smollen, M. 1984. Theory, design and operation of Nutrient removal Activated Sludge Process, South African Water Research Commission, Pretoria, South Africa.

Ekama, G.A. & Marais, G.v.R. 1979. Dynamic behaviour of the activated sludge process, Journal Water Pollution Control Federation, 51: 534-556.
Englezos, P. & Kalogerakis, N. 2001. Applied Parameter Estimation for Chemical Engineers, New York, Marcel Dekker.

Enns, D.F. 1984. Model reduction with balanced realizations: an error bound and a frequency weighted generalization. In: Proceedings 23rd Conference Decision Control, Las Vegas, NV: 127-1321.

Farza, M., Hammouri, H., Othman, S. & Busawon, K. 1997. Nonlinear observers for parameter estimation in bioprocesses. Chemical Engineering Science, 52(23): 4251-4267.

Fausett, L.V. 1999. Applied Numerical Analysis using MATLAB, Englewood Cliffs, Prentice-Hall.

Feller, W. 1971. An Introduction to Probability Theory and Its Application, New York, Wiley.

Fernando, K.V. & Nicholson, H. 1982. Singular perturbation model reduction of balance systems. IEEE Transactions Automatic Control, AC-27(2): 466-468.

Ferreira, E., Rocha, I. & Veloso, A.C., 2005. Design of On-line State Estimators for Recombinant E. Coli fed-batch Fermentation. Preprints from Proceedings of the 16th IFAC World Congress, 4 July – 8 July, Prague, Czech Republic.

Fisher, W.R., Doherty, M.F. & Douglas, J.M. 1988. The Interface between Design and Control. 1. Process Controllability. Industrial Engineering Chemical Research, 27: 597-605.

Fletcher, R. 1987. Practical Methods of Optimization, Chichester, Great Britain. John Wiley and Sons, Ltd.

Ford, D.L. & Eckenfelder Jr., W.W. 1967.The role of enzymes in the contact stabilization process-discussion. Advances in Water Pollution Research , 2. Article by Siddinqi, R.H., Engelbrecht, R.S. & Speece R.E. Journal Water Pollution Control Federation, 39: 1211-1222.

Fossard, A.J. & Normand-Cyrot, D. 1995. Nonlinear Systems, vol. 1 Modeling and Estimation, London, Chapman and Hall.

Francisco, M., Vega, P. & Perez, O. 2005. Process Integrated Design within a Model Predictive Control Framework. Preprints from Proceedings of the 16th IFAC World Congress, 4 July – 8 July, Prague, Czech Republic.

Francisco, M., Vega, P., Perez, O. & Poch, M. 2003. Dynamic Optimization for Activated Sludge Integrated Design. European Control Conference, UK.

Fuchard, M., Bernard, O. & Gouze, J. 2002. Interval observers with guaranteed confidence levels: Application to Activated Sludge Process.

Fuerhacker, M., Bauer, H., Ellinger, R., Sree, U., Schmid, H., Zibuschka, F. & Puxbaum, H. 2000. Approach for a novel control strategy for simultaneous nitrification/denitrification in activated sludge reactors. Water Research, 34(9): 2499-2506.

Gardener, W. 1990. Introduction to Random Processes, 2nd ed., New York, McGraw-Hill.

Gaslan, E.H., Voros, S., Banks, J., Wilson, D., Hillis, P., Campbell, A.T. & Parsons, S.A. 2003. A model for predicting dissolved organic carbon distribution. Water Research, 38: 783-791.

Gaudy, A.F., Obayashi, O. & Gaudy, E.T. (1971). Control of growth rate by initial substrate concentration at values below maximum rate. Applied Microbiology, 22: 1041-1047.

Gauthier, J.-P. & Kupka, I. 1994. Observability and observer for nonlinear systems. SIAM J. Control Optimization, 32: 975-994.

Gauthier, J.-P., Hammouri, H. & Othman, S. 1992. A simple observer for nonlinear systems applications to bioreactors. IEEE Transactions. Automation Control, 37: 875-880.

Gawthrop, P.J. & Wang, L. 2004 Estimation of physical parameters of stable and unstable systems via estimation of step response. Proceedings of 8th International Conference on Control, Automation, Robotics and Vision, Kumin, China.

Gehan, O., M'Saad, M., Farza, M. & Pigeon, E. 1999. Robust Control and Nonlinear Estimation for Bioprocess Monitoring, 14th Triennial IFAC World Congress, Beijing, P.R. China: 445-450.

Geladi, P. & Kowalski, B.R. 1986. Partial Least Squares Regression: A Tutorial. Analytica Chimica Acta, 185: 1-17.

Gerksie, S., Vrecko, D. & Huala, N. 2005. Improving oxygen control in activated sludge process with estimation of respiration and scheduling control. http://www.sciencedirect.com

Gernaey, K.V., van Loosdrecht, C.M., Henze, M., Lind, M. & Jorgensen, S.B. 2004: Activated sludge wastewater treatment plant modelling and simulation: state of the art. Environmental Modelling & Software, 19: 763-783.

Gernshenfeld, 1999. The Nature of Mathematical Modeling, Cambridge, Cambridge University.

Gillijns, S. & de Moor, B. 2007. Unbiased minimum-variance input and state estimation for linear discrete-time systems, Automatica, 43, 111-116.

Glover, K. 1984. All optimal Hankel-norm approximations of linear multivariable systems and their L_∞ error bounds. International Journal Control, 39(6): 1115-1193.

Goldbic, L., Gerkes, H., Bajsic, I. & Malensk, J. 2000. Software sensor for biomass concentration concentration monitoring during industrial fermentation. Instrumentation Science Technology, 28(4): 323-334.

Godfrey, K. & Di Stefano, J. 1985. Identifiability of model parameters, in: Identification and system parameter estimation, Oxford:Pergamon Press, 89-144.

Golub, G. & van Loon, C. 1996. Matrix Computations, 3rd ed., Baltimore, Maryland, The John Hopkins University Press.

Gomez-Quintero, C. & Queinnec, I. 2002. Robust estimation for an uncertain model of an activated sludge model. Proceedings of the 2002 IEEE International Conference on Control Applications, Glasgow, 972-977.

Gomez-Quintero, C. & Queinnec, I. 2002. State and disturbance estimation for an alternating activated sludge process. Proceedings of the 15th IFAC Congress, Barcelona, CD-ROM, 1-6.

Goodman, R. 1988. Introduction to Stochastic Models, Menlo Park, California, Benjamin-Cummings.

Goodwin, G.C., Mcinnis, B.C. & Long, R.S. 1980. Adaptive control algorithms for waste water treatment and pH neutralization. Optimization Control Applied Methods, 3: 443-459.

Gouze, J.L., Rapaport, A. & Hadj-Sadok, Z. 2000. Interval observers for uncertain biological systems. Ecological Modelling, 133: 45-56.

Green, M. & Limbeer, D.J.N. 1995. Linear Robust Control, Englewood Cliffs, NJ, Prentice Hall, Inc.

Gude, R.D., Shah, S.L. & Gray, M.R. 1995. Adaptive multirate state and parameter estimation strategies with application to a bioreactor. American Institute of Chemical Engineers Journal, 41(11): 2451-2464.

Gugercin, S. & Antoulas, A.C. 2000. A comparative study of 7 algorithms for model reduction. In: Proceedings of 39th IEEE Conference of Decision Control, 2367-2372.

Gujer, W., Henze, M., Mino, T. & Van Loosdrecht, M.C.M. 1999. The Activated Sludge Model No. 3. IAWQ Task Group Mathematical Modelling for Design and Operation of Biological Wastewater Treatment. Kollekolle.

Haarsma, G. & Keesman, K. 1995. Robust model predictive dissolving oxygen control, Proceedings of the 9th Forum Applied Biotechnology, Gent, Belgium, 2715-2725.

Hadj-Sadok, M.Z. & Gouze, J.L. 2001. Estimation of uncertain models of activated sludge processes with internal observers. Journal of Process Control, 11: 299-310.

Halevi, Y., Zlochevsky, A. & Gilat, T. 1997. Parameter-dependent model order reduction. International Journal Control, 66(3): 463-485.

Hart, C.W. 1998. On-line first principle models-state estimation. Presented to the IchemE, The Fifth Conference on Advances in Process Control, 2 –3 September in Swansea.

Helstrom, C.W. 1991. Probability and Stochastic Processes for Engineers, 2nd ed, New York, MacMillan.

Henze, M., Gujer, W., Mino, T., Matsuo, T., Wentzel, M.C., Marais, G.v.R. & Loosdrecht, M.C.M. March, 1998. Outline Activated Sludge Model No. 2d. IAWQ Task Group on Mathematical Modelling for Design and Operation of Biological Wastewater Treatment Processes. Kollekolle.

Henze, M., Gujer, W., Mino, T., Matsuo, T., Wentzel, M.C. & Marais, G.v.R. 1995. Activated sludge model No. 2. IAWQ Scientific and Technical Report No. 3, IAWQ, London.

Henze, M., Gujer, W., Mino, T., Matsuo, T., Wentzel, M.C. & Marais, G.v.R. 1994. Activated sludge model No. 2. IAWQ Scientific and Technical Report No. 2, IAWQ, London.

Henze, M., Grady Jr., C.P.L., Gujer, W., Marais, G.v.R. & Matsuo, T.. 1987. Activated sludge model No. 1. IAWPRC Scientific and Technical Report No. 1, IAWPRC task group on mathematical modeling for design and operation of biological wastewater treatment, London.

Hoel, P.G. 1971. Introduction to Mathematical Statistics, 4th ed, New York, Wiley.

Holmberg, A. 1983b. A microprocessor-based estimation and control system for the activated sludge process. Halme, A., Modelling and Control of Biotechnical Processes, Oxford, Pergamon: 111-120.

Holmberg, A. 1982. On the practical identifiability of microbial growth models incorporating Michaelis-Menten type nonlinearities. Mathematics Biosciences, 62:23-43.

Holmberg, A. & Ranta, J. 1982. Procedures for parameter and state estimation of microbial growth process models. Automatica, 18: 181-193.

Holmberg, A., Selkainako, T., Pallasvuo,O. & Halme, A. 1980. Microprocessor based estimation and control of the activated sludge wastewater treatment process- experimental testing at the Shomonoje research plant, System Theory Laboratory, Report Series B59, 10.6-2.7.1980, Helsinki University of Technology.

Holmberg, U. 1990. On identiability of dissolved oxygen concentration dynamics, Proceedings of the IAWPRC's 25th Anniversary Conference and Exhibition, Kyoto, Japan, 113-119.

Holmberg, U. & Olsson, G. 1986. Simultaneous on-line estimation of oxygen transfer rate and respiration rate. Johnson, A., Modelling and Control of Biotechnological Processes, Oxford, Pergamon: 205-209.

Holmberg, U. & Olsson, G. 1985. Simultaneous on-line estimation of oxygen transfer rate and respiration rate, Proceedings of the 1st IFAC Symposium on Modelling and Control of Biotechnological processes, 185-189.

Hong, Y-S. & Bhamidimarri, R. 2003. Evolutionary self-organising modeling of a municipal wastewater treatment plant. Water Research, 37: 1199-1212.

Hou, M. & Muller, P. 1991. Design of observers for linear systems with unknown inputs. IEEE Transaction Automatic Control, AC-37(6), 871-875.

Hou, M. & Muller, P. 1992. Design of observers for linear systems with unknown inputs. IEEE Transaction Automatic Control, AC-37(6), 871-875.

Hu, Z., Wentzel, M.C. & Ekama, G.A. 2003. Modelling biological nutrient removal activated sludge systems – A review. Water Research, 37: 3430-3444.

Huffel, S.Van. & van de Walle, J. 1991. The Total Least Squares Problem, Computational Aspects and Analysis, SIAM, Philadelphia.

Hulhoven, X. & Bogaerts, P. 2005. Maximum Likelihood adaptive observer for bioprocesses. Preprints from Proceedings of the 16th IFAC World Congress, 4 July – 8 July, Prague, Czech Republic.

Hulhoven, X. & Bogaerts, Ph. 2004. Stochastic full horizon-asymptotic hybrid observer applied to a simulated cell culture, In : Proceedings of the Computer Application in Biotechnology Conference Cab'9), IFAC, Nancy.

Ikonen, E. & Najim, K. 2002. Advanced Process Identification and Control, New York, Marcel Dekker.

Ingilsen, P. 2002a. Realising Full-Scale Control in Watewater Treatment Systems Using In situ Nutrient Sensors, Ph.D. thesis, Dept of Industrial Electrical Engineering and Automation, Lund University, Sweden.

Ingildsen, P., Jeppson, U. & Olsson, G. 2002b. Dissolved oxygen controller based on on-line measurements of ammonia combining feedforward and feedback, Water Science Technology., 45(4-

5): 453-460.

Jacquart, J.C., Lefort, D. & Lovel, J.M. 1973. An attempt to take account of biological storage in the mathematical analysis of activated sludge behaviour. In Jenkins S.H. (Ed.) Advances in Water Pollution Research, New York, Pergamon Press.

James,S., Legge, R. & Budman, H. 2002. Comparative study of blackbox and hybrid estimation methods in fed-batch fermentation. J. Process Control, 12(1): 113-121.

Jannssen, M.J.M., Hopkins, L.N., Petersen, B. & Vanrolleghem, P.A. 2000. Reduction of an activated sludge process model to facilitate controller tuning. In Van Landeghem, R. (Ed.), Proceedings of the 14th European Simulation Multiconference, Society for Computer Simulation International (SCS): 697-701.

Jeppsson, U. 1996. Modelling Aspects of Wastewater Treatment Processes, Lund University, Lund, Sweden. Reprocentralen.

Jeppsson, U. & Olsson, G. 1993. Reduced order models for on-line parameter identifications of the activated sludge process. Water Science Technology, 28(11/12): 173-183.

Johnson, A. & Tiedeman, A.R., 1985. Model reduction of an oxygen enriched industrial waste-water treatment process, IFAC Modelling and Control of Biotechnological Processes, Noordwijkerhout: 167-173.

Juang, J.-N. 1994. Applied System Identification, Englewood Cliffs, Prentice-Hall.

Junkins, J. 1969. On the Optimization and Estimation of Powered Rocket Trajectories using Parametric Differential Correction Processes. Tech. Rep. SM 61793, McDonnell Douglas Astronautics.

Kabouris, J.C. & Georgakakos, A.P. 1996. Parameter and state estimation of the activated sludge process: On-line algorithm. Water Research, 30(12): 3115-3129.

Kabouris, J.C.& Georgakakos, A.P. 1996. Parameter and state estimation of the activated sludge process-I. Model development. Water Research, 30(12): 2853-2865.

Kabouris, J.C. & Georgakakos, A.P. 1996. Parameter and state estimation of the activated sludge process-II. Applications. Water Research, 30(12): 2867-2882.

Kalman, R.E. 1960. New approach linear filtering and prediction problems, Transaction of the ASME Journal of Basic Engineering, 35-45.

Kalman, R. & Busy, R. 1961. New results in linearing filtering and prediction theory. Journal of Basic Engineering, March, 95-108.

Kalmus, H. 1966. Regulation and Control in Living Systems, New York, Wiley.

Katebi, M.R., Johnson, M.A. & Wilke, J. 1999. Control and Instrumentation for Wastewater treatment Plant, Springer-Verlag, London, ISBN 1-85233-054-6.

Katoh, M.H.K. & Masubuchi, M. 1981. Analysis and state estimation of enzyme kinetic model for microbial growth processes. In Preprints 8th triennal IFAC World Congress, Kyoto, Japan, 22: 159-164.

Keesman, K.J. 2002. State and parameter estimation in biotechnical batch reactors. Control Engineering Practice, 10: 219-225.

Keirn-Jesperson, J.P. & Henze, M. 1993. Biological phosphorus removal from wastewater by aerobic-anoxic sequencing batch reactors. Water Research, 27: 617-624.

Khalil, H.K. 2002. Nonlinear Systems. 3rd ed., Upper Saddle River, N.J., Prentice-Hall.

Kim, H., McAvoy, T.J., Anderson, J.S. & Hao, O.J. 2000. Control of alternating aerobic-anoxic activated sludge system- Part 2: optimization using a linearized model. Control Engineering Practice, 8: 279-289.

Ko, K.Y., Mc Innis, B.C. & Goodwin, G.C. 1982. Adaptive control and identification of the dissolved oxygen process. Automatica, 18(6): 727-730.

Kokotovic, P.V., O'Malley, R.C. & Sannuti, P.I. 1976. Singular perturbation and order reduction in control theory- an overview. Automatica, 12: 123-132.

Kotob, S., Albrecht, C., Jaridan, M. & Kafeety, H. 1987. Adaptive Bioreactor Identification Using Sensitivity of Process Stoichiometry, Proc. 10th IFAC World congress, Munich, July 27-31, 2: 344-349.

Krauss, P., Dass, K. & Rake, H. 1994. Model Based Predictive Controller with Kalman Filtering for State Estimation, Advances in model based predictive control, Oxford University Press: 69-83.

Kreisselmeier, G. 1977. Adaptive observers with exponential rate of convergence. IEEE Transaction Automation Control, AC-22,1: 2-8.

Kumar, R. & Moore, J.B. 1979. Towards Bias Elimination in Least Squares Identification via Detection Techniques. In Iserman, R., Identification and System Parameter Estimation, Oxford, Pergamon Press, 1: 315-322.

Kwakernaak, H. & Sivan, R. 1972. Linear Optimal control systems, New York, John Wiley.

Lakshminarayanan, S., Gudi, R., Shah, S.L. & Nandakumar, K. 1996. Monitoring batch processes using multivariate statistical tools : extensions and practical issues. Proceedings of IFAC World Congress, San Francisco: 241-246.

Langholz, G. & Feinmesser, D. 1978. Model reductions by Routh Approximations. International Journal System Scinence, 9(5): 493-496.

Latham, A. & Anderson, B.D.O. 1985. Frequency-weighted optimal Hankel-norm approximation of stable transfer functions. System Control Letters, 5: 229-236.

Law, A. & Kelton, D. 1991. Simulation, Modeling and Analysis, New York, McGraw-Hill.

Lawrence, A.W. & McCarty, P.L. 1970. Unified Basis for biological treatment, design and operation. Journal of Sanitation Engineering Division, ASCE, 96(SA3): 757- 778.

Larrea, L., Garcia-Heras, J.L., Ayesa, E. & Florez, J. 1992. Designing experiments to determine the coefficients of activated sludge models by identification algorithms. Water Science Technology, 25: 149-165.

Lee, T.T., Wang, F.Y. & Newell, R.B. 1999. Dynamic modelling and simulation of activated sludge process using orthogonal collocation approach. Water Research, 32(1): 73-86.

Lee, T.T., Wang, F.Y. & Newell, R.B. 1999. Dynamic simulation of bioreactor systems using orthogonal collocation on finite elements. Computers and Chemical Engineering, 23: 1247-1262.

Lee, T.T., Wang, F.Y. & Newell, R.B. 1999. Distributed parameter approach to the dynamics of complex biological processes. American Institute of Chemical Engineers, 45(10): 2245-2268.

Lee, T.T., Wang, F.Y. & Newell, R.B. Robust multivariable control of complex biological process (in

preparation).

Lefevre, L., Dochain, D., Feyo de Azevedo, S. & Magnus, A. 2000. Optimal selection of orthogonal polynomials applied to the integration of chemical reactor equations by collocation methods. Computers and Chemical Engineering, 24: 2571-2588.

Leigh, J.R. & Ng, M.H. 1984. Estimation of biomass and secondary product in batch fermentation. In A. Bensoussan and L.L. Lions (Ed.), Analysis and Optimization of Systems, Berlin, Springer Verlag, 2: 456-467.

Leigh, J.R. & Ng, M.H. 1984. Estimation of biomass and secondary product in batch fermentation. 6th International Conference of Analysis & Optimization Systems, Nice, France: 19-22.

Lennox, B., Montague, G.A., Hiden, H.G., Kornfeld, G. & Goulding, P.R. 2001. Process monitoring of an industrial fed-batch fermentation. Biotechnology Bioengineering, 74(2): 125-135.

Leon-Garcia, A. 1989. Probability and Random Processes for Electrical Engineering, Reading, Mass, Addison-Wesley.

Lepschy, A., Mian, G.A. & Viaro, U. 1987. A method for optimal linear model reduction. System Control Letters, 8: 405-410.

Lesouef, A., Payraudeau, M., Rogalla, F. & Kleiber, B., 1992. Optimizing nitrogen removal reactor configurations by on-site calibration of the IAWPRC activated sludge model. Water Science Technology, 25: 105-123.

Levenberg, K. 1944. A method for the solution of certain nonlinear problems in least squares, Quarterly of applied Mathematics, 2: 164-168.

Lewis, R. 1986. Otimal estimation with an introduction to stochastic control theory, New York, John Wiley & Sons, Inc.

Lindberg, C. 1997. Control and estimation strategies. Applied to the Activated Sludge Process, Ph.D. Thesis, Uppsala University, Uppsala.

Lindberg, C.-F. & Carlson, B. 1996. Estimation of the respiration rate and oxygen transfer function utilizing a slow do sensor. Water Science Technology, 33(1):325-333.

Lindberg, C. & Carlson, B. 1996. Nonlinear and set point control of the dissolved oxygen dynamic in an Activated Sludge Process. Water Science Technology, 34, 135-140.

Lira, V., Barros, P., Nero, J. & van Haandel, A. 2004. Estimation of Dissolved oxygen Dynamics for Sequencing Batch Aerobic Reactors. IMTC 2004 – Instrumentation and Measurement Technology Conference, Como.

Ljung, L. 1987. System Identification: Theory for the User, Englewood Cliffs, New Jersey, USA. Prentice Hall, Inc.

Luenberger, D.G. 1984. Linear and Nonlinear Programming, 2nd ed., Addison-Wesley Publishing Company.

Luenberger, D.G. 1969 Optimization by Vector Space Methods, New York, John Wiley and Sons.

Lukasse, L.J.S., Keesman, K.J. & van Straten, G. 1999. A recursively identified model for short-term predictions of NH_4/NO_3 - Concentrations in alternating activated sludge processes. Journal of Process Control, 9: 87-100.

Lukasse, L.J.S., Keesman, K.J. & van Straten, G. 1997. Estimation of BOD_{st}, respiration rate and kinetics of activated sludge. Water Research, 31(9): 2278-2286.

Lukasse, L.J.S., Keesman, K.J. & van Straten, G. 1996. Grey-box identification of dissolved oxygen dynamics in activated sludge process, Proceedings of the 13th World Congress of IFAC, San Francisco, USA, 485-490.

Luus, R. 1980. Optimization in model reduction. International Journal Control, 32(5): 741-747.

Luyben, M.L. 1993 Analyzing the Interaction between Process Design and Process Control. Ph.D. Thesis, Princeton University.

Maciejowski, J.M. 2002. Predictive Control with constraints, England, Prentice-Hall, Pearson Education: 74-88.

Mailleret, L., Bernard, O. & Steyer, J.-P. 2004. Robust nonlinear adaptive control for bioreactors with unknown kinetics. Automatica, 40(8): 365-383.

Makinia, J. & Wells, S.A. 2000. A general model of the activated sludge reactor with dispersive flow- I. Model development and parameter estimation. Water Research, 34(16): 3987-3996.

Manesis, S.A., Sapidis, D.J. & King, R.E. 1998. Intelligent control of wastewater treatment plants. Artificial Intelligence. Engineering, 12: 275-281.

Marais, G.v.R., Ekama, G.A. 1976: "The activated sludge process Part 1 – steady state behaviour". Water S.A., 2(4): 163.

Marcos, N., Guay, M., Dochain, D. & Zhang, T. 2004. Adaptive Extremum-Seeking Controlof a Continuous Bioreactor. Journal of Process Control, 14(3): 317-328.

Mareels, I.M.Y., Gevers, M., Bastin, G. & Dochain, D. 1987 Exponential convergence of a new error system arising from adaptive observers. Proc. 26th IEEE Conference December Control, Los Angeles: 16-19.

Margaria, G., Kiccomagno, E., Chapell, M. & Wynn, H. 2001. Differential algebra methods for the study of the structural identifiablity fo rational function state space models in the biosciences, Mathematics Biosciences, 1-26.

Marsili-Libelli, S., Guerrizio, S. & Checchi, N. 2003. Confidence regions of estimated parameters for ecological systems. Ecological Modelling, 165: 127-146.

Marsile-Leblli, S. & Guinti, L. 2002. Fuzzy predictive control for nitrogen removal in biological wastewater treatment. Water Science Technology, 45(4 – 5): 37-44.

Marsili-Libelli, S. & Tabani, F. 2002. Accuracy analysis of a respirometer for activated sludge dynamic modelling. Water Research, 36: 1181-1192.

Marsili-Libelli, S., Ratini, P., Spagni, A. & Bortone, G. 2000. Implementation, study and calibration of a modified ASM2d for the simulation of SBR processes. Water Science Technology, 43(3): 69-76.

Marsili-Libelli, S. & Giovannini, F. 1997. On-line estimation of the nitrification process. Water Research, 31(1): 179-185.

Marsili-Libelli, S.& Vaggi, A. 1997. Estimation of respirometric activities in bioprocesses. Journal of Biotechnology, 52: 181-192.

Marsili-Libelli, S. 1992. Parameter estimation of ecological models. Ecological Modelling, 62: 233-258.

Marsili-Libelli, S. 1990. Adaptive estimation of bioactivities in the activated sludge process, In : IEEE Proceeding Control Theory and Applications, 37-6: 349-356.

Marsili-Libeili, S., Giardi, R. & Lasagni, M. 1985. Self-tuning control of activated sludge process. Environmental Technology Letters.

Marsili-Libeili, S. 1983. On-line estimation of bioactivities in activated sludge processes. In Halme, A., Modelling and Control of Biotechnical Processes, Oxford, Pergamon: 121-126.

Marsili-Libelli, S. 1980. Reduced-order modelling of the activated-sludge process. Ecological Modelling, 9: 15-32.

Marquardt, D. 1963. Algorithm for Least-Squares Estimation of Nonlinear parameters. Journal of the Society for Industrial and Applied Mathematics, June, 11(2).

Mathieu, S. & Etienne, P. 2000. Estimation of wastewater biodegradable COD fractions by combining respirometric experiments in various SO/XO ratios. Water Research, 34(4): 1233-1246.

Maurer, M. & Gujer, W. 1994. Prediction of the performance of enhanced biological phosphorus removal plants. Water Science Technology, 30(6): 333-44.

Mazouni, D., Ignatova, M. & Harmand, J. 2004 (an accepted for oral presentation). A simple mass balance for biological sequence batch reactor used for carbon and nitrogen removal. In the proceedings of IFAC – DECOM04, 3 – 5 October, Bansko, Bulgaria.
Mehra, R.K. 1979. Nonlinear System Identification: Selected Survey and Recent Trends. In Iserman, R., Identification and System Parameter Estimation, Oxford, Pergamon Press, 1: 77-83.

Mesarovic, M.D. 1968. Systems Theory and Biology, Berlin, Springer-Verlag.

McInnis, B.C., Lin, C.-Y. & Butler, P.B. 1979. Adaptive Microcomputer dissolved Oxygen Control for Wastewater Treatment. In Iserman, R., Identification and System Parameter Estimation, Oxford, Pergamon Press, 1: 789-793.

McKinney, R.E. 1962. Mathematics of complete mixing activated sludge. Journal of Sanitation Engineering Division, ASCE., 88(SA3), Proceedings Paper 3133: 87.

Mkondweni, N. 2002. Modelling and Optimal Control of Fed-batch Fermentation Process for the Production of Yeast. Submitted towards the Mtech: Electrical Engineering.

Moilanen, U.R. 1981. State and parameter estimation experiments by a fermentation process. In preprints 8th triennal IFAC World Congress, Kyoto, Japan, 22: 185-191.

Moisan, M. & Bernard, O. 2005. Interval Observers for Non Monotone Systems. Application to Bioprocesses. Preprints from Proceedings of the 16th IFAC World Congress, 4 July – 8 July, Prague, Czech Republic.

Montague, G.A. 1997. Monitoring and control of fermenters, Institution of Chemical Engineers.

Montgomery, D.C. 1997. The Use of Statistical Process Control and Design of Experiments in Product and Process Improvement, IIE Transactions, 24, 479, In Al-Sultan Khaled S. & Rahim, M.A., Optimization in Quality Control, Technology & Engineering

Moore, B.C. 1981. Principal component analysis in linear system: Controllability, observability and model reduction. IEEE Transactions Automatic Control AC-26: 17-32.

Moreno, J. 1999. "Optimal control of bioreactors for wastewater treatment". Optimal Control Applications and Methods, 20: 145-164.

Morris, J.C. & Stumm, W. 1960. Colloidal aspects of waste treatment. Proceedings. Rudolphs Research Conference, Rutgers University.

Murnleitner, E., Kuba, T., van Loosdrecht, M.C.M. & Heijnen, J.J. 1997. An integrated metabolic model for aerobic and denitrifying biological phosphorus removal. Biotechnology Bioengineering, 54: 434-450.

Narendra, K.S. & Annaswany, A.M. 1989. Stable Adaptive Systems. Englewood Cliffs, Prentice-Hall.

Neff, H.P. 1984. Continuous and Discrete Linear System, New York, Harper and Row.

Nejjari, F., Roux, G., Dahhou, B. & Benhammou, A. 1999. Estimation and optimal control design of biological wastewater treatment process. Mathematics Control Simulation, 48: 269-280.

Nejjari, F., Benhammou, A., Dahhou, B. & Roux, G. 1999 Nonlinear multivariable adaptive control of an activated sludge wastewater treatment process, International Journal of Adaptive Control and Signal Processing, 13(5): 347-365.

Nejjari, F., Benhammou, A., Dahhou, B. & Roux, G. 1997. Nonlinear multivariable control of a biological wastewater treatment process, Proceedings of EEC 97, Brussels.

Nejjari, F., BenYoussef, C., Benhammou, A. & Dahhou, B. 1996. Procedures for state and parameter estimation of a biological wastewater treatment, CESA'96 IMACS, Lille, France, 9-12 July, 1: 238-243.

Nelson, B. 1995. Stochastic Modeling, Analysis and Simulation, New York, McGraw-Hill.

Newell, R.B. & Cameron, I.T. 2000. DaeSim Studio Modelling and Simulation Environment. DaeSim Technologies Pty Ltd, Brisbane, Australia. Available from http://www.daesim.com.

Newell, R.B. & Cameron, I.T. 1991. NIMBUS Users manual. Computer-Aided Process Engineering Centre, Department of Chemical Engineering, The University of Queensland, Brisbane, Australia.

Nihtila, M., Harmo, P. & Perttula, M. 1984. Real-time growth estimation in batch fermentation. Proc. 9th IFAC World Congress, Budapest, July 2-6: 225-230.

Nomikas, P. & MacGregor, J.F. 1994. Monitoring batch processes using multiway principal component analysis. American Institute of Chemical Engineers. Journal, 40(8): 1361-1373.

Norgaard, M., Poulsen, N. & Raun, O. Easy and accurate state estimation for nonlinear systems, Preprints of the 14th World Congress, China, J-3d-04-4, 343-348.

O'Brien, M., Castillo, S.E.P. & Katebi, R. 2005. Model Based Predictive Control for Wastewater Applications. Preprints from Proceedings of the 16th IFAC World Congress, 4 July – 8 July, Prague, Czech Republic.

Ohlsson, H., Roll, J., Glad, T. & Ljung, L. 2007. Using manifold learning for nonlinear system identification, Preprints of the 7th IFAC Symposium of Nonlinear Control Systems, Pretoria, South Africa, 706-711.

Oliveira, R., Ferreira, E.C. & Feyode Azevedo, S., 2002. Stability dynamics of convergence and tuning of observer-based kinetics estimators. Journal of Process Control, 12: 311-323.

Oliveira, R., Ferreira, E.C., Oliveira, F. & Feyo Azevedo, S. 1996. A study on the convergence of

observer-based kinetics estimators in stirred tank bioreactors. Journal of Process Control, 6: 367-371.

Olsson, G. 1993. Advancing ICA Technology by Eliminating the Constraints. Water Science Technology, 28(11-12): 1-7.

Olsson, G. 1992. Control of wastewater treatment systems. ISA Transactions, 31(1): 87-96.

Orupold, K., Masirin, A. & Tenno, T. 2001. Estimation of biodegradation parameters of phenolic compounds on activated sludge by respirometry. Chemosphere, 44: 1273-1280.

Ossenbruggen, P.J., Spanjers, H., Aspergren, H. & Klapwijk, A. 1991. Designing experiments for model identification of the nitrification process. Water Science Technology, 24: 9-16.

Otterpohl, R., Raak, M. & Rolfs, Th. July, 1994. A Mathematical Model for the Efficiency of the Primary Clarification. Proceedings of the IAWQ 17th Biennial Int. Conference, Budapest, Hungary.

Otterpohl, R. & Freund, M. 1992. Dynamic Models for Clarifiers of Activated Sludge Plants with Dry and Weather Flows . Water Science & Technology, 26(5-6): 1391-1400.

Ozkan, L., Romijn, R., Weiland, S., Marquardt, W. & Ludlage, J. 2007. Model reduction of nonlinear systems: a grey box modeling approach. Preprints of the 7th IFAC Symposium on Nonlinear Control Systems, Pretoria, South Africa, 760-765.

Pala, A. & *Bölükbas, Ö.* 2005. Evaluation of kinetic parameters for biological CNP removal from a municipal wastewater through batch tests. Process Biochemistry, 40: 629-635.

Papastratos, S., Hart, C., Speaks, K. & Hayot, P. 1999. State estimation for on-line fisrt principle models. Presented at the 2nd European Congress of Chemical Engineering, 5 – 7 October, Montpellier, France.

Pernebo, L. & Silverman, I.M. 1982. Model reduction via balanced state space representations. IEEE Transactions Automatic Control, AC-27: 2.

Perrier, M., Feyo Azevedo, S., Ferreira, E.C. & Dochain, D. 2000. Tuning of observer-based estimators: theory and application to on-line estimation of kinetic parameters. Control Engineering Practice, 8: 377-388.

Petersen, B., Gernaey, K., Devisscher, M., Dochain, D. & Vanrolleghem, P.A. 2003. A simplified method to assess structurally identifiable parameters in Monod-based activated sludge models. Water Research, 37: 2893-2904.

Pohjanpalo, H. 1978. System identifiability based on the power series expansion of the solution , Mathematics Biosciences, 41, 21-26.

Pomerieau, Y. 1990. Modelisation et controle d'un prodece fed-batch de culture des levures a pain., Ph. D. Thesis, Ecole Polytechnique de Montreal, Canada.

Pomerieau, Y. & Perrier, M. 1989. Estimation of multiple specific growth rates in bioprocess. American Institute of Chemical Engineers Journal, in press.

Pomerieau, Y. & Perrier, M. 1988. Non-linear estimation of specific growth rates in Baker's yeast fed-batch fermentation. AICHE 1988 Annual Meeting, Washington, DC, paper 132B.

Pomerieau, Y. 1988. Modelisation et controle d'un procede fed-batch de culture des levures a pain (Saccharomyces cerevisiae). Ecole Polytechnique de Montreal, Canada, Internal report.

Pons, M.-N., Wu, J. & Potier, O. 2005. Chemometric Estimation of Wastewater Compostion for the on-line Control of Treatment Plants. Preprints from Proceedings of the 16th IFAC World Congress, 4 July – 8 July, Prague, Czech Republic.

Porges, N., Jasewicz, L. & Hoover, S.R. 1956. Principles of biological oxidations. In McCabe, B.J. & Eckenfelder, Jr. W.W. (Eds.) Biological Treatment of Sewage and Industrial Wastes, New York, Reinhold Publishers Company,1: 35-48.

Press, W.H., Flannery, B.P., Teukolsky, S.A. & Vettering, W.T. 1986. Numerical Recipes: The Art of Scientific Computing, Cambridge, Cambridge University Press.

Proakis, J.G. & Manolakis, D.G. 1996. Digital Signal Processing, Principles, Algorithms and Applications 3rd ed., Englewood Cliff, Prentice-Hall.

Profozich, P.M. 1997. Managing Change with Business Process Simulation, Englewood Cliffs, Prentice-Hall.

Rapaport, A. & Gouze, J.-L. 2003. Parallotopic and practical observers for nonlinear uncertain systems. International Journal of Control, 76(3): 237-251.

Rapaport, A. & Gouze, J. 1999. Practical observers for uncertain affine outputs injection systems, Proceedings of the ECC'99 Karlsruhe, Germany.

Rauh, A., Kletting, M., Aschemann, H. & Hofer, E.P. 2004a. Application of Interval Arithmetic Simulation Techniques to Wastewater Treatment Processes. In the Proceedings of MIC 2004, Grindelwald, Switzerland: 287-293.

Rauh, A., Kletting, M., Aschemann, H. & Hofer, E.P. 2004b. Reduction of Overestimation in Interval Arithmetic Simulation of Biological Wastewater Treatment Processes. Proceedings of SCAN 2004, Fukuoka, Japan.

Richardson, C.H. 1954. An Introduction to the Calculus of Finite Differences, New York, Van Nostrand-Reinhold.

Roberts, N., Andersen, D., Deal, R., Garet, M. & Shaffer, W. 1983. Introduction to Computer Simulation, Reading, Mass, Addison-Wesley.

Rocha, I. & Ferreira, E.C. 2004. Yield and kinetic parameter estimation and model reduction in a recombinant E. coli fermentation. ESCAPE – 14, Lisbon, Portugal, 16-19 May, (CD-ROM).

Rosen, R. 1970. Dynamical System Theory in Biology, New York, Wiley Interscience.

Saaty, T. 1981. Modern Nonlinear Equations, New York, Dover Publications.

Safanov, M.G. & Chiang, R.Y. 1991. Robust Control Toolbox Users Guide. The Mathworks Inc., Natick.

Safanov, M.G., Chiang, R.Y. & Limebeer, D.J.N. 1990. Optimal Hankel model reduction for non minimal systems. IEEE Transaction Automatic Control, 35(4): 494-502.

Safanov, M.G. & Chiang, R.Y. 1989. A schur method for balanced-truncation method reduction. IEEE Automatic Control, AC-34: 729-733.

Sage, A.P. 1995. Systems Engineering, New York, Wiley.

Sage, A.P. 1991. Decision Support Systems Engineering, New York, McGraw-Hill.

Sakizlis, V., Perkin, J.D. & Pistikopoulos, E.N. 2004. Recent advances in optimization-based simultaneous process and control design. Computational Chemical Engineering, 28: 2069-2086.

Sandquist, G.M. 1985. Introduction to System Science, Englewood Cliffs, Prentice-Hall.

Sato, J. & Ohmori, H. 2002. Sensitivity analysis and parameter identification of wastewater treatment based on Activated Sludge Model No. 1 (ASM 1), Proceedings of SICE 2002, Osaka, 434-439.

Scheid, F. 1968. Theory and Problems of Numerical Analysis [Schaum's Outline Series], New York, McGraw-Hill.

Schermann, P.S. & Garag-Gabin, W. 2005. Process Gain, Time Lags and Reaction Curves. In Bela G. Liptak, Instrument Engineer's Handbook: Process Control and Optimization, Pergamon Press, New York

Schutze, M., Butler, D. & Beck, M.B. 2002. Modelling, Simulation and Control of Urban Wastewater Systems, Springer.

Shimizu, H., Takamatsu, T., Shioya, S. & Suga, K.I. 1989. An algorithmic approach to constructing the on-line estimation system for specific growth rate, Biotechnology Bioengineering, 33: 354-364.

Siegrist, H. & Tschui, M. 1992. Interpretation of experimental data with regard to the activated sludge model no. 1 and calibration of the model for municipal wastewater treatment plants. Water Science Technology, 25: 167-183.

SIMBA 4, Userguide 2001. Simulation of biological wastewater treatment. IFAK system GmbH, Magdeburg, Germany.

Slotine, J.-J.E., Li W. 1991. Applied Nonlinear Control, Upper Saddle River, New Jersey, Prentice Hall.

Smits, I.Y.M., Versyck, K.J.E. & van Impe, J.F.M. 2002. Optimal control theory: a generic tool for identification and control of (bio-)chemical reactors. Annual Reviews in Control, 26: 57-73.

Smolder, G.J.F., van Loosdrecht, M.C.M. & Heijnen, J.J. 1995. A metabolic model for biological phosphorus removal process. Water Science Technology, 31(2): 79-93.

Soderstrom, T. & Stoica, P. 1989. System Identification, Hemel Hempstead, UK, Prentice Hall International.

Soderstrom, T. 1974. Convergence properties of generalised least squares method. Automatica, 10: 617-626.

Sorenson, H.W. 1970. Least squares estimation: from Gauss to Kalman, IEEE Spectrum, 7, 63-68.

Sotomayor, O.A.Z. & Garcia, C. 2002. Model-Based Predictive Control of a pre-nitrification plant: a linear state-space in model approach. Proceedings of the IFAC World Congress, Barcelona, Spain.

Spagni,A., Buday, J., Ratini, P. & Bortone, G. 2001. Experimental considerations on the monitoring ORP, pH, conductivity and dissolved oxygen in nitrogen and phosphorus biological removal processes. Water Science Technology, 43(11): 197-204.

Spanjers, H., Olsson, G. & Klapwijk, A. 1994. Determining short-term biochemical oxygen demand and respiration rate in an aeration tank by using respirometry and estimation. Water Research, 28: 1571-1583.

Spiegel, M.R. 1975. Probability and Statistics [Schaum's Outline Series], New York, McGraw-Hill.

Spiegel, M.R. 1968. Theory and Problems of Fourier Analysis with Boundary Value Problems, New York, McGraw-Hill.

Staniskis, J. & Simutis, R.1986 A measuring System for Biotechnical Processes Based on Discrete Methods of Estimation. Biotechnology Bioengineering, 28: 362-371.

Stecha, J., Cepak, M., Pekar, J. & Pachner, D. 2005. System Parameter estimation using p-norm minimization. Preprints from Proceedings of the 16th IFAC World Congress, 4 July – 8 July, Prague, Czech Republic.

Steffens, M.A., Lant, P.A. & Newell, R.B. 1997. A systematic approach for reducing complex biological wastewater treatment models. Water Research 31(3): 590-606.

Sveshnikov, A. 1978. Problems in Probability Theory. Mathematical Statistics and Theory of Random Functions, New York, Dover Publications.

Takacs, G., Patry, G.G. & Nolasco, D. 1991. A dynamic model of the clarification-thickening processes. Water Research, 25(10): 1263-1271.

Takacs, I., Patry, G.G. & Nolasco, D., 1990. A Generalized Dynamic Model of the Thickening/Clarification Process. Briggs, R., Instrumentation, Control and Automation of Water and Wastewater Treatment and Transport Systems, Oxford : 487-494, Pergamon Press.

Takahashi, R. & Peres, P. 1999. Unknown input observers for uncertain systems. A unifying approach, European Journal of Control, 5, 261-275.

Takamatsu, T., Shioya, S., Yokoyama, K., Kurome, Y. & Monsaki, K. 1981. On-line monitoring and control of biochemical reaction processes. Proceedings of 8th triennal IFAC World Congress, Kyoto, Japan, 22: 146-151.

Tenno, R. & Uronen, P. 1996. State estimation for a large-scale wastewater treatment system. Automatica, 32(3): 305-317.

Tenno, R. & Uronen, P. 1995. State and parameter estimation for wastewater treatment processes using a stochastic model. Control Eng. Practice, 3(6): 793-804.

Thompson, R. 2000. Simulation: a Modeler's Approach, New York, Wiley Interscience.

Titica, M., Dochain, D. & Guay, M. 2003. Adaptive Extremum-Seeking Control of Fed-Batch Bioreactors. European Journal of Control, 9: 614-627.

Tromans, D. 1999. Oxygen solubility modelling in aqueous solutions, In: Proceedings of the 2nd International Conference on Intelligent Processing and Manufacturing of Materials (IPMM 99), 1: 411-416.

Valdes, H., Flaus,J. & Acuna, G. 2003. Moving horizon state estimation with global convergence using interval techniques: application to biotechnological processes. Journal of Process Control, 13: 325-336.

Van den Bos, A. 1979. Small Sample Properties of a Class of Nonlinear Least Squares Problems. In Iserman, R., Identification and System Parameter Estimation, Oxford, Pergamon Press, 1: 341-347.

Van Haandel, A.P.C., Ekama, G.A. & Marais, G.v.R. 1981. The activated sludge process 3-single sludge dentrification. Water Research, 15: 1135-52.

Van Impe, J.F.M. 1998. Optimal control of fed-batch fermentation processes. In : Advanced Instrumentation, Data Interpretation and Control of Biotechnological Processes, In van Impe, J.,

vanrolleghem, P. & Iserentant, D., Dordrecht-Boston-London., Kluwer Academic Publishers.

Van Impe, J.F.M. & Bastin, G. 1995. Optimal adaptive control of fed-batch fermentation processes. Control Engineering Practice, 3(7): 939-954.

Vega, P. & Gutierrez, G. 1999. Optimal design Control and Operation of wastewater treatment plants. European Control Conference, Germany

Vemuri, V. 1978. Modeling of Complex Systems, New York, Academic Press.

Villadsen, J. & Michelsen, M.L. 1978. Solution of Differential Equation Models by Polynomial Approximation. Englewood Cliff, NJ, Prentice Hall.

Vogelaar, J.C.T., Klawijk, A., van Lier, J.B. & Rulkens, W. H. 1996. Temperature effects on the oxygen transfer rate between 20 and 55 C. Water Research, 34(3): 1037-1041.

Von Mises, R. 1919. Fundamentalsatze der Wahrscheinlichkeitsrechnung. Math. Zeitschrift, 4: 1-97.

Wang, L., Gawthrop, P.J. & Young, P.C. 2005. Continuous time system identification of Nonparametric models with constraint. Preprints from Proceedings of the 16th IFAC World Congress, 4 July – 8 July, Prague, Czech Republic.

Wang, L. & Gawthrop, P.J. 2001. On the estimation of continuous time transfer functions. International Journal Control, 74: 889-904.

Wang, L., Desarmo, M. & Cluett, W.R. 1999. Real-time estimation of process frequency response and step response from feedback experiments. Automatica, 35: 1427-1436.

Watanabe, T., Yasude, K. & Yokoyama, R. 1996. Balanced truncating preserving poles in a specified disk and it's application to the reduction of H_ω controller. IECON Proceedings, 3: 1359-1364.

Watson, H.J. 1989. Computer Simulation, 2nd ed., New York, Wiley.

Wentzel, M.C., Ekama, G.A. & Marais, G.v.R. 1992. Processes and modelling of nitrification denitrification biological excess phophorus removal systems. Water Science Technology, 25(6): 59-82.

Wentzel, M.C., Dold, P.L., Ekama, G.A. & Marais, G.v.R. 1990. Biological excess phosphorus removal-steady state process design. Water SA,16(1): 29-48.

Williamson, D. 1977. Observation of bilinear systems with application to biological control. Automatica, 13: 243-254.

Willoughby, R. 1974. Stiff Differential Systems, New York, New York, USA. Plenum Press.

Wilson, D.A. 1974. Model reduction for multivariable systems. International Journal Control, 20: 57-64.

Wilson, D.E. & Marais, G.v.R. 1976. Adsorption phase in biological dentrification. Research report No W 11. Dept of Civil Eng. Univ. of Cape Town.

Wimberger, D. & Verde, R.C. 2005. On-line Monitoring of an Aerobic SBR Process based on dissolved oxygen measurement. Preprints from Proceedings of the 16th IFAC World Congress, 4 July – 8 July, Prague, Czech Republic.

Winkin, J.J., Dochain, D. & Ligarius, P. 2000. Dynamical analysis of distributed parameter tubular reactors. Automatica,36: 349-361.

Winston, P.H. 1992. Artificial Intelligence, New York, McGraw-Hill.

Wisnewski, P.A. & Doyle III, F.J. 1996. A reduced model approach to estimation and control of a Kamyr digester. Computers Chemical Engineering, 20(Suppl.): S1053-S1058.

WRC. 1984. Theory, design and operation of nutrient removal activated sludge processes. Water Research Commission, P.O. Box 824, Pretoria 0001, South Africa.

Yakowitz, S. & Szidarovszky, F. 1986. An Introduction to Numerical Computations, New York, Macmillan.

Yoo, C., Cho, J., Kwak, H., Choi, S., Chuh, H. & Lee, I. 2001. Closed loop identification and control for DO concentration in the full-scale cones WWTP, Water Science Technology, 43(7), 207-212.

Yoo, C., Lee, H. & Lee, I. 2002. Comparisons of process identification methods and supervisory DO control in the full scale wastewater treatment plant. Proceedings of the 15th IFAC World Congress, Barcelona, CD-ROM.

Yoo, C., Lee, J. & Lee, I. 2004. Nonlinear Model-based Dissolved oxygen control in a biological wastewater treatment process, Korean Journal of Chemical Engineering, 21(1), 17-19.

Yoo, Y.J., Hong, J. & Hatch, R.T. 1985. Sequential estimation of states and kinetic parameters and optimization of fermentation processes, Proceedings of ACC, Boston, USA, 2: 866-871.

Young, P. 1979. Parameter Estimation for Continuous-time models – A Survey. In Iserman, R., Identification and System Parameter Estimation, Oxford, Pergamon Press, 1: 17-41.

Youssef, C., Dahhou, B., Zeng, F. & Rols, T. 1996. Estimation and filtering of nonlinear systems. Application to a wastewater treatment process. In International Journal System Science, 27, 497-505.

Zeigler, B.P. 2000. Theory of Modeling and Simulation, 2nd ed., New York, Academic Press.

Zeng, F. & Dahhou, B. 1993. Adaptive observer estimator design for a class of nonlinear systems, Applied Mathematics Modelling, 17, 58-69.

Zhang, H., Zouaoui, Z. & Lennox, B. 2005. A Comparative Study of Soft-sensing Methods for Fed-batch Fermentation Processes. Preprints from Proceedings of the 16th IFAC World Congress, 4 July – 8 July, Prague, Czech Republic.

Zhao, H. & *Kümmel, M.* 1995. State and parameter estimation for phosphorus removal in an alternating activated sludge process. Journal of Process Control, 5(5): 341-351.

Zhu, Y. 2001. Multivariable System Identification for Process Control, Oxford. Elsevier Science.

APPENDICES

APPENDIX A: CALCULATION OF THE INFLUENT OF THE UCT MODEL

```
function [sys]=uct_influent(Q)

%           Calculates the inflow for uct modells
%
%           evaluate the daily hydrograph of an example plant

% i f a k   Institut fuer Automation und Kommunikation e.V. Magdeburg
%           Steinfeldstr. (IGZ), 39179 Barleben
%
%
% Aenderungen  Autor, Datum, Version, Anlass
%
%           S. du Plessis, 19.05.2004, Simba 4.2, File setup


% Inflöw rate m^3/d
Qzu = 24*Q/6733*[125 130 137 144 169 195 250 330 270 368 340 313 340 370 338
302 340 377 388 400 370 338 275 200 125]';

% Concentration of COD
COD = 1*[570 580 610 620 630 640 650 630 600 580 560 555 565 555 555 560 600
640 650 640 630 620 610 580 570]'

% Concentration of TKN
TKN = 1*[52 57 63 68 72 67 62 57 53 52 51 55 60 55 51 56 61 66 71 67 62 57 63
58 52]';

% Concentration in alkalinity
SALK = [6.4 6.3 6.4 7.2 6.7 6.8 7.0 6.8 6.6 6.3 6.7 8.0 7.1 6.6 7.4 7.4 7.4
6.6 6.6 7.3 7.3 7.4 6.5 6.5 6.4]';

%COD=555;       % g COD/m^3
%TKN=55;        % g N/m^3
fbs=0.200;     % g COD g-1 COD
fsus=0.050;  % g COD g-1 COD
fsup=kali('fsup');%0.130;  % g COD g-1 COD
fszbh=0.000; % g Zbh COD g-1 COD
fna=0.750;   % g N g-1 N
fnobp=0.500; % g N g-1 N
fnous=0.0300;% g N g-1 N
fzBN=0.068;  % g N/g COD
fzn=0.148;   % g N/g COD



ti=[ 0:(1/24):1]';

SI=fsus*COD;
XBH=fszbh*COD;
```

```
XBA=0*ones(size(ti));
XP=0.000*ones(size(ti));
XI=fsup*COD;
XSA=0.000*ones(size(ti));
SNH=fna*TKN;
NO=TKN-SNH-fzBN*(XBA+XBH);
Nob=NO-fnous*(TKN)-(fzn*XI);
XND=fnobp*Nob;
SND=Nob-XND;
SNO=0.000*ones(size(ti));
SALK=7.000*ones(size(ti));
Sb=COD-XP-XBA-SI-XI-XBH;
SS=fbs*Sb;
XSE=Sb-SS;
SO=0.000*ones(size(ti));

sys=[ti,XBH,XBA,XP,XI,XSA,XSE,XND,SS,SNH,SND,SNO,SALK,SI,SO,Qzu];
```

APPENDIX B: SET THE BIOLOGICAL PARAMETERS FOR UCT MODEL

```
function [p]=p_uct(T)
% set the biological parameters for model UCT model
% automatically generated by fox3edit
% Author: Sidney du Plessis
% Date: 01-Jun-2004 11:21:29

p=[...
.666;                                                    %YH - [g COD/g COD]
0.068;                                                   %iXB - [g N/g COD]
0.068;                                                   %iXP - [g N/g COD]
0.15;                                                    %YA - [g COD/g N]
0.08;                                                    %fP - [-]
2.5*1.2^(T-20);                                          %myH - [-]
0.5*1.123^(T-20);                                        %myA - [-]
5*1^(T-20);                                              %KSH - [g COD/m^3]
0.1;                                                     %KNO - [g N/m^3]
0.002;                                                   %KOH - [g O/m^3]
0.01;                                                    %KNA - [g N/m^3]
1.35*1.080^(T-20);                                       %KMP - [-]
0.027*0.91^(T-20);                                       %KSP - [-]
0.33;                                                    %nyG - [-]
0.62*1.029^(T-20);                                       %bH - [1/d]
0.04*1.029^(T-20);                                       %bA - [1/d]
0.17*1.029^(T-20);                                       %KA - [g COD/g COD]
1.0*1^(T-20);                                            %fMA - [-]
0.032*1.029^(T-20);                                      %KR - [m^3/g COD]
1.0*1.123^(T-20);                                        %KSA - [g N/m^3]
0.002;                                                   %KOA - [g O/m^3]
1.024^(T-20);                                            %fTS Temperatur term for kla [-
]
13.89-T*0.3825+T*T*0.007311-T*T*T*0.00006588]; %SOsat DO Saturation
Concentration for 20 grd C [g/m^3]
```

APPENDIX C : BENCHMARK AND ATHLONE PROCESSES WITH ASM1 AND UCT REDUCED BIOLOGICAL MODELS FOR SENSITIVITY STUDIES

Benchmark process with ASM1 reduced biological model

Figure 9.2: Process variable S_{NH1} and its sensitivity functions towards the model parameters

The process variable Snh1, trajectory reaches a value of 8 at discrete time of zero then becomes unstable and oscillating between discrete time of 1 and 20. Then finally the trajectory drops down to zero at constant value. For the sensitivity function Snh1f, the trajectory quickly increases from zero value and reaches a maximum at 0.18 value for discrete time of 25. Finally the trajectory drops down at a value of 0.1 at a discrete time of 50 then remains constant at that value of 0.1. For variable Snh1YH, the trajectory reaches a minimum of -1 at discrete time of 32 which is slightly oscillating reaching a stable trajectory after discrete time of 60 at a minimum value of – 0.05. After this the trajectory is ever increasing at a slight angle to a discrete time of 100. For variable Snh1YA, the trajectory reaches a maximum of 490 then stabilizes to a constant value of zero. For sensitivity function Snh1iXB, the trajectory reaches a minimum value of – 300 at discrete time of 30 then the trajectory smoothes out at above the value of – 200. For sensitivity function Snh1muA, the trajectory reaches a minimum value of – 200 at the discrete time of 20 then increase to zero and remains constant at that value. For sensitivity function Snh1muH, the trajectory reaches a minimum value of - 45 at discrete time of 30 then increase at a slight angle with a trajectory of – 20 at discrete time of 100. For sensitivity function Snh1KS, the trajectory reaches a maximum value of 1 at discrete time of 25 while the trajectory drops down at slight angle. For sensitivity function Snh1KOH, the trajectory does a S-shaped curve reaching a maximum at 8 at discrete time of 100. For sensitivity function Snh1KNO, the trajectory reaches a maximum of 1.2 at discrete time of 80. For sensitivity function Snh1KNH, the trajectory reaches a maximum value at 100 at discrete time of 20 and drops down to a constant value of zero. For sensitivity function Snh1KOA, the trajectory reaches a maximum value of 80 at discrete time of 25 which slightly oscillates then smoothes out. For sensitivity function Snh1etag, the trajectory reaches a minimum value of – 5 at discrete time of 30 then the trajectory increases to - 0.05 at discrete time of 100. For sensitivity function Snh1etah, the trajectory reaches a minimum value of – 5 at discrete time of 30 then the trajectory increases to – 0.05 at discrete time of 100. For sensitivity function Snh1Kh, the trajectory is oscillating slightly reaching a minimum of - 0.6 at discrete time of 25 then the trajectory becomes stable reaching a steady state. For sensitivity function Snh1Kx, the trajectory reaches a maximum value of 2 at discrete time of 25 and then the trajectory reaches a steady state value of 0.4.

Figure 9.3: Process variable S_{NH2} and its sensitivity functions towards the model parameters

The process variable Snh2, trajectory reaches a value of 8 at discrete time of zero then becomes unstable and oscillating between discrete time of 1 and 20. Then finally the trajectory drops down to zero at constant value. For the sensitivity function Snh2f, the trajectory quickly increases from zero value and reaches a maximum at 0.18 value for discrete time of 25. Finally the trajectory drops down at a value of 0.1 at a discrete time of 50 then remains constant at that value of 0.1. For variable Snh2YH, the trajectory reaches a minimum of -1 at discrete time of 32 and is slightly oscillating reaching a stable trajectory after discrete time of 60 at a minimum value of – 0.05. After this the trajectory is ever increasing at a slight angle to a discrete time of 100. For variable Snh2YA, the trajectory reaches a maximum of 490 then stabilizes to a constant value of zero. For sensitivity function Snh2iXB, the trajectory reaches a minimum value of – 300 at discrete time of 30 then the trajectory smoothes out at above the value of – 200. For sensitivity function Snh2muA, the trajectory reaches a minimum value of – 200 at the discrete time of 20 then increase to zero and remains constant at that value. For sensitivity function Snh2muH, the trajectory reaches a minimum value of - 45 at discrete time of 30 then increase at a slight angle with a trajectory of – 20 at discrete time of 100. For sensitivity function Snh2KS, the trajectory reaches a maximum value of 1 at discrete time of 25 while the trajectory drops down at slight angle. For sensitivity function Snh2KOH, the trajectory does a S-shaped curve reaching a maximum at 8 at discrete time of 100. For sensitivity function Snh2KNO, the trajectory reaches a maximum of 1.2 at discrete time of 80. For sensitivity function Snh2KNH, the trajectory reaches a maximum value at 100 at discrete time of 20 and drops down to a

constant value of zero. For sensitivity function Snh2KOA, the trajectory reaches a maximum value of 80 at discrete time of 25 which slightly oscillates then smoothes out. For sensitivity function Snh2etag, the trajectory reaches a minimum value of – 5 at discrete time of 30 then the trajectory increases to - 0.05 at discrete time of 100. For sensitivity function Snh2etah, the trajectory oscillates in its path reaching a minimum value of – 3 at discrete time of 25 then the trajectory increases to – 0.05 at discrete time of 100. For sensitivity function Snh2Kh, the trajectory is oscillating slightly reaching a minimum of - 0.6 at discrete time of 25 then the trajectory becomes stable reaching a steady state. For sensitivity function Snh2Kx, the trajectory reaches a maximum value of 2 at discrete time of 25 and then the trajectory reaches a steady state value of 0.4.

Figure 9.4: Process variable S_{NH3} and its sensitivity functions towards the model parameters

The process variable Snh3, trajectory reaches a value of 8 at discrete time of zero then becomes unstable and oscillating between discrete time of 1 and 20. Then finally the trajectory drops down to zero at constant value. For the sensitivity function Snh3f, the trajectory quickly increases from zero value and reaches a maximum at 0.18 value for discrete time of 25. Finally the trajectory drops down at a value of 0.1 at a discrete time of 50 then remains constant at that value of 0.1. For variable Snh3YH, the trajectory reaches a minimum of -1 at discrete time of 32 which is slightly oscillating reaching a stable trajectory after discrete time of 60 at a minimum value of – 0.05. After this the trajectory is ever increasing at a slight angle to a discrete time of 100. For variable Snh3YA, the trajectory reaches a maximum of 490 then stabilizes to a constant value of zero. For sensitivity function Snh3iXB, the trajectory reaches a minimum value of – 300 at discrete time of 30 then the trajectory smoothes out at above the value of – 200. For sensitivity function Snh3muA, the trajectory reaches a minimum value of – 200 at the discrete time of 20 then increase to zero and remains constant at that value. For sensitivity function Snh3muH, the trajectory reaches a minimum value of - 45 at discrete time of 30 then increase at a slight angle with a trajectory of – 20 at discrete time of 100. For sensitivity function Snh3KS, the trajectory reaches a maximum value of 1 at discrete time of 25 while the trajectory drops down at slight angle. For sensitivity function Snh3KOH, the trajectory does a S-shaped curve reaching a maximum at 8 at discrete time of 100. For sensitivity function Snh3KNO, the trajectory reaches a maximum of 1.2 at discrete time of 80. For sensitivity function Snh3KNH, the trajectory reaches a maximum value at 100 at discrete time of 20 and drops down to a constant value of zero. For sensitivity function Snh3KOA, the trajectory reaches a maximum value of 80 at discrete time of 25 which slightly oscillates then smoothes out. For sensitivity function Snh3etag, the trajectory reaches a minimum value of – 5 at discrete time of 30 then the trajectory increases to - 0.05 at discrete time of 100. For sensitivity function Snh3etah, the trajectory oscillates in its path reaching a minimum value of – 3 at discrete time of 25 then the trajectory increases to – 0.05 at discrete time of 100. For sensitivity function Snh3Kh, the trajectory is oscillating slightly reaching a minimum of - 0.6 at discrete time of 25 then the trajectory becomes stable reaching a steady state. For sensitivity function Snh3Kx, the trajectory reaches a maximum value of 2 at discrete time of 25 and then the trajectory reaches a steady state value of 0.4.

Figure 9.5: Process variable S_{NH4} and its sensitivity functions towards the model parameters

The process variable Snh4, trajectory reaches a value from zero to 7 at discrete time of zero then becomes unstable and oscillating between discrete time of 1 and 20. Then finally the trajectory drops down to zero at constant value. For the sensitivity function Snh4f, the trajectory quickly increases from zero value and reaches a maximum at 0.18 value for discrete time of 25. Finally the trajectory drops down at a value of 0.1 at a discrete time of 50 then remains constant at that value of 0.1. For variable Snh4YH, the trajectory reaches a minimum of -1 at discrete time of 32 which is slightly oscillating reaching a stable trajectory after discrete time of 60 at a minimum value of – 0.05. After this the trajectory is ever increasing at a slight angle to a discrete time of 100. For variable Snh4YA, the trajectory reaches a maximum of 490 then stabilizes to a

constant value of zero. For sensitivity function Snh4iXB, the trajectory reaches a minimum value of – 300 at discrete time of 30 then the trajectory smoothes out at above the value of – 200. For sensitivity function Snh4muA, the trajectory reaches a minimum value of – 200 at the discrete time of 20 then increase to zero and remains constant at that value. For sensitivity function Snh4muH, the trajectory reaches a minimum value of - 45 at discrete time of 30 then increase at a slight angle with a trajectory of – 20 at discrete time of 100. For sensitivity function Snh4KS, the trajectory reaches a maximum value of 1 at discrete time of 25 while the trajectory drops down at slight angle. For sensitivity function Snh4KOH, the trajectory does a S-shaped curve reaching a maximum at 8 at discrete time of 100. For sensitivity function Snh4KNO, the trajectory reaches a maximum of 1.2 at discrete time of 80. For sensitivity function Snh4KNH, the trajectory reaches a maximum value at 100 at discrete time of 20 and drops down to a constant value of zero. For sensitivity function Snh4KOA, the trajectory reaches a maximum value of 80 at discrete time of 25 which slightly oscillates then smoothes out. For sensitivity function Snh4etag, the trajectory reaches a minimum value of – 5 at discrete time of 30 then the trajectory increases to - 0.05 at discrete time of 100. For sensitivity function Snh4etah, the trajectory oscillates in its path reaching a minimum value of – 3 at discrete time of 25 then the trajectory increases to – 0.05 at discrete time of 100. For sensitivity function Snh4Kh, the trajectory is oscillating slightly reaching a minimum of - 0.6 at discrete time of 25 then the trajectory becomes stable reaching a steady state. For sensitivity function Snh4Kx, the trajectory reaches a maximum value of 2 at discrete time of 25 and then the trajectory reaches a steady state value of 0.4.

Figure 9.6: Process variable S_{NH5} and its sensitivity functions towards the model parameters
The process variable Snh5, trajectory reaches a value from zero to 7 at discrete time of zero then becomes unstable and oscillating between discrete time of 1 and 20. Then finally the trajectory drops down to zero at constant value. For the sensitivity function Snh5f, the trajectory quickly increases from zero value and reaches a maximum at 0.18 value for discrete time of 25. Finally the trajectory drops down at a value of 0.1 at a discrete time of 50 then remains constant at that value of 0.1. For variable Snh5YH, the trajectory reaches a minimum of -1 at discrete time of 32 which is slightly oscillating reaching a stable trajectory after discrete time of 60 at a minimum value of – 0.05. After this the trajectory is ever increasing at a slight angle to a discrete time of 100. For variable Snh5YA, the trajectory reaches a maximum of 490 then stabilizes to a constant value of zero. For sensitivity function Snh5iXB, the trajectory reaches a minimum value of – 300 at discrete time of 30 then the trajectory smoothes out at above the value of – 200. For sensitivity function Snh5muA, the trajectory reaches a minimum value of – 200 at the discrete time of 20 then increase to zero and remains constant at that value. For sensitivity function Snh5muH, the trajectory reaches a minimum value of - 45 at discrete time of 30 then increase at a slight angle with a trajectory of – 20 at discrete time of 100. For sensitivity function Snh5KS, the trajectory reaches a maximum value of 1 at discrete time of 25 while the trajectory drops down at slight angle. For sensitivity function Snh5KOH, the trajectory does a S-shaped curve reaching a maximum at 8 at discrete time of 100. For sensitivity function Snh5KNO, the trajectory reaches a maximum of 1.2 at discrete time of 80. For sensitivity function Snh5KNH, the trajectory reaches a maximum value at 100 at discrete time of 20 and drops down to a constant value of zero. For sensitivity function Snh5KOA, the trajectory reaches a maximum value of 80 at discrete time of 25 which slightly oscillates then smoothes out. For sensitivity function Snh5etag, the trajectory reaches a minimum value of – 5 at discrete time of 30 then the trajectory increases to - 0.05 at discrete time of 100. For sensitivity function Snh5etah, the trajectory oscillates in its path reaching a minimum value of – 3 at discrete time of 25 then the trajectory increases to – 0.05 at discrete time of 100. For sensitivity function Snh5Kh, the trajectory is oscillating slightly reaching a minimum of - 0.6 at discrete time of 25 then the trajectory becomes stable reaching a steady state. For sensitivity function Snh5Kx, the trajectory reaches a maximum value of 2 at discrete time of 25 and then the trajectory reaches a steady state value of 0.4.

Figure 9.7: Process variable S_{NO1} and its sensitivity functions towards the model parameters
The process variable SNO1, trajectory increases from 5 to 8 then decreases to zero at discrete time of 100. For sensitivity function SNO1f, the trajectory follows a reverse S-shaped curve to the value of 0.2 and reaches a steady state at this value. For variable SNO1YH, the trajectory reaches a minimum of - 15 at discrete time of 60. For variable SNO1YA, the trajectory reaches a minimum value of – 490 at a discrete time of 20 and reaches a steady state after discrete time of 60. For sensitivity function SNO1iXB, the trajectory follows a S- shaped curve and drops down to – 400 at steady state. For sensitivity function SNO1muA, the trajectory reaches a maximum value of 200 at discrete time of 20 and reaches a steady state at zero after discrete time of 60. For sensitivity function SNO1muH, the trajectory follows a S-shaped curve with a minimum at – 95 at discrete time of 80. For sensitivity function SNO1KS, the trajectory has a maximum value of 8 at discrete time of 60. For sensitivity function SNO1KOH, the trajectory has a minimum value of - 18 at discrete time of 50. For sensitivity function SNO1KNO, the trajectory continually increases to a value of 6 and level off after discrete time of 90. For sensitivity function SNO1KNH, the trajectory reaches a minimum value of – 98 at discrete time of 25 and reaches a steady state after discrete time of 60. For sensitivity function SNO1KOA, the trajectory reaches a minimum of – 50 at discrete time of 25 and reaches a steady state after discrete time of 60. For sensitivity function SNO1etag, the trajectory reaches a minimum of – 15 at discrete time of 70. For sensitivity function SNO1etah, the trajectory reaches a minimum of – 15 at discrete time of 70. For sensitivity function SNO1Kh, the trajectory follows a S-shaped curve and reaches a minimum of – 1 at discrete time of 65. For sensitivity function SNO1Kx, the trajectory follows a reverse S-shaped curve and reaches a maximum of 3 at discrete time of 60.

Figure 9.8: Process variable S_{NO2} and its sensitivity functions towards the model parameters
The process variable SNO2, trajectory increases from 5 to 8 then decreases to zero at discrete time of 100. For sensitivity function SNO2f, the trajectory follows a reverse S-shaped curve to the value of 0.2 and reaches a steady state at this value. For variable SNO2YH, the trajectory reaches a minimum of - 15 at discrete time of 60. For variable SNO2YA, the trajectory reaches a minimum value of – 490 at a discrete time of 20 and reaches a steady state after discrete time of 60. For sensitivity function SNO2iXB, the trajectory follows a S- shaped curve and drops down to – 400 at steady state. For sensitivity function SNO2muA, the trajectory reaches a maximum value of 200 at discrete time of 20 and reaches a steady state at zero after discrete time of 60. For sensitivity function SNO2muH, the trajectory follows a S-shaped curve with a minimum at – 95 at discrete time of 80. For sensitivity function SNO2KS, the trajectory has a maximum value of 8 at discrete time of 60. For sensitivity function SNO2KOH, the trajectory has a minimum value of - 18 at discrete time of 50. For sensitivity function SNO2KNO, the trajectory continually increases to a value of 6 and level off after discrete time of 90. For sensitivity function SNO2KNH, the trajectory reaches a minimum value of – 98 at discrete time of 25 and reaches a steady state after discrete time of 60. For sensitivity function SNO21KOA, the trajectory reaches a minimum of – 50 at discrete time of 25 and reaches a steady state after discrete time of 60. For sensitivity function SNO2etag, the trajectory reaches a minimum of – 15 at discrete time of 70. For sensitivity function SNO2etah, the trajectory reaches a minimum of – 0.4 at discrete time of 60. For sensitivity function SNO2Kh, the trajectory follows a S-shaped curve and reaches a minimum of – 1 at discrete time of 65. For sensitivity function SNO2Kx, the trajectory follows a reverse S-shaped curve and reaches a maximum of 3 at discrete time of 60.

Figure 9.9: Process variable S_{NO3} and its sensitivity functions towards the model parameters
The process variable SNO3, trajectory increases from 5 to 8 then decreases to zero at discrete time of 100. For sensitivity function SNO3f, the trajectory follows a reverse S-shaped curve to the value of 0.2 and reaches a steady state at this value. For variable SNO3YH, the trajectory reaches a minimum of - 15 at discrete time of 60. For variable SNO3YA, the trajectory reaches a minimum value of – 490 at a discrete time of 20 and reaches a steady state after discrete time of

60. For sensitivity function SNO3iXB, the trajectory follows a S- shaped curve and drops down to – 400 at steady state. For sensitivity function SNO3muA, the trajectory reaches a maximum value of 200 at discrete time of 20 and reaches a steady state at zero after discrete time of 60. For sensitivity function SNO3muH, the trajectory follows a S-shaped curve with a minimum at – 95 at discrete time of 80. For sensitivity function SNO3KS, the trajectory has a maximum value of 8 at discrete time of 60. For sensitivity function SNO3KOH, the trajectory has a minimum value of - 18 at discrete time of 50. For sensitivity function SNO3KNO, the trajectory continually increases to a value of 6 and level off after discrete time of 90. For sensitivity function SNO3KNH, the trajectory reaches a minimum value of – 98 at discrete time of 25 and reaches a steady state after discrete time of 60. For sensitivity function SNO3KOA, the trajectory reaches a minimum of – 50 at discrete time of 25 and reaches a steady state after discrete time of 60. For sensitivity function SNO3etag, the trajectory reaches a minimum of – 15 at discrete time of 70. For sensitivity function SNO3etah, the trajectory reaches a minimum of – 0.4 at discrete time of 60. For sensitivity function SNO3Kh, the trajectory follows a S-shaped curve and reaches a minimum of – 1 at discrete time of 65. For sensitivity function SNO3Kx, the trajectory follows a reverse S-shaped curve and reaches a maximum of 3 at discrete time of 60.

Figure 9.10: Process variable S_{NO4} and its sensitivity functions towards the model parameters
The process variable SNO4, trajectory decreases from 10 in an unstable manner in a discrete time of 20 and further decrease to zero at discrete time of 100. For sensitivity function SNO4f, the trajectory follows a reverse S-shaped curve to the value of 0.2 and reaches a steady state at this value. For variable SNO4YH, the trajectory reaches a minimum of -15 at discrete time of 60. For variable SNO4YA, the trajectory reaches a minimum value of – 490 at a discrete time of 20 and reaches a steady state after discrete time of 60. For sensitivity function SNO4iXB, the trajectory follows a S- shaped curve and drops down to – 400 at steady state. For sensitivity function SNO4muA, the trajectory reaches a maximum value of 200 at discrete time of 20 and reaches a steady state at zero after discrete time of 60. For sensitivity function SNO4muH, the trajectory follows a S-shaped curve with a minimum at – 95 at discrete time of 80. For sensitivity function SNO4KS, the trajectory has a maximum value of 8 at discrete time of 60. For sensitivity function SNO4KOH, the trajectory has a minimum value of - 18 at discrete time of 50. For sensitivity function SNO4KNO, the trajectory continually increases to a value of 6 and level off after discrete time of 90. For sensitivity function SNO4KNH, the trajectory reaches a minimum value of – 98 at discrete time of 25 and reaches a steady state after discrete time of 60. For sensitivity function SNO4KOA, the trajectory reaches a minimum of – 50 at discrete time of 25 and reaches a steady state after discrete time of 60. For sensitivity function SNO4etag, the trajectory reaches a minimum of – 15 at discrete time of 70. For sensitivity function SNO4etah, the trajectory reaches a minimum of – 0.4 at discrete time of 60. For sensitivity function SNO4Kh, the trajectory follows a S-shaped curve and reaches a minimum of – 1 at discrete time of 65. For sensitivity function SNO4Kx, the trajectory follows a reverse S-shaped curve and reaches a maximum of 3 at discrete time of 60.

Figure 9.11: Process variable S_{NO5} and its sensitivity functions towards the model parameters
The process variable SNO5, trajectory decreases from 10 in an unstable manner in a discrete time of 20 and further decrease to zero at discrete time of 100. For sensitivity function SNO5f, the trajectory follows a reverse S-shaped curve to the value of 0.2 and reaches a steady state at this value. For variable SNO5YH, the trajectory reaches a minimum of - 15 at discrete time of 60. For variable SNO5YA, the trajectory reaches a minimum value of – 490 at a discrete time of 20 and reaches a steady state after discrete time of 60. For sensitivity function SNO5iXB, the trajectory follows a S- shaped curve and drops down to – 400 at steady state. For sensitivity function SNO5muA, the trajectory reaches a maximum value of 200 at discrete time of 20 and reaches a steady state at zero after discrete time of 60. For sensitivity function SNO5muH, the trajectory follows a S-shaped curve with a minimum at – 95 at discrete time of 80. For sensitivity function SNO5KS, the trajectory has a maximum value of 8 at discrete time of 60. For sensitivity

function SNO5KOH, the trajectory has a minimum value of - 18 at discrete time of 50. For sensitivity function SNO5KNO, the trajectory continually increases to a value of 6 and level off after discrete time of 90. For sensitivity function SNO5KNH, the trajectory reaches a minimum value of – 98 at discrete time of 25 and reaches a steady state after discrete time of 60. For sensitivity function SNO5KOA, the trajectory reaches a minimum of – 50 at discrete time of 25 and reaches a steady state after discrete time of 60. For sensitivity function SNO5etag, the trajectory reaches a minimum of – 15 at discrete time of 70. For sensitivity function SNO5etah, the trajectory reaches a minimum of – 0.4 at discrete time of 60. For sensitivity function SNO5Kh, the trajectory follows a S-shaped curve and reaches a minimum of – 1 at discrete time of 65. For sensitivity function SNO5Kx, the trajectory follows a reverse S-shaped curve and reaches a maximum of 3 at discrete time of 60.

Figure 9.12: Process variable S_{S1} and its sensitivity functions towards the model parameters
The process variable SS1, the trajectory increases from 2 to 9 and reaches a steady state after discrete time of 60. For sensitivity function SS1f, the trajectory drops steeply to - 0.04 at discrete time of 100. For variable SS1YH, the trajectory oscillates till it reaches a steady state of 100 at discrete time of 60. For variable SS1YA, the trajectory reaches a maximum value of 1.5 at discrete time of 40 and then decrease to – 1.8 at discrete time of 100. For sensitivity function SS1iXB, the trajectory increases from zero to 75 at discrete time of 100. For sensitivity function SS1muA, the trajectory reaches a minimum value of – 0.75 at discrete time of 40 and a high value of 1 at discrete time of 100. For sensitivity function SS1muH, the trajectory oscillates from zero and becomes stable at - 200 at discrete time of 60 and reaches a steady state. For sensitivity function SS1KS, the trajectory oscillates from zero to downwards value of 4 at discrete time of 100. For sensitivity function SS1KOH, the trajectory oscillates from zero to – 50 then becomes stable at discrete time of 60 and decrease to – 90 at discrete time 100. For sensitivity function SS1KNO, the trajectory oscillates from zero to – 10 and becomes stable after – 10 at discrete time of 60 and reaches a minimum of - 10.5 For sensitivity function SS1KNH, the trajectory reaches a maximum of 0.4 at discrete time of 40 and drops down to – 0.4 at discrete time of 100. For sensitivity function SS1KOA, the trajectory reaches a maximum of 0.25 at discrete time of 35. For sensitivity function SS1etag, the trajectory constantly increases from zero at discrete time of 40 to 1.9 at discrete time of 100. For sensitivity function SS1etah, the trajectory constantly increases from zero at discrete time of 40 to 1.9 at discrete time of 100. For sensitivity function SS1Kh, the trajectory oscillates from zero to 50 at a discrete time of 60 whereby it remains stable and reaches steady state. For sensitivity function SS1Kx, the trajectory oscillates from zero to – 150 then after at discrete value of 65 it remains stable and reaches a steady state.

Figure 9.13: Process variable S_{S2} and its sensitivity functions towards the model parameters
The process variable SS2, the trajectory increases from 2 to 9 and reaches a steady state after discrete time of 60. For sensitivity function SS2f, the trajectory drops steeply to - 0.04 at discrete time of 100. For variable SS2YH, the trajectory oscillates till it reaches a steady state of 100 at discrete time of 60. For variable SS2YA, the trajectory reaches a maximum value of 1.5 at discrete time of 40 and then decrease to – 1.8 at discrete time of 100. For sensitivity function SS2iXB, the trajectory increases from zero to 75 at discrete time of 100. For sensitivity function SS2muA, the trajectory reaches a minimum value of – 0.75 at discrete time of 40 and a high value of 1 at discrete time of 100. For sensitivity function SS2muH, the trajectory oscillates from zero and becomes stable at - 200 at discrete time of 60 and reaches a steady state. For sensitivity function SS2KS, the trajectory oscillates from zero to downwards value of 4 at discrete time of 100. For sensitivity function SS2KOH, the trajectory oscillates from zero to – 50 then becomes stable at discrete time of 60 and decrease to – 90 at discrete time 100. For sensitivity function SS2KNO, the trajectory oscillates from zero to – 10 and becomes stable after – 10 at discrete time of 60 and reaches a minimum of - 10.5 For sensitivity function SS2KNH, the trajectory reaches a maximum of 0.4 at discrete time of 40 and drops down to –

0.4 at discrete time of 100. For sensitivity function SS2KOA, the trajectory reaches a maximum of 0.25 at discrete time of 35. For sensitivity function SS2etag, the trajectory constantly increases from zero at discrete time of 40 increases to 3 at discrete time of 100. For sensitivity function SS2etah, the trajectory rapidly oscillates from zero to 25 until a discrete time of 60 then remains stable afterwards. For sensitivity function SS1Kh, the trajectory oscillates from zero to 50 at a discrete time of 60 whereby it remains stable and reaches steady state. For sensitivity function SS1Kx, the trajectory oscillates from zero to – 150 then after at discrete value of 65 it remains stable and reaches a steady state.

Figure 9.14: Process variable S_{S3} and its sensitivity functions towards the model parameters
The process variable SS3, the trajectory increases from 2 to 9 and reaches a steady state after discrete time of 60. For sensitivity function SS3f, the trajectory drops steeply to - 0.04 at discrete time of 100. For variable SS3YH, the trajectory oscillates till it reaches a steady state of 150 at discrete time of 60. For variable SS3YA, the trajectory reaches a maximum value of 1.5 at discrete time of 40 and then decrease to – 1.8 at discrete time of 100. For sensitivity function SS3iXB, the trajectory increases from zero to 75 at discrete time of 100. For sensitivity function SS3muA, the trajectory reaches a minimum value of – 0.75 at discrete time of 40 and a high value of 1 at discrete time of 100. For sensitivity function SS3muH, the trajectory oscillates from zero and becomes stable at - 200 at discrete time of 60 and reaches a steady state. For sensitivity function SS3KS, the trajectory oscillates from zero to downwards value of 4 at discrete time of 100. For sensitivity function SS3KOH, the trajectory oscillates from zero to – 50 then becomes stable at discrete time of 60 and decrease to – 90 at discrete time 100. For sensitivity function SS3KNO, the trajectory oscillates from zero to – 10 and becomes stable after – 10 at discrete time of 60 and reaches a minimum of - 10.5 For sensitivity function SS3KNH, the trajectory reaches a maximum of 0.4 at discrete time of 40 and drops down to – 0.4 at discrete time of 100. For sensitivity function SS3KOA, the trajectory reaches a maximum of 0.25 at discrete time of 35. For sensitivity function SS3etag, the trajectory constantly increases from zero at discrete time of 40 increases to 2 at discrete time of 100. For sensitivity function SS3etah, the trajectory rapidly oscillates from zero to 25 until a discrete time of 60 then remains stable afterwards. For sensitivity function SS3Kh, the trajectory oscillates from zero to 50 at a discrete time of 60 whereby it remains stable and reaches steady state. For sensitivity function SS3Kx, the trajectory oscillates from zero to – 150 then after at discrete value of 65 it remains stable and reaches a steady state.

Figure 9.15: Process variable S_{S4} and its sensitivity functions towards the model parameters
The process variable SS4, the trajectory increases from 2 to 9 and reaches a steady state after discrete time of 60. For sensitivity function SS4f, the trajectory drops steeply to 0.02 at discrete time of 100. For variable SS4YH, the trajectory oscillates till it reaches a steady state of 150 at discrete time of 60. For variable SS4YA, the trajectory reaches a maximum value of 1.5 at discrete time of 40 and then decrease to – 1.8 at discrete time of 100. For sensitivity function SS4iXB, the trajectory increases from zero to 75 at discrete time of 100. For sensitivity function SS4muA, the trajectory reaches a minimum value of – 0.75 at discrete time of 40 and a high value of 1 at discrete time of 100. For sensitivity function SS4muH, the trajectory oscillates from zero and becomes stable at - 200 at discrete time of 60 and reaches a steady state. For sensitivity function SS4KS, the trajectory oscillates from zero to downwards value of 4 at discrete time of 100. For sensitivity function SS4KOH, the trajectory oscillates from zero to – 50 then becomes stable at discrete time of 60 and decrease to – 90 at discrete time 100. For sensitivity function SS4KNO, the trajectory oscillates from zero to – 10 and becomes stable after – 10 at discrete time of 60 and reaches a minimum of - 10.5 For sensitivity function SS4KNH, the trajectory reaches a maximum of 0.4 at discrete time of 40 and drops down to – 0.4 at discrete time of 100. For sensitivity function SS4KOA, the trajectory reaches a maximum of 0.25 at discrete time of 35. For sensitivity function SS4etag, the trajectory constantly increases from zero at discrete time of 40 increases to 1.5 at discrete time of 100. For sensitivity

function SS4etah, the trajectory rapidly oscillates from zero to 20 until a discrete time of 60 then remains stable afterwards. For sensitivity function SS4Kh, the trajectory oscillates from zero to 50 at a discrete time of 60 whereby it remains stable and reaches steady state. For sensitivity function SS4Kx, the trajectory oscillates from zero to – 150 then after at discrete value of 65 it remains stable and reaches a steady state.

Figure 9.16: Process variable S_{S5} and its sensitivity functions towards the model parameters
The process variable SS5, the trajectory increases from 2 to 9 and reaches a steady state after discrete time of 60. For sensitivity function SS5f, the trajectory drops steeply to 0.02 at discrete time of 100. For variable SS5YH, the trajectory oscillates till it reaches a steady state of 150 at discrete time of 60. For variable SS5YA, the trajectory reaches a maximum value of 1.5 at discrete time of 40 and then decrease to – 1.8 at discrete time of 100. For sensitivity function SS5iXB, the trajectory increases from zero to 75 at discrete time of 100. For sensitivity function SS5muA, the trajectory reaches a minimum value of – 0.75 at discrete time of 40 and a high value of 1 at discrete time of 100. For sensitivity function SS5muH, the trajectory oscillates from zero and becomes stable at - 200 at discrete time of 60 and reaches a steady state. For sensitivity function SS5KS, the trajectory oscillates from zero to downwards value of 4 at discrete time of 100. For sensitivity function SS5KOH, the trajectory oscillates from zero to – 50 then becomes stable at discrete time of 60 and decrease to – 90 at discrete time 100. For sensitivity function SS5KNO, the trajectory oscillates from zero to – 10 and becomes stable after – 10 at discrete time of 60 and reaches a minimum of - 10.5 For sensitivity function SS5KNH, the trajectory reaches a maximum of 0.4 at discrete time of 40 and drops down to – 0.4 at discrete time of 100. For sensitivity function SS5KOA, the trajectory reaches a maximum of 0.25 at discrete time of 35. For sensitivity function SS5etag, the trajectory constantly increases from zero at discrete time of 40 increases to 1 at discrete time of 100. For sensitivity function SS5etah, the trajectory rapidly oscillates from zero to 15 until a discrete time of 60 then remains stable afterwards. For sensitivity function SS5Kh, the trajectory oscillates from zero to 50 at a discrete time of 60 whereby it remains stable and reaches steady state. For sensitivity function SS5Kx, the trajectory oscillates from zero to – 150 then after at discrete value of 65 it remains stable and reaches a steady state.

Benchmark process with UCT reduced biological model

Figure 9.17: Process variable S_{NH1} and its sensitivity functions towards the model parameters
The process variable Snh1, the trajectory decreases from zero to – 5000 at discrete time of 100. For the sensitivity function Snh1f, the trajectory increases from zero to 35 at discrete time of 80 and remains stable. For variable Snh1YZH, the trajectory follows a S-shaped curve from zero to – 0.8 at discrete time of 100. For variable Snh1YZA, the trajectory increases from zero to 275 at discrete time of 100. For sensitivity function Snh1fZBH, the trajectory decreases from zero to – 1900 at discrete time of 100. For sensitivity function Snh1muA, the trajectory decreases from zero to – 500 at discrete time of 100. For sensitivity function Snh1muH, the trajectory decreases from zero to – 39 at discrete time of 100. For sensitivity function Snh1KS, the trajectory decreases from zero to – 0.4 at discrete time of 100. For sensitivity function Snh1KOH, the trajectory increases from zero to 190 at discrete time of 100. For sensitivity function Snh1KNO, the trajectory at first oscillates around zero then stabilizes and slightly decreased to - 0.1×10^{-3} at discrete time of 100. For sensitivity function Snh1KNH, the trajectory increases from zero to 110 at discrete time of 100. For sensitivity function Snh1KOA, the trajectory increases from zero to 500 at discrete time of 100. For sensitivity function Snh1etag, the trajectory decreases from zero to – 0.5 at discrete time of 100. For sensitivity function Snh1KMP, the trajectory increases from zero to 95 at discrete time of 100. For sensitivity function Snh1KSP, the trajectory increases from zero to 105 at discrete time of 100. For sensitivity function Snh1KSA, the trajectory increases rapidly from zero to 2 at discrete time of 5 then decreases back to zero reaching a steady state at 80. For sensitivity function Snh1fMA, the trajectory increases from

zero to 0.5×10^{-3} at discrete time of 100. For sensitivity function Snh1KA, the trajectory increases from zero to 0.02 at discrete time of 100.

Figure 9.18: Process variable S_{NH2} and its sensitivity functions towards the model parameters
The process variable Snh2, the trajectory decreases from zero to – 5000 at discrete time of 100. For the sensitivity function Snh2f, the trajectory increases from zero to 35 at discrete time of 80 and remains stable. For variable Snh2YZH, the trajectory follows a S-shaped curve from zero to – 0.8 at discrete time of 100. For variable Snh2YZA, the trajectory increases from zero to 275 at discrete time of 100. For sensitivity function Snh2fZBH, the trajectory decreases from zero to – 1900 at discrete time of 100. For sensitivity function Snh2muA, the trajectory decreases from zero to – 500 at discrete time of 100. For sensitivity function Snh2muH, the trajectory decreases from zero to – 39 at discrete time of 100. For sensitivity function Snh2KS, the trajectory decreases from zero to – 0.4 at discrete time of 100. For sensitivity function Snh2KOH, the trajectory increases from zero to 190 at discrete time of 100. For sensitivity function Snh2KNO, the trajectory at first oscillates around zero then stabilizes and slightly decreased to - 0.1×10^{-3} at discrete time of 100. For sensitivity function Snh2KNH, the trajectory increases from zero to 110 at discrete time of 100. For sensitivity function Snh2KOA, the trajectory increases from zero to 500 at discrete time of 100. For sensitivity function Snh2etag, the trajectory decreases from zero to – 0.5 at discrete time of 100. For sensitivity function Snh2KMP, the trajectory increases from zero to 95 at discrete time of 100. For sensitivity function Snh2KSP, the trajectory increases from zero to 105 at discrete time of 100. For sensitivity function Snh2KSA, the trajectory increases rapidly from zero to 2 at discrete time of 5 then decreases back to zero reaching a steady state at 80. For sensitivity function Snh2fMA, the trajectory increases from zero to 0.5×10^{-3} at discrete time of 100. For sensitivity function Snh2KA, the trajectory increases from zero to 0.02 at discrete time of 100.

Figure 9.19: Process variable S_{NH3} and its sensitivity functions towards the model parameters
The process variable Snh3, the trajectory decreases from zero to – 5000 at discrete time of 100. For the sensitivity function Snh3f, the trajectory increases from zero to 35 at discrete time of 80 and remains stable. For variable Snh3YZH, the trajectory follows a S-shaped curve from zero to – 0.8 at discrete time of 100. For variable Snh3YZA, the trajectory increases from zero to 275 at discrete time of 100. For sensitivity function Snh3fZBH, the trajectory decreases from zero to – 1900 at discrete time of 100. For sensitivity function Snh3muA, the trajectory decreases from zero to – 500 at discrete time of 100. For sensitivity function Snh3muH, the trajectory decreases from zero to – 39 at discrete time of 100. For sensitivity function Snh3KS, the trajectory decreases from zero to – 0.4 at discrete time of 100. For sensitivity function Snh3KOH, the trajectory increases from zero to 190 at discrete time of 100. For sensitivity function Snh3KNO, the trajectory at first oscillates around zero then stabilizes and slightly decreased to - 0.1×10^{-3} at discrete time of 100. For sensitivity function Snh3KNH, the trajectory increases from zero to 110 at discrete time of 100. For sensitivity function Snh3KOA, the trajectory increases from zero to 500 at discrete time of 100. For sensitivity function Snh3etag, the trajectory decreases from zero to – 0.5 at discrete time of 100. For sensitivity function Snh3KMP, the trajectory increases from zero to 100 at discrete time of 100. For sensitivity function Snh3KSP, the trajectory increases from zero to 105 at discrete time of 100. For sensitivity function Snh3KSA, the trajectory oscillates unsteadily from zero to 1.8 at discrete time of 5 then decreases back to zero reaching a steady state at 80. For sensitivity function Snh1fMA, the trajectory increases from zero to 0.5×10^{-3} at discrete time of 100. For sensitivity function Snh1KA, the trajectory increases from zero to 0.02 at discrete time of 100.

Figure 9.20: Process variable S_{NH4} and its sensitivity functions towards the model parameters
The process variable Snh4, the trajectory decreases from zero to – 5000 at discrete time of 100. For the sensitivity function Snh4f, the trajectory increases from zero to 35 at discrete time of 80

and remains stable. For variable Snh4YZH, the trajectory follows a S-shaped curve from zero to – 0.8 at discrete time of 100. For variable Snh4YZA, the trajectory increases from zero to 275 at discrete time of 100. For sensitivity function Snh4fZBH, the trajectory decreases from zero to – 1900 at discrete time of 100. For sensitivity function Snh4muA, the trajectory decreases from zero to – 500 at discrete time of 100. For sensitivity function Snh4muH, the trajectory decreases from zero to – 39 at discrete time of 100. For sensitivity function Snh4KS, the trajectory decreases from zero to – 0.4 at discrete time of 100. For sensitivity function Snh4KOH, the trajectory increases from zero to 190 at discrete time of 100. For sensitivity function Snh4KNO, the trajectory at first oscillates around zero then stabilizes and slightly decreased to - 0.1×10^{-3} at discrete time of 100. For sensitivity function Snh4KNH, the trajectory increases from zero to 110 at discrete time of 100. For sensitivity function Snh4KOA, the trajectory increases from zero to 500 at discrete time of 100. For sensitivity function Snh4etag, the trajectory decreases from zero to – 0.5 at discrete time of 100. For sensitivity function Snh4KMP, the trajectory increases from zero to 100 at discrete time of 100. For sensitivity function Snh4KSP, the trajectory increases from zero to 105 at discrete time of 100. For sensitivity function Snh4KSA, the trajectory increases rapidly from zero to 2 at discrete time of 5 then decreases back to zero reaching a steady state at 80. For sensitivity function Snh4fMA, the trajectory increases from zero to 0.5×10^{-3} at discrete time of 100. For sensitivity function Snh4KA, the trajectory increases from zero to 0.02 at discrete time of 100.

Figure 9.21: Process variable S_{NH5} and its sensitivity functions towards the model parameters
The process variable Snh5, the trajectory decreases from zero to – 5000 at discrete time of 100. For the sensitivity function Snh5f, the trajectory increases from zero to 35 at discrete time of 80 and remains stable. For variable Snh5YZH, the trajectory follows a S-shaped curve from zero to – 0.8 at discrete time of 100. For variable Snh5YZA, the trajectory increases from zero to 275 at discrete time of 100. For sensitivity function Snh5fZBH, the trajectory decreases from zero to – 1900 at discrete time of 100. For sensitivity function Snh5muA, the trajectory decreases from zero to – 500 at discrete time of 100. For sensitivity function Snh5muH, the trajectory decreases from zero to – 39 at discrete time of 100. For sensitivity function Snh5KS, the trajectory decreases from zero to – 0.4 at discrete time of 100. For sensitivity function Snh5KOH, the trajectory increases from zero to 190 at discrete time of 100. For sensitivity function Snh5KNO, the trajectory at first oscillates around zero then stabilizes and slightly decreased to - 0.1×10^{-3} at discrete time of 100. For sensitivity function Snh5KNH, the trajectory increases from zero to 110 at discrete time of 100. For sensitivity function Snh5KOA, the trajectory increases from zero to 500 at discrete time of 100. For sensitivity function Snh5etag, the trajectory decreases from zero to – 0.5 at discrete time of 100. For sensitivity function Snh5KMP, the trajectory increases from zero to 100 at discrete time of 100. For sensitivity function Snh5KSP, the trajectory increases from zero to 105 at discrete time of 100. For sensitivity function Snh5KSA, the trajectory increases rapidly from zero to 2 at discrete time of 5 then decreases back to zero reaching a steady state at 80. For sensitivity function Snh5fMA, the trajectory increases from zero to 0.5×10^{-3} at discrete time of 100. For sensitivity function Snh5KA, the trajectory increases from zero to 0.03 at discrete time of 100.

Figure 9.22: Process variable S_{NO1} and its sensitivity functions towards the model parameters
The process variables SNO1, the trajectory increases from zero to 4900 at discrete time of 100. For sensitivity function SNO1f, the trajectory increases from zero to 4×10^{-3} at discrete time of 5 then slowly oscillates until it reaches zero whereby it stabilizes. For variable SNO1YZH, the trajectory remains at zero until discrete value of 20 then decreases to – 4 at discrete time of 100. For variable SNO1YZA, the trajectory increases from zero to 30 at discrete time of 60 and reaches a steady state at this value. For sensitivity function SNO1fZBH, the trajectory initially oscillates slightly around zero then decreases to – 0.1 then reaches a steady state at zero at discrete time of 30. For sensitivity function SNO1muA, the trajectory increases to 4 at discrete

time of 5 and decreases to zero at discrete time of 40 and reaches a steady state at this value. For sensitivity function SNO1muH, the trajectory decreases from zero to – 0.3 at discrete time of 100. For sensitivity functions SNO1KS, the trajectory increases from zero to 0.015 at discrete time of 60 then reaches a steady state after this value. For sensitivity function SNO1KOH, the trajectory decreases from zero to – 0.8 at discrete time of 100. For sensitivity function SNO1KNO, the trajectory initially oscillates from zero to 3×10^{-3} at discrete time of 3 then settles down to zero at discrete time of 80. For sensitivity function SNO1KNH, the trajectory increases from zero to 4 at discrete time of 5 then drops down to zero reaching a steady state at discrete time of 60. For sensitivity function SNO1KOA, the trajectory increases from zero to 2 at discrete time of 5 then decreases to zero reaching a steady state at discrete time of 60. For sensitivity function SNO1etag, the trajectory decreases from zero to – 0.5 at discrete time of 60 and reaches a steady state at this value. For sensitivity function SNO1KMP, the trajectory increases from zero to 3 at discrete time of 100. For sensitivity function SNO1KSP the trajectory oscillates around zero then increases to 0.49 at discrete time of 100. For sensitivity function SNO1KSA, the trajectory decreases from zero to – 4 at discrete time of 5 then increases to zero at discrete time of 20 and reaches a steady state after this value. For sensitivity function SNo1fMA, the trajectory follows a slight S-shaped curve from zero to – 0.4 at discrete time of 100. For sensitivity function SNO1KA, the trajectory follows a slight S-shaped curve from zero to 17 at discrete time of 100.

Figure 9.23: Process variable S_{NO2} and its sensitivity functions towards the model parameters
The process variables SNO2, the trajectory increases from zero to 4900 at discrete time of 100. For sensitivity function SNO2f, the trajectory increases from zero to 4×10^{-3} at discrete time of 5 then slowly oscillates until it reaches zero whereby it stabilizes. For variable SNO2YZH, the trajectory remains at zero until discrete value of 20 then decreases to – 4 at discrete time of 100. For variable SNO2YZA, the trajectory increases from zero to 30 at discrete time of 60 and reaches a steady state at this value. For sensitivity function SNO2fZBH, the trajectory initially oscillates slightly around zero then decreases to – 0.1 then reaches a steady state at zero at discrete time of 30. For sensitivity function SNO2muA, the trajectory increases to 4 at discrete time of 5 and decreases to zero at discrete time of 40 and reaches a steady state at this value. For sensitivity function SNO2muH, the trajectory decreases from zero to – 0.3 at discrete time of 100. For sensitivity functions SNO2KS, the trajectory increases from zero to 0.015 at discrete time of 60 then reaches a steady state after this value. For sensitivity function SNO2KOH, the trajectory decreases from zero to – 0.8 at discrete time of 100. For sensitivity function SNO2KNO, the trajectory initially oscillates from zero to 3×10^{-3} at discrete time of 3 then settles down to zero at discrete time of 80. For sensitivity function SNO2KNH, the trajectory increases from zero to -120 reaching a steady state at discrete time of 60. For sensitivity function SNO2KOA, the trajectory increases from zero to 2 at discrete time of 5 then decreases to zero reaching a steady state at discrete time of 60. For sensitivity function SNO2etag, the trajectory decreases from zero to – 0.5 at discrete time of 60 and reaches a steady state at this value. For sensitivity function SNO2KMP, the trajectory increases from zero to 3 at discrete time of 100. For sensitivity function SNO2KSP the trajectory oscillates around zero then increases to 0.49 at discrete time of 100. For sensitivity function SNO2KSA, the trajectory decreases from zero to – 4 at discrete time of 5 then increases to zero at discrete time of 20 and reaches a steady state after this value. For sensitivity function SNo2fMA, the trajectory follows a slight S-shaped curve from zero to – 0.4 at discrete time of 100. For sensitivity function SNO2KA, the trajectory follows a slight S-shaped curve from zero to 17 at discrete time of 100.

Figure 9.24: Process variable S_{NO3} and its sensitivity functions towards the model parameters
The process variables SNO3, the trajectory increases from zero to 4900 at discrete time of 100. For sensitivity function SNO3f, the trajectory increases from zero to 3.5×10^{-3} at discrete time of 5 then slowly oscillates until it reaches zero whereby it stabilizes. For variable SNO3YZH, the

trajectory remains at zero until discrete value of 20 then decreases to – 4 at discrete time of 100. For variable SNO3YZA, the trajectory increases from zero to 30 at discrete time of 60 and reaches a steady state at this value. For sensitivity function SNO3fZBH, the trajectory initially oscillates slightly around zero then decreases to – 0.1 reaches a steady state at zero at discrete time of 30. For sensitivity function SNO3muA, the trajectory increases to 4 at discrete time of 5 and decreases to zero at discrete time of 40 and reaches a steady state at this value. For sensitivity function SNO3muH, the trajectory decreases from zero to – 0.3 at discrete time of 100. For sensitivity functions SNO3KS, the trajectory increases from zero to 0.015 at discrete time of 60 then reaches a steady state after this value. For sensitivity function SNO3KOH, the trajectory decreases from zero to – 0.8 at discrete time of 100. For sensitivity function SNO3KNO, the trajectory initially oscillates from zero to 3×10^{-3} at discrete time of 3 then settles down to zero at discrete time of 80. For sensitivity function SNO3KNH, the trajectory increases from zero to -120 reaching a steady state at discrete time of 60. For sensitivity function SNO3KOA, the trajectory increases from zero to 2 at discrete time of 5 then decreases to zero reaching a steady state at discrete time of 60. For sensitivity function SNO3etag, the trajectory decreases from zero to – 0.5 at discrete time of 60 and reaches a steady state at this value. For sensitivity function SNO3KMP, the trajectory increases from zero to 3 at discrete time of 100. For sensitivity function SNO3KSP the trajectory oscillates around zero then increases to 0.49 at discrete time of 100. For sensitivity function SNO3KSA, the trajectory decreases from zero to – 4 at discrete time of 5 then increases to zero at discrete time of 20 and reaches a steady state after this value. For sensitivity function SNO3fMA, the trajectory follows a slight S-shaped curve from zero to – 0.4 at discrete time of 100. For sensitivity function SNO3KA, the trajectory follows a slight S-shaped curve from zero to 17 at discrete time of 100.

Figure 9.25: Process variable S_{NO4} and its sensitivity functions towards the model parameters

The process variables SNO4, the trajectory increases from zero to 4900 at discrete time of 100. For sensitivity function SNO4f, the trajectory increases from zero to 2×10^{-3} at discrete time of 5 then slowly oscillates until it reaches zero whereby it stabilizes. For variable SNO4YZH, the trajectory remains at zero until discrete value of 20 then decreases to – 4 at discrete time of 100. For variable SNO4YZA, the trajectory increases from zero to 30 at discrete time of 60 and reaches a steady state at this value. For sensitivity function SNO4fZBH, the trajectory initially oscillates slightly around zero then reaches a steady state at zero at discrete time of 30. For sensitivity function SNO4muA, the trajectory increases to 4 at discrete time of 5 and decreases to zero at discrete time of 40 and reaches a steady state at this value. For sensitivity function SNO4muH, the trajectory decreases from zero to – 0.3 at discrete time of 100. For sensitivity functions SNO4KS, the trajectory increases from zero to 0.015 at discrete time of 60 then reaches a steady state after this value. For sensitivity function SNO4KOH, the trajectory decreases from zero to – 0.8 at discrete time of 100. For sensitivity function SNO4KNO, the trajectory initially oscillates from zero to 3×10^{-3} at discrete time of 3 then settles down to zero at discrete time of 80. For sensitivity function SNO4KNH, the trajectory increases from zero to -120 reaching a steady state at discrete time of 60. For sensitivity function SNO4KOA, the trajectory increases from zero to 2 at discrete time of 5 then decreases to zero reaching a steady state at discrete time of 60. For sensitivity function SNO4etag, the trajectory decreases from zero to – 0.5 at discrete time of 60 and reaches a steady state at this value. For sensitivity function SNO4KMP, the trajectory increases from zero to 3 at discrete time of 100. For sensitivity function SNO4KSP the trajectory oscillates around zero then increases to 0.49 at discrete time of 100. For sensitivity function SNO4KSA, the trajectory decreases from zero to – 4 at discrete time of 5 then increases to zero at discrete time of 20 and reaches a steady state after this value. For sensitivity function SNO4fMA, the trajectory follows a slight S-shaped curve from zero to – 0.4 at discrete time of 100. For sensitivity function SNO4KA, the trajectory follows a slight S-shaped curve from zero to 17 at discrete time of 100.

Figure 9.26.Process variable S_{NO5} and its sensitivity functions towards the model parameters

The process variables SNO5, the trajectory increases from zero to 4900 at discrete time of 100. For sensitivity function SNO5f, the trajectory increase from zero to 2×10^{-3} at discrete time of 5 then slowly oscillating until it reaches zero whereby it stabilizes. For variable SNO5YZH, the trajectory remains at zero until discrete value of 20 then decreases to – 4 at discrete time of 100. For variable SNO5YZA, the trajectory increases from zero to 30 at discrete time of 60 and reaches a steady state at this value. For sensitivity function SNO5fZBH, the trajectory initially oscillates slightly around zero then reaches a steady state at zero at discrete time of 30. For sensitivity function SNO5muA, the trajectory increases to 4 at discrete time of 5 and decreases to zero at discrete time of 40 and reaches a steady state at this value. For sensitivity function SNO5muH, the trajectory decreases from zero to – 0.3 at discrete time of 100. For sensitivity functions SNO5KS, the trajectory increases from zero to 0.015 at discrete time of 60 then reaches a steady state after this value. For sensitivity function SNO5KOH, the trajectory decreases from zero to – 0.8 at discrete time of 100. For sensitivity function SNO5KNO, the trajectory initially oscillates from zero to 3×10^{-3} at discrete time of 3 then settles down to zero at discrete time of 80. For sensitivity function SNO5KNH, the trajectory increases from zero to -120 reaching a steady state at discrete time of 60. For sensitivity function SNO5KOA, the trajectory increases from zero to 2 at discrete time of 5 then decreases to zero reaching a steady state at discrete time of 60. For sensitivity function SNO5etag, the trajectory decreases from zero to – 0.5 at discrete time of 60 and reaches a steady state at this value. For sensitivity function SNO5KMP, the trajectory increases from zero to 3 at discrete time of 100. For sensitivity function SNO5KSP the trajectory oscillates around zero then increases to 0.49 at discrete time of 100. For sensitivity function SNO5KSA, the trajectory decreases from zero to – 4 at discrete time of 5 then increases to zero at discrete time of 20 and reaches a steady state after this value. For sensitivity function SNO5fMA, the trajectory follows a slight S-shaped curve from zero to – 0.4 at discrete time of 100. For sensitivity function SNO5KA, the trajectory follows a slight S-shaped curve from zero to 17 at discrete time of 100.

Figure 9.27: Process variable S_{S1} and its sensitivity functions towards the model parameters

The process variable SS1, the trajectory increases from zero to 10 then is slightly increasing to 15 and remaining at steady state at this value. For sensitivity function SS1f, the trajectory decreases from zero to - 0.5×10^{-10} oscillating then is reaching zero at steady state. For variable SS1YZH, the trajectory increases from zero to 38 at discrete time of 60 reaching a steady state after this value. For variable SS1YZA, the trajectory oscillates slightly from zero to - 1×10^{-9} then reaches steady state at discrete time of 60. For sensitivity function SS1fZBH, the trajectory is slightly oscillating from zero to 0.5×10^{-9} then decreasing to zero at discrete time of 60. For sensitivity function SS1muA, the trajectory oscillates slightly around zero then decreases to - 1×10^{-9} and remains stable around zero from discrete time of 20. For sensitivity function SS1muH, the trajectory decreases from zero to – 500 at discrete time of 60 and reaches a steady state at this value. For sensitivity function SS1KS, the trajectory increases from zero to 35 at discrete time of 60 and reaches a steady state at this value. For sensitivity function SS1KOH, the trajectory increases from zero to 0.25 then decreases to 0.01 reaching zero at a discrete time of 60. For sensitivity function SS1KNO, the trajectory increases from zero to 0.06 at discrete time of 60 and reaches a steady state at this value. For sensitivity function SS1KNH, the trajectory increases from zero to 3.5×10^{-3} and decreases to zero at discrete time of 60. For sensitivity function SS1KOA, the trajectory decreases from zero to - 1.5×10^{-9} and oscillates until it reaches zero at discrete time of 50 and remains there. For sensitivity function SS1etag, the trajectory increases from zero to 5×10^{-11} at a discrete time of 5 then oscillating finally reaching a steady state value of 1×10^{-11} at discrete time of 60. For sensitivity function SS1KMP, the trajectory decrease from zero to - 3×10^{-11} then increasing to - 1×10^{-11} and finally decreasing to - 2×10^{-11} at a discrete time of 100. For sensitivity function SS1KSP, the trajectory

oscillates from zero to - 5×10^{-11} then settling down to zero after a discrete time of 40. For sensitivity function SS1KSA, the trajectory oscillates from zero to 1.5×10^{-9} then settles down to zero at a discrete time of 60. For sensitivity function SS1fMA, the trajectory increases from zero to 3×10^{-12} at a discrete time of 100. For sensitivity function SS1KA, the trajectory increases from zero to 1.5×10^{-10} at a discrete time of 100.

Figure 9.28: Process variable S_{S2} and its sensitivity functions towards the model parameters

The process variable SS2, the trajectory increases from zero to 10 then is slightly increasing to 15 and remaining at steady state at this value. For sensitivity function SS2f, the trajectory decreases from zero to - 0.5×10^{-10} oscillating then is reaching zero at steady state. For variable SS2YZH, the trajectory increases from zero to 38 at discrete time of 60 reaching a steady state after this value. For variable SS2YZA, the trajectory oscillates slightly from zero to - 1×10^{-9} then reaches steady state at discrete time of 60. For sensitivity function SS2fZBH, the trajectory is slightly oscillating from zero to 0.5×10^{-9} then decreasing to zero at discrete time of 60. For sensitivity function SS2muA, the trajectory oscillates slightly around zero then decreases to - 1×10^{-9} and remains stable around zero from discrete time of 20. For sensitivity function SS2muH, the trajectory decreases from zero to – 500 at discrete time of 60 and reaches a steady state at this value. For sensitivity function SS2KS, the trajectory increases from zero to 35 at discrete time of 60 and reaches a steady state at this value. For sensitivity function SS2KOH, the trajectory increases from zero to 0.25 then decreases to 0.01 reaching zero at a discrete time of 60. For sensitivity function SS2KNO, the trajectory increases from zero to 0.06 at discrete time of 60 and reaches a steady state at this value. For sensitivity function SS2KNH, the trajectory increases from zero to 3.5×10^{-3} and decreases to zero at discrete time of 60. For sensitivity function SS2KOA, the trajectory decreases from zero to - 1.5×10^{-9} and oscillates until it reaches zero at discrete time of 50 and remains there. For sensitivity function SS2etag, the trajectory increases from zero to 0.6×10^{-10} at a discrete time of 5 then oscillating finally reaching a steady state value of 1×10^{-11} at discrete time of 60. For sensitivity function SS2KMP, the trajectory decrease from zero to - 3×10^{-11} then increasing to - 1×10^{-11} and finally decreasing to - 2×10^{-11} at a discrete time of 100. For sensitivity function SS2KSP, the trajectory oscillates from zero to - 5×10^{-11} then settling down to zero after a discrete time of 40. For sensitivity function SS2KSA, the trajectory oscillates from zero to 1.5×10^{-9} then settles down to zero at a discrete time of 60. For sensitivity function SS2fMA, the trajectory increases from zero to 3×10^{-12} at a discrete time of 100. For sensitivity function SS2KA, the trajectory increases from zero to 1.5×10^{-10} at a discrete time of 100.

Figure 9.29: Process variable S_{S3} and its sensitivity functions towards the model parameters

The process variable SS3, the trajectory increases from zero to 7 then is slightly increasing to 8 and remaining at steady state at this value. For sensitivity function SS1f, the trajectory decreases from zero to - 4×10^{-11} oscillating then is reaching zero at steady state. For variable SS3YZH, the trajectory increases from zero to 38 at discrete time of 60 reaching a steady state after this value. For variable SS3YZA, the trajectory oscillates slightly from zero to - 1×10^{-9} then reaches steady state at discrete time of 60. For sensitivity function SS3fZBH, the trajectory is slightly oscillating from zero to 0.5×10^{-9} then decreasing to zero at discrete time of 60. For sensitivity function SS3muA, the trajectory oscillates slightly around zero then decreases to - 1×10^{-9} and remains stable around zero from discrete time of 20. For sensitivity function SS3muH, the trajectory decreases from zero to – 500 at discrete time of 60 and reaches a steady state at this value. For sensitivity function SS3KS, the trajectory increases from zero to 35 at discrete time of 60 and reaches a steady state at this value. For sensitivity function

SS3KOH, the trajectory increases from zero to 0.25 then decreases to 0.01 reaching zero at a discrete time of 60. For sensitivity function SS3KNO, the trajectory increases from zero to 0.06 at discrete time of 60 and reaches a steady state at this value. For sensitivity function SS3KNH, the trajectory increases from zero to 3.5×10^{-3} and decreases to zero at discrete time of 60. For sensitivity function SS3KOA, the trajectory decreases from zero to - 1.5×10^{-9} and oscillates until it reaches zero at discrete time of 50 and remains there. For sensitivity function SS3etag, the trajectory increases from zero to 5×10^{-11} at a discrete time of 5 then oscillating finally reaching a steady state value of 1×10^{-11} at discrete time of 60. For sensitivity function SS3KMP, the trajectory decrease from zero to - 3×10^{-11} then increasing to - 1×10^{-11} and finally decreasing to - 2×10^{-11} at a discrete time of 100. For sensitivity function SS3KSP, the trajectory oscillates from zero to - 5×10^{-11} then settling down to zero after a discrete time of 40. For sensitivity function SS3KSA, the trajectory oscillates from zero to 1.5×10^{-9} then settles down to zero at a discrete time of 60. For sensitivity function SS3fMA, the trajectory increases from zero to 3×10^{-12} at a discrete time of 100. For sensitivity function SS3KA, the trajectory increases from zero to 1.5×10^{-10} at a discrete time of 100.

Figure 9.30: Process variable S_{S4} and its sensitivity functions towards the model parameters

The process variable SS4, the trajectory increases from zero to 7 then is decreasing to 5 then slightly increasing to 8 and remaining at steady state at this value. For sensitivity function SS4f, the trajectory decreases from zero to - 3×10^{-11} oscillating then is reaching zero at steady state. For variable SS4YZH, the trajectory increases from zero to 38 at discrete time of 60 reaching a steady state after this value. For variable SS4YZA, the trajectory oscillates slightly from zero to - 1×10^{-9} then reaches steady state at discrete time of 60. For sensitivity function SS4fZBH, the trajectory is slightly oscillating from zero to 0.5×10^{-9} then decreasing to zero at discrete time of 60. For sensitivity function SS4muA, the trajectory oscillates slightly around zero then decreases to - 1×10^{-9} and remains stable around zero from discrete time of 20. For sensitivity function SS4muH, the trajectory decreases from zero to – 500 at discrete time of 60 and reaches a steady state at this value. For sensitivity function SS4KS, the trajectory increases from zero to 35 at discrete time of 60 and reaches a steady state at this value. For sensitivity function SS4KOH, the trajectory increases from zero to 0.25 then decreases to 0.01 reaching zero at a discrete time of 60. For sensitivity function SS4KNO, the trajectory increases from zero to 0.06 at discrete time of 60 and reaches a steady state at this value. For sensitivity function SS4KNH, the trajectory increases from zero to 3.5×10^{-3} and decreases to zero at discrete time of 60. For sensitivity function SS4KOA, the trajectory decreases from zero to - 1.5×10^{-9} and oscillates until it reaches zero at discrete time of 50 and remains there. For sensitivity function SS4etag, the trajectory increases from zero to 5×10^{-11} at a discrete time of 5 then oscillating finally reaching a steady state value of 1×10^{-11} at discrete time of 60. For sensitivity function SS4KMP, the trajectory decrease from zero to - 3×10^{-11} then increasing to - 1×10^{-11} and finally decreasing to - 2×10^{-11} at a discrete time of 100. For sensitivity function SS4KSP, the trajectory oscillates from zero to - 5×10^{-11} then settling down to zero after a discrete time of 40. For sensitivity function SS4KSA, the trajectory oscillates from zero to 1.5×10^{-9} then settles down to zero at a discrete time of 60. For sensitivity function SS4fMA, the trajectory increases from zero to 3×10^{-12} at a discrete time of 100. For sensitivity function SS4KA, the trajectory increases from zero to 1.5×10^{-10} at a discrete time of 100.

Figure 9.31: Process variable S_{S5} and its sensitivity functions towards the model parameters

The process variable SS5, the trajectory increases from zero to 3.9 then is decreasing to 2.5 then slightly increasing to 3 and remaining at steady state at this value. For sensitivity function SS5f, the trajectory decreases from zero to - 3×10^{-11} oscillating then is reaching zero at steady state. For variable SS5YZH, the trajectory increases from zero to 38 at discrete time of 60 reaching a steady state after this value. For variable SS5YZA, the trajectory oscillates slightly from zero to - 1×10^{-9} then reaches steady state at discrete time of 60. For sensitivity function SS5fZBH, the trajectory is slightly oscillating from zero to 0.4×10^{-9} then decreasing to zero at discrete time of 80. For sensitivity function SS5muA, the trajectory oscillates slightly around zero then decreases to - 1×10^{-9} and remains stable around zero from discrete time of 20. For sensitivity function SS5muH, the trajectory decreases from zero to – 500 at discrete time of 60 and reaches a steady state at this value. For sensitivity function SS5KS, the trajectory increases from zero to 35 at discrete time of 60 and reaches a steady state at this value. For sensitivity function SS5KOH, the trajectory increases from zero to 0.015 then decreases to zero at a discrete time of 80. For sensitivity function SS5KNO, the trajectory increases from zero to 0.06 at discrete time of 60 and reaches a steady state at this value. For sensitivity function SS5KNH, the trajectory increases from zero to 3.5×10^{-3} and decreases to zero at discrete time of 60. For sensitivity function SS5KOA, the trajectory decreases from zero to - 1×10^{-9} and oscillates until it reaches zero at discrete time of 60 and remains there. For sensitivity function SS5etag, the trajectory increases from zero to 3.8×10^{-11} at a discrete time of 5 then oscillating finally reaching a steady state value of 0.75×10^{-11} at discrete time of 60. For sensitivity function SS5KMP, the trajectory decrease from zero to - 3×10^{-11} then increasing to - 1×10^{-11} and finally decreasing to - 2×10^{-11} at a discrete time of 100. For sensitivity function SS5KSP, the trajectory oscillates from zero to - 5×10^{-11} then settling down to zero after a discrete time of 40. For sensitivity function SS5KSA, the trajectory oscillates from zero to 1.5×10^{-9} then settles down to zero at a discrete time of 60. For sensitivity function SS5fMA, the trajectory increases from zero to 3×10^{-12} at a discrete time of 100. For sensitivity function SS5KA, the trajectory increases from zero to 1.5×10^{-10} at a discrete time of 100.

Figure 9.32: Process variable S_{Sads1} and its sensitivity functions towards the model parameters

The process variable Sads1, the trajectory decreases from zero to – 250 at a discrete time of 40 and remains at a steady state. For sensitivity function Sads1f, the trajectory oscillates from zero to - 2×10^{-9} at a discrete time of 5 then stabilizes to zero at a discrete time of 20. For variable Sads1YZH, the trajectory increases from zero to 4000 at a discrete time of 80 then reaches a steady state. For variable Sads1YZA, the trajectory decreases from zero - 0.5×10^{-7} then slightly oscillates around - 0.5×10^{-7} then is increasing to - 0.2×10^{-7} at a discrete time of 100. For sensitivity function Sads1fZBH, the trajectory increases from zero to 4×10^{-8} at a discrete time of 5 then is decreasing back to zero at a discrete time of 100. For sensitivity function Sads1muA, the trajectory oscillates slightly from zero to - 0.8×10^{-7} at a discrete time of 5 then increases to zero at a discrete time of 80. For sensitivity function Sads1muH, the trajectory oscillates slightly from zero to 1.2×10^{-9} at a discrete time of 5 and decreases further to 0.2×10^{-9} at a discrete time of 100. For sensitivity function Sads1KS, the trajectory oscillates slightly from zero to - 3×10^{-11} at a discrete time of 5 then increases to - 0.8×10^{-11} at a discrete time of 100. For sensitivity function Sads1KOH, the trajectory is unstable increasing from zero to 6 at a discrete time of 3 then decreasing to zero at a discrete time of 100. For sensitivity function Sads1KNO, the trajectory increases from zero to 0.039 at a discrete time of 4 then decreases to 0.03 and slowly increases to 0.038 at a discrete time of 100. For sensitivity function Sads1KNH, the trajectory increases from zero to 0.38 at a discrete time of 3 then decreases gradually to zero at a discrete time of 100. For sensitivity function Sads1KOA, the trajectory oscillates from

zero to - 0.5×10^{-7} and increases to - 0.25×10^{-7} then reaches zero at a discrete time of 60. For sensitivity function Sads1etag, the trajectory decreases from zero to – 3.8 at a discrete time of 100. For sensitivity function Sads1KMP, the trajectory decreases from zero to – 2000 at a discrete time of 100. For sensitivity function Sads1KSP, the trajectory is unstable around zero then reaches – 200 at a discrete time of 40 and reaches a steady state after this value. For sensitivity function Sads1KSA, the trajectory is increasing from zero to around 0.7×10^{-7} at a discrete time of 5 then reaches zero at a discrete time of 80. For sensitivity function Sads1fMA, the trajectory increases from zero to 350 at a discrete time of 60 and remains at steady state. For sensitivity function Sads1KA, the trajectory increases from zero to 1.2×10^{4} at a discrete time of 60 and reaches a steady state.

Figure 9.33: Process variable S_{Sads2} and its sensitivity functions towards the model parameters
The process variable Sads2, the trajectory decreases from zero to – 250 at a discrete time of 40 and remains at a steady state. For sensitivity function Sads2f, the trajectory oscillates from zero to - 2×10^{-9} at a discrete time of 5 then stabilizes to zero at a discrete time of 20. For variable Sads2YZH, the trajectory increases from zero to 4000 at a discrete time of 80 then reaches a steady state. For variable Sads2YZA, the trajectory decreases from zero - 0.5×10^{-7} then slightly oscillates around - 0.5×10^{-7} then is increasing to - 0.2×10^{-7} at a discrete time of 100. For sensitivity function Sads2fZBH, the trajectory increases from zero to 4×10^{-8} at a discrete time of 5 then is decreasing back to zero at a discrete time of 100. For sensitivity function Sads2muA, the trajectory oscillates slightly from zero to - 0.8×10^{-7} at a discrete time of 5 then increases to zero at a discrete time of 80. For sensitivity function Sads2muH, the trajectory oscillates slightly from zero to 1.2×10^{-9} at a discrete time of 5 and decreases further to 0.2×10^{-9} at a discrete time of 100. For sensitivity function Sads2KS, the trajectory oscillates slightly from zero to - 3×10^{-11} at a discrete time of 5 then increases to - 0.8×10^{-11} at a discrete time of 100. For sensitivity function Sads2KOH, the trajectory oscillates increasing from zero to 10 at a discrete time of 3 then decreasing to zero at a discrete time of 100. For sensitivity function Sads2KNO, the trajectory increases from zero to 0.039 at a discrete time of 4 then decreases to 0.03 and slowly increases to 0.038 at a discrete time of 100. For sensitivity function Sads2KNH, the trajectory increases from zero to 0.38 at a discrete time of 3 then decreases gradually to zero at a discrete time of 100. For sensitivity function Sads2KOA, the trajectory oscillates from zero to - 0.5×10^{-7} and increases to - 0.25×10^{-7} then reaches zero at a discrete time of 60. For sensitivity function Sads2etag, the trajectory decreases from zero to – 3.8 at a discrete time of 100. For sensitivity function Sads2KMP, the trajectory decreases from zero to – 2000 at a discrete time of 100. For sensitivity function Sads2KSP, the trajectory increases from zero 1000 at a discrete time of 5 and decreases to – 200 at a discrete time of 40 and reaches a steady state after this value. For sensitivity function Sads2KSA, the trajectory is increasing from zero to around 1×10^{-7} at a discrete time of 5 then reaches zero at a discrete time of 80. For sensitivity function Sads2fMA, the trajectory increases from zero to 350 at a discrete time of 60 and remains at steady state. For sensitivity function Sads2KA, the trajectory increases from zero to 1.2×10^{4} at a discrete time of 60 and reaches a steady state.

Figure 9.34: Process variable S_{Sads3} and its sensitivity functions towards the model parameters
The process variable Sads3, the trajectory decreases from zero to – 250 at a discrete time of 40 and remains at a steady state. For sensitivity function Sads3f, the trajectory oscillates from zero to - 4×10^{-11} at a discrete time of 8 then stabilizes to zero at a discrete time of 20. For variable Sads3YZH, the trajectory increases from zero to 4500 at a discrete time of 80 then reaches a steady state. For variable Sads3YZA, the trajectory decreases from zero - 0.5×10^{-7} then slightly oscillates around - 0.5×10^{-7} then is increasing to - 0.2×10^{-7} at a discrete time of 100.

For sensitivity function Sads3fZBH, the trajectory increases from zero to 4×10^{-8} at a discrete time of 5 then is decreasing back to zero at a discrete time of 100. For sensitivity function Sads3muA, the trajectory oscillates slightly from zero to - 0.8×10^{-7} at a discrete time of 5 then increases to zero at a discrete time of 80. For sensitivity function Sads3muH, the trajectory oscillates slightly from zero to 1.2×10^{-9} at a discrete time of 5 and decreases further to 0.2×10^{-9} at a discrete time of 100. For sensitivity function Sads3KS, the trajectory oscillates slightly from zero to - 3×10^{-11} at a discrete time of 5 then increases to - 0.8×10^{-11} at a discrete time of 100. For sensitivity function Sads3KOH, the trajectory oscillates increasing from zero to 10 at a discrete time of 3 then decreasing to zero at a discrete time of 100. For sensitivity function Sads3KNO, the trajectory increases from zero to 0.039 at a discrete time of 4 then decreases to 0.03 and slowly increases to 0.038 at a discrete time of 100. For sensitivity function Sads3KNH, the trajectory increases from zero to 0.38 at a discrete time of 3 then decreases gradually to zero at a discrete time of 100. For sensitivity function Sads3KOA, the trajectory oscillates from zero to - 0.5×10^{-7} and increases to - 0.25×10^{-7} then reaches zero at a discrete time of 60. For sensitivity function Sads3etag, the trajectory decreases from zero to – 3.8 at a discrete time of 100. For sensitivity function Sads3KMP, the trajectory decreases from zero to – 2000 at a discrete time of 100. For sensitivity function Sads3KSP, the trajectory increases from zero 1000 at a discrete time of 5 and decreases to – 200 at a discrete time of 40 and reaches a steady state after this value. For sensitivity function Sads3KSA, the trajectory is increasing from zero to around 1×10^{-7} at a discrete time of 5 then reaches zero at a discrete time of 80. For sensitivity function Sads3fMA, the trajectory increases from zero to 350 at a discrete time of 60 and remains at steady state. For sensitivity function Sads3KA, the trajectory increases from zero to 1.2×10^{4} at a discrete time of 60 and reaches a steady state.

Figure 9.35:Process variable S_{Sads4} and its sensitivity functions towards the model parameters
The process variable Sads4, the trajectory decreases from zero to – 350 at a discrete time of 40 and remains at a steady state. For sensitivity function Sads4f, the trajectory oscillates from zero to - 1×10^{-9} at a discrete time of 8 then stabilizes to zero at a discrete time of 50. For variable Sads4YZH, the trajectory increases from zero to 4500 at a discrete time of 80 then reaches a steady state. For variable Sads4YZA, the trajectory decreases from zero - 0.5×10^{-7} then slightly oscillates around - 0.5×10^{-7} then is increasing to - 0.2×10^{-7} at a discrete time of 100. For sensitivity function Sads4fZBH, the trajectory increases from zero to 4×10^{-8} at a discrete time of 5 then is decreasing back to zero at a discrete time of 100. For sensitivity function Sads4muA, the trajectory oscillates slightly from zero to - 0.8×10^{-7} at a discrete time of 5 then increases to zero at a discrete time of 80. For sensitivity function Sads4muH, the trajectory oscillates slightly from zero to 1.2×10^{-9} at a discrete time of 5 and decreases further to 0.2×10^{-9} at a discrete time of 100. For sensitivity function Sads4KS, the trajectory oscillates slightly from zero to - 3×10^{-11} at a discrete time of 5 then increases to - 0.8×10^{-11} at a discrete time of 100. For sensitivity function Sads4KOH, the trajectory oscillates increasing from zero to 10 at a discrete time of 3 then decreasing to zero at a discrete time of 100. For sensitivity function Sads4KNO, the trajectory increases from zero to 0.039 at a discrete time of 4 then decreases to 0.03 and slowly increases to 0.038 at a discrete time of 100. For sensitivity function Sads4KNH, the trajectory increases from zero to 0.38 at a discrete time of 3 then decreases gradually to zero at a discrete time of 100. For sensitivity function Sads4KOA, the trajectory oscillates from zero to - 0.5×10^{-7} and increases to - 0.25×10^{-7} then reaches zero at a discrete time of 60. For sensitivity function Sads4etag, the trajectory decreases from zero to – 3.8 at a discrete time of 100. For sensitivity function Sads4KMP, the trajectory decreases from zero to – 2000 at a discrete time of 100. For sensitivity function Sads4KSP, the trajectory increases from zero 1000 at a discrete time of 5 and decreases to – 200 at a discrete time of 40 and reaches a

steady state after this value. For sensitivity function Sads4KSA, the trajectory is increasing from zero to around 1×10^{-7} at a discrete time of 5 then reaches zero at a discrete time of 80. For sensitivity function Sads4fMA, the trajectory increases from zero to 350 at a discrete time of 60 and remains at steady state. For sensitivity function Sads4KA, the trajectory increases from zero to 1.2×10^{4} at a discrete time of 60 and reaches a steady state.

Figure 9.36: Process variable S_{Sads5} and its sensitivity functions towards the model parameters
The process variable Sads5, the trajectory decreases from zero to – 450 at a discrete time of 40 and remains at a steady state. For sensitivity function Sads5f, the trajectory oscillates from zero to - 1×10^{-9} at a discrete time of 8 then stabilizes to zero at a discrete time of 90. For variable Sads5YZH, the trajectory increases from zero to 5000 at a discrete time of 100. For variable Sads5YZA, the trajectory decreases from zero - 0.5×10^{-7} then slightly oscillates around - 0.5×10^{-7} then is increasing to - 0.2×10^{-7} at a discrete time of 100. For sensitivity function Sads5fZBH, the trajectory increases from zero to 4×10^{-8} at a discrete time of 5 then is decreasing back to zero at a discrete time of 100. For sensitivity function Sads5muA, the trajectory oscillates slightly from zero to - 0.8×10^{-7} at a discrete time of 5 then increases to zero at a discrete time of 80. For sensitivity function Sads5muH, the trajectory oscillates slightly from zero to 1.2×10^{-9} at a discrete time of 5 and decreases further to 0.2×10^{-9} at a discrete time of 100. For sensitivity function Sads5KS, the trajectory oscillates slightly from zero to - 3×10^{-11} at a discrete time of 5 then increases to - 0.8×10^{-11} at a discrete time of 100. For sensitivity function Sads5KOH, the trajectory oscillates increasing from zero to 10 at a discrete time of 3 then decreasing to zero at a discrete time of 100. For sensitivity function Sads5KNO, the trajectory increases from zero to 0.039 at a discrete time of 4 then decreases to 0.03 and slowly increases to 0.038 at a discrete time of 100. For sensitivity function Sads5KNH, the trajectory increases from zero to 0.38 at a discrete time of 3 then decreases gradually to zero at a discrete time of 100. For sensitivity function Sads5KOA, the trajectory oscillates from zero to - 0.5×10^{-7} and increases to - 0.25×10^{-7} then reaches zero at a discrete time of 60. For sensitivity function Sads5etag, the trajectory decreases from zero to – 3.8 at a discrete time of 100. For sensitivity function Sads5KMP, the trajectory decreases from zero to – 2000 at a discrete time of 100. For sensitivity function Sads5KSP, the trajectory increases from zero 1000 at a discrete time of 5 and decreases to – 200 at a discrete time of 40 and reaches a steady state after this value. For sensitivity function Sads5KSA, the trajectory is increasing from zero to around 1×10^{-7} at a discrete time of 5 then reaches zero at a discrete time of 80. For sensitivity function Sads5fMA, the trajectory increases from zero to 350 at a discrete time of 60 and remains at steady state. For sensitivity function Sads5KA, the trajectory increases from zero to 1.2×10^{4} at a discrete time of 60 and reaches a steady state.

1Athlone process with ASM1 reduced biological model

Figure 9.37: Process variable S_{SNH1} and its sensitivity functions towards the model parameters
The process variable Snh1, the trajectory decreases from 3.7 at a discrete time of 1 then decreases to 0.8 at a discrete time of 3 reaches a steady state of 0.7 at a discrete time of 40. For sensitivity function Snh1f, the trajectory increases from zero to 0.35 reaching a steady state at a discrete time of 60. For variable Snh1YH, the trajectory decreases from zero to – 0.04 reaching a steady state after a discrete time of 40. For variable Snh1YA, the trajectory increases from zero to 5 at a discrete time of 20 then decreases slowly to 4 at a discrete time of 100. For sensitivity function Snh1iXB, the trajectory decreases from – 9 at a discrete time of 25 then increases to – 8 at a discrete time of 100. For sensitivity function Snh1muA, the trajectory decreases from zero to – 2 at a discrete time of 20 then slightly increases and reaches a steady state value of - 2.0 at a discrete time of 60. For sensitivity function Snh1muH, the trajectory decreases from zero to - 1.8 at a discrete time of 25 then slightly increases to - 1.6 at a discrete

time of 80 after this time reaching a steady state. For sensitivity function Snh1KS, the trajectory increases from zero to 0.06 at a discrete time of 20 then reaches 0.05 at a discrete time of 100. For sensitivity function Snh1KOH, the trajectory increases from zero to 0.7 at a discrete time of 80 then reaches a steady state. For sensitivity function Snh1KNO, the trajectory increases from zero to a maximum of 0.09 at a discrete time of 35 then decreases to 0.015 at a discrete time of 100. For sensitivity function Snh1KNH, the trajectory increases from zero to 1.2 at a discrete time of 20 then decreases to 1 at a discrete time of 80 and reaches steady state. For sensitivity function Snh1KOA, the trajectory increases from zero to 0.5 then oscillates rapidly to 0.8 at a discrete time of 20 then reaches a value of 0.6 at a steady state at a discrete time of 80. For sensitivity function Snh1etag, the trajectory decreases from zero to - 0.16 at a discrete time of 20 then increases to zero at a discrete time of 100. For sensitivity function Snh1etah, the trajectory decreases from zero to - 0.16 at a discrete time of 20 then increases to zero at a discrete time of 100. For sensitivity function Snh1Kh, the trajectory decreases from zero to – 0.05 at a discrete time of 40 and reaches a steady state after this value. For sensitivity function Snh1Kx, the trajectory increases from zero to 0.18 at a discrete time of 40 then reaches a steady state after this value.

Figure 9.38: Process variable S_{SNH2} and its sensitivity functions towards the model parameters
The process variable Snh2, the trajectory increases from zero to 2 at a discrete time of 1 then decreases to 0.8 at a discrete time of 10 reaches a steady state of 0.7 at a discrete time of 40. For sensitivity function Snh2f, the trajectory increases from zero to 0.35 reaching a steady state at a discrete time of 60. For variable Snh2YH, the trajectory decreases from zero to – 0.08 in an unstable manner a discrete time of 40 and reaches a steady state after a discrete time of 60. For variable Snh2YA, the trajectory increases from zero to 9.5 at a discrete time of 20 then decreases slowly to 6 at a discrete time of 100. For sensitivity function Snh2iXB, the trajectory decreases from - 18 at a discrete time of 25 then slightly increases to – 17 at a discrete time of 80 then reaches a steady state after this value. For sensitivity function Snh2muA, the trajectory decreases from zero to – 4 at a discrete time of 20 then slightly increases and reaches a steady state value of – 3 at a discrete time of 60. For sensitivity function Snh2muH, the trajectory decreases from zero to – 3 at a discrete time of 25 then slightly increases to – 2.8 at a discrete time of 80 after this time reaching a steady state. For sensitivity function Snh2KS, the trajectory increases from zero to 0.1 at a discrete time of 30 then reaches 0.09 at a discrete time of 100. For sensitivity function Snh2KOH, the trajectory increases from zero to 0.8 at a discrete time of 60 then reaches a steady state at 1 after a discrete time of 80. For sensitivity function Snh2KNO, the trajectory increases from zero to a maximum of 0.12 at a discrete time of 35 then decreases to 0.015 at a discrete time of 100. For sensitivity function Snh2KNH, the trajectory increases from zero to 2 at a discrete time of 15 then decreases to 1.8 at a discrete time of 80 and reaches steady state. For sensitivity function Snh2KOA, the trajectory increases from zero to 0.5 then oscillates rapidly from 0.8 to 1.2 at a discrete time of 20 then decreases to a value of 1 at a discrete time of 60 then reaches a steady state after this value. For sensitivity function Snh2etag, the trajectory decreases from zero to a minimum of – 0.2 at a discrete time of 20 then increases to zero at a discrete time of 100. For sensitivity function Snh2etah, the trajectory decreases from zero to a minimum of – 0.03 at a discrete time of 30 then increases to – 0.002 at a discrete time of 100. For sensitivity function Snh2Kh, the trajectory decreases from zero to – 0.09 at a discrete time of 80 and reaches a steady state after this value. For sensitivity function Snh2Kx, the trajectory increases from zero to 0.18 at a discrete time of 40 then reaches a steady state after this value.

Figure 9.39: Process variable S_{SNH3} and its sensitivity functions towards the model parameters
The process variable Snh3, the trajectory increases from 0.8 to 1.2 at a discrete time of 2 then decreases to 0.4 at a discrete time of 60 reaches a steady state after this value. For sensitivity function Snh3f, the trajectory increases from zero to 0.35 reaching a steady state at a discrete time of 60. For variable Snh3YH, the trajectory decreases from zero to – 0.1 at a discrete time of 40 and reaches a steady state after this value. For variable Snh3YA, the trajectory increases

from zero to 9.5 at a discrete time of 20 then decreases slowly to 6 at a discrete time of 100. For sensitivity function Snh3iXB, the trajectory decreases from - 20 at a discrete time of 40 then reaches a steady state after this value. For sensitivity function Snh3muA, the trajectory decreases from zero to – 5.5 at a discrete time of 15 then slightly increases and reaches a steady state value of – 6 at a discrete time of 60. For sensitivity function Snh3muH, the trajectory decreases from zero to – 4 at a discrete time of 30 then slightly increases to – 3.8 at a discrete time of 100. For sensitivity function Snh3KS, the trajectory increases from zero to 0.1 at a discrete time of 30 then reaches 0.09 at a discrete time of 100. For sensitivity function Snh3KOH, the trajectory increases from zero to 0.8 at a discrete time of 60 then reaches a steady state at 1 after a discrete time of 80. For sensitivity function Snh3KNO, the trajectory increases from zero to a maximum of 0.15 at a discrete time of 35 then decreases to 0.015 at a discrete time of 100. For sensitivity function Snh3KNH, the trajectory increases from zero to 3 at a discrete time of 20 then decreases to 2 at a discrete time of 80 and reaches steady state. For sensitivity function Snh3KOA, the trajectory increases from zero to 0.5 then oscillates rapidly from 0.8 to 1.2 at a discrete time of 20 then decreases to a value of 1 at a discrete time of 60 then reaches a steady state after this value. For sensitivity function Snh3etag, the trajectory decreases from zero to a minimum of – 0.2 at a discrete time of 20 then increases to zero at a discrete time of 100. For sensitivity function Snh3etah, the trajectory decreases from zero to a minimum of – 0.038 at a discrete time of 30 then increases to – 0.002 at a discrete time of 100. For sensitivity function Snh3Kh, the trajectory decreases from zero to – 0.13 at a discrete time of 80 and reaches a steady state after this value. For sensitivity function Snh3Kx, the trajectory increases from zero to 0.4 at a discrete time of 60 then reaches a steady state after this value.

Figure 9.40: Process variable S_{SNO1} and its sensitivity functions towards the model parameters
The process variable SNO1, the trajectory decreases from 5 to zero at a discrete time of 40 then reaches a steady state after this value. For sensitivity function SNO1f, the trajectory increases from zero to 0.007 at a discrete time of 60 then reaches a steady state at this value. For variable SNO1YH, the trajectory decreases from zero to a minimum of – 0.26 at a discrete time of 20 then reaches zero at a discrete time of 100. For variable SNO1YA, the trajectory decreases from zero to – 5 at a discrete time of 20 then increases to – 4 at a discrete time of 60 reaches a steady state at this value. For sensitivity function SNO1iXB, the trajectory decreases from zero to – 0.4 at a discrete time of 60 reaches a steady state at this value. For sensitivity function SNO1muA, the trajectory increases from zero to 2 at a discrete time of 20 then slightly decreases to 1.8 at a discrete time of 100. For sensitivity function SNO1muH, the trajectory decreases from zero to a minimum of – 0.4 at discrete time of 20 then increases to – 0.05 at a discrete time of 100. For sensitivity function SNO1KS, the trajectory increases from zero to a maximum of 0.12 at a discrete time of 20 then decreases to zero at a discrete time of 100. For sensitivity function SNO1KOH, the trajectory decreases from zero to minimum of – 0.4 then increases to zero at discrete time of 100. For sensitivity function SNO1KNO, the trajectory increases from zero to maximum of 0.08 at a discrete time of 35 then decreases to 0.02 at a discrete time of 100. For sensitivity function SNO1KNH, the trajectory decreases from zero to – 1 at a discrete time of 20 then reaches a steady state around – 0.8 at a discrete time of 80. For sensitivity function SNO1KOA, the trajectory decreases from zero to – 0.8 at a discrete time of 20 then slightly increases to – 0.6 at a discrete time of 60 then reaches a steady state at this value. For sensitivity function SNO1etag, the trajectory decreases from zero to a minimum of – 0.15 at a discrete time of 20 then increases to zero at discrete time of 100. For sensitivity function SNO1etah, the trajectory decreases from zero to a minimum of – 0.15 at a discrete time of 20 then increases to zero at discrete time of 100. For sensitivity function SNO1Kh, the trajectory decreases from zero to a minimum of – 0.01 at a discrete time of 25 then increases to – 0.0025 at a discrete time of 100. For sensitivity function SNO1Kx, the trajectory increases from zero to a maximum of 0.03 at a discrete time of 20 then decreases to 0.01 at discrete time of 100.

Figure 9.41: Process variable S_{SNO2} and its sensitivity functions towards the model parameters
The process variable SNO2, the trajectory decreases from 8 to zero at a discrete time of 40 then reaches a steady state after this value. For sensitivity function SNO2f, the trajectory increases from zero to 0.012 at a discrete time of 80 then reaches a steady state at this value. For variable SNO2YH, the trajectory decreases from zero to a minimum of – 0.4 at a discrete time of 20 then reaches – 0.01 at a discrete time of 100. For variable SNO2YA, the trajectory decreases from zero to – 8 at a discrete time of 20 then slightly increases to – 6.5 at a discrete time of 80 reaches a steady state at this value. For sensitivity function SNO2iXB, the trajectory decreases from zero to – 0.7 at a discrete time of 80 reaches a steady state at this value. For sensitivity function SNO2muA, the trajectory increases from zero to 4 at a discrete time of 20 then slightly decreases to 3 at a discrete time of 100. For sensitivity function SNO2muH, the trajectory decreases from zero to a minimum of – 0.5 at discrete time of 20 then increases to – 0.2 at a discrete time of 100. For sensitivity function SNO2KS, the trajectory increases from zero to a maximum of 0.2 at a discrete time of 20 then decreases to 0.02 at a discrete time of 100. For sensitivity function SNO2KOH, the trajectory decreases from zero to minimum of – 0.4 then increases to zero at discrete time of 100. For sensitivity function SNO2KNO, the trajectory increases from zero to maximum of 0.12 at a discrete time of 35 then decreases to 0.02 at a discrete time of 100. For sensitivity function SNO2KNH, the trajectory decreases from zero to – 2 at a discrete time of 20 then reaches a steady state around – 1.8 at a discrete time of 80. For sensitivity function SNO2KOA, the trajectory decreases from zero to – 1 at a discrete time of 20 then slightly increases to – 0.9 at a discrete time of 60 then reaches a steady state at this value. For sensitivity function SNO2etag, the trajectory decreases from zero to a minimum of – 0.2 at a discrete time of 20 then increases to zero at discrete time of 100. For sensitivity function SNO2etah, the trajectory decreases from zero to a minimum of – 0.007 at a discrete time of 20 then increases to zero at discrete time of 100. For sensitivity function SNO2Kh, the trajectory decreases from zero to a minimum of – 0.015 at a discrete time of 25 then increases to – 0.005 at a discrete time of 100. For sensitivity function SNO2Kx, the trajectory increases from zero to a maximum of 0.048 at a discrete time of 25 then decreases to 0.02 at discrete time of 100.

Figure 9.42: Process variable S_{SNO3} and its sensitivity functions towards the model parameters
The process variable SNO3, the trajectory decreases from 6.5 to zero at a discrete time of 40 then reaches a steady state after this value. For sensitivity function SNO3f, the trajectory increases from zero to 0.018 at a discrete time of 60 then reaches a steady state at this value. For variable SNO3YH, the trajectory decreases from zero to a minimum of – 0.4 at a discrete time of 20 then reaches – 0.01 at a discrete time of 100. For variable SNO3YA, the trajectory decreases from zero to – 8 at a discrete time of 20 then slightly increases to – 6.5 at a discrete time of 80 reaches a steady state at this value. For sensitivity function SNO3iXB, the trajectory decreases from zero to – 1 at a discrete time of 60 reaches a steady state at this value. For sensitivity function SNO3muA, the trajectory increases from zero to 5 at a discrete time of 20 then slightly decreases to 4.9 at a discrete time of 100. For sensitivity function SNO3muH, the trajectory decreases from zero to a minimum of – 0.5 at discrete time of 20 then increases to – 0.2 at a discrete time of 100. For sensitivity function SNO3KS, the trajectory increases from zero to a maximum of 0.2 at a discrete time of 20 then decreases to 0.02 at a discrete time of 100. For sensitivity function SNO3KOH, the trajectory decreases from zero to minimum of – 0.4 then increases to zero at discrete time of 100. For sensitivity function SNO3KNO, the trajectory increases from zero to maximum of 0.15 at a discrete time of 35 then decreases to 0.02 at a discrete time of 100. For sensitivity function SNO3KNH, the trajectory decreases from zero to – 2 at a discrete time of 20 then reaches a steady state around – 1.8 at a discrete time of 80. For sensitivity function SNO3KOA, the trajectory decreases from zero to – 1 at a discrete time of 20 then slightly increases to – 0.9 at a discrete time of 60 then reaches a steady state at this value. For sensitivity function SNO3etag, the trajectory decreases from zero to a minimum of – 0.2 at a discrete time of 20 then increases to zero at discrete time of 100. For sensitivity function SNO3etah, the trajectory decreases from zero to a minimum of – 0.007 at a discrete time of 20

then increases to zero at discrete time of 100. For sensitivity function SNO3Kh, the trajectory decreases from zero to a minimum of – 0.015 at a discrete time of 25 then increases to – 0.005 at a discrete time of 100. For sensitivity function SNO3Kx, the trajectory increases from zero to a maximum of 0.048 at a discrete time of 25 then decreases to 0.02 at discrete time of 100.

Figure 9.43: Process variable S_{SS1} and its sensitivity functions towards the model parameters
The process variable SS1, the trajectory decreases from 4 to 1.8 slightly decreasing to 1.7 at a discrete time of 100. For sensitivity function SS1f, the trajectory follows an S-shaped curve from zero to - 1.8×10^{-4} at a discrete time of 100. For variable SS1YH, the trajectory increases from zero to 10 then decrease to 9.8 at a discrete time of 100. For variable SS1YA, the trajectory follows a reverse S-shaped curve from zero to 0.1 at a discrete time of 100. For sensitivity function SS1iXB, the trajectory follows a reverse S-shaped curve from zero to 0.01 at a discrete time of 100. For sensitivity function SS1muA, the trajectory follows an S-shaped curve from zero to – 0.05 at discrete time of 100. For sensitivity function SS1muH, the trajectory decreases from zero to – 18 at a discrete time of 20 slightly increasing to – 14 at a discrete time of 80 reaching a steady state after this value. For sensitivity function SS1KS, the trajectory increases from zero to 0.5 then slowly decreasing to 0.45 at a discrete time of 100. For sensitivity function SS1KOH, the trajectory gradually decreases from zero to – 40 at a discrete time of 100. For sensitivity function SS1KNO, the trajectory decreases from zero to a minimum of – 5 at a discrete time of 30 and increases to – 0.02 at a discrete time of 100. For sensitivity function SS1KNH, the trajectory follows a reverse S-shaped curve from zero to 0.025 at a discrete time of 100. For sensitivity function SS1KOA, the trajectory follows a reverse S-shaped curve from zero to 0.018 at a discrete time of 100. For sensitivity function SS1etag, the trajectory increases from zero to a maximum of 1.8×10^{-3} at a discrete time of 45 then decreases to 0.2×10^{-3} at a discrete time of 100. For sensitivity function SS1etah, the trajectory increases from zero to a maximum of 1.8×10^{-3} at a discrete time of 45 then decreases to 0.2×10^{-3} at a discrete time of 100. For sensitivity function SS1Kh, the trajectory increases from zero to 11 at a discrete time of 10 then slightly decreases to 10 at a discrete time of 100. For SS1Kx, the trajectory decreases from zero to – 38 at a discrete time of 10 then slightly increases to – 36 at a discrete time of 100.

Figure 9.44: Process variable S_{SS2} and its sensitivity functions towards the model parameters
The process variable SS2, the trajectory decreases from 2.7 to 2 at a discrete time of 5 then slightly decreasing to 1.8 at a discrete time of 100. For sensitivity function SS2f, the trajectory follows an S-shaped curve from zero to - 2×10^{-4} at a discrete time of 100. For variable SS2YH, the trajectory increases from zero to 18 oscillating at a discrete time of 20 then slightly decreasing to 16 at a discrete time of 100. For variable SS2YA, the trajectory follows a reverse S-shaped curve from zero to 0.18 at a discrete time of 100. For sensitivity function SS2iXB, the trajectory follows a reverse S-shaped curve from zero to 0.018 at a discrete time of 100. For sensitivity function SS2muA, the trajectory follows an S-shaped curve from zero to – 0.075 at discrete time of 100. For sensitivity function SS2muH, the trajectory decreases from zero to – 30 at a discrete time of 15 slightly increasing to – 22 at a discrete time of 100. For sensitivity function SS2KS, the trajectory increases from zero to 1 oscillating at a discrete time of 20 then slowly decreasing to 0.7 at a discrete time of 100. For sensitivity function SS2KOH, the trajectory gradually decreases from zero to – 40 at a discrete time of 100. For sensitivity function SS2KNO, the trajectory decreases from zero to a minimum of – 5 at a discrete time of 30 and increases to – 0.02 at a discrete time of 100. For sensitivity function SS2KNH, the trajectory follows a reverse S-shaped curve from zero to 0.035 at a discrete time of 100. For sensitivity function SS2KOA, the trajectory follows a reverse S-shaped curve from zero to 0.02 at a discrete time of 100. For sensitivity function SS2etag, the trajectory increases from zero to a maximum of 2×10^{-3} at a discrete time of 45 then decreases to 0.2×10^{-3} at a discrete time of 100. For sensitivity function SS2etah, the trajectory increases from zero to a maximum of 8 at a discrete time of 10 then decreases to zero at a discrete time of 100. For sensitivity function SS2Kh, the

trajectory increases from zero to 18 at a discrete time of 10 then slightly decreases to 17 at a discrete time of 100. For SS2Kx, the trajectory decreases from zero to – 50 at a discrete time of 10 then reaches a steady state at this value.

Figure 9.45: Process variable S_{SS3} and its sensitivity functions towards the model parameters
The process variable SS3, the trajectory decreases from 1 to 2.2 at a discrete time of 2 then slightly decreasing to 2 at a discrete time of 100. For sensitivity function SS3f, the trajectory follows an S-shaped curve from zero to - 2×10^{-4} at a discrete time of 100. For variable SS3YH, the trajectory increases from zero to 20 at a discrete time of 20 then slightly decreasing to 18 at a discrete time of 100. For variable SS3YA, the trajectory follows a reverse S-shaped curve from zero to 0.16 at a discrete time of 100. For sensitivity function SS3iXB, the trajectory follows a reverse S-shaped curve from zero to 0.016 at a discrete time of 100. For sensitivity function SS3muA, the trajectory follows an S-shaped curve from zero to – 0.075 at discrete time of 100. For sensitivity function SS3muH, the trajectory decreases from zero to – 30 at a discrete time of 10 slightly increasing to – 26 at a discrete time of 100. For sensitivity function SS3KS, the trajectory increases from zero to 1 at a discrete time of 20 then slowly decreasing to 0.7 at a discrete time of 100. For sensitivity function SS3KOH, the trajectory gradually decreases from zero to – 40 at a discrete time of 100. For sensitivity function SS3KNO, the trajectory decreases from zero to a minimum of – 5 at a discrete time of 30 and increases to – 0.02 at a discrete time of 100. For sensitivity function SS3KNH, the trajectory follows a reverse S-shaped curve from zero to 0.03 at a discrete time of 100. For sensitivity function SS3KOA, the trajectory follows a reverse S-shaped curve from zero to 0.018 at a discrete time of 100. For sensitivity function SS3etag, the trajectory increases from zero to a maximum of 1.8×10^{-3} at a discrete time of 45 then decreases to 0.3×10^{-3} at a discrete time of 100. For sensitivity function SS3etah, the trajectory increases from zero to a maximum of 6 at a discrete time of 15 then decreases to zero at a discrete time of 100. For sensitivity function SS3Kh, the trajectory increases from zero to 18 at a discrete time of 10 then slightly decreases to 17 at a discrete time of 100. For SS3Kx, the trajectory decreases from zero to – 50 at a discrete time of 10 then reaches a steady state at this value.

Athlone process with the UCT reduced biological model

Figure 9.46: Process variable S_{SNH1} and its sensitivity functions towards the model parameters
The process variable Snh1, the trajectory decreases from zero to – 800 at a discrete time of 40 then reaches a steady state after this value. For sensitivity function Snh1f, the trajectory decreases from zero to 3.8 at a discrete time of 60 then reaches a steady state after this value. For variable Snh1YZH, the trajectory increases from zero to 1.8 at a discrete time of 60 then reaches a steady state after this value. For variable Snh1YZA, the trajectory increases from zero to 39 at a discrete time of 60 then reaches a steady state after this value. For sensitivity function Snh1fZBH, the trajectory decreases from zero to – 520 at a discrete time of 60 then reaches a steady state after this value. For sensitivity function Snh1muA, the trajectory decreases from zero to – 75 at a discrete time of 60 then reaches a steady state after this value. For sensitivity function Snh1muH, the trajectory decreases from zero to – 15 at a discrete time of 60 then reaches a steady state after this value. For sensitivity function Snh1KS, the trajectory increases from zero to 1 at a discrete time of 40 then reaches a steady state after this value. For sensitivity function Snh1KOH, the trajectory increases from zero to 38 at a discrete time of 40 then reaches a steady state after this value. For sensitivity function Snh1KNO, the trajectory increases from zero to 3×10^{-3} at a discrete time of 3 then decreases to 0.2×10^{-3} at a discrete time of 60 then reaches a steady state after this value. For sensitivity function Snh1KNH, the trajectory increases from zero to 38 at a discrete time of 60 then reaches a steady state after this value. For sensitivity function Snh1KOA, the trajectory increases from zero to 100 at a discrete time of 60 then reaches a steady state after this value. For sensitivity function Snh1etag, the trajectory decreases from zero to – 0.1 at a discrete time of 40 then reaches a steady state after this value. For sensitivity function Snh1KMP, the trajectory increases from zero to 15 at a discrete time of

60 then reaches a steady state after this value. For sensitivity function Snh1KSP, the trajectory increases from zero to 18 at a discrete time of 60 then reaches a steady state after this value. For sensitivity function Snh1KSA, the trajectory increases from zero to 0.5 at a discrete time of 3 then decreases to zero reaching a steady state. For sensitivity function Snh1fMA, the trajectory slightly increases from zero to 3×10^{-5} at a discrete time of 40 then reaches a steady state at a value of 3.2×10^{-5} at a discrete time of 60 then reaches a steady state after this value. For sensitivity function Snh1KA, the trajectory follows a reverse S-shaped curve from zero to 2×10^{-3} at a discrete time of 100.

Figure 9.47: Process variable S_{SNH2} and its sensitivity functions towards the model parameters
The process variable Snh2, the trajectory decreases from zero to – 1500 at a discrete time of 60 then reaches a steady state after this value. For sensitivity function Snh2f, the trajectory decreases from zero to 3.8 at a discrete time of 60 then reaches a steady state after this value. For variable Snh2YZH, the trajectory increases from zero to 2.6 at a discrete time of 60 then reaches a steady state after this value. For variable Snh2YZA, the trajectory increases from zero to 50 at a discrete time of 60 then reaches a steady state after this value. For sensitivity function Snh2fZBH, the trajectory decreases from zero to – 800 at a discrete time of 60 then reaches a steady state after this value. For sensitivity function Snh2muA, the trajectory decreases from zero to – 110 at a discrete time of 60 then reaches a steady state after this value. For sensitivity function Snh2muH, the trajectory decreases from zero to – 20 at a discrete time of 60 then reaches a steady state after this value. For sensitivity function Snh2KS, the trajectory increases from zero to 1.8 at a discrete time of 40 then reaches a steady state after this value. For sensitivity function Snh2KOH, the trajectory increases from zero to 48 at a discrete time of 60 then reaches a steady state after this value. For sensitivity function Snh2KNO, the trajectory increases from zero then to 3×10^{-3} at a discrete time of 3 then oscillating decreases to 0.2×10^{-3} at a discrete time of 60 then reaches a steady state after this value. For sensitivity function Snh2KNH, the trajectory increases from zero to 60 at a discrete time of 60 then reaches a steady state after this value. For sensitivity function Snh2KOA, the trajectory increases from zero to 170 at a discrete time of 60 then reaches a steady state after this value. For sensitivity function Snh2etag, the trajectory decreases from zero to – 0.15 at a discrete time of 60 then reaches a steady state after this value. For sensitivity function Snh2KMP, the trajectory increases from zero to 20 at a discrete time of 60 then reaches a steady state after this value. For sensitivity function Snh2KSP, the trajectory increases from zero to 30 at a discrete time of 60 then reaches a steady state after this value. For sensitivity function Snh2KSA, the trajectory increases from zero to 0.75 at a discrete time of 3 then decreases to zero reaching a steady state. For sensitivity function Snh2fMA, the trajectory slightly increases from zero to 0.75×10^{-4} at a discrete time of 100. For sensitivity function Snh2KA, the trajectory follows a reverse S-shaped curve from zero to 4×10^{-3} at a discrete time of 100.

Figure 9.48: Process variable S_{SNH3} and its sensitivity functions towards the model parameters
The process variable Snh3, the trajectory decreases from zero to – 1500 at a discrete time of 60 then reaches a steady state after this value. For sensitivity function Snh3f, the trajectory decreases from zero to 3.8 at a discrete time of 60 then reaches a steady state after this value. For variable Snh3YZH, the trajectory increases from zero to 3.8 at a discrete time of 60 then reaches a steady state after this value. For variable Snh3YZA, the trajectory increases from zero to 80 at a discrete time of 60 then reaches a steady state after this value. For sensitivity function Snh3fZBH, the trajectory decreases from zero to – 1000 at a discrete time of 60 then reaches a steady state after this value. For sensitivity function Snh3muA, the trajectory decreases from zero to – 180 at a discrete time of 60 then reaches a steady state after this value. For sensitivity function Snh3muH, the trajectory decreases from zero to – 30 at a discrete time of 60 then reaches a steady state after this value. For sensitivity function Snh3KS, the trajectory increases

from zero to 1.8 at a discrete time of 40 then reaches a steady state after this value. For sensitivity function Snh3KOH, the trajectory increases from zero to 48 at a discrete time of 60 then reaches a steady state after this value. For sensitivity function Snh3KNO, the trajectory increases from zero then to 2×10^{-3} at a discrete time of 3 then decreases to 0.2×10^{-3} at a discrete time of 60 then reaches a steady state after this value. For sensitivity function Snh3KNH, the trajectory increases from zero to 80 at a discrete time of 60 then reaches a steady state after this value. For sensitivity function Snh3KOA, the trajectory increases from zero to 170 at a discrete time of 60 then reaches a steady state after this value. For sensitivity function Snh3etag, the trajectory decreases from zero to – 0.15 at a discrete time of 60 then reaches a steady state after this value. For sensitivity function Snh3KMP, the trajectory increases from zero to 20 at a discrete time of 60 then reaches a steady state after this value. For sensitivity function Snh3KSP, the trajectory increases from zero to 39 at a discrete time of 60 then reaches a steady state after this value. For sensitivity function Snh3KSA, the trajectory increases from zero to 0.75 at a discrete time of 3 then decreases to zero reaching a steady state. For sensitivity function Snh3fMA, the trajectory slightly increases from zero to 0.75×10^{-4} at a discrete time of 100. For sensitivity function Snh3KA, the trajectory follows a reverse S-shaped curve from zero to 4×10^{-3} at a discrete time of 100.

Figure 9.49: Process variable S_{SNO1} and its sensitivity functions towards the model parameters

The process variables SNO1, the trajectory increases from zero to 600 at a discrete time of 60 then reaches a steady state after this value. For sensitivity function SNO1f, the trajectory increases from zero to 1.8×10^{-9} then decreases to zero at a discrete time of 60 then reaches a steady state after this value. For variable SNO1YZH, the trajectory increases from zero to 1.7 at a discrete time of 60 then reaches a steady state after this value. For variable SNO1YZA, the trajectory increases from zero to 4.8 at a discrete time of 60 then reaches a steady state after this value. For sensitivity function SNO1fZBH, the trajectory suddenly decreases from zero then increases after – 0.04 at a discrete time of 3 back to zero then reaches a steady state. For sensitivity function SNO1muA, the trajectory increases from zero to 1 at a discrete time of 3 then decreases back to zero reaching a steady state. For sensitivity function SNO1muH, the trajectory decreases from zero to – 0.8 at a discrete time of 60 then reaches a steady state after this value. For sensitivity function SNO1KS, the trajectory increases from zero to 0.18 at a discrete time of 80 then reaches a steady state after this value. For sensitivity function SNO1KOH, the trajectory decreases from zero to – 0.8 at a discrete time of 60 then reaches a steady state after this value. For sensitivity function SNO1KNO, the trajectory increases from zero to 4×10^{-3} at a discrete time of 2 then decreases to 0.2×10^{-3} at a discrete time of 60 then reaches a steady state after this value. For sensitivity function SNO1KNH, then trajectory suddenly increases from zero to 1 at a discrete time of 3 then decreases to zero at a steady state. For sensitivity function SNO1KOA, the trajectory suddenly increases from zero to 0.5 at a discrete time of 3 then decreases to zero at steady state. For sensitivity function SNO1etag, the trajectory decreases from zero to – 0.12 at a discrete time of 60 then reaches a steady state after this value. For sensitivity function SNO1KMP, the trajectory increases from zero to 0.19 at a discrete time of 80 then reaches a steady state after this value. For sensitivity function SNO1KSP, the trajectory slightly oscillates from zero then increases to 0.08 in a stable regime then reaches a steady state at a discrete time of 60 and after this value. For sensitivity function SNO1KSA, the trajectory decreases from zero to – 0.5 at a discrete time of 2 then increases to zero reaching a steady state. For sensitivity function SNO1fMA, the trajectory decreases from zero to – 0.017 at a discrete time of 80 then reaches a steady state after this value. For sensitivity function SNO1KA, the trajectory follows an S-shaped curve from zero to – 0.08 at a discrete time of 100.

Figure 9.50: Process variable S_{SNO2} and its sensitivity functions towards the model parameters

The process variables SNO2, the trajectory increases from zero to 1000 at a discrete time of 60 then reaches a steady state after this value. For sensitivity function SNO2f, the trajectory increases from zero at unstable manner to 1.8×10^{-9} then decreases to zero at a discrete time of 60 then reaches a steady state after this value. For variable SNO2YZH, the trajectory increases from zero to 1.9 at a discrete time of 60 then reaches a steady state after this value. For variable SNO2YZA, the trajectory increases from zero to 8 at a discrete time of 60 then reaches a steady state after this value. For sensitivity function SNO2fZBH, the trajectory suddenly decreases from zero then increases after – 0.04 at a discrete time of 3 back to zero then reaches a steady state. For sensitivity function SNO2muA, the trajectory increases from zero to 1 at a discrete time of 3 then decreases back to zero reaching a steady state. For sensitivity function SNO2muH, the trajectory decreases from zero to – 0.12 at a discrete time of 60 then reaches a steady state after this value. For sensitivity function SNO2KS, the trajectory increases from zero to 0.18 at a discrete time of 60 then reaches a steady state after this value. For sensitivity function SNO2KOH, the trajectory decreases from zero to – 1 at a discrete time of 60 then reaches a steady state after this value. For sensitivity function SNO2KNO, the trajectory increases from zero to 4.9×10^{-3} at a discrete time of 2 then decreases to 0.2×10^{-3} at a discrete time of 60 then reaches a steady state after this value. For sensitivity function SNO2KNH, then trajectory decreases from zero to – 60 at a discrete time of 60 then reaches a steady state after this value. For sensitivity function SNO2KOA, the trajectory suddenly increases from zero to 0.5 at a discrete time of 3 then decreases to zero at steady state. For sensitivity function SNO2etag, the trajectory decreases from zero to – 0.17 at a discrete time of 60 then reaches a steady state after this value. For sensitivity function SNO2KMP, the trajectory increases from zero to 0.4 at a discrete time of 100. For sensitivity function SNO2KSP, the trajectory slightly oscillates from zero then increases to 0.09 in a stable regime then reaches a steady state at a discrete time of 60 and after this value. For sensitivity function SNO2KSA, the trajectory decreases from zero to – 1 at a discrete time of 2 then increases to zero reaching a steady state. For sensitivity function SNO2fMA, the trajectory decreases from zero to – 0.02 at a discrete time of 60 then reaches a steady state after this value. For sensitivity function SNO2KA, the trajectory follows an S-shaped curve from zero to – 1.2 at a discrete time of 100.

Figure 9.51: Process variable S_{SNO3} and its sensitivity functions towards the model parameters

The process variables SNO3, the trajectory increases from zero to 1000 at a discrete time of 60 then reaches a steady state after this value. For sensitivity function SNO3f, the trajectory increases from zero at unstable manner to 0.5×10^{-9} then decreases to 0.1×10^{-9} at a discrete time of 60 then reaches a steady state after this value. For variable SNO3YZH, the trajectory increases from zero to 1.9 at a discrete time of 60 then reaches a steady state after this value. For variable SNO3YZA, the trajectory increases from zero to 8 at a discrete time of 60 then reaches a steady state after this value. For sensitivity function SNO3fZBH, the trajectory suddenly decreases from zero then increases after – 0.04 at a discrete time of 3 back to zero then reaches a steady state. For sensitivity function SNO3muA, the trajectory increases from zero to 1 at a discrete time of 3 then decreases back to zero reaching a steady state. For sensitivity function SNO3muH, the trajectory decreases from zero to – 0.12 at a discrete time of 60 then reaches a steady state after this value. For sensitivity function SNO3KS, the trajectory increases from zero to 0.18 at a discrete time of 60 then reaches a steady state after this value. For sensitivity function SNO3KOH, the trajectory decreases from zero to – 1 at a discrete time of 60 then reaches a steady state after this value. For sensitivity function SNO3KNO, the trajectory increases from zero to 2×10^{-3} at a discrete time of 7 then decreases to 0.2×10^{-3} at a discrete time of 60 then reaches a steady state after this value. For sensitivity function SNO3KNH, then trajectory decreases from zero to – 80 at a discrete time of 60 then reaches a steady state after this value. For sensitivity function SNO3KOA, the trajectory suddenly increases from zero to 0.5 at a discrete time of 3 then decreases to zero at steady state. For sensitivity function SNO3etag, the trajectory decreases from zero to – 0.17 at a discrete time of 60 then reaches a steady state

after this value. For sensitivity function SNO3KMP, the trajectory increases from zero to 0.4 at a discrete time of 100. For sensitivity function SNO3KSP, the trajectory follows a reverse S-shaped curve from zero to 0.09 at a discrete time of 100. For sensitivity function SNO3KSA, the trajectory decreases from zero to – 1 at a discrete time of 2 then increases to zero reaching a steady state. For sensitivity function SNO3fMA, the trajectory decreases from zero to – 0.02 at a discrete time of 60 then reaches a steady state after this value. For sensitivity function SNO3KA, the trajectory follows an S-shaped curve from zero to – 1.2 at a discrete time of 100.

Figure 9.52: Process variable S_{SS1} and its sensitivity functions towards the model parameters
The process variable SS1, the trajectory decreases from zero to -680 at a discrete time of 60 then reaches a steady state after this value. For sensitivity function SS1f, the trajectory decreases from zero to -2.2×10^{-9} then increases to zero at a discrete time of 20 then reaches a steady state. For variable SS1YZH, the trajectory increases from zero to 600 at a discrete time of 60 then reaches a steady state after this value. For variable SS1YZA, the trajectory decreases from zero to -0.7×10^{-7} then increases to -0.25×10^{-7} at a discrete time of 60 then reaches a steady state after this value. For sensitivity function SS1fZBH, the trajectory increases from zero to 1×10^{-7} then decreases to zero at a discrete time of 60 then reaches a steady state after this value. For sensitivity function SS1muA, the trajectory slightly decreases from zero to -1×10^{-8} then suddenly back to zero at a discrete time of 100 then reaching a steady state after this value. For sensitivity function SS1muH, the trajectory decreases from zero to – 300 at a discrete time of 60 then reaches a steady state after this value. For sensitivity function SS1KS, the trajectory increases from zero to 480 at a discrete time of 60 then reaches a steady state after this value. For sensitivity function SS1KOH, the trajectory increases from zero to 0.4 at a discrete time of 2 then decreases to 0.05 at a discrete time of 60 then reaches a steady state after this value. For sensitivity function SS1KNO, the trajectory increases from zero to 0.038 at a discrete time of 3 then suddenly decreases to 0.02 at a discrete time of 5 then increases to 0.04 at a discrete time of 60 then reaches a steady state after this value. For sensitivity function SS1KNH, the trajectory increases from zero to 0.05 at a discrete time of 3 then decrease to zero at a discrete time of 80 then reaches a steady state after this value. For sensitivity function SS1KOA, the trajectory decreases from zero to -1×10^{-7} at a discrete time of 5 then increases to zero at a discrete time of 40 then reaches a steady state after this value. For sensitivity function SS1etag, the trajectory increases from zero to 4×10^{-9} at a discrete time of 5 then decreases to 0.05×10^{-9} at a discrete time of 60 then reaches a steady state after this value. For sensitivity function SS1KMP, the trajectory decreases from zero to -3.8×10^{-9} at a discrete time of 5 then increases to -0.5×10^{-9} at a discrete time of 60 then reaches a steady state after this value. For sensitivity function SS1KSP, the trajectory decreases from zero to -0.5×10^{-9} at a discrete time of 5 then increases to zero at a discrete time of 40 then reaches a steady state after this value. For sensitivity function SS1KSA, the trajectory increases from zero to 0.9×10^{-7} at a discrete time of 5 then decreases to zero at a discrete time of 40 then reaches a steady state after this value. For sensitivity function SS1fMA, the trajectory increases from zero to 0.8×10^{-10} at a discrete time of 80 then reaches a steady state after this value. For sensitivity function SS1KA, the trajectory increases from zero to 5×10^{-9} at a discrete time of 100.

Figure 9.53: Process variable S_{SS2} and its sensitivity functions towards the model parameters
The process variable SS2, the trajectory decreases from zero to -800 at a discrete time of 60 then reaches a steady state after this value. For sensitivity function SS2f, the trajectory decreases from zero to -2.2×10^{-9} then increases to zero at a discrete time of 20 then reaches a steady state. For variable SS2YZH, the trajectory increases from zero to 1000 at a discrete time of 60 then reaches a steady state after this value. For variable SS2YZA, the trajectory

decreases from zero to -0.7×10^{-7} then increases to -0.25×10^{-7} at a discrete time of 60 then reaches a steady state after this value. For sensitivity function SS2fZBH, the trajectory increases from zero to 1.4×10^{-7} at a discrete time of 5 then decreases to zero at a discrete time of 60 then reaches a steady state after this value. For sensitivity function SS2muA, the trajectory slightly decreases from zero to -1×10^{-8} then suddenly back to zero at a discrete time of 100 then reaching a steady state after this value. For sensitivity function SS2muH, the trajectory decreases from zero to – 420 at a discrete time of 60 then reaches a steady state after this value. For sensitivity function SS2KS, the trajectory increases from zero to 750 at a discrete time of 60 then reaches a steady state after this value. For sensitivity function SS2KOH, the trajectory increases from zero to 0.4 at a discrete time of 2 then decreases to 0.05 at a discrete time of 60 then reaches a steady state after this value. For sensitivity function SS2KNO, the trajectory increases from zero to 0.038 at a discrete time of 3 then suddenly decreases to 0.02 at a discrete time of 5 then increases to 0.05 at a discrete time of 60 then reaches a steady state after this value. For sensitivity function SS2KNH, the trajectory increases from zero to 0.05 at a discrete time of 3 then decrease to zero at a discrete time of 80 then reaches a steady state after this value. For sensitivity function SS2KOA, the trajectory decreases from zero to -1×10^{-7} at a discrete time of 5 then increases to zero at a discrete time of 40 then reaches a steady state after this value. For sensitivity function SS2etag, the trajectory increases from zero oscillating to 4×10^{-9} at a discrete time of 5 then decreases to 0.05×10^{-9} at a discrete time of 60 then reaches a steady state after this value. For sensitivity function SS2KMP, the trajectory decreases from zero to -3.8×10^{-9} at a discrete time of 5 then increases to -0.5×10^{-9} at a discrete time of 60 then reaches a steady state after this value. For sensitivity function SS2KSP, the trajectory decreases from zero to -0.5×10^{-9} at a discrete time of 5 then increases to zero at a discrete time of 40 then reaches a steady state after this value. For sensitivity function SS2KSA, the trajectory increases from zero to 0.9×10^{-7} at a discrete time of 5 then decreases to zero at a discrete time of 40 then reaches a steady state after this value. For sensitivity function SS2fMA, the trajectory increases from zero to 0.8×10^{-10} at a discrete time of 80 then reaches a steady state after this value. For sensitivity function SS2KA, the trajectory increases from zero to 5×10^{-9} at a discrete time of 100.

Figure 9.54: Process variable S_{SS3} and its sensitivity functions towards the model parameters

The process variable SS3, the trajectory decreases from zero to – 950 at a discrete time of 60 then reaches a steady state after this value. For sensitivity function SS3f, the trajectory decreases from zero to -0.5×10^{-9} then increases to zero at a discrete time of 60 then reaches a steady state. For variable SS3YZH, the trajectory increases from zero to 1000 at a discrete time of 60 then reaches a steady state after this value. For variable SS3YZA, the trajectory decreases from zero to -0.7×10^{-7} then increases to -0.25×10^{-7} at a discrete time of 60 then reaches a steady state after this value. For sensitivity function SS3fZBH, the trajectory increases from zero to 1.4×10^{-7} at a discrete time of 5 then decreases to zero at a discrete time of 60 then reaches a steady state after this value. For sensitivity function SS3muA, the trajectory slightly decreases from zero to -1×10^{-8} at a discrete time of 8 then suddenly back to zero at a discrete time of 60 then reaching a steady state after this value. For sensitivity function SS3muH, the trajectory decreases from zero to – 500 at a discrete time of 60 then reaches a steady state after this value. For sensitivity function SS3KS, the trajectory increases from zero to 900 at a discrete time of 60 then reaches a steady state after this value. For sensitivity function SS3KOH, the trajectory increases from zero to 0.4 at a discrete time of 2 then decreases to 0.05 at a discrete time of 60 then reaches a steady state after this value. For sensitivity function SS3KNO, the trajectory increases from zero to 0.038 at a discrete time of 3 then suddenly decreases to 0.02 at a discrete time of 5 then increases to 0.05 at a discrete time of 60 then reaches a steady state after this value. For sensitivity function SS3KNH, the trajectory increases

from zero to 0.05 at a discrete time of 3 then decrease to zero at a discrete time of 80 then reaches a steady state after this value. For sensitivity function SS3KOA, the trajectory decreases from zero to – 0.5×10^{-7} at a discrete time of 5 then increases to zero at a discrete time of 60 then reaches a steady state after this value. For sensitivity function SS3etag, the trajectory increases from zero to 2.2×10^{-9} at a discrete time of 10 then decreases to 0.8×10^{-9} at a discrete time of 60 then reaches a steady state after this value. For sensitivity function SS3KMP, the trajectory decreases from zero to – 3.8×10^{-9} at a discrete time of 5 then increases to – 0.5×10^{-9} at a discrete time of 60 then reaches a steady state after this value. For sensitivity function SS3KSP, the trajectory decreases from zero to – 0.5×10^{-9} at a discrete time of 5 then increases to zero at a discrete time of 40 then reaches a steady state after this value. For sensitivity function SS3KSA, the trajectory increases from zero to 0.5×10^{-7} at a discrete time of 5 then decreases to zero at a discrete time of 40 then reaches a steady state after this value. For sensitivity function SS3fMA, the trajectory increases from zero to 0.8×10^{-10} at a discrete time of 80 then reaches a steady state after this value. For sensitivity function SS3KA, the trajectory increases from zero to 5×10^{-9} at a discrete time of 100.

Figure 9.55: Process variable S_{Sads1} and its sensitivity functions towards the model parameters
The process variable Sads1, the trajectory decreases from zero to – 180 at a discrete time of 40 then reaches a steady state after this value. For sensitivity function Sads1f, the trajectory decreases from zero to – 1.5×10^{-9} at a discrete time of 5 then increases to zero at a discrete time of 40 then reaches a steady state after this value. For variable Sads1YZH, the trajectory increases from zero to 500 at a discrete time of 40 then reaches a steady state after this value. For variable Sads1YZA, the trajectory decreases from zero to – 0.5×10^{-7} at a discrete time of 5 then reaches – 0.25×10^{-7} at a discrete time of 60 then reaches a steady state after this value. For sensitivity function Sads1fZBH, the trajectory increases from zero to 0.6×10^{-7} at a discrete time of 5 then decreases to zero at a discrete time of 100. For sensitivity function Sads1muA, the trajectory initially remains constant then decreases to – 0.8×10^{-7} at a discrete time of 5 then increases to zero at a discrete time of 20 then reaches a steady state after this value. For sensitivity function Sads1muH, the trajectory increases from zero to 2.4×10^{-9} at a discrete time of 7 then decreases to 0.4×10^{-9} at a discrete time of 60 then reaches a steady state after this value. For sensitivity function Sads1KS, the trajectory decreases from zero to – 2×10^{-9} at a discrete time of 5 then increases – 0.6×10^{-9} at a discrete time of 60 then reaches a steady state after this value. For sensitivity function Sads1KOH, the trajectory increases from zero to 4.8 at a discrete time of 3 then decreases to zero at a discrete time of 60 then reaches a steady state after this value. For sensitivity function Sads1KNO, the trajectory rapidly increases from zero to 0.014 at a discrete time of 3 then slightly increases to 0.016 at a discrete time of 100. For sensitivity function Sads1KNH, the trajectory rapidly increases from zero to 0.1 at a discrete time of 5 then decreases z_0, zero at a discrete time of 40 then reaches a steady state after this value. For sensitivity function Sads1KOA, the trajectory decreases from zero to – 0.75×10^{-7} at a discrete time of 5 then increases to zero at a discrete time of 40 then reaches a steady state after this value. For sensitivity function Sads1etag, the trajectory decreases from zero to – 0.75 at a discrete time of 60 then reaches a steady state after this value. For sensitivity function Sads1KMP, the trajectory decreases from zero to – 300 at a discrete time of 60 then reaches a steady state after this value. For sensitivity function Sads1KSP, the trajectory rapidly increases from zero to 200 at a discrete time of 2 then decreases to – 50 at a discrete time of 100. For sensitivity function Sads1KSA, the trajectory increases from zero to 5×10^{-9} at a discrete time of 5 then decreases to zero at a discrete time of 40 then reaches a steady state after this value. For sensitivity function Sads1fMA, the trajectory increases from zero to 20 at a discrete time of

60 then reaches a steady state after this value. For sensitivity function Sads1KA, the trajectory increases from zero to 1200 at a discrete time of 60 then reaches a steady state after this value.

Figure 9.56: Process variable S_{Sads2} and its sensitivity functions towards the model parameters
The process variable Sads2, the trajectory decreases from zero to – 180 at a discrete time of 40 then reaches a steady state after this value. For sensitivity function Sads2f, the trajectory decreases from zero to -1.5×10^{-9} at a discrete time of 5 then increases to zero at a discrete time of 40 then reaches a steady state after this value. For variable Sads2YZH, the trajectory increases from zero to 980 at a discrete time of 60 then reaches a steady state after this value. For variable Sads2YZA, the trajectory decreases from zero to -0.5×10^{-7} at a discrete time of 5 then reaches -0.25×10^{-7} at a discrete time of 60 then reaches a steady state after this value. For sensitivity function Sads2fZBH, the trajectory increases from zero to 0.8×10^{-7} at a discrete time of 5 then decreases to 0.02×10^{-7} at a discrete time of 60 then reaches a steady state after this value. For sensitivity function Sads2muA, the trajectory initially remains constant then decreases to -0.8×10^{-7} at a discrete time of 5 then increases to zero at a discrete time of 20 then reaches a steady state after this value. For sensitivity function Sads2muH, the trajectory increases from zero to 2.4×10^{-9} at a discrete time of 7 then decreases to 0.4×10^{-9} at a discrete time of 60 then reaches a steady state after this value. For sensitivity function Sads2KS, the trajectory decreases from zero to -2×10^{-9} at a discrete time of 5 then increases -0.6×10^{-9} at a discrete time of 60 then reaches a steady state after this value. For sensitivity function Sads2KOH, the trajectory increases from zero to 5 at a discrete time of 3 then decreases to zero at a discrete time of 60 then reaches a steady state after this value. For sensitivity function Sads2KNO, the trajectory rapidly increases from zero to 0.019 at a discrete time of 3 then slightly increases to 0.02 at a discrete time of 60 then reaches a steady state after this value. For sensitivity function Sads2KNH, the trajectory rapidly increases from zero to 0.1 at a discrete time of 5 then decreases z_0, zero at a discrete time of 40 then reaches a steady state after this value. For sensitivity function Sads2KOA, the trajectory decreases from zero to -0.6×10^{-7} at a discrete time of 5 then increases to zero at a discrete time of 60 then reaches a steady state after this value. For sensitivity function Sads2etag, the trajectory decreases from zero to – 1 at a discrete time of 60 then reaches a steady state after this value. For sensitivity function Sads2KMP, the trajectory decreases from zero to – 420 at a discrete time of 60 then reaches a steady state after this value. For sensitivity function Sads2KSP, the trajectory rapidly increases from zero to 250 at a discrete time of 3 then decreases to – 100 at a discrete time of 100. For sensitivity function Sads2KSA, the trajectory increases from zero to 0.7×10^{-7} at a discrete time of 5 then decreases to zero at a discrete time of 40 then reaches a steady state after this value. For sensitivity function Sads2fMA, the trajectory increases from zero to 39 at a discrete time of 60 then reaches a steady state after this value. For sensitivity function Sads2KA, the trajectory increases from zero to 2000 at a discrete time of 60 then reaches a steady state after this value.

Figure 9.57: Process variable S_{Sads3} and its sensitivity functions towards the model parameters
The process variable Sads3, the trajectory decreases from zero to – 180 at a discrete time of 40 then reaches a steady state after this value. For sensitivity function Sads3f, the trajectory decreases from zero to -1.5×10^{-9} at a discrete time of 5 then increases to zero at a discrete time of 40 then reaches a steady state after this value. For variable Sads3YZH, the trajectory increases from zero to 980 at a discrete time of 60 then reaches a steady state after this value. For variable Sads3YZA, the trajectory decreases from zero to -0.5×10^{-7} at a discrete time of 5 then reaches -0.25×10^{-7} at a discrete time of 60 then reaches a steady state after this value. For sensitivity function Sads3fZBH, the trajectory increases from zero to 0.8×10^{-7} at a discrete

time of 5 then decreases to 0.02×10^{-7} at a discrete time of 60 then reaches a steady state after this value. For sensitivity function Sads3muA, the trajectory initially remains constant then decreases to – 0.8×10^{-7} at a discrete time of 5 then increases to zero at a discrete time of 20 then reaches a steady state after this value. For sensitivity function Sads3muH, the trajectory increases from zero to 2.4×10^{-9} at a discrete time of 7 then decreases to 0.4×10^{-9} at a discrete time of 60 then reaches a steady state after this value. For sensitivity function Sads3KS, the trajectory decreases from zero to – 2×10^{-9} at a discrete time of 5 then increases – 0.6×10^{-9} at a discrete time of 60 then reaches a steady state after this value. For sensitivity function Sads3KOH, the trajectory increases from zero to 2 at a discrete time of 5 then decreases to zero at a discrete time of 100. For sensitivity function Sads3KNO, the trajectory rapidly increases from zero to 0.019 at a discrete time of 3 then slightly increases to 0.02 at a discrete time of 60 then reaches a steady state after this value. For sensitivity function Sads3KNH, the trajectory rapidly increases from zero to 0.1 at a discrete time of 5 then decreases z_0, zero at a discrete time of 40 then reaches a steady state after this value. For sensitivity function Sads3KOA, the trajectory decreases from zero to a minimum of – 3.8×10^{-9} at a discrete time of 8 then increases to zero at a discrete time of 100. For sensitivity function Sads3etag, the trajectory decreases from zero to – 1 at a discrete time of 60 then reaches a steady state after this value. For sensitivity function Sads3KMP, the trajectory decreases from zero to – 500 at a discrete time of 60 then reaches a steady state after this value. For sensitivity function Sads3KSP, the trajectory rapidly increases from zero to 250 at a discrete time of 3 then decreases to – 100 at a discrete time of 100. For sensitivity function Sads3KSA, the trajectory increases from zero to 0.7×10^{-7} at a discrete time of 5 then decreases to zero at a discrete time of 40 then reaches a steady state after this value. For sensitivity function Sads3fMA, the trajectory increases from zero to 49 at a discrete time of 100. For sensitivity function Sads3KA, the trajectory increases from zero to 3000 at a discrete time of 60 then reaches a steady state after this value.

APPENDIX D: SOFTWARE FOR SIMULATION OF SENSITIVITY FUNCTIONS OF THE PROCESS VARIABLES OF THE BENCHMARK AND ATHLONE MASS BALANCES MODEL BASED ON THE REDUCED ASM1 AND UCT BIOLOGICAL MODELS TOWARDS THEIR PARAMETERS

SOFTWARE FOR SIMULATION OF SENSITIVITY FUNCTIONS OF THE PROCESS VARIABLES OF THE BENCHMARK MASS BALANCE MODEL BASED ON THE REDUCED ASM1 BIOLOGICAL MODEL TOWARDS ITS PARAMETERS

1.Main program

```
%PROGRAM BASM1S.m
%Aim - the program calculates the sensitivity model and simulates the
%sensitivity functions for the process variables of the Benchmark process
%based on ASM1 reduced biological model towards the model parameters. The
%program call the function subroutine rateASM1.m. The calculation uses
%reduced biological model with 3 variables SNH, Sno and SS
%The program uses global definition of the model parameters

global Ks KOH KNO KNH KOA Kx muH etag muA Kh etah iXB YH YA
%Process parameters
f=1.2;YA = 0.24;YH = 0.67;iXB = 0.08;muH = 0.4;Ks = 10;KOH = 0.2;KNO = 0.5;etag = 0.8;etah = 0.8;Kh = 3;Kx = 0.1;muA = 0.5;KNH =
1;KOA = 0.4;
%Tanks volumes and flow rates
V1 = 1000;V2 = 1000;V3 = 1333;V4 = 1333;V5 = 1333;
Qo = 18446;Qa = 55338;Qr = 18446;Qw = 385;Sosat = 8;
%Average values of the inflow concentrations for dry weather
SSi=69.5;SNHi=31.56;SNOi=0.0;
%Determination of the sampling period
DT = 0.01042;days=0.1042*10;K=days/DT
k=0:DT:days
%Average influent concentrations trajectories for SNH, SNO, SS
Xi  =[SNHi*ones(1,K);SNOi*ones(1,K);SSi*ones(1,K)]*0.01
%Initial conditions- steady state values for the Snh, Sno,Ss and zero for the sensitivity functions
XS0
=[7.918;5.37;2.808;zeros(45,1);8.344;3.662;1.459;zeros(45,1);5.548;6.541;1.15;zeros(45,1);2.967;9.299;0.995;zeros(45,1);1.733;10.4
15;0.889;zeros(45,1)];% initial conditions for the differential equations
% Steady state values for the biomass XBH, XBA, XS
XBH = 0.05*[2551.76*ones(1,K);2553.38*ones(1,K);2557.13*ones(1,K);2559.18*ones(1,K);2559.34*ones(1,K)];% XBH steady state COD/m^3
XBA = 0.05*[148.389*ones(1,K);148.309*ones(1,K);148.941*ones(1,K);149.527*ones(1,K);149.797*ones(1,K)];% XBA steady state g all
COD/m^3
XS = 0.05*[82.135*ones(1,K);76.386*ones(1,K);64.855*ones(1,K);55.694*ones(1,K);49.306*ones(1,K)]; % XS steady state all COD/m^3
%trajectory of the control signal
SO1 = [0.2*ones(1,K);0.2*ones(1,K)];SO2=[2.0*ones(1,K);2.29*ones(1,K);1.91*ones(1,K)]*1;
U=[SO1;SO2];

% calculation of the initial trajectory for the state vector X and for the sensitivity vector XSS
X =[[7.918;5.37;2.808;8.344;3.662;1.459;5.548;6.541;1.15;2.967;9.299;0.995;1.733;10.415;0.889] zeros(15,K)];XSS = [XS0
zeros(240,K)];
%Calculation of the state space process model matrices
%Calculation of the matrix A
IV1 = DT/V1;IV2 = DT/V2;IV3 = DT/V3;IV4 = DT/V4;IV5 = DT/V5;IV=IV1*Qo;IVV=IV*f;Q=Qo+Qa+Qr
IV21=IV2*Q;IV32=IV3*Q;IV43=IV4*Q;IV54=IV5*Q
IV11=1-IV1*Q;IV22=1-IV21;IV33=1-IV32;IV44=1-IV43;IV55=1-IV54;IV15=IV1*(Qa+Qr)
A=[[IV11 0.0 0.0;0.0 IV11 0.0;0.0 0.0 IV11] zeros(3,9) [IV15 0.0 0.0;0.0 IV15 0.0;0.0 0.0 IV15];
    [IV21 0.0 0.0;0.0 IV21 0.0;0.0 0.0 IV21] [IV22 0.0 0.0;0.0 IV22 0.0;0.0 0.0 IV22] zeros(3,9);
    zeros(3,3) [IV32 0.0 0.0;0.0 IV32 0.0;0.0 0.0 IV32] [IV33 0.0 0.0;0.0 IV33 0.0;0.0 0.0 IV33] zeros(3,6);
    zeros(3,6) [IV43 0.0 0.0;0.0 IV43 0.0;0.0 0.0 IV43] [IV44 0.0 0.0;0.0 IV44 0.0;0.0 0.0 IV44] zeros(3,3);
    zeros(3,9) [IV54 0.0 0.0;0.0 IV54 0.0;0.0 0.0 IV54] [IV55 0.0 0.0;0.0 IV55 0.0;0.0 0.0 IV55]]
A11=A(1:3,1:3);A15=A(1:3,13:15);A21=A(4:6,1:3);A22=A(4:6,4:6);A32=A(7:9,4:6);A33=A(7:9,7:9)
A43=A(10:12,7:9);A44=A(10:12,10:12);A54=A(13:15,10:12);A55=A(13:15,13:15)

%Calculation of the matrice B1,B and Cn and C
B1=[IVV 0.0 0.0;0.0 IV 0.0;0.0 0.0 IV]
B=[IVV 0.0 0.0;0.0 IV 0.0;0.0 0.0 IV;zeros(12,3)]
Cn=DT*[(-iXB) 0.0 (-1/YH);(-iXB) (-(1-YH))/(2.86*YH) -1/YH;-(iXB+1/YA) 1/YA 0.0;0.0 0.0 1.0];
C=[Cn zeros(4,12);zeros(4,3) Cn zeros(4,9);zeros(4,6) Cn zeros(4,6);zeros(4,9) Cn zeros(4,3);zeros(4,12) Cn]

%Simulation of the sensitivity model
for k = 1:K
    XSSk = XSS(:,k);
    Xk=X(:,k);
    Uk =U(:,k);
    XBHk = XBH(:,k);
    XBAk = XBA(:,k);
    XSk = XS(:,k);
    Xik = Xi(:,k);
```

```
   [ROASM1,AS,BS,CS,DS]=rateASM1(Xk,Uk,XBHk,XBAk,XSk,DT,A11,A15,A21,A22,A32,A33,A43,A44,A54,A55,B1,Cn);

    XSS(:,k+1) = AS*XSS(:,k) + CS'*ROASM1 + BS*Xi(:,k)+DS;
    X(:,k+1) = [XSS(1:3,k+1);XSS(49:51,k+1);XSS(97:99,k+1);XSS(145:147,k+1);XSS(193:195,k+1)];
end

%vector of sensitivity for the first tank variables SNH, SNO,SS
SNH1=XSS(1,:);SNO1=XSS(2,:);SS1=XSS(3,:);
SNH1f=XSS(4,:);SNO1f=XSS(5,:);SS1f=XSS(6,:);
SNH1YH=XSS(7,:);SNO1YH=XSS(8,:);SS1YH=XSS(9,:);
SNH1YA=XSS(10,:);SNO1YA=XSS(11,:);SS1YA=XSS(12,:);
SNH1iXB=XSS(13,:);SNO1iXB=XSS(14,:);SS1iXB=XSS(15,:);
SNH1muA=XSS(16,:);SNO1muA=XSS(17,:);SS1muA=XSS(18,:);
SNH1muH=XSS(19,:);SNO1muH=XSS(20,:);SS1muH=XSS(21,:);
SNH1KS=XSS(22,:);SNO1KS=XSS(23,:);SS1KS=XSS(24,:);
SNH1KOH=XSS(25,:);SNO1KOH=XSS(26,:);SS1KOH=XSS(27,:);
SNH1KNO=XSS(28,:);SNO1KNO=XSS(29,:);SS1KNO=XSS(30,:);
SNH1KNH=XSS(31,:);SNO1KNH=XSS(32,:);SS1KNH=XSS(33,:);
SNH1KOA=XSS(34,:);SNO1KOA=XSS(35,:);SS1KOA=XSS(36,:);
SNH1etag=XSS(37,:);SNO1etag=XSS(38,:);SS1etag=XSS(39,:);
SNH1etah=XSS(40,:);SNO1etah=XSS(41,:);SS1etah=XSS(42,:);
SNH1Kh=XSS(43,:);SNO1Kh=XSS(44,:);SS1Kh=XSS(45,:);
SNH1Kx=XSS(46,:);SNO1Kx=XSS(47,:);SS1Kx=XSS(48,:);

%vector of sensitivity for the second tank variables SNH, SNO,SS
SNH2=XSS(49,:);SNO2=XSS(50,:);SS2=XSS(51,:);
SNH2f=XSS(52,:);SNO2f=XSS(53,:);SS2f=XSS(54,:);
SNH2YH=XSS(55,:);SNO2YH=XSS(56,:);SS2YH=XSS(57,:);
SNH2YA=XSS(58,:);SNO2YA=XSS(59,:);SS2YA=XSS(60,:);
SNH2iXB=XSS(61,:);SNO2iXB=XSS(62,:);SS2iXB=XSS(63,:);
SNH2muA=XSS(64,:);SNO2muA=XSS(65,:);SS2muA=XSS(66,:);
SNH2muH=XSS(67,:);SNO2muH=XSS(68,:);SS2muH=XSS(69,:);
SNH2KS=XSS(70,:);SNO2KS=XSS(71,:);SS2KS=XSS(72,:);
SNH2KOH=XSS(73,:);SNO2KOH=XSS(74,:);SS2KOH=XSS(75,:);
SNH2KNO=XSS(76,:);SNO2KNO=XSS(77,:);SS2KNO=XSS(78,:);
SNH2KNH=XSS(79,:);SNO2KNH=XSS(80,:);SS2KNH=XSS(81,:);
SNH2KOA=XSS(82,:);SNO2KOA=XSS(83,:);SS2KOA=XSS(84,:);
SNH2etag=XSS(85,:);SNO2etag=XSS(86,:);SS2etag=XSS(87,:);
SNH2etah=XSS(88,:);SNO2etah=XSS(89,:);SS2etah=XSS(90,:);
SNH2Kh=XSS(91,:);SNO2Kh=XSS(92,:);SS2Kh=XSS(93,:);
SNH2Kx=XSS(94,:);SNO2Kx=XSS(95,:);SS2Kx=XSS(96,:);

%vector of sensitivity for the third tank variables SNH, SNO,SS
SNH3=XSS(97,:);SNO3=XSS(98,:);SS3=XSS(99,:);
SNH3f=XSS(100,:);SNO3f=XSS(101,:);SS3f=XSS(102,:);
SNH3YH=XSS(103,:);SNO3YH=XSS(104,:);SS3YH=XSS(105,:);
SNH3YA=XSS(106,:);SNO3YA=XSS(107,:);SS3YA=XSS(108,:);
SNH3iXB=XSS(109,:);SNO3iXB=XSS(110,:);SS3iXB=XSS(111,:);
SNH3muA=XSS(112,:);SNO3muA=XSS(113,:);SS3muA=XSS(114,:);
SNH3muH=XSS(115,:);SNO3muH=XSS(116,:);SS3muH=XSS(117,:);
SNH3KS=XSS(118,:);SNO3KS=XSS(119,:);SS3KS=XSS(120,:);
SNH3KOH=XSS(121,:);SNO3KOH=XSS(122,:);SS3KOH=XSS(123,:);
SNH3KNO=XSS(124,:);SNO3KNO=XSS(125,:);SS3KNO=XSS(126,:);
SNH3KNH=XSS(127,:);SNO3KNH=XSS(128,:);SS3KNH=XSS(129,:);
SNH3KOA=XSS(130,:);SNO3KOA=XSS(131,:);SS3KOA=XSS(132,:);
SNH3etag=XSS(133,:);SNO3etag=XSS(134,:);SS3etag=XSS(135,:);
SNH3etah=XSS(136,:);SNO3etah=XSS(137,:);SS3etah=XSS(138,:);
SNH3Kh=XSS(139,:);SNO3Kh=XSS(140,:);SS3Kh=XSS(141,:);
SNH3Kx=XSS(142,:);SNO3Kx=XSS(143,:);SS3Kx=XSS(144,:);

%vector of sensitivity for the fourth tank variables SNH, SNO,SS
SNH4=XSS(145,:);SNO4=XSS(146,:);SS4=XSS(147,:);
SNH4f=XSS(148,:);SNO4f=XSS(149,:);SS4f=XSS(150,:);
SNH4YH=XSS(151,:);SNO4YH=XSS(152,:);SS4YH=XSS(153,:);
SNH4YA=XSS(154,:);SNO4YA=XSS(155,:);SS4YA=XSS(156,:);
SNH4iXB=XSS(157,:);SNO4iXB=XSS(158,:);SS4iXB=XSS(159,:);
SNH4muA=XSS(160,:);SNO4muA=XSS(161,:);SS4muA=XSS(162,:);
SNH4muH=XSS(163,:);SNO4muH=XSS(164,:);SS4muH=XSS(165,:);
SNH4KS=XSS(166,:);SNO4KS=XSS(167,:);SS4KS=XSS(168,:);
SNH4KOH=XSS(169,:);SNO4KOH=XSS(170,:);SS4KOH=XSS(171,:);
SNH4KNO=XSS(172,:);SNO4KNO=XSS(173,:);SS4KNO=XSS(174,:);
SNH4KNH=XSS(175,:);SNO4KNH=XSS(176,:);SS4KNH=XSS(177,:);
SNH4KOA=XSS(178,:);SNO4KOA=XSS(179,:);SS4KOA=XSS(180,:);
SNH4etag=XSS(181,:);SNO4etag=XSS(182,:);SS4etag=XSS(183,:);
SNH4etah=XSS(184,:);SNO4etah=XSS(185,:);SS4etah=XSS(186,:);
SNH4Kh=XSS(187,:);SNO4Kh=XSS(188,:);SS4Kh=XSS(189,:);
SNH4Kx=XSS(190,:);SNO4Kx=XSS(191,:);SS4Kx=XSS(192,:);

%vector of sensitivity for the fifth tank variables SNH, SNO,SS
SNH5=XSS(193,:);SNO5=XSS(194,:);SS5=XSS(195,:);
SNH5f=XSS(196,:);SNO5f=XSS(197,:);SS5f=XSS(198,:);
SNH5YH=XSS(199,:);SNO5YH=XSS(200,:);SS5YH=XSS(201,:);
SNH5YA=XSS(202,:);SNO5YA=XSS(203,:);SS5YA=XSS(204,:);
SNH5iXB=XSS(205,:);SNO5iXB=XSS(206,:);SS5iXB=XSS(207,:);
SNH5muA=XSS(208,:);SNO5muA=XSS(209,:);SS5muA=XSS(210,:);
SNH5muH=XSS(211,:);SNO5muH=XSS(212,:);SS5muH=XSS(213,:);
SNH5KS=XSS(214,:);SNO5KS=XSS(215,:);SS5KS=XSS(216,:);
SNH5KOH=XSS(217,:);SNO5KOH=XSS(218,:);SS5KOH=XSS(219,:);
SNH5KNO=XSS(220,:);SNO5KNO=XSS(221,:);SS5KNO=XSS(222,:);
SNH5KNH=XSS(223,:);SNO5KNH=XSS(224,:);SS5KNH=XSS(225,:);
SNH5KOA=XSS(226,:);SNO5KOA=XSS(227,:);SS5KOA=XSS(228,:);
SNH5etag=XSS(229,:);SNO5etag=XSS(230,:);SS5etag=XSS(231,:);
SNH5etah=XSS(232,:);SNO5etah=XSS(233,:);SS5etah=XSS(234,:);
SNH5Kh=XSS(235,:);SNO5Kh=XSS(236,:);SS5Kh=XSS(237,:);
SNH5Kx=XSS(238,:);SNO5Kx=XSS(239,:);SS5Kx=XSS(240,:);

k=1:101
%Graphs of the sensitivity functions for the SNH for the first tank
figure(1)
```

```
subplot(8,2,1);plot(k,SNH1,'k')
title('Process variable Snh1')
ylabel('\fontsize{8}SNH1')
xlabel('\fontsize{8}discrete time k')

subplot(8,2,2); plot(k,SNH1f,'k')
title('Sensitivity function Snh1f')
ylabel('\fontsize{8}SNH1f')
xlabel('\fontsize{8}discrete time,k')

subplot(8,2,3); plot(k,SNH1YH,'k')
title('Variable Snh1YH')
ylabel('\fontsize{8}SNH1YH')
xlabel('\fontsize{8}discrete time,k')

subplot(8,2,4); plot(k,SNH1YA,'k')
title('Variable Snh1YA')
ylabel('\fontsize{8}SNH1YA')
xlabel('\fontsize{8}discrete time,k')

subplot(8,2,5); plot(k,SNH1iXB,'k')
title('Sensitivity function Snh1iXB')
ylabel('\fontsize{8}SNH1iXB')
xlabel('discrete time,k')

subplot(8,2,6); plot(k,SNH1muA,'k')
title('Sensitivity function Snh1muA')
ylabel('\fontsize{8}SNH1muA')
xlabel('\fontsize{8}discrete time,k')

subplot(8,2,7); plot(k,SNH1muH,'k')
title('Sensitivity function Snh1muH')
ylabel('\fontsize{8}SNH1muH')
xlabel('discrete time,k')

subplot(8,2,8); plot(k,SNH1KS,'k')
title('Sensitivity function Snh1KS')
ylabel('\fontsize{8}SNH1KS')
xlabel('discrete time,k')

subplot(8,2,9); plot(k,SNH1KOH,'k')
title('Sensitivity function Snh1KOH')
ylabel('\fontsize{8}SNH1KOH')
xlabel('\fontsize{8}discrete time,k')

subplot(8,2,10); plot(k,SNH1KNO,'k')
title('Sensitivity function Snh1KNO')
ylabel('\fontsize{8}SNH1KNO')
xlabel('\fontsize{8}discrete time,k')

subplot(8,2,11); plot(k,SNH1KNH,'k')
title('Sensitivity function Snh1KNH')
ylabel('\fontsize{8}SNH1KNH')
xlabel('\fontsize{8}discrete time,k')

subplot(8,2,12); plot(k,SNH1KOA,'k')
title('Sensitivity function Snh1KOA')
ylabel('\fontsize{8}SNH1KOA')
xlabel('\fontsize{8}discrete time,k')

subplot(8,2,13); plot(k,SNH1etag,'k')
title('Sensitivity function Snh1etag')
ylabel('\fontsize{8}SNH1etag')
xlabel('\fontsize{8}discrete time,k')

subplot(8,2,14); plot(k,SNH1etag,'k')
title('Sensitivity function Snh1etah')
ylabel('\fontsize{8}SNH1etah')
xlabel('\fontsize{8}discrete time,k')

subplot(8,2,15); plot(k,SNH1Kh,'k')
title('Sensitivity function Snh1Kh')
ylabel('\fontsize{8}SNH1Kh')
xlabel('\fontsize{8}discrete time,k')

subplot(8,2,16); plot(k,SNH1Kx,'k')
title('Sensitivity function Snh1Kx')
ylabel('\fontsize{8}SNH1Kx')
xlabel('\fontsize{8}discrete time,k')
%Graphs of the sensitivity functions for the SNH for the
second tank
figure(2)
subplot(8,2,1);plot(k,SNH2,'k')
title('Process variable Snh2')
ylabel('\fontsize{8}SNH2')
xlabel('\fontsize{8}discrete time k')

subplot(8,2,2); plot(k,SNH2f,'k')
title('Sensitivity function Snh2f')
ylabel('\fontsize{8}SNH2f')
xlabel('\fontsize{8}discrete time,k')

subplot(8,2,3); plot(k,SNH2YH,'k')
title('Variable Snh2YH')
ylabel('\fontsize{8}SNH2YH')
xlabel('\fontsize{8}discrete time,k')

subplot(8,2,4); plot(k,SNH2YA,'k')
title('Variable Snh2YA')
ylabel('\fontsize{8}SNH2YA')
xlabel('\fontsize{8}discrete time,k')

subplot(8,2,5); plot(k,SNH2iXB,'k')
title('Sensitivity function Snh1iXB')
ylabel('\fontsize{8}SNH2iXB')
xlabel('discrete time,k')

subplot(8,2,6); plot(k,SNH2muA,'k')
title('Sensitivity function Snh2muA')
ylabel('\fontsize{8}SNH2muA')
xlabel('\fontsize{8}discrete time,k')

subplot(8,2,7); plot(k,SNH2muH,'k')
title('Sensitivity function Snh2muH')
ylabel('\fontsize{8}SNH2muH')
xlabel('discrete time,k')

subplot(8,2,8); plot(k,SNH2KS,'k')
title('Sensitivity function Snh2KS')
ylabel('\fontsize{8}SNH2KS')
xlabel('discrete time,k')

subplot(8,2,9); plot(k,SNH2KOH,'k')
title('Sensitivity function Snh2KOH')
ylabel('\fontsize{8}SNH2KOH')
xlabel('\fontsize{8}discrete time,k')

subplot(8,2,10); plot(k,SNH2KNO,'k')
title('Sensitivity function Snh2KNO')
ylabel('\fontsize{8}SNH2KNO')
xlabel('\fontsize{8}discrete time,k')

subplot(8,2,11); plot(k,SNH2KNH,'k')
title('Sensitivity function Snh2KNH')
ylabel('\fontsize{8}SNH2KNH')
xlabel('\fontsize{8}discrete time,k')

subplot(8,2,12); plot(k,SNH2KOA,'k')
title('Sensitivity function Snh2KOA')
ylabel('\fontsize{8}SNH2KOA')
xlabel('\fontsize{8}discrete time,k')

subplot(8,2,13); plot(k,SNH2etag,'k')
title('Sensitivity function Snh2etag')
ylabel('\fontsize{8}SNH2etag')
xlabel('\fontsize{8}discrete time,k')

subplot(8,2,14); plot(k,SNH2etah,'k')
title('Sensitivity function Snh2etah')
ylabel('\fontsize{8}SNH2etah')
xlabel('\fontsize{8}discrete time,k')

subplot(8,2,15); plot(k,SNH2Kh,'k')
title('Sensitivity function Snh2Kh')
ylabel('\fontsize{8}SNH2Kh')
xlabel('\fontsize{8}discrete time,k')

subplot(8,2,16); plot(k,SNH2Kx,'k')
```

```
title('Sensitivity function Snh2Kx')
ylabel('\fontsize{8}SNH2Kx')
xlabel('\fontsize{8}discrete time,k')
%Graphs of the sensitivity functions for the SNH for the
third tank
figure(3)
subplot(8,2,1);plot(k,SNH3,'k')
title('Process variable Snh3')
ylabel('\fontsize{8}SNH3')
xlabel('\fontsize{8}discrete time k')

subplot(8,2,2); plot(k,SNH3f,'k')
title('Sensitivity function Snh3f')
ylabel('\fontsize{8}SNH3f')
xlabel('\fontsize{8}discrete time,k')

subplot(8,2,3); plot(k,SNH3YH,'k')
title('Variable Snh3YH')
ylabel('\fontsize{8}SNH3YH')
xlabel('\fontsize{8}discrete time,k')

subplot(8,2,4); plot(k,SNH3YA,'k')
title('Variable Snh3YA')
ylabel('\fontsize{8}SNH3YA')
xlabel('\fontsize{8}discrete time,k')

subplot(8,2,5); plot(k,SNH3iXB,'k')
title('Sensitivity function Snh3iXB')
ylabel('\fontsize{8}SNH3iXB')
xlabel('discrete time,k')

subplot(8,2,6); plot(k,SNH3muA,'k')
title('Sensitivity function Snh3muA')
ylabel('\fontsize{8}SNH3muA')
xlabel('\fontsize{8}discrete time,k')

subplot(8,2,7); plot(k,SNH3muH,'k')
title('Sensitivity function Snh3muH')
ylabel('\fontsize{8}SNH3muH')
xlabel('discrete time,k')

subplot(8,2,8); plot(k,SNH3KS,'k')
title('Sensitivity function Snh3KS')
ylabel('\fontsize{8}SNH3KS')
xlabel('discrete time,k')

subplot(8,2,9); plot(k,SNH3KOH,'k')
title('Sensitivity function Snh3KOH')
ylabel('\fontsize{8}SNH3KOH')
xlabel('\fontsize{8}discrete time,k')

subplot(8,2,10); plot(k,SNH3KNO,'k')
title('Sensitivity function Snh3KNO')
ylabel('\fontsize{8}SNH3KNO')
xlabel('\fontsize{8}discrete time,k')

subplot(8,2,11); plot(k,SNH3KNH,'k')
title('Sensitivity function Snh3KNH')
ylabel('\fontsize{8}SNH3KNH')
xlabel('\fontsize{8}discrete time,k')

subplot(8,2,12); plot(k,SNH3KOA,'k')
title('Sensitivity function Snh3KOA')
ylabel('\fontsize{8}SNH3KOA')
xlabel('\fontsize{8}discrete time,k')

subplot(8,2,13); plot(k,SNH3etag,'k')
title('Sensitivity function Snh3etag')
ylabel('\fontsize{8}SNH3etag')
xlabel('\fontsize{8}discrete time,k')

subplot(8,2,14); plot(k,SNH3etah,'k')
title('Sensitivity function Snh3etah')
ylabel('\fontsize{8}SNH3etah')
xlabel('\fontsize{8}discrete time,k')

subplot(8,2,15); plot(k,SNH3Kh,'k')
title('Sensitivity function Snh3Kh')
ylabel('\fontsize{8}SNH3Kh')
xlabel('\fontsize{8}discrete time,k')

subplot(8,2,16); plot(k,SNH3Kx,'k')
title('Sensitivity function Snh3Kx')
ylabel('\fontsize{8}SNH3Kx')
xlabel('\fontsize{8}discrete time,k')

%Graphs for the sensitivity functions for SNH in the tank 4
figure(4)
subplot(8,2,1);plot(k,SNH4,'k')
title('Process variable Snh4')
ylabel('\fontsize{8}SNH4')
xlabel('\fontsize{8}discrete time k')

subplot(8,2,2); plot(k,SNH4f,'k')
title('Sensitivity function Snh4f')
ylabel('\fontsize{8}SNH4f')
xlabel('\fontsize{8}discrete time,k')

subplot(8,2,3); plot(k,SNH4YH,'k')
title('Variable Snh4YH')
ylabel('\fontsize{8}SNH4YH')
xlabel('\fontsize{8}discrete time,k')

subplot(8,2,4); plot(k,SNH4YA,'k')
title('Variable Snh4YA')
ylabel('\fontsize{8}SNH4YA')
xlabel('\fontsize{8}discrete time,k')

subplot(8,2,5); plot(k,SNH4iXB,'k')
title('Sensitivity function Snh4iXB')
ylabel('\fontsize{8}SNH4iXB')
xlabel('discrete time,k')

subplot(8,2,6); plot(k,SNH4muA,'k')
title('Sensitivity function Snh4muA')
ylabel('\fontsize{8}SNH4muA')
xlabel('\fontsize{8}discrete time,k')

subplot(8,2,7); plot(k,SNH4muH,'k')
title('Sensitivity function Snh4muH')
ylabel('\fontsize{8}SNH4muH')
xlabel('discrete time,k')

subplot(8,2,8); plot(k,SNH4KS,'k')
title('Sensitivity function Snh4KS')
ylabel('\fontsize{8}SNH4KS')
xlabel('discrete time,k')

subplot(8,2,9); plot(k,SNH4KOH,'k')
title('Sensitivity function Snh4KOH')
ylabel('\fontsize{8}SNH4KOH')
xlabel('\fontsize{8}discrete time,k')

subplot(8,2,10); plot(k,SNH4KNO,'k')
title('Sensitivity function Snh4KNO')
ylabel('\fontsize{8}SNH4KNO')
xlabel('\fontsize{8}discrete time,k')

subplot(8,2,11); plot(k,SNH4KNH,'k')
title('Sensitivity function Snh4KNH')
ylabel('\fontsize{8}SNH4KNH')
xlabel('\fontsize{8}discrete time,k')

subplot(8,2,12); plot(k,SNH4KOA,'k')
title('Sensitivity function Snh4KOA')
ylabel('\fontsize{8}SNH4KOA')
xlabel('\fontsize{8}discrete time,k')

subplot(8,2,13); plot(k,SNH4etag,'k')
title('Sensitivity function Snh4etag')
ylabel('\fontsize{8}SNH4etag')
xlabel('\fontsize{8}discrete time,k')

subplot(8,2,14); plot(k,SNH4etah,'k')
title('Sensitivity function Snh4etah')
ylabel('\fontsize{8}SNH4etah')
xlabel('\fontsize{8}discrete time,k')

subplot(8,2,15); plot(k,SNH4Kh,'k')
title('Sensitivity function Snh4Kh')
ylabel('\fontsize{8}SNH4Kh')
xlabel('\fontsize{8}discrete time,k')

subplot(8,2,16); plot(k,SNH4Kx,'k')
title('Sensitivity function Snh4Kx')
ylabel('\fontsize{8}SNH4Kx')
xlabel('\fontsize{8}discrete time,k')

%Grapf for the sensitivity functions of the variable SNH in
the tank 5
figure(5)
subplot(8,2,1);plot(k,SNH5,'k')
title('Process variable Snh5')
ylabel('\fontsize{8}SNH5')
xlabel('\fontsize{8}discrete time k')

subplot(8,2,2); plot(k,SNH5f,'k')
title('Sensitivity function Snh5f')
ylabel('\fontsize{8}SNH5f')
xlabel('\fontsize{8}discrete time,k')

subplot(8,2,3); plot(k,SNH5YH,'k')
title('Variable Snh5YH')
ylabel('\fontsize{8}SNH5YH')
xlabel('\fontsize{8}discrete time,k')

subplot(8,2,4); plot(k,SNH5YA,'k')
title('Variable Snh5YA')
ylabel('\fontsize{8}SNH5YA')
xlabel('\fontsize{8}discrete time,k')

subplot(8,2,5); plot(k,SNH5iXB,'k')
title('Sensitivity function Snh5iXB')
ylabel('\fontsize{8}SNH5iXB')
xlabel('discrete time,k')

subplot(8,2,6); plot(k,SNH5muA,'k')
title('Sensitivity function Snh5muA')
```

```
ylabel('\fontsize{8}SNH5muA')
xlabel('\fontsize{8}discrete time,k')

subplot(8,2,7); plot(k,SNH5muH,'k')
title('Sensitivity function Snh5muH')
ylabel('\fontsize{8}SNH5muH')
xlabel('discrete time,k')

subplot(8,2,8); plot(k,SNH5KS,'k')
title('Sensitivity function Snh5KS')
ylabel('\fontsize{8}SNH5KS')
xlabel('discrete time,k')

subplot(8,2,9); plot(k,SNH5KOH,'k')
title('Sensitivity function Snh5KOH')
ylabel('\fontsize{8}SNH5KOH')
xlabel('\fontsize{8}discrete time,k')

subplot(8,2,10); plot(k,SNH5KNO,'k')
title('Sensitivity function Snh5KNO')
ylabel('\fontsize{8}SNH5KNO')
xlabel('\fontsize{8}discrete time,k')

subplot(8,2,11); plot(k,SNH5KNH,'k')
title('Sensitivity function Snh5KNH')
ylabel('\fontsize{8}SNH5KNH')
xlabel('\fontsize{8}discrete time,k')

subplot(8,2,12); plot(k,SNH5KOA,'k')
title('Sensitivity function Snh5KOA')
ylabel('\fontsize{8}SNH5KOA')
xlabel('\fontsize{8}discrete time,k')

subplot(8,2,13); plot(k,SNH5etag,'k')
title('Sensitivity function Snh5etag')
ylabel('\fontsize{8}SNH5etag')
xlabel('\fontsize{8}discrete time,k')

subplot(8,2,14); plot(k,SNH5etah,'k')
title('Sensitivity function Snh5etah')
ylabel('\fontsize{8}SNH5etah')
xlabel('\fontsize{8}discrete time,k')

subplot(8,2,15); plot(k,SNH5Kh,'k')
title('Sensitivity function Snh5Kh')
ylabel('\fontsize{8}SNH5Kh')
xlabel('\fontsize{8}discrete time,k')

subplot(8,2,16); plot(k,SNH5Kx,'k')
title('Sensitivity function Snh5Kx')
ylabel('\fontsize{8}SNH5Kx')
xlabel('\fontsize{8}discrete time,k')

%Graphs of the sensitivity functions for the SNO
%Graphs of the sensitivity functions of the variable SNO in
the tank 1
figure(6)
subplot(8,2,1);plot(k,SNO1,'k')
title('Process variable SNO1')
ylabel('\fontsize{8}SNO1')
xlabel('\fontsize{8}discrete time k')

subplot(8,2,2); plot(k,SNO1f,'k')
title('Sensitivity function SNO1f')
ylabel('\fontsize{8}SNO1f')
xlabel('\fontsize{8}discrete time,k')

subplot(8,2,3); plot(k,SNO1YH,'k')
title('Variable SNO1YH')
ylabel('\fontsize{8}SNO1YH')
xlabel('\fontsize{8}discrete time,k')

subplot(8,2,4); plot(k,SNO1YA,'k')
title('Variable SNO1YA')
ylabel('\fontsize{8}SNO1YA')
xlabel('\fontsize{8}discrete time,k')

subplot(8,2,5); plot(k,SNO1iXB,'k')
title('Sensitivity function SNO1iXB')
ylabel('\fontsize{8}SNO1iXB')
xlabel('discrete time,k')

subplot(8,2,6); plot(k,SNO1muA,'k')
title('Sensitivity function SNO1muA')
ylabel('\fontsize{8}SNO1muA')
xlabel('\fontsize{8}discrete time,k')

subplot(8,2,7); plot(k,SNO1muH,'k')
title('Sensitivity function SNO1muH')
ylabel('\fontsize{8}SNO1muH')
xlabel('discrete time,k')

subplot(8,2,8); plot(k,SNO1KS,'k')
title('Sensitivity function SNO1KS')
ylabel('\fontsize{8}SNO1KS')
xlabel('discrete time,k')

subplot(8,2,9); plot(k,SNO1KOH,'k')
title('Sensitivity function SNO1KOH')
ylabel('\fontsize{8}SNO1KOH')
xlabel('\fontsize{8}discrete time,k')

subplot(8,2,10); plot(k,SNO1KNO,'k')
title('Sensitivity function SNO1KNO')
ylabel('\fontsize{8}SNO1KNO')
xlabel('\fontsize{8}discrete time,k')

subplot(8,2,11); plot(k,SNO1KNH,'k')
title('Sensitivity function SNO1KNH')
ylabel('\fontsize{8}SNO1KNH')
xlabel('\fontsize{8}discrete time,k')

subplot(8,2,12); plot(k,SNO1KOA,'k')
title('Sensitivity function SNO1KOA')
ylabel('\fontsize{8}SNO1KOA')
xlabel('\fontsize{8}discrete time,k')

subplot(8,2,13); plot(k,SNO1etag,'k')
title('Sensitivity function SNO1etag')
ylabel('\fontsize{8}SNO1etag')
xlabel('\fontsize{8}discrete time,k')

subplot(8,2,14); plot(k,SNO1etag,'k')
title('Sensitivity function SNO1etah')
ylabel('\fontsize{8}SNO1etah')
xlabel('\fontsize{8}discrete time,k')

subplot(8,2,15); plot(k,SNO1Kh,'k')
title('Sensitivity function SNO1Kh')
ylabel('\fontsize{8}SNO1Kh')
xlabel('\fontsize{8}discrete time,k')

subplot(8,2,16); plot(k,SNO1Kx,'k')
title('Sensitivity function SNO1Kx')
ylabel('\fontsize{8}SNO1Kx')
xlabel('\fontsize{8}discrete time,k')

%Graphs of the sensitivity functions for the variable SNO in
the tank 2
figure(7)
subplot(8,2,1);plot(k,SNO2,'k')
title('Process variable SNO2')
ylabel('\fontsize{8}SNO2')
xlabel('\fontsize{8}discrete time k')

subplot(8,2,2); plot(k,SNO2f,'k')
title('Sensitivity function SNO2f')
ylabel('\fontsize{8}SNO2f')
xlabel('\fontsize{8}discrete time,k')

subplot(8,2,3); plot(k,SNO2YH,'k')
title('Variable SNO2YH')
ylabel('\fontsize{8}SNO2YH')
xlabel('\fontsize{8}discrete time,k')

subplot(8,2,4); plot(k,SNO2YA,'k')
title('Variable SNO2YA')
ylabel('\fontsize{8}SNO2YA')
xlabel('\fontsize{8}discrete time,k')

subplot(8,2,5); plot(k,SNO2iXB,'k')
title('Sensitivity function SNO1iXB')
ylabel('\fontsize{8}SNO2iXB')
xlabel('discrete time,k')

subplot(8,2,6); plot(k,SNO2muA,'k')
title('Sensitivity function SNO2muA')
ylabel('\fontsize{8}SNO2muA')
xlabel('\fontsize{8}discrete time,k')

subplot(8,2,7); plot(k,SNO2muH,'k')
title('Sensitivity function SNO2muH')
ylabel('\fontsize{8}SNO2muH')
xlabel('discrete time,k')

subplot(8,2,8); plot(k,SNO2KS,'k')
title('Sensitivity function SNO2KS')
ylabel('\fontsize{8}SNO2KS')
xlabel('discrete time,k')

subplot(8,2,9); plot(k,SNO2KOH,'k')
title('Sensitivity function SNO2KOH')
ylabel('\fontsize{8}SNOKOH')
xlabel('\fontsize{8}discrete time,k')

subplot(8,2,10); plot(k,SNO2KNO,'k')
title('Sensitivity function SNO2KNO')
ylabel('\fontsize{8}SNO2KNO')
xlabel('\fontsize{8}discrete time,k')

subplot(8,2,11); plot(k,SNO2KNH,'k')
title('Sensitivity function SNO2KNH')
ylabel('\fontsize{8}SNO2KNH')
xlabel('\fontsize{8}discrete time,k')

subplot(8,2,12); plot(k,SNO2KOA,'k')
title('Sensitivity function SNO2KOA')
ylabel('\fontsize{8}SNO2KOA')
```

```
xlabel('\fontsize{8}discrete time,k')

subplot(8,2,13); plot(k,SNO2etag,'k')
title('Sensitivity function SNO2etag')
ylabel('\fontsize{8}SNO2etag')
xlabel('\fontsize{8}discrete time,k')

subplot(8,2,14); plot(k,SNO2etah,'k')
title('Sensitivity function SNO2etah')
ylabel('\fontsize{8}SNO2etah')
xlabel('\fontsize{8}discrete time,k')

subplot(8,2,15); plot(k,SNO2Kh,'k')
title('Sensitivity function SNO2Kh')
ylabel('\fontsize{8}SNO2Kh')
xlabel('\fontsize{8}discrete time,k')

subplot(8,2,16); plot(k,SNO2Kx,'k')
title('Sensitivity function SNO2Kx')
ylabel('\fontsize{8}SNO2Kx')
xlabel('\fontsize{8}discrete time,k')

%Graphs for the variable SNO  in the  tank 3
figure(8)
subplot(8,2,1);plot(k,SNO3,'k')
title('Process variable SNO3')
ylabel('\fontsize{8}SNO3')
xlabel('\fontsize{8}discrete time k')

subplot(8,2,2); plot(k,SNO3f,'k')
title('Sensitivity function SNO3f')
ylabel('\fontsize{8}SNO3f')
xlabel('\fontsize{8}discrete time,k')

subplot(8,2,3); plot(k,SNO3YH,'k')
title('Variable SNO3YH')
ylabel('\fontsize{8}SNO3YH')
xlabel('\fontsize{8}discrete time,k')

subplot(8,2,4); plot(k,SNO3YA,'k')
title('Variable SNO3YA')
ylabel('\fontsize{8}SNO3YA')
xlabel('\fontsize{8}discrete time,k')

subplot(8,2,5); plot(k,SNO3iXB,'k')
title('Sensitivity function SNO3iXB')
ylabel('\fontsize{8}SNO3iXB')
xlabel('discrete time,k')

subplot(8,2,6); plot(k,SNO3muA,'k')
title('Sensitivity function SNO3muA')
ylabel('\fontsize{8}SNO3muA')
xlabel('\fontsize{8}discrete time,k')

subplot(8,2,7); plot(k,SNO3muH,'k')
title('Sensitivity function SNO3muH')
ylabel('\fontsize{8}SNO3muH')
xlabel('discrete time,k')

subplot(8,2,8); plot(k,SNO3KS,'k')
title('Sensitivity function SNO3KS')
ylabel('\fontsize{8}SNO3KS')
xlabel('discrete time,k')

subplot(8,2,9); plot(k,SNO3KOH,'k')
title('Sensitivity function SNO3KOH')
ylabel('\fontsize{8}SNO3KOH')
xlabel('\fontsize{8}discrete time,k')

subplot(8,2,10); plot(k,SNO3KNO,'k')
title('Sensitivity function SNO3KNO')
ylabel('\fontsize{8}SNO3KNO')
xlabel('\fontsize{8}discrete time,k')

subplot(8,2,11); plot(k,SNO3KNH,'k')
title('Sensitivity function SNO3KNH')
ylabel('\fontsize{8}SNO3KNH')
xlabel('\fontsize{8}discrete time,k')

subplot(8,2,12); plot(k,SNO3KOA,'k')
title('Sensitivity function SNO3KOA')
ylabel('\fontsize{8}SNO3KOA')
xlabel('\fontsize{8}discrete time,k')

subplot(8,2,13); plot(k,SNO3etag,'k')
title('Sensitivity function SNO3etag')
ylabel('\fontsize{8}SNO3etag')
xlabel('\fontsize{8}discrete time,k')

subplot(8,2,14); plot(k,SNO3etah,'k')
title('Sensitivity function SNO3etah')
ylabel('\fontsize{8}SNO3etah')
xlabel('\fontsize{8}discrete time,k')

subplot(8,2,15); plot(k,SNO3Kh,'k')
title('Sensitivity function SNO3Kh')
ylabel('\fontsize{8}SNO3Kh')
xlabel('\fontsize{8}discrete time,k')

subplot(8,2,16); plot(k,SNO3Kx,'k')
title('Sensitivity function SNO3Kx')
ylabel('\fontsize{8}SNO3Kx')
xlabel('\fontsize{8}discrete time,k')

%Graphs for the sensitivity functions for SNO in the tank 4
figure(9)
subplot(8,2,1);plot(k,SNO4,'k')
title('Process variable SNO4')
ylabel('\fontsize{8}SNO4')
xlabel('\fontsize{8}discrete time k')

subplot(8,2,2); plot(k,SNO4f,'k')
title('Sensitivity function SNO4f')
ylabel('\fontsize{8}SNO4f')
xlabel('\fontsize{8}discrete time,k')

subplot(8,2,3); plot(k,SNO4YH,'k')
title('Variable SNO4YH')
ylabel('\fontsize{8}SNO4YH')
xlabel('\fontsize{8}discrete time,k')

subplot(8,2,4); plot(k,SNO4YA,'k')
title('Variable SNO4YA')
ylabel('\fontsize{8}SNN4YA')
xlabel('\fontsize{8}discrete time,k')

subplot(8,2,5); plot(k,SNO4iXB,'k')
title('Sensitivity function SNO4iXB')
ylabel('\fontsize{8}SNO4iXB')
xlabel('discrete time,k')

subplot(8,2,6); plot(k,SNO4muA,'k')
title('Sensitivity function SNO4muA')
ylabel('\fontsize{8}SNO4muA')
xlabel('\fontsize{8}discrete time,k')

subplot(8,2,7); plot(k,SNO4muH,'k')
title('Sensitivity function SNO4muH')
ylabel('\fontsize{8}SNO4muH')
xlabel('discrete time,k')

subplot(8,2,8); plot(k,SNO4KS,'k')
title('Sensitivity function SNO4KS')
ylabel('\fontsize{8}SNO4KS')
xlabel('discrete time,k')

subplot(8,2,9); plot(k,SNO4KOH,'k')
title('Sensitivity function SNO4KOH')
ylabel('\fontsize{8}SNO4KOH')
xlabel('\fontsize{8}discrete time,k')

subplot(8,2,10); plot(k,SNO4KNO,'k')
title('Sensitivity function SNO4KNO')
ylabel('\fontsize{8}SNO4KNO')
xlabel('\fontsize{8}discrete time,k')

subplot(8,2,11); plot(k,SNO4KNH,'k')
title('Sensitivity function SNO4KNH')
ylabel('\fontsize{8}SNO4KNH')
xlabel('\fontsize{8}discrete time,k')

subplot(8,2,12); plot(k,SNO4KOA,'k')
title('Sensitivity function SNO4KOA')
ylabel('\fontsize{8}SNO4KOA')
xlabel('\fontsize{8}discrete time,k')

subplot(8,2,13); plot(k,SNO4etag,'k')
title('Sensitivity function SNO4etag')
ylabel('\fontsize{8}SNO4etag')
xlabel('\fontsize{8}discrete time,k')

subplot(8,2,14); plot(k,SNO4etah,'k')
title('Sensitivity function SNO4etah')
ylabel('\fontsize{8}SNO4etah')
xlabel('\fontsize{8}discrete time,k')

subplot(8,2,15); plot(k,SNO4Kh,'k')
title('Sensitivity function SNO4Kh')
ylabel('\fontsize{8}SNO4Kh')
xlabel('\fontsize{8}discrete time,k')

subplot(8,2,16); plot(k,SNO4Kx,'k')
title('Sensitivity function SNO4Kx')
ylabel('\fontsize{8}SNO4Kx')
xlabel('\fontsize{8}discrete time,k')

%Grapf for the sensitivity functions of the variable SNO in
the tank 5
figure(10)
subplot(8,2,1);plot(k,SNO5,'k')
title('Process variable SNO5')
ylabel('\fontsize{8}SNO5')
xlabel('\fontsize{8}discrete time k')

subplot(8,2,2); plot(k,SNO5f,'k')
title('Sensitivity function SNO5f')
ylabel('\fontsize{8}SNO5f')
xlabel('\fontsize{8}discrete time,k')
```

```
subplot(8,2,3); plot(k,SNO5YH,'k')
title('Variable SNO5YH')
ylabel('\fontsize{8}SNO5YH')
xlabel('\fontsize{8}discrete time,k')

subplot(8,2,4); plot(k,SNO5YA,'k')
title('Variable SNO5YA')
ylabel('\fontsize{8}SNO5YA')
xlabel('\fontsize{8}discrete time,k')

subplot(8,2,5); plot(k,SNO5iXB,'k')
title('Sensitivity function SNO5iXB')
ylabel('\fontsize{8}SNO5iXB')
xlabel('discrete time,k')

subplot(8,2,6); plot(k,SNO5muA,'k')
title('Sensitivity function SNO5muA')
ylabel('\fontsize{8}SNO5muA')
xlabel('\fontsize{8}discrete time,k')

subplot(8,2,7); plot(k,SNO5muH,'k')
title('Sensitivity function SNO5muH')
ylabel('\fontsize{8}SNO5muH')
xlabel('discrete time,k')

subplot(8,2,8); plot(k,SNO5KS,'k')
title('Sensitivity function SNO5KS')
ylabel('\fontsize{8}SNO5KS')
xlabel('discrete time,k')

subplot(8,2,9); plot(k,SNO5KOH,'k')
title('Sensitivity function SNO5KOH')
ylabel('\fontsize{8}SNO5KOH')
xlabel('\fontsize{8}discrete time,k')

subplot(8,2,10); plot(k,SNO5KNO,'k')
title('Sensitivity function SNO5KNO')
ylabel('\fontsize{8}SNO5KNO')
xlabel('\fontsize{8}discrete time,k')

subplot(8,2,11); plot(k,SNO5KNH,'k')
title('Sensitivity function SNO5KNH')
ylabel('\fontsize{8}SNO5KNH')
xlabel('\fontsize{8}discrete time,k')

subplot(8,2,12); plot(k,SNO5KOA,'k')
title('Sensitivity function SNO5KOA')
ylabel('\fontsize{8}SNO5KOA')
xlabel('\fontsize{8}discrete time,k')

subplot(8,2,13); plot(k,SNO5etag,'k')
title('Sensitivity function SNO5etag')
ylabel('\fontsize{8}SNO5etag')
xlabel('\fontsize{8}discrete time,k')

subplot(8,2,14); plot(k,SNO5etah,'k')
title('Sensitivity function SNO5etah')
ylabel('\fontsize{8}SNO5etah')
xlabel('\fontsize{8}discrete time,k')

subplot(8,2,15); plot(k,SNO5Kh,'k')
title('Sensitivity function SNO5Kh')
ylabel('\fontsize{8}SNO5Kh')
xlabel('\fontsize{8}discrete time,k')

subplot(8,2,16); plot(k,SNO5Kx,'k')
title('Sensitivity function SNO5Kx')
ylabel('\fontsize{8}SNO5Kx')
xlabel('\fontsize{8}discrete time,k')

%Graphs of the sensitivity unctions for the SS
%Graphs of the sensitivity functions for the SS in the tank
1
figure(11)
subplot(8,2,1);plot(k,SS1,'k')
title('Process variable SS1')
ylabel('\fontsize{8}SS1')
xlabel('\fontsize{8}discrete time k')

subplot(8,2,2); plot(k,SS1f,'k')
title('Sensitivity function SS1f')
ylabel('\fontsize{8}SS1f')
xlabel('\fontsize{8}discrete time,k')

subplot(8,2,3); plot(k,SS1YH,'k')
title('Variable SS1YH')
ylabel('\fontsize{8}SS1YH')
xlabel('\fontsize{8}discrete time,k')

subplot(8,2,4); plot(k,SS1YA,'k')
title('Variable SS1YA')
ylabel('\fontsize{8}SS1YA')
xlabel('\fontsize{8}discrete time,k')

subplot(8,2,5); plot(k,SS1iXB,'k')
title('Sensitivity function SS1iXB')
ylabel('\fontsize{8}SS1iXB')
xlabel('discrete time,k')

subplot(8,2,6); plot(k,SS1muA,'k')
title('Sensitivity function SS1muA')
ylabel('\fontsize{8}SS1muA')
xlabel('\fontsize{8}discrete time,k')

subplot(8,2,7); plot(k,SS1muH,'k')
title('Sensitivity function SS1muH')
ylabel('\fontsize{8}SS1muH')
xlabel('discrete time,k')

subplot(8,2,8); plot(k,SS1KS,'k')
title('Sensitivity function SS1KS')
ylabel('\fontsize{8}SS1KS')
xlabel('discrete time,k')

subplot(8,2,9); plot(k,SS1KOH,'k')
title('Sensitivity function SS1KOH')
ylabel('\fontsize{8}SS1KOH')
xlabel('\fontsize{8}discrete time,k')

subplot(8,2,10); plot(k,SS1KNO,'k')
title('Sensitivity function SS1KNO')
ylabel('\fontsize{8}SS1KNO')
xlabel('\fontsize{8}discrete time,k')

subplot(8,2,11); plot(k,SS1KNH,'k')
title('Sensitivity function SS1KNH')
ylabel('\fontsize{8}SS1KNH')
xlabel('\fontsize{8}discrete time,k')

subplot(8,2,12); plot(k,SS1KOA,'k')
title('Sensitivity function SS1KOA')
ylabel('\fontsize{8}SS1KOA')
xlabel('\fontsize{8}discrete time,k')

subplot(8,2,13); plot(k,SS1etag,'k')
title('Sensitivity function SS1etag')
ylabel('\fontsize{8}SS1etag')
xlabel('\fontsize{8}discrete time,k')

subplot(8,2,14); plot(k,SS1etag,'k')
title('Sensitivity function SS1etah')
ylabel('\fontsize{8}SS1etah')
xlabel('\fontsize{8}discrete time,k')

subplot(8,2,15); plot(k,SS1Kh,'k')
title('Sensitivity function SS1Kh')
ylabel('\fontsize{8}SS1Kh')
xlabel('\fontsize{8}discrete time,k')

subplot(8,2,16); plot(k,SS1Kx,'k')
title('Sensitivity function SS1Kx')
ylabel('\fontsize{8}SS1Kx')
xlabel('\fontsize{8}discrete time,k')

%Graphs of the sensitivity functions of the varible SS in
the tank 2
figure(12)
subplot(8,2,1);plot(k,SS2,'k')
title('Process variable SS2')
ylabel('\fontsize{8}SS2')
xlabel('\fontsize{8}discrete time k')

subplot(8,2,2); plot(k,SS2f,'k')
title('Sensitivity function SS2f')
ylabel('\fontsize{8}SS2f')
xlabel('\fontsize{8}discrete time,k')

subplot(8,2,3); plot(k,SS2YH,'k')
title('Variable SS2YH')
ylabel('\fontsize{8}SS2YH')
xlabel('\fontsize{8}discrete time,k')

subplot(8,2,4); plot(k,SS2YA,'k')
title('Variable SS2YA')
ylabel('\fontsize{8}SS2YA')
xlabel('\fontsize{8}discrete time,k')

subplot(8,2,5); plot(k,SS2iXB,'k')
title('Sensitivity function SS1iXB')
ylabel('\fontsize{8}SS2iXB')
xlabel('discrete time,k')

subplot(8,2,6); plot(k,SS2muA,'k')
title('Sensitivity function SS2muA')
ylabel('\fontsize{8}SS2muA')
xlabel('\fontsize{8}discrete time,k')

subplot(8,2,7); plot(k,SS2muH,'k')
title('Sensitivity function SS2muH')
ylabel('\fontsize{8}SS2muH')
xlabel('discrete time,k')

subplot(8,2,8); plot(k,SS2KS,'k')
title('Sensitivity function SS2KS')
ylabel('\fontsize{8}SS2KS')
xlabel('discrete time,k')
```

```
subplot(8,2,9); plot(k,SS2KOH,'k')
title('Sensitivity function SS2KOH')
ylabel('\fontsize{8}SS2KOH')
xlabel('\fontsize{8}discrete time,k')

subplot(8,2,10); plot(k,SS2KNO,'k')
title('Sensitivity function SS2KNO')
ylabel('\fontsize{8}SS2KNO')
xlabel('\fontsize{8}discrete time,k')

subplot(8,2,11); plot(k,SS2KNH,'k')
title('Sensitivity function SS2KNH')
ylabel('\fontsize{8}SS2KNH')
xlabel('\fontsize{8}discrete time,k')

subplot(8,2,12); plot(k,SS2KOA,'k')
title('Sensitivity function SS2KOA')
ylabel('\fontsize{8}SS2KOA')
xlabel('\fontsize{8}discrete time,k')

subplot(8,2,13); plot(k,SS2etag,'k')
title('Sensitivity function SS2etag')
ylabel('\fontsize{8}SS2etag')
xlabel('\fontsize{8}discrete time,k')

subplot(8,2,14); plot(k,SS2etah,'k')
title('Sensitivity function SS2etah')
ylabel('\fontsize{8}SS2etah')
xlabel('\fontsize{8}discrete time,k')

subplot(8,2,15); plot(k,SS2Kh,'k')
title('Sensitivity function SS2Kh')
ylabel('\fontsize{8}SS2Kh')
xlabel('\fontsize{8}discrete time,k')

subplot(8,2,16); plot(k,SS2Kx,'k')
title('Sensitivity function SS2Kx')
ylabel('\fontsize{8}SS2Kx')
xlabel('\fontsize{8}discrete time,k')

%Graphs for SS variable in the tank 3
figure(13)
subplot(8,2,1);plot(k,SS3,'k')
title('Process variable SS3')
ylabel('\fontsize{8}SS3')
xlabel('\fontsize{8}discrete time k')

subplot(8,2,2); plot(k,SS3f,'k')
title('Sensitivity function SS3f')
ylabel('\fontsize{8}SS3f')
xlabel('\fontsize{8}discrete time,k')

subplot(8,2,3); plot(k,SS3YH,'k')
title('Variable SS3YH')
ylabel('\fontsize{8}SS3YH')
xlabel('\fontsize{8}discrete time,k')

subplot(8,2,4); plot(k,SS3YA,'k')
title('Variable SS3YA')
ylabel('\fontsize{8}SS3YA')
xlabel('\fontsize{8}discrete time,k')

subplot(8,2,5); plot(k,SS3iXB,'k')
title('Sensitivity function SS3iXB')
ylabel('\fontsize{8}SS3iXB')
xlabel('discrete time,k')

subplot(8,2,6); plot(k,SS3muA,'k')
title('Sensitivity function SS3muA')
ylabel('\fontsize{8}SS3muA')
xlabel('\fontsize{8}discrete time,k')

subplot(8,2,7); plot(k,SS3muH,'k')
title('Sensitivity function SS3muH')
ylabel('\fontsize{8}SS3muH')
xlabel('discrete time,k')

subplot(8,2,8); plot(k,SS3KS,'k')
title('Sensitivity function SS3KS')
ylabel('\fontsize{8}SS3KS')
xlabel('discrete time,k')

subplot(8,2,9); plot(k,SS3KOH,'k')
title('Sensitivity function SS3KOH')
ylabel('\fontsize{8}SS3KOH')
xlabel('\fontsize{8}discrete time,k')

subplot(8,2,10); plot(k,SS3KNO,'k')
title('Sensitivity function SS3KNO')
ylabel('\fontsize{8}SS3KNO')
xlabel('\fontsize{8}discrete time,k')

subplot(8,2,11); plot(k,SS3KNH,'k')
title('Sensitivity function SS3KNH')
ylabel('\fontsize{8}SS3KNH')
xlabel('\fontsize{8}discrete time,k')

subplot(8,2,12); plot(k,SS3KOA,'k')
title('Sensitivity function SS3KOA')
ylabel('\fontsize{8}SS3KOA')
xlabel('\fontsize{8}discrete time,k')

subplot(8,2,13); plot(k,SS3etag,'k')
title('Sensitivity function SS3etag')
ylabel('\fontsize{8}SS3etag')
xlabel('\fontsize{8}discrete time,k')

subplot(8,2,14); plot(k,SS3etah,'k')
title('Sensitivity function SS3etah')
ylabel('\fontsize{8}SS3etah')
xlabel('\fontsize{8}discrete time,k')

subplot(8,2,15); plot(k,SS3Kh,'k')
title('Sensitivity function SS3Kh')
ylabel('\fontsize{8}SS3Kh')
xlabel('\fontsize{8}discrete time,k')

subplot(8,2,16); plot(k,SS3Kx,'k')
title('Sensitivity function SS3Kx')
ylabel('\fontsize{8}SS3Kx')
xlabel('\fontsize{8}discrete time,k')

%Graphs for the sensitivity functions for SS in the tank 4
figure(14)
subplot(8,2,1);plot(k,SS4,'k')
title('Process variable SS4')
ylabel('\fontsize{8}SS4')
xlabel('\fontsize{8}discrete time k')

subplot(8,2,2); plot(k,SS4f,'k')
title('Sensitivity function SS4f')
ylabel('\fontsize{8}SS4f')
xlabel('\fontsize{8}discrete time,k')

subplot(8,2,3); plot(k,SS4YH,'k')
title('Variable SS4YH')
ylabel('\fontsize{8}SS4YH')
xlabel('\fontsize{8}discrete time,k')

subplot(8,2,4); plot(k,SS4YA,'k')
title('Variable SS4YA')
ylabel('\fontsize{8}SS4YA')
xlabel('\fontsize{8}discrete time,k')

subplot(8,2,5); plot(k,SS4iXB,'k')
title('Sensitivity function SS4iXB')
ylabel('\fontsize{8}SS4iXB')
xlabel('discrete time,k')

subplot(8,2,6); plot(k,SS4muA,'k')
title('Sensitivity function SS4muA')
ylabel('\fontsize{8}SS4muA')
xlabel('\fontsize{8}discrete time,k')

subplot(8,2,7); plot(k,SS4muH,'k')
title('Sensitivity function SS4muH')
ylabel('\fontsize{8}SS4muH')
xlabel('discrete time,k')

subplot(8,2,8); plot(k,SS4KS,'k')
title('Sensitivity function SS4KS')
ylabel('\fontsize{8}SS4KS')
xlabel('discrete time,k')

subplot(8,2,9); plot(k,SS4KOH,'k')
title('Sensitivity function SS4KOH')
ylabel('\fontsize{8}SS4KOH')
xlabel('\fontsize{8}discrete time,k')

subplot(8,2,10); plot(k,SS4KNO,'k')
title('Sensitivity function SS4KNO')
ylabel('\fontsize{8}SS4KNO')
xlabel('\fontsize{8}discrete time,k')

subplot(8,2,11); plot(k,SS4KNH,'k')
title('Sensitivity function SS4KNH')
ylabel('\fontsize{8}SS4KNH')
xlabel('\fontsize{8}discrete time,k')

subplot(8,2,12); plot(k,SS4KOA,'k')
title('Sensitivity function SS4KOA')
ylabel('\fontsize{8}SS4KOA')
xlabel('\fontsize{8}discrete time,k')

subplot(8,2,13); plot(k,SS4etag,'k')
title('Sensitivity function SS4etag')
ylabel('\fontsize{8}SS4etag')
xlabel('\fontsize{8}discrete time,k')

subplot(8,2,14); plot(k,SS4etah,'k')
title('Sensitivity function SS4etah')
ylabel('\fontsize{8}SS4etah')
xlabel('\fontsize{8}discrete time,k')

subplot(8,2,15); plot(k,SS4Kh,'k')
title('Sensitivity function SS4Kh')
ylabel('\fontsize{8}SS4Kh')
xlabel('\fontsize{8}discrete time,k')
```

```
subplot(8,2,16); plot(k,SS4Kx,'k')
title('Sensitivity function SS4Kx')
ylabel('\fontsize{8}SS4Kx')
xlabel('\fontsize{8}discrete time,k')

%Grapf for the sensitivity functions of the variable SNH in
the tank 5
figure(15)
subplot(8,2,1);plot(k,SS5,'k')
title('Process variable SS5')
ylabel('\fontsize{8}SS5')
xlabel('\fontsize{8}discrete time k')

subplot(8,2,2); plot(k,SS5f,'k')
title('Sensitivity function SS5f')
ylabel('\fontsize{8}SS5f')
xlabel('\fontsize{8}discrete time,k')

subplot(8,2,3); plot(k,SS5YH,'k')
title('Variable SS5YH')
ylabel('\fontsize{8}SS5YH')
xlabel('\fontsize{8}discrete time,k')

subplot(8,2,4); plot(k,SS5YA,'k')
title('Variable SS5YA')
ylabel('\fontsize{8}SS5YA')
xlabel('\fontsize{8}discrete time,k')

subplot(8,2,5); plot(k,SS5iXB,'k')
title('Sensitivity function SS5iXB')
ylabel('\fontsize{8}SS5iXB')
xlabel('discrete time,k')

subplot(8,2,6); plot(k,SS5muA,'k')
title('Sensitivity function SS5muA')
ylabel('\fontsize{8}SS5muA')
xlabel('\fontsize{8}discrete time,k')

subplot(8,2,7); plot(k,SS5muH,'k')
title('Sensitivity function SS5muH')
ylabel('\fontsize{8}SS5muH')
xlabel('discrete time,k')

subplot(8,2,8); plot(k,SS5KS,'k')
title('Sensitivity function SS5KS')
ylabel('\fontsize{8}SS5KS')
xlabel('discrete time,k')

subplot(8,2,9); plot(k,SS5KOH,'k')
title('Sensitivity function SS5KOH')
ylabel('\fontsize{8}SS5KOH')
xlabel('\fontsize{8}discrete time,k')

subplot(8,2,10); plot(k,SS5KNO,'k')
title('Sensitivity function SS5KNO')
ylabel('\fontsize{8}SS5KNO')
xlabel('\fontsize{8}discrete time,k')

subplot(8,2,11); plot(k,SS5KNH,'k')
title('Sensitivity function SS5KNH')
ylabel('\fontsize{8}SS5KNH')
xlabel('\fontsize{8}discrete time,k')

subplot(8,2,12); plot(k,SS5KOA,'k')
title('Sensitivity function SS5KOA')
ylabel('\fontsize{8}SS5KOA')
xlabel('\fontsize{8}discrete time,k')

subplot(8,2,13); plot(k,SS5etag,'k')
title('Sensitivity function SS5etag')
ylabel('\fontsize{8}SS5etag')
xlabel('\fontsize{8}discrete time,k')

subplot(8,2,14); plot(k,SS5etah,'k')
title('Sensitivity function SS5etah')
ylabel('\fontsize{8}SS5etah')
xlabel('\fontsize{8}discrete time,k')

subplot(8,2,15); plot(k,SS5Kh,'k')
title('Sensitivity function SS5Kh')
ylabel('\fontsize{8}SS5Kh')
xlabel('\fontsize{8}discrete time,k')

subplot(8,2,16); plot(k,SS5Kx,'k')
title('Sensitivity function SS5Kx')
ylabel('\fontsize{8}SS5Kx')
xlabel('\fontsize{8}discrete time,k')
```

2. Subprogram

```
%SUBPROGRAM rateASM1.m
%AIM:The program function rateASM1.m calculates the process rates, derivatives of the process
rates towards the model parameters and variables and forms the sensitivity model matrices
necessary for simulation of the process variables and the sensitivity functions for the Benchmark
process based on the reduced ASM1 biological model.
%The program uses global definition of the model parameters

function [ROASM1,AS,BS,CS,DS] =rateASM1(Xk,Uk,XBHk,XBAk,XSk,DT,A11,A15,A21,A22,A32,A33,A43,A44,A54,A55,B1,Cn)
%Calculation of the process rates at every moment of the time

global Ks KOH KNO KNH KOA Kx muH etag muA Kh etah iXB YH YA

%Process rates for every tank
ROASM1(1)=muH*(Xk(3)/(Ks+Xk(3)))*(Uk(1)/(KOH+Uk(1)))*XBHk(1);
ROASM1(2)=muH*(Xk(3)/(Ks+Xk(3)))*(KOH/(KOH+Uk(1)))*(Xk(2)/(KNO+Xk(2)))*etag*XBHk(1);
ROASM1(3)=muA*(Xk(1)/(KNH+Xk(1)))*(Uk(1)/(KOA+Uk(1)))*XBAk(1);x1=XSk(1)/XBHk(1);
ROASM1(4)=Kh*XBHk(1)*(x1/(Kx+x1))*((Uk(1)/(KOH+Uk(1)))+etah*(KOH/(KOH+Uk(1)))*(Xk(2)/(KNO+Xk(2))));

ROASM1(5)=muH*(Xk(6)/(Ks+Xk(6)))*(Uk(2)/(KOH+Uk(2)))*XBHk(2);
ROASM1(6)=muH*(Xk(6)/(Ks+Xk(6)))*(KOH/(KOH+Uk(2)))*(Xk(5)/(KNO+Xk(5)))*etag*XBHk(2);
ROASM1(7)=muA*(Xk(4)/(KNH+Xk(4)))*(Uk(2)/(KOA+Uk(2)))*XBAk(2);x1=XSk(2)/XBHk(2);
ROASM1(8)=Kh*XBHk(2)*(x1/(Kx+x1))*((Uk(2)/(KOH+Uk(2)))+etah*(KOH/(KOH+Uk(2)))*(Xk(5)/(KNO+Xk(5))));

ROASM1(9)=muH*(Xk(9)/(Ks+Xk(9)))*(Uk(3)/(KOH+Uk(3)))*XBHk(3);
ROASM1(10)=muH*(Xk(9)/(Ks+Xk(9)))*(KOH/(KOH+Uk(3)))*(Xk(8)/(KNO+Xk(8)))*etag*XBHk(3);
ROASM1(11)=muA*(Xk(7)/(KNH+Xk(7)))*(Uk(3)/(KOA+Uk(3)))*XBAk(3);x1=XSk(3)/XBHk(3);
ROASM1(12)=Kh*XBHk(3)*(x1/(Kx+x1))*((Uk(3)/(KOH+Uk(3)))+etah*(KOH/(KOH+Uk(3)))*(Xk(8)/(KNO+Xk(8))));

ROASM1(13)=muH*(Xk(12)/(Ks+Xk(12)))*(Uk(4)/(KOH+Uk(4)))*XBHk(4);
ROASM1(14)=muH*(Xk(12)/(Ks+Xk(12)))*(KOH/(KOH+Uk(4)))*(Xk(11)/(KNO+Xk(11)))*etag*XBHk(4);
ROASM1(15)=muA*(Xk(10)/(KNH+Xk(10)))*(Uk(4)/(KOA+Uk(4)))*XBAk(4);x1=XSk(4)/XBHk(4);
ROASM1(16)=Kh*XBHk(4)*(x1/(Kx+x1))*((Uk(4)/(KOH+Uk(4)))+etah*(KOH/(KOH+Uk(4)))*(Xk(11)/(KNO+Xk(11))));

ROASM1(17)=muH*(Xk(15)/(Ks+Xk(15)))*(Uk(5)/(KOH+Uk(5)))*XBHk(5);
ROASM1(18)=muH*(Xk(15)/(Ks+Xk(15)))*(KOH/(KOH+Uk(5)))*(Xk(14)/(KNO+Xk(14)))*etag*XBHk(5);
ROASM1(19)=muA*(Xk(13)/(KNH+Xk(13)))*(Uk(5)/(KOA+Uk(5)))*XBAk(5);x1=XSk(5)/XBHk(5);
ROASM1(20)=Kh*XBHk(5)*(x1/(Kx+x1))*((Uk(5)/(KOH+Uk(5)))+etah*(KOH/(KOH+Uk(5)))*(Xk(14)/(KNO+Xk(14))));
ROASM1=[ROASM1(1) ROASM1(2) ROASM1(3) ROASM1(4) ROASM1(5) ROASM1(6) ROASM1(7) ROASM1(8) ROASM1(9) ROASM1(10) ROASM1(11) ROASM1(12)
ROASM1(13) ROASM1(14) ROASM1(15) ROASM1(16) ROASM1(17) ROASM1(18) ROASM1(19) ROASM1(20)]';

%Calculations for the Sensitivity Analysis
% Calcualation of the derivatives of the process rates toward the process  variables for the Tank 1
rSNH1SNH1=-(iXB+1/YA)*muA*XBAk(1)*(Uk(1)/(KOA+Uk(1)))*(KNH/(KNH+Xk(1)))^2);
rSNH1SNO1=-iXB*muH*(Xk(3)/(Ks+Xk(3)))*(KOH/(KOH+Uk(1)))*XBHk(1)*etag*(KNO/(KNO+Xk(2))^2);
rSNH1SS1=-iXB*muH*XBHk(1)*(Uk(1)/(KOH+Uk(1)))*(Ks/(Ks+Xk(3))^2);
rSNO1SNH1=(1/YA)*muA*XBAk(1)*(Uk(1)/(KOA+Uk(1)))*(KNH/(KNH+Xk(1))^2);
rSNO1SNO1=-((1-YH)/2.86*YH)*XBHk(1)*muH*etag*(Xk(3)/(Ks+Xk(3)))*(KOH/(KOH+Uk(1)))*(KNO/(KNO+Xk(2))^2);
rSNO1SS1=-((1-YH)/2.86*YH)*XBHk(1)*muH*etag*(KOH/(KOH+Uk(1)))*(Xk(2)/(KNO+Xk(2)))*(Ks/(Ks+Xk(3))^2);rSS1SNH1=0;
```

```
rSS1SNO1=-
(1/YH)*muH*(Xk(3)/(Ks+Xk(3)))*Kh*etah*((XSk(1)/XBHk(1))/(Kx+(XSk(1)/XBHk(1))))*XBHk(1)*(KOH/(KOH+Uk(1)))*(KNO/(KNO+Xk(2))^2);
rSS1SS1=-(1/YH)*muH*XBHk(1)*((Uk(1)/(KOH+Uk(1)))+(Xk(2)/(KNO+Xk(2)))*(KOH/(KOH+Uk(1))))*(Ks/(Ks+Xk(3)));
% Calculation of the derivatives of the process rates toward the process  variables for the Tank 2
rSNH2SNH2=-(iXB+1/YA)*muA*XBAk(2)*(Uk(2)/(KOA+Uk(2)))*(KNH/(KNH+Xk(4))^2);
rSNH2SNO2=-iXB*muH*(Xk(6)/(Ks+Xk(6)))*(KOH/(KOH+Uk(2)))*XBHk(2)*etag*(KNO/(KNO+Xk(5))^2);
rSNH2SS2=-iXB*muH*XBHk(2)*(Uk(2)/(KOH+Uk(2)))*(Ks/(Ks+Xk(6))^2);
rSNO2SNH2=(1/YA)*muA*XBAk(2)*(Uk(2)/(KOA+Uk(2)))*(KNH/(KNH+Xk(4))^2);
rSNO2SNO2=-((1-YH)/2.86*YH)*XBHk(2)*muH*etag*(Xk(6)/(Ks+Xk(6)))*(KOH/(KOH+Uk(2)))*(KNO/(KNO+Xk(5))^2);
rSNO2SS2=-((1-YH)/2.86*YH)*XBHk(2)*muH*etag*(KOH/(KOH+Uk(2)))*(Xk(5)/(KNO+Xk(5)))*(Ks/(Ks+Xk(6))^2);rSS2SNH2=0;
rSS2SNO2=-
(1/YH)*muH*(Xk(6)/(Ks+Xk(6)))*Kh*etah*((XSk(2)/XBHk(2))/(Kx+(XSk(2)/XBHk(2))))*XBHk(2)*(KOH/(KOH+Uk(2)))*(KNO/(KNO+Xk(5))^2);
rSS2SS2=-(1/YH)*muH*XBHk(2)*((Uk(2)/(KOH+Uk(2)))+(Xk(5)/(KNO+Xk(5)))*(KOH/(KOH+Uk(2))))*(Ks/(Ks+Xk(6)));
% Calculation of the derivatives of the process rates toward the process  variables for the Tank 3
rSNH3SNH3=-(iXB+1/YA)*muA*XBAk(3)*(Uk(3)/(KOA+Uk(3)))*(KNH/(KNH+Xk(7))^2);
rSNH3SNO3=-iXB*muH*(Xk(9)/(Ks+Xk(9)))*(KOH/(KOH+Uk(3)))*XBHk(3)*etag*(KNO/(KNO+Xk(8))^2);
rSNH3SS3=-iXB*muH*XBHk(3)*(Uk(3)/(KOH+Uk(3)))*(Ks/(Ks+Xk(9))^2);
rSNO3SNH3=(1/YA)*muA*XBAk(3)*(Uk(3)/(KOA+Uk(3)))*(KNH/(KNH+Xk(7))^2);
rSNO3SNO3=-((1-YH)/2.86*YH)*XBHk(3)*muH*etag*(Xk(9)/(Ks+Xk(9)))*(KOH/(KOH+Uk(3)))*(KNO/(KNO+Xk(8))^2);
rSNO3SS3=-((1-YH)/2.86*YH)*XBHk(3)*muH*etag*(KOH/(KOH+Uk(3)))*(Xk(8)/(KNO+Xk(8)))*(Ks/(Ks+Xk(9))^2);rSS3SNH3=0;
rSS3SNO3=-
(1/YH)*muH*(Xk(9)/(Ks+Xk(9)))*Kh*etah*((XSk(3)/XBHk(3))/(Kx+(XSk(3)/XBHk(3))))*XBHk(3)*(KOH/(KOH+Uk(3)))*(KNO/(KNO+Xk(8))^2);
rSS3SS3=-(1/YH)*muH*XBHk(3)*((Uk(3)/(KOH+Uk(3)))+(Xk(8)/(KNO+Xk(8)))*(KOH/(KOH+Uk(3))))*(Ks/(Ks+Xk(9)));
% Calculation of the derivatives of the process rates toward the process  variables for the Tank 4
rSNH4SNH4=-(iXB+1/YA)*muA*XBAk(4)*(Uk(4)/(KOA+Uk(4)))*(KNH/(KNH+Xk(10))^2);
rSNH4SNO4=-iXB*muH*(Xk(12)/(Ks+Xk(12)))*(KOH/(KOH+Uk(4)))*XBHk(4)*etag*(KNO/(KNO+Xk(11))^2);
rSNH4SS4=-iXB*muH*XBHk(4)*(Uk(4)/(KOH+Uk(4)))*(Ks/(Ks+Xk(12))^2);
rSNO4SNH4=(1/YA)*muA*XBAk(4)*(Uk(4)/(KOA+Uk(4)))*(KNH/(KNH+Xk(10))^2);
rSNO4SNO4=-((1-YH)/2.86*YH)*XBHk(4)*muH*etag*(Xk(12)/(Ks+Xk(12)))*(KOH/(KOH+Uk(4)))*(KNO/(KNO+Xk(11))^2);
rSNO4SS4=-((1-YH)/2.86*YH)*XBHk(4)*muH*etag*(KOH/(KOH+Uk(4)))*(Xk(11)/(KNO+Xk(11)))*(Ks/(Ks+Xk(12))^2);rSS4SNH4=0;
rSS4SNO4=-
(1/YH)*muH*(Xk(12)/(Ks+Xk(12)))*Kh*etah*((XSk(4)/XBHk(4))/(Kx+(XSk(4)/XBHk(4))))*XBHk(4)*(KOH/(KOH+Uk(4)))*(KNO/(KNO+Xk(11))^2);
rSS4SS4=-(1/YH)*muH*XBHk(4)*((Uk(4)/(KOH+Uk(4)))+(Xk(11)/(KNO+Xk(11)))*(KOH/(KOH+Uk(4))))*(Ks/(Ks+Xk(12)));
% Calculation of the derivatives of the process rates toward the process  variables for the Tank 5
rSNH5SNH5=-(iXB+1/YA)*muA*XBAk(5)*(Uk(5)/(KOA+Uk(5)))*(KNH/(KNH+Xk(13))^2);
rSNH5SNO5=-iXB*muH*(Xk(15)/(Ks+Xk(15)))*(KOH/(KOH+Uk(5)))*XBHk(5)*etag*(KNO/(KNO+Xk(14))^2);
rSNH5SS5=-iXB*muH*XBHk(5)*(Uk(5)/(KOH+Uk(5)))*(Ks/(Ks+Xk(15))^2);
rSNO5SNH5=(1/YA)*muA*XBAk(5)*(Uk(5)/(KOA+Uk(5)))*(KNH/(KNH+Xk(13))^2);
rSNO5SNO5=-((1-YH)/2.86*YH)*XBHk(5)*muH*etag*(Xk(15)/(Ks+Xk(15)))*(KOH/(KOH+Uk(5)))*(KNO/(KNO+Xk(14))^2);
rSNO5SS5=-((1-YH)/2.86*YH)*XBHk(5)*muH*etag*(KOH/(KOH+Uk(5)))*(Xk(14)/(KNO+Xk(14)))*(Ks/(Ks+Xk(15))^2);rSS5SNH5=0;
rSS5SNO5=-
(1/YH)*muH*(Xk(15)/(Ks+Xk(15)))*Kh*etah*((XSk(5)/XBHk(5))/(Kx+(XSk(5)/XBHk(5))))*XBHk(5)*(KOH/(KOH+Uk(5)))*(KNO/(KNO+Xk(14))^2);
rSS5SS5=-(1/YH)*muH*XBHk(5)*((Uk(5)/(KOH+Uk(5)))+(Xk(14)/(KNO+Xk(14)))*(KOH/(KOH+Uk(5))))*(Ks/(Ks+Xk(15)));


% Calculation of the derivatives of the process rates toward the process  parameter YH for the tank 1
rSNH1f=0.0;rSNO1f=0.0;rSS1f=0.0;rSNH1YH=0;
rSNO1YH=-muH*etag*XBHk(1)*(Xk(3)/(Ks+Xk(3)))*(KOH/(KOH+Uk(1)))*(Xk(2)/(KNO+Xk(2)))*(1/2.86*YH^2);
rSS1YH=(1/YH^2)*muH*XBHk(1)*(Xk(3)/(Ks+Xk(3)))*((Uk(1)/(KOH+Uk(1)))+(Xk(2)/(KNO+Xk(2)))*(KOH/(KOH+Uk(1))));
% Calculation of the derivatives of the process rates toward the process  parameter YA for the tank 1
rSNH1YA=(1/YA^2)*muA*(Uk(1)/(KOA+Uk(1)))*(Xk(1)/(KNH+Xk(1)))*XBAk(1);
rSNO1YA=-(1/YA^2)*muA*(Uk(1)/(KOA+Uk(1)))*(Xk(1)/(KNH+Xk(1)))*XBAk(1);rSS1YA=0;
% Calculation of the derivatives of the process rates toward the process  parameter iXB for the tank 1
rSNH1iXB=-muH*XBHk(1)*(Xk(3)/(Ks+Xk(3)))*((Uk(1)/(KOH+Uk(1)))+(Xk(2)/(KNO+Xk(2)))*(KOH/(KOH+Uk(1)))*etag)-
muA*(Uk(1)/(KOA+Uk(1)))*(Xk(1)/(KNH+Xk(1)))*XBAk(1);rSNO1iXB=0;rSS1iXB=0;
% Calculation of the derivatives of the process rates toward the process  parameter muA for the tank 1
rSNH1muA=-(iXB+1/YA)*(Uk(1)/(KOA+Uk(1)))*(Xk(1)/(KNH+Xk(1)))*XBAk(1);
rSNO1muA=(1/YA)*(Uk(1)/(KOA+Uk(1)))*(Xk(1)/(KNH+Xk(1)))*XBAk(1);rSS1muA=0;
% Calculation of the derivatives of the process rates toward the process  parameter muH for the tank 1
rSNH1muH=-iXB*XBHk(1)*(Xk(3)/(Ks+Xk(3)))*((Uk(1)/(KOH+Uk(1)))+etag*(Xk(2)/(KNO+Xk(2)))*(KOH/(KOH+Uk(1))));
rSNO1muH=-((1-YH)/2.86*YH)*XBHk(1)*(Xk(3)/(Ks+Xk(3)))*(KOH/(KOH+Uk(1)))*(Xk(2)/(KNO+Xk(2)));
rSS1muH=-(1/YH)*XBHk(1)*(Xk(3)/(Ks+Xk(3)))*((Uk(1)/(KOH+Uk(1)))+(Xk(2)/(KNO+Xk(2)))*(KOH/(KOH+Uk(1))));
% Calculation of the derivatives of the process rates toward the process  parameter KS for the tank 1
rSNH1KS=iXB*muH*XBHk(1)*(Xk(3)/(Ks+Xk(3)))^2)*((Uk(1)/(KOH+Uk(1)))+etag*(Xk(2)/(KNO+Xk(2)))*(KOH/(KOH+Uk(1))));
rSNO1KS=((1-YH)/2.86*YH)*XBHk(1)*muH*(Xk(3)/(Ks+Xk(3)))*(KOH/(KOH+Uk(1)))*(Xk(2)/(KNO+Xk(2)))*etag;
rSS1KS=(1/YH)*muH*XBHk(1)*(Xk(3)/(Ks+Xk(3)))^2)*((Uk(1)/(KOH+Uk(1)))+(Xk(2)/(KNO+Xk(2)))*(KOH/(KOH+Uk(1))));
% Calculation of the derivatives of the process rates toward the process  parameter KOH for the tank 1
rSNH1KOH=iXB*muH*XBHk(1)*(Xk(3)/(Ks+Xk(3)))*(Uk(1)/(KOH+Uk(1))^2)*(1-etag*(Xk(2)/(KNO+Xk(2))));
rSNO1KOH=-((1-YH)/2.86*YH)*XBHk(1)*muH*(Xk(3)/(Ks+Xk(3)))*(Uk(1)/(KOH+Uk(1))^2)*(Xk(2)/(KNO+Xk(2)));
rSS1KOH=(1/YH)*muH*XBHk(1)*(Xk(3)/(Ks+Xk(3)))*(Uk(1)/(KOH+Uk(1))^2)*(1-
(Xk(2)/(KNO+Xk(2))))+Kh*XBHk(1)*((XSk(1)/XBHk(1))/(Kx+(XSk(1)/XBHk(1))))*(Uk(1)/(KOH+Uk(1))^2)*(-1+etah*(Xk(2)/(KNO+Xk(2))));
% Calculation of the derivatives of the process rates toward the process  parameter KNO for the tank 1
rSNH1KNO=iXB*muH*XBHk(1)*etag*(Xk(3)/(Ks+Xk(3)))*(Xk(2)/(KNO+Xk(2))^2)*(KOH/(KOH+Uk(1)));
rSNO1KNO=((1-YH)/2.86*YH)*muH*XBHk(1)*etag*(Xk(3)/(Ks+Xk(3)))*(Xk(2)/(KNO+Xk(2))^2)*(KOH/(KOH+Uk(1)));
rSS1KNO=(1/YH)*muH*XBHk(1)*(Xk(3)/(Ks+Xk(3)))*(Xk(2)/(KNO+Xk(2))^2)*(KOH/(KOH+Uk(1)))-
Kh*XBHk(1)*etah*((XSk(1)/XBHk(1))/(Kx+(XSk(1)/XBHk(1))))*(Xk(2)/(KNO+Xk(2))^2)*(KOH/(KOH+Uk(1)));
% Calculation of the derivatives of the process rates toward the process  parameter KNH for the tank 1
rSNH1KNH=(iXB+1/YA)*muA*(Uk(1)/(KOA+Uk(1)))*(Xk(1)/(KNH+Xk(1)))*XBAk(1);
rSNO1KNH=-(1/YA)*muA*(Uk(1)/(KOA+Uk(1)))*(Xk(1)/(KNH+Xk(1)))*XBAk(1);rSS1KNH=0;
% Calculation of the derivatives of the process rates toward the process  parameter KOA for the tank 1
rSNH1KOA=(iXB+1/YA)*muA*(Uk(1)/(KOA+Uk(1))^2)*(Xk(1)/(KNH+Xk(1)))*XBAk(1);
rSNO1KOA=-(1/YA)*muA*(Uk(1)/(KOA+Uk(1))^2)*(Xk(1)/(KNH+Xk(1)))*XBAk(1);rSS1KOA=0;
% Calculation of the derivatives of the process rates toward the process  parameter etag for the tank 1
rSNH1etag=-iXB*muH*(Xk(3)/(Ks+Xk(3)))*(Xk(2)/(KNO+Xk(2)))*(KOH/(KOH+Uk(1)))*XBHk(1);
rSNO1etag=-((1-YH)/2.86*YH)*muH*(Xk(3)/(Ks+Xk(3)))*(Xk(2)/(KNO+Xk(2)))*(KOH/(KOH+Uk(1)))*XBHk(1);rSS1etag=0;
% Calculation of the derivatives of the process rates toward the process  parameter etah for the tank 1
rSNH1etah=0;rSNO1etah=0;
rSS1etah=Kh*((XSk(1)/XBHk(1))/(Kx+(XSk(1)/XBHk(1))))*(Uk(1)/(KOH+Uk(1)))*(Xk(2)/(KNO+Xk(2)))*(KOH/(KOH+Uk(1)))*XBHk(1);
% Calculation of the derivatives of the process rates toward the process  parameter Kh for the tank 1
rSNH1Kh=0;rSNO1Kh=0;
rSS1Kh=((XSk(1)/XBHk(1))/(Kx+(XSk(1)/XBHk(1))))*((Uk(1)/(KOH+Uk(1)))+etah*(Xk(2)/(KNO+Xk(2)))*(KOH/(KOH+Uk(1))))*XBHk(1);
% Calculation of the derivatives of the process rates toward the process  parameter Kx for the tank 1
rSNH1Kx=0;rSNO1Kx=0;
rSS1Kx=-Kh*((Uk(1)/(KOH+Uk(1)))+etah*(Xk(2)/(KNO+Xk(2)))*(KOH/(KOH+Uk(1))))*XBHk(1)*((XSk(1)/XBHk(1))/(Kx+(XSk(1)/XBHk(1))));

% Calculation of the derivatives of the process rates toward the process  parameter YH for the tank 2
rSNH2f=0.0;rSNO2f=0.0;rSS2f=0.0;rSNH2YH=0;
rSNO2YH=-muH*etag*XBHk(2)*(Xk(6)/(Ks+Xk(6)))*(KOH/(KOH+Uk(2)))*(Xk(5)/(KNO+Xk(5)))*(1/2.86*YH^2);
rSS2YH=(1/YH^2)*muH*XBHk(2)*(Xk(6)/(Ks+Xk(6)))*((Uk(2)/(KOH+Uk(2)))+(Xk(5)/(KNO+Xk(5)))*(KOH/(KOH+Uk(2))));
```

```
% Calculation of the derivatives of the process rates toward the process  parameter YA for the tank 2
rSNH2YA=(1/YA^2)*muA*(Uk(2)/(KOA+Uk(2)))*(Xk(4)/(KNH+Xk(4)))*XBAk(2);
rSNO2YA=-(1/YA^2)*muA*(Uk(2)/(KOA+Uk(2)))*(Xk(4)/(KNH+Xk(4)))*XBAk(2);rSS2YA=0;
% Calculation of the derivatives of the process rates toward the process  parameter iXB for the tank 2
rSNH2iXB=-muH*XBHk(2)*(Xk(6)/(Ks+Xk(6)))*((Uk(2)/(KOH+Uk(2)))+(Xk(5)/(KNO+Xk(5)))*(KOH/(KOH+Uk(2)))*etag)-
muA*(Uk(2)/(KOA+Uk(2)))*(Xk(4)/(KNH+Xk(4)))*XBAk(2);rSNO2iXB=0;rSS2iXB=0;
% Calculation of the derivatives of the process rates toward the process  parameter muA for the tank 2
rSNH2muA=-(iXB+1/YA)*(Uk(2)/(KOA+Uk(2)))*(Xk(4)/(KNH+Xk(4)))*XBAk(2);
rSNO2muA=(1/YA)*(Uk(2)/(KOA+Uk(2)))*(Xk(4)/(KNH+Xk(4)))*XBAk(2);rSS2muA=0;
% Calculation of the derivatives of the process rates toward the process  parameter muH for the tank 2
rSNH2muH=-iXB*XBHk(2)*(Xk(6)/(Ks+Xk(6)))*((Uk(2)/(KOH+Uk(2)))+etag*(Xk(5)/(KNO+Xk(5)))*(KOH/(KOH+Uk(2))));
rSNO2muH=-((1-YH)/2.86*YH)*XBHk(2)*(Xk(6)/(Ks+Xk(6)))*(KOH/(KOH+Uk(2)))*(Xk(5)/(KNO+Xk(5)));
rSS2muH=-(1/YH)*XBHk(2)*(Xk(6)/(Ks+Xk(6)))*((Uk(2)/(KOH+Uk(2)))+(Xk(5)/(KNO+Xk(5)))*(KOH/(KOH+Uk(2))));
% Calculation of the derivatives of the process rates toward the process  parameter KS for the tank 2
rSNH2KS=iXB*muH*XBHk(2)*(Xk(6)/(Ks+Xk(6))^2)*((Uk(2)/(KOH+Uk(2)))+etag*(Xk(5)/(KNO+Xk(5)))*(KOH/(KOH+Uk(2))));
rSNO2KS=((1-YH)/2.86*YH)*XBHk(2)*muH*(Xk(6)/(Ks+Xk(6)))*(KOH/(KOH+Uk(2)))*(Xk(5)/(KNO+Xk(5)))*etag;
rSS2KS=(1/YH)*muH*XBHk(2)*(Xk(6)/(Ks+Xk(6))^2)*((Uk(2)/(KOH+Uk(2)))+(Xk(5)/(KNO+Xk(5)))*(KOH/(KOH+Uk(2))));
% Calculation of the derivatives of the process rates toward the process  parameter KOH for the tank 2
rSNH2KOH=iXB*muH*XBHk(2)*(Xk(6)/(Ks+Xk(6)))*(Uk(2)/(KOH+Uk(2))^2)*(1-etag*(Xk(5)/(KNO+Xk(5))));
rSNO2KOH=-((1-YH)/2.86*YH)*XBHk(2)*muH*(Xk(6)/(Ks+Xk(6)))*(Uk(2)/(KOH+Uk(2))^2)*(Xk(5)/(KNO+Xk(5)));
rSS2KOH=(1/YH)*muH*XBHk(2)*(Xk(6)/(Ks+Xk(6)))*(Uk(2)/(KOH+Uk(2))^2)*(1-
(Xk(5)/(KNO+Xk(5))))+Kh*XBHk(2)*((XSk(2)/XBHk(2))/(Kx+(XSk(2)/XBHk(2))))*(Uk(2)/(KOH+Uk(2))^2)*(-1+etah*(Xk(5)/(KNO+Xk(5))));
% Calculation of the derivatives of the process rates toward the process  parameter KNO for the tank 2
rSNH2KNO=iXB*muH*XBHk(2)*etag*(Xk(6)/(Ks+Xk(6)))*(Xk(5)/(KNO+Xk(5))^2)*(KOH/(KOH+Uk(2)));
rSNO2KNO=((1-YH)/2.86*YH)*muH*XBHk(2)*etag*(Xk(6)/(Ks+Xk(6)))*(Xk(5)/(KNO+Xk(5))^2)*(KOH/(KOH+Uk(2)));
rSS2KNO=(1/YH)*muH*XBHk(2)*(Xk(6)/(Ks+Xk(6)))*(Xk(5)/(KNO+Xk(5))^2)*(KOH/(KOH+Uk(2)))-
Kh*XBHk(2)*etah*((XSk(2)/XBHk(2))/(Kx+(XSk(2)/XBHk(2))))*(Xk(5)/(KNO+Xk(5))^2)*(KOH/(KOH+Uk(2)));
% Calculation of the derivatives of the process rates toward the process  parameter KNH for the tank 2
rSNH2KNH=(iXB+1/YA)*muA*(Uk(2)/(KOA+Uk(2)))*(Xk(4)/(KNH+Xk(4)))*XBAk(2);
rSNO2KNH=-(1/YA)*muA*(Uk(2)/(KOA+Uk(2)))*(Xk(4)/(KNH+Xk(4)))*XBAk(2);rSS2KNH=0;
% Calculation of the derivatives of the process rates toward the process  parameter KOA for the tank 2
rSNH2KOA=(iXB+1/YA)*muA*(Uk(2)/(KOA+Uk(2))^2)*(Xk(4)/(KNH+Xk(4)))*XBAk(2);
rSNO2KOA=-(1/YA)*muA*(Uk(2)/(KOA+Uk(2))^2)*(Xk(4)/(KNH+Xk(4)))*XBAk(2);rSS2KOA=0;
% Calculationof the derivatives of the process rates toward the process  parameter  etag for the tank 2
rSNH2etag=-iXB*muH*(Xk(6)/(Ks+Xk(6)))*(Xk(5)/(KNO+Xk(5)))*(KOH/(KOH+Uk(2)))*XBHk(2);
rSNO2etag=-((1-YH)/2.86*YH)*muH*(Xk(6)/(Ks+Xk(6)))*(Xk(5)/(KNO+Xk(5)))*(KOH/(KOH+Uk(2)))*XBHk(2);rSS2etag=0;
% Calculation of the derivatives of the process rates toward the process  parameter etah for the tank 2
rSNH2etah=0;rSNO2etah=0;
rSS2etah=Kh*((XSk(2)/XBHk(2))/(Kx+(XSk(2)/XBHk(2))))*(Uk(2)/(KOH+Uk(2)))*(Xk(5)/(KNO+Xk(5)))*(KOH/(KOH+Uk(2)))*XBHk(2);
% Calculation for Kh for the tank 2
rSNH2Kh=0;rSNO2Kh=0;
rSS2Kh=((XSk(2)/XBHk(2))/(Kx+(XSk(2)/XBHk(2))))*((Uk(2)/(KOH+Uk(2)))+etah*(Xk(5)/(KNO+Xk(5)))*(KOH/(KOH+Uk(2))))*XBHk(2);
% Calculation of the derivatives of the process rates toward the process  parameter Kx for the tank 2
rSNH2Kx=0;rSNO2Kx=0;
rSS2Kx=-Kh*((Uk(2)/(KOH+Uk(2)))+etah*(Xk(5)/(KNO+Xk(5)))*(KOH/(KOH+Uk(2))))*XBHk(2)*((XSk(2)/XBHk(2))/(Kx+(XSk(2)/XBHk(2))));


% Calculation of the derivatives of the process rates toward the process  parameter YH for the tank 3
rSNH3f=0.0;rSNO3f=0.0;rSS3f=0.0;rSNH3YH=0;
rSNO3YH=-muH*etag*XBHk(3)*(Xk(9)/(Ks+Xk(9)))*(KOH/(KOH+Uk(3)))*(Xk(8)/(KNO+Xk(8)))*(1/2.86*YH^2);
rSS3YH=(1/YH^2)*muH*XBHk(3)*(Xk(9)/(Ks+Xk(9)))*((Uk(3)/(KOH+Uk(3)))+(Xk(8)/(KNO+Xk(8)))*(KOH/(KOH+Uk(3))));
% Calculation of the derivatives of the process rates toward the process  parameter YA for the tank 3
rSNH3YA=(1/YA^2)*muA*(Uk(3)/(KOA+Uk(3)))*(Xk(7)/(KNH+Xk(7)))*XBAk(3);
rSNO3YA=-(1/YA^2)*muA*(Uk(3)/(KOA+Uk(3)))*(Xk(7)/(KNH+Xk(7)))*XBAk(3);rSS3YA=0;
% Calculation of the derivatives of the process rates toward the process  parameter iXB for the tank 3
rSNH3iXB=-muH*XBHk(3)*(Xk(9)/(Ks+Xk(9)))*((Uk(3)/(KOH+Uk(3)))+(Xk(8)/(KNO+Xk(8)))*(KOH/(KOH+Uk(3)))*etag)-
muA*(Uk(3)/(KOA+Uk(3)))*(Xk(7)/(KNH+Xk(7)))*XBAk(3);rSNO3iXB=0;rSS3iXB=0;
% Calculation of the derivatives of the process rates toward the process  parameter muA for the tank 3
rSNH3muA=-(iXB+1/YA)*(Uk(3)/(KOA+Uk(3)))*(Xk(7)/(KNH+Xk(7)))*XBAk(3);
rSNO3muA=(1/YA)*(Uk(3)/(KOA+Uk(3)))*(Xk(7)/(KNH+Xk(7)))*XBAk(3);rSS3muA=0;
% Calculation of the derivatives of the process rates toward the process  parameter muH for the tank 3
rSNH3muH=-iXB*XBHk(3)*(Xk(9)/(Ks+Xk(9)))*((Uk(3)/(KOH+Uk(3)))+etag*(Xk(8)/(KNO+Xk(8)))*(KOH/(KOH+Uk(3))));
rSNO3muH=-((1-YH)/2.86*YH)*XBHk(3)*(Xk(9)/(Ks+Xk(9)))*(KOH/(KOH+Uk(3)))*(Xk(8)/(KNO+Xk(8)));
rSS3muH=-(1/YH)*XBHk(3)*(Xk(9)/(Ks+Xk(9)))*((Uk(3)/(KOH+Uk(3)))+(Xk(8)/(KNO+Xk(8)))*(KOH/(KOH+Uk(3))));
% Calculation of the derivatives of the process rates toward the process  parameter KS for the tank 3
rSNH3KS=iXB*muH*XBHk(3)*(Xk(9)/(Ks+Xk(9))^2)*((Uk(3)/(KOH+Uk(3)))+etag*(Xk(8)/(KNO+Xk(8)))*(KOH/(KOH+Uk(3))));
rSNO3KS=((1-YH)/2.86*YH)*XBHk(3)*muH*(Xk(9)/(Ks+Xk(9)))*(KOH/(KOH+Uk(3)))*(Xk(8)/(KNO+Xk(8)))*etag;
rSS3KS=(1/YH)*muH*XBHk(3)*(Xk(9)/(Ks+Xk(9))^2)*((Uk(3)/(KOH+Uk(3)))+(Xk(8)/(KNO+Xk(8)))*(KOH/(KOH+Uk(3))));
% Calculation of the derivatives of the process rates toward the process  parameter KOH for the tank 3
rSNH3KOH=iXB*muH*XBHk(3)*(Xk(9)/(Ks+Xk(9)))*(Uk(3)/(KOH+Uk(3))^2)*(1-etag*(Xk(8)/(KNO+Xk(8))));
rSNO3KOH=-((1-YH)/2.86*YH)*XBHk(3)*muH*(Xk(9)/(Ks+Xk(9)))*(Uk(3)/(KOH+Uk(3))^2)*(Xk(8)/(KNO+Xk(8)));
rSS3KOH=(1/YH)*muH*XBHk(3)*(Xk(9)/(Ks+Xk(9)))*(Uk(3)/(KOH+Uk(3))^2)*(1-
(Xk(8)/(KNO+Xk(8))))+Kh*XBHk(3)*((XSk(3)/XBHk(3))/(Kx+(XSk(3)/XBHk(3))))*(Uk(3)/(KOH+Uk(3))^2)*(-1+etah*(Xk(8)/(KNO+Xk(8))));
% Calculation of the derivatives of the process rates toward the process  parameter KNO for the tank 3
rSNH3KNO=iXB*muH*XBHk(3)*etag*(Xk(9)/(Ks+Xk(9)))*(Xk(8)/(KNO+Xk(8))^2)*(KOH/(KOH+Uk(3)));
rSNO3KNO=((1-YH)/2.86*YH)*muH*XBHk(3)*etag*(Xk(9)/(Ks+Xk(9)))*(Xk(8)/(KNO+Xk(8))^2)*(KOH/(KOH+Uk(3)));
rSS3KNO=(1/YH)*muH*XBHk(3)*(Xk(9)/(Ks+Xk(9)))*(Xk(8)/(KNO+Xk(8))^2)*(KOH/(KOH+Uk(3)))-
Kh*XBHk(3)*etah*((XSk(3)/XBHk(3))/(Kx+(XSk(3)/XBHk(3))))*(Xk(8)/(KNO+Xk(8))^2)*(KOH/(KOH+Uk(3)));
% Calculation of the derivatives of the process rates toward the process  parameter  KNH for the tank 3
rSNH3KNH=(iXB+1/YA)*muA*(Uk(3)/(KOA+Uk(3)))*(Xk(7)/(KNH+Xk(7)))*XBAk(3);
rSNO3KNH=-(1/YA)*muA*(Uk(3)/(KOA+Uk(3)))*(Xk(7)/(KNH+Xk(7)))*XBAk(3);rSS3KNH=0;
% Calculation of the derivatives of the process rates toward the process  parameter KOA for the tank 3
rSNH3KOA=(iXB+1/YA)*muA*(Uk(3)/(KOA+Uk(3))^2)*(Xk(7)/(KNH+Xk(7)))*XBAk(3);
rSNO3KOA=-(1/YA)*muA*(Uk(3)/(KOA+Uk(3))^2)*(Xk(7)/(KNH+Xk(7)))*XBAk(3);rSS3KOA=0;
% Calculation of the derivatives of the process rates toward the process  parameter etag for the tank 3
rSNH3etag=-iXB*muH*(Xk(9)/(Ks+Xk(9)))*(Xk(8)/(KNO+Xk(8)))*(KOH/(KOH+Uk(3)))*XBHk(3);
rSNO3etag=-((1-YH)/2.86*YH)*muH*(Xk(9)/(Ks+Xk(9)))*(Xk(8)/(KNO+Xk(8)))*(KOH/(KOH+Uk(3)))*XBHk(3);rSS3etag=0;
% Calculation  of the derivatives of the process rates toward the process  parameter etah for the tank 3
rSNH3etah=0;rSNO3etah=0;
rSS3etah=Kh*((XSk(3)/XBHk(3))/(Kx+(XSk(3)/XBHk(3))))*(Uk(3)/(KOH+Uk(3)))*(Xk(8)/(KNO+Xk(8)))*(KOH/(KOH+Uk(3)))*XBHk(3);
% Calculation of the derivatives of the process rates toward the process  parameter Kh for the tank 3
rSNH3Kh=0;rSNO3Kh=0;
rSS3Kh=((XSk(3)/XBHk(3))/(Kx+(XSk(3)/XBHk(3))))*((Uk(3)/(KOH+Uk(3)))+etah*(Xk(8)/(KNO+Xk(8)))*(KOH/(KOH+Uk(3))))*XBHk(3);
% Calculation of the derivatives of the process rates toward the process  parameter Kx for the tank 3
rSNH3Kx=0;rSNO3Kx=0;
rSS3Kx=-Kh*((Uk(3)/(KOH+Uk(3)))+etah*(Xk(8)/(KNO+Xk(8)))*(KOH/(KOH+Uk(3))))*XBHk(3)*((XSk(3)/XBHk(3))/(Kx+(XSk(3)/XBHk(3))));

% Calculation of the derivatives of the process rates toward the process  parameter YH for the tank 4
rSNH4f=0.0;rSNO4f=0.0;rSS4f=0.0;rSNH4YH=0;
```

```
rSNO4YH=-muH*etag*XBHk(4)*(Xk(12)/(Ks+Xk(12)))*(KOH/(KOH+Uk(4)))*(Xk(11)/(KNO+Xk(11)))*(1/2.86*YH^2);
rSS4YH=(1/YH^2)*muH*XBHk(4)*(Xk(12)/(Ks+Xk(12)))*((Uk(4)/(KOH+Uk(4)))+(Xk(11)/(KNO+Xk(11)))*(KOH/(KOH+Uk(4))));
% Calculation of the derivatives of the process rates toward the process  parameter YA for the tank 4
rSNH4YA=(1/YA^2)*muA*(Uk(4)/(KOA+Uk(4)))*(Xk(10)/(KNH+Xk(10)))*XBAk(4);
rSNO4YA=-(1/YA^2)*muA*(Uk(4)/(KOA+Uk(4)))*(Xk(10)/(KNH+Xk(10)))*XBAk(4);rSS4YA=0;
% Calculation of the derivatives of the process rates toward the process  parameter iXB for the tank 4
rSNH4iXB=-muH*XBHk(4)*(Xk(12)/(Ks+Xk(12)))*((Uk(4)/(KOH+Uk(4)))+(Xk(11)/(KNO+Xk(11)))*(KOH/(KOH+Uk(4)))*etag)-
muA*(Uk(4)/(KOA+Uk(4)))*(Xk(10)/(KNH+Xk(10)))*XBAk(4);rSNO4iXB=0;rSS4iXB=0;
% Calculation of the derivatives of the process rates toward the process  parameter muA for the tank 4
rSNH4muA=-(iXB+1/YA)*(Uk(4)/(KOA+Uk(4)))*(Xk(10)/(KNH+Xk(10)))*XBAk(4);
rSNO4muA=(1/YA)*(Uk(4)/(KOA+Uk(4)))*(Xk(10)/(KNH+Xk(10)))*XBAk(4);rSS4muA=0;
% Calculation of the derivatives of the process rates toward the process  parameter muH for the tank 4
rSNH4muH=-iXB*XBHk(4)*(Xk(12)/(Ks+Xk(12)))*((Uk(4)/(KOH+Uk(4)))+etag*(Xk(11)/(KNO+Xk(11)))*(KOH/(KOH+Uk(4))));
rSNO4muH=-((1-YH)/2.86*YH)*XBHk(4)*(Xk(12)/(Ks+Xk(12)))*(KOH/(KOH+Uk(4)))*(Xk(11)/(KNO+Xk(11)));
rSS4muH=-(1/YH)*XBHk(4)*(Xk(12)/(Ks+Xk(12)))*((Uk(4)/(KOH+Uk(4)))+(Xk(11)/(KNO+Xk(11)))*(KOH/(KOH+Uk(4))));
% Calculation of the derivatives of the process rates toward the process  parameter KS for the tank 4
rSNH4KS=iXB*muH*XBHk(4)*(Xk(12)/(Ks+Xk(12))^2)*((Uk(4)/(KOH+Uk(4)))+etag*(Xk(11)/(KNO+Xk(11)))*(KOH/(KOH+Uk(4))));
rSNO4KS=((1-YH)/2.86*YH)*XBHk(4)*muH*(Xk(12)/(Ks+Xk(12)))*(KOH/(KOH+Uk(4)))*(Xk(11)/(KNO+Xk(11)))*etag;
rSS4KS=(1/YH)*muH*XBHk(4)*(Xk(12)/(Ks+Xk(12))^2)*((Uk(4)/(KOH+Uk(4)))+(Xk(11)/(KNO+Xk(11)))*(KOH/(KOH+Uk(4))));
% Calculation of the derivatives of the process rates toward the process  parameter KOH for the tank 4
rSNH4KOH=iXB*muH*XBHk(4)*(Xk(12)/(Ks+Xk(12)))*(Uk(4)/(KOH+Uk(4))^2)*(1-etag*(Xk(11)/(KNO+Xk(11))));
rSNO4KOH=-((1-YH)/2.86*YH)*XBHk(4)*muH*(Xk(12)/(Ks+Xk(12)))*(Uk(4)/(KOH+Uk(4))^2)*(Xk(11)/(KNO+Xk(11)));
rSS4KOH=(1/YH)*muH*XBHk(4)*(Xk(12)/(Ks+Xk(12)))*(Uk(4)/(KOH+Uk(4))^2)*(1-
(Xk(11)/(KNO+Xk(11))))+Kh*XBHk(4)*((XSk(4)/XBHk(4))/(Kx+(XSk(4)/XBHk(4))))*(Uk(4)/(KOH+Uk(4))^2)*(-1+etah*(Xk(11)/(KNO+Xk(11))));
% Calculation of the derivatives of the process rates toward the process  parameter KNO for the tank 4
rSNH4KNO=iXB*muH*XBHk(4)*etag*(Xk(12)/(Ks+Xk(12)))*(Xk(11)/(KNO+Xk(11))^2)*(KOH/(KOH+Uk(4)));
rSNO4KNO=((1-YH)/2.86*YH)*muH*XBHk(4)*etag*(Xk(12)/(Ks+Xk(12)))*(Xk(11)/(KNO+Xk(11))^2)*(KOH/(KOH+Uk(4)));
rSS4KNO=(1/YH)*muH*XBHk(4)*(Xk(12)/(Ks+Xk(12)))*(Xk(11)/(KNO+Xk(11))^2)*(KOH/(KOH+Uk(4)))-
Kh*XBHk(4)*etah*((XSk(4)/XBHk(4))/(Kx+(XSk(4)/XBHk(4))))*(Xk(11)/(KNO+Xk(11))^2)*(KOH/(KOH+Uk(4)));
% Calculation of the derivatives of the process rates toward the process  parameter KNH for the tank 4
rSNH4KNH=(iXB+1/YA)*muA*(Uk(4)/(KOA+Uk(4)))*(Xk(10)/(KNH+Xk(10)))*XBAk(4);
rSNO4KNH=-(1/YA)*muA*(Uk(4)/(KOA+Uk(4)))*(Xk(10)/(KNH+Xk(10)))*XBAk(4);rSS4KNH=0;
% Calculation of the derivatives of the process rates toward the process  parameter KOA for the tank 4
rSNH4KOA=(iXB+1/YA)*muA*(Uk(4)/(KOA+Uk(4))^2)*(Xk(10)/(KNH+Xk(10)))*XBAk(4);
rSNO4KOA=-(1/YA)*muA*(Uk(4)/(KOA+Uk(4))^2)*(Xk(10)/(KNH+Xk(10)))*XBAk(4);rSS4KOA=0;
% Calculation of the derivatives of the process rates toward the process  parameter etag for the tank 4
rSNH4etag=-iXB*muH*(Xk(12)/(Ks+Xk(12)))*(Xk(11)/(KNO+Xk(11)))*(KOH/(KOH+Uk(4)))*XBHk(4);
rSNO4etag=-((1-YH)/2.86*YH)*muH*(Xk(12)/(Ks+Xk(12)))*(Xk(11)/(KNO+Xk(11)))*(KOH/(KOH+Uk(4)))*XBHk(4);rSS4etag=0;
% Calculation of the derivatives of the process rates toward the process  parameter etah for the tank 4
rSNH4etah=0;rSNO4etah=0;
rSS4etah=Kh*((XSk(4)/XBHk(4))/(Kx+(XSk(4)/XBHk(4))))*(Uk(4)/(KOH+Uk(4)))*(Xk(11)/(KNO+Xk(11)))*(KOH/(KOH+Uk(4)))*XBHk(4);
% Calculation of the derivatives of the process rates toward the process  parameter Kh for the tank 4
rSNH4Kh=0;rSNO4Kh=0;
rSS4Kh=((XSk(4)/XBHk(4))/(Kx+(XSk(4)/XBHk(4))))*((Uk(4)/(KOH+Uk(4)))+etah*(Xk(11)/(KNO+Xk(11)))*(KOH/(KOH+Uk(4))))*XBHk(4);
% Calculation of the derivatives of the process rates toward the process  parameter Kx for the tank 4
rSNH4Kx=0;rSNO4Kx=0;
rSS4Kx=-Kh*((Uk(4)/(KOH+Uk(4)))+etah*(Xk(11)/(KNO+Xk(11)))*(KOH/(KOH+Uk(4))))*XBHk(4)*((XSk(4)/XBHk(4))/(Kx+(XSk(4)/XBHk(4))));

% Calculation of the derivatives of the process rates toward the process  parameter YH for the tank 5
rSNH5f=0.0;rSNO5f=0.0;rSS5f=0.0;rSNH5YH=0;
rSNO5YH=-muH*etag*XBHk(5)*(Xk(15)/(Ks+Xk(15)))*(KOH/(KOH+Uk(5)))*(Xk(14)/(KNO+Xk(14)))*(1/2.86*YH^2);
rSS5YH=(1/YH^2)*muH*XBHk(5)*(Xk(15)/(Ks+Xk(15)))*((Uk(5)/(KOH+Uk(5)))+(Xk(14)/(KNO+Xk(14)))*(KOH/(KOH+Uk(5))));
% Calculation of the derivatives of the process rates toward the process  parameter  YA for the tank 5
rSNH5YA=(1/YA^2)*muA*(Uk(5)/(KOA+Uk(5)))*(Xk(13)/(KNH+Xk(13)))*XBAk(5);
rSNO5YA=-(1/YA^2)*muA*(Uk(5)/(KOA+Uk(5)))*(Xk(13)/(KNH+Xk(13)))*XBAk(5);rSS5YA=0;
% Calculation  of the derivatives of the process rates toward the process  parameter iXB for the tank 5
rSNH5iXB=-muH*XBHk(5)*(Xk(15)/(Ks+Xk(15)))*((Uk(5)/(KOH+Uk(5)))+(Xk(14)/(KNO+Xk(14)))*(KOH/(KOH+Uk(5)))*etag)-
muA*(Uk(5)/(KOA+Uk(5)))*(Xk(13)/(KNH+Xk(13)))*XBAk(5);rSNO5iXB=0;rSS5iXB=0;
% Calculation of the derivatives of the process rates toward the process  parameter muA for the tank 5
rSNH5muA=-(iXB+1/YA)*(Uk(5)/(KOA+Uk(5)))*(Xk(13)/(KNH+Xk(13)))*XBAk(5);
rSNO5muA=(1/YA)*(Uk(4)/(KOA+Uk(5)))*(Xk(13)/(KNH+Xk(13)))*XBAk(5);rSS5muA=0;
% Calculation of the derivatives of the process rates toward the process  parameter muH for the tank 5
rSNH5muH=-iXB*XBHk(5)*(Xk(15)/(Ks+Xk(15)))*((Uk(5)/(KOH+Uk(5)))+etag*(Xk(14)/(KNO+Xk(14)))*(KOH/(KOH+Uk(5))));
rSNO5muH=-((1-YH)/2.86*YH)*XBHk(5)*(Xk(15)/(Ks+Xk(15)))*(KOH/(KOH+Uk(5)))*(Xk(14)/(KNO+Xk(14)));
rSS5muH=-(1/YH)*XBHk(5)*(Xk(15)/(Ks+Xk(15)))*((Uk(5)/(KOH+Uk(5)))+(Xk(14)/(KNO+Xk(14)))*(KOH/(KOH+Uk(5))));
% Calculation of the derivatives of the process rates toward the process  parameter KS for the tank 5
rSNH5KS=iXB*muH*XBHk(5)*(Xk(15)/(Ks+Xk(15))^2)*((Uk(5)/(KOH+Uk(5)))+etag*(Xk(14)/(KNO+Xk(14)))*(KOH/(KOH+Uk(5))));
rSNO5KS=((1-YH)/2.86*YH)*XBHk(5)*muH*(Xk(15)/(Ks+Xk(15)))*(KOH/(KOH+Uk(5)))*(Xk(14)/(KNO+Xk(14)))*etag;
rSS5KS=(1/YH)*muH*XBHk(5)*(Xk(15)/(Ks+Xk(15))^2)*((Uk(5)/(KOH+Uk(5)))+(Xk(14)/(KNO+Xk(14)))*(KOH/(KOH+Uk(5))));
% Calculation of the derivatives of the process rates toward the process  parameter KOH for the tank 5
rSNH5KOH=iXB*muH*XBHk(5)*(Xk(15)/(Ks+Xk(15)))*(Uk(5)/(KOH+Uk(5))^2)*(1-etag*(Xk(14)/(KNO+Xk(14))));
rSNO5KOH=-((1-YH)/2.86*YH)*XBHk(5)*muH*(Xk(15)/(Ks+Xk(15)))*(Uk(5)/(KOH+Uk(5))^2)*(Xk(14)/(KNO+Xk(14)));
rSS5KOH=(1/YH)*muH*XBHk(4)*(Xk(15)/(Ks+Xk(15)))*(Uk(5)/(KOH+Uk(5))^2)*(1-
(Xk(14)/(KNO+Xk(14))))+Kh*XBHk(5)*((XSk(5)/XBHk(5))/(Kx+(XSk(5)/XBHk(5))))*(Uk(5)/(KOH+Uk(5))^2)*(-1+etah*(Xk(14)/(KNO+Xk(14))));
% Calculation of the derivatives of the process rates toward the process  parameter KNO for the tank 5
rSNH5KNO=iXB*muH*XBHk(5)*etag*(Xk(15)/(Ks+Xk(15)))*(Xk(14)/(KNO+Xk(14))^2)*(KOH/(KOH+Uk(5)));
rSNO5KNO=((1-YH)/2.86*YH)*muH*XBHk(5)*etag*(Xk(15)/(Ks+Xk(15)))*(Xk(14)/(KNO+Xk(14))^2)*(KOH/(KOH+Uk(5)));
rSS5KNO=(1/YH)*muH*XBHk(5)*(Xk(15)/(Ks+Xk(15)))*(Xk(14)/(KNO+Xk(14))^2)*(KOH/(KOH+Uk(5)))-
Kh*XBHk(5)*etah*((XSk(5)/XBHk(5))/(Kx+(XSk(5)/XBHk(5))))*(Xk(14)/(KNO+Xk(14))^2)*(KOH/(KOH+Uk(5)));
% Calculation of the derivatives of the process rates toward the process  parameter KNH for the tank 5
rSNH5KNH=(iXB+1/YA)*muA*(Uk(5)/(KOA+Uk(5)))*(Xk(13)/(KNH+Xk(13)))*XBAk(5);
rSNO5KNH=-(1/YA)*muA*(Uk(5)/(KOA+Uk(5)))*(Xk(13)/(KNH+Xk(13)))*XBAk(5);rSS5KNH=0;
% Calculation of the derivatives of the process rates toward the process  parameter KOA for the tank 5
rSNH5KOA=(iXB+1/YA)*muA*(Uk(5)/(KOA+Uk(5))^2)*(Xk(13)/(KNH+Xk(13)))*XBAk(5);
rSNO5KOA=-(1/YA)*muA*(Uk(5)/(KOA+Uk(5))^2)*(Xk(13)/(KNH+Xk(13)))*XBAk(5);rSS5KOA=0;
% Calculation of the derivatives of the process rates toward the process  parameter etag for the tank 5
rSNH5etag=-iXB*muH*(Xk(15)/(Ks+Xk(15)))*(Xk(14)/(KNO+Xk(14)))*(KOH/(KOH+Uk(5)))*XBHk(5);
rSNO5etag=-((1-YH)/2.86*YH)*muH*(Xk(15)/(Ks+Xk(15)))*(Xk(14)/(KNO+Xk(14)))*(KOH/(KOH+Uk(5)))*XBHk(5);rSS5etag=0;
% Calculation of the derivatives of the process rates toward the process  parameter etah for the tank 5
rSNH5etah=0;rSNO5etah=0;
rSS5etah=Kh*((XSk(5)/XBHk(5))/(Kx+(XSk(5)/XBHk(5))))*(Uk(5)/(KOH+Uk(5)))*(Xk(14)/(KNO+Xk(14)))*(KOH/(KOH+Uk(5)))*XBHk(5);
% Calculation of the derivatives of the process rates toward the process  parameter Kh for the tank 5
rSNH5Kh=0;rSNO5Kh=0;
rSS5Kh=((XSk(5)/XBHk(5))/(Kx+(XSk(5)/XBHk(5))))*((Uk(5)/(KOH+Uk(5)))+etah*(Xk(14)/(KNO+Xk(14)))*(KOH/(KOH+Uk(5))))*XBHk(5);
% Calculation of the derivatives of the process rates toward the process  parameter Kx for the tank 5
rSNH5Kx=0;rSNO5Kx=0;
rSS5Kx=-Kh*((Uk(5)/(KOH+Uk(5)))+etah*(Xk(14)/(KNO+Xk(14)))*(KOH/(KOH+Uk(5))))*XBHk(5)*((XSk(5)/XBHk(5))/(Kx+(XSk(5)/XBHk(5))));

% Development of the matrix AS of the sensitivity model
```

```
A1f=[A11(1,1)+DT*rSNH1SNH1 DT*rSNH1SNO1 DT*rSNH1SS1;
   DT*rSNO1SNH1 A11(2,2)+DT*rSNO1SNO1 DT*rSNO1SS1;
   DT*rSS1SNH1 DT*rSS1SNO1 A11(3,3)+DT*rSS1SS1];
A1S=[A11 zeros(3,45);zeros(3,3) A1f zeros(3,42);zeros(3,6) A1f zeros(3,39);zeros(3,9) A1f zeros(3,36);zeros(3,12) A1f
zeros(3,33);zeros(3,15) A1f zeros(3,30);zeros(3,18) A1f zeros(3,27);zeros(3,21) A1f zeros(3,24);zeros(3,24) A1f
zeros(3,21);zeros(3,27) A1f zeros(3,18);zeros(3,30) A1f zeros(3,15);zeros(3,33) A1f zeros(3,12);zeros(3,36) A1f
zeros(3,9);zeros(3,39) A1f zeros(3,6);zeros(3,42) A1f zeros(3,3);zeros(3,45) A1f];
A2f=[A22(1,1)+DT*rSNH2SNH2 DT*rSNH2SNO2 DT*rSNH2SS2;
   DT*rSNO2SNH2 A22(2,2)+DT*rSNO2SNO2 DT*rSNO2SS2;
   DT*rSS2SNH2 DT*rSS2SNO2 A22(3,3)+DT*rSS2SS2];
A2S=[A22 zeros(3,45);zeros(3,3) A2f zeros(3,42);zeros(3,6) A2f zeros(3,39);zeros(3,9) A2f zeros(3,36);zeros(3,12) A2f
zeros(3,33);zeros(3,15) A2f zeros(3,30);zeros(3,18) A2f zeros(3,27);zeros(3,21) A2f zeros(3,24);zeros(3,24) A2f
zeros(3,21);zeros(3,27) A2f zeros(3,18);zeros(3,30) A2f zeros(3,15);zeros(3,33) A2f zeros(3,12);zeros(3,36) A2f
zeros(3,9);zeros(3,39) A2f zeros(3,6);zeros(3,42) A2f zeros(3,3);zeros(3,45) A2f];
A3f=[A33(1,1)+DT*rSNH3SNH3 DT*rSNH3SNO3 DT*rSNH3SS3;
   DT*rSNO3SNH3 A33(2,2)+DT*rSNO3SNO3 DT*rSNO3SS3;
   DT*rSS3SNH3 DT*rSS3SNO3 A33(3,3)+DT*rSS3SS3];
A3S=[A33 zeros(3,45);zeros(3,3) A3f zeros(3,42);zeros(3,6) A3f zeros(3,39);zeros(3,9) A3f zeros(3,36);zeros(3,12) A3f
zeros(3,33);zeros(3,15) A3f zeros(3,30);zeros(3,18) A3f zeros(3,27);zeros(3,21) A3f zeros(3,24);zeros(3,24) A3f
zeros(3,21);zeros(3,27) A3f zeros(3,18);zeros(3,30) A3f zeros(3,15);zeros(3,33) A3f zeros(3,12);zeros(3,36) A3f
zeros(3,9);zeros(3,39) A3f zeros(3,6);zeros(3,42) A3f zeros(3,3);zeros(3,45) A3f];
A4f=[A44(1,1)+DT*rSNH4SNH4 DT*rSNH4SNO4 DT*rSNH4SS4;
   DT*rSNO4SNH4 A44(2,2)+DT*rSNO4SNO4 DT*rSNO4SS4;
   DT*rSS4SNH4 DT*rSS4SNO4 A44(3,3)+DT*rSS4SS4];
A4S=[A44 zeros(3,45);zeros(3,3) A4f zeros(3,42);zeros(3,6) A4f zeros(3,39);zeros(3,9) A4f zeros(3,36);zeros(3,12) A4f
zeros(3,33);zeros(3,15) A4f zeros(3,30);zeros(3,18) A4f zeros(3,27);zeros(3,21) A4f zeros(3,24);zeros(3,24) A4f
zeros(3,21);zeros(3,27) A4f zeros(3,18);zeros(3,30) A4f zeros(3,15);zeros(3,33) A4f zeros(3,12);zeros(3,36) A4f
zeros(3,9);zeros(3,39) A4f zeros(3,6);zeros(3,42) A4f zeros(3,3);zeros(3,45) A4f];
A5f=[A55(1,1)+DT*rSNH5SNH5 DT*rSNH5SNO5 DT*rSNH5SS5;
   DT*rSNO5SNH5 A55(2,2)+DT*rSNO5SNO5 DT*rSNO5SS5;
   DT*rSS5SNH5 DT*rSS5SNO5 A55(3,3)+DT*rSS5SS5];
A5S=[A55 zeros(3,45);zeros(3,3) A5f zeros(3,42);zeros(3,6) A5f zeros(3,39);zeros(3,9) A5f zeros(3,36);zeros(3,12) A5f
zeros(3,33);zeros(3,15) A5f zeros(3,30);zeros(3,18) A5f zeros(3,27);zeros(3,21) A5f zeros(3,24);zeros(3,24) A5f
zeros(3,21);zeros(3,27) A5f zeros(3,18);zeros(3,30) A5f zeros(3,15);zeros(3,33) A5f zeros(3,12);zeros(3,36) A5f
zeros(3,9);zeros(3,39) A5f zeros(3,6);zeros(3,42) A5f zeros(3,3);zeros(3,45) A5f];

%matrices of the interconnections
A15S=[A15 zeros(3,45);zeros(3,3) A15 zeros(3,42);zeros(3,6) A15 zeros(3,39);zeros(3,9) A15 zeros(3,36);zeros(3,12) A15
zeros(3,33);zeros(3,15) A15 zeros(3,30);zeros(3,18) A15 zeros(3,27);zeros(3,21) A15 zeros(3,24);zeros(3,24) A15
zeros(3,21);zeros(3,27) A15 zeros(3,18);zeros(3,30) A15 zeros(3,15);zeros(3,33) A15 zeros(3,12);zeros(3,36) A15
zeros(3,9);zeros(3,39) A15 zeros(3,6);zeros(3,42) A15 zeros(3,3);zeros(3,45) A15];
A21S=[A21 zeros(3,45);zeros(3,3) A21 zeros(3,42);zeros(3,6) A21 zeros(3,39);zeros(3,9) A21 zeros(3,36);zeros(3,12) A21
zeros(3,33);zeros(3,15) A21 zeros(3,30);zeros(3,18) A21 zeros(3,27);zeros(3,21) A21 zeros(3,24);zeros(3,24) A21
zeros(3,21);zeros(3,27) A21 zeros(3,18);zeros(3,30) A21 zeros(3,15);zeros(3,33) A21 zeros(3,12);zeros(3,36) A21
zeros(3,9);zeros(3,39) A21 zeros(3,6);zeros(3,42) A21 zeros(3,3);zeros(3,45) A21];
A32S=[A32 zeros(3,45);zeros(3,3) A32 zeros(3,42);zeros(3,6) A32 zeros(3,39);zeros(3,9) A32 zeros(3,36);zeros(3,12) A32
zeros(3,33);zeros(3,15) A32 zeros(3,30);zeros(3,18) A32 zeros(3,27);zeros(3,21) A32 zeros(3,24);zeros(3,24) A32
zeros(3,21);zeros(3,27) A32 zeros(3,18);zeros(3,30) A32 zeros(3,15);zeros(3,33) A32 zeros(3,12);zeros(3,36) A32
zeros(3,9);zeros(3,39) A32 zeros(3,6);zeros(3,42) A32 zeros(3,3);zeros(3,45) A32];
A43S=[A43 zeros(3,45);zeros(3,3) A43 zeros(3,42);zeros(3,6) A43 zeros(3,39);zeros(3,9) A43 zeros(3,36);zeros(3,12) A43
zeros(3,33);zeros(3,15) A43 zeros(3,30);zeros(3,18) A43 zeros(3,27);zeros(3,21) A43 zeros(3,24);zeros(3,24) A43
zeros(3,21);zeros(3,27) A43 zeros(3,18);zeros(3,30) A43 zeros(3,15);zeros(3,33) A43 zeros(3,12);zeros(3,36) A43
zeros(3,9);zeros(3,39) A43 zeros(3,6);zeros(3,42) A43 zeros(3,3);zeros(3,45) A43];
A54S=[A54 zeros(3,45);zeros(3,3) A54 zeros(3,42);zeros(3,6) A54 zeros(3,39);zeros(3,9) A54 zeros(3,36);zeros(3,12) A54
zeros(3,33);zeros(3,15) A54 zeros(3,30);zeros(3,18) A54 zeros(3,27);zeros(3,21) A54 zeros(3,24);zeros(3,24) A54
zeros(3,21);zeros(3,27) A54 zeros(3,18);zeros(3,30) A54 zeros(3,15);zeros(3,33) A54 zeros(3,12);zeros(3,36) A54
zeros(3,9);zeros(3,39) A54 zeros(3,6);zeros(3,42) A54 zeros(3,3);zeros(3,45) A54];

%the matrix of the state sensitivity
AS=[A1S zeros(48,144) A15S;A21S A2S zeros(48,144);zeros(48,48) A32S A3S zeros(48,96);zeros(48,96) A43S A4S
zeros(48,48);zeros(48,144) A54S A5S];

%matrix of the rates of the sensitivity model
C1S=[Cn zeros(4,45)];
CS=[C1S zeros(4,192);zeros(4,48) C1S zeros(4,144);zeros(4,96) C1S zeros(4,96); zeros(4,144) C1S zeros(4,48);zeros(4,192) C1S];

% Development of the matrix BS of the sensitivity model
B1theta=[B1(2,2) 0 0;zeros(44,3)];
B1S=[B1;B1theta];
BS=[B1S;zeros(192,3)];

% Development of the vector DS of the sensitivity model
% Calculation of the first tank
D1S=[zeros(1,3) rSNH1f rSNO1f rSS1f rSNH1YH rSNO1YH rSS1YH rSNH1YA rSNO1YA rSS1YA rSNH1iXB rSNO1iXB rSS1iXB rSNH1muA rSNO1muA
rSS1muA rSNH1muH rSNO1muH rSS1muH rSNH1KS rSNO1KS rSS1KS rSNH1KOH rSNO1KOH rSS1KOH rSNH1KNO rSNO1KNO rSS1KNO rSNH1KNH rSNO1KNH
rSS1KNH rSNH1KOA rSNO1KOA rSS1KOA rSNH1etag rSNO1etag rSS1etag rSNH1etah rSNO1etah rSS1etah rSNH1Kh rSNO1Kh rSS1Kh rSNH1Kx rSNO1Kx
rSS1Kx]';
% Calculation of the second tank
D2S=[zeros(1,3) rSNH2f rSNO2f rSS2f rSNH2YH rSNO2YH rSS2YH rSNH2YA rSNO2YA rSS2YA rSNH2iXB rSNO2iXB rSS2iXB rSNH2muA rSNO2muA
rSS2muA rSNH2muH rSNO2muH rSS2muH rSNH2KS rSNO2KS rSS2KS rSNH2KOH rSNO2KOH rSS2KOH rSNH2KNO rSNO2KNO rSS2KNO rSNH2KNH rSNO2KNH
rSS2KNH rSNH2KOA rSNO2KOA rSS2KOA rSNH2etag rSNO2etag rSS2etag rSNH2etah rSNO2etah rSS2etah rSNH2Kh rSNO2Kh rSS2Kh rSNH2Kx rSNO2Kx
rSS2Kx]';
% Calculation of the third tank
D3S=[zeros(1,3) rSNH3f rSNO3f rSS3f rSNH3YH rSNO3YH rSS3YH rSNH3YA rSNO3YA rSS3YA rSNH3iXB rSNO3iXB rSS3iXB rSNH3muA rSNO3muA
rSS3muA rSNH3muH rSNO3muH rSS3muH rSNH3KS rSNO3KS rSS3KS rSNH3KOH rSNO3KOH rSS3KOH rSNH3KNO rSNO3KNO rSS3KNO rSNH3KNH rSNO3KNH
rSS3KNH rSNH3KOA rSNO3KOA rSS3KOA rSNH3etag rSNO3etag rSS3etag rSNH3etah rSNO3etah rSS3etah rSNH3Kh rSNO3Kh rSS3Kh rSNH3Kx rSNO3Kx
rSS3Kx]';
% Calculation of the forth tank
D4S=[zeros(1,3) rSNH4f rSNO4f rSS4f rSNH4YH rSNO4YH rSS4YH rSNH4YA rSNO4YA rSS4YA rSNH4iXB rSNO4iXB rSS4iXB rSNH4muA rSNO4muA
rSS4muA rSNH4muH rSNO4muH rSS4muH rSNH4KS rSNO4KS rSS4KS rSNH4KOH rSNO4KOH rSS4KOH rSNH4KNO rSNO4KNO rSS4KNO rSNH4KNH rSNO4KNH
rSS4KNH rSNH4KOA rSNO4KOA rSS4KOA rSNH4etag rSNO4etag rSS4etag rSNH4etah rSNO4etah rSS4etah rSNH4Kh rSNO4Kh rSS4Kh rSNH4Kx rSNO4Kx
rSS4Kx]';
% Calculation of the fifth tank
D5S=[zeros(1,3) rSNH5f rSNO5f rSS5f rSNH5YH rSNO5YH rSS5YH rSNH5YA rSNO5YA rSS5YA rSNH5iXB rSNO5iXB rSS5iXB rSNH5muA rSNO5muA
rSS5muA rSNH5muH rSNO5muH rSS5muH rSNH5KS rSNO5KS rSS5KS rSNH5KOH rSNO5KOH rSS5KOH rSNH5KNO rSNO5KNO rSS5KNO rSNH5KNH rSNO5KNH
rSS5KNH rSNH5KOA rSNO5KOA rSS5KOA rSNH5etag rSNO5etag rSS5etag rSNH5etah rSNO5etah rSS5etah rSNH5Kh rSNO5Kh rSS5Kh rSNH5Kx rSNO5Kx
rSS5Kx]';
DS=[D1S;D2S;D3S;D4S;D5S]
```

SOFTWARE FOR SIMULATION OF SENSITIVITY FUNCTIONS OF THE PROCESS VARIABLES OF THE BENCHMARK MASS BALANCE MODEL BASED ON THE REDUCED UCT BIOLOGICAL MODEL TOWARDS ITS PARAMETERS

1.Main program

```
%PROGRAM BUCTS1.m
%Aim - the program calculates the sensitivity model and simulates the
%sensitivity functions for the process variables of the Benchmark process
%based on UCT reduced biological model towards the model parameters. The
%program call the function subroutine rateBUCTS.m. The calculation uses
%reduced biological model with 3 variables SNH, Sno,SS and Sads
%The program uses global definition of the model parameters

global Ks KOH KNO KNA KOA muH etag muA KMP fZBH YZH YZA KA KSA KSP fMA
%Process model parameters
f=1.2;YZA = 0.15;YZH = 0.67;fZBH = 0.068;muH = 0.05;Ks = 5;KOH = 0.002;KNO = 0.1;etag = 0.33KMP = 1.35;
muA = 0.5;KNA = 0.01;KA = 0.17;KOA = 0.002;fMA=1;KSP=0.027;KSA=1;
%Process tanks volumes and flowrates
V1 = 1000;V2 = 1000;V3 = 1333;V4 = 1333;V5 = 1333;Qo = 18446;Qa = 55338;Qr = 18446;Qw = 385;
%Average values of the influent variables
SSi=69.5;SNHi=31.56;SNOi=0.0;XSi=202.3;
%Determination of the sampling period
DT = 0.01042;days=0.1042*10;
K=days/DT
k=0:DT:days
%Influent concentrations trajectoriesfor SNH, SNO, SS and XS
Xi  =[SNHi*ones(1,K);SNOi*ones(1,K);SSi*ones(1,K);XSi*ones(1,K)]*1
%Initial conditions- steady state values for the Snh, Sno,Ss and zero for the sensitivity functions
XS0
=[7.918;5.37;2.808;82.135;zeros(68,1);8.344;3.662;1.459;5.15;zeros(68,1);5.548;6.541;1.15;5.1;zeros(68,1);2.967;9.299;0.995;4.8;ze
ros(68,1);1.733;10.415;0.889;4.2;zeros(68,1)];
% Steady state values for the biomass XBH, XBA, XS
XBH = 0.02*[2551.76*ones(1,K);2553.38*ones(1,K);2557.13*ones(1,K);2559.18*ones(1,K);2559.34*ones(1,K)];% XBH steady state COD/m^3
XBA = 0.02*[148.389*ones(1,K);148.309*ones(1,K);148.941*ones(1,K);149.527*ones(1,K);149.797*ones(1,K)];% XBA steady state g all
COD/m^3
XS = 0.02*[82.135*ones(1,K);76.386*ones(1,K);64.855*ones(1,K);55.694*ones(1,K);49.306*ones(1,K)]; % XS steady state all COD/m^3
%trajectory of the control signal
SO1 = [0.2*ones(1,K);0.2*ones(1,K)];
SO2=[2.0*ones(1,K);2.29*ones(1,K);1.91*ones(1,K)];
U=[SO1;SO2];
% calculation of the initial trajectory for the state vector X and for the sensitivity vector XSS
X =[[7.918;5.37;2.808;5.3;8.344;3.662;1.459;5.15;5.548;6.541;1.15;5.1;2.967;9.299;0.995;4.8;1.733;10.415;0.889;4.2] zeros(20,K)];
XSS = [XS0 zeros(360,K
%Calculation of the process state space model matrices
%calculation of the matrix Au
IV1 = DT/V1;IV2 = DT/V2;IV3 = DT/V3;IV4 = DT/V4;IV5 = DT/V5;IV=IV1*Qo;IVV=IV*f;Q=Qo+Qa+Qr;
IV21=IV2*Q;IV32=IV3*Q;IV43=IV4*Q;IV54=IV5*Q;IV11=1-IV1*Q;IV22=1-IV21;IV33=1-IV32;IV44=1-IV43;IV55=1-IV54;IV15=IV1*(Qa+Qr);

Au=[[IV11 0.0 0.0 0.0;0.0 IV11 0.0 0.0;0.0 0.0 IV11 0.0;0.0 0.0 0.0 IV11] zeros(4,12) [IV15 0.0 0.0 0.0;0.0 IV15 0.0 0.0;0.0 0.0
IV15 0.0;0.0 0.0 0.0 IV15];
    [IV21 0.0 0.0 0.0;0.0 IV21 0.0 0.0;0.0 0.0 IV21 0.0;0.0 0.0 0.0 IV21] [IV22 0.0 0.0 0.0;0.0 IV22 0.0 0.0;0.0 0.0 IV22 0.0;0.0
0.0 0.0 IV22] zeros(4,12);
    zeros(4,4) [IV32 0.0 0.0 0.0;0.0 IV32 0.0 0.0;0.0 0.0 IV32 0.0;0.0 0.0 0.0 IV32] [IV33 0.0 0.0 0.0;0.0 IV33 0.0 0.0;0.0 0.0
IV33 0.0;0.0 0.0 0.0 IV33] zeros(4,8);
    zeros(4,8) [IV43 0.0 0.0 0.0;0.0 IV43 0.0 0.0;0.0 0.0 IV43 0.0;0.0 0.0 0.0 IV43] [IV44 0.0 0.0 0.0;0.0 IV44 0.0 0.0;0.0 0.0
IV44 0.0;0.0 0.0 0.0 IV44] zeros(4,4);
    zeros(4,12) [IV54 0.0 0.0 0.0;0.0 IV54 0.0 0.0;0.0 0.0 IV54 0.0;0.0 0.0 0.0 IV54] [IV55 0.0 0.0 0.0;0.0 IV55 0.0 0.0;0.0 0.0
IV55 0.0;0.0 0.0 0.0 IV55]]
A11u=Au(1:4,1:4);A15u=Au(1:4,17:20);A21u=Au(5:8,1:4);A22u=Au(5:8,5:8);A32u=Au(9:12,5:8);A33u=Au(9:12,9:12);
A43u=Au(13:16,9:12);A44u=Au(13:16,13:16);A54u=Au(17:20,13:16);A55u=Au(17:20,17:20);
% Development of the matrix Bu
B1u=[IVV 0.0 0.0 0.0;0.0 IV 0.0 0.0;0.0 0.0 IV 0.0;0.0 0.0 0.0 IV];
Bu=[B1u;zeros(16,4)];
% Development of the matrix Cu
x1=-1/YZH;x2=1/YZA;x3=(1-YZH)/(2.86*YZH);x4=x3-fZBH;x5=-x2-fZBH;
Cnu=[-fZBH 0 x1 0;0 -fZBH x1 0;-fZBH -x3 x1 0;0 x3-fZBH x1 0;-fZBH 0 0 x1;0 -fZBH 0 x1;-fZBH -x3 0 x1;0 x3-fZBH 0 x1;0 0 0 1;-x2-
fZBH x2 0 0];
Cu=[Cnu zeros(10,16);zeros(10,4) Cnu zeros(10,12);zeros(10,8) Cnu zeros(10,8);zeros(10,12) Cnu zeros(10,4);zeros(10,16) Cnu];
%Simulation of the sensitivity model
for k = 1:K
    XSSk = XSS(:,k);
    Xk=X(:,k);
    Uk =U(:,k);
```

```
    XBHk = XBH(:,k);
    XBAk = XBA(:,k);
    XSk = XS(:,k);
    Xik = Xi(:,k);
   [ROUCT,ASu,BSu,CSu,DSu]=rateBUCTS(Xk,Uk,XBHk,XBAk,XSk,DT,A11u,A15u,A21u,A22u,A32u,A33u,A43u,A44u,A54u,A55u,B1u,Cnu);

    XSS(:,k+1) = ASu*XSS(:,k) + CSu'*ROUCT + BSu*Xi(:,k)+DSu;
    X(:,k+1) = [XSS(1:4,k+1);XSS(73:76,k+1);XSS(145:148,k+1);XSS(217:220,k+1);XSS(289:292,k+1)];
end

%vector of sensitivity for the first tank XStheta
SNH1=XSS(1,:);SNO1=XSS(2,:);SS1=XSS(3,:);Sads1=XSS(4,:);
SNH1f=XSS(5,:);SNO1f=XSS(6,:);SS1f=XSS(7,:);Sads1f=XSS(8,:);
SNH1YZH=XSS(9,:);SNO1YZH=XSS(10,:);SS1YZH=XSS(11,:);Sads1YZH=XSS(12,:);
SNH1YZA=XSS(13,:);SNO1YZA=XSS(14,:);SS1YZA=XSS(15,:);Sads1YZA=XSS(16,:);
SNH1fZBH=XSS(17,:);SNO1fZBH=XSS(18,:);SS1fZBH=XSS(19,:);Sads1fZBH=XSS(20,:);
SNH1muA=XSS(21,:);SNO1muA=XSS(22,:);SS1muA=XSS(23,:);Sads1muA=XSS(24,:);
SNH1muH=XSS(25,:);SNO1muH=XSS(26,:);SS1muH=XSS(27,:);Sads1muH=XSS(28,:);
SNH1KS=XSS(29,:);SNO1KS=XSS(30,:);SS1KS=XSS(31,:);Sads1KS=XSS(32,:);
SNH1KOH=XSS(33,:);SNO1KOH=XSS(34,:);SS1KOH=XSS(35,:);Sads1KOH=XSS(36,:);
SNH1KNO=XSS(37,:);SNO1KNO=XSS(38,:);SS1KNO=XSS(39,:);Sads1KNO=XSS(40,:);
SNH1KNH=XSS(41,:);SNO1KNH=XSS(22,:);SS1KNH=XSS(43,:);Sads1KNH=XSS(44,:);
SNH1KOA=XSS(45,:);SNO1KOA=XSS(46,:);SS1KOA=XSS(47,:);Sads1KOA=XSS(48,:);
SNH1etag=XSS(49,:);SNO1etag=XSS(50,:);SS1etag=XSS(51,:);Sads1etag=XSS(52,:);
SNH1KMP=XSS(53,:);SNO1KMP=XSS(54,:);SS1KMP=XSS(55,:);Sads1KMP=XSS(56,:);
SNH1KSP=XSS(57,:);SNO1KSP=XSS(58,:);SS1KSP=XSS(59,:);Sads1KSP=XSS(60,:);
SNH1KSA=XSS(61,:);SNO1KSA=XSS(62,:);SS1KSA=XSS(63,:);Sads1KSA=XSS(64,:);
SNH1fMA=XSS(65,:);SNO1fMA=XSS(66,:);SS1fMA=XSS(67,:);Sads1fMA=XSS(68,:);
SNH1KA=XSS(69,:);SNO1KA=XSS(70,:);SS1KA=XSS(71,:);Sads1KA=XSS(72,:);
%vector of sensitivity for the second tank XStheta
SNH2=XSS(73,:);SNO2=XSS(74,:);SS2=XSS(75,:);Sads2=XSS(76,:)
SNH2f=XSS(77,:);SNO2f=XSS(78,:);SS2f=XSS(79,:);Sads2f=XSS(80,:);
SNH2YZH=XSS(81,:);SNO2YZH=XSS(82,:);SS2YZH=XSS(83,:);Sads2YZH=XSS(84,:);
SNH2YZA=XSS(85,:);SNO2YZA=XSS(86,:);SS2YZA=XSS(87,:);Sads2YZA=XSS(88,:);
SNH2fZBH=XSS(89,:);SNO2fZBH=XSS(90,:);SS2fZBH=XSS(91,:);Sads2fZBH=XSS(92,:);
SNH2muA=XSS(93,:);SNO2muA=XSS(94,:);SS2muA=XSS(95,:);Sads2muA=XSS(96,:);
SNH2muH=XSS(97,:);SNO2muH=XSS(98,:);SS2muH=XSS(99,:);Sads2muH=XSS(100,:);
SNH2KS=XSS(101,:);SNO2KS=XSS(102,:);SS2KS=XSS(103,:);Sads2KS=XSS(104,:);
SNH2KOH=XSS(105,:);SNO2KOH=XSS(106,:);SS2KOH=XSS(107,:);Sads2KOH=XSS(108,:);
SNH2KNO=XSS(109,:);SNO2KNO=XSS(110,:);SS2KNO=XSS(111,:);Sads2KNO=XSS(112,:);
SNH2KNH=XSS(113,:);SNO2KNH=XSS(114,:);SS2KNH=XSS(115,:);Sads2KNH=XSS(116,:);
SNH2KOA=XSS(117,:);SNO2KOA=XSS(118,:);SS2KOA=XSS(119,:);Sads2KOA=XSS(120,:);
SNH2etag=XSS(121,:);SNO2etag=XSS(122,:);SS2etag=XSS(123,:);Sads2etag=XSS(124,:);
SNH2KMP=XSS(125,:);SNO2KMP=XSS(126,:);SS2KMP=XSS(127,:);Sads2KMP=XSS(128,:);
SNH2KSP=XSS(129,:);SNO2KSP=XSS(130,:);SS2KSP=XSS(131,:);Sads2KSP=XSS(132,:);
SNH2KSA=XSS(133,:);SNO2KSA=XSS(134,:);SS2KSA=XSS(135,:);Sads2KSA=XSS(136,:);
SNH2fMA=XSS(137,:);SNO2fMA=XSS(138,:);SS2fMA=XSS(139,:);Sads2fMA=XSS(140,:);
SNH2KA=XSS(141,:);SNO2KA=XSS(142,:);SS2KA=XSS(143,:);Sads2KA=XSS(144,:);

%vector of sensitivity for the third tank XStheta
SNH3=XSS(145,:);SNO3=XSS(146,:);SS3=XSS(147,:);Sads3=XSS(148,:)
SNH3f=XSS(149,:);SNO3f=XSS(150,:);SS3f=XSS(151,:);Sads3f=XSS(152,:);
SNH3YZH=XSS(153,:);SNO3YZH=XSS(154,:);SS3YZH=XSS(155,:);Sads3YZH=XSS(156,:);
SNH3YZA=XSS(157,:);SNO3YZA=XSS(158,:);SS3YZA=XSS(159,:);Sads3YZA=XSS(160,:);
SNH3fZBH=XSS(161,:);SNO3fZBH=XSS(162,:);SS3fZBH=XSS(163,:);Sads3fZBH=XSS(164,:);
SNH3muA=XSS(165,:);SNO3muA=XSS(166,:);SS3muA=XSS(167,:);Sads3muA=XSS(168,:);
SNH3muH=XSS(169,:);SNO3muH=XSS(170,:);SS3muH=XSS(171,:);Sads3muH=XSS(172,:);
SNH3KS=XSS(173,:);SNO3KS=XSS(174,:);SS3KS=XSS(175,:);Sads3KS=XSS(176,:);
SNH3KOH=XSS(177,:);SNO3KOH=XSS(178,:);SS3KOH=XSS(179,:);Sads3KOH=XSS(180,:);
SNH3KNO=XSS(181,:);SNO3KNO=XSS(182,:);SS3KNO=XSS(183,:);Sads3KNO=XSS(184,:);
SNH3KNH=XSS(185,:);SNO3KNH=XSS(186,:);SS3KNH=XSS(187,:);Sads3KNH=XSS(188,:);
SNH3KOA=XSS(189,:);SNO3KOA=XSS(190,:);SS3KOA=XSS(191,:);Sads3KOA=XSS(192,:);
SNH3etag=XSS(193,:);SNO3etag=XSS(194,:);SS3etag=XSS(195,:);Sads3etag=XSS(196,:);
SNH3KMP=XSS(197,:);SNO3KMP=XSS(198,:);SS3KMP=XSS(199,:);Sads3KMP=XSS(200,:);
SNH3KSP=XSS(201,:);SNO3KSP=XSS(202,:);SS3KSP=XSS(203,:);Sads3KSP=XSS(204,:);
SNH3KSA=XSS(205,:);SNO3KSA=XSS(206,:);SS3KSA=XSS(207,:);Sads3KSA=XSS(208,:);
SNH3fMA=XSS(209,:);SNO3fMA=XSS(210,:);SS3fMA=XSS(211,:);Sads3fMA=XSS(212,:);
SNH3KA=XSS(213,:);SNO3KA=XSS(214,:);SS3KA=XSS(215,:);Sads3KA=XSS(216,:);

%vector of sensitivity for the fourth tank XStheta
SNH4=XSS(217,:);SNO4=XSS(218,:);SS4=XSS(219,:);Sads4=XSS(220,:)
SNH4f=XSS(221,:);SNO4f=XSS(222,:);SS4f=XSS(223,:);Sads4f=XSS(224,:);
SNH4YZH=XSS(225,:);SNO4YZH=XSS(226,:);SS4YZH=XSS(227,:);Sads4YZH=XSS(228,:);
SNH4YZA=XSS(229,:);SNO4YZA=XSS(230,:);SS4YZA=XSS(231,:);Sads4YZA=XSS(232,:);
SNH4fZBH=XSS(233,:);SNO4fZBH=XSS(234,:);SS4fZBH=XSS(235,:);Sads4fZBH=XSS(236,:);
SNH4muA=XSS(237,:);SNO4muA=XSS(238,:);SS4muA=XSS(239,:);Sads4muA=XSS(240,:);
SNH4muH=XSS(241,:);SNO4muH=XSS(242,:);SS4muH=XSS(243,:);Sads4muH=XSS(244,:);
SNH4KS=XSS(245,:);SNO4KS=XSS(246,:);SS4KS=XSS(247,:);Sads4KS=XSS(248,:);
SNH4KOH=XSS(249,:);SNO4KOH=XSS(250,:);SS4KOH=XSS(251,:);Sads4KOH=XSS(252,:);
SNH4KNO=XSS(253,:);SNO4KNO=XSS(254,:);SS4KNO=XSS(255,:);Sads4KNO=XSS(256,:);
SNH4KNH=XSS(257,:);SNO4KNH=XSS(258,:);SS4KNH=XSS(259,:);Sads4KNH=XSS(260,:);
SNH4KOA=XSS(261,:);SNO4KOA=XSS(262,:);SS4KOA=XSS(263,:);Sads4KOA=XSS(264,:);
SNH4etag=XSS(265,:);SNO4etag=XSS(266,:);SS4etag=XSS(267,:);Sads4etag=XSS(268,:);
SNH4KMP=XSS(269,:);SNO4KMP=XSS(270,:);SS4KMP=XSS(271,:);Sads4KMP=XSS(272,:);
SNH4KSP=XSS(273,:);SNO4KSP=XSS(274,:);SS4KSP=XSS(275,:);Sads4KSP=XSS(276,:);
SNH4KSA=XSS(277,:);SNO4KSA=XSS(278,:);SS4KSA=XSS(279,:);Sads4KSA=XSS(280,:);
SNH4fMA=XSS(281,:);SNO4fMA=XSS(282,:);SS4fMA=XSS(283,:);Sads4fMA=XSS(284,:);
SNH4KA=XSS(285,:);SNO4KA=XSS(286,:);SS4KA=XSS(287,:);Sads4KA=XSS(288,:);

%vector of sensitivity for the fifth tank XStheta
SNH5=XSS(289,:);SNO5=XSS(290,:);SS5=XSS(291,:);Sads5=XSS(292,:)
SNH5f=XSS(293,:);SNO5f=XSS(294,:);SS5f=XSS(295,:);Sads5f=XSS(296,:);
SNH5YZH=XSS(297,:);SNO5YZH=XSS(298,:);SS5YZH=XSS(299,:);Sads5YZH=XSS(300,:);
SNH5YZA=XSS(301,:);SNO5YZA=XSS(302,:);SS5YZA=XSS(303,:);Sads5YZA=XSS(304,:);
SNH5fZBH=XSS(305,:);SNO5fZBH=XSS(306,:);SS5fZBH=XSS(307,:);Sads5fZBH=XSS(308,:);
SNH5muA=XSS(309,:);SNO5muA=XSS(310,:);SS5muA=XSS(311,:);Sads5muA=XSS(312,:);
SNH5muH=XSS(313,:);SNO5muH=XSS(314,:);SS5muH=XSS(315,:);Sads5muH=XSS(316,:);
SNH5KS=XSS(317,:);SNO5KS=XSS(318,:);SS5KS=XSS(319,:);Sads5KS=XSS(320,:);
SNH5KOH=XSS(321,:);SNO5KOH=XSS(322,:);SS5KOH=XSS(323,:);Sads5KOH=XSS(324,:);
```

```
SNH5KNO=XSS(325,:);SNO5KNO=XSS(326,:);SS5KNO=XSS(327,:);Sads5KNO=XSS(328,:);
SNH5KNH=XSS(329,:);SNO5KNH=XSS(330,:);SS5KNH=XSS(331,:);Sads5KNH=XSS(332,:);
SNH5KOA=XSS(333,:);SNO5KOA=XSS(334,:);SS5KOA=XSS(335,:);Sads5KOA=XSS(336,:);
SNH5etag=XSS(337,:);SNO5etag=XSS(338,:);SS5etag=XSS(339,:);Sads5etag=XSS(340,:);
SNH5KMP=XSS(341,:);SNO5KMP=XSS(342,:);SS5KMP=XSS(343,:);Sads5KMP=XSS(344,:);
SNH5KSP=XSS(345,:);SNO5KSP=XSS(346,:);SS5KSP=XSS(347,:);Sads5KSP=XSS(348,:);
SNH5KSA=XSS(349,:);SNO5KSA=XSS(350,:);SS5KSA=XSS(351,:);Sads5KSA=XSS(352,:);
SNH5fMA=XSS(353,:);SNO5fMA=XSS(354,:);SS5fMA=XSS(355,:);Sads5fMA=XSS(356,:);
SNH5KA=XSS(357,:);SNO5KA=XSS(358,:);SS5KA=XSS(359,:);Sads5KA=XSS(360,:);

k=1:101
%Graphs of the sensitivity functions for the SNH
%Graphs for the first tank
figure(1)
subplot(9,2,1);plot(k,SNH1,'k')
title('Process variable Snh1')
ylabel('\fontsize{8}SNH1')
xlabel('\fontsize{8}discrete time k')

subplot(9,2,2); plot(k,SNH1f,'k')
title('Sensitivity function Snh1f')
ylabel('\fontsize{8}SNH1f')
xlabel('\fontsize{8}discrete time,k')

subplot(9,2,3); plot(k,SNH1YZH,'k')
title('Variable Snh1YZH')
ylabel('\fontsize{8}SNH1YZH')
xlabel('\fontsize{8}discrete time,k')

subplot(9,2,4); plot(k,SNH1YZA,'k')
title('Variable Snh1YZA')
ylabel('\fontsize{8}SNH1YZA')
xlabel('\fontsize{8}discrete time,k')

subplot(9,2,5); plot(k,SNH1fZBH,'k')
title('Sensitivity function Snh1fZBH')
ylabel('\fontsize{8}SNH1fZBH')
xlabel('discrete time,k')

subplot(9,2,6); plot(k,SNH1muA,'k')
title('Sensitivity function Snh1muA')
ylabel('\fontsize{8}SNH1muA')
xlabel('\fontsize{8}discrete time,k')

subplot(9,2,7); plot(k,SNH1muH,'k')
title('Sensitivity function Snh1muH')
ylabel('\fontsize{8}SNH1muH')
xlabel('discrete time,k')

subplot(9,2,8); plot(k,SNH1KS,'k')
title('Sensitivity function Snh1KS')
ylabel('\fontsize{8}SNH1KS')
xlabel('discrete time,k')

subplot(9,2,9); plot(k,SNH1KOH,'k')
title('Sensitivity function Snh1KOH')
ylabel('\fontsize{8}SNH1KOH')
xlabel('\fontsize{8}discrete time,k')

subplot(9,2,10); plot(k,SNH1KNO,'k')
title('Sensitivity function Snh1KNO')
ylabel('\fontsize{8}SNH1KNO')
xlabel('\fontsize{8}discrete time,k')

subplot(9,2,11); plot(k,SNH1KNH,'k')
title('Sensitivity function Snh1KNH')
ylabel('\fontsize{8}SNH1KNH')
xlabel('\fontsize{8}discrete time,k')

subplot(9,2,12); plot(k,SNH1KOA,'k')
title('Sensitivity function Snh1KOA')
ylabel('\fontsize{8}SNH1KOA')
xlabel('\fontsize{8}discrete time,k')

subplot(9,2,13); plot(k,SNH1etag,'k')
title('Sensitivity function Snh1etag')
ylabel('\fontsize{8}SNH1etag')
xlabel('\fontsize{8}discrete time,k')

subplot(9,2,14); plot(k,SNH1KMP,'k')
title('Sensitivity function Snh1KMP')
ylabel('\fontsize{8}SNH1KMP')
xlabel('\fontsize{8}discrete time,k')

subplot(9,2,15); plot(k,SNH1KSP,'k')
title('Sensitivity function Snh1KSP')
ylabel('\fontsize{8}SNH1KSP')
xlabel('\fontsize{8}discrete time,k')

subplot(9,2,16); plot(k,SNH1KSA,'k')
title('Sensitivity function Snh1KSA')
ylabel('\fontsize{8}SNH1KSA')
xlabel('\fontsize{8}discrete time,k')

subplot(9,2,17); plot(k,SNH1fMA,'k')
title('Sensitivity function Snh1fMA')
ylabel('\fontsize{8}SNH1fMA')
xlabel('\fontsize{8}discrete time,k')

subplot(9,2,18); plot(k,SNH1KA,'k')
title('Sensitivity function Snh1KA')
ylabel('\fontsize{8}SNH1KA')
xlabel('\fontsize{8}discrete time,k')

%Graphs for the second tank

figure(2)
subplot(9,2,1);plot(k,SNH2,'k')
title('Process variable Snh2')
ylabel('\fontsize{8}SNH2')
xlabel('\fontsize{8}discrete time k')

subplot(9,2,2); plot(k,SNH2f,'k')
title('Sensitivity function Snh2f')
ylabel('\fontsize{8}SNH2f')
xlabel('\fontsize{8}discrete time,k')

subplot(9,2,3); plot(k,SNH2YZH,'k')
title('Variable Snh2YZH')
ylabel('\fontsize{8}SNH2YZH')
xlabel('\fontsize{8}discrete time,k')

subplot(9,2,4); plot(k,SNH2YZA,'k')
title('Variable Snh2YZA')
ylabel('\fontsize{8}SNH2YZA')
xlabel('\fontsize{8}discrete time,k')

subplot(9,2,5); plot(k,SNH2fZBH,'k')
title('Sensitivity function Snh2fZBH')
ylabel('\fontsize{8}SNH2fZBH')
xlabel('discrete time,k')

subplot(9,2,6); plot(k,SNH2muA,'k')
title('Sensitivity function Snh2muA')
ylabel('\fontsize{8}SNH2muA')
xlabel('\fontsize{8}discrete time,k')

subplot(9,2,7); plot(k,SNH2muH,'k')
title('Sensitivity function Snh2muH')
ylabel('\fontsize{8}SNH2muH')
xlabel('discrete time,k')

subplot(9,2,8); plot(k,SNH2KS,'k')
title('Sensitivity function Snh2KS')
ylabel('\fontsize{8}SNH2KS')
xlabel('discrete time,k')

subplot(9,2,9); plot(k,SNH2KOH,'k')
title('Sensitivity function Snh2KOH')
ylabel('\fontsize{8}SNH2KOH')
xlabel('\fontsize{8}discrete time,k')

subplot(9,2,10); plot(k,SNH2KNO,'k')
title('Sensitivity function Snh2KNO')
ylabel('\fontsize{8}SNH2KNO')
xlabel('\fontsize{8}discrete time,k')

subplot(9,2,11); plot(k,SNH2KNH,'k')
title('Sensitivity function Snh2KNH')
ylabel('\fontsize{8}SNH2KNH')
xlabel('\fontsize{8}discrete time,k')

subplot(9,2,12); plot(k,SNH2KOA,'k')
title('Sensitivity function Snh2KOA')
ylabel('\fontsize{8}SNH2KOA')
xlabel('\fontsize{8}discrete time,k')

subplot(9,2,13); plot(k,SNH2etag,'k')
title('Sensitivity function Snh2etag')
ylabel('\fontsize{8}SNH2etag')
xlabel('\fontsize{8}discrete time,k')

subplot(9,2,14); plot(k,SNH2KMP,'k')
title('Sensitivity function Snh2KMP')
ylabel('\fontsize{8}SNH2KMP')
xlabel('\fontsize{8}discrete time,k')

subplot(9,2,15); plot(k,SNH2KSP,'k')
title('Sensitivity function Snh2KSP')
ylabel('\fontsize{8}SNH2KSP')
xlabel('\fontsize{8}discrete time,k')

subplot(9,2,16); plot(k,SNH2KSA,'k')
title('Sensitivity function Snh2KSA')
ylabel('\fontsize{8}SNH2KSA')
xlabel('\fontsize{8}discrete time,k')

subplot(9,2,17); plot(k,SNH2fMA,'k')
```

```
title('Sensitivity function Snh2fMA')
ylabel('\fontsize{8}SNH2fMA')
xlabel('\fontsize{8}discrete time,k')

subplot(9,2,18); plot(k,SNH2KA,'k')
title('Sensitivity function Snh2KA')
ylabel('\fontsize{8}SNH2KA')
xlabel('\fontsize{8}discrete time,k')


%graphs for SNH variable in the third tank

figure(3)
subplot(9,2,1);plot(k,SNH3,'k')
title('Process variable Snh3')
ylabel('\fontsize{8}SNH3')
xlabel('\fontsize{8}discrete time k')

subplot(9,2,2); plot(k,SNH3f,'k')
title('Sensitivity function Snh3f')
ylabel('\fontsize{8}SNH3f')
xlabel('\fontsize{8}discrete time,k')

subplot(9,2,3); plot(k,SNH3YZH,'k')
title('Variable Snh3YZH')
ylabel('\fontsize{8}SNH3YZH')
xlabel('\fontsize{8}discrete time,k')

subplot(9,2,4); plot(k,SNH3YZA,'k')
title('Variable Snh3YZA')
ylabel('\fontsize{8}SNH3YZA')
xlabel('\fontsize{8}discrete time,k')

subplot(9,2,5); plot(k,SNH3fZBH,'k')
title('Sensitivity function Snh3fZBH')
ylabel('\fontsize{8}SNH3fZBH')
xlabel('discrete time,k')

subplot(9,2,6); plot(k,SNH3muA,'k')
title('Sensitivity function Snh3muA')
ylabel('\fontsize{8}SNH3muA')
xlabel('\fontsize{8}discrete time,k')

subplot(9,2,7); plot(k,SNH3muH,'k')
title('Sensitivity function Snh3muH')
ylabel('\fontsize{8}SNH3muH')
xlabel('discrete time,k')

subplot(9,2,8); plot(k,SNH3KS,'k')
title('Sensitivity function Snh3KS')
ylabel('\fontsize{8}SNH3KS')
xlabel('discrete time,k')

subplot(9,2,9); plot(k,SNH3KOH,'k')
title('Sensitivity function Snh3KOH')
ylabel('\fontsize{8}SNH3KOH')
xlabel('\fontsize{8}discrete time,k')

subplot(9,2,10); plot(k,SNH3KNO,'k')
title('Sensitivity function Snh3KNO')
ylabel('\fontsize{8}SNH3KNO')
xlabel('\fontsize{8}discrete time,k')

subplot(9,2,11); plot(k,SNH3KNH,'k')
title('Sensitivity function Snh3KNH')
ylabel('\fontsize{8}SNH3KNH')
xlabel('\fontsize{8}discrete time,k')

subplot(9,2,12); plot(k,SNH3KOA,'k')
title('Sensitivity function Snh3KOA')
ylabel('\fontsize{8}SNH3KOA')
xlabel('\fontsize{8}discrete time,k')

subplot(9,2,13); plot(k,SNH3etag,'k')
title('Sensitivity function Snh3etag')
ylabel('\fontsize{8}SNH3etag')
xlabel('\fontsize{8}discrete time,k')

subplot(9,2,14); plot(k,SNH3KMP,'k')
title('Sensitivity function Snh3KMP')
ylabel('\fontsize{8}SNH3KMP')
xlabel('\fontsize{8}discrete time,k')

subplot(9,2,15); plot(k,SNH3KSP,'k')
title('Sensitivity function Snh3KSP')
ylabel('\fontsize{8}SNH3KSP')
xlabel('\fontsize{8}discrete time,k')

subplot(9,2,16); plot(k,SNH3KSA,'k')
title('Sensitivity function Snh3KSA')
ylabel('\fontsize{8}SNH3KSA')
xlabel('\fontsize{8}discrete time,k')

subplot(9,2,17); plot(k,SNH3fMA,'k')
title('Sensitivity function Snh3fMA')
ylabel('\fontsize{8}SNH3fMA')
xlabel('\fontsize{8}discrete time,k')

subplot(9,2,18); plot(k,SNH3KA,'k')
title('Sensitivity function Snh3KA')
ylabel('\fontsize{8}SNH3KA')
xlabel('\fontsize{8}discrete time,k')

%Graphs for the sensitivity functions for SNH in the tank 4

figure(4)
subplot(9,2,1);plot(k,SNH4,'k')
title('Process variable Snh4')
ylabel('\fontsize{8}SNH4')
xlabel('\fontsize{8}discrete time k')

subplot(9,2,2); plot(k,SNH4f,'k')
title('Sensitivity function Snh4f')
ylabel('\fontsize{8}SNH4f')
xlabel('\fontsize{8}discrete time,k')

subplot(9,2,3); plot(k,SNH4YZH,'k')
title('Variable Snh4YZH')
ylabel('\fontsize{8}SNH4YZH')
xlabel('\fontsize{8}discrete time,k')

subplot(9,2,4); plot(k,SNH4YZA,'k')
title('Variable Snh4YZA')
ylabel('\fontsize{8}SNH4YZA')
xlabel('\fontsize{8}discrete time,k')

subplot(9,2,5); plot(k,SNH4fZBH,'k')
title('Sensitivity function Snh4fZBH')
ylabel('\fontsize{8}SNH4fZBH')
xlabel('discrete time,k')

subplot(9,2,6); plot(k,SNH4muA,'k')
title('Sensitivity function Snh4muA')
ylabel('\fontsize{8}SNH4muA')
xlabel('\fontsize{8}discrete time,k')

subplot(9,2,7); plot(k,SNH4muH,'k')
title('Sensitivity function Snh4muH')
ylabel('\fontsize{8}SNH4muH')
xlabel('discrete time,k')

subplot(9,2,8); plot(k,SNH4KS,'k')
title('Sensitivity function Snh4KS')
ylabel('\fontsize{8}SNH4KS')
xlabel('discrete time,k')

subplot(9,2,9); plot(k,SNH4KOH,'k')
title('Sensitivity function Snh4KOH')
ylabel('\fontsize{8}SNH4KOH')
xlabel('\fontsize{8}discrete time,k')

subplot(9,2,10); plot(k,SNH4KNO,'k')
title('Sensitivity function Snh4KNO')
ylabel('\fontsize{8}SNH4KNO')
xlabel('\fontsize{8}discrete time,k')

subplot(9,2,11); plot(k,SNH4KNH,'k')
title('Sensitivity function Snh4KNH')
ylabel('\fontsize{8}SNH4KNH')
xlabel('\fontsize{8}discrete time,k')

subplot(9,2,12); plot(k,SNH4KOA,'k')
title('Sensitivity function Snh4KOA')
ylabel('\fontsize{8}SNH4KOA')
xlabel('\fontsize{8}discrete time,k')

subplot(9,2,13); plot(k,SNH4etag,'k')
title('Sensitivity function Snh4etag')
ylabel('\fontsize{8}SNH4etag')
xlabel('\fontsize{8}discrete time,k')

subplot(9,2,14); plot(k,SNH4KMP,'k')
title('Sensitivity function Snh4KMP')
ylabel('\fontsize{8}SNH4KMP')
xlabel('\fontsize{8}discrete time,k')

subplot(9,2,15); plot(k,SNH4KSP,'k')
title('Sensitivity function Snh4KSP')
ylabel('\fontsize{8}SNH4KSP')
xlabel('\fontsize{8}discrete time,k')

subplot(9,2,16); plot(k,SNH4KSA,'k')
title('Sensitivity function Snh4KSA')
ylabel('\fontsize{8}SNH4KSA')
xlabel('\fontsize{8}discrete time,k')

subplot(9,2,17); plot(k,SNH4fMA,'k')
title('Sensitivity function Snh4fMA')
ylabel('\fontsize{8}SNH4fMA')
xlabel('\fontsize{8}discrete time,k')

subplot(9,2,18); plot(k,SNH4KA,'k')
title('Sensitivity function Snh4KA')
ylabel('\fontsize{8}SNH4KA')
xlabel('\fontsize{8}discrete time,k')
```

```
%Grapf for the sensitivity functions of the variable SNH in
the tank 5
figure(5)
subplot(9,2,1);plot(k,SNH5,'k')
title('Process variable Snh5')
ylabel('\fontsize{8}SNH5')
xlabel('\fontsize{8}discrete time k')

subplot(9,2,2); plot(k,SNH5f,'k')
title('Sensitivity function Snh5f')
ylabel('\fontsize{8}SNH5f')
xlabel('\fontsize{8}discrete time,k')

subplot(9,2,3); plot(k,SNH5YZH,'k')
title('Variable Snh5YZH')
ylabel('\fontsize{8}SNH5YZH')
xlabel('\fontsize{8}discrete time,k')

subplot(9,2,4); plot(k,SNH5YZA,'k')
title('Variable Snh5YZA')
ylabel('\fontsize{8}SNH5YZA')
xlabel('\fontsize{8}discrete time,k')

subplot(9,2,5); plot(k,SNH5fZBH,'k')
title('Sensitivity function Snh5fZBH')
ylabel('\fontsize{8}SNH5fZBH')
xlabel('discrete time,k')

subplot(9,2,6); plot(k,SNH5muA,'k')
title('Sensitivity function Snh5muA')
ylabel('\fontsize{8}SNH5muA')
xlabel('\fontsize{8}discrete time,k')

subplot(9,2,7); plot(k,SNH5muH,'k')
title('Sensitivity function Snh5muH')
ylabel('\fontsize{8}SNH5muH')
xlabel('discrete time,k')

subplot(9,2,8); plot(k,SNH5KS,'k')
title('Sensitivity function Snh5KS')
ylabel('\fontsize{8}SNH5KS')
xlabel('discrete time,k')

subplot(9,2,9); plot(k,SNH5KOH,'k')
title('Sensitivity function Snh5KOH')
ylabel('\fontsize{8}SNH5KOH')
xlabel('\fontsize{8}discrete time,k')

subplot(9,2,10); plot(k,SNH5KNO,'k')
title('Sensitivity function Snh5KNO')
ylabel('\fontsize{8}SNH5KNO')
xlabel('\fontsize{8}discrete time,k')

subplot(9,2,11); plot(k,SNH5KNH,'k')
title('Sensitivity function Snh5KNH')
ylabel('\fontsize{8}SNH5KNH')
xlabel('\fontsize{8}discrete time,k')

subplot(9,2,12); plot(k,SNH5KOA,'k')
title('Sensitivity function Snh5KOA')
ylabel('\fontsize{8}SNH5KOA')
xlabel('\fontsize{8}discrete time,k')

subplot(9,2,13); plot(k,SNH5etag,'k')
title('Sensitivity function Snh5etag')
ylabel('\fontsize{8}SNH5etag')
xlabel('\fontsize{8}discrete time,k')

subplot(9,2,14); plot(k,SNH5KMP,'k')
title('Sensitivity function Snh5KMP')
ylabel('\fontsize{8}SNH5KMP')
xlabel('\fontsize{8}discrete time,k')

subplot(9,2,15); plot(k,SNH5KSP,'k')
title('Sensitivity function Snh5KSP')
ylabel('\fontsize{8}SNH5KSP')
xlabel('\fontsize{8}discrete time,k')

subplot(9,2,16); plot(k,SNH5KSA,'k')
title('Sensitivity function Snh5KSA')
ylabel('\fontsize{8}SNH5KSA')
xlabel('\fontsize{8}discrete time,k')

subplot(9,2,17); plot(k,SNH5fMA,'k')
title('Sensitivity function Snh5fMA')
ylabel('\fontsize{8}SNH5fMA')
xlabel('\fontsize{8}discrete time,k')

subplot(9,2,18); plot(k,SNH5KA,'k')
title('Sensitivity function Snh5KA')
ylabel('\fontsize{8}SNH5KA')
xlabel('\fontsize{8}discrete time,k')


%Graphs of the sensitivity functions for the SNO
%Graphs of the sensitivity functions of the cariable SNO in
the tank 1
figure(6)
subplot(9,2,1);plot(k,SNO1,'k')
title('Process variable SNO1')
ylabel('\fontsize{8}SNO1')
xlabel('\fontsize{8}discrete time k')

subplot(9,2,2); plot(k,SNO1f,'k')
title('Sensitivity function SNO1f')
ylabel('\fontsize{8}SNO1f')
xlabel('\fontsize{8}discrete time,k')

subplot(9,2,3); plot(k,SNO1YZH,'k')
title('Variable SNO1YZH')
ylabel('\fontsize{8}SNO1YZH')
xlabel('\fontsize{8}discrete time,k')

subplot(9,2,4); plot(k,SNO1YZA,'k')
title('Variable SNO1YZA')
ylabel('\fontsize{8}SNO1YZA')
xlabel('\fontsize{8}discrete time,k')

subplot(9,2,5); plot(k,SNO1fZBH,'k')
title('Sensitivity function SNO1fZBH')
ylabel('\fontsize{8}SNO1fZBH')
xlabel('discrete time,k')

subplot(9,2,6); plot(k,SNO1muA,'k')
title('Sensitivity function SNO1muA')
ylabel('\fontsize{8}SNO1muA')
xlabel('\fontsize{8}discrete time,k')

subplot(9,2,7); plot(k,SNO1muH,'k')
title('Sensitivity function SNO1muH')
ylabel('\fontsize{8}SNO1muH')
xlabel('discrete time,k')

subplot(9,2,8); plot(k,SNO1KS,'k')
title('Sensitivity function SNO1KS')
ylabel('\fontsize{8}SNO1KS')
xlabel('discrete time,k')

subplot(9,2,9); plot(k,SNO1KOH,'k')
title('Sensitivity function SNO1KOH')
ylabel('\fontsize{8}SNO1KOH')
xlabel('\fontsize{8}discrete time,k')

subplot(9,2,10); plot(k,SNO1KNO,'k')
title('Sensitivity function SNO1KNO')
ylabel('\fontsize{8}SNO1KNO')
xlabel('\fontsize{8}discrete time,k')

subplot(9,2,11); plot(k,SNO1KNH,'k')
title('Sensitivity function SNO1KNH')
ylabel('\fontsize{8}SNO1KNH')
xlabel('\fontsize{8}discrete time,k')

subplot(9,2,12); plot(k,SNO1KOA,'k')
title('Sensitivity function SNO1KOA')
ylabel('\fontsize{8}SNO1KOA')
xlabel('\fontsize{8}discrete time,k')

subplot(9,2,13); plot(k,SNO1etag,'k')
title('Sensitivity function SNO1etag')
ylabel('\fontsize{8}SNO1etag')
xlabel('\fontsize{8}discrete time,k')

subplot(9,2,14); plot(k,SNO1KMP,'k')
title('Sensitivity function SNO1KMP')
ylabel('\fontsize{8}SNO1KMP')
xlabel('\fontsize{8}discrete time,k')

subplot(9,2,15); plot(k,SNO1KSP,'k')
title('Sensitivity function SNO1KSP')
ylabel('\fontsize{8}SNO1KSP')
xlabel('\fontsize{8}discrete time,k')

subplot(9,2,16); plot(k,SNO1KSA,'k')
title('Sensitivity function SNO1KSA')
ylabel('\fontsize{8}SNO1KSA')
xlabel('\fontsize{8}discrete time,k')

subplot(9,2,17); plot(k,SNO1fMA,'k')
title('Sensitivity function SNO1fMA')
ylabel('\fontsize{8}SNO1fMA')
xlabel('\fontsize{8}discrete time,k')

subplot(9,2,18); plot(k,SNO1KA,'k')
title('Sensitivity function SNO1KA')
ylabel('\fontsize{8}SNO1KA')
xlabel('\fontsize{8}discrete time,k')


%Graphs of the sensitivity functions for the variable SNO in
the tank 2
figure(7)
subplot(9,2,1);plot(k,SNO2,'k')
title('Process variable SNO2')
ylabel('\fontsize{8}SNO2')
xlabel('\fontsize{8}discrete time k')

subplot(9,2,2); plot(k,SNO2f,'k')
```

```
title('Sensitivity function SNO2f')
ylabel('\fontsize{8}SNO2f')
xlabel('\fontsize{8}discrete time,k')

subplot(9,2,3); plot(k,SNO2YZH,'k')
title('Variable SNO2YZH')
ylabel('\fontsize{8}SNO2YZH')
xlabel('\fontsize{8}discrete time,k')

subplot(9,2,4); plot(k,SNO2YZA,'k')
title('Variable SNO2YZA')
ylabel('\fontsize{8}SNO2YZA')
xlabel('\fontsize{8}discrete time,k')

subplot(9,2,5); plot(k,SNO2fZBH,'k')
title('Sensitivity function SNO2fZBH')
ylabel('\fontsize{8}SNO2fZBH')
xlabel('discrete time,k')

subplot(9,2,6); plot(k,SNO2muA,'k')
title('Sensitivity function SNO2muA')
ylabel('\fontsize{8}SNO2muA')
xlabel('\fontsize{8}discrete time,k')

subplot(9,2,7); plot(k,SNO2muH,'k')
title('Sensitivity function SNO2muH')
ylabel('\fontsize{8}SNO2muH')
xlabel('discrete time,k')

subplot(9,2,8); plot(k,SNO2KS,'k')
title('Sensitivity function SNO2KS')
ylabel('\fontsize{8}SNO2KS')
xlabel('discrete time,k')

subplot(9,2,9); plot(k,SNO2KOH,'k')
title('Sensitivity function SNO2KOH')
ylabel('\fontsize{8}SNO2KOH')
xlabel('\fontsize{8}discrete time,k')

subplot(9,2,10); plot(k,SNO2KNO,'k')
title('Sensitivity function SNO2KNO')
ylabel('\fontsize{8}SNO2KNO')
xlabel('\fontsize{8}discrete time,k')

subplot(9,2,11); plot(k,SNO2KNH,'k')
title('Sensitivity function SNO2KNH')
ylabel('\fontsize{8}SNH2KNH')
xlabel('\fontsize{8}discrete time,k')

subplot(9,2,12); plot(k,SNO2KOA,'k')
title('Sensitivity function SNO2KOA')
ylabel('\fontsize{8}SNO2KOA')
xlabel('\fontsize{8}discrete time,k')

subplot(9,2,13); plot(k,SNO2etag,'k')
title('Sensitivity function SNO2etag')
ylabel('\fontsize{8}SNO2etag')
xlabel('\fontsize{8}discrete time,k')

subplot(9,2,14); plot(k,SNO2KMP,'k')
title('Sensitivity function SNO2KMP')
ylabel('\fontsize{8}SNO2KMP')
xlabel('\fontsize{8}discrete time,k')

subplot(9,2,15); plot(k,SNO2KSP,'k')
title('Sensitivity function SNO2KSP')
ylabel('\fontsize{8}SNO2KSP')
xlabel('\fontsize{8}discrete time,k')

subplot(9,2,16); plot(k,SNO2KSA,'k')
title('Sensitivity function SNO2KSA')
ylabel('\fontsize{8}SNO2KSA')
xlabel('\fontsize{8}discrete time,k')

subplot(9,2,17); plot(k,SNO2fMA,'k')
title('Sensitivity function SNO2fMA')
ylabel('\fontsize{8}SNO2fMA')
xlabel('\fontsize{8}discrete time,k')

subplot(9,2,18); plot(k,SNO2KA,'k')
title('Sensitivity function SNO2KA')
ylabel('\fontsize{8}SNO2KA')
xlabel('\fontsize{8}discrete time,k')

%Graphs for the variable SNO  in the  tank 3

figure(8)
subplot(9,2,1);plot(k,SNO3,'k')
title('Process variable SNO3')
ylabel('\fontsize{8}SNO3')
xlabel('\fontsize{8}discrete time k')

subplot(9,2,2); plot(k,SNO3f,'k')
title('Sensitivity function SNO3f')
ylabel('\fontsize{8}SNO3f')
xlabel('\fontsize{8}discrete time,k')

subplot(9,2,3); plot(k,SNO3YZH,'k')
title('Variable SNO3YZH')
ylabel('\fontsize{8}SNO3YZH')
xlabel('\fontsize{8}discrete time,k')

subplot(9,2,4); plot(k,SNO3YZA,'k')
title('Variable SNO3YZA')
ylabel('\fontsize{8}SNO3YZA')
xlabel('\fontsize{8}discrete time,k')

subplot(9,2,5); plot(k,SNO3fZBH,'k')
title('Sensitivity function SNO3fZBH')
ylabel('\fontsize{8}SNO3fZBH')
xlabel('discrete time,k')

subplot(9,2,6); plot(k,SNO3muA,'k')
title('Sensitivity function SNO3muA')
ylabel('\fontsize{8}SNO3muA')
xlabel('\fontsize{8}discrete time,k')

subplot(9,2,7); plot(k,SNO3muH,'k')
title('Sensitivity function SNO3muH')
ylabel('\fontsize{8}SNO3muH')
xlabel('discrete time,k')

subplot(9,2,8); plot(k,SNO3KS,'k')
title('Sensitivity function SNO3KS')
ylabel('\fontsize{8}SNO3KS')
xlabel('discrete time,k')

subplot(9,2,9); plot(k,SNO3KOH,'k')
title('Sensitivity function SNO3KOH')
ylabel('\fontsize{8}SNO3KOH')
xlabel('\fontsize{8}discrete time,k')

subplot(9,2,10); plot(k,SNO3KNO,'k')
title('Sensitivity function SNO3KNO')
ylabel('\fontsize{8}SNO3KNO')
xlabel('\fontsize{8}discrete time,k')

subplot(9,2,11); plot(k,SNO3KNH,'k')
title('Sensitivity function SNO3KNH')
ylabel('\fontsize{8}SNO3KNH')
xlabel('\fontsize{8}discrete time,k')

subplot(9,2,12); plot(k,SNO3KOA,'k')
title('Sensitivity function SNO3KOA')
ylabel('\fontsize{8}SNO3KOA')
xlabel('\fontsize{8}discrete time,k')

subplot(9,2,13); plot(k,SNO3etag,'k')
title('Sensitivity function SNO3etag')
ylabel('\fontsize{8}SNO3etag')
xlabel('\fontsize{8}discrete time,k')

subplot(9,2,14); plot(k,SNO3KMP,'k')
title('Sensitivity function SNO3KMP')
ylabel('\fontsize{8}SNO3KMP')
xlabel('\fontsize{8}discrete time,k')

subplot(9,2,15); plot(k,SNO3KSP,'k')
title('Sensitivity function SNO3KSP')
ylabel('\fontsize{8}SNO3KSP')
xlabel('\fontsize{8}discrete time,k')

subplot(9,2,16); plot(k,SNO3KSA,'k')
title('Sensitivity function SNO3KSA')
ylabel('\fontsize{8}SNO3KSA')
xlabel('\fontsize{8}discrete time,k')

subplot(9,2,17); plot(k,SNO3fMA,'k')
title('Sensitivity function SNO3fMA')
ylabel('\fontsize{8}SNO3fMA')
xlabel('\fontsize{8}discrete time,k')

subplot(9,2,18); plot(k,SNO3KA,'k')
title('Sensitivity function SNO3KA')
ylabel('\fontsize{8}SNO3KA')
xlabel('\fontsize{8}discrete time,k')

%Graphs for the sensitivity functions for SNO in the tank 4

figure(9)
subplot(9,2,1);plot(k,SNO4,'k')
title('Process variable SNO4')
ylabel('\fontsize{8}SNO4')
subplot(9,2,3); plot(k,SNO4YZH,'k')
title('Variable SNO4YZH')
ylabel('\fontsize{8}SNO4YZH')
xlabel('\fontsize{8}discrete time,k')

subplot(9,2,4); plot(k,SNO4YZA,'k')
title('Variable SNO4YZA')
ylabel('\fontsize{8}SNO4YZA')
xlabel('\fontsize{8}discrete time,k')

subplot(9,2,5); plot(k,SNO4fZBH,'k')
title('Sensitivity function SNO4fZBH')
ylabel('\fontsize{8}SNO4fZBH')
xlabel('discrete time,k')
```

```
subplot(9,2,6); plot(k,SNO4muA,'k')
title('Sensitivity function SNO4muA')
ylabel('\fontsize{8}SNO4muA')
xlabel('\fontsize{8}discrete time,k')

subplot(9,2,7); plot(k,SNO4muH,'k')
title('Sensitivity function SNO4muH')
ylabel('\fontsize{8}SNO4muH')
xlabel('discrete time,k')

subplot(9,2,8); plot(k,SNO4KS,'k')
title('Sensitivity function SNO4KS')
ylabel('\fontsize{8}SNO4KS')
xlabel('discrete time,k')

subplot(9,2,9); plot(k,SNO4KOH,'k')
title('Sensitivity function SNO4KOH')
ylabel('\fontsize{8}SNO4KOH')
xlabel('\fontsize{8}discrete time,k')

subplot(9,2,10); plot(k,SNO4KNO,'k')
title('Sensitivity function SNO4KNO')
ylabel('\fontsize{8}SNO4KNO')
xlabel('\fontsize{8}discrete time,k')

subplot(9,2,11); plot(k,SNO4KNH,'k')
title('Sensitivity function SNO4KNH')
ylabel('\fontsize{8}SNO4KNH')
xlabel('\fontsize{8}discrete time,k')

subplot(9,2,12); plot(k,SNO4KOA,'k')
title('Sensitivity function SNO4KOA')
ylabel('\fontsize{8}SNO4KOA')
xlabel('\fontsize{8}discrete time,k')

subplot(9,2,13); plot(k,SNO4etag,'k')
title('Sensitivity function SNO4etag')
ylabel('\fontsize{8}SNO4etag')
xlabel('\fontsize{8}discrete time,k')

subplot(9,2,14); p
xlabel('\fontsize{8}discrete time k')

subplot(9,2,2); plot(k,SNO4f,'k')
title('Sensitivity function SNO4f')
ylabel('\fontsize{8}SNO4f')
xlabel('\fontsize{8}discrete time,k')
lot(k,SNO4KMP,'k')
title('Sensitivity function SNO4KMP')
ylabel('\fontsize{8}SNO4KMP')
xlabel('\fontsize{8}discrete time,k')

subplot(9,2,15); plot(k,SNO4KSP,'k')
title('Sensitivity function SNO4KSP')
ylabel('\fontsize{8}SNO4KSP')
xlabel('\fontsize{8}discrete time,k')

subplot(9,2,16); plot(k,SNO4KSA,'k')
title('Sensitivity function SNO4KSA')
ylabel('\fontsize{8}SNO4KSA')
xlabel('\fontsize{8}discrete time,k')

subplot(9,2,17); plot(k,SNO4fMA,'k')
title('Sensitivity function SNO4fMA')
ylabel('\fontsize{8}SNO4fMA')
xlabel('\fontsize{8}discrete time,k')

subplot(9,2,18); plot(k,SNO4KA,'k')
title('Sensitivity function SNO4KA')
ylabel('\fontsize{8}SNO4KA')
xlabel('\fontsize{8}discrete time,k')

%Grapf for the sensitivity functions of the variable SNO in
the tank 5
figure(10)
subplot(9,2,1);plot(k,SNO5,'k')
title('Process variable SNO5')
ylabel('\fontsize{8}SNO5')
xlabel('\fontsize{8}discrete time k')

subplot(9,2,2); plot(k,SNO5f,'k')
title('Sensitivity function SNO5f')
ylabel('\fontsize{8}SNO5f')
xlabel('\fontsize{8}discrete time,k')

subplot(9,2,3); plot(k,SNO5YZH,'k')
title('Variable SNO5YZH')
ylabel('\fontsize{8}SNO5YZH')
xlabel('\fontsize{8}discrete time,k')

subplot(9,2,4); plot(k,SNO5YZA,'k')
title('Variable SNO5YZA')
ylabel('\fontsize{8}SNO5YZA')
xlabel('\fontsize{8}discrete time,k')

subplot(9,2,5); plot(k,SNO5fZBH,'k')
title('Sensitivity function SNO5fZBH')
ylabel('\fontsize{8}SNO5fZBH')
xlabel('discrete time,k')

subplot(9,2,6); plot(k,SNO5muA,'k')
title('Sensitivity function SNO5muA')
ylabel('\fontsize{8}SNO5muA')
xlabel('\fontsize{8}discrete time,k')

subplot(9,2,7); plot(k,SNO5muH,'k')
title('Sensitivity function SNO5muH')
ylabel('\fontsize{8}SNO5muH')
xlabel('discrete time,k')

subplot(9,2,8); plot(k,SNO5KS,'k')
title('Sensitivity function SNO5KS')
ylabel('\fontsize{8}SNO5KS')
xlabel('discrete time,k')

subplot(9,2,9); plot(k,SNO5KOH,'k')
title('Sensitivity function SNO5KOH')
ylabel('\fontsize{8}SNO5KOH')
xlabel('\fontsize{8}discrete time,k')

subplot(9,2,10); plot(k,SNO5KNO,'k')
title('Sensitivity function SNO5KNO')
ylabel('\fontsize{8}SNO5KNO')
xlabel('\fontsize{8}discrete time,k')

subplot(9,2,11); plot(k,SNO5KNH,'k')
title('Sensitivity function SNO5KNH')
ylabel('\fontsize{8}SNO5KNH')
xlabel('\fontsize{8}discrete time,k')

subplot(9,2,12); plot(k,SNO5KOA,'k')
title('Sensitivity function SNO5KOA')
ylabel('\fontsize{8}SNO5KOA')
xlabel('\fontsize{8}discrete time,k')

subplot(9,2,13); plot(k,SNO5etag,'k')
title('Sensitivity function SNO5etag')
ylabel('\fontsize{8}SNO5etag')
xlabel('\fontsize{8}discrete time,k')

subplot(9,2,14); plot(k,SNO5KMP,'k')
title('Sensitivity function SNO5KMP')
ylabel('\fontsize{8}SNO5KMP')
xlabel('\fontsize{8}discrete time,k')

subplot(9,2,15); plot(k,SNO5KSP,'k')
title('Sensitivity function SNO5KSP')
ylabel('\fontsize{8}SNO5KSP')
xlabel('\fontsize{8}discrete time,k')

subplot(9,2,16); plot(k,SNO5KSA,'k')
title('Sensitivity function SNO5KSA')
ylabel('\fontsize{8}SNO5KSA')
xlabel('\fontsize{8}discrete time,k')

subplot(9,2,17); plot(k,SNO5fMA,'k')
title('Sensitivity function SNO5fMA')
ylabel('\fontsize{8}SNO5fMA')
xlabel('\fontsize{8}discrete time,k')

subplot(9,2,18); plot(k,SNO5KA,'k')
title('Sensitivity function SNO5KA')
ylabel('\fontsize{8}SNO5KA')
xlabel('\fontsize{8}discrete time,k')

%Graphs of the sensitivity unctions for the SS

%Graphs of the sensitivity functions for the SS in the tank
1
figure(11)
subplot(9,2,1);plot(k,SS1,'k')
title('Process variable SS1')
ylabel('\fontsize{8}SS1')
xlabel('\fontsize{8}discrete time k')

subplot(9,2,2); plot(k,SS1f,'k')
title('Sensitivity function SS1f')
ylabel('\fontsize{8}SS1f')
xlabel('\fontsize{8}discrete time,k')

subplot(9,2,3); plot(k,SS1YZH,'k')
title('Variable SS1YZH')
ylabel('\fontsize{8}SS1YZH')
xlabel('\fontsize{8}discrete time,k')

subplot(9,2,4); plot(k,SS1YZA,'k')
title('Variable SS1YZA')
ylabel('\fontsize{8}SS1YZA')
xlabel('\fontsize{8}discrete time,k')

subplot(9,2,5); plot(k,SS1fZBH,'k')
title('Sensitivity function SS1fZBH')
ylabel('\fontsize{8}SS1fZBH')
xlabel('discrete time,k')

subplot(9,2,6); plot(k,SS1muA,'k')
title('Sensitivity function SS1muA')
ylabel('\fontsize{8}SS1muA')
```

```
xlabel('\fontsize{8}discrete time,k')

subplot(9,2,7); plot(k,SS1muH,'k')
title('Sensitivity function SS1muH')
ylabel('\fontsize{8}SS1muH')
xlabel('discrete time,k')

subplot(9,2,8); plot(k,SS1KS,'k')
title('Sensitivity function SS1KS')
ylabel('\fontsize{8}SS1KS')
xlabel('discrete time,k')

subplot(9,2,9); plot(k,SS1KOH,'k')
title('Sensitivity function SS1KOH')
ylabel('\fontsize{8}SS1KOH')
xlabel('\fontsize{8}discrete time,k')

subplot(9,2,10); plot(k,SS1KNO,'k')
title('Sensitivity function SS1KNO')
ylabel('\fontsize{8}SS1KNO')
xlabel('\fontsize{8}discrete time,k')

subplot(9,2,11); plot(k,SS1KNH,'k')
title('Sensitivity function SS1KNH')
ylabel('\fontsize{8}SS1KNH')
xlabel('\fontsize{8}discrete time,k')

subplot(9,2,12); plot(k,SS1KOA,'k')
title('Sensitivity function SS1KOA')
ylabel('\fontsize{8}SS1KOA')
xlabel('\fontsize{8}discrete time,k')

subplot(9,2,13); plot(k,SS1etag,'k')
title('Sensitivity function SS1etag')
ylabel('\fontsize{8}SS1etag')
xlabel('\fontsize{8}discrete time,k')

subplot(9,2,14); plot(k,SS1KMP,'k')
title('Sensitivity function SS1KMP')
ylabel('\fontsize{8}SS1KMP')
xlabel('\fontsize{8}discrete time,k')

subplot(9,2,15); plot(k,SS1KSP,'k')
title('Sensitivity function SS1KSP')
ylabel('\fontsize{8}SS1KSP')
xlabel('\fontsize{8}discrete time,k')

subplot(9,2,16); plot(k,SS1KSA,'k')
title('Sensitivity function SS1KSA')
ylabel('\fontsize{8}SS1KSA')
xlabel('\fontsize{8}discrete time,k')

subplot(9,2,17); plot(k,SS1fMA,'k')
title('Sensitivity function SS1fMA')
ylabel('\fontsize{8}SS1fMA')
xlabel('\fontsize{8}discrete time,k')

subplot(9,2,18); plot(k,SS1KA,'k')
title('Sensitivity function SS1KA')
ylabel('\fontsize{8}SS1KA')
xlabel('\fontsize{8}discrete time,k')


%Graphs of the sensitivity functions of the varible SS in
the tank 2
figure(12)
subplot(9,2,1);plot(k,SS2,'k')
title('Process variable SS2')
ylabel('\fontsize{8}SS2')
xlabel('\fontsize{8}discrete time k')

subplot(9,2,2); plot(k,SS2f,'k')
title('Sensitivity function SS2f')
ylabel('\fontsize{8}SS2f')
xlabel('\fontsize{8}discrete time,k')

subplot(9,2,3); plot(k,SS2YZH,'k')
title('Variable SS2YZH')
ylabel('\fontsize{8}SS2YZH')
xlabel('\fontsize{8}discrete time,k')

subplot(9,2,4); plot(k,SS2YZA,'k')
title('Variable SS2YZA')
ylabel('\fontsize{8}SS2YZA')
xlabel('\fontsize{8}discrete time,k')

subplot(9,2,5); plot(k,SS2fZBH,'k')
title('Sensitivity function SS2fZBH')
ylabel('\fontsize{8}SS2fZBH')
xlabel('discrete time,k')

subplot(9,2,6); plot(k,SS2muA,'k')
title('Sensitivity function SS2muA')
ylabel('\fontsize{8}SS2muA')
xlabel('\fontsize{8}discrete time,k')

subplot(9,2,7); plot(k,SS2muH,'k')
title('Sensitivity function SS2muH')
ylabel('\fontsize{8}SS2muH')
xlabel('discrete time,k')

subplot(9,2,8); plot(k,SS2KS,'k')
title('Sensitivity function SS2KS')
ylabel('\fontsize{8}SS2KS')
xlabel('discrete time,k')

subplot(9,2,9); plot(k,SS2KOH,'k')
title('Sensitivity function SS2KOH')
ylabel('\fontsize{8}SS2KOH')
xlabel('\fontsize{8}discrete time,k')

subplot(9,2,10); plot(k,SS2KNO,'k')
title('Sensitivity function SS2KNO')
ylabel('\fontsize{8}SS2KNO')
xlabel('\fontsize{8}discrete time,k')

subplot(9,2,11); plot(k,SS2KNH,'k')
title('Sensitivity function SS2KNH')
ylabel('\fontsize{8}SS2KNH')
xlabel('\fontsize{8}discrete time,k')

subplot(9,2,12); plot(k,SS2KOA,'k')
title('Sensitivity function SS2KOA')
ylabel('\fontsize{8}SS2KOA')
xlabel('\fontsize{8}discrete time,k')

subplot(9,2,13); plot(k,SS2etag,'k')
title('Sensitivity function SS2etag')
ylabel('\fontsize{8}SS2etag')
xlabel('\fontsize{8}discrete time,k')

subplot(9,2,14); plot(k,SS2KMP,'k')
title('Sensitivity function SS2KMP')
ylabel('\fontsize{8}SS2KMP')
xlabel('\fontsize{8}discrete time,k')

subplot(9,2,15); plot(k,SS2KSP,'k')
title('Sensitivity function SS2KSP')
ylabel('\fontsize{8}SS2KSP')
xlabel('\fontsize{8}discrete time,k')

subplot(9,2,16); plot(k,SS2KSA,'k')
title('Sensitivity function SS2KSA')
ylabel('\fontsize{8}SS2KSA')
xlabel('\fontsize{8}discrete time,k')

subplot(9,2,17); plot(k,SS2fMA,'k')
title('Sensitivity function SS2fMA')
ylabel('\fontsize{8}SS2fMA')
xlabel('\fontsize{8}discrete time,k')

subplot(9,2,18); plot(k,SS2KA,'k')
title('Sensitivity function SS2KA')
ylabel('\fontsize{8}SS2KA')
xlabel('\fontsize{8}discrete time,k')

%Graphs for SS variable in the tank 3

figure(13)
subplot(9,2,1);plot(k,SS3,'k')
title('Process variable SS3')
ylabel('\fontsize{8}SS3')
xlabel('\fontsize{8}discrete time k')

subplot(9,2,2); plot(k,SS3f,'k')
title('Sensitivity function SS3f')
ylabel('\fontsize{8}SS3f')
xlabel('\fontsize{8}discrete time,k')

subplot(9,2,3); plot(k,SS3YZH,'k')
title('Variable SS3YZH')
ylabel('\fontsize{8}SS3YZH')
xlabel('\fontsize{8}discrete time,k')

subplot(9,2,4); plot(k,SS3YZA,'k')
title('Variable SS3YZA')
ylabel('\fontsize{8}SS3YZA')
xlabel('\fontsize{8}discrete time,k')

subplot(9,2,5); plot(k,SS3fZBH,'k')
title('Sensitivity function SS3fZBH')
ylabel('\fontsize{8}SS3fZBH')
xlabel('discrete time,k')

subplot(9,2,6); plot(k,SS3muA,'k')
title('Sensitivity function SS3muA')
ylabel('\fontsize{8}SS3muA')
xlabel('\fontsize{8}discrete time,k')

subplot(9,2,7); plot(k,SS3muH,'k')
title('Sensitivity function SS3muH')
ylabel('\fontsize{8}SS3muH')
xlabel('discrete time,k')

subplot(9,2,8); plot(k,SS3KS,'k')
title('Sensitivity function SS3KS')
ylabel('\fontsize{8}SS3KS')
xlabel('discrete time,k')
```

```
subplot(9,2,9); plot(k,SS3KOH,'k')
title('Sensitivity function SS3KOH')
ylabel('\fontsize{8}SS3KOH')
xlabel('\fontsize{8}discrete time,k')

subplot(9,2,10); plot(k,SS3KNO,'k')
title('Sensitivity function SS3KNO')
ylabel('\fontsize{8}SS3KNO')
xlabel('\fontsize{8}discrete time,k')

subplot(9,2,11); plot(k,SS3KNH,'k')
title('Sensitivity function SS3KNH')
ylabel('\fontsize{8}SS3KNH')
xlabel('\fontsize{8}discrete time,k')

subplot(9,2,12); plot(k,SS3KOA,'k')
title('Sensitivity function SS3KOA')
ylabel('\fontsize{8}SS3KOA')
xlabel('\fontsize{8}discrete time,k')

subplot(9,2,13); plot(k,SS3etag,'k')
title('Sensitivity function SS3etag')
ylabel('\fontsize{8}SS3etag')
xlabel('\fontsize{8}discrete time,k')

subplot(9,2,14); plot(k,SS3KMP,'k')
title('Sensitivity function SS3KMP')
ylabel('\fontsize{8}SS3KMP')
xlabel('\fontsize{8}discrete time,k')

subplot(9,2,15); plot(k,SS3KSP,'k')
title('Sensitivity function SS3KSP')
ylabel('\fontsize{8}SS3KSP')
xlabel('\fontsize{8}discrete time,k')

subplot(9,2,16); plot(k,SS3KSA,'k')
title('Sensitivity function SS3KSA')
ylabel('\fontsize{8}SS3KSA')
xlabel('\fontsize{8}discrete time,k')

subplot(9,2,17); plot(k,SS3fMA,'k')
title('Sensitivity function SS3fMA')
ylabel('\fontsize{8}SS3fMA')
xlabel('\fontsize{8}discrete time,k')

subplot(9,2,18); plot(k,SS3KA,'k')
title('Sensitivity function SS3KA')
ylabel('\fontsize{8}SS3KA')
xlabel('\fontsize{8}discrete time,k')

%Graphs for the sensitivity functions for SS in the tank 4

figure(14)
subplot(9,2,1);plot(k,SS4,'k')
title('Process variable SS4')
ylabel('\fontsize{8}SS4')
xlabel('\fontsize{8}discrete time k')

subplot(9,2,2); plot(k,SS4f,'k')
title('Sensitivity function SS4f')
ylabel('\fontsize{8}SS4f')
xlabel('\fontsize{8}discrete time,k')

subplot(9,2,3); plot(k,SS4YZH,'k')
title('Variable SS4YZH')
ylabel('\fontsize{8}SS4YZH')
xlabel('\fontsize{8}discrete time,k')

subplot(9,2,4); plot(k,SS4YZA,'k')
title('Variable SS4YZA')
ylabel('\fontsize{8}SS4YZA')
xlabel('\fontsize{8}discrete time,k')

subplot(9,2,5); plot(k,SS4fZBH,'k')
title('Sensitivity function SS4fZBH')
ylabel('\fontsize{8}SS4fZBH')
xlabel('discrete time,k')

subplot(9,2,6); plot(k,SS4muA,'k')
title('Sensitivity function SS4muA')
ylabel('\fontsize{8}SS4muA')
xlabel('\fontsize{8}discrete time,k')

subplot(9,2,7); plot(k,SS4muH,'k')
title('Sensitivity function SS4muH')
ylabel('\fontsize{8}SS4muH')
xlabel('discrete time,k')

subplot(9,2,8); plot(k,SS4KS,'k')
title('Sensitivity function SS4KS')
ylabel('\fontsize{8}SS4KS')
xlabel('discrete time,k')

subplot(9,2,9); plot(k,SS4KOH,'k')
title('Sensitivity function SS4KOH')
ylabel('\fontsize{8}SS4KOH')
xlabel('\fontsize{8}discrete time,k')

subplot(9,2,10); plot(k,SS4KNO,'k')
title('Sensitivity function SS4KNO')
ylabel('\fontsize{8}SS4KNO')
xlabel('\fontsize{8}discrete time,k')

subplot(9,2,11); plot(k,SS4KNH,'k')
title('Sensitivity function SS4KNH')
ylabel('\fontsize{8}SS4KNH')
xlabel('\fontsize{8}discrete time,k')

subplot(9,2,12); plot(k,SS4KOA,'k')
title('Sensitivity function SS4KOA')
ylabel('\fontsize{8}SS4KOA')
xlabel('\fontsize{8}discrete time,k')

subplot(9,2,13); plot(k,SS4etag,'k')
title('Sensitivity function SS4etag')
ylabel('\fontsize{8}SS4etag')
xlabel('\fontsize{8}discrete time,k')

subplot(9,2,14); plot(k,SS4KMP,'k')
title('Sensitivity function SS4KMP')
ylabel('\fontsize{8}SS4KMP')
xlabel('\fontsize{8}discrete time,k')

subplot(9,2,15); plot(k,SS4KSP,'k')
title('Sensitivity function SS4KSP')
ylabel('\fontsize{8}SS4KSP')
xlabel('\fontsize{8}discrete time,k')

subplot(9,2,16); plot(k,SS4KSA,'k')
title('Sensitivity function SS4KSA')
ylabel('\fontsize{8}SS4KSA')
xlabel('\fontsize{8}discrete time,k')

subplot(9,2,17); plot(k,SS4fMA,'k')
title('Sensitivity function SS4fMA')
ylabel('\fontsize{8}SS4fMA')
xlabel('\fontsize{8}discrete time,k')

subplot(9,2,18); plot(k,SS4KA,'k')
title('Sensitivity function SS4KA')
ylabel('\fontsize{8}SS4KA')
xlabel('\fontsize{8}discrete time,k')

%Grapf for the sensitivity functions of the variable SNH in
the tank 5
figure(15)
subplot(9,2,1);plot(k,SS5,'k')
title('Process variable SS5')
ylabel('\fontsize{8}SS5')
xlabel('\fontsize{8}discrete time k')

subplot(9,2,2); plot(k,SS5f,'k')
title('Sensitivity function SS5f')
ylabel('\fontsize{8}SS5f')
xlabel('\fontsize{8}discrete time,k')

subplot(9,2,3); plot(k,SS5YZH,'k')
title('Variable SS5YZH')
ylabel('\fontsize{8}SS5YZH')
xlabel('\fontsize{8}discrete time,k')

subplot(9,2,4); plot(k,SS5YZA,'k')
title('Variable SS5YZA')
ylabel('\fontsize{8}SS5YZA')
xlabel('\fontsize{8}discrete time,k')

subplot(9,2,5); plot(k,SS5fZBH,'k')
title('Sensitivity function SS5fZBH')
ylabel('\fontsize{8}SS5fZBH')
xlabel('discrete time,k')

subplot(9,2,6); plot(k,SS5muA,'k')
title('Sensitivity function SS5muA')
ylabel('\fontsize{8}SS5muA')
xlabel('\fontsize{8}discrete time,k')

subplot(9,2,7); plot(k,SS5muH,'k')
title('Sensitivity function SS5muH')
ylabel('\fontsize{8}SS5muH')
xlabel('discrete time,k')

subplot(9,2,8); plot(k,SS5KS,'k')
title('Sensitivity function SS5KS')
ylabel('\fontsize{8}SS5KS')
xlabel('discrete time,k')

subplot(9,2,9); plot(k,SS5KOH,'k')
title('Sensitivity function SS5KOH')
ylabel('\fontsize{8}SS5KOH')
xlabel('\fontsize{8}discrete time,k')

subplot(9,2,10); plot(k,SS5KNO,'k')
title('Sensitivity function SS5KNO')
ylabel('\fontsize{8}SS5KNO')
xlabel('\fontsize{8}discrete time,k')

subplot(9,2,11); plot(k,SS5KNH,'k')
```

```
title('Sensitivity function SS5KNH')
ylabel('\fontsize{8}SS5KNH')
xlabel('\fontsize{8}discrete time,k')

subplot(9,2,12); plot(k,SS5KOA,'k')
title('Sensitivity function SS5KOA')
ylabel('\fontsize{8}SS5KOA')
xlabel('\fontsize{8}discrete time,k')

subplot(9,2,13); plot(k,SS5etag,'k')
title('Sensitivity function SS5etag')
ylabel('\fontsize{8}SS5etag')
xlabel('\fontsize{8}discrete time,k')

subplot(9,2,14); plot(k,SS5KMP,'k')
title('Sensitivity function SS5KMP')
ylabel('\fontsize{8}SS5KMP')
xlabel('\fontsize{8}discrete time,k')

subplot(9,2,15); plot(k,SS5KSP,'k')
title('Sensitivity function SS5KSP')
ylabel('\fontsize{8}SS5KSP')
xlabel('\fontsize{8}discrete time,k')

subplot(9,2,16); plot(k,SS5KSA,'k')
title('Sensitivity function SS5KSA')
ylabel('\fontsize{8}SS5KSA')
xlabel('\fontsize{8}discrete time,k')

subplot(9,2,17); plot(k,SS5fMA,'k')
title('Sensitivity function SS5fMA')
ylabel('\fontsize{8}SS5fMA')
xlabel('\fontsize{8}discrete time,k')

subplot(9,2,18); plot(k,SS5KA,'k')
title('Sensitivity function SS5KA')
ylabel('\fontsize{8}SS5KA')
xlabel('\fontsize{8}discrete time,k')

%Graphs of the sensitivity functions for the Sads in the
tank 1
figure(16)
subplot(9,2,1);plot(k,Sads1,'k')
title('Process variable Sads1')
ylabel('\fontsize{8}Sads1')
xlabel('\fontsize{8}discrete time k')

subplot(9,2,2); plot(k,Sads1f,'k')
title('Sensitivity function Sads1f')
ylabel('\fontsize{8}Sads1f')
xlabel('\fontsize{8}discrete time,k')

subplot(9,2,3); plot(k,Sads1YZH,'k')
title('Variable Sads1YZH')
ylabel('\fontsize{8}Sads1YZH')
xlabel('\fontsize{8}discrete time,k')

subplot(9,2,4); plot(k,Sads1YZA,'k')
title('Variable Sads1YZA')
ylabel('\fontsize{8}Sads1YZA')
xlabel('\fontsize{8}discrete time,k')

subplot(9,2,5); plot(k,Sads1fZBH,'k')
title('Sensitivity function Sads1fZBH')
ylabel('\fontsize{8}Sads1fZBH')
xlabel('discrete time,k')

subplot(9,2,6); plot(k,Sads1muA,'k')
title('Sensitivity function Sads1muA')
ylabel('\fontsize{8}Sads1muA')
xlabel('\fontsize{8}discrete time,k')

subplot(9,2,7); plot(k,Sads1muH,'k')
title('Sensitivity function Sads1muH')
ylabel('\fontsize{8}Sads1muH')
xlabel('discrete time,k')

subplot(9,2,8); plot(k,Sads1KS,'k')
title('Sensitivity function Sads1KS')
ylabel('\fontsize{8}Sads1KS')
xlabel('discrete time,k')

subplot(9,2,9); plot(k,Sads1KOH,'k')
title('Sensitivity function Sads1KOH')
ylabel('\fontsize{8}Sads1KOH')
xlabel('\fontsize{8}discrete time,k')

subplot(9,2,10); plot(k,Sads1KNO,'k')
title('Sensitivity function Sads1KNO')
ylabel('\fontsize{8}Sads1KNO')
xlabel('\fontsize{8}discrete time,k')

subplot(9,2,11); plot(k,Sads1KNH,'k')
title('Sensitivity function Sads1KNH')
ylabel('\fontsize{8}Sads1KNH')
xlabel('\fontsize{8}discrete time,k')

subplot(9,2,12); plot(k,Sads1KOA,'k')
title('Sensitivity function Sads1KOA')
ylabel('\fontsize{8}Sads1KOA')
xlabel('\fontsize{8}discrete time,k')

subplot(9,2,13); plot(k,Sads1etag,'k')
title('Sensitivity function Sads1etag')
ylabel('\fontsize{8}Sads1etag')
xlabel('\fontsize{8}discrete time,k')

subplot(9,2,14); plot(k,Sads1KMP,'k')
title('Sensitivity function Sads1KMP')
ylabel('\fontsize{8}Sads1KMP')
xlabel('\fontsize{8}discrete time,k')

subplot(9,2,15); plot(k,Sads1KSP,'k')
title('Sensitivity function Sads1KSP')
ylabel('\fontsize{8}Sads1KSP')
xlabel('\fontsize{8}discrete time,k')

subplot(9,2,16); plot(k,Sads1KSA,'k')
title('Sensitivity function Sads1KSA')
ylabel('\fontsize{8}Sads1KSA')
xlabel('\fontsize{8}discrete time,k')

subplot(9,2,17); plot(k,Sads1fMA,'k')
title('Sensitivity function Sads1fMA')
ylabel('\fontsize{8}Sads1fMA')
xlabel('\fontsize{8}discrete time,k')

subplot(9,2,18); plot(k,Sads1KA,'k')
title('Sensitivity function Sads1KA')
ylabel('\fontsize{8}Sads1KA')
xlabel('\fontsize{8}discrete time,k')


%Graphs of the sensitivity functions of the varible SS in
the tank 2
figure(17)
subplot(9,2,1);plot(k,Sads2,'k')
title('Process variable Sads2')
ylabel('\fontsize{8}Sads2')
xlabel('\fontsize{8}discrete time k')

subplot(9,2,2); plot(k,Sads2f,'k')
title('Sensitivity function Sads2f')
ylabel('\fontsize{8}Sads2f')
xlabel('\fontsize{8}discrete time,k')

subplot(9,2,3); plot(k,Sads2YZH,'k')
title('Variable Sads2YZH')
ylabel('\fontsize{8}Sads2YZH')
xlabel('\fontsize{8}discrete time,k')

subplot(9,2,4); plot(k,Sads2YZA,'k')
title('Variable Sads2YZA')
ylabel('\fontsize{8}Sads2YZA')
xlabel('\fontsize{8}discrete time,k')

subplot(9,2,5); plot(k,Sads2fZBH,'k')
title('Sensitivity function Sads2fZBH')
ylabel('\fontsize{8}Sads2fZBH')
xlabel('discrete time,k')

subplot(9,2,6); plot(k,Sads2muA,'k')
title('Sensitivity function Sads2muA')
ylabel('\fontsize{8}Sads2muA')
xlabel('\fontsize{8}discrete time,k')

subplot(9,2,7); plot(k,Sads2muH,'k')
title('Sensitivity function Sads2muH')
ylabel('\fontsize{8}Sads2muH')
xlabel('discrete time,k')

subplot(9,2,8); plot(k,Sads2KS,'k')
title('Sensitivity function Sads2KS')
ylabel('\fontsize{8}Sads2KS')
xlabel('discrete time,k')

subplot(9,2,9); plot(k,Sads2KOH,'k')
title('Sensitivity function Sads2KOH')
ylabel('\fontsize{8}Sads2KOH')
xlabel('\fontsize{8}discrete time,k')

subplot(9,2,10); plot(k,Sads2KNO,'k')
title('Sensitivity function Sads2KNO')
ylabel('\fontsize{8}Sads2KNO')
xlabel('\fontsize{8}discrete time,k')

subplot(9,2,11); plot(k,Sads2KNH,'k')
title('Sensitivity function Sads2KNH')
ylabel('\fontsize{8}Sads2KNH')
xlabel('\fontsize{8}discrete time,k')

subplot(9,2,12); plot(k,Sads2KOA,'k')
title('Sensitivity function Sads2KOA')
ylabel('\fontsize{8}Sads2KOA')
xlabel('\fontsize{8}discrete time,k')

subplot(9,2,13); plot(k,Sads2etag,'k')
title('Sensitivity function Sads2etag')
```

```
ylabel('\fontsize{8}Sads2etag')
xlabel('\fontsize{8}discrete time,k')

subplot(9,2,14); plot(k,Sads2KMP,'k')
title('Sensitivity function Sads2KMP')
ylabel('\fontsize{8}Sads2KMP')
xlabel('\fontsize{8}discrete time,k')

subplot(9,2,15); plot(k,Sads2KSP,'k')
title('Sensitivity function Sads2KSP')
ylabel('\fontsize{8}Sads2KSP')
xlabel('\fontsize{8}discrete time,k')

subplot(9,2,16); plot(k,Sads2KSA,'k')
title('Sensitivity function Sads2KSA')
ylabel('\fontsize{8}Sads2KSA')
xlabel('\fontsize{8}discrete time,k')

subplot(9,2,17); plot(k,Sads2fMA,'k')
title('Sensitivity function Sads2fMA')
ylabel('\fontsize{8}Sads2fMA')
xlabel('\fontsize{8}discrete time,k')

subplot(9,2,18); plot(k,Sads2KA,'k')
title('Sensitivity function Sads2KA')
ylabel('\fontsize{8}Sads2KA')
xlabel('\fontsize{8}discrete time,k')

%Graphs for SS variable in the tank 3

figure(18)
subplot(9,2,1);plot(k,Sads3,'k')
title('Process variable Sads3')
ylabel('\fontsize{8}Sads3')
xlabel('\fontsize{8}discrete time k')

subplot(9,2,2); plot(k,SS3f,'k')
title('Sensitivity function Sads3f')
ylabel('\fontsize{8}Sads3f')
xlabel('\fontsize{8}discrete time,k')

subplot(9,2,3); plot(k,Sads3YZH,'k')
title('Variable Sads3YZH')
ylabel('\fontsize{8}Sads3YZH')
xlabel('\fontsize{8}discrete time,k')

subplot(9,2,4); plot(k,Sads3YZA,'k')
title('Variable Sads3YZA')
ylabel('\fontsize{8}Sads3YZA')
xlabel('\fontsize{8}discrete time,k')

subplot(9,2,5); plot(k,Sads3fZBH,'k')
title('Sensitivity function Sads3fZBH')
ylabel('\fontsize{8}Sads3fZBH')
xlabel('discrete time,k')

subplot(9,2,6); plot(k,Sads3muA,'k')
title('Sensitivity function Sads3muA')
ylabel('\fontsize{8}Sads3muA')
xlabel('\fontsize{8}discrete time,k')

subplot(9,2,7); plot(k,Sads3muH,'k')
title('Sensitivity function Sads3muH')
ylabel('\fontsize{8}Sads3muH')
xlabel('discrete time,k')

subplot(9,2,8); plot(k,Sads3KS,'k')
title('Sensitivity function Sads3KS')
ylabel('\fontsize{8}Sads3KS')
xlabel('discrete time,k')

subplot(9,2,9); plot(k,Sads3KOH,'k')
title('Sensitivity function Sads3KOH')
ylabel('\fontsize{8}Sads3KOH')
xlabel('\fontsize{8}discrete time,k')

subplot(9,2,10); plot(k,Sads3KNO,'k')
title('Sensitivity function Sads3KNO')
ylabel('\fontsize{8}Sads3KNO')
xlabel('\fontsize{8}discrete time,k')

subplot(9,2,11); plot(k,Sads3KNH,'k')
title('Sensitivity function Sads3KNH')
ylabel('\fontsize{8}Sads3KNH')
xlabel('\fontsize{8}discrete time,k')

subplot(9,2,12); plot(k,Sads3KOA,'k')
title('Sensitivity function Sads3KOA')
ylabel('\fontsize{8}Sads3KOA')
xlabel('\fontsize{8}discrete time,k')

subplot(9,2,13); plot(k,Sads3etag,'k')
title('Sensitivity function Sads3etag')
ylabel('\fontsize{8}Sads3etag')
xlabel('\fontsize{8}discrete time,k')

subplot(9,2,14); plot(k,Sads3KMP,'k')
title('Sensitivity function Sads3KMP')
ylabel('\fontsize{8}Sads3KMP')
xlabel('\fontsize{8}discrete time,k')

subplot(9,2,15); plot(k,Sads3KSP,'k')
title('Sensitivity function Sads3KSP')
ylabel('\fontsize{8}Sads3KSP')
xlabel('\fontsize{8}discrete time,k')

subplot(9,2,16); plot(k,Sads3KSA,'k')
title('Sensitivity function Sads3KSA')
ylabel('\fontsize{8}Sads3KSA')
xlabel('\fontsize{8}discrete time,k')

subplot(9,2,17); plot(k,Sads3fMA,'k')
title('Sensitivity function Sads3fMA')
ylabel('\fontsize{8}Sads3fMA')
xlabel('\fontsize{8}discrete time,k')

subplot(9,2,18); plot(k,Sads3KA,'k')
title('Sensitivity function Sads3KA')
ylabel('\fontsize{8}Sads3KA')
xlabel('\fontsize{8}discrete time,k')

%Graphs for the sensitivity functions for SS in the tank 4

figure(19)
subplot(9,2,1);plot(k,Sads4,'k')
title('Process variable Sads4')
ylabel('\fontsize{8}Sads4')
xlabel('\fontsize{8}discrete time k')

subplot(9,2,2); plot(k,Sads4f,'k')
title('Sensitivity function Sads4f')
ylabel('\fontsize{8}Sads4f')
xlabel('\fontsize{8}discrete time,k')

subplot(9,2,3); plot(k,Sads4YZH,'k')
title('Variable Sads4YZH')
ylabel('\fontsize{8}Sads4YZH')
xlabel('\fontsize{8}discrete time,k')

subplot(9,2,4); plot(k,Sads4YZA,'k')
title('Variable Sads4YZA')
ylabel('\fontsize{8}Sads4YZA')
xlabel('\fontsize{8}discrete time,k')

subplot(9,2,5); plot(k,Sads4fZBH,'k')
title('Sensitivity function Sads4fZBH')
ylabel('\fontsize{8}Sads4fZBH')
xlabel('discrete time,k')

subplot(9,2,6); plot(k,Sads4muA,'k')
title('Sensitivity function Sads4muA')
ylabel('\fontsize{8}Sads4muA')
xlabel('\fontsize{8}discrete time,k')

subplot(9,2,7); plot(k,Sads4muH,'k')
title('Sensitivity function Sads4muH')
ylabel('\fontsize{8}Sads4muH')
xlabel('discrete time,k')

subplot(9,2,8); plot(k,Sads4KS,'k')
title('Sensitivity function Sads4KS')
ylabel('\fontsize{8}Sads4KS')
xlabel('discrete time,k')

subplot(9,2,9); plot(k,Sads4KOH,'k')
title('Sensitivity function Sads4KOH')
ylabel('\fontsize{8}Sads4KOH')
xlabel('\fontsize{8}discrete time,k')

subplot(9,2,10); plot(k,Sads4KNO,'k')
title('Sensitivity function Sads4KNO')
ylabel('\fontsize{8}Sads4KNO')
xlabel('\fontsize{8}discrete time,k')

subplot(9,2,11); plot(k,Sads4KNH,'k')
title('Sensitivity function Sads4KNH')
ylabel('\fontsize{8}Sads4KNH')
xlabel('\fontsize{8}discrete time,k')

subplot(9,2,12); plot(k,Sads4KOA,'k')
title('Sensitivity function Sads4KOA')
ylabel('\fontsize{8}Sads4KOA')
xlabel('\fontsize{8}discrete time,k')

subplot(9,2,13); plot(k,Sads4etag,'k')
title('Sensitivity function Sads4etag')
ylabel('\fontsize{8}Sads4etag')
xlabel('\fontsize{8}discrete time,k')

subplot(9,2,14); plot(k,Sads4KMP,'k')
title('Sensitivity function Sads4KMP')
ylabel('\fontsize{8}Sads4KMP')
xlabel('\fontsize{8}discrete time,k')

subplot(9,2,15); plot(k,Sads4KSP,'k')
title('Sensitivity function Sads4KSP')
ylabel('\fontsize{8}Sads4KSP')
xlabel('\fontsize{8}discrete time,k')
```

```
subplot(9,2,16); plot(k,Sads4KSA,'k')
title('Sensitivity function Sads4KSA')
ylabel('\fontsize{8}Sads4KSA')
xlabel('\fontsize{8}discrete time,k')

subplot(9,2,17); plot(k,Sads4fMA,'k')
title('Sensitivity function Sads4fMA')
ylabel('\fontsize{8}Sads4fMA')
xlabel('\fontsize{8}discrete time,k')

subplot(9,2,18); plot(k,Sads4KA,'k')
title('Sensitivity function Sads4KA')
ylabel('\fontsize{8}Sads4KA')
xlabel('\fontsize{8}discrete time,k')

%Grapf for the sensitivity functions of the variable SNH in
the tank 5
figure(20)
subplot(9,2,1);plot(k,Sads5,'k')
title('Process variable Sads5')
ylabel('\fontsize{8}Sads5')
xlabel('\fontsize{8}discrete time k')

subplot(9,2,2); plot(k,Sads5f,'k')
title('Sensitivity function Sads5f')
ylabel('\fontsize{8}Sads5f')
xlabel('\fontsize{8}discrete time,k')

subplot(9,2,3); plot(k,Sads5YZH,'k')
title('Variable Sads5YZH')
ylabel('\fontsize{8}Sads5YZH')
xlabel('\fontsize{8}discrete time,k')

subplot(9,2,4); plot(k,Sads5YZA,'k')
title('Variable Sads5YZA')
ylabel('\fontsize{8}Sads5YZA')
xlabel('\fontsize{8}discrete time,k')

subplot(9,2,5); plot(k,Sads5fZBH,'k')
title('Sensitivity function Sads5fZBH')
ylabel('\fontsize{8}Sads5fZBH')
xlabel('discrete time,k')

subplot(9,2,6); plot(k,Sads5muA,'k')
title('Sensitivity function Sads5muA')
ylabel('\fontsize{8}Sads5muA')
xlabel('\fontsize{8}discrete time,k')

subplot(9,2,7); plot(k,Sads5muH,'k')
title('Sensitivity function Sads5muH')
ylabel('\fontsize{8}Sads5muH')
xlabel('discrete time,k')

subplot(9,2,8); plot(k,Sads5KS,'k')
title('Sensitivity function Sads5KS')
ylabel('\fontsize{8}Sads5KS')
xlabel('discrete time,k')

subplot(9,2,9); plot(k,Sads5KOH,'k')
title('Sensitivity function Sads5KOH')
ylabel('\fontsize{8}Sads5KOH')
xlabel('\fontsize{8}discrete time,k')

subplot(9,2,10); plot(k,Sads5KNO,'k')
title('Sensitivity function Sads5KNO')
ylabel('\fontsize{8}Sads5KNO')
xlabel('\fontsize{8}discrete time,k')

subplot(9,2,11); plot(k,Sads5KNH,'k')
title('Sensitivity function Sads5KNH')
ylabel('\fontsize{8}Sads5KNH')
xlabel('\fontsize{8}discrete time,k')

subplot(9,2,12); plot(k,Sads5KOA,'k')
title('Sensitivity function Sads5KOA')
ylabel('\fontsize{8}Sads5KOA')
xlabel('\fontsize{8}discrete time,k')

subplot(9,2,13); plot(k,Sads5etag,'k')
title('Sensitivity function Sads5etag')
ylabel('\fontsize{8}Sads5etag')
xlabel('\fontsize{8}discrete time,k')

subplot(9,2,14); plot(k,Sads5KMP,'k')
title('Sensitivity function Sads5KMP')
ylabel('\fontsize{8}Sads5KMP')
xlabel('\fontsize{8}discrete time,k')

subplot(9,2,15); plot(k,Sads5KSP,'k')
title('Sensitivity function Sads5KSP')
ylabel('\fontsize{8}Sads5KSP')
xlabel('\fontsize{8}discrete time,k')

subplot(9,2,16); plot(k,Sads5KSA,'k')
title('Sensitivity function Sads5KSA')
ylabel('\fontsize{8}Sads5KSA')
xlabel('\fontsize{8}discrete time,k')

subplot(9,2,17); plot(k,Sads5fMA,'k')
title('Sensitivity function Sads5fMA')
ylabel('\fontsize{8}Sads5fMA')
xlabel('\fontsize{8}discrete time,k')

subplot(9,2,18); plot(k,Sads5KA,'k')
title('Sensitivity function Sads5KA')
ylabel('\fontsize{8}Sads5KA')
xlabel('\fontsize{8}discrete time,k')
```

2.Subprogram

```
%SUBPROGRAM rateBUCTS.m
%AIM:The program function rateASM1.m calculates the process rates, derivatives of the proces rates towards the model parameters
and variables and forms the sensitivity model matrices necessary for simulation of theprocess variables and the sensitivity
functions for the Benchmark process based on the reduced UCT biological model.
%The program uses global definition of the model parameters

function [ROUCT,ASu,BSu,CSu,DSu]=rateBUCTS(Xk,Uk,XBHk,XBAk,XSk,DT,A11u,A15u,A21u,A22u,A32u,A33u,A43u,A44u,A54u,A55u,B1u,Cnu)
global Ks KOH KNO KNA KOA muH etag muA KMP fZBH YZH YZA KA KSA KSP fMA

%Calculation of the process rates at every moment of the time
% reactions in tank 1
ROUCT(1)=muH*(Xk(3)/(Ks+Xk(3)))*(Uk(1)/(KOH+Uk(1)))*(Xk(1)/(KNA+Xk(1)))*XBHk(1);
ROUCT(2)=muH*(Xk(3)/(Ks+Xk(3)))*(Uk(1)/(KOH+Uk(1)))*(KNA/(KNA+Xk(1)))*(Xk(2)/(KNO+Xk(2)))*XBHk(1);
ROUCT(3)=muH*(Xk(3)/(Ks+Xk(3)))*(KOH/(KOH+Uk(1)))*(Xk(1)/(KNA+Xk(1)))*(Xk(2)/(KNO+Xk(2)))*XBHk(1);
ROUCT(4)=muH*(Xk(3)/(Ks+Xk(3)))*(KOH/(KOH+Uk(1)))*(KNA/(KNA+Xk(1)))*(Xk(2)/(KNO+Xk(2)))*XBHk(1);
ROUCT(5)=KMP*((Xk(4)/XBHk(1))/(KSP+Xk(4)/XBHk(1)))*(Uk(1)/(KOH+Uk(1)))*(Xk(1)/(KNA+Xk(1)))*XBHk(1);
ROUCT(6)=KMP*((Xk(4)/XBHk(1))/(KSP+Xk(4)/XBHk(1)))*(Uk(1)/(KOH+Uk(1)))*(KNA/(KNA+Xk(1)))*(Xk(2)/(KNO+Xk(2)))*XBHk(1);
ROUCT(7)=KMP*((Xk(4)/XBHk(1))/(KSP+Xk(4)/XBHk(1)))*(KOH/(KOH+Uk(1)))*(Xk(1)/(KNA+Xk(1)))*(Xk(2)/(KNO+Xk(2)))*etag*XBHk(1);
ROUCT(8)=KMP*((Xk(4)/XBHk(1))/(KSP+Xk(4)/XBHk(1)))*(KOH/(KOH+Uk(1)))*(KNA/(KNA+Xk(1)))*(Xk(2)/(KNO+Xk(2)))*etag*XBHk(1);
ROUCT(9)=KA*XSk(1)*XBHk(1)*(fMA-(Xk(4)/XBHk(1)));
ROUCT(10)=muA*(Uk(1)/(KOA+Uk(1)))*(Xk(1)/(KSA+Xk(1)))*XBHk(1);

% reactions in tank 2
ROUCT(11)=muH*(Xk(7)/(Ks+Xk(7)))*(Uk(2)/(KOH+Uk(2)))*(Xk(5)/(KNA+Xk(5)))*XBHk(2);
ROUCT(12)=muH*(Xk(7)/(Ks+Xk(7)))*(Uk(2)/(KOH+Uk(2)))*(KNA/(KNA+Xk(5)))*(Xk(6)/(KNO+Xk(6)))*XBHk(2);
ROUCT(13)=muH*(Xk(7)/(Ks+Xk(7)))*(KOH/(KOH+Uk(2)))*(Xk(5)/(KNA+Xk(5)))*(Xk(6)/(KNO+Xk(6)))*XBHk(2);
ROUCT(14)=muH*(Xk(7)/(Ks+Xk(7)))*(KOH/(KOH+Uk(2)))*(KNA/(KNA+Xk(5)))*(Xk(6)/(KNO+Xk(6)))*XBHk(2);
ROUCT(15)=KMP*((Xk(8)/XBHk(2))/(KSP+Xk(8)/XBHk(2)))*(Uk(2)/(KOH+Uk(2)))*(Xk(5)/(KNA+Xk(5)))*XBHk(2);
ROUCT(16)=KMP*((Xk(8)/XBHk(2))/(KSP+Xk(8)/XBHk(2)))*(Uk(2)/(KOH+Uk(2)))*(KNA/(KNA+Xk(5)))*(Xk(6)/(KNO+Xk(6)))*XBHk(2);
ROUCT(17)=KMP*((Xk(8)/XBHk(2))/(KSP+Xk(8)/XBHk(2)))*(KOH/(KOH+Uk(2)))*(Xk(5)/(KNA+Xk(5)))*(Xk(6)/(KNO+Xk(6)))*etag*XBHk(2);
ROUCT(18)=KMP*((Xk(8)/XBHk(2))/(KSP+Xk(8)/XBHk(2)))*(KOH/(KOH+Uk(2)))*(KNA/(KNA+Xk(5)))*(Xk(6)/(KNO+Xk(6)))*etag*XBHk(2);
ROUCT(19)=KA*XSk(2)*XBHk(2)*(fMA-(Xk(8)/XBHk(2)));
ROUCT(20)=muA*(Uk(2)/(KOA+Uk(2)))*(Xk(5)/(KSA+Xk(5)))*XBHk(2);

% reactions in tank 3
ROUCT(21)=muH*(Xk(11)/(Ks+Xk(11)))*(Uk(3)/(KOH+Uk(3)))*(Xk(9)/(KNA+Xk(9)))*XBHk(3);
ROUCT(22)=muH*(Xk(11)/(Ks+Xk(11)))*(Uk(3)/(KOH+Uk(3)))*(KNA/(KNA+Xk(9)))*(Xk(10)/(KNO+Xk(10)))*XBHk(3);
ROUCT(23)=muH*(Xk(11)/(Ks+Xk(11)))*(KOH/(KOH+Uk(3)))*(Xk(9)/(KNA+Xk(9)))*(Xk(10)/(KNO+Xk(10)))*XBHk(3);
ROUCT(24)=muH*(Xk(11)/(Ks+Xk(11)))*(KOH/(KOH+Uk(3)))*(KNA/(KNA+Xk(9)))*(Xk(10)/(KNO+Xk(10)))*XBHk(3);
ROUCT(25)=KMP*((Xk(12)/XBHk(3))/(KSP+Xk(12)/XBHk(3)))*(Uk(3)/(KOH+Uk(3)))*(Xk(9)/(KNA+Xk(9)))*XBHk(3);
```

```
ROUCT(26)=KMP*((Xk(12)/XBHk(3))/(KSP+Xk(12)/XBHk(3)))*(Uk(3)/(KOH+Uk(3)))*(KNA/(KNA+Xk(9)))*(Xk(10)/(KNO+Xk(10)))*XBHk(3);
ROUCT(27)=KMP*((Xk(12)/XBHk(3))/(KSP+Xk(12)/XBHk(3)))*(KOH/(KOH+Uk(3)))*(Xk(9)/(KNA+Xk(9)))*(Xk(10)/(KNO+Xk(10)))*etag*XBHk(3);
ROUCT(28)=KMP*((Xk(12)/XBHk(3))/(KSP+Xk(12)/XBHk(3)))*(KOH/(KOH+Uk(3)))*(KNA/(KNA+Xk(9)))*(Xk(10)/(KNO+Xk(10)))*etag*XBHk(3);
ROUCT(29)=KA*XSk(3)*XBHk(3)*(fMA-(Xk(12)/XBHk(3)));
ROUCT(30)=muA*(Uk(3)/(KOA+Uk(3)))*(Xk(9)/(KSA+Xk(9)))*XBHk(3);

% reactions in tank 4
ROUCT(31)=muH*(Xk(15)/(Ks+Xk(15)))*(Uk(4)/(KOH+Uk(4)))*(Xk(13)/(KNA+Xk(13)))*XBHk(4);
ROUCT(32)=muH*(Xk(15)/(Ks+Xk(15)))*(Uk(4)/(KOH+Uk(4)))*(KNA/(KNA+Xk(13)))*(Xk(14)/(KNO+Xk(14)))*XBHk(4);
ROUCT(33)=muH*(Xk(15)/(Ks+Xk(15)))*(KOH/(KOH+Uk(4)))*(Xk(13)/(KNA+Xk(13)))*(Xk(14)/(KNO+Xk(14)))*XBHk(4);
ROUCT(34)=muH*(Xk(15)/(Ks+Xk(15)))*(KOH/(KOH+Uk(4)))*(KNA/(KNA+Xk(13)))*(Xk(14)/(KNO+Xk(14)))*XBHk(4);
ROUCT(35)=KMP*((Xk(16)/XBHk(4))/(KSP+Xk(16)/XBHk(4)))*(Uk(4)/(KOH+Uk(4)))*(Xk(13)/(KNA+Xk(13)))*XBHk(4);
ROUCT(36)=KMP*((Xk(16)/XBHk(4))/(KSP+Xk(16)/XBHk(4)))*(Uk(4)/(KOH+Uk(4)))*(KNA/(KNA+Xk(13)))*(Xk(14)/(KNO+Xk(14)))*XBHk(4);
ROUCT(37)=KMP*((Xk(16)/XBHk(4))/(KSP+Xk(16)/XBHk(4)))*(KOH/(KOH+Uk(4)))*(Xk(13)/(KNA+Xk(13)))*(Xk(14)/(KNO+Xk(14)))*etag*XBHk(4);
ROUCT(38)=KMP*((Xk(16)/XBHk(4))/(KSP+Xk(16)/XBHk(4)))*(KOH/(KOH+Uk(4)))*(KNA/(KNA+Xk(13)))*(Xk(14)/(KNO+Xk(14)))*etag*XBHk(4);
ROUCT(39)=KA*XSk(4)*XBHk(4)*(fMA-(Xk(16)/XBHk(4)));
ROUCT(40)=muA*(Uk(4)/(KOA+Uk(4)))*(Xk(13)/(KSA+Xk(13)))*XBHk(4);

% reactions in tank 5
ROUCT(41)=muH*(Xk(19)/(Ks+Xk(19)))*(Uk(5)/(KOH+Uk(5)))*(Xk(17)/(KNA+Xk(17)))*XBHk(5);
ROUCT(42)=muH*(Xk(19)/(Ks+Xk(19)))*(Uk(5)/(KOH+Uk(5)))*(KNA/(KNA+Xk(17)))*(Xk(18)/(KNO+Xk(18)))*XBHk(5);
ROUCT(43)=muH*(Xk(19)/(Ks+Xk(19)))*(KOH/(KOH+Uk(5)))*(Xk(17)/(KNA+Xk(17)))*(Xk(18)/(KNO+Xk(18)))*XBHk(5);
ROUCT(44)=muH*(Xk(19)/(Ks+Xk(19)))*(KOH/(KOH+Uk(5)))*(KNA/(KNA+Xk(17)))*(Xk(18)/(KNO+Xk(18)))*XBHk(5);
ROUCT(45)=KMP*((Xk(20)/XBHk(5))/(KSP+Xk(20)/XBHk(5)))*(Uk(5)/(KOH+Uk(5)))*(Xk(17)/(KNA+Xk(17)))*XBHk(5);
ROUCT(46)=KMP*((Xk(20)/XBHk(5))/(KSP+Xk(20)/XBHk(5)))*(Uk(5)/(KOH+Uk(5)))*(KNA/(KNA+Xk(17)))*(Xk(18)/(KNO+Xk(18)))*XBHk(5);
ROUCT(47)=KMP*((Xk(20)/XBHk(5))/(KSP+Xk(20)/XBHk(5)))*(KOH/(KOH+Uk(5)))*(Xk(17)/(KNA+Xk(17)))*(Xk(18)/(KNO+Xk(18)))*etag*XBHk(5);
ROUCT(48)=KMP*((Xk(20)/XBHk(5))/(KSP+Xk(20)/XBHk(5)))*(KOH/(KOH+Uk(5)))*(KNA/(KNA+Xk(17)))*(Xk(18)/(KNO+Xk(18)))*etag*XBHk(5);
ROUCT(49)=KA*XSk(5)*XBHk(5)*(fMA-(Xk(20)/XBHk(5)));
ROUCT(50)=muA*(Uk(5)/(KOA+Uk(5)))*(Xk(17)/(KSA+Xk(17)))*XBHk(5);

ROUCT=[ROUCT(1) ROUCT(2) ROUCT(3) ROUCT(4) ROUCT(5) ROUCT(6) ROUCT(7) ROUCT(8) ROUCT(9) ROUCT(10) ROUCT(11) ROUCT(12) ROUCT(13)
ROUCT(14) ROUCT(15) ROUCT(16) ROUCT(17) ROUCT(18) ROUCT(19) ROUCT(20) ROUCT(21) ROUCT(22) ROUCT(23) ROUCT(24) ROUCT(25) ROUCT(26)
ROUCT(27) ROUCT(28) ROUCT(29) ROUCT(30) ROUCT(31) ROUCT(32) ROUCT(33) ROUCT(34) ROUCT(35) ROUCT(36) ROUCT(37) ROUCT(38) ROUCT(39)
ROUCT(40) ROUCT(41) ROUCT(42) ROUCT(43) ROUCT(44) ROUCT(45) ROUCT(46) ROUCT(47) ROUCT(48) ROUCT(49) ROUCT(50)]';

%Calculation for the Sensitivity Analysis
% Calculation of the derivatives of the process rates towards the process variables
%Calculations for the tank 1
rUSNH1SNH1=-
fZBH*XBHk(1)*(KNA/(KNA+Xk(1)))^2)*(Uk(1)/(KOH+Uk(1)))*(muH*(Xk(3)/(Ks+Xk(3)))+KMP*((Xk(4)/XBHk(1))/(KSP+(Xk(4)/XBHk(1)))))+(KOH/(KO
H+Uk(1)))*(Xk(2)/(KNO+Xk(2)))*muH*(Xk(3)/(Ks+Xk(3)))*KMP*etag*((Xk(4)/XBHk(1))/(KSP+(Xk(4)/XBHk(1))))-
(1/YZA+fZBH)*muA*(Uk(1)/(KOA+Uk(1)))*(KSA/(KSA+Xk(1)))*XBAk(1);
rUSNH1SNO1=-
fZBH*XBHk(1)*(KNO/(KNO+Xk(2))^2)*(KOH/(KOH+Uk(1)))*(Xk(1)/(KNA+Xk(1)))*(muH*(Xk(3)/(Ks+Xk(3)))+etag*KMP*((Xk(4)/XBHk(1))/(KSP+(Xk(
4)/XBHk(1)))));
rUSNH1SS1=-fZBH*muH*(Ks/(Ks+Xk(3)))*XBHk(1)*(Xk(1)/(KSA+Xk(1)))*((Uk(1)/(KOH+Uk(1)))+(KOH/(KOH+Uk(1)))*(Xk(2)/(KNO+Xk(2))));
rUSNH1Sads1=-
fZBH*KMP*((KSP/XBHk(1))/(KSP+(Xk(4)/XBHk(1))))*(Xk(1)/(KNA+Xk(1)))*((Uk(1)/(KOH+Uk(1)))+etag*(KOH/(KOH+Uk(1)))*(Xk(2)/(KNO+Xk(2)))
);
rUSNO1SNH1=fZBH*(Uk(1)/(KOH+Uk(1)))*(KNA/(KNA+Xk(1))^2)*(Xk(2)/(KNO+Xk(2)))*XBHk(1)*(muH*(Xk(3)/(Ks+Xk(3)))+KMP*((Xk(4)/XBHk(1))/(
KSP+(Xk(4)/XBHk(1))))+fZBH*(KOH/(KOH+Uk(1)))*(KNA/(KNA+Xk(1))^2)*(Xk(2)/(KNO+Xk(2)))*XBHk(1)*(muH*(Xk(3)/(Ks+Xk(3)))+KMP*etag*((Xk
(4)/XBHk(1))/(KSP+(Xk(4)/XBHk(1)))))+(1/YZA)*muA*(KSA/(KSA+Xk(1))^2)*(Xk(2)/KOA+Xk(2)))*XBAk(1);
rUSNO1SNO1=-
fZBH*(Uk(1)/(KOH+Uk(1)))*(KSA/(KSA+Xk(1)))*(KNO/(KNO+Xk(2))^2)*XBHk(1)*(muH*(Xk(3)/(Ks+Xk(3)))+KMP*((Xk(4)/XBHk(1))/(KSP+(Xk(4)/XB
Hk(1)))))-
(KOH/(KOH+Uk(1)))*(KNO/(KNO+Xk(2))^2)*XBHk(1)*(muH*(Xk(3)/(Ks+Xk(3)))+KMP*etag*((Xk(4)/XBHk(1))/(KSP+(Xk(4)/XBHk(1)))))*(((1-
YZH)/2.86*YZH)*(Xk(1)/(KNA+Xk(1)))+(((1-YZH)/2.86*YZH)+fZBH)*(KNA/(KNA+Xk(1))));
rUSNO1SS1=-muH*(Ks/(Ks+Xk(3))^2)*(Xk(2)/(KNO+Xk(2)))*XBHk(1)*(fZBH*(Uk(1)/(KOH+Uk(1)))*(KNA/(KNA+Xk(1)))+((1-
YZH)/2.86*YZH)*(KOH/(KOH+Uk(1)))*(Xk(1)/(KNA+Xk(1)))+((1-YZH)/2.86*YZH)+fZBH)*(KOH/(KOH+Uk(1)))*(KNA/(KNA+Xk(1)));
rUSNO1Sads1=-
KMP*((KSP/XBHk(1))/(KSP+(KSP/XBHk(1)))^2)*(Xk(2)/(KNO+Xk(2)))*XBHk(1)*(fZBH*(Uk(1)/(KOH+Uk(1)))*(KNA/(KNA+Xk(1)))+((1-
YZH)/2.86*YZH)*(KOH/(KOH+Uk(1)))*(Xk(1)/(KNA+Xk(1)))*etag+(((1-YZH)/2.86*YZH)+fZBH)*(KOH/(KOH+Uk(1)))*(KNA/(KNA+Xk(1)))*etag);
rUSS1SNH1=-(1/YZH)*muH*(Xk(3)/(Ks+Xk(3)))*(Uk(1)/(KOH+Uk(1)))*(KNA/(KNA+Xk(1))^2)*XBHk(1)*(1-(Xk(2)/(KNO+Xk(2))));
rUSS1SNO1=-
(1/YZH)*muH*(Xk(3)/(Ks+Xk(3)))*(KNO/(KNO+Xk(2)^2)*XBHk(1)*((Uk(1)/(KOH+Uk(1)))*(KNA/(KNA+Xk(1)))+(KOH/(KOH+Uk(1)))*(Xk(1)/(KNA+Xk
(1)))+(KOH/(KOH+Uk(1)))*(KNA/(KNA+Xk(1))));
rUSS1SS1=-
(1/YZH)*(Ks/(Ks+Xk(3))^2)*((Uk(1)/(KOH+Uk(1)))*((Xk(1)/(KNA+Xk(1)))+(KNA/(KNA+Xk(1)))*(Xk(2)/(KNO+Xk(2))))+(KOH/(KOH+Uk(1)))*(Xk(2
)/(KNO+Xk(2)))*((Xk(1)/(KNA+Xk(1)))+(KNA/(KNA+Xk(1)))))*XBHk(1);
rUSS1Sads1=0;
rUSads1SNH1=-(1/YZH)*KMP*((Xk(4)/XBHk(1))/(KSP+(Xk(4)/XBHk(1))))*(Uk(1)/(KOH+Uk(1)))*(KNA/(KNA+Xk(1))^2)*XBHk(1)*(1-
(Xk(2)/(KNO+Xk(2))));
rUSads1SNO1=-
(1/YZH)*KMP*((Xk(4)/XBHk(1))/(KSP+(Xk(4)/XBHk(1))))*(KNO/(KNO+Xk(2))^2)*XBHk(1)*((Uk(1)/(KOH+Uk(1)))*(KNA/(KNA+Xk(1)))+(KOH/(KOH+U
k(1)))*(Xk(1)/(KNA+Xk(1)))+(KOH/(KOH+Uk(1)))*(KNA/(KNA+Xk(1)))); rUSads1SS1=0;
rUSads1Sads1=-
(1/YZH)*KMP*((KSP/XBHk(1))/(KSP+(Xk(4)/XBHk(1)))^2)*(Uk(1)/(KOH+Uk(1)))*XBHk(1)*((Xk(1)/(KNA+Xk(1)))*+(KNA/(KNA+Xk(1)))*(Xk(2)/(KN
O+Xk(2))))-
(1/YZH)*KMP*((KSP/XBHk(1))/(KSP+(Xk(4)/XBHk(1)))^2)*(KOH/(KOH+Uk(1)))*(Xk(2)/(KNO+Xk(2)))*etag*XBHk(1)*((Xk(1)/(KNA+Xk(1)))+(KNA/(
KNA+Xk(1))));

% Calculation fo the tank 2
rUSNH2SNH2=-
fZBH*XBHk(2)*(KNA/(KNA+Xk(5))^2)*(Uk(2)/(KOH+Uk(2)))*(muH*(Xk(7)/(Ks+Xk(7)))+KMP*((Xk(8)/XBHk(2))/(KSP+(Xk(8)/XBHk(2)))))+(KOH/(KO
H+Uk(2)))*(Xk(6)/(KNO+Xk(6)))*muH*(Xk(7)/(Ks+Xk(7)))*KMP*etag*((Xk(8)/XBHk(2))/(KSP+(Xk(8)/XBHk(2))))-
(1/YZA+fZBH)*muA*(Uk(2)/(KOA+Uk(2)))*(KSA/(KSA+Xk(5)))*XBAk(2);
rUSNH2SNO2=-
fZBH*XBHk(2)*(KNO/(KNO+Xk(6))^2)*(KOH/(KOH+Uk(2)))*(Xk(5)/(KNA+Xk(5)))*(muH*(Xk(7)/(Ks+Xk(7)))+etag*KMP*((Xk(8)/XBHk(2))/(KSP+(Xk(
8)/XBHk(2)))));
rUSNH2SS2=-fZBH*muH*(Ks/(Ks+Xk(7)))*XBHk(2)*(Xk(5)/(KSA+Xk(5)))*((Uk(2)/(KOH+Uk(2)))+(KOH/(KOH+Uk(2)))*(Xk(6)/(KNO+Xk(6))));
rUSNH2Sads2=-
fZBH*KMP*((KSP/XBHk(2))/(KSP+(Xk(8)/XBHk(2))))*(Xk(5)/(KNA+Xk(5)))*((Uk(2)/(KOH+Uk(2)))+etag*(KOH/(KOH+Uk(2)))*(Xk(6)/(KNO+Xk(6)))
);
rUSNO2SNH2=fZBH*(Uk(2)/(KOH+Uk(2)))*(KNA/(KNA+Xk(5))^2)*(Xk(6)/(KNO+Xk(6)))*XBHk(2)*(muH*(Xk(7)/(Ks+Xk(7)))+KMP*((Xk(8)/XBHk(2))/(
KSP+(Xk(8)/XBHk(2))))+fZBH*(KOH/(KOH+Uk(2)))*(KNA/(KNA+Xk(5))^2)*(Xk(6)/(KNO+Xk(6)))*XBHk(2)*(muH*(Xk(7)/(Ks+Xk(7)))+KMP*etag*((Xk
(8)/XBHk(2))/(KSP+(Xk(8)/XBHk(2)))))+(1/YZA)*muA*(KSA/(KSA+Xk(5))^2)*(Xk(6)/KOA+Xk(6)))*XBAk(2);
rUSNO2SNO2=-
fZBH*(Uk(2)/(KOH+Uk(2)))*(KSA/(KSA+Xk(5)))*(KNO/(KNO+Xk(6))^2)*XBHk(2)*(muH*(Xk(7)/(Ks+Xk(7)))+KMP*((Xk(8)/XBHk(2))/(KSP+(Xk(8)/XB
Hk(2)))))-
```

```
(KOH/(KOH+Uk(2)))*(KNO/(KNO+Xk(6))^2)*XBHk(2)*(muH*(Xk(7)/(Ks+Xk(7)))+KMP*etag*((Xk(8)/XBHk(2))/(KSP+(Xk(8)/XBHk(2)))))*(((1-
YZH)/2.86*YZH)*(Xk(5)/(KNA+Xk(5)))+(((1-YZH)/2.86*YZH)+fZBH)*(KNA/(KNA+Xk(5))));
rUSNO2SS2=-muH*(Ks/(Ks+Xk(7))^2)*(Xk(6)/(KNO+Xk(6)))*XBHk(2)*(fZBH*(Uk(2)/(KOH+Uk(2)))*(KNA/(KNA+Xk(5)))+((1-
YZH)/2.86*YZH)*(KOH/(KOH+Uk(2)))*(Xk(5)/(KNA+Xk(5)))+((1-YZH)/2.86*YZH)+fZBH)*(KOH/(KOH+Uk(2)))*(KNA/(KNA+Xk(5)));
rUSNO2Sads2=-
KMP*((KSP/XBHk(2))/(KSP+(KSP/XBHk(2)))^2)*(Xk(6)/(KNO+Xk(6)))*XBHk(2)*(fZBH*(Uk(2)/(KOH+Uk(2)))*(KNA/(KNA+Xk(5)))+((1-
YZH)/2.86*YZH)*(KOH/(KOH+Uk(2)))*(Xk(5)/(KNA+Xk(5)))*etag+(((1-YZH)/2.86*YZH)+fZBH)*(KOH/(KOH+Uk(2)))*(KNA/(KNA+Xk(5)))*etag);
rUSS2SNH2=-(1/YZH)*muH*(Xk(7)/(Ks+Xk(7)))*(Uk(2)/(KOH+Uk(2)))*(KNA/(KNA+Xk(5))^2)*XBHk(2)*(1-(Xk(6)/(KNO+Xk(6))));
rUSS2SNO2=-
(1/YZH)*muH*(Xk(7)/(Ks+Xk(7)))*(KNO/(KNO+Xk(6))^2)*XBHk(2)*((Uk(2)/(KOH+Uk(2)))*(KNA/(KNA+Xk(5)))+(KOH/(KOH+Uk(2)))*(Xk(5)/(KNA+Xk
(5)))+(KOH/(KOH+Uk(2)))*(KNA/(KNA+Xk(5))));
rUSS2SS2=-
(1/YZH)*(Ks/(Ks+Xk(7))^2)*((Uk(2)/(KOH+Uk(2)))*((Xk(5)/(KNA+Xk(5)))+(KNA/(KNA+Xk(5)))*(Xk(6)/(KNO+Xk(6))))+(KOH/(KOH+Uk(2)))*(Xk(6
)/(KNO+Xk(6)))*((Xk(5)/(KNA+Xk(5)))+(KNA/(KNA+Xk(5)))))*XBHk(2); rUSS2Sads2=0;
rUSads2SNH2=-(1/YZH)*KMP*((Xk(8)/XBHk(2))/(KSP+(Xk(8)/XBHk(2))))*(Uk(2)/(KOH+Uk(2)))*(KNA/(KNA+Xk(5))^2)*XBHk(2)*(1-
(Xk(6)/(KNO+Xk(6))));
rUSads2SNO2=-
(1/YZH)*KMP*((Xk(8)/XBHk(2))/(KSP+(Xk(8)/XBHk(2))))*(KNO/(KNO+Xk(6))^2)*XBHk(2)*((Uk(2)/(KOH+Uk(2)))*(KNA/(KNA+Xk(5)))+(KOH/(KOH+U
k(2)))*(Xk(5)/(KNA+Xk(5)))+(KOH/(KOH+Uk(2)))*(KNA/(KNA+Xk(5))));rUSads2SS2=0;
rUSads2Sads2=-
(1/YZH)*KMP*((KSP/XBHk(2))/(KSP+(Xk(8)/XBHk(2)))^2)*(Uk(2)/(KOH+Uk(2)))*XBHk(2)*((Xk(5)/(KNA+Xk(5)))*+(KNA/(KNA+Xk(5)))*(Xk(6)/(KN
O+Xk(6))))-
(1/YZH)*KMP*((KSP/XBHk(2))/(KSP+(Xk(8)/XBHk(2)))^2)*(KOH/(KOH+Uk(2)))*(Xk(6)/(KNO+Xk(6)))*etag*XBHk(2)*((Xk(5)/(KNA+Xk(5)))+(KNA/(
KNA+Xk(5))));

% Calculation for the tank 3
rUSNH3SNH3=-
fZBH*XBHk(3)*(KNA/(KNA+Xk(9))^2)*(Uk(3)/(KOH+Uk(3)))*(muH*(Xk(11)/(Ks+Xk(11)))+KMP*((Xk(12)/XBHk(3))/(KSP+(Xk(12)/XBHk(3)))))+(KOH
/(KOH+Uk(3)))*(Xk(10)/(KNO+Xk(10)))*muH*(Xk(11)/(Ks+Xk(11)))*KMP*etag*((Xk(12)/XBHk(3))/(KSP+(Xk(12)/XBHk(3))))-
(1/YZA+fZBH)*muA*(Uk(3)/(KOA+Uk(3)))*(KSA/(KSA+Xk(9)))*XBAk(3);
rUSNH3SNO3=-
fZBH*XBHk(3)*(KNO/(KNO+Xk(10))^2)*(KOH/(KOH+Uk(3)))*(Xk(9)/(KNA+Xk(9)))*(muH*(Xk(11)/(Ks+Xk(11)))+etag*KMP*((Xk(12)/XBHk(3))/(KSP+
(Xk(12)/XBHk(3)))));
rUSNH3SS3=-fZBH*muH*(Ks/(Ks+Xk(11)))*XBHk(3)*(Xk(9)/(KSA+Xk(9)))*((Uk(3)/(KOH+Uk(3)))+(KOH/(KOH+Uk(3)))*(Xk(10)/(KNO+Xk(10))));
rUSNH3Sads3=-
fZBH*KMP*((KSP/XBHk(3))/(KSP+(Xk(12)/XBHk(3))))*(Xk(9)/(KNA+Xk(9)))*((Uk(3)/(KOH+Uk(3)))+etag*(KOH/(KOH+Uk(3)))*(Xk(10)/(KNO+Xk(10
))));
rUSNO3SNH3=fZBH*(Uk(3)/(KOH+Uk(3)))*(KNA/(KNA+Xk(9))^2)*(Xk(10)/(KNO+Xk(10)))*XBHk(3)*(muH*(Xk(11)/(Ks+Xk(11)))+KMP*((Xk(12)/XBHk(
3))/(KSP+(Xk(12)/XBHk(3))))+fZBH*(KOH/(KOH+Uk(3)))*(KNA/(KNA+Xk(9))^2)*(Xk(10)/(KNO+Xk(10)))*XBHk(3)*(muH*(Xk(11)/(Ks+Xk(11)))+KMP
*etag*((Xk(12)/XBHk(3))/(KSP+(Xk(12)/XBHk(3)))))+(1/YZA)*muA*(KSA/(KSA+Xk(9))^2)*(Xk(10)/KOA+Xk(10)))*XBAk(3);
rUSNO3SNO3=-
fZBH*(Uk(3)/(KOH+Uk(3)))*(KSA/(KSA+Xk(9)))*(KNO/(KNO+Xk(10))^2)*XBHk(3)*(muH*(Xk(11)/(Ks+Xk(11)))+KMP*((Xk(12)/XBHk(3))/(KSP+(Xk(1
2)/XBHk(3)))))-
(KOH/(KOH+Uk(3)))*(KNO/(KNO+Xk(10))^2)*XBHk(3)*(muH*(Xk(11)/(Ks+Xk(11)))+KMP*etag*((Xk(12)/XBHk(3))/(KSP+(Xk(12)/XBHk(3)))))*(((1-
YZH)/2.86*YZH)*(Xk(9)/(KNA+Xk(9)))+(((1-YZH)/2.86*YZH)+fZBH)*(KNA/(KNA+Xk(9))));
rUSNO3SS3=-muH*(Ks/(Ks+Xk(11))^2)*(Xk(10)/(KNO+Xk(10)))*XBHk(3)*(fZBH*(Uk(3)/(KOH+Uk(3)))*(KNA/(KNA+Xk(9)))+((1-
YZH)/2.86*YZH)*(KOH/(KOH+Uk(3)))*(Xk(9)/(KNA+Xk(9)))+((1-YZH)/2.86*YZH)+fZBH)*(KOH/(KOH+Uk(3)))*(KNA/(KNA+Xk(9)));
rUSNO3Sads3=-
KMP*((KSP/XBHk(3))/(KSP+(KSP/XBHk(3)))^2)*(Xk(10)/(KNO+Xk(10)))*XBHk(3)*(fZBH*(Uk(3)/(KOH+Uk(3)))*(KNA/(KNA+Xk(9)))+((1-
YZH)/2.86*YZH)*(KOH/(KOH+Uk(3)))*(Xk(9)/(KNA+Xk(9)))*etag+(((1-YZH)/2.86*YZH)+fZBH)*(KOH/(KOH+Uk(3)))*(KNA/(KNA+Xk(9)))*etag);
rUSS3SNH3=-(1/YZH)*muH*(Xk(11)/(Ks+Xk(11)))*(Uk(3)/(KOH+Uk(3)))*(KNA/(KNA+Xk(9))^2)*XBHk(3)*(1-(Xk(10)/(KNO+Xk(10))));
rUSS3SNO3=-
(1/YZH)*muH*(Xk(11)/(Ks+Xk(11)))*(KNO/(KNO+Xk(10))^2)*XBHk(3)*((Uk(3)/(KOH+Uk(3)))*(KNA/(KNA+Xk(9)))+(KOH/(KOH+Uk(3)))*(Xk(9)/(KNA
+Xk(9)))+(KOH/(KOH+Uk(3)))*(KNA/(KNA+Xk(9))));
rUSS3SS3=-
(1/YZH)*(Ks/(Ks+Xk(11))^2)*((Uk(3)/(KOH+Uk(3)))*((Xk(9)/(KNA+Xk(9)))+(KNA/(KNA+Xk(9)))*(Xk(10)/(KNO+Xk(10)))+(KOH/(KOH+Uk(3)))*(X
k(10)/(KNO+Xk(10)))*((Xk(9)/(KNA+Xk(9)))+(KNA/(KNA+Xk(9)))))*XBHk(3);rUSS3Sads3=0;
rUSads3SNH3=-(1/YZH)*KMP*((Xk(12)/XBHk(3))/(KSP+(Xk(12)/XBHk(3))))*(Uk(3)/(KOH+Uk(3)))*(KNA/(KNA+Xk(9))^2)*XBHk(3)*(1-
(Xk(10)/(KNO+Xk(10))));
rUSads3SNO3=-
(1/YZH)*KMP*((Xk(12)/XBHk(3))/(KSP+(Xk(12)/XBHk(3))))*(KNO/(KNO+Xk(10))^2)*XBHk(3)*((Uk(3)/(KOH+Uk(3)))*(KNA/(KNA+Xk(9)))+(KOH/(KO
H+Uk(3)))*(Xk(9)/(KNA+Xk(9)))+(KOH/(KOH+Uk(3)))*(KNA/(KNA+Xk(9))));rUSads3SS3=0;
rUSads3Sads3=-
(1/YZH)*KMP*((KSP/XBHk(3))/(KSP+(Xk(12)/XBHk(3)))^2)*(Uk(3)/(KOH+Uk(3)))*XBHk(3)*((Xk(9)/(KNA+Xk(9)))*+(KNA/(KNA+Xk(9)))*(Xk(10)/(
KNO+Xk(10))))-
(1/YZH)*KMP*((KSP/XBHk(3))/(KSP+(Xk(12)/XBHk(3)))^2)*(KOH/(KOH+Uk(3)))*(Xk(10)/(KNO+Xk(10)))*etag*XBHk(3)*((Xk(9)/(KNA+Xk(9)))+(KN
A/(KNA+Xk(9))));

% Calculation for the tank 4
rUSNH4SNH4=-
fZBH*XBHk(4)*(KNA/(KNA+Xk(13))^2)*(Uk(4)/(KOH+Uk(4)))*(muH*(Xk(15)/(Ks+Xk(15)))+KMP*((Xk(16)/XBHk(4))/(KSP+(Xk(16)/XBHk(4)))))+(KO
H/(KOH+Uk(4)))*(Xk(14)/(KNO+Xk(14)))*muH*(Xk(15)/(Ks+Xk(15)))*KMP*etag*((Xk(16)/XBHk(4))/(KSP+(Xk(16)/XBHk(4))))-
(1/YZA+fZBH)*muA*(Uk(4)/(KOA+Uk(4)))*(KSA/(KSA+Xk(13)))*XBAk(4);
rUSNH4SNO4=-
fZBH*XBHk(4)*(KNO/(KNO+Xk(14))^2)*(KOH/(KOH+Uk(4)))*(Xk(13)/(KNA+Xk(13)))*(muH*(Xk(15)/(Ks+Xk(15)))+etag*KMP*((Xk(16)/XBHk(4))/(KS
P+(Xk(16)/XBHk(4)))));
rUSNH4SS4=-fZBH*muH*(Ks/(Ks+Xk(15)))*XBHk(4)*(Xk(13)/(KSA+Xk(13)))*((Uk(4)/(KOH+Uk(4)))+(KOH/(KOH+Uk(4)))*(Xk(14)/(KNO+Xk(14))));
rUSNH4Sads4=-
fZBH*KMP*((KSP/XBHk(4))/(KSP+(Xk(16)/XBHk(4))))*(Xk(1)/(KNA+Xk(13)))*((Uk(4)/(KOH+Uk(4)))+etag*(KOH/(KOH+Uk(4)))*(Xk(14)/(KNO+Xk(1
4))));
rUSNO4SNH4=fZBH*(Uk(4)/(KOH+Uk(4)))*(KNA/(KNA+Xk(13))^2)*(Xk(14)/(KNO+Xk(14)))*XBHk(4)*(muH*(Xk(15)/(Ks+Xk(15)))+KMP*((Xk(16)/XBHk
(4))/(KSP+(Xk(16)/XBHk(4))))+fZBH*(KOH/(KOH+Uk(4)))*(KNA/(KNA+Xk(13))^2)*(Xk(14)/(KNO+Xk(14)))*XBHk(4)*(muH*(Xk(15)/(Ks+Xk(15)))+K
MP*etag*((Xk(16)/XBHk(4))/(KSP+(Xk(16)/XBHk(4)))))+(1/YZA)*muA*(KSA/(KSA+Xk(13))^2)*(Xk(14)/KOA+Xk(14)))*XBAk(4);
rUSNO4SNO4=-
fZBH*(Uk(4)/(KOH+Uk(4)))*(KSA/(KSA+Xk(13)))*(KNO/(KNO+Xk(14))^2)*XBHk(4)*(muH*(Xk(15)/(Ks+Xk(15)))+KMP*((Xk(16)/XBHk(4))/(KSP+(Xk(
16)/XBHk(4)))))-
(KOH/(KOH+Uk(4)))*(KNO/(KNO+Xk(14))^2)*XBHk(4)*(muH*(Xk(15)/(Ks+Xk(15)))+KMP*etag*((Xk(16)/XBHk(4))/(KSP+(Xk(16)/XBHk(4)))))*(((1-
YZH)/2.86*YZH)*(Xk(13)/(KNA+Xk(13)))+(((1-YZH)/2.86*YZH)+fZBH)*(KNA/(KNA+Xk(13))));
rUSNO4SS4=-muH*(Ks/(Ks+Xk(15))^2)*(Xk(14)/(KNO+Xk(14)))*XBHk(4)*(fZBH*(Uk(4)/(KOH+Uk(4)))*(KNA/(KNA+Xk(13)))+((1-
YZH)/2.86*YZH)*(KOH/(KOH+Uk(4)))*(Xk(13)/(KNA+Xk(13)))+(((1-YZH)/2.86*YZH)+fZBH)*(KOH/(KOH+Uk(4)))*(KNA/(KNA+Xk(13)));
rUSNO4Sads4=-
KMP*((KSP/XBHk(4))/(KSP+(KSP/XBHk(4)))^2)*(Xk(14)/(KNO+Xk(14)))*XBHk(4)*(fZBH*(Uk(4)/(KOH+Uk(4)))*(KNA/(KNA+Xk(13)))+((1-
YZH)/2.86*YZH)*(KOH/(KOH+Uk(4)))*(Xk(13)/(KNA+Xk(13)))*etag+(((1-YZH)/2.86*YZH)+fZBH)*(KOH/(KOH+Uk(4)))*(KNA/(KNA+Xk(13)))*etag);
rUSS4SNH4=-(1/YZH)*muH*(Xk(15)/(Ks+Xk(15)))*(Uk(4)/(KOH+Uk(4)))*(KNA/(KNA+Xk(13))^2)*XBHk(4)*(1-(Xk(14)/(KNO+Xk(14))));
rUSS4SNO4=-
(1/YZH)*muH*(Xk(15)/(Ks+Xk(15)))*(KNO/(KNO+Xk(14))^2)*XBHk(4)*((Uk(4)/(KOH+Uk(4)))*(KNA/(KNA+Xk(13)))+(KOH/(KOH+Uk(4)))*(Xk(13)/(K
NA+Xk(13)))+(KOH/(KOH+Uk(4)))*(KNA/(KNA+Xk(13))));
```

```
rUSS4SS4=-
(1/YZH)*(Ks/(Ks+Xk(15))^2)*((Uk(4)/(KOH+Uk(4)))*((Xk(13)/(KNA+Xk(13)))+(KNA/(KNA+Xk(13)))*(Xk(14)/(KNO+Xk(14))))+(KOH/(KOH+Uk(4)))
*(Xk(14)/(KNO+Xk(14))))*((Xk(13)/(KNA+Xk(13)))+(KNA/(KNA+Xk(13))))*XBHk(4);rUSS4Sads4=0;
rUSads4SNH4=-(1/YZH)*KMP*((Xk(16)/XBHk(4))/(KSP+(Xk(16)/XBHk(4))))*(Uk(4)/(KOH+Uk(4)))*(KNA/(KNA+Xk(13))^2)*XBHk(4)*(1-
(Xk(14)/(KNO+Xk(14))));
rUSads4SNO4=-
(1/YZH)*KMP*((Xk(16)/XBHk(4))/(KSP+(Xk(16)/XBHk(4))))*(KNO/(KNO+Xk(14))^2)*XBHk(4)*((Uk(4)/(KOH+Uk(4)))*(KNA/(KNA+Xk(13)))+(KOH/(K
OH+Uk(4)))*(Xk(13)/(KNA+Xk(13))))+(KOH/(KOH+Uk(4)))*(KNA/(KNA+Xk(13))));rUSads4SS4=0;
rUSads4Sads4=-
(1/YZH)*KMP*((KSP/XBHk(4))/(KSP+(Xk(16)/XBHk(4)))^2)*(Uk(4)/(KOH+Uk(4)))*XBHk(4)*((Xk(1)/(KNA+Xk(13)))*+(KNA/(KNA+Xk(13)))*(Xk(14)
/(KNO+Xk(14))))-
(1/YZH)*KMP*((KSP/XBHk(4))/(KSP+(Xk(16)/XBHk(4)))^2)*(KOH/(KOH+Uk(4)))*(Xk(14)/(KNO+Xk(14)))*etag*XBHk(4)*((Xk(13)/(KNA+Xk(13)))+(
KNA/(KNA+Xk(13))));

% Calculation for the tank 5
rUSNH5SNH5=-
fZBH*XBHk(5)*(KNA/(KNA+Xk(17))^2)*(Uk(5)/(KOH+Uk(5)))*(muH*(Xk(19)/(Ks+Xk(19)))+KMP*((Xk(20)/XBHk(5))/(KSP+(Xk(20)/XBHk(5)))))+(KO
H/(KOH+Uk(5)))*(Xk(18)/(KNO+Xk(18)))*muH*(Xk(19)/(Ks+Xk(19)))*KMP*etag*((Xk(20)/XBHk(5))/(KSP+(Xk(20)/XBHk(5))))-
(1/YZA+fZBH)*muA*(Uk(5)/(KOA+Uk(5)))*(KSA/(KSA+Xk(17)))*XBAk(5);
rUSNH5SNO5=-
fZBH*XBHk(5)*(KNO/(KNO+Xk(18))^2)*(KOH/(KOH+Uk(5)))*(Xk(17)/(KNA+Xk(17)))*(muH*(Xk(19)/(Ks+Xk(19)))+etag*KMP*((Xk(20)/XBHk(5))/(KS
P+(Xk(20)/XBHk(5)))));
rUSNH5SS5=-fZBH*muH*(Ks/(Ks+Xk(19)))*XBHk(5)*(Xk(17)/(KSA+Xk(17)))*((Uk(5)/(KOH+Uk(5)))+(KOH/(KOH+Uk(5)))*(Xk(18)/(KNO+Xk(18))));
rUSNH5Sads5=-
fZBH*KMP*((KSP/XBHk(5))/(KSP+(Xk(20)/XBHk(5))))*(Xk(17)/(KNA+Xk(17)))*((Uk(5)/(KOH+Uk(5)))+etag*(KOH/(KOH+Uk(5)))*(Xk(18)/(KNO+Xk(
18))));
rUSNO5SNH5=fZBH*(Uk(5)/(KOH+Uk(5)))*(KNA/(KNA+Xk(17))^2)*(Xk(18)/(KNO+Xk(18)))*XBHk(5)*(muH*(Xk(19)/(Ks+Xk(19)))+KMP*((Xk(20)/XBHk
(5))/(KSP+(Xk(20)/XBHk(5))))+fZBH*(KOH/(KOH+Uk(5)))*(KNA/(KNA+Xk(17)))^2)*(Xk(18)/(KNO+Xk(18)))*XBHk(5)*(muH*(Xk(19)/(Ks+Xk(19)))+K
MP*etag*((Xk(20)/XBHk(5))/(KSP+(Xk(20)/XBHk(5))))+(1/YZA)*muA*(KSA/(KSA+Xk(17)))^2)*(Xk(18)/KOA+Xk(18)))*XBAk(5);
rUSNO5SNO5=-
fZBH*(Uk(5)/(KOH+Uk(5)))*(KSA/(KSA+Xk(17)))*(KNO/(KNO+Xk(18))^2)*XBHk(5)*(muH*(Xk(19)/(Ks+Xk(19)))+KMP*((Xk(20)/XBHk(5))/(KSP+(Xk(
20)/XBHk(5))))-
(KOH/(KOH+Uk(5)))*(KNO/(KNO+Xk(18))^2)*XBHk(5)*(muH*(Xk(19)/(Ks+Xk(19)))+KMP*etag*((Xk(20)/XBHk(5))/(KSP+(Xk(20)/XBHk(5))))*(((1-
YZH)/2.86*YZH)*(Xk(17)/(KNA+Xk(17)))+fZBH)*(KNA/(KNA+Xk(17))));
rUSNO5SS5=-muH*(Ks/(Ks+Xk(19))^2)*(Xk(18)/(KNO+Xk(18)))*XBHk(5)*(fZBH*(Uk(5)/(KOH+Uk(5)))*(KNA/(KNA+Xk(17)))+((1-
YZH)/2.86*YZH)*(KOH/(KOH+Uk(5)))*(Xk(17)/(KNA+Xk(17)))+(((1-YZH)/2.86*YZH)+fZBH)*(KOH/(KOH+Uk(5)))*(KNA/(KNA+Xk(17)));
rUSNO5Sads5=-
KMP*((KSP/XBHk(5))/(KSP+(KSP/XBHk(5))))^2)*(Xk(18)/(KNO+Xk(18)))*XBHk(5)*(fZBH*(Uk(5)/(KOH+Uk(5)))*(KNA/(KNA+Xk(17)))+((1-
YZH)/2.86*YZH)*(KOH/(KOH+Uk(5)))*(Xk(17)/(KNA+Xk(17)))*etag+(((1-YZH)/2.86*YZH)+fZBH)*(KOH/(KOH+Uk(5)))*(KNA/(KNA+Xk(17)))*etag);
rUSS5SNH5=-(1/YZH)*muH*(Xk(19)/(Ks+Xk(19)))*(Uk(5)/(KOH+Uk(5)))*(KNA/(KNA+Xk(17))^2)*XBHk(5)*(1-(Xk(18)/(KNO+Xk(18))));
rUSS5SNO5=-
(1/YZH)*muH*(Xk(19)/(Ks+Xk(19)))*(KNO/(KNO+Xk(18))^2)*XBHk(5)*((Uk(5)/(KOH+Uk(5)))*(KNA/(KNA+Xk(17)))+(KOH/(KOH+Uk(5)))*(Xk(17)/(K
NA+Xk(17)))+(KOH/(KOH+Uk(5)))*(KNA/(KNA+Xk(17))));
rUSS5SS5=-
(1/YZH)*(Ks/(Ks+Xk(19))^2)*((Uk(5)/(KOH+Uk(5)))*((Xk(17)/(KNA+Xk(17)))+(KNA/(KNA+Xk(17)))*(Xk(18)/(KNO+Xk(18))))+(KOH/(KOH+Uk(5)))
*(Xk(18)/(KNO+Xk(18)))*((Xk(17)/(KNA+Xk(17)))+(KNA/(KNA+Xk(17))))*XBHk(5);rUSS5Sads5=0;
rUSads5SNH5=-(1/YZH)*KMP*((Xk(20)/XBHk(5))/(KSP+(Xk(20)/XBHk(5))))*(Uk(5)/(KOH+Uk(5)))*(KNA/(KNA+Xk(17))^2)*XBHk(5)*(1-
(Xk(18)/(KNO+Xk(18))));
rUSads5SNO5=-
(1/YZH)*KMP*((Xk(20)/XBHk(5))/(KSP+(Xk(20)/XBHk(5))))*(KNO/(KNO+Xk(18))^2)*XBHk(5)*((Uk(5)/(KOH+Uk(5)))*(KNA/(KNA+Xk(17)))+(KOH/(K
OH+Uk(5)))*(Xk(17)/(KNA+Xk(17)))+(KOH/(KOH+Uk(5)))*(KNA/(KNA+Xk(17))));rUSads5SS5=0;
rUSads5Sads5=-
(1/YZH)*KMP*((KSP/XBHk(5))/(KSP+(Xk(20)/XBHk(5))))^2)*(Uk(5)/(KOH+Uk(5)))*XBHk(5)*((Xk(17)/(KNA+Xk(17)))*+(KNA/(KNA+Xk(17)))*(Xk(18
)/(KNO+Xk(18))))-
(1/YZH)*KMP*((KSP/XBHk(5))/(KSP+(Xk(20)/XBHk(5))))^2)*(KOH/(KOH+Uk(5)))*(Xk(18)/(KNO+Xk(18)))*etag*XBHk(5)*((Xk(17)/(KNA+Xk(17)))+(
KNA/(KNA+Xk(17))));

%Calculation of the derivatives of the process rates towards the process parameters
% Calculation for model parameters of rUSNH for the tank 1
rUSNH1f=0.0; rUSNH1YZH=0;rUSNH1YZA=(1/YZA)*muA*(Xk(1)/(KSA+Xk(1)))*(Uk(1)/(KOA+Uk(1)))*XBAk(1);
rUSNH1fZBH=-(Uk(1)/(KOH+Uk(1)))*(Xk(1)/(KNA+Xk(1)))*XBHk(1)*(muH*(Xk(3)/(Ks+Xk(3)))+KMP*((Xk(4)/XBHk(1))/(KSP+(Xk(4)/XBHk(1)))))-
(KOH/(KOH+Uk(1)))*(Xk(1)/(KNA+Xk(1)))*(Xk(2)/(KNO+Xk(2)))*XBHk(1)*(muH*(Xk(3)/(Ks+Xk(3)))+KMP*etag*((Xk(4)/XBHk(1))/(KSP+(Xk(4)/XB
Hk(1)))))-muA*(Xk(1)/(KSA+Xk(1)))*(Uk(1)/(KOA+Uk(1)))*XBAk(1);
rUSNH1muH=-fZBH*(Xk(3)/(Ks+Xk(3)))*XBHk(1)*((Xk(1)/(KNA+Xk(1)))*(Uk(1)/(KOH+Uk(1)))+(KOH/(KOH+Uk(1)))*(Xk(2)/(KNO+Xk(2))));
rUSNH1muA=-((1/YZA)-fZBH)*(Xk(1)/(KSA+Xk(1)))*(Uk(1)/(KOA+Uk(1)))*XBAk(1);
rUSNH1Ks=fZBH*muH*(Xk(3)/(Ks+Xk(3))^2)*((Xk(1)/(KNA+Xk(1)))*XBHk(1)*((Uk(1)/(KOH+Uk(1)))+(KOH/(KOH+Uk(1)))*(Xk(2)/(KNO+Xk(2)))));
rUSNH1KOH=fZBH*(Uk(1)/(KOH+Uk(1))^2)*(Xk(1)/(KNA+Xk(1)))*XBHk(1)*(muH*(Xk(3)/(Ks+Xk(3)))+KMP*((Xk(4)/XBHk(1))/(KSP+(Xk(4)/XBHk(1))
)))-
fZBH*(Uk(1)/(KOH+Uk(1))^2)*(Xk(1)/(KNA+Xk(1)))*(Xk(2)/(KNO+Xk(2)))*XBHk(1)*(muH*(Xk(3)/(Ks+Xk(3)))+KMP*etag*((Xk(4)/XBHk(1))/(KSP+
(Xk(4)/XBHk(1)))));
rUSNH1KNO=fZBH*(KOH/(KOH+Uk(1)))*(Xk(1)/(KNA+Xk(1)))*(Xk(2)/(KNO+Xk(2))^2)*XBHk(1)*(muH*(Xk(3)/(Ks+Xk(3)))+KMP*etag*((Xk(4)/XBHk(1
))/(KSP+(Xk(4)/XBHk(1)))));
rUSNH1KNA=fZBH*(Uk(1)/(KOH+Uk(1)))*(Xk(1)/(KNA+Xk(1)))*XBHk(1)*(muH*(Xk(3)/(Ks+Xk(3)))+KMP*((Xk(4)/XBHk(1))/(KSP+(Xk(4)/XBHk(1))))
)+fZBH*(KOH/(KOH+Uk(1)))*(Xk(1)/(KNA+Xk(1)))^2)*(Xk(2)/(KNO+Xk(2)))*XBHk(1)*(muH*(Xk(3)/(Ks+Xk(3)))+KMP*etag*((Xk(4)/XBHk(1))/(KSP+
(Xk(4)/XBHk(1)))));
rUSNH1KOA=((1/YZA)+fZBH)*muA*(Xk(1)/(KSA+Xk(1)))*(Uk(1)/(KOA+Uk(1)))^2)*XBAk(1);
rUSNH1etag=-KMP*((Xk(4)/XBHk(1))/(KSP+(Xk(4)/XBHk(1))))*(KOH/(KOH+Uk(1)))*(Xk(1)/(KNA+Xk(1)))*(Xk(2)/(KNO+Xk(2)))*XBHk(1)*fZBH;
rUSNH1KMP=((Xk(4)/XBHk(1))/(KSP+(Xk(4)/XBHk(1))))*(Xk(1)/(KNA+Xk(1)))*XBHk(1)*fZBH*((Uk(1)/(KOH+Uk(1)))+(KOH/(KOH+Uk(1)))*(Xk(2)/(
KNO+Xk(2)))*etag);
rUSNH1KSP=fZBH*KMP*((Xk(4)/XBHk(1))/(KSP+(Xk(4)/XBHk(1))))*((Xk(1)/(KNA+Xk(1)))*(Uk(1)/(KOH+Uk(1)))+(KOH/(KOH+Uk(1)))*(Xk(2)/(KNO+
Xk(2))))*XBHk(1);
rUSNH1KSA=((1/YZA)+fZBH)*muA*(Xk(1)/(KSA+Xk(1)))^2)*(Uk(1)/(KOA+Uk(1)))*XBAk(1); rUSNH1fMA=0.0;rUSNH1KA=0.0;

% Calculation for model parameters of rUSNO for the tank 1
rUSNO1f=0.0;
rUSNO1YZH=(1/(2.86*YZH^2))*(KOH/(KOH+Uk(1)))*(Xk(2)/(KNO+Xk(2)))*XBHk(1)*(muH*(Xk(3)/(Ks+Xk(3)))+KMP*etag*((Xk(4)/XBHk(1))/(KSP+(X
k(4)/XBHk(1)))))*((Xk(1)/(KNA+Xk(1)))+(KNA/(KNA+Xk(1))));
rUSNO1YZA=(1/(2.86*YZH^2))*muA*(Xk(1)/(KSA+Xk(1)))*(Uk(1)/(KOA+Uk(1)))*XBAk(1);
rUSNO1fZBH=-
(Uk(1)/(KOH+Uk(1)))*(KNA/(KNA+Xk(1)))*(Xk(2)/(KNO+Xk(2)))*XBHk(1)*(muH*(Xk(3)/(Ks+Xk(3)))+KMP*((Xk(4)/XBHk(1))/(KSP+(Xk(4)/XBHk(1)
))));
rUSNO1muH=-2*fZBH*(Xk(3)/(Ks+Xk(3)))*(KNA/(KNA+Xk(1)))*(Xk(2)/(KNO+Xk(2)))*XBHk(1)*((Uk(1)/(KOH+Uk(1)))+(KOH/(KOH+Uk(1))))-((1-
YZH)/2.86*YZH)*(Xk(3)/(Ks+Xk(3)))*(KOH/(KOH+Uk(1)))*(Xk(2)/(KNO+Xk(2)))*XBHk(1)*((Xk(1)/(KNA+Xk(1)))+(KNA/(KNA+Xk(1))));
rUSNO1muA=(1/YZA)*(Xk(1)/(KSA+Xk(1)))^2)*(Uk(1)/(KOA+Uk(1)))*XBAk(1);
rUSNO1Ks=fZBH*muH*(Xk(3)/(Ks+Xk(3)))^2)*(KNA/(KNA+Xk(1)))*(Xk(2)/(KNO+Xk(2)))*XBHk(1)*((Uk(1)/(KOH+Uk(1)))+(KOH/(KOH+Uk(1))))+((1-
YZH)/2.86*YZH)*muH*(Xk(3)/(Ks+Xk(3)))*(KOH/(KOH+Uk(1)))*(Xk(2)/(KNO+Xk(2)))*XBHk(1)*((Xk(1)/(KNA+Xk(1)))+(KNA/(KNA+Xk(1))));
rUSNO1KOH=-((1-
YZH)/2.86*YZH)*(KOH/(KOH+Uk(1)))^2)*(Xk(2)/(KNO+Xk(2)))*XBHk(1)*(muH*(Xk(3)/(Ks+Xk(3)))+KMP*etag*((Xk(4)/XBHk(1))/(KSP+(Xk(4)/XBHk(
```

```
1)))))+fZBH*(Uk(1)/(KOH+Uk(1))^2)*(KNA/(KNA+Xk(1)))*(Xk(2)/(KNO+Xk(2)))*XBHk(1)*KMP*((Xk(4)/XBHk(1))/(KSP+(Xk(4)/XBHk(1))))*(1-
etag);
rUSNO1KNO=fZBH*(Uk(1)/(KOH+Uk(1)))*(KNA/(KNA+Xk(1)))*(Xk(2)/(KNO+Xk(2))^2)*XBHk(1)*(muH*(Xk(3)/(Ks+Xk(3)))+KMP*((Xk(4)/XBHk(1))/(K
SP+(Xk(4)/XBHk(1)))))+((1-
YZH)/2.86*YZH)*(KOH/(KOH+Uk(1)))*(Xk(1)/(KNA+Xk(1)))*(Xk(2)/(KNO+Xk(2))^2)*XBHk(1)*(muH*(Xk(3)/(Ks+Xk(3)))+KMP*etag*((Xk(4)/XBHk(1
))/(KSP+(Xk(4)/XBHk(1)))))+((1-
YZH)/2.86*YZH)+fZBH)*(KOH/(KOH+Uk(1)))*(KNA/(KNA+Xk(1)))*(Xk(2)/(KNO+Xk(2))^2)*XBHk(1)*(muH*(Xk(3)/(Ks+Xk(3)))+KMP*etag*((Xk(4)/XB
Hk(1))/(KSP+(Xk(4)/XBHk(1)))));
rUSNO1KNA=-
fZBH*(Uk(1)/(KOH+Uk(1)))*(Xk(1)/(KNA+Xk(1)))*(Xk(2)/(KNO+Xk(2)))*XBHk(1)*(muH*(Xk(3)/(Ks+Xk(3)))+KMP*((Xk(4)/XBHk(1))/(KSP+(Xk(4)/
XBHk(1)))))-
fZBH*(KOH/(KOH+Uk(1)))*(Xk(1)/(KNA+Xk(1))^2)*(Xk(2)/(KNO+Xk(2)))*XBHk(1)*(muH*(Xk(3)/(Ks+Xk(3)))+KMP*etag*((Xk(4)/XBHk(1))/(KSP+(X
k(4)/XBHk(1)))));
rUSNO1KOA=(1/YZA)*muA*(Xk(1)/(KSA+Xk(1))^2)*(Uk(1)/(KOA+Uk(1)))*XBAk(1);
rUSNO1etag=-((1-
YZH)/2.86*YZH)*KMP*((Xk(4)/XBHk(1))/(KSP+(Xk(4)/XBHk(1))))*(KOH/(KOH+Uk(1)))*(Xk(2)/(KNO+Xk(2)))*XBHk(1)*((Xk(1)/(KNA+Xk(1)))+(KNA
/(KNA+Xk(1))))-fZBH*KMP*((Xk(4)/XBHk(1))/(KSP+(Xk(4)/XBHk(1))))*(KOH/(KOH+Uk(1)))*(KNA/(KNA+Xk(1)))*(Xk(2)/(KNO+Xk(2)))*XBHk(1);
rUSNO1KMP=-
fZBH*((Xk(4)/XBHk(1))/(KSP+(Xk(4)/XBHk(1))))*(KNA/(KNA+Xk(1)))*(Xk(2)/(KNO+Xk(2)))*XBHk(1)*((Uk(1)/(KOH+Uk(1)))+etag*(KOH/(KOH+Uk(
1))))+((1-
YZH)/2.86*YZH)*((Xk(4)/XBHk(1))/(KSP+(Xk(4)/XBHk(1))))*(KOH/(KOH+Uk(1)))*(Xk(2)/(KNO+Xk(2)))*etag*XBHk(1)*((Xk(1)/(KNA+Xk(1)))+(KN
A/(KNA+Xk(1))));
rUSNO1KSP=fZBH*KMP*((Xk(4)/XBHk(1))/(KSP+(Xk(4)/XBHk(1))))*(KNA/(KNA+Xk(1)))*(Xk(2)/(KNO+Xk(2)))*XBHk(1)*((Uk(1)/(KOH+Uk(1)))+etag
*(KOH/(KOH+Uk(1))))+((1-
YZH)/2.86*YZH)*((Xk(4)/XBHk(1))/(KSP+(Xk(4)/XBHk(1))))*(KOH/(KOH+Uk(1)))*(Xk(2)/(KNO+Xk(2)))*etag*XBHk(1)*((Xk(1)/(KNA+Xk(1)))+(KN
A/(KNA+Xk(1)))); rUSNO1KSA=-(1/YZA)*muA*(Xk(1)/(KSA+Xk(1))^2)*(Uk(1)/(KOA+Uk(1)))*XBAk(1);rUSNO1fMA=0;rUSNO1KA=0;

% Calculation for model parameters of rUSS for the tank 1
rUSS1f=0.0;
rUSS1YZH=(1/(YZH^2))*muH*(Xk(3)/(Ks+Xk(3)))*XBHk(1)*(Uk(1)/(KOH+Uk(1)))*((Xk(1)/(KNA+Xk(1)))+(KNA/(KNA+Xk(1))))*(Xk(2)/(KNO+Xk(2))
)+(KOH/(KOH+Uk(1)))*(Xk(2)/(KNO+Xk(2)))*((Xk(1)/(KNA+Xk(1)))+(KNA/(KNA+Xk(1))));
rUSS1YZA=0;rUSS1fZBH=0;
rUSS1muH=-
(1/YZH)*(Xk(3)/(Ks+Xk(3)))*XBHk(1)*(Uk(1)/(KOH+Uk(1)))*((Xk(1)/(KNA+Xk(1)))+(KNA/(KNA+Xk(1))))*(Xk(2)/(KNO+Xk(2)))+(Uk(1)/(KOH+Uk(
1)))*((Xk(1)/(KNA+Xk(1)))+(KNA/(KNA+Xk(1))))*(Xk(2)/(KNO+Xk(2)));
rUSS1muA=0;
rUSS1Ks=(1/YZH)*muH*(Xk(3)/(Ks+Xk(3)))*XBHk(1)*(Uk(1)/(KOH+Uk(1)))*((Xk(1)/(KNA+Xk(1)))+(KNA/(KNA+Xk(1))))*(Xk(2)/(KNO+Xk(2)))+(KO
H/(KOH+Uk(1)))*(Xk(2)/(KNO+Xk(2)))*((Xk(1)/(KNA+Xk(1)))+(KNA/(KNA+Xk(1))));
rUSS1KOH=(1/YZH)*muH*(Xk(3)/(Ks+Xk(3)))*(Uk(1)/(KOH+Uk(1)))*XBHk(1)*(Xk(1)/(KNA+Xk(1)))*(1-(Xk(2)/(KNO+Xk(2))));
rUSS1KNO=(1/YZH)*muH*(Xk(3)/(Ks+Xk(3)))*(Xk(2)/(KNO+Xk(2)))*XBHk(1)*(Uk(1)/(KOH+Uk(1)))*((Xk(1)/(KNA+Xk(1)))+(KNA/(KNA+Xk(1))));
rUSS1KNA=(1/YZH)*muH*(Xk(3)/(Ks+Xk(3)))*(Xk(1)/(KNA+Xk(1))^2)*XBHk(1)*(Uk(1)/(KOH+Uk(1)))*(1-(Xk(2)/(KNO+Xk(2))));
rUSS1KOA=0;rUSS1etag=0;rUSS1KMP=0;rUSS1KSP=0;rUSS1KSA=0;rUSS1fMA=0;rUSS1KA=0;

% Calculation for model parameters of rUSads for the tank 1
rUSads1f=0.0;
rUSads1YZH=(1/(YZH^2))*KMP*((Xk(4)/XBHk(1))/(KSP+(Xk(4)/XBHk(1))))*XBHk(1)*(Uk(1)/(KOH+Uk(1)))*((Xk(1)/(KNA+Xk(1)))+(KNA/(KNA+Xk(1
))))*(Xk(2)/(KNO+Xk(2)))+etag*(KOH/(KOH+Uk(1)))*(Xk(2)/(KNO+Xk(2)))*((Xk(1)/(KNA+Xk(1)))+(KNA/(KNA+Xk(1))));
rUSads1YZA=0;rUSads1fZBH=0;rUSads1muH=0;rUSads1muA=0;rUSads1Ks=0;
rUSads1KOH=(1/YZH)*KMP*((Xk(4)/XBHk(1))/(KSP+(Xk(4)/XBHk(1))))*(Uk(1)/(KOH+Uk(1))^2)*XBHk(1)*(Xk(1)/(KNA+Xk(1)))*(1-
(Xk(2)/(KNO+Xk(2))));
rUSads1KNO=(1/YZH)*KMP*((Xk(4)/XBHk(1))/(KSP+(Xk(4)/XBHk(1))))*(Xk(2)/(KNO+Xk(2))^2)*XBHk(1)*(Uk(1)/(KOH+Uk(1)))*(KNA/(KNA+Xk(1)))
+etag*(KOH/(KOH+Uk(1)))*((Xk(1)/(KNA+Xk(1)))+(KNA/(KNA+Xk(1))));
rUSads1KNA=(1/YZH)*KMP*((Xk(4)/XBHk(1))/(KSP+(Xk(4)/XBHk(1))))*(Xk(1)/(KNA+Xk(1))^2)*XBHk(1)*(Uk(1)/(KOH+Uk(1)))*(1-
(Xk(2)/(KNO+Xk(2))));rUSads1KOA=0;
rUSads1etag=-
(1/YZH)*KMP*((Xk(4)/XBHk(1))/(KSP+(Xk(4)/XBHk(1))))*(KOH/(KOH+Uk(1)))*(Xk(2)/(KNO+Xk(2)))*etag*XBHk(1)*((Xk(1)/(KNA+Xk(1)))+(KNA/(
KNA+Xk(1))));
rUSads1KMP=-
(1/YZH)*((Xk(4)/XBHk(1))/(KSP+(Xk(4)/XBHk(1))))*XBHk(1)*(Uk(1)/(KOH+Uk(1)))*((Xk(1)/(KNA+Xk(1)))+(KNA/(KNA+Xk(1))))*(Xk(2)/(KNO+Xk
(2)))+etag*(KOH/(KOH+Uk(1)))*(Xk(2)/(KNO+Xk(2)))*((Xk(1)/(KNA+Xk(1)))+(KNA/(KNA+Xk(1))));
rUSads1KSP=(1/YZH)*KMP*((Xk(4)/XBHk(1))/(KSP+(Xk(4)/XBHk(1)))^2)*XBHk(1)*(Uk(1)/(KOH+Uk(1)))*((Xk(1)/(KNA+Xk(1)))+(KNA/(KNA+Xk(1))
))*(Xk(2)/(KNO+Xk(2)))+etag*(KOH/(KOH+Uk(1)))*(Xk(2)/(KNO+Xk(2)))*((Xk(1)/(KNA+Xk(1)))+(KNA/(KNA+Xk(1))));
rUSads1KSA=0;rUSads1fMA=KA*XSk(1)*XBHk(1);rUSads1KA=XSk(1)*XBHk(1)*(fMA-(Xk(4)/XBHk(1)));

% Calculation for model parameters of rUSNH for the tank 2
rUSNH2f=0.0;rUSNH2YZH=0;
rUSNH2YZA=(1/YZA)*muA*(Xk(5)/(KSA+Xk(5)))*(Uk(2)/(KOA+Uk(2)))*XBAk(2);
rUSNH2fZBH=-(Uk(2)/(KOH+Uk(2)))*(Xk(5)/(KNA+Xk(5)))*XBHk(2)*(muH*(Xk(7)/(Ks+Xk(7)))+KMP*((Xk(8)/XBHk(2))/(KSP+(Xk(8)/XBHk(2)))))-
(KOH/(KOH+Uk(2)))*(Xk(5)/(KNA+Xk(5)))*(Xk(6)/(KNO+Xk(6)))*XBHk(2)*(muH*(Xk(7)/(Ks+Xk(7)))+KMP*etag*((Xk(8)/XBHk(2))/(KSP+(Xk(8)/XB
Hk(2)))))-muA*(Xk(5)/(KSA+Xk(5)))*(Uk(2)/(KOA+Uk(2)))*XBAk(2);
rUSNH2muH=-fZBH*(Xk(7)/(Ks+Xk(7)))*XBHk(2)*((Xk(5)/(KNA+Xk(5)))*(Uk(2)/(KOH+Uk(2)))+(KOH/(KOH+Uk(2)))*(Xk(6)/(KNO+Xk(6))));
rUSNH2muA=-((1/YZA)-fZBH)*(Xk(5)/(KSA+Xk(5)))*(Uk(2)/(KOA+Uk(2)))*XBAk(2);
rUSNH2Ks=fZBH*muH*(Xk(7)/(Ks+Xk(7))^2)*(Xk(5)/(KNA+Xk(5)))*XBHk(2)*((Uk(2)/(KOH+Uk(2)))+(KOH/(KOH+Uk(2)))*(Xk(6)/(KNO+Xk(6))));
rUSNH2KOH=fZBH*(Uk(2)/(KOH+Uk(2))^2)*(Xk(5)/(KNA+Xk(5)))*XBHk(2)*(muH*(Xk(7)/(Ks+Xk(7)))+KMP*((Xk(8)/XBHk(2))/(KSP+(Xk(8)/XBHk(2))
)))-
fZBH*(Uk(2)/(KOH+Uk(2))^2)*(Xk(5)/(KNA+Xk(5)))*(Xk(6)/(KNO+Xk(6)))*XBHk(2)*(muH*(Xk(7)/(Ks+Xk(7)))+KMP*etag*((Xk(8)/XBHk(2))/(KSP+
(Xk(8)/XBHk(2)))));
rUSNH2KNO=fZBH*(KOH/(KOH+Uk(2)))*(Xk(5)/(KNA+Xk(5)))*(Xk(6)/(KNO+Xk(6))^2)*XBHk(2)*(muH*(Xk(7)/(Ks+Xk(7)))+KMP*etag*((Xk(8)/XBHk(2
))/(KSP+(Xk(8)/XBHk(2)))));
rUSNH2KNA=fZBH*(Uk(2)/(KOH+Uk(2)))*(Xk(5)/(KNA+Xk(5)))*XBHk(2)*(muH*(Xk(7)/(Ks+Xk(7)))+KMP*((Xk(8)/XBHk(2))/(KSP+(Xk(8)/XBHk(2))))
)+fZBH*(KOH/(KOH+Uk(2)))*(Xk(5)/(KNA+Xk(5)))^2)*(Xk(6)/(KNO+Xk(6)))*XBHk(2)*(muH*(Xk(7)/(Ks+Xk(7)))+KMP*etag*((Xk(8)/XBHk(2))/(KSP+
(Xk(8)/XBHk(2)))));
rUSNH2KOA=((1/YZA)+fZBH)*muA*(Xk(5)/(KSA+Xk(5)))*(Uk(2)/(KOA+Uk(2))^2)*XBAk(2);
rUSNH2etag=-KMP*((Xk(8)/XBHk(2))/(KSP+(Xk(8)/XBHk(2))))*(KOH/(KOH+Uk(2)))*(Xk(5)/(KNA+Xk(5)))*(Xk(6)/(KNO+Xk(6)))*XBHk(2)*fZBH;
rUSNH2KMP=((Xk(8)/XBHk(2))/(KSP+(Xk(8)/XBHk(2))))*(Xk(5)/(KNA+Xk(5)))*XBHk(2)*fZBH*((Uk(2)/(KOH+Uk(2)))+(KOH/(KOH+Uk(2)))*(Xk(6)/(
KNO+Xk(6)))*etag);
rUSNH2KSP=fZBH*KMP*((Xk(8)/XBHk(2))/(KSP+(Xk(8)/XBHk(2))))*((Xk(5)/(KNA+Xk(5)))*(Uk(2)/(KOH+Uk(2)))+(KOH/(KOH+Uk(2)))*(Xk(6)/(KNO+
Xk(6))))*XBHk(2);
rUSNH2KSA=((1/YZA)+fZBH)*muA*(Xk(5)/(KSA+Xk(5))^2)*(Uk(2)/(KOA+Uk(2)))*XBAk(2);rUSNH2fMA=0.0;rUSNH2KA=0.0;

% Calculation for model parameters of rUSNO for the tank 2
rUSNO2f=0.0;
rUSNO2YZH=(1/(2.86*YZH^2))*(KOH/(KOH+Uk(2)))*(Xk(6)/(KNO+Xk(6)))*XBHk(2)*(muH*(Xk(7)/(Ks+Xk(7)))+KMP*etag*((Xk(8)/XBHk(2))/(KSP+(X
k(8)/XBHk(2)))))*((Xk(5)/(KNA+Xk(5)))+(KNA/(KNA+Xk(5))));
rUSNO2YZA=(1/(2.86*YZH^2))*muA*(Xk(5)/(KSA+Xk(5)))*(Uk(2)/(KOA+Uk(2)))*XBAk(2);
rUSNO2fZBH=-
(Uk(2)/(KOH+Uk(2)))*(KNA/(KNA+Xk(5)))*(Xk(6)/(KNO+Xk(6)))*XBHk(2)*(muH*(Xk(7)/(Ks+Xk(7)))+KMP*((Xk(8)/XBHk(2))/(KSP+(Xk(8)/XBHk(2)
))));
```

```
rUSNO2muH=-2*fZBH*(Xk(7)/(Ks+Xk(7)))*(KNA/(KNA+Xk(5)))*(Xk(6)/(KNO+Xk(6)))*XBHk(2)*((Uk(2)/(KOH+Uk(2)))+(KOH/(KOH+Uk(2))))-((1-
YZH)/2.86*YZH)*(Xk(7)/(Ks+Xk(7)))*(KOH/(KOH+Uk(2)))*(Xk(6)/(KNO+Xk(6)))*XBHk(2)*((Xk(5)/(KNA+Xk(5)))+(KNA/(KNA+Xk(5))));
rUSNO2muA=(1/YZA)*(Xk(5)/(KSA+Xk(5))^2)*(Uk(2)/(KOA+Uk(2)))*XBAk(2);
rUSNO2Ks=fZBH*muH*(Xk(7)/(Ks+Xk(7))^2)*(KNA/(KNA+Xk(5)))*(Xk(6)/(KNO+Xk(6)))*XBHk(2)*((Uk(2)/(KOH+Uk(2)))+(KOH/(KOH+Uk(2))))+((1-
YZH)/2.86*YZH)*muH*(Xk(7)/(Ks+Xk(7)))*(KOH/(KOH+Uk(2)))*(Xk(6)/(KNO+Xk(6)))*XBHk(2)*((Xk(5)/(KNA+Xk(5)))+(KNA/(KNA+Xk(5))));
rUSNO2KOH=-((1-
YZH)/2.86*YZH)*(KOH/(KOH+Uk(2))^2)*(Xk(6)/(KNO+Xk(6)))*XBHk(2)*(muH*(Xk(7)/(Ks+Xk(7)))+KMP*etag*((Xk(8)/XBHk(2))/(KSP+(Xk(8)/XBHk(
2)))))+fZBH*(Uk(2)/(KOH+Uk(2))^2)*(KNA/(KNA+Xk(5)))*(Xk(6)/(KNO+Xk(6)))*XBHk(2)*KMP*((Xk(8)/XBHk(2))/(KSP+(Xk(8)/XBHk(2))))*(1-
etag);
rUSNO2KNO=fZBH*(Uk(2)/(KOH+Uk(2)))*(KNA/(KNA+Xk(5)))*(Xk(6)/(KNO+Xk(6))^2)*XBHk(2)*(muH*(Xk(7)/(Ks+Xk(7)))+KMP*((Xk(8)/XBHk(2))/(K
SP+(Xk(8)/XBHk(2)))))+((1-
YZH)/2.86*YZH)*(KOH/(KOH+Uk(2)))*(Xk(5)/(KNA+Xk(5)))*(Xk(6)/(KNO+Xk(6))^2)*XBHk(2)*(muH*(Xk(7)/(Ks+Xk(7)))+KMP*etag*((Xk(8)/XBHk(2
))/(KSP+(Xk(8)/XBHk(2)))))+(((1-
YZH)/2.86*YZH)+fZBH)*(KOH/(KOH+Uk(2)))*(KNA/(KNA+Xk(5)))*(Xk(6)/(KNO+Xk(6))^2)*XBHk(2)*(muH*(Xk(7)/(Ks+Xk(7)))+KMP*etag*((Xk(8)/XB
Hk(2))/(KSP+(Xk(8)/XBHk(2))));
rUSNO2KNA=-
fZBH*(Uk(2)/(KOH+Uk(2)))*(Xk(5)/(KNA+Xk(5)))*(Xk(6)/(KNO+Xk(6)))*XBHk(2)*(muH*(Xk(7)/(Ks+Xk(7)))+KMP*((Xk(8)/XBHk(2))/(KSP+(Xk(8)/
XBHk(2)))))-
fZBH*(KOH/(KOH+Uk(2)))*(Xk(5)/(KNA+Xk(5))^2)*(Xk(6)/(KNO+Xk(6)))*XBHk(2)*(muH*(Xk(7)/(Ks+Xk(7)))+KMP*etag*((Xk(8)/XBHk(2))/(KSP+(X
k(8)/XBHk(2)))));
rUSNO2KOA=(1/YZA)*muA*(Xk(5)/(KSA+Xk(5))^2)*(Uk(2)/(KOA+Uk(2)))*XBAk(2);
rUSNO2etag=-((1-
YZH)/2.86*YZH)*KMP*((Xk(8)/XBHk(2))/(KSP+(Xk(8)/XBHk(2))))*(KOH/(KOH+Uk(2)))*(Xk(6)/(KNO+Xk(6)))*XBHk(2)*((Xk(5)/(KNA+Xk(5)))+(KNA
/(KNA+Xk(5))))-fZBH*KMP*((Xk(8)/XBHk(2))/(KSP+(Xk(8)/XBHk(2))))*(KOH/(KOH+Uk(2)))*(KNA/(KNA+Xk(5)))*(Xk(6)/(KNO+Xk(6)))*XBHk(2);
rUSNO2KMP=-
fZBH*((Xk(8)/XBHk(2))/(KSP+(Xk(8)/XBHk(2))))*(KNA/(KNA+Xk(5)))*(Xk(6)/(KNO+Xk(6)))*XBHk(2)*((Uk(2)/(KOH+Uk(2)))+etag*(KOH/(KOH+Uk(
2))))-((1-
YZH)/2.86*YZH)*((Xk(8)/XBHk(2))/(KSP+(Xk(8)/XBHk(2))))*(KOH/(KOH+Uk(2)))*(Xk(6)/(KNO+Xk(6)))*etag*XBHk(2)*((Xk(5)/(KNA+Xk(5)))+(KN
A/(KNA+Xk(5))));
rUSNO2KSP=fZBH*KMP*((Xk(8)/XBHk(2))/(KSP+(Xk(8)/XBHk(2))))*(KNA/(KNA+Xk(5)))*(Xk(6)/(KNO+Xk(6)))*XBHk(2)*((Uk(2)/(KOH+Uk(2)))+etag
*(KOH/(KOH+Uk(2))))+((1-
YZH)/2.86*YZH)*((Xk(8)/XBHk(2))/(KSP+(Xk(8)/XBHk(2))))*(KOH/(KOH+Uk(2)))*(Xk(6)/(KNO+Xk(6)))*etag*XBHk(2)*((Xk(5)/(KNA+Xk(5)))+(KN
A/(KNA+Xk(5))));
rUSNO2KSA=-(1/YZA)*(Xk(5)/(KSA+Xk(5))^2)*(Uk(2)/(KOA+Uk(2)))*XBAk(2);rUSNO2fMA=0;rUSNO2KA=0;

% Calculation for model parameters of rUSS for the tank 2
rUSS2f=0.0;
rUSS2YZH=(1/(YZH^2))*muH*(Xk(7)/(Ks+Xk(7)))*XBHk(2)*(Uk(2)/(KOH+Uk(2)))*((Xk(5)/(KNA+Xk(5)))+(KNA/(KNA+Xk(5))))*(Xk(6)/(KNO+Xk(6))
)+(KOH/(KOH+Uk(2)))*(Xk(6)/(KNO+Xk(6)))*((Xk(5)/(KNA+Xk(5)))+(KNA/(KNA+Xk(5))));
rUSS2YZA=0;rUSS2fZBH=0;
rUSS2muH=-
(1/YZH)*(Xk(7)/(Ks+Xk(7)))*XBHk(1)*(Uk(2)/(KOH+Uk(2)))*((Xk(5)/(KNA+Xk(5)))+(KNA/(KNA+Xk(5))))*(Xk(6)/(KNO+Xk(6)))+(Uk(2)/(KOH+Uk(
2)))*((Xk(5)/(KNA+Xk(5)))+(KNA/(KNA+Xk(5))))*(Xk(6)/(KNO+Xk(6)));rUSS2muA=0;
rUSS2Ks=(1/YZH)*muH*(Xk(7)/(Ks+Xk(7)))*XBHk(2)*(Uk(2)/(KOH+Uk(2)))*((Xk(5)/(KNA+Xk(5)))+(KNA/(KNA+Xk(5))))*(Xk(6)/(KNO+Xk(6)))+(KO
H/(KOH+Uk(2)))*(Xk(6)/(KNO+Xk(6)))*((Xk(5)/(KNA+Xk(5)))+(KNA/(KNA+Xk(5))));
rUSS2KOH=(1/YZH)*muH*(Xk(7)/(Ks+Xk(7)))*(Uk(2)/(KOH+Uk(2)))*XBHk(2)*(Xk(5)/(KNA+Xk(5)))*(1-(Xk(6)/(KNO+Xk(6))));
rUSS2KNO=(1/YZH)*muH*(Xk(7)/(Ks+Xk(7)))*(Xk(6)/(KNO+Xk(6)))*XBHk(2)*(Uk(1)/(KOH+Uk(2)))*(KNA/(KNA+Xk(5)))+(KOH/(KOH+Uk(2)))*((Xk(5
)/(KNA+Xk(5)))+(KNA/(KNA+Xk(5))));
rUSS2KNA=(1/YZH)*muH*(Xk(7)/(Ks+Xk(7)))*(Xk(5)/(KNA+Xk(5))^2)*XBHk(2)*(Uk(2)/(KOH+Uk(2)))*(1-(Xk(6)/(KNO+Xk(6))));
rUSS2KOA=0;rUSS2etag=0;rUSS2KMP=0;rUSS2KSP=0;rUSS2KSA=0;rUSS2fMA=0;rUSS2KA=0;

% Calculation for model parameters of rUSads for the tank 2
rUSads2f=0.0;
rUSads2YZH=(1/(YZH^2))*KMP*((Xk(8)/XBHk(2))/(KSP+(Xk(8)/XBHk(2))))*XBHk(2)*(Uk(2)/(KOH+Uk(2)))*((Xk(5)/(KNA+Xk(5)))+(KNA/(KNA+Xk(5
))))*(Xk(6)/(KNO+Xk(6)))+etag*(KOH/(KOH+Uk(2)))*(Xk(6)/(KNO+Xk(6)))*((Xk(5)/(KNA+Xk(5)))+(KNA/(KNA+Xk(5))));
rUSads2YZA=0;rUSads2fZBH=0;rUSads2muH=0;rUSads2muA=0;rUSads2Ks=0;
rUSads2KOH=(1/YZH)*KMP*((Xk(8)/XBHk(2))/(KSP+(Xk(8)/XBHk(2))))*(Uk(2)/(KOH+Uk(2)))^2)*XBHk(2)*(Xk(5)/(KNA+Xk(5)))*(1-
(Xk(6)/(KNO+Xk(6))));
rUSads2KNO=(1/YZH)*KMP*((Xk(8)/XBHk(2))/(KSP+(Xk(8)/XBHk(2))))*(Xk(6)/(KNO+Xk(6))^2)*XBHk(2)*(Uk(2)/(KOH+Uk(2)))*(KNA/(KNA+Xk(5)))
+etag*(KOH/(KOH+Uk(2)))*((Xk(5)/(KNA+Xk(5)))+(KNA/(KNA+Xk(5))));
rUSads2KNA=(1/YZH)*KMP*((Xk(8)/XBHk(2))/(KSP+(Xk(8)/XBHk(2))))*(Xk(5)/(KNA+Xk(5))^2)*XBHk(2)*(Uk(2)/(KOH+Uk(2)))*(1-
(Xk(6)/(KNO+Xk(6))));rUSads2KOA=0;
rUSads2etag=-
(1/YZH)*KMP*((Xk(8)/XBHk(2))/(KSP+(Xk(8)/XBHk(2))))*(KOH/(KOH+Uk(2)))*(Xk(6)/(KNO+Xk(6)))*etag*XBHk(2)*((Xk(5)/(KNA+Xk(5)))+(KNA/(
KNA+Xk(5))));
rUSads2KMP=-
(1/YZH)*((Xk(8)/XBHk(2))/(KSP+(Xk(8)/XBHk(2))))*XBHk(2)*(Uk(2)/(KOH+Uk(2)))*((Xk(5)/(KNA+Xk(5)))+(KNA/(KNA+Xk(5))))*(Xk(6)/(KNO+Xk
(6)))+etag*(KOH/(KOH+Uk(2)))*(Xk(6)/(KNO+Xk(6)))*((Xk(5)/(KNA+Xk(5)))+(KNA/(KNA+Xk(5))));
rUSads2KSP=(1/YZH)*KMP*((Xk(8)/XBHk(2))/(KSP+(Xk(8)/XBHk(2))))^2)*XBHk(2)*(Uk(2)/(KOH+Uk(2)))*((Xk(5)/(KNA+Xk(5)))+(KNA/(KNA+Xk(5))
))*(Xk(6)/(KNO+Xk(6)))+etag*(KOH/(KOH+Uk(2)))*(Xk(6)/(KNO+Xk(6)))*((Xk(5)/(KNA+Xk(5)))+(KNA/(KNA+Xk(5))));
rUSads2KSA=0;rUSads2fMA=KA*XSk(2)*XBHk(2);rUSads2KA=XSk(2)*XBHk(2)*(fMA-(Xk(8)/XBHk(2)));

% Calculation for model parameters of rUSNH for the tank 3
rUSNH3f=0.0;rUSNH3YZH=0;rUSNH3YZA=(1/YZA)*muA*(Xk(9)/(KSA+Xk(9)))*(Uk(3)/(KOA+Uk(3)))*XBAk(3);
rUSNH3fZBH=-
(Uk(3)/(KOH+Uk(3)))*(Xk(9)/(KNA+Xk(9)))*XBHk(3)*(muH*(Xk(11)/(Ks+Xk(11)))+KMP*((Xk(12)/XBHk(3))/(KSP+(Xk(12)/XBHk(3)))))-
(KOH/(KOH+Uk(3)))*(Xk(9)/(KNA+Xk(9)))*(Xk(10)/(KNO+Xk(10)))*XBHk(3)*(muH*(Xk(11)/(Ks+Xk(11)))+KMP*etag*((Xk(12)/XBHk(3))/(KSP+(Xk(
12)/XBHk(3)))))-muA*(Xk(9)/(KSA+Xk(9)))*(Uk(3)/(KOA+Uk(3)))*XBAk(3);
rUSNH3muH=-fZBH*(Xk(11)/(Ks+Xk(11)))*XBHk(3)*((Xk(9)/(KNA+Xk(9)))*(Uk(3)/(KOH+Uk(3)))+(KOH/(KOH+Uk(3)))*(Xk(10)/(KNO+Xk(10))));
rUSNH3muA=-((1/YZA)-fZBH)*(Xk(9)/(KSA+Xk(9)))*(Uk(3)/(KOA+Uk(3)))*XBAk(3);
rUSNH3Ks=fZBH*muH*(Xk(11)/(Ks+Xk(11)))^2)*(Xk(9)/(KNA+Xk(9)))*XBHk(3)*((Uk(3)/(KOH+Uk(3)))+(KOH/(KOH+Uk(3)))*(Xk(10)/(KNO+Xk(10))))
;
rUSNH3KOH=fZBH*(Uk(3)/(KOH+Uk(3)))^2)*(Xk(9)/(KNA+Xk(9)))*XBHk(3)*(muH*(Xk(11)/(Ks+Xk(11)))+KMP*((Xk(12)/XBHk(3))/(KSP+(Xk(12)/XBHk
(3)))))-
fZBH*(Uk(3)/(KOH+Uk(3)))^2)*(Xk(9)/(KNA+Xk(9)))*(Xk(10)/(KNO+Xk(10)))*XBHk(3)*(muH*(Xk(11)/(Ks+Xk(11)))+KMP*etag*((Xk(12)/XBHk(3))/
(KSP+(Xk(12)/XBHk(3)))));
rUSNH3KNO=fZBH*(KOH/(KOH+Uk(3)))*(Xk(9)/(KNA+Xk(9)))*(Xk(10)/(KNO+Xk(10)))^2)*XBHk(3)*(muH*(Xk(11)/(Ks+Xk(11)))+KMP*etag*((Xk(12)/X
BHk(3))/(KSP+(Xk(12)/XBHk(3)))));
rUSNH3KNA=fZBH*(Uk(3)/(KOH+Uk(3)))*(Xk(9)/(KNA+Xk(9)))*XBHk(3)*(muH*(Xk(11)/(Ks+Xk(11)))+KMP*((Xk(12)/XBHk(3))/(KSP+(Xk(12)/XBHk(3
)))))+fZBH*(KOH/(KOH+Uk(3)))*(Xk(9)/(KNA+Xk(9)))^2)*(Xk(10)/(KNO+Xk(10)))*XBHk(3)*(muH*(Xk(11)/(Ks+Xk(11)))+KMP*etag*((Xk(12)/XBHk(
3))/(KSP+(Xk(12)/XBHk(3)))));
rUSNH3KOA=((1/YZA)+fZBH)*muA*(Xk(9)/(KSA+Xk(9)))*(Uk(3)/(KOA+Uk(3)))^2)*XBAk(3);
rUSNH3etag=-
KMP*((Xk(12)/XBHk(3))/(KSP+(Xk(12)/XBHk(3))))*(KOH/(KOH+Uk(3)))*(Xk(9)/(KNA+Xk(9)))*(Xk(10)/(KNO+Xk(10)))*XBHk(3)*fZBH;
rUSNH3KMP=((Xk(12)/XBHk(3))/(KSP+(Xk(12)/XBHk(3))))*(Xk(9)/(KNA+Xk(9)))*XBHk(3)*fZBH*((Uk(3)/(KOH+Uk(3)))+(KOH/(KOH+Uk(3)))*(Xk(10
)/(KNO+Xk(10)))*etag);
rUSNH3KSP=fZBH*KMP*((Xk(12)/XBHk(3))/(KSP+(Xk(12)/XBHk(3))))*((Xk(9)/(KNA+Xk(9)))*(Uk(3)/(KOH+Uk(3)))+(KOH/(KOH+Uk(3)))*(Xk(10)/(K
NO+Xk(10))))*XBHk(3);
rUSNH3KSA=((1/YZA)+fZBH)*muA*(Xk(9)/(KSA+Xk(9))^2)*(Uk(3)/(KOA+Uk(3)))*XBAk(3);rUSNH3fMA=0.0;rUSNH3KA=0.0;
```

```
% Calculation for model parameters of rUSNO for the tank 3
rUSNO3f=0.0;
rUSNO3YZH=(1/(2.86*YZH^2))*(KOH/(KOH+Uk(3)))*(Xk(10)/(KNO+Xk(10)))*XBHk(3)*(muH*(Xk(11)/(Ks+Xk(11)))+KMP*etag*((Xk(12)/XBHk(3))/(K
SP+(Xk(12)/XBHk(3)))))*((Xk(9)/(KNA+Xk(9)))+(KNA/(KNA+Xk(9))));
rUSNO3YZA=(1/(2.86*YZH^2))*muA*(Xk(9)/(KSA+Xk(9)))*(Uk(3)/(KOA+Uk(3)))*XBAk(3);
rUSNO3fZBH=-
(Uk(3)/(KOH+Uk(3)))*(KNA/(KNA+Xk(9)))*(Xk(10)/(KNO+Xk(10)))*XBHk(3)*(muH*(Xk(11)/(Ks+Xk(11)))+KMP*((Xk(12)/XBHk(3))/(KSP+(Xk(12)/X
BHk(3)))));
rUSNO3muH=-2*fZBH*(Xk(11)/(Ks+Xk(11)))*(KNA/(KNA+Xk(9)))*(Xk(10)/(KNO+Xk(10)))*XBHk(3)*((Uk(3)/(KOH+Uk(3)))+(KOH/(KOH+Uk(3))))-
((1-YZH)/2.86*YZH)*(Xk(11)/(Ks+Xk(11)))*(KOH/(KOH+Uk(3)))*(Xk(10)/(KNO+Xk(10)))*XBHk(3)*((Xk(9)/(KNA+Xk(9)))+(KNA/(KNA+Xk(9))));
rUSNO3muA=(1/YZA)*(Xk(9)/(KSA+Xk(9))^2)*(Uk(3)/(KOA+Uk(3)))*XBAk(3);
rUSNO3Ks=fZBH*muH*(Xk(11)/(Ks+Xk(11))^2)*(KNA/(KNA+Xk(9)))*(Xk(10)/(KNO+Xk(10)))*XBHk(3)*((Uk(3)/(KOH+Uk(3)))+(KOH/(KOH+Uk(3))))+(
(1-
YZH)/2.86*YZH)*muH*(Xk(11)/(Ks+Xk(11)))*(KOH/(KOH+Uk(3)))*(Xk(10)/(KNO+Xk(10)))*XBHk(3)*((Xk(9)/(KNA+Xk(9)))+(KNA/(KNA+Xk(9))));
rUSNO3KOH=-((1-
YZH)/2.86*YZH)*(KOH/(KOH+Uk(3))^2)*(Xk(10)/(KNO+Xk(10)))*XBHk(3)*(muH*(Xk(11)/(Ks+Xk(11)))+KMP*etag*((Xk(12)/XBHk(3))/(KSP+(Xk(12)
/XBHk(3)))))+fZBH*(Uk(3)/(KOH+Uk(3))^2)*(KNA/(KNA+Xk(9)))*(Xk(10)/(KNO+Xk(10)))*XBHk(3)*KMP*((Xk(12)/XBHk(3))/(KSP+(Xk(12)/XBHk(3)
)))*(1-etag);
rUSNO3KNO=fZBH*(Xk(11)/(Ks+Xk(11)))*(KNA/(KNA+Xk(9)))*(Xk(10)/(KNO+Xk(10))^2)*XBHk(3)*(muH*(Xk(11)/(Ks+Xk(11)))+KMP*((Xk(12)/XBHk(
3))/(KSP+(Xk(12)/XBHk(3)))))+((1-
YZH)/2.86*YZH)*(KOH/(KOH+Uk(3)))*(Xk(9)/(KNA+Xk(9)))*(Xk(10)/(KNO+Xk(10))^2)*XBHk(3)*(muH*(Xk(11)/(Ks+Xk(11)))+KMP*etag*((Xk(12)/X
BHk(3))/(KSP+(Xk(12)/XBHk(3)))))+(((1-
YZH)/2.86*YZH)+fZBH)*(KOH/(KOH+Uk(3)))*(KNA/(KNA+Xk(9)))*(Xk(10)/(KNO+Xk(10))^2)*XBHk(3)*(muH*(Xk(11)/(Ks+Xk(11)))+KMP*etag*((Xk(1
2)/XBHk(3))/(KSP+(Xk(12)/XBHk(3)))));
rUSNO3KNA=-
fZBH*(Uk(3)/(KOH+Uk(3)))*(Xk(9)/(KNA+Xk(9)))*(Xk(10)/(KNO+Xk(10)))*XBHk(3)*(muH*(Xk(11)/(Ks+Xk(11)))+KMP*((Xk(12)/XBHk(3))/(KSP+(X
k(12)/XBHk(3)))))-
fZBH*(KOH/(KOH+Uk(3)))*(Xk(9)/(KNA+Xk(9))^2)*(Xk(10)/(KNO+Xk(10)))*XBHk(3)*(muH*(Xk(11)/(Ks+Xk(11)))+KMP*etag*((Xk(12)/XBHk(3))/(K
SP+(Xk(12)/XBHk(3)))));
rUSNO3KOA=(1/YZA)*muA*(Xk(9)/(KSA+Xk(9))^2)*(Uk(3)/(KOA+Uk(3)))*XBAk(3);
rUSNO3etag=-((1-
YZH)/2.86*YZH)*KMP*((Xk(12)/XBHk(3))/(KSP+(Xk(12)/XBHk(3))))*(KOH/(KOH+Uk(3)))*(Xk(10)/(KNO+Xk(10)))*XBHk(3)*((Xk(9)/(KNA+Xk(9)))+
(KNA/(KNA+Xk(9))))-
fZBH*KMP*((Xk(12)/XBHk(3))/(KSP+(Xk(12)/XBHk(3))))*(KOH/(KOH+Uk(3)))*(KNA/(KNA+Xk(9)))*(Xk(10)/(KNO+Xk(10)))*XBHk(3);
rUSNO3KMP=-
fZBH*((Xk(12)/XBHk(3))/(KSP+(Xk(12)/XBHk(3))))*(KNA/(KNA+Xk(9)))*(Xk(10)/(KNO+Xk(10)))*XBHk(3)*((Uk(3)/(KOH+Uk(3)))+etag*(KOH/(KOH
+Uk(3))))-((1-
YZH)/2.86*YZH)*((Xk(12)/XBHk(3))/(KSP+(Xk(12)/XBHk(3))))*(KOH/(KOH+Uk(3)))*(Xk(10)/(KNO+Xk(10)))*etag*XBHk(3)*((Xk(9)/(KNA+Xk(9)))
+(KNA/(KNA+Xk(9))));
rUSNO3KSP=fZBH*KMP*((Xk(12)/XBHk(3))/(KSP+(Xk(12)/XBHk(3))))*(KNA/(KNA+Xk(9)))*(Xk(10)/(KNO+Xk(10)))*XBHk(3)*((Uk(3)/(KOH+Uk(3)))+
etag*(KOH/(KOH+Uk(3))))+((1-
YZH)/2.86*YZH)*((Xk(12)/XBHk(3))/(KSP+(Xk(12)/XBHk(3))))*(KOH/(KOH+Uk(3)))*(Xk(10)/(KNO+Xk(10)))*etag*XBHk(3)*((Xk(9)/(KNA+Xk(9)))
+(KNA/(KNA+Xk(9))));
rUSNO3KSA=-(1/YZA)*(Xk(9)/(KSA+Xk(9))^2)*(Uk(3)/(KOA+Uk(3)))*XBAk(3);rUSNO3fMA=0;rUSNO3KA=0;

% Calculation for model parameters of rUSS for the tank 3
rUSS3f=0.0;
rUSS3YZH=(1/(YZH^2))*muH*(Xk(11)/(Ks+Xk(11)))*XBHk(3)*(Uk(3)/(KOH+Uk(3)))*((Xk(9)/(KNA+Xk(9)))+(KNA/(KNA+Xk(9))))*(Xk(10)/(KNO+Xk(
10)))+(KOH/(KOH+Uk(3)))*(Xk(10)/(KNO+Xk(10)))*((Xk(9)/(KNA+Xk(9)))+(KNA/(KNA+Xk(9))));
rUSS3YZA=0;rUSS3fZBH=0;
rUSS3muH=-
(1/YZH)*(Xk(11)/(Ks+Xk(11)))*XBHk(3)*(Uk(3)/(KOH+Uk(3)))*((Xk(9)/(KNA+Xk(9)))+(KNA/(KNA+Xk(9))))*(Xk(10)/(KNO+Xk(10)))+(Uk(3)/(KOH
+Uk(3)))*((Xk(9)/(KNA+Xk(9)))+(KNA/(KNA+Xk(9))))*(Xk(10)/(KNO+Xk(10)));rUSS3muA=0;
rUSS3Ks=(1/YZH)*muH*(Xk(11)/(Ks+Xk(11)))*XBHk(3)*(Uk(3)/(KOH+Uk(3)))*((Xk(9)/(KNA+Xk(9)))+(KNA/(KNA+Xk(9))))*(Xk(10)/(KNO+Xk(10)))
+(KOH/(KOH+Uk(3)))*(Xk(10)/(KNO+Xk(10)))*((Xk(9)/(KNA+Xk(9)))+(KNA/(KNA+Xk(9))));
rUSS3KOH=(1/YZH)*muH*(Xk(11)/(Ks+Xk(11)))*(Uk(3)/(KOH+Uk(3)))*XBHk(3)*(Xk(9)/(KNA+Xk(9)))*(1-(Xk(10)/(KNO+Xk(10))));
rUSS3KNO=(1/YZH)*muH*(Xk(11)/(Ks+Xk(11)))*(Xk(10)/(KNO+Xk(10)))*XBHk(3)*(Uk(3)/(KOH+Uk(3)))*(KNA/(KNA+Xk(9)))+(KOH/(KOH+Uk(3)))*((
Xk(9)/(KNA+Xk(9)))+(KNA/(KNA+Xk(9))));
rUSS3KNA=(1/YZH)*muH*(Xk(11)/(Ks+Xk(11)))*(Xk(9)/(KNA+Xk(9))^2)*XBHk(3)*(Uk(3)/(KOH+Uk(3)))*(1-(Xk(10)/(KNO+Xk(10))));
rUSS3KOA=0;rUSS3etag=0;rUSS3KMP=0;rUSS3KSP=0;rUSS3KSA=0;rUSS3fMA=0;rUSS3KA=0;

% Calculation for model parameters of rUSads for the tank 3
rUSads3f=0.0;
rUSads3YZH=(1/(YZH^2))*KMP*((Xk(12)/XBHk(3))/(KSP+(Xk(12)/XBHk(3))))*XBHk(3)*(Uk(3)/(KOH+Uk(3)))*((Xk(9)/(KNA+Xk(9)))+(KNA/(KNA+Xk
(9))))*(Xk(10)/(KNO+Xk(10)))+etag*(KOH/(KOH+Uk(3)))*(Xk(10)/(KNO+Xk(10)))*((Xk(9)/(KNA+Xk(9)))+(KNA/(KNA+Xk(9))));
rUSads3YZA=0;rUSads3fZBH=0;rUSads3muH=0;rUSads3muA=0;rUSads3Ks=0;
rUSads3KOH=(1/YZH)*KMP*((Xk(12)/XBHk(3))/(KSP+(Xk(12)/XBHk(3))))*(Uk(3)/(KOH+Uk(3))^2)*XBHk(3)*(Xk(9)/(KNA+Xk(9)))*(1-
(Xk(10)/(KNO+Xk(10))));
rUSads3KNO=(1/YZH)*KMP*((Xk(12)/XBHk(3))/(KSP+(Xk(12)/XBHk(3))))*(Xk(10)/(KNO+Xk(10))^2)*XBHk(3)*(Uk(3)/(KOH+Uk(3)))*(KNA/(KNA+Xk(
9)))+etag*(KOH/(KOH+Uk(3)))*((Xk(9)/(KNA+Xk(9)))+(KNA/(KNA+Xk(9))));
rUSads3KNA=(1/YZH)*KMP*((Xk(12)/XBHk(3))/(KSP+(Xk(12)/XBHk(3))))*(Xk(9)/(KNA+Xk(9))^2)*XBHk(3)*(Uk(3)/(KOH+Uk(3)))*(1-
(Xk(10)/(KNO+Xk(10))));rUSads3KOA=0;
rUSads3etag=-
(1/YZH)*KMP*((Xk(12)/XBHk(3))/(KSP+(Xk(12)/XBHk(3))))*(KOH/(KOH+Uk(3)))*(Xk(10)/(KNO+Xk(10)))*etag*XBHk(3)*((Xk(9)/(KNA+Xk(9)))+(K
NA/(KNA+Xk(9))));
rUSads3KMP=-
(1/YZH)*((Xk(12)/XBHk(3))/(KSP+(Xk(12)/XBHk(3))))*XBHk(3)*(Uk(3)/(KOH+Uk(3)))*((Xk(9)/(KNA+Xk(9)))+(KNA/(KNA+Xk(9))))*(Xk(10)/(KNO
+Xk(10)))+etag*(KOH/(KOH+Uk(3)))*(Xk(10)/(KNO+Xk(10)))*((Xk(9)/(KNA+Xk(9)))+(KNA/(KNA+Xk(9))));
rUSads3KSP=(1/YZH)*KMP*((Xk(12)/XBHk(3))/(KSP+(Xk(12)/XBHk(3))))^2)*XBHk(3)*(Uk(3)/(KOH+Uk(3)))*((Xk(9)/(KNA+Xk(9)))+(KNA/(KNA+Xk(9
))))*(Xk(10)/(KNO+Xk(10)))+etag*(KOH/(KOH+Uk(3)))*(Xk(10)/(KNO+Xk(10)))*((Xk(9)/(KNA+Xk(9)))+(KNA/(KNA+Xk(9))));
rUSads3KSA=0;rUSads3fMA=KA*XSk(3)*XBHk(3);rUSads3KA=XSk(3)*XBHk(3)*(fMA-(Xk(12)/XBHk(3)));

% Calculation for model parameters of rUSNH for the tank 4
rUSNH4f=0.0;rUSNH4YZH=0;rUSNH4YZA=(1/YZA)*muA*(Xk(13)/(KSA+Xk(13)))*(Uk(4)/(KOA+Uk(4)))*XBAk(4);
rUSNH4fZBH=-
(Uk(4)/(KOH+Uk(4)))*(Xk(13)/(KNA+Xk(13)))*XBHk(4)*(muH*(Xk(15)/(Ks+Xk(15)))+KMP*((Xk(16)/XBHk(4))/(KSP+(Xk(16)/XBHk(4)))))-
(KOH/(KOH+Uk(4)))*(Xk(13)/(KNA+Xk(13)))*(Xk(14)/(KNO+Xk(14)))*XBHk(4)*(muH*(Xk(15)/(Ks+Xk(15)))+KMP*etag*((Xk(16)/XBHk(4))/(KSP+(X
k(16)/XBHk(4)))))-muA*(Xk(13)/(KSA+Xk(13)))*(Uk(4)/(KOA+Uk(4)))*XBAk(4);
rUSNH4muH=-fZBH*(Xk(15)/(Ks+Xk(15)))*XBHk(4)*((Xk(13)/(KNA+Xk(13)))*(Uk(4)/(KOH+Uk(4)))+(KOH/(KOH+Uk(4)))*(Xk(14)/(KNO+Xk(14))));
rUSNH4muA=-((1/YZA)-fZBH)*(Xk(13)/(KSA+Xk(13)))*(Uk(4)/(KOA+Uk(4)))*XBAk(4);
rUSNH4Ks=fZBH*muH*(Xk(15)/(Ks+Xk(15))^2)*(Xk(13)/(KNA+Xk(13)))*XBHk(4)*((Uk(4)/(KOH+Uk(4)))+(KOH/(KOH+Uk(4)))*(Xk(14)/(KNO+Xk(14)))
);
rUSNH4KOH=fZBH*(Uk(4)/(KOH+Uk(4))^2)*(Xk(13)/(KNA+Xk(13)))*XBHk(4)*(muH*(Xk(15)/(Ks+Xk(15)))+KMP*((Xk(16)/XBHk(4))/(KSP+(Xk(16)/XB
Hk(4)))))-
fZBH*(Uk(4)/(KOH+Uk(4))^2)*(Xk(13)/(KNA+Xk(13)))*(Xk(14)/(KNO+Xk(14)))*XBHk(4)*(muH*(Xk(15)/(Ks+Xk(15)))+KMP*etag*((Xk(16)/XBHk(4))
)/(KSP+(Xk(16)/XBHk(4)))));
rUSNH4KNO=fZBH*(KOH/(KOH+Uk(4)))*(Xk(13)/(KNA+Xk(13)))*(Xk(14)/(KNO+Xk(14))^2)*XBHk(4)*(muH*(Xk(15)/(Ks+Xk(15)))+KMP*etag*((Xk(16)
/XBHk(4))/(KSP+(Xk(16)/XBHk(4)))));
```

```
rUSNH4KNA=fZBH*(Uk(4)/(KOH+Uk(4)))*(Xk(13)/(KNA+Xk(13)))*XBHk(4)*(muH*(Xk(15)/(Ks+Xk(15)))+KMP*((Xk(16)/XBHk(4))/(KSP+(Xk(16)/XBHk
(4)))))+fZBH*(KOH/(KOH+Uk(4)))*(Xk(13)/(KNA+Xk(13))^2)*(Xk(14)/(KNO+Xk(14)))*XBHk(4)*(muH*(Xk(15)/(Ks+Xk(15)))+KMP*etag*((Xk(16)/X
BHk(4))/(KSP+(Xk(16)/XBHk(4)))));
rUSNH4KOA=((1/YZA)+fZBH)*muA*(Xk(13)/(KSA+Xk(13)))*(Uk(4)/(KOA+Uk(4))^2)*XBAk(4);
rUSNH4etag=-
KMP*((Xk(16)/XBHk(4))/(KSP+(Xk(16)/XBHk(4))))*(KOH/(KOH+Uk(4)))*(Xk(13)/(KNA+Xk(13)))*(Xk(14)/(KNO+Xk(14)))*XBHk(4)*fZBH;
rUSNH4KMP=((Xk(16)/XBHk(4))/(KSP+(Xk(16)/XBHk(4))))*(Xk(13)/(KNA+Xk(13)))*XBHk(4)*fZBH*((Uk(4)/(KOH+Uk(4)))+(KOH/(KOH+Uk(4)))*(Xk(
14)/(KNO+Xk(14)))*etag);
rUSNH4KSP=fZBH*KMP*((Xk(16)/XBHk(4))/(KSP+(Xk(16)/XBHk(4))))*((Xk(13)/(KNA+Xk(13)))*(Uk(4)/(KOH+Uk(4)))+(KOH/(KOH+Uk(4)))*(Xk(14)/
(KNO+Xk(14))))*XBHk(4);
rUSNH4KSA=((1/YZA)+fZBH)*muA*(Xk(13)/(KSA+Xk(13))^2)*(Uk(4)/(KOA+Uk(4)))*XBAk(4);rUSNH4fMA=0.0;rUSNH4KA=0.0;

% Calculation for model parameters of rUSNO for the tank 4
rUSNO4f=0.0;
rUSNO4YZH=(1/(2.86*YZH^2))*(KOH/(KOH+Uk(4)))*(Xk(14)/(KNO+Xk(14)))*XBHk(4)*(muH*(Xk(15)/(Ks+Xk(15)))+KMP*etag*((Xk(16)/XBHk(4))/(K
SP+(Xk(16)/XBHk(4)))))*((Xk(13)/(KNA+Xk(13)))+(KNA/(KNA+Xk(13))));
rUSNO4YZA=(1/(2.86*YZH^2))*muA*(Xk(13)/(KSA+Xk(13)))*(Uk(4)/(KOA+Uk(4)))*XBAk(4);
rUSNO4fZBH=-
(Uk(4)/(KOH+Uk(4)))*(KNA/(KNA+Xk(13)))*(Xk(14)/(KNO+Xk(14)))*XBHk(4)*(muH*(Xk(15)/(Ks+Xk(15)))+KMP*((Xk(16)/XBHk(4))/(KSP+(Xk(16)/
XBHk(4)))));
rUSNO4muH=-2*fZBH*(Xk(15)/(Ks+Xk(15)))*(KNA/(KNA+Xk(13)))*(Xk(14)/(KNO+Xk(14)))*XBHk(4)*((Uk(4)/(KOH+Uk(4)))+(KOH/(KOH+Uk(4))))-
((1-
YZH)/2.86*YZH)*(Xk(15)/(Ks+Xk(15)))*(KOH/(KOH+Uk(4)))*(Xk(14)/(KNO+Xk(14)))*XBHk(4)*((Xk(13)/(KNA+Xk(13)))+(KNA/(KNA+Xk(13))));
rUSNO4muA=(1/YZA)*(Xk(13)/(KSA+Xk(13))^2)*(Uk(4)/(KOA+Uk(4)))*XBAk(4);
rUSNO4Ks=fZBH*muH*(Xk(15)/(Ks+Xk(15))^2)*(KNA/(KNA+Xk(13)))*(Xk(14)/(KNO+Xk(14)))*XBHk(4)*((Uk(4)/(KOH+Uk(4)))+(KOH/(KOH+Uk(4))))+
((1-
YZH)/2.86*YZH)*muH*(Xk(15)/(Ks+Xk(15)))*(KOH/(KOH+Uk(4)))*(Xk(14)/(KNO+Xk(14)))*XBHk(4)*((Xk(13)/(KNA+Xk(13)))+(KNA/(KNA+Xk(13))))
;
rUSNO4KOH=-((1-
YZH)/2.86*YZH)*(KOH/(KOH+Uk(4))^2)*(Xk(14)/(KNO+Xk(14)))*XBHk(4)*(muH*(Xk(15)/(Ks+Xk(15)))+KMP*etag*((Xk(16)/XBHk(4))/(KSP+(Xk(16)
/XBHk(4)))))+fZBH*(Uk(4)/(KOH+Uk(4))^2)*(KNA/(KNA+Xk(13)))*(Xk(14)/(KNO+Xk(14)))*XBHk(4)*KMP*((Xk(16)/XBHk(4))/(KSP+(Xk(16)/XBHk(4
))))*(1-etag);
rUSNO4KNO=fZBH*(Xk(15)/(Ks+Xk(15)))*(KNA/(KNA+Xk(13)))*(Xk(14)/(KNO+Xk(14))^2)*XBHk(4)*(muH*(Xk(15)/(Ks+Xk(15)))+KMP*((Xk(16)/XBHk
(4))/(KSP+(Xk(16)/XBHk(4)))))+((1-
YZH)/2.86*YZH)*(KOH/(KOH+Uk(4)))*(Xk(13)/(KNA+Xk(13)))*(Xk(14)/(KNO+Xk(14))^2)*XBHk(4)*(muH*(Xk(15)/(Ks+Xk(15)))+KMP*etag*((Xk(16)
/XBHk(4))/(KSP+(Xk(16)/XBHk(4)))))+(((1-
YZH)/2.86*YZH)+fZBH)*(KOH/(KOH+Uk(4)))*(KNA/(KNA+Xk(13)))*(Xk(14)/(KNO+Xk(14))^2)*XBHk(4)*(muH*(Xk(15)/(Ks+Xk(15)))+KMP*etag*((Xk(
16)/XBHk(4))/(KSP+(Xk(16)/XBHk(4)))));
rUSNO4KNA=-
fZBH*(Uk(4)/(KOH+Uk(4)))*(Xk(13)/(KNA+Xk(13)))*(Xk(14)/(KNO+Xk(14)))*XBHk(4)*(muH*(Xk(15)/(Ks+Xk(15)))+KMP*((Xk(16)/XBHk(4))/(KSP+
(Xk(16)/XBHk(4)))))-
fZBH*(KOH/(KOH+Uk(4)))*(Xk(13)/(KNA+Xk(13))^2)*(Xk(14)/(KNO+Xk(14)))*XBHk(4)*(muH*(Xk(15)/(Ks+Xk(15)))+KMP*etag*((Xk(16)/XBHk(4))/
(KSP+(Xk(16)/XBHk(4)))));
rUSNO4KOA=(1/YZA)*muA*(Xk(13)/(KSA+Xk(13))^2)*(Uk(4)/(KOA+Uk(4)))*XBAk(4);
rUSNO4etag=-((1-
YZH)/2.86*YZH)*KMP*((Xk(16)/XBHk(4))/(KSP+(Xk(16)/XBHk(4))))*(KOH/(KOH+Uk(4)))*(Xk(14)/(KNO+Xk(14)))*XBHk(4)*((Xk(13)/(KNA+Xk(13))
)+(KNA/(KNA+Xk(13))))-
fZBH*KMP*((Xk(16)/XBHk(4))/(KSP+(Xk(16)/XBHk(4))))*(KOH/(KOH+Uk(4)))*(KNA/(KNA+Xk(13)))*(Xk(14)/(KNO+Xk(14)))*XBHk(4);
rUSNO4KMP=-
fZBH*((Xk(16)/XBHk(4))/(KSP+(Xk(16)/XBHk(4))))*(KNA/(KNA+Xk(13)))*(Xk(14)/(KNO+Xk(14)))*XBHk(1)*((Uk(4)/(KOH+Uk(4)))+etag*(KOH/(KO
H+Uk(4))))-((1-
YZH)/2.86*YZH)*((Xk(16)/XBHk(4))/(KSP+(Xk(16)/XBHk(4))))*(KOH/(KOH+Uk(4)))*(Xk(14)/(KNO+Xk(14)))*etag*XBHk(4)*((Xk(13)/(KNA+Xk(13)
))+(KNA/(KNA+Xk(13))));
rUSNO4KSP=fZBH*KMP*((Xk(16)/XBHk(4))/(KSP+(Xk(16)/XBHk(4))))*(KNA/(KNA+Xk(13)))*(Xk(14)/(KNO+Xk(14)))*XBHk(4)*((Uk(4)/(KOH+Uk(4)))
+etag*(KOH/(KOH+Uk(4))))+((1-
YZH)/2.86*YZH)*((Xk(16)/XBHk(4))/(KSP+(Xk(16)/XBHk(4))))*(KOH/(KOH+Uk(4)))*(Xk(14)/(KNO+Xk(14)))*etag*XBHk(4)*((Xk(13)/(KNA+Xk(13)
))+(KNA/(KNA+Xk(13))));
rUSNO4KSA=-(1/YZA)*(Xk(13)/(KSA+Xk(13))^2)*(Uk(4)/(KOA+Uk(4)))*XBAk(4);rUSNO4fMA=0;rUSNO4KA=0;

% Calculation for model parameters of rUSS for the tank 4
rUSS4f=0.0;
rUSS4YZH=(1/(YZH^2))*muH*(Xk(15)/(Ks+Xk(15)))*XBHk(4)*(Uk(4)/(KOH+Uk(4)))*((Xk(13)/(KNA+Xk(13)))+(KNA/(KNA+Xk(13))))*(Xk(14)/(KNO+
Xk(14)))+(KOH/(KOH+Uk(4)))*(Xk(14)/(KNO+Xk(14)))*((Xk(13)/(KNA+Xk(13)))+(KNA/(KNA+Xk(13))));
rUSS4YZA=0;rUSS4fZBH=0;
rUSS4muH=-
(1/YZH)*(Xk(15)/(Ks+Xk(15)))*XBHk(4)*(Uk(4)/(KOH+Uk(4)))*((Xk(13)/(KNA+Xk(13)))+(KNA/(KNA+Xk(13))))*(Xk(14)/(KNO+Xk(14)))+(Uk(4)/(
KOH+Uk(4)))*((Xk(13)/(KNA+Xk(13)))+(KNA/(KNA+Xk(13))))*(Xk(14)/(KNO+Xk(14)));
rUSS4muA=0;
rUSS4Ks=(1/YZH)*muH*(Xk(15)/(Ks+Xk(15)))*XBHk(4)*(Uk(4)/(KOH+Uk(4)))*((Xk(13)/(KNA+Xk(13)))+(KNA/(KNA+Xk(13))))*(Xk(14)/(KNO+Xk(14
)))+(KOH/(KOH+Uk(4)))*(Xk(14)/(KNO+Xk(14)))*((Xk(13)/(KNA+Xk(13)))+(KNA/(KNA+Xk(13))));
rUSS4KOH=(1/YZH)*muH*(Xk(15)/(Ks+Xk(15)))*(Uk(4)/(KOH+Uk(4)))*XBHk(4)*(Xk(13)/(KNA+Xk(13)))*(1-(Xk(14)/(KNO+Xk(14))));
rUSS4KNO=(1/YZH)*muH*(Xk(15)/(Ks+Xk(15)))*(Xk(14)/(KNO+Xk(14)))*XBHk(4)*(Uk(4)/(KOH+Uk(4)))*(KNA/(KNA+Xk(13)))+(KOH/(KOH+Uk(4)))*(
(Xk(13)/(KNA+Xk(13)))+(KNA/(KNA+Xk(13))));
rUSS4KNA=(1/YZH)*muH*(Xk(15)/(Ks+Xk(15)))*(Xk(13)/(KNA+Xk(13))^2)*XBHk(4)*(Uk(4)/(KOH+Uk(4)))*(1-(Xk(14)/(KNO+Xk(14))));
rUSS4KOA=0;rUSS4etag=0;rUSS4KMP=0;rUSS4KSP=0;rUSS4KSA=0;rUSS4fMA=0;rUSS4KA=0;

% Calculation for model parameters of rUSads for the tank 4
rUSads4f=0.0;
rUSads4YZH=(1/(YZH^2))*KMP*((Xk(16)/XBHk(4))/(KSP+(Xk(16)/XBHk(4))))*XBHk(4)*(Uk(4)/(KOH+Uk(4)))*((Xk(13)/(KNA+Xk(13)))+(KNA/(KNA+
Xk(13))))*(Xk(14)/(KNO+Xk(14)))+etag*(KOH/(KOH+Uk(4)))*(Xk(14)/(KNO+Xk(14)))*((Xk(13)/(KNA+Xk(13)))+(KNA/(KNA+Xk(13))));
rUSads4YZA=0;rUSads4fZBH=0;rUSads4muH=0;rUSads4muA=0;rUSads4Ks=0;
rUSads4KOH=(1/YZH)*KMP*((Xk(16)/XBHk(4))/(KSP+(Xk(16)/XBHk(4))))*(Uk(4)/(KOH+Uk(4))^2)*XBHk(4)*(Xk(13)/(KNA+Xk(13)))*(1-
(Xk(14)/(KNO+Xk(14))));
rUSads4KNO=(1/YZH)*KMP*((Xk(16)/XBHk(4))/(KSP+(Xk(16)/XBHk(4))))*(Xk(14)/(KNO+Xk(14))^2)*XBHk(4)*(Uk(4)/(KOH+Uk(4)))*(KNA/(KNA+Xk(
13)))+etag*(KOH/(KOH+Uk(4)))*((Xk(13)/(KNA+Xk(13)))+(KNA/(KNA+Xk(13))));
rUSads4KNA=(1/YZH)*KMP*((Xk(16)/XBHk(4))/(KSP+(Xk(16)/XBHk(4))))*(Xk(13)/(KNA+Xk(13))^2)*XBHk(4)*(Uk(4)/(KOH+Uk(4)))*(1-
(Xk(14)/(KNO+Xk(14))));rUSads4KOA=0;
rUSads4etag=-
(1/YZH)*KMP*((Xk(16)/XBHk(4))/(KSP+(Xk(16)/XBHk(4))))*(KOH/(KOH+Uk(4)))*(Xk(14)/(KNO+Xk(14)))*etag*XBHk(4)*((Xk(13)/(KNA+Xk(13)))+
(KNA/(KNA+Xk(13))));
rUSads4KMP=-
(1/YZH)*((Xk(16)/XBHk(4))/(KSP+(Xk(16)/XBHk(4))))*XBHk(4)*(Uk(4)/(KOH+Uk(4)))*((Xk(13)/(KNA+Xk(13)))+(KNA/(KNA+Xk(13))))*(Xk(14)/(
KNO+Xk(14)))+etag*(KOH/(KOH+Uk(4)))*(Xk(14)/(KNO+Xk(14)))*((Xk(13)/(KNA+Xk(13)))+(KNA/(KNA+Xk(13))));
rUSads4KSP=(1/YZH)*((Xk(16)/XBHk(4))/(KSP+(Xk(16)/XBHk(4))))^2)*XBHk(4)*(Uk(4)/(KOH+Uk(4)))*((Xk(13)/(KNA+Xk(13)))+(KNA/(KNA+Xk(13)
)))*(Xk(14)/(KNO+Xk(14)))+etag*(KOH/(KOH+Uk(4)))*(Xk(14)/(KNO+Xk(14)))*((Xk(13)/(KNA+Xk(13)))+(KNA/(KNA+Xk(13))));
rUSads4KSA=0;rUSads4fMA=KA*XSk(4)*XBHk(4);rUSads4KA=XSk(4)*XBHk(4)*(fMA-(Xk(16)/XBHk(4)));

% Calculation for model parameters of rUSNH for the tank 5
rUSNH5f=0.0;rUSNH5YZH=0;
```

```
rUSNH5YZA=(1/YZA)*muA*(Xk(17)/(KSA+Xk(17)))*(Uk(5)/(KOA+Uk(5)))*XBAk(5);
rUSNH5fZBH=-
(Uk(5)/(KOH+Uk(5)))*(Xk(17)/(KNA+Xk(17)))*XBHk(5)*(muH*(Xk(19)/(Ks+Xk(19)))+KMP*((Xk(20)/XBHk(5))/(KSP+(Xk(20)/XBHk(5)))))-
(KOH/(KOH+Uk(5)))*(Xk(17)/(KNA+Xk(17)))*(Xk(18)/(KNO+Xk(18)))*XBHk(5)*(muH*(Xk(19)/(Ks+Xk(19)))+KMP*etag*((Xk(20)/XBHk(5))/(KSP+(X
k(20)/XBHk(5)))))-muA*(Xk(17)/(KSA+Xk(17)))*(Uk(5)/(KOA+Uk(5)))*XBAk(5);
rUSNH5muH=-fZBH*(Xk(19)/(Ks+Xk(19)))*XBHk(5)*((Xk(17)/(KNA+Xk(17)))*(Uk(5)/(KOH+Uk(5)))+(KOH/(KOH+Uk(5)))*(Xk(18)/(KNO+Xk(18))));
rUSNH5muA=-((1/YZA)-fZBH)*(Xk(17)/(KSA+Xk(17)))*(Uk(5)/(KOA+Uk(5)))*XBAk(5);
rUSNH5Ks=fZBH*muH*(Xk(19)/(Ks+Xk(19))^2)*(Xk(17)/(KNA+Xk(17)))*XBHk(5)*((Uk(5)/(KOH+Uk(5)))+(KOH/(KOH+Uk(5)))*(Xk(18)/(KNO+Xk(18)))
);
rUSNH5KOH=fZBH*(Uk(5)/(KOH+Uk(5))^2)*(Xk(17)/(KNA+Xk(17)))*XBHk(5)*(muH*(Xk(19)/(Ks+Xk(19)))+KMP*((Xk(20)/XBHk(5))/(KSP+(Xk(20)/XB
Hk(5)))))-
fZBH*(Uk(5)/(KOH+Uk(5))^2)*(Xk(17)/(KNA+Xk(17)))*(Xk(18)/(KNO+Xk(18)))*XBHk(5)*(muH*(Xk(19)/(Ks+Xk(19)))+KMP*etag*((Xk(20)/XBHk(5)
)/(KSP+(Xk(20)/XBHk(5)))));
rUSNH3KOH=fZBH*(Uk(3)/(KOH+Uk(3))^2)*(Xk(9)/(KNA+Xk(9)))*XBHk(3)*(muH*(Xk(11)/(Ks+Xk(11)))+KMP*((Xk(12)/XBHk(3))/(KSP+(Xk(12)/XBHk
(3)))))-
fZBH*(Uk(3)/(KOH+Uk(3))^2)*(Xk(9)/(KNA+Xk(9)))*(Xk(10)/(KNO+Xk(10)))*XBHk(3)*(muH*(Xk(11)/(Ks+Xk(11)))+KMP*etag*((Xk(12)/XBHk(3))/
(KSP+(Xk(12)/XBHk(3)))));
rUSNH5KNO=fZBH*(KOH/(KOH+Uk(5)))*(Xk(17)/(KNA+Xk(17)))*(Xk(18)/(KNO+Xk(18))^2)*XBHk(5)*(muH*(Xk(19)/(Ks+Xk(19)))+KMP*etag*((Xk(20)
/XBHk(5))/(KSP+(Xk(20)/XBHk(5)))));
rUSNH5KNA=fZBH*(Uk(5)/(KOH+Uk(5)))*(Xk(17)/(KNA+Xk(17)))*XBHk(5)*(muH*(Xk(19)/(Ks+Xk(19)))+KMP*((Xk(20)/XBHk(5))/(KSP+(Xk(20)/XBHk
(5)))))+fZBH*(KOH/(KOH+Uk(5)))*(Xk(17)/(KNA+Xk(17))^2)*(Xk(18)/(KNO+Xk(18)))*XBHk(5)*(muH*(Xk(19)/(Ks+Xk(19)))+KMP*etag*((Xk(20)/X
BHk(5))/(KSP+(Xk(20)/XBHk(5)))));
rUSNH5KOA=((1/YZA)+fZBH)*muA*(Xk(17)/(KSA+Xk(17)))*(Uk(5)/(KOA+Uk(5))^2)*XBAk(5);
rUSNH5etag=-
KMP*((Xk(20)/XBHk(5))/(KSP+(Xk(20)/XBHk(5))))*(KOH/(KOH+Uk(5)))*(Xk(17)/(KNA+Xk(17)))*(Xk(18)/(KNO+Xk(18)))*XBHk(5)*fZBH;
rUSNH5KMP=((Xk(20)/XBHk(5))/(KSP+(Xk(20)/XBHk(5))))*(Xk(17)/(KNA+Xk(17)))*XBHk(5)*fZBH*((Uk(5)/(KOH+Uk(5)))+(KOH/(KOH+Uk(5)))*(Xk(
18)/(KNO+Xk(18)))*etag);
rUSNH5KSP=fZBH*KMP*((Xk(20)/XBHk(5))/(KSP+(Xk(20)/XBHk(5))))*((Xk(17)/(KNA+Xk(17)))*(Uk(5)/(KOH+Uk(5)))+(KOH/(KOH+Uk(5)))*(Xk(18)/
(KNO+Xk(18))))*XBHk(5);
rUSNH5KSA=((1/YZA)+fZBH)*muA*(Xk(17)/(KSA+Xk(17)))^2)*(Uk(5)/(KOA+Uk(5)))*XBAk(5);rUSNH5fMA=0.0;rUSNH5KA=0.0;

% Calculation for model parameters of rUSNO for the tank 5
rUSNO5f=0.0;
rUSNO5YZH=(1/(2.86*YZH^2))*(KOH/(KOH+Uk(5)))*(Xk(18)/(KNO+Xk(18)))*XBHk(5)*(muH*(Xk(19)/(Ks+Xk(19)))+KMP*etag*((Xk(20)/XBHk(5))/(K
SP+(Xk(20)/XBHk(5))))*((Xk(17)/(KNA+Xk(17)))+(KNA/(KNA+Xk(17))));
rUSNO5YZA=(1/(2.86*YZH^2))*muA*(Xk(17)/(KSA+Xk(17)))*(Uk(5)/(KOA+Uk(5)))*XBAk(5);
rUSNO5fZBH=-
(Uk(1)/(KOH+Uk(5)))*(KNA/(KNA+Xk(17)))*(Xk(18)/(KNO+Xk(18)))*XBHk(5)*(muH*(Xk(19)/(Ks+Xk(19)))+KMP*((Xk(20)/XBHk(5))/(KSP+(Xk(20)/
XBHk(5)))));
rUSNO5muH=-2*fZBH*(Xk(19)/(Ks+Xk(19)))*(KNA/(KNA+Xk(17)))*(Xk(18)/(KNO+Xk(18)))*XBHk(5)*((Uk(5)/(KOH+Uk(5)))+(KOH/(KOH+Uk(5))))-
((1-
YZH)/2.86*YZH)*(Xk(19)/(Ks+Xk(19)))*(KOH/(KOH+Uk(5)))*(Xk(18)/(KNO+Xk(18)))*XBHk(5)*((Xk(17)/(KNA+Xk(17)))+(KNA/(KNA+Xk(17))));
rUSNO5muA=(1/YZA)*(Xk(17)/(KSA+Xk(17)))^2)*(Uk(5)/(KOA+Uk(5)))*XBAk(5);
rUSNO5Ks=fZBH*muH*(Xk(19)/(Ks+Xk(19))^2)*(KNA/(KNA+Xk(17)))*(Xk(18)/(KNO+Xk(18)))*XBHk(5)*((Uk(5)/(KOH+Uk(5)))+(KOH/(KOH+Uk(5))))+
((1-
YZH)/2.86*YZH)*muH*(Xk(19)/(Ks+Xk(19)))*(KOH/(KOH+Uk(5)))*(Xk(18)/(KNO+Xk(18)))*XBHk(5)*((Xk(17)/(KNA+Xk(17)))+(KNA/(KNA+Xk(17))))
;
rUSNO5KOH=-((1-
YZH)/2.86*YZH)*(KOH/(KOH+Uk(5))^2)*(Xk(18)/(KNO+Xk(18)))*XBHk(5)*(muH*(Xk(19)/(Ks+Xk(19)))+KMP*etag*((Xk(20)/XBHk(5))/(KSP+(Xk(20)
/XBHk(5))))+fZBH*(Uk(5)/(KOH+Uk(5))^2)*(KNA/(KNA+Xk(17)))*(Xk(18)/(KNO+Xk(18)))*XBHk(5)*KMP*((Xk(20)/XBHk(5))/(KSP+(Xk(20)/XBHk(5
))))*(1-etag);
rUSNO5KNO=fZBH*(Xk(19)/(Ks+Xk(19)))*(KNA/(KNA+Xk(17)))*(Xk(18)/(KNO+Xk(18))^2)*XBHk(1)*(muH*(Xk(19)/(Ks+Xk(19)))+KMP*((Xk(20)/XBHk
(5))/(KSP+(Xk(20)/XBHk(5)))))+((1-
YZH)/2.86*YZH)*(KOH/(KOH+Uk(5)))*(Xk(17)/(KNA+Xk(17)))*(Xk(18)/(KNO+Xk(18))^2)*XBHk(5)*(muH*(Xk(19)/(Ks+Xk(19)))+KMP*etag*((Xk(20)
/XBHk(5))/(KSP+(Xk(20)/XBHk(5)))))+(((1-
YZH)/2.86*YZH)+fZBH)*(KOH/(KOH+Uk(5)))*(KNA/(KNA+Xk(17)))*(Xk(18)/(KNO+Xk(18))^2)*XBHk(5)*(muH*(Xk(19)/(Ks+Xk(19)))+KMP*etag*((Xk(
20)/XBHk(5))/(KSP+(Xk(20)/XBHk(5)))));
rUSNO5KNA=-
fZBH*(Uk(5)/(KOH+Uk(5)))*(Xk(17)/(KNA+Xk(17)))*(Xk(18)/(KNO+Xk(18)))*XBHk(5)*(muH*(Xk(19)/(Ks+Xk(19)))+KMP*((Xk(20)/XBHk(5))/(KSP+
(Xk(20)/XBHk(5)))))-
fZBH*(KOH/(KOH+Uk(5)))*(Xk(17)/(KNA+Xk(17)))^2)*(Xk(18)/(KNO+Xk(18)))*XBHk(5)*(muH*(Xk(19)/(Ks+Xk(19)))+KMP*etag*((Xk(20)/XBHk(5))/
(KSP+(Xk(20)/XBHk(5)))));
rUSNO5KOA=(1/YZA)*muA*(Xk(17)/(KSA+Xk(17))^2)*(Uk(5)/(KOA+Uk(5)))*XBAk(5);
rUSNO5etag=-((1-
YZH)/2.86*YZH)*KMP*((Xk(20)/XBHk(5))/(KSP+(Xk(20)/XBHk(5))))*(KOH/(KOH+Uk(5)))*(Xk(18)/(KNO+Xk(18)))*XBHk(5)*((Xk(17)/(KNA+Xk(17)))
)+(KNA/(KNA+Xk(17))))-
fZBH*KMP*((Xk(20)/XBHk(5))/(KSP+(Xk(20)/XBHk(5))))*(KOH/(KOH+Uk(5)))*(KNA/(KNA+Xk(17)))*(Xk(18)/(KNO+Xk(18)))*XBHk(5);
rUSNO5KMP=-
fZBH*((Xk(20)/XBHk(5))/(KSP+(Xk(20)/XBHk(5))))*(KNA/(KNA+Xk(17)))*(Xk(18)/(KNO+Xk(18)))*XBHk(5)*((Uk(5)/(KOH+Uk(5)))+etag*(KOH/(KO
H+Uk(5))))-((1-
YZH)/2.86*YZH)*((Xk(20)/XBHk(5))/(KSP+(Xk(20)/XBHk(5))))*(KOH/(KOH+Uk(5)))*(Xk(18)/(KNO+Xk(18)))*etag*XBHk(5)*((Xk(17)/(KNA+Xk(17)
)))+(KNA/(KNA+Xk(17))));
rUSNO5KSP=fZBH*KMP*((Xk(20)/XBHk(5))/(KSP+(Xk(20)/XBHk(5))))*(KNA/(KNA+Xk(17)))*(Xk(18)/(KNO+Xk(18)))*XBHk(5)*((Uk(5)/(KOH+Uk(5)))
+etag*(KOH/(KOH+Uk(5))))+((1-
YZH)/2.86*YZH)*((Xk(20)/XBHk(5))/(KSP+(Xk(20)/XBHk(5))))*(KOH/(KOH+Uk(5)))*(Xk(18)/(KNO+Xk(18)))*etag*XBHk(5)*((Xk(17)/(KNA+Xk(17)
)))+(KNA/(KNA+Xk(17))));
rUSNO5KSA=-(1/YZA)*(Xk(17)/(KSA+Xk(17))^2)*(Uk(5)/(KOA+Uk(5)))*XBAk(5);rUSNO5fMA=0;rUSNO5KA=0;

% Calculation for model parameters of rUSS for the tank 5
rUSS5f=0.0;
rUSS5YZH=(1/(YZH^2))*muH*(Xk(19)/(Ks+Xk(19)))*XBHk(5)*(Uk(1)/(KOH+Uk(5)))*((Xk(17)/(KNA+Xk(17)))+(KNA/(KNA+Xk(17))))*(Xk(18)/(KNO+
Xk(18)))+(KOH/(KOH+Uk(5)))*(Xk(18)/(KNO+Xk(18)))*((Xk(17)/(KNA+Xk(17)))+(KNA/(KNA+Xk(17))));
rUSS5YZA=0;rUSS5fZBH=0;
rUSS5muH=-
(1/YZH)*(Xk(19)/(Ks+Xk(19)))*XBHk(5)*(Uk(5)/(KOH+Uk(5)))*((Xk(17)/(KNA+Xk(17)))+(KNA/(KNA+Xk(17))))*(Xk(18)/(KNO+Xk(18)))+(Uk(5)/(
KOH+Uk(5)))*((Xk(17)/(KNA+Xk(17)))+(KNA/(KNA+Xk(17))))*Xk(18)/(KNO+Xk(18)));
rUSS5muA=0;
rUSS5Ks=(1/YZH)*muH*(Xk(19)/(Ks+Xk(19)))*XBHk(5)*(Uk(5)/(KOH+Uk(5)))*((Xk(17)/(KNA+Xk(17)))+(KNA/(KNA+Xk(17))))*(Xk(18)/(KNO+Xk(18
)))+(KOH/(KOH+Uk(5)))*(Xk(18)/(KNO+Xk(18)))*((Xk(17)/(KNA+Xk(17)))+(KNA/(KNA+Xk(17))));
rUSS5KOH=(1/YZH)*muH*(Xk(19)/(Ks+Xk(19)))*(Uk(5)/(KOH+Uk(5)))*XBHk(5)*(Xk(17)/(KNA+Xk(17)))*(1-(Xk(18)/(KNO+Xk(18))));
rUSS5KNO=(1/YZH)*muH*(Xk(19)/(Ks+Xk(19)))*(Xk(18)/(KNO+Xk(18)))*XBHk(5)*(Uk(5)/(KOH+Uk(5)))*(KNA/(KNA+Xk(17)))+(KOH/(KOH+Uk(5)))*(
(Xk(17)/(KNA+Xk(17)))+(KNA/(KNA+Xk(17))));
rUSS5KNA=(1/YZH)*muH*(Xk(19)/(Ks+Xk(19)))*(Xk(17)/(KNA+Xk(17)))^2)*XBHk(5)*(Uk(5)/(KOH+Uk(5)))*(1-(Xk(18)/(KNO+Xk(18))));
rUSS5KOA=0;rUSS5etag=0;rUSS5KMP=0;rUSS5KSP=0;rUSS5KSA=0;rUSS5fMA=0;rUSS5KA=0;

% Calculation for model parameters of rUSads for the tank 5
rUSads5f=0.0;
rUSads5YZH=(1/(YZH^2))*KMP*((Xk(20)/XBHk(5))/(KSP+(Xk(20)/XBHk(5))))*XBHk(5)*(Uk(5)/(KOH+Uk(5)))*((Xk(17)/(KNA+Xk(17)))+(KNA/(KNA+
Xk(17))))*(Xk(18)/(KNO+Xk(18)))+etag*(KOH/(KOH+Uk(5)))*(Xk(18)/(KNO+Xk(18)))*((Xk(17)/(KNA+Xk(17)))+(KNA/(KNA+Xk(17))));
```

```
rUSads5YZA=0;rUSads5fZBH=0;rUSads5muH=0;rUSads5muA=0;rUSads5Ks=0;
rUSads5KOH=(1/YZH)*KMP*((Xk(20)/XBHk(5))/(KSP+(Xk(20)/XBHk(5))))*(Uk(5)/(KOH+Uk(5))^2)*XBHk(5)*(Xk(17)/(KNA+Xk(17)))*(1-
(Xk(18)/(KNO+Xk(18))));
rUSads5KNO=(1/YZH)*KMP*((Xk(20)/XBHk(5))/(KSP+(Xk(20)/XBHk(5))))*(Xk(18)/(KNO+Xk(18))^2)*XBHk(5)*(Uk(5)/(KOH+Uk(5)))*(KNA/(KNA+Xk(
17)))+etag*(KOH/(KOH+Uk(5)))*((Xk(17)/(KNA+Xk(17)))+(KNA/(KNA+Xk(17))));
rUSads5KNA=(1/YZH)*KMP*((Xk(20)/XBHk(5))/(KSP+(Xk(20)/XBHk(5))))*(Xk(17)/(KNA+Xk(17))^2)*XBHk(5)*(Uk(5)/(KOH+Uk(5)))*(1-
(Xk(18)/(KNO+Xk(18))));rUSads5KOA=0;
rUSads5etag=-
(1/YZH)*KMP*((Xk(20)/XBHk(5))/(KSP+(Xk(20)/XBHk(5))))*(KOH/(KOH+Uk(5)))*(Xk(18)/(KNO+Xk(18)))*etag*XBHk(5)*((Xk(17)/(KNA+Xk(17)))+
(KNA/(KNA+Xk(17))));
rUSads5KMP=-
(1/YZH)*((Xk(20)/XBHk(5))/(KSP+(Xk(20)/XBHk(5))))*XBHk(5)*(Uk(5)/(KOH+Uk(5)))*((Xk(17)/(KNA+Xk(17)))+(KNA/(KNA+Xk(17))))*(Xk(18)/(
KNO+Xk(18)))+etag*(KOH/(KOH+Uk(5)))*(Xk(18)/(KNO+Xk(18)))*((Xk(17)/(KNA+Xk(17)))+(KNA/(KNA+Xk(17))));
rUSads5KSP=-
(1/YZH)*KMP*((Xk(20)/XBHk(5))/(KSP+(Xk(20)/XBHk(5)))^2)*XBHk(5)*(Uk(5)/(KOH+Uk(5)))*((Xk(17)/(KNA+Xk(17)))+(KNA/(KNA+Xk(17))))*(Xk
(18)/(KNO+Xk(18)))+etag*(KOH/(KOH+Uk(5)))*(Xk(18)/(KNO+Xk(18)))*((Xk(17)/(KNA+Xk(17)))+(KNA/(KNA+Xk(17))));
rUSads5KSA=0;rUSads5fMA=KA*XSk(5)*XBHk(5);rUSads5KA=XSk(5)*XBHk(5)*(fMA-(Xk(20)/XBHk(5)));

%Calculation of the process matrices
%Calculation of the matrix ASu of the sensitivity model
A1fu=[A11u(1,1)+DT*rUSNH1SNH1 DT*rUSNH1SNO1 DT*rUSNH1SS1 DT*rUSNH1Sads1;
   DT*rUSNO1SNH1 A11u(2,2)+DT*rUSNO1SNO1 DT*rUSNO1SS1 DT*rUSNO1Sads1;
   DT*rUSS1SNH1 DT*rUSS1SNO1 A11u(3,3)+DT*rUSS1SS1 DT*rUSS1Sads1;
   DT*rUSads1SNH1 DT*rUSads1SNO1 DT*rUSads1SS1 A11u(4,4)+DT*rUSads1Sads1];
A1S=[A11u zeros(4,68);zeros(4,4) A1fu zeros(4,64);zeros(4,8) A1fu zeros(4,60);
    zeros(4,12) A1fu zeros(4,56);zeros(4,16) A1fu zeros(4,52);zeros(4,20) A1fu zeros(4,48);
    zeros(4,24) A1fu zeros(4,44);zeros(4,28) A1fu zeros(4,40);zeros(4,32) A1fu zeros(4,36);
    zeros(4,36) A1fu zeros(4,32);zeros(4,40) A1fu zeros(4,28);zeros(4,44) A1fu zeros(4,24);
    zeros(4,48) A1fu zeros(4,20);zeros(4,52) A1fu zeros(4,16);zeros(4,56) A1fu zeros(4,12);
    zeros(4,60) A1fu zeros(4,8);zeros(4,64) A1fu zeros(4,4);zeros(4,68) A1fu];

A2fu=[A22u(1,1)+DT*rUSNH2SNH2 DT*rUSNH2SNO2 DT*rUSNH2SS2 DT*rUSNH2Sads2;
   DT*rUSNO2SNH2 A22u(2,2)+DT*rUSNO2SNO2 DT*rUSNO2SS2 DT*rUSNO2Sads2;
   DT*rUSS2SNH2 DT*rUSS2SNO2 A22u(3,3)+DT*rUSS2SS2 DT*rUSS2Sads2;
   DT*rUSads2SNH2 DT*rUSads2SNO2 DT*rUSads2SS2 A22u(4,4)+DT*rUSads2Sads2];
A2S=[A22u zeros(4,68);zeros(4,4) A2fu zeros(4,64);zeros(4,8) A2fu zeros(4,60);
    zeros(4,12) A2fu zeros(4,56);zeros(4,16) A2fu zeros(4,52);zeros(4,20) A2fu zeros(4,48);
    zeros(4,24) A2fu zeros(4,44);zeros(4,28) A2fu zeros(4,40);zeros(4,32) A2fu zeros(4,36);
    zeros(4,36) A2fu zeros(4,32);zeros(4,40) A2fu zeros(4,28);zeros(4,44) A2fu zeros(4,24);
    zeros(4,48) A2fu zeros(4,20);zeros(4,52) A2fu zeros(4,16);zeros(4,56) A2fu zeros(4,12);
    zeros(4,60) A2fu zeros(4,8);zeros(4,64) A2fu zeros(4,4);zeros(4,68) A2fu];

A3fu=[A33u(1,1)+DT*rUSNH3SNH3 DT*rUSNH3SNO3 DT*rUSNH3SS3 DT*rUSNH3Sads3;
   DT*rUSNO3SNH3 A33u(2,2)+DT*rUSNO3SNO3 DT*rUSNO3SS3 DT*rUSNO3Sads3;
   DT*rUSS3SNH3 DT*rUSS3SNO3 A33u(3,3)+DT*rUSS3SS3 DT*rUSS3Sads3;
   DT*rUSads3SNH3 DT*rUSads3SNO3 DT*rUSads3SS3 A33u(4,4)+DT*rUSads3Sads3];
A3S=[A33u zeros(4,68);zeros(4,4) A3fu zeros(4,64);zeros(4,8) A3fu zeros(4,60);
    zeros(4,12) A3fu zeros(4,56);zeros(4,16) A3fu zeros(4,52);zeros(4,20) A3fu zeros(4,48);
    zeros(4,24) A3fu zeros(4,44);zeros(4,28) A3fu zeros(4,40);zeros(4,32) A3fu zeros(4,36);
    zeros(4,36) A3fu zeros(4,32);zeros(4,40) A3fu zeros(4,28);zeros(4,44) A3fu zeros(4,24);
    zeros(4,48) A3fu zeros(4,20);zeros(4,52) A3fu zeros(4,16);zeros(4,56) A3fu zeros(4,12);
    zeros(4,60) A3fu zeros(4,8);zeros(4,64) A3fu zeros(4,4);zeros(4,68) A3fu];

A4fu=[A44u(1,1)+DT*rUSNH4SNH4 DT*rUSNH4SNO4 DT*rUSNH4SS4 DT*rUSNH4Sads4;
   DT*rUSNO4SNH4 A44u(2,2)+DT*rUSNO4SNO4 DT*rUSNO4SS4 DT*rUSNO4Sads4;
   DT*rUSS4SNH4 DT*rUSS4SNO4 A44u(3,3)+DT*rUSS4SS4 DT*rUSS4Sads4;
   DT*rUSads4SNH4 DT*rUSads4SNO4 DT*rUSads4SS4 A44u(4,4)+DT*rUSads4Sads4];
A4S=[A44u zeros(4,68);zeros(4,4) A4fu zeros(4,64);zeros(4,8) A4fu zeros(4,60);
    zeros(4,12) A4fu zeros(4,56);zeros(4,16) A4fu zeros(4,52);zeros(4,20) A4fu zeros(4,48);
    zeros(4,24) A4fu zeros(4,44);zeros(4,28) A4fu zeros(4,40);zeros(4,32) A4fu zeros(4,36);
    zeros(4,36) A4fu zeros(4,32);zeros(4,40) A4fu zeros(4,28);zeros(4,44) A4fu zeros(4,24);
    zeros(4,48) A4fu zeros(4,20);zeros(4,52) A4fu zeros(4,16);zeros(4,56) A4fu zeros(4,12);
    zeros(4,60) A4fu zeros(4,8);zeros(4,64) A4fu zeros(4,4);zeros(4,68) A4fu];

A5fu=[A55u(1,1)+DT*rUSNH5SNH5 DT*rUSNH5SNO5 DT*rUSNH5SS5 DT*rUSNH5Sads5;
   DT*rUSNO5SNH5 A55u(2,2)+DT*rUSNO5SNO5 DT*rUSNO5SS5 DT*rUSNO5Sads5;
   DT*rUSS5SNH5 DT*rUSS5SNO5 A55u(3,3)+DT*rUSS5SS5 DT*rUSS5Sads5;
   DT*rUSads5SNH5 DT*rUSads5SNO5 DT*rUSads5SS5 A55u(4,4)+DT*rUSads5Sads5];
A5S=[A55u zeros(4,68);zeros(4,4) A5fu zeros(4,64);zeros(4,8) A5fu zeros(4,60);
    zeros(4,12) A5fu zeros(4,56);zeros(4,16) A5fu zeros(4,52);zeros(4,20) A5fu zeros(4,48);
    zeros(4,24) A5fu zeros(4,44);zeros(4,28) A5fu zeros(4,40);zeros(4,32) A5fu zeros(4,36);
    zeros(4,36) A5fu zeros(4,32);zeros(4,40) A5fu zeros(4,28);zeros(4,44) A5fu zeros(4,24);
    zeros(4,48) A5fu zeros(4,20);zeros(4,52) A5fu zeros(4,16);zeros(4,56) A5fu zeros(4,12);
    zeros(4,60) A5fu zeros(4,8);zeros(4,64) A5fu zeros(4,4);zeros(4,68) A5fu];

A15S=[A15u zeros(4,68);zeros(4,4) A15u zeros(4,64);zeros(4,8) A15u zeros(4,60);
    zeros(4,12) A15u zeros(4,56);zeros(4,16) A15u zeros(4,52);zeros(4,20) A15u zeros(4,48);
    zeros(4,24) A15u zeros(4,44);zeros(4,28) A15u zeros(4,40);zeros(4,32) A15u zeros(4,36);
    zeros(4,36) A15u zeros(4,32);zeros(4,40) A15u zeros(4,28);zeros(4,44) A15u zeros(4,24);
    zeros(4,48) A15u zeros(4,20);zeros(4,52) A15u zeros(4,16);zeros(4,56) A15u zeros(4,12);
    zeros(4,60) A15u zeros(4,8);zeros(4,64) A15u zeros(4,4);zeros(4,68) A15u];
A21S=[A21u zeros(4,68);zeros(4,4) A21u zeros(4,64);zeros(4,8) A21u zeros(4,60);
    zeros(4,12) A21u zeros(4,56);zeros(4,16) A21u zeros(4,52);zeros(4,20) A21u zeros(4,48);
    zeros(4,24) A21u zeros(4,44);zeros(4,28) A21u zeros(4,40);zeros(4,32) A21u zeros(4,36);
    zeros(4,36) A21u zeros(4,32);zeros(4,40) A21u zeros(4,28);zeros(4,44) A21u zeros(4,24);
    zeros(4,48) A21u zeros(4,20);zeros(4,52) A21u zeros(4,16);zeros(4,56) A21u zeros(4,12);
    zeros(4,60) A21u zeros(4,8);zeros(4,64) A21u zeros(4,4);zeros(4,68) A21u];
A32S=[A32u zeros(4,68);zeros(4,4) A32u zeros(4,64);zeros(4,8) A32u zeros(4,60);
    zeros(4,12) A32u zeros(4,56);zeros(4,16) A32u zeros(4,52);zeros(4,20) A32u zeros(4,48);
    zeros(4,24) A32u zeros(4,44);zeros(4,28) A32u zeros(4,40);zeros(4,32) A32u zeros(4,36);
    zeros(4,36) A32u zeros(4,32);zeros(4,40) A32u zeros(4,28);zeros(4,44) A32u zeros(4,24);
    zeros(4,48) A32u zeros(4,20);zeros(4,52) A32u zeros(4,16);zeros(4,56) A32u zeros(4,12);
    zeros(4,60) A32u zeros(4,8);zeros(4,64) A32u zeros(4,4);zeros(4,68) A32u];
A43S=[A43u zeros(4,68);zeros(4,4) A43u zeros(4,64);zeros(4,8) A43u zeros(4,60);
    zeros(4,12) A43u zeros(4,56);zeros(4,16) A43u zeros(4,52);zeros(4,20) A43u zeros(4,48);
    zeros(4,24) A43u zeros(4,44);zeros(4,28) A43u zeros(4,40);zeros(4,32) A43u zeros(4,36);
    zeros(4,36) A43u zeros(4,32);zeros(4,40) A43u zeros(4,28);zeros(4,44) A43u zeros(4,24);
    zeros(4,48) A43u zeros(4,20);zeros(4,52) A43u zeros(4,16);zeros(4,56) A43u zeros(4,12);
    zeros(4,60) A43u zeros(4,8);zeros(4,64) A43u zeros(4,4);zeros(4,68) A43u];
```

```
A54S=[A54u zeros(4,68);zeros(4,4) A54u zeros(4,64);zeros(4,8) A54u zeros(4,60);
    zeros(4,12) A54u zeros(4,56);zeros(4,16) A54u zeros(4,52);zeros(4,20) A54u zeros(4,48);
    zeros(4,24) A54u zeros(4,44);zeros(4,28) A54u zeros(4,40);zeros(4,32) A54u zeros(4,36);
    zeros(4,36) A54u zeros(4,32);zeros(4,40) A54u zeros(4,28);zeros(4,44) A54u zeros(4,24);
    zeros(4,48) A54u zeros(4,20);zeros(4,52) A54u zeros(4,16);zeros(4,56) A54u zeros(4,12);
    zeros(4,60) A54u zeros(4,8);zeros(4,64) A54u zeros(4,4);zeros(4,68) A54u];
ASu=[A1S zeros(72,216) A15S;A21S A2S zeros(72,216);zeros(72,72) A32S A3S zeros(72,144);zeros(72,144) A43S A4S
zeros(72,72);zeros(72,216) A54S A5S];

%matrix of the rates of the sensitivity model CSu
C1Su=[Cnu zeros(10,68)];
CSu=[C1Su zeros(10,288);zeros(10,72) C1Su zeros(10,216);zeros(10,144) C1Su zeros(10,144); zeros(10,216) C1Su
zeros(10,72);zeros(10,288) C1Su];

% Development of the matrix BSu of the sensitivity model
B1thetau=[B1u(2,2) 0 0 0;zeros(67,4)];B1Su=[B1u;B1thetau];BSu=[B1Su;zeros(288,4)];

% Development of the vector DSu of the sensitivity model
% Calculation of the first tank
D1Su=[zeros(1,4) rUSNH1f rUSNO1f rUSS1f rUSads1f rUSNH1YZH rUSNO1YZH rUSS1YZH rUSads1YZH rUSNH1YZA rUSNO1YZA rUSS1YZA rUSads1YZA
rUSNH1fZBH rUSNO1fZBH...
   rUSS1fZBH rUSads1fZBH rUSNH1muA rUSNO1muA rUSS1muA rUSads1muA rUSNH1muH rUSNO1muH rUSS1muH rUSads1muH rUSNH1Ks rUSNO1Ks rUSS1Ks
rUSads1Ks rUSNH1KOH...
   rUSNO1KOH rUSS1KOH rUSads1KOH rUSNH1KNO rUSNO1KNO rUSS1KNO rUSads1KNO rUSNH1KNA rUSNO1KNA rUSS1KNA rUSads1KNA rUSNH1KOA
rUSNO1KOA rUSS1KOA rUSads1KOA...
   rUSNH1etag rUSNO1etag rUSS1etag rUSads1etag rUSNH1KMP rUSNO1KMP rUSS1KMP rUSads1KMP rUSNH1KSP rUSNO1KSP rUSS1KSP rUSads1KSP
rUSNH1KSA rUSNO1KSA rUSS1KSA...
   rUSads1KSA rUSNH1fMA rUSNO1fMA rUSS1fMA rUSads1fMA rUSNH1KA rUSNO1KA rUSS1KA rUSads1KA]';
% Calculation of the second tank
D2Su=[zeros(1,4) rUSNH2f rUSNO2f rUSS2f rUSads2f rUSNH2YZH rUSNO2YZH rUSS2YZH rUSads2YZH rUSNH2YZA rUSNO2YZA rUSS2YZA rUSads2YZA
rUSNH2fZBH rUSNO2fZBH...
   rUSS2fZBH rUSads2fZBH rUSNH2muA rUSNO2muA rUSS2muA rUSads2muA rUSNH2muH rUSNO2muH rUSS2muH rUSads2muH rUSNH2Ks rUSNO2Ks rUSS2Ks
rUSads2Ks rUSNH2KOH...
   rUSNO2KOH rUSS2KOH rUSads2KOH rUSNH2KNO rUSNO2KNO rUSS2KNO rUSads2KNO rUSNH2KNA rUSNO2KNA rUSS2KNA rUSads2KNA rUSNH2KOA
rUSNO2KOA rUSS2KOA rUSads2KOA...
   rUSNH2etag rUSNO2etag rUSS2etag rUSads2etag rUSNH2KMP rUSNO2KMP rUSS2KMP rUSads2KMP rUSNH2KSP rUSNO2KSP rUSS2KSP rUSads2KSP
rUSNH2KSA rUSNO2KSA rUSS2KSA...
   rUSads2KSA rUSNH2fMA rUSNO2fMA rUSS2fMA rUSads2fMA rUSNH2KA rUSNO2KA rUSS2KA rUSads2KA]';
% Calculation of the third tank
D3Su=[zeros(1,4) rUSNH3f rUSNO3f rUSS3f rUSads3f rUSNH3YZH rUSNO3YZH rUSS3YZH rUSads3YZH rUSNH3YZA rUSNO3YZA rUSS3YZA rUSads3YZA
rUSNH3fZBH rUSNO3fZBH...
   rUSS3fZBH rUSads3fZBH rUSNH3muA rUSNO3muA rUSS3muA rUSads3muA rUSNH3muH rUSNO3muH rUSS3muH rUSads3muH rUSNH3Ks rUSNO3Ks rUSS3Ks
rUSads3Ks rUSNH3KOH...
   rUSNO3KOH rUSS3KOH rUSads3KOH rUSNH3KNO rUSNO3KNO rUSS3KNO rUSads3KNO rUSNH3KNA rUSNO3KNA rUSS3KNA rUSads3KNA rUSNH3KOA
rUSNO3KOA rUSS3KOA rUSads3KOA...
   rUSNH3etag rUSNO3etag rUSS3etag rUSads3etag rUSNH3KMP rUSNO3KMP rUSS3KMP rUSads3KMP rUSNH3KSP rUSNO3KSP rUSS3KSP rUSads3KSP
rUSNH3KSA rUSNO3KSA rUSS3KSA...
   rUSads3KSA rUSNH3fMA rUSNO3fMA rUSS3fMA rUSads3fMA rUSNH3KA rUSNO3KA rUSS3KA rUSads3KA]';
% Calculation of the fourth tank
D4Su=[zeros(1,4) rUSNH4f rUSNO4f rUSS4f rUSads4f rUSNH4YZH rUSNO4YZH rUSS4YZH rUSads4YZH rUSNH4YZA rUSNO4YZA rUSS4YZA rUSads4YZA
rUSNH4fZBH rUSNO4fZBH...
   rUSS4fZBH rUSads4fZBH rUSNH4muA rUSNO4muA rUSS4muA rUSads4muA rUSNH4muH rUSNO4muH rUSS4muH rUSads4muH rUSNH4Ks rUSNO4Ks rUSS4Ks
rUSads4Ks rUSNH4KOH...
   rUSNO4KOH rUSS4KOH rUSads4KOH rUSNH4KNO rUSNO4KNO rUSS4KNO rUSads4KNO rUSNH4KNA rUSNO4KNA rUSS4KNA rUSads4KNA rUSNH4KOA
rUSNO4KOA rUSS4KOA rUSads4KOA...
   rUSNH4etag rUSNO4etag rUSS4etag rUSads4etag rUSNH4KMP rUSNO4KMP rUSS4KMP rUSads4KMP rUSNH4KSP rUSNO4KSP rUSS4KSP rUSads4KSP
rUSNH4KSA rUSNO4KSA rUSS4KSA...
   rUSads4KSA rUSNH4fMA rUSNO4fMA rUSS4fMA rUSads4fMA rUSNH4KA rUSNO4KA rUSS4KA rUSads4KA]';
% Calculation of the fifth tank
D5Su=[zeros(1,4) rUSNH5f rUSNO5f rUSS5f rUSads5f rUSNH5YZH rUSNO5YZH rUSS5YZH rUSads5YZH rUSNH5YZA rUSNO5YZA rUSS5YZA rUSads5YZA
rUSNH5fZBH rUSNO5fZBH...
   rUSS5fZBH rUSads5fZBH rUSNH5muA rUSNO5muA rUSS5muA rUSads5muA rUSNH5muH rUSNO5muH rUSS5muH rUSads5muH rUSNH5Ks rUSNO5Ks rUSS5Ks
rUSads5Ks rUSNH5KOH...
   rUSNO5KOH rUSS5KOH rUSads5KOH rUSNH5KNO rUSNO5KNO rUSS5KNO rUSads5KNO rUSNH5KNA rUSNO5KNA rUSS5KNA rUSads5KNA rUSNH5KOA
rUSNO5KOA rUSS5KOA rUSads5KOA...
   rUSNH5etag rUSNO5etag rUSS5etag rUSads5etag rUSNH5KMP rUSNO5KMP rUSS5KMP rUSads5KMP rUSNH5KSP rUSNO5KSP rUSS5KSP rUSads5KSP
rUSNH5KSA rUSNO5KSA rUSS5KSA...
   rUSads5KSA rUSNH5fMA rUSNO5fMA rUSS5fMA rUSads5fMA rUSNH5KA rUSNO5KA rUSS5KA rUSads5KA]';
DSu=[D1Su;D2Su;D3Su;D4Su;D5Su];
```

SOFTWARE FOR SIMULATION OF SENSITIVITY FUNCTIONS OF THE PROCESS VARIABLES OF THE ATHLONE MASS BALANCE MODEL BASED ON THE REDUCED ASM1 BIOLOGICAL MODEL TOWARDS ITS PARAMETERS

1.Main program

```
%PROGRAM AASM1S.m
%Aim - the program calculates the sensitivity model and simulates the sensitivity functions for the process variables of the
Athlone process based on ASM1 reduced biological model towards the model parameters. The %program call the function subroutine
rateAASM1.m. The calculation uses %reduced biological model with 3 variables SNH, SNo and SS
%The program uses global definition of the model parameters

global Ks KOH KNO KNH KOA Kx muH etag muA Kh etah iXB YH YA
%Values of the model parameters
f=1.2;YA = 0.24;YH = 0.67;iXB = 0.08;muH = 0.4;Ks = 10;KOH = 0.2;KNO = 0.5;bH = 0.3;etag = 0.8;etah = 0.8;Kh = 3;Kx = 0.1;
muA = 0.5;KNH = 1;KOA = 0.4;
% Values of the process Flowrates
Qo = 40003;Qa = 39916.8;Qp = 39916.8;Qr = 40003;Qw = 3840.0;
% Volumes of the process tanks
V1=1148;V2=1148;V3=5273;
%Influent average concentrations
SSi=69.5;SNHi=31.56;SNOi=0.0;
%Definition of the sampling period
DT = 0.01042;days=0.1042*10;
```

```
K=days/DT
k=0:DT:days
%Average influent concentrations for SNH, SNO, SS
Xi  =0.01*[SNHi*ones(1,K);SNOi*ones(1,K);SSi*ones(1,K)]
%Initial conditions- steady state values for the Snh, Sno,Ss and zero for the sensitivity functions
XS0 =[3.2;5.28;3.808;zeros(45,1);1.344;7.662;2.459;zeros(45,1);0.548;6.541;1.15;zeros(45,1)];% initial conditions for the
differential equations
% Steady state values for the biomass XBH, XBA, XS
XBH = 0.01*[2551.76*ones(1,K);2553.38*ones(1,K);2557.13*ones(1,K)];% XBH steady state COD/m^3
XBA = 0.01*[37.389*ones(1,K);40.309*ones(1,K);40.941*ones(1,K)];% XBA steady state g all COD/m^3
XS = 0.01*[60.135*ones(1,K);55.386*ones(1,K);50.855*ones(1,K)]; % XS steady state all COD/m^3
%trajectory of the control signal
SO1 = [0.2*ones(1,K);0.2*ones(1,K)];SO2=[4.0*ones(1,K)];U=[SO1;SO2];
% calculation of the initial trajectory for the state vector X and for the sensitivity vector XSS
X =[[3.2;5.28;3.808;1.344;7.662;2.459;0.548;6.541;1.15] zeros(9,K)];% initial conditions for
XSS = [XS0 zeros(144,K)]; %Calculation of the process matrices
IV1 = DT/V1;IV2 = DT/V2;IV3 = DT/V3;IV=IV1*Qo;IVV=IV*f
B=[IVV 0.0 0.0;0.0 IV 0.0;0.0 0.0 IV;zeros(6,3)];
Q1=Qo+Qp;Q2=Q1+Qa+Qr;Q3=Q2;IV221=IV2*Q2;IV331=IV3*Q3
IV11=1-IV1*Q1 %element of A11
IV12=IV1*Qp    %element of A12
IV21=IV2*Q1     %element of A21
IV22=1-IV221   %element of A22
IV23=IV2*(Qa+Qr)  %element of A23
IV32=IV3*Q2  %element of A32
IV33=1-IV331   %element of A33

A=[[IV11 0.0 0.0;0.0 IV11 0.0;0.0 0.0 IV11] [IV12 0.0 0.0;0.0 IV12 0.0;0.0 0.0 IV12] zeros(3,3) ;[IV21 0.0 0.0;0.0 IV21 0.0;0.0
0.0 IV21] [IV22 0.0 0.0;0.0 IV22 0.0;0.0 0.0 IV22] [IV23 0.0 0.0;0.0 IV23 0.0;0.0 0.0 IV23];zeros(3,3) [IV32 0.0 0.0;0.0 IV32
0.0;0.0 0.0 IV32] [IV33 0.0 0.0;0.0 IV33 0.0;0.0 0.0 IV33]]
A11=A(1:3,1:3);A12=A(1:3,4:6);A13=zeros(3,3);A21=A(4:6,1:3);A22=A(4:6,4:6);A23=A(4:6,7:9);A31=zeros(3,3);A32=A(7:9,4:6);
A33=A(7:9,7:9);

B1=[IVV 0.0 0.0;0.0 IV 0.0;0.0 0.0 IV]
Cn=DT*[(-iXB) 0.0 (-1/YH);(-iXB) (-(1-YH))/(2.86*YH) -1/YH;-(iXB+1/YA) 1/YA 0.0;0.0 0.0 1.0];
C=[Cn zeros(4,6);zeros(4,3) Cn zeros(4,3);zeros(4,6) Cn]

for k = 1:K
    XSSk = XSS(:,k);
    Xk=X(:,k);
    Uk =U(:,k);
    XBHk = XBH(:,k);
    XBAk = XBA(:,k);
    XSk = XS(:,k);
    Xik = Xi(:,k);
   [ROASM1,AS,BS,CS,DS]=rateAASM1(Xk,Uk,XBHk,XBAk,XSk,DT,A11,A12,A21,A22,A23,A32,A33,B1,Cn);

    XSS(:,k+1) = AS*XSS(:,k) + CS'*ROASM1 + BS*Xi(:,k)+DS;
    X(:,k+1) = [XSS(1:3,k+1);XSS(49:51,k+1);XSS(97:99,k+1)];
end

%vector of sensitivity for the first tank variables SNH,SNO,SS
SNH1=XSS(1,:);SNO1=XSS(2,:);SS1=XSS(3,:);
SNH1f=XSS(4,:);SNO1f=XSS(5,:);SS1f=XSS(6,:);
SNH1YH=XSS(7,:);SNO1YH=XSS(8,:);SS1YH=XSS(9,:);
SNH1YA=XSS(10,:);SNO1YA=XSS(11,:);SS1YA=XSS(12,:);
SNH1iXB=XSS(13,:);SNO1iXB=XSS(14,:);SS1iXB=XSS(15,:);
SNH1muA=XSS(16,:);SNO1muA=XSS(17,:);SS1muA=XSS(18,:);
SNH1muH=XSS(19,:);SNO1muH=XSS(20,:);SS1muH=XSS(21,:);
SNH1KS=XSS(22,:);SNO1KS=XSS(23,:);SS1KS=XSS(24,:);
SNH1KOH=XSS(25,:);SNO1KOH=XSS(26,:);SS1KOH=XSS(27,:);
SNH1KNO=XSS(28,:);SNO1KNO=XSS(29,:);SS1KNO=XSS(30,:);
SNH1KNH=XSS(31,:);SNO1KNH=XSS(32,:);SS1KNH=XSS(33,:);
SNH1KOA=XSS(34,:);SNO1KOA=XSS(35,:);SS1KOA=XSS(36,:);
SNH1etag=XSS(37,:);SNO1etag=XSS(38,:);SS1etag=XSS(39,:);
SNH1etah=XSS(40,:);SNO1etah=XSS(41,:);SS1etah=XSS(42,:);
SNH1Kh=XSS(43,:);SNO1Kh=XSS(44,:);SS1Kh=XSS(45,:);
SNH1Kx=XSS(46,:);SNO1Kx=XSS(47,:);SS1Kx=XSS(48,:);

%vector of sensitivity for the second tank variables SNH,SNO,SS
SNH2=XSS(49,:);SNO2=XSS(50,:);SS2=XSS(51,:);
SNH2f=XSS(52,:);SNO2f=XSS(53,:);SS2f=XSS(54,:);
SNH2YH=XSS(55,:);SNO2YH=XSS(56,:);SS2YH=XSS(57,:);
SNH2YA=XSS(58,:);SNO2YA=XSS(59,:);SS2YA=XSS(60,:);
SNH2iXB=XSS(61,:);SNO2iXB=XSS(62,:);SS2iXB=XSS(63,:);
SNH2muA=XSS(64,:);SNO2muA=XSS(65,:);SS2muA=XSS(66,:);
SNH2muH=XSS(67,:);SNO2muH=XSS(68,:);SS2muH=XSS(69,:);
SNH2KS=XSS(70,:);SNO2KS=XSS(71,:);SS2KS=XSS(72,:);
SNH2KOH=XSS(73,:);SNO2KOH=XSS(74,:);SS2KOH=XSS(75,:);
SNH2KNO=XSS(76,:);SNO2KNO=XSS(77,:);SS2KNO=XSS(78,:);
SNH2KNH=XSS(79,:);SNO2KNH=XSS(80,:);SS2KNH=XSS(81,:);
SNH2KOA=XSS(82,:);SNO2KOA=XSS(83,:);SS2KOA=XSS(84,:);
SNH2etag=XSS(85,:);SNO2etag=XSS(86,:);SS2etag=XSS(87,:);
SNH2etah=XSS(88,:);SNO2etah=XSS(89,:);SS2etah=XSS(90,:);
SNH2Kh=XSS(91,:);SNO2Kh=XSS(92,:);SS2Kh=XSS(93,:);
SNH2Kx=XSS(94,:);SNO2Kx=XSS(95,:);SS2Kx=XSS(96,:);

%vector of sensitivity for the third tank variables SNH3, SNO, SS
SNH3=XSS(97,:);SNO3=XSS(98,:);SS3=XSS(99,:);
SNH3f=XSS(100,:);SNO3f=XSS(101,:);SS3f=XSS(102,:);
SNH3YH=XSS(103,:);SNO3YH=XSS(104,:);SS3YH=XSS(105,:);
SNH3YA=XSS(106,:);SNO3YA=XSS(107,:);SS3YA=XSS(108,:);
SNH3iXB=XSS(109,:);SNO3iXB=XSS(110,:);SS3iXB=XSS(111,:);
SNH3muA=XSS(112,:);SNO3muA=XSS(113,:);SS3muA=XSS(114,:);
SNH3muH=XSS(115,:);SNO3muH=XSS(116,:);SS3muH=XSS(117,:);
SNH3KS=XSS(118,:);SNO3KS=XSS(119,:);SS3KS=XSS(120,:);
SNH3KOH=XSS(121,:);SNO3KOH=XSS(122,:);SS3KOH=XSS(123,:);
SNH3KNO=XSS(124,:);SNO3KNO=XSS(125,:);SS3KNO=XSS(126,:);
SNH3KNH=XSS(127,:);SNO3KNH=XSS(128,:);SS3KNH=XSS(129,:);
```

```
SNH3KOA=XSS(130,:);SNO3KOA=XSS(131,:);SS3KOA=XSS(132,:);
SNH3etag=XSS(133,:);SNO3etag=XSS(134,:);SS3etag=XSS(135,:);
SNH3etah=XSS(136,:);SNO3etah=XSS(137,:);SS3etah=XSS(138,:);
SNH3Kh=XSS(139,:);SNO3Kh=XSS(140,:);SS3Kh=XSS(141,:);
SNH3Kx=XSS(142,:);SNO3Kx=XSS(143,:);SS3Kx=XSS(144,:);


k=1:101
%Graphs of the sensitivity functions for the SNH
%Graphs of the sensitivity of the variable SNH in the tank 1
figure(1)
subplot(8,2,1);plot(k,SNH1,'k')
title('Process variable Snh1')
ylabel('\fontsize{8}SNH1')
xlabel('\fontsize{8}discrete time k')

subplot(8,2,2); plot(k,SNH1f,'k')
title('Sensitivity function Snh1f')
ylabel('\fontsize{8}SNH1f')
xlabel('\fontsize{8}discrete time,k')

subplot(8,2,3); plot(k,SNH1YH,'k')
title('Variable Snh1YH')
ylabel('\fontsize{8}SNH1YH')
xlabel('\fontsize{8}discrete time,k')

subplot(8,2,4); plot(k,SNH1YA,'k')
title('Variable Snh1YA')
ylabel('\fontsize{8}SNH1YA')
xlabel('\fontsize{8}discrete time,k')

subplot(8,2,5); plot(k,SNH1iXB,'k')
title('Sensitivity function Snh1iXB')
ylabel('\fontsize{8}SNH1iXB')
xlabel('discrete time,k')

subplot(8,2,6); plot(k,SNH1muA,'k')
title('Sensitivity function Snh1muA')
ylabel('\fontsize{8}SNH1muA')
xlabel('\fontsize{8}discrete time,k')

subplot(8,2,7); plot(k,SNH1muH,'k')
title('Sensitivity function Snh1muH')
ylabel('\fontsize{8}SNH1muH')
xlabel('discrete time,k')

subplot(8,2,8); plot(k,SNH1KS,'k')
title('Sensitivity function Snh1KS')
ylabel('\fontsize{8}SNH1KS')
xlabel('discrete time,k')

subplot(8,2,9); plot(k,SNH1KOH,'k')
title('Sensitivity function Snh1KOH')
ylabel('\fontsize{8}SNH1KOH')
xlabel('\fontsize{8}discrete time,k')

subplot(8,2,10); plot(k,SNH1KNO,'k')
title('Sensitivity function Snh1KNO')
ylabel('\fontsize{8}SNH1KNO')
xlabel('\fontsize{8}discrete time,k')

subplot(8,2,11); plot(k,SNH1KNH,'k')
title('Sensitivity function Snh1KNH')
ylabel('\fontsize{8}SNH1KNH')
xlabel('\fontsize{8}discrete time,k')

subplot(8,2,12); plot(k,SNH1KOA,'k')
title('Sensitivity function Snh1KOA')
ylabel('\fontsize{8}SNH1KOA')
xlabel('\fontsize{8}discrete time,k')

subplot(8,2,13); plot(k,SNH1etag,'k')
title('Sensitivity function Snh1etag')
ylabel('\fontsize{8}SNH1etag')
xlabel('\fontsize{8}discrete time,k')

subplot(8,2,14); plot(k,SNH1etag,'k')
title('Sensitivity function Snh1etah')
ylabel('\fontsize{8}SNH1etah')
xlabel('\fontsize{8}discrete time,k')

subplot(8,2,15); plot(k,SNH1Kh,'k')
title('Sensitivity function Snh1Kh')
ylabel('\fontsize{8}SNH1Kh')
xlabel('\fontsize{8}discrete time,k')

subplot(8,2,16); plot(k,SNH1Kx,'k')
title('Sensitivity function Snh1Kx')
ylabel('\fontsize{8}SNH1Kx')
xlabel('\fontsize{8}discrete time,k')

%Graphs of sensitivity of the variable SNH2 in the tank 2
figure(2)
subplot(8,2,1);plot(k,SNH2,'k')
title('Process variable Snh2')
ylabel('\fontsize{8}SNH2')
xlabel('\fontsize{8}discrete time k')

subplot(8,2,2); plot(k,SNH2f,'k')
title('Sensitivity function Snh2f')
ylabel('\fontsize{8}SNH2f')
xlabel('\fontsize{8}discrete time,k')

subplot(8,2,3); plot(k,SNH2YH,'k')
title('Variable Snh2YH')
ylabel('\fontsize{8}SNH2YH')
xlabel('\fontsize{8}discrete time,k')

subplot(8,2,4); plot(k,SNH2YA,'k')
title('Variable Snh2YA')
ylabel('\fontsize{8}SNH2YA')
xlabel('\fontsize{8}discrete time,k')

subplot(8,2,5); plot(k,SNH2iXB,'k')
title('Sensitivity function Snh1iXB')
ylabel('\fontsize{8}SNH2iXB')
xlabel('discrete time,k')

subplot(8,2,6); plot(k,SNH2muA,'k')
title('Sensitivity function Snh2muA')
ylabel('\fontsize{8}SNH2muA')
xlabel('\fontsize{8}discrete time,k')

subplot(8,2,7); plot(k,SNH2muH,'k')
title('Sensitivity function Snh2muH')
ylabel('\fontsize{8}SNH2muH')
xlabel('discrete time,k')

subplot(8,2,8); plot(k,SNH2KS,'k')
title('Sensitivity function Snh2KS')
ylabel('\fontsize{8}SNH2KS')
xlabel('discrete time,k')

subplot(8,2,9); plot(k,SNH2KOH,'k')
title('Sensitivity function Snh2KOH')
ylabel('\fontsize{8}SNH2KOH')
xlabel('\fontsize{8}discrete time,k')

subplot(8,2,10); plot(k,SNH2KNO,'k')
title('Sensitivity function Snh2KNO')
ylabel('\fontsize{8}SNH2KNO')
xlabel('\fontsize{8}discrete time,k')

subplot(8,2,11); plot(k,SNH2KNH,'k')
title('Sensitivity function Snh2KNH')
ylabel('\fontsize{8}SNH2KNH')
xlabel('\fontsize{8}discrete time,k')

subplot(8,2,12); plot(k,SNH2KOA,'k')
title('Sensitivity function Snh2KOA')
ylabel('\fontsize{8}SNH2KOA')
xlabel('\fontsize{8}discrete time,k')

subplot(8,2,13); plot(k,SNH2etag,'k')
title('Sensitivity function Snh2etag')
ylabel('\fontsize{8}SNH2etag')
xlabel('\fontsize{8}discrete time,k')

subplot(8,2,14); plot(k,SNH2etah,'k')
title('Sensitivity function Snh2etah')
ylabel('\fontsize{8}SNH2etah')
xlabel('\fontsize{8}discrete time,k')

subplot(8,2,15); plot(k,SNH2Kh,'k')
title('Sensitivity function Snh2Kh')
ylabel('\fontsize{8}SNH2Kh')
xlabel('\fontsize{8}discrete time,k')

subplot(8,2,16); plot(k,SNH2Kx,'k')
title('Sensitivity function Snh2Kx')
ylabel('\fontsize{8}SNH2Kx')
xlabel('\fontsize{8}discrete time,k')

%Graphs of sensitivity of the variables SNH  in the tank 3

figure(3)
subplot(8,2,1);plot(k,SNH3,'k')
title('Process variable Snh3')
ylabel('\fontsize{8}SNH3')
xlabel('\fontsize{8}discrete time k')

subplot(8,2,2); plot(k,SNH3f,'k')
title('Sensitivity function Snh3f')
ylabel('\fontsize{8}SNH3f')
xlabel('\fontsize{8}discrete time,k')

subplot(8,2,3); plot(k,SNH3YH,'k')
title('Variable Snh3YH')
ylabel('\fontsize{8}SNH3YH')
xlabel('\fontsize{8}discrete time,k')
```

```
subplot(8,2,4); plot(k,SNH3YA,'k')
title('Variable Snh3YA')
ylabel('\fontsize{8}SNH3YA')
xlabel('\fontsize{8}discrete time,k')

subplot(8,2,5); plot(k,SNH3iXB,'k')
title('Sensitivity function Snh3iXB')
ylabel('\fontsize{8}SNH3iXB')
xlabel('discrete time,k')

subplot(8,2,6); plot(k,SNH3muA,'k')
title('Sensitivity function Snh3muA')
ylabel('\fontsize{8}SNH3muA')
xlabel('\fontsize{8}discrete time,k')

subplot(8,2,7); plot(k,SNH3muH,'k')
title('Sensitivity function Snh3muH')
ylabel('\fontsize{8}SNH3muH')
xlabel('discrete time,k')

subplot(8,2,8); plot(k,SNH3KS,'k')
title('Sensitivity function Snh3KS')
ylabel('\fontsize{8}SNH3KS')
xlabel('discrete time,k')

subplot(8,2,9); plot(k,SNH3KOH,'k')
title('Sensitivity function Snh3KOH')
ylabel('\fontsize{8}SNH3KOH')
xlabel('\fontsize{8}discrete time,k')

subplot(8,2,10); plot(k,SNH3KNO,'k')
title('Sensitivity function Snh3KNO')
ylabel('\fontsize{8}SNH3KNO')
xlabel('\fontsize{8}discrete time,k')

subplot(8,2,11); plot(k,SNH3KNH,'k')
title('Sensitivity function Snh3KNH')
ylabel('\fontsize{8}SNH3KNH')
xlabel('\fontsize{8}discrete time,k')

subplot(8,2,12); plot(k,SNH3KOA,'k')
title('Sensitivity function Snh3KOA')
ylabel('\fontsize{8}SNH3KOA')
xlabel('\fontsize{8}discrete time,k')

subplot(8,2,13); plot(k,SNH3etag,'k')
title('Sensitivity function Snh3etag')
ylabel('\fontsize{8}SNH3etag')
xlabel('\fontsize{8}discrete time,k')

subplot(8,2,14); plot(k,SNH3etah,'k')
title('Sensitivity function Snh3etah')
ylabel('\fontsize{8}SNH3etah')
xlabel('\fontsize{8}discrete time,k')

subplot(8,2,15); plot(k,SNH3Kh,'k')
title('Sensitivity function Snh3Kh')
ylabel('\fontsize{8}SNH3Kh')
xlabel('\fontsize{8}discrete time,k')

subplot(8,2,16); plot(k,SNH3Kx,'k')
title('Sensitivity function Snh3Kx')
ylabel('\fontsize{8}SNH3Kx')
xlabel('\fontsize{8}discrete time,k')

%Graphs of the sensitivity functions for the SNO
%Graphs of the sensitivity functions of the cariable SNO in
the tank 1
figure(4)
subplot(8,2,1);plot(k,SNO1,'k')
title('Process variable SNO1')
ylabel('\fontsize{8}SNO1')
xlabel('\fontsize{8}discrete time k')

subplot(8,2,2); plot(k,SNO1f,'k')
title('Sensitivity function SNO1f')
ylabel('\fontsize{8}SNO1f')
xlabel('\fontsize{8}discrete time,k')

subplot(8,2,3); plot(k,SNO1YH,'k')
title('Variable SNO1YH')
ylabel('\fontsize{8}SNO1YH')
xlabel('\fontsize{8}discrete time,k')

subplot(8,2,4); plot(k,SNO1YA,'k')
title('Variable SNO1YA')
ylabel('\fontsize{8}SNO1YA')
xlabel('\fontsize{8}discrete time,k')

subplot(8,2,5); plot(k,SNO1iXB,'k')
title('Sensitivity function SNO1iXB')
ylabel('\fontsize{8}SNO1iXB')
xlabel('discrete time,k')

subplot(8,2,6); plot(k,SNO1muA,'k')
title('Sensitivity function SNO1muA')
ylabel('\fontsize{8}SNO1muA')
xlabel('\fontsize{8}discrete time,k')

subplot(8,2,7); plot(k,SNO1muH,'k')
title('Sensitivity function SNO1muH')
ylabel('\fontsize{8}SNO1muH')
xlabel('discrete time,k')

subplot(8,2,8); plot(k,SNO1KS,'k')
title('Sensitivity function SNO1KS')
ylabel('\fontsize{8}SNO1KS')
xlabel('discrete time,k')

subplot(8,2,9); plot(k,SNO1KOH,'k')
title('Sensitivity function SNO1KOH')
ylabel('\fontsize{8}SNO1KOH')
xlabel('\fontsize{8}discrete time,k')

subplot(8,2,10); plot(k,SNO1KNO,'k')
title('Sensitivity function SNO1KNO')
ylabel('\fontsize{8}SNO1KNO')
xlabel('\fontsize{8}discrete time,k')

subplot(8,2,11); plot(k,SNO1KNH,'k')
title('Sensitivity function SNO1KNH')
ylabel('\fontsize{8}SNO1KNH')
xlabel('\fontsize{8}discrete time,k')

subplot(8,2,12); plot(k,SNO1KOA,'k')
title('Sensitivity function SNO1KOA')
ylabel('\fontsize{8}SNO1KOA')
xlabel('\fontsize{8}discrete time,k')

subplot(8,2,13); plot(k,SNO1etag,'k')
title('Sensitivity function SNO1etag')
ylabel('\fontsize{8}SNO1etag')
xlabel('\fontsize{8}discrete time,k')

subplot(8,2,14); plot(k,SNO1etag,'k')
title('Sensitivity function SNO1etah')
ylabel('\fontsize{8}SNO1etah')
xlabel('\fontsize{8}discrete time,k')

subplot(8,2,15); plot(k,SNO1Kh,'k')
title('Sensitivity function SNO1Kh')
ylabel('\fontsize{8}SNO1Kh')
xlabel('\fontsize{8}discrete time,k')

subplot(8,2,16); plot(k,SNO1Kx,'k')
title('Sensitivity function SNO1Kx')
ylabel('\fontsize{8}SNO1Kx')
xlabel('\fontsize{8}discrete time,k')

%Graphs of the sensitivity functions for the variable SNO in
the tank 2
figure(5)
subplot(8,2,1);plot(k,SNO2,'k')
title('Process variable SNO2')
ylabel('\fontsize{8}SNO2')
xlabel('\fontsize{8}discrete time k')

subplot(8,2,2); plot(k,SNO2f,'k')
title('Sensitivity function SNO2f')
ylabel('\fontsize{8}SNO2f')
xlabel('\fontsize{8}discrete time,k')

subplot(8,2,3); plot(k,SNO2YH,'k')
title('Variable SNO2YH')
ylabel('\fontsize{8}SNO2YH')
xlabel('\fontsize{8}discrete time,k')

subplot(8,2,4); plot(k,SNO2YA,'k')
title('Variable SNO2YA')
ylabel('\fontsize{8}SNO2YA')
xlabel('\fontsize{8}discrete time,k')

subplot(8,2,5); plot(k,SNO2iXB,'k')
title('Sensitivity function SNO1iXB')
ylabel('\fontsize{8}SNO2iXB')
xlabel('discrete time,k')

subplot(8,2,6); plot(k,SNO2muA,'k')
title('Sensitivity function SNO2muA')
ylabel('\fontsize{8}SNO2muA')
xlabel('\fontsize{8}discrete time,k')

subplot(8,2,7); plot(k,SNO2muH,'k')
title('Sensitivity function SNO2muH')
ylabel('\fontsize{8}SNO2muH')
xlabel('discrete time,k')

subplot(8,2,8); plot(k,SNO2KS,'k')
title('Sensitivity function SNO2KS')
ylabel('\fontsize{8}SNO2KS')
xlabel('discrete time,k')

subplot(8,2,9); plot(k,SNO2KOH,'k')
title('Sensitivity function SNO2KOH')
ylabel('\fontsize{8}SNOKOH')
xlabel('\fontsize{8}discrete time,k')

subplot(8,2,10); plot(k,SNO2KNO,'k')
```

```
title('Sensitivity function SNO2KNO')
ylabel('\fontsize{8}SNO2KNO')
xlabel('\fontsize{8}discrete time,k')

subplot(8,2,11); plot(k,SNO2KNH,'k')
title('Sensitivity function SNO2KNH')
ylabel('\fontsize{8}SNO2KNH')
xlabel('\fontsize{8}discrete time,k')

subplot(8,2,12); plot(k,SNO2KOA,'k')
title('Sensitivity function SNO2KOA')
ylabel('\fontsize{8}SNO2KOA')
xlabel('\fontsize{8}discrete time,k')

subplot(8,2,13); plot(k,SNO2etag,'k')
title('Sensitivity function SNO2etag')
ylabel('\fontsize{8}SNO2etag')
xlabel('\fontsize{8}discrete time,k')

subplot(8,2,14); plot(k,SNO2etah,'k')
title('Sensitivity function SNO2etah')
ylabel('\fontsize{8}SNO2etah')
xlabel('\fontsize{8}discrete time,k')

subplot(8,2,15); plot(k,SNO2Kh,'k')
title('Sensitivity function SNO2Kh')
ylabel('\fontsize{8}SNO2Kh')
xlabel('\fontsize{8}discrete time,k')

subplot(8,2,16); plot(k,SNO2Kx,'k')
title('Sensitivity function SNO2Kx')
ylabel('\fontsize{8}SNO2Kx')
xlabel('\fontsize{8}discrete time,k')

%Graphs for the variable SNO  in the  tank 3

figure(6)
subplot(8,2,1);plot(k,SNO3,'k')
title('Process variable SNO3')
ylabel('\fontsize{8}SNO3')
xlabel('\fontsize{8}discrete time k')

subplot(8,2,2); plot(k,SNO3f,'k')
title('Sensitivity function SNO3f')
ylabel('\fontsize{8}SNO3f')
xlabel('\fontsize{8}discrete time,k')

subplot(8,2,3); plot(k,SNO3YH,'k')
title('Variable SNO3YH')
ylabel('\fontsize{8}SNO3YH')
xlabel('\fontsize{8}discrete time,k')

subplot(8,2,4); plot(k,SNO3YA,'k')
title('Variable SNO3YA')
ylabel('\fontsize{8}SNO3YA')
xlabel('\fontsize{8}discrete time,k')

subplot(8,2,5); plot(k,SNO3iXB,'k')
title('Sensitivity function SNO3iXB')
ylabel('\fontsize{8}SNO3iXB')
xlabel('discrete time,k')

subplot(8,2,6); plot(k,SNO3muA,'k')
title('Sensitivity function SNO3muA')
ylabel('\fontsize{8}SNO3muA')
xlabel('\fontsize{8}discrete time,k')

subplot(8,2,7); plot(k,SNO3muH,'k')
title('Sensitivity function SNO3muH')
ylabel('\fontsize{8}SNO3muH')
xlabel('discrete time,k')

subplot(8,2,8); plot(k,SNO3KS,'k')
title('Sensitivity function SNO3KS')
ylabel('\fontsize{8}SNO3KS')
xlabel('discrete time,k')

subplot(8,2,9); plot(k,SNO3KOH,'k')
title('Sensitivity function SNO3KOH')
ylabel('\fontsize{8}SNO3KOH')
xlabel('\fontsize{8}discrete time,k')

subplot(8,2,10); plot(k,SNO3KNO,'k')
title('Sensitivity function SNO3KNO')
ylabel('\fontsize{8}SNO3KNO')
xlabel('\fontsize{8}discrete time,k')

subplot(8,2,11); plot(k,SNO3KNH,'k')
title('Sensitivity function SNO3KNH')
ylabel('\fontsize{8}SNO3KNH')
xlabel('\fontsize{8}discrete time,k')

subplot(8,2,12); plot(k,SNO3KOA,'k')
title('Sensitivity function SNO3KOA')
ylabel('\fontsize{8}SNO3KOA')
xlabel('\fontsize{8}discrete time,k')

subplot(8,2,13); plot(k,SNO3etag,'k')
title('Sensitivity function SNO3etag')
ylabel('\fontsize{8}SNO3etag')
xlabel('\fontsize{8}discrete time,k')

subplot(8,2,14); plot(k,SNO3etah,'k')
title('Sensitivity function SNO3etah')
ylabel('\fontsize{8}SNO3etah')
xlabel('\fontsize{8}discrete time,k')

subplot(8,2,15); plot(k,SNO3Kh,'k')
title('Sensitivity function SNO3Kh')
ylabel('\fontsize{8}SNO3Kh')
xlabel('\fontsize{8}discrete time,k')

subplot(8,2,16); plot(k,SNO3Kx,'k')
title('Sensitivity function SNO3Kx')
ylabel('\fontsize{8}SNO3Kx')
xlabel('\fontsize{8}discrete time,k')


%Graphs of the sensitivity unctions for the SS

%Graphs of the sensitivity functions for the SS in the tank
1
figure(7)
subplot(8,2,1);plot(k,SS1,'k')
title('Process variable SS1')
ylabel('\fontsize{8}SS1')
xlabel('\fontsize{8}discrete time k')

subplot(8,2,2); plot(k,SS1f,'k')
title('Sensitivity function SS1f')
ylabel('\fontsize{8}SS1f')
xlabel('\fontsize{8}discrete time,k')

subplot(8,2,3); plot(k,SS1YH,'k')
title('Variable SS1YH')
ylabel('\fontsize{8}SS1YH')
xlabel('\fontsize{8}discrete time,k')

subplot(8,2,4); plot(k,SS1YA,'k')
title('Variable SS1YA')
ylabel('\fontsize{8}SS1YA')
xlabel('\fontsize{8}discrete time,k')

subplot(8,2,5); plot(k,SS1iXB,'k')
title('Sensitivity function SS1iXB')
ylabel('\fontsize{8}SS1iXB')
xlabel('discrete time,k')

subplot(8,2,6); plot(k,SS1muA,'k')
title('Sensitivity function SS1muA')
ylabel('\fontsize{8}SS1muA')
xlabel('\fontsize{8}discrete time,k')

subplot(8,2,7); plot(k,SS1muH,'k')
title('Sensitivity function SS1muH')
ylabel('\fontsize{8}SS1muH')
xlabel('discrete time,k')

subplot(8,2,8); plot(k,SS1KS,'k')
title('Sensitivity function SS1KS')
ylabel('\fontsize{8}SS1KS')
xlabel('discrete time,k')

subplot(8,2,9); plot(k,SS1KOH,'k')
title('Sensitivity function SS1KOH')
ylabel('\fontsize{8}SS1KOH')
xlabel('\fontsize{8}discrete time,k')

subplot(8,2,10); plot(k,SS1KNO,'k')
title('Sensitivity function SS1KNO')
ylabel('\fontsize{8}SS1KNO')
xlabel('\fontsize{8}discrete time,k')

subplot(8,2,11); plot(k,SS1KNH,'k')
title('Sensitivity function SS1KNH')
ylabel('\fontsize{8}SS1KNH')
xlabel('\fontsize{8}discrete time,k')

subplot(8,2,12); plot(k,SS1KOA,'k')
title('Sensitivity function SS1KOA')
ylabel('\fontsize{8}SS1KOA')
xlabel('\fontsize{8}discrete time,k')

subplot(8,2,13); plot(k,SS1etag,'k')
title('Sensitivity function SS1etag')
ylabel('\fontsize{8}SS1etag')
xlabel('\fontsize{8}discrete time,k')

subplot(8,2,14); plot(k,SS1etag,'k')
title('Sensitivity function SS1etah')
ylabel('\fontsize{8}SS1etah')
xlabel('\fontsize{8}discrete time,k')

subplot(8,2,15); plot(k,SS1Kh,'k')
title('Sensitivity function SS1Kh')
ylabel('\fontsize{8}SS1Kh')
xlabel('\fontsize{8}discrete time,k')
```

```
subplot(8,2,16); plot(k,SS1Kx,'k')
title('Sensitivity function SS1Kx')
ylabel('\fontsize{8}SS1Kx')
xlabel('\fontsize{8}discrete time,k')

%Graphs of the sensitivity functions of the varible SS in
the tank 2
figure(8)
subplot(8,2,1);plot(k,SS2,'k')
title('Process variable SS2')
ylabel('\fontsize{8}SS2')
xlabel('\fontsize{8}discrete time k')

subplot(8,2,2); plot(k,SS2f,'k')
title('Sensitivity function SS2f')
ylabel('\fontsize{8}SS2f')
xlabel('\fontsize{8}discrete time,k')

subplot(8,2,3); plot(k,SS2YH,'k')
title('Variable SS2YH')
ylabel('\fontsize{8}SS2YH')
xlabel('\fontsize{8}discrete time,k')

subplot(8,2,4); plot(k,SS2YA,'k')
title('Variable SS2YA')
ylabel('\fontsize{8}SS2YA')
xlabel('\fontsize{8}discrete time,k')

subplot(8,2,5); plot(k,SS2iXB,'k')
title('Sensitivity function SS1iXB')
ylabel('\fontsize{8}SS2iXB')
xlabel('discrete time,k')

subplot(8,2,6); plot(k,SS2muA,'k')
title('Sensitivity function SS2muA')
ylabel('\fontsize{8}SS2muA')
xlabel('\fontsize{8}discrete time,k')

subplot(8,2,7); plot(k,SS2muH,'k')
title('Sensitivity function SS2muH')
ylabel('\fontsize{8}SS2muH')
xlabel('discrete time,k')

subplot(8,2,8); plot(k,SS2KS,'k')
title('Sensitivity function SS2KS')
ylabel('\fontsize{8}SS2KS')
xlabel('discrete time,k')

subplot(8,2,9); plot(k,SS2KOH,'k')
title('Sensitivity function SS2KOH')
ylabel('\fontsize{8}SS2KOH')
xlabel('\fontsize{8}discrete time,k')

subplot(8,2,10); plot(k,SS2KNO,'k')
title('Sensitivity function SS2KNO')
ylabel('\fontsize{8}SS2KNO')
xlabel('\fontsize{8}discrete time,k')

subplot(8,2,11); plot(k,SS2KNH,'k')
title('Sensitivity function SS2KNH')
ylabel('\fontsize{8}SS2KNH')
xlabel('\fontsize{8}discrete time,k')

subplot(8,2,12); plot(k,SS2KOA,'k')
title('Sensitivity function SS2KOA')
ylabel('\fontsize{8}SS2KOA')
xlabel('\fontsize{8}discrete time,k')

subplot(8,2,13); plot(k,SS2etag,'k')
title('Sensitivity function SS2etag')
ylabel('\fontsize{8}SS2etag')
xlabel('\fontsize{8}discrete time,k')

subplot(8,2,14); plot(k,SS2etah,'k')
title('Sensitivity function SS2etah')
ylabel('\fontsize{8}SS2etah')
xlabel('\fontsize{8}discrete time,k')

subplot(8,2,15); plot(k,SS2Kh,'k')
title('Sensitivity function SS2Kh')
ylabel('\fontsize{8}SS2Kh')
xlabel('\fontsize{8}discrete time,k')

subplot(8,2,16); plot(k,SS2Kx,'k')
title('Sensitivity function SS2Kx')
ylabel('\fontsize{8}SS2Kx')
xlabel('\fontsize{8}discrete time,k')

%Graphs for SS variable in the tank 3

figure(9)
subplot(8,2,1);plot(k,SS3,'k')
title('Process variable SS3')
ylabel('\fontsize{8}SS3')
xlabel('\fontsize{8}discrete time k')

subplot(8,2,2); plot(k,SS3f,'k')
title('Sensitivity function SS3f')
ylabel('\fontsize{8}SS3f')
xlabel('\fontsize{8}discrete time,k')

subplot(8,2,3); plot(k,SS3YH,'k')
title('Variable SS3YH')
ylabel('\fontsize{8}SS3YH')
xlabel('\fontsize{8}discrete time,k')

subplot(8,2,4); plot(k,SS3YA,'k')
title('Variable SS3YA')
ylabel('\fontsize{8}SS3YA')
xlabel('\fontsize{8}discrete time,k')

subplot(8,2,5); plot(k,SS3iXB,'k')
title('Sensitivity function SS3iXB')
ylabel('\fontsize{8}SS3iXB')
xlabel('discrete time,k')

subplot(8,2,6); plot(k,SS3muA,'k')
title('Sensitivity function SS3muA')
ylabel('\fontsize{8}SS3muA')
xlabel('\fontsize{8}discrete time,k')

subplot(8,2,7); plot(k,SS3muH,'k')
title('Sensitivity function SS3muH')
ylabel('\fontsize{8}SS3muH')
xlabel('discrete time,k')

subplot(8,2,8); plot(k,SS3KS,'k')
title('Sensitivity function SS3KS')
ylabel('\fontsize{8}SS3KS')
xlabel('discrete time,k')

subplot(8,2,9); plot(k,SS3KOH,'k')
title('Sensitivity function SS3KOH')
ylabel('\fontsize{8}SS3KOH')
xlabel('\fontsize{8}discrete time,k')

subplot(8,2,10); plot(k,SS3KNO,'k')
title('Sensitivity function SS3KNO')
ylabel('\fontsize{8}SS3KNO')
xlabel('\fontsize{8}discrete time,k')

subplot(8,2,11); plot(k,SS3KNH,'k')
title('Sensitivity function SS3KNH')
ylabel('\fontsize{8}SS3KNH')
xlabel('\fontsize{8}discrete time,k')

subplot(8,2,12); plot(k,SS3KOA,'k')
title('Sensitivity function SS3KOA')
ylabel('\fontsize{8}SS3KOA')
xlabel('\fontsize{8}discrete time,k')

subplot(8,2,13); plot(k,SS3etag,'k')
title('Sensitivity function SS3etag')
ylabel('\fontsize{8}SS3etag')
xlabel('\fontsize{8}discrete time,k')

subplot(8,2,14); plot(k,SS3etah,'k')
title('Sensitivity function SS3etah')
ylabel('\fontsize{8}SS3etah')
xlabel('\fontsize{8}discrete time,k')

subplot(8,2,15); plot(k,SS3Kh,'k')
title('Sensitivity function SS3Kh')
ylabel('\fontsize{8}SS3Kh')
xlabel('\fontsize{8}discrete time,k')

subplot(8,2,16); plot(k,SS3Kx,'k')
title('Sensitivity function SS3Kx')
ylabel('\fontsize{8}SS3Kx')
xlabel('\fontsize{8}discrete time,k')
```

2.Subprogram

```
%SUBPROGRAM rateAASM1.m
AIM:The program function rateAASM1.m calculates the process rates, derivatives of the proces rates towards the model parameters
and variables and forms the sensitivity model matrices necessary for simulation of theprocess variables and the sensitivity
functions for the Athlone process based on the reduced ASM1 biological model.
%The program uses global definition of the model parameters

function [ROASM1,AS,BS,CS,DS]=rateAASM1(Xk,Uk,XBHk,XBAk,XSk,DT,A11,A12,A21,A22,A23,A32,A33,B1,Cn)
%Calculation of the process rates at every moment of the time

global Ks KOH KNO KNH KOA Kx muH etag muA Kh etah iXB YH YA
```

```
%Calculation of the process rates for every tank
ROASM1(1)=muH*(Xk(3)/(Ks+Xk(3)))*(Uk(1)/(KOH+Uk(1)))*XBHk(1);
ROASM1(2)=muH*(Xk(3)/(Ks+Xk(3)))*(KOH/(KOH+Uk(1)))*(Xk(2)/(KNO+Xk(2)))*etag*XBHk(1);
ROASM1(3)=muA*(Xk(1)/(KNH+Xk(1)))*(Uk(1)/(KOA+Uk(1)))*XBAk(1);
x1=XSk(1)/XBHk(1);
ROASM1(4)=Kh*XBHk(1)*(x1/(Kx+x1))*((Uk(1)/(KOH+Uk(1)))+etah*(KOH/(KOH+Uk(1)))*(Xk(2)/(KNO+Xk(2))));

ROASM1(5)=muH*(Xk(6)/(Ks+Xk(6)))*(Uk(2)/(KOH+Uk(2)))*XBHk(2);
ROASM1(6)=muH*(Xk(6)/(Ks+Xk(6)))*(KOH/(KOH+Uk(2)))*(Xk(5)/(KNO+Xk(5)))*etag*XBHk(2);
ROASM1(7)=muA*(Xk(4)/(KNH+Xk(4)))*(Uk(2)/(KOA+Uk(2)))*XBAk(2);
x1=XSk(2)/XBHk(2);
ROASM1(8)=Kh*XBHk(2)*(x1/(Kx+x1))*((Uk(2)/(KOH+Uk(2)))+etah*(KOH/(KOH+Uk(2)))*(Xk(5)/(KNO+Xk(5))));

ROASM1(9)=muH*(Xk(9)/(Ks+Xk(9)))*(Uk(3)/(KOH+Uk(3)))*XBHk(3);
ROASM1(10)=muH*(Xk(9)/(Ks+Xk(9)))*(KOH/(KOH+Uk(3)))*(Xk(8)/(KNO+Xk(8)))*etag*XBHk(3);
ROASM1(11)=muA*(Xk(7)/(KNH+Xk(7)))*(Uk(3)/(KOA+Uk(3)))*XBAk(3);
x1=XSk(3)/XBHk(3);
ROASM1(12)=Kh*XBHk(3)*(x1/(Kx+x1))*((Uk(3)/(KOH+Uk(3)))+etah*(KOH/(KOH+Uk(3)))*(Xk(8)/(KNO+Xk(8))));
ROASM1=[ROASM1(1) ROASM1(2) ROASM1(3) ROASM1(4) ROASM1(5) ROASM1(6) ROASM1(7) ROASM1(8) ROASM1(9) ROASM1(10) ROASM1(11)
ROASM1(12)]';

%Calculation for the Sensitivity Analysis
% Calcualation of the derivatives of the process rates toward the process  variables for the Tank 1
rSNH1SNH1=-(iXB+1/YA)*muA*XBAk(1)*(Uk(1)/(KOA+Uk(1)))*(KNH/(KNH+Xk(1))^2);
rSNH1SNO1=-iXB*muH*(Xk(3)/(Ks+Xk(3)))*(KOH/(KOH+Uk(1)))*XBHk(1)*etag*(KNO/(KNO+Xk(2))^2);
rSNH1SS1=-iXB*muH*XBHk(1)*(Uk(1)/(KOH+Uk(1)))*(Ks/(Ks+Xk(3))^2);
rSNO1SNH1=(1/YA)*muA*XBAk(1)*(Uk(1)/(KOA+Uk(1)))*(KNH/(KNH+Xk(1))^2);
rSNO1SNO1=-((1-YH)/2.86*YH)*XBHk(1)*muH*etag*(Xk(3)/(Ks+Xk(3)))*(KOH/(KOH+Uk(1)))*(KNO/(KNO+Xk(2))^2);
rSNO1SS1=-((1-YH)/2.86*YH)*XBHk(1)*muH*etag*(KOH/(KOH+Uk(1)))*(Xk(2)/(KNO+Xk(2)))*(Ks/(Ks+Xk(3))^2);rSS1SNH1=0;
rSS1SNO1=-
(1/YH)*muH*(Xk(3)/(Ks+Xk(3)))*Kh*etah*((XSk(1)/XBHk(1))/(Kx+(XSk(1)/XBHk(1))))*XBHk(1)*(KOH/(KOH+Uk(1)))*(KNO/(KNO+Xk(2))^2);
rSS1SS1=-(1/YH)*muH*XBHk(1)*((Uk(1)/(KOH+Uk(1)))+(Xk(2)/(KNO+Xk(2)))*(KOH/(KOH+Uk(1))))*(Ks/(Ks+Xk(3)));
% Calculation of the derivatives of the process rates toward the process  variables for the Tank 2
rSNH2SNH2=-(iXB+1/YA)*muA*XBAk(2)*(Uk(2)/(KOA+Uk(2)))*(KNH/(KNH+Xk(4))^2);
rSNH2SNO2=-iXB*muH*(Xk(6)/(Ks+Xk(6)))*(KOH/(KOH+Uk(2)))*XBHk(2)*etag*(KNO/(KNO+Xk(5))^2);
rSNH2SS2=-iXB*muH*XBHk(2)*(Uk(2)/(KOH+Uk(2)))*(Ks/(Ks+Xk(6))^2);
rSNO2SNH2=(1/YA)*muA*XBAk(2)*(Uk(2)/(KOA+Uk(2)))*(KNH/(KNH+Xk(4))^2);
rSNO2SNO2=-((1-YH)/2.86*YH)*XBHk(2)*muH*etag*(Xk(6)/(Ks+Xk(6)))*(KOH/(KOH+Uk(2)))*(KNO/(KNO+Xk(5))^2);
rSNO2SS2=-((1-YH)/2.86*YH)*XBHk(2)*muH*etag*(KOH/(KOH+Uk(2)))*(Xk(5)/(KNO+Xk(5)))*(Ks/(Ks+Xk(6))^2);rSS2SNH2=0;
rSS2SNO2=-
(1/YH)*muH*(Xk(6)/(Ks+Xk(6)))*Kh*etah*((XSk(2)/XBHk(2))/(Kx+(XSk(2)/XBHk(2))))*XBHk(2)*(KOH/(KOH+Uk(2)))*(KNO/(KNO+Xk(5))^2);
rSS2SS2=-(1/YH)*muH*XBHk(2)*((Uk(2)/(KOH+Uk(2)))+(Xk(5)/(KNO+Xk(5)))*(KOH/(KOH+Uk(2))))*(Ks/(Ks+Xk(6)));
% Calculation of the derivatives of the process rates toward the process  variables  for the Tank 3
rSNH3SNH3=-(iXB+1/YA)*muA*XBAk(3)*(Uk(3)/(KOA+Uk(3)))*(KNH/(KNH+Xk(7))^2);
rSNH3SNO3=-iXB*muH*(Xk(9)/(Ks+Xk(9)))*(KOH/(KOH+Uk(3)))*XBHk(3)*etag*(KNO/(KNO+Xk(8))^2);
rSNH3SS3=-iXB*muH*XBHk(3)*(Uk(3)/(KOH+Uk(3)))*(Ks/(Ks+Xk(9))^2);
rSNO3SNH3=(1/YA)*muA*XBAk(3)*(Uk(3)/(KOA+Uk(3)))*(KNH/(KNH+Xk(7))^2);
rSNO3SNO3=-((1-YH)/2.86*YH)*XBHk(3)*muH*etag*(Xk(9)/(Ks+Xk(9)))*(KOH/(KOH+Uk(3)))*(KNO/(KNO+Xk(8))^2);
rSNO3SS3=-((1-YH)/2.86*YH)*XBHk(3)*muH*etag*(KOH/(KOH+Uk(3)))*(Xk(8)/(KNO+Xk(8)))*(Ks/(Ks+Xk(9))^2);rSS3SNH3=0;
rSS3SNO3=-
(1/YH)*muH*(Xk(9)/(Ks+Xk(9)))*Kh*etah*((XSk(3)/XBHk(3))/(Kx+(XSk(3)/XBHk(3))))*XBHk(3)*(KOH/(KOH+Uk(3)))*(KNO/(KNO+Xk(8))^2);
rSS3SS3=-(1/YH)*muH*XBHk(3)*((Uk(3)/(KOH+Uk(3)))+(Xk(8)/(KNO+Xk(8)))*(KOH/(KOH+Uk(3))))*(Ks/(Ks+Xk(9)));

% Calculation of the derivatives of the process rates toward the process  parameter YH for the tank 1
rSNH1f=0.0;rSNO1f=0.0;rSS1f=0.0;rSNH1YH=0;
rSNO1YH=-muH*etag*XBHk(1)*(Xk(3)/(Ks+Xk(3)))*(KOH/(KOH+Uk(1)))*(Xk(2)/(KNO+Xk(2)))*(1/2.86*YH^2);
rSS1YH=(1/YH^2)*muH*XBHk(1)*(Xk(3)/(Ks+Xk(3)))*((Uk(1)/(KOH+Uk(1)))+(Xk(2)/(KNO+Xk(2)))*(KOH/(KOH+Uk(1))));
% Calculation of the derivatives of the process rates toward the process  variables for YA for the tank 1
rSNH1YA=(1/YA^2)*muA*(Uk(1)/(KOA+Uk(1)))*(Xk(1)/(KNH+Xk(1)))*XBAk(1);
rSNO1YA=-(1/YA^2)*muA*(Uk(1)/(KOA+Uk(1)))*(Xk(1)/(KNH+Xk(1)))*XBAk(1);rSS1YA=0;
% Calculation of the derivatives of the process rates toward the process parameter iXB for the tank 1
rSNH1iXB=-muH*XBHk(1)*(Xk(3)/(Ks+Xk(3)))*((Uk(1)/(KOH+Uk(1)))+(Xk(2)/(KNO+Xk(2)))*(KOH/(KOH+Uk(1)))*etag)-
muA*(Uk(1)/(KOA+Uk(1)))*(Xk(1)/(KNH+Xk(1)))*XBAk(1);rSNO1iXB=0;rSS1iXB=0;
% Calculation of the derivatives of the process rates toward the process  parameter muA for the tank 1
rSNH1muA=-(iXB+1/YA)*(Uk(1)/(KOA+Uk(1)))*(Xk(1)/(KNH+Xk(1)))*XBAk(1);
rSNO1muA=(1/YA)*(Uk(1)/(KOA+Uk(1)))*(Xk(1)/(KNH+Xk(1)))*XBAk(1);rSS1muA=0;
% Calculation of the derivatives of the process rates toward the process  parameter muH for the tank 1
rSNH1muH=-iXB*XBHk(1)*(Xk(3)/(Ks+Xk(3)))*((Uk(1)/(KOH+Uk(1)))+etag*(Xk(2)/(KNO+Xk(2)))*(KOH/(KOH+Uk(1))));
rSNO1muH=-((1-YH)/2.86*YH)*XBHk(1)*(Xk(3)/(Ks+Xk(3)))*(KOH/(KOH+Uk(1)))*(Xk(2)/(KNO+Xk(2)));
rSS1muH=-(1/YH)*XBHk(1)*(Xk(3)/(Ks+Xk(3)))*((Uk(1)/(KOH+Uk(1)))+(Xk(2)/(KNO+Xk(2)))*(KOH/(KOH+Uk(1))));
% Calculation of the derivatives of the process rates toward the process  parameter KS for the tank 1
rSNH1KS=iXB*muH*XBHk(1)*(Xk(3)/(Ks+Xk(3))^2)*((Uk(1)/(KOH+Uk(1)))+etag*(Xk(2)/(KNO+Xk(2)))*(KOH/(KOH+Uk(1))));
rSNO1KS=((1-YH)/2.86*YH)*XBHk(1)*muH*(Xk(3)/(Ks+Xk(3)))*(KOH/(KOH+Uk(1)))*(Xk(2)/(KNO+Xk(2)))*etag;
rSS1KS=(1/YH)*muH*XBHk(1)*(Xk(3)/(Ks+Xk(3))^2)*((Uk(1)/(KOH+Uk(1)))+(Xk(2)/(KNO+Xk(2)))*(KOH/(KOH+Uk(1))));
% Calculation of the derivatives of the process rates toward the process  parameter KOH for the tank 1
rSNH1KOH=iXB*muH*XBHk(1)*(Xk(3)/(Ks+Xk(3)))*(Uk(1)/(KOH+Uk(1))^2)*(1-etag*(Xk(2)/(KNO+Xk(2))));
rSNO1KOH=-((1-YH)/2.86*YH)*XBHk(1)*muH*(Xk(3)/(Ks+Xk(3)))*(Uk(1)/(KOH+Uk(1))^2)*(Xk(2)/(KNO+Xk(2)));
rSS1KOH=(1/YH)*muH*XBHk(1)*(Xk(3)/(Ks+Xk(3)))*(Uk(1)/(KOH+Uk(1))^2)*(1-
(Xk(2)/(KNO+Xk(2))))+Kh*XBHk(1)*((XSk(1)/XBHk(1))/(Kx+(XSk(1)/XBHk(1))))*(Uk(1)/(KOH+Uk(1))^2)*(-1+etah*(Xk(2)/(KNO+Xk(2))));
% Calculation of the derivatives of the process rates toward the process  parameter KNO for the tank 1
rSNH1KNO=iXB*muH*XBHk(1)*etag*(Xk(3)/(Ks+Xk(3)))*(Xk(2)/(KNO+Xk(2))^2)*(KOH/(KOH+Uk(1)));
rSNO1KNO=((1-YH)/2.86*YH)*muH*XBHk(1)*etag*(Xk(3)/(Ks+Xk(3)))*(Xk(2)/(KNO+Xk(2))^2)*(KOH/(KOH+Uk(1)));
rSS1KNO=(1/YH)*muH*XBHk(1)*(Xk(3)/(Ks+Xk(3)))*(Xk(2)/(KNO+Xk(2))^2)*(KOH/(KOH+Uk(1)))-
Kh*XBHk(1)*etah*((XSk(1)/XBHk(1))/(Kx+(XSk(1)/XBHk(1))))*(Xk(2)/(KNO+Xk(2))^2)*(KOH/(KOH+Uk(1)));
% Calculation of the derivatives of the process rates toward the process  parameter KNH for the tank 1
rSNH1KNH=(iXB+1/YA)*muA*(Uk(1)/(KOA+Uk(1)))*(Xk(1)/(KNH+Xk(1)))*XBAk(1);
rSNO1KNH=-(1/YA)*muA*(Uk(1)/(KOA+Uk(1)))*(Xk(1)/(KNH+Xk(1)))*XBAk(1);rSS1KNH=0;
% Calculation of the derivatives of the process rates toward the process  parameter KOA for the tank 1
rSNH1KOA=(iXB+1/YA)*muA*(Uk(1)/(KOA+Uk(1))^2)*(Xk(1)/(KNH+Xk(1)))*XBAk(1);
rSNO1KOA=-(1/YA)*muA*(Uk(1)/(KOA+Uk(1))^2)*(Xk(1)/(KNH+Xk(1)))*XBAk(1);rSS1KOA=0;
% Calculation of the derivatives of the process rates toward the process  parameter etag for the tank 1
rSNH1etag=-iXB*muH*(Xk(3)/(Ks+Xk(3)))*(Xk(2)/(KNO+Xk(2)))*(KOH/(KOH+Uk(1)))*XBHk(1);
rSNO1etag=-((1-YH)/2.86*YH)*muH*(Xk(3)/(Ks+Xk(3)))*(Xk(2)/(KNO+Xk(2)))*(KOH/(KOH+Uk(1)))*XBHk(1);rSS1etag=0;
% Calculation of the derivatives of the process rates toward the process  parameter etah for the tank 1
rSNH1etah=0;rSNO1etah=0;
rSS1etah=Kh*((XSk(1)/XBHk(1))/(Kx+(XSk(1)/XBHk(1))))*(Uk(1)/(KOH+Uk(1)))*(Xk(2)/(KNO+Xk(2)))*(KOH/(KOH+Uk(1)))*XBHk(1);
% Calculation of the derivatives of the process rates toward the process  parameter Kh for the tank 1
rSNH1Kh=0;rSNO1Kh=0;
```

```
rSS1Kh=((XSk(1)/XBHk(1))/(Kx+(XSk(1)/XBHk(1))))*((Uk(1)/(KOH+Uk(1)))+etah*(Xk(2)/(KNO+Xk(2)))*(KOH/(KOH+Uk(1))))*XBHk(1);
% Calculation of the derivatives of the process rates toward the process  parameter Kx for the tank 1
rSNH1Kx=0;rSNO1Kx=0;
rSS1Kx=-Kh*((Uk(1)/(KOH+Uk(1)))+etah*(Xk(2)/(KNO+Xk(2)))*(KOH/(KOH+Uk(1))))*XBHk(1)*((XSk(1)/XBHk(1))/(Kx+(XSk(1)/XBHk(1))));

% Calculation of the derivatives of the process rates toward the process  parameter f for the tank 2
rSNH2f=0.0;rSNO2f=0.0;rSS2f=0.0;
% Calculation of the derivatives of the process rates toward the process  parameter YH for the tank 2
rSNH2YH=0;rSNO2YH=-muH*etag*XBHk(2)*(Xk(6)/(Ks+Xk(6)))*(KOH/(KOH+Uk(2)))*(Xk(5)/(KNO+Xk(5)))*(1/2.86*YH^2);
rSS2YH=(1/YH^2)*muH*XBHk(2)*(Xk(6)/(Ks+Xk(6)))*((Uk(2)/(KOH+Uk(2)))+(Xk(5)/(KNO+Xk(5)))*(KOH/(KOH+Uk(2))));
% Calculation of the derivatives of the process rates toward the process  parameter YA for the tank 2
rSNH2YA=(1/YA^2)*muA*(Uk(2)/(KOA+Uk(2)))*(Xk(4)/(KNH+Xk(4)))*XBAk(2);
rSNO2YA=-(1/YA^2)*muA*(Uk(2)/(KOA+Uk(2)))*(Xk(4)/(KNH+Xk(4)))*XBAk(2);rSS2YA=0;
% Calculation of the derivatives of the process rates toward the process  parameter iXB for the tank 2
rSNH2iXB=-muH*XBHk(2)*(Xk(6)/(Ks+Xk(6)))*((Uk(2)/(KOH+Uk(2)))+(Xk(5)/(KNO+Xk(5)))*(KOH/(KOH+Uk(2)))*etag)-
muA*(Uk(2)/(KOA+Uk(2)))*(Xk(4)/(KNH+Xk(4)))*XBAk(2);rSNO2iXB=0;rSS2iXB=0;
% Calculation of the derivatives of the process rates toward the process  parameter muA for the tank 2
rSNH2muA=-(iXB+1/YA)*(Uk(2)/(KOA+Uk(2)))*(Xk(4)/(KNH+Xk(4)))*XBAk(2);
rSNO2muA=(1/YA)*(Uk(2)/(KOA+Uk(2)))*(Xk(4)/(KNH+Xk(4)))*XBAk(2);rSS2muA=0;
% Calculation of the derivatives of the process rates toward the process  parameter muH for the tank 2
rSNH2muH=-iXB*XBHk(2)*(Xk(6)/(Ks+Xk(6)))*((Uk(2)/(KOH+Uk(2)))+etag*(Xk(5)/(KNO+Xk(5)))*(KOH/(KOH+Uk(2))));
rSNO2muH=-((1-YH)/2.86*YH)*XBHk(2)*(Xk(6)/(Ks+Xk(6)))*(KOH/(KOH+Uk(2)))*(Xk(5)/(KNO+Xk(5)));
rSS2muH=-(1/YH)*XBHk(2)*(Xk(6)/(Ks+Xk(6)))*((Uk(2)/(KOH+Uk(2)))+(Xk(5)/(KNO+Xk(5)))*(KOH/(KOH+Uk(2))));
% Calculation  of the derivatives of the process rates toward the process  parameter KS for the tank 2
rSNH2KS=iXB*muH*XBHk(2)*(Xk(6)/(Ks+Xk(6))^2)*((Uk(2)/(KOH+Uk(2)))+etag*(Xk(5)/(KNO+Xk(5)))*(KOH/(KOH+Uk(2))));
rSNO2KS=((1-YH)/2.86*YH)*XBHk(2)*muH*(Xk(6)/(Ks+Xk(6)))*(KOH/(KOH+Uk(2)))*(Xk(5)/(KNO+Xk(5)))*etag;
rSS2KS=(1/YH)*muH*XBHk(2)*(Xk(6)/(Ks+Xk(6))^2)*((Uk(2)/(KOH+Uk(2)))+(Xk(5)/(KNO+Xk(5)))*(KOH/(KOH+Uk(2))));
% Calculation of the derivatives of the process rates toward the process  parameter  KOH for the tank 2
rSNH2KOH=iXB*muH*XBHk(2)*(Xk(6)/(Ks+Xk(6)))*(Uk(2)/(KOH+Uk(2))^2)*(1-etag*(Xk(5)/(KNO+Xk(5))));
rSNO2KOH=-((1-YH)/2.86*YH)*XBHk(2)*muH*(Xk(6)/(Ks+Xk(6)))*(Uk(2)/(KOH+Uk(2))^2)*(Xk(5)/(KNO+Xk(5)));
rSS2KOH=(1/YH)*muH*XBHk(2)*(Xk(6)/(Ks+Xk(6)))*(Uk(2)/(KOH+Uk(2))^2)*(1-
(Xk(5)/(KNO+Xk(5))))+Kh*XBHk(2)*((XSk(2)/XBHk(2))/(Kx+(XSk(2)/XBHk(2))))*(Uk(2)/(KOH+Uk(2))^2)*(-1+etah*(Xk(5)/(KNO+Xk(5))));
% Calculation of the derivatives of the process rates toward the process  parameter  KNO for the tank 2
rSNH2KNO=iXB*muH*XBHk(2)*etag*(Xk(6)/(Ks+Xk(6)))*(Xk(5)/(KNO+Xk(5))^2)*(KOH/(KOH+Uk(2)));
rSNO2KNO=((1-YH)/2.86*YH)*muH*XBHk(2)*etag*(Xk(6)/(Ks+Xk(6)))*(Xk(5)/(KNO+Xk(5))^2)*(KOH/(KOH+Uk(2)));
rSS2KNO=(1/YH)*muH*XBHk(2)*(Xk(6)/(Ks+Xk(6)))*(Xk(5)/(KNO+Xk(5))^2)*(KOH/(KOH+Uk(2)))-
Kh*XBHk(2)*etah*((XSk(2)/XBHk(2))/(Kx+(XSk(2)/XBHk(2))))*(Xk(5)/(KNO+Xk(5))^2)*(KOH/(KOH+Uk(2)));
% Calculation  of the derivatives of the process rates toward the process  parameter KNH for the tank 2
rSNH2KNH=(iXB+1/YA)*muA*(Uk(2)/(KOA+Uk(2)))*(Xk(4)/(KNH+Xk(4)))*XBAk(2);
rSNO2KNH=-(1/YA)*muA*(Uk(2)/(KOA+Uk(2)))*(Xk(4)/(KNH+Xk(4)))*XBAk(2);rSS2KNH=0;
% Calculation of the derivatives of the process rates toward the process  parameter  KOA for the tank 2
rSNH2KOA=(iXB+1/YA)*muA*(Uk(2)/(KOA+Uk(2))^2)*(Xk(4)/(KNH+Xk(4)))*XBAk(2);
rSNO2KOA=-(1/YA)*muA*(Uk(2)/(KOA+Uk(2))^2)*(Xk(4)/(KNH+Xk(4)))*XBAk(2);rSS2KOA=0;
% Calculation of the derivatives of the process rates toward the process  parameter  etag for the tank 2
rSNH2etag=-iXB*muH*(Xk(6)/(Ks+Xk(6)))*(Xk(5)/(KNO+Xk(5)))*(KOH/(KOH+Uk(2)))*XBHk(2);
rSNO2etag=-((1-YH)/2.86*YH)*muH*(Xk(6)/(Ks+Xk(6)))*(Xk(5)/(KNO+Xk(5)))*(KOH/(KOH+Uk(2)))*XBHk(2);rSS2etag=0;
% Calculation of the derivatives of the process rates toward the process  parameter  etah for the tank 2
rSNH2etah=0;rSNO2etah=0;
rSS2etah=Kh*((XSk(2)/XBHk(2))/(Kx+(XSk(2)/XBHk(2))))*(Uk(2)/(KOH+Uk(2)))*(Xk(5)/(KNO+Xk(5)))*(KOH/(KOH+Uk(2)))*XBHk(2);
% Calculation of the derivatives of the process rates toward the process  parameter  Kh for the tank 2
rSNH2Kh=0;rSNO2Kh=0;
rSS2Kh=((XSk(2)/XBHk(2))/(Kx+(XSk(2)/XBHk(2))))*((Uk(2)/(KOH+Uk(2)))+etah*(Xk(5)/(KNO+Xk(5)))*(KOH/(KOH+Uk(2))))*XBHk(2);
% Calculation of the derivatives of the process rates toward the process  parameter  Kx for the tank 2
rSNH2Kx=0;rSNO2Kx=0;
rSS2Kx=-Kh*((Uk(2)/(KOH+Uk(2)))+etah*(Xk(5)/(KNO+Xk(5)))*(KOH/(KOH+Uk(2))))*XBHk(2)*((XSk(2)/XBHk(2))/(Kx+(XSk(2)/XBHk(2))));

% Calculation of the derivatives of the process rates toward the process  parameter YH for the tank 3
rSNH3f=0.0;rSNO3f=0.0;rSS3f=0.0;rSNH3YH=0;
rSNO3YH=-muH*etag*XBHk(3)*(Xk(9)/(Ks+Xk(9)))*(KOH/(KOH+Uk(3)))*(Xk(8)/(KNO+Xk(8)))*(1/2.86*YH^2);
rSS3YH=(1/YH^2)*muH*XBHk(3)*(Xk(9)/(Ks+Xk(9)))*((Uk(3)/(KOH+Uk(3)))+(Xk(8)/(KNO+Xk(8)))*(KOH/(KOH+Uk(3))));
% Calculation of the derivatives of the process rates toward the process  parameter  YA for the tank 3
rSNH3YA=(1/YA^2)*muA*(Uk(3)/(KOA+Uk(3)))*(Xk(7)/(KNH+Xk(7)))*XBAk(3);
rSNO3YA=-(1/YA^2)*muA*(Uk(3)/(KOA+Uk(3)))*(Xk(7)/(KNH+Xk(7)))*XBAk(3);rSS3YA=0;
% Calculation of the derivatives of the process rates toward the process  parameter  iXB for the tank 3
rSNH3iXB=-muH*XBHk(3)*(Xk(9)/(Ks+Xk(9)))*((Uk(3)/(KOH+Uk(3)))+(Xk(8)/(KNO+Xk(8)))*(KOH/(KOH+Uk(3)))*etag)-
muA*(Uk(3)/(KOA+Uk(3)))*(Xk(7)/(KNH+Xk(7)))*XBAk(3);
rSNO3iXB=0;rSS3iXB=0;
% Calculation of the derivatives of the process rates toward the process  parameter  muA for the tank 3
rSNH3muA=-(iXB+1/YA)*(Uk(3)/(KOA+Uk(3)))*(Xk(7)/(KNH+Xk(7)))*XBAk(3);
rSNO3muA=(1/YA)*(Uk(3)/(KOA+Uk(3)))*(Xk(7)/(KNH+Xk(7)))*XBAk(3);rSS3muA=0;
% Calculation of the derivatives of the process rates toward the process  parameter  muH for the tank 3
rSNH3muH=-iXB*XBHk(3)*(Xk(9)/(Ks+Xk(9)))*((Uk(3)/(KOH+Uk(3)))+etag*(Xk(8)/(KNO+Xk(8)))*(KOH/(KOH+Uk(3))));
rSNO3muH=-((1-YH)/2.86*YH)*XBHk(3)*(Xk(9)/(Ks+Xk(9)))*(KOH/(KOH+Uk(3)))*(Xk(8)/(KNO+Xk(8)));
rSS3muH=-(1/YH)*XBHk(3)*(Xk(9)/(Ks+Xk(9)))*((Uk(3)/(KOH+Uk(3)))+(Xk(8)/(KNO+Xk(8)))*(KOH/(KOH+Uk(3))));
% Calculation of the derivatives of the process rates toward the process  parameter  KS for the tank 3
rSNH3KS=iXB*muH*XBHk(3)*(Xk(9)/(Ks+Xk(9))^2)*((Uk(3)/(KOH+Uk(3)))+etag*(Xk(8)/(KNO+Xk(8)))*(KOH/(KOH+Uk(3))));
rSNO3KS=((1-YH)/2.86*YH)*XBHk(3)*muH*(Xk(9)/(Ks+Xk(9)))*(KOH/(KOH+Uk(3)))*(Xk(8)/(KNO+Xk(8)))*etag;
rSS3KS=(1/YH)*muH*XBHk(3)*(Xk(9)/(Ks+Xk(9))^2)*((Uk(3)/(KOH+Uk(3)))+(Xk(8)/(KNO+Xk(8)))*(KOH/(KOH+Uk(3))));
% Calculation of the derivatives of the process rates toward the process  parameter  KOH for the tank 3
rSNH3KOH=iXB*muH*XBHk(3)*(Xk(9)/(Ks+Xk(9)))*(Uk(3)/(KOH+Uk(3))^2)*(1-etag*(Xk(8)/(KNO+Xk(8))));
rSNO3KOH=-((1-YH)/2.86*YH)*XBHk(3)*muH*(Xk(9)/(Ks+Xk(9)))*(Uk(3)/(KOH+Uk(3))^2)*(Xk(8)/(KNO+Xk(8)));
rSS3KOH=(1/YH)*muH*XBHk(3)*(Xk(9)/(Ks+Xk(9)))*(Uk(3)/(KOH+Uk(3))^2)*(1-
(Xk(8)/(KNO+Xk(8))))+Kh*XBHk(3)*((XSk(3)/XBHk(3))/(Kx+(XSk(3)/XBHk(3))))*(Uk(3)/(KOH+Uk(3))^2)*(-1+etah*(Xk(8)/(KNO+Xk(8))));
% Calculation of the derivatives of the process rates toward the process  parameter  KNO for the tank 3
rSNH3KNO=iXB*muH*XBHk(3)*etag*(Xk(9)/(Ks+Xk(9)))*(Xk(8)/(KNO+Xk(8))^2)*(KOH/(KOH+Uk(3)));
rSNO3KNO=((1-YH)/2.86*YH)*muH*XBHk(3)*etag*(Xk(9)/(Ks+Xk(9)))*(Xk(8)/(KNO+Xk(8))^2)*(KOH/(KOH+Uk(3)));
rSS3KNO=(1/YH)*muH*XBHk(3)*(Xk(9)/(Ks+Xk(9)))*(Xk(8)/(KNO+Xk(8))^2)*(KOH/(KOH+Uk(3)))-
Kh*XBHk(3)*etah*((XSk(3)/XBHk(3))/(Kx+(XSk(3)/XBHk(3))))*(Xk(8)/(KNO+Xk(8))^2)*(KOH/(KOH+Uk(3)));
% Calculation of the derivatives of the process rates toward the process  parameter  KNH for the tank 3
rSNH3KNH=(iXB+1/YA)*muA*(Uk(3)/(KOA+Uk(3)))*(Xk(7)/(KNH+Xk(7)))*XBAk(3);
rSNO3KNH=-(1/YA)*muA*(Uk(3)/(KOA+Uk(3)))*(Xk(7)/(KNH+Xk(7)))*XBAk(3);rSS3KNH=0;
% Calculation of the derivatives of the process rates toward the process  parameter  KOA for the tank 3
rSNH3KOA=(iXB+1/YA)*muA*(Uk(3)/(KOA+Uk(3))^2)*(Xk(7)/(KNH+Xk(7)))*XBAk(3);
rSNO3KOA=-(1/YA)*muA*(Uk(3)/(KOA+Uk(3))^2)*(Xk(7)/(KNH+Xk(7)))*XBAk(3);rSS3KOA=0;
% Calculation of the derivatives of the process rates toward the process  parameter  etag for the tank 3
rSNH3etag=-iXB*muH*(Xk(9)/(Ks+Xk(9)))*(Xk(8)/(KNO+Xk(8)))*(KOH/(KOH+Uk(3)))*XBHk(3);
rSNO3etag=-((1-YH)/2.86*YH)*muH*(Xk(9)/(Ks+Xk(9)))*(Xk(8)/(KNO+Xk(8)))*(KOH/(KOH+Uk(3)))*XBHk(3);rSS3etag=0;
% Calculation of the derivatives of the process rates toward the process  parameter  etah for the tank 3
rSNH3etah=0;rSNO3etah=0;
```

```
rSS3etah=Kh*((XSk(3)/XBHk(3))/(Kx+(XSk(3)/XBHk(3))))*(Uk(3)/(KOH+Uk(3)))*(Xk(8)/(KNO+Xk(8)))*(KOH/(KOH+Uk(3)))*XBHk(3);
% Calculation of the derivatives of the process rates toward the process  parameter Kh for the tank 3
rSNH3Kh=0;rSNO3Kh=0;
rSS3Kh=((XSk(3)/XBHk(3))/(Kx+(XSk(3)/XBHk(3))))*((Uk(3)/(KOH+Uk(3)))+etah*(Xk(8)/(KNO+Xk(8)))*(KOH/(KOH+Uk(3))))*XBHk(3);
% Calculation of the derivatives of the process rates toward the process  parameter  Kx for the tank 3
rSNH3Kx=0;rSNO3Kx=0;
rSS3Kx=-Kh*((Uk(3)/(KOH+Uk(3)))+etah*(Xk(8)/(KNO+Xk(8)))*(KOH/(KOH+Uk(3))))*XBHk(3)*((XSk(3)/XBHk(3))/(Kx+(XSk(3)/XBHk(3))));

% Development of the matrix AS of the model of sensitivity
A1f=[A11(1,1)+DT*rSNH1SNH1 DT*rSNH1SNO1 DT*rSNH1SS1;
   DT*rSNO1SNH1 A11(2,2)+DT*rSNO1SNO1 DT*rSNO1SS1;
   DT*rSS1SNH1 DT*rSS1SNO1 A11(3,3)+DT*rSS1SS1];
A1S=[A11 zeros(3,45);zeros(3,3) A1f zeros(3,42);zeros(3,6) A1f zeros(3,39);zeros(3,9) A1f zeros(3,36);zeros(3,12) A1f
zeros(3,33);zeros(3,15) A1f zeros(3,30);zeros(3,18) A1f zeros(3,27);zeros(3,21) A1f zeros(3,24);zeros(3,24) A1f
zeros(3,21);zeros(3,27) A1f zeros(3,18);zeros(3,30) A1f zeros(3,15);zeros(3,33) A1f zeros(3,12);zeros(3,36) A1f
zeros(3,9);zeros(3,39) A1f zeros(3,6);zeros(3,42) A1f zeros(3,3);zeros(3,45) A1f];
A2f=[A22(1,1)+DT*rSNH2SNH2 DT*rSNH2SNO2 DT*rSNH2SS2;
   DT*rSNO2SNH2 A22(2,2)+DT*rSNO2SNO2 DT*rSNO2SS2;
   DT*rSS2SNH2 DT*rSS2SNO2 A22(3,3)+DT*rSS2SS2];
A2S=[A22 zeros(3,45);zeros(3,3) A2f zeros(3,42);zeros(3,6) A2f zeros(3,39);zeros(3,9) A2f zeros(3,36);zeros(3,12) A2f
zeros(3,33);zeros(3,15) A2f zeros(3,30);zeros(3,18) A2f zeros(3,27);zeros(3,21) A2f zeros(3,24);zeros(3,24) A2f
zeros(3,21);zeros(3,27) A2f zeros(3,18);zeros(3,30) A2f zeros(3,15);zeros(3,33) A2f zeros(3,12);zeros(3,36) A2f
zeros(3,9);zeros(3,39) A2f zeros(3,6);zeros(3,42) A2f zeros(3,3);zeros(3,45) A2f];
A3f=[A33(1,1)+DT*rSNH3SNH3 DT*rSNH3SNO3 DT*rSNH3SS3;
   DT*rSNO3SNH3 A33(2,2)+DT*rSNO3SNO3 DT*rSNO3SS3;
   DT*rSS3SNH3 DT*rSS3SNO3 A33(3,3)+DT*rSS3SS3];
A3S=[A33 zeros(3,45);zeros(3,3) A3f zeros(3,42);zeros(3,6) A3f zeros(3,39);zeros(3,9) A3f zeros(3,36);zeros(3,12) A3f
zeros(3,33);zeros(3,15) A3f zeros(3,30);zeros(3,18) A3f zeros(3,27);zeros(3,21) A3f zeros(3,24);zeros(3,24) A3f
zeros(3,21);zeros(3,27) A3f zeros(3,18);zeros(3,30) A3f zeros(3,15);zeros(3,33) A3f zeros(3,12);zeros(3,36) A3f
zeros(3,9);zeros(3,39) A3f zeros(3,6);zeros(3,42) A3f zeros(3,3);zeros(3,45) A3f];
%matrices of the interconnections
A12S=[A12 zeros(3,45);zeros(3,3) A12 zeros(3,42);zeros(3,6) A12 zeros(3,39);zeros(3,9) A12 zeros(3,36);zeros(3,12) A12
zeros(3,33);zeros(3,15) A12 zeros(3,30);zeros(3,18) A12 zeros(3,27);zeros(3,21) A12 zeros(3,24);zeros(3,24) A12
zeros(3,21);zeros(3,27) A12 zeros(3,18);zeros(3,30) A12 zeros(3,15);zeros(3,33) A12 zeros(3,12);zeros(3,36) A12
zeros(3,9);zeros(3,39) A12 zeros(3,6);zeros(3,42) A12 zeros(3,3);zeros(3,45) A12];
A21S=[A21 zeros(3,45);zeros(3,3) A21 zeros(3,42);zeros(3,6) A21 zeros(3,39);zeros(3,9) A21 zeros(3,36);zeros(3,12) A21
zeros(3,33);zeros(3,15) A21 zeros(3,30);zeros(3,18) A21 zeros(3,27);zeros(3,21) A21 zeros(3,24);zeros(3,24) A21
zeros(3,21);zeros(3,27) A21 zeros(3,18);zeros(3,30) A21 zeros(3,15);zeros(3,33) A21 zeros(3,12);zeros(3,36) A21
zeros(3,9);zeros(3,39) A21 zeros(3,6);zeros(3,42) A21 zeros(3,3);zeros(3,45) A21];
A23S=[A23 zeros(3,45);zeros(3,3) A23 zeros(3,42);zeros(3,6) A23 zeros(3,39);zeros(3,9) A23 zeros(3,36);zeros(3,12) A23
zeros(3,33);zeros(3,15) A23 zeros(3,30);zeros(3,18) A23 zeros(3,27);zeros(3,21) A23 zeros(3,24);zeros(3,24) A23
zeros(3,21);zeros(3,27) A23 zeros(3,18);zeros(3,30) A23 zeros(3,15);zeros(3,33) A23 zeros(3,12);zeros(3,36) A23
zeros(3,9);zeros(3,39) A23 zeros(3,6);zeros(3,42) A23 zeros(3,3);zeros(3,45) A23];
A32S=[A32 zeros(3,45);zeros(3,3) A32 zeros(3,42);zeros(3,6) A32 zeros(3,39);zeros(3,9) A32 zeros(3,36);zeros(3,12) A32
zeros(3,33);zeros(3,15) A32 zeros(3,30);zeros(3,18) A32 zeros(3,27);zeros(3,21) A32 zeros(3,24);zeros(3,24) A32
zeros(3,21);zeros(3,27) A32 zeros(3,18);zeros(3,30) A32 zeros(3,15);zeros(3,33) A32 zeros(3,12);zeros(3,36) A32
zeros(3,9);zeros(3,39) A32 zeros(3,6);zeros(3,42) A32 zeros(3,3);zeros(3,45) A32];
%the matrix of the state of sensitivity
AS=[A1S A12S zeros(48,48) ;A21S A2S A23S;zeros(48,48) A32S A3S];

%matrix of the rates for the model of sensitivity
C1S=[Cn zeros(4,45)];CS=[C1S zeros(4,96);zeros(4,48) C1S zeros(4,48);zeros(4,96) C1S];

% Development of the matrix BS of the model of sensitivity
B1theta=[B1(2,2) 0 0;zeros(44,3)];B1S=[B1;B1theta];BS=[B1S;zeros(96,3)];

% Development of the vector DS of the model of sensitivity
% Calculation of the first tank
D1S=[zeros(1,3) rSNH1f rSNO1f rSS1f rSNH1YH rSNO1YH rSS1YH rSNH1YA rSNO1YA rSS1YA rSNH1iXB rSNO1iXB rSS1iXB rSNH1muA rSNO1muA
rSS1muA rSNH1muH rSNO1muH rSS1muH rSNH1KS rSNO1KS rSS1KS rSNH1KOH rSNO1KOH rSS1KOH rSNH1KNO rSNO1KNO rSS1KNO rSNH1KNH rSNO1KNH
rSS1KNH rSNH1KOA rSNO1KOA rSS1KOA rSNH1etag rSNO1etag rSS1etag rSNH1etah rSNO1etah rSS1etah rSNH1Kh rSNO1Kh rSS1Kh rSNH1Kx rSNO1Kx
rSS1Kx]';
% Calculation of the second tank
D2S=[zeros(1,3) rSNH2f rSNO2f rSS2f rSNH2YH rSNO2YH rSS2YH rSNH2YA rSNO2YA rSS2YA rSNH2iXB rSNO2iXB rSS2iXB rSNH2muA rSNO2muA
rSS2muA rSNH2muH rSNO2muH rSS2muH rSNH2KS rSNO2KS rSS2KS rSNH2KOH rSNO2KOH rSS2KOH rSNH2KNO rSNO2KNO rSS2KNO rSNH2KNH rSNO2KNH
rSS2KNH rSNH2KOA rSNO2KOA rSS2KOA rSNH2etag rSNO2etag rSS2etag rSNH2etah rSNO2etah rSS2etah rSNH2Kh rSNO2Kh rSS2Kh rSNH2Kx rSNO2Kx
rSS2Kx]';
% Calculation of the third tank
D3S=[zeros(1,3) rSNH3f rSNO3f rSS3f rSNH3YH rSNO3YH rSS3YH rSNH3YA rSNO3YA rSS3YA rSNH3iXB rSNO3iXB rSS3iXB rSNH3muA rSNO3muA
rSS3muA rSNH3muH rSNO3muH rSS3muH rSNH3KS rSNO3KS rSS3KS rSNH3KOH rSNO3KOH rSS3KOH rSNH3KNO rSNO3KNO rSS3KNO rSNH3KNH rSNO3KNH
rSS3KNH rSNH3KOA rSNO3KOA rSS3KOA rSNH3etag rSNO3etag rSS3etag rSNH3etah rSNO3etah rSS3etah rSNH3Kh rSNO3Kh rSS3Kh rSNH3Kx rSNO3Kx
rSS3Kx]';

DS=[D1S;D2S;D3S];
```

SOFTWARE FOR SIMULATION OF SENSITIVITY FUNCTIONS OF THE PROCESS VARIABLES OF THE ATHLONE MASS BALANCE MODEL BASED ON THE REDUCED UCT BIOLOGICAL MODEL TOWARDS ITS PARAMETERS

1.Main program

```
%PROGRAM AUCTS.m
%AIM:The program function rateAUCTS.m calculates the process rates, derivatives of the proces rates towards the model parameters
and variables and forms the sensitivity model matrices necessary for simulation of theprocess variables and the sensitivity
functions for the Athlone process based on the reduced UCT biological model.
%The program uses global definition of the model parameters

global Ks KOH KNO KNA KOA muH etag muA KMP fZBH YZH YZA KA KSA KSP fMA

%Process model parameters
f=1.2;YZA = 0.15;YZH = 0.67;fZBH = 0.068;muH = 1.5;Ks = 5;KOH = 0.002;KNO = 0.1;etag = 0.33;KMP = 1.35;muA = 0.5;
KNA = 0.01;KA = 0.17;KOA = 0.002;fMA=1;KSP=0.027;KSA=1;
% Flowrates
Qo = 40003;Qa = 39916.8;Qp = 39916.8;Qr = 40003;Qw = 384.0;
```

```
% Volumes
V1=1148;V2=1148;V3=5273;
 %Influent average concentrations
SSi=69.5;SNHi=31.56;SNOi=0.0;XSi=202.3;
%Determination of the sampling period
DT = 0.01042;days=0.1042*10
K=days/DT
k=0:DT:days
%Influent concentrations trajectories for SNH, SNO, SS, Sads
Xi  =[SNHi*ones(1,K);SNOi*ones(1,K);SSi*ones(1,K);XSi*ones(1,K)]*0.1
%Initial conditions- steady state values for the Snh, Sno,Ss and zero for the sensitivity functions
XS0 =[7.918;5.37;2.808;82.135;zeros(68,1);8.344;3.662;1.459;5.15;zeros(68,1);5.548;6.541;1.15;5.1;zeros(68,1)]% initial conditions
for the differential equations
% Steady state values for the biomass XBH, XBA, XS
XBH = 0.01*[2551.76*ones(1,K);2553.38*ones(1,K);2557.13*ones(1,K)]% XBH steady state COD/m^3
XBA = 0.01*[148.389*ones(1,K);148.309*ones(1,K);148.941*ones(1,K)]% XBA steady state g all COD/m^3
XS = 0.01*[82.135*ones(1,K);76.386*ones(1,K);64.855*ones(1,K)] % XS steady state all COD/m^3
%trajectory of the control signal
SO1 = [0.2*ones(1,K);0.2*ones(1,K)];SO2=[4.0*ones(1,K)];U=[SO1;SO2];
% Calculation of the initial trajectory for the state vector X and for the sensitivity vector XSS
X =[[7.918;5.37;2.808;5.3;8.344;3.662;1.459;5.15;5.548;6.541;1.15;5.1] zeros(12,K)];% initial conditions for the differential
equations
XSS = [XS0 zeros(216,K)];
%Calculation of the process state space model matrices
%Calculation of the matrix A
IV1 = DT/V1;IV2 = DT/V2;IV3 = DT/V3;IV=IV1*Qo;IVV=IV*f;
B=[IVV 0.0 0.0 0.0;0.0 IV 0.0 0.0;0.0 0.0 IV 0.0;0.0 0.0 0.0 IV;zeros(8,4)]
Q1=Qo+Qp;Q2=Q1+Qa+Qr;Q3=Q2;IV221=IV2*Q2;IV331=IV3*Q3
IV11=1-IV1*Q1 %element of A11
IV12=IV1*Qp    %element of A12
IV21=IV2*Q1     %element of A21
IV22=1-IV221   %element of A22
IV23=IV2*(Qa+Qr)  %element of A23
IV32=IV3*Q2  %element of A32
IV33=1-IV331   %element of A33

A=[[IV11 0.0 0.0 0.0;0.0 IV11 0.0 0.0;0.0 0.0 IV11 0.0;0.0 0.0 0.0 IV11] [IV12 0.0 0.0 0.0;0.0 IV12 0.0 0.0;0.0 0.0 IV12 0.0;0.0
0.0 0.0 IV12] zeros(4,4);
    [IV21 0.0 0.0 0.0;0.0 IV21 0.0 0.0;0.0 0.0 IV21 0.0;0.0 0.0 0.0 IV21] [IV22 0.0 0.0 0.0;0.0 IV22 0.0 0.0;0.0 0.0 IV22 0.0;0.0
0.0 0.0 IV22] [IV23 0.0 0.0 0.0;0.0 IV23 0.0 0.0;0.0 0.0 IV23 0.0;0.0 0.0 0.0 IV23];
    zeros(4,4) [IV32 0.0 0.0 0.0;0.0 IV32 0.0 0.0;0.0 0.0 IV32 0.0;0.0 0.0 0.0 IV32] [IV33 0.0 0.0 0.0;0.0 IV33 0.0 0.0;0.0 0.0
IV33 0.0;0.0 0.0 0.0 IV33]]
A11u=A(1:4,1:4);A12u=A(1:4,5:8);A13u=zeros(4,4);A21u=A(5:8,1:4);A22u=A(5:8,5:8);A23u=A(5:8,9:12);A31u=zeros(4,4);
A32u=A(9:12,5:8);A33u=A(9:12,9:12);
%Calculation of the matrix B1u and Cu
B1u=[IVV 0.0 0.0 0.0;0.0 IV 0.0 0.0;0.0 0.0 IV 0.0;0.0 0.0 0.0 IV];
x1=-1/YZH;x2=1/YZA;x3=(1-YZH)/(2.86*YZH);x4=x3-fZBH;x5=-x2-fZBH;
Cnu=[-fZBH 0 x1 0;0 -fZBH x1 0;-fZBH -x3 x1 0;0 x3-fZBH x1 0;-fZBH 0 0 x1;0 -fZBH 0 x1;-fZBH -x3 0 x1;0 x3-fZBH 0 x1;0 0 0 1;-x2-
fZBH x2 0 0];
Cu=[Cnu zeros(10,8);zeros(10,4) Cnu zeros(10,4);zeros(10,8) Cnu];

%Simulation of the process sensitivity model
for k = 1:K
    XSSk = XSS(:,k);
    Xk=X(:,k);
    Uk =U(:,k);
    XBHk = XBH(:,k);
    XBAk = XBA(:,k);
    XSk = XS(:,k);
    Xik = Xi(:,k);
   [ROUCT,ASu,BSu,CSu,DSu]=rateAUCTS(Xk,Uk,XBHk,XBAk,XSk,DT,A11u,A12u,A21u,A22u,A23u,A32u,A33u,B1u,Cnu);

    XSS(:,k+1) = ASu*XSS(:,k) + CSu'*ROUCT + BSu*Xi(:,k)+DSu;
    X(:,k+1) = [XSS(1:4,k+1);XSS(73:76,k+1);XSS(145:148,k+1)];
end

%vector of sensitivity for the first tank XStheta
SNH1=XSS(1,:);SNO1=XSS(2,:);SS1=XSS(3,:);Sads1=XSS(4,:);
SNH1f=XSS(5,:);SNO1f=XSS(6,:);SS1f=XSS(7,:);Sads1f=XSS(8,:);
SNH1YZH=XSS(9,:);SNO1YZH=XSS(10,:);SS1YZH=XSS(11,:);Sads1YZH=XSS(12,:);
SNH1YZA=XSS(13,:);SNO1YZA=XSS(14,:);SS1YZA=XSS(15,:);Sads1YZA=XSS(16,:);
SNH1fZBH=XSS(17,:);SNO1fZBH=XSS(18,:);SS1fZBH=XSS(19,:);Sads1fZBH=XSS(20,:);
SNH1muA=XSS(21,:);SNO1muA=XSS(22,:);SS1muA=XSS(23,:);Sads1muA=XSS(24,:);
SNH1muH=XSS(25,:);SNO1muH=XSS(26,:);SS1muH=XSS(27,:);Sads1muH=XSS(28,:);
SNH1KS=XSS(29,:);SNO1KS=XSS(30,:);SS1KS=XSS(31,:);Sads1KS=XSS(32,:);
SNH1KOH=XSS(33,:);SNO1KOH=XSS(34,:);SS1KOH=XSS(35,:);Sads1KOH=XSS(36,:);
SNH1KNO=XSS(37,:);SNO1KNO=XSS(38,:);SS1KNO=XSS(39,:);Sads1KNO=XSS(40,:);
SNH1KNH=XSS(41,:);SNO1KNH=XSS(22,:);SS1KNH=XSS(43,:);Sads1KNH=XSS(44,:);
SNH1KOA=XSS(45,:);SNO1KOA=XSS(46,:);SS1KOA=XSS(47,:);Sads1KOA=XSS(48,:);
SNH1etag=XSS(49,:);SNO1etag=XSS(50,:);SS1etag=XSS(51,:);Sads1etag=XSS(52,:);
SNH1KMP=XSS(53,:);SNO1KMP=XSS(54,:);SS1KMP=XSS(55,:);Sads1KMP=XSS(56,:);
SNH1KSP=XSS(57,:);SNO1KSP=XSS(58,:);SS1KSP=XSS(59,:);Sads1KSP=XSS(60,:);
SNH1KSA=XSS(61,:);SNO1KSA=XSS(62,:);SS1KSA=XSS(63,:);Sads1KSA=XSS(64,:);
SNH1fMA=XSS(65,:);SNO1fMA=XSS(66,:);SS1fMA=XSS(67,:);Sads1fMA=XSS(68,:);
SNH1KA=XSS(69,:);SNO1KA=XSS(70,:);SS1KA=XSS(71,:);Sads1KA=XSS(72,:);


%vector of sensitivity for the second tank XStheta
SNH2=XSS(73,:);SNO2=XSS(74,:);SS2=XSS(75,:);Sads2=XSS(76,:);
SNH2f=XSS(77,:);SNO2f=XSS(78,:);SS2f=XSS(79,:);Sads2f=XSS(80,:);
SNH2YZH=XSS(81,:);SNO2YZH=XSS(82,:);SS2YZH=XSS(83,:);Sads2YZH=XSS(84,:);
SNH2YZA=XSS(85,:);SNO2YZA=XSS(86,:);SS2YZA=XSS(87,:);Sads2YZA=XSS(88,:);
SNH2fZBH=XSS(89,:);SNO2fZBH=XSS(90,:);SS2fZBH=XSS(91,:);Sads2fZBH=XSS(92,:);
SNH2muA=XSS(93,:);SNO2muA=XSS(94,:);SS2muA=XSS(95,:);Sads2muA=XSS(96,:);
SNH2muH=XSS(97,:);SNO2muH=XSS(98,:);SS2muH=XSS(99,:);Sads2muH=XSS(100,:);
SNH2KS=XSS(101,:);SNO2KS=XSS(102,:);SS2KS=XSS(103,:);Sads2KS=XSS(104,:);
SNH2KOH=XSS(105,:);SNO2KOH=XSS(106,:);SS2KOH=XSS(107,:);Sads2KOH=XSS(108,:);
SNH2KNO=XSS(109,:);SNO2KNO=XSS(110,:);SS2KNO=XSS(111,:);Sads2KNO=XSS(112,:);
SNH2KNH=XSS(113,:);SNO2KNH=XSS(114,:);SS2KNH=XSS(115,:);Sads2KNH=XSS(116,:);
```

```
SNH2KOA=XSS(117,:);SNO2KOA=XSS(118,:);SS2KOA=XSS(119,:);Sads2KOA=XSS(120,:);
SNH2etag=XSS(121,:);SNO2etag=XSS(122,:);SS2etag=XSS(123,:);Sads2etag=XSS(124,:);
SNH2KMP=XSS(125,:);SNO2KMP=XSS(126,:);SS2KMP=XSS(127,:);Sads2KMP=XSS(128,:);
SNH2KSP=XSS(129,:);SNO2KSP=XSS(130,:);SS2KSP=XSS(131,:);Sads2KSP=XSS(132,:);
SNH2KSA=XSS(133,:);SNO2KSA=XSS(134,:);SS2KSA=XSS(135,:);Sads2KSA=XSS(136,:);
SNH2fMA=XSS(137,:);SNO2fMA=XSS(138,:);SS2fMA=XSS(139,:);Sads2fMA=XSS(140,:);
SNH2KA=XSS(141,:);SNO2KA=XSS(142,:);SS2KA=XSS(143,:);Sads2KA=XSS(144,:);

%vector of sensitivity for the third tank XStheta
SNH3=XSS(145,:);SNO3=XSS(146,:);SS3=XSS(147,:);Sads3=XSS(148,:);
SNH3f=XSS(149,:);SNO3f=XSS(150,:);SS3f=XSS(151,:);Sads3f=XSS(152,:);
SNH3YZH=XSS(153,:);SNO3YZH=XSS(154,:);SS3YZH=XSS(155,:);Sads3YZH=XSS(156,:);
SNH3YZA=XSS(157,:);SNO3YZA=XSS(158,:);SS3YZA=XSS(159,:);Sads3YZA=XSS(160,:);
SNH3fZBH=XSS(161,:);SNO3fZBH=XSS(162,:);SS3fZBH=XSS(163,:);Sads3fZBH=XSS(164,:);
SNH3muA=XSS(165,:);SNO3muA=XSS(166,:);SS3muA=XSS(167,:);Sads3muA=XSS(168,:);
SNH3muH=XSS(169,:);SNO3muH=XSS(170,:);SS3muH=XSS(171,:);Sads3muH=XSS(172,:);
SNH3KS=XSS(173,:);SNO3KS=XSS(174,:);SS3KS=XSS(175,:);Sads3KS=XSS(176,:);
SNH3KOH=XSS(177,:);SNO3KOH=XSS(178,:);SS3KOH=XSS(179,:);Sads3KOH=XSS(180,:);
SNH3KNO=XSS(181,:);SNO3KNO=XSS(182,:);SS3KNO=XSS(183,:);Sads3KNO=XSS(184,:);
SNH3KNH=XSS(185,:);SNO3KNH=XSS(186,:);SS3KNH=XSS(187,:);Sads3KNH=XSS(188,:);
SNH3KOA=XSS(189,:);SNO3KOA=XSS(190,:);SS3KOA=XSS(191,:);Sads3KOA=XSS(192,:);
SNH3etag=XSS(193,:);SNO3etag=XSS(194,:);SS3etag=XSS(195,:);Sads3etag=XSS(196,:);
SNH3KMP=XSS(197,:);SNO3KMP=XSS(198,:);SS3KMP=XSS(199,:);Sads3KMP=XSS(200,:);
SNH3KSP=XSS(201,:);SNO3KSP=XSS(202,:);SS3KSP=XSS(203,:);Sads3KSP=XSS(204,:);
SNH3KSA=XSS(205,:);SNO3KSA=XSS(206,:);SS3KSA=XSS(207,:);Sads3KSA=XSS(208,:);
SNH3fMA=XSS(209,:);SNO3fMA=XSS(210,:);SS3fMA=XSS(211,:);Sads3fMA=XSS(212,:);
SNH3KA=XSS(213,:);SNO3KA=XSS(214,:);SS3KA=XSS(215,:);Sads3KA=XSS(216,:);

k=1:101
%Graphs of the sensitivity functions for the SNH
%Graph for the first tank
figure(1)
subplot(9,2,1);plot(k,SNH1,'k')
title('Process variable Snh1')
ylabel('\fontsize{8}SNH1')
xlabel('\fontsize{8}discrete time k')

subplot(9,2,2); plot(k,SNH1f,'k')
title('Sensitivity function Snh1f')
ylabel('\fontsize{8}SNH1f')
xlabel('\fontsize{8}discrete time,k')

subplot(9,2,3); plot(k,SNH1YZH,'k')
title('Variable Snh1YZH')
ylabel('\fontsize{8}SNH1YZH')
xlabel('\fontsize{8}discrete time,k')

subplot(9,2,4); plot(k,SNH1YZA,'k')
title('Variable Snh1YZA')
ylabel('\fontsize{8}SNH1YZA')
xlabel('\fontsize{8}discrete time,k')

subplot(9,2,5); plot(k,SNH1fZBH,'k')
title('Sensitivity function Snh1fZBH')
ylabel('\fontsize{8}SNH1fZBH')
xlabel('discrete time,k')

subplot(9,2,6); plot(k,SNH1muA,'k')
title('Sensitivity function Snh1muA')
ylabel('\fontsize{8}SNH1muA')
xlabel('\fontsize{8}discrete time,k')

subplot(9,2,7); plot(k,SNH1muH,'k')
title('Sensitivity function Snh1muH')
ylabel('\fontsize{8}SNH1muH')
xlabel('discrete time,k')

subplot(9,2,8); plot(k,SNH1KS,'k')
title('Sensitivity function Snh1KS')
ylabel('\fontsize{8}SNH1KS')
xlabel('discrete time,k')

subplot(9,2,9); plot(k,SNH1KOH,'k')
title('Sensitivity function Snh1KOH')
ylabel('\fontsize{8}SNH1KOH')
xlabel('\fontsize{8}discrete time,k')

subplot(9,2,10); plot(k,SNH1KNO,'k')
title('Sensitivity function Snh1KNO')
ylabel('\fontsize{8}SNH1KNO')
xlabel('\fontsize{8}discrete time,k')

subplot(9,2,11); plot(k,SNH1KNH,'k')
title('Sensitivity function Snh1KNH')
ylabel('\fontsize{8}SNH1KNH')
xlabel('\fontsize{8}discrete time,k')

subplot(9,2,12); plot(k,SNH1KOA,'k')
title('Sensitivity function Snh1KOA')
ylabel('\fontsize{8}SNH1KOA')
xlabel('\fontsize{8}discrete time,k')

subplot(9,2,13); plot(k,SNH1etag,'k')
title('Sensitivity function Snh1etag')
ylabel('\fontsize{8}SNH1etag')
xlabel('\fontsize{8}discrete time,k')

subplot(9,2,14); plot(k,SNH1KMP,'k')
title('Sensitivity function Snh1KMP')
ylabel('\fontsize{8}SNH1KMP')
xlabel('\fontsize{8}discrete time,k')

subplot(9,2,15); plot(k,SNH1KSP,'k')
title('Sensitivity function Snh1KSP')
ylabel('\fontsize{8}SNH1KSP')
xlabel('\fontsize{8}discrete time,k')

subplot(9,2,16); plot(k,SNH1KSA,'k')
title('Sensitivity function Snh1KSA')
ylabel('\fontsize{8}SNH1KSA')
xlabel('\fontsize{8}discrete time,k')

subplot(9,2,17); plot(k,SNH1fMA,'k')
title('Sensitivity function Snh1fMA')
ylabel('\fontsize{8}SNH1fMA')
xlabel('\fontsize{8}discrete time,k')

subplot(9,2,18); plot(k,SNH1KA,'k')
title('Sensitivity function Snh1KA')
ylabel('\fontsize{8}SNH1KA')
xlabel('\fontsize{8}discrete time,k')

%Graphs for the second tank

figure(2)
subplot(9,2,1);plot(k,SNH2,'k')
title('Process variable Snh2')
ylabel('\fontsize{8}SNH2')
xlabel('\fontsize{8}discrete time k')

subplot(9,2,2); plot(k,SNH2f,'k')
title('Sensitivity function Snh2f')
ylabel('\fontsize{8}SNH2f')
xlabel('\fontsize{8}discrete time,k')

subplot(9,2,3); plot(k,SNH2YZH,'k')
title('Variable Snh2YZH')
ylabel('\fontsize{8}SNH2YZH')
xlabel('\fontsize{8}discrete time,k')

subplot(9,2,4); plot(k,SNH2YZA,'k')
title('Variable Snh2YZA')
ylabel('\fontsize{8}SNH2YZA')
xlabel('\fontsize{8}discrete time,k')

subplot(9,2,5); plot(k,SNH2fZBH,'k')
title('Sensitivity function Snh2fZBH')
ylabel('\fontsize{8}SNH2fZBH')
xlabel('discrete time,k')

subplot(9,2,6); plot(k,SNH2muA,'k')
title('Sensitivity function Snh2muA')
ylabel('\fontsize{8}SNH2muA')
xlabel('\fontsize{8}discrete time,k')

subplot(9,2,7); plot(k,SNH2muH,'k')
title('Sensitivity function Snh2muH')
ylabel('\fontsize{8}SNH2muH')
xlabel('discrete time,k')

subplot(9,2,8); plot(k,SNH2KS,'k')
title('Sensitivity function Snh2KS')
ylabel('\fontsize{8}SNH2KS')
xlabel('discrete time,k')

subplot(9,2,9); plot(k,SNH2KOH,'k')
title('Sensitivity function Snh2KOH')
ylabel('\fontsize{8}SNH2KOH')
xlabel('\fontsize{8}discrete time,k')
```

```
subplot(9,2,10); plot(k,SNH2KNO,'k')
title('Sensitivity function Snh2KNO')
ylabel('\fontsize{8}SNH2KNO')
xlabel('\fontsize{8}discrete time,k')

subplot(9,2,11); plot(k,SNH2KNH,'k')
title('Sensitivity function Snh2KNH')
ylabel('\fontsize{8}SNH2KNH')
xlabel('\fontsize{8}discrete time,k')

subplot(9,2,12); plot(k,SNH2KOA,'k')
title('Sensitivity function Snh2KOA')
ylabel('\fontsize{8}SNH2KOA')
xlabel('\fontsize{8}discrete time,k')

subplot(9,2,13); plot(k,SNH2etag,'k')
title('Sensitivity function Snh2etag')
ylabel('\fontsize{8}SNH2etag')
xlabel('\fontsize{8}discrete time,k')

subplot(9,2,14); plot(k,SNH2KMP,'k')
title('Sensitivity function Snh2KMP')
ylabel('\fontsize{8}SNH2KMP')
xlabel('\fontsize{8}discrete time,k')

subplot(9,2,15); plot(k,SNH2KSP,'k')
title('Sensitivity function Snh2KSP')
ylabel('\fontsize{8}SNH2KSP')
xlabel('\fontsize{8}discrete time,k')

subplot(9,2,16); plot(k,SNH2KSA,'k')
title('Sensitivity function Snh2KSA')
ylabel('\fontsize{8}SNH2KSA')
xlabel('\fontsize{8}discrete time,k')

subplot(9,2,17); plot(k,SNH2fMA,'k')
title('Sensitivity function Snh2fMA')
ylabel('\fontsize{8}SNH2fMA')
xlabel('\fontsize{8}discrete time,k')

subplot(9,2,18); plot(k,SNH2KA,'k')
title('Sensitivity function Snh2KA')
ylabel('\fontsize{8}SNH2KA')
xlabel('\fontsize{8}discrete time,k')


%graphs for SNH variable in the third tank

figure(3)
subplot(9,2,1);plot(k,SNH3,'k')
title('Process variable Snh3')
ylabel('\fontsize{8}SNH3')
xlabel('\fontsize{8}discrete time k')

subplot(9,2,2); plot(k,SNH3f,'k')
title('Sensitivity function Snh3f')
ylabel('\fontsize{8}SNH3f')
xlabel('\fontsize{8}discrete time,k')

subplot(9,2,3); plot(k,SNH3YZH,'k')
title('Variable Snh3YZH')
ylabel('\fontsize{8}SNH3YZH')
xlabel('\fontsize{8}discrete time,k')

subplot(9,2,4); plot(k,SNH3YZA,'k')
title('Variable Snh3YZA')
ylabel('\fontsize{8}SNH3YZA')
xlabel('\fontsize{8}discrete time,k')

subplot(9,2,5); plot(k,SNH3fZBH,'k')
title('Sensitivity function Snh3fZBH')
ylabel('\fontsize{8}SNH3fZBH')
xlabel('discrete time,k')

subplot(9,2,6); plot(k,SNH3muA,'k')
title('Sensitivity function Snh3muA')
ylabel('\fontsize{8}SNH3muA')
xlabel('\fontsize{8}discrete time,k')

subplot(9,2,7); plot(k,SNH3muH,'k')
title('Sensitivity function Snh3muH')
ylabel('\fontsize{8}SNH3muH')
xlabel('discrete time,k')

subplot(9,2,8); plot(k,SNH3KS,'k')
title('Sensitivity function Snh3KS')
ylabel('\fontsize{8}SNH3KS')
xlabel('discrete time,k')

subplot(9,2,9); plot(k,SNH3KOH,'k')
title('Sensitivity function Snh3KOH')
ylabel('\fontsize{8}SNH3KOH')
xlabel('\fontsize{8}discrete time,k')

subplot(9,2,10); plot(k,SNH3KNO,'k')
title('Sensitivity function Snh3KNO')
ylabel('\fontsize{8}SNH3KNO')
xlabel('\fontsize{8}discrete time,k')

subplot(9,2,11); plot(k,SNH3KNH,'k')
title('Sensitivity function Snh3KNH')
ylabel('\fontsize{8}SNH3KNH')
xlabel('\fontsize{8}discrete time,k')

subplot(9,2,12); plot(k,SNH3KOA,'k')
title('Sensitivity function Snh3KOA')
ylabel('\fontsize{8}SNH3KOA')
xlabel('\fontsize{8}discrete time,k')

subplot(9,2,13); plot(k,SNH3etag,'k')
title('Sensitivity function Snh3etag')
ylabel('\fontsize{8}SNH3etag')
xlabel('\fontsize{8}discrete time,k')

subplot(9,2,14); plot(k,SNH3KMP,'k')
title('Sensitivity function Snh3KMP')
ylabel('\fontsize{8}SNH3KMP')
xlabel('\fontsize{8}discrete time,k')

subplot(9,2,15); plot(k,SNH3KSP,'k')
title('Sensitivity function Snh3KSP')
ylabel('\fontsize{8}SNH3KSP')
xlabel('\fontsize{8}discrete time,k')

subplot(9,2,16); plot(k,SNH3KSA,'k')
title('Sensitivity function Snh3KSA')
ylabel('\fontsize{8}SNH3KSA')
xlabel('\fontsize{8}discrete time,k')

subplot(9,2,17); plot(k,SNH3fMA,'k')
title('Sensitivity function Snh3fMA')
ylabel('\fontsize{8}SNH3fMA')
xlabel('\fontsize{8}discrete time,k')

subplot(9,2,18); plot(k,SNH3KA,'k')
title('Sensitivity function Snh3KA')
ylabel('\fontsize{8}SNH3KA')
xlabel('\fontsize{8}discrete time,k')


%Graphs of the sensitivity functions for the SNO
%Graphs of the sensitivity functions of the variable SNO in
the tank 1
figure(4)
subplot(9,2,1);plot(k,SNO1,'k')
title('Process variable SNO1')
ylabel('\fontsize{8}SNO1')
xlabel('\fontsize{8}discrete time k')

subplot(9,2,2); plot(k,SNO1f,'k')
title('Sensitivity function SNO1f')
ylabel('\fontsize{8}SNO1f')
xlabel('\fontsize{8}discrete time,k')

subplot(9,2,3); plot(k,SNO1YZH,'k')
title('Variable SNO1YZH')
ylabel('\fontsize{8}SNO1YZH')
xlabel('\fontsize{8}discrete time,k')

subplot(9,2,4); plot(k,SNO1YZA,'k')
title('Variable SNO1YZA')
ylabel('\fontsize{8}SNO1YZA')
xlabel('\fontsize{8}discrete time,k')

subplot(9,2,5); plot(k,SNO1fZBH,'k')
title('Sensitivity function SNO1fZBH')
ylabel('\fontsize{8}SNO1fZBH')
xlabel('discrete time,k')

subplot(9,2,6); plot(k,SNO1muA,'k')
title('Sensitivity function SNO1muA')
ylabel('\fontsize{8}SNO1muA')
xlabel('\fontsize{8}discrete time,k')

subplot(9,2,7); plot(k,SNO1muH,'k')
title('Sensitivity function SNO1muH')
ylabel('\fontsize{8}SNO1muH')
xlabel('discrete time,k')

subplot(9,2,8); plot(k,SNO1KS,'k')
title('Sensitivity function SNO1KS')
ylabel('\fontsize{8}SNO1KS')
xlabel('discrete time,k')

subplot(9,2,9); plot(k,SNO1KOH,'k')
title('Sensitivity function SNO1KOH')
ylabel('\fontsize{8}SNO1KOH')
xlabel('\fontsize{8}discrete time,k')

subplot(9,2,10); plot(k,SNO1KNO,'k')
title('Sensitivity function SNO1KNO')
ylabel('\fontsize{8}SNO1KNO')
xlabel('\fontsize{8}discrete time,k')

subplot(9,2,11); plot(k,SNO1KNH,'k')
title('Sensitivity function SNO1KNH')
ylabel('\fontsize{8}SNO1KNH')
xlabel('\fontsize{8}discrete time,k')
```

```
subplot(9,2,12); plot(k,SNO1KOA,'k')
title('Sensitivity function SNO1KOA')
ylabel('\fontsize{8}SNO1KOA')
xlabel('\fontsize{8}discrete time,k')

subplot(9,2,13); plot(k,SNO1etag,'k')
title('Sensitivity function SNO1etag')
ylabel('\fontsize{8}SNO1etag')
xlabel('\fontsize{8}discrete time,k')

subplot(9,2,14); plot(k,SNO1KMP,'k')
title('Sensitivity function SNO1KMP')
ylabel('\fontsize{8}SNO1KMP')
xlabel('\fontsize{8}discrete time,k')

subplot(9,2,15); plot(k,SNO1KSP,'k')
title('Sensitivity function SNO1KSP')
ylabel('\fontsize{8}SNO1KSP')
xlabel('\fontsize{8}discrete time,k')

subplot(9,2,16); plot(k,SNO1KSA,'k')
title('Sensitivity function SNO1KSA')
ylabel('\fontsize{8}SNO1KSA')
xlabel('\fontsize{8}discrete time,k')

subplot(9,2,17); plot(k,SNO1fMA,'k')
title('Sensitivity function SNO1fMA')
ylabel('\fontsize{8}SNO1fMA')
xlabel('\fontsize{8}discrete time,k')

subplot(9,2,18); plot(k,SNO1KA,'k')
title('Sensitivity function SNO1KA')
ylabel('\fontsize{8}SNO1KA')
xlabel('\fontsize{8}discrete time,k')


%Graphs of the sensitivity functions for the variable SNO in
the tank 2
figure(5)
subplot(9,2,1);plot(k,SNO2,'k')
title('Process variable SNO2')
ylabel('\fontsize{8}SNO2')
xlabel('\fontsize{8}discrete time k')

subplot(9,2,2); plot(k,SNO2f,'k')
title('Sensitivity function SNO2f')
ylabel('\fontsize{8}SNO2f')
xlabel('\fontsize{8}discrete time,k')

subplot(9,2,3); plot(k,SNO2YZH,'k')
title('Variable SNO2YZH')
ylabel('\fontsize{8}SNO2YZH')
xlabel('\fontsize{8}discrete time,k')

subplot(9,2,4); plot(k,SNO2YZA,'k')
title('Variable SNO2YZA')
ylabel('\fontsize{8}SNO2YZA')
xlabel('\fontsize{8}discrete time,k')

subplot(9,2,5); plot(k,SNO2fZBH,'k')
title('Sensitivity function SNO2fZBH')
ylabel('\fontsize{8}SNO2fZBH')
xlabel('discrete time,k')

subplot(9,2,6); plot(k,SNO2muA,'k')
title('Sensitivity function SNO2muA')
ylabel('\fontsize{8}SNO2muA')
xlabel('\fontsize{8}discrete time,k')

subplot(9,2,7); plot(k,SNO2muH,'k')
title('Sensitivity function SNO2muH')
ylabel('\fontsize{8}SNO2muH')
xlabel('discrete time,k')

subplot(9,2,8); plot(k,SNO2KS,'k')
title('Sensitivity function SNO2KS')
ylabel('\fontsize{8}SNO2KS')
xlabel('discrete time,k')

subplot(9,2,9); plot(k,SNO2KOH,'k')
title('Sensitivity function SNO2KOH')
ylabel('\fontsize{8}SNO2KOH')
xlabel('\fontsize{8}discrete time,k')

subplot(9,2,10); plot(k,SNO2KNO,'k')
title('Sensitivity function SNO2KNO')
ylabel('\fontsize{8}SNO2KNO')
xlabel('\fontsize{8}discrete time,k')

subplot(9,2,11); plot(k,SNO2KNH,'k')
title('Sensitivity function SNO2KNH')
ylabel('\fontsize{8}SNH2KNH')
xlabel('\fontsize{8}discrete time,k')

subplot(9,2,12); plot(k,SNO2KOA,'k')
title('Sensitivity function SNO2KOA')
ylabel('\fontsize{8}SNO2KOA')
xlabel('\fontsize{8}discrete time,k')

subplot(9,2,13); plot(k,SNO2etag,'k')
title('Sensitivity function SNO2etag')
ylabel('\fontsize{8}SNO2etag')
xlabel('\fontsize{8}discrete time,k')

subplot(9,2,14); plot(k,SNO2KMP,'k')
title('Sensitivity function SNO2KMP')
ylabel('\fontsize{8}SNO2KMP')
xlabel('\fontsize{8}discrete time,k')

subplot(9,2,15); plot(k,SNO2KSP,'k')
title('Sensitivity function SNO2KSP')
ylabel('\fontsize{8}SNO2KSP')
xlabel('\fontsize{8}discrete time,k')

subplot(9,2,16); plot(k,SNO2KSA,'k')
title('Sensitivity function SNO2KSA')
ylabel('\fontsize{8}SNO2KSA')
xlabel('\fontsize{8}discrete time,k')

subplot(9,2,17); plot(k,SNO2fMA,'k')
title('Sensitivity function SNO2fMA')
ylabel('\fontsize{8}SNO2fMA')
xlabel('\fontsize{8}discrete time,k')

subplot(9,2,18); plot(k,SNO2KA,'k')
title('Sensitivity function SNO2KA')
ylabel('\fontsize{8}SNO2KA')
xlabel('\fontsize{8}discrete time,k')

%Graphs for the variable SNO  in the  tank 3

figure(6)
subplot(9,2,1);plot(k,SNO3,'k')
title('Process variable SNO3')
ylabel('\fontsize{8}SNO3')
xlabel('\fontsize{8}discrete time k')

subplot(9,2,2); plot(k,SNO3f,'k')
title('Sensitivity function SNO3f')
ylabel('\fontsize{8}SNO3f')
xlabel('\fontsize{8}discrete time,k')

subplot(9,2,3); plot(k,SNO3YZH,'k')
title('Variable SNO3YZH')
ylabel('\fontsize{8}SNO3YZH')
xlabel('\fontsize{8}discrete time,k')

subplot(9,2,4); plot(k,SNO3YZA,'k')
title('Variable SNO3YZA')
ylabel('\fontsize{8}SNO3YZA')
xlabel('\fontsize{8}discrete time,k')

subplot(9,2,5); plot(k,SNO3fZBH,'k')
title('Sensitivity function SNO3fZBH')
ylabel('\fontsize{8}SNO3fZBH')
xlabel('discrete time,k')

subplot(9,2,6); plot(k,SNO3muA,'k')
title('Sensitivity function SNO3muA')
ylabel('\fontsize{8}SNO3muA')
xlabel('\fontsize{8}discrete time,k')

subplot(9,2,7); plot(k,SNO3muH,'k')
title('Sensitivity function SNO3muH')
ylabel('\fontsize{8}SNO3muH')
xlabel('discrete time,k')

subplot(9,2,8); plot(k,SNO3KS,'k')
title('Sensitivity function SNO3KS')
ylabel('\fontsize{8}SNO3KS')
xlabel('discrete time,k')

subplot(9,2,9); plot(k,SNO3KOH,'k')
title('Sensitivity function SNO3KOH')
ylabel('\fontsize{8}SNO3KOH')
xlabel('\fontsize{8}discrete time,k')

subplot(9,2,10); plot(k,SNO3KNO,'k')
title('Sensitivity function SNO3KNO')
ylabel('\fontsize{8}SNO3KNO')
xlabel('\fontsize{8}discrete time,k')

subplot(9,2,11); plot(k,SNO3KNH,'k')
title('Sensitivity function SNO3KNH')
ylabel('\fontsize{8}SNO3KNH')
xlabel('\fontsize{8}discrete time,k')

subplot(9,2,12); plot(k,SNO3KOA,'k')
title('Sensitivity function SNO3KOA')
ylabel('\fontsize{8}SNO3KOA')
xlabel('\fontsize{8}discrete time,k')

subplot(9,2,13); plot(k,SNO3etag,'k')
title('Sensitivity function SNO3etag')
ylabel('\fontsize{8}SNO3etag')
xlabel('\fontsize{8}discrete time,k')
```

```
subplot(9,2,14); plot(k,SNO3KMP,'k')
title('Sensitivity function SNO3KMP')
ylabel('\fontsize{8}SNO3KMP')
xlabel('\fontsize{8}discrete time,k')

subplot(9,2,15); plot(k,SNO3KSP,'k')
title('Sensitivity function SNO3KSP')
ylabel('\fontsize{8}SNO3KSP')
xlabel('\fontsize{8}discrete time,k')

subplot(9,2,16); plot(k,SNO3KSA,'k')
title('Sensitivity function SNO3KSA')
ylabel('\fontsize{8}SNO3KSA')
xlabel('\fontsize{8}discrete time,k')

subplot(9,2,17); plot(k,SNO3fMA,'k')
title('Sensitivity function SNO3fMA')
ylabel('\fontsize{8}SNO3fMA')
xlabel('\fontsize{8}discrete time,k')

subplot(9,2,18); plot(k,SNO3KA,'k')
title('Sensitivity function SNO3KA')
ylabel('\fontsize{8}SNO3KA')
xlabel('\fontsize{8}discrete time,k')

%Graphs of the sensitivity unctions for the SS

%Graphs of the sensitivity functions for the SS in the tank
1
figure(7)
subplot(9,2,1);plot(k,SS1,'k')
title('Process variable SS1')
ylabel('\fontsize{8}SS1')
xlabel('\fontsize{8}discrete time k')

subplot(9,2,2); plot(k,SS1f,'k')
title('Sensitivity function SS1f')
ylabel('\fontsize{8}SS1f')
xlabel('\fontsize{8}discrete time,k')

subplot(9,2,3); plot(k,SS1YZH,'k')
title('Variable SS1YZH')
ylabel('\fontsize{8}SS1YZH')
xlabel('\fontsize{8}discrete time,k')

subplot(9,2,4); plot(k,SS1YZA,'k')
title('Variable SS1YZA')
ylabel('\fontsize{8}SS1YZA')
xlabel('\fontsize{8}discrete time,k')

subplot(9,2,5); plot(k,SS1fZBH,'k')
title('Sensitivity function SS1fZBH')
ylabel('\fontsize{8}SS1fZBH')
xlabel('discrete time,k')

subplot(9,2,6); plot(k,SS1muA,'k')
title('Sensitivity function SS1muA')
ylabel('\fontsize{8}SS1muA')
xlabel('\fontsize{8}discrete time,k')

subplot(9,2,7); plot(k,SS1muH,'k')
title('Sensitivity function SS1muH')
ylabel('\fontsize{8}SS1muH')
xlabel('discrete time,k')

subplot(9,2,8); plot(k,SS1KS,'k')
title('Sensitivity function SS1KS')
ylabel('\fontsize{8}SS1KS')
xlabel('discrete time,k')

subplot(9,2,9); plot(k,SS1KOH,'k')
title('Sensitivity function SS1KOH')
ylabel('\fontsize{8}SS1KOH')
xlabel('\fontsize{8}discrete time,k')

subplot(9,2,10); plot(k,SS1KNO,'k')
title('Sensitivity function SS1KNO')
ylabel('\fontsize{8}SS1KNO')
xlabel('\fontsize{8}discrete time,k')

subplot(9,2,11); plot(k,SS1KNH,'k')
title('Sensitivity function SS1KNH')
ylabel('\fontsize{8}SS1KNH')
xlabel('\fontsize{8}discrete time,k')

subplot(9,2,12); plot(k,SS1KOA,'k')
title('Sensitivity function SS1KOA')
ylabel('\fontsize{8}SS1KOA')
xlabel('\fontsize{8}discrete time,k')

subplot(9,2,13); plot(k,SS1etag,'k')
title('Sensitivity function SS1etag')
ylabel('\fontsize{8}SS1etag')
xlabel('\fontsize{8}discrete time,k')

subplot(9,2,14); plot(k,SS1KMP,'k')
title('Sensitivity function SS1KMP')
ylabel('\fontsize{8}SS1KMP')
xlabel('\fontsize{8}discrete time,k')

subplot(9,2,15); plot(k,SS1KSP,'k')
title('Sensitivity function SS1KSP')
ylabel('\fontsize{8}SS1KSP')
xlabel('\fontsize{8}discrete time,k')

subplot(9,2,16); plot(k,SS1KSA,'k')
title('Sensitivity function SS1KSA')
ylabel('\fontsize{8}SS1KSA')
xlabel('\fontsize{8}discrete time,k')

subplot(9,2,17); plot(k,SS1fMA,'k')
title('Sensitivity function SS1fMA')
ylabel('\fontsize{8}SS1fMA')
xlabel('\fontsize{8}discrete time,k')

subplot(9,2,18); plot(k,SS1KA,'k')
title('Sensitivity function SS1KA')
ylabel('\fontsize{8}SS1KA')
xlabel('\fontsize{8}discrete time,k')


%Graphs of the sensitivity functions of the varible SS in
the tank 2
figure(8)
subplot(9,2,1);plot(k,SS2,'k')
title('Process variable SS2')
ylabel('\fontsize{8}SS2')
xlabel('\fontsize{8}discrete time k')

subplot(9,2,2); plot(k,SS2f,'k')
title('Sensitivity function SS2f')
ylabel('\fontsize{8}SS2f')
xlabel('\fontsize{8}discrete time,k')

subplot(9,2,3); plot(k,SS2YZH,'k')
title('Variable SS2YZH')
ylabel('\fontsize{8}SS2YZH')
xlabel('\fontsize{8}discrete time,k')

subplot(9,2,4); plot(k,SS2YZA,'k')
title('Variable SS2YZA')
ylabel('\fontsize{8}SS2YZA')
xlabel('\fontsize{8}discrete time,k')

subplot(9,2,5); plot(k,SS2fZBH,'k')
title('Sensitivity function SS2fZBH')
ylabel('\fontsize{8}SS2fZBH')
xlabel('discrete time,k')

subplot(9,2,6); plot(k,SS2muA,'k')
title('Sensitivity function SS2muA')
ylabel('\fontsize{8}SS2muA')
xlabel('\fontsize{8}discrete time,k')

subplot(9,2,7); plot(k,SS2muH,'k')
title('Sensitivity function SS2muH')
ylabel('\fontsize{8}SS2muH')
xlabel('discrete time,k')

subplot(9,2,8); plot(k,SS2KS,'k')
title('Sensitivity function SS2KS')
ylabel('\fontsize{8}SS2KS')
xlabel('discrete time,k')

subplot(9,2,9); plot(k,SS2KOH,'k')
title('Sensitivity function SS2KOH')
ylabel('\fontsize{8}SS2KOH')
xlabel('\fontsize{8}discrete time,k')

subplot(9,2,10); plot(k,SS2KNO,'k')
title('Sensitivity function SS2KNO')
ylabel('\fontsize{8}SS2KNO')
xlabel('\fontsize{8}discrete time,k')

subplot(9,2,11); plot(k,SS2KNH,'k')
title('Sensitivity function SS2KNH')
ylabel('\fontsize{8}SS2KNH')
xlabel('\fontsize{8}discrete time,k')

subplot(9,2,12); plot(k,SS2KOA,'k')
title('Sensitivity function SS2KOA')
ylabel('\fontsize{8}SS2KOA')
xlabel('\fontsize{8}discrete time,k')

subplot(9,2,13); plot(k,SS2etag,'k')
title('Sensitivity function SS2etag')
ylabel('\fontsize{8}SS2etag')
xlabel('\fontsize{8}discrete time,k')

subplot(9,2,14); plot(k,SS2KMP,'k')
title('Sensitivity function SS2KMP')
ylabel('\fontsize{8}SS2KMP')
xlabel('\fontsize{8}discrete time,k')

subplot(9,2,15); plot(k,SS2KSP,'k')
title('Sensitivity function SS2KSP')
ylabel('\fontsize{8}SS2KSP')
xlabel('\fontsize{8}discrete time,k')
```

```
subplot(9,2,16); plot(k,SS2KSA,'k')
title('Sensitivity function SS2KSA')
ylabel('\fontsize{8}SS2KSA')
xlabel('\fontsize{8}discrete time,k')

subplot(9,2,17); plot(k,SS2fMA,'k')
title('Sensitivity function SS2fMA')
ylabel('\fontsize{8}SS2fMA')
xlabel('\fontsize{8}discrete time,k')

subplot(9,2,18); plot(k,SS2KA,'k')
title('Sensitivity function SS2KA')
ylabel('\fontsize{8}SS2KA')
xlabel('\fontsize{8}discrete time,k')

%Graphs for SS variable in the tank 3

figure(9)
subplot(9,2,1);plot(k,SS3,'k')
title('Process variable SS3')
ylabel('\fontsize{8}SS3')
xlabel('\fontsize{8}discrete time k')

subplot(9,2,2); plot(k,SS3f,'k')
title('Sensitivity function SS3f')
ylabel('\fontsize{8}SS3f')
xlabel('\fontsize{8}discrete time,k')

subplot(9,2,3); plot(k,SS3YZH,'k')
title('Variable SS3YZH')
ylabel('\fontsize{8}SS3YZH')
xlabel('\fontsize{8}discrete time,k')

subplot(9,2,4); plot(k,SS3YZA,'k')
title('Variable SS3YZA')
ylabel('\fontsize{8}SS3YZA')
xlabel('\fontsize{8}discrete time,k')

subplot(9,2,5); plot(k,SS3fZBH,'k')
title('Sensitivity function SS3fZBH')
ylabel('\fontsize{8}SS3fZBH')
xlabel('discrete time,k')

subplot(9,2,6); plot(k,SS3muA,'k')
title('Sensitivity function SS3muA')
ylabel('\fontsize{8}SS3muA')
xlabel('\fontsize{8}discrete time,k')

subplot(9,2,7); plot(k,SS3muH,'k')
title('Sensitivity function SS3muH')
ylabel('\fontsize{8}SS3muH')
xlabel('discrete time,k')

subplot(9,2,8); plot(k,SS3KS,'k')
title('Sensitivity function SS3KS')
ylabel('\fontsize{8}SS3KS')
xlabel('discrete time,k')

subplot(9,2,9); plot(k,SS3KOH,'k')
title('Sensitivity function SS3KOH')
ylabel('\fontsize{8}SS3KOH')
xlabel('\fontsize{8}discrete time,k')

subplot(9,2,10); plot(k,SS3KNO,'k')
title('Sensitivity function SS3KNO')
ylabel('\fontsize{8}SS3KNO')
xlabel('\fontsize{8}discrete time,k')

subplot(9,2,11); plot(k,SS3KNH,'k')
title('Sensitivity function SS3KNH')
ylabel('\fontsize{8}SS3KNH')
xlabel('\fontsize{8}discrete time,k')

subplot(9,2,12); plot(k,SS3KOA,'k')
title('Sensitivity function SS3KOA')
ylabel('\fontsize{8}SS3KOA')
xlabel('\fontsize{8}discrete time,k')

subplot(9,2,13); plot(k,SS3etag,'k')
title('Sensitivity function SS3etag')
ylabel('\fontsize{8}SS3etag')
xlabel('\fontsize{8}discrete time,k')

subplot(9,2,14); plot(k,SS3KMP,'k')
title('Sensitivity function SS3KMP')
ylabel('\fontsize{8}SS3KMP')
xlabel('\fontsize{8}discrete time,k')

subplot(9,2,15); plot(k,SS3KSP,'k')
title('Sensitivity function SS3KSP')
ylabel('\fontsize{8}SS3KSP')
xlabel('\fontsize{8}discrete time,k')

subplot(9,2,16); plot(k,SS3KSA,'k')
title('Sensitivity function SS3KSA')
ylabel('\fontsize{8}SS3KSA')
xlabel('\fontsize{8}discrete time,k')

subplot(9,2,17); plot(k,SS3fMA,'k')
title('Sensitivity function SS3fMA')
ylabel('\fontsize{8}SS3fMA')
xlabel('\fontsize{8}discrete time,k')

subplot(9,2,18); plot(k,SS3KA,'k')
title('Sensitivity function SS3KA')
ylabel('\fontsize{8}SS3KA')
xlabel('\fontsize{8}discrete time,k')

%Graphs of the sensitivity functions for the Sads in the
tank 1
figure(10)
subplot(9,2,1);plot(k,Sads1,'k')
title('Process variable Sads1')
ylabel('\fontsize{8}Sads1')
xlabel('\fontsize{8}discrete time k')

subplot(9,2,2); plot(k,Sads1f,'k')
title('Sensitivity function Sads1f')
ylabel('\fontsize{8}Sads1f')
xlabel('\fontsize{8}discrete time,k')

subplot(9,2,3); plot(k,Sads1YZH,'k')
title('Variable Sads1YZH')
ylabel('\fontsize{8}Sads1YZH')
xlabel('\fontsize{8}discrete time,k')

subplot(9,2,4); plot(k,Sads1YZA,'k')
title('Variable Sads1YZA')
ylabel('\fontsize{8}Sads1YZA')
xlabel('\fontsize{8}discrete time,k')

subplot(9,2,5); plot(k,Sads1fZBH,'k')
title('Sensitivity function Sads1fZBH')
ylabel('\fontsize{8}Sads1fZBH')
xlabel('discrete time,k')

subplot(9,2,6); plot(k,Sads1muA,'k')
title('Sensitivity function Sads1muA')
ylabel('\fontsize{8}Sads1muA')
xlabel('\fontsize{8}discrete time,k')

subplot(9,2,7); plot(k,Sads1muH,'k')
title('Sensitivity function Sads1muH')
ylabel('\fontsize{8}Sads1muH')
xlabel('discrete time,k')

subplot(9,2,8); plot(k,Sads1KS,'k')
title('Sensitivity function Sads1KS')
ylabel('\fontsize{8}Sads1KS')
xlabel('discrete time,k')

subplot(9,2,9); plot(k,Sads1KOH,'k')
title('Sensitivity function Sads1KOH')
ylabel('\fontsize{8}Sads1KOH')
xlabel('\fontsize{8}discrete time,k')

subplot(9,2,10); plot(k,Sads1KNO,'k')
title('Sensitivity function Sads1KNO')
ylabel('\fontsize{8}Sads1KNO')
xlabel('\fontsize{8}discrete time,k')

subplot(9,2,11); plot(k,Sads1KNH,'k')
title('Sensitivity function Sads1KNH')
ylabel('\fontsize{8}Sads1KNH')
xlabel('\fontsize{8}discrete time,k')

subplot(9,2,12); plot(k,Sads1KOA,'k')
title('Sensitivity function Sads1KOA')
ylabel('\fontsize{8}Sads1KOA')
xlabel('\fontsize{8}discrete time,k')

subplot(9,2,13); plot(k,Sads1etag,'k')
title('Sensitivity function Sads1etag')
ylabel('\fontsize{8}Sads1etag')
xlabel('\fontsize{8}discrete time,k')

subplot(9,2,14); plot(k,Sads1KMP,'k')
title('Sensitivity function Sads1KMP')
ylabel('\fontsize{8}Sads1KMP')
xlabel('\fontsize{8}discrete time,k')

subplot(9,2,15); plot(k,Sads1KSP,'k')
title('Sensitivity function Sads1KSP')
ylabel('\fontsize{8}Sads1KSP')
xlabel('\fontsize{8}discrete time,k')

subplot(9,2,16); plot(k,Sads1KSA,'k')
title('Sensitivity function Sads1KSA')
ylabel('\fontsize{8}Sads1KSA')
xlabel('\fontsize{8}discrete time,k')

subplot(9,2,17); plot(k,Sads1fMA,'k')
title('Sensitivity function Sads1fMA')
ylabel('\fontsize{8}Sads1fMA')
xlabel('\fontsize{8}discrete time,k')

subplot(9,2,18); plot(k,Sads1KA,'k')
```

```
title('Sensitivity function Sads1KA')
ylabel('\fontsize{8}Sads1KA')
xlabel('\fontsize{8}discrete time,k')


%Graphs of the sensitivity functions of the varible SS in
the tank 2
figure(11)
subplot(9,2,1);plot(k,Sads2,'k')
title('Process variable Sads2')
ylabel('\fontsize{8}Sads2')
xlabel('\fontsize{8}discrete time k')

subplot(9,2,2); plot(k,Sads2f,'k')
title('Sensitivity function Sads2f')
ylabel('\fontsize{8}Sads2f')
xlabel('\fontsize{8}discrete time,k')

subplot(9,2,3); plot(k,Sads2YZH,'k')
title('Variable Sads2YZH')
ylabel('\fontsize{8}Sads2YZH')
xlabel('\fontsize{8}discrete time,k')

subplot(9,2,4); plot(k,Sads2YZA,'k')
title('Variable Sads2YZA')
ylabel('\fontsize{8}Sads2YZA')
xlabel('\fontsize{8}discrete time,k')

subplot(9,2,5); plot(k,Sads2fZBH,'k')
title('Sensitivity function Sads2fZBH')
ylabel('\fontsize{8}Sads2fZBH')
xlabel('discrete time,k')

subplot(9,2,6); plot(k,Sads2muA,'k')
title('Sensitivity function Sads2muA')
ylabel('\fontsize{8}Sads2muA')
xlabel('\fontsize{8}discrete time,k')

subplot(9,2,7); plot(k,Sads2muH,'k')
title('Sensitivity function Sads2muH')
ylabel('\fontsize{8}Sads2muH')
xlabel('discrete time,k')

subplot(9,2,8); plot(k,Sads2KS,'k')
title('Sensitivity function Sads2KS')
ylabel('\fontsize{8}Sads2KS')
xlabel('discrete time,k')

subplot(9,2,9); plot(k,Sads2KOH,'k')
title('Sensitivity function Sads2KOH')
ylabel('\fontsize{8}Sads2KOH')
xlabel('\fontsize{8}discrete time,k')

subplot(9,2,10); plot(k,Sads2KNO,'k')
title('Sensitivity function Sads2KNO')
ylabel('\fontsize{8}Sads2KNO')
xlabel('\fontsize{8}discrete time,k')

subplot(9,2,11); plot(k,Sads2KNH,'k')
title('Sensitivity function Sads2KNH')
ylabel('\fontsize{8}Sads2KNH')
xlabel('\fontsize{8}discrete time,k')

subplot(9,2,12); plot(k,Sads2KOA,'k')
title('Sensitivity function Sads2KOA')
ylabel('\fontsize{8}Sads2KOA')
xlabel('\fontsize{8}discrete time,k')

subplot(9,2,13); plot(k,Sads2etag,'k')
title('Sensitivity function Sads2etag')
ylabel('\fontsize{8}Sads2etag')
xlabel('\fontsize{8}discrete time,k')

subplot(9,2,14); plot(k,Sads2KMP,'k')
title('Sensitivity function Sads2KMP')
ylabel('\fontsize{8}Sads2KMP')
xlabel('\fontsize{8}discrete time,k')

subplot(9,2,15); plot(k,Sads2KSP,'k')
title('Sensitivity function Sads2KSP')
ylabel('\fontsize{8}Sads2KSP')
xlabel('\fontsize{8}discrete time,k')

subplot(9,2,16); plot(k,Sads2KSA,'k')
title('Sensitivity function Sads2KSA')
ylabel('\fontsize{8}Sads2KSA')
xlabel('\fontsize{8}discrete time,k')

subplot(9,2,17); plot(k,Sads2fMA,'k')
title('Sensitivity function Sads2fMA')
ylabel('\fontsize{8}Sads2fMA')
xlabel('\fontsize{8}discrete time,k')

subplot(9,2,18); plot(k,Sads2KA,'k')
title('Sensitivity function Sads2KA')
ylabel('\fontsize{8}Sads2KA')
xlabel('\fontsize{8}discrete time,k')

%Graphs for SS variable in the tank 3

figure(12)
subplot(9,2,1);plot(k,Sads3,'k')
title('Process variable Sads3')
ylabel('\fontsize{8}Sads3')
xlabel('\fontsize{8}discrete time k')

subplot(9,2,2); plot(k,SS3f,'k')
title('Sensitivity function Sads3f')
ylabel('\fontsize{8}Sads3f')
xlabel('\fontsize{8}discrete time,k')

subplot(9,2,3); plot(k,Sads3YZH,'k')
title('Variable Sads3YZH')
ylabel('\fontsize{8}Sads3YZH')
xlabel('\fontsize{8}discrete time,k')

subplot(9,2,4); plot(k,Sads3YZA,'k')
title('Variable Sads3YZA')
ylabel('\fontsize{8}Sads3YZA')
xlabel('\fontsize{8}discrete time,k')

subplot(9,2,5); plot(k,Sads3fZBH,'k')
title('Sensitivity function Sads3fZBH')
ylabel('\fontsize{8}Sads3fZBH')
xlabel('discrete time,k')

subplot(9,2,6); plot(k,Sads3muA,'k')
title('Sensitivity function Sads3muA')
ylabel('\fontsize{8}Sads3muA')
xlabel('\fontsize{8}discrete time,k')

subplot(9,2,7); plot(k,Sads3muH,'k')
title('Sensitivity function Sads3muH')
ylabel('\fontsize{8}Sads3muH')
xlabel('discrete time,k')

subplot(9,2,8); plot(k,Sads3KS,'k')
title('Sensitivity function Sads3KS')
ylabel('\fontsize{8}Sads3KS')
xlabel('discrete time,k')

subplot(9,2,9); plot(k,Sads3KOH,'k')
title('Sensitivity function Sads3KOH')
ylabel('\fontsize{8}Sads3KOH')
xlabel('\fontsize{8}discrete time,k')

subplot(9,2,10); plot(k,Sads3KNO,'k')
title('Sensitivity function Sads3KNO')
ylabel('\fontsize{8}Sads3KNO')
xlabel('\fontsize{8}discrete time,k')

subplot(9,2,11); plot(k,Sads3KNH,'k')
title('Sensitivity function Sads3KNH')
ylabel('\fontsize{8}Sads3KNH')
xlabel('\fontsize{8}discrete time,k')

subplot(9,2,12); plot(k,Sads3KOA,'k')
title('Sensitivity function Sads3KOA')
ylabel('\fontsize{8}Sads3KOA')
xlabel('\fontsize{8}discrete time,k')

subplot(9,2,13); plot(k,Sads3etag,'k')
title('Sensitivity function Sads3etag')
ylabel('\fontsize{8}Sads3etag')
xlabel('\fontsize{8}discrete time,k')

subplot(9,2,14); plot(k,Sads3KMP,'k')
title('Sensitivity function Sads3KMP')
ylabel('\fontsize{8}Sads3KMP')
xlabel('\fontsize{8}discrete time,k')

subplot(9,2,15); plot(k,Sads3KSP,'k')
title('Sensitivity function Sads3KSP')
ylabel('\fontsize{8}Sads3KSP')
xlabel('\fontsize{8}discrete time,k')

subplot(9,2,16); plot(k,Sads3KSA,'k')
title('Sensitivity function Sads3KSA')
ylabel('\fontsize{8}Sads3KSA')
xlabel('\fontsize{8}discrete time,k')

subplot(9,2,17); plot(k,Sads3fMA,'k')
title('Sensitivity function Sads3fMA')
ylabel('\fontsize{8}Sads3fMA')
xlabel('\fontsize{8}discrete time,k')

subplot(9,2,18); plot(k,Sads3KA,'k')
title('Sensitivity function Sads3KA')
ylabel('\fontsize{8}Sads3KA')
xlabel('\fontsize{8}discrete time,k')
```

2.Subprogram

```
%SUBPROGRAM rateAUCTS.m
%AIM:The program function rateASM1.m calculates the process rates, derivatives of the proces rates towards the model
parameters and variables and forms the sensitivity model matrices necessary for simulation of theprocess variables and
the sensitivity functions for the Athlone process based on the reduced UCT biological model.
%The program uses global definition of the model parameters

function [ROUCT,ASu,BSu,CSu,DSu]=rateAUCTS(Xk,Uk,XBHk,XBAk,XSk,DT,A11u,A12u,A21u,A22u,A23u,A32u,A33u,B1u,Cnu)
global Ks KOH KNO KNA KOA muH etag muA KMP fZBH YZH YZA KA KSA KSP fMA

%Calculation of the process rates at every moment of the time
% reactions in tank 1
ROUCT(1)=muH*(Xk(3)/(Ks+Xk(3)))*(Uk(1)/(KOH+Uk(1)))*(Xk(1)/(KNA+Xk(1)))*XBHk(1);
ROUCT(2)=muH*(Xk(3)/(Ks+Xk(3)))*(Uk(1)/(KOH+Uk(1)))*(KNA/(KNA+Xk(1)))*(Xk(2)/(KNO+Xk(2)))*XBHk(1);
ROUCT(3)=muH*(Xk(3)/(Ks+Xk(3)))*(KOH/(KOH+Uk(1)))*(Xk(1)/(KNA+Xk(1)))*(Xk(2)/(KNO+Xk(2)))*XBHk(1);
ROUCT(4)=muH*(Xk(3)/(Ks+Xk(3)))*(KOH/(KOH+Uk(1)))*(KNA/(KNA+Xk(1)))*(Xk(2)/(KNO+Xk(2)))*XBHk(1);
ROUCT(5)=KMP*((Xk(4)/XBHk(1))/(KSP+Xk(4)/XBHk(1)))*(Uk(1)/(KOH+Uk(1)))*(Xk(1)/(KNA+Xk(1)))*XBHk(1);
ROUCT(6)=KMP*((Xk(4)/XBHk(1))/(KSP+Xk(4)/XBHk(1)))*(Uk(1)/(KOH+Uk(1)))*(KNA/(KNA+Xk(1)))*(Xk(2)/(KNO+Xk(2)))*XBHk(1);
ROUCT(7)=KMP*((Xk(4)/XBHk(1))/(KSP+Xk(4)/XBHk(1)))*(KOH/(KOH+Uk(1)))*(Xk(1)/(KNA+Xk(1)))*(Xk(2)/(KNO+Xk(2)))*etag*XBHk(
1);
ROUCT(8)=KMP*((Xk(4)/XBHk(1))/(KSP+Xk(4)/XBHk(1)))*(KOH/(KOH+Uk(1)))*(KNA/(KNA+Xk(1)))*(Xk(2)/(KNO+Xk(2)))*etag*XBHk(1)
;
ROUCT(9)=KA*XSk(1)*XBHk(1)*(fMA-(Xk(4)/XBHk(1)));
ROUCT(10)=muA*(Uk(1)/(KOA+Uk(1)))*(Xk(1)/(KSA+Xk(1)))*XBHk(1);

% reactions in tank 2
ROUCT(11)=muH*(Xk(7)/(Ks+Xk(7)))*(Uk(2)/(KOH+Uk(2)))*(Xk(5)/(KNA+Xk(5)))*XBHk(2);
ROUCT(12)=muH*(Xk(7)/(Ks+Xk(7)))*(Uk(2)/(KOH+Uk(2)))*(KNA/(KNA+Xk(5)))*(Xk(6)/(KNO+Xk(6)))*XBHk(2);
ROUCT(13)=muH*(Xk(7)/(Ks+Xk(7)))*(KOH/(KOH+Uk(2)))*(Xk(5)/(KNA+Xk(5)))*(Xk(6)/(KNO+Xk(6)))*XBHk(2);
ROUCT(14)=muH*(Xk(7)/(Ks+Xk(7)))*(KOH/(KOH+Uk(2)))*(KNA/(KNA+Xk(5)))*(Xk(6)/(KNO+Xk(6)))*XBHk(2);
ROUCT(15)=KMP*((Xk(8)/XBHk(2))/(KSP+Xk(8)/XBHk(2)))*(Uk(2)/(KOH+Uk(2)))*(Xk(5)/(KNA+Xk(5)))*XBHk(2);
ROUCT(16)=KMP*((Xk(8)/XBHk(2))/(KSP+Xk(8)/XBHk(2)))*(Uk(2)/(KOH+Uk(2)))*(KNA/(KNA+Xk(5)))*(Xk(6)/(KNO+Xk(6)))*XBHk(2);
ROUCT(17)=KMP*((Xk(8)/XBHk(2))/(KSP+Xk(8)/XBHk(2)))*(KOH/(KOH+Uk(2)))*(Xk(5)/(KNA+Xk(5)))*(Xk(6)/(KNO+Xk(6)))*etag*XBHk
(2);
ROUCT(18)=KMP*((Xk(8)/XBHk(2))/(KSP+Xk(8)/XBHk(2)))*(KOH/(KOH+Uk(2)))*(KNA/(KNA+Xk(5)))*(Xk(6)/(KNO+Xk(6)))*etag*XBHk(2
);
ROUCT(19)=KA*XSk(2)*XBHk(2)*(fMA-(Xk(8)/XBHk(2)));
ROUCT(20)=muA*(Uk(2)/(KOA+Uk(2)))*(Xk(5)/(KSA+Xk(5)))*XBHk(2);

% reactions in tank 3
ROUCT(21)=muH*(Xk(11)/(Ks+Xk(11)))*(Uk(3)/(KOH+Uk(3)))*(Xk(9)/(KNA+Xk(9)))*XBHk(3);
ROUCT(22)=muH*(Xk(11)/(Ks+Xk(11)))*(Uk(3)/(KOH+Uk(3)))*(KNA/(KNA+Xk(9)))*(Xk(10)/(KNO+Xk(10)))*XBHk(3);
ROUCT(23)=muH*(Xk(11)/(Ks+Xk(11)))*(KOH/(KOH+Uk(3)))*(Xk(9)/(KNA+Xk(9)))*(Xk(10)/(KNO+Xk(10)))*XBHk(3);
ROUCT(24)=muH*(Xk(11)/(Ks+Xk(11)))*(KOH/(KOH+Uk(3)))*(KNA/(KNA+Xk(9)))*(Xk(10)/(KNO+Xk(10)))*XBHk(3);
ROUCT(25)=KMP*((Xk(12)/XBHk(3))/(KSP+Xk(12)/XBHk(3)))*(Uk(3)/(KOH+Uk(3)))*(Xk(9)/(KNA+Xk(9)))*XBHk(3);
ROUCT(26)=KMP*((Xk(12)/XBHk(3))/(KSP+Xk(12)/XBHk(3)))*(Uk(3)/(KOH+Uk(3)))*(KNA/(KNA+Xk(9)))*(Xk(10)/(KNO+Xk(10)))*XBHk(
3);
ROUCT(27)=KMP*((Xk(12)/XBHk(3))/(KSP+Xk(12)/XBHk(3)))*(KOH/(KOH+Uk(3)))*(Xk(9)/(KNA+Xk(9)))*(Xk(10)/(KNO+Xk(10)))*etag*
XBHk(3);
ROUCT(28)=KMP*((Xk(12)/XBHk(3))/(KSP+Xk(12)/XBHk(3)))*(KOH/(KOH+Uk(3)))*(KNA/(KNA+Xk(9)))*(Xk(10)/(KNO+Xk(10)))*etag*XB
Hk(3);
ROUCT(29)=KA*XSk(3)*XBHk(3)*(fMA-(Xk(12)/XBHk(3)));
ROUCT(30)=muA*(Uk(3)/(KOA+Uk(3)))*(Xk(9)/(KSA+Xk(9)))*XBHk(3);

ROUCT=[ROUCT(1) ROUCT(2) ROUCT(3) ROUCT(4) ROUCT(5) ROUCT(6) ROUCT(7) ROUCT(8) ROUCT(9) ROUCT(10) ROUCT(11) ROUCT(12)
ROUCT(13) ROUCT(14) ROUCT(15) ROUCT(16) ROUCT(17) ROUCT(18) ROUCT(19) ROUCT(20) ROUCT(21) ROUCT(22) ROUCT(23) ROUCT(24)
ROUCT(25) ROUCT(26) ROUCT(27) ROUCT(28) ROUCT(29) ROUCT(30)]';

%Calculation for the Sensitivity Analysis
% Calculation of the derivatives of the process rates towards the process variables
%Calculations for the tank 1
rUSNH1SNH1=-
fZBH*XBHk(1)*(KNA/(KNA+Xk(1))^2)*(Uk(1)/(KOH+Uk(1)))*(muH*(Xk(3)/(Ks+Xk(3)))+KMP*((Xk(4)/XBHk(1))/(KSP+(Xk(4)/XBHk(1)))
))+(KOH/(KOH+Uk(1)))*(Xk(2)/(KNO+Xk(2)))*muH*(Xk(3)/(Ks+Xk(3)))*KMP*etag*((Xk(4)/XBHk(1))/(KSP+(Xk(4)/XBHk(1)))))-
(1/YZA+fZBH)*muA*(Uk(1)/(KOA+Uk(1)))*(KSA/(KSA+Xk(1)))*XBAk(1);
rUSNH1SNO1=-
fZBH*XBHk(1)*(KNO/(KNO+Xk(2))^2)*(KOH/(KOH+Uk(1)))*(Xk(1)/(KNA+Xk(1)))*(muH*(Xk(3)/(Ks+Xk(3)))+etag*KMP*((Xk(4)/XBHk(1)
))/(KSP+(Xk(4)/XBHk(1)))));
rUSNH1SS1=-
fZBH*muH*(Ks/(Ks+Xk(3)))*XBHk(1)*(Xk(1)/(KSA+Xk(1)))*((Uk(1)/(KOH+Uk(1)))+(KOH/(KOH+Uk(1)))*(Xk(2)/(KNO+Xk(2))));
rUSNH1Sads1=-
fZBH*KMP*((KSP/XBHk(1))/(KSP+(Xk(4)/XBHk(1))))*(Xk(1)/(KNA+Xk(1)))*((Uk(1)/(KOH+Uk(1)))+etag*(KOH/(KOH+Uk(1)))*(Xk(2)/(
KNO+Xk(2))));
rUSNO1SNH1=fZBH*(Uk(1)/(KOH+Uk(1)))*(KNA/(KNA+Xk(1))^2)*(Xk(2)/(KNO+Xk(2)))*XBHk(1)*(muH*(Xk(3)/(Ks+Xk(3)))+KMP*((Xk(4)
/XBHk(1))/(KSP+(Xk(4)/XBHk(1))))+fZBH*(KOH/(KOH+Uk(1)))*(KNA/(KNA+Xk(1))^2)*(Xk(2)/(KNO+Xk(2)))*XBHk(1)*(muH*(Xk(3)/(Ks
+Xk(3)))+KMP*etag*((Xk(4)/XBHk(1))/(KSP+(Xk(4)/XBHk(1)))))+(1/YZA)*muA*(KSA/(KSA+Xk(1))^2)*(Xk(2)/KOA+Xk(2)))*XBAk(1);
rUSNO1SNO1=-
fZBH*(Uk(1)/(KOH+Uk(1)))*(KSA/(KSA+Xk(1)))*(KNO/(KNO+Xk(2))^2)*XBHk(1)*(muH*(Xk(3)/(Ks+Xk(3)))+KMP*((Xk(4)/XBHk(1))/(KS
P+(Xk(4)/XBHk(1)))))-
(KOH/(KOH+Uk(1)))*(KNO/(KNO+Xk(2))^2)*XBHk(1)*(muH*(Xk(3)/(Ks+Xk(3)))+KMP*etag*((Xk(4)/XBHk(1))/(KSP+(Xk(4)/XBHk(1)))))
*(((1-YZH)/2.86*YZH)*(Xk(1)/(KNA+Xk(1)))+(((1-YZH)/2.86*YZH)+fZBH)*(KNA/(KNA+Xk(1))));
rUSNO1SS1=-muH*(Ks/(Ks+Xk(3))^2)*(Xk(2)/(KNO+Xk(2)))*XBHk(1)*(fZBH*(Uk(1)/(KOH+Uk(1)))*(KNA/(KNA+Xk(1)))+((1-
YZH)/2.86*YZH)*(KOH/(KOH+Uk(1)))*(Xk(1)/(KNA+Xk(1)))+((1-YZH)/2.86*YZH)+fZBH)*(KOH/(KOH+Uk(1)))*(KNA/(KNA+Xk(1)));
rUSNO1Sads1=-
KMP*((KSP/XBHk(1))/(KSP+(KSP/XBHk(1)))^2)*(Xk(2)/(KNO+Xk(2)))*XBHk(1)*(fZBH*(Uk(1)/(KOH+Uk(1)))*(KNA/(KNA+Xk(1)))+((1-
YZH)/2.86*YZH)*(KOH/(KOH+Uk(1)))*(Xk(1)/(KNA+Xk(1)))*etag+(((1-
YZH)/2.86*YZH)+fZBH)*(KOH/(KOH+Uk(1)))*(KNA/(KNA+Xk(1)))*etag);
rUSS1SNH1=-(1/YZH)*muH*(Xk(3)/(Ks+Xk(3)))*(Uk(1)/(KOH+Uk(1)))*(KNA/(KNA+Xk(1))^2)*XBHk(1)*(1-(Xk(2)/(KNO+Xk(2))));
rUSS1SNO1=-
(1/YZH)*muH*(Xk(3)/(Ks+Xk(3)))*(KNO/(KNO+Xk(2))^2)*XBHk(1)*((Uk(1)/(KOH+Uk(1)))*(KNA/(KNA+Xk(1)))+(KOH/(KOH+Uk(1)))*(Xk
(1)/(KNA+Xk(1)))+(KOH/(KOH+Uk(1)))*(KNA/(KNA+Xk(1))));
```

```
rUSS1SS1=-
(1/YZH)*(Ks/(Ks+Xk(3))^2)*((Uk(1)/(KOH+Uk(1)))*((Xk(1)/(KNA+Xk(1)))+(KNA/(KNA+Xk(1)))*(Xk(2)/(KNO+Xk(2))))+(KOH/(KOH+Uk
(1)))*(Xk(2)/(KNO+Xk(2)))*((Xk(1)/(KNA+Xk(1)))+(KNA/(KNA+Xk(1)))))*XBHk(1);rUSS1Sads1=0;
rUSads1SNH1=-(1/YZH)*KMP*((Xk(4)/XBHk(1))/(KSP+(Xk(4)/XBHk(1))))*(Uk(1)/(KOH+Uk(1)))*(KNA/(KNA+Xk(1))^2)*XBHk(1)*(1-
(Xk(2)/(KNO+Xk(2))));
rUSads1SNO1=-
(1/YZH)*KMP*((Xk(4)/XBHk(1))/(KSP+(Xk(4)/XBHk(1))))*(KNO/(KNO+Xk(2))^2)*XBHk(1)*((Uk(1)/(KOH+Uk(1)))*(KNA/(KNA+Xk(1)))+
(KOH/(KOH+Uk(1)))*(Xk(1)/(KNA+Xk(1)))+(KOH/(KOH+Uk(1)))*(KNA/(KNA+Xk(1))));rUSads1SS1=0;
rUSads1Sads1=-
(1/YZH)*KMP*((KSP/XBHk(1))/(KSP+(Xk(4)/XBHk(1)))^2)*(Uk(1)/(KOH+Uk(1)))*XBHk(1)*((Xk(1)/(KNA+Xk(1)))*+(KNA/(KNA+Xk(1)))
*(Xk(2)/(KNO+Xk(2))))-
(1/YZH)*KMP*((KSP/XBHk(1))/(KSP+(Xk(4)/XBHk(1)))^2)*(KOH/(KOH+Uk(1)))*(Xk(2)/(KNO+Xk(2)))*etag*XBHk(1)*((Xk(1)/(KNA+Xk(
1)))+(KNA/(KNA+Xk(1))));

% Calculation fo the tank 2
rUSNH2SNH2=-
fZBH*XBHk(2)*(KNA/(KNA+Xk(5))^2)*(Uk(2)/(KOH+Uk(2)))*(muH*(Xk(7)/(Ks+Xk(7)))+KMP*((Xk(8)/XBHk(2))/(KSP+(Xk(8)/XBHk(2)))
))+(KOH/(KOH+Uk(2)))*(Xk(6)/(KNO+Xk(6)))*muH*(Xk(7)/(Ks+Xk(7)))*KMP*etag*((Xk(8)/XBHk(2))/(KSP+(Xk(8)/XBHk(2))))-
(1/YZA+fZBH)*muA*(Uk(2)/(KOA+Uk(2)))*(KSA/(KSA+Xk(5)))*XBAk(2);
rUSNH2SNO2=-
fZBH*XBHk(2)*(KNO/(KNO+Xk(6))^2)*(KOH/(KOH+Uk(2)))*(Xk(5)/(KNA+Xk(5)))*(muH*(Xk(7)/(Ks+Xk(7)))+etag*KMP*((Xk(8)/XBHk(2)
)/(KSP+(Xk(8)/XBHk(2)))));
rUSNH2SS2=-
fZBH*muH*(Ks/(Ks+Xk(7)))*XBHk(2)*(Xk(5)/(KSA+Xk(5)))*((Uk(2)/(KOH+Uk(2)))+(KOH/(KOH+Uk(2)))*(Xk(6)/(KNO+Xk(6))));
rUSNH2Sads2=-
fZBH*KMP*((KSP/XBHk(2))/(KSP+(Xk(8)/XBHk(2))))*(Xk(5)/(KNA+Xk(5)))*((Uk(2)/(KOH+Uk(2)))+etag*(KOH/(KOH+Uk(2)))*(Xk(6)/(
KNO+Xk(6))));
rUSNO2SNH2=fZBH*(Uk(2)/(KOH+Uk(2)))*(KNA/(KNA+Xk(5))^2)*(Xk(6)/(KNO+Xk(6)))*XBHk(2)*(muH*(Xk(7)/(Ks+Xk(7)))+KMP*((Xk(8)
/XBHk(2))/(KSP+(Xk(8)/XBHk(2))))+fZBH*(KOH/(KOH+Uk(2)))*(KNA/(KNA+Xk(5))^2)*(Xk(6)/(KNO+Xk(6)))*XBHk(2)*(muH*(Xk(7)/(Ks
+Xk(7)))+KMP*etag*((Xk(8)/XBHk(2))/(KSP+(Xk(8)/XBHk(2)))))+(1/YZA)*muA*(KSA/(KSA+Xk(5))^2)*(Xk(6)/KOA+Xk(6)))*XBAk(2);
rUSNO2SNO2=-
fZBH*(Uk(2)/(KOH+Uk(2)))*(KSA/(KSA+Xk(5)))*(KNO/(KNO+Xk(6))^2)*XBHk(2)*(muH*(Xk(7)/(Ks+Xk(7)))+KMP*((Xk(8)/XBHk(2))/(KS
P+(Xk(8)/XBHk(2)))))-
(KOH/(KOH+Uk(2)))*(KNO/(KNO+Xk(6))^2)*XBHk(2)*(muH*(Xk(7)/(Ks+Xk(7)))+KMP*etag*((Xk(8)/XBHk(2))/(KSP+(Xk(8)/XBHk(2)))))
*(((1-YZH)/2.86*YZH)*(Xk(5)/(KNA+Xk(5)))+(((1-YZH)/2.86*YZH)+fZBH)*(KNA/(KNA+Xk(5))));
rUSNO2SS2=-muH*(Ks/(Ks+Xk(7))^2)*(Xk(6)/(KNO+Xk(6)))*XBHk(2)*(fZBH*(Uk(2)/(KOH+Uk(2)))*(KNA/(KNA+Xk(5)))+((1-
YZH)/2.86*YZH)*(KOH/(KOH+Uk(2)))*(Xk(5)/(KNA+Xk(5)))+((1-YZH)/2.86*YZH)+fZBH)*(KOH/(KOH+Uk(2)))*(KNA/(KNA+Xk(5)));
rUSNO2Sads2=-
KMP*((KSP/XBHk(2))/(KSP+(KSP/XBHk(2)))^2)*(Xk(6)/(KNO+Xk(6)))*XBHk(2)*(fZBH*(Uk(2)/(KOH+Uk(2)))*(KNA/(KNA+Xk(5)))+((1-
YZH)/2.86*YZH)*(KOH/(KOH+Uk(2)))*(Xk(5)/(KNA+Xk(5)))*etag+(((1-
YZH)/2.86*YZH)+fZBH)*(KOH/(KOH+Uk(2)))*(KNA/(KNA+Xk(5)))*etag);
rUSS2SNH2=-(1/YZH)*muH*(Xk(7)/(Ks+Xk(7)))*(Uk(2)/(KOH+Uk(2)))*(KNA/(KNA+Xk(5))^2)*XBHk(2)*(1-(Xk(6)/(KNO+Xk(6))));
rUSS2SNO2=-
(1/YZH)*muH*(Xk(7)/(Ks+Xk(7)))*(KNO/(KNO+Xk(6))^2)*XBHk(2)*((Uk(2)/(KOH+Uk(2)))*(KNA/(KNA+Xk(5)))+(KOH/(KOH+Uk(2)))*(Xk
(5)/(KNA+Xk(5)))+(KOH/(KOH+Uk(2)))*(KNA/(KNA+Xk(5))));
rUSS2SS2=-
(1/YZH)*(Ks/(Ks+Xk(7))^2)*((Uk(2)/(KOH+Uk(2)))*((Xk(5)/(KNA+Xk(5)))+(KNA/(KNA+Xk(5)))*(Xk(6)/(KNO+Xk(6))))+(KOH/(KOH+Uk
(2)))*(Xk(6)/(KNO+Xk(6)))*((Xk(5)/(KNA+Xk(5)))+(KNA/(KNA+Xk(5))))*XBHk(2);rUSS2Sads2=0;
rUSads2SNH2=-(1/YZH)*KMP*((Xk(8)/XBHk(2))/(KSP+(Xk(8)/XBHk(2))))*(Uk(2)/(KOH+Uk(2)))*(KNA/(KNA+Xk(5))^2)*XBHk(2)*(1-
(Xk(6)/(KNO+Xk(6))));
rUSads2SNO2=-
(1/YZH)*KMP*((Xk(8)/XBHk(2))/(KSP+(Xk(8)/XBHk(2))))*(KNO/(KNO+Xk(6))^2)*XBHk(2)*((Uk(2)/(KOH+Uk(2)))*(KNA/(KNA+Xk(5)))+
(KOH/(KOH+Uk(2)))*(Xk(5)/(KNA+Xk(5)))+(KOH/(KOH+Uk(2)))*(KNA/(KNA+Xk(5))));rUSads2SS2=0;
rUSads2Sads2=-
(1/YZH)*KMP*((KSP/XBHk(2))/(KSP+(Xk(8)/XBHk(2)))^2)*(Uk(2)/(KOH+Uk(2)))*XBHk(2)*((Xk(5)/(KNA+Xk(5)))*+(KNA/(KNA+Xk(5)))
*(Xk(6)/(KNO+Xk(6))))-
(1/YZH)*KMP*((KSP/XBHk(2))/(KSP+(Xk(8)/XBHk(2)))^2)*(KOH/(KOH+Uk(2)))*(Xk(6)/(KNO+Xk(6)))*etag*XBHk(2)*((Xk(5)/(KNA+Xk(
5)))+(KNA/(KNA+Xk(5))));

% Calculation for the tank 3
rUSNH3SNH3=-
fZBH*XBHk(3)*(KNA/(KNA+Xk(9))^2)*(Uk(3)/(KOH+Uk(3)))*(muH*(Xk(11)/(Ks+Xk(11)))+KMP*((Xk(12)/XBHk(3))/(KSP+(Xk(12)/XBHk(
3)))))+(KOH/(KOH+Uk(3)))*(Xk(10)/(KNO+Xk(10)))*muH*(Xk(11)/(Ks+Xk(11)))*KMP*etag*((Xk(12)/XBHk(3))/(KSP+(Xk(12)/XBHk(3)
))))-(1/YZA+fZBH)*muA*(Uk(3)/(KOA+Uk(3)))*(KSA/(KSA+Xk(9)))*XBAk(3);
rUSNH3SNO3=-
fZBH*XBHk(3)*(KNO/(KNO+Xk(10))^2)*(KOH/(KOH+Uk(3)))*(Xk(9)/(KNA+Xk(9)))*(muH*(Xk(11)/(Ks+Xk(11)))+etag*KMP*((Xk(12)/XBH
k(3))/(KSP+(Xk(12)/XBHk(3)))));
rUSNH3SS3=-
fZBH*muH*(Ks/(Ks+Xk(11)))*XBHk(3)*(Xk(9)/(KSA+Xk(9)))*((Uk(3)/(KOH+Uk(3)))+(KOH/(KOH+Uk(3)))*(Xk(10)/(KNO+Xk(10))));
rUSNH3Sads3=-
fZBH*KMP*((KSP/XBHk(3))/(KSP+(Xk(12)/XBHk(3))))*(Xk(9)/(KNA+Xk(9)))*((Uk(3)/(KOH+Uk(3)))+etag*(KOH/(KOH+Uk(3)))*(Xk(10)
/(KNO+Xk(10))));
rUSNO3SNH3=fZBH*(Uk(3)/(KOH+Uk(3)))*(KNA/(KNA+Xk(9))^2)*(Xk(10)/(KNO+Xk(10)))*XBHk(3)*(muH*(Xk(11)/(Ks+Xk(11)))+KMP*((X
k(12)/XBHk(3))/(KSP+(Xk(12)/XBHk(3))))+fZBH*(KOH/(KOH+Uk(3)))*(KNA/(KNA+Xk(9))^2)*(Xk(10)/(KNO+Xk(10)))*XBHk(3)*(muH*(X
k(11)/(Ks+Xk(11)))+KMP*etag*((Xk(12)/XBHk(3))/(KSP+(Xk(12)/XBHk(3))))+(1/YZA)*muA*(KSA/(KSA+Xk(9))^2)*(Xk(10)/KOA+Xk(10
)))*XBAk(3);
rUSNO3SNO3=-
fZBH*(Uk(3)/(KOH+Uk(3)))*(KSA/(KSA+Xk(9)))*(KNO/(KNO+Xk(10))^2)*XBHk(3)*(muH*(Xk(11)/(Ks+Xk(11)))+KMP*((Xk(12)/XBHk(3))
/(KSP+(Xk(12)/XBHk(3)))))-
(KOH/(KOH+Uk(3)))*(KNO/(KNO+Xk(10))^2)*XBHk(3)*(muH*(Xk(11)/(Ks+Xk(11)))+KMP*etag*((Xk(12)/XBHk(3))/(KSP+(Xk(12)/XBHk(3
)))))*(((1-YZH)/2.86*YZH)*(Xk(9)/(KNA+Xk(9)))+(((1-YZH)/2.86*YZH)+fZBH)*(KNA/(KNA+Xk(9))));
rUSNO3SS3=-muH*(Ks/(Ks+Xk(11))^2)*(Xk(10)/(KNO+Xk(10)))*XBHk(3)*(fZBH*(Uk(3)/(KOH+Uk(3)))*(KNA/(KNA+Xk(9)))+((1-
YZH)/2.86*YZH)*(KOH/(KOH+Uk(3)))*(Xk(9)/(KNA+Xk(9)))+((1-YZH)/2.86*YZH)+fZBH)*(KOH/(KOH+Uk(3)))*(KNA/(KNA+Xk(9)));
rUSNO3Sads3=-
KMP*((KSP/XBHk(3))/(KSP+(KSP/XBHk(3)))^2)*(Xk(10)/(KNO+Xk(10)))*XBHk(3)*(fZBH*(Uk(3)/(KOH+Uk(3)))*(KNA/(KNA+Xk(9)))+((1
-YZH)/2.86*YZH)*(KOH/(KOH+Uk(3)))*(Xk(9)/(KNA+Xk(9)))*etag+(((1-
YZH)/2.86*YZH)+fZBH)*(KOH/(KOH+Uk(3)))*(KNA/(KNA+Xk(9)))*etag);
rUSS3SNH3=-(1/YZH)*muH*(Xk(11)/(Ks+Xk(11)))*(Uk(3)/(KOH+Uk(3)))*(KNA/(KNA+Xk(9))^2)*XBHk(3)*(1-(Xk(10)/(KNO+Xk(10))));
rUSS3SNO3=-
(1/YZH)*muH*(Xk(11)/(Ks+Xk(11)))*(KNO/(KNO+Xk(10))^2)*XBHk(3)*((Uk(3)/(KOH+Uk(3)))*(KNA/(KNA+Xk(9)))+(KOH/(KOH+Uk(3)))*
(Xk(9)/(KNA+Xk(9)))+(KOH/(KOH+Uk(3)))*(KNA/(KNA+Xk(9))));
rUSS3SS3=-
(1/YZH)*(Ks/(Ks+Xk(11))^2)*((Uk(3)/(KOH+Uk(3)))*((Xk(9)/(KNA+Xk(9)))+(KNA/(KNA+Xk(9)))*(Xk(10)/(KNO+Xk(10))))+(KOH/(KOH
+Uk(3)))*(Xk(10)/(KNO+Xk(10)))*((Xk(9)/(KNA+Xk(9)))+(KNA/(KNA+Xk(9))))*XBHk(3);rUSS3Sads3=0;
```

```
rUSads3SNH3=-(1/YZH)*KMP*((Xk(12)/XBHk(3))/(KSP+(Xk(12)/XBHk(3))))*(Uk(3)/(KOH+Uk(3)))*(KNA/(KNA+Xk(9))^2)*XBHk(3)*(1-
(Xk(10)/(KNO+Xk(10))));
rUSads3SNO3=-
(1/YZH)*KMP*((Xk(12)/XBHk(3))/(KSP+(Xk(12)/XBHk(3))))*(KNO/(KNO+Xk(10))^2)*XBHk(3)*((Uk(3)/(KOH+Uk(3)))*(KNA/(KNA+Xk(9)
))+(KOH/(KOH+Uk(3)))*(Xk(9)/(KNA+Xk(9)))+(KOH/(KOH+Uk(3)))*(KNA/(KNA+Xk(9))));rUSads3SS3=0;
rUSads3Sads3=-
(1/YZH)*KMP*((KSP/XBHk(3))/(KSP+(Xk(12)/XBHk(3)))^2)*(Uk(3)/(KOH+Uk(3)))*XBHk(3)*((Xk(9)/(KNA+Xk(9)))*+(KNA/(KNA+Xk(9))
)*(Xk(10)/(KNO+Xk(10))))-
(1/YZH)*KMP*((KSP/XBHk(3))/(KSP+(Xk(12)/XBHk(3)))^2)*(KOH/(KOH+Uk(3)))*(Xk(10)/(KNO+Xk(10)))*etag*XBHk(3)*((Xk(9)/(KNA+
Xk(9)))+(KNA/(KNA+Xk(9))));


%Calculation of the derivatives of the process rates towards the process parameters
% Calculation for model parameters of rUSNH for the tank 1
rUSNH1f=0.0;rUSNH1YZH=0;rUSNH1YZA=(1/YZA)*muA*(Xk(1)/(KSA+Xk(1)))*(Uk(1)/(KOA+Uk(1)))*XBAk(1);
rUSNH1fZBH=-
(Uk(1)/(KOH+Uk(1)))*(Xk(1)/(KNA+Xk(1)))*XBHk(1)*(muH*(Xk(3)/(Ks+Xk(3)))+KMP*((Xk(4)/XBHk(1))/(KSP+(Xk(4)/XBHk(1)))))-
(KOH/(KOH+Uk(1)))*(Xk(1)/(KNA+Xk(1)))*(Xk(2)/(KNO+Xk(2)))*XBHk(1)*(muH*(Xk(3)/(Ks+Xk(3)))+KMP*etag*((Xk(4)/XBHk(1))/(KS
P+(Xk(4)/XBHk(1)))))-muA*(Xk(1)/(KSA+Xk(1)))*(Uk(1)/(KOA+Uk(1)))*XBAk(1);
rUSNH1muH=-
fZBH*(Xk(3)/(Ks+Xk(3)))*XBHk(1)*((Xk(1)/(KNA+Xk(1)))*(Uk(1)/(KOH+Uk(1)))+(KOH/(KOH+Uk(1)))*(Xk(2)/(KNO+Xk(2))));
rUSNH1muA=-((1/YZA)-fZBH)*(Xk(1)/(KSA+Xk(1)))*(Uk(1)/(KOA+Uk(1)))*XBAk(1);
rUSNH1Ks=fZBH*muH*(Xk(3)/(Ks+Xk(3))^2)*((Xk(1)/(KNA+Xk(1)))*XBHk(1)*((Uk(1)/(KOH+Uk(1)))+(KOH/(KOH+Uk(1)))*(Xk(2)/(KNO+
Xk(2)))));
rUSNH1KOH=fZBH*(Uk(1)/(KOH+Uk(1))^2)*(Xk(1)/(KNA+Xk(1)))*XBHk(1)*(muH*(Xk(3)/(Ks+Xk(3)))+KMP*((Xk(4)/XBHk(1))/(KSP+(Xk(
4)/XBHk(1)))))-
fZBH*(Uk(1)/(KOH+Uk(1))^2)*(Xk(1)/(KNA+Xk(1)))*(Xk(2)/(KNO+Xk(2)))*XBHk(1)*(muH*(Xk(3)/(Ks+Xk(3)))+KMP*etag*((Xk(4)/XBH
k(1))/(KSP+(Xk(4)/XBHk(1)))));
rUSNH1KNO=fZBH*(KOH/(KOH+Uk(1)))*(Xk(1)/(KNA+Xk(1)))*(Xk(2)/(KNO+Xk(2))^2)*XBHk(1)*(muH*(Xk(3)/(Ks+Xk(3)))+KMP*etag*((X
k(4)/XBHk(1))/(KSP+(Xk(4)/XBHk(1)))));
rUSNH1KNA=fZBH*(Uk(1)/(KOH+Uk(1)))*(Xk(1)/(KNA+Xk(1)))*XBHk(1)*(muH*(Xk(3)/(Ks+Xk(3)))+KMP*((Xk(4)/XBHk(1))/(KSP+(Xk(4)
/XBHk(1)))))+fZBH*(KOH/(KOH+Uk(1)))*(Xk(1)/(KNA+Xk(1))^2)*(Xk(2)/(KNO+Xk(2)))*XBHk(1)*(muH*(Xk(3)/(Ks+Xk(3)))+KMP*etag*
((Xk(4)/XBHk(1))/(KSP+(Xk(4)/XBHk(1)))));
rUSNH1KOA=((1/YZA)+fZBH)*muA*(Xk(1)/(KSA+Xk(1)))*(Uk(1)/(KOA+Uk(1))^2)*XBAk(1);
rUSNH1etag=-
KMP*((Xk(4)/XBHk(1))/(KSP+(Xk(4)/XBHk(1))))*(KOH/(KOH+Uk(1)))*(Xk(1)/(KNA+Xk(1)))*(Xk(2)/(KNO+Xk(2)))*XBHk(1)*fZBH;
rUSNH1KMP=((Xk(4)/XBHk(1))/(KSP+(Xk(4)/XBHk(1))))*(Xk(1)/(KNA+Xk(1)))*XBHk(1)*fZBH*((Uk(1)/(KOH+Uk(1)))+(KOH/(KOH+Uk(1)
)))*(Xk(2)/(KNO+Xk(2)))*etag);
rUSNH1KSP=fZBH*KMP*((Xk(4)/XBHk(1))/(KSP+(Xk(4)/XBHk(1))))*((Xk(1)/(KNA+Xk(1)))*(Uk(1)/(KOH+Uk(1)))+(KOH/(KOH+Uk(1)))*(
Xk(2)/(KNO+Xk(2))))*XBHk(1);
rUSNH1KSA=((1/YZA)+fZBH)*muA*(Xk(1)/(KSA+Xk(1))^2)*(Uk(1)/(KOA+Uk(1)))*XBAk(1);rUSNH1fMA=0.0;rUSNH1KA=0.0;

% Calculation for model parameters of rUSNO for the tank 1
rUSNO1f=0.0;
rUSNO1YZH=(1/(2.86*YZH^2))*(KOH/(KOH+Uk(1)))*(Xk(2)/(KNO+Xk(2)))*XBHk(1)*(muH*(Xk(3)/(Ks+Xk(3)))+KMP*etag*((Xk(4)/XBHk(
1))/(KSP+(Xk(4)/XBHk(1)))))*((Xk(1)/(KNA+Xk(1)))+(KNA/(KNA+Xk(1))));
rUSNO1YZA=(1/(2.86*YZH^2))*muA*(Xk(1)/(KSA+Xk(1)))*(Uk(1)/(KOA+Uk(1)))*XBAk(1);
rUSNO1fZBH=-
(Uk(1)/(KOH+Uk(1)))*(KNA/(KNA+Xk(1)))*(Xk(2)/(KNO+Xk(2)))*XBHk(1)*(muH*(Xk(3)/(Ks+Xk(3)))+KMP*((Xk(4)/XBHk(1))/(KSP+(Xk
(4)/XBHk(1)))));
rUSNO1muH=-
2*fZBH*(Xk(3)/(Ks+Xk(3)))*(KNA/(KNA+Xk(1)))*(Xk(2)/(KNO+Xk(2)))*XBHk(1)*((Uk(1)/(KOH+Uk(1)))+(KOH/(KOH+Uk(1))))-((1-
YZH)/2.86*YZH)*(Xk(3)/(Ks+Xk(3)))*(KOH/(KOH+Uk(1)))*(Xk(2)/(KNO+Xk(2)))*XBHk(1)*((Xk(1)/(KNA+Xk(1)))+(KNA/(KNA+Xk(1))))
;
rUSNO1muA=(1/YZA)*(Xk(1)/(KSA+Xk(1))^2)*(Uk(1)/(KOA+Uk(1)))*XBAk(1);
rUSNO1Ks=fZBH*muH*(Xk(3)/(Ks+Xk(3))^2)*(KNA/(KNA+Xk(1)))*(Xk(2)/(KNO+Xk(2)))*XBHk(1)*((Uk(1)/(KOH+Uk(1)))+(KOH/(KOH+Uk(
1))))+((1-
YZH)/2.86*YZH)*muH*(Xk(3)/(Ks+Xk(3)))*(KOH/(KOH+Uk(1)))*(Xk(2)/(KNO+Xk(2)))*XBHk(1)*((Xk(1)/(KNA+Xk(1)))+(KNA/(KNA+Xk(1
))));
rUSNO1KOH=-((1-
YZH)/2.86*YZH)*(KOH/(KOH+Uk(1))^2)*(Xk(2)/(KNO+Xk(2)))*XBHk(1)*(muH*(Xk(3)/(Ks+Xk(3)))+KMP*etag*((Xk(4)/XBHk(1))/(KSP+(
Xk(4)/XBHk(1)))))+fZBH*(Uk(1)/(KOH+Uk(1))^2)*(KNA/(KNA+Xk(1)))*(Xk(2)/(KNO+Xk(2)))*XBHk(1)*KMP*((Xk(4)/XBHk(1))/(KSP+(X
k(4)/XBHk(1))))*(1-etag);
rUSNO1KNO=fZBH*(Uk(1)/(KOH+Uk(1)))*(KNA/(KNA+Xk(1)))*(Xk(2)/(KNO+Xk(2))^2)*XBHk(1)*(muH*(Xk(3)/(Ks+Xk(3)))+KMP*((Xk(4)/
XBHk(1))/(KSP+(Xk(4)/XBHk(1)))))+((1-
YZH)/2.86*YZH)*(KOH/(KOH+Uk(1)))*(Xk(1)/(KNA+Xk(1)))*(Xk(2)/(KNO+Xk(2))^2)*XBHk(1)*(muH*(Xk(3)/(Ks+Xk(3)))+KMP*etag*((X
k(4)/XBHk(1))/(KSP+(Xk(4)/XBHk(1)))))+((1-
YZH)/2.86*YZH)+fZBH)*(KOH/(KOH+Uk(1)))*(KNA/(KNA+Xk(1)))*(Xk(2)/(KNO+Xk(2))^2)*XBHk(1)*(muH*(Xk(3)/(Ks+Xk(3)))+KMP*etag
*((Xk(4)/XBHk(1))/(KSP+(Xk(4)/XBHk(1)))));
rUSNO1KNA=-
fZBH*(Uk(1)/(KOH+Uk(1)))*(Xk(1)/(KNA+Xk(1)))*(Xk(2)/(KNO+Xk(2)))*XBHk(1)*(muH*(Xk(3)/(Ks+Xk(3)))+KMP*((Xk(4)/XBHk(1))/(
KSP+(Xk(4)/XBHk(1)))))-
fZBH*(KOH/(KOH+Uk(1)))*(Xk(1)/(KNA+Xk(1))^2)*(Xk(2)/(KNO+Xk(2)))*XBHk(1)*(muH*(Xk(3)/(Ks+Xk(3)))+KMP*etag*((Xk(4)/XBHk(
1))/(KSP+(Xk(4)/XBHk(1)))));
rUSNO1KOA=(1/YZA)*muA*(Xk(1)/(KSA+Xk(1))^2)*(Uk(1)/(KOA+Uk(1)))*XBAk(1);
rUSNO1etag=-((1-
YZH)/2.86*YZH)*KMP*((Xk(4)/XBHk(1))/(KSP+(Xk(4)/XBHk(1))))*(KOH/(KOH+Uk(1)))*(Xk(2)/(KNO+Xk(2)))*XBHk(1)*((Xk(1)/(KNA+X
k(1)))+(KNA/(KNA+Xk(1))))-
fZBH*KMP*((Xk(4)/XBHk(1))/(KSP+(Xk(4)/XBHk(1))))*(KOH/(KOH+Uk(1)))*(KNA/(KNA+Xk(1)))*(Xk(2)/(KNO+Xk(2)))*XBHk(1);
rUSNO1KMP=-
fZBH*((Xk(4)/XBHk(1))/(KSP+(Xk(4)/XBHk(1))))*(KNA/(KNA+Xk(1)))*(Xk(2)/(KNO+Xk(2)))*XBHk(1)*((Uk(1)/(KOH+Uk(1)))+etag*(K
OH/(KOH+Uk(1))))+((1-
YZH)/2.86*YZH)*((Xk(4)/XBHk(1))/(KSP+(Xk(4)/XBHk(1))))*(KOH/(KOH+Uk(1)))*(Xk(2)/(KNO+Xk(2)))*etag*XBHk(1)*((Xk(1)/(KNA+
Xk(1)))+(KNA/(KNA+Xk(1))));
rUSNO1KSP=fZBH*KMP*((Xk(4)/XBHk(1))/(KSP+(Xk(4)/XBHk(1))))*(KNA/(KNA+Xk(1)))*(Xk(2)/(KNO+Xk(2)))*XBHk(1)*((Uk(1)/(KOH+U
k(1)))+etag*(KOH/(KOH+Uk(1))))+((1-
YZH)/2.86*YZH)*((Xk(4)/XBHk(1))/(KSP+(Xk(4)/XBHk(1))))*(KOH/(KOH+Uk(1)))*(Xk(2)/(KNO+Xk(2)))*etag*XBHk(1)*((Xk(1)/(KNA+
Xk(1)))+(KNA/(KNA+Xk(1))));
rUSNO1KSA=-(1/YZA)*muA*(Xk(1)/(KSA+Xk(1))^2)*(Uk(1)/(KOA+Uk(1)))*XBAk(1);rUSNO1fMA=0;rUSNO1KA=0;

% Calculation for model parameters of rUSS for the tank 1
rUSS1f=0.0;
rUSS1YZH=(1/(YZH^2))*muH*(Xk(3)/(Ks+Xk(3)))*XBHk(1)*(Uk(1)/(KOH+Uk(1)))*((Xk(1)/(KNA+Xk(1)))+(KNA/(KNA+Xk(1))))*(Xk(2)/
(KNO+Xk(2)))+(KOH/(KOH+Uk(1)))*(Xk(2)/(KNO+Xk(2)))*((Xk(1)/(KNA+Xk(1)))+(KNA/(KNA+Xk(1))));rUSS1YZA=0;rUSS1fZBH=0;
```

```
rUSS1muH=-
(1/YZH)*(Xk(3)/(Ks+Xk(3)))*XBHk(1)*(Uk(1)/(KOH+Uk(1)))*((Xk(1)/(KNA+Xk(1)))+(KNA/(KNA+Xk(1))))*(Xk(2)/(KNO+Xk(2)))+(Uk(
1)/(KOH+Uk(1)))*((Xk(1)/(KNA+Xk(1)))+(KNA/(KNA+Xk(1))))*(Xk(2)/(KNO+Xk(2)));rUSS1muA=0;
rUSS1Ks=(1/YZH)*muH*(Xk(3)/(Ks+Xk(3)))*XBHk(1)*(Uk(1)/(KOH+Uk(1)))*((Xk(1)/(KNA+Xk(1)))+(KNA/(KNA+Xk(1))))*(Xk(2)/(KNO+
Xk(2)))+(KOH/(KOH+Uk(1)))*(Xk(2)/(KNO+Xk(2)))*((Xk(1)/(KNA+Xk(1)))+(KNA/(KNA+Xk(1))));
rUSS1KOH=(1/YZH)*muH*(Xk(3)/(Ks+Xk(3)))*(Uk(1)/(KOH+Uk(1)))*XBHk(1)*(Xk(1)/(KNA+Xk(1)))*(1-(Xk(2)/(KNO+Xk(2))));
rUSS1KNO=(1/YZH)*muH*(Xk(3)/(Ks+Xk(3)))*(Xk(2)/(KNO+Xk(2)))*XBHk(1)*(Uk(1)/(KOH+Uk(1)))*(KNA/(KNA+Xk(1)))+(KOH/(KOH+Uk(
1)))*((Xk(1)/(KNA+Xk(1)))+(KNA/(KNA+Xk(1))));
rUSS1KNA=(1/YZH)*muH*(Xk(3)/(Ks+Xk(3)))*(Xk(1)/(KNA+Xk(1))^2)*XBHk(1)*(Uk(1)/(KOH+Uk(1)))*(1-(Xk(2)/(KNO+Xk(2))));
rUSS1KOA=0;rUSS1etag=0;rUSS1KMP=0;rUSS1KSP=0;rUSS1KSA=0;rUSS1fMA=0;rUSS1KA=0;

% Calculation for model parameters of rUSads for the tank 1
rUSads1f=0.0;
rUSads1YZH=(1/(YZH^2))*KMP*((Xk(4)/XBHk(1))/(KSP+(Xk(4)/XBHk(1))))*XBHk(1)*(Uk(1)/(KOH+Uk(1)))*((Xk(1)/(KNA+Xk(1)))+(KN
A/(KNA+Xk(1))))*(Xk(2)/(KNO+Xk(2)))+etag*(KOH/(KOH+Uk(1)))*(Xk(2)/(KNO+Xk(2)))*((Xk(1)/(KNA+Xk(1)))+(KNA/(KNA+Xk(1))));
rUSads1YZA=0;rUSads1fZBH=0;rUSads1muH=0;rUSads1muA=0;rUSads1Ks=0;
rUSads1KOH=(1/YZH)*KMP*((Xk(4)/XBHk(1))/(KSP+(Xk(4)/XBHk(1))))*(Uk(1)/(KOH+Uk(1))^2)*XBHk(1)*(Xk(1)/(KNA+Xk(1)))*(1-
(Xk(2)/(KNO+Xk(2))));
rUSads1KNO=(1/YZH)*KMP*((Xk(4)/XBHk(1))/(KSP+(Xk(4)/XBHk(1))))*(Xk(2)/(KNO+Xk(2))^2)*XBHk(1)*(Uk(1)/(KOH+Uk(1)))*(KNA/(
KNA+Xk(1)))+etag*(KOH/(KOH+Uk(1)))*((Xk(1)/(KNA+Xk(1)))+(KNA/(KNA+Xk(1))));
rUSads1KNA=(1/YZH)*KMP*((Xk(4)/XBHk(1))/(KSP+(Xk(4)/XBHk(1))))*(Xk(1)/(KNA+Xk(1))^2)*XBHk(1)*(Uk(1)/(KOH+Uk(1)))*(1-
(Xk(2)/(KNO+Xk(2))));rUSads1KOA=0;
rUSads1etag=-
(1/YZH)*KMP*((Xk(4)/XBHk(1))/(KSP+(Xk(4)/XBHk(1))))*(KOH/(KOH+Uk(1)))*(Xk(2)/(KNO+Xk(2)))*etag*XBHk(1)*((Xk(1)/(KNA+Xk(
1)))+(KNA/(KNA+Xk(1))));
rUSads1KMP=-
(1/YZH)*((Xk(4)/XBHk(1))/(KSP+(Xk(4)/XBHk(1))))*XBHk(1)*(Uk(1)/(KOH+Uk(1)))*((Xk(1)/(KNA+Xk(1)))+(KNA/(KNA+Xk(1))))*(Xk
(2)/(KNO+Xk(2)))+etag*(KOH/(KOH+Uk(1)))*(Xk(2)/(KNO+Xk(2)))*((Xk(1)/(KNA+Xk(1)))+(KNA/(KNA+Xk(1))));
rUSads1KSP=(1/YZH)*KMP*((Xk(4)/XBHk(1))/(KSP+(Xk(4)/XBHk(1))))^2)*XBHk(1)*(Uk(1)/(KOH+Uk(1)))*((Xk(1)/(KNA+Xk(1)))+(KNA/
(KNA+Xk(1))))*(Xk(2)/(KNO+Xk(2)))+etag*(KOH/(KOH+Uk(1)))*(Xk(2)/(KNO+Xk(2)))*((Xk(1)/(KNA+Xk(1)))+(KNA/(KNA+Xk(1))));
rUSads1KSA=0;rUSads1fMA=KA*XSk(1)*XBHk(1);rUSads1KA=XSk(1)*XBHk(1)*(fMA-(Xk(4)/XBHk(1)));

% Calculation for model parameters of rUSNH for the tank 2
rUSNH2f=0.0;rUSNH2YZH=0;
rUSNH2YZA=(1/YZA)*muA*(Xk(5)/(KSA+Xk(5)))*(Uk(2)/(KOA+Uk(2)))*XBAk(2);
rUSNH2fZBH=-
(Uk(2)/(KOH+Uk(2)))*(Xk(5)/(KNA+Xk(5)))*XBHk(2)*(muH*(Xk(7)/(Ks+Xk(7)))+KMP*((Xk(8)/XBHk(2))/(KSP+(Xk(8)/XBHk(2)))))-
(KOH/(KOH+Uk(2)))*(Xk(5)/(KNA+Xk(5)))*(Xk(6)/(KNO+Xk(6)))*XBHk(2)*(muH*(Xk(7)/(Ks+Xk(7)))+KMP*etag*((Xk(8)/XBHk(2))/(KS
P+(Xk(8)/XBHk(2)))))-muA*(Xk(5)/(KSA+Xk(5)))*(Uk(2)/(KOA+Uk(2)))*XBAk(2);
rUSNH2muH=-
fZBH*(Xk(7)/(Ks+Xk(7)))*XBHk(2)*((Xk(5)/(KNA+Xk(5)))*(Uk(2)/(KOH+Uk(2)))+(KOH/(KOH+Uk(2)))*(Xk(6)/(KNO+Xk(6))));
rUSNH2muA=-((1/YZA)-fZBH)*(Xk(5)/(KSA+Xk(5)))*(Uk(2)/(KOA+Uk(2)))*XBAk(2);
rUSNH2Ks=fZBH*muH*(Xk(7)/(Ks+Xk(7)))^2)*(Xk(5)/(KNA+Xk(5)))*XBHk(2)*((Uk(2)/(KOH+Uk(2)))+(KOH/(KOH+Uk(2)))*(Xk(6)/(KNO+X
k(6))));
rUSNH2KOH=fZBH*(Uk(2)/(KOH+Uk(2))^2)*(Xk(5)/(KNA+Xk(5)))*XBHk(2)*(muH*(Xk(7)/(Ks+Xk(7)))+KMP*((Xk(8)/XBHk(2))/(KSP+(Xk(
8)/XBHk(2)))))-
fZBH*(Uk(2)/(KOH+Uk(2))^2)*(Xk(5)/(KNA+Xk(5)))*(Xk(6)/(KNO+Xk(6)))*XBHk(2)*(muH*(Xk(7)/(Ks+Xk(7)))+KMP*etag*((Xk(8)/XBH
k(2))/(KSP+(Xk(8)/XBHk(2)))));
rUSNH2KNO=fZBH*(KOH/(KOH+Uk(2)))*(Xk(5)/(KNA+Xk(5)))*(Xk(6)/(KNO+Xk(6))^2)*XBHk(2)*(muH*(Xk(7)/(Ks+Xk(7)))+KMP*etag*((X
k(8)/XBHk(2))/(KSP+(Xk(8)/XBHk(2)))));
rUSNH2KNA=fZBH*(Uk(2)/(KOH+Uk(2)))*(Xk(5)/(KNA+Xk(5)))*XBHk(2)*(muH*(Xk(7)/(Ks+Xk(7)))+KMP*((Xk(8)/XBHk(2))/(KSP+(Xk(8)
/XBHk(2)))))+fZBH*(KOH/(KOH+Uk(2)))*(Xk(5)/(KNA+Xk(5))^2)*(Xk(6)/(KNO+Xk(6)))*XBHk(2)*(muH*(Xk(7)/(Ks+Xk(7)))+KMP*etag*
((Xk(8)/XBHk(2))/(KSP+(Xk(8)/XBHk(2)))));
rUSNH2KOA=((1/YZA)+fZBH)*muA*(Xk(5)/(KSA+Xk(5)))*(Uk(2)/(KOA+Uk(2))^2)*XBAk(2);
rUSNH2etag=-
KMP*((Xk(8)/XBHk(2))/(KSP+(Xk(8)/XBHk(2))))*(KOH/(KOH+Uk(2)))*(Xk(5)/(KNA+Xk(5)))*(Xk(6)/(KNO+Xk(6)))*XBHk(2)*fZBH;
rUSNH2KMP=((Xk(8)/XBHk(2))/(KSP+(Xk(8)/XBHk(2))))*(Xk(5)/(KNA+Xk(5)))*XBHk(2)*fZBH*((Uk(2)/(KOH+Uk(2)))+(KOH/(KOH+Uk(2)
))*(Xk(6)/(KNO+Xk(6)))*etag);
rUSNH2KSP=fZBH*KMP*((Xk(8)/XBHk(2))/(KSP+(Xk(8)/XBHk(2))))*((Xk(5)/(KNA+Xk(5)))*(Uk(2)/(KOH+Uk(2)))+(KOH/(KOH+Uk(2)))*(
Xk(6)/(KNO+Xk(6))))*XBHk(2);
rUSNH2KSA=((1/YZA)+fZBH)*muA*(Xk(5)/(KSA+Xk(5))^2)*(Uk(2)/(KOA+Uk(2)))*XBAk(2);rUSNH2fMA=0.0;rUSNH2KA=0.0;

% Calculation for model parameters of rUSNO for the tank 2
rUSNO2f=0.0;
rUSNO2YZH=(1/(2.86*YZH^2))*(KOH/(KOH+Uk(2)))*(Xk(6)/(KNO+Xk(6)))*XBHk(2)*(muH*(Xk(7)/(Ks+Xk(7)))+KMP*etag*((Xk(8)/XBHk(
2))/(KSP+(Xk(8)/XBHk(2)))))*((Xk(5)/(KNA+Xk(5)))+(KNA/(KNA+Xk(5))));
rUSNO2YZA=(1/(2.86*YZH^2))*muA*(Xk(5)/(KSA+Xk(5)))*(Uk(2)/(KOA+Uk(2)))*XBAk(2);
rUSNO2fZBH=-
(Uk(2)/(KOH+Uk(2)))*(KNA/(KNA+Xk(5)))*(Xk(6)/(KNO+Xk(6)))*XBHk(2)*(muH*(Xk(7)/(Ks+Xk(7)))+KMP*((Xk(8)/XBHk(2))/(KSP+(Xk
(8)/XBHk(2)))));
rUSNO2muH=-
2*fZBH*(Xk(7)/(Ks+Xk(7)))*(KNA/(KNA+Xk(5)))*(Xk(6)/(KNO+Xk(6)))*XBHk(2)*((Uk(2)/(KOH+Uk(2)))+(KOH/(KOH+Uk(2))))-((1-
YZH)/2.86*YZH)*(Xk(7)/(Ks+Xk(7)))*(KOH/(KOH+Uk(2)))*(Xk(6)/(KNO+Xk(6)))*XBHk(2)*((Xk(5)/(KNA+Xk(5)))+(KNA/(KNA+Xk(5))))
;
rUSNO2muA=(1/YZA)*(Xk(5)/(KSA+Xk(5)))^2)*(Uk(2)/(KOA+Uk(2)))*XBAk(2);
rUSNO2Ks=fZBH*muH*(Xk(7)/(Ks+Xk(7)))^2)*(KNA/(KNA+Xk(5)))*(Xk(6)/(KNO+Xk(6)))*XBHk(2)*((Uk(2)/(KOH+Uk(2)))+(KOH/(KOH+Uk(
2))))+((1-
YZH)/2.86*YZH)*muH*(Xk(7)/(Ks+Xk(7)))*(KOH/(KOH+Uk(2)))*(Xk(6)/(KNO+Xk(6)))*XBHk(2)*((Xk(5)/(KNA+Xk(5)))+(KNA/(KNA+Xk(5
))));
rUSNO2KOH=-((1-
YZH)/2.86*YZH)*(KOH/(KOH+Uk(2)))^2)*(Xk(6)/(KNO+Xk(6)))*XBHk(2)*(muH*(Xk(7)/(Ks+Xk(7)))+KMP*etag*((Xk(8)/XBHk(2))/(KSP+(
Xk(8)/XBHk(2)))))+fZBH*(Uk(2)/(KOH+Uk(2)))^2)*(KNA/(KNA+Xk(5)))*(Xk(6)/(KNO+Xk(6)))*XBHk(2)*KMP*((Xk(8)/XBHk(2))/(KSP+(X
k(8)/XBHk(2))))*(1-etag);
rUSNO2KNO=fZBH*(Uk(2)/(KOH+Uk(2)))*(KNA/(KNA+Xk(5)))*(Xk(6)/(KNO+Xk(6)))^2)*XBHk(2)*(muH*(Xk(7)/(Ks+Xk(7)))+KMP*((Xk(8)/
XBHk(2))/(KSP+(Xk(8)/XBHk(2)))))+((1-
YZH)/2.86*YZH)*(KOH/(KOH+Uk(2)))*(Xk(5)/(KNA+Xk(5)))*(Xk(6)/(KNO+Xk(6)))^2)*XBHk(2)*(muH*(Xk(7)/(Ks+Xk(7)))+KMP*etag*((X
k(8)/XBHk(2))/(KSP+(Xk(8)/XBHk(2)))))+(((1-
YZH)/2.86*YZH)+fZBH)*(KOH/(KOH+Uk(2)))*(KNA/(KNA+Xk(5)))*(Xk(6)/(KNO+Xk(6)))^2)*XBHk(2)*(muH*(Xk(7)/(Ks+Xk(7)))+KMP*etag
*((Xk(8)/XBHk(2))/(KSP+(Xk(8)/XBHk(2)))));
rUSNO2KNA=-
fZBH*(Uk(2)/(KOH+Uk(2)))*(Xk(5)/(KNA+Xk(5)))*(Xk(6)/(KNO+Xk(6)))*XBHk(2)*(muH*(Xk(7)/(Ks+Xk(7)))+KMP*((Xk(8)/XBHk(2))/(
KSP+(Xk(8)/XBHk(2)))))-
fZBH*(KOH/(KOH+Uk(2)))*(Xk(5)/(KNA+Xk(5))^2)*(Xk(6)/(KNO+Xk(6)))*XBHk(2)*(muH*(Xk(7)/(Ks+Xk(7)))+KMP*etag*((Xk(8)/XBHk(
2))/(KSP+(Xk(8)/XBHk(2)))));
rUSNO2KOA=(1/YZA)*muA*(Xk(5)/(KSA+Xk(5))^2)*(Uk(2)/(KOA+Uk(2)))*XBAk(2);
```

```
rUSNO2etag=-((1-
YZH)/2.86*YZH)*KMP*((Xk(8)/XBHk(2))/(KSP+(Xk(8)/XBHk(2))))*(KOH/(KOH+Uk(2)))*(Xk(6)/(KNO+Xk(6)))*XBHk(2)*((Xk(5)/(KNA+X
k(5)))+(KNA/(KNA+Xk(5))))-
fZBH*KMP*((Xk(8)/XBHk(2))/(KSP+(Xk(8)/XBHk(2))))*(KOH/(KOH+Uk(2)))*(KNA/(KNA+Xk(5)))*(Xk(6)/(KNO+Xk(6)))*XBHk(2);
rUSNO2KMP=-
fZBH*((Xk(8)/XBHk(2))/(KSP+(Xk(8)/XBHk(2))))*(KNA/(KNA+Xk(5)))*(Xk(6)/(KNO+Xk(6)))*XBHk(2)*((Uk(2)/(KOH+Uk(2)))+etag*(K
OH/(KOH+Uk(2))))-((1-
YZH)/2.86*YZH)*((Xk(8)/XBHk(2))/(KSP+(Xk(8)/XBHk(2))))*(KOH/(KOH+Uk(2)))*(Xk(6)/(KNO+Xk(6)))*etag*XBHk(2)*((Xk(5)/(KNA+
Xk(5)))+(KNA/(KNA+Xk(5))));
rUSNO2KSP=fZBH*KMP*((Xk(8)/XBHk(2))/(KSP+(Xk(8)/XBHk(2))))*(KNA/(KNA+Xk(5)))*(Xk(6)/(KNO+Xk(6)))*XBHk(2)*((Uk(2)/(KOH+U
k(2)))+etag*(KOH/(KOH+Uk(2))))+((1-
YZH)/2.86*YZH)*((Xk(8)/XBHk(2))/(KSP+(Xk(8)/XBHk(2))))*(KOH/(KOH+Uk(2)))*(Xk(6)/(KNO+Xk(6)))*etag*XBHk(2)*((Xk(5)/(KNA+
Xk(5)))+(KNA/(KNA+Xk(5))));
rUSNO2KSA=-(1/YZA)*(Xk(5)/(KSA+Xk(5))^2)*(Uk(2)/(KOA+Uk(2)))*XBAk(2);rUSNO2fMA=0;rUSNO2KA=0;

% Calculation for model parameters of rUSS for the tank 2
rUSS2f=0.0;
rUSS2YZH=(1/(YZH^2))*muH*(Xk(7)/(Ks+Xk(7)))*XBHk(2)*(Uk(2)/(KOH+Uk(2)))*((Xk(5)/(KNA+Xk(5)))+(KNA/(KNA+Xk(5))))*(Xk(6)/
(KNO+Xk(6)))+(KOH/(KOH+Uk(2)))*(Xk(6)/(KNO+Xk(6)))*((Xk(5)/(KNA+Xk(5)))+(KNA/(KNA+Xk(5))));
rUSS2YZA=0;rUSS2fZBH=0;
rUSS2muH=-
(1/YZH)*(Xk(7)/(Ks+Xk(7)))*XBHk(1)*(Uk(2)/(KOH+Uk(2)))*((Xk(5)/(KNA+Xk(5)))+(KNA/(KNA+Xk(5))))*(Xk(6)/(KNO+Xk(6)))+(Uk(
2)/(KOH+Uk(2)))*((Xk(5)/(KNA+Xk(5)))+(KNA/(KNA+Xk(5))))*(Xk(6)/(KNO+Xk(6)));rUSS2muA=0;
rUSS2Ks=(1/YZH)*muH*(Xk(7)/(Ks+Xk(7)))*XBHk(2)*(Uk(2)/(KOH+Uk(2)))*((Xk(5)/(KNA+Xk(5)))+(KNA/(KNA+Xk(5))))*(Xk(6)/(KNO+
Xk(6)))+(KOH/(KOH+Uk(2)))*(Xk(6)/(KNO+Xk(6)))*((Xk(5)/(KNA+Xk(5)))+(KNA/(KNA+Xk(5))));
rUSS2KOH=(1/YZH)*muH*(Xk(7)/(Ks+Xk(7)))*(Uk(2)/(KOH+Uk(2)))*XBHk(2)*(Xk(5)/(KNA+Xk(5)))*(1-(Xk(6)/(KNO+Xk(6))));
rUSS2KNO=(1/YZH)*muH*(Xk(7)/(Ks+Xk(7)))*(Xk(6)/(KNO+Xk(6)))*XBHk(2)*(Uk(1)/(KOH+Uk(2)))*(KNA/(KNA+Xk(5)))+(KOH/(KOH+Uk(
2)))*((Xk(5)/(KNA+Xk(5)))+(KNA/(KNA+Xk(5))));
rUSS2KNA=(1/YZH)*muH*(Xk(7)/(Ks+Xk(7)))*(Xk(5)/(KNA+Xk(5))^2)*XBHk(2)*(Uk(2)/(KOH+Uk(2)))*(1-(Xk(6)/(KNO+Xk(6))));
rUSS2KOA=0;rUSS2etag=0;rUSS2KMP=0;rUSS2KSP=0;rUSS2KSA=0;rUSS2fMA=0;rUSS2KA=0;

% Calculation for model parameters of rUSads for the tank 2
rUSads2f=0.0;
rUSads2YZH=(1/(YZH^2))*KMP*((Xk(8)/XBHk(2))/(KSP+(Xk(8)/XBHk(2))))*XBHk(2)*(Uk(2)/(KOH+Uk(2)))*((Xk(5)/(KNA+Xk(5)))+(KN
A/(KNA+Xk(5))))*(Xk(6)/(KNO+Xk(6)))+etag*(KOH/(KOH+Uk(2)))*(Xk(6)/(KNO+Xk(6)))*((Xk(5)/(KNA+Xk(5)))+(KNA/(KNA+Xk(5))));
rUSads2YZA=0;rUSads2fZBH=0;rUSads2muH=0;rUSads2muA=0;rUSads2Ks=0;
rUSads2KOH=(1/YZH)*KMP*((Xk(8)/XBHk(2))/(KSP+(Xk(8)/XBHk(2))))*(Uk(2)/(KOH+Uk(2))^2)*XBHk(2)*(Xk(5)/(KNA+Xk(5)))*(1-
(Xk(6)/(KNO+Xk(6))));
rUSads2KNO=(1/YZH)*KMP*((Xk(8)/XBHk(2))/(KSP+(Xk(8)/XBHk(2))))*(Xk(6)/(KNO+Xk(6))^2)*XBHk(2)*(Uk(2)/(KOH+Uk(2)))*(KNA/(
KNA+Xk(5)))+etag*(KOH/(KOH+Uk(2)))*((Xk(5)/(KNA+Xk(5)))+(KNA/(KNA+Xk(5))));
rUSads2KNA=(1/YZH)*KMP*((Xk(8)/XBHk(2))/(KSP+(Xk(8)/XBHk(2))))*(Xk(5)/(KNA+Xk(5))^2)*XBHk(2)*(Uk(2)/(KOH+Uk(2)))*(1-
(Xk(6)/(KNO+Xk(6))));rUSads2KOA=0;
rUSads2etag=-
(1/YZH)*KMP*((Xk(8)/XBHk(2))/(KSP+(Xk(8)/XBHk(2))))*(KOH/(KOH+Uk(2)))*(Xk(6)/(KNO+Xk(6)))*etag*XBHk(2)*((Xk(5)/(KNA+Xk(
5)))+(KNA/(KNA+Xk(5))));
rUSads2KMP=-
(1/YZH)*((Xk(8)/XBHk(2))/(KSP+(Xk(8)/XBHk(2))))*XBHk(2)*(Uk(2)/(KOH+Uk(2)))*((Xk(5)/(KNA+Xk(5)))+(KNA/(KNA+Xk(5))))*(Xk
(6)/(KNO+Xk(6)))+etag*(KOH/(KOH+Uk(2)))*(Xk(6)/(KNO+Xk(6)))*((Xk(5)/(KNA+Xk(5)))+(KNA/(KNA+Xk(5))));
rUSads2KSP=(1/YZH)*KMP*((Xk(8)/XBHk(2))/(KSP+(Xk(8)/XBHk(2)))^2)*XBHk(2)*(Uk(2)/(KOH+Uk(2)))*((Xk(5)/(KNA+Xk(5)))+(KNA/
(KNA+Xk(5))))*(Xk(6)/(KNO+Xk(6)))+etag*(KOH/(KOH+Uk(2)))*(Xk(6)/(KNO+Xk(6)))*((Xk(5)/(KNA+Xk(5)))+(KNA/(KNA+Xk(5))));
rUSads2KSA=0;rUSads2fMA=KA*XSk(2)*XBHk(2);rUSads2KA=XSk(2)*XBHk(2)*(fMA-(Xk(8)/XBHk(2)));

% Calculation for model parameters of rUSNH for the tank 3
rUSNH3f=0.0;rUSNH3YZH=0;rUSNH3YZA=(1/YZA)*muA*(Xk(9)/(KSA+Xk(9)))*(Uk(3)/(KOA+Uk(3)))*XBAk(3);
rUSNH3fZBH=-
(Uk(3)/(KOH+Uk(3)))*(Xk(9)/(KNA+Xk(9)))*XBHk(3)*(muH*(Xk(11)/(Ks+Xk(11)))+KMP*((Xk(12)/XBHk(3))/(KSP+(Xk(12)/XBHk(3))))
)-
(KOH/(KOH+Uk(3)))*(Xk(9)/(KNA+Xk(9)))*(Xk(10)/(KNO+Xk(10)))*XBHk(3)*(muH*(Xk(11)/(Ks+Xk(11)))+KMP*etag*((Xk(12)/XBHk(3)
)/(KSP+(Xk(12)/XBHk(3)))))-muA*(Xk(9)/(KSA+Xk(9)))*(Uk(3)/(KOA+Uk(3)))*XBAk(3);
rUSNH3muH=-
fZBH*(Xk(11)/(Ks+Xk(11)))*XBHk(3)*((Xk(9)/(KNA+Xk(9)))*(Uk(3)/(KOH+Uk(3)))+(KOH/(KOH+Uk(3)))*(Xk(10)/(KNO+Xk(10))));
rUSNH3muA=-((1/YZA)-fZBH)*(Xk(9)/(KSA+Xk(9)))*(Uk(3)/(KOA+Uk(3)))*XBAk(3);
rUSNH3Ks=fZBH*muH*(Xk(11)/(Ks+Xk(11)))^2)*(Xk(9)/(KNA+Xk(9)))*XBHk(3)*((Uk(3)/(KOH+Uk(3)))+(KOH/(KOH+Uk(3)))*(Xk(10)/(KN
O+Xk(10))));
rUSNH3KOH=fZBH*(Uk(3)/(KOH+Uk(3))^2)*(Xk(9)/(KNA+Xk(9)))*XBHk(3)*(muH*(Xk(11)/(Ks+Xk(11)))+KMP*((Xk(12)/XBHk(3))/(KSP+(
Xk(12)/XBHk(3)))))-
fZBH*(Uk(3)/(KOH+Uk(3))^2)*(Xk(9)/(KNA+Xk(9)))*(Xk(10)/(KNO+Xk(10)))*XBHk(3)*(muH*(Xk(11)/(Ks+Xk(11)))+KMP*etag*((Xk(12
)/XBHk(3))/(KSP+(Xk(12)/XBHk(3)))));
rUSNH3KNO=fZBH*(KOH/(KOH+Uk(3)))*(Xk(9)/(KNA+Xk(9)))*(Xk(10)/(KNO+Xk(10))^2)*XBHk(3)*(muH*(Xk(11)/(Ks+Xk(11)))+KMP*etag
*((Xk(12)/XBHk(3))/(KSP+(Xk(12)/XBHk(3)))));
rUSNH3KNA=fZBH*(Uk(3)/(KOH+Uk(3)))*(Xk(9)/(KNA+Xk(9)))*XBHk(3)*(muH*(Xk(11)/(Ks+Xk(11)))+KMP*((Xk(12)/XBHk(3))/(KSP+(Xk
(12)/XBHk(3)))))+fZBH*(KOH/(KOH+Uk(3)))*(Xk(9)/(KNA+Xk(9))^2)*(Xk(10)/(KNO+Xk(10)))*XBHk(3)*(muH*(Xk(11)/(Ks+Xk(11)))+K
MP*etag*((Xk(12)/XBHk(3))/(KSP+(Xk(12)/XBHk(3)))));
rUSNH3KOA=((1/YZA)+fZBH)*muA*(Xk(9)/(KSA+Xk(9)))*(Uk(3)/(KOA+Uk(3))^2)*XBAk(3);
rUSNH3etag=-
KMP*((Xk(12)/XBHk(3))/(KSP+(Xk(12)/XBHk(3))))*(KOH/(KOH+Uk(3)))*(Xk(9)/(KNA+Xk(9)))*(Xk(10)/(KNO+Xk(10)))*XBHk(3)*fZBH;
rUSNH3KMP=((Xk(12)/XBHk(3))/(KSP+(Xk(12)/XBHk(3))))*(Xk(9)/(KNA+Xk(9)))*XBHk(3)*fZBH*((Uk(3)/(KOH+Uk(3)))+(KOH/(KOH+Uk(
3)))*(Xk(10)/(KNO+Xk(10)))*etag);
rUSNH3KSP=fZBH*KMP*((Xk(12)/XBHk(3))/(KSP+(Xk(12)/XBHk(3))))*((Xk(9)/(KNA+Xk(9)))*(Uk(3)/(KOH+Uk(3)))+(KOH/(KOH+Uk(3)))
*(Xk(10)/(KNO+Xk(10))))*XBHk(3);
rUSNH3KSA=((1/YZA)+fZBH)*muA*(Xk(9)/(KSA+Xk(9)))^2)*(Uk(3)/(KOA+Uk(3)))*XBAk(3);rUSNH3fMA=0.0;rUSNH3KA=0.0;

% Calculation for model parameters of rUSNO for the tank 3
rUSNO3f=0.0;
rUSNO3YZH=(1/(2.86*YZH^2))*(KOH/(KOH+Uk(3)))*(Xk(10)/(KNO+Xk(10)))*XBHk(3)*(muH*(Xk(11)/(Ks+Xk(11)))+KMP*etag*((Xk(12)/
XBHk(3))/(KSP+(Xk(12)/XBHk(3)))))*((Xk(9)/(KNA+Xk(9)))+(KNA/(KNA+Xk(9))));
rUSNO3YZA=(1/(2.86*YZH^2))*muA*(Xk(9)/(KSA+Xk(9)))*(Uk(3)/(KOA+Uk(3)))*XBAk(3);
rUSNO3fZBH=-
(Uk(3)/(KOH+Uk(3)))*(KNA/(KNA+Xk(9)))*(Xk(10)/(KNO+Xk(10)))*XBHk(3)*(muH*(Xk(11)/(Ks+Xk(11)))+KMP*((Xk(12)/XBHk(3))/(KS
P+(Xk(12)/XBHk(3)))));
rUSNO3muH=-
2*fZBH*(Xk(11)/(Ks+Xk(11)))*(KNA/(KNA+Xk(9)))*(Xk(10)/(KNO+Xk(10)))*XBHk(3)*((Uk(3)/(KOH+Uk(3)))+(KOH/(KOH+Uk(3))))-
((1-
YZH)/2.86*YZH)*(Xk(11)/(Ks+Xk(11)))*(KOH/(KOH+Uk(3)))*(Xk(10)/(KNO+Xk(10)))*XBHk(3)*((Xk(9)/(KNA+Xk(9)))+(KNA/(KNA+Xk(9
))));
```

```
rUSNO3muA=(1/YZA)*(Xk(9)/(KSA+Xk(9))^2)*(Uk(3)/(KOA+Uk(3)))*XBAk(3);
rUSNO3Ks=fZBH*muH*(Xk(11)/(Ks+Xk(11))^2)*(KNA/(KNA+Xk(9)))*(Xk(10)/(KNO+Xk(10)))*XBHk(3)*((Uk(3)/(KOH+Uk(3)))+(KOH/(KOH
+Uk(3))))+((1-
YZH)/2.86*YZH)*muH*(Xk(11)/(Ks+Xk(11)))*(KOH/(KOH+Uk(3)))*(Xk(10)/(KNO+Xk(10)))*XBHk(3)*((Xk(9)/(KNA+Xk(9)))+(KNA/(KNA+
Xk(9))));
rUSNO3KOH=-((1-
YZH)/2.86*YZH)*(KOH/(KOH+Uk(3))^2)*(Xk(10)/(KNO+Xk(10)))*XBHk(3)*(muH*(Xk(11)/(Ks+Xk(11)))+KMP*etag*((Xk(12)/XBHk(3))/(
KSP+(Xk(12)/XBHk(3)))))+fZBH*(Uk(3)/(KOH+Uk(3))^2)*(KNA/(KNA+Xk(9)))*(Xk(10)/(KNO+Xk(10)))*XBHk(3)*KMP*((Xk(12)/XBHk(3)
)/(KSP+(Xk(12)/XBHk(3))))*(1-etag);
rUSNO3KNO=fZBH*(Xk(11)/(Ks+Xk(11)))*(KNA/(KNA+Xk(9)))*(Xk(10)/(KNO+Xk(10))^2)*XBHk(3)*(muH*(Xk(11)/(Ks+Xk(11)))+KMP*((X
k(12)/XBHk(3))/(KSP+(Xk(12)/XBHk(3)))))+((1-
YZH)/2.86*YZH)*(KOH/(KOH+Uk(3)))*(Xk(9)/(KNA+Xk(9)))*(Xk(10)/(KNO+Xk(10))^2)*XBHk(3)*(muH*(Xk(11)/(Ks+Xk(11)))+KMP*etag
*((Xk(12)/XBHk(3))/(KSP+(Xk(12)/XBHk(3)))))+(((1-
YZH)/2.86*YZH)+fZBH)*(KOH/(KOH+Uk(3)))*(KNA/(KNA+Xk(9)))*(Xk(10)/(KNO+Xk(10))^2)*XBHk(3)*(muH*(Xk(11)/(Ks+Xk(11)))+KMP*
etag*((Xk(12)/XBHk(3))/(KSP+(Xk(12)/XBHk(3)))));
rUSNO3KNA=-
fZBH*(Uk(3)/(KOH+Uk(3)))*(Xk(9)/(KNA+Xk(9)))*(Xk(10)/(KNO+Xk(10)))*XBHk(3)*(muH*(Xk(11)/(Ks+Xk(11)))+KMP*((Xk(12)/XBHk(
3))/(KSP+(Xk(12)/XBHk(3)))))-
fZBH*(KOH/(KOH+Uk(3)))*(Xk(9)/(KNA+Xk(9))^2)*(Xk(10)/(KNO+Xk(10)))*XBHk(3)*(muH*(Xk(11)/(Ks+Xk(11)))+KMP*etag*((Xk(12)/
XBHk(3))/(KSP+(Xk(12)/XBHk(3)))));
rUSNO3KOA=(1/YZA)*muA*(Xk(9)/(KSA+Xk(9))^2)*(Uk(3)/(KOA+Uk(3)))*XBAk(3);
rUSNO3etag=-((1-
YZH)/2.86*YZH)*KMP*((Xk(12)/XBHk(3))/(KSP+(Xk(12)/XBHk(3))))*(KOH/(KOH+Uk(3)))*(Xk(10)/(KNO+Xk(10)))*XBHk(3)*((Xk(9)/(K
NA+Xk(9)))+(KNA/(KNA+Xk(9))))-
fZBH*KMP*((Xk(12)/XBHk(3))/(KSP+(Xk(12)/XBHk(3))))*(KOH/(KOH+Uk(3)))*(KNA/(KNA+Xk(9)))*(Xk(10)/(KNO+Xk(10)))*XBHk(3);
rUSNO3KMP=-
fZBH*((Xk(12)/XBHk(3))/(KSP+(Xk(12)/XBHk(3))))*(KNA/(KNA+Xk(9)))*(Xk(10)/(KNO+Xk(10)))*XBHk(3)*((Uk(3)/(KOH+Uk(3)))+eta
g*(KOH/(KOH+Uk(3))))-((1-
YZH)/2.86*YZH)*((Xk(12)/XBHk(3))/(KSP+(Xk(12)/XBHk(3))))*(KOH/(KOH+Uk(3)))*(Xk(10)/(KNO+Xk(10)))*etag*XBHk(3)*((Xk(9)/(
KNA+Xk(9)))+(KNA/(KNA+Xk(9))));
rUSNO3KSP=fZBH*KMP*((Xk(12)/XBHk(3))/(KSP+(Xk(12)/XBHk(3))))*(KNA/(KNA+Xk(9)))*(Xk(10)/(KNO+Xk(10)))*XBHk(3)*((Uk(3)/(K
OH+Uk(3)))+etag*(KOH/(KOH+Uk(3))))+((1-
YZH)/2.86*YZH)*((Xk(12)/XBHk(3))/(KSP+(Xk(12)/XBHk(3))))*(KOH/(KOH+Uk(3)))*(Xk(10)/(KNO+Xk(10)))*etag*XBHk(3)*((Xk(9)/(
KNA+Xk(9)))+(KNA/(KNA+Xk(9))));
rUSNO3KSA=-(1/YZA)*(Xk(9)/(KSA+Xk(9))^2)*(Uk(3)/(KOA+Uk(3)))*XBAk(3);rUSNO3fMA=0;rUSNO3KA=0;

% Calculation for model parameters of rUSS for the tank 3
rUSS3f=0.0;
rUSS3YZH=(1/(YZH^2))*muH*(Xk(11)/(Ks+Xk(11)))*XBHk(3)*(Uk(3)/(KOH+Uk(3)))*((Xk(9)/(KNA+Xk(9)))+(KNA/(KNA+Xk(9))))*(Xk(1
0)/(KNO+Xk(10)))+(KOH/(KOH+Uk(3)))*(Xk(10)/(KNO+Xk(10)))*((Xk(9)/(KNA+Xk(9)))+(KNA/(KNA+Xk(9))));
rUSS3YZA=0;rUSS3fZBH=0;
rUSS3muH=-
(1/YZH)*(Xk(11)/(Ks+Xk(11)))*XBHk(3)*(Uk(3)/(KOH+Uk(3)))*((Xk(9)/(KNA+Xk(9)))+(KNA/(KNA+Xk(9))))*(Xk(10)/(KNO+Xk(10)))+
(Uk(3)/(KOH+Uk(3)))*((Xk(9)/(KNA+Xk(9)))+(KNA/(KNA+Xk(9))))*(Xk(10)/(KNO+Xk(10)));
rUSS3muA=0;
rUSS3Ks=(1/YZH)*muH*(Xk(11)/(Ks+Xk(11)))*XBHk(3)*(Uk(3)/(KOH+Uk(3)))*((Xk(9)/(KNA+Xk(9)))+(KNA/(KNA+Xk(9))))*(Xk(10)/(K
NO+Xk(10)))+(KOH/(KOH+Uk(3)))*(Xk(10)/(KNO+Xk(10)))*((Xk(9)/(KNA+Xk(9)))+(KNA/(KNA+Xk(9))));
rUSS3KOH=(1/YZH)*muH*(Xk(11)/(Ks+Xk(11)))*(Uk(3)/(KOH+Uk(3)))*XBHk(3)*(Xk(9)/(KNA+Xk(9)))*(1-(Xk(10)/(KNO+Xk(10))));
rUSS3KNO=(1/YZH)*muH*(Xk(11)/(Ks+Xk(11)))*(Xk(10)/(KNO+Xk(10)))*XBHk(3)*(Uk(3)/(KOH+Uk(3)))*(KNA/(KNA+Xk(9)))+(KOH/(KOH
+Uk(3)))*((Xk(9)/(KNA+Xk(9)))+(KNA/(KNA+Xk(9))));
rUSS3KNA=(1/YZH)*muH*(Xk(11)/(Ks+Xk(11)))*(Xk(9)/(KNA+Xk(9))^2)*XBHk(3)*(Uk(3)/(KOH+Uk(3)))*(1-(Xk(10)/(KNO+Xk(10))));
rUSS3KOA=0;rUSS3etag=0;rUSS3KMP=0;rUSS3KSP=0;rUSS3KSA=0;rUSS3fMA=0;rUSS3KA=0;

% Calculation for model parameters of rUSads for the tank 3
rUSads3f=0.0;
rUSads3YZH=(1/(YZH^2))*KMP*((Xk(12)/XBHk(3))/(KSP+(Xk(12)/XBHk(3))))*XBHk(3)*(Uk(3)/(KOH+Uk(3)))*((Xk(9)/(KNA+Xk(9)))+(
KNA/(KNA+Xk(9))))*(Xk(10)/(KNO+Xk(10)))+etag*(KOH/(KOH+Uk(3)))*(Xk(10)/(KNO+Xk(10)))*((Xk(9)/(KNA+Xk(9)))+(KNA/(KNA+Xk(
9))));
rUSads3YZA=0;rUSads3fZBH=0;rUSads3muH=0;rUSads3muA=0;rUSads3Ks=0;
rUSads3KOH=(1/YZH)*KMP*((Xk(12)/XBHk(3))/(KSP+(Xk(12)/XBHk(3))))*(Uk(3)/(KOH+Uk(3))^2)*XBHk(3)*(Xk(9)/(KNA+Xk(9)))*(1-
(Xk(10)/(KNO+Xk(10))));
rUSads3KNO=(1/YZH)*KMP*((Xk(12)/XBHk(3))/(KSP+(Xk(12)/XBHk(3))))*(Xk(10)/(KNO+Xk(10))^2)*XBHk(3)*(Uk(3)/(KOH+Uk(3)))*(K
NA/(KNA+Xk(9)))+etag*(KOH/(KOH+Uk(3)))*((Xk(9)/(KNA+Xk(9)))+(KNA/(KNA+Xk(9))));
rUSads3KNA=(1/YZH)*KMP*((Xk(12)/XBHk(3))/(KSP+(Xk(12)/XBHk(3))))*(Xk(9)/(KNA+Xk(9))^2)*XBHk(3)*(Uk(3)/(KOH+Uk(3)))*(1-
(Xk(10)/(KNO+Xk(10))));rUSads3KOA=0;
rUSads3etag=-
(1/YZH)*KMP*((Xk(12)/XBHk(3))/(KSP+(Xk(12)/XBHk(3))))*(KOH/(KOH+Uk(3)))*(Xk(10)/(KNO+Xk(10)))*etag*XBHk(3)*((Xk(9)/(KNA
+Xk(9)))+(KNA/(KNA+Xk(9))));
rUSads3KMP=-
(1/YZH)*((Xk(12)/XBHk(3))/(KSP+(Xk(12)/XBHk(3))))*XBHk(3)*(Uk(3)/(KOH+Uk(3)))*((Xk(9)/(KNA+Xk(9)))+(KNA/(KNA+Xk(9))))*(
Xk(10)/(KNO+Xk(10)))+etag*(KOH/(KOH+Uk(3)))*(Xk(10)/(KNO+Xk(10)))*((Xk(9)/(KNA+Xk(9)))+(KNA/(KNA+Xk(9))));
rUSads3KSP=(1/YZH)*KMP*((Xk(12)/XBHk(3))/(KSP+(Xk(12)/XBHk(3)))^2)*XBHk(3)*(Uk(3)/(KOH+Uk(3)))*((Xk(9)/(KNA+Xk(9)))+(KN
A/(KNA+Xk(9))))*(Xk(10)/(KNO+Xk(10)))+etag*(KOH/(KOH+Uk(3)))*(Xk(10)/(KNO+Xk(10)))*((Xk(9)/(KNA+Xk(9)))+(KNA/(KNA+Xk(9)
)));
rUSads3KSA=0;rUSads3fMA=KA*XSk(3)*XBHk(3);rUSads3KA=XSk(3)*XBHk(3)*(fMA-(Xk(12)/XBHk(3)));


%Calculation of the process sensitivity model matrices
%Calculation of the matrix ASu
A1fu=[A11u(1,1)+DT*rUSNH1SNH1 DT*rUSNH1SNO1 DT*rUSNH1SS1 DT*rUSNH1Sads1;
   DT*rUSNO1SNH1 A11u(2,2)+DT*rUSNO1SNO1 DT*rUSNO1SS1 DT*rUSNO1Sads1;
   DT*rUSS1SNH1 DT*rUSS1SNO1 A11u(3,3)+DT*rUSS1SS1 DT*rUSS1Sads1;
   DT*rUSads1SNH1 DT*rUSads1SNO1 DT*rUSads1SS1 A11u(4,4)+DT*rUSads1Sads1];
A1S=[A11u zeros(4,68);zeros(4,4) A1fu zeros(4,64);zeros(4,8) A1fu zeros(4,60);
    zeros(4,12) A1fu zeros(4,56);zeros(4,16) A1fu zeros(4,52);zeros(4,20) A1fu zeros(4,48);
    zeros(4,24) A1fu zeros(4,44);zeros(4,28) A1fu zeros(4,40);zeros(4,32) A1fu zeros(4,36);
    zeros(4,36) A1fu zeros(4,32);zeros(4,40) A1fu zeros(4,28);zeros(4,44) A1fu zeros(4,24);
    zeros(4,48) A1fu zeros(4,20);zeros(4,52) A1fu zeros(4,16);zeros(4,56) A1fu zeros(4,12);
    zeros(4,60) A1fu zeros(4,8);zeros(4,64) A1fu zeros(4,4);zeros(4,68) A1fu];

A2fu=[A22u(1,1)+DT*rUSNH2SNH2 DT*rUSNH2SNO2 DT*rUSNH2SS2 DT*rUSNH2Sads2;
   DT*rUSNO2SNH2 A22u(2,2)+DT*rUSNO2SNO2 DT*rUSNO2SS2 DT*rUSNO2Sads2;
   DT*rUSS2SNH2 DT*rUSS2SNO2 A22u(3,3)+DT*rUSS2SS2 DT*rUSS2Sads2;
   DT*rUSads2SNH2 DT*rUSads2SNO2 DT*rUSads2SS2 A22u(4,4)+DT*rUSads2Sads2];
A2S=[A22u zeros(4,68);zeros(4,4) A2fu zeros(4,64);zeros(4,8) A2fu zeros(4,60);
```

```
    zeros(4,12) A2fu zeros(4,56);zeros(4,16) A2fu zeros(4,52);zeros(4,20) A2fu zeros(4,48);
    zeros(4,24) A2fu zeros(4,44);zeros(4,28) A2fu zeros(4,40);zeros(4,32) A2fu zeros(4,36);
    zeros(4,36) A2fu zeros(4,32);zeros(4,40) A2fu zeros(4,28);zeros(4,44) A2fu zeros(4,24);
    zeros(4,48) A2fu zeros(4,20);zeros(4,52) A2fu zeros(4,16);zeros(4,56) A2fu zeros(4,12);
    zeros(4,60) A2fu zeros(4,8);zeros(4,64) A2fu zeros(4,4);zeros(4,68) A2fu];

A3fu=[A33u(1,1)+DT*rUSNH3SNH3 DT*rUSNH3SNO3 DT*rUSNH3SS3 DT*rUSNH3Sads3;
   DT*rUSNO3SNH3 A33u(2,2)+DT*rUSNO3SNO3 DT*rUSNO3SS3 DT*rUSNO3Sads3;
   DT*rUSS3SNH3 DT*rUSS3SNO3 A33u(3,3)+DT*rUSS3SS3 DT*rUSS3Sads3;
   DT*rUSads3SNH3 DT*rUSads3SNO3 DT*rUSads3SS3 A33u(4,4)+DT*rUSads3Sads3];
A3S=[A33u zeros(4,68);zeros(4,4) A3fu zeros(4,64);zeros(4,8) A3fu zeros(4,60);
    zeros(4,12) A3fu zeros(4,56);zeros(4,16) A3fu zeros(4,52);zeros(4,20) A3fu zeros(4,48);
    zeros(4,24) A3fu zeros(4,44);zeros(4,28) A3fu zeros(4,40);zeros(4,32) A3fu zeros(4,36);
    zeros(4,36) A3fu zeros(4,32);zeros(4,40) A3fu zeros(4,28);zeros(4,44) A3fu zeros(4,24);
    zeros(4,48) A3fu zeros(4,20);zeros(4,52) A3fu zeros(4,16);zeros(4,56) A3fu zeros(4,12);
    zeros(4,60) A3fu zeros(4,8);zeros(4,64) A3fu zeros(4,4);zeros(4,68) A3fu];

A12S=[A12u zeros(4,68);zeros(4,4) A12u zeros(4,64);zeros(4,8) A12u zeros(4,60);
    zeros(4,12) A12u zeros(4,56);zeros(4,16) A12u zeros(4,52);zeros(4,20) A12u zeros(4,48);
    zeros(4,24) A12u zeros(4,44);zeros(4,28) A12u zeros(4,40);zeros(4,32) A12u zeros(4,36);
    zeros(4,36) A12u zeros(4,32);zeros(4,40) A12u zeros(4,28);zeros(4,44) A12u zeros(4,24);
    zeros(4,48) A12u zeros(4,20);zeros(4,52) A12u zeros(4,16);zeros(4,56) A12u zeros(4,12);
    zeros(4,60) A12u zeros(4,8);zeros(4,64) A12u zeros(4,4);zeros(4,68) A12u];


A21S=[A21u zeros(4,68);zeros(4,4) A21u zeros(4,64);zeros(4,8) A21u zeros(4,60);
    zeros(4,12) A21u zeros(4,56);zeros(4,16) A21u zeros(4,52);zeros(4,20) A21u zeros(4,48);
    zeros(4,24) A21u zeros(4,44);zeros(4,28) A21u zeros(4,40);zeros(4,32) A21u zeros(4,36);
    zeros(4,36) A21u zeros(4,32);zeros(4,40) A21u zeros(4,28);zeros(4,44) A21u zeros(4,24);
    zeros(4,48) A21u zeros(4,20);zeros(4,52) A21u zeros(4,16);zeros(4,56) A21u zeros(4,12);
    zeros(4,60) A21u zeros(4,8);zeros(4,64) A21u zeros(4,4);zeros(4,68) A21u];

A23S=[A23u zeros(4,68);zeros(4,4) A23u zeros(4,64);zeros(4,8) A23u zeros(4,60);
    zeros(4,12) A23u zeros(4,56);zeros(4,16) A23u zeros(4,52);zeros(4,20) A23u zeros(4,48);
    zeros(4,24) A23u zeros(4,44);zeros(4,28) A23u zeros(4,40);zeros(4,32) A23u zeros(4,36);
    zeros(4,36) A23u zeros(4,32);zeros(4,40) A23u zeros(4,28);zeros(4,44) A23u zeros(4,24);
    zeros(4,48) A23u zeros(4,20);zeros(4,52) A23u zeros(4,16);zeros(4,56) A23u zeros(4,12);
    zeros(4,60) A23u zeros(4,8);zeros(4,64) A23u zeros(4,4);zeros(4,68) A23u];

A32S=[A32u zeros(4,68);zeros(4,4) A32u zeros(4,64);zeros(4,8) A32u zeros(4,60);
    zeros(4,12) A32u zeros(4,56);zeros(4,16) A32u zeros(4,52);zeros(4,20) A32u zeros(4,48);
    zeros(4,24) A32u zeros(4,44);zeros(4,28) A32u zeros(4,40);zeros(4,32) A32u zeros(4,36);
    zeros(4,36) A32u zeros(4,32);zeros(4,40) A32u zeros(4,28);zeros(4,44) A32u zeros(4,24);
    zeros(4,48) A32u zeros(4,20);zeros(4,52) A32u zeros(4,16);zeros(4,56) A32u zeros(4,12);
    zeros(4,60) A32u zeros(4,8);zeros(4,64) A32u zeros(4,4);zeros(4,68) A32u];

ASu=[A1S A12S zeros(72,72);A21S A2S A23S;zeros(72,72) A32S A3S];

%matrix of the rates CSu of the sensitivity model
C1Su=[Cnu zeros(10,68)];CSu=[C1Su zeros(10,144);zeros(10,72) C1Su zeros(10,72);zeros(10,144) C1Su];

% Development of the matrix BSu of the sensitivity model
B1thetau=[B1u(2,2) 0 0 0;zeros(67,4)];B1Su=[B1u;B1thetau];BSu=[B1Su;zeros(144,4)];

% Development of the vector DSu of the sensitivity model
% Calculation of the first tank
D1Su=[zeros(1,4) rUSNH1f rUSNO1f rUSS1f rUSads1f rUSNH1YZH rUSNO1YZH rUSS1YZH rUSads1YZH rUSNH1YZA rUSNO1YZA rUSS1YZA
rUSads1YZA rUSNH1fZBH rUSNO1fZBH...
   rUSS1fZBH rUSads1fZBH rUSNH1muA rUSNO1muA rUSS1muA rUSads1muA rUSNH1muH rUSNO1muH rUSS1muH rUSads1muH rUSNH1Ks
rUSNO1Ks rUSS1Ks rUSads1Ks rUSNH1KOH...
   rUSNO1KOH rUSS1KOH rUSads1KOH rUSNH1KNO rUSNO1KNO rUSS1KNO rUSads1KNO rUSNH1KNA rUSNO1KNA rUSS1KNA rUSads1KNA
rUSNH1KOA rUSNO1KOA rUSS1KOA rUSads1KOA...
   rUSNH1etag rUSNO1etag rUSS1etag rUSads1etag rUSNH1KMP rUSNO1KMP rUSS1KMP rUSads1KMP rUSNH1KSP rUSNO1KSP rUSS1KSP
rUSads1KSP rUSNH1KSA rUSNO1KSA rUSS1KSA...
   rUSads1KSA rUSNH1fMA rUSNO1fMA rUSS1fMA rUSads1fMA rUSNH1KA rUSNO1KA rUSS1KA rUSads1KA]';
% Calculation of the second tank
D2Su=[zeros(1,4) rUSNH2f rUSNO2f rUSS2f rUSads2f rUSNH2YZH rUSNO2YZH rUSS2YZH rUSads2YZH rUSNH2YZA rUSNO2YZA rUSS2YZA
rUSads2YZA rUSNH2fZBH rUSNO2fZBH...
   rUSS2fZBH rUSads2fZBH rUSNH2muA rUSNO2muA rUSS2muA rUSads2muA rUSNH2muH rUSNO2muH rUSS2muH rUSads2muH rUSNH2Ks
rUSNO2Ks rUSS2Ks rUSads2Ks rUSNH2KOH...
   rUSNO2KOH rUSS2KOH rUSads2KOH rUSNH2KNO rUSNO2KNO rUSS2KNO rUSads2KNO rUSNH2KNA rUSNO2KNA rUSS2KNA rUSads2KNA
rUSNH2KOA rUSNO2KOA rUSS2KOA rUSads2KOA...
   rUSNH2etag rUSNO2etag rUSS2etag rUSads2etag rUSNH2KMP rUSNO2KMP rUSS2KMP rUSads2KMP rUSNH2KSP rUSNO2KSP rUSS2KSP
rUSads2KSP rUSNH2KSA rUSNO2KSA rUSS2KSA...
   rUSads2KSA rUSNH2fMA rUSNO2fMA rUSS2fMA rUSads2fMA rUSNH2KA rUSNO2KA rUSS2KA rUSads2KA]';
% Calculation of the third tank
D3Su=[zeros(1,4) rUSNH3f rUSNO3f rUSS3f rUSads3f rUSNH3YZH rUSNO3YZH rUSS3YZH rUSads3YZH rUSNH3YZA rUSNO3YZA rUSS3YZA
rUSads3YZA rUSNH3fZBH rUSNO3fZBH...
   rUSS3fZBH rUSads3fZBH rUSNH3muA rUSNO3muA rUSS3muA rUSads3muA rUSNH3muH rUSNO3muH rUSS3muH rUSads3muH rUSNH3Ks
rUSNO3Ks rUSS3Ks rUSads3Ks rUSNH3KOH...
   rUSNO3KOH rUSS3KOH rUSads3KOH rUSNH3KNO rUSNO3KNO rUSS3KNO rUSads3KNO rUSNH3KNA rUSNO3KNA rUSS3KNA rUSads3KNA
rUSNH3KOA rUSNO3KOA rUSS3KOA rUSads3KOA...
   rUSNH3etag rUSNO3etag rUSS3etag rUSads3etag rUSNH3KMP rUSNO3KMP rUSS3KMP rUSads3KMP rUSNH3KSP rUSNO3KSP rUSS3KSP
rUSads3KSP rUSNH3KSA rUSNO3KSA rUSS3KSA...
   rUSads3KSA rUSNH3fMA rUSNO3fMA rUSS3fMA rUSads3fMA rUSNH3KA rUSNO3KA rUSS3KA rUSads3KA]';

DSu=[D1Su;D2Su;D3Su];
```

APPENDIX E: REDUCED ASM1 AND UCT MODEL PARAMETER ESTIMATION USED FOR THE BENCHMARK AND ATHLONE PROCESS MASS BALANCE MODELS

Figure 9.59: Trajectories of the reduced ASM1 biological model applied for the Benchmark process

The trajectory of estimated muH starts from zero decreasing to – 0.19 at a discrete time of 4 then reaches a maximum of 0.05 at a discrete time of 10 and continues to – 0.04 at a discrete time of 100. The trajectory of estimated muA starts from zero increasing to a maximum of 0.12 at a discrete time of 3 then decreases to 0.0395 at a discrete time of 8 and continues to 0.0595 at a discrete time of 100. The trajectory of estimated Kh starts from zero decreasing to a minimum of – 0.2 at a discrete time of 5 then reaches a maximum of 0.95 at a discrete time of 9.5 and continues to 0.598 at a discrete time of 100.

Figure 9.60: Trajectories of the ASM1 full (solid line), reduced estimated (dashed line) and the error between them as applied for the Benchmark process for the process variable SNH

The trajectories of process variables, ASM1 full Snh1 and reduced estimated, Snh1E are approximately identical whilst the estimation error, ERRSnh1 decreases from zero to – 1 and oscillates slightly then dramatically increases to 1 at a discrete time of 100. The trajectories of process variables, ASM1 full Snh2 and reduced estimated, Snh2E differs slightly from each other whilst the estimation error, ERRSnh2 decreases from zero to – 1 then dramatically increases to 1.9 at a discrete time of 100. The trajectories of process variables, ASM1 full Snh3 and reduced estimated, Snh3E differs slightly from each other whilst the estimation error, ERRSnh3 increases to 0.25 then decreases to – 0.6 at a discrete time of 3 and dramatically increases to 2.2 at a discrete time of 100. The trajectories of process variables, ASM1 full Snh4 and reduced estimated, Snh4E differs slightly from each other whilst the estimation error, ERRSnh4 increases from zero to 0.25 then decreases to – 0.5 at a discrete time of 3 and increases to 2.6 at a discrete time of 100. The trajectories of process variables, ASM1 full Snh5 and reduced estimated, Snh5E differs slightly from each other whilst the estimation error, ERRSnh2 increases from zero to 0.25 then decreases to – 0.25 at a discrete time of 4 then dramatically increases to 2.95 at a discrete time of 100.

Figure 9.61: Trajectories of the ASM1 full (solid line), reduced estimated (dashed line) and the error between them as applied for the Benchmark process for the process variable SNO

The trajectories of process variables, ASM1 full SNO1 and reduced estimated, SNO1E are the same till the discrete time of 40 and after this they start to diverge a little whilst the estimation error, ERRSNO1 decreases from zero to – 0.7 then increases to 1.5 at a discrete time of 100. The trajectories of process variables, ASM1 full SNO2 and reduced estimated, SNO2E are the same till the discrete time of 40 and after this they start to diverge a little whilst the estimation error, ERRSNO2 decreases from zero to – 0.7 then increases to 1.8 at a discrete time of 100. The trajectories of process variables, ASM1 full SNO3 and reduced estimated, SNO3E are the same till the discrete time of 40 and

after this they start to diverge a little whilst the estimation error, ERRSNO3 decreases from zero to – 0.9 then increases to 1.85 at a discrete time of 100. The trajectories of process variables, ASM1 full SNO4 and reduced estimated, SNO4E are the same till the discrete time of 40 and after this they start to diverge a little whilst the estimation error, ERRSNO4 decreases from zero to – 1 then increases to 1.9 at a discrete time of 100. The trajectories of process variables, ASM1 full SNO5 and reduced estimated, SNO5E are the same till the discrete time of 40 and after this they start to diverge a little whilst the estimation error, ERRSNO5 decreases from zero to – 0.8 then increases to 1.95 at a discrete time of 100.

Figure 9.62: Trajectories of the ASM1 full (solid line), reduced estimated (dashed line) and the error between them as applied for the Benchmark process for the process variable SS

The trajectories of process variables, ASM1 full SS1 and reduced estimated, SS1E are identical whilst the estimation error, ERRSS1 oscillates from zero to 0.8 then remains stable and increases to 1.5 at a discrete time of 100. The trajectories of process variables, ASM1 full SS2 and reduced estimated, SS2E are identical whilst the estimation error, ERRSS2 oscillates from zero to 0.8 then remains stable and increases to 1.4 at a discrete time of 100. The trajectories of process variables, ASM1 full SS3 and reduced estimated, SS3E are identical whilst the estimation error, ERRSS3 oscillates from zero to 1 then remains stable and increases to 1.45 at a discrete time of 100. The trajectories of process variables, ASM1 full SS4 and reduced estimated, SS4E are identical whilst the estimation error, ERRSS4 oscillates from zero to 1.1 then remains stable and increases to 1.49 at a discrete time of 100. The trajectories of process variables, ASM1 full SS5 and reduced estimated, SS5E are identical whilst the estimation error, ERRSS5 oscillates from zero to 1 then remains stable and increases to 1.5 at a discrete time of 100.

Figure 9.63: Trajectories of the reduced ASM1 biological model parameters for the Athlone process

The trajectory of estimated muH decreases from 65 to zero at a discrete time of 2 then remains constant then decreases to -7 at a discrete time of 5 and increases to 4 at a discrete time of 7 then remains at a constant value of 2 until a discrete time of 100. The trajectory of estimated muA increases from 0.5 to 1.8 at a discrete time of 2 then decreases to 1.2 at a discrete time of 4 and increases to 1.48 at a discrete time of 6 then decreases to 0.65 at a discrete time of 8 and steadily increases from this value to 3.2 at a discrete time of 100. The trajectory of estimated Kh decreases from 3.6 to zero at a discrete time of 5 and increases to 4.8 at a discrete time of 8 then decreases to 3.7 at a discrete time of 9 and steadily increases to 6.5 at a discrete time of 100.

Figure 9.64: Trajectories of the ASM1 full (solid line), reduced estimated (dashed line) and the error between them as applied for the Athlone process for the process variable SNH

The trajectories of process variables, ASM1 full Snh1 and reduced estimated Snh1E are slightly different having the same profile with the reduced estimated Snh1E having a maximum of 0.3 at a discrete time of 20 whilst ASM1 full Snh1 have a maximum of 0.28 at a discrete time of 20. The estimated error ERRSnh1 decreases from zero to -0.04 at a discrete time of 8 and increases to 0.0285 at a discrete time of 100. The trajectories of process variables, ASM1 full Snh2 and reduced estimated Snh2E are slightly different having the same profile with the reduced estimated Snh2E having a maximum of 0.22 at a discrete time of 20 whilst ASM1 full Snh2 have a maximum of 0.225 at a discrete time of 30. The estimated error ERRSnh2 decreases from zero to -0.002 at a discrete time of 8 and increases to 0.095 at a discrete time of 100. The trajectories of process variables, ASM1 full Snh3 and reduced estimated Snh3E are slightly different having the same

profile with the reduced estimated Snh3E having a maximum of 0.16 at a discrete time of 20 whilst ASM1 full Snh3 have a maximum of 0.19 at a discrete time of 30. The estimated error ERRSnh3 increases slightly at zero then decreases to -0.01 and increases to 0.16 at a discrete time of 100.

Figure 9.65. Trajectories of the ASM1 full (solid line), reduced estimated (dashed line) and the error between them as applied for the Athlone process for the process variable SNO

The trajectories of process variables, ASM1 full SNO1 and reduced estimated SNO1E are slightly different having the same profile with the reduced estimated SNO1E increasing from 0.037 to 0.13 at a discrete time of 100 whilst ASM1 full SNO1 decreases from 0.056 to 0.019 at a discrete time of 8 then increases to 0.144 at a discrete time of 100. The estimated error ERRSNO1 decreases from zero to a minimum of - 19×10^{-3} at a discrete time of 11 and increases to 5×10^{-3} at a discrete time of 100. The trajectories of process variables, ASM1 full SNO2 and reduced estimated SNO2E are slightly different having the same profile with the reduced estimated SNO2E increasing from 0.05 to 0.24 at a discrete time of 100 whilst ASM1 full SNO2 increases slightly from 0.04 to 0.06 at a discrete time of 2 and decreases to 0.0495 at a discrete time of 10 then increases to 0.348 at a discrete time of 100. The estimated error ERRSNO2 decreases from zero to -0.0198 at a discrete time of 8 and decreases to a minimum of -0.0199 at a discrete time of 17 then increases to 0.102 at a discrete time of 100. The trajectories of process variables, ASM1 full SNO3 and reduced estimated SNO3E are slightly different having the same profile with the reduced estimated SNO3E increasing from 0.065 to 0.3 at a discrete time of 100 whilst ASM1 full SNO3 reaches a minimum of 0.065 at a discrete time of 10 then increases to 0.46 at a discrete time of 100. The estimated error ERRSNO3 decreases from zero to a minimum of – 0.02 at a discrete time of 11 and increases to 0.155 at a discrete time of 100.

Figure 9.66. Trajectories of the ASM1 full (solid line), reduced estimated (dashed line) and the error between them as applied for the Athlone process for the process variable SS

The trajectories of process variables, ASM1 full SS1 and reduced estimated SS1E are completely identical with increasing from zero to 2.1 at a discrete time of 100 whilst estimated error ERRSS1 decreases from zero to a minimum of -0.02 at a discrete time of 17 then increases to 0.076 at a discrete time of 100. The trajectories of process variables, ASM1 full SS2 and reduced estimated SS2E are completely identical with increasing from zero to 3.25 at a discrete time of 100 whilst estimated error ERRSS2 increases from zero to 0.022 then decreases to a minimum of -0.03 at a discrete time of 25 then increases to 0.074 at a discrete time of 100. The trajectories of process variables, ASM1 full SS3 and reduced estimated SS3E are completely identical with increasing from zero to 4 at a discrete time of 100 whilst estimated error ERRSS3 decreases from zero to a minimum of -0.06 at a discrete time of 20 then increases to 0.18 at a discrete time of 100.

Figure 9.67: Trajectories of the reduced UCT biological model parameters for the

Benchmark process

The trajectory of estimated muH decreases from 0.4 to 0.21 at a discrete time of 2 and increases to 0.44 at a discrete time of 100. The trajectory of estimated KMP decreases from 0.8 to 0.48 at a discrete time of 2 and increases to a maximum of 0.99 at a discrete time of 7 then decreases to 0.24 at discrete time of 100. The trajectory of estimated KA decreases from 0.006 to 0.0018 at a discrete time of 2 and increases to 0.009 at a discrete time of 7 then increases to 0.0098 at a discrete time of 100. The trajectory of estimated muA increases from 0.095 to 0.16 at a discrete time of 2 then decreases to

0.025 at a discrete time of 30 then remains at this steady state until a discrete time of 100.

Figure 9.68: Trajectories of the UCT full (solid line), reduced estimated (dashed line) and the error between them as applied for the Benchmark process for the process variable SNH

The trajectories of process variables, UCT full Snh1 and reduced estimated Snh1E are slightly different with same profile from zero to approximately 3 at a discrete time of 100 whilst the estimated error ERRSnh1 decreases from zero to -0.14 at a discrete time of 6 then increases to 0.24 at a discrete time of 100. The trajectories of process variables, UCT full Snh2 and reduced estimated Snh2E are slightly different with same profile from zero to approximately 3 at a discrete time of 100 whilst the estimated error ERRSnh2 decreases from zero to -0.15 at a discrete time of 4 then increases to 0.26 at a discrete time of 100. The trajectories of process variables, UCT full Snh3 and reduced estimated Snh3E are slightly different with same profile from zero to approximately 3 at a discrete time of 100 whilst the estimated error ERRSnh3 decreases from zero to -0.08 at a discrete time of 6 then increases to 0.36 at a discrete time of 100. The trajectories of process variables, UCT full Snh4 and reduced estimated Snh4E are slightly different with same profile from zero to approximately 3 at a discrete time of 100 whilst the estimated error ERRSnh4 decreases from zero to -0..006 at a discrete time of 6 then increases to 0.38 at a discrete time of 100. The trajectories of process variables, UCT full Snh5 and reduced estimated Snh5E are slightly different with same profile from zero to approximately 3 at a discrete time of 100 whilst the estimated error ERRSnh5 decreases from zero to -0.04 at a discrete time of 6 then increases to 0.4 at a discrete time of 100.

Figure 9.69: Trajectories of the UCT full (solid line), reduced estimated (dashed line) and the error between them as applied for the Benchmark process for the process variable SNO

The trajectories of process variables, UCT full SNO1 and reduced estimated SNO1E are slightly different with UCT full SNO1 increases from zero to 0.6 at a discrete time of 100 and reduced estimated SNO1E increases from zero to 0.5 at a discrete time of 100 whilst the estimated error ERRSNO1 decreases from zero to -0.005 at a discrete time of 4 then increases to 0.08 at a discrete time of 100. The trajectories of process variables, UCT full SNO2 and reduced estimated SNO2E are slightly different with UCT full SNO2 increases from zero to 0.6 at a discrete time of 100 and reduced estimated SNO2E increases from zero to 0.52 at a discrete time of 100 whilst the estimated error ERRSNO2 decreases from zero to -0.075 at a discrete time of 4 then increases to 0.095 at a discrete time of 100. The trajectories of process variables, UCT full SNO3 and reduced estimated SNO3E are slightly different with UCT full SNO3 increases from zero to 0.64 at a discrete time of 100 and reduced estimated SNO3E increases from zero to 0.56 at a discrete time of 100 whilst the estimated error ERRSNO3 decreases from zero to -0.07 at a discrete time of 4 then increases to 0.096 at a discrete time of 100. The trajectories of process variables, UCT full SNO4 and reduced estimated SNO4E are slightly different with UCT full SNO4 increases from zero to 0.66 at a discrete time of 100 and reduced estimated SNO4E increases from zero to 0.58 at a discrete time of 100 whilst the estimated error ERRSNO4 decreases from zero to -0.065 at a discrete time of 6 then increases to 0.098 at a discrete time of 100. The trajectories of process variables, UCT full SNO5 and reduced estimated SNO5E are slightly different with UCT full SNO5 increases from zero to 0.68 at a discrete time of 100 and reduced estimated SNO5E increases from zero to 0.59 at a discrete time of 100 whilst the estimated error

ERRSNO5 decreases from zero to -0.07 at a discrete time of 6 then increases to 0.1 at a discrete time of 100.

Figure 9.70: Trajectories of the UCT full (solid line), reduced estimated (dashed line) and the error between them as applied for the Benchmark process for the process variable SS

The trajectories of process variables, UCT full SS1 and reduced estimated SS1E are completely identical where they increases from zero to a maximum of 1.85 at a discrete time of 20 then decreases to 1.35 at a discrete time of 100 whilst the estimated error ERRSS1 oscillates from zero to 0.008 at a discrete time of 50 then reaches a steady state until a discrete time of 100. The trajectories of process variables, UCT full SS2 and reduced estimated SS2E are completely identical where they increases from zero to a maximum of 1.7 at a discrete time of 20 then decreases to 1 at a discrete time of 100 whilst the estimated error ERRSS2 oscillates from zero to 0.0075 at a discrete time of 40 then reaches a steady state until a discrete time of 100. The trajectories of process variables, UCT full SS3 and reduced estimated SS3E are completely identical where they increases from zero to a maximum of 1.4 at a discrete time of 20 then decreases to 0.75 at a discrete time of 100 whilst the estimated error ERRSS3 oscillates from zero to 0.008 at a discrete time of 50 then reaches a steady state until a discrete time of 100. The trajectories of process variables, UCT full SS4 and reduced estimated SS4E are completely identical where they increases from zero to a maximum of 1.2 at a discrete time of 20 then decreases to 0.5 at a discrete time of 100 whilst the estimated error ERRSS4 oscillates from zero to 0.009 at a discrete time of 50 then reaches a steady state until a discrete time of 100. The trajectories of process variables, UCT full SS5 and reduced estimated SS5E are completely identical where they increases from zero to a maximum of 0.95 at a discrete time of 20 then decreases to 0.35 at a discrete time of 100 whilst the estimated error ERRSS5 oscillates from zero to 0.011 at a discrete time of 50 then reaches a steady state until a discrete time of 100.

Figure 9.71: Trajectories of the UCT full (solid line), reduced estimated (dashed line) and the error between them as applied for the Benchmark process for the process variable XSA

The trajectories of process variables, UCT full XSA1 and reduced estimated XSA1E are completely identical where they decreases from 0.75 to 0.35 at a discrete time of 2 then increases to 1 at a discrete time of 100 whilst the estimated error ERRXSA1 displays noise from zero to 0.0025 at a discrete time of 40 then slowly decreases to -0.0025 at a discrete time of 100. The trajectories of process variables, UCT full XSA2 and reduced estimated XSA2E are completely identical where they increases from 0.8 to 0.9 at a discrete time of 1 and decreases to 0.25 at a discrete time of 2 then increases to 1.1 at a discrete time of 100 whilst the estimated error ERRXSA2 displays noise around zero to discrete time of 40 then slowly decreases to -0.0095 at a discrete time of 100. The trajectories of process variables, UCT full XSA3 and reduced estimated XSA3E are completely identical where they increases from 0.6 to 0.7 at a discrete time of 1 and decreases to 0.25 at a discrete time of 2 then increases to 1.15 at a discrete time of 100 whilst the estimated error ERRXSA3 displays noise from zero to 0.0025 at a discrete time of 40 then slowly decreases to -0.01 at a discrete time of 100. The trajectories of process variables, UCT full XSA4 and reduced estimated XSA4E are completely identical where they decreases from 0.55 to 0.5 at a discrete time of 1 and increases to 0.55 at a discrete time of 2 then decreases to 0.25 at a discrete time of 3 then increases to 1.2 at a discrete time of 100 whilst the estimated error ERRXSA4 displays noise around zero until a discrete time of 40 then slowly decreases to -0.01 at a discrete time of 100. The trajectories of process variables, UCT full XSA5 and reduced estimated

XSA5E are completely identical where they decreases from 0.5 to 0.25 at a discrete time of 8 and increases to 1.2 at a discrete time of 100 whilst the estimated error ERRXSA5 decreases from zero to -0.025 then displays noise around zero until discrete time of 40 then slowly decreases to -0.018 at a discrete time of 100.

APPENDIX F: SOFTWARE FOR PARAMETER ESTIMATION OF THE BENCHMARK MASS BALANCES MODEL FOR THE CASE OF ASM1 AND UCT REDUCED MODELS

1. SOFTWARE FOR PARAMETER ESTIMATION OF THE BENCHMARK MASS-BALANCE MODEL FOR THE CASE OF ASM1 REDUCED MODEL

1.1. Main program

```
%PROGRAM BASM1parest.m
%Aim - the program estimates the reduced ASM1 model parameters for the Benchmark process and calculates the errors
between the process variables behaviour for the full and reduced ASM1 models. The
%program call the function subroutines rateASM1F.m, prateASM1R.m and rateASM1RE.m. The calculation uses
%reduced biological model with 3 variables SNH, SNO and SS
%The program uses global definition of the model parameters

global Ks KOH KNO KNH KOA Kx muH etag muA Kh etah iXB YH YA fP iXP bH bA Ka
%Process parameters
f=1.2;YA = 0.24;YH = 0.67;iXB = 0.08;muH = 0.4;Ks = 10;KOH = 0.2;KNO = 0.5;etag = 0.8;etah = 0.8;Kh = 3;Kx = 0.1;muA =
0.5;KNH = 1;KOA = 0.4;fP = 0.08;iXP = 0.06;bH = 0.3;bA = 0.05;Ka = 0.05;
%Tanks volumes and flow rates
V1 = 1000;V2 = 1000;V3 = 1333;V4 = 1333;V5 = 1333;
Qo = 18446;Qa = 55338;Qr = 18446;Qw = 385;Sosat = 8;LAMBDA = (Qo+Qr)/(Qr+Qw);
%Oxygen parameters
S0sat = 8;Kla1=4.8;Kla2=4.8;Kla3 = 240;Kla4=240;Kla5 = 84;
Kl=[Kla1 Kla2 Kla3 Kla4 Kla5];Kla=diag(Kl);

%Determination of the sampling period
DT = 0.01042;days=0.1042*10;K=days/DT;k=0:DT:days;

%calculation of the model matrices
%Calculation of the matrix CF

YH1 = -1/YH;YA1 = 1/YA;YH2 = -(1-YH)/YH;YA2 = -(4.57/YA)+1;YH3 = -(1-YH)/(2.86*YH);fP1 = 1-fP;
iXB1 = -(iXB+YA1);iXB2 = iXB-(fP*iXP);iXB3 = -iXB/14;YH4 = (1-YH)/(14*2.86*YH)+iXB3;YA3 = iXB-YA1/7;YH5 = 1/14;
YZSI = [0 0 0 0 0 0 0 0]';
YZSS = [YH1 YH1 0 0 0 0 1 0]';
YZXI = [0 0 0 0 0 0 0 0]';
YZXS = [0 0 0 fP1 fP1 0 -1 0]';
YZXBH = [1 1 0 -1 0 0 0 0]';
YZXBA = [0 0 1 0 -1 0 0 0]';
YZXP = [0 0 0 fP fP 0 0 0]';
YZSO = [YH2 0 YA2 0 0 0 0 0]';
YZSNO = [0 YH3 YA1 0 0 0 0 0]';
YZSNH = [-iXB -iXB iXB1 0 0 1 0 0]';
YZSND = [0 0 0 0 0 -1 0 1]';
YZXND = [0 0 0 iXB2 iXB2 0 0 -1]';
YZSALK = [iXB3 YH4 YA3 0 0 YH5 0 0]';
Cn = DT*[YZSI  YZSS  YZXI  YZXS  YZXBH  YZXBA  YZXP  YZSO  YZSNO  YZSNH  YZSND  YZXND  YZSALK];
CF=[Cn zeros(8,52);zeros(8,13) Cn zeros(8,39);zeros(8,26) Cn zeros(8,26);zeros(8,39) Cn zeros(8,13);zeros(8,52) Cn];
%Calculation of the matrix AF
IV1 = DT/V1;IV2 = DT/V2;IV3 = DT/V3;IV4 = DT/V4;IV5 = DT/V5;IV=IV1*Qo;IVV=IV*f;
Q=Qo+Qa+Qr;
IV21=IV2*Q;IV32=IV3*Q;IV43=IV4*Q;IV54=IV5*Q;
IV11=1-IV1*Q;IV22=1-IV21;IV33=1-IV32;IV44=1-IV43;IV55=1-IV54;IV15=IV1*(Qa+Qr);IV15p=IV1*(Qa+LAMBDA*Qr);
a1=[IV11,IV11,IV11,IV11,IV11,IV11,IV11,IV11,IV11,IV11,IV11,IV11,IV11];
A11=diag(a1);
a2=[IV22,IV22,IV22,IV22,IV22,IV22,IV22,IV22,IV22,IV22,IV22,IV22,IV22];
A22=diag(a2);
a3=[IV33,IV33,IV33,IV33,IV33,IV33,IV33,IV33,IV33,IV33,IV33,IV33,IV33];
A33=diag(a3);
a4=[IV44,IV44,IV44,IV44,IV44,IV44,IV44,IV44,IV44,IV44,IV44,IV44,IV44];
A44=diag(a4);
a5=[IV55,IV55,IV55,IV55,IV55,IV55,IV55,IV55,IV55,IV55,IV55,IV55,IV55];
A55=diag(a5);
a15=[IV15,IV15,IV15p,IV15,IV15p,IV15p,IV15p,IV15,IV15,IV15,IV15,IV15p,IV15];
A15=diag(a15);
a21=[IV21,IV21,IV21,IV21,IV21,IV21,IV21,IV21,IV21,IV21,IV21,IV21,IV21];
A21=diag(a21);
a32=[IV32,IV32,IV32,IV32,IV32,IV32,IV32,IV32,IV32,IV32,IV32,IV32,IV32];
A32=diag(a32);
a43=[IV43,IV43,IV43,IV43,IV43,IV43,IV43,IV43,IV43,IV43,IV43,IV43,IV43];
A43=diag(a43);
a54=[IV54,IV54,IV54,IV54,IV54,IV54,IV54,IV54,IV54,IV54,IV54,IV54,IV54];
A54=diag(a54);
AF=[A11 zeros(13,39) A15;A21 A22 zeros(13,39);zeros(13,13) A32 A33 zeros(13,26);zeros(13,26) A43 A44
zeros(13,13);zeros(13,39) A54 A55];
%Calculation of the matrix BF
b1=[IV,IV,IV,IV,IV,IV,IV,IV,IV,IV,IV,IV,IV];
B1=diag(b1);
BF=[B1;zeros(52,13)];

%Average influent concentrations trajectories for the process variables
SSi=69.5;XBHi=28.17;XSi=202.32;XIi=51.2;SNHi=31.56;SIi=30.0;SNDi=6.95;XNDi=10.59;S0i=0.0;
XBAi=0.0;XPi=0.0;SNOi=0.0;SALKi=7.0;
Zi=[SIi*ones(1,K);SSi*ones(1,K);XIi*ones(1,K);XSi*ones(1,K);XBHi*ones(1,K);XBAi*ones(1,K);XPi*ones(1,K);S0i*ones(1,K);S
NOi*ones(1,K);SNHi*ones(1,K);SNDi*ones(1,K);XNDi*ones(1,K);SALKi*ones(1,K)];

%Determination of the initial conditions
Si_1    =   3.0000000e+01;Ss_1      =   2.8082131e+00;Xi_1      =   1.1491252e+03;Xs_1     =   8.2134908e+01;
Xbh_1   =   2.5517658e+03;Xba_1    =   1.4838943e+02;Xp_1     =   4.4885186e+02;So_1     =   4.2984433e-03;
Sno_1   =   5.3699400e+00;Snh_1    =   7.9178845e+00;Snd_1    =   1.2166405e+00;Xnd_1    =   5.2848894e+00;
Salk_1  =   4.9277103e+00;
Z10 = [Si_1 ;Ss_1 ;Xi_1 ;Xs_1 ;Xbh_1 ;Xba_1 ;Xp_1 ;So_1 ;Sno_1 ;Snh_1 ;Snd_1 ;Xnd_1 ;Salk_1 ];

Si_2    =   3.0000000e+01;Ss_2      =   1.4587940e+00;Xi_2      =   1.1491252e+03;Xs_2     =   7.6386187e+01;
```

```
Xbh_2    =   2.5533851e+03;Xba_2    =   1.4830914e+02;Xp_2     =   4.4952273e+02;So_2     =   6.3131911e-05;
Sno_2    =   3.6619672e+00;Snh_2    =   8.3444148e+00;Snd_2     =  8.8206477e-01;Xnd_2    =   5.0290873e+00;
Salk_2   =   5.0801748e+00;
Z20 = [Si_2 ;Ss_2 ;Xi_2 ;Xs_2 ;Xbh_2 ;Xba_2 ;Xp_2 ;So_2 ;Sno_2 ;Snh_2 ;Snd_2 ;Xnd_2 ;Salk_2 ];

Si_3     =   3.0000000e+01;Ss_3     =   1.1495418e+00;Xi_3     =   1.1491252e+03;Xs_3     =   6.4854922e+01;
Xbh_3    =   2.5571314e+03;Xba_3    =   1.4894126e+02;Xp_3     =   4.5041834e+02;So_3     =   1.7183778e+00;
Sno_3    =   6.5408820e+00;Snh_3    =   5.5479452e+00;Snd_3    =   8.2888682e-01;Xnd_3    =   4.3924277e+00;
Salk_3   =   4.6747902e+00;
Z30 = [Si_3 ;Ss_3 ;Xi_3 ;Xs_3 ;Xbh_3 ;Xba_3 ;Xp_3 ;So_3 ;Sno_3 ;Snh_3 ;Snd_3 ;Xnd_3 ;Salk_3 ];

Si_4     =   3.0000000e+01;Ss_4     =   9.9532389e-01;Xi_4     =   1.1491252e+03;Xs_4     =   5.5693982e+01;
Xbh_4    =   2.5591826e+03;Xba_4    =   1.4952712e+02;Xp_4     =   4.5131469e+02;So_4     =   2.4288838e+00;
Sno_4    =   9.2989988e+00;Snh_4    =   2.9673854e+00;Snd_4    =   7.6678656e-01;Xnd_4    =   3.8790101e+00;
Salk_4   =   4.2934562e+00;
Z40 = [Si_4 ;Ss_4 ;Xi_4 ;Xs_4 ;Xbh_4 ;Xba_4 ;Xp_4 ;So_4 ;Sno_4 ;Snh_4 ;Snd_4 ;Xnd_4 ;Salk_4 ];


Si_5     =   3.0000000e+01;Ss_5     =   8.8949280e-01;Xi_5     =   1.1491252e+03;Xs_5     =   4.9305586e+01;
Xbh_5    =   2.5593436e+03;Xba_5    =   1.4979714e+02;Xp_5     =   4.5221112e+02;So_5     =   4.9094351e-01;
Sno_5    =   1.0415220e+01;Snh_5    =   1.7333316e+00;Snd_5    =   6.8828001e-01;Xnd_5    =   3.5271755e+00;
Salk_5   =   4.1255794e+00;
Z50 = [Si_5 ;Ss_5 ;Xi_5 ;Xs_5 ;Xbh_5 ;Xba_5 ;Xp_5 ;So_5 ;Sno_5 ;Snh_5 ;Snd_5 ;Xnd_5 ;Salk_5 ];
% Vector of the initial values
Z0=[Z10;Z20;Z30;Z40;Z50]*0.1
Z=[Z0 zeros(65,K)];

%Simulation of the full model behavior
for k = 1:K
% calculation of the initial trajectory for the state vector Z

    Zk=Z(:,k);
    S0k=[Zk(8,1);Zk(21,1);Zk(34,1);Zk(47,1);Zk(60,1)];
    Zik = Zi(:,k);
   [ROASM1F]=rateASM1F(Zk);
    ZZk=DT*Kla*(S0sat-S0k);
    ZZ1k=[zeros(7,1);ZZk(1);zeros(12,1);ZZk(2);zeros(12,1);ZZk(3);zeros(12,1);ZZk(4);zeros(12,1);ZZk(5);zeros(5,1)];
    Z(:,k+1) = AF*Z(:,k) + CF'*ROASM1F + BF*Zi(:,k)+ZZ1k;
end
Z
%Selection of the measured variables of state space SNH,SNO,SS
X=[Z(10,:);Z(9,:);Z(2,:);Z(23,:);Z(22,:);Z(15,:);Z(36,:);Z(35,:);Z(28,:);Z(49,:);Z(48,:);Z(41,:);Z(62,:);
Z(61,:);Z(54,:)]
%trajectory of the control signal
U=[Z(8,:);Z(21,:);Z(34,:);Z(47,:);Z(60,:)]

%Calculation of the vector P

%Average values of the inflow concentrations for dry weather
Xi  =[SNHi*ones(1,K);SNOi*ones(1,K);SSi*ones(1,K)]

% Steady state values for the biomass XBH, XBA, XS
XBH = [2551.76*ones(1,K);2553.38*ones(1,K);2557.13*ones(1,K);2559.18*ones(1,K);2559.34*ones(1,K)];% XBH steady state
COD/m^3
XBA = [148.389*ones(1,K);148.309*ones(1,K);148.941*ones(1,K);149.527*ones(1,K);149.797*ones(1,K)];% XBA steady state g
all COD/m^3
XS = [82.135*ones(1,K);76.386*ones(1,K);64.855*ones(1,K);55.694*ones(1,K);49.306*ones(1,K)]; % XS steady state all
COD/m^3

%Calculation of the state space process model matrices
%Calculation of the matrix A

AR=[[IV11 0.0 0.0;0.0 IV11 0.0;0.0 0.0 IV11] zeros(3,9) [IV15 0.0 0.0;0.0 IV15 0.0;0.0 0.0 IV15];
    [IV21 0.0 0.0;0.0 IV21 0.0;0.0 0.0 IV21] [IV22 0.0 0.0;0.0 IV22 0.0;0.0 0.0 IV22] zeros(3,9);
    zeros(3,3) [IV32 0.0 0.0;0.0 IV32 0.0;0.0 0.0 IV32] [IV33 0.0 0.0;0.0 IV33 0.0;0.0 0.0 IV33] zeros(3,6);
    zeros(3,6) [IV43 0.0 0.0;0.0 IV43 0.0;0.0 0.0 IV43] [IV44 0.0 0.0;0.0 IV44 0.0;0.0 0.0 IV44] zeros(3,3);
    zeros(3,9) [IV54 0.0 0.0;0.0 IV54 0.0;0.0 0.0 IV54] [IV55 0.0 0.0;0.0 IV55 0.0;0.0 0.0 IV55]]

%Calculation of the matrices B1,B and Cn and C
B1R=[IVV 0.0 0.0;0.0 IV 0.0;0.0 0.0 IV]
BR=[IVV 0.0 0.0;0.0 IV 0.0;0.0 0.0 IV;zeros(12,3)]
CnR=DT*[(-iXB) 0.0 (-1/YH);(-iXB) (-(1-YH))/(2.86*YH) -1/YH;-(iXB+1/YA) 1/YA 0.0;0.0 0.0 1.0];
CR=[CnR zeros(4,12);zeros(4,3) CnR zeros(4,9);zeros(4,6) CnR zeros(4,6);zeros(4,9) CnR zeros(4,3);zeros(4,12) CnR];

%Calculation of the estimated coefficients
for k = 1:K
    Xk=X(:,k);
    Uk =U(:,k);
    XBHk = XBH(:,k);
    XBAk = XBA(:,k);
    XSk = XS(:,k);
    Xik = Xi(:,k);
   [Pk]=prateASM1R(Xk,Uk,XBHk,XBAk,XSk);
    FIk=CR'*Pk;
    Y(:,k) = X(:,k+1)-AR*X(:,k)-BR*Xi(:,k);
    theta(:,k)=(FIk'*FIk)^(-1)*FIk'*Y(:,k);
end

muHE(1,:)=theta(1,:);muAE(1,:)=theta(2,:);KhE(1,:)=theta(3,:);

 %Simulation of the reduced model with the estimated parameters

XE=[Z(10,1);Z(9,1);Z(2,1);Z(23,1);Z(22,1);Z(15,1);Z(36,1);Z(35,1);Z(28,1);Z(49,1);Z(48,1);Z(41,1);Z(62,1);Z(61,1);
Z(54,1)];
ERR=X(:,1)-XE;
```

```
for k = 1:K
    Xk=X(:,k);
    Uk =U(:,k);
    XBHk = XBH(:,k);
    XBAk = XBA(:,k);
    XSk = XS(:,k);
    Xik = Xi(:,k);
    thetak=theta(:,k);
   [ROASM1E]=rateASM1RE(Xk,Uk,XBHk,XBAk,XSk,thetak);

    XE(:,k+1)=AR*XE(:,k)+CR'*ROASM1E+BR*Xi(:,k);
    ERR(:,k+1)=X(:,k+1)-XE(:,k+1);
end

%vector of process full, estimated and error variables SNH, SNO,SS, Tank 1
SNH1=X(1,:);SNO1=X(2,:);SS1=X(3,:);
SNH1E=XE(1,:);SNO1E=XE(2,:);SS1E=XE(3,:);
ERRSNH1=ERR(1,:);ERRSNO1=ERR(2,:);ERRSS1=ERR(3,:);
%Calculation of the weighted errors for tank1
eSNH1=(ERRSNH1*ERRSNH1')/(SNH1*SNH1')
eSNO1=(ERRSNO1*ERRSNO1')/(SNO1*SNO1')
eSS1=(ERRSS1*ERRSS1')/(SS1*SS1')

%vector of process full, estimated and error variables SNH, SNO,SS, Tank 2
SNH2=X(4,:);SNO2=X(5,:);SS2=X(6,:);
SNH2E=XE(4,:);SNO2E=XE(5,:);SS2E=XE(6,:);
ERRSNH2=ERR(4,:);ERRSNO2=ERR(5,:);ERRSS2=ERR(6,:);
%Calculation of the weighted errors for tank 2
eSNH2=(ERRSNH2*ERRSNH2')/(SNH2*SNH2')
eSNO2=(ERRSNO2*ERRSNO2')/(SNO2*SNO2')
eSS2=(ERRSS2*ERRSS2')/(SS2*SS2')

%vector of process full, estimated and error variables SNH, SNO,SS, Tank 3
SNH3=X(7,:);SNO3=X(8,:);SS3=X(9,:);
SNH3E=XE(7,:);SNO3E=XE(8,:);SS3E=XE(9,:);
ERRSNH3=ERR(7,:);ERRSNO3=ERR(8,:);ERRSS3=ERR(9,:);
%Calculation of the weighted errors for tank 3
eSNH3=(ERRSNH3*ERRSNH3')/(SNH3*SNH3')
eSNO3=(ERRSNO3*ERRSNO3')/(SNO3*SNO3')
eSS3=(ERRSS3*ERRSS3')/(SS3*SS3')

%vector of process full, estimated and error variables SNH, SNO,SS, Tank 4
SNH4=X(10,:);SNO4=X(11,:);SS4=X(12,:);
SNH4E=XE(10,:);SNO4E=XE(11,:);SS4E=XE(12,:);
ERRSNH4=ERR(10,:);ERRSNO4=ERR(11,:);ERRSS4=ERR(12,:);
%Calculation of the weighted errors for tank 4
eSNH4=(ERRSNH4*ERRSNH4')/(SNH4*SNH4')
eSNO4=(ERRSNO4*ERRSNO4')/(SNO4*SNO4')
eSS4=(ERRSS4*ERRSS4')/(SS4*SS4')

%vector of process full, estimated and error variables SNH, SNO,SS, Tank 5
SNH5=X(13,:);SNO5=X(14,:);SS5=X(15,:);
SNH5E=XE(13,:);SNO5E=XE(14,:);SS5E=XE(15,:);
ERRSNH5=ERR(13,:);ERRSNO5=ERR(14,:);ERRSS5=ERR(15,:);
%Calculation of the weighted errors for tank 5
eSNH5=(ERRSNH5*ERRSNH5')/(SNH5*SNH5')
eSNO5=(ERRSNO5*ERRSNO5')/(SNO5*SNO5')
eSS5=(ERRSS5*ERRSS5')/(SS5*SS5')

k=1:100;
%Graphs of the estimated parameters
figure(1)
subplot(3,1,1);plot(k,muHE,'k')
title('Estimated muH')
ylabel('\fontsize{8}muHE')
xlabel('\fontsize{8}discrete time k')

subplot(3,1,2);plot(k,muAE,'k')
title('Estimated muA')
ylabel('\fontsize{8}muAE')
xlabel('\fontsize{8}discrete time k')

subplot(3,1,3);plot(k,KhE,'k')
title('Estimated Kh')
ylabel('\fontsize{8}KhE')
xlabel('\fontsize{8}discrete time k')

k=1:101;
figure(2)
subplot(5,2,1);plot(k,SNH1,'k-',k,SNH1E,'k-.')
title('Process variables Snh1 and Snh1E')
ylabel('\fontsize{8}SNH1,SNH1E')
xlabel('\fontsize{8}discrete time k')

subplot(5,2,2); plot(k,ERRSNH1,'k')
title('Estmation error ERRSnh1')
ylabel('\fontsize{8}ERRSNH1')
xlabel('\fontsize{8}discrete time,k')

subplot(5,2,3);plot(k,SNH2,'k-',k,SNH2E,'k-.')
title('Process variables Snh2 and Snh2E')
ylabel('\fontsize{8}SNH2,SNH2E')
xlabel('\fontsize{8}discrete time k')

subplot(5,2,4); plot(k,ERRSNH2,'k')
title('Estmation error ERRSnh2')
ylabel('\fontsize{8}ERRSNH2')
xlabel('\fontsize{8}discrete time,k')

subplot(5,2,5);plot(k,SNH3,'k-',k,SNH3E,'k-.')
title('Process variables Snh3 and Snh3E')
ylabel('\fontsize{8}SNH3,SNH3E')
xlabel('\fontsize{8}discrete time k')

subplot(5,2,6); plot(k,ERRSNH3,'k')
title('Estmation error ERRSnh3')
ylabel('\fontsize{8}ERRSNH3')
xlabel('\fontsize{8}discrete time,k')

subplot(5,2,7);plot(k,SNH4,'k-',k,SNH4E,'k-.')
title('Process variables Snh4 and Snh4E')
ylabel('\fontsize{8}SNH4,SNH4E')
xlabel('\fontsize{8}discrete time k')

subplot(5,2,8); plot(k,ERRSNH4,'k')
title('Estmation error ERRSnh4')
ylabel('\fontsize{8}ERRSNH4')
xlabel('\fontsize{8}discrete time,k')

subplot(5,2,9);plot(k,SNH5,'k-',k,SNH5E,'k-.')
title('Process variables Snh5 and Snh5E')
ylabel('\fontsize{8}SNH5,SNH5E')
xlabel('\fontsize{8}discrete time k')

subplot(5,2,10); plot(k,ERRSNH5,'k')
title('Estmation error ERRSnh5')
ylabel('\fontsize{8}ERRSNH5')
xlabel('\fontsize{8}discrete time,k')

figure(3)
subplot(5,2,1);plot(k,SNO1,'k-',k,SNO1E,'k-.')
```

```
title('Process variables SNO1 and SNO1E')
ylabel('\fontsize{8}SNO1,SNO1E')
xlabel('\fontsize{8}discrete time k')

subplot(5,2,2); plot(k,ERRSNO1,'k')
title('Estmation error ERRSNO1')
ylabel('\fontsize{8}ERRSNO1')
xlabel('\fontsize{8}discrete time,k')

subplot(5,2,3);plot(k,SNO2,'k-',k,SNO2E,'k-.')
title('Process variables SNO2 and SNO2E')
ylabel('\fontsize{8}SNO2,SNO2E')
xlabel('\fontsize{8}discrete time k')

subplot(5,2,4); plot(k,ERRSNO2,'k')
title('Estmation error ERRSNO2')
ylabel('\fontsize{8}ERRSNO2')
xlabel('\fontsize{8}discrete time,k')

subplot(5,2,5);plot(k,SNO3,'k-',k,SNO3E,'k-.')
title('Process variables SNO3 and SNO3E')
ylabel('\fontsize{8}SNO3,SNO3E')
xlabel('\fontsize{8}discrete time k')

subplot(5,2,6); plot(k,ERRSNO3,'k')
title('Estmation error ERRSNO3')
ylabel('\fontsize{8}ERRSNO3')
xlabel('\fontsize{8}discrete time,k')

subplot(5,2,7);plot(k,SNO4,'k-',k,SNO4E,'k-.')
title('Process variables SNO4 and SNO4E')
ylabel('\fontsize{8}SNO4,SNO4E')
xlabel('\fontsize{8}discrete time k')

subplot(5,2,8); plot(k,ERRSNO4,'k')
title('Estmation error ERRSNO4')
ylabel('\fontsize{8}ERRSNO4')
xlabel('\fontsize{8}discrete time,k')

subplot(5,2,9);plot(k,SNO5,'k-',k,SNO5E,'k-.')
title('Process variables SNO5 and SNO5E')
ylabel('\fontsize{8}SNO5,SNO5E')
xlabel('\fontsize{8}discrete time k')

subplot(5,2,10); plot(k,ERRSNO5,'k')
title('Estmation error ERRSNO5')
ylabel('\fontsize{8}ERRSNO5')
xlabel('\fontsize{8}discrete time,k')
```

```
figure(4)
subplot(5,2,1);plot(k,SS1,'k-',k,SS1E,'k-.')
title('Process variables SS1 and SS1E')
ylabel('\fontsize{8}SS1,SS1E')
xlabel('\fontsize{8}discrete time k')

subplot(5,2,2); plot(k,ERRSS1,'k')
title('Estmation error ERRSS1')
ylabel('\fontsize{8}ERRSS1')
xlabel('\fontsize{8}discrete time,k')

subplot(5,2,3);plot(k,SS2,'k-',k,SS2E,'k-.')
title('Process variables SS2 and SS2E')
ylabel('\fontsize{8}SS2,SS2E')
xlabel('\fontsize{8}discrete time k')

subplot(5,2,4); plot(k,ERRSS2,'k')
title('Estmation error ERRSS2')
ylabel('\fontsize{8}ERRSS2')
xlabel('\fontsize{8}discrete time,k')

subplot(5,2,5);plot(k,SS3,'k-',k,SS3E,'k-.')
title('Process variables SS3 and SS3E')
ylabel('\fontsize{8}SS3,SS3E')
xlabel('\fontsize{8}discrete time k')

subplot(5,2,6); plot(k,ERRSS3,'k')
title('Estmation error ERRSS3')
ylabel('\fontsize{8}ERRSS3')
xlabel('\fontsize{8}discrete time,k')

subplot(5,2,7);plot(k,SS4,'k-',k,SS4E,'k-.')
title('Process variables SS4 and SS4E')
ylabel('\fontsize{8}SS4,SS4E')
xlabel('\fontsize{8}discrete time k')

subplot(5,2,8); plot(k,ERRSS4,'k')
title('Estmation error ERRSS4')
ylabel('\fontsize{8}ERRSS4')
xlabel('\fontsize{8}discrete time,k')

subplot(5,2,9);plot(k,SS5,'k-',k,SS5E,'k-.')
title('Process variables SS5 and SS5E')
ylabel('\fontsize{8}SS5,SS5E')
xlabel('\fontsize{8}discrete time k')

subplot(5,2,10); plot(k,ERRSS5,'k')
title('Estmation error ERRSS5')
ylabel('\fontsize{8}ERRSS5')
xlabel('\fontsize{8}discrete time,k')
```

1.2.Subprograms

%SUBPROGRAM rateAASM1F.m

```
%AIM:The program function rateASM1F.m calculates the process rates of the full ASM1 biological model at every moment of
the time.The program uses global definition of the model parameters

function [ROASM1F]=rateAASM1F(Zk)
global Ks KOH KNO KNH KOA Kx muH etag muA Kh etah iXB YH YA fP iXP bH bA Ka

%Process rates for the tank 1
ROASM1F(1)=muH*(Zk(2)/(Ks+Zk(2)))*(Zk(8)/(KOH+Zk(8)))*Zk(5);
ROASM1F(2)=muH*(Zk(2)/(Ks+Zk(2)))*(KOH/(KOH+Zk(8)))*(Zk(9)/(KNO+Zk(9)))*etag*Zk(5);
ROASM1F(3)=muA*(Zk(10)/(KNH+Zk(10)))*(Zk(8)/(KOA+Zk(8)))*Zk(6);
ROASM1F(4)=bH*Zk(5);
ROASM1F(5)=bA*Zk(6);
ROASM1F(6)=Ka*Zk(11)*Zk(5);
x1=Zk(4)/Zk(5);
ROASM1F(7)=Kh*Zk(5)*(x1/(Kx+x1))*((Zk(8)/(KOH+Zk(8)))+etah*(KOH/(KOH+Zk(8)))*(Zk(9)/(KNO+Zk(9))));
ROASM1F(8)=ROASM1F(7)*Zk(12)/Zk(4);

%Process rates for the tank 2
ROASM1F(9)=muH*(Zk(15)/(Ks+Zk(15)))*(Zk(21)/(KOH+Zk(21)))*Zk(18);
ROASM1F(10)=muH*(Zk(15)/(Ks+Zk(15)))*(KOH/(KOH+Zk(21)))*(Zk(22)/(KNO+Zk(22)))*etag*Zk(18);
ROASM1F(11)=muA*(Zk(23)/(KNH+Zk(23)))*(Zk(21)/(KOA+Zk(21)))*Zk(19);
ROASM1F(12)=bH*Zk(18);
ROASM1F(13)=bA*Zk(19);
ROASM1F(14)=Ka*Zk(24)*Zk(18);
x1=Zk(17)/Zk(18);
ROASM1F(15)=Kh*Zk(18)*(x1/(Kx+x1))*((Zk(21)/(KOH+Zk(21)))+etah*(KOH/(KOH+Zk(21)))*(Zk(22)/(KNO+Zk(22))));
ROASM1F(16)=ROASM1F(15)*Zk(25)/Zk(17);

%Process rates for the tank 3
ROASM1F(17)=muH*(Zk(28)/(Ks+Zk(28)))*(Zk(34)/(KOH+Zk(34)))*Zk(31);
ROASM1F(18)=muH*(Zk(28)/(Ks+Zk(28)))*(KOH/(KOH+Zk(34)))*(Zk(35)/(KNO+Zk(35)))*etag*Zk(31);
ROASM1F(19)=muA*(Zk(36)/(KNH+Zk(36)))*(Zk(34)/(KOA+Zk(34)))*Zk(32);
ROASM1F(20)=bH*Zk(31);
ROASM1F(21)=bA*Zk(32);
ROASM1F(22)=Ka*Zk(37)*Zk(31);
x1=Zk(30)/Zk(31);
ROASM1F(23)=Kh*Zk(31)*(x1/(Kx+x1))*((Zk(34)/(KOH+Zk(34)))+etah*(KOH/(KOH+Zk(34)))*(Zk(35)/(KNO+Zk(35))));
ROASM1F(24)=ROASM1F(23)*Zk(38)/Zk(30);

ROASM1F=[ROASM1F(1);ROASM1F(2);ROASM1F(3);ROASM1F(4);ROASM1F(5);ROASM1F(6);ROASM1F(7);ROASM1F(8);ROASM1F(9);
```

```
ROASM1F(10);
ROASM1F(11);ROASM1F(12);ROASM1F(13);ROASM1F(14);ROASM1F(15);ROASM1F(16);ROASM1F(17);ROASM1F(18);ROASM1F(19);
ROASM1F(20);ROASM1F(21);ROASM1F(22);ROASM1F(23);ROASM1F(24)];
```

%SUBPROGRAM prateASM1R.m

```
%AIM:The program function prateASM1.m calculates the functions of the process rates which multiply
%the process estimated parameters for the Benchmark process based on the reduced ASM1 biological model at every moment
of time.The program uses global definition of the model parameters

function [Pk]=prateASM1R(Xk,Uk,XBHk,XBAk,XSk)
global Ks KOH KNO KNH KOA Kx muH etag muA Kh etah iXB YH YA fP iXP bH bA Ka

%Tank 1
P11=(Xk(3)/(Ks+Xk(3)))*(Uk(1)/(KOH+Uk(1)))*XBHk(1);
P12=(Xk(3)/(Ks+Xk(3)))*(KOH/(KOH+Uk(1)))*(Xk(2)/(KNO+Xk(2)))*etag*XBHk(1);
P13=(Xk(1)/(KNH+Xk(1)))*(Uk(1)/(KOA+Uk(1)))*XBAk(1);
x1=XSk(1)/XBHk(1);
P14=XBHk(1)*(x1/(Kx+x1))*((Uk(1)/(KOH+Uk(1)))+etah*(KOH/(KOH+Uk(1)))*(Xk(2)/(KNO+Xk(2))));
P1k=[P11 0 0;P12 0 0;0 P13 0;0 0 P14];
 %Tank 2
P21=(Xk(6)/(Ks+Xk(6)))*(Uk(2)/(KOH+Uk(2)))*XBHk(2);
P22=(Xk(6)/(Ks+Xk(6)))*(KOH/(KOH+Uk(2)))*(Xk(5)/(KNO+Xk(5)))*etag*XBHk(2);
P23=(Xk(4)/(KNH+Xk(4)))*(Uk(2)/(KOA+Uk(2)))*XBAk(2);
x1=XSk(2)/XBHk(2);
P24=XBHk(2)*(x1/(Kx+x1))*((Uk(2)/(KOH+Uk(2)))+etah*(KOH/(KOH+Uk(2)))*(Xk(5)/(KNO+Xk(5))));
P2k=[P21 0 0;P22 0 0;0 P23 0;0 0 P24];
 %Tank 3
P31=(Xk(9)/(Ks+Xk(9)))*(Uk(3)/(KOH+Uk(3)))*XBHk(3);
P32=(Xk(9)/(Ks+Xk(9)))*(KOH/(KOH+Uk(3)))*(Xk(8)/(KNO+Xk(8)))*etag*XBHk(3);
P33=(Xk(7)/(KNH+Xk(7)))*(Uk(3)/(KOA+Uk(3)))*XBAk(3);
x1=XSk(3)/XBHk(3);
P34=XBHk(3)*(x1/(Kx+x1))*((Uk(3)/(KOH+Uk(3)))+etah*(KOH/(KOH+Uk(3)))*(Xk(8)/(KNO+Xk(8))));
P3k=[P31 0 0;P32 0 0;0 P33 0;0 0 P34];
 %Tank 4
P41=(Xk(12)/(Ks+Xk(12)))*(Uk(4)/(KOH+Uk(4)))*XBHk(4);
P42=(Xk(12)/(Ks+Xk(12)))*(KOH/(KOH+Uk(4)))*(Xk(11)/(KNO+Xk(11)))*etag*XBHk(4);
P43=(Xk(10)/(KNH+Xk(10)))*(Uk(4)/(KOA+Uk(4)))*XBAk(4);
x1=XSk(4)/XBHk(4);
P44=XBHk(4)*(x1/(Kx+x1))*((Uk(4)/(KOH+Uk(4)))+etah*(KOH/(KOH+Uk(4)))*(Xk(11)/(KNO+Xk(11))));
P4k=[P41 0 0;P42 0 0;0 P43 0;0 0 P44];
 %Tank 5
P51=(Xk(15)/(Ks+Xk(15)))*(Uk(5)/(KOH+Uk(5)))*XBHk(5);
P52=(Xk(15)/(Ks+Xk(15)))*(KOH/(KOH+Uk(5)))*(Xk(14)/(KNO+Xk(14)))*etag*XBHk(5);
P53=(Xk(13)/(KNH+Xk(13)))*(Uk(5)/(KOA+Uk(5)))*XBAk(5);
x1=XSk(5)/XBHk(5);
P54=XBHk(5)*(x1/(Kx+x1))*((Uk(5)/(KOH+Uk(5)))+etah*(KOH/(KOH+Uk(5)))*(Xk(14)/(KNO+Xk(14))));
P5k=[P51 0 0;P52 0 0;0 P53 0;0 0 P44];

%Matrix Pk for the whole process
Pk=[P1k;P2k;P3k;P4k;P5k];
```

%SUBPROGRAM rateASM1RE.m

```
%AIM:The program function rateASM1.m calculates at every moment the process rates of the reduced ASM1 model using the
estimated values of the model parameters. The program uses global definition of the parameters

function [ROASM1E]=rateASM1RE(Xk,Uk,XBHk,XBAk,XSk,thetak)
global Ks KOH KNO KNH KOA Kx muH etag muA Kh etah iXB YH YA fP iXP bH bA Ka

%Process rates for every tank
ROASM1(1)=thetak(1)*(Xk(3)/(Ks+Xk(3)))*(Uk(1)/(KOH+Uk(1)))*XBHk(1);
ROASM1(2)=thetak(1)*(Xk(3)/(Ks+Xk(3)))*(KOH/(KOH+Uk(1)))*(Xk(2)/(KNO+Xk(2)))*etag*XBHk(1);
ROASM1(3)=thetak(2)*(Xk(1)/(KNH+Xk(1)))*(Uk(1)/(KOA+Uk(1)))*XBAk(1);
x1=XSk(1)/XBHk(1);
ROASM1(4)=thetak(3)*XBHk(1)*(x1/(Kx+x1))*((Uk(1)/(KOH+Uk(1)))+etah*(KOH/(KOH+Uk(1)))*(Xk(2)/(KNO+Xk(2))));

ROASM1(5)=thetak(1)*(Xk(6)/(Ks+Xk(6)))*(Uk(2)/(KOH+Uk(2)))*XBHk(2);
ROASM1(6)=thetak(1)*(Xk(6)/(Ks+Xk(6)))*(KOH/(KOH+Uk(2)))*(Xk(5)/(KNO+Xk(5)))*etag*XBHk(2);
ROASM1(7)=thetak(2)*(Xk(4)/(KNH+Xk(4)))*(Uk(2)/(KOA+Uk(2)))*XBAk(2);
x1=XSk(2)/XBHk(2);
ROASM1(8)=thetak(3)*XBHk(2)*(x1/(Kx+x1))*((Uk(2)/(KOH+Uk(2)))+etah*(KOH/(KOH+Uk(2)))*(Xk(5)/(KNO+Xk(5))));

ROASM1(9)=thetak(1)*(Xk(9)/(Ks+Xk(9)))*(Uk(3)/(KOH+Uk(3)))*XBHk(3);
ROASM1(10)=thetak(1)*(Xk(9)/(Ks+Xk(9)))*(KOH/(KOH+Uk(3)))*(Xk(8)/(KNO+Xk(8)))*etag*XBHk(3);
ROASM1(11)=thetak(2)*(Xk(7)/(KNH+Xk(7)))*(Uk(3)/(KOA+Uk(3)))*XBAk(3);
x1=XSk(3)/XBHk(3);
ROASM1(12)=thetak(3)*XBHk(3)*(x1/(Kx+x1))*((Uk(3)/(KOH+Uk(3)))+etah*(KOH/(KOH+Uk(3)))*(Xk(8)/(KNO+Xk(8))));

ROASM1(13)=thetak(1)*(Xk(12)/(Ks+Xk(12)))*(Uk(4)/(KOH+Uk(4)))*XBHk(4);
ROASM1(14)=thetak(1)*(Xk(12)/(Ks+Xk(12)))*(KOH/(KOH+Uk(4)))*(Xk(11)/(KNO+Xk(11)))*etag*XBHk(4);
ROASM1(15)=thetak(2)*(Xk(10)/(KNH+Xk(10)))*(Uk(4)/(KOA+Uk(4)))*XBAk(4);
x1=XSk(4)/XBHk(4);
ROASM1(16)=thetak(3)*XBHk(4)*(x1/(Kx+x1))*((Uk(4)/(KOH+Uk(4)))+etah*(KOH/(KOH+Uk(4)))*(Xk(11)/(KNO+Xk(11))));

ROASM1(17)=thetak(1)*(Xk(15)/(Ks+Xk(15)))*(Uk(5)/(KOH+Uk(5)))*XBHk(5);
ROASM1(18)=thetak(1)*(Xk(15)/(Ks+Xk(15)))*(KOH/(KOH+Uk(5)))*(Xk(14)/(KNO+Xk(14)))*etag*XBHk(5);
ROASM1(19)=thetak(2)*(Xk(13)/(KNH+Xk(13)))*(Uk(5)/(KOA+Uk(5)))*XBAk(5);
x1=XSk(5)/XBHk(5);
ROASM1(20)=thetak(3)*XBHk(5)*(x1/(Kx+x1))*((Uk(5)/(KOH+Uk(5)))+etah*(KOH/(KOH+Uk(5)))*(Xk(14)/(KNO+Xk(14))));

%Vector of the process rates
 ROASM1E=[ROASM1(1) ROASM1(2) ROASM1(3) ROASM1(4) ROASM1(5) ROASM1(6) ROASM1(7) ROASM1(8) ROASM1(9) ROASM1(10)
ROASM1(11) ROASM1(12) ROASM1(13) ROASM1(14) ROASM1(15) ROASM1(16) ROASM1(17) ROASM1(18) ROASM1(19) ROASM1(20)]';
```

2. SOFTWARE FOR PARAMETER ESTIMATION OF THE ATHLONE MASS-BALANCE MODEL FOR THE CASE OF ASM1 REDUCED MODEL

2.1.Main program

%PROGRAM BASM1parest.m

```
%Aim - the program estimates the reduced ASM1 model parameters for the Athlone process and calculates the errors
between the process variables behaviour for the full and reduced models. The program call the function subroutines
rateASM1F.m, prateASM1R.m and rateASM1RE.m. The calculation uses the reduced biological model with 3 variables SNH, SNO
and SS. The program uses global definition of the model parameters

global Ks KOH KNO KNH KOA Kx muH etag muA Kh etah iXB YH YA fP iXP bH bA Ka
%Process parameters
f=1.2;YA = 0.24;YH = 0.67;iXB = 0.08;muH = 0.4;Ks = 10;KOH = 0.2;KNO = 0.5;etag = 0.8;etah = 0.8;Kh = 3;Kx = 0.1;muA =
0.5;KNH = 1;KOA = 0.4;fP = 0.08;iXP = 0.06;bH = 0.3;bA = 0.05;Ka = 0.05;
% Values of the process Flowrates
Qo = 40003.2;Qa = 39916.8*0.5;Qp = 39916.8*0.45;Qr = 40003.2;Qw = 3840.0*1;
% Volumes of the process tanks
V1=1148;V2=1148;V3=5273;LAMBDA = (Qo+Qp+Qr-Qw)/Qr
%Oxygen parameters
SOsat = 8;Kla1=4.8;Kla2=4.8;Kla3=240.0;
Kl=[Kla1 Kla2 Kla3];
Kla=diag(Kl);

%Determination of the sampling period
DT = 0.01042;days=0.1042*10;K=days/DT;k=0:DT:days;

%calculation of the model matrices
%Calculation of the matrix CF

YH1 = -1/YH;YA1 = 1/YA;YH2 = -(1-YH)/YH;YA2 = -(4.57/YA)+1;YH3 = -(1-YH)/(2.86*YH);fP1 = 1-fP;iXB1 = -(iXB+YA1);
iXB2 = iXB-(fP*iXP);iXB3 = -iXB/14;YH4 = (1-YH)/(14*2.86*YH)+iXB3;YA3 = iXB3-YA1/7;YH5 = 1/14;
YZSI = [0 0 0 0 0 0 0 0]';
YZSS = [YH1 YH1 0 0 0 0 1 0]';
YZXI = [0 0 0 0 0 0 0 0]';
YZXS = [0 0 0 fP1 fP1 0 -1 0]';
YZXBH = [1 1 0 -1 0 0 0 0]';
YZXBA = [0 0 1 0 -1 0 0 0]';
YZXP = [0 0 0 fP fP 0 0 0]';
YZSO = [YH2 0 YA2 0 0 0 0 0]';
YZSNO = [0 YH3 YA1 0 0 0 0 0]';
YZSNH = [-iXB -iXB iXB1 0 0 1 0 0]';
YZSND = [0 0 0 0 0 -1 0 1]';
YZXND = [0 0 0 iXB2 iXB2 0 0 -1]';
YZSALK = [iXB3 YH4 YA3 0 0 YH5 0 0]';
Cn = DT*[YZSI  YZSS  YZXI  YZXS  YZXBH  YZXBA  YZXP  YZSO  YZSNO  YZSNH  YZSND  YZXND  YZSALK];
CF=[Cn zeros(8,26);zeros(8,13) Cn zeros(8,13);zeros(8,26) Cn];

%Calculation of matrix AF
%Calculation of the process matrices
IV1 = DT/V1;IV2 = DT/V2;IV3 = DT/V3;IV=IV1*Qo;IVV=IV*f
B=[IVV 0.0 0.0;0.0 IV 0.0;0.0 0.0 IV;zeros(6,3)];
Q1=Qo+Qp;Q2=Q1+Qa+Qr;Q3=Q2

IV221=IV2*Q2;IV331=IV3*Q3
IV11=1-IV1*Q1 %element of A11
IV12=IV1*Qp    %element of A12
IV21=IV2*Q1    %element of A21
IV22=1-IV221   %element of A22
IV23=IV2*(Qa+Qr)  %element of A23 soluble
IV23p=IV2*(Qa+LAMBDA*Qr)
IV32=IV3*Q2  %element of A32
IV33=1-IV331   %element of A33

a1=[IV11,IV11,IV11,IV11,IV11,IV11,IV11,IV11,IV11,IV11,IV11,IV11,IV11,IV11];
A11=diag(a1);
a2=[IV22,IV22,IV22,IV22,IV22,IV22,IV22,IV22,IV22,IV22,IV22,IV22,IV22,IV22];
A22=diag(a2);
a3=[IV33,IV33,IV33,IV33,IV33,IV33,IV33,IV33,IV33,IV33,IV33,IV33,IV33,IV33];
A33=diag(a3);
a12=[IV12,IV12,IV12,IV12,IV12,IV12,IV12,IV12,IV12,IV12,IV12,IV12,IV12,IV12];
A12=diag(a12);
a21=[IV21,IV21,IV21,IV21,IV21,IV21,IV21,IV21,IV21,IV21,IV21,IV21,IV21,IV21];
A21=diag(a21);
a23=[IV23,IV23,IV23p,IV23,IV23p,IV23p,IV23p,IV23,IV23,IV23,IV23,IV23p,IV23];
A23=diag(a23);
a32=[IV32,IV32,IV32,IV32,IV32,IV32,IV32,IV32,IV32,IV32,IV32,IV32,IV32,IV32];
A32=diag(a32);

AF=[A11 A12 zeros(13,13);A21 A22 A23;zeros(13,13) A32 A33]
%Calculation of the matrix BF
b1=[IV,IV,IV,IV,IV,IV,IV,IV,IV,IV,IV,IV,IV,IV]
B1=diag(b1);BF=[B1;zeros(26,13)]

%Average influent concentrations trajectories for the process variables
SSi=69.5;XBHi=28.17;XSi=202.32;XIi=51.2;SNHi=31.56;SIi=30.0;SNDi=6.95;XNDi=10.59;S0i=0.0;XBAi=0.0;XPi=0.0;SNOi=0.0;
SALKi=7.0;
Zi=[SIi*ones(1,K);SSi*ones(1,K);XIi*ones(1,K);XSi*ones(1,K);XBHi*ones(1,K);XBAi*ones(1,K);XPi*ones(1,K);S0i*ones(1,K);S
NOi*ones(1,K);SNHi*ones(1,K);SNDi*ones(1,K);XNDi*ones(1,K);SALKi*ones(1,K)]*0.01;

%Determination of the initial conditions
Si_1    =   3.0000000e+01;Ss_1     =  2.8082131e+00;Xi_1      = 1.1491252e+03;Xs_1    =   8.2134908e+01;
```

```
Xbh_1   =   2.5517658e+03;Xba_1   =   1.4838943e+02;Xp_1    =   4.4885186e+02;So_1    =   4.2984433e-03;
Sno_1   =   5.3699400e+00;Snh_1   =   7.9178845e+00;Snd_1   =   1.2166405e+00;Xnd_1   =   5.2848894e+00;
Salk_1  =   4.9277103e+00;
Z10 = [Si_1 ;Ss_1 ;Xi_1 ;Xs_1 ;Xbh_1 ;Xba_1 ;Xp_1 ;So_1 ;Sno_1 ;Snh_1 ;Snd_1 ;Xnd_1 ;Salk_1 ];

Si_2    =   3.0000000e+01;Ss_2    =   1.4587940e+00;Xi_2    =   1.1491252e+03;Xs_2    =   7.6386187e+01;
Xbh_2   =   2.5533851e+03;Xba_2   =   1.4830914e+02;Xp_2    =   4.4952273e+02;So_2    =   6.3131911e-05;
Sno_2   =   3.6619672e+00;Snh_2   =   8.3444148e+00;Snd_2    =   8.8206477e-01;Xnd_2   =   5.0290873e+00;
Salk_2  =   5.0801748e+00;
Z20 = [Si_2 ;Ss_2 ;Xi_2 ;Xs_2 ;Xbh_2 ;Xba_2 ;Xp_2 ;So_2 ;Sno_2 ;Snh_2 ;Snd_2 ;Xnd_2 ;Salk_2 ];

Si_3    =   3.0000000e+01;Ss_3    =   1.1495418e+00;Xi_3    =   1.1491252e+03;Xs_3    =   6.4854922e+01;
Xbh_3   =   2.5571314e+03;Xba_3   =   1.4894126e+02;Xp_3    =   4.5041834e+02;So_3    =   1.7183778e+00;
Sno_3   =   6.5408820e+00;Snh_3   =   5.5479452e+00;Snd_3   =   8.2888682e-01;Xnd_3   =   4.3924277e+00;
Salk_3  =   4.6747902e+00;
Z30 = [Si_3 ;Ss_3 ;Xi_3 ;Xs_3 ;Xbh_3 ;Xba_3 ;Xp_3 ;So_3 ;Sno_3 ;Snh_3 ;Snd_3 ;Xnd_3 ;Salk_3 ];
Z0=[Z10;Z20;Z30]*0.01
% calculation of the initial trajectory for the state vector Z
Z=[Z0 zeros(39,K)];
%Simulation of the full model behavior
for k = 1:K
    Zk=Z(:,k);
    S0k=[Zk(8,1);Zk(21,1);Zk(34,1)];
    Zik = Zi(:,k);
   [ROASM1F]=rateAASM1F(Zk);
    ZZk=DT*Kla*(S0sat-S0k);
    ZZ1k=[zeros(7,1);ZZk(1);zeros(12,1);ZZk(2);zeros(12,1);ZZk(3);zeros(5,1)];
    Z(:,k+1) = AF*Z(:,k) + CF''*ROASM1F + BF*Zi(:,k)+ZZ1k;
end
%Selection of the measured variables of state space SNH,SNO,SS
X=[Z(10,:);Z(9,:);Z(2,:);Z(23,:);Z(22,:);Z(15,:);Z(36,:);Z(35,:);Z(28,:)]
%trajectory of the control signal
U=[Z(8,:);Z(21,:);Z(34,:)]

%Calculation of the vector P

%Average values of the inflow concentrations for dry weather
Xi  =[SNHi*ones(1,K);SNOi*ones(1,K);SSi*ones(1,K)]*0.01

% Steady state values for the biomass XBH, XBA, XS
XBH = [2551.76*ones(1,K);2553.38*ones(1,K);2557.13*ones(1,K)]*0.01;% XBH steady state COD/m^3
XBA = [148.389*ones(1,K);148.309*ones(1,K);148.941*ones(1,K)]*0.01;% XBA steady state g all COD/m^3
XS = [82.135*ones(1,K);76.386*ones(1,K);64.855*ones(1,K)]*0.01; % XS steady state all COD/m^3

%Calculation of the state space process model matrices
%Calculation of the matrix A
AR=[[IV11 0.0 0.0;0.0 IV11 0.0;0.0 0.0 IV11] [IV12 0.0 0.0;0.0 IV12 0.0;0.0 0.0 IV12] zeros(3,3) ;
    [IV21 0.0 0.0;0.0 IV21 0.0;0.0 0.0 IV21] [IV22 0.0 0.0;0.0 IV22 0.0;0.0 0.0 IV22] [IV23 0.0 0.0;0.0 IV23 0.0;0.0
0.0 IV23];zeros(3,3) [IV32 0.0 0.0;0.0 IV32 0.0;0.0 0.0 IV32] [IV33 0.0 0.0;0.0 IV33 0.0;0.0 0.0 IV33]]
%Calculation of the matrices B1,BR and Cn and CR
B1R=[IVV 0.0 0.0;0.0 IV 0.0;0.0 0.0 IV]
BR=[IVV 0.0 0.0;0.0 IV 0.0;0.0 0.0 IV;zeros(6,3)]
CnR=DT*[(-iXB) 0.0 (-1/YH);(-iXB) (-(1-YH))/(2.86*YH) -1/YH;-(iXB+1/YA) 1/YA 0.0;0.0 0.0 1.0];
CR=[CnR zeros(4,6);zeros(4,3) CnR zeros(4,3);zeros(4,6) CnR];

%Calculation of the estimated coefficients
for k = 1:K
    Xk=X(:,k);
    Uk =U(:,k);
    XBHk = XBH(:,k);
    XBAk = XBA(:,k);
    XSk = XS(:,k);
    Xik = Xi(:,k);
   [Pk]=prateAASM1R(Xk,Uk,XBHk,XBAk,XSk);
    FIk=CR''*Pk;
    Yk = X(:,k+1)-AR*X(:,k)-BR*Xi(:,k);
    theta(:,k)=(FIk''*FIk)^(-1)*FIk''*Yk;
end

muHE(1,:)=theta(1,:);muAE(1,:)=theta(2,:);KhE(1,:)=theta(3,:);

 %Simulation of the reduced model with the estimated parameters

XE=[Z(10,1);Z(9,1);Z(2,1);Z(23,1);Z(22,1);Z(15,1);Z(36,1);Z(35,1);Z(28,1)];
ERR=X(:,1)-XE;
for k = 1:K
    Xk=X(:,k);
    Uk =U(:,k);
    XBHk = XBH(:,k);
    XBAk = XBA(:,k);
    XSk = XS(:,k);
    Xik = Xi(:,k);
    thetak=theta(:,k);
   [ROASM1E]=rateAASM1RE(Xk,Uk,XBHk,XBAk,XSk,thetak);

    XE(:,k+1)=AR*XE(:,k)+CR''*ROASM1E+BR*Xi(:,k);
    ERR(:,k+1)=X(:,k+1)-XE(:,k+1);
end

%vector of process full, estimated and error variables SNH, SNO,SS, Tank 1
SNH1=X(1,:);SNO1=X(2,:);SS1=X(3,:);
SNH1E=XE(1,:);SNO1E=XE(2,:);SS1E=XE(3,:);
ERRSNH1=ERR(1,:);ERRSNO1=ERR(2,:);ERRSS1=ERR(3,:);
%Calculation of the weighted errors for tank1
eSNH1=(ERRSNH1*ERRSNH1')/(SNH1*SNH1')
```

```
eSNO1=(ERRSNO1*ERRSNO1')/(SNO1*SNO1')
eSS1=(ERRSS1*ERRSS1')/(SS1*SS1')

%vector of process full, estimated and error variables SNH, SNO,SS, Tank 2
SNH2=X(4,:);SNO2=X(5,:);SS2=X(6,:);
SNH2E=XE(4,:);SNO2E=XE(5,:);SS2E=XE(6,:);
ERRSNH2=ERR(4,:);ERRSNO2=ERR(5,:);ERRSS2=ERR(6,:);
%Calculation of the weighted errors for tank 2
eSNH2=(ERRSNH2*ERRSNH2')/(SNH2*SNH2')
eSNO2=(ERRSNO2*ERRSNO2')/(SNO2*SNO2')
eSS2=(ERRSS2*ERRSS2')/(SS2*SS2')

%vector of process full, estimated and error variables SNH, SNO,SS, Tank 3
SNH3=X(7,:);SNO3=X(8,:);SS3=X(9,:);
SNH3E=XE(7,:);SNO3E=XE(8,:);SS3E=XE(9,:);
ERRSNH3=ERR(7,:);ERRSNO3=ERR(8,:);ERRSS3=ERR(9,:);
%Calculation of the weighted errors for tank 3
eSNH3=(ERRSNH3*ERRSNH3')/(SNH3*SNH3')
eSNO3=(ERRSNO3*ERRSNO3')/(SNO3*SNO3')
eSS3=(ERRSS3*ERRSS3')/(SS3*SS3')


k=1:100;
%Graphs of the estimated parameters
figure(1)
subplot(3,1,1);plot(k,muHE,'k')
title('Estimated muH')
ylabel('\fontsize{8}muHE')
xlabel('\fontsize{8}discrete time k')

subplot(3,1,2);plot(k,muAE,'k')
title('Estimated muA')
ylabel('\fontsize{8}muAE')
xlabel('\fontsize{8}discrete time k')

subplot(3,1,3);plot(k,KhE,'k')
title('Estimated Kh')
ylabel('\fontsize{8}KhE')
xlabel('\fontsize{8}discrete time k')

k=1:101;
figure(2)
subplot(3,2,1);plot(k,SNH1,'k-',k,SNH1E,'k-.')
title('Process variables Snh1 and Snh1E')
ylabel('\fontsize{8}SNH1,SNH1E')
xlabel('\fontsize{8}discrete time k')

subplot(3,2,2); plot(k,ERRSNH1,'k')
title('Estmation error ERRSnh1')
ylabel('\fontsize{8}ERRSNH1')
xlabel('\fontsize{8}discrete time,k')

subplot(3,2,3);plot(k,SNH2,'k-',k,SNH2E,'k-.')
title('Process variables Snh2 and Snh2E')
ylabel('\fontsize{8}SNH2,SNH2E')
xlabel('\fontsize{8}discrete time k')

subplot(3,2,4); plot(k,ERRSNH2,'k')
title('Estmation error ERRSnh2')
ylabel('\fontsize{8}ERRSNH2')
xlabel('\fontsize{8}discrete time,k')

subplot(3,2,5);plot(k,SNH3,'k-',k,SNH3E,'k-.')
title('Process variables Snh3 and Snh3E')
ylabel('\fontsize{8}SNH3,SNH3E')
xlabel('\fontsize{8}discrete time k')

subplot(3,2,6); plot(k,ERRSNH3,'k')
title('Estmation error ERRSnh3')
ylabel('\fontsize{8}ERRSNH3')
xlabel('\fontsize{8}discrete time,k')

figure(3)
subplot(3,2,1);plot(k,SNO1,'k-',k,SNO1E,'k-.')
title('Process variables SNO1 and SNO1E')
ylabel('\fontsize{8}SNO1,SNO1E')
xlabel('\fontsize{8}discrete time k')

subplot(3,2,2); plot(k,ERRSNO1,'k')
title('Estmation error ERRSNO1')
ylabel('\fontsize{8}ERRSNO1')
xlabel('\fontsize{8}discrete time,k')

subplot(3,2,3);plot(k,SNO2,'k-',k,SNO2E,'k-.')
title('Process variables SNO2 and SNO2E')
ylabel('\fontsize{8}SNO2,SNO2E')
xlabel('\fontsize{8}discrete time k')

subplot(3,2,4); plot(k,ERRSNO2,'k')
title('Estmation error ERRSNO2')
ylabel('\fontsize{8}ERRSNO2')
xlabel('\fontsize{8}discrete time,k')

subplot(3,2,5);plot(k,SNO3,'k-',k,SNO3E,'k-.')
title('Process variables SNO3 and SNO3E')
ylabel('\fontsize{8}SNO3,SNO3E')
xlabel('\fontsize{8}discrete time k')

subplot(3,2,6); plot(k,ERRSNO3,'k')
title('Estmation error ERRSNO3')
ylabel('\fontsize{8}ERRSNO3')
xlabel('\fontsize{8}discrete time,k')

figure(4)
subplot(3,2,1);plot(k,SS1,'k-',k,SS1E,'k-.')
title('Process variables SS1 and SS1E')
ylabel('\fontsize{8}SS1,SS1E')
xlabel('\fontsize{8}discrete time k')

subplot(3,2,2); plot(k,ERRSS1,'k')
title('Estmation error ERRSS1')
ylabel('\fontsize{8}ERRSS1')
xlabel('\fontsize{8}discrete time,k')

subplot(3,2,3);plot(k,SS2,'k-',k,SS2E,'k-.')
title('Process variables SS2 and SS2E')
ylabel('\fontsize{8}SNH2,SS2E')
xlabel('\fontsize{8}discrete time k')

subplot(3,2,4); plot(k,ERRSS2,'k')
title('Estmation error ERRSS2')
ylabel('\fontsize{8}ERRSS2')
xlabel('\fontsize{8}discrete time,k')

subplot(3,2,5);plot(k,SS3,'k-',k,SS3E,'k-.')
title('Process variables SS3 and SS3E')
ylabel('\fontsize{8}SS3,SS3E')
xlabel('\fontsize{8}discrete time k')

subplot(3,2,6); plot(k,ERRSS3,'k')
title('Estmation error ERRSS3')
ylabel('\fontsize{8}ERRSS3')
xlabel('\fontsize{8}discrete time,k')
```

2.2. Subprograms

%SUBPROGRAM rateAASM1F.m

```
%AIM:The program function rateASM1F.m calculates the process rates of the full ASM1 biological model for the Athlone
process. The program uses global definition of the model parameters
function [ROASM1F]=rateAASM1F(Zk)
global Ks KOH KNO KNH KOA Kx muH etag muA Kh etah iXB YH YA fP iXP bH bA Ka

%Process rates for the tank 1
ROASM1F(1)=muH*(Zk(2)/(Ks+Zk(2)))*(Zk(8)/(KOH+Zk(8)))*Zk(5);
ROASM1F(2)=muH*(Zk(2)/(Ks+Zk(2)))*(KOH/(KOH+Zk(8)))*(Zk(9)/(KNO+Zk(9)))*etag*Zk(5);
ROASM1F(3)=muA*(Zk(10)/(KNH+Zk(10)))*(Zk(8)/(KOA+Zk(8)))*Zk(6);
ROASM1F(4)=bH*Zk(5);
ROASM1F(5)=bA*Zk(6);
ROASM1F(6)=Ka*Zk(11)*Zk(5);
xl=Zk(4)/Zk(5);
```

```
ROASM1F(7)=Kh*Zk(5)*(x1/(Kx+x1))*((Zk(8)/(KOH+Zk(8)))+etah*(KOH/(KOH+Zk(8)))*(Zk(9)/(KNO+Zk(9))));
ROASM1F(8)=ROASM1F(7)*Zk(12)/Zk(4);

%Process rates for the tank 2
ROASM1F(9)=muH*(Zk(15)/(Ks+Zk(15)))*(Zk(21)/(KOH+Zk(21)))*Zk(18);
ROASM1F(10)=muH*(Zk(15)/(Ks+Zk(15)))*(KOH/(KOH+Zk(21)))*(Zk(22)/(KNO+Zk(22)))*etag*Zk(18);
ROASM1F(11)=muA*(Zk(23)/(KNH+Zk(23)))*(Zk(21)/(KOA+Zk(21)))*Zk(19);
ROASM1F(12)=bH*Zk(18);
ROASM1F(13)=bA*Zk(19);
ROASM1F(14)=Ka*Zk(24)*Zk(18);
x1=Zk(17)/Zk(18);
ROASM1F(15)=Kh*Zk(18)*(x1/(Kx+x1))*((Zk(21)/(KOH+Zk(21)))+etah*(KOH/(KOH+Zk(21)))*(Zk(22)/(KNO+Zk(22))));
ROASM1F(16)=ROASM1F(15)*Zk(25)/Zk(17);

%Process rates for the tank 3
ROASM1F(17)=muH*(Zk(28)/(Ks+Zk(28)))*(Zk(34)/(KOH+Zk(34)))*Zk(31);
ROASM1F(18)=muH*(Zk(28)/(Ks+Zk(28)))*(KOH/(KOH+Zk(34)))*(Zk(35)/(KNO+Zk(35)))*etag*Zk(31);
ROASM1F(19)=muA*(Zk(36)/(KNH+Zk(36)))*(Zk(34)/(KOA+Zk(34)))*Zk(32);
ROASM1F(20)=bH*Zk(31);
ROASM1F(21)=bA*Zk(32);
ROASM1F(22)=Ka*Zk(37)*Zk(31);
x1=Zk(30)/Zk(31);
ROASM1F(23)=Kh*Zk(31)*(x1/(Kx+x1))*((Zk(34)/(KOH+Zk(34)))+etah*(KOH/(KOH+Zk(34)))*(Zk(35)/(KNO+Zk(35))));
ROASM1F(24)=ROASM1F(23)*Zk(38)/Zk(30);
 %Vector of the process rates
ROASM1F=[ROASM1F(1);ROASM1F(2);ROASM1F(3);ROASM1F(4);ROASM1F(5);ROASM1F(6);ROASM1F(7);ROASM1F(8);
ROASM1F(9);ROASM1F(10);
ROASM1F(11);ROASM1F(12);ROASM1F(13);ROASM1F(14);ROASM1F(15);ROASM1F(16);ROASM1F(17);ROASM1F(18);ROASM1F(19);ROASM1F(20)
;ROASM1F(21);ROASM1F(22);ROASM1F(23);ROASM1F(24)];
```

%SUBPROGRAM prateASM1R.m

```
%AIM:The program function prateASM1.m calculates at every moment the functions of the process rates which multiply
%the process estimated parameters for the Athlone process based on the reduced ASM1 biological model.
%The program uses global definition of the model parameters

function [Pk]=prateASM1R(Xk,Uk,XBHk,XBAk,XSk)
global Ks KOH KNO KNH KOA Kx muH etag muA Kh etah iXB YH YA fP iXP bH bA Ka

%P functions for every tank
%Tank 1
P11=(Xk(3)/(Ks+Xk(3)))*(Uk(1)/(KOH+Uk(1)))*XBHk(1);
P12=(Xk(3)/(Ks+Xk(3)))*(KOH/(KOH+Uk(1)))*(Xk(2)/(KNO+Xk(2)))*etag*XBHk(1);
P13=(Xk(1)/(KNH+Xk(1)))*(Uk(1)/(KOA+Uk(1)))*XBAk(1);
x1=XSk(1)/XBHk(1);
P14=XBHk(1)*(x1/(Kx+x1))*((Uk(1)/(KOH+Uk(1)))+etah*(KOH/(KOH+Uk(1)))*(Xk(2)/(KNO+Xk(2))));
P1k=[P11 0 0;P12 0 0;0 P13 0;0 0 P14];
%Tank 2
P21=(Xk(6)/(Ks+Xk(6)))*(Uk(2)/(KOH+Uk(2)))*XBHk(2);
P22=(Xk(6)/(Ks+Xk(6)))*(KOH/(KOH+Uk(2)))*(Xk(5)/(KNO+Xk(5)))*etag*XBHk(2);
P23=(Xk(4)/(KNH+Xk(4)))*(Uk(2)/(KOA+Uk(2)))*XBAk(2);
x1=XSk(2)/XBHk(2);
P24=XBHk(2)*(x1/(Kx+x1))*((Uk(2)/(KOH+Uk(2)))+etah*(KOH/(KOH+Uk(2)))*(Xk(5)/(KNO+Xk(5))));
P2k=[P21 0 0;P22 0 0;0 P23 0;0 0 P24];
 %Tank 3
P31=(Xk(9)/(Ks+Xk(9)))*(Uk(3)/(KOH+Uk(3)))*XBHk(3);
P32=(Xk(9)/(Ks+Xk(9)))*(KOH/(KOH+Uk(3)))*(Xk(8)/(KNO+Xk(8)))*etag*XBHk(3);
P33=(Xk(7)/(KNH+Xk(7)))*(Uk(3)/(KOA+Uk(3)))*XBAk(3);
x1=XSk(3)/XBHk(3);
P34=XBHk(3)*(x1/(Kx+x1))*((Uk(3)/(KOH+Uk(3)))+etah*(KOH/(KOH+Uk(3)))*(Xk(8)/(KNO+Xk(8))));
P3k=[P31 0 0;P32 0 0;0 P33 0;0 0 P34];
 %Matrix Pk for the whole process
Pk=[P1k;P2k;P3k];
```

%SUBPROGRAM rateASM1RE.m

```
%AIM:The program function rateASM1.m calculates at every moment the process rates of the reduced ASM1 model using the
estimated parameters. The program uses global definition of the model parameters

function [ROASM1E]=rateASM1RE(Xk,Uk,XBHk,XBAk,XSk,thetak)
global Ks KOH KNO KNH KOA Kx muH etag muA Kh etah iXB YH YA fP iXP bH bA Ka

%Process rates for every tank
ROASM1(1)=thetak(1)*(Xk(3)/(Ks+Xk(3)))*(Uk(1)/(KOH+Uk(1)))*XBHk(1);
ROASM1(2)=thetak(1)*(Xk(3)/(Ks+Xk(3)))*(KOH/(KOH+Uk(1)))*(Xk(2)/(KNO+Xk(2)))*etag*XBHk(1);
ROASM1(3)=thetak(2)*(Xk(1)/(KNH+Xk(1)))*(Uk(1)/(KOA+Uk(1)))*XBAk(1);
x1=XSk(1)/XBHk(1);
ROASM1(4)=thetak(3)*XBHk(1)*(x1/(Kx+x1))*((Uk(1)/(KOH+Uk(1)))+etah*(KOH/(KOH+Uk(1)))*(Xk(2)/(KNO+Xk(2))));

ROASM1(5)=thetak(1)*(Xk(6)/(Ks+Xk(6)))*(Uk(2)/(KOH+Uk(2)))*XBHk(2);
ROASM1(6)=thetak(1)*(Xk(6)/(Ks+Xk(6)))*(KOH/(KOH+Uk(2)))*(Xk(5)/(KNO+Xk(5)))*etag*XBHk(2);
ROASM1(7)=thetak(2)*(Xk(4)/(KNH+Xk(4)))*(Uk(2)/(KOA+Uk(2)))*XBAk(2);
x1=XSk(2)/XBHk(2);
ROASM1(8)=thetak(3)*XBHk(2)*(x1/(Kx+x1))*((Uk(2)/(KOH+Uk(2)))+etah*(KOH/(KOH+Uk(2)))*(Xk(5)/(KNO+Xk(5))));

ROASM1(9)=thetak(1)*(Xk(9)/(Ks+Xk(9)))*(Uk(3)/(KOH+Uk(3)))*XBHk(3);
ROASM1(10)=thetak(1)*(Xk(9)/(Ks+Xk(9)))*(KOH/(KOH+Uk(3)))*(Xk(8)/(KNO+Xk(8)))*etag*XBHk(3);
ROASM1(11)=thetak(2)*(Xk(7)/(KNH+Xk(7)))*(Uk(3)/(KOA+Uk(3)))*XBAk(3);
x1=XSk(3)/XBHk(3);
ROASM1(12)=thetak(3)*XBHk(3)*(x1/(Kx+x1))*((Uk(3)/(KOH+Uk(3)))+etah*(KOH/(KOH+Uk(3)))*(Xk(8)/(KNO+Xk(8))));
%Vector of the process rates
ROASM1E=[ROASM1(1) ROASM1(2) ROASM1(3) ROASM1(4) ROASM1(5) ROASM1(6) ROASM1(7) ROASM1(8) ROASM1(9) ROASM1(10)
ROASM1(11) ROASM1(12)]';
```

3.1 SOFTWARE FOR PARAMETER ESTIMATION OF THE BENCHMARK MASS-BALANCE MODEL FOR THE CASE OF UCT REDUCED MODEL

3.1.Main program

```
%PROGRAM BUCTparest.m
%Aim - the program calculates the trajectories of the full mass-balance model, the estimations of the kinetic
parameters muH, muA, KMP and KA, and the trajectories of the process variables of the reduced mass-balance model for
the Benchmark process with the UCT reduced biological model. The program calls the function subroutines rateBUCTF.m,
rateBUCTE.m and prateBUCTR.m. The calculation uses the reduced biological model with 4 variables SNH, SNO,SS and Sads
%The program uses global definition of the model parameters
global Ks KOH KNO KNA KOA muH etag muA KMP fZBH YZH YZA KA KSA KSP fMA bH KR bA

f=1.2;YZA = 0.15;YZH = 0.67;fZBH = 0.068;fZEH=0.068;fP=0.08;muH = 2.0;Ks = 5;KOH = 0.002;KNO = 0.1;etag = 0.33;
KMP = 1.35;muA = 0.3;KNA = 0.01;KA = 0.17;KOA = 0.002;fMA=1;KSP=0.027;KSA=1;bH=0.3;bA=0.05;KR=0.032
%Process model parameters

%Process tanks volumes and flowrates
V1 = 1000;V2 = 1000;V3 = 1333;V4 = 1333;V5 = 1333;Qo = 18446;Qa = 55338;Qr = 18446;Qw = 385;LAMBDA = (Qo+Qr)/(Qr+Qw);
%Oxygen parameters
SOsat = 8;Kla1=4.8;Kla2=4.8;Kla3 = 240;Kla4=240;Kla5 = 84;
 Kl=[Kla1 Kla2 Kla3 Kla4 Kla5];Kla=diag(Kl);
%Determination of the sampling period
DT = 0.01042;days=0.1042*10;K=days/DT;k=0:DT:days

%Calculation of the matrix C
x1=-1/YZH;x2=1/YZA;x3=(1-YZH)/(2.86*YZH);x4=x3-fZBH;x5=-x2-fZBH;x13=x3/2.86;x14=(4.57-YZA)/YZA;
x6=1-fP;x7=fZBH-fP*fZEH;x8=fZBH/14;x9=x3/14-x8;x10=(x3+fZBH)/14;x11=1/14;x12=-x8-1/(7*YZA);
YZXBH = [1 1 1 1 1 1 1 1 -1 0 0 0 0 0]';
YZXBA = [0 0 0 0 0 0 0 0 0 0 0 0 1 -1]';
YZXP = [0 0 0 0 0 0 0 0 fP 0 0 0 0 fP]';
YZXI = [0 0 0 0 0 0 0 0 0 0 0 0 0 0]';
YZXSA=[0 0 0 0 x1 x1 x1 x1 0 1 0 0 0 0]';
YZXSE=[0 0 0 0 0 0 0 0 x6 -1 0 0 0 x6]';
YZXND = [0 0 0 0 0 0 0 0 x7 0 -1 0 0 x7]';
YZSS = [x1 x1 x1 x1 0 0 0 0 0 0 0 0 0 0]';
YZSNH = [-fZBH 0 -fZBH 0 -fZBH 0 -fZBH 0 0 0 0 1 x2 x5]';
YZSND = [0 0 0 0 0 0 0 0 0 0 1 -1 0 0]';
YZSNO = [0 -fZBH -x3 x4 0 -fZBH -x3 x4 0 0 0 0 x2 0]';
YZSALK=[-x8 x8 x9 x10 -x8 x8 x9 x10 0 0 0 x11 x12 0]';
YZSI = [0 0 0 0 0 0 0 0 0 0 0 0 0 0]';
YZS0 = [-x13 -x13 0 0 -x13 -x13 0 0 0 0 0 0 -x14 0]';
Cnu = [YZXBH YZXBA YZXP YZXI YZXSA YZXSE YZXND YZSS YZSNH YZSND YZSNO YZSALK YZSI YZS0];
CF=DT*[Cnu zeros(14,56);zeros(14,14) Cnu zeros(14,42);zeros(14,28) Cnu zeros(14,28);zeros(14,42) Cnu
zeros(14,14);zeros(14,56) Cnu];

%Calculation of matrix AF
IV1 = DT/V1;IV2 = DT/V2;IV3 = DT/V3;IV4 = DT/V4;IV5 = DT/V5;IV=IV1*Qo;IVV=IV*f;
Q=Qo+Qa+Qr;
IV21=IV2*Q;IV32=IV3*Q;IV43=IV4*Q;IV54=IV5*Q;
IV11=1-IV1*Q;IV22=1-IV21;IV33=1-IV32;IV44=1-IV43;IV55=1-IV54;IV15=IV1*(Qa+Qr);IV15p=IV1*(Qa+LAMBDA*Qr);
a1=[IV11,IV11,IV11,IV11,IV11,IV11,IV11,IV11,IV11,IV11,IV11,IV11,IV11,IV11];
A11=diag(a1);
a2=[IV22,IV22,IV22,IV22,IV22,IV22,IV22,IV22,IV22,IV22,IV22,IV22,IV22,IV22];
A22=diag(a2);
a3=[IV33,IV33,IV33,IV33,IV33,IV33,IV33,IV33,IV33,IV33,IV33,IV33,IV33,IV33];
A33=diag(a3);
a4=[IV44,IV44,IV44,IV44,IV44,IV44,IV44,IV44,IV44,IV44,IV44,IV44,IV44,IV44];
A44=diag(a4);
a5=[IV55,IV55,IV55,IV55,IV55,IV55,IV55,IV55,IV55,IV55,IV55,IV55,IV55,IV55];
A55=diag(a5);
a15=[IV15p,IV15p,IV15p,IV15p,IV15,IV15,IV15p,IV15,IV15,IV15,IV15,IV15,IV15,IV15];
A15=diag(a15);
a21=[IV21,IV21,IV21,IV21,IV21,IV21,IV21,IV21,IV21,IV21,IV21,IV21,IV21,IV21];
A21=diag(a21);
a32=[IV32,IV32,IV32,IV32,IV32,IV32,IV32,IV32,IV32,IV32,IV32,IV32,IV32,IV32];
A32=diag(a32);
a43=[IV43,IV43,IV43,IV43,IV43,IV43,IV43,IV43,IV43,IV43,IV43,IV43,IV43,IV43];
A43=diag(a43);
a54=[IV54,IV54,IV54,IV54,IV54,IV54,IV54,IV54,IV54,IV54,IV54,IV54,IV54,IV54];
A54=diag(a54);
AF=[A11 zeros(14,42) A15;A21 A22 zeros(14,42);zeros(14,14) A32 A33 zeros(14,28);zeros(14,28) A43 A44
zeros(14,14);zeros(14,42) A54 A55];
%Calculation of the matrix BF
b1=[IV,IV,IV,IV,IV,IV,IV,IV,IV,IV,IV,IV,IV,IV];
B1=diag(b1);
BF=[B1;zeros(56,14)];

%Average influent concentrations trajectories for the process variables
SSi=69.5;XBHi=28.17;XSEi=202.32;XIi=51.2;SNHi=31.56;SIi=30.0;SNDi=6.95;XNDi=10.59;SOi=0.0;XBAi=0.0;XPi=0.0;SNOi=0.0;
SALKi=7.0;XSAi=0.0;
Zi=[XBHi*ones(1,K);XBAi*ones(1,K);XPi*ones(1,K);XIi*ones(1,K);XSAi*ones(1,K);XSEi*ones(1,K);XNDi*ones(1,K);
SSi*ones(1,K);SNHi*ones(1,K);SNDi*ones(1,K);SNOi*ones(1,K);SALKi*ones(1,K);SIi*ones(1,K);SOi*ones(1,K)]*0.1;

%Determination of the initial conditions
Si_1    =   3.0000000e+01;Ss_1     =   2.8082131e+00;Xi_1      =  1.1491252e+03;Xsa_1    =   8.2134908e+01;
Xbh_1   =   2.5517658e+03;Xba_1    =   1.4838943e+02;Xp_1     =   4.4885186e+02;Xse_1=500.0;So_1     =   4.2984433e-
03;Sno_1   =   5.3699400e+00;Snh_1    =   7.9178845e+00;Snd_1    =   1.2166405e+00;Xnd_1    =   5.2848894e+00;
Salk_1  =   4.9277103e+00;
Z10 = [Xbh_1 ;Xba_1 ;Xp_1 ;Xi_1 ;Xsa_1 ;Xse_1;Xnd_1 ;Ss_1 ;Snh_1 ;Snd_1 ;Sno_1 ;Salk_1;Si_1 ;So_1];

Si_2    =   3.0000000e+01;Ss_2     =   1.4587940e+00;Xi_2      =  1.1491252e+03;Xsa_2    =   7.6386187e+01;
Xse_2=480.0;Xbh_2   =   2.5533851e+03;Xba_2    =   1.4830914e+02;Xp_2     =   4.4952273e+02;So_2     =   6.3131911e-05;
```

```
Sno_2   =   3.6619672e+00;Snh_2   =   8.3444148e+00;Snd_2    =  8.8206477e-01;Xnd_2   =   5.0290873e+00;
Salk_2  =   5.0801748e+00;

Z20 = [Xbh_2 ;Xba_2 ;Xp_2 ;Xi_2 ;Xsa_2 ;Xse_2;Xnd_2 ;Ss_2 ;Snh_2 ;Snd_2 ;Sno_2 ;Salk_2;Si_2 ;So_2];

Si_3    =   3.0000000e+01;Ss_3    =   1.1495418e+00;Xi_3    =   1.1491252e+03;Xsa_3   =   6.4854922e+01;Xse_3=420.0;
Xbh_3   =   2.5571314e+03;Xba_3   =   1.4894126e+02;Xp_3    =   4.5041834e+02;So_3    =   1.7183778e+00;
Sno_3   =   6.5408820e+00;Snh_3   =   5.5479452e+00;Snd_3   =   8.2888682e-01;Xnd_3   =   4.3924277e+00;
Salk_3  =   4.6747902e+00;
Z30 = [Xbh_3 ;Xba_3 ;Xp_3 ;Xi_3 ;Xsa_3 ;Xse_3;Xnd_3 ;Ss_3 ;Snh_3 ;Snd_3 ;Sno_3 ;Salk_3;Si_3 ;So_3];

Si_4    =   3.0000000e+01;Ss_4    =   9.9532389e-01;Xi_4    =   1.1491252e+03;Xsa_4   =   5.5693982e+01;Xse_4=350.0;
Xbh_4   =   2.5591826e+03;Xba_4   =   1.4952712e+02;Xp_4    =   4.5131469e+02;So_4    =   2.4288838e+00;
Sno_4   =   9.2989988e+00;Snh_4   =   2.9673854e+00;Snd_4   =   7.6678656e-01;Xnd_4   =   3.8790101e+00;
Salk_4  =   4.2934562e+00;

Z40 = [Xbh_4 ;Xba_4 ;Xp_4 ;Xi_4 ;Xsa_4 ;Xse_4;Xnd_4 ;Ss_4 ;Snh_4 ;Snd_4 ;Sno_4 ;Salk_4;Si_4 ;So_4];


Si_5    =   3.0000000e+01;Ss_5    =   8.8949280e-01;Xi_5    =   1.1491252e+03;Xsa_5   =   4.9305586e+01;Xse_5=250.0;
Xbh_5   =   2.5593436e+03;Xba_5   =   1.4979714e+02;Xp_5    =   4.5221112e+02;So_5    =   4.9094351e-01;
Sno_5   =   1.0415220e+01;Snh_5   =   1.7333316e+00;Snd_5   =   6.8828001e-01;Xnd_5   =   3.5271755e+00;
Salk_5  =   4.1255794e+00;

Z50 = [Xbh_5 ;Xba_5 ;Xp_5 ;Xi_5 ;Xsa_5 ;Xse_5;Xnd_5 ;Ss_5 ;Snh_5 ;Snd_5 ;Sno_5 ;Salk_5;Si_5 ;So_5];

%Vector of the initial conditions
Z0=[Z10;Z20;Z30;Z40;Z50]*0.1;
X=[Z0 zeros(70,K)]*0.1;

%Simulation of the full model behavior
for k = 1:K
    Xk=X(:,k);
    S0k=[Xk(14,1);Xk(28,1);Xk(42,1);Xk(56,1);Xk(70,1)];
    Zik = Zi(:,k);
   [ROUCTF]=rateBUCTF(Xk);
    ZZk=DT*Kla*(S0sat-S0k);
    ZZ1k=[zeros(13,1);ZZk(1);zeros(13,1);ZZk(2);zeros(13,1);ZZk(3);zeros(13,1);ZZk(4);zeros(13,1);ZZk(5)];
    X(:,k+1) = AF*X(:,k) + CF'*ROUCTF + BF*Zi(:,k)+ZZ1k;
end

%Selection of the measured variables of state space SNH,SNO,SS,Sads
XR=[X(9,:);X(11,:);X(8,:);X(5,:);X(23,:);X(25,:);X(22,:);X(19,:);X(37,:);X(39,:);X(36,:);X(33,:);X(51,:);X(53,:);
X(50,:);X(47,:);X(65,:);X(67,:);X(64,:);X(61,:)]
%trajectory of the control signal
U=[X(14,:);X(28,:);X(42,:);X(56,:);X(70,:)]

%Calculation of the vector P

%Average values of the influent variables
SSi=69.5;SNHi=31.56;SNOi=0.0;XSAi=0.0;

%Influent concentrations trajectories for SNH, SNO, SS and XSA
Xi  =[SNHi*ones(1,K);SNOi*ones(1,K);SSi*ones(1,K);XSAi*ones(1,K)]*0.1;

 % Steady state values for the biomass XBH, XBA, XSA
XBH = 0.1*[2551.76*ones(1,K);2553.38*ones(1,K);2557.13*ones(1,K);2559.18*ones(1,K);2559.34*ones(1,K)];% XBH steady
state COD/m^3
XBA = 0.1*[148.389*ones(1,K);148.309*ones(1,K);148.941*ones(1,K);149.527*ones(1,K);149.797*ones(1,K)];% XBA steady
state g all COD/m^3
XSE = 0.1*[82.135*ones(1,K);76.386*ones(1,K);64.855*ones(1,K);55.694*ones(1,K);49.306*ones(1,K)]; % XS steady state all
COD/m^3

%Calculation of the state space process model matrices
%Calculation of the matrix A

AR=[[IV11 0.0 0.0 0.0;0.0 IV11 0.0 0.0;0.0 0.0 IV11 0.0;0.0 0.0 0.0 IV11] zeros(4,12) [IV15 0.0 0.0 0.0;0.0 IV15 0.0
0.0;0.0 0.0 IV15 0.0;0.0 0.0 0.0 IV15];
    [IV21 0.0 0.0 0.0;0.0 IV21 0.0 0.0;0.0 0.0 IV21 0.0;0.0 0.0 0.0 IV21] [IV22 0.0 0.0 0.0;0.0 IV22 0.0 0.0;0.0 0.0
IV22 0.0;0.0 0.0 0.0 IV22] zeros(4,12);
    zeros(4,4) [IV32 0.0 0.0 0.0;0.0 IV32 0.0 0.0;0.0 0.0 IV32 0.0;0.0 0.0 0.0 IV32] [IV33 0.0 0.0 0.0;0.0 IV33 0.0
0.0;0.0 0.0 IV33 0.0;0.0 0.0 0.0 IV33] zeros(4,8);
    zeros(4,8) [IV43 0.0 0.0 0.0;0.0 IV43 0.0 0.0;0.0 0.0 IV43 0.0;0.0 0.0 0.0 IV43] [IV44 0.0 0.0 0.0;0.0 IV44 0.0
0.0;0.0 0.0 IV44 0.0;0.0 0.0 0.0 IV44] zeros(4,4);
    zeros(4,12) [IV54 0.0 0.0 0.0;0.0 IV54 0.0 0.0;0.0 0.0 IV54 0.0;0.0 0.0 0.0 IV54] [IV55 0.0 0.0 0.0;0.0 IV55 0.0
0.0;0.0 0.0 IV55 0.0;0.0 0.0 0.0 IV55]]

%Calculation of the matrice B1,B and Cn and C
B1R=[IVV 0.0 0.0 0.0;0.0 IV 0.0 0.0;0.0 0.0 IV 0.0;0.0 0.0 0.0 IV];
BR=[IVV 0.0 0.0 0.0;0.0 IV 0.0 0.0;0.0 0.0 IV 0.0;0.0 0.0 0.0 IV;zeros(16,4)];

x1=-1/YZH;x2=1/YZA;x3=(1-YZH)/(2.86*YZH);x4=x3-fZBH;x5=-x2-fZBH;
Cnu=[-fZBH 0 x1 0;0 -fZBH x1 0;-fZBH -x3 x1 0;0 x3-fZBH x1 0;-fZBH 0 0 x1;0 -fZBH 0 x1;-fZBH -x3 0 x1;0 x3-fZBH 0 x1;0
0 0 1;-x2-fZBH x2 0 0]
CR=DT*[Cnu zeros(10,16);zeros(10,4) Cnu zeros(10,12);zeros(10,8) Cnu zeros(10,8);zeros(10,12) Cnu
zeros(10,4);zeros(10,16) Cnu];

%Calculation of the estimated coefficients
for k = 1:K
    XRk=XR(:,k);
    Uk =U(:,k);
    XBHk = XBH(:,k);
    XBAk = XBA(:,k);
    XSEk = XSE(:,k);
    Xik = Xi(:,k);
```

```
   [Pk]=prateBUCTR(XRk,Uk,XBHk,XBAk,XSEk);
    FIk=CR'*Pk;
    Y(:,k) = XR(:,k+1)-AR*XR(:,k)-BR*Xi(:,k);
    theta(:,k)=(FIk'*FIk)^(-1)*FIk'*Y(:,k);
end

muHE(1,:)=theta(1,:);KMPE(1,:)=theta(2,:);KAE(1,:)=theta(3,:);muAE(1,:)=theta(4,:);

%Simulation of the reduced model with the estimated parameters
XE=[X(9,:);X(11,:);X(8,:);X(5,:);X(23,:);X(25,:);X(22,:);X(19,:);X(37,:);X(39,:);X(36,:);X(33,:);X(51,:);X(53,:);
X(50,:);X(47,:);X(65,:);X(67,:);X(64,:);X(61,:)]
ERR=XR(:,1)-XE(:,1);
for k = 1:K
    XRk=XR(:,k);
    Uk =U(:,k);
    XBHk = XBH(:,k);
    XBAk = XBA(:,k);
    XSEk = XSE(:,k);
    Xik = Xi(:,k);
    thetak=theta(:,k);
   [ROUCTE]=rateBUCTE(XRk,Uk,XBHk,XBAk,XSEk,thetak);
    XE(:,k+1)=AR*XE(:,k)+CR'*ROUCTE+BR*Xi(:,k);
    ERR(:,k+1)=XR(:,k+1)-XE(:,k+1);
end

X=XR
%vector of process full, estimated and error variables SNH, SNO,SS,xsA Tank 1
SNH1=X(1,:);SNO1=X(2,:);SS1=X(3,:);XSA1=X(4,:);
SNH1E=XE(1,:);SNO1E=XE(2,:);SS1E=XE(3,:);XSA1E=XE(4,:);
ERRSNH1=ERR(1,:);ERRSNO1=ERR(2,:);ERRSS1=ERR(3,:);ERRXSA1=ERR(4,:);
%Calculation of the weighted errors for tank1
eSNH1=(ERRSNH1*ERRSNH1')/(SNH1*SNH1')
eSNO1=(ERRSNO1*ERRSNO1')/(SNO1*SNO1')
eSS1=(ERRSS1*ERRSS1')/(SS1*SS1')
eXSA1=(ERRXSA1*ERRXSA1')/(XSA1*XSA1')
 %vector of process full, estimated and error variables SNH, SNO,SS, Tank 2
SNH2=X(5,:);SNO2=X(6,:);SS2=X(7,:);XSA2=X(8,:);
SNH2E=XE(5,:);SNO2E=XE(6,:);SS2E=XE(7,:);XSA2E=XE(8,:);
ERRSNH2=ERR(5,:);ERRSNO2=ERR(6,:);ERRSS2=ERR(7,:);ERRXSA2=ERR(8,:);
%Calculation of the weighted errors for tank 2
eSNH2=(ERRSNH2*ERRSNH2')/(SNH2*SNH2')
eSNO2=(ERRSNO2*ERRSNO2')/(SNO2*SNO2')
eSS2=(ERRSS2*ERRSS2')/(SS2*SS2')
eXSA2=(ERRXSA2*ERRXSA2')/(XSA2*XSA2')
 %vector of process full, estimated and error variables SNH, SNO,SS, Tank 3
SNH3=X(9,:);SNO3=X(10,:);SS3=X(11,:);XSA3=X(12,:);
SNH3E=XE(9,:);SNO3E=XE(10,:);SS3E=XE(11,:);XSA3E=XE(12,:);
ERRSNH3=ERR(9,:);ERRSNO3=ERR(10,:);ERRSS3=ERR(11,:);ERRXSA3=ERR(12,:);
%Calculation of the weighted errors for tank 3
eSNH3=(ERRSNH3*ERRSNH3')/(SNH3*SNH3')
eSNO3=(ERRSNO3*ERRSNO3')/(SNO3*SNO3')
eSS3=(ERRSS3*ERRSS3')/(SS3*SS3')
eXSA3=(ERRXSA3*ERRXSA3')/(XSA3*XSA3')
 %vector of process full, estimated and error variables SNH, SNO,SS, Tank 4
SNH4=X(13,:);SNO4=X(14,:);SS4=X(15,:);XSA4=X(16,:);
SNH4E=XE(13,:);SNO4E=XE(14,:);SS4E=XE(15,:);XSA4E=XE(16,:);
ERRSNH4=ERR(13,:);ERRSNO4=ERR(14,:);ERRSS4=ERR(15,:);ERRXSA4=ERR(16,:);
%Calculation of the weighted errors for tank 4
eSNH4=(ERRSNH4*ERRSNH4')/(SNH4*SNH4')
eSNO4=(ERRSNO4*ERRSNO4')/(SNO4*SNO4')
eSS4=(ERRSS4*ERRSS4')/(SS4*SS4')
eXSA4=(ERRXSA4*ERRXSA4')/(XSA4*XSA4')
 %vector of process full, estimated and error variables SNH, SNO,SS, Tank 5
SNH5=X(17,:);SNO5=X(18,:);SS5=X(19,:);XSA5=X(20,:);
SNH5E=XE(17,:);SNO5E=XE(18,:);SS5E=XE(19,:);XSA5E=XE(20,:);
ERRSNH5=ERR(17,:);ERRSNO5=ERR(18,:);ERRSS5=ERR(19,:);ERRXSA5=ERR(20,:);
%Calculation of the weighted errors for tank 5
eSNH5=(ERRSNH5*ERRSNH5')/(SNH5*SNH5')
eSNO5=(ERRSNO5*ERRSNO5')/(SNO5*SNO5')
eSS5=(ERRSS5*ERRSS5')/(SS5*SS5')
eXSA5=(ERRXSA5*ERRXSA5')/(XSA5*XSA5')

k=1:100
%Graphs of the estimated parameters
figure(1)
subplot(4,1,1);plot(k,muHE,'k')
title('Estimated muH')
ylabel('\fontsize{8}muHE')
xlabel('\fontsize{8}discrete time k')

subplot(4,1,2);plot(k,KMPE,'k')
title('Estimated KMP')
ylabel('\fontsize{8}KMPE')
xlabel('\fontsize{8}discrete time k')

subplot(4,1,3);plot(k,KAE,'k')
title('Estimated KA')
ylabel('\fontsize{8}KAE')
xlabel('\fontsize{8}discrete time k')

subplot(4,1,4);plot(k,muAE,'k')
title('Estimated muA')
ylabel('\fontsize{8}muAE')
xlabel('\fontsize{8}discrete time k')

k=1:101;
figure(2)
subplot(5,2,1);plot(k,SNH1,'k-',k,SNH1E,'k-.')
title('Process variables Snh1 and Snh1E')
ylabel('\fontsize{8}SNH1,SNH1E')
xlabel('\fontsize{8}discrete time k')

subplot(5,2,2); plot(k,ERRSNH1,'k')
title('Estmation error ERRSnh1')
ylabel('\fontsize{8}ERRSNH1')
xlabel('\fontsize{8}discrete time,k')

subplot(5,2,3);plot(k,SNH2,'k-',k,SNH2E,'k-.')
title('Process variables Snh2 and Snh2E')
ylabel('\fontsize{8}SNH2,SNH2E')
xlabel('\fontsize{8}discrete time k')

subplot(5,2,4); plot(k,ERRSNH2,'k')
title('Estmation error ERRSnh2')
ylabel('\fontsize{8}ERRSNH2')
xlabel('\fontsize{8}discrete time,k')

subplot(5,2,5);plot(k,SNH3,'k-',k,SNH3E,'k-.')
```

```
title('Process variables Snh3 and Snh3E')
ylabel('\fontsize{8}SNH3,SNH3E')
xlabel('\fontsize{8}discrete time k')

subplot(5,2,6); plot(k,ERRSNH3,'k')
title('Estmation error ERRSnh3')
ylabel('\fontsize{8}ERRSNH3')
xlabel('\fontsize{8}discrete time,k')

subplot(5,2,7);plot(k,SNH4,'k-',k,SNH4E,'k-.')
title('Process variables Snh4 and Snh4E')
ylabel('\fontsize{8}SNH4,SNH4E')
xlabel('\fontsize{8}discrete time k')

subplot(5,2,8); plot(k,ERRSNH4,'k')
title('Estmation error ERRSnh4')
ylabel('\fontsize{8}ERRSNH4')
xlabel('\fontsize{8}discrete time,k')

subplot(5,2,9);plot(k,SNH5,'k-',k,SNH5E,'k-.')
title('Process variables Snh5 and Snh5E')
ylabel('\fontsize{8}SNH5,SNH5E')
xlabel('\fontsize{8}discrete time k')

subplot(5,2,10); plot(k,ERRSNH5,'k')
title('Estmation error ERRSnh5')
ylabel('\fontsize{8}ERRSNH5')
xlabel('\fontsize{8}discrete time,k')

figure(3)
subplot(5,2,1);plot(k,SNO1,'k-',k,SNO1E,'k-.')
title('Process variables SNO1 and SNO1E')
ylabel('\fontsize{8}SNO1,SNO1E')
xlabel('\fontsize{8}discrete time k')

subplot(5,2,2); plot(k,ERRSNO1,'k')
title('Estmation error ERRSNO1')
ylabel('\fontsize{8}ERRSNO1')
xlabel('\fontsize{8}discrete time,k')

subplot(5,2,3);plot(k,SNO2,'k-',k,SNO2E,'k-.')
title('Process variables SNO2 and SNO2E')
ylabel('\fontsize{8}SNO2,SNO2E')
xlabel('\fontsize{8}discrete time k')

subplot(5,2,4); plot(k,ERRSNO2,'k')
title('Estmation error ERRSNO2')
ylabel('\fontsize{8}ERRSNO2')
xlabel('\fontsize{8}discrete time,k')

subplot(5,2,5);plot(k,SNO3,'k-',k,SNO3E,'k-.')
title('Process variables SNO3 and SNO3E')
ylabel('\fontsize{8}SNO3,SNO3E')
xlabel('\fontsize{8}discrete time k')

subplot(5,2,6); plot(k,ERRSNO3,'k')
title('Estmation error ERRSNO3')
ylabel('\fontsize{8}ERRSNO3')
xlabel('\fontsize{8}discrete time,k')

subplot(5,2,7);plot(k,SNO4,'k-',k,SNO4E,'k-.')
title('Process variables SNO4 and SNO4E')
ylabel('\fontsize{8}SNO4,SNO4E')
xlabel('\fontsize{8}discrete time k')

subplot(5,2,8); plot(k,ERRSNO4,'k')
title('Estmation error ERRSNO4')
ylabel('\fontsize{8}ERRSNO4')
xlabel('\fontsize{8}discrete time,k')

subplot(5,2,9);plot(k,SNO5,'k-',k,SNO5E,'k-.')
title('Process variables SNO5 and SNO5E')
ylabel('\fontsize{8}SNO5,SNO5E')
xlabel('\fontsize{8}discrete time k')

subplot(5,2,10); plot(k,ERRSNO5,'k')
title('Estmation error ERRSNO5')
ylabel('\fontsize{8}ERRSNO5')
xlabel('\fontsize{8}discrete time,k')
 figure(4)
subplot(5,2,1);plot(k,SS1,'k-',k,SS1E,'k-.')
title('Process variables SS1 and SS1E')
ylabel('\fontsize{8}SS1,SS1E')
xlabel('\fontsize{8}discrete time k')

subplot(5,2,2); plot(k,ERRSS1,'k')
title('Estmation error ERRSS1')
ylabel('\fontsize{8}ERRSS1')
xlabel('\fontsize{8}discrete time,k')

subplot(5,2,3);plot(k,SS2,'k-',k,SS2E,'k-.')
title('Process variables SS2 and SS2E')
ylabel('\fontsize{8}SS2,SS2E')
xlabel('\fontsize{8}discrete time k')

subplot(5,2,4); plot(k,ERRSS2,'k')
title('Estmation error ERRSS2')
ylabel('\fontsize{8}ERRSS2')
xlabel('\fontsize{8}discrete time,k')

subplot(5,2,5);plot(k,SS3,'k-',k,SS3E,'k-.')
title('Process variables SS3 and SS3E')
ylabel('\fontsize{8}SS3,SS3E')
xlabel('\fontsize{8}discrete time k')

subplot(5,2,6); plot(k,ERRSS3,'k')
title('Estmation error ERRSS3')
ylabel('\fontsize{8}ERRSS3')
xlabel('\fontsize{8}discrete time,k')

subplot(5,2,7);plot(k,SS4,'k-',k,SS4E,'k-.')
title('Process variables SS4 and SS4E')
ylabel('\fontsize{8}SS4,SS4E')
xlabel('\fontsize{8}discrete time k')

subplot(5,2,8); plot(k,ERRSS4,'k')
title('Estmation error ERRSS4')
ylabel('\fontsize{8}ERRSS4')
xlabel('\fontsize{8}discrete time,k')

subplot(5,2,9);plot(k,SS5,'k-',k,SS5E,'k-.')
title('Process variables SS5 and SS5E')
ylabel('\fontsize{8}SS5,SS5E')
xlabel('\fontsize{8}discrete time k')

subplot(5,2,10); plot(k,ERRSS5,'k')
title('Estmation error ERRSS5')
ylabel('\fontsize{8}ERRSS5')
xlabel('\fontsize{8}discrete time,k')

 figure(5)
subplot(5,2,1);plot(k,XSA1,'k-',k,XSA1E,'k-.')
title('Process variables XSA1 and XSA1E')
ylabel('\fontsize{8}XSA1,XSA1E')
xlabel('\fontsize{8}discrete time k')

subplot(5,2,2); plot(k,ERRXSA1,'k')
title('Estmation error ERRXSA1')
ylabel('\fontsize{8}ERRXSA1')
xlabel('\fontsize{8}discrete time,k')

subplot(5,2,3);plot(k,XSA2,'k-',k,XSA2E,'k-.')
title('Process variables XSA2 and XSA2E')
ylabel('\fontsize{8}XSA2,XSA2E')
xlabel('\fontsize{8}discrete time k')

subplot(5,2,4); plot(k,ERRXSA2,'k')
title('Estmation error ERRXSA2')
ylabel('\fontsize{8}ERRXSA2')
xlabel('\fontsize{8}discrete time,k')

subplot(5,2,5);plot(k,XSA3,'k-',k,XSA3E,'k-.')
title('Process variables XSA3 and XSA3E')
ylabel('\fontsize{8}XSA3,XSA3E')
xlabel('\fontsize{8}discrete time k')

subplot(5,2,6); plot(k,ERRXSA3,'k')
title('Estmation error ERRXSA3')
ylabel('\fontsize{8}ERRXSA3')
xlabel('\fontsize{8}discrete time,k')

subplot(5,2,7);plot(k,XSA4,'k-',k,XSA4E,'k-.')
title('Process variables XSA4 and XSA4E')
ylabel('\fontsize{8}XSA4,XSA4E')
xlabel('\fontsize{8}discrete time k')

subplot(5,2,8); plot(k,ERRXSA4,'k')
title('Estmation error ERRXSA4')
ylabel('\fontsize{8}ERRXSA4')
xlabel('\fontsize{8}discrete time,k')

subplot(5,2,9);plot(k,XSA5,'k-',k,XSA5E,'k-.')
title('Process variables XSA5 and XSA5E')
ylabel('\fontsize{8}XSA5,XSA5E')
xlabel('\fontsize{8}discrete time k')

subplot(5,2,10); plot(k,ERRXSA5,'k')
title('Estmation error ERRXSA5')
ylabel('\fontsize{8}ERRXSA5')
xlabel('\fontsize{8}discrete time,k')
```

3.2. Subprograms

%SUBPROGRAM rateBUCTF.m

```
%AIM:The program function rateBUCTF.m calculates at every moment the process rates of the full UCT biological model for
the Benchmark process. The program uses global definition of the model parameters

function [ROUCTF]=rateBUCTF(Xk)
global Ks KOH KNO KNA KOA muH etag muA KMP fZBH YZH YZA KA KSA KSP fMA bH KR bA

%Calculation of the process rates at every moment of the time
% reactions in tank 1
ROUCTF(1)=muH*(Xk(8)/(Ks+Xk(8)))*(Xk(14)/(KOH+Xk(14)))*(Xk(9)/(KNA+Xk(9)))*Xk(1);
ROUCTF(2)=muH*(Xk(8)/(Ks+Xk(8)))*(Xk(14)/(KOH+Xk(14)))*(KNA/(KNA+Xk(9)))*(Xk(11)/(KNO+Xk(11)))*Xk(1);
ROUCTF(3)=muH*(Xk(8)/(Ks+Xk(8)))*(KOH/(KOH+Xk(14)))*(Xk(9)/(KNA+Xk(9)))*(Xk(11)/(KNO+Xk(11)))*Xk(1);
ROUCTF(4)=muH*(Xk(8)/(Ks+Xk(8)))*(KOH/(KOH+Xk(14)))*(KNA/(KNA+Xk(9)))*(Xk(11)/(KNO+Xk(11)))*Xk(1);
ROUCTF(5)=KMP*((Xk(5)/Xk(1))/(KSP+Xk(5)/Xk(1)))*(Xk(14)/(KOH+Xk(14)))*(Xk(9)/(KNA+Xk(9)))*Xk(1);
ROUCTF(6)=KMP*((Xk(5)/Xk(1))/(KSP+Xk(5)/Xk(1)))*(Xk(14)/(KOH+Xk(14)))*(KNA/(KNA+Xk(9)))*(Xk(11)/(KNO+Xk(11)))*Xk(1);
ROUCTF(7)=KMP*((Xk(5)/Xk(1))/(KSP+Xk(5)/Xk(1)))*(KOH/(KOH+Xk(14)))*(Xk(9)/(KNA+Xk(9)))*(Xk(11)/(KNO+Xk(11)))*etag*Xk(1)
ROUCTF(8)=KMP*((Xk(5)/Xk(1))/(KSP+Xk(5)/Xk(1)))*(KOH/(KOH+Xk(14)))*(KNA/(KNA+Xk(9)))*(Xk(11)/(KNO+Xk(11)))*etag*Xk(1);
ROUCTF(9)=bH*Xk(1);
ROUCTF(10)=KA*Xk(6)*Xk(1)*(fMA-(Xk(4)/Xk(1)));
ROUCTF(11)=(ROUCTF(5)+ROUCTF(6)+ROUCTF(7)+ROUCTF(8))*(Xk(7)/Xk(1));
ROUCTF(12)=KR*Xk(10)*Xk(1);
ROUCTF(13)=muA*(Xk(14)/(KOA+Xk(14)))*(Xk(9)/(KSA+Xk(9)))*Xk(2);
ROUCTF(14)=bA*Xk(2);
 % reactions in tank 2
ROUCTF(15)=muH*(Xk(22)/(Ks+Xk(22)))*(Xk(28)/(KOH+Xk(28)))*(Xk(23)/(KNA+Xk(23)))*Xk(15);
ROUCTF(16)=muH*(Xk(22)/(Ks+Xk(22)))*(Xk(28)/(KOH+Xk(28)))*(KNA/(KNA+Xk(23)))*(Xk(25)/(KNO+Xk(25)))*Xk(15);
ROUCTF(17)=muH*(Xk(22)/(Ks+Xk(22)))*(KOH/(KOH+Xk(28)))*(Xk(23)/(KNA+Xk(23)))*(Xk(25)/(KNO+Xk(25)))*Xk(15);
ROUCTF(18)=muH*(Xk(22)/(Ks+Xk(22)))*(KOH/(KOH+Xk(28)))*(KNA/(KNA+Xk(23)))*(Xk(25)/(KNO+Xk(25)))*Xk(15);
ROUCTF(19)=KMP*((Xk(19)/Xk(15))/(KSP+Xk(19)/Xk(15)))*(Xk(28)/(KOH+Xk(28)))*(Xk(23)/(KNA+Xk(23)))*Xk(15);
ROUCTF(20)=KMP*((Xk(19)/Xk(15))/(KSP+Xk(19)/Xk(15)))*(Xk(28)/(KOH+Xk(28)))*(KNA/(KNA+Xk(23)))*(Xk(25)/(KNO+Xk(25)))*
Xk(15);
ROUCTF(21)=KMP*((Xk(19)/Xk(15))/(KSP+Xk(19)/Xk(15)))*(KOH/(KOH+Xk(28)))*(Xk(23)/(KNA+Xk(23)))*(Xk(25)/(KNO+Xk(25)))*
etag*Xk(15);
ROUCTF(22)=KMP*((Xk(19)/Xk(15))/(KSP+Xk(19)/Xk(15)))*(KOH/(KOH+Xk(28)))*(KNA/(KNA+Xk(23)))*(Xk(25)/(KNO+Xk(25)))*
etag*Xk(15);
ROUCTF(23)=bH*Xk(15);
ROUCTF(24)=KA*Xk(20)*Xk(15)*(fMA-(Xk(18)/Xk(15)));
ROUCTF(25)=(ROUCTF(19)+ROUCTF(20)+ROUCTF(21)+ROUCTF(22))*(Xk(21)/Xk(15));
ROUCTF(26)=KR*Xk(24)*Xk(15);
ROUCTF(27)=muA*(Xk(28)/(KOA+Xk(28)))*(Xk(23)/(KSA+Xk(23)))*Xk(16);
ROUCTF(28)=bA*Xk(16);
 % reactions in tank 3
ROUCTF(29)=muH*(Xk(36)/(Ks+Xk(36)))*(Xk(42)/(KOH+Xk(42)))*(Xk(37)/(KNA+Xk(37)))*Xk(29);
ROUCTF(30)=muH*(Xk(36)/(Ks+Xk(36)))*(Xk(42)/(KOH+Xk(42)))*(KNA/(KNA+Xk(37)))*(Xk(39)/(KNO+Xk(39)))*Xk(29);
ROUCTF(31)=muH*(Xk(36)/(Ks+Xk(36)))*(KOH/(KOH+Xk(42)))*(Xk(37)/(KNA+Xk(37)))*(Xk(39)/(KNO+Xk(39)))*Xk(29);
ROUCTF(32)=muH*(Xk(36)/(Ks+Xk(36)))*(KOH/(KOH+Xk(42)))*(KNA/(KNA+Xk(37)))*(Xk(39)/(KNO+Xk(39)))*Xk(29);
ROUCTF(33)=KMP*((Xk(33)/Xk(29))/(KSP+Xk(33)/Xk(29)))*(Xk(42)/(KOH+Xk(42)))*(Xk(37)/(KNA+Xk(37)))*Xk(29);
ROUCTF(34)=KMP*((Xk(33)/Xk(29))/(KSP+Xk(33)/Xk(29)))*(Xk(42)/(KOH+Xk(42)))*(KNA/(KNA+Xk(37)))*(Xk(39)/(KNO+Xk(39)))*
Xk(29);
ROUCTF(35)=KMP*((Xk(33)/Xk(29))/(KSP+Xk(33)/Xk(29)))*(KOH/(KOH+Xk(42)))*(Xk(37)/(KNA+Xk(37)))*(Xk(39)/(KNO+Xk(39)))*
etag*Xk(29);
ROUCTF(36)=KMP*((Xk(33)/Xk(29))/(KSP+Xk(33)/Xk(29)))*(KOH/(KOH+Xk(42)))*(KNA/(KNA+Xk(37)))*(Xk(39)/(KNO+Xk(39)))*
etag*Xk(29);
ROUCTF(37)=bH*Xk(29);
ROUCTF(38)=KA*Xk(34)*Xk(29)*(fMA-(Xk(32)/Xk(29)));
ROUCTF(39)=(ROUCTF(33)+ROUCTF(34)+ROUCTF(35)+ROUCTF(36))*(Xk(35)/Xk(29));
ROUCTF(40)=KR*Xk(38)*Xk(29);
ROUCTF(41)=muA*(Xk(42)/(KOA+Xk(42)))*(Xk(37)/(KSA+Xk(37)))*Xk(30);
ROUCTF(42)=bA*Xk(30);
% reactions in tank 4
ROUCTF(43)=muH*(Xk(50)/(Ks+Xk(50)))*(Xk(56)/(KOH+Xk(56)))*(Xk(51)/(KNA+Xk(51)))*Xk(43);
ROUCTF(44)=muH*(Xk(50)/(Ks+Xk(50)))*(Xk(56)/(KOH+Xk(56)))*(KNA/(KNA+Xk(51)))*(Xk(53)/(KNO+Xk(53)))*Xk(43);
ROUCTF(45)=muH*(Xk(50)/(Ks+Xk(50)))*(KOH/(KOH+Xk(56)))*(Xk(51)/(KNA+Xk(51)))*(Xk(53)/(KNO+Xk(53)))*Xk(43);
ROUCTF(46)=muH*(Xk(50)/(Ks+Xk(50)))*(KOH/(KOH+Xk(56)))*(KNA/(KNA+Xk(51)))*(Xk(53)/(KNO+Xk(53)))*Xk(43);
ROUCTF(47)=KMP*((Xk(47)/Xk(43))/(KSP+Xk(47)/Xk(43)))*(Xk(56)/(KOH+Xk(56)))*(Xk(51)/(KNA+Xk(51)))*Xk(43);
ROUCTF(48)=KMP*((Xk(47)/Xk(43))/(KSP+Xk(47)/Xk(43)))*(Xk(56)/(KOH+Xk(56)))*(KNA/(KNA+Xk(51)))*(Xk(53)/(KNO+Xk(53)))*
Xk(43);
ROUCTF(49)=KMP*((Xk(47)/Xk(43))/(KSP+Xk(47)/Xk(43)))*(KOH/(KOH+Xk(56)))*(Xk(51)/(KNA+Xk(51)))*(Xk(53)/(KNO+Xk(53)))*
etag*Xk(43);
ROUCTF(50)=KMP*((Xk(47)/Xk(43))/(KSP+Xk(47)/Xk(43)))*(KOH/(KOH+Xk(56)))*(KNA/(KNA+Xk(51)))*(Xk(53)/(KNO+Xk(53)))*
etag*Xk(43);
ROUCTF(51)=bH*Xk(43);
ROUCTF(52)=KA*Xk(48)*Xk(43)*(fMA-(Xk(46)/Xk(43)));
ROUCTF(53)=(ROUCTF(47)+ROUCTF(48)+ROUCTF(49)+ROUCTF(50))*(Xk(49)/Xk(43));
ROUCTF(54)=KR*Xk(52)*Xk(43);
ROUCTF(55)=muA*(Xk(56)/(KOA+Xk(56)))*(Xk(51)/(KSA+Xk(51)))*Xk(44);
ROUCTF(56)=bA*Xk(44);
 % reactions in tank 5
ROUCTF(57)=muH*(Xk(64)/(Ks+Xk(64)))*(Xk(70)/(KOH+Xk(70)))*(Xk(65)/(KNA+Xk(65)))*Xk(57);
ROUCTF(58)=muH*(Xk(64)/(Ks+Xk(64)))*(Xk(70)/(KOH+Xk(70)))*(KNA/(KNA+Xk(65)))*(Xk(67)/(KNO+Xk(67)))*Xk(57);
ROUCTF(59)=muH*(Xk(64)/(Ks+Xk(64)))*(KOH/(KOH+Xk(70)))*(Xk(65)/(KNA+Xk(65)))*(Xk(67)/(KNO+Xk(67)))*Xk(57);
ROUCTF(60)=muH*(Xk(64)/(Ks+Xk(64)))*(KOH/(KOH+Xk(70)))*(KNA/(KNA+Xk(65)))*(Xk(67)/(KNO+Xk(67)))*Xk(57);
ROUCTF(61)=KMP*((Xk(61)/Xk(57))/(KSP+Xk(61)/Xk(57)))*(Xk(70)/(KOH+Xk(70)))*(Xk(65)/(KNA+Xk(65)))*Xk(57);
ROUCTF(62)=KMP*((Xk(61)/Xk(57))/(KSP+Xk(61)/Xk(57)))*(Xk(70)/(KOH+Xk(70)))*(KNA/(KNA+Xk(65)))*(Xk(67)/(KNO+Xk(67)))*
Xk(57);
ROUCTF(63)=KMP*((Xk(61)/Xk(57))/(KSP+Xk(61)/Xk(57)))*(KOH/(KOH+Xk(70)))*(Xk(65)/(KNA+Xk(65)))*(Xk(67)/(KNO+Xk(67)))*
etag*Xk(57);
```

```
ROUCTF(64)=KMP*((Xk(61)/Xk(57))/(KSP+Xk(61)/Xk(57)))*(KOH/(KOH+Xk(70)))*(KNA/(KNA+Xk(65)))*(Xk(67)/(KNO+Xk(67)))*
etag*Xk(57);
ROUCTF(65)=bH*Xk(57);
ROUCTF(66)=KA*Xk(62)*Xk(57)*(fMA-(Xk(60)/Xk(57)));
ROUCTF(67)=(ROUCTF(61)+ROUCTF(62)+ROUCTF(63)+ROUCTF(64))*(Xk(63)/Xk(57));
ROUCTF(68)=KR*Xk(66)*Xk(57);
ROUCTF(69)=muA*(Xk(70)/(KOA+Xk(70)))*(Xk(65)/(KSA+Xk(65)))*Xk(58);
ROUCTF(70)=bA*Xk(58);
 %Vector of the process rates
ROUCTF=[ROUCTF(1);ROUCTF(2);ROUCTF(3);ROUCTF(4);ROUCTF(5);ROUCTF(6);ROUCTF(7);ROUCTF(8);ROUCTF(9);ROUCTF(10);ROUCTF(11)
;ROUCTF(12);ROUCTF(13);ROUCTF(14);
ROUCTF(15);ROUCTF(16);ROUCTF(17);ROUCTF(18);ROUCTF(19);ROUCTF(20);ROUCTF(21);ROUCTF(22);ROUCTF(23);ROUCTF(24);
ROUCTF(25);ROUCTF(26);ROUCTF(27);ROUCTF(28);
ROUCTF(29);ROUCTF(30);ROUCTF(31);ROUCTF(32);ROUCTF(33);ROUCTF(34);ROUCTF(35);ROUCTF(36);ROUCTF(37);ROUCTF(38);
ROUCTF(39);ROUCTF(40);ROUCTF(41);ROUCTF(42);
ROUCTF(43);ROUCTF(44);ROUCTF(45);ROUCTF(46);ROUCTF(47);ROUCTF(48);ROUCTF(49);ROUCTF(50);ROUCTF(51);ROUCTF(52);
ROUCTF(53);ROUCTF(54);ROUCTF(55);ROUCTF(56);
ROUCTF(57);ROUCTF(58);ROUCTF(59);ROUCTF(60);ROUCTF(61);ROUCTF(62);ROUCTF(63);ROUCTF(64);ROUCTF(65);ROUCTF(66);
ROUCTF(67);ROUCTF(68);ROUCTF(69);ROUCTF(70)];
```

%SUBPROGRAM prateBUCTR.m

```
%AIM:The program function prateBUCTR.m calculates at every moment the function P, which multiplies the estimated
parameters for the reduced UCT biological model and Benchmark process.
%The program uses global definition of the model parameters

function [Pk]=prateBUCTR(Xk,Uk,XBHk,XBAk,XSEk)
global Ks KOH KNO KNA KOA muH etag muA KMP fZBH YZH YZA KA KSA KSP fMA bH KR bA

%Calculation of the process rates function Pk at every moment of the time
% tank 1
P11=(Xk(3)/(Ks+Xk(3)))*(Uk(1)/(KOH+Uk(1)))*(Xk(1)/(KNA+Xk(1)))*XBHk(1);
P12=(Xk(3)/(Ks+Xk(3)))*(Uk(1)/(KOH+Uk(1)))*(KNA/(KNA+Xk(1)))*(Xk(2)/(KNO+Xk(2)))*XBHk(1);
P13=(Xk(3)/(Ks+Xk(3)))*(KOH/(KOH+Uk(1)))*(Xk(1)/(KNA+Xk(1)))*(Xk(2)/(KNO+Xk(2)))*XBHk(1);
P14=(Xk(3)/(Ks+Xk(3)))*(KOH/(KOH+Uk(1)))*(KNA/(KNA+Xk(1)))*(Xk(2)/(KNO+Xk(2)))*XBHk(1);
P15=((Xk(4)/XBHk(1))/(KSP+Xk(4)/XBHk(1)))*(Uk(1)/(KOH+Uk(1)))*(Xk(1)/(KNA+Xk(1)))*XBHk(1);
P16=((Xk(4)/XBHk(1))/(KSP+Xk(4)/XBHk(1)))*(Uk(1)/(KOH+Uk(1)))*(KNA/(KNA+Xk(1)))*(Xk(2)/(KNO+Xk(2)))*XBHk(1);
P17=((Xk(4)/XBHk(1))/(KSP+Xk(4)/XBHk(1)))*(KOH/(KOH+Uk(1)))*(Xk(1)/(KNA+Xk(1)))*(Xk(2)/(KNO+Xk(2)))*etag*XBHk(1);
P18=((Xk(4)/XBHk(1))/(KSP+Xk(4)/XBHk(1)))*(KOH/(KOH+Uk(1)))*(KNA/(KNA+Xk(1)))*(Xk(2)/(KNO+Xk(2)))*etag*XBHk(1);
P19=XSEk(1)*XBHk(1)*(fMA-(Xk(4)/XBHk(1)));
P110=(Uk(1)/(KOA+Uk(1)))*(Xk(1)/(KSA+Xk(1)))*XBAk(1);
P1k=[P11 0 0 0;P12 0 0 0;P13 0 0 0;P14 0 0 0;0 P15 0 0;0 P16 0 0;0 P17 0 0;0 P18 0 0;0 0 P19 0;0 0 0 P110];
 % tank 2
P21=(Xk(7)/(Ks+Xk(7)))*(Uk(2)/(KOH+Uk(2)))*(Xk(5)/(KNA+Xk(5)))*XBHk(2);
P22=(Xk(7)/(Ks+Xk(7)))*(Uk(2)/(KOH+Uk(2)))*(KNA/(KNA+Xk(5)))*(Xk(6)/(KNO+Xk(6)))*XBHk(2);
P23=(Xk(7)/(Ks+Xk(7)))*(KOH/(KOH+Uk(2)))*(Xk(5)/(KNA+Xk(5)))*(Xk(6)/(KNO+Xk(6)))*XBHk(2);
P24=(Xk(7)/(Ks+Xk(7)))*(KOH/(KOH+Uk(2)))*(KNA/(KNA+Xk(5)))*(Xk(6)/(KNO+Xk(6)))*XBHk(2);
P25=((Xk(8)/XBHk(2))/(KSP+Xk(8)/XBHk(2)))*(Uk(2)/(KOH+Uk(2)))*(Xk(5)/(KNA+Xk(5)))*XBHk(2);
P26=((Xk(8)/XBHk(2))/(KSP+Xk(8)/XBHk(2)))*(Uk(2)/(KOH+Uk(2)))*(KNA/(KNA+Xk(5)))*(Xk(6)/(KNO+Xk(6)))*XBHk(2);
P27=((Xk(8)/XBHk(2))/(KSP+Xk(8)/XBHk(2)))*(KOH/(KOH+Uk(2)))*(Xk(5)/(KNA+Xk(5)))*(Xk(6)/(KNO+Xk(6)))*etag*XBHk(2);
P28=((Xk(8)/XBHk(2))/(KSP+Xk(8)/XBHk(2)))*(KOH/(KOH+Uk(2)))*(KNA/(KNA+Xk(5)))*(Xk(6)/(KNO+Xk(6)))*etag*XBHk(2);
P29=XSEk(2)*XBHk(2)*(fMA-(Xk(8)/XBHk(2)));
P210=(Uk(2)/(KOA+Uk(2)))*(Xk(5)/(KSA+Xk(5)))*XBAk(2);
P2k=[P21 0 0 0;P22 0 0 0;P23 0 0 0;P24 0 0 0;0 P25 0 0;0 P26 0 0;0 P27 0 0;0 P28 0 0;0 0 P29 0;0 0 0 P210];
 % tank 3
P31=(Xk(11)/(Ks+Xk(11)))*(Uk(3)/(KOH+Uk(3)))*(Xk(9)/(KNA+Xk(9)))*XBHk(3);
P32=(Xk(11)/(Ks+Xk(11)))*(Uk(3)/(KOH+Uk(3)))*(KNA/(KNA+Xk(9)))*(Xk(10)/(KNO+Xk(10)))*XBHk(3);
P33=(Xk(11)/(Ks+Xk(11)))*(KOH/(KOH+Uk(3)))*(Xk(9)/(KNA+Xk(9)))*(Xk(10)/(KNO+Xk(10)))*XBHk(3);
P34=(Xk(11)/(Ks+Xk(11)))*(KOH/(KOH+Uk(3)))*(KNA/(KNA+Xk(9)))*(Xk(10)/(KNO+Xk(10)))*XBHk(3);
P35=((Xk(12)/XBHk(3))/(KSP+Xk(12)/XBHk(3)))*(Uk(3)/(KOH+Uk(3)))*(Xk(9)/(KNA+Xk(9)))*XBHk(3);
P36=((Xk(12)/XBHk(3))/(KSP+Xk(12)/XBHk(3)))*(Uk(3)/(KOH+Uk(3)))*(KNA/(KNA+Xk(9)))*(Xk(10)/(KNO+Xk(10)))*XBHk(3);
P37=((Xk(12)/XBHk(3))/(KSP+Xk(12)/XBHk(3)))*(KOH/(KOH+Uk(3)))*(Xk(9)/(KNA+Xk(9)))*(Xk(10)/(KNO+Xk(10)))*etag*XBHk(3);
P38=((Xk(12)/XBHk(3))/(KSP+Xk(12)/XBHk(3)))*(KOH/(KOH+Uk(3)))*(KNA/(KNA+Xk(9)))*(Xk(10)/(KNO+Xk(10)))*etag*XBHk(3);
P39=XSEk(3)*XBHk(3)*(fMA-(Xk(12)/XBHk(3)));
P310=(Uk(3)/(KOA+Uk(3)))*(Xk(9)/(KSA+Xk(9)))*XBAk(3);
P3k=[P31 0 0 0;P32 0 0 0;P33 0 0 0;P34 0 0 0;0 P35 0 0;0 P36 0 0;0 P37 0 0;0 P38 0 0;0 0 P39 0;0 0 0 P310];
 % tank 4
P41=(Xk(15)/(Ks+Xk(15)))*(Uk(4)/(KOH+Uk(4)))*(Xk(13)/(KNA+Xk(13)))*XBHk(4);
P42=(Xk(15)/(Ks+Xk(15)))*(Uk(4)/(KOH+Uk(4)))*(KNA/(KNA+Xk(13)))*(Xk(14)/(KNO+Xk(14)))*XBHk(4);
P43=(Xk(15)/(Ks+Xk(15)))*(KOH/(KOH+Uk(4)))*(Xk(13)/(KNA+Xk(13)))*(Xk(14)/(KNO+Xk(14)))*XBHk(4);
P44=(Xk(15)/(Ks+Xk(15)))*(KOH/(KOH+Uk(4)))*(KNA/(KNA+Xk(13)))*(Xk(14)/(KNO+Xk(14)))*XBHk(4);
P45=((Xk(16)/XBHk(4))/(KSP+Xk(16)/XBHk(4)))*(Uk(4)/(KOH+Uk(4)))*(Xk(13)/(KNA+Xk(13)))*XBHk(4);
P46=((Xk(16)/XBHk(4))/(KSP+Xk(16)/XBHk(4)))*(Uk(4)/(KOH+Uk(4)))*(KNA/(KNA+Xk(13)))*(Xk(14)/(KNO+Xk(14)))*XBHk(4);
P47=((Xk(16)/XBHk(4))/(KSP+Xk(16)/XBHk(4)))*(KOH/(KOH+Uk(4)))*(Xk(13)/(KNA+Xk(13)))*(Xk(14)/(KNO+Xk(14)))*etag*XBHk(4);
P48=((Xk(16)/XBHk(4))/(KSP+Xk(16)/XBHk(4)))*(KOH/(KOH+Uk(4)))*(KNA/(KNA+Xk(13)))*(Xk(14)/(KNO+Xk(14)))*etag*XBHk(4);
P49=XSEk(4)*XBHk(4)*(fMA-(Xk(16)/XBHk(4)));
P410=(Uk(4)/(KOA+Uk(4)))*(Xk(13)/(KSA+Xk(13)))*XBAk(4);
P4k=[P41 0 0 0;P42 0 0 0;P43 0 0 0;P44 0 0 0;0 P45 0 0;0 P46 0 0;0 P47 0 0;0 P48 0 0;0 0 P49 0;0 0 0 P410];
 % reactions in tank 5
P51=(Xk(19)/(Ks+Xk(19)))*(Uk(5)/(KOH+Uk(5)))*(Xk(17)/(KNA+Xk(17)))*XBHk(5);
P52=(Xk(19)/(Ks+Xk(19)))*(Uk(5)/(KOH+Uk(5)))*(KNA/(KNA+Xk(17)))*(Xk(18)/(KNO+Xk(18)))*XBHk(5);
P53=(Xk(19)/(Ks+Xk(19)))*(KOH/(KOH+Uk(5)))*(Xk(17)/(KNA+Xk(17)))*(Xk(18)/(KNO+Xk(18)))*XBHk(5);
P54=(Xk(19)/(Ks+Xk(19)))*(KOH/(KOH+Uk(5)))*(KNA/(KNA+Xk(17)))*(Xk(18)/(KNO+Xk(18)))*XBHk(5);
P55=((Xk(20)/XBHk(5))/(KSP+Xk(20)/XBHk(5)))*(Uk(5)/(KOH+Uk(5)))*(Xk(17)/(KNA+Xk(17)))*XBHk(5);
P56=((Xk(20)/XBHk(5))/(KSP+Xk(20)/XBHk(5)))*(Uk(5)/(KOH+Uk(5)))*(KNA/(KNA+Xk(17)))*(Xk(18)/(KNO+Xk(18)))*XBHk(5);
P57=((Xk(20)/XBHk(5))/(KSP+Xk(20)/XBHk(5)))*(KOH/(KOH+Uk(5)))*(Xk(17)/(KNA+Xk(17)))*(Xk(18)/(KNO+Xk(18)))*etag*XBHk(5);
P58=((Xk(20)/XBHk(5))/(KSP+Xk(20)/XBHk(5)))*(KOH/(KOH+Uk(5)))*(KNA/(KNA+Xk(17)))*(Xk(18)/(KNO+Xk(18)))*etag*XBHk(5);
P59=XSEk(5)*XBHk(5)*(fMA-(Xk(20)/XBHk(5)));
P510=muA*(Uk(5)/(KOA+Uk(5)))*(Xk(17)/(KSA+Xk(17)))*XBAk(5);
P5k=[P51 0 0 0;P52 0 0 0;P53 0 0 0;P54 0 0 0;0 P55 0 0;0 P56 0 0;0 P57 0 0;0 P58 0 0;0 0 P59 0;0 0 0 P510];
 %Matrix Pk
Pk=[P1k;P2k;P3k;P4k;P5k];
```

```
%SUBPROGRAM rateBUCTE.m
%AIM:The program function rateBUCTE.m calculates at every moment the process rates using the estimated values of the
parameters for the reduced UCT biological model and the Benchmark process.
%The program uses global definition of the model parameters

function [ROBUCTE]=rateBUCTE(Xk,Uk,XBHk,XBAk,XSEk,thetak)
global Ks KOH KNO KNA KOA muH etag muA KMP fZBH YZH YZA KA KSA KSP fMA bH KR bA

%Calculation of the process rates at every moment of the time
% reactions in tank 1
ROUCT(1)=thetak(1)*(Xk(3)/(Ks+Xk(3)))*(Uk(1)/(KOH+Uk(1)))*(Xk(1)/(KNA+Xk(1)))*XBHk(1);
ROUCT(2)=thetak(1)*(Xk(3)/(Ks+Xk(3)))*(Uk(1)/(KOH+Uk(1)))*(KNA/(KNA+Xk(1)))*(Xk(2)/(KNO+Xk(2)))*XBHk(1);
ROUCT(3)=thetak(1)*(Xk(3)/(Ks+Xk(3)))*(KOH/(KOH+Uk(1)))*(Xk(1)/(KNA+Xk(1)))*(Xk(2)/(KNO+Xk(2)))*XBHk(1);
ROUCT(4)=thetak(1)*(Xk(3)/(Ks+Xk(3)))*(KOH/(KOH+Uk(1)))*(KNA/(KNA+Xk(1)))*(Xk(2)/(KNO+Xk(2)))*XBHk(1);
ROUCT(5)=thetak(2)*((Xk(4)/XBHk(1))/(KSP+Xk(4)/XBHk(1)))*(Uk(1)/(KOH+Uk(1)))*(Xk(1)/(KNA+Xk(1)))*XBHk(1);
ROUCT(6)=thetak(2)*((Xk(4)/XBHk(1))/(KSP+Xk(4)/XBHk(1)))*(Uk(1)/(KOH+Uk(1)))*(KNA/(KNA+Xk(1)))*(Xk(2)/(KNO+Xk(2)))*
XBHk(1);
ROUCT(7)=thetak(2)*((Xk(4)/XBHk(1))/(KSP+Xk(4)/XBHk(1)))*(KOH/(KOH+Uk(1)))*(Xk(1)/(KNA+Xk(1)))*(Xk(2)/(KNO+Xk(2)))*
etag*XBHk(1);
ROUCT(8)=thetak(2)*((Xk(4)/XBHk(1))/(KSP+Xk(4)/XBHk(1)))*(KOH/(KOH+Uk(1)))*(KNA/(KNA+Xk(1)))*(Xk(2)/(KNO+Xk(2)))*
etag*XBHk(1);
ROUCT(9)=thetak(3)*XSEk(1)*XBHk(1)*(fMA-(Xk(4)/XBHk(1)));
ROUCT(10)=thetak(4)*(Uk(1)/(KOA+Uk(1)))*(Xk(1)/(KSA+Xk(1)))*XBAk(1);
 % reactions in tank 2
ROUCT(11)=thetak(1)*(Xk(7)/(Ks+Xk(7)))*(Uk(2)/(KOH+Uk(2)))*(Xk(5)/(KNA+Xk(5)))*XBHk(2);
ROUCT(12)=thetak(1)*(Xk(7)/(Ks+Xk(7)))*(Uk(2)/(KOH+Uk(2)))*(KNA/(KNA+Xk(5)))*(Xk(6)/(KNO+Xk(6)))*XBHk(2);
ROUCT(13)=thetak(1)*(Xk(7)/(Ks+Xk(7)))*(KOH/(KOH+Uk(2)))*(Xk(5)/(KNA+Xk(5)))*(Xk(6)/(KNO+Xk(6)))*XBHk(2);
ROUCT(14)=thetak(1)*(Xk(7)/(Ks+Xk(7)))*(KOH/(KOH+Uk(2)))*(KNA/(KNA+Xk(5)))*(Xk(6)/(KNO+Xk(6)))*XBHk(2);
ROUCT(15)=thetak(2)*((Xk(8)/XBHk(2))/(KSP+Xk(8)/XBHk(2)))*(Uk(2)/(KOH+Uk(2)))*(Xk(5)/(KNA+Xk(5)))*XBHk(2);
ROUCT(16)=thetak(2)*((Xk(8)/XBHk(2))/(KSP+Xk(8)/XBHk(2)))*(Uk(2)/(KOH+Uk(2)))*(KNA/(KNA+Xk(5)))*(Xk(6)/(KNO+Xk(6)))*
XBHk(2);
ROUCT(17)=thetak(2)*((Xk(8)/XBHk(2))/(KSP+Xk(8)/XBHk(2)))*(KOH/(KOH+Uk(2)))*(Xk(5)/(KNA+Xk(5)))*(Xk(6)/(KNO+Xk(6)))*
etag*XBHk(2);
ROUCT(18)=thetak(2)*((Xk(8)/XBHk(2))/(KSP+Xk(8)/XBHk(2)))*(KOH/(KOH+Uk(2)))*(KNA/(KNA+Xk(5)))*(Xk(6)/(KNO+Xk(6)))*
etag*XBHk(2);
ROUCT(19)=thetak(3)*XSEk(2)*XBHk(2)*(fMA-(Xk(8)/XBHk(2)));
ROUCT(20)=thetak(4)*(Uk(2)/(KOA+Uk(2)))*(Xk(5)/(KSA+Xk(5)))*XBAk(2);
% reactions in tank 3
ROUCT(21)=thetak(1)*(Xk(11)/(Ks+Xk(11)))*(Uk(3)/(KOH+Uk(3)))*(Xk(9)/(KNA+Xk(9)))*XBHk(3);
ROUCT(22)=thetak(1)*(Xk(11)/(Ks+Xk(11)))*(Uk(3)/(KOH+Uk(3)))*(KNA/(KNA+Xk(9)))*(Xk(10)/(KNO+Xk(10)))*XBHk(3);
ROUCT(23)=thetak(1)*(Xk(11)/(Ks+Xk(11)))*(KOH/(KOH+Uk(3)))*(Xk(9)/(KNA+Xk(9)))*(Xk(10)/(KNO+Xk(10)))*XBHk(3);
ROUCT(24)=thetak(1)*(Xk(11)/(Ks+Xk(11)))*(KOH/(KOH+Uk(3)))*(KNA/(KNA+Xk(9)))*(Xk(10)/(KNO+Xk(10)))*XBHk(3);
ROUCT(25)=thetak(2)*((Xk(12)/XBHk(3))/(KSP+Xk(12)/XBHk(3)))*(Uk(3)/(KOH+Uk(3)))*(Xk(9)/(KNA+Xk(9)))*XBHk(3);
ROUCT(26)=thetak(2)*((Xk(12)/XBHk(3))/(KSP+Xk(12)/XBHk(3)))*(Uk(3)/(KOH+Uk(3)))*(KNA/(KNA+Xk(9)))*(Xk(10)/(KNO+Xk(10)))
*XBHk(3);
ROUCT(27)=thetak(2)*((Xk(12)/XBHk(3))/(KSP+Xk(12)/XBHk(3)))*(KOH/(KOH+Uk(3)))*(Xk(9)/(KNA+Xk(9)))*(Xk(10)/(KNO+Xk(10)))
*etag*XBHk(3);
ROUCT(28)=thetak(2)*((Xk(12)/XBHk(3))/(KSP+Xk(12)/XBHk(3)))*(KOH/(KOH+Uk(3)))*(KNA/(KNA+Xk(9)))*(Xk(10)/(KNO+Xk(10)))*
etag*XBHk(3);
ROUCT(29)=thetak(3)*XSEk(3)*XBHk(3)*(fMA-(Xk(12)/XBHk(3)));
ROUCT(30)=thetak(4)*(Uk(3)/(KOA+Uk(3)))*(Xk(9)/(KSA+Xk(9)))*XBAk(3);
 % reactions in tank 4
ROUCT(31)=thetak(1)*(Xk(15)/(Ks+Xk(15)))*(Uk(4)/(KOH+Uk(4)))*(Xk(13)/(KNA+Xk(13)))*XBHk(4);
ROUCT(32)=thetak(1)*(Xk(15)/(Ks+Xk(15)))*(Uk(4)/(KOH+Uk(4)))*(KNA/(KNA+Xk(13)))*(Xk(14)/(KNO+Xk(14)))*XBHk(4);
ROUCT(33)=thetak(1)*(Xk(15)/(Ks+Xk(15)))*(KOH/(KOH+Uk(4)))*(Xk(13)/(KNA+Xk(13)))*(Xk(14)/(KNO+Xk(14)))*XBHk(4);
ROUCT(34)=thetak(1)*(Xk(15)/(Ks+Xk(15)))*(KOH/(KOH+Uk(4)))*(KNA/(KNA+Xk(13)))*(Xk(14)/(KNO+Xk(14)))*XBHk(4);
ROUCT(35)=thetak(2)*((Xk(16)/XBHk(4))/(KSP+Xk(16)/XBHk(4)))*(Uk(4)/(KOH+Uk(4)))*(Xk(13)/(KNA+Xk(13)))*XBHk(4);
ROUCT(36)=thetak(2)*((Xk(16)/XBHk(4))/(KSP+Xk(16)/XBHk(4)))*(Uk(4)/(KOH+Uk(4)))*(KNA/(KNA+Xk(13)))*
(Xk(14)/(KNO+Xk(14)))*XBHk(4);
ROUCT(37)=thetak(2)*((Xk(16)/XBHk(4))/(KSP+Xk(16)/XBHk(4)))*(KOH/(KOH+Uk(4)))*(Xk(13)/(KNA+Xk(13)))*
(Xk(14)/(KNO+Xk(14)))*etag*XBHk(4);
ROUCT(38)=thetak(2)*((Xk(16)/XBHk(4))/(KSP+Xk(16)/XBHk(4)))*(KOH/(KOH+Uk(4)))*(KNA/(KNA+Xk(13)))*(Xk(14)/(KNO+Xk(14)))*
etag*XBHk(4);
ROUCT(39)=thetak(3)*XSEk(4)*XBHk(4)*(fMA-(Xk(16)/XBHk(4)));
ROUCT(40)=thetak(4)*(Uk(4)/(KOA+Uk(4)))*(Xk(13)/(KSA+Xk(13)))*XBAk(4);

% reactions in tank 5
ROUCT(41)=thetak(1)*(Xk(19)/(Ks+Xk(19)))*(Uk(5)/(KOH+Uk(5)))*(Xk(17)/(KNA+Xk(17)))*XBHk(5);
ROUCT(42)=thetak(1)*(Xk(19)/(Ks+Xk(19)))*(Uk(5)/(KOH+Uk(5)))*(KNA/(KNA+Xk(17)))*(Xk(18)/(KNO+Xk(18)))*XBHk(5);
ROUCT(43)=thetak(1)*(Xk(19)/(Ks+Xk(19)))*(KOH/(KOH+Uk(5)))*(Xk(17)/(KNA+Xk(17)))*(Xk(18)/(KNO+Xk(18)))*XBHk(5);
ROUCT(44)=thetak(1)*(Xk(19)/(Ks+Xk(19)))*(KOH/(KOH+Uk(5)))*(KNA/(KNA+Xk(17)))*(Xk(18)/(KNO+Xk(18)))*XBHk(5);
ROUCT(45)=thetak(2)*((Xk(20)/XBHk(5))/(KSP+Xk(20)/XBHk(5)))*(Uk(5)/(KOH+Uk(5)))*(Xk(17)/(KNA+Xk(17)))*XBHk(5);
ROUCT(46)=thetak(2)*((Xk(20)/XBHk(5))/(KSP+Xk(20)/XBHk(5)))*(Uk(5)/(KOH+Uk(5)))*(KNA/(KNA+Xk(17)))*(Xk(18)/(KNO+Xk(18))
)*XBHk(5);
ROUCT(47)=thetak(2)*((Xk(20)/XBHk(5))/(KSP+Xk(20)/XBHk(5)))*(KOH/(KOH+Uk(5)))*(Xk(17)/(KNA+Xk(17)))*(Xk(18)/(KNO+Xk(18)
))*etag*XBHk(5);
ROUCT(48)=thetak(2)*((Xk(20)/XBHk(5))/(KSP+Xk(20)/XBHk(5)))*(KOH/(KOH+Uk(5)))*(KNA/(KNA+Xk(17)))*(Xk(18)/(KNO+Xk(18)))*
etag*XBHk(5);
ROUCT(49)=thetak(3)*XSEk(5)*XBHk(5)*(fMA-(Xk(20)/XBHk(5)));
ROUCT(50)=thetak(4)*(Uk(5)/(KOA+Uk(5)))*(Xk(17)/(KSA+Xk(17)))*XBAk(5);
 %Vector of the process rates
ROBUCTE=[ROUCT(1);ROUCT(2);ROUCT(3);ROUCT(4);ROUCT(5);ROUCT(6);ROUCT(7);ROUCT(8);ROUCT(9);ROUCT(10);ROUCT(11);ROUCT(12)
;ROUCT(13);ROUCT(14);
ROUCT(15);ROUCT(16);ROUCT(17);ROUCT(18);ROUCT(19);ROUCT(20);ROUCT(21);ROUCT(22);ROUCT(23);ROUCT(24);ROUCT(25);ROUCT(26)
;ROUCT(27);ROUCT(28);
ROUCT(29);ROUCT(30);ROUCT(31);ROUCT(32);ROUCT(33);ROUCT(34);ROUCT(35);ROUCT(36);ROUCT(37);ROUCT(38);ROUCT(39);ROUCT(40)
;ROUCT(41);ROUCT(42);ROUCT(43);ROUCT(44);ROUCT(45);ROUCT(46);ROUCT(47);ROUCT(48);ROUCT(49);ROUCT(50)];
```

CAPE PENINSULA
UNIVERSITY OF TECHNOLOGY